

DEC 18 1958

FORD MOTOR COMPANY  
ENGINEERING LIBRARY  
Dearborn, Michigan

SHELF

Volume 18, No. 1

January 1957

АВТОМАТИКА  
и  
ТЕЛЕМЕХАНИКА

SOVIET INSTRUMENTATION AND  
CONTROL TRANSLATION SERIES

# Automation and Remote Control

(The Soviet Journal *Avtomatika i Telemekhanika* in English Translation)

■ This translation of a Soviet Journal on automatic control is published as a service to American science and industry. It is sponsored by the Massachusetts Institute of Technology under a grant in aid from the National Science Foundation, and is distributed by the Instrument Society of America.





## SOVIET INSTRUMENTATION AND CONTROL TRANSLATION SERIES

### *Instrument Society of America Executive Board*

Robert J. Jeffries  
*President*  
Justus T. Vollbrecht  
*Past President*  
Henry C. Frost  
*President-Elect-Secretary*  
Edward C. Baran  
*Dept. Vice President*  
John Johnston, Jr.  
*Dept. Vice President*  
Philip A. Sprague  
*Dept. Vice President*  
Ralph H. Tripp  
*Dept. Vice President*  
Howard W. Hudson  
*Treasurer*  
Carl W. Gram, Jr.  
*Dist. I Vice President*  
E. Albert Adler  
*Dist. II Vice President*  
John T. Elder  
*Dist. III Vice President*  
Mifflin S. Jacobs  
*Dist. IV Vice President*  
Gordon D. Carnegie  
*Dist. V Vice President*  
Willard A. Kates  
*Dist. VI Vice President*  
John F. Draffen  
*Dist. VII Vice President*  
John V. Opie  
*Dist. VIII Vice President*  
Adelbert Carpenter  
*Dist. IX Vice President*  
John J. Hillen  
*Dist. X Vice President*

### *Headquarters Office*

William H. Kushnick  
*Executive Director*  
Charles W. Covey  
*Editor, ISA Journal*  
George A. Hall  
*Assistant Editor, ISA Journal*  
Herbert S. Kindler  
*Director Technical Programs*  
Ralph M. Stotsenburg  
*Director Section Activities*  
Thomas K. Hodges  
*Director Promotional Services*

### *ISA Publications Committee*

Nathan Cohn, *Chairman*  
Jere E. Brophy    George A. Larsen    Frank S. Swaney  
Floyd E. Bryan    John E. Read    Richard A. Terry  
Richard W. Jones    Joshua Stern    Benjamin W. Thomas

■ This translation of the Soviet Journal *Avtomatika i Telemekhanika* is published and distributed at nominal subscription rates under a grant in aid to the Massachusetts Institute of Technology from the National Science Foundation. The translated journal will enable American scientists and engineers to be informed of work in the fields of instrumentation and automatic control reported in the Soviet Union.

The original Russian articles are translated by competent technical personnel. The translations are on a cover-to-cover basis, permitting readers to appraise for themselves the scope, status and importance of the Soviet work.

Publication of *Avtomatika i Telemekhanika* in English translation started under the present auspices in April 1958 with Russian Vol. 18, No. 1, of January 1957. The eleven remaining Russian issues of 1957 will be published in English translation prior to the end of 1958. English translations will carry the same volume and issue numbers as the Russian originals.

All views expressed in the translated material are intended to be those of the original authors, and not those of the translators, the Massachusetts Institute of Technology, nor the Instrument Society of America.

Readers are invited to submit communications on the quality of the translations and the content of the articles to ISA headquarters. Pertinent correspondence will be published in the "Letters" section of the ISA Journal. Space will also be made available in the ISA Journal for such replies as may be received from Russian authors to comments or questions by American readers.

### *Subscription Prices:*

Per year (12 issues), starting with Vol. 18, No. 1

General: United States and Canada . . . . . \$30.00  
Elsewhere . . . . . 33.00

*Libraries of academic and other non-profit institutions:*  
United States and Canada . . . . . \$15.00  
Elsewhere . . . . . 18.00

Single issues to everyone, each . . . . . \$ 3.50

### *Subscriptions should be addressed to the:*

Instrument Society of America  
313 Sixth Avenue, Pittsburgh 22, Penna.

*Translated and printed by Consultants Bureau, Inc.  
Copyright by Massachusetts Institute of Technology 1958*







# THE APPROXIMATE DERIVATION OF PARTIAL "SLIDING" PERIODIC MODES IN RELAY SYSTEMS\*

Yu. V. Dolgolenko

(Leningrad)

An automatic control system in which a relay link with a symmetric characteristic is the control element for an amplifier is considered; an internal feedback loop which includes the relay is also present. It is shown that in order to detect symmetric partially sliding periodic modes (i.e., modes in which the relay system oscillates during part of a half-period) in such a system we must apply an approximate harmonic balance method, while the non-linear link is taken to be the amplifier unit made up of amplifier, relay and internal feedback loop. Simple partially sliding periodic modes are classified, formulas are derived and hodographs presented for the harmonic transfer coefficient of the amplifier unit. Examples of determining partially sliding periodic modes by harmonic balance methods are given.

## 1. The Equation of Motion for the Relay System. Sliding Mode

Let us consider an automatic control system in which a relay link having the characteristic shown in Fig. 1 is the control element for an amplifier. Three types of internal feedback encompassing the relay are in

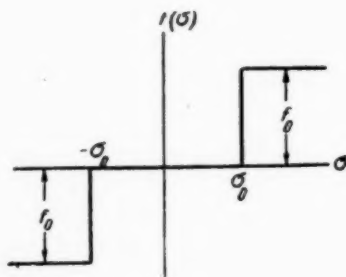


Fig. 1

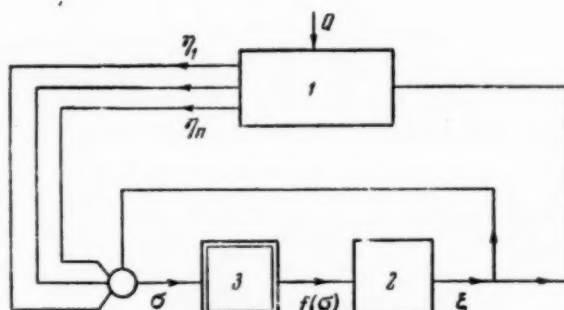


Fig. 2. 1) linear part; 2) amplifier; 3) relay.

practice found in such systems: a) strong feedback from amplifier output to relay input, the transfer function being  $K(p) = 1$ ; b) weak feedback from amplifier output to relay input, the transfer function being  $K(p) = \rho \frac{T_p}{T_p + 1}$ ; c) a static delay between relay output and input  $K(p) = \frac{\rho}{T_p + 1}$ . It has been shown [1] that in

\* Presented at a seminar at the Institute of Automation and Remote Control, Academy of Sciences of the USSR.

all three cases the system can be referred to the block diagram shown in Fig. 2, while the equation of motion can be written in the following form:

$$\begin{aligned}\dot{\eta}_k &= \sum_{a=1}^n b_{ka} \eta_a + n_k \xi + h_k Q, \quad (k=1, 2, \dots, n), \\ \sigma &= \sum_{k=1}^n j_k \eta_k - r \xi, \quad \dot{\xi} = f(\sigma),\end{aligned}\quad (1.1)$$

where  $b$ ,  $n$ ,  $h$ ,  $j$ , and  $r$  are constants, and  $Q$  is the external disturbance applied to the linear part.

The motion of the system described by (1.1) may be considered as that of the image point in the  $(n+1)$  dimensional phase space of the variables  $\eta_k$ ,  $(k=1, 2, \dots, n)$  and  $\xi$ . The threshold values of the variables at the relay input,  $\sigma = \pm \sigma_0$  define the surfaces.

$$\pm \sigma_0 = \sum_{k=1}^n j_k \eta_k - r \xi. \quad (1.2)$$

The surfaces of (1.2) divide the phase space into three regions.\* In region  $S$ ,  $\xi = \text{const}$ ; the amplifier is here dead. In the  $G^{(+)}$  and  $G^{(-)}$  regions we have  $\dot{\xi} = f_0$  and  $\dot{\xi} = -f_0$ , respectively, these being regions of relay motion.

The motion may be termed "sliding" if the image point moves over one of the surfaces defined by (1.2). The sliding mode areas are those areas on the surfaces  $\sigma = \pm \sigma_0$  in which the image point trajectories lie in the surfaces and do not pass through them, unlike what occurs in the other areas of the (1.2) surfaces. We shall denote these regions by  $R^{(+)}$  and  $R^{(-)}$ , respectively. The  $R$  regions exist if  $r \neq 0$  in the relay system equations when these are given in the form of (1.1).

It has been shown [1] that for a sliding mode to exist in a relay automatic control system the necessary and sufficient conditions that have to be fulfilled are

$$\begin{aligned}\pm \sigma_0 &= \sum_{k=1}^n j_k \eta_k - r \xi, \\ r f_0 + \frac{l}{r} \sigma_0 &\geq \pm \left[ \sum_{a=1}^n \eta_a \sum_{k=1}^n j_k v_{ka} + m Q \right] \geq \frac{l}{r} \sigma_0,\end{aligned}\quad (1.3)$$

where the symbols used are

$$v_{ka} = b_{ka} + \frac{1}{r} n_k j_a, \quad m = \sum_{k=1}^n j_k h_k, \quad l = \sum_{k=1}^n j_k n_k. \quad (1.4)$$

If (1.3) is fulfilled with the positive sign where an alternative exists the sliding mode falls in region  $R^{(+)}$ , being accompanied by a monotonic increase in the  $\xi$  coordinate of the amplifier. When the minus sign applies the sliding occurs in  $R^{(-)}$  and  $\xi$  decreases monotonically.

Another formula, equivalent to (1.3), has been given [1]. It is as follows:

$$f_0 \geq \pm \xi \geq 0. \quad (1.5)$$

\* See Figs. 6-10.

(1.5) was derived by G. N. Nikolsky [2].

The boundary  $g^{(+)}$  to the region  $R^{(+)}$  (on attaining which the image point passes into the  $G^{(+)}$  region) is defined by the equations

$$\sum_{k=1}^n j_k \eta_k - r \xi = \sigma_0, \quad \sum_{\alpha=1}^n \eta_{\alpha} \sum_{k=1}^n j_k v_{k\alpha} = r f_0 + \frac{l}{r} \sigma_0 - mQ, \quad (1.6)$$

while the boundary  $s^{(+)}$  to the region  $R^{(+)}$  (on attaining which the image point passes into the  $S$  region) is defined by the equations

$$\sum_{k=1}^n j_k \eta_k - r \xi = \sigma_0, \quad \sum_{\alpha=1}^n \eta_{\alpha} \sum_{k=1}^n j_k v_{k\alpha} = \frac{l}{r} \sigma_0 - mQ. \quad (1.7)$$

The  $R^{(-)}$  region has a boundary  $g^{(-)}$  which is defined by the equations

$$\sum_{k=1}^n j_k \eta_k - r \xi = -\sigma_0, \quad \sum_{\alpha=1}^n \eta_{\alpha} \sum_{k=1}^n j_k v_{k\alpha} = -r f_0 - \frac{l}{r} \sigma_0 - mQ, \quad (1.8)$$

and the boundary  $s^{(-)}$  is defined by the equations

$$\sum_{k=1}^n j_k \eta_k - r \xi = -\sigma_0, \quad \sum_{\alpha=1}^n \eta_{\alpha} \sum_{k=1}^n j_k v_{k\alpha} = -\frac{l}{r} \sigma_0 - mQ. \quad (1.9)$$

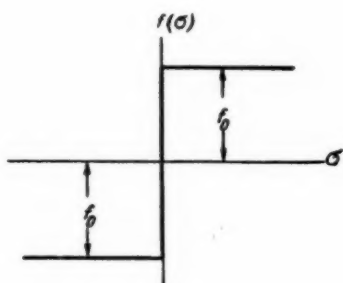


Fig. 3

With a relay characteristic such as is shown in Fig. 3 the surface of (1.2), when  $\sigma_0 = 0$ , divides the phase space into  $G^{(+)}$  and  $G^{(-)}$  regions.\* The sliding mode region  $R$  on the surface  $\sigma = 0$  has boundaries  $g^{(+)}$  and  $g^{(-)}$  which are defined by (1.6) and (1.8), respectively, with  $\sigma_0 = 0$ .  $s^{(+)}$  and  $s^{(-)}$  combine into one boundary  $s$ , which divides the area within  $R$  into a part where the motion occurs as  $\xi$  increases and another where the motion involves  $\xi$  decreasing.  $s$  is defined by (1.7) or (1.9) with  $\sigma_0 = 0$ .

With a relay characteristic such as is shown in Fig. 3, the first form of the condition for sliding to exist becomes

$$\sum_{k=1}^n j_k \eta_k - r \xi = 0, \quad r f_0 \geq \sum_{\alpha=1}^n \eta_{\alpha} \sum_{k=1}^n j_k v_{k\alpha} + mQ \geq -r f_0, \quad (1.10)$$

while the second becomes

$$f_0 \geq \dot{\xi} \geq -f_0. \quad (1.11)$$

\* See Figs. 4 and 5.



## 2. Classification of Symmetric Periodic Modes

A periodic mode is one in which there is a steady-state oscillation. When a periodic mode is symmetric (1.11) has a solution which satisfies the following conditions:

$$\begin{aligned} \eta_k(t) &= -\eta_k(t+T) \quad (k=1, 2, \dots, n), \\ \xi(t) &= -\xi(t+T), \\ \sigma(t) &= -\sigma(t+T), \\ Q(t) &= -Q(t+T), \end{aligned} \quad (2.1)$$

where  $T$  is the half-period of oscillation.

When  $Q(t) \equiv 0$ , self-oscillation occurs, while forced oscillation occurs if there is a periodic external disturbance. In future we will suppose that any external disturbance is sinusoidal:

$$Q = A \sin(\omega t + \varphi). \quad (2.2)$$

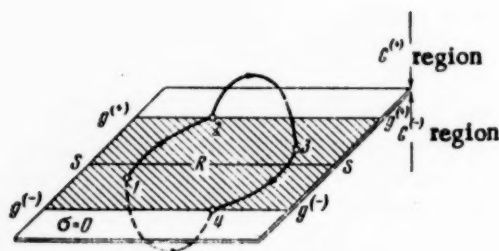


Fig. 4. Phase trajectory for the SR periodic mode.

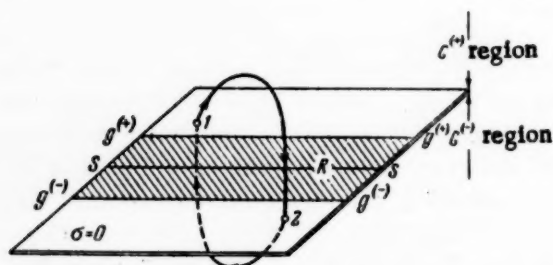


Fig. 5. Phase trajectory for the R periodic mode.

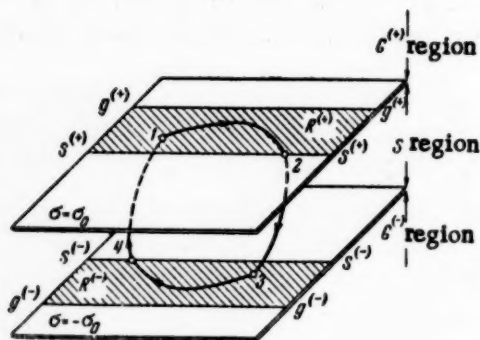


Fig. 6. Phase trajectory for the SD periodic mode.

We shall term periodic modes simple if the image point in the phase space passes once through the S region (dead region) or once through G (region of relay motion) during a half-period.

A periodic mode is termed partially sliding if a sliding action occurs during part of a half-period.

With a relay characteristic as shown in Fig. 3 two simple periodic modes can exist.

a) A partially sliding periodic mode, SR (sliding - relay). A typical phase trajectory for this mode is shown in Fig. 4. In the SR mode the image point moves in the R region along the trajectory 1-2, and on reaching position 2 on the  $g^{(+)}$  boundary the relay motion alters, the image point then moving along 2-3 in the  $G^{(+)}$  region.  $T$  is then equal to the time for the point to follow the track 1-2-3.

b) R periodic mode (relay). A typical phase trajectory for this mode is shown in Fig. 5.  $T$  is then equal to the time for the point to follow the track 1-2.

With a relay characteristic as shown in Fig. 1, five simple symmetric periodic modes can exist.

a) A partially sliding periodic mode SD (sliding - dead). The trajectory for this is shown in Fig. 6. Figure 6 shows that here the sliding mode which is represented by the motion of the image point in the  $R^{(+)}$  region along the area 1-2 later changes to a "dead" mode in which the image point moves along 2-3 in the S region. The time taken for the image point to move from 1-3 is equal to  $T$ .

b) A partially sliding periodic mode SRSD (sliding - relay - sliding - dead). The phase trajectory for this is shown in Fig. 7. The time taken for the image point to move from 1-5 is equal to  $T$ .

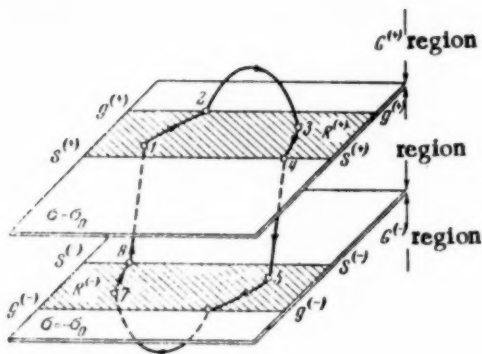


Fig. 7. Phase trajectory for the SRSD periodic mode.

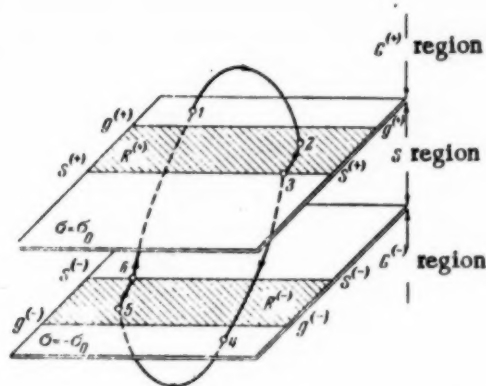


Fig. 8. Phase trajectory for the SDR periodic mode.

c) A partially sliding periodic mode SDR. The phase trajectory for this is shown in Fig. 8. The time taken for the image point to move from 1-4 is equal to  $T$ .

d) A partially sliding periodic mode SRD with a phase trajectory as shown in Fig. 9, and having  $T$  equal to the time taken for the image point to move from 1-4.

e) A periodic mode RD with a phase trajectory as shown in Fig. 10, and having  $T$  equal to the time taken for the image point to move along the arcs 1-2-3.

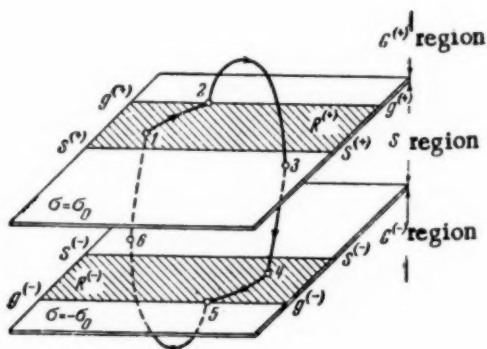


Fig. 9. Phase trajectory for the SRD periodic mode.

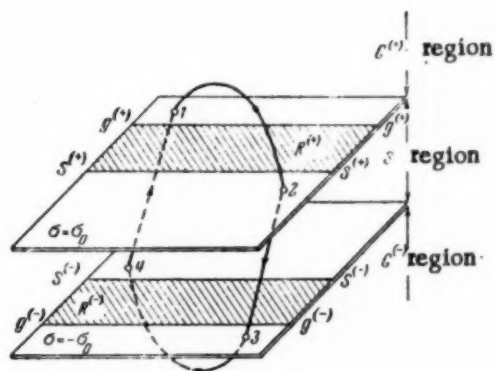


Fig. 10. Phase trajectory for the RD periodic mode.

Yu. I. Neimark [3] and the present writer [4] have considered the exact determination of certain partially sliding periodic modes. Great computational difficulties are encountered in applying exact methods to partially sliding periodic modes in real control systems, since systems of transcendental equations have to be solved. These methods are therefore of no practical value in engineering problems.

### 3. Determination of Periodic Regimes by Harmonic Balance Methods

The following symbolism will be used:

$$\tilde{\xi} = r\dot{\xi}, \quad \tilde{n}_k = \frac{n_k}{r}, \quad \tilde{f}(\sigma) = rf(\sigma). \quad (3.1)$$

Then the system of equations in (1.1) goes over to the following form when the sinusoidal external action of (2.2) is applied:

$$\dot{\eta}_k = \sum_{\alpha=1}^n b_{k\alpha} \eta_{\alpha} + \tilde{n}_k \tilde{\xi} + h_k A \sin(\omega t + \varphi) \quad (k=1, 2, \dots, n),$$

$$\dot{v} = \sum_{k=1}^n j_k \eta_k, \quad (3.2)$$

$$\sigma = v - \tilde{\xi}, \quad \dot{\tilde{\xi}} = \tilde{f}(\sigma). \quad (3.3)$$

(3.2) is the equation for the linear part of the control system, while (3.3) is that for the amplifier unit consisting of relay, amplifier plus integrating link, and strong over-all feedback loop. The block diagram of the system corresponding to (3.2) and (3.3) is shown in Fig. 11, b.

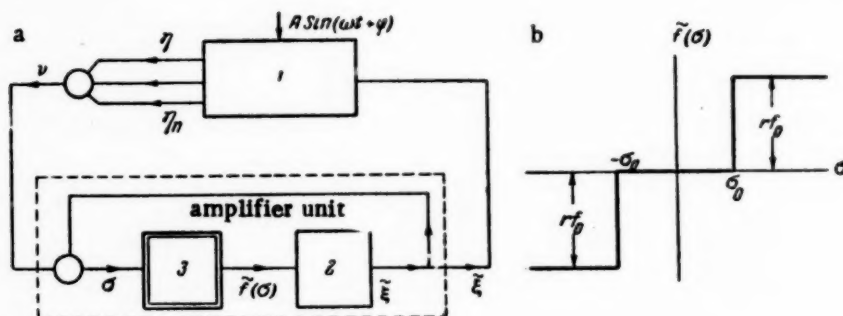


Fig. 11. 1) Linear part; 2) amplifier; 3) relay.

In the sliding mode the input and output variables  $v$  and  $\tilde{\xi}$  from the amplifier unit are related in the following way:

$$\dot{\tilde{\xi}} = v - \sigma_0 \operatorname{sign} \dot{v}, \quad r f_0 > |\dot{v}|, \quad (3.4)$$

since in the sliding mode  $\tilde{\xi} = v$ .

In the relay mode

$$\dot{\tilde{\xi}} = r f_0 \operatorname{sign}(\sigma_0 + v - \tilde{\xi}), \quad |v - \tilde{\xi}| > \sigma_0. \quad (3.5)$$

In the dead mode

$$\dot{\tilde{\xi}} = 0, \quad \sigma_0 > |v - \tilde{\xi}|. \quad (3.6)$$

(3.4) and (3.6) show that the amplifier unit may be considered on the whole as a linear link, the output coordinate  $\tilde{\xi}$  being related to the input by the nonlinear equation

$$\tilde{\xi} = F(v, \dot{v}). \quad (3.7)$$



Assuming that the control system described by (3.2) and (3.7) is operating in a forced oscillatory mode of frequency  $\omega$ , we can use the harmonic balance method [5-8] to derive the periodic mode.

We shall assume that the linear part of the system acts as a low-frequency filter, and that  $\omega$  is such that the higher harmonics of the variables  $\eta_k, (k = 1, 2, \dots, n)$  and  $\tilde{\xi}$  have frequencies falling outside the filter pass-band.

Then, neglecting the higher harmonics in the expressions for  $\eta_k$  and  $v$  we put

$$v = S \sin \omega t, \eta_k = a_k \cos \omega t + c_k \sin \omega t. \quad (3.8)$$

Substituting (3.8) into (3.7), expanding as a Fourier series, and cutting out the higher harmonics, we get

$$\tilde{\xi} = F(S \sin \omega t, S \omega \cos \omega t) = S [g(S, \omega) \sin \omega t + b(S, \omega) \cos \omega t], \quad (3.9)$$

where

$$g(S, \omega) = \frac{1}{\pi S} \int_0^{2\pi} F(S \sin \psi, S \omega \cos \psi) \sin \psi d\psi, \quad (3.10)$$

$$b(S, \omega) = \frac{1}{\pi S} \int_0^{2\pi} F(S \sin \psi, S \omega \cos \psi) \cos \psi d\psi.$$

We now substitute (3.8) and (3.9) into (3.2). After equating the coefficients to  $\sin \omega t$  and  $\cos \omega t$  on the left and right we get

$$-a_k \omega = \sum_{\alpha=1}^n b_{k\alpha} c_\alpha + \tilde{n}_k S g(S, \omega) + h_k A \cos \varphi, \quad (k = 1, 2, \dots, n),$$

$$c_k \omega = \sum_{\alpha=1}^n b_{k\alpha} a_\alpha + \tilde{n}_k S b(S, \omega) + h_k A \sin \varphi, \quad (3.11)$$

$$S = \sum_{k=1}^n j_k c_k, \quad 0 = \sum_{k=1}^n j_k a_k. \quad (3.12)$$

Multiplying the second equations in (3.11) and (3.12) by  $\underline{i}$  and combining these with the first equations we get

$$i \omega R_k = \sum_{\alpha=1}^n b_{k\alpha} R_\alpha + \tilde{n}_k S \vartheta(S, \omega) + h_k A e^{j\varphi} \quad (k = 1, 2, \dots, n), \quad (3.13)$$

$$S = \sum_{k=1}^n j_k R_k, \quad (3.14)$$

where  $R_k = c_k + i a_k$ ,  $\vartheta(S, \omega) = g(S, \omega) + i b(S, \omega)$ .

The system in (3.13) is rewritten as

$$\sum_{\alpha=1}^n (b_{k\alpha} - \delta_{k\alpha} i \omega) R_\alpha = -\tilde{n}_k S \vartheta(S, \omega) - h_k A e^{j\varphi} \quad (k = 1, 2, \dots, n), \quad (3.15)$$

and hence we find  $R_k$ :

$$R_k = -\frac{N_k(i\omega)}{D(i\omega)} S \Phi(S, \omega) - \frac{H_k(i\omega)}{D(i\omega)} A e^{i\varphi} \quad (k = 1, 2, \dots, n). \quad (3.16)$$

In (3.16)  $D(i\omega)$  is the determinant of the left-hand side of (3.15), while  $N_k(i\omega)$  and  $H_k(i\omega)$  are obtained from  $D(i\omega)$  by replacing  $k$  by  $\tilde{n}_1, \tilde{n}_2, \dots, \tilde{n}_n$  and  $h_1, h_2, \dots, h_k$ , respectively.

By substituting (3.16) into (3.14) and using the symbols

$$K(i\omega) = -\frac{\sum_{k=1}^n i_k N_k(i\omega)}{D(i\omega)}, \quad \tilde{K}(i\omega) = -\frac{\sum_{k=1}^n i_k H_k(i\omega)}{D(i\omega)}, \quad (3.17)$$

we have

$$K^{-1}(i\omega) = \Phi(S, \omega) + \frac{A}{S} e^{i\varphi} \frac{\tilde{K}(i\omega)}{K(i\omega)}, \quad (3.18)$$

where  $K(i\omega)$  is the frequency function (amplitude - phase characteristic) for the linear part,  $\tilde{K}(i\omega)$  is the frequency function for the linear part of the system between the point at which the external signal is applied and the output, and  $\Phi(S, \omega)$  is the harmonic transfer for the amplifier unit.

$A$  and  $\omega$  are given in (3.18);  $S$  and  $\varphi$  have to be determined. In the self-oscillation mode  $A \equiv 0$ ; then from (3.18) we have

$$K^{-1}(i\omega) = \Phi(S, \omega), \quad (3.19)$$

where  $S$  and  $\omega$  are to be determined.

To solve (3.18) and (3.19) we must expand the formulas and construct hodographs for the harmonic transfer coefficient of the amplifier unit for the various types of symmetric periodic mode.

#### 4. Determination of the Harmonic Transfer Coefficient of the Amplifier Unit. Relay Without An Insensitive Zone

a. Harmonic transfer coefficient of the amplifier unit for the SR mode. Figure 12 shows  $\nu$  and  $\tilde{\xi}$  for the amplifier unit as functions of  $\psi = \omega t$ , when

$$\nu = S \sin \psi, \quad \dot{\nu} = S\omega \cos \psi. \quad (4.1)$$

When  $-\pi + \beta \leq \psi \leq -\alpha$ ,  $\beta \leq \psi \leq \pi - \alpha$ ,  $\pi + \beta \leq \psi \leq 2\pi - \alpha$  a sliding mode occurs, and when  $\alpha \leq \psi \leq \beta$ ,  $\pi - \alpha \leq \psi \leq \pi + \beta$  relay operation occurs.

When  $\psi = -\alpha$ ,  $\dot{\nu} = r f_0$ , and so, from (4.1)

$$\cos \alpha = \frac{r f_0}{S\omega} \quad (4.2)$$

and from Fig. 12 it is clear that  $\alpha \leq 0$ .

We now find  $\tilde{\xi}$  when  $-\alpha \leq \psi \leq \beta$ :

$$\tilde{\xi} = \nu|_{\psi=-\alpha} + r f_0 \frac{\psi + \alpha}{\omega} = S [(\psi + \alpha) \cos \alpha - \sin \alpha]. \quad (4.3)$$

$\beta$  is found from the condition  $v = \tilde{\xi}$  when  $\psi = \beta$ . From (4.1) and (4.3) we get

$$\sin \alpha + \sin \beta = (\alpha + \beta) \cos \alpha, \quad (4.4)$$

and Fig. 12 shows that  $0 \leq \beta \leq \pi - \alpha$ .

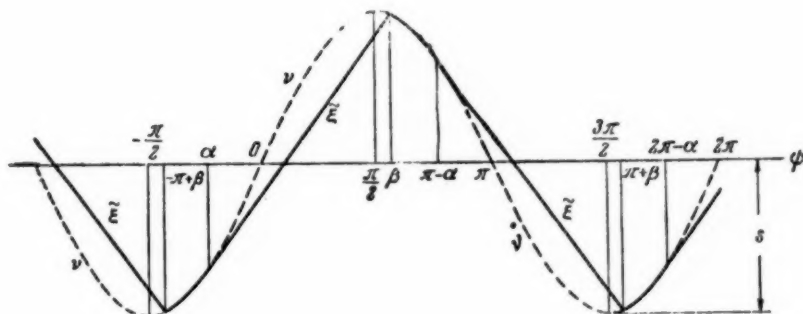


Fig. 12. Determination of the harmonic transfer coefficient of the amplifier unit for the SR periodic mode.

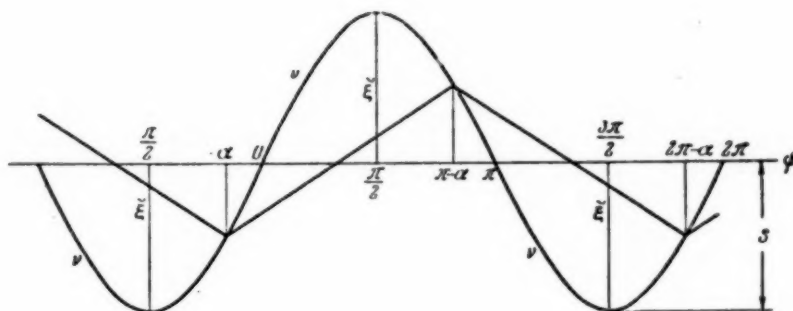


Fig. 13. Determination of the harmonic transfer coefficient of the amplifier unit for the R periodic mode.

When  $\beta = \pi - \alpha$  the SR periodic mode goes over to the R mode. (4.4) gives

$$\operatorname{tg} \alpha = \frac{\pi}{2}, \quad \cos \alpha = \frac{r/\omega}{S\omega} = \frac{2}{V\pi^2 + 4}.$$

Thus, the SR mode can only occur when

$$1 \geq \frac{r/\omega}{S\omega} \geq \frac{2}{V\pi^2 + 4}. \quad (4.5)$$

Since the periodic mode is symmetric

$$g(S, \omega) = \frac{2}{\pi S} \int_{-\alpha}^{\pi-\alpha} \tilde{\xi} \sin \psi d\psi, \quad b(S, \omega) = \frac{2}{\pi S} \int_{-\alpha}^{\pi-\alpha} \tilde{\xi} \cos \psi d\psi, \quad (4.6)$$



where

$$\tilde{\xi} = \begin{cases} S[(\psi + \alpha) \cos \alpha - \sin \alpha] & \text{if } -\alpha \leq \psi \leq \beta, \\ S \sin \psi & \text{if } \beta \leq \psi \leq \pi - \beta. \end{cases} \quad (4.7)$$

Substituting (4.7) into (4.6), integrating, and using (4.4), we get (after certain simple manipulations)

$$g(S, \omega) = \frac{2}{\pi} \left( \frac{\pi - \alpha - \beta}{2} + \frac{1}{4} \sin 2\alpha - \frac{1}{4} \sin 2\beta + \cos \alpha \sin \beta \right), \quad (4.8)$$

$$b(S, \omega) = -\frac{2}{\pi} \left( \frac{1}{2} + \frac{1}{4} \cos 2\alpha + \frac{1}{4} \cos 2\beta - \cos \alpha \cos \beta \right).$$

When  $\alpha = \beta = 0$  the SR mode is purely a sliding one. Then from (4.8) we get

$$g(S, \omega) = 1, \quad b(S, \omega) = 0 \quad (4.9)$$

When  $\beta = \pi - \alpha$ ,  $\cos \alpha = \frac{2}{\sqrt{\pi^2 + 4}}$  the SR mode goes over to the R mode. Then from (4.8) we get

$$g(S, \omega) = \frac{8}{\pi^2 + 4}, \quad b(S, \omega) = -\frac{16}{\pi(\pi^2 + 4)}. \quad (4.10)$$

**b. Determination of the harmonic transfer coefficient of the amplifier unit for the R mode.** The periodic R mode can be determined by harmonic balance methods as usually interpreted [5]. But we shall undertake the determination of the harmonic transfer coefficient for the amplifier unit for the R mode, since by constructing the hodographs of  $\Phi(S, \omega)$  for the SR and R periodic modes for one quadrant we can at once find all types of simple periodic mode in the system without resort to further calculations or constructions when the relay has no insensitive zone.

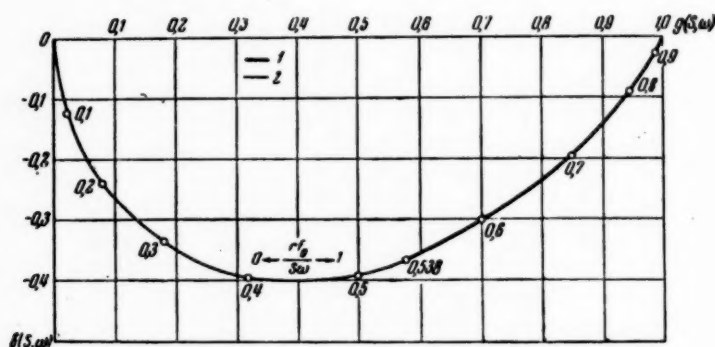


Fig. 14. Hodograph for the harmonic transfer coefficient of the amplifier unit when the relay has no insensitive zone.

1) SR periodic mode; 2) R periodic mode.

Figure 13 shows  $\nu$  and  $\tilde{\xi}$  as functions of  $\psi = \omega t$  when (4.1) is complied with.

If the R periodic mode is to exist we must have  $\dot{\nu} \geq r f_0$  when  $\psi = -\alpha$ . Hence

$$\cos \alpha \geq \frac{rf_0}{S\omega}. \quad (4.11)$$

We now find  $\tilde{\xi}$  when  $-\alpha \leq \psi \leq \pi - \alpha$ :

$$\tilde{\xi} = v|_{\psi=-\alpha} + rf_0 \frac{\psi + \alpha}{\omega} = S \left[ (\psi + \alpha) \frac{rf_0}{S\omega} - \sin \alpha \right]. \quad (4.12)$$

$\alpha$  is found from the condition  $v = \tilde{\xi}$  when  $\psi = \pi - \alpha$ . Using this, we get

$$\sin \alpha = \frac{rf_0}{S\omega} \frac{\pi}{2}. \quad (4.13)$$

At the boundary of the SR mode we get, from (4.11) and (4.13), that

$$\frac{rf_0}{S\omega} = \frac{2}{\sqrt{\pi^2 + 4}}.$$

On the other hand when  $\alpha = 0$ ,  $\tilde{\xi} \equiv 0$  and so this condition also gives the boundary of the R mode. We have from (4.13)

$$rf_0/S\omega = 0.$$

Thus, the R mode can only occur when

$$0 \leq \frac{rf_0}{S\omega} \leq \frac{2}{\sqrt{\pi^2 + 4}}. \quad (4.14)$$

Substituting (4.12) into (4.6), integrating and using (4.13) we have

$$g(S, \omega) = 2 \left( \frac{rf_0}{S\omega} \right)^2, \quad b(S, \omega) = -\frac{4}{\pi^2} \sin 2\alpha. \quad (4.15)$$

When  $\alpha = 0$ ,  $\frac{rf_0}{S\omega} = 0$  and from (4.15) we will have

$$g(S, \omega) = 0, \quad b(S, \omega) = 0. \quad (4.16)$$

When  $g(S, \omega)$  and  $b(S, \omega)$  have been determined numerically [from (4.8) for the SR mode and from (4.15) for the R mode] the hodograph for  $\theta(S, \omega)$  can be drawn up as in Fig. 14. Figure 14 shows that  $\theta(S, \omega)$  is a function of the parameter  $\frac{rf_0}{S\omega}$ .

## 5. Determination of the Harmonic Transfer Coefficient for the Amplifier Unit. Relay With an Insensitive Zone

a. Harmonic transfer coefficient for the amplifier unit in the SD mode. Figure 15 shows  $v$  and  $\tilde{\xi}$  as functions of  $\psi = \omega t$  when

$$v = S \sin \psi, \quad \dot{v} = S\omega \cos \psi. \quad (5.1)$$

When  $\alpha \leq \psi \leq \frac{\pi}{2}$ ,  $\pi - \alpha \leq \psi \leq \frac{3\pi}{2}$  the sliding mode occurs; and when  $-\frac{\pi}{2} \leq \psi \leq -\alpha$ ,

$\frac{\pi}{2} \leq \psi \leq \pi - \alpha$ ,  $\frac{3\pi}{2} \leq \psi \leq 2\pi - \alpha$  we get the dead mode.

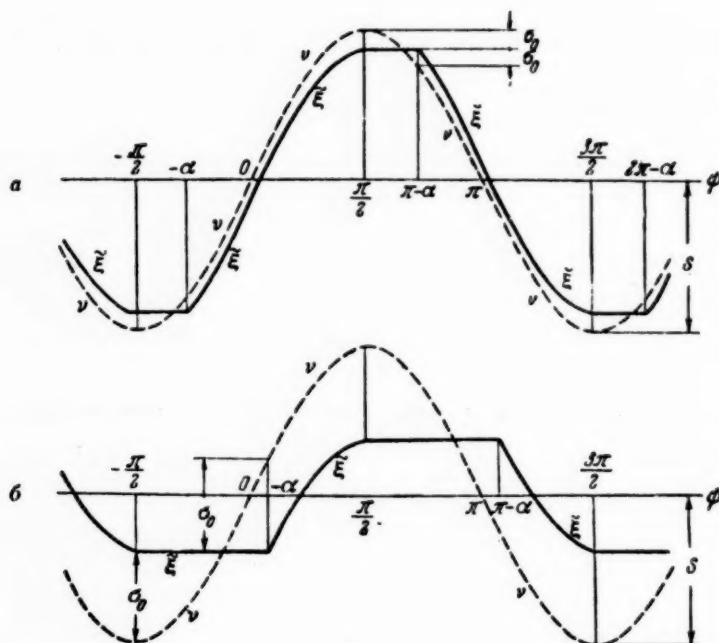


Fig. 15. Determination of the harmonic transfer coefficient for the amplifier unit in the SD mode.

When  $\psi = \pi - \alpha$ ,  $v = S - 2\sigma_0$  and from (5.1)

$$\sin \alpha = 1 - 2 \frac{\sigma_0}{S}, \quad \cos \alpha = 2 \frac{\sigma_0}{S} \sqrt{\frac{S}{\sigma_0} - 1}. \quad (5.2)$$

Figure 15 shows that  $-\frac{\pi}{2} \leq \alpha \leq \frac{\pi}{2}$ .

In the case shown in Fig. 15, a, i.e., when  $\alpha \geq 0$ ,  $0 \leq \sin \alpha \leq 1$ , if a sliding mode is to exist we must have  $\dot{v}_{\max} = S \omega \cos 0 \leq r f_0$ . Hence we have, taking into account (5.2), that a necessary condition for the SD mode to exist is

$$\frac{r f_0}{\omega \sigma_0} \geq \frac{S}{\sigma_0} \quad \text{when } 0 \leq \frac{\sigma_0}{S} \leq \frac{1}{2}. \quad (5.3)$$

In the case shown in Fig. 15, b, i.e., when  $\alpha \leq 0$ ,  $-1 \leq \sin \alpha \leq 0$ , if a sliding mode is to exist we must have  $\dot{v} \big|_{\psi = -\alpha} = S \omega \cos(-\alpha) \leq r f_0$ . Hence we have, that a necessary condition for the SD mode to exist is

$$\frac{r f_0}{\omega \sigma_0} \geq 2 \sqrt{\frac{S}{\sigma_0} - 1} \quad \text{when } \frac{1}{2} \leq \frac{\sigma_0}{S} \leq 1. \quad (5.4)$$

Figure 15 shows that

$$\varphi = \begin{cases} S \sin \psi - \sigma_0 & \text{when } -\alpha \leq \psi \leq \frac{\pi}{2}, \\ S - \sigma_0 & \text{when } \frac{\pi}{2} \leq \psi \leq \pi - \alpha \end{cases} \quad (5.5)$$

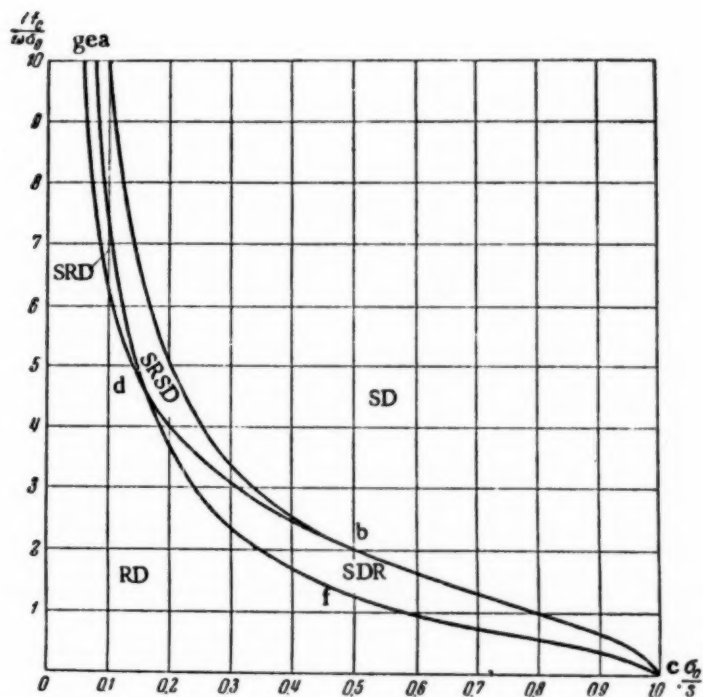


Fig. 16. Division of the plane of  $\frac{\sigma_0}{S}$  and  $\frac{r f_0}{\omega \sigma_0}$  for the amplifier unit harmonic transfer coefficient into regions where different types of periodic mode exist; b) 0.5, 2.0; and d) 0.155, 4.67.

Substituting (5.5) into (4.6), integrating and using (5.2) we have (after certain simple manipulations)

$$g(S, \omega) = \frac{1}{2\pi} (\pi + 2\alpha + \sin 2\alpha), \quad b(S, \omega) = -\frac{1}{2\pi} (1 + \cos 2\alpha). \quad (5.6)$$

It is clear from (5.6) and (5.2) that  $g(S, \omega)$  and  $b(S, \omega)$  do not depend directly on  $\omega$ . But these formulas are applicable only if (5.3) and (5.4) are fulfilled, and these latter depend on  $\omega$ , and so  $g(S, \omega)$  and  $b(S, \omega)$  are not only functions of  $S$  but also of  $\omega$ .

The calculation shows that the amplifier unit harmonic transfer coefficient for the SD mode is a function of  $\frac{\sigma_0}{S}$  and  $\frac{r f_0}{\omega \sigma_0}$ . The following curves have been drawn in the plane of these parameters in Fig. 16:

a) from the equation

$$\frac{r f_0}{\omega \sigma_0} = \frac{S}{\sigma_0} \quad \text{when } 0 \leq \frac{\sigma_0}{S} \leq \frac{1}{2}; \quad (5.7)$$

bc from the equation

$$\frac{r f_0}{\omega \sigma_0} = 2 \sqrt{\frac{S}{\sigma_0} - 1} \quad \text{when} \quad \frac{1}{2} \leq \frac{\sigma_0}{S} \leq 1. \quad (5.8)$$

The SD region lies between (5.7) and (5.8) and the straight line  $\frac{\sigma_0}{S} = 1$ . Within these limits the harmonic coefficient is independent of  $\frac{r f_0}{\omega \sigma_0}$ .

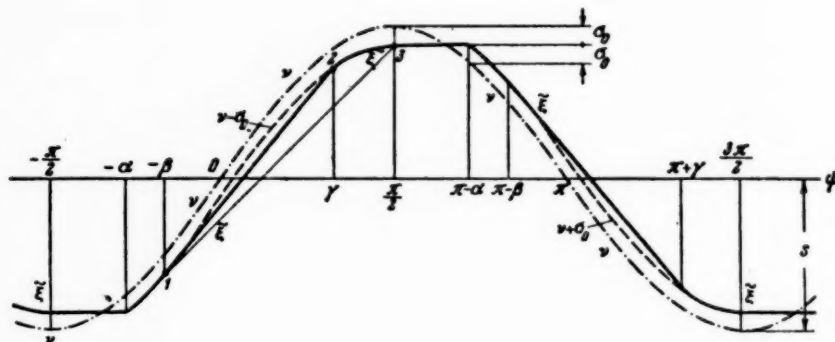


Fig. 17. Determination of the amplifier unit harmonic transfer coefficient for the SRSD mode.

b. Harmonic transfer coefficient for the amplifier unit in the SRSD mode. Figure 17 shows  $\nu$  and  $\tilde{\xi}$  as functions of  $\psi = \omega t$  when (5.1) is fulfilled.

When  $-\alpha \leq \psi \leq -\beta$ ,  $\gamma \leq \psi \leq \frac{\pi}{2}$ ,  $\pi - \alpha \leq \psi \leq \pi - \beta$ ,  $\pi + \gamma \leq \psi \leq \frac{3\pi}{2}$  we gave a sliding mode, when  $-\beta \leq \psi \leq \gamma$ ,  $\pi - \beta \leq \psi \leq \pi - \gamma$  — a relay mode, and when  $-\frac{\pi}{2} \leq \psi \leq -\alpha$ ,

$\frac{\pi}{2} \leq \psi \leq \pi - \alpha$  a dead mode.

$\alpha$  is found from the condition that  $\nu = S - 2\sigma_0$  when  $\psi = \pi - \alpha$ :

$$\sin \alpha = 1 - 2 \frac{\sigma_0}{S}, \quad \cos \alpha = 2 \frac{\sigma_0}{S} \sqrt{\frac{S}{\sigma_0} - 1}, \quad (5.9)$$

whence  $0 \leq \alpha \leq \frac{\pi}{2}$ ,  $0 \leq \sin \alpha \leq 1$ . Using (5.9) we get

$$0 \leq \frac{\sigma_0}{S} \leq \frac{1}{2}. \quad (5.10)$$

$\beta$  is found from the condition  $\tilde{\nu} = r f_0$  when  $\psi = -\beta$ . From (5.1) we get

$$\cos \beta = \frac{rf_0}{\omega \sigma_0} \frac{\sigma_0}{S}, \quad (5.11)$$

whence we must have  $0 \leq \beta \leq \alpha$ .

The above limits for  $\beta$  show that  $1 \geq \cos \beta \geq \cos \alpha$ . Substituting (5.9) and (5.11) into this inequality we have

$$\frac{S}{\sigma_0} \geq \frac{rf_0}{\omega \sigma_0} \geq 2 \sqrt{\frac{S}{\sigma_0} - 1}. \quad (5.12)$$

We now find  $\tilde{\xi}$  when  $-\beta \leq \psi \leq \gamma$ , i.e., the equation of the straight line 1-2 in Fig. 17.

$$\tilde{\xi} = v|_{\psi=\beta} - \sigma_0 + rf_0 \frac{\psi + \beta}{\omega} = \sigma_0 \left[ -\frac{S}{\sigma_0} \sin \beta - 1 + \frac{rf_0}{\omega \sigma_0} (\psi + \beta) \right]. \quad (5.13)$$

$\gamma$  is found from the condition  $\tilde{\xi} = v - \sigma_0$  when  $\psi = \gamma$ . From these conditions we get from (5.13) and (5.1) [allowing for (5.11)]:

$$\sin \beta + \sin \gamma = (\beta + \gamma) \cos \beta, \quad (5.14)$$

where  $\gamma$  must satisfy  $0 \leq \gamma \leq \frac{\pi}{2}$ .

In Fig. 17 we produce the straight line 1-3, and, denoting its ordinate by  $x$ , we find its equation to be:

$$x = S \frac{1 + \sin \beta}{\beta + \frac{\pi}{2}} (\psi + \beta) - S \sin \beta - \sigma_0. \quad (5.15)$$

$\gamma$  will be less than  $\frac{\pi}{2}$  if

$$\left. \frac{d\tilde{\xi}}{d\psi} \right|_{-\beta < \psi < \gamma} \geq \frac{dx}{d\psi}$$

Substituting (5.13) and (5.15) into this, and allowing for (5.11) we have

$$\cos \beta \geq 2 \frac{1 + \sin \beta}{\beta + \frac{\pi}{2}}. \quad (5.16)$$

Calculations show that (5.16) is satisfied when  $\beta \leq 0.76$ ,  $\cos \beta \geq 0.725$ . Substituting (5.11) into the latter inequality we have

$$\frac{rf_0}{\omega \sigma_0} \geq 0.725 \frac{S}{\sigma_0}. \quad (5.17)$$

(5.10), (5.12), and (5.17) define the SRSD region in the plane of  $\frac{\sigma_0}{S}$  and  $\frac{rf_0}{\omega \sigma_0}$  in Fig. 16.

The upper boundary of this region — curve ab — is defined by

$$\frac{rf_0}{\omega \sigma_0} = \frac{S}{\sigma_0} \text{ when } 0 \leq \frac{\sigma_0}{S} \leq \frac{1}{2}. \quad (5.18)$$



The lower ones are defined by:

curve bc

$$\frac{r/o}{\omega\sigma_0} = 2 \sqrt{\frac{S}{\sigma_0} - 1} \quad \text{when} \quad 0,155 \leq \frac{\sigma_0}{S} \leq \frac{1}{2}; \quad (5.19)$$

curve cd

$$\frac{r/o}{\omega\sigma_0} = 0,725 \frac{S}{\sigma_0} \quad \text{when} \quad 0 \leq \frac{\sigma_0}{S} \leq 0,155. \quad (5.20)$$

The harmonic transfer coefficient is determined by (4.6), where

$$\tilde{\xi} = \begin{cases} S \sin \psi - \sigma_0 & \text{when } -\alpha \leq \psi \leq -\beta, \\ \sigma_0 \left[ -\frac{S}{\sigma_0} \sin \beta - 1 + \frac{r/o}{\omega\sigma_0} (\psi + \beta) \right] & \text{when } -\beta \leq \psi \leq \gamma, \\ S \sin \psi - \sigma_0 & \text{when } \gamma \leq \psi \leq \frac{\pi}{2}, \\ S - \sigma_0 & \text{when } \frac{\pi}{2} \leq \psi \leq \pi - \alpha. \end{cases} \quad (5.21)$$

Substituting (5.2) into (4.6), integrating and using (5.9), (5.11), and (5.14), manipulation gives

$$\begin{aligned} g(S, \omega) &= \frac{1}{2\pi} (\pi + 2\alpha - 2\beta - 2\gamma + \sin 2\alpha + \sin 2\beta - \sin 2\gamma + 4 \cos \beta \sin \gamma), \\ b(S, \omega) &= -\frac{1}{2\pi} (3 + \cos 2\alpha + \cos 2\beta + \cos 2\gamma - 4 \cos \beta \cos \gamma). \end{aligned} \quad (5.22)$$

The SRSD mode reaches the boundary of the SD mode when  $\beta$  and  $\gamma = 0$ . Under these conditions (5.22) gives (5.6).

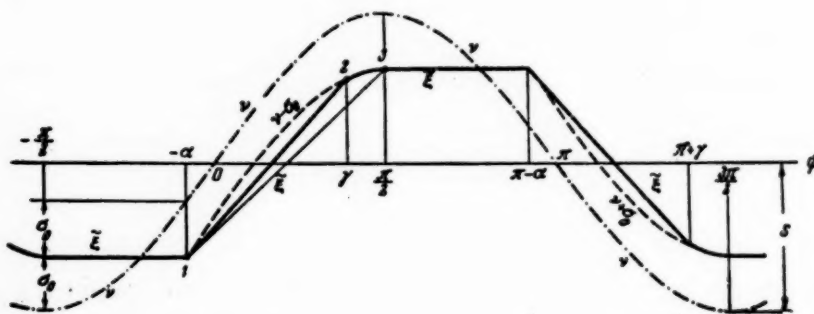


Fig. 18. Determination of the harmonic transfer coefficient for the amplifier in the SDR mode.

The SRSD mode reaches the boundary of the SDR mode when  $\beta = \alpha$ , and (5.22) takes the form:

$$\begin{aligned} g(S, \omega) &= \frac{1}{2\pi} (\pi - 2\gamma + 2 \sin 2\alpha - \sin 2\gamma + 4 \cos \alpha \sin \gamma), \\ b(S, \omega) &= -\frac{1}{2\pi} (3 + 2 \cos 2\alpha + \cos 2\gamma - 4 \cos \alpha \cos \gamma). \end{aligned} \quad (5.23)$$

The SRSD mode reaches the boundary of the SRD mode when  $\gamma = \frac{\pi}{2}$ , and (5.22) takes the form:

$$\begin{aligned} g(S, \omega) &= \frac{1}{2\pi} (2\alpha - 2\beta + \sin 2\alpha + \sin 2\beta + 4 \cos \beta), \\ b(S, \omega) &= -\frac{1}{2\pi} (2 + \cos 2\alpha + \cos 2\beta). \end{aligned} \quad (5.24)$$

c. The harmonic transfer coefficient of the amplifier unit in the SDR mode. Figure 18 shows  $\nu$  and  $\tilde{\xi}$  as functions of  $\psi - \omega t$  when (5.1) is fulfilled.

When  $\gamma \leq \psi \leq \frac{\pi}{2}$ ,  $\pi + \gamma \leq \psi \leq \frac{3\pi}{2}$  sliding occurs, when  $-\alpha \leq \psi \leq \gamma$ ,  $\pi - \alpha \leq \psi \leq \pi + \gamma$ .

we get relay action, and when  $-\frac{\pi}{2} \leq \psi \leq -\alpha$ ,  $\frac{\pi}{2} \leq \psi \leq \pi - \alpha$ , a dead mode.

$\alpha$  is defined by (5.9), and Fig. 18 shows that  $-\frac{\pi}{2} < \alpha < \frac{\pi}{2}$ .

We now find  $\tilde{\xi}$  when  $-\alpha \leq \psi \leq \gamma$ , i.e., the equation of the straight line 1-2 in Fig. 18:

$$\tilde{\xi} = \nu|_{\psi=-\alpha} - \sigma_0 + r f_0 \frac{\psi + \alpha}{\omega} = \sigma_0 \left[ -\frac{S}{\sigma_0} + 1 + \frac{r f_0}{\omega \sigma_0} (\psi + \alpha) \right]. \quad (5.25)$$

$\gamma$  is found from the condition  $\tilde{\xi} = \nu - \sigma_0$  when  $\psi = \gamma$ . Under these conditions (5.25) and (5.1), taking into account (5.9) gives

$$\sin \alpha + \sin \gamma = \frac{\sigma_0}{S} \frac{r f_0}{\omega \sigma_0} (\alpha + \gamma), \quad (5.26)$$

where  $\gamma$  lies within the range  $-\alpha < \gamma < \frac{\pi}{2}$ .

Figure 18 shows the straight line 1-3, and denoting the ordinate by  $x$  the equation of the straight line is found to be:

$$x = S \frac{1 + \sin \alpha}{\alpha + \frac{\pi}{2}} (\psi + \alpha) - S \sin \alpha - \sigma_0. \quad (5.27)$$

If the SDR mode is to exist we must have

$$\left. \frac{d(\nu - \sigma_0)}{d\psi} \right|_{\psi=-\alpha} \geq \left. \frac{d\tilde{\xi}}{d\psi} \right|_{-\alpha < \psi < \gamma} \geq \frac{dx}{d\psi}.$$

Hence substituting (5.1), (5.25), and (5.27) we get, incorporating (5.9):

$$2 \sqrt{\frac{S}{\sigma_0} - 1} \geq \frac{r f_0}{\omega \sigma_0} \geq \frac{4 \left( \frac{S}{\sigma_0} - 1 \right)}{\pi + 2 \sin^{-1} \left( 1 - 2 \frac{\sigma_0}{S} \right)}. \quad (5.28)$$

(5.28) defined the SDR region in the plane of  $\frac{\sigma_0}{S}$  and  $\frac{r f_0}{\omega \sigma_0}$  in Fig. 16. Curve cbd (the upper boundary) is defined by

$$\frac{r/o}{\omega\sigma_0} = 2 \sqrt{\frac{S}{\sigma_0} - 1} \quad \text{when } 0,155 \leq \frac{\sigma_0}{S} \leq 1, \quad (5.29)$$

while cfd (lower boundary) is defined by

$$\frac{r/o}{\omega\sigma_0} = 4 \frac{\frac{S}{\sigma_0} - 1}{\pi + 2 \sin^{-1} \left( 1 - 2 \frac{\sigma_0}{S} \right)} \quad \text{when } 0,155 \leq \frac{\sigma_0}{S} \leq 1. \quad (5.30)$$

The harmonic transfer coefficient is determined by (4.6) where

$$\tilde{\xi} = \begin{cases} \sigma_0 \left[ 1 - \frac{S}{\sigma_0} + \frac{r/o}{\omega\sigma_0} (\psi + \alpha) \right] & \text{when } -\alpha \leq \psi \leq \gamma, \\ S \sin \psi - \sigma_0 & \text{when } \gamma \leq \psi \leq \frac{\pi}{2}, \\ S - \sigma_0 & \text{when } \frac{\pi}{2} \leq \psi \leq \pi - \alpha \end{cases} \quad (5.31)$$

Substituting (5.31) into (4.6), integrating and using (5.26), we have

$$\begin{aligned} g(S, \omega) &= \frac{1}{2\pi} \left[ \pi - 2\gamma - \sin 2\gamma + 4 \frac{\sigma_0}{S} \frac{r/o}{\omega\sigma_0} (\sin \alpha + \sin \gamma) \right], \\ b(S, \omega) &= -\frac{1}{2\pi} \left[ 1 + \cos 2\gamma + 4 \frac{\sigma_0}{S} \frac{r/o}{\omega\sigma_0} (\cos \alpha - \cos \gamma) \right]. \end{aligned} \quad (5.32)$$

When  $\frac{r/o}{\omega\sigma_0} \frac{\sigma_0}{S} = \cos \alpha$  we come to the upper boundary of the SDR mode. If  $\alpha > 0$  here, then the SDR region adjoins that of the SRSD region. Under these conditions we get (5.23) from (5.32). On the other hand, if  $\alpha < 0$ , we get  $\gamma = -\alpha$  at the same time, and then the SDR region adjoins the SD region. Under these conditions we get (5.6) from (5.32). Finally, when  $\gamma = \pi/2$ , the SDR mode adjoins the RD mode. Under these conditions, (5.32) gives

$$g(S, \omega) = \frac{2}{\pi} \frac{\sigma_0}{S} \frac{r/o}{\omega\sigma_0} (1 + \sin \alpha), \quad b(S, \omega) = -\frac{2}{\pi} \frac{\sigma_0}{S} \frac{r/o}{\omega\sigma_0} \cos \alpha. \quad (5.33)$$

d. The harmonic transfer coefficient for the amplifier unit in the SDR mode. Figure 19 shows  $\nu$  and  $\tilde{\xi}$  as functions of  $\psi = \omega t$  when (5.1) is fulfilled.

When  $-\alpha \leq \psi \leq -\beta$ ,  $\pi - \alpha \leq \psi \leq \pi - \beta$ ,  $2\pi - \alpha \leq \psi \leq 2\pi - \beta$  sliding occurs, when

$\beta \leq \psi \leq \gamma$ ,  $\pi - \beta \leq \psi \leq \pi + \gamma$  we have relay action, and when  $-\pi + \gamma \leq \psi \leq -\alpha$ ,

$\gamma \leq \psi \leq \pi - \alpha$ ,  $\pi + \gamma \leq \psi \leq 2\pi - \alpha$ , a dead mode.

$\beta$  is defined by (5.11) being such that  $0 < \beta < \alpha$ .

The straight line 1-2 in Fig. 19 is described by (5.13), and 1-3 by (5.15).

If the SDR mode is to exist we must have that

$$\frac{dx}{d\psi} \geq \frac{d\tilde{\xi}}{d\psi} \Big|_{-\beta \leq \psi \leq \gamma}. \quad (5.34)$$

Substituting (5.13) and (5.15) into (5.14) and allowing for (5.11) we get

$$\cos \beta \leq 2 \frac{1 + \sin \beta}{\pi + 2\beta}. \quad (5.35)$$

(5.35) is satisfied when  $\beta > 0.76$ ,  $\cos \beta < 0.725$ . Substituting (5.11) into the latter inequality we have

$$\frac{r/\sigma_0}{\omega \sigma_0} \leq 0.725 \frac{S}{\sigma_0}. \quad (5.36)$$

$\gamma$  is determined from (5.14) whence  $\frac{\pi}{2} \leq \gamma < \pi$ .

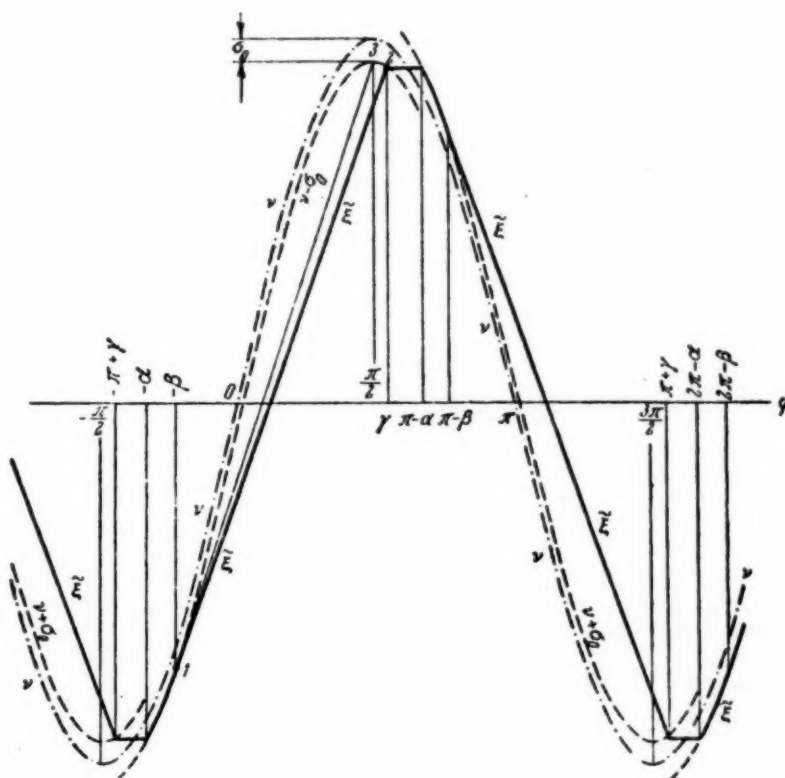


Fig. 19. Determination of the harmonic transfer coefficient for the amplifier unit in the SRD mode.

$\alpha$  is determined from the condition  $v + \sigma_0 = S \sin \gamma - \sigma_0$  when  $\psi = \pi - \alpha$ . Using (5.1) we get

$$\sin \alpha = \sin \gamma - 2 \frac{\sigma_0}{S}, \quad (5.37)$$

whence  $\beta \leq \alpha < \frac{\pi}{2}$  and hence  $\cos \beta \geq \cos \alpha$ .

Substituting  $\cos \beta$  from (5.11) we get

$$\frac{rf_0}{\omega\sigma_0} \geq \frac{S}{\sigma_0} \cos \alpha. \quad (5.38)$$

(5.36) and (5.38) define the SRD region in the  $\frac{\sigma_0}{S}$  and  $\frac{rf_0}{\omega\sigma_0}$  plane in Fig. 16. The upper boundary - curve dc - is defined by

$$\frac{rf_0}{\omega\sigma_0} = 0,725 \frac{S}{\sigma_0} \quad \text{when} \quad 0 \leq \frac{\sigma_0}{S} \leq 0,155. \quad (5.39)$$

The lower boundary - curve dg - is determined from (5.38) when the inequality becomes an equality, i.e., when

$$\alpha = \beta. \quad (5.40)$$

Substituting (5.40) into (5.37) we get, together with (5.11) and (5.14), a system of equations which define the lower boundary of the SRD region:

$$\begin{aligned} \sin \beta + \sin \gamma &= (\beta + \gamma) \cos \beta, \\ \sin \beta - \sin \gamma &= -2 \frac{\sigma_0}{S}, \\ \cos \beta &= \frac{rf_0}{\omega\sigma_0} \frac{\sigma_0}{S} \end{aligned} \quad (5.41)$$

or

$$\begin{aligned} \frac{\sigma_0}{S} + \sqrt{1 - \left(\frac{rf_0}{\omega\sigma_0} \frac{\sigma_0}{S}\right)^2} &= \frac{1}{2} \frac{rf_0}{\omega\sigma_0} \frac{\sigma_0}{S} \left\{ \arccos \frac{rf_0}{\omega\sigma_0} \frac{\sigma_0}{S} + \right. \\ &\quad \left. + \arcsin \left[ 2 \frac{\sigma_0}{S} + \sqrt{1 - \left(\frac{rf_0}{\omega\sigma_0} \frac{\sigma_0}{S}\right)^2} \right] \right\}. \end{aligned} \quad (5.42)$$

It is easy to perceive that when  $\frac{\sigma_0}{S} = 0,155$  and  $\frac{rf_0}{\omega\sigma_0} = 4,67$ , (5.42) is satisfied, i.e., the lower boundary to the SRD region passes through point d in Fig. 16.

The harmonic transfer coefficient is defined by (4.16) where

$$\tilde{\xi} = \begin{cases} S \sin \psi - \sigma_0 & \text{when } -\alpha \leq \psi \leq -\beta, \\ \sigma_0 \left[ -\frac{S}{\sigma_0} - 1 + \frac{rf_0}{\omega\sigma_0} (\psi + \beta) \right] & \text{when } -\beta \leq \psi \leq \gamma, \\ S \sin \gamma - \sigma_0 & \text{when } \gamma \leq \psi \leq \pi - \alpha, \end{cases} \quad (5.43)$$

Substituting (5.43) into (4.16), integrating and using (5.11), (5.14), and (5.37) we obtain, after certain transformations,

$$\begin{aligned} g(S, \omega) &= \frac{1}{2\pi} (2\alpha - 2\beta + \sin 2\alpha + \sin 2\beta + 4 \cos \beta \sin \gamma), \\ b(S, \omega) &= -\frac{1}{2\pi} (2 + \cos 2\alpha + \cos 2\beta - 4 \cos \beta \cos \gamma). \end{aligned} \quad (5.44)$$

When  $\gamma = \frac{\pi}{2}$  the SRD mode adjoins the SRSD mode. Under these conditions (5.44) gives (5.24).

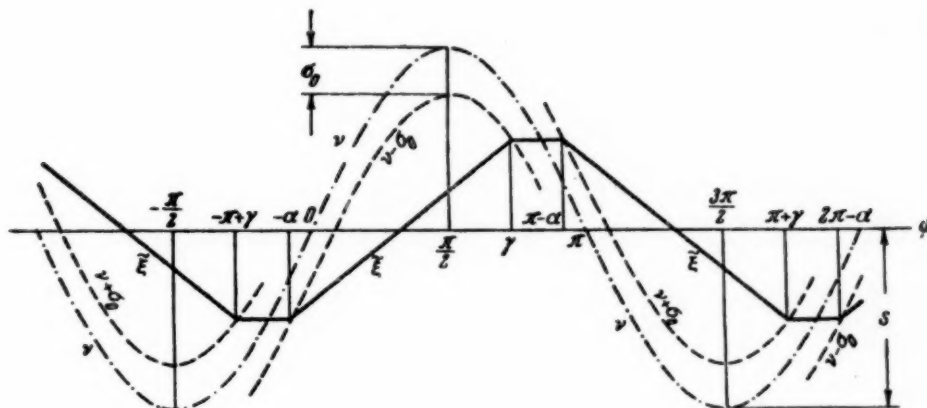


Fig. 20. Determination of the harmonic transfer coefficient for the amplifier unit in the RD mode.

When  $\beta = \alpha$ , the SRD mode adjoins the RD mode. Then, using (5.11), (5.44) gives

$$\begin{aligned} g(S, \omega) &= \frac{2}{\pi} \frac{rf_0}{\omega\sigma_0} \frac{\sigma_0}{S} (\sin \alpha + \sin \gamma), \\ b(S, \omega) &= -\frac{2}{\pi} \frac{rf_0}{\omega\sigma_0} \frac{\sigma_0}{S} (\cos \alpha - \cos \gamma). \end{aligned} \quad (5.45)$$

e. The harmonic transfer coefficient for the amplifier unit in the RD mode. Figure 20 shows  $\nu$  and  $\tilde{\xi}$  as functions of  $\psi = \omega t$  when (5.1) is fulfilled.

When  $-\alpha \leq \psi \leq \gamma$ ,  $\pi - \alpha \leq \psi \leq \pi + \gamma$  a relay mode occurs, and when  $-\pi + \gamma \leq \psi \leq -\alpha$ ,

$\gamma \leq \psi \leq \pi - \alpha$ ,  $\pi + \gamma \leq \psi \leq 2\pi - \alpha$ , we get a dead mode.

When  $-\alpha \leq \psi \leq \gamma$ ,  $\tilde{\xi}$  is defined by (5.25).  $\alpha$  and  $\gamma$  are related by the following conditions:  
 a)  $\nu - \sigma_0 = \tilde{\xi}$  when  $\psi = \gamma$ ; b)  $S \sin \gamma - \sigma_0 = \nu + \sigma_0$  when  $\psi = \pi - \alpha$ . By using these conditions we get (5.26) and (5.37) from (5.1) and (5.5).

The harmonic transfer coefficient is defined by (4.16), where

$$\xi_1 = \begin{cases} \sigma_0 \left[ -\frac{S}{\sigma_0} - 1 + \frac{r f_0}{\omega \sigma_0} (\psi + \alpha) \right] & \text{when } -\alpha \leq \psi \leq \gamma, \\ S \sin \gamma - \sigma_0 & \text{when } \gamma \leq \psi \leq \pi - \alpha. \end{cases} \quad (5.46)$$

Substituting (5.46) into (4.16), integrating and using (5.26) and (5.37), we get (5.45).



When  $\gamma = \frac{\pi}{2}$ , the RD mode adjoins the SRD mode. We then get (5.33) from (5.45).

The boundary dg in the plane of  $\frac{\sigma_0}{S}$  and  $\frac{rf_0}{\omega\sigma_0}$  in Fig. 16 is defined by (5.42) when  $0 \leq \frac{\sigma_0}{S} \leq 0.155$ , while the boundary cfd is defined by (5.30).

When  $g(S, \omega)$  and  $b(S, \omega)$  have been determined numerically from (5.6) for the SD mode, from (5.23) for the SRSD mode, (5.32) for the SDR mode, (5.44) for the SRD mode and (5.45) for the RD mode, (5.32) for the SDR mode, (5.44) for the SRD mode and (5.45) for the RD mode, the family of hodographs for  $\vartheta(S, \omega)$  given in Fig. 21 can be constructed.\* Each hodograph is constructed for  $0 \leq \frac{\sigma_0}{S} \leq 1$  and  $\rho = \frac{rf_0}{\omega\sigma_0} = \text{const.}$  Figure 21 shows that each hodograph is a loop having points with the values  $\frac{\sigma_0}{S} = 0$  and  $\frac{\sigma_0}{S} = 1$  at the origin. The family of hodographs  $\vartheta(S, \omega)$  need only be drawn once and for all, and can then be used to deal with all particular problems in which the equations of motion for the relay system can be given in the form of (1.1).

## 6. Examples of Determining Self-Oscillation Modes

1. Let us consider a relay system with the following equation of motion:

$$T_1 \ddot{\varphi} + \varphi = -k_1 \xi, \quad T_2 \ddot{\mu} + \mu = k_2 \varphi, \quad \sigma = \mu - \xi, \quad \dot{\xi} = f(\sigma) \quad (6.1)$$

the relay characteristics being as in Fig. 3.

The transfer function of the linear part is determined from the first two equations in (6.1):

$$K(p) = -\frac{k}{(T_1 p + 1)(T_2 p + 1)}, \quad (6.2)$$

where  $k = k_1 k_2$  is the over-all gain of the linear part.

The inverse amplitude-phase characteristic of the linear part is

$$K^{-1}(i\omega) = -\frac{1}{k} (1 + iT_1 \omega)(1 + iT_2 \omega) \quad (6.3)$$

this being a parabola with its apex in the real axis at the point,  $-\frac{1}{k}$ , the real axis being its axis of symmetry, the parabola intersecting the positive imaginary axis at the point,  $-i \frac{T_1 + T_2}{k \sqrt{T_1 T_2}}$ .

It is quite obvious that when  $\frac{k}{\omega}$  is sufficiently large the parabola intersects the hodograph of the harmonic transfer coefficient shown in Fig. 14, twice. If  $T_1 = 4 T_2$  then when  $k > 1.336$  one intersection will lie in the R mode region, while the other will fall in the SR mode region, as shown in Fig. 22.

Let the intersections on  $K^{-1}(i\omega)$  have frequency values  $\omega_1$  and  $\omega_2$ , and those on  $\vartheta(S, \omega)$ , values  $\rho_1$  and  $\rho_2$  in the parameter  $\rho = \frac{f_0}{S \omega}$ . Figure 22 shows that  $\omega_1 < \omega_2$ ,  $\rho_1 < \rho_2$ , and hence

$$S_1 = \frac{f_0}{\rho_1 \omega_1} > S_2 = \frac{f_0}{\rho_2 \omega_2}.$$

Hence when  $T_1 = 4 T_2$  and  $k > 1.336$  two modes occur: the R mode of low  $\omega_1$  and large amplitude  $S_1$  (at the amplifier unit input), and the SR mode with high  $\omega_2$  and low amplitude  $S_2$ .

\* The numerical calculations used to draw up Figs. 14, 16, and 17 were carried out by N. N. Vinogradov and A. A. Karymov.

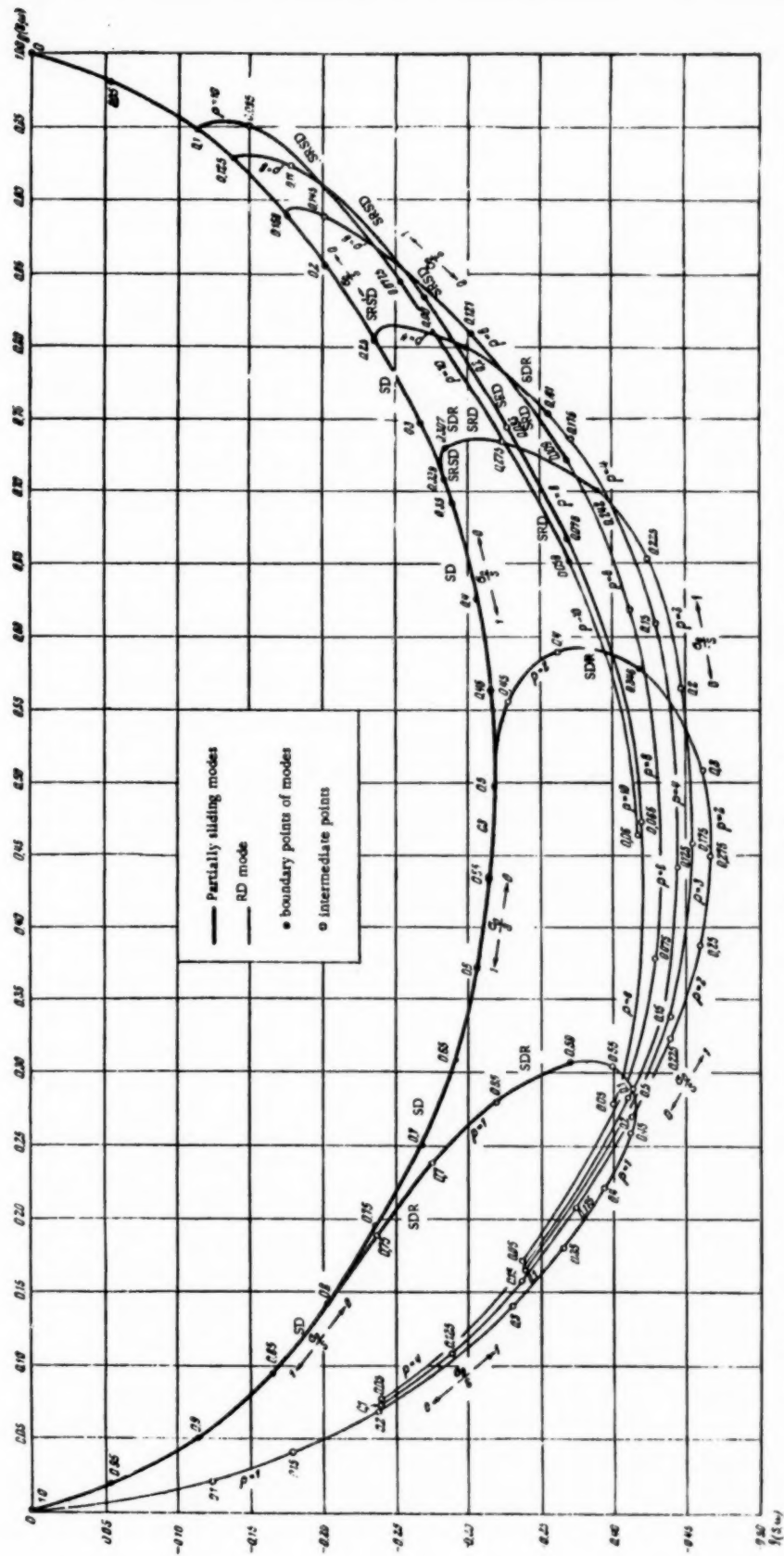


Fig. 21. The family of hodographs of the harmonic transfer coefficient for an amplifier unit which has a relay with an insensitive zone.

Their stabilities may be determined from Goldfarb's conditions [5] which have been formulated for  $K^{-1}(i\omega)$ ,  $\Phi(S, \omega)$  by Smirnov [9]; the self-oscillation is stable if at the point where  $K^{-1}(i\omega)$  and  $\Phi(S, \omega)$  intersect, the angle  $\alpha$  between the tangent  $T$  to  $\Phi(S, \omega)$ , directed toward increasing  $S$  values, and the normal  $N$  to  $K^{-1}(i\omega)$ , directed within the region enclosed by the hodograph, is less than  $\pi/2$ , and unstable if  $\alpha$  is greater than  $\frac{\pi}{2}$ .

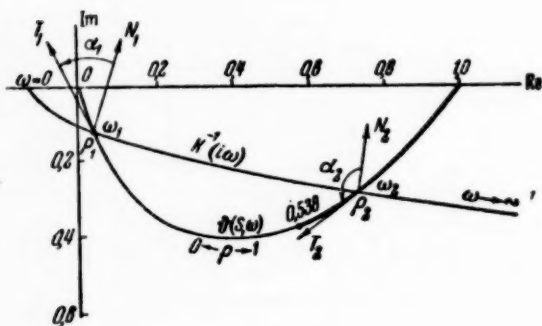


Fig. 22

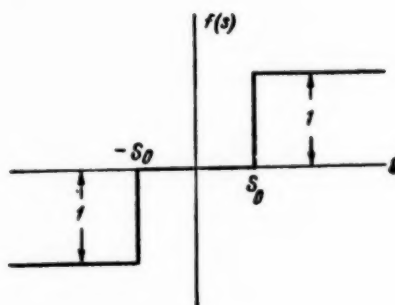


Fig. 23

The constructions given in Fig. 22 show that the R mode is stable and the SR mode unstable.

2. Determine the SD self-oscillation modes in a control system having the following equation of motion

$$\delta T_a \dot{x} = -z, \quad s = x - y, \quad T \dot{y} = f(s), \quad T_c \dot{z} + z = y \quad (6.4)$$

and a relay characteristic as in Fig. 23.

The following new variables will be used:

$$\eta_1 = \frac{Tx}{\delta T_a}, \quad \eta_2 = \frac{Tz}{\delta T_a}, \quad \xi = \frac{T y}{\delta T_a}, \quad \sigma = \frac{T s}{\delta T_a}, \quad \tau = \frac{t}{\delta T_a}; \quad (6.5)$$

then (6.4) takes the following form:

$$\dot{\eta}_1 = -\eta_2, \quad \dot{\eta}_2 = -\psi \eta_2 + \psi \xi, \quad \sigma = \eta_1 - \xi, \quad \dot{\xi} = f(\sigma), \quad (6.6)$$

where

$$\psi = \frac{\delta T_a}{T_c}, \quad \sigma_0 = \frac{T s_0}{\delta T_a}, \quad (6.7)$$

the dots denoting the derivatives with respect to  $\tau$ .

$$K(p) = -\frac{\psi}{p(p + \psi)}$$

\* Aizerman [10] has shown that this condition is sufficient for systems in which the linear parts satisfy the autoresonance condition. In systems with linear parts which satisfy the filter condition the condition is a necessary one; no simple formulation of the necessary and sufficient conditions is at present known.

and hence

$$K^{-1}(i\omega) = -i \frac{\omega}{\psi} (\psi + i\omega) = \frac{\omega^2}{\psi} - i\omega. \quad (6.8)$$

Substituting (6.8) into (3.19) we get

$$\frac{\omega^2}{\psi} - i\omega = g(S, \omega) + ib(S, \omega)$$

and hence

$$\frac{\omega^2}{\psi} = g(S, \omega), \quad \omega = -b(S, \omega). \quad (6.9)$$

Elimination of  $\omega$  from (6.9) gives

$$\psi = \frac{b^2(S, \omega)}{g(S, \omega)}. \quad (6.10)$$

Substituting (5.6) into (6.10) we get

$$\psi = \frac{1}{2\pi} \cdot \frac{(1 + \cos 2\alpha)^2}{\pi + 2\alpha + \sin 2\alpha} = f(\alpha), \quad (6.11)$$

where

$$-\frac{\pi}{2} \leq \alpha \leq \frac{\pi}{2}.$$

The right hand side of (6.11) is shown in Fig. 24, whence it is clear that (6.11) only applies when  $\psi \leq 0.293$ . Thus the SD self-oscillation modes exist when  $\psi \leq 0.293$ . Then the line  $\psi = \text{const}$  intersects the curve  $f(\alpha)$  of Fig. 24 twice; when  $-0.5\pi < \alpha < -0.18\pi$ , and when  $-0.18\pi < \alpha < 0.5\pi$ .

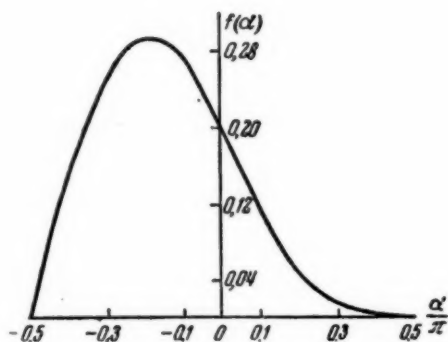


Fig. 24

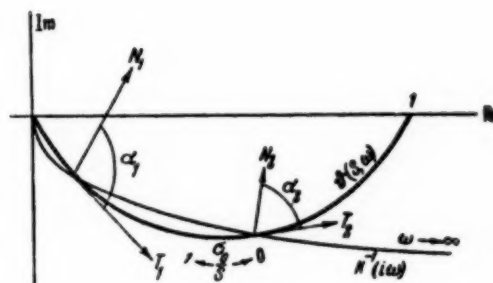


Fig. 25

The approximate solution gives two periodic SD solutions.

(5.2) gives an expression for the amplitude of the coordinate  $\nu$  at the amplifier unit input

$$S = \frac{2\sigma_0}{1 - \sin \alpha}, \quad (6.12)$$

which shows that the solution for  $-0.5\pi < \alpha < -0.18\pi$  gives a value of  $S$  less than that for  $-0.18\pi < \alpha < 0.5\pi$ .

The problem of self-oscillation stability is solved by showing in Fig. 25 the relative dispositions of  $K^{-1}(i\omega)$  and  $\Theta(S, \omega)$ . Fig. 25 makes it clear that the self-oscillations of large amplitude are stable, the other being unstable.

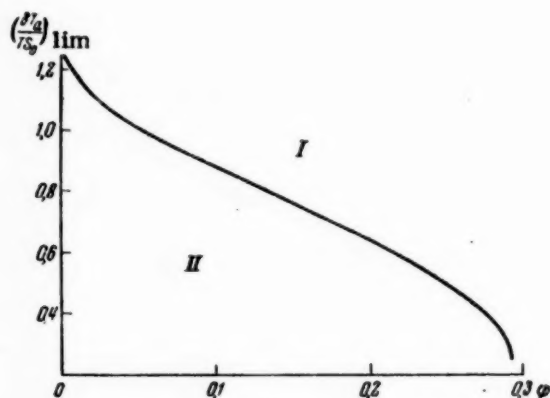


Fig. 26. I) Region of SD self-oscillation modes. II) Region where SD self-oscillation modes are absent.

An exact solution to this problem has been obtained [4]. It shows that when  $\psi \leq 0.33$ , there is one self-oscillatory SD mode. The approximate value  $\psi \leq 0.293$  obtained here is 11% different from the accurate one. The unstable SD mode is absent from the exact solution, so it would appear false and should be rejected.

The self-oscillatory mode which occurs when  $-0.18\pi < \alpha < 0.5\pi$  exist, though, when (5.3) and (5.4) are complied with. These conditions take the following form in our case ( $r = 1$ ,  $f_0 = 1$ ):

$$\begin{aligned} \frac{1}{\omega\sigma_0} &\geq \frac{S}{\sigma_0} \text{ if } 0 \leq \alpha \leq 0.5\pi, \\ \frac{1}{\omega\sigma_0} &\geq 2\sqrt{\frac{S}{\sigma_0} - 1} \text{ if } -0.18\pi \leq \alpha \leq 0. \end{aligned} \quad (6.13)$$

By substituting the value of  $\frac{S}{\sigma_0}$  from (6.12) and  $\omega$  (6.9) into (6.13), and taking into account (5.6), and replacing  $\sigma_0$  by its value, found from (6.7), we get

$$\frac{\delta T_a}{T s_0} \geq \frac{2}{\pi} \frac{\cos^2 \alpha}{1 - \sin \alpha}$$

when

$$0 \leq \alpha \leq 0.5\pi,$$

$$\frac{\delta T_a}{T s_0} \geq \frac{2}{\pi} \cos^2 \alpha \sqrt{\frac{1 + \sin \alpha}{1 - \sin \alpha}}$$

when

$$-0.18\pi \leq \alpha \leq 0.$$

In Fig. 26 we show the right hand sides of (6.14) as functions of  $\psi$ , the relation between  $\alpha$  and  $\psi$  being taken from Fig. 24. Figure 26 shows that the SD self-oscillation mode can be eliminated by increasing the width of the relay's insensitive zone or by increasing the amplifier constant  $T$ . The limiting value of  $\frac{\delta T a}{T s_0}$  (here derived approximately) differs by 10-12% from the exact values found for the range  $0 < \psi < 0.27$  by the present author [4]. This must be considered satisfactory for an approximate solution.

#### LITERATURE CITED

- [1] Yu. V. Dolgolenko, Sliding Modes in Indirect Relay-Controlled Systems. Trans. Second All-Union Conference on the Theory of Automatic Control, Vol. 1, Acad. Sci. USSR Press, 1955.
- [2] G. N. Nikolsky, Stabilizing the Set Course of a Ship Automatically. Trans. Central Communication Lab., Vol. 1, State Power Press, 1934.
- [3] Yu. I. Neimark, Sliding and Periodic Modes in Relay Systems. Trans. Gorky Phys.-Tech. Research Institute and Radiophysics Faculty of Gorky State University, Scientific Reports, Vol. 30, Physics Series, Soviet Radio Press, 1956.
- [4] Yu. V. Dolgolenko, Sliding Modes in Indirect Relay-Controlled Systems, Dissertation for doctorate, Kalinin Polytechnical Institute, Leningrad, 1955.
- [5] L. S. Goldfarb, Certain Nonlinearities in Automatic Control Systems, Automation and Remote Control, 8, 5 (1947).
- [6] A. I. Lurye, Some Nonlinear Problems in Automatic Control Theory, Tech.-Theor. Press, 1951.
- [7] M. A. Aizerman, The Construction of Resonance Curves for Systems With Nonlinear Feedback, Engineering Symposium, 13, 1952.
- [8] E. P. Popov, An Approximate Study of Self- and Forced Oscillation in Nonlinear Systems, Bull. Acad. Sci. USSR, Tech. Sciences Section, No. 5, 1954.
- [9] I. M. Smirnova, The Stability of Periodic Modes in Automatic Control Systems Found by Approximate Methods, Trans. Second All-Union Conference on the Theory of Automatic Control, Vol. 1, Acad. Sci. USSR Press, 1955.
- [10] M. A. Aizerman, Comparison of the Approximate Methods for Studying Periodic Modes and Their Region of Applicability, in "Fundamentals of Automatic Control," edited by V. V. Solodovnikov, State Machine Press, 1954.

Received June 25, 1956.





# OSCILLATORY PROCESSES (RAMP ACTION) IN RELAY AUTOMATIC CONTROL SYSTEMS

Yu. I. Neimark

(Gorky)

The conditions under which self-oscillation starts and stops and under which it is stable and independent of external forces are derived for relay systems, using the integral form of the equations of motion. Considerable attention is devoted to physical interpretation of the simplifying assumptions made in deriving an idealized conception of this type of behavior.

Many papers have already appeared on self-maintained oscillations in automatic control systems. The phase-space interpretation given by Andronov and Bautin [1] has latterly been generalized for an arbitrary discrete relay system [2-4].

A new method of dealing with the phenomenon is given here in which the concept of the transition conductivity in the linear link and the integral form of the equations of motion are used. This approach enables one to eliminate the assumption that the relay system is discrete, and elucidates the character and permissibility of the simplifying assumptions which lead to an idealized conception of the phenomenon.\*

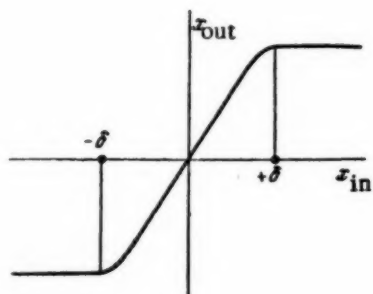


Fig. 1

Discontinuities in nonlinear circuit elements incorporated in automatic control systems may cause peculiar modes of operation which have latterly been called jump or "sliding action." If we include constant speed servomotor systems with relay systems this phenomenon can be divided into two types. The first occurs particularly in relay systems in which (we assume) the relay output can only take the values +1 and -1, while the second occurs in constant-speed servomotor systems where the output coordinate can have any value lying between the limits of +1 and -1, although this occurs only over a very narrow range of input coordinates

2δ. (Fig. 1). In the first case the "sliding action" occurs via fairly rapid (in theory, infinitely rapid) relay switch-over. In the second case the servomotor output coordinate changes between its extreme values while the input varies within the given limits (-δ, δ), the range being taken as infinitely small in the idealized picture. Delays are either neglected or taken as very small, since time-constants confuse the clear idealized picture. All the same it is of interest to give preliminary consideration to each of these types of behaviors.

\* A more detailed discussion of certain questions discussed here, and a generalization for a system with several relays can be found in [4].

Consider the operation of the relay system (Fig. 2) which has the characteristic shown in Fig. 3. Let the input coordinate  $y$  be zero at some instant  $t_0$ . The output coordinate  $x$  can as of  $t_0$  take the values either  $+1$  or  $-1$ . Now suppose that when  $x = +1$ ,  $y = y_+(t, t_0)$  and that when  $x = -1$ ,  $y = y_-(t, t_0)$ , and that

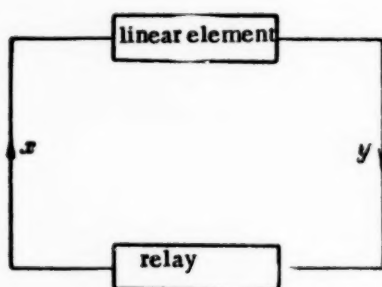


Fig. 2

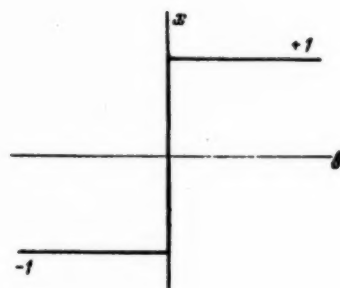


Fig. 3

$y = y_-$  goes upward, while  $y = y_+$  goes downward as shown in Fig. 4. What will the subsequent behavior of the system be? When the relay switches over to  $+1$ ,  $y$  will at once become negative, and so the relay output must be  $-1$ , while on switching to  $-1$ ,  $y$  at once becomes positive, the corresponding value of  $x$  being  $+1$ . Hence the relay can switch neither to  $+1$  nor to  $-1$ . To discover what occurs we assume that there is a very small backlash  $2\delta$  corresponding to the relay characteristic shown in Fig. 5, or else a very short time-constant  $\tau$ .

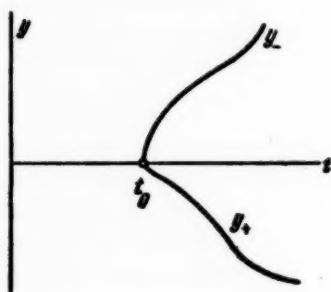


Fig. 4

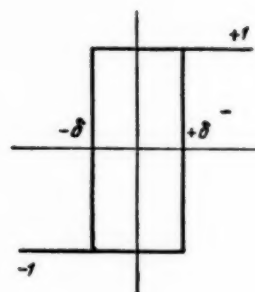


Fig. 5

In the first case  $x$  will be either  $+1$  or  $-1$  when  $y = 0$ . Suppose that  $x = +1$ . The changes in  $y$  will follow the curve  $y = y_+(t, t_0)$ , and on reaching the straight line  $y = -\delta$  at time  $t_1$ , the relay will switch over to  $-1$ .  $y$  will then follow  $y = y_-(t, t_1)$ , and if  $t_1 - t_0$  is small this curve will be close to  $y = y_-(t, t_0)$  for time  $t_0$ . So  $y$  begins to fall and at some time  $t_2$  attains the value  $+\delta$ . Continuing in this fashion we find that  $y$  will alternate between  $-\delta$  and  $+\delta$ , as shown in Fig. 6, and this will continue, the alternate movements being along the initial sections of the  $y = y_-$  and  $y = y_+$  curves respectively at each switchover. If now  $\delta$  tends to zero we arrive at an oscillatory motion with  $y = 0$  and infinitely rapid relay operation. This will continue until either  $y = y_-$  no longer proceeds downward or  $y = y_+$  upward, after which the relay will switch to either  $+1$  or  $-1$  as appropriate.

When  $\tau$  is finite we suppose that when the relay switches over to  $+1$  at time  $t$  the linear link output  $y$  does not at once begin to alter, but does so only after a time  $\tau$ , then following the curve  $y = y_+$ . Up to this time  $y$  is rising to some positive value, after which it begins to fall, passing through zero at time  $t_1$ . The

relay switches over to  $-1$ , but  $y$  continues to fall along  $y = y_+$  for a time  $\tau$ , then commencing to rise, attaining  $y = 0$  at time  $t_2$ , etc. Thus, here again  $y$  oscillates about zero (Fig. 7). As the delay is reduced without limit we arrive at the same result, namely a limiting infinitely rapid oscillatory motion of the relay.

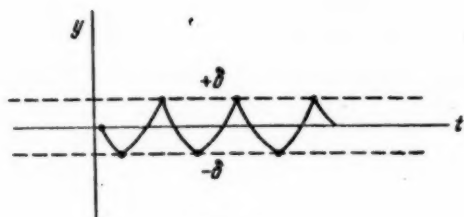


Fig. 6

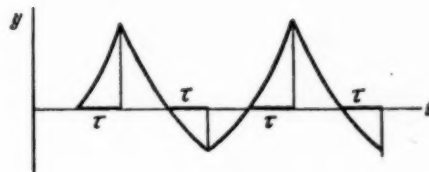


Fig. 7

Thus when  $y = y_+$  and  $y = y_-$  are as described and  $\delta$  and  $\tau$  are sufficiently small, we find that the behavior is such as to maintain the output  $x$ , thanks to relay oscillation around the zero region. This gives the so-called "ramp (or sliding) action" when  $\delta \rightarrow 0$  and  $\tau \rightarrow 0$ .

In any real system the "ramp action" is a somewhat idealized and simplified concept which is more realistic the less the time delay and backlash. We must here specify how small  $\delta$  and  $\tau$  have to be. The restrictions on  $\delta$  and  $\tau$  arise firstly from the requirement that the excursions in  $y$  be negligibly small, and secondly that changes occurring during the transit in  $y = y_+$  and  $y = y_-$  are extremely slight. To specify these demands quantitatively we shall estimate the excursions of  $y$  around zero and the time between successive relay operations.

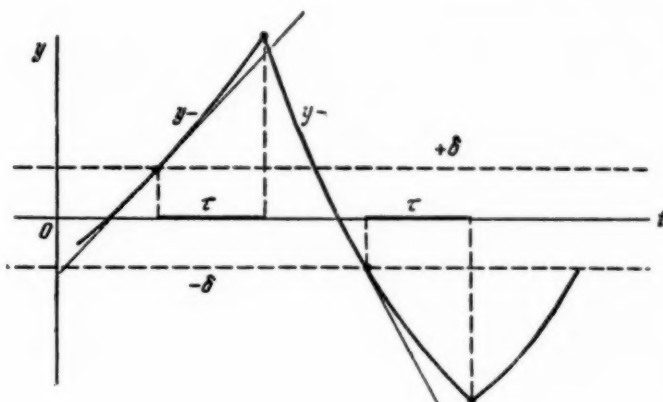


Fig. 8

If we denote the slopes of the initial sections of  $y = y_+$  and  $y = y_-$  by  $k_+$  and  $k_-$ , respectively, in accordance with Fig. 8, the swings in  $y$  are approximately equal to  $-k_+ \tau + 2\delta + k_- \tau = A$ , while the total time of one oscillation is about  $(-k_+ \tau + 2\delta + k_- \tau) \left( \frac{1}{k_-} - \frac{1}{k_+} \right) = T$ .  $A$  must, on the one hand, be negligibly small, and on the other, the main time constants of the linear link must be much greater than  $T$ .

If  $\varphi(t)$  is the so-called transition conductance of the linear element,  $x(t)$  its input and  $y(t)$  the output coordinate, then

$$y(t) = \int_{-\infty}^t \varphi'(t - \tau) x(\tau) d\tau.$$

When  $x(t)$  and  $y(t)$  are considered as from some time  $t_0$ , we may put this in the form

$$y(t) = y_0(t) + \int_{t_0}^t \varphi'(t - \tau) x(\tau) d\tau,$$

where  $y_0(t)$  is the linear link output caused by the so-called initial perturbation in this link.

Then the equations of motion for our relay systems may be written in the form

$$\begin{aligned} y(t) &= y_0(t) + \int_{t_0}^t \varphi'(t - \tau) x(\tau) d\tau + f(t), \\ x(t) &= \Omega[y(t)], \end{aligned} \quad (1)$$

where  $\Omega(y)$  is the nonlinear element characteristic and  $f(t)$  is the component of the linear link output corresponding to the external perturbation applied to the link.

From the earlier discussion for "ramp action" starting at a time  $t_0$  we must have that the function

$$y_+(t, t_0) = y_0(t) + \int_{t_0}^t \varphi'(t - \tau) d\tau + f(t) \quad (2)$$

has a negative derivative at  $t = t_0$ , i.e., that

$$y'_0(t_0) + \varphi'(0) + f'(t_0) < 0, \quad (3)$$

and that

$$y_-(t, t_0) = y_0(t) - \int_{t_0}^t \varphi'(t - \tau) d\tau + f(t) \quad (4)$$

has a positive derivative at  $t = t_0$ , i.e., that

$$y'_0(t_0) - \varphi'(0) + f'(t_0) > 0. \quad (5)$$

(3) and (5) in particular show that for "ramp action" to arise the inequality

$$\varphi'(0) < 0, \quad (6)$$

must be complied with.

When (3) and (5) are fulfilled, since  $y = 0$  in "ramp action," (1) takes the form \*

\* We note (although this condition will never be used) that  $x(t)$  must be considered as the relay output coordinate averaged over a time interval which is extremely small compared with the time-constant of the linear link in the relay system.

$$y_0(t) + \int_{t_0}^t \varphi'(t-\tau)x(\tau)d\tau + f(t) = 0. \quad (7)$$

If the solution to this equation,  $x(t)$ , is known, the conditions for "ramp action" to start, (3) and (5), may be written as

$$|x(t_0)| < 1. \quad (8)$$

Thus, "ramp action" will occur at  $t_0$ , if firstly, (6) is fulfilled for the linear part of the circuit, and secondly if (8) applies to the solution to (7),  $x(t)$ . In fact, by replacing  $y_0(t) + f(t)$  in (3) and (5) by

$$-\int_{t_0}^t \varphi'(t-\tau)x(\tau)d\tau, \quad \text{in accordance with (7) we arrive at } \varphi'(0)[1-x(t_0)] < 0, \quad \varphi'(0)[-1-x(t_0)] > 0$$

or in accordance with (6) at  $|x(t_0)| < 1$ .

The oscillations once set up will continue while the modulus of  $x(t)$  remains less than 1. If only this condition is violated the relay will switch over to  $+1$  or  $-1$  depending on whether  $x(t)$  passes through  $+1$  or  $-1$  when (8) is violated.

With constant-speed servomotors the picture of how the oscillation is set up is in a certain sense simpler, i.e., if the solution to a system of equations such as

$$y = L(x), \quad x = \Omega(y) \quad (9)$$

is  $x(t)$ , and this has a modulus less than unity during a certain time interval, then it is implied that  $y$  then falls between  $-\delta$  and  $+\delta$ , and oscillation occurs. In the limit when  $\delta \rightarrow 0$  the oscillatory motion corresponds to the solution of  $L(x) = 0$  satisfying the condition  $|x(t)| < 1$ . As previously, if  $y$  is to lie between  $+\delta$  and  $-\delta$  we must have that the  $y = y_+$  and  $y = y_-$  curves satisfy the conditions  $y'_+ < 0$  and  $y'_- > 0$  at any moment, which implies, as before, that  $\varphi(0)$  is negative.

Thus "ramp action" is formally described by the same equations in both cases, and the conditions for it to arise are the same.

In order that oscillatory motion should not only always be possible in the system but that the system should actually operate in this way (i.e., that the motion of the system should at all times be oscillatory in spite of external disturbances) we must have a solution to (7) such that at all times  $|x(t)| < 1$ . This requirement primarily implies that the equilibrium state  $x = 0$  of the linear system is described by the equation

$$f(t) + \int_0^t \varphi'(t-\tau)x(\tau)d\tau = 0, \quad (10)$$

and must be stable against sufficiently small external disturbances. Rewriting (10) in the form

$$K(p)x = -F \quad \text{or} \quad x = -K^{-1}(p)F, \quad (11)$$

we have directly that the poles of  $K^{-1}(p)$  or, which is the same thing, that the zeros of  $K(p)$  must lie in the left half-plane. In particular, if the linear link is of itself stable, this means that the transfer coefficient hodograph  $w = K(i\omega)$  must not enclose the point  $w = 0$ . The requirement that the equilibrium state should of itself be stable is still not sufficient for a continuous oscillatory regime to exist in the system. It is further necessary that the external forces acting on a real system do not upset this regime. To discuss this problem we resort to Bulgakov's perturbation accumulation method [5].

Let  $D(p)$ , the transfer coefficient from the input (to which the action  $g(t)$  is applied) to the output of the linear link, be such that



$$F = D(p)G. \quad (12)$$

After substituting (12) into (11) we get in image terms

$$x = -\frac{D(p)}{K(p)}G \quad (13)$$

or alternatively in the original terms

$$x(t) = -\int_0^t \psi(t-\tau)g(\tau)d\tau, \quad (14)$$

where  $\psi(t)$  is the original of  $\frac{D(p)}{K(p)}$ , (14) shows that

$$|x(t)| \leq \int_0^t |\psi(\tau)| \max_{\tau < t} |g(\tau)| d\tau.$$

Hence for the system to be at all times oscillatory it is sufficient for the inequality

$$\max |g(t)| < \left( \int_0^\infty |\psi(\tau)| d\tau \right)^{-1}. \quad (15)$$

to be complied with.

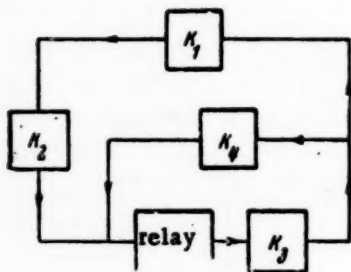


Fig. 9

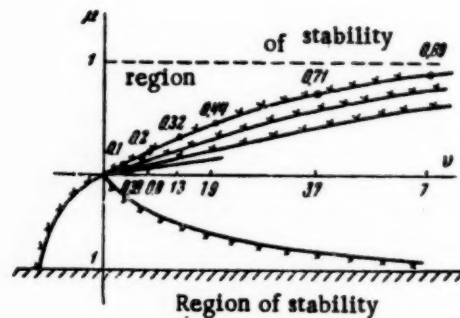


Fig. 10

As an example we will consider an automatic control system in which a relay controller with strong feedback indirectly controls the temperature of a furnace. The block diagram of such a system is shown in Fig. 9. The transfer coefficient of the linear part is

$$K(p) = -K_3(K_1K_2 + K_4) = -\frac{K_aK_i}{T_ap(T_ap+1)}e^{-p\tau} - \frac{p}{T_ap}, \quad (16)$$

where  $K_1$ ,  $K_2$ ,  $K_3$ , and  $K_4$  are the transfer coefficients for the controlled object, measuring element, servomotor and feedback respectively, being as follows:

$$K_1 = \frac{K_a}{T_a p + 1} e^{-p\tau}, \quad K_2 = K_1, \quad K_3 = \frac{1}{T_s p}, \quad K_4 = \rho.$$

Let the equation for the relay element of input  $y$  and output  $x$  be

$$x = \text{sign } y.$$

An oscillatory mode can occur in this system if  $\varphi'(0)$  is negative for the linear part of the system. Using known relationships we have

$$\varphi'(0) = \lim_{p \rightarrow \infty} pK(p) = -\frac{\rho}{T_s}$$

and hence for oscillation to begin we must have that

$$\varphi'(0) = -\frac{\rho}{T_s} < 0. \quad (17)$$

When (17) is fulfilled the state of equilibrium in the relay system will be stable only if the zeros of  $K(p)$  lie to the left of the imaginary axis, i.e., if the quasipolynomial

$$K_i K_a + \rho (T_a p + 1) e^{p\tau} \quad (18)$$

has no roots in the right half-plane.

Let us introduce the fresh parameters

$$\nu = \frac{\tau}{T_a} \text{ and } \mu = \frac{\rho}{K_a K_i}$$

and rewrite (18) in the form

$$1 + \mu(1 + z)e^{\nu z}.$$

The corresponding D-scheme in the parameters  $\mu$  and  $\nu$ , and the equilibrium state stability region, are shown in Fig. 10.

#### LITERATURE CITED

- [1] A. A. Andronov and N. N. Bautin, The Motion of a Neutral Aircraft Controlled by an Autopilot, and the Theory of Point Transformations of Surfaces, Proc. Acad. Sci. USSR 43, 5 (1944).
- [2] Yu. V. Dolgolenko, Oscillatory Modes in Relay Indirect Control Systems, Acad. Sci. USSR Press, 1955, Vol. 1.
- [3] Yu. V. Dolgolenko, Oscillatory Modes in Relay Indirect Control Systems, Author's abstract of doctorate dissertation, Leningrad, 1955.
- [4] Yu. I. Neimark, "Ramp Action" and Periodic Motions in Relay Systems, Trans. Gorky Inst. Phys. Tech. Research and Radio Faculty Gorky State Univ., Vol. 30, Phys. Series, 1956.
- [5] B. V. Bulgakov, Oscillation, State Technical Press, 1954.

Received June 2, 1956



# STUDY OF PULSED CONTACTOR AUTOMATIC CONTROL SYSTEM DYNAMICS

V. P. Kazakov

(Moscow)

Methods of defining self-oscillation and transient processes in pulsed contactor systems are described which are based on the frequency and time characteristics of the continuous section in the system.

An approximate method of defining self-oscillation which is based on the first harmonic of the output from the pulsed contactor is also described, and a method of allowing for higher harmonics is also given. The calculated results are compared with experiment.

## INTRODUCTION

Control systems using a pulsed relay to transform the input variable into a train of pulses of constant magnitude and duration and of polarity defined by the input polarity at the instant of connection have been considered by several workers [1-4]. This was first dealt with in [1] in relation to dynamics studies on a multi-channel controller for a boiler assembly. A simple pulsed relay control system was analyzed using difference equation equipment. A similar method was used in [2], in which transient processes were analyzed for the discontinuous control systems used on cutting machines and coal combines which had auxiliary constant-speed mechanisms; nonlinear difference equations of orders one and two were studied.

A method of analyzing self-oscillation in pulsed relay systems was proposed in [3], in which pulse circuit theory was used [5]. The solutions, which were obtained in a closed form, required that the poles of the transfer function for the linear part of the system be found, and hence the difficulty of determining the self-oscillation parameters increased rapidly with the order of the equations describing the linear part. Harmonic balance methods [4] have been used to deal with similar systems. By constructing a nonlinear complex gain for the pulsed relay element, which has an insensitive zone and  $\gamma$  equal to 1, the frequency and amplitude of the first self-oscillation harmonic were derived.

The present paper deals with a method of studying pulsed relay automatic control systems which provides the self-oscillation parameters to the desired degree of accuracy independent of the complexity in the linear part, and also with a graphic method of considering transients in such systems.

### 1. Determination of Self-Oscillation

A pulsed-relay control system is represented schematically as a circuit consisting of the pulsed element and the linear part, all the elements other than the relay being included in the latter (Fig. 1).

The external disturbance  $f(t)$ , which may in general act at any point in the system, is supposed applied to the pulsed element input, and all quantities are taken as functions of the dimensionless time  $\bar{t} = \frac{t}{T_p}$ , where  $T_p$  is the repetition period of the pulsed element.

By representing the pulsed relay element as a series combination of a two-position relay with a Z-type characteristic and an amplitude-modulated pulsed element (Fig. 2), we can apply the method of studying self-oscillation given in [6].

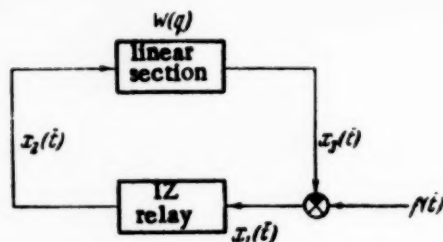


Fig. 1

We shall suppose that a self-oscillation of relative half-period  $N$  (a whole number) occurs in the automatic control system, and that  $f(\bar{t}) = 0$ . Then all the quantities specifying the state of the system  $x_1(\bar{t})$ ,  $x_2(\bar{t})$  and  $x_3(\bar{t})$ , will change periodically, with half-period  $N$ . The desired periodic solution will exist if the conditions that the instant and direction of switchover are appropriate, are fulfilled: 1)  $x_1(N-1) > 0$ ; 2)  $x_1(N) < 0$  and also if the condition that no switching occurs within a half-period  $N$ ; 3)  $x_1(n) > 0$  when  $0 \leq n \leq N$  or, since the condition of closure implies  $x_1(\bar{t}) = -x_3(\bar{t})$ :

$$\begin{aligned} x_3(N-1) &< 0, \\ x_3(N) &> 0, \\ x_3(n) &< 0 \text{ when } 0 \leq n \leq N. \end{aligned} \quad (1)$$

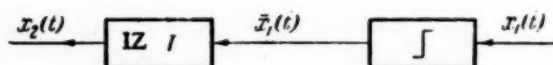


Fig. 2

A periodic pulse series acts on the linear part during self-oscillation, as shown in Fig. 3 (for  $N = 3$ ). The Fourier series for the periodic series of cross-hatched pulses  $\bar{x}_2(\bar{t})$  takes the form

$$\bar{x}_2(\bar{t}) = \sum_{m=-\infty}^{\infty} C_{2m-1} e^{j(2m-1)\frac{\pi}{N}\bar{t}},$$

where

$$C_{2m-1} = \frac{k_p}{j\pi(2m-1)} \left[ 1 - e^{-j(2m-1)\frac{\pi}{N}\gamma} \right],$$

where  $k_p$  is the pulsed element gain and  $\gamma$  is the relative pulse length.

The signal to the linear part is found as the sum of analogous pulse series displaced relative to the first along the time axis by  $k$  whole intervals of time  $\bar{T}$ , where  $k = 1, 2, 3, \dots, (N-1)$ . Then

$$x_2(\bar{t}) = \sum_{k=0}^{N-1} \bar{x}_2(\bar{t} - k) = \sum_{m=-\infty}^{\infty} C_{2m-1} e^{j(2m-1)\frac{\pi}{N}\bar{t}} \times \sum_{k=0}^{N-1} e^{-j(2m-1)\frac{\pi}{N}k}$$

and finally

$$x_2(\bar{t}) = \sum_{m=-\infty}^{\infty} \bar{C}_{2m-1} e^{j(2m-1)\frac{\pi}{N}\bar{t}},$$

$$\bar{C}_{2m-1} = \frac{2k_p}{j\pi(2m-1)} \frac{1 - e^{-j(2m-1)\frac{\pi}{N}\gamma}}{1 - e^{-j(2m-1)\frac{\pi}{N}}}$$

$x_3(\bar{t})$  is found as the sum of the responses from the linear part to each harmonic in the expansion of  $x_2(\bar{t})$ . If  $W(j\omega) = K(\omega)e^{j\theta(\omega)}$  is the frequency characteristic of the linear part, then

$$x_3(\bar{t}) = \sum_{m=-\infty}^{\infty} \bar{C}_{2m-1} K\left[(2m-1)\frac{\pi}{N}\right] e^{j\left\{(2m-1)\frac{\pi}{N}\bar{t} + \theta\left[(2m-1)\frac{\pi}{N}\right]\right\}}$$

Here  $\frac{\pi}{N} = \omega T_p = \chi$  is the relative oscillation frequency. Elementary operations transform this to the following form:

$$x_3(\bar{t}) = \frac{4k_p}{\pi} \sum_{m=1}^{\infty} \bar{M} K\left[(2m-1)\frac{\pi}{N}\right] \sin\left\{(2m-1)\frac{\pi}{N}\bar{t} + \psi + \theta\left[(2m-1)\frac{\pi}{N}\right]\right\},$$

where

$$\bar{M} = \frac{1}{2m-1} \frac{\sin(2m-1)\frac{\pi}{2N}\gamma}{\sin(2m-1)\frac{\pi}{2N}}, \quad \psi = (2m-1)\frac{\pi}{2N}(1-\gamma).$$

The linear part frequently acts as a low-frequency filter, i.e., it practically rejects harmonic components with relative frequencies equal to or greater than  $\chi_c = \frac{\pi}{N_c}$ . We can thus restrict ourselves to a finite number of terms in the expression for  $x_3(\bar{t})$ . But even then major computational difficulties are encountered in applying  $x_3(\bar{t})$  directly.

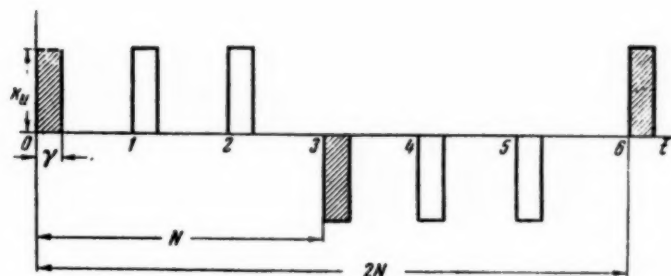


Fig. 3

Periodic solutions can easily be found by considering only the first harmonic in  $x_3(\bar{t})$ . Hence a method of solution in a first approximation is given below (i.e., one for the main harmonic) and the way to allow for the effects of higher harmonics on the self-oscillation parameters is then indicated.

Let us consider the first harmonic of the output from the linear part:

$$x_3(\bar{t})_I = \frac{4k_p}{\pi} \frac{\sin \frac{\pi}{2N}\gamma}{\sin \frac{\pi}{2N}} K\left(\frac{\pi}{N}\right) \sin\left\{\frac{\pi}{N}\bar{t} + \frac{\pi}{2N}(1-\gamma) + \theta\left(\frac{\pi}{N}\right)\right\}.$$

The amplitude  $A_I = \frac{4k_p}{\pi} \frac{\sin \frac{\pi}{2N} \gamma}{\sin \frac{\pi}{2N}} K\left(\frac{\pi}{N}\right)$  is always greater than zero when  $N \geq 1$ . By subjecting  $x_3(\bar{t})_I$  to the conditions in (1) at  $\bar{t} = N-1$  and  $\bar{t} = N$ , we get

$$\begin{aligned} -2(k+1)\pi < \theta\left(\frac{\pi}{N}\right) < -\pi \left[ (2k+1) - \frac{1+\gamma}{2N} \right], \\ -\pi \left[ (2k+1) + \frac{1-\gamma}{2N} \right] < \theta\left(\frac{\pi}{N}\right) < -2\pi k \quad (k=0, 1, 2, \dots, \infty). \end{aligned} \quad (2)$$

Thus if a point on the frequency characteristic of the linear part at some value  $\chi = \chi_1 = \frac{\pi}{N_1}$  has a phase  $\theta\left(\frac{\pi}{N_1}\right)$ , which satisfies the above inequalities the system will have a periodic solution of relative half-period  $N = N_1$ . Geometrically, (2) define a sector of the complex plane bounded by straight lines passing through the origin for each value of  $\chi$ .

The position of each sector on the complex plane is specified by the angle  $\alpha_0 = -\pi \left(1 - \frac{\gamma}{2N}\right)$  formed by the bisectrix of the sector and the positive direction of the real semiaxis, while the sector angle  $\beta$  is numerically equal to the relative frequency  $\pi/N$  for which it is drawn (Fig. 4). The amplitude of the first harmonic is found by multiplying the frequency characteristic modulus  $K(\pi/N)$  by  $k_p a$ , where

$$a = \frac{4}{\pi} \left( \sin \frac{\pi}{2N} \gamma / \sin \frac{\pi}{2N} \right).$$

$a$  has been calculated for various  $N$  and  $\gamma$  and is given in Table 1, which latter shows that when  $N > 6$  we may, to a sufficient accuracy, assume  $a = \frac{\pi \gamma}{4}$ .

If more than one point on  $W(j \frac{\pi}{N})$  falls

within the corresponding sectors, more than one periodic solution can exist for the system.

$x_3(N-1)_I$  and  $x_3(N)_I$  can be found for any value of  $N$  from the frequency characteristic of the linear part. In fact when  $k_p = 1$

$$x_3(N-1)_I = -aK\left(\frac{\pi}{N}\right) \sin \left\{ -\frac{\pi}{N} \frac{1+\gamma}{2} + \theta\left(\frac{\pi}{N}\right) \right\}$$

and

$$x_3(N)_I = -aK\left(\frac{\pi}{N}\right) \sin \left\{ \frac{\pi}{N} \frac{1-\gamma}{2} + \theta\left(\frac{\pi}{N}\right) \right\},$$

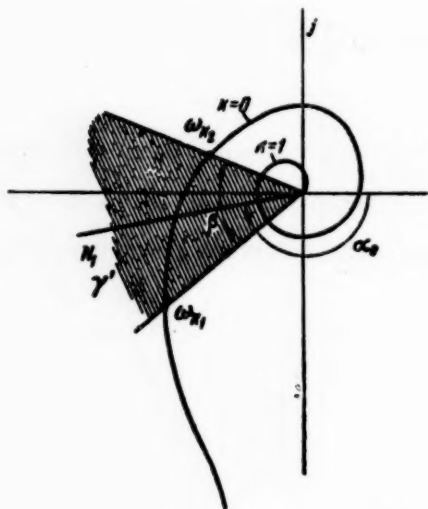


Fig. 4



and the projection on the imaginary axis of the radius vector for  $W(j \frac{\pi}{N})$  (for some  $N$ ), turned through the angle  $b_1 = \frac{\pi}{N} \frac{1+\gamma}{2}$  in a negative sense and multiplied by  $a$ , is  $-x_3(N-1)_I$  (section  $OA'$  in Fig. 5).

TABLE 1

$$a = \frac{4}{\pi} \frac{\sin \frac{\pi}{2N} \gamma}{\sin \frac{\pi}{2N}}$$

$\gamma \backslash N$	$\frac{1}{5}$	$\frac{1}{3}$	$\frac{2}{5}$	$\frac{3}{5}$	$\frac{2}{3}$	$\frac{4}{5}$	1	2	3	4	5	$6 - \infty$
0.05	0.483	-0.292	0.343	0.341	0.216	0.0134	0.099	0.0706	0.0665	0.0653	0.0645	0.0635
0.1	0.897	-0.571	0.686	0.660	0.419	0.267	0.198	0.139	0.133	0.131	0.129	0.127
0.2	1.27	-1.03	1.27	1.27	0.813	0.521	0.392	0.281	0.264	0.260	0.258	0.254
0.3	0.897	-1.26	1.66	1.79	1.168	0.749	0.576	0.418	0.396	0.391	0.386	0.381
0.4	0	-1.21	1.79	2.209	1.46	0.978	0.747	0.555	0.528	0.517	0.513	0.508
0.5	0.897	-0.897	1.66	2.43	1.65	1.14	0.897	0.688	0.658	0.646	0.641	0.631
0.6	-1.27	-0.391	1.27	2.54	1.78	1.27	1.027	0.815	0.785	0.772	0.768	0.762
0.7	-0.897	0.203	0.686	2.43	1.78	1.35	1.13	0.937	0.909	0.897	0.895	0.889
0.8	0	0.749	0	2.21	1.71	1.37	1.21	1.056	1.03	1.02	1.023	1.016
0.9	0.897	1.130	0.686	1.79	1.52	1.35	1.25	1.16	1.15	1.14	1.14	1.14
1	1.27	1.27	0.897	0.63	1.27	1.27	1.27	1.27	1.27	1.27	1.27	1.27

The projection of this same vector,  $ak(\frac{\pi}{N})$ , when turned in the positive direction by an angle  $b_2 = \frac{\pi}{N} \frac{1-\gamma}{2}$  is  $-x_3(N)_I$  (section  $OB'$  in Fig. 5).

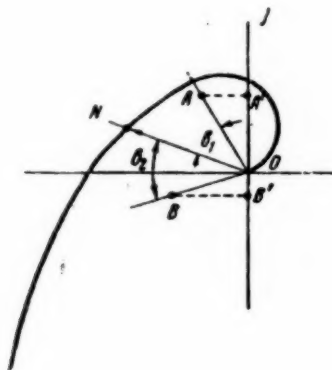


Fig. 5

By representing  $x_3(N-1)_I$  and  $x_3(N)_I$  as projections on the imaginary axis we are able to derive a simple expression for the necessary condition for self-oscillation to occur.

Since the effector unit in a pulsed relay system is usually a mechanism without feedback, i.e., an integrating element, the self-oscillation amplitude increases with  $N$ .

Hence, a self-oscillation of half-period  $N_k$  must comply with the following relations:

$$x_3[N_k] > 0$$

and

$$x_3[N_{k1}] < 0,$$

where  $N_{k1} = N_k - 1$ , i.e., the stepwise curve  $x_3[N] = f[N]$  intersects the  $N$  axis from below upwards at  $N_k$ . Then any deviation from the  $N$  axis causes the system to react in such a way that the self-oscillation returns to  $N_k$ . Figure 5 shows that the periodic solution with half-period  $N_k$  will be stable if the point on the frequency characteristic at which  $N = N_{k1}$  has a phase

$$\theta\left(\frac{\pi}{N_{k1}}\right) < -(2k+1)\pi\left(1 + \frac{1-\gamma}{2N_{k1}}\right).$$

TABLE 2a

$$b_1 = \frac{\pi}{2N} (1 + \gamma)$$

$\gamma$	$\frac{1}{5}$	$\frac{1}{3}$	$\frac{2}{5}$	$\frac{3}{5}$	$\frac{2}{3}$	$\frac{4}{5}$	1	2	3	4	5	6	7	8	9	10	12	15	18	20
0.05	472°30'	283°30'	236°15'	157°30'	141°45'	118°7'	94°30'	47°15'	31°30'	23°30'	18°55'	15°45'	13°13'	11°48'	10°30'	9°24'	7°52'	6°30'	5°15'	4°45'
0.1	495°	297°	247°30'	165°	148°30'	123°45'	99°	49°30'	33°	24°45'	19°48'	16°30'	13°48'	12°18'	11°	9°54'	8°15'	6°36'	5°30'	4°55'
0.2	540°	324°	270°	180°	162°	135°	108°	54°	36°	27°	21°36'	18°	15°8'	13°30'	12°	10°48'	9°	7°12'	6°	5°24'
0.3	585°	351°	295°30'	195°	175°30'	146°15'	117°	58°30'	39°	29°30'	23°24'	19°30'	16°20'	14°48'	13°	11°42'	9°45'	7°48'	6°30'	5°48'
0.4	630°	378°	315°	210°	189°	157°30'	126°	63°	42°	31°30'	25°12'	21°	17°36'	15°45'	14°	12°36'	10°30'	8°24'	7°	6°18'
0.5	675°	405°	337°30'	225°	202°30'	168°45'	135°	67°30'	45°	33°45'	27°	22°30'	18°54'	16°48'	15°	13°30'	11°15'	9°	7°30'	6°45'
0.6	720°	432°	360°	240°	216°	180°	144°	72°	48°	36°	28°48'	24°	20°8'	18°	16°	14°24'	12°	9°36'	8°	7°15'
0.7	765°	459°	382°30'	255°	229°30'	191°15'	153°	76°30'	51°	38°20'	30°36'	25°35'	21°25'	19°10'	17°	15°15'	12°45'	10°12'	8°30'	7°45'
0.8	810°	486°	405°	270°	243°	202°30'	162°	81°	54°	40°30'	32°24'	27°	22°42'	20°15'	18°	16°12'	13°30'	10°48'	9°	8°6'
0.9	855°	513°	427°30'	285°	256°30'	213°45'	171°	85°30'	57°	42°45'	34°12'	28°30'	23°54'	21°20'	19°	17°6'	14°15'	11°24'	9°30'	8°30'
1.0	900°	540°	450°	300°	270°	225°	180°	90°	60°	45°	36°	30°	25°12'	22°30'	20°	18°	15°	12°	10°	9°

TABLE 2b

$$b_2 = \frac{\pi}{2N} (1 - \gamma)$$

$\gamma$	$\frac{1}{5}$	$\frac{1}{3}$	$\frac{2}{5}$	$\frac{3}{5}$	$\frac{2}{3}$	$\frac{4}{5}$	1	2	3	4	5	6	7	8	9	10	12	15	18	20
0.05	427°30'	256°30'	213°45'	142°30'	128°15'	106°50'	85°30'	42°45'	28°30'	21°18'	17°6'	14°15'	12°12'	10°38'	9°30'	8°31'	7°8'	5°42'	4°45'	4°18'
0.1	405°	243°	202°30'	135°	121°30'	101°15'	81°	40°30'	27°	20°15'	16°12'	13°30'	11°35'	10°6'	9°	8°6'	6°42'	5°24'	4°30'	4°1'
0.2	360°	216°	180°	120°	108°	90°	72°	36°	24°	18°	14°24'	12°	10°14'	9°	8°	7°12'	6°	4°48'	4°	3°36'
0.3	315°	189°	157°30'	105°	94°30'	78°45'	63°	31°30'	21°	15°45'	12°36'	10°30'	8°55'	7°49'	7°	6°18'	5°15'	4°12'	3°30'	3°9'
0.4	270°	162°	135°	90°	81°	67°30'	54°	27°	18°	13°30'	10°48'	9°	7°43'	6°45'	6°	5°24'	4°30'	3°36'	3°	2°42'
0.5	225°	135°	112°30'	75°	67°30'	56°15'	45°	22°30'	15°	11°15'	9°	7°30'	6°25'	5°38'	5°	4°30'	3°44'	3°	2°30'	2°15'
0.6	180°	108°	90°	60°	54°	45°	36°	18°30'	12°	9°	7°12'	6°	5°8'	4°30'	4°	3°36'	3°	2°24'	2°	1°48'
0.7	135°	81°	67°30'	45°	40°30'	33°45'	27°	13°30'	9°	6°45'	5°24'	4°30'	3°50'	3°19'	3°	2°42'	2°14'	1°48'	1°30'	1°19'
0.8	90°	54°	45°	30°	27°	22°30'	18°	9°	6°	4°30'	3°36'	3°	2°32'	2°15'	2°	1°48'	1°30'	1°12'	1°	0°54'
0.9	45°	27°	22°30'	15°	13°30'	11°15'	9°	4°30'	3°	2°15'	1°48'	1°30'	1°16'	1°8'	1°	0°54'	0°45'	0°36'	0°30'	0°26'

By drawing  $x_3(N-1)_1$  and  $x_3(N)_1$  as graphs we may check up on the effect of higher harmonics on the self-oscillation frequency. Any component in the expressions

$$x_3(N-1) = -\frac{4k_p}{\pi} \sum_{m=1}^{\infty} \bar{M}K \left[ (2m-1) \frac{\pi}{N} \right] \times \\ \times \sin \left\{ -(2m-1) \frac{\pi}{N} \frac{1+\gamma}{2} + \theta \left[ (2m-1) \frac{\pi}{N} \right] \right\}$$

and

$$x_3(N) = -\frac{4k_p}{\pi} \sum_{m=1}^{\infty} \bar{M}K \left[ (2m-1) \frac{\pi}{N} \right] \times \\ \times \sin \left\{ (2m-1) \frac{\pi}{N} \frac{1-\gamma}{2} + \theta \left[ (2m-1) \frac{\pi}{N} \right] \right\}$$

can be found if we know the values of

$$\bar{M}, \bar{b}_1 = (2m-1) \frac{\pi}{N} \frac{1+\gamma}{2} \text{ and } \bar{b}_2 = (2m-1) \frac{\pi}{N} \frac{1-\gamma}{2}$$

for the  $(2m-1)$ -th harmonic. These can be found from the respective coefficients  $\underline{a}$ ,  $b_1$  and  $b_2$  in  $x_3(N-1)_1$  and  $x_3(N)_1$  by simply reducing the  $N$  axis scale by a factor  $(2m-1)$  and  $\bar{M}$  by doing the same with the  $\underline{a}$  axis. Tables 2a and 2b give  $b_1$  and  $b_2$  for various  $N$  and  $\gamma$ . Figures 6, a and 6, b show graphs of  $\underline{a}$ ,  $b_1$  and  $b_2$ .

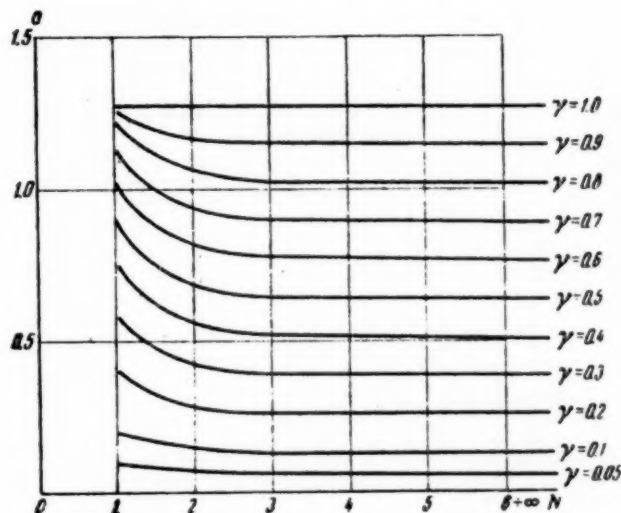


Fig. 6, a

Hence to check up on the influence of higher harmonics on the accuracy with which  $N$  is determined we need to find  $x_3(N-1)_1$  and  $x_3(N)_1$  for points on the frequency characteristic with  $N = \frac{N_1}{(2m-1)}$  as well as these same functions at  $N = N_1$ . By summing these values of  $x_3(N-1)_1$  and  $x_3(N)_1$ , we get values of  $x_3(N-1)$  and  $x_3(N)$  which allow for the requisite number of higher harmonics.

In most practical cases there is no need to determine  $x_3(N-1)_1$  and  $x_3(N)_1$  for  $m > 3$ , i.e., to consider harmonics above the fifth. Only in systems where the frequency characteristics of the linear part has a fairly

large modulus in the first and fourth quadrants can high self-oscillation harmonic corrections alter the value of  $N$  found in the first approximation.

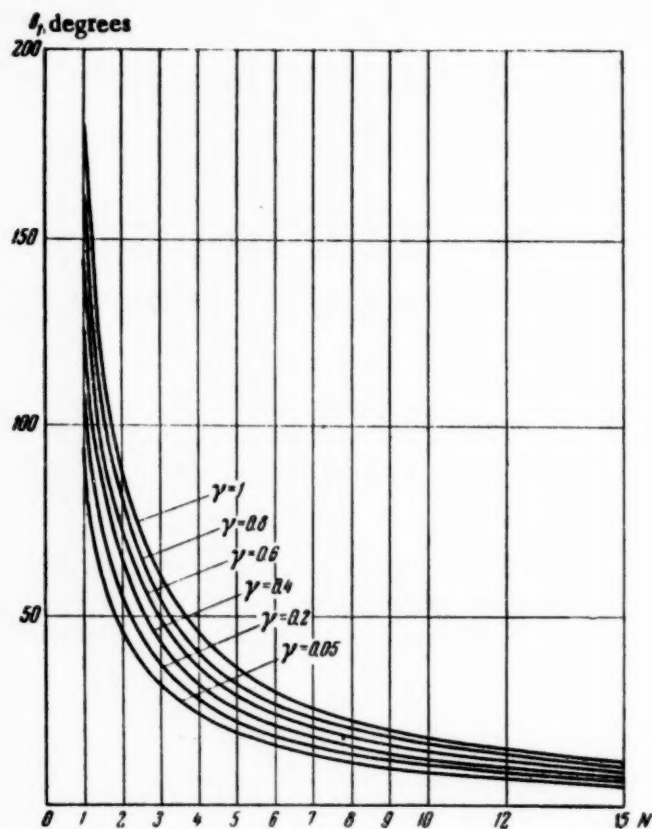


Fig. 6, b

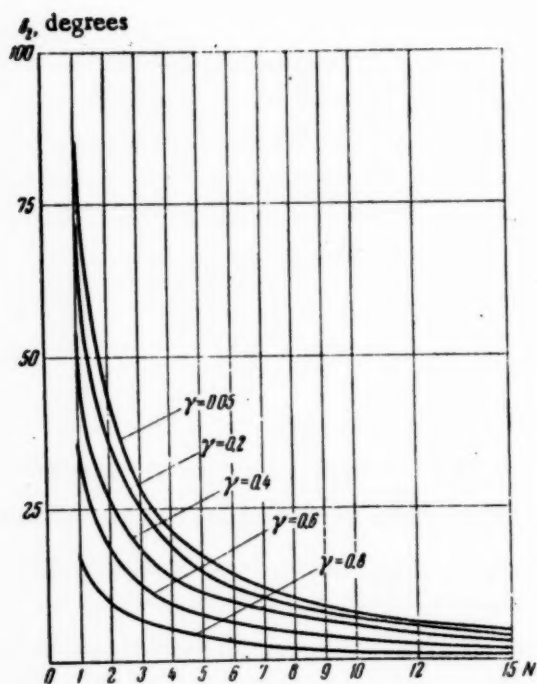


Fig. 6, c

The highest self-oscillation frequency possible in a pulsed relay system is one-half the pulse repetition frequency. Since the self-oscillation period  $T = 2NT_p$  we have to determine the minimum possible control interval  $T_p$  at which  $N = N_1$ . We may see from the expression for  $\alpha_0$  that, as  $\gamma$  changes from zero to unity, each sector rotates through an angle  $\frac{\pi}{2N}$  in the positive sense, and so increasing  $\gamma$  can only reduce the self-oscillation frequency. Since  $\chi = \omega T_p$  we can, by appropriate choice of  $T_p$  at any point on the frequency characteristic, obtain the desired value for  $\chi$  (or  $N$ ). We shall show how to choose  $T_p$  such that the system self-oscillates at  $N = N_1$ , and with the minimum period  $T = 2N_1 T_p$ . Then the point at which  $\chi_1 = \frac{\pi}{N_1}$  must be found in the appropriate sector in the complex plane with sector angle  $\beta = \frac{\pi}{N_1}$ . At the selected value  $\gamma = \gamma_1$  we determine the sector position, i.e.,  $\alpha_0$ . Within the sector lies an arc of the frequency characteristic with frequencies from  $\omega_{k1}$  to  $\omega_{k2}$  (Fig. 4). The required value of  $T_p$  is found from  $T_p = \frac{\chi_1}{\omega_{k1}}$ , where  $\omega_{k2} > \omega_1 > \omega_{k1}$ . If the self-oscillation period at a given  $N$  is to be minimal,  $\omega_1$  must be chosen as close as possible to  $\omega_{k2}$ , i.e., the control period is determined from  $T_p \geq \frac{\pi}{N_1 \omega_{k2}}$ .

## 2. Drawing Out Transients and Self-Oscillation Forms

The special feature of pulsed relay control systems is that the linear part is always fed with trains of rectangular pulses identical in amplitude and duration, the pulses succeeding one another at closely defined

time intervals; this enables one to draw out processes occurring in such systems by simple graphical methods. At each instant when the contacts close the linear part responds in the same way if the error signal at the pulsed unit input falls outside the insensitive zone. The polarity is determined by the error signal polarity. Hence if the way the linear part responds to a rectangular pulse of given height and duration is known any process in the system can be drawn out by summing the responses according to sign.

The response to a rectangular pulse is simply determined by the time characteristic of the linear part, which can be derived in any of the usual ways. When the linear part is complex this determination is best done experimentally if the system actually exists, or by the trapezoidal characteristic method if the frequency characteristic of the linear part is known. The proposed method of drawing out the transient processes and self-oscillation wave shapes for pulsed relay systems is illustrated in Fig. 7.

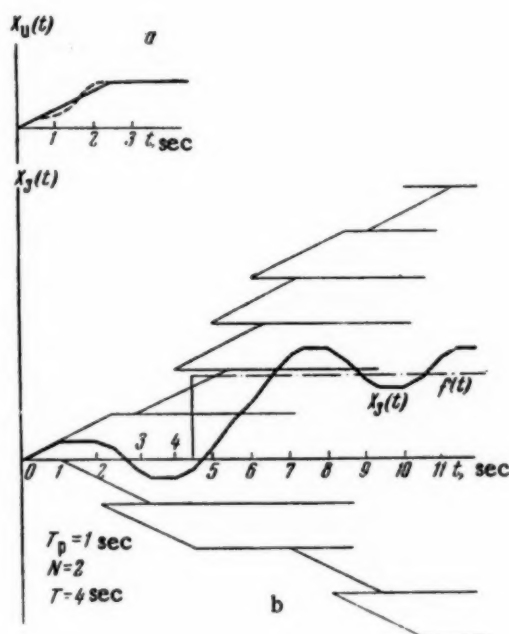


Fig. 7

Figure 7, *a* shows the pulse characteristic of the linear part in some system (dashed curve), this being approximated by trapezia for simplicity and clarity. Figure 7, *b* shows how the closed-loop response to a stepwise change of external action can be found for an arbitrarily chosen  $T_p$ . This construction involves the assumption that  $x_3(t)$  (linear part output) at the instant of contact is equal to the external signal  $f(t)$ . It is further supposed that minute fluctuations at the input or in the pulse unit amplifier cause this latter to emit a control pulse of a given sign at this instant, and hence the stable periodic motion about the set equilibrium position is initiated.



An external stepwise signal arising at some instant is only perceived at the next instant of contact. The sign of the error signal at the pulse unit input is determined by the relative positions of  $x_3(t)$  and  $f(t)$  (Fig. 7, b).

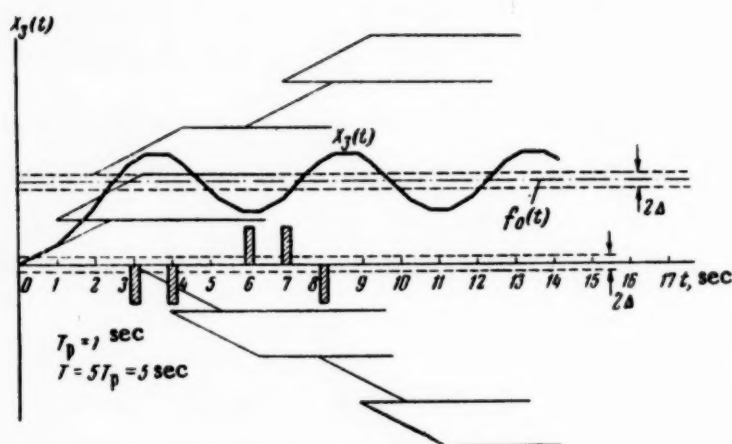


Fig. 8

If there is an insensitive zone it can alter the character of an oscillation setup in the system, and can even prevent oscillation. If the system is initially at rest a definite impetus is required to disturb it. The self-oscillations which then occur after the transient has died away will depend on the relative magnitudes of the

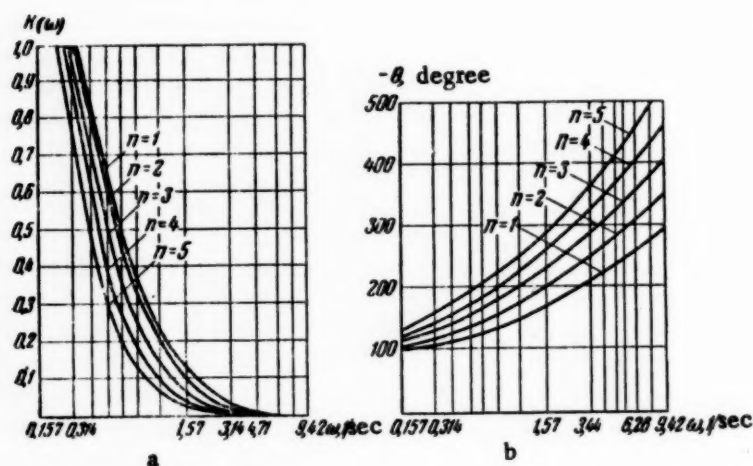


Fig. 9

insensitive zone and step stimulus. Figure 8 shows that a system of this type which has the same values of  $T_p$  and  $\gamma$  will show quite a different self-oscillation picture. We show here a case where the oscillation period is an odd multiple of the pulse repetition period and thus cannot be specified by  $N$  since this is an even number, equal to the half-period of self-oscillation.

This way of drawing out processes in relay pulse systems can be used to determine self-oscillation parameters when the oscillations become established after relatively few pulse repetition periods.

This method has also been applied to study the dynamics of an experimental three-channel relay control system. Each channel has an independent pulsed relay system, the linear part containing the constant-speed

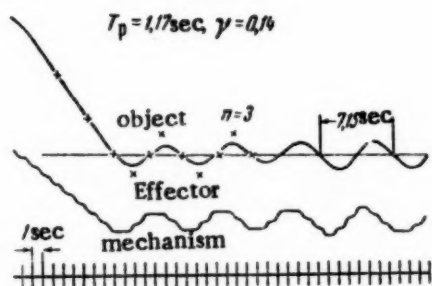


Fig. 10

effector mechanism, the object being a chain of RC links; the number of  $n$  links may be changed from one to five as desired. Figures 9, a and b show  $K(\omega)$  and  $\theta(\omega)$  for each channel. Figure 10 shows oscillograms for the first channel, and Fig. 11 shows  $K(\chi)$  and  $\theta(\chi)$  for

the linear part when  $T_p = 1.17$  sec and  $n = 3$ . Figure 12 shows  $W(j\chi)$  for the linear part and the sectors in the complex plane for  $N = 1, 2, 3, 4$ , and  $5$ . The values of  $N$  corresponding to the frequencies are given in brackets.

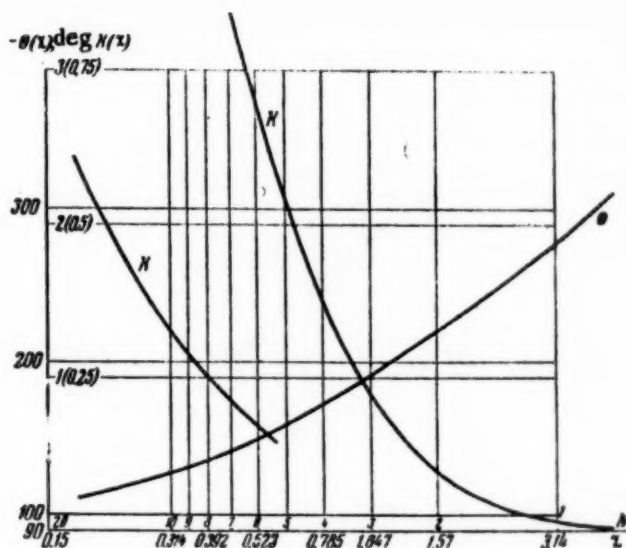


Fig. 11

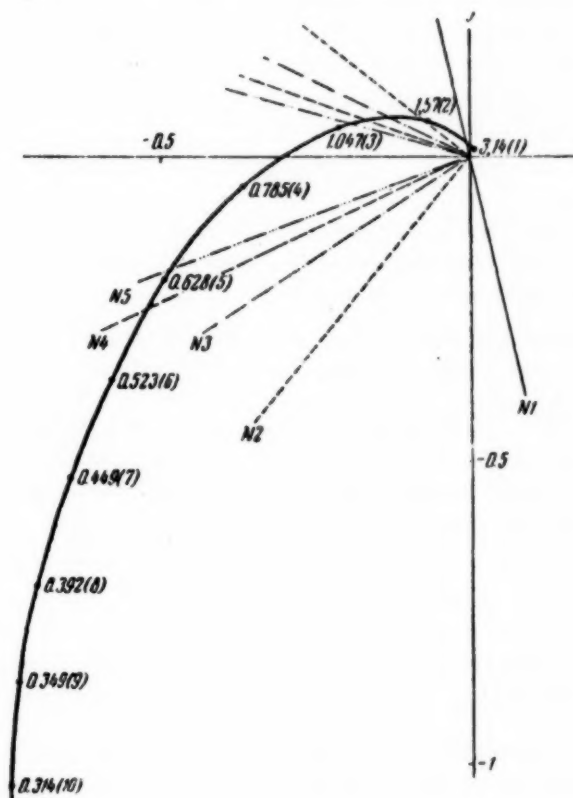


Fig. 12



The relative disposition of  $W(j\chi)$  and the sectors shows that two periodic modes can exist with half-periods  $N = 3$  and  $N = 4$ . Checks on the stability showed that the periodic mode with  $N = 3$  is the only one that can exist, as the oscillograms confirm.

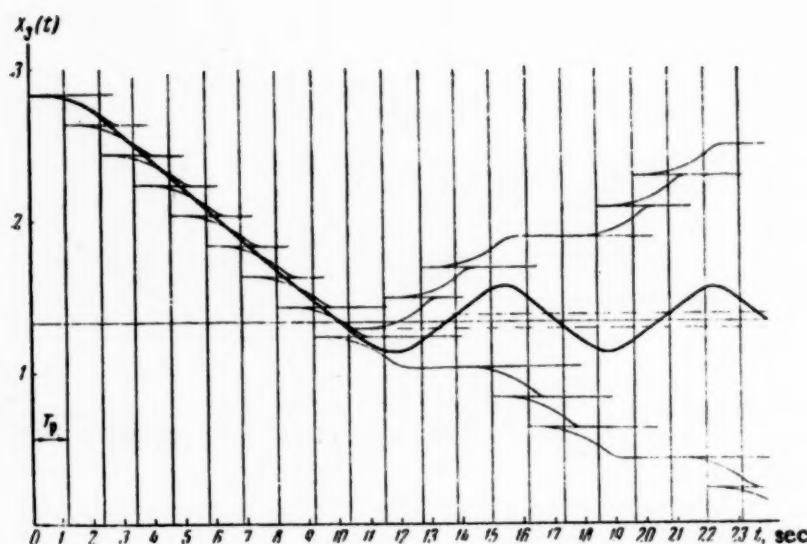


Fig. 13

Figure 13 illustrates the process occurring in the system on a stepwise change of input. The crosses on Fig. 10 show the calculated points for the process. The differences between the experimental and calculated amplitudes was due to the system having a narrow insensitive zone of magnitude changing randomly from zero up to a certain value; this could not be allowed for in the construction.

#### SUMMARY

1. A way of deriving the first harmonic of periodic modes is considered in relation to pulsed relay systems with any pulse repetition frequency and any mark-space ratio which only requires a knowledge of the frequency characteristics for the linear part of the system.
2. It is shown that simple constructions can be used to check the effect of higher harmonics on the self-oscillation period determined in a first approximation.
3. A simple graphic method of deriving transients and self-oscillation wave shapes in pulsed relay systems is given; this can also be used to determine the self-oscillation parameters. This latter feature is particularly important in systems where the pulse element has an insensitive zone, since other methods of studying periodic modes becomes very laborious and inefficient.

#### LITERATURE CITED

- [1] Yu. G. Kornilov, The Analytic Theory of Pulsed Control Applied to an Eight-Point Temperature Regulator for a Dust-Fired Cylinder Boiler, Engineering Symposium, 1, 2 (1941).
- [2] O. M. Krizhanovsky, A Comparison of Pulse Control Systems on Cutting Machines and Coal Combines Using Supply-Frequency Pulsing and Constant-Speed Servomotors, Proc. Akad. Nauk Ukraine SSR, No. 4, 1953.

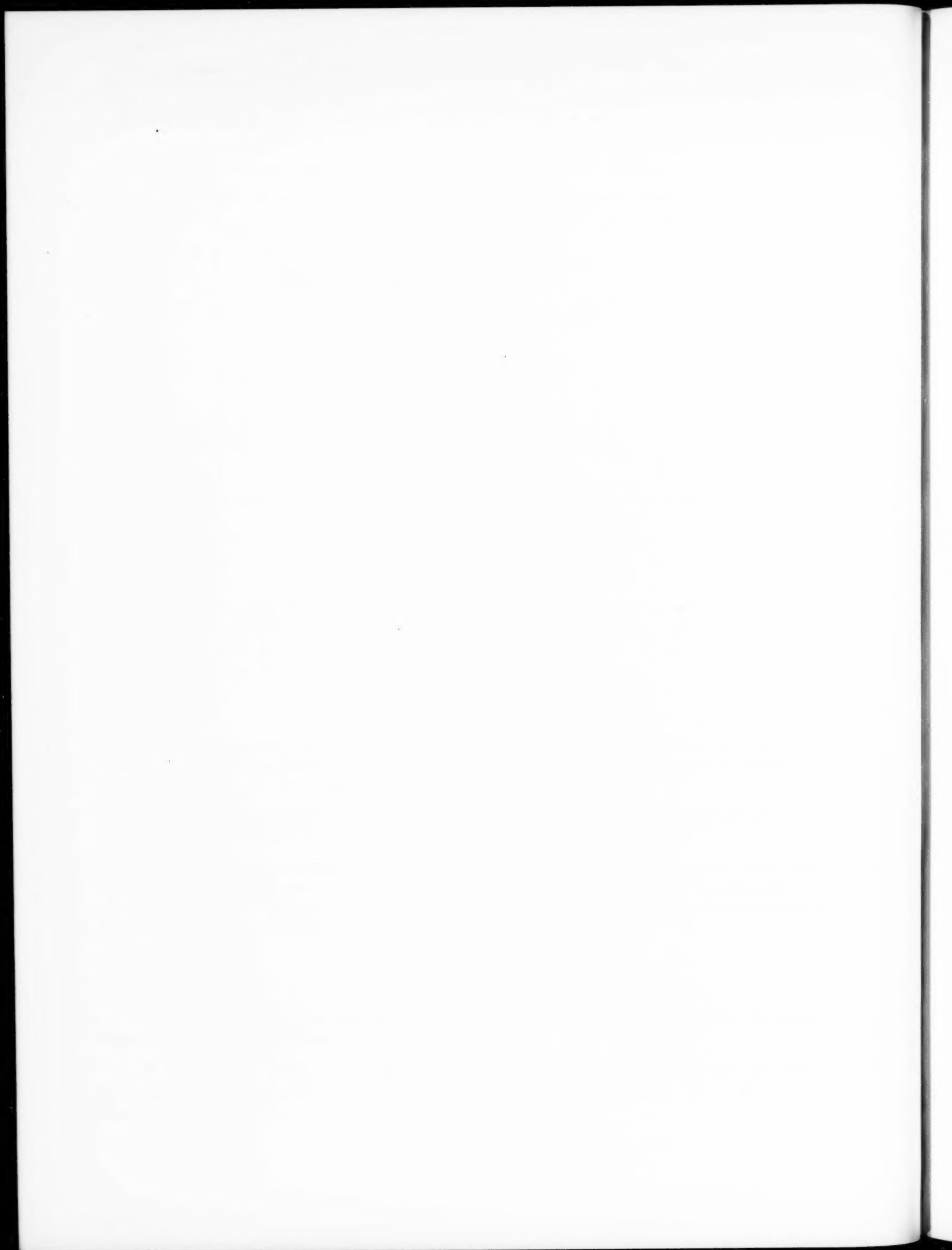
[3] Yu. V. Dolgolenko, Stability and Self-Oscillation in One Type of Pulsed Relay Automatic Control System, Engineering Symposium, Vol. 13, 1952.

[4] C. K. Chow, Contactor Servomechanisms Employing Sampled Data, Trans. of AJEE Applications and Industry March, 1954.

[5] Ya. Z. Tsypkin, Transient and Steady-State Processes in Pulse Circuits, State Power Press, 1951.

[6] Ya. Z. Tsypkin, Relay Automatic Control System Theory, Trans. Second All-Union Conference on Automatic Control Theory, Vol. 1, Acad. Sci. USSR Press, 1955.

Received July 20, 1956.



## GENERALIZATION OF THE DYNAMIC EQUATIONS FOR A COMPLEX POWER SYSTEM AND A STABILITY ANALYSIS BY ELECTRONIC COMPUTER

L. V. Tsukernik

(Kiev)

The equations for a perturbed complex power system are generalized in matrix form (the automatic excitation control applied to parallel-operated synchronous machines being also allowed for) with a view to applying them to the analysis of the stability of units. Algorithms are derived which facilitate programming the computation of the coefficients in the characteristic equation.

The logical scheme of the program for computing the boundaries of the stability region in the parameter plane electronically is given for the parameters appearing in the coefficients of the characteristic equation. The program may with advantage be used with any dynamic system for which the perturbation equation can be derived.

Current computing and mathematical analog techniques enable one to study the stabilities (vide Lyapunov) of dynamic systems with many degrees of freedom, such as complex power systems.

By power system we imply some system of synchronous machines (station equivalents) operated in parallel and connected by a grid of arbitrary form in which automatic excitation control (AEC) is applied for certain parameters and their derivatives (automatic speed control applied to the prime movers can also be allowed for).

Linearized differential equations for the perturbed motion must be set up if the stability is to be analyzed. Such equations have until recently only been derived for the simplest cases, e. g., one machine operated in parallel with a system of infinite capacity [1-5] or several machines without AEC [2, 5].

The generalized equations for the oscillations of synchronous machines derived by Kron [5] in tensor form only apply to unregulated machines. Kron only remarks that AEC can be allowed for in an analogous fashion, and does not derive the equations. AEC is also not considered in certain papers [7, 8] concerned with the choice of coordinate systems for setting up the equations for synchronous machines operated in parallel. The transfer from tensor symbolism to the real physical parameters required for practical calculations is carried out in these latter papers. This shows that even when the most convenient coordinate system is selected it is in practice impossible to obtain suitable equations for the perturbed motion of the whole system when there are two or more machines with AEC.

In 1954-1955 calculations were performed in the USSR on the stabilities of systems containing two and three stations in which automatic control was applied to two stations [9-12]. The hypotheses first formulated by Lebedev [3] were here assumed: these suppose that transients related to the stator circuit leakage inductances are neglected in the primary differential equations, and that the electromagnetic momentum of a parallel-operated synchronous unit may simultaneously be represented as functions of the relative rotor angle and the corresponding synchronous emf, transient emf and machine voltage.

$$P = f(\delta, E_d) = f(\delta, E'_d) = f(\delta, V).$$

Lebedev linearized the small deviations in the electromagnetic momentum and described them by the equations

$$\Delta P = \frac{\partial P}{\partial \delta} \Delta \delta + \frac{\partial P}{\partial E_d} \Delta E_d = \frac{\partial P}{\partial \delta} \Delta \delta + \frac{\partial P}{\partial E'_d} \Delta E'_d = \frac{\partial P}{\partial \delta} \Delta \delta + \frac{\partial P}{\partial V} \Delta V. \quad (1)$$

$(E_d = \text{const}) \quad (E'_d = \text{const}) \quad (V = \text{const})$

The partial derivatives in (1) are constants (for a given grid and operating mode) and can be computed when the appropriate primary data are provided. Thus, it will not be necessary to write out all the partial derivatives in full in deriving the perturbation equations for the system, which simplifies matters considerably.

When transferring our attention to a large power system in which several stations are regulated by the combined regulation method now commonly used with synchronous units it is convenient to generalize (1) by treating it as a system of equations for the link reactions in the system, in accordance with the concepts of theoretical mechanics. These equations relate the number of degrees of freedom to the number of independent coordinates, and can be expressed with the aid of various partial derivatives. An expedient choice of system link reaction equations is very important if the equations derived from them are to be simple and excessive labor in calculating the partial derivatives is to be avoided. The equations for a system consisting of  $n$  phaneropolar synchronous units of which  $m \leq n$  are subject to AEC, are quite convenient for this purpose [12]:

$$\Delta N_k = \sum_{i=1}^n \frac{\partial N_k}{\partial \delta_{1i}} \Delta \delta_{1i} + \sum_{i=1}^m \frac{\partial N_k}{\partial E_{Qi}} \Delta E_{Qi} \quad (N = P; E'_d; V; I; I_d) \quad (2)$$

( $k = 1, 2, \dots, n$  when  $N = P$  and  $k = 1, 2, \dots, m$  for other values of  $N$ ).

All the relative angles  $\delta_{1s} = \delta_1 - \delta_s$  are reckoned from the axis of the rotor poles in machine 1; this does not limit the generality of the analysis.

Instead of the equation in (2) for  $N = E'_d$  we can, by starting from the relation  $P_k = f(\delta_{1s}, E_{Qj}, E'_d)$ , ( $j \neq k$ ), use the following equation:

$$\Delta P_k = \sum_{i=1}^n \frac{\partial P_k}{\partial \delta_{1i}} \Delta \delta_{1i} + \sum_{j=1}^m \frac{\partial P_k}{\partial E_{Qj}} \Delta E_{Qj} + \frac{\partial P_k}{\partial E'_d} \Delta E'_d \quad (j \neq k). \quad (3)$$

The final results are the same in both cases.

The primary equations for each synchronous unit in a large power system (using combined AEC) have been given [11], together with the preferred method of combining them with the link equations to give two generalized equations (sets of equations).

1. Equations derived from d'Alembert's general dynamic equations which describe the motion of the individual rotors, which are transformed together with the link reaction equations for the electromagnetic momentum of the machine. These equations may be termed the equations for the electromechanical momenta.

$$(M_k p^2 + D_k p) \Delta \delta_k + \sum_{i=1}^n \frac{\partial P_k}{\partial \delta_{1i}} \Delta \delta_{1i} + \sum_{i=1}^m \frac{\partial P_k}{\partial E_{Qi}} \Delta E_{Qi} = 0 \quad (k = 1, 2, \dots, n). \quad (4)$$

2. Equations derived from the differential equations describing the electrical (mainly electromagnetic) transient processes in each synchronous unit, including therein the exciter and regulator, and also describing the control and feedback laws in the exciter circuits. These equations are also transformed together with the rest of the link reaction equations. This gives a set of equations which may be termed the electromagnetic process equations:

$$\dot{F}_{bk} \dot{F}_{\delta k} \Delta \delta_k + \sum_{s=2}^n (\dot{R}_{1s}^{(k)} + T_{1s}^{(k)} p) \Delta \delta_{1s} + \sum_{i=1}^m (\dot{Q}_i^{(k)} + T_i^{(k)} p) \Delta E_{Qi} - \Delta E_{Qk} = 0 \quad (5)$$

$(k = 1, 2, \dots, m).$

The symbols  $\Delta \delta_k$  and  $\Delta E_{Qi}$  used in (4) and (5) (which are expressed in relative units in operator form) denote the deviations in the rotor angle and the emf in the cross-field synchronizer resistance (these being the mechanical and electromagnetic coordinates respectively); the  $\Delta \delta_{1s} = \Delta \delta_1 - \Delta \delta_s$  are the deviations in the relative angles;  $M_k$  and  $D_k$  are the inertial constant and damping factor respectively, which also allow for the speed-torque characteristic of the prime mover;  $P_k$  is the power (taken as numerically equal to the torque);  $\dot{F}_{bk}$  and  $\dot{F}_{\delta k}$  are the transfer operators for exciter and excitation regulator as functions of  $\Delta \delta_k$  and its derivatives;  $\dot{R}_{1s}^{(k)}$  and  $\dot{Q}_i^{(k)}$  are operator expressions mainly dependent on the transfer functions of the exciter regulator for deviations in stator current ( $\dot{F}_{Ik}$ ) and voltage ( $\dot{F}_{V_k}$ ) and their respective derivatives;

$$\dot{R}_{1s}^{(k)} = \dot{F}_{bk} \left( \dot{F}_{Ik} \frac{\partial I_k}{\partial \delta_{1s}} + \dot{F}_{V_k} \frac{\partial V_k}{\partial \delta_{1s}} \right) + (x_{qk} - x_{dk}) \frac{\partial I_{dk}}{\partial \delta_{1s}}, \quad (6)$$

$$\dot{Q}_i^{(k)} = \dot{F}_{bk} \left( \dot{F}_{Ik} \frac{\partial I_k}{\partial E_{Qi}} + \dot{F}_{V_k} \frac{\partial V_k}{\partial E_{Qi}} \right) + (x_{qk} - x_{dk}) \frac{\partial I_{dk}}{\partial E_{Qi}} \quad (7)$$

(the latter terms in (6) and (7) represent the effect of the phaneropolar rotors);  $T_{1s}^{(k)}$  and  $T_i^{(k)}$  are coefficients dependent on the rotor time-constants  $T_{0k}$  and on the effect of the stator circuit on the electromagnetic processes in the rotor;

$$T_{1s}^{(k)} = T_{0k} (x_{qk} - x'_{dk}) \frac{\partial I_{dk}}{\partial \delta_{1s}}, \quad (8)$$

$$T_k^{(k)} = T_{0k} [(x_{qk} - x'_{dk}) \frac{\partial I_{dk}}{\partial E_{Qk}} - 1] = -T'_{dk}, \quad (9)$$

$$T_j^{(k)} = T_{0k} (x_{qk} - x'_{dk}) \frac{\partial I_{dk}}{\partial E_{Qj}} \quad \left( \begin{matrix} j = 1, 2, \dots, n \\ j \neq k \end{matrix} \right). \quad (10)$$

The terms in (5) which contain  $T_{1s}^{(k)}$  and  $T_j^{(k)}$  allow for the mutual components in the transient electromagnetic process, while those with  $T_k^{(k)} = -T'_{dk}$  deal with the inherent components of the transient process in a given machine.

(6) - (9) show that if  $\frac{\partial I_{dk}}{\partial \delta_{1s}}$  and  $\frac{\partial I_{dk}}{\partial E_{Qj}}$  are small (the mutual impedances in the equivalent circuit of the system being high) the last terms in (6) and (7), together with  $T_{1s}^{(k)}$  and  $T_j^{(k)}$ , may be taken as being zero, which materially simplifies the calculations.

There is no difficulty in allowing for the various steady-state load characteristics (variation of conductance with voltage and frequency) in setting up the equations from which the stability of the power system is to be analyzed. Then when setting up the equations for the perturbed motion and deriving stability criteria we can allow for the load characteristics by replacing the loads at grid points by fictitious stations [2, 5]. But the problem becomes very complicated even if only the steady-state characteristics are introduced and the motor load dynamics are neglected. The desirability of introducing such complexities in practice requires special consideration.



Matrix theory can be advantageously applied to the subsequent analysis of the power system, particularly as we have in mind programming an electronic computer.

(4) and (5) take the following matrix forms:

$$\mathbf{M}_\delta \dot{\delta} + \mathbf{M}_\epsilon \dot{\epsilon} = 0, \quad (11)$$

$$\mathbf{E}_\delta \dot{\delta} + \mathbf{E}_\epsilon \dot{\epsilon} = 0. \quad (12)$$

$\delta$  and  $\epsilon$  in (11) and (12) are the matrix columns for the mechanical and electromagnetic coordinates respectively:

$$\delta = \begin{bmatrix} \Delta \delta_1 \\ \Delta \delta_2 \\ \dots \\ \Delta \delta_n \end{bmatrix}, \quad \epsilon = \begin{bmatrix} \Delta E_{Q1} \\ \Delta E_{Q2} \\ \dots \\ \Delta E_{Qm} \end{bmatrix}, \quad (13)$$

$\mathbf{M}_\delta, \mathbf{M}_\epsilon, \mathbf{E}_\delta, \mathbf{E}_\epsilon$  are matrices derived from (4) and (5) (bearing in mind that  $\delta_{1s} = \delta_1 - \delta_s$ ):

$$\mathbf{M}_\delta = \begin{bmatrix} M_1 p^2 + D_1 p & 0 & \dots & 0 \\ 0 & M_2 p^2 + D_2 p & \dots & 0 \\ \dots & \dots & \dots & \dots \\ 0 & 0 & \dots & M_n p^2 + D_n p \end{bmatrix} -$$

$$- \begin{bmatrix} \sum_{s=2}^n \frac{\partial P_1}{\partial \delta_{1s}} \frac{\partial P_1}{\partial \delta_{12}} \dots \frac{\partial P_1}{\partial \delta_{1n}} \\ \sum_{s=2}^n \frac{\partial P_2}{\partial \delta_{1s}} \frac{\partial P_2}{\partial \delta_{12}} \dots \frac{\partial P_2}{\partial \delta_{1n}} \\ \dots \\ \sum_{s=2}^n \frac{\partial P_n}{\partial \delta_{1s}} \frac{\partial P_n}{\partial \delta_{12}} \dots \frac{\partial P_n}{\partial \delta_{1n}} \end{bmatrix} \quad (14)$$

$$\mathbf{M}_\epsilon = \begin{bmatrix} \frac{\partial P_1}{\partial E_{Q1}} \frac{\partial P_1}{\partial E_{Q2}} \dots \frac{\partial P_1}{\partial E_{Qm}} \\ \frac{\partial P_2}{\partial E_{Q1}} \frac{\partial P_2}{\partial E_{Q2}} \dots \frac{\partial P_2}{\partial E_{Qm}} \\ \dots \\ \frac{\partial P_n}{\partial E_{Q1}} \frac{\partial P_n}{\partial E_{Q2}} \dots \frac{\partial P_n}{\partial E_{Qm}} \end{bmatrix} \quad (15)$$



$$\begin{aligned}
\mathbf{E}_\delta = & \begin{vmatrix} \dot{F}_{b1}\dot{F}_{\delta 1} & 0 & \dots & 0 \\ 0 & \dot{F}_{b2}\dot{F}_{\delta 2} & \dots & 0 \\ \dots & \dots & \dots & \dots \\ 0 & 0 & \dots & \dot{F}_{bm}\dot{F}_{\delta m} \end{vmatrix} - \\
& - \begin{vmatrix} -\sum_{s=2}^n (\dot{R}_{1s}^{(1)} + T_{1s}^{(1)}p) & \dot{R}_{12}^{(1)} + T_{12}^{(1)}p & \dots & \dot{R}_{1n}^{(1)} + T_{1n}^{(1)}p \\ -\sum_{s=2}^n (\dot{R}_{1s}^{(2)} + T_{1s}^{(2)}p) & \dot{R}_{12}^{(2)} + T_{12}^{(2)}p & \dots & \dot{R}_{1n}^{(2)} + T_{1n}^{(2)}p \\ \dots & \dots & \dots & \dots \\ -\sum_{s=2}^n (\dot{R}_{1s}^{(m)} + T_{1s}^{(m)}p) & \dot{R}_{12}^{(m)} + T_{12}^{(m)}p & \dots & \dot{R}_{1n}^{(m)} + T_{1n}^{(m)}p \end{vmatrix} \quad (16) \\
\mathbf{E}_\epsilon = & - \begin{vmatrix} 1 & 0 & \dots & 0 \\ 0 & 1 & \dots & 0 \\ \dots & \dots & \dots & \dots \\ 0 & 0 & \dots & 1 \end{vmatrix} + \begin{vmatrix} \dot{Q}_1^{(1)} + T_1^{(1)}p & \dot{Q}_2^{(1)} + T_2^{(1)}p & \dots & \dot{Q}_m^{(1)} + T_m^{(1)}p \\ \dot{Q}_1^{(2)} + T_1^{(2)}p & \dot{Q}_2^{(2)} + T_2^{(2)}p & \dots & \dot{Q}_m^{(2)} + T_m^{(2)}p \\ \dots & \dots & \dots & \dots \\ \dot{Q}_1^{(m)} + T_1^{(m)}p & \dot{Q}_2^{(m)} + T_2^{(m)}p & \dots & \dot{Q}_m^{(m)} + T_m^{(m)}p \end{vmatrix} \quad (17)
\end{aligned}$$

$\mathbf{M}_\delta$  and  $\mathbf{E}_\delta$  are square matrices of  $(n \times n)$  and  $(m \times m)$  types respectively; the first index denotes the number of lines and the second the number of columns.  $\mathbf{M}_\epsilon$  and  $\mathbf{E}_\epsilon$  are rectangular matrices of types  $(n \times m)$  and  $(m \times n)$ .

When automatic regulators are absent and electromagnetic transients in the machines are neglected, and supposing that  $\Delta E_{Qi} = \Delta E_{di} = 0$ , we get:

$$\mathbf{M}_\delta \delta = 0, \quad (18)$$

i.e., the system as regards its electromagnetic coordinates is described by the well-known equations derived on the assumption of constant exciter current in all machines [5].

By analogy  $\Delta \delta_i = 0$  (which corresponds to the assumption of infinitely great moments of inertia for all machines) the mechanical coordinate system is described by the equations

$$\mathbf{E}_\epsilon \epsilon = 0. \quad (19)$$

Solving (12) for  $\epsilon$  and substituting this latter in (11) we get

$$(\mathbf{M}_\delta - \mathbf{M}_\epsilon \mathbf{E}_\epsilon^{-1} \mathbf{E}_\delta) \delta = 0. \quad (20)$$

In the general case where the electromagnetic transients are not present at all stations ( $n > m$ ) it is not possible to eliminate all the  $\delta$  coordinates from (11) and (12) in an analogous fashion.

The characteristic equation of the system is obtained by expanding the determinant of order  $\underline{n}$ :

$$|\mathbf{M}_\delta - \mathbf{M}_\epsilon \mathbf{E}_\epsilon^{-1} \mathbf{E}_\delta| = 0. \quad (21)$$

The inverse matrix  $\mathbf{E}_\epsilon^{-1}$  is

$$E_{\epsilon}^{-1} = \frac{\tilde{E}_{\epsilon}}{|E_{\epsilon}|}, \quad (22)$$

where  $\tilde{E}_{\epsilon}$  is the so-called mutual matrix, in which the elements are the algebraic complements of the transposed matrix  $E_{\epsilon}$ .

Since, according to (17), derivatives of the transfer functions of exciter and regulator appear in the elements of  $E_{\epsilon}$  laborious calculations are required to transform it.

To avoid a difficult transformation of  $E_{\epsilon}$  we use compound (adjoint) matrices. (11) and (12) can be combined in the form

$$L\gamma = 0, \quad (23)$$

where  $L$  is a compound square matrix of type  $(m+n) \times (m+n)$ , and  $\gamma$  is a compound matrix-column in generalized coordinates:

$$L = \left\| \begin{array}{c|c} M_{\delta} & M_{\epsilon} \\ \hline (n \times n) & (n \times m) \\ E_{\delta} & E_{\epsilon} \\ \hline (m \times n) & (m \times m) \end{array} \right\|, \quad \gamma = \left\| \begin{array}{c} \delta \\ \hline (n \times 1) \\ \epsilon \\ \hline (m \times 1) \end{array} \right\|, \quad (24)$$

Separate out of the first lines of  $M_{\delta}$  and  $M_{\epsilon}$  as the submatrices  $M_1$  of type  $(m \times n)$  and  $M_2$  of type  $(m \times m)$ . Then  $L$  and  $\gamma$  can be thrown into the following form:

$$L = \left\| \begin{array}{c|c} M_1 & M_2 \\ \hline (m \times n) & (m \times m) \\ E_1 & E_2 \\ \hline (n \times n) & (n \times m) \end{array} \right\|, \quad \gamma = \left\| \begin{array}{c} \gamma_1 \\ \hline (m \times 1) \\ \gamma_2 \\ \hline (n \times 1) \end{array} \right\|. \quad (25)$$

The characteristic equation of the system is found from the determinant

$$|E_1 - E_2 M_2^{-1} M_1| = 0. \quad (26)$$

(26) is a very convenient algorithm for programming a computer to calculate the coefficients in the characteristic equation, since the elements of  $M_2$  are numbers.

In the particular case where the determinant of  $M_2$  is zero and it cannot be transformed,  $L$  can be divided into other submatrices:

$$L = \left\| \begin{array}{c|c} M_a & M_b \\ \hline (m \times m) & (m \times n) \\ E_a & E_b \\ \hline (n \times m) & (n \times n) \end{array} \right\|, \quad \gamma = \left\| \begin{array}{c} \gamma_1 \\ \hline (m \times 1) \\ \gamma_2 \\ \hline (n \times 1) \end{array} \right\|. \quad (27)$$

The characteristic equation then takes a structure analogous to that of (26):

$$|E_b - E_a M_a^{-1} M_b| = 0. \quad (28)$$

It is usual to study the stability against relative displacement of stations in a power system. When there are two or more stations the number of such degrees of freedom is  $n-1$ ; hence the order of the characteristic determinant (26) can be reduced by one by passing from  $n$  coordinates for the absolute angles  $\Delta \delta_k$  to  $(n-1)$  independent coordinates for the relative angles [11].

This transformation can sometimes be conveniently performed on a hand machine, the reduced determinant order then greatly facilitating expansion. For programming computers it is more important to retain the comparatively simple structure of (26). When computations are performed with this algorithm the free term in the characteristic equation must be zero, thus reducing the order of the equation by one; this also serves to check the correctness of the calculation.

The Appendix gives an example of setting-up the characteristic determinant (26) for a system of four equivalent units (stations) with AEC applied to two. This hypothetical scheme enables one to analyze a number of questions related to the choice of AEC design parameters for generators and synchronous long-range transmission compensators in a unified power system.

Naturally the determination of the coefficients in the characteristic equation is only a preparatory step. But the importance and difficulty of this stage make it very desirable to use a computer. One difficulty in programming such a problem lies in the fact that polynomials in  $p$  enter into the expanded determinant [e.g., from (26)] as well as pure numbers, while the coefficients in the polynomial may contain both numbers and parameter symbols (e.g., two parameters defining a plane within which it is sought to define the region of stability).

The stability is analyzed by computing certain criteria (e.g., those of Rothe-Hurewitz or Mikhailov-Nyquist) and by delineating the stability region in the parameter plane (e.g., Neimark's D-analysis, or other methods). The Institutes of Electrical Engineering and Mathematics of the Academy of Sciences of the Ukrainian SSR have used computers very efficiently for this purpose. As would have been expected the most convenient method is to compute Rothe's criterion because the system is recurrent and defines the boundary of the stability region directly.

The basic principles used in programming this problem which are applicable to any dynamic system may be given in the following form:

- a) the data supplied to the machine are the coefficients of the characteristic equation, represented as functions of two parameters (e.g., the excitation control coefficients for the generators).
- b) the parameters are successively given small increments during the calculation. Rothe's criterion is computed continuously for each pair of values.
- c) the machine automatically follows the changes in sign of the criterion. The results are presented as parameter pairs for the ends of the range over which the sign changes. These values are the limiting coordinates between which the stability boundary lies. The arrangement of stable and unstable regions relative to the boundary are found directly by calculating the criterion at any point.

The computation of points bounding the stability region in the two-parameter plane ( $k'$  and  $k''$ ) is shown schematically in the figure (p. 58).

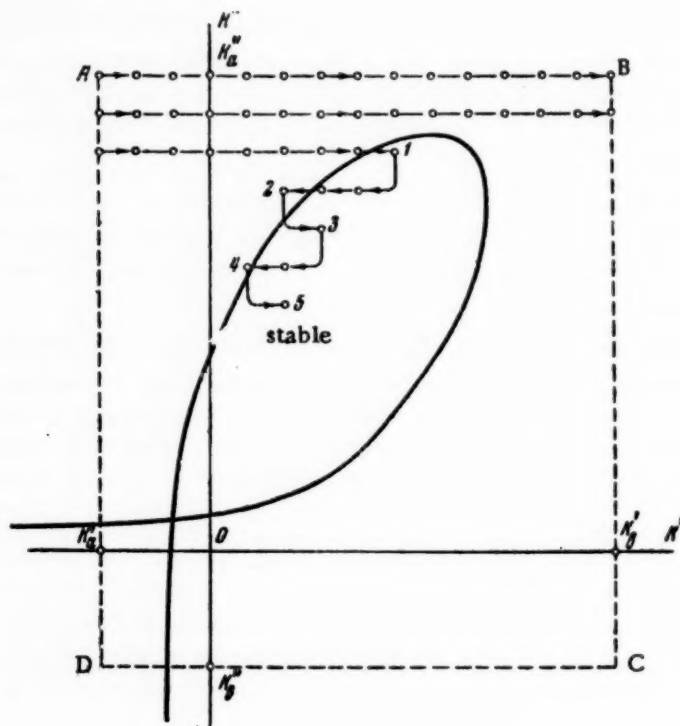
First of all the extreme values of  $k'$  and  $k''$  are computed — these define a rectangle within which the boundary of the stability region lies. General arguments bearing on the signs and magnitudes of  $k'_a$ ,  $k'_b$  and  $k''_a$ ,  $k''_b$  are available — if not they are assumed arbitrarily.

Possible restrictions on  $k'$  and  $k''$  arising from the condition that all the coefficients in the characteristic equation must be positive are simultaneously incorporated.

The pitch of the intervals on the  $k'$  and  $k''$  axes is then selected.

An arbitrary starting-point can be used (e.g., A) — the machine calculates the criterion and remembers the result without giving any external reading (e.g., without printing). A step is then taken along the  $k'$  axis. The calculation is again performed, and the result compared with the previous one. If the sign is unchanged a fresh calculation is performed, etc.

If the sign changes, i.e., if the boundary of the stability region is intersected, the machine prints the coordinates of the point (the values of  $k'$  and  $k''$ ).



The machine then begins to follow the boundary automatically. It takes a step along the axis perpendicular to the first and computes the criterion again, working in the reverse direction without printing until the sign changes. The coordinates are printed when the interval within which the boundary lies is located. The calculation then proceeds as before. If one of the limits to  $k'$  is reached without a change of sign the machine begins to work along the same direction again having taken one step along AD (see figure). If the boundary is not located the pitch can be reduced in case the stability region lies inside a rectangle with sides equal to the initial pitches.

By assembling pairs of readings for planes containing the stability region boundary, and successively altering the other parameters, an assembly of planes lying in the stability region can be collected from which the problem can be very completely analyzed.

Power systems represented by three equivalent stations in which the characteristic equations cover ten orders of magnitude have been examined at the Institute and sample calculations performed to derive stability statistics. AEC applied to one or two of the distant generators or to an intermediate synchronous compensator has been considered. The main regulation was assumed to be against current and voltage deviations, with additional control either on the first and second current derivatives or on the slip and acceleration. A series of stability regions in the planes of either regulation by current and angle derivatives (slip and acceleration) or regulation against deviations in current and voltage were obtained. The initial modes ( $P_0 = 0, 0.5, 1.0, 1.1$ ) and system circuit were also varied (presence and absence of longitudinal compensation on long-distance lines, etc.).

The results were in fairly good agreement with analog studies made on three systems for which experimental data were available.

All calculations were carried out using the above equations for the perturbed motion of a power system. The principal participants in the calculations were: from the Institute of Electrical Technology - N. A. Kachanova

$$\begin{array}{c}
\begin{array}{c}
M^{(1)}(p) + \sum_{s=2}^4 \frac{\partial P_1}{\partial \delta_{1s}} \\
\hline
\sum_{s=2}^4 \frac{\partial P_2}{\partial \delta_{1s}} M^{(s)}(p) - \frac{\partial P_2}{\partial \delta_{13}} \\
\hline
\sum_{s=2}^4 \frac{\partial P_3}{\partial \delta_{1s}} M^{(s)}(p) - \frac{\partial P_3}{\partial \delta_{13}} \\
\hline
\sum_{s=2}^4 \frac{\partial P_4}{\partial \delta_{1s}} M^{(s)}(p) - \frac{\partial P_4}{\partial \delta_{13}} \\
\hline
\sum_{s=2}^4 E_{1s}^{(3)}(p) \\
\hline
\sum_{s=2}^4 E_{1s}^{(4)}(p)
\end{array}
\quad
\begin{array}{c}
-\frac{\partial P_1}{\partial \delta_{13}} \\
\hline
M^{(s)}(p) - \frac{\partial P_2}{\partial \delta_{13}} \\
\hline
M^{(s)}(p) - \frac{\partial P_3}{\partial \delta_{13}} \\
\hline
M^{(s)}(p) - \frac{\partial P_4}{\partial \delta_{13}} \\
\hline
E_{13}^{(3)}(p) - E_{13}^{(3)}(p) \\
\hline
E_{13}^{(4)}(p) - E_{13}^{(4)}(p)
\end{array}
\quad
\begin{array}{c}
-\frac{\partial P_1}{\partial \delta_{14}} \\
\hline
-\frac{\partial P_2}{\partial \delta_{13}} \\
\hline
-\frac{\partial P_3}{\partial \delta_{14}} \\
\hline
M^{(4)}(p) - \frac{\partial P_4}{\partial \delta_{14}} \\
\hline
-E_{13}^{(3)}(p) - E_{13}^{(3)}(p) \\
\hline
-E_{13}^{(4)}(p) - E_{13}^{(4)}(p)
\end{array}
\quad
\begin{array}{c}
\frac{\partial P_1}{\partial E_{Q4}} \\
\hline
\frac{\partial P_2}{\partial E_{Q3}} \\
\hline
\frac{\partial P_3}{\partial E_{Q4}} \\
\hline
\frac{\partial P_4}{\partial E_{Q3}} \\
\hline
E_3^{(3)}(p) - T^{(3)}(p) E_4^{(3)}(p) \\
\hline
E_3^{(4)}(p) - T^{(4)}(p)
\end{array}
\end{array}
\quad (A.3)$$

(A.6)

### Symbols

$$M^{(k)}(p) = M_k p^2 + D_k p \quad (k=1, 2, 3, 4) \quad (A.4)$$

$$E^{(l)}(p) = (c_l^* p^2 + c_l' p) (1 + T_{1l} p) (1 + T_{vl} p) \quad (A.5)$$

$$E_{1s}^{(l)}(p) = (k_l^* p^2 + k_l' p + k_l) (1 + T_{sl} p) (1 + T_{vl} p) \frac{\partial I_l}{\partial \delta_{1s}} + (b_l^* p^2 + b_l' p - b_l) (1 + T_{sl} p) (1 + T_{vl} p) \frac{\partial V_l}{\partial \delta_{1s}} + [(x_{ql} - x_{dl}) \frac{\partial I_{dl}}{\partial \delta_{1s}} + T_{1s}^{(l)} p] T^{(l)}(p)$$

(A.7)

$$E_1^{(l)}(p) = (k_1^* p^2 + k_1' p + k_1) (1 + T_{sl} p) (1 + T_{vl} p) \frac{\partial I_l}{\partial E_{Ql}} + (b_1^* p^2 + b_1' p - b_1) (1 + T_{sl} p) (1 + T_{vl} p) \frac{\partial V_l}{\partial E_{Ql}} + [(x_{ql} - x_{dl}) \frac{\partial I_{dl}}{\partial E_{Ql}} + T_1^{(l)} p] T^{(l)}(p) \quad (l=3, 4; s=2, 3, 4; i=3, 4)$$

(A.8)



and L. N. Dashevsky; from the Institute of Mathematics — E. L. Yushchenko and V. S. Korolyuk; the latter programmed the computer.

## APPENDIX

### Derivation of the Characteristic Equation for a Power System Consisting of Four Stations, in Two of Which AEC is Used

AEC is supposed applied in stations 3 and 4, the angles being taken as relative to station 1. The regulated station parameters will be indicated by the indices  $l = 3, 4$ , and  $i = 3, 4$ , of the previously used indices  $1, 2, \dots, m$ .

For generality we assume that AEC is applied for current and voltage deviations, for the first and second derivatives of these deviations, and for rotor slip and acceleration relative to an axis rotating with the initial synchronous speed. In the general case the parameters controlled may be different in each circuit. If the regulators are identical the expressions are much simplified.

Thus, the transfer functions  $\dot{F} = W(p)$  for the AEC may be put in the following form:

$$\dot{F}_{il} = \frac{k_l p^2 + k_l' p + k_l}{1 + T_{il} p}, \quad \dot{F}_{vl} = \frac{b_l p^2 + b_l' p - b_l}{1 + T_{vl} p}; \quad \dot{F}_{sl} = \frac{c_l p^2 + c_l' p}{1 + T_{sl} p} \quad (l = 3, 4). \quad (A.1)$$

The exciter transfer functions, represented as first-order inertial links in the equivalent circuit, are

$$\dot{F}_{bl} = \frac{1}{1 + T_{bl} p}. \quad (A.2)$$

(A.1) and (A.2) are substituted into (6) and (7), supposing that  $k = l$ , and then the expressions obtained for  $\dot{R}_{is}^{(l)}$  and  $\dot{Q}_i^{(l)}$  ( $l = 3, 4$ ;  $s = 2, 3, 4$ ;  $i = 3, 4$ ) are substituted into (16) and (17) for  $\dot{E}_\delta$  and  $\dot{E}_\epsilon$  (supposing also that  $n = 4$ ).

All elements of these matrices can be referred to a general denominator, denoted in future by (A.6). The denominator can then be contracted, since  $\dot{E}_\delta$  and  $\dot{E}_\epsilon$  are the matrix coefficients of (12).

Then the compound matrix  $L$  can, from (24), be written in the form of a table (A.3) in which  $M_\delta$  and  $M_\epsilon$  enter directly from (14) and (15), remembering that the partial derivatives with respect to emf may be taken only with respect to  $E_{Q3}$  and  $E_{Q4}$ .

(A.3) gives the submatrices  $M_1, M_2, E_1$  and  $E_2$  separated in accordance with (25).

For convenience we also give (A.4) - (A.8) for the symbols, which, taken together with (8) - (9) can be used to contract the elements of (A.3).

The formulas for the partial derivatives have been given [12].

The determinant of  $M_2$  is denoted by the scalar  $\underline{a}$ , as its elements are only numbers.

The mutual matrix  $\tilde{M}_2$  is

$$\tilde{M}_2 = \left\| \begin{array}{cc} \frac{\partial P_2}{\partial F_{Q4}} & - \frac{\partial P_1}{\partial E_{Q4}} \\ - \frac{\partial P_2}{\partial F_{Q3}} & \frac{\partial P_1}{\partial E_{Q3}} \end{array} \right\| \quad (A.9)$$

Then the matrix characteristic Equation (26), after contraction with  $\underline{a}$ , takes the form:

$$a M_1 - M_2 \bar{M}_2 M_1 = 0. \quad (A.10)$$

(A.10) is a convenient algorithm for computing the coefficients in the characteristic equation after replacing the appropriate parts of the algebraic expressions in (A.3) by numbers.

### SUMMARY

The stabilities of complex regulated dynamic systems can be efficiently analyzed by using a computer to construct a series of boundaries to the stability region in the various parameter planes.

The generalized perturbed motion equations are of great value in a form which enables one to obtain an algorithm convenient for programming the calculation of coefficients in the characteristic equation.

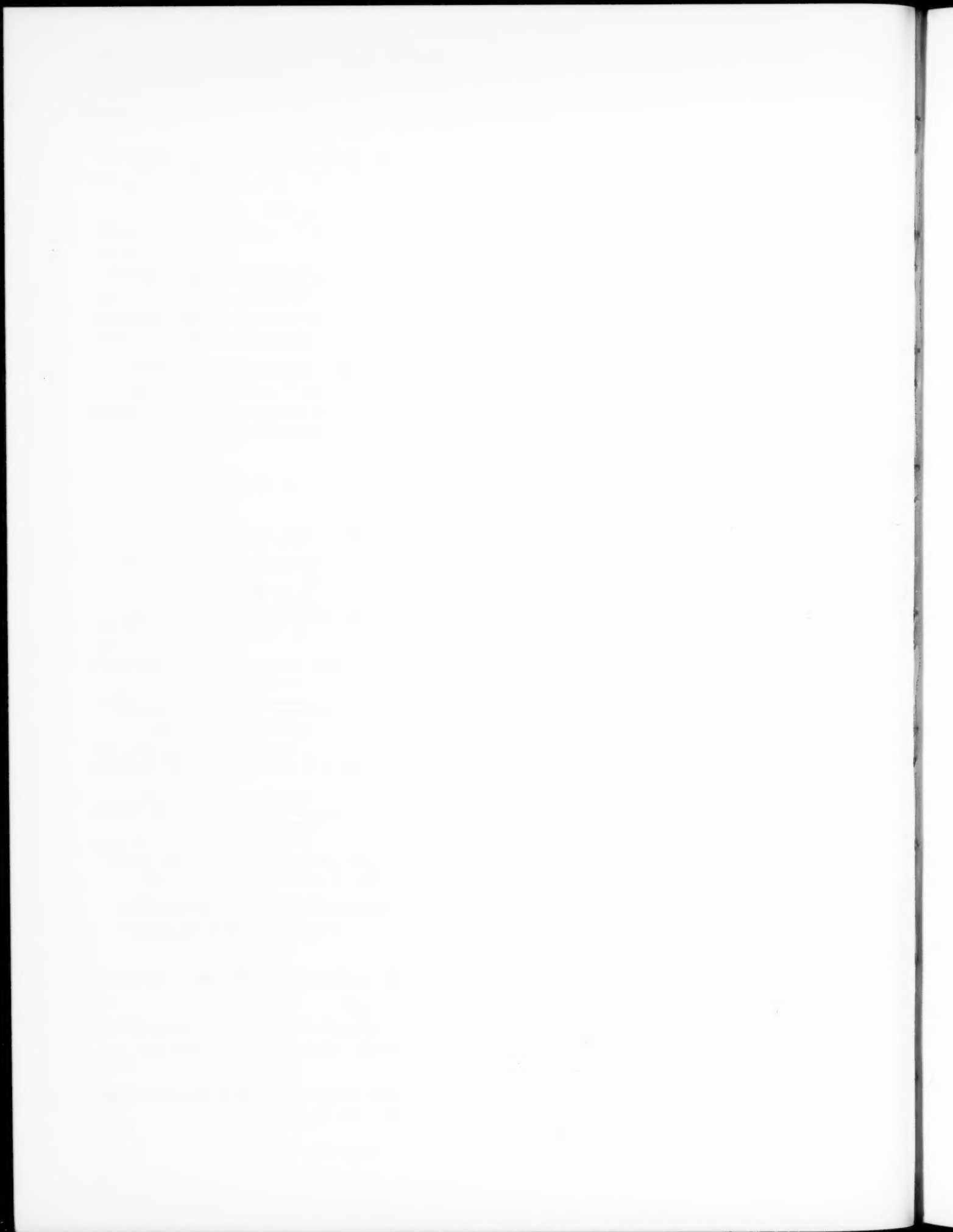
Such an algorithm may be obtained for a complex power system containing synchronous units with automatic excitation control operated in parallel by generalizing the equations of motion in matrix form. This generalization facilitates the analysis much more than does the use of the known equations for the separate elements and links in the system. There is no need to use tensor analysis for generalizing the equations of motion of a perturbed power system.

### LITERATURE CITED

- [1] A. A. Gorev, *Transients in Synchronous Machines*, State Electrical Press, 1950.
- [2] A. A. Gorev, *The Steady-State Stability of Systems with Two Synchronous Units Working into a Common Load of Known Characteristics*, *Trans. Leningrad Polytech. Inst.*, No. 1, 1954.
- [3] S. A. Lebedev, *Study of Artificial Stability*, Symposium of the All-Union Power Institute, State Electrical Press, 1940.
- [4] S. A. Lebedev, *Artificial Stability in Synchronous Machines*, Report to the International Conference on Large Electricity Grids, State Electrical Press, 1948.
- [5] P. S. Zhdanov, *The Steady-State Stability of Complex Electrical Systems*, State Electrical Press, 1940.
- [6] G. Kron, *A New Theory of Hunting*, *Trans. AIEE*, Vol. 71, 3, 1952; also G. Kron, *Use of Tensor Analysis in Electrical Engineering*, State Electrical Press, 1955.
- [7] S. V. Strakhov, *The Choice of Coordinates for Predicting Transients in Synchronous Machine Circuits*, *Electricity*, No. 6, 1954.
- [8] W. G. Heffron, G. M. Rosenberry, and F. S. Rothe, *Generalized Hunting Equations of Power System*, *Trans. AIEE*, Vol. 71, 3, 1952; also W. G. Heffron, Discussion in [6].
- [9] M. V. Meerov, *Some Design Principles for Multicircuit Systems Containing Controlled Quantities With High Degrees of Steady-State Accuracy*, *Trans. Second All-Union Conference on the Theory of Automatic Control*, Vol. 1, Acad. Sci. Press, 1955.
- [10] M. N. Rozanov, *The Analysis of Stability in Complex Automatically Controlled Systems*, Symposium of Contributions from the Moscow Power Institute, No. 20, 1956.
- [11] L. V. Tsukernik, *Differential Equations for the Perturbed Motion of a Complex Power System for Use in the Analysis of Steady-State Stability*, *Bull. Tech.-Sciences Section, Acad. Sci. USSR, Tech. Sci. Section*, No. 3, 1956.
- [12] L. V. Tsukernik, *The Analysis of Stability in Complex Power Systems*, Symposium of Contributions from the Institute of Electrical Engineering, Acad. Sci. of the Ukrainian SSR, No. 13, 1956.

Received May 14, 1956.





## TRANSIENTS IN CONTACTOR SYSTEMS

Ya. I. Mekler

(Moscow)

Circuit disturbances due to adding zero and multiplying by one are considered, and a method of avoiding these disturbances and producing safe circuits is given. This method enables one to transform circuits requiring make-before-break (or break-before-make) contacts into normal ones free from such requirements.

### 1. Aspects of Adding Zero and Multiplying by One

Certain transformations are required in order to transform electrical circuits with the object of simplifying analytic expressions for their operations. Adding zero and multiplying by one are among such transformations; these operations should not change the analytic expressions for the circuit, and hence should not alter their operation.

It has frequently been observed in practice that such operations do in fact alter the relations between circuits, and disturb their operation.

Contact circuit theory shows [1] that the product of mutually exclusive contacts, e. g.,  $x\bar{x}$ , is zero, the sum  $x + \bar{x}$  being unity.\* But this relation is only correct if no transient operations occur in the circuit [1, 2].

Transient operations can sometimes be neglected, e. g.:

- 1) if the intermediate or output relays in multistage circuits are unaffected by short-period circuit interruptions or brief energization when the preceeding relay in the chain changes its state of operation;
- 2) when single-stage systems are used.

Transient regimes must be considered in relation to the convenience of current multistage circuits. The above relations will only always be correct when the following conditions are observed:

- 1)  $x\bar{x} = 0$  if the opening and closing contacts do not overlap;
- 2)  $x + \bar{x} = 1$  if the opening and closing contacts overlap, i.e., are bridging contacts.

Hence the transpositions introduced by inserting zero or one into the analytic expressions give rise to additional conditions to be satisfied by the contacts during transient operations.

Both bridging and normal contacts are available in telephone relays. The above conditions can also be disturbed if the contacts are maladjusted. It is essentially impossible to produce bridging contacts in the so-called "precision" relays.\*\*

\* This is also true for entire expressions relating to the operation of a contact group.

\*\* Use of bridge contacts, e. g., with RE or EP relays, changes the normal pressure and is not recommended.

The object of the present communication is to indicate when circuit changes involving zero and one disturb the operation and demand special contact designs, and also to give a method of designing circuits which avoid these disturbances, no matter whether normal or bridging contacts are used.

## 2. Sequential Operation of Make and Break Contacts. $x \bar{x} = 0$

The conditions for an element  $X$  to operate may be written in general form as:

$$f = \Sigma F_1 + x \Sigma \bar{F}_2 = F_{1_1} + F_{1_2} + \dots + F_{1_n} + x \bar{F}_{2_1} \bar{F}_{2_2} \dots \bar{F}_{2_n}, \quad (1)$$

where  $F_1$  is the state of the circuit elements preceding operation of  $X$ ,  $F_2$  being the same, but preceding release of  $X$ .

The indices 1, 2, ...,  $n$  in  $F_1 (F_{1_1}, F_{1_2}, \dots, F_{1_n})$  and in  $F_2 (F_{2_1}, F_{2_2}, \dots, F_{2_n})$  indicate 1st, 2nd, ...,  $n$ th times of operation of  $X$  during the cycle.

(1) presupposes that  $X$  operates  $n$  times.

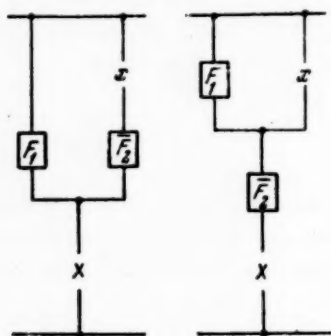


Fig. 1

The case most frequently encountered in practice is where  $X$  operates once during the cycle. The expression for its operations then becomes simpler, reducing to the expression

$$f = F_1 + x \bar{F}_2 \quad (2)$$

or, for instance:

$$f = (F_1 + x) \bar{F}_2. \quad (2')$$

It is convenient to consider (2), in which  $X$  operates once, for simplicity.

The results will also be correct when  $X$  operates repeatedly.

The circuits corresponding to (2) and (2') are given in Fig. 1.

We shall consider (2).

The following symbolism will be used.

$\underline{a}$  is the state of a circuit element which switches on the main element  $X$ .

$\underline{a}'$  is the state of a circuit element which switches off the main element  $X$ .

$\underline{y}$  is the 1st state of the circuit elements which change position once during the period that  $X$  changes its position:  $y = y_1 y_2 \dots y_n$  where  $y_1, y_2, \dots, y_n$  are separate circuit elements of category  $Y$ , arranged in order of increasing index in the switch-in table.

$\underline{y}'$  is the 2nd state of these elements after  $X$  has changed its state:  $y' = \bar{y}_1 \bar{y}_2 \dots \bar{y}_n$ .

$x_1, \dots, x_n$  are other circuit elements;  $X_1, X_2, X_3, \dots, X_n$  are the separate elements in this category arranged in order of increasing index in the switch-in table.

The sign  $\sim$  denotes that the circuit element (contact) can be of either make or break type.

(1) can be put in the following form:

$$\begin{aligned}
 f_X &= \tilde{a}\tilde{y}_1 \dots \tilde{y}_n \tilde{x}_1 \tilde{x}_2 \dots \tilde{x}_n + x \overline{\tilde{a}'\tilde{y}'\tilde{x}_1\tilde{x}_2 \dots \tilde{x}_n} = \\
 &= \tilde{a}\tilde{y}_1 \dots \tilde{y}_n \tilde{x}_1 \tilde{x}_2 \dots \tilde{x}_n + x (\tilde{a}' + \tilde{y}' + \tilde{x}_1 + \tilde{x}_2 + \dots + \tilde{x}_n) = \\
 &= \tilde{a}\tilde{y}_1 \dots \tilde{y}_n \tilde{x}_1 \tilde{x}_2 \dots \tilde{x}_n + x (\tilde{a}' + \tilde{y}_n + \tilde{x}_1 + \tilde{x}_2 + \dots + \tilde{x}_n). *
 \end{aligned} \tag{3}$$

The corresponding circuit is given in Fig. 2.

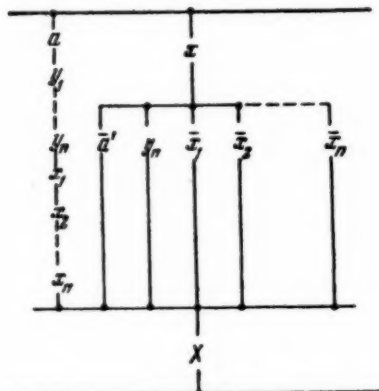


Fig. 2

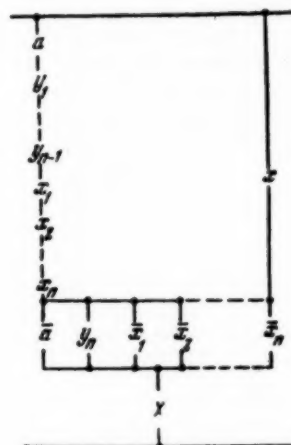


Fig. 3

(3) can be transformed to reduce the number of contacts. If  $a = a'$  then

$$\begin{aligned}
 f_X &= \tilde{a}\tilde{y}_1 \dots \tilde{y}_n \tilde{x}_1 \tilde{x}_2 \dots \tilde{x}_n + x (\tilde{a} + \tilde{y}_n + \tilde{x}_1 + \tilde{x}_2 + \dots + \tilde{x}_n) = \\
 &= \tilde{a}\tilde{y}_1 \dots \tilde{y}_n \tilde{x}_1 \tilde{x}_2 \dots \tilde{x}_n + \tilde{a}\tilde{y}_1 \dots \tilde{y}_{n-1} \tilde{x}_1 \tilde{x}_2 \dots \tilde{x}_n \tilde{a} + \tilde{a}\tilde{y}_1 \dots \tilde{y}_{n-1} \tilde{x}_1 \tilde{x}_2 \dots \tilde{x}_n \tilde{x}_1 + \\
 &\quad + \tilde{a}\tilde{y}_1 \dots \tilde{y}_{n-1} \tilde{x}_1 \tilde{x}_2 \dots \tilde{x}_n \tilde{x}_2 + \dots + \tilde{a}\tilde{y}_1 \dots \tilde{y}_{n-1} \tilde{x}_1 \tilde{x}_2 \dots \tilde{x}_n \tilde{x}_n + \\
 &\quad + x (\tilde{a} + \tilde{y}_n + \tilde{x}_1 + \tilde{x}_2 + \dots + \tilde{x}_n) = \\
 &= (\tilde{a}\tilde{y}_1 \dots \tilde{y}_{n-1} \tilde{x}_1 \tilde{x}_2 \dots \tilde{x}_n + x) (\tilde{a} + \tilde{y}_n + \tilde{x}_1 + \tilde{x}_2 + \dots + \tilde{x}_n).
 \end{aligned} \tag{4}$$

The corresponding circuit is given in Fig. 3.

The following terms have been added for transformation purposes:

$$\begin{aligned}
 &\tilde{a}\tilde{y}_1 \dots \tilde{y}_{n-1} \tilde{x}_1 \tilde{x}_2 \dots \tilde{x}_n \tilde{a}, \tilde{a}\tilde{y}_1 \dots \tilde{y}_{n-1} \tilde{x}_1 \tilde{x}_2 \dots \tilde{x}_n \tilde{x}_1, \\
 &\tilde{a}\tilde{y}_1 \dots \tilde{y}_{n-1} \tilde{x}_1 \tilde{x}_2 \dots \tilde{x}_n \tilde{x}_2, \dots, \tilde{a}\tilde{y}_1 \dots \tilde{y}_{n-1} \tilde{x}_1 \tilde{x}_2 \dots \tilde{x}_n \tilde{x}_n,
 \end{aligned}$$

these being zero.

\* The author has shown that if the number of elements in category Y is greater than one, only  $y_n$  remains in the hold-on circuits, this element being the last in the cut-in table sequence.

The addition of such terms should not be reflected in the circuit operations. Analysis shows that for this to be so  $\underline{a}$  and  $\bar{a}$  must not overlap if the circuits of Figs. 2 and 3 are to be identical.

This condition, which is not present in Fig. 2, enters because  $\bar{a} \bar{y}_1 \dots \bar{y}_{n-1} \bar{x}_1 \bar{x}_2 \dots \bar{x}_n \bar{a} = 0$  was added to (4).

If  $\underline{a}$  and  $\bar{a}$  are bridge-type contacts or overlap because of faulty adjustment a false pulse may cause X to operate.

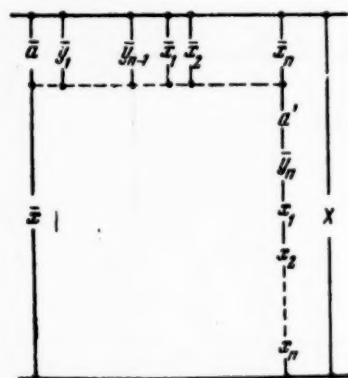


Fig. 4

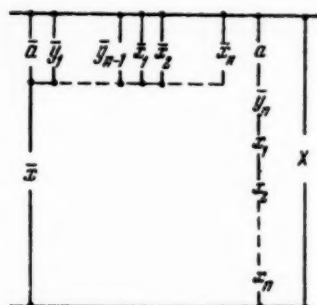


Fig. 5

Thus, if zero terms are added to the analytic expression, an extra condition is applicable to the circuit operation; mutually exclusive contacts must not overlap.

If we invert (3) and (4) they can be put in the form

$$f = (\bar{a} + \bar{y}_1 + \dots + \bar{y}_{n-1} + \bar{x}_1 + \bar{x}_2 + \dots + \bar{x}_n) (\bar{x} + \bar{a} \bar{y}_1 \bar{y}_2 \dots \bar{y}_n) + X, \quad (5)$$

$$f = (\bar{a} + \bar{y}_1 + \dots + \bar{y}_{n-1} + \bar{x}_1 + \bar{x}_2 + \dots + \bar{x}_n) \bar{x} + \bar{a} \bar{y}_1 \bar{y}_2 \dots \bar{y}_n + X. \quad (6)$$

The corresponding circuits are given in Figs. 4 and 5.

oper. stage	0	1	2	3	4	5	6	7	8	9	10	11	12	13	14	15	16	17	18	19	20
circuit elements state	-a	+a	-a	+a	-a	+a	-a	+a	-a	+a	-a	+a	-a	+a	-a	+a	-a	+a	-a	+a	-a
-x1																					
-x2																					
-x3																					
-x4																					
-x5																					
-x6																					
-x7																					
-x8																					
-x9																					
-x10																					
-x11																					
-x12																					
-x13																					
-x14																					
-x15																					
-x16																					
-x17																					
-x18																					
-x19																					
-x20																					

Fig. 6

(6) shows that if X is not to be incorrectly operated,  $\underline{a}$  and  $\bar{a}$  must be of bridge type.

Hence the condition  $x\bar{x} = 0$  in (4) becomes  $\bar{a}\bar{a} = \bar{0} = 1$  in (6) after inversion.

In the light of the above it would seem that the terms  $\bar{a} \bar{y}_1 \dots \bar{y}_{n-1} \bar{x}_1 \bar{x}_2 \dots \bar{x}_n \bar{a}$  introduced into (4) introduce additional conditions into the circuit.

But if  $x_1$  and  $\bar{x}_1$  overlap while  $X_2 \dots X_n$  are cut off then  $\bar{a} \bar{y}_1 \dots \bar{y}_{n-1} \bar{x}_1 \bar{x}_2 \dots \bar{x}_n \bar{x}_1 = 0$ .

No extra condition for  $X_1$  is then introduced into the circuit. The same holds for the other elements.

Consider the operations table given in Fig. 6. The condition for  $X_3$  to operate is written as follows:

$$\begin{aligned} f_{X_3} &= \bar{a} \bar{x}_1 \bar{x}_2 \bar{x}_4 + x_3 \bar{a} \bar{x}_1 \bar{x}_2 \bar{x}_4 = \bar{a} \bar{x}_1 \bar{x}_2 \bar{x}_4 + x_3 (a + x_1 + x_2 + x_4) = \\ &= \bar{a} \bar{x}_1 \bar{x}_2 \bar{x}_4 + x_3 (a + x_2 + x_4). \end{aligned} \quad (7)$$

$x_1 x_3 = 0$ , since  $X_1$  and  $X_3$  are not cut in simultaneously.

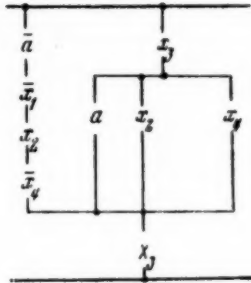


Fig. 7

The circuit corresponding to this expression is given in Fig. 7. This circuit can be drawn in another fashion and the number of contacts reduced. Two zero terms  $\bar{a} \bar{x}_1 \bar{x}_4 a$  and  $\bar{a} \bar{x}_1 \bar{x}_4 x_4$  are introduced into (4) for this purpose.

The expression takes the form

$$\begin{aligned} f_{X_3} &= \bar{a} \bar{x}_1 \bar{x}_2 \bar{x}_4 + \bar{a} \bar{x}_1 \bar{x}_4 a + \bar{a} \bar{x}_1 \bar{x}_4 x_4 + x_3 (a + x_2 + x_4) = \\ &= (\bar{a} \bar{x}_1 \bar{x}_4 + x_3) (a + x_2 + x_4). \end{aligned} \quad (8)$$

The circuit corresponding to this expression is given in Fig. 8. The contacts are here reduced to seven.

Both circuits can be given the inverse expression:

$$f = \bar{a} \bar{x}_1 \bar{x}_2 \bar{x}_4 + x_3 (a + x_2 + x_4) X_3 = (a + x_1 + \bar{x}_2 + x_4) (\bar{x}_3 + \bar{a} \bar{x}_2 \bar{x}_4) + X_3, \quad (9)$$

$$f = (\bar{a} \bar{x}_1 \bar{x}_4 + x_3) (a + x_2 + x_4) X_3 = (a + x_1 + x_4) \bar{x}_3 + \bar{a} \bar{x}_2 \bar{x}_4 + X_3. \quad (10)$$

These circuits are given in Fig. 9.

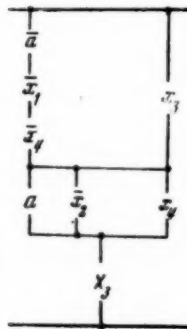


Fig. 8

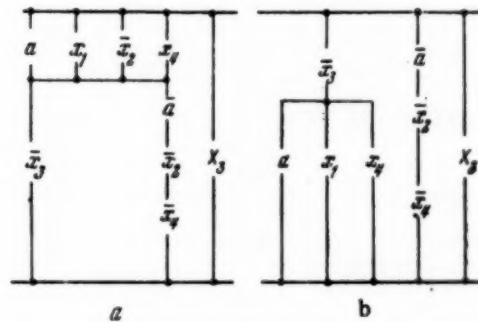


Fig. 9

Consideration of Fig. 8 shows that if  $X_3$  is not to be incorrectly cut in at stage 16,  $a$  and  $\bar{a}$  must not overlap. Figure 7 is free from this condition, which appears because the expression  $\bar{a} \bar{x}_1 \bar{x}_4 a = 0$  was introduced into (8). If the additional term is zero  $\bar{a}$  and  $a$  must not overlap, otherwise,  $\bar{a} \bar{x}_1 \bar{x}_4 a \neq 0$ .



Consideration of Fig. 9, b which is an inversion of the circuit of Fig. 8, shows that if  $X_3$  is not to be incorrectly cut in,  $\underline{a}$  and  $\bar{a}$  must be of bridge type.

Thus, the condition  $\bar{a}a = 0$  in (8) becomes  $\bar{\bar{a}}a = \bar{0} = 1$  after inversion in (10).

In the circuit of Fig. 9, a, contact  $\underline{a}$  can be of any type, since (9) is inverted relative to (7), but the latter does not imply any restrictive conditions for  $\underline{a}$ .

Addition of  $\bar{a}\bar{x}_1\bar{x}_4x_4 = 0$  does not introduce an additional condition since the overlap between  $x_4$  and  $\bar{x}_4$  occurs when  $\bar{a}$  is open (stages 10 and 14), i.e., there is an extra reserve break in this circuit because of the cut-in state of  $\underline{a}$ .

$X_3$  is of course cut-in in stages 10 and 14 and this element would not operate incorrectly if  $\bar{a}$  did not introduce an additional break. But the appearance of a cut-in pulse in the coil of the hold-on relay would indicate a nonrational circuit.

The presence of an extra break in the form of an open-circuit contact  $\bar{a}$  in stages 10 and 14 enables one to have any contacts on  $X_4$ , i.e.,  $\bar{x}_4x_4$  on switch-over may be either zero or one, since in both cases  $\bar{a}\bar{x}_1\bar{x}_4x_4 = 0$ .

Hence there will be no false cut-in pulse on  $X_3$  in stages 10 and 14.

### 3. Parallel Operation of Make and Break Contacts $x + \bar{x} = 1$

The problem of the relative states of contacts on the same element during transition movements may arise in setting up the analytic expression for the operation by the method, known from contactor circuit theory, in which the states of the elements are determined stage by stage. Since the circuits differ only in the state of one element at some stages it is clear that the analytic expression, being the sum of certain constituent units, will require bridge contacts on all elements which change their states during operation.

The demand for overlapping contacts indicates that  $x + \bar{x} = 1$  exists in latent form in the analytic expression. If this is eliminated without upsetting the sequential operation then the demand for contact overlap on  $X$  will be eliminated.

Expressions of the type  $x + \bar{x} = 1$  can be eliminated from the analytic expression by pairing the separate constituents:

$$\begin{aligned} \Sigma K^{(1)} = & \bar{x}_1\bar{x}_2 \dots \bar{x}_{n-1}\bar{x}_n + \bar{x}_1\bar{x}_2 \dots \bar{x}_{n-1}x_n + \bar{x}_1\bar{x}_2 \dots x_{n-1}\bar{x}_n + \\ & + \bar{x}_1\bar{x}_2 \dots x_{n-1}x_n + \dots + x_1x_2 \dots \bar{x}_{n-1}\bar{x}_n + x_1x_2 \dots \bar{x}_{n-1}x_n + \\ & + x_1x_2 \dots x_{n-1}\bar{x}_n + x_1x_2 \dots x_{n-1}x_n. \end{aligned} \quad (11)$$

If it is possible to separate  $x_n + \bar{x}_n$  and eliminate it by this pairing process, then

$$\Sigma K^{(1)} = \bar{x}_1\bar{x}_2 \dots \bar{x}_{n-1} + \bar{x}_1\bar{x}_2 \dots x_{n-1} + \dots + x_1x_2 \dots \bar{x}_{n-1} + x_1x_2 \dots x_{n-1}. \quad (12)$$

This is the sum of unit constituents with terms from  $X_1$  to  $X_{n-1}$ .

But elimination of expressions such as  $x + \bar{x} = 1$  does not lead to the desired result, since the demand for bridge contacts remains.

A method which enables one to avoid removing terms in constituents and frees the circuit from contact overlap requirements is given below.

The terms in the expression should be arranged in the order given in column 5 of Table 1. The constituents in this column are arranged in one of the possible ways in which only one term in the series of constituents is different.

If by  $\Sigma K^{(1)}(x_1, x_2, x_3, \dots, x_n)$  we denote the sum of the unit constituents of the elements  $X_1, X_2, X_3, \dots, X_n$ , then

$$\Sigma K^{(1)}(x_1, x_2, x_3, \dots, x_n) = x_1 \Sigma K^{(1)}(x_2, x_3, \dots, x_n) + \bar{x}_1 \Sigma K^{(1)}(x_2, x_3, \dots, x_n). \quad (13)$$



$$\begin{aligned} \Sigma K^{(1)}(x_1, x_2, x_3, \dots, x_n) &= x_1 \Sigma K^{(1)}(x_2, x_3, \dots, x_n) + \\ &+ \bar{x}_1 \Sigma K^{(1)}(x_2, x_3, \dots, x_n) + x_1 K^{(1)}(x_2, x_3, \dots, x_n) + \\ &+ \bar{x}_1 K^{(1)}(x_2, x_3, \dots, x_n). \end{aligned} \quad (14) \quad (14)$$

	$\bar{x}_1 \bar{x}_2 \bar{x}_3 \dots \bar{x}_n$	1-st constituent
	$\bar{x}_1 \bar{x}_2 \bar{x}_3 \dots \bar{x}_n$	2nd constituent
	$\bar{x}_1 \bar{x}_2 \bar{x}_3 \dots \bar{x}_n$	$(j-1)$ th constituent
	$\bar{x}_1 \bar{x}_2 \bar{x}_3 \dots \bar{x}_n$	$j$ -th constituent
	$\bar{x}_1 \bar{x}_2 \bar{x}_3 \dots \bar{x}_n$	$j$ -th constituent
	$\bar{x}_1 \bar{x}_2 \bar{x}_3 \dots \bar{x}_n$	$(j+1)$ -th constituent
	$\bar{x}_1 \bar{x}_2 \bar{x}_3 \dots \bar{x}_n$	$(j+1)$ -th constituent
	$\bar{x}_1 \bar{x}_2 \bar{x}_3 \dots \bar{x}_n$	$(i-1)$ -th constituent
	$\bar{x}_1 \bar{x}_2 \bar{x}_3 \dots \bar{x}_n$	$i$ -th constituent

The above arguments also apply to the other circuit elements.

$$\begin{aligned} \Sigma K^{(1)} &= \overline{x_1} \overline{x_2} \dots \overline{x_{n-1}} \overline{x_n} + \overline{x_1} \overline{x_2} \dots \overline{x_{n-1}} x_n + \overline{x_1} \overline{x_2} \dots \overline{x_{n-1}} x_n + \overline{x_1} \overline{x_2} \dots x_{n-1} \overline{x_n} + \\ &+ \overline{x_1} \overline{x_2} \dots x_{n-1} x_n + \overline{x_1} \overline{x_2} \dots x_{n-1} \overline{x_n} + \overline{x_1} \overline{x_2} \dots x_{n-1} \overline{x_n} \dots + \\ &+ x_1 x_2 \dots \overline{x_{n-1}} \overline{x_n} + x_1 x_2 \dots \overline{x_{n-1}} x_n + x_1 x_2 \dots \overline{x_{n-1}} x_n + x_1 x_2 \dots x_{n-1} \overline{x_n} + \\ &+ x_1 x_2 \dots x_{n-1} x_n + x_1 x_2 \dots x_{n-1} \overline{x_n} = \\ &= \overline{x_1} \overline{x_2} \dots \overline{x_{n-1}} + \overline{x_1} \overline{x_2} \dots x_n + \overline{x_1} \overline{x_2} \dots x_{n-1} + \dots + \\ &+ x_1 x_2 \dots \overline{x_{n-1}} + x_1 x_2 \dots x_n + x_1 x_2 \dots x_{n-1}. \end{aligned} \quad (15)$$

The first and third terms show open and closed contacts on  $X_{n-1}$  respectively. It might appear that a bridge contact is required. But this is not necessary because when the contacts on  $X_{n-1}$  change over the circuit will be closed by  $x_n$  (second term).

TABLE 1

Decimal number	Old description		Recommended	
	binary number	constituent of the unit expansion	binary number	constituent of the unit expansion
0	00...00	$\bar{x}_1 \bar{x}_2 \dots \bar{x}_{n-1} \bar{x}_n$	00...00	$\bar{x}_1 \bar{x}_2 \dots \bar{x}_{n-1} \bar{x}_n$
1	00...01	$\bar{x}_1 \bar{x}_2 \dots \bar{x}_{n-1} x_n$	00...01	$\bar{x}_1 \bar{x}_2 \dots \bar{x}_{n-1} x_n$
2	00...10	$x_1 \bar{x}_2 \dots \bar{x}_{n-1} \bar{x}_n$	00...11	$x_1 \bar{x}_2 \dots \bar{x}_{n-1} x_n$
3	00...11	$x_1 \bar{x}_2 \dots \bar{x}_{n-1} x_n$	00...10	$x_1 \bar{x}_2 \dots \bar{x}_{n-1} \bar{x}_n$
.	.....	.	.....	.
.	.....	.	.....	.
.	.....	.	.....	.
$m+1$	01...00	$\bar{x}_1 x_2 \dots \bar{x}_{n-1} \bar{x}_n$	01...10	$\bar{x}_1 x_2 \dots \bar{x}_{n-1} \bar{x}_n$
$m+2$	01...01	$\bar{x}_1 x_2 \dots \bar{x}_{n-1} x_n$	01...11	$\bar{x}_1 x_2 \dots \bar{x}_{n-1} x_n$
$m+3$	01...10	$x_1 x_2 \dots \bar{x}_{n-1} \bar{x}_n$	01...01	$x_1 x_2 \dots \bar{x}_{n-1} \bar{x}_n$
$m+4$	01...11	$x_1 x_2 \dots \bar{x}_{n-1} x_n$	01...00	$x_1 x_2 \dots \bar{x}_{n-1} x_n$
$m+5$	11...00	$x_1 x_2 \dots x_{n-1} \bar{x}_n$	11...00	$x_1 x_2 \dots x_{n-1} \bar{x}_n$
$m+6$	11...01	$x_1 x_2 \dots x_{n-1} x_n$	11...01	$x_1 x_2 \dots x_{n-1} x_n$
$m+7$	11...10	$x_1 x_2 \dots x_{n-1} \bar{x}_n$	11...11	$x_1 x_2 \dots x_{n-1} x_n$
$m+8$	11...11	$x_1 x_2 \dots x_{n-1} x_n$	11...10	$x_1 x_2 \dots x_{n-1} \bar{x}_n$

Note. Some series expansion constituents in column 3 differ in the states of several terms, while all those in column 5 differ in one term only.

Further transformations are analogous and are therefore omitted.

The constituents for circuits composed of three elements  $X_1$ ,  $X_2$ , and  $X_3$  only are given in Table 2.

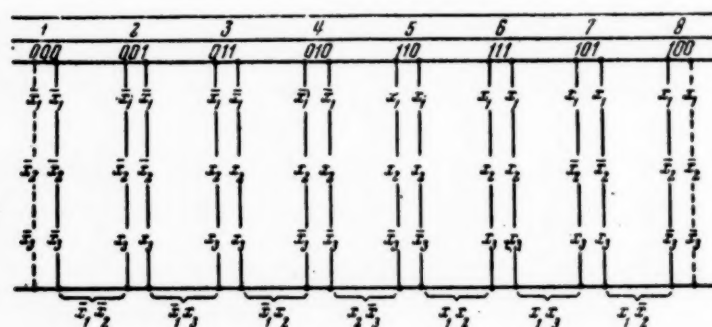


Fig. 10

Figure 10 gives the scheme corresponding to Table 2, in which constituents 2, 3, 4, 5, 6, and 7 enter twice:

$$\Sigma K^{(1)} = \bar{x}_1 \bar{x}_2 (\bar{x}_3 + x_3) + \bar{x}_1 x_2 (\bar{x}_3 + x_3) + \bar{x}_1 x_2 (x_3 + \bar{x}_3) + x_2 \bar{x}_3 (\bar{x}_1 + x_1) + x_2 x_3 (\bar{x}_1 + x_1) + x_1 x_2 (\bar{x}_3 + x_3) + x_1 x_3 (\bar{x}_2 + x_2) + x_1 \bar{x}_2 (x_3 + \bar{x}_3). \quad (16)$$

It is readily seen that:

1) when  $\bar{x}_2$  and  $x_2$  are switched over (terms 1 and 3 in the expression) there is a risk of breaking the  $\bar{x}_1 \bar{x}_2$  circuit, but the second term  $\bar{x}_1 x_2$  preserves the continuity;

2) when  $x_3$  and  $\bar{x}_3$  are switched over (terms 2 and 4 in the expression) there is a risk of breaking the  $\bar{x}_1 x_3$  circuit but the third term  $\bar{x}_1 x_2$  preserves the continuity;

3) when  $\bar{x}_1$  and  $x_1$  are switched over (terms 3 and 5 in the expression) there is a risk of breaking the  $\bar{x}_1 x_2$  circuit but the fourth term  $x_2 \bar{x}_3$  preserves the continuity, etc.

Circuits designed in accordance with the above expression do not require bridge contacts.

The expression can be further simplified:

$$\Sigma K^{(1)} = \bar{x}_1 \bar{x}_2 + \bar{x}_1 x_3 + \bar{x}_1 x_2 + x_2 \bar{x}_3 + x_1 x_2 + x_1 x_3 + x_1 \bar{x}_2 = x_3 (\bar{x}_1 + x_1) + \bar{x}_1 (\bar{x}_2 + x_2) + x_1 (\bar{x}_3 + x_3) + x_2 = x_3 + \bar{x}_1 + x_1 + x_2. \quad (17)$$

Circuits designed in accordance with the above expression do not require bridge contacts.

If we add constituents 1 and 8 in accordance with the above argument (shown by dashes in Fig. 10) we get

$$\begin{aligned} \Sigma K^{(1)} &= \bar{x}_1 \bar{x}_2 + \bar{x}_1 x_3 + \bar{x}_1 x_2 + x_2 \bar{x}_3 + x_1 x_2 + x_1 x_3 + x_1 \bar{x}_2 + \bar{x}_2 \bar{x}_3 = \\ &= x_3 (\bar{x}_1 + x_1) + \bar{x}_1 (\bar{x}_2 + x_2) + x_1 (\bar{x}_3 + x_3) + \bar{x}_3 (x_2 + \bar{x}_2) = \\ &= x_3 + \bar{x}_1 + x_1 + \bar{x}_3. \end{aligned} \quad (18)$$

It is then clear that in spite of the total number of constituents and the presence of mutually exclusive contacts the circuit does not require that the contacts should overlap.

TABLE 2

Decimal number	Binary number	Constituents of the layout of units
0	000	$\bar{x}_1 \bar{x}_2 \bar{x}_3$
1	001	$\bar{x}_1 \bar{x}_2 x_3$
2	011	$\bar{x}_1 x_2 \bar{x}_3$
3	010	$\bar{x}_1 x_2 x_3$
4	110	$x_1 \bar{x}_2 \bar{x}_3$
5	111	$x_1 \bar{x}_2 x_3$
6	101	$x_1 x_2 \bar{x}_3$
7	100	$x_1 x_2 x_3$

It might appear that there is no practical significance in considering a circuit which is exactly equal to unity. But the above argument shows that the circuit re-

presented as  $\sum_{i=1}^{2^n} K^{(1)}$  is not always unity, but is so

only when bridging contacts are present. By using the method presented here the circuit can be transformed to one which is always unity, no matter what contact designs are used.

A circuit of this type can be used to check the operation of another circuit. The checking circuit will then be equivalent to unity only when the checked one operates correctly, and will detect disturbances in the operation of the checked circuit.

The above argument was derived from methodological considerations in a general form for all constituents. The results are evidently correct for any number of constituents, since the analytic expression can be given the form

$$x_1 \Sigma K^{(1)}(x_2, x_3, \dots, x_n) + \bar{x}_1 \Sigma K^{(1)}(x_2, x_3, \dots, x_n) + x_1 K^{(1)}(x_2, x_3, \dots, x_n) + \bar{x}_1 K^{(1)}(x_2, x_3, \dots, x_n).$$

The following correct transformation of multistage circuits can be derived from the above argument.

1. The circuits of multistage units are represented by the separate unit constituents.
2. The constituent units are arranged in the order given in column 5 of Table 1. The order is such that adjacent constituents differ from each other by their state of only one element.
3. In the analytic expression of the scheme only those constituents repeat themselves which differ in the state of an element on which the contacts must overlap (considering energized or deenergized states).

oper. stage	0	1	2	3	4	5	6	7	8	9	10	11	12	13	14	15	16	17	18	19	20	21	22	23					18	19	20			
	circuit elements state																																	
-a	-a	+a		-a	+a		-a	+a		-a	+a		-a	+a		-a	+a		-a	+a		-a	+a		-a	+a		-a	+a		-a	+a		
-x <sub>1</sub>																			-x <sub>1</sub>		x <sub>1</sub>								-x <sub>1</sub>		x <sub>1</sub>			
-x <sub>2</sub>																			-x <sub>2</sub>		x <sub>2</sub>								-x <sub>2</sub>		x <sub>2</sub>			
-x <sub>3</sub>																			-x <sub>3</sub>		x <sub>3</sub>								-x <sub>3</sub>		x <sub>3</sub>			
-x <sub>4</sub>																			-x <sub>4</sub>		x <sub>4</sub>								-x <sub>4</sub>		x <sub>4</sub>			
-x <sub>5</sub>																			-x <sub>5</sub>		x <sub>5</sub>								-x <sub>5</sub>		x <sub>5</sub>			
1st cycle																							2nd cycle				n-th cycle							

To remove this condition for  $\underline{a}$  and  $\bar{a}$  we must add the 2nd, 3rd, 4th, and 5th terms to (20):

$$\begin{aligned}
 f_X &= ax_1\bar{x}_3\bar{x}_4\bar{x}_5 + ax_1\bar{x}_3\bar{x}_4x_5 + ax_1\bar{x}_3x_4\bar{x}_5 + ax_1\bar{x}_3x_4x_5 + \bar{a}x_1\bar{x}_3\bar{x}_4\bar{x}_5 + \bar{a}x_1\bar{x}_3\bar{x}_4x_5 + \\
 &\quad + \bar{a}x_1\bar{x}_3x_4\bar{x}_5 + \bar{a}x_1\bar{x}_3x_4x_5 + ax_1x_3\bar{x}_4\bar{x}_5 + ax_1x_3\bar{x}_4x_5 + ax_1x_3x_4\bar{x}_5 + ax_1x_3x_4x_5 = \\
 &= ax_1\bar{x}_4\bar{x}_5(\bar{x}_3 + x_3) + x_1\bar{x}_3\bar{x}_4\bar{x}_5(a + \bar{a}) + \bar{a}x_1x_3\bar{x}_4(\bar{x}_5 + x_5) + x_1x_3\bar{x}_4x_5(\bar{a} + a) + \\
 &\quad + ax_1x_3x_5(\bar{x}_4 + x_4) = x_1\bar{x}_4\bar{x}_5(a + x_3) + x_1\bar{x}_3\bar{x}_4(\bar{a} + x_5) + ax_1x_3x_5 = \\
 &= x_1[\bar{x}_4(\bar{x}_5a + x_3) + ax_3x_5].
 \end{aligned}
 \tag{21}$$

The hold-on circuits do not need bridge contacts for  $\underline{a}$ ,  $x_3$ ,  $x_4$ , and  $x_5$ , from (21). The number of contacts is reduced to eight.

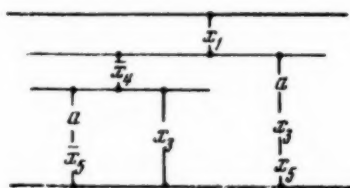


Fig. 12

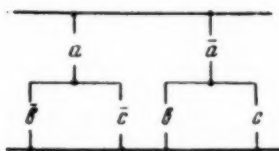


Fig. 13



Fig. 14

The layout corresponding to (21) is given in Fig. 12.

TABLE 3

Binary number	Con-stituent	$a(\bar{b} + \bar{c}) + \bar{a}(b + c)$	$f_X$
000	$\bar{a} \bar{b} \bar{c}$	$0(1 + 1) + 1(0 + 0)$	0
001	$\bar{a} \bar{b} c$	$0(1 + 0) + 1(0 + 1)$	1
011	$\bar{a} b c$	$0(0 + 0) + 1(1 + 1)$	1
010	$\bar{a} b \bar{c}$	$0(0 + 1) + 1(1 + 0)$	1
110	$a b \bar{c}$	$1(0 + 1) + 0(1 + 0)$	1
111	$a b c$	$1(0 + 0) + 0(1 + 1)$	0
101	$a \bar{b} c$	$1(1 + 0) + 0(0 + 1)$	1
100	$a \bar{b} \bar{c}$	$1(1 + 1) + 0(0 + 0)$	1

Suppose there is a layout such as is given in Fig. 13 [1]. Its structural formula is of the form:

$$f_X = a(b + \bar{c}) + \bar{a}(b + c). \tag{22}$$

This expression refers back to the form:

$$x_1 \Sigma K^{(1)}(x_2, x_3) + \bar{x}_1 \Sigma K^{(1)}(x_2, x_3),$$

which we have considered above.

The unit constituents of the analytic expression are determined by evaluating the coefficients of the circuit. Table 3 gives the results.

On splitting the expression up into its unit constituents it takes the form:

$$f_X = \bar{a}\bar{b}\bar{c} + \bar{a}b\bar{c} + \bar{a}b\bar{c} + \bar{a}b\bar{c} + \bar{a}b\bar{c} + \bar{a}b\bar{c}. \tag{23}$$

To remove this condition for  $\underline{a}$  and  $\bar{a}$  to overlap we must, in accordance with the above argument, add  $\bar{a}\bar{b}\bar{c}$ ,  $\bar{a}b\bar{c}$ ,  $\bar{a}b\bar{c}$ , and  $\bar{a}b\bar{c}$ :

$$\begin{aligned}
 f_X &= \bar{a}\bar{b}\bar{c} + \bar{a}b\bar{c} + \bar{a}b\bar{c} + \bar{a}b\bar{c} + \bar{a}b\bar{c} + \bar{a}b\bar{c} + \bar{a}b\bar{c} + \bar{a}b\bar{c} + \bar{a}b\bar{c} + \bar{a}b\bar{c} = \\
 &= \bar{a}(\bar{b}\bar{c} + b\bar{c} + \bar{b}\bar{c}) + b\bar{c}(\bar{a} + a) + a(\bar{b}\bar{c} + \bar{b}\bar{c} + \bar{b}\bar{c}) + \bar{b}\bar{c}(a + \bar{a}) = \\
 &= \bar{a}(c + b) + b\bar{c} + a(\bar{c} + \bar{b}) + \bar{b}\bar{c}.
 \end{aligned}
 \tag{24}$$



It is readily seen that this requires no contact overlap. The contacts can be of any type. The number of springs is 15.

The above scheme can be simplified:

$$\begin{aligned} f_X &= \bar{a}(c+b) + b\bar{c} + a(\bar{c}+\bar{b}) + \bar{b}c = \bar{a}c + \bar{a}b + b\bar{c} + a\bar{c} + a\bar{b} + \bar{b}c + \\ &+ a\bar{a} + b\bar{b} + c\bar{c} = \bar{a}(a+b+c) + \bar{b}(a+b+c) + \bar{c}(a+b+c) = \\ &= (a+b+c)(\bar{a}+\bar{b}+\bar{c}). \end{aligned} \quad (25)$$

The layout corresponding to this is given in Fig. 14. The number of springs is reduced to nine.

#### SUMMARY

1. If  $x\bar{x} = 0$  is added to the analytic expression representing any circuit, or the expression is multiplied by  $x + \bar{x} = 1$ , a new expression is obtained which implies the conditions inherent in the added expressions. In the first case these conditions denote that on changing the state of relay  $X$  its make and break contacts must not overlap, while in the second they mean that they must overlap, i.e., must be bridge-type. But these requirements can sometimes be obviated by selecting a definite sequence of element switching.

2. If any circuit requires overlap (bridge contacts) this implies that the corresponding analytic expression contains  $x + \bar{x} = 1$  in concealed form. If the circuit inherently demands nonoverlapping contacts, then  $x\bar{x} = 0$  must be present in the corresponding analytic expression in concealed form.

3. If any circuit requires overlap (bridge contacts) or nonoverlapping contacts on a given relay, then to eliminate this requirement so the circuit can be built with any contacts, we have to obtain, by multiplying or compounding the corresponding analytic expression as regards its separate constituents: a)  $x\bar{x} = 0$  as a factor multiplying the constituents and b)  $x + \bar{x} = 1$  as a factor on collecting constituents, and eliminate these from the expression and from the circuit.

4. If the circuit requires overlapping contacts on certain elements  $X_1, X_2$ , etc., this implies that in concealed form we have in the analytic expression

$$x_1 + \bar{x}_1 = 1, \quad x_2 + \bar{x}_2 = 1, \dots, \quad x_n + \bar{x}_n = 1.$$

Hence to separate these term-pairs as factors and eliminate them we should add the constituents already present in them which differ as regards the state of the element on which contact overlap is required. The overlap requirement can thereby be eliminated.

5. If the circuit requires overlapping make and break contacts, then on inversion this condition changes to one of no contact overlap, and conversely if the circuit requires nonoverlapping contacts, then on inversion the contacts must be of bridge type.

#### LITERATURE CITED

- [1] M. A. Gavrilov, Theory of Contactor Circuits, Acad. Sci. USSR Press, 1950.
- [2] G. Mountgomerie, Sketch for an Algebra and Contactor Circuits, The Journal of the Institute of Electrical Engineers, Vol. 95, June 1948.

Received November 23, 1955.



# A METHOD OF DETERMINING DESIRED LOG FREQUENCY CHARACTERISTICS

P. S. Matveev

(Moscow)

A method of determining desired log frequency characteristics is given. A nomogram for estimating overshoot is presented, together with some examples illustrating the practical application of the method.

The published [1-3] method of designing correcting units involves the prior choice of log frequency characteristics to satisfy known requirements.

One such possible method of choice is given below for a system in which the given parameters are as follows:

- 1) the response time,  $T$  for a stepwise change;
- 2) the error coefficients  $C_1, C_2, \dots, C_i$ .

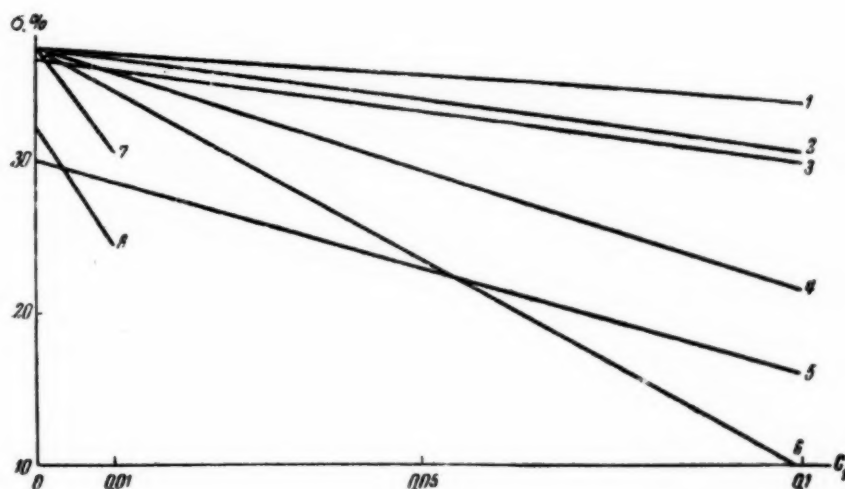


Fig. 1

The desired result is obtained if the pulse transient function for the system is taken as

$$K(t) = a_0 + a_1 t + a_2 t^2 + \dots + a_n t^n \quad (1)$$

and it is supposed that

$$K(t) = 0 \quad (t \leq 0^-), \quad (2)$$

$$K(t) = 0 \quad (t \geq T^+). \quad (3)$$

(2) is evidently the condition that the system is physically possible while (3) is the condition for the system to be of the required quality. When the control action is slow the error can, to an adequate accuracy, be represented as

$$e(t) = C_0 g(t) + C_1 \dot{g}(t) + \frac{C_2}{2} \ddot{g}(t) + \dots + \frac{C_n}{n!} g^{(n)}(t), \quad (4)$$

where  $g(t)$  is the control action, and

$$C_0 = 1 - \int_0^T K(\tau) d\tau, \\ C_i = (-1)^{(i+1)} \int_0^T \tau^i K(\tau) d\tau \quad (i = 1, 2, \dots, n). \quad (5)$$

If the error coefficients are given, then by substituting (5) into  $K(t)$  taken from (1) we get a system of  $(n+1)$  linear algebraic equations:

$$a_0 T + \frac{a_1}{2} T^2 + \dots + \frac{a_n}{n+1} T^{n+1} = 1, \\ \frac{a_0 T^2}{2} + \frac{a_1}{3} T^3 + \dots + \frac{a_n T^{n+2}}{n+2} = C_1, \\ \dots \dots \dots \\ (-1)^{(i+1)} \left( \frac{a_0 T^{n+1}}{n+1} + \frac{a_1 T^{n+2}}{n+2} + \dots + \frac{a_n T^{2n+1}}{2n+1} \right) = C_n. \quad (6)$$

The solution to this system gives the unknowns in (1). From the known expression for  $K(t)$  the closed-loop transfer function is determined:

$$\Phi(S) = \int_0^T e^{-ST} K(t) dt, \quad (7)$$

and from  $\Phi(S)$  the transfer function for the open-loop system  $KW(S)$  is determined by the usual methods.  $KW(S)$  is then a transcendental function of  $S$ . This difficulty is avoided by replacing  $KW(S)$  by the approximate desired frequency characteristics, without allowing for the oscillatory components due to the dissected character of the pulse transient function. This method also enables one to estimate the overshoot. The following arguments are used to derive the overshoot.

The system output  $x(t)$  can be represented via the pulse transient and its effect  $f(t)$  in the form

$$x(t) = \int_0^t f(t-\tau) K(\tau) d\tau. \quad (8)$$

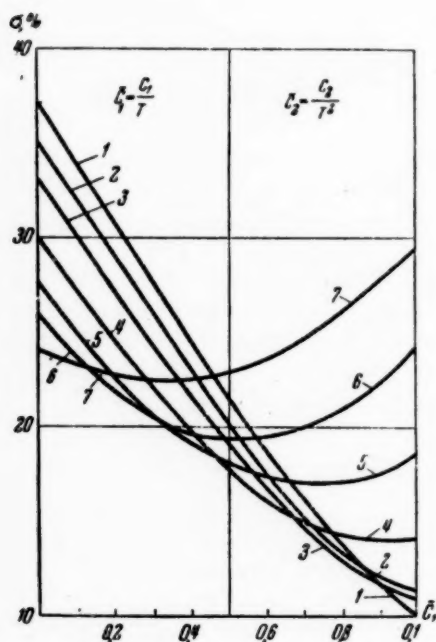


Fig. 2

If we suppose that  $f(t) = 1[t]$ , and incorporates (1), we get

$$x(t) = a_0 t + \frac{a_1 t^2}{2} + \dots + \frac{a_n t^n}{n!} \quad (0 \leq t \leq T). \quad (9)$$

As (9) is a general form for the transient process we can always estimate the overshoot by finding the roots derived from  $x(t)$ , i.e.,  $K(t)$ , and substituting the least of these in (9).

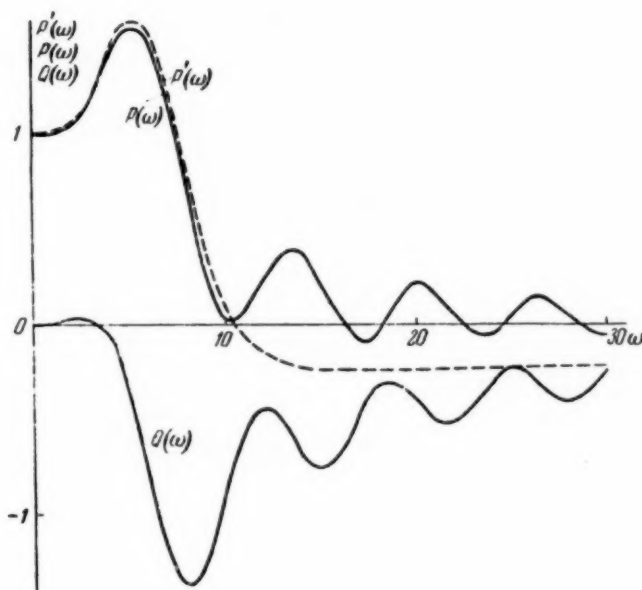


Fig. 3

A particular case, which occurs in a number of practical problems, will be considered to illustrate the method; here only the velocity and acceleration error coefficients  $C_1$  and  $C_2$  are of interest. The expression for  $K(t)$  then becomes much simpler, taking the form:

$$K(t) = a_0 + a_1 t + a_2 t^2 \quad (0 \leq t \leq T). \quad (10)$$

When  $f(t) = 1[t]$ ,  $x(t)$  is given by

$$x(t) = a_0 t + \frac{a_1 t^2}{2} + \frac{a_2 t^3}{3} \quad (0 \leq t \leq T). \quad (11)$$

The unknown constants  $a_0$ ,  $a_1$  and  $a_2$  in (10) and (11) are determined from the equations

$$a_0 T + \frac{a_1 T^2}{2} + \frac{a_2 T^3}{3} = 1, \quad \frac{a_0 T^2}{2} + \frac{a_1 T^3}{3} + \frac{a_2 T^4}{4} = C_1, \quad \frac{a_0 T^3}{3} + \frac{a_1 T^4}{4} + \frac{a_2 T^5}{5} = -C_2, \quad (12)$$

whence

(13)

$$a_0 = \frac{9T^2 - 36C_1T - 30C_2}{T^3}, \quad a_1 = \frac{-36T^2 + 192C_1T + 180C_2}{T^4},$$

$$a_2 = \frac{30T^2 - 180C_1T - 180C_2}{T^5}.$$

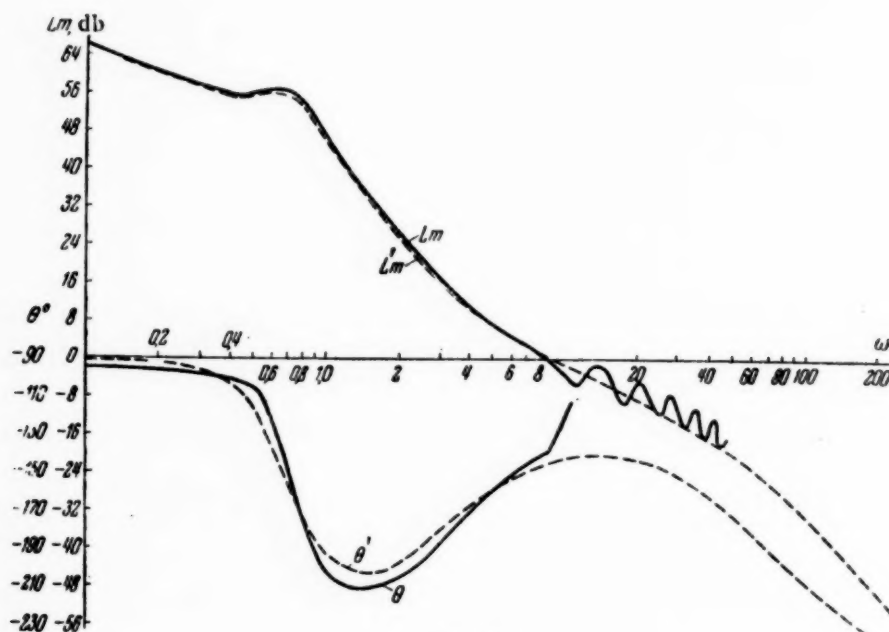


Fig. 4

The overshoot is estimated by equating (10) to zero; the roots of

$$t_{1,2} = \frac{-a_1 \pm \sqrt{a_1^2 - 4a_0a_2}}{2a_2}$$

are found and the lesser substituted in (11).

Figure 1 shows the curves from which the overshoot can be estimated when  $C_1$ ,  $C_2$ , and  $T$  are known, wide ranges of these parameters being covered. It shows that the overshoot does not exceed 40% when  $C_1$ ,  $C_2$ , and  $T$  vary within these limits.

Figure 2 shows a more general form of nomogram for this case:  $T$  has been eliminated by making the substitutions  $\bar{C}_1 = \frac{C_1}{T}$  and  $\bar{C}_2 = \frac{C_2}{T^2}$ . An analogous nomogram can be constructed

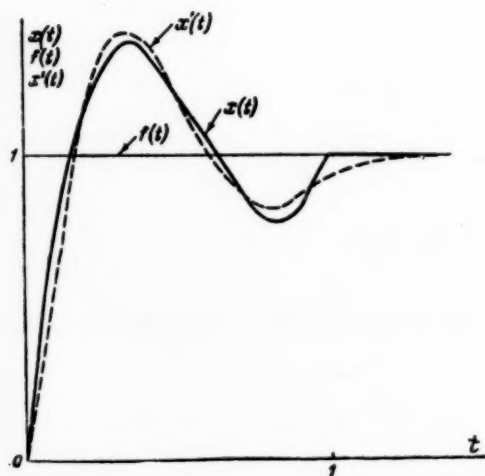


Fig. 5

when  $C_3$  is also present. When conditions change slowly the nomograms can be used to determine the form of  $K(t)$  by using compromise values for  $T$ ,  $\sigma$ ,  $C_1$ , and  $C_2$ , as well as to estimate the overshoot.

We shall now consider a few examples illustrating the use of this method.

**Example 1.** Find the requisite frequency characteristics of a system satisfying the following requirements:  $T \approx 1$  sec;  $C_1 = 0.005$ ,  $C_2 = 0.0015$ ; overshoot not to exceed 40%. Then  $a_0 = 8.775$ ,  $a_1 = -34.77$  and  $a_2 = 28.83$  in (10) and (11).

Figures 3, 4, and 5 show the characteristics of the closed loop, the log characteristics of the open loop, and the transients corresponding to (10) (full line) and the approximate ones in which no allowance is made for the discontinuity in the transient function (dashed line).

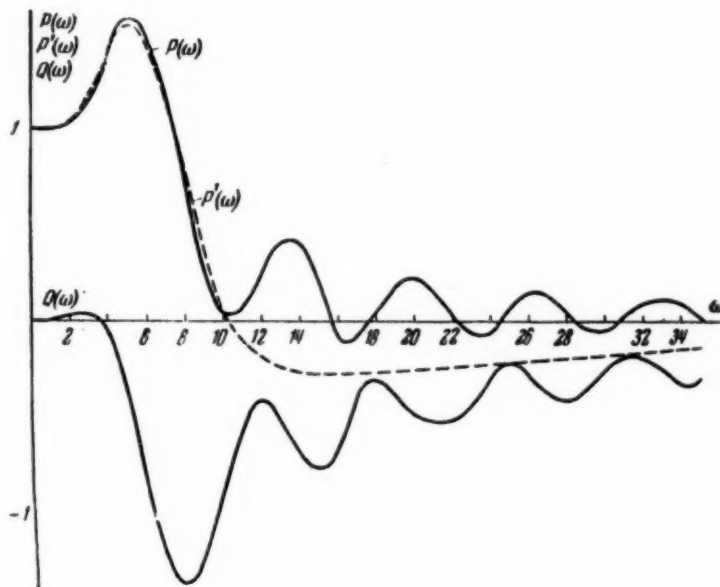


Fig. 6

The approximate frequency curve is

$$KW(S) = \frac{200(0.455S + 1)(0.2S + 1)}{S(1.42^2 S^2 + 2 \times 0.272 \times 1.42S + 1)(0.02S + 1)(0.01S + 1)} \quad (14)$$

$C_1 = 0.005$ ,  $C_2 = 0.0015$ ,  $T \approx 1.1$  sec and  $\sigma \approx 40\%$  from (14).

**Example 2.** The other error coefficients may sometimes be of interest when  $C_1$  and  $C_2$  are given. It is then convenient to use (5) and (10) to estimate them. The following relations, which are consequences of (5) and (10), can also be used.

$$C_3 = \frac{a_0 T^4}{4} + \frac{a_1 T^5}{5} + \frac{a_2 T^6}{6}, \quad -C = \frac{a_0 T^3}{5} + \frac{a_1 T^4}{6} + \frac{a_2 T^5}{7},$$

$$C_5 = \frac{a_0 T^6}{6} + \frac{a_1 T^7}{7} + \frac{a_2 T^8}{8} \text{ etc.} \quad (15)$$

Suppose we are required to find the characteristics of a system with the following parameters:  $T \approx 1$  sec;  $C_1 = 0.0033$ ,  $C_2 = 0.0015$ ; overshoot not to exceed 40%.

Then  $a_0 = 8.8362$ ,  $a_1 = -35.0964$ ,  $a_2 = 29.136$ , and using (15) we have  $C_3 = 0.0456$ ,  $C_4 = -0.081$ ,  $C_5 = 0.101$ .

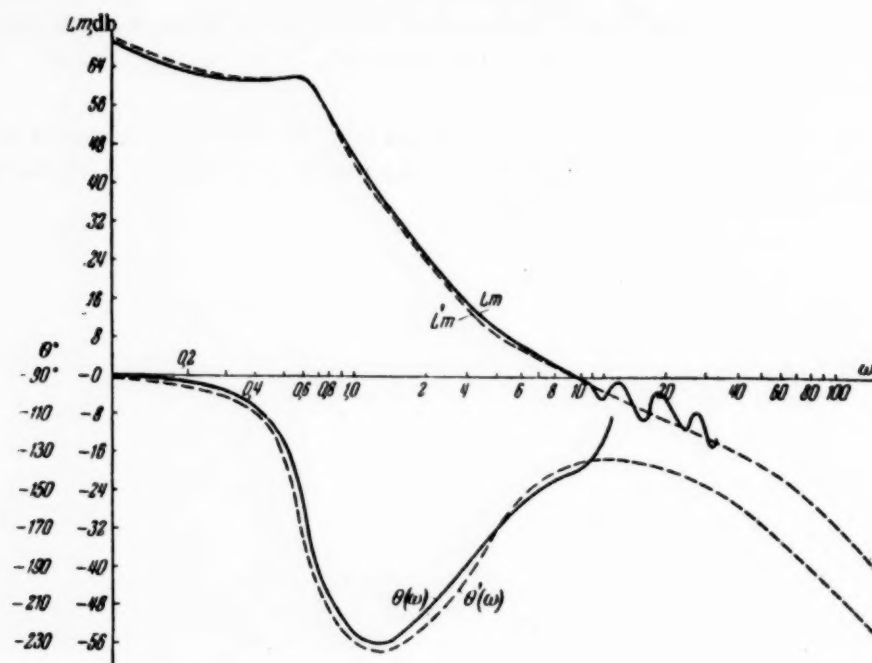


Fig. 7

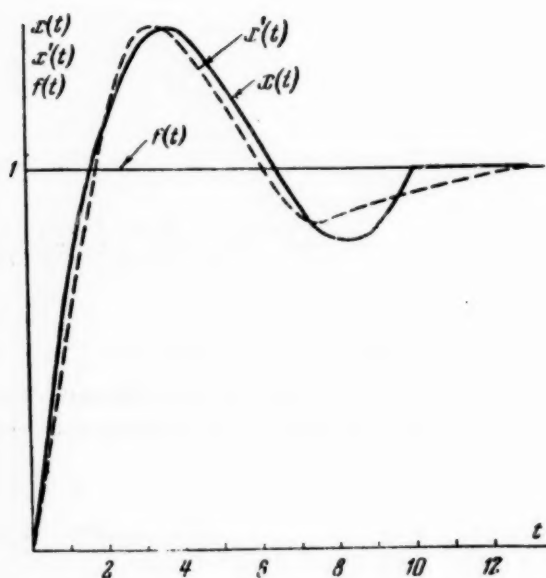


Fig. 8



The approximate characteristic of the open system is

$$KW(S) = \frac{303 (0,28^2 S^2 + 2 \times 0,6 \times 0,28 S + 1)}{S (1,68^2 S^2 + 2 \times 0,16 \times 1,68 S + 1) (0,02 S + 1) (0,01 S + 1)}, \quad (16)$$

with the following parameters:

$$C_1 = 0,0033, \quad C_2 = 0,0015, \quad C_3 = 0,052, \quad C_4 = -0,066, \quad C_5 = 0,03.$$

Figures 6 - 8 show the same characteristics as for Example 1.

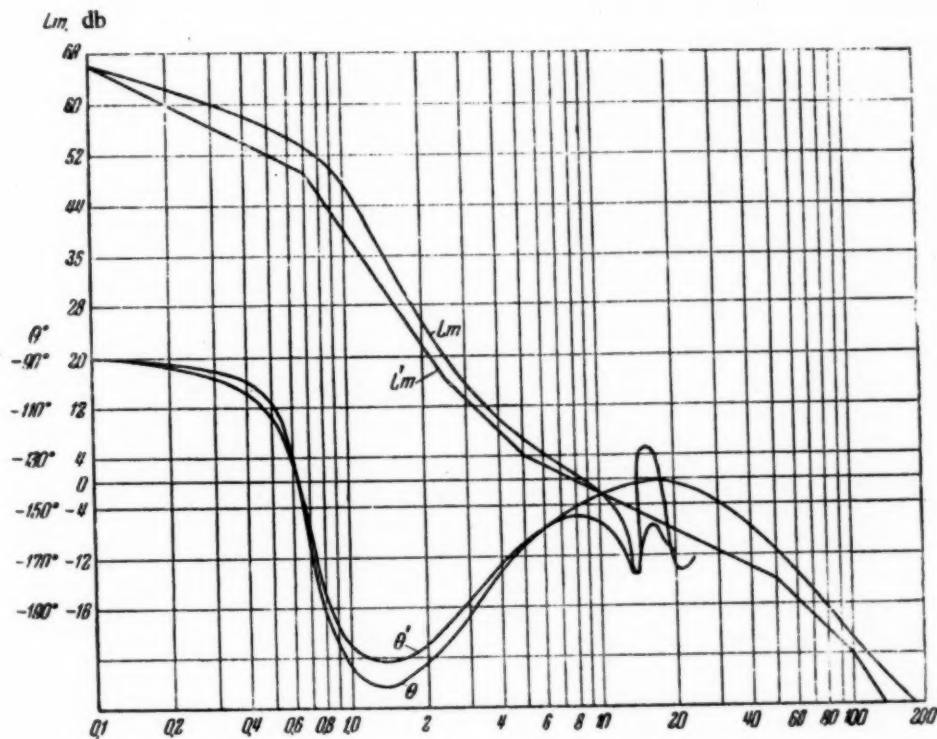


Fig. 9

**Example 3.** Suppose we are required to find the characteristics of a system with the following parameters:

- 1)  $T = 1$  sec;
- 2)  $C_1 = 0,005, \quad C_2 = 0,0015, \quad C_3 = 0,05, \quad C_4 = -0,08.$

Figure 9 shows the characteristics corresponding to (10) and

$$KW(S) = \frac{200 (0,2 S + 1) (0,4 S + 1)}{S (1,415^2 S^2 + 2 \times 0,26 \times 1,415 S + 1) (0,02 S + 1) (0,01 S + 1)}. \quad (17)$$

For (17),  $C_1 = 0,005, \quad C_2 = 0,0016, \quad C_3 = 0,055$  and  $C_4 = -0,11$  and  $T \approx 1$  sec.

Comparison of the required and approximate log frequency curves and the corresponding dynamic parameters shows that they are in adequately exact agreement.

#### SUMMARY

A method of selecting the parameters of an automatic control system has been developed to give parameters which satisfy the demand for dynamic accuracy (given error coefficients  $C_1$ ,  $C_2$ , and  $C_3$ ) and also the demand for system quality ( $T$  and  $\sigma$ ).

#### LITERATURE CITED

- [1] The Basis of Automatic Control, edited by V. V. Solodnikov, State Machine Press, 1954.
- [2] V. V. Solodnikov, Design of Follower System Correction Units Using Optimal and Typical Frequency Characteristics, Automation and Remote Control 14, 5 (1953).
- [3] V. V. Solodnikov, Design of Follower System Correction Units with Typical Actions, Automation and Remote Control 12, 5 (1951).

Received May 5, 1955.

# SUPPLY-VOLTAGE DEPENDENT ZERO SHIFTS IN MAGNETIC NULL DETECTORS

A. M. Pshenichnikov

(Moscow)

The supply-voltage dependent zero shifts in magnetic modulators used as null detectors are considered, and methods of reducing or balancing-out the shifts are described.

The zero shifts due to voltage changes in recording and telemetering equipment are more important than those due to supply frequency and ambient temperature changes. For example in a magnetic modulator (in which the zero shift is very marked) the shift may be  $220 \mu V$  for a 20% change in supply voltage when

the input sensitivity is  $\pm 25 \mu V$ , while the shift due to a frequency change from 45 to 50 cps may not be as large as  $50 \mu V$ . The supply-voltage dependent zero shifts in magnetic null detectors are due to the magnetic parameters of the four coils not being identical. These differences are found even when permalloy from a given batch given the same annealing treatment is used. The permeabilities vary differently when the supply voltage alters, and a first harmonic unbalance appears at the amplifier output, which displaces the zero. Hence, in making magnetic null detectors the magnetic characteristics of the coils are sometimes recorded on ac after winding and those with identical characteristics chosen, which ensures good results. When such a magnetic modulator was constructed at the Institute of Automation and Remote Control (Academy of Sciences of the USSR) the zero shift due to supply voltage changes of  $\pm 20\%$  did not exceed  $15 \mu V$ . Coil selection is somewhat inconvenient under factory conditions.

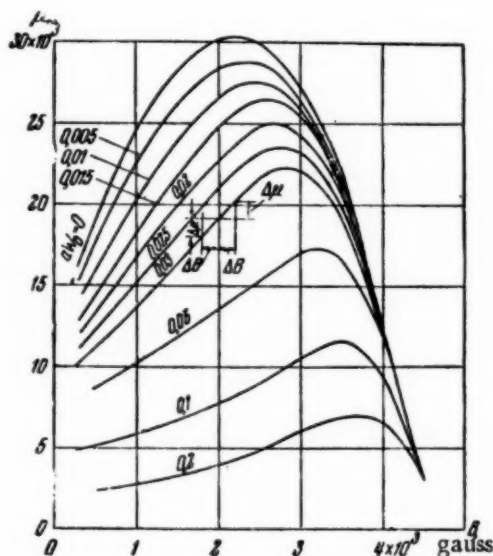


Fig. 1. Relation of magnetic permeability to induction and dc magnetization for annealed 78% molybdenum permalloy.

magnetization characteristics under both ac and dc magnetization showed that when the changes in both types of magnetization are the same the permeability of permalloy varies differently.

Curves relating the permeability of the induction at various dc magnetizations were used to elucidate the permeability changes (Fig. 1). Curves relating the permeability to the induction at constant dc magnetizations were drawn up from the above. Further, the relative increase in permeability\* due to a 10%

The author has proposed a method of balancing out these zero shifts due to supply voltage variations. Examination of permalloy

\* A method proposed by S. A. Ginzburg was used for this purpose.

Comparison of the required and approximate log frequency curves and the corresponding dynamic parameters shows that they are in adequately exact agreement.

#### SUMMARY

A method of selecting the parameters of an automatic control system has been developed to give parameters which satisfy the demand for dynamic accuracy (given error coefficients  $C_1$ ,  $C_2$ , and  $C_3$ ) and also the demand for system quality ( $T$  and  $\sigma$ ).

#### LITERATURE CITED

- [1] The Basis of Automatic Control, edited by V. V. Solodnikov, State Machine Press, 1954.
- [2] V. V. Solodnikov, Design of Follower System Correction Units Using Optimal and Typical Frequency Characteristics, Automation and Remote Control 14, 5 (1953).
- [3] V. V. Solodnikov, Design of Follower System Correction Units with Typical Actions, Automation and Remote Control 12, 5 (1951).

Received May 5, 1955.

# SUPPLY-VOLTAGE DEPENDENT ZERO SHIFTS IN MAGNETIC NULL DETECTORS

A. M. Pshenichnikov

(Moscow)

The supply-voltage dependent zero shifts in magnetic modulators used as null detectors are considered, and methods of reducing or balancing-out the shifts are described.

The zero shifts due to voltage changes in recording and telemetering equipment are more important than those due to supply frequency and ambient temperature changes. For example in a magnetic modulator (in which the zero shift is very marked) the shift may be  $220 \mu V$  for a 20% change in supply voltage when

the input sensitivity is  $\pm 25 \mu V$ , while the shift due to a frequency change from 45 to 50 cps may not be as large as  $50 \mu V$ . The supply-voltage dependent zero shifts in magnetic null detectors are due to the magnetic parameters of the four coils not being identical. These differences are found even when permalloy from a given batch given the same annealing treatment is used. The permeabilities vary differently when the supply voltage alters, and a first harmonic unbalance appears at the amplifier output, which displaces the zero. Hence, in making magnetic null detectors the magnetic characteristics of the coils are sometimes recorded on ac after winding and those with identical characteristics chosen, which ensures good results. When such a magnetic modulator was constructed at the Institute of Automation and Remote Control (Academy of Sciences of the USSR) the zero shift due to supply voltage changes of  $\pm 20\%$  did not exceed  $15 \mu V$ . Coil selection is somewhat inconvenient under factory conditions.

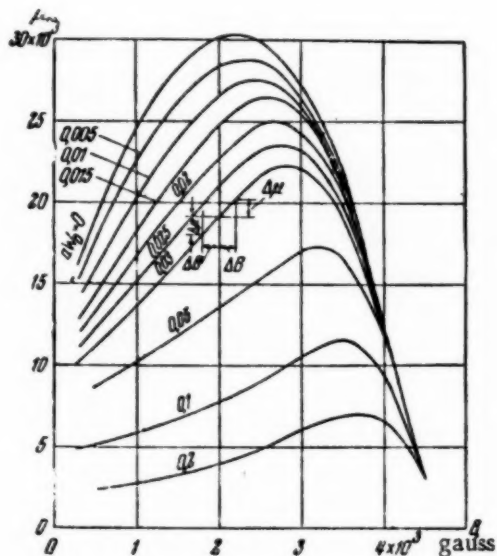


Fig. 1. Relation of magnetic permeability to induction and dc magnetization for annealed 78% molybdenum permalloy.

magnetization characteristics under both ac and dc magnetization showed that when the changes in both types of magnetization are the same the permeability of permalloy varies differently.

Curves relating the permeability of the induction at various dc magnetizations were used to elucidate the permeability changes (Fig. 1). Curves relating the permeability to the induction at constant dc magnetizations were drawn up from the above. Further, the relative increase in permeability\* due to a 10%

The author has proposed a method of balancing out these zero shifts due to supply voltage variations. Examination of permalloy

\* A method proposed by S. A. Ginzburg was used for this purpose.

change in induction,  $\frac{\Delta \mu}{\mu} / \frac{\Delta B}{B}$ , was calculated for various dc magnetizations over  $\pm 10\%$  induction ranges. The relative increase in permeability due to a 10% change in dc magnetization,  $\frac{\Delta \mu}{\mu} / \frac{\Delta a W_0}{a W_0}$ .

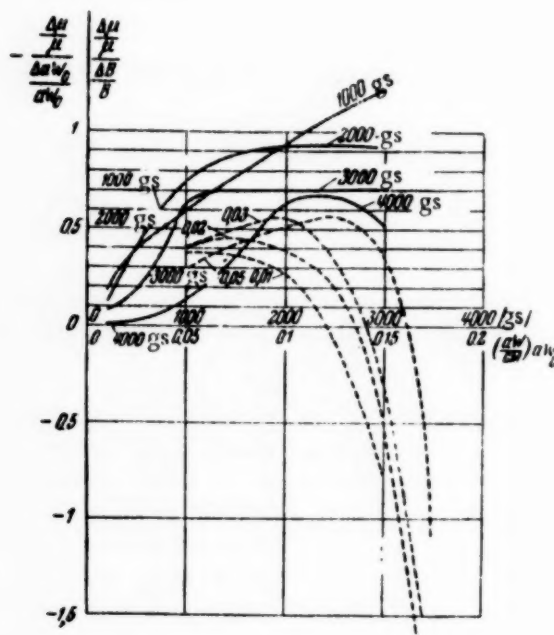


Fig. 2. Relations for the relative permeability increase in 78% molybdenum permalloy. 1) On 10% increase in induction at various  $a W_0$  as a function of induction; 2) on 10% increase in magnetization at various inductions as a function of  $a W_0$ .

was also determined at various inductions. Figure 2 shows  $\frac{\Delta \mu}{\mu} / \frac{\Delta B}{B} = F_1(B)$  when  $a W_0 = \text{const}$  and  $-\frac{\Delta \mu}{\mu} / \frac{\Delta a W_0}{a W_0} = F_2(a W_0)$  when  $B = \text{const}$ . Then by producing the lines of equal relative increase in  $\frac{\Delta \mu}{\mu} / \frac{\Delta B}{B}$  and  $-\frac{\Delta \mu}{\mu} / \frac{\Delta a W_0}{a W_0}$  (which are straight lines parallel to the abscissa) we get the values of  $B_{\sim}$  and  $H_0$  at which  $\frac{\Delta \mu}{\mu} / \frac{\Delta B}{B}$  and  $-\frac{\Delta \mu}{\mu} / \frac{\Delta a W_0}{a W_0}$  remain constant. Figure 3 shows  $\frac{\Delta \mu}{\mu} / \frac{\Delta B}{B} = C_1$  and  $\frac{\Delta \mu}{\mu} / \frac{\Delta a W_0}{a W_0} = C_2$  in  $(B_{\sim}, H_0)$  coordinates. The intersection of the  $\frac{\Delta \mu}{\mu} / \frac{\Delta B}{B} = C_1 = F_3(B_{\sim}, H_0)$  and  $-\frac{\Delta \mu}{\mu} / \frac{\Delta a W_0}{a W_0} = C_2 = F_4(B_{\sim}, H_0)$  when curves at  $C_1 = C_2$  gives a line which is the locus along which a simultaneous 10% change in induction (ac induced) and dc magnetization (magnetizing current) produces no change in permeability. This line divides the  $B_{\sim}, H_0$  plane into two zones: I and II (Fig. 3).

In zones I and II the relative permeability changes due to simultaneous changes in the ac and dc currents are of opposite signs. In zone I the relative permeability changes due to the ac changes are greater than those due to changes in the magnetizing current, while in zone II the converse holds.



The curve  $\frac{\Delta \mu}{\mu} / \frac{\Delta B}{B} = 0$  is the locus along which the permeability change due to a 10% change in induction is zero; this separates zone III. In zone III the permeability changes due to changes in the ac and dc currents are of the same sign.

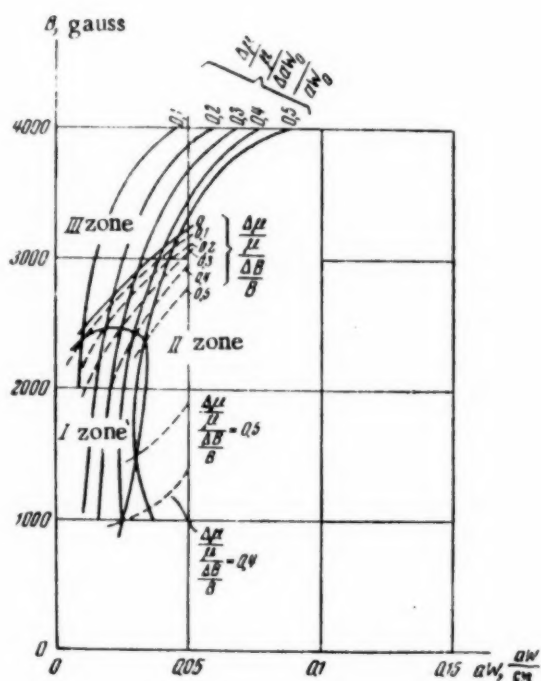


Fig. 3. Curves of equal relative increase in permeability on a 10% change in magnetization,  $\frac{\Delta \mu}{\mu} / \frac{\Delta a W_0}{a W_0}$ , and on a 10% change in induction,  $\frac{\Delta \mu}{\mu} / \frac{\Delta B}{B}$ .

to be at the boundary of zones I and II. All four coils will then change in inductance when the magnetizing dc and ac currents alter simultaneously by amounts that are smaller than under any other circumstances. This usually implies a large increase in initial magnetization and a reduction in induction, which reduces the sensitivity of the null detector.

If the working point cannot be set at the boundary between zones I and II, zero displacements can be balanced-out in zone I by using a saturated choke Ch in series with the full-wave bridge rectifier (Fig. 4). Since the choke is saturated its over-all impedance depends on the supply voltage. Hence, the magnetizing current alters more rapidly than simple proportionality to the supply voltage would imply. The zero displacement due to change in the dc magnetization increases and balances out that due to supply voltage change. The zero shift in magnetic null detectors can therefore be reduced by about a factor 4 even when the coil characteristics are very different.

When the magnetic amplifier is operated in zone III zero shift can only be eliminated by selecting coils of identical magnetic characteristics.

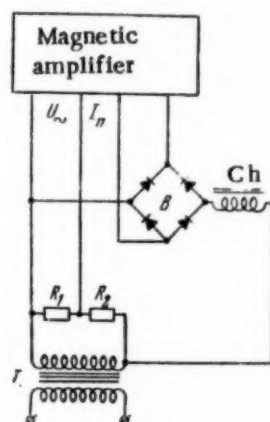
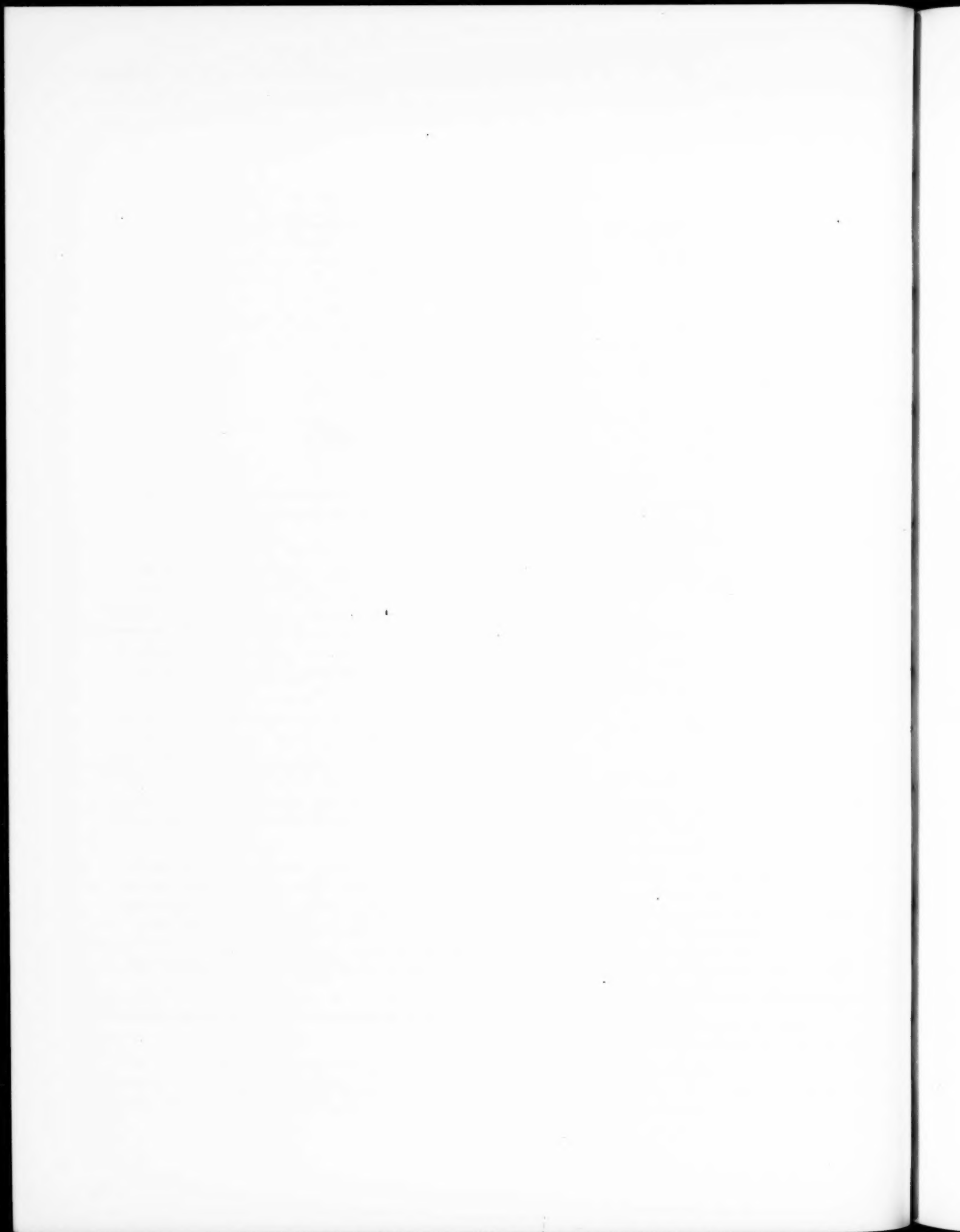


Fig. 4. Circuit for balancing-out zero shift on working in zone I.

Since slight differences in the inductances suffice to shift the zero, it is found in practice that such slight differences do not cause any material differences between the values of B and  $(a W_0)$  corresponding to the boundaries of zones I and II for the separate coils.

When the magnetizing circuit is fed from the ac supply via a rectifier the operating region should therefore be chosen



# DETERMINATION OF HYDRAULIC LOSS COEFFICIENTS IN THROTTLE RESISTANCES IN HYDRAULIC SYSTEMS

I. N. Kichin

(Moscow)

A method based on experimental data is given for determining hydraulic loss coefficients in hydraulic system throttle resistances of sleeve or block type.

Throttle resistances of designs such as that shown in Fig. 1 are used to restrict the flow of working fluid in hydraulic systems, including automatic regulators.

The resistance dimensions and flow regime are frequently such that the fluid flows under laminar flow conditions. The input profile has a considerable influence on this.

The formulas available for established laminar or turbulent flow cannot be applied to such resistances. But, as will be shown below, when laminar flow has not been established, Weisbach's universal formula can be used:

$$\Delta P = k \frac{v^2}{2g} \gamma, \quad (1)$$

where  $k$  is a general hydraulic loss coefficient which allows for both local and viscous resistances. We only have to assign a definite value to  $k$ .

TABLE 1

Resistance	d, cm	l, cm	l/d	Resistance	d, cm	l, cm	l/d
1	0.12	0.08	0.66	18	0.04	2.0	50
2	0.12	0.36	2.8	24	0.04	4.0	100
3	0.10	0.08	0.8	14	0.035	0.09	2.57
4	0.10	0.29	2.9	19	0.035	1.0	28.5
5	0.08	0.03	0.37	23	0.035	2.0	58
6	0.08	0.192	2.4	25	0.035	4.0	114
7	0.075	0.018	2.4	16	0.03	0.083	2.67
8	0.06	0.03	0.5	17	0.03	0.5	16.5
9	0.06	0.15	2.5	22	0.03	1.0	33.3
10	0.06	0.5	8.0	26	0.03	2.0	67
12	0.06	1.0	16.1	20	0.02	0.06	3.0
15	0.06	2.0	32.2	21	0.02	0.5	25
11	0.05	0.13	2.6	27	0.02	1.0	50
13	0.04	0.1	2.5				

$k$  may be represented as a single-valued function of  $\frac{l}{l_1}$ , where  $l$  is the working channel length in the coil, and  $l_1$  is the length of the initial laminar flow region,  $0.05 d Re$  [1], and so

$$\frac{l}{l_1} = \frac{l}{0.05 d Re} \quad (2)$$

where  $Re$  is Reynold's number for the channel flow and  $d$  is the channel diameter.

The dimensions of the 27 resistances tested are given in Table 1 [3].

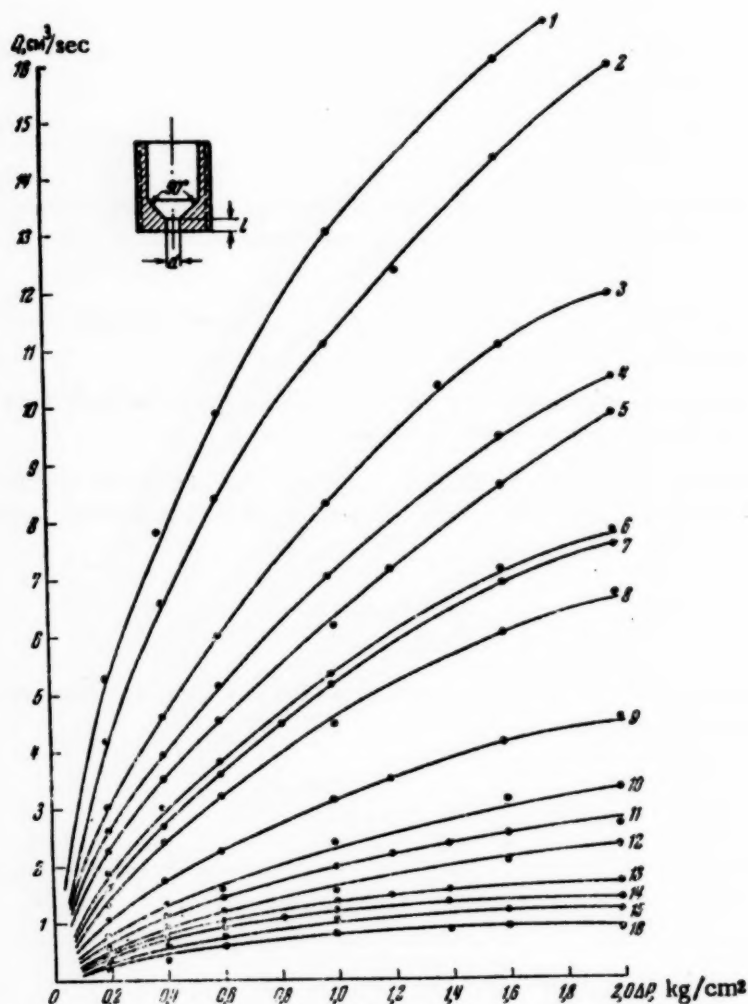


Fig. 1

Transformer oil of kinematic viscosity  $\nu = 27 \times 10^{-2}$  stokes and density  $\gamma = 0.876 \text{ g/cm}^3$  was used. The pressure drop across the throttle was varied from 0 to 2  $\text{kg/cm}^2$  by steps of 0.2  $\text{kg/cm}^2$  during the tests. The efflux variation with pressure drop across the resistance is shown in Figs. 1 and 2, the horizontal axis being the pressure drop and the vertical the volume efflux.  $k$  and  $l/l_1$  were determined for sixty points on the characteristics, using (1) and (2) where  $v_{Av} = \frac{4Q}{\pi d^2}$  and  $Re = \frac{v_{Av} d}{\nu}$ . Figure 3 shows the relation  $k = f(l/l_1)$ , (Curve 1), which is a single curve for all the resistances tested under these conditions.

$k$  (the hydraulic loss coefficient) is made up of local losses, defined by  $k_1$ , and viscous losses,  $k_2$ . For  $k_1$  we used the relation to  $l/l_1$  calculated from the Shiller-Bussinesk theory\* (Curves 6 and 7 of Fig. 3).

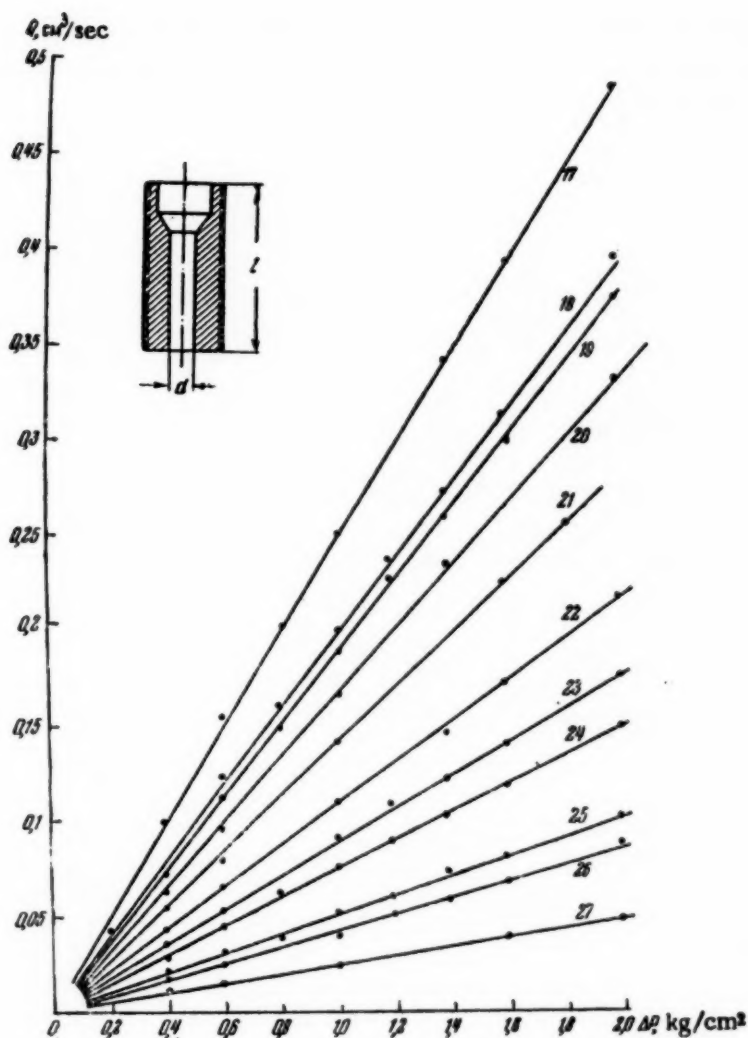


Fig. 2

$k_2$  is determined from

$$k_2 = \frac{48}{\text{Re}} \frac{l}{d},$$

which is derived from experiments on resistances with  $l/d > 16$  in which the local losses were enormously less than the viscous loss (Curve 3). Curve 8 is the sum of  $k_1$  and  $k_2$ . In the initial section  $\left(0 < \frac{l}{l_1} < 1\right)$  the curve agrees closely with 1, but when laminar flow is established  $\frac{l}{l_1} > 1$  the two

\* Data taken from [2].

part company. If we use the law

$$k_2 = \frac{\Lambda}{\text{Re}} \frac{l}{d}.$$

to determine  $k_2$ , where  $\Lambda$  is 64 from Poiseuille's law for a laminar flow regime, but is greater than 64 if calculated from the data of [2] as a function of  $\frac{l}{l_1}$  (the corresponding curves for  $k_2$  being Nos. 4 and 5 in Fig. 3), then on adding  $k_2$  and  $k_1$  (Curves 6 or 7) we get 2, from which we see that the hydraulic losses exceed the computed ones (Curve 1) by about 25% on the average.

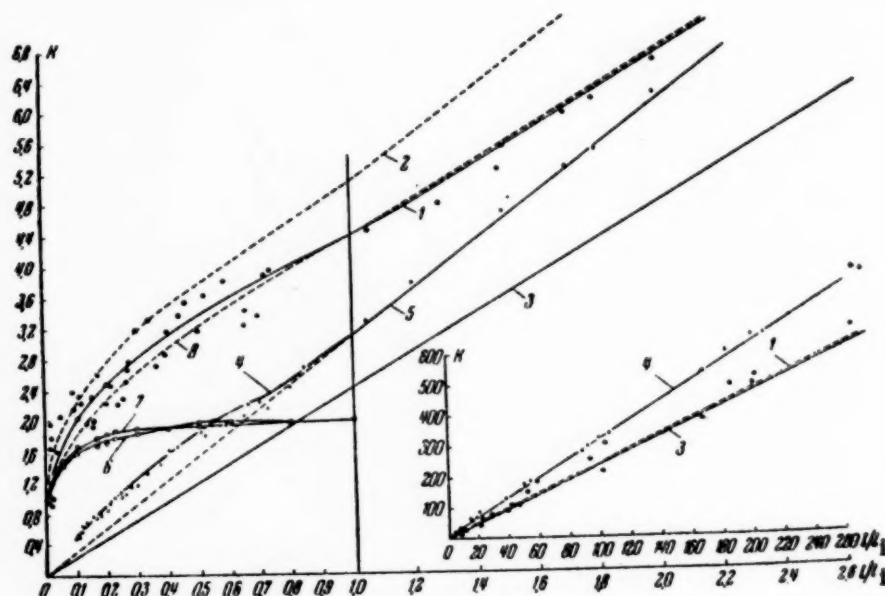


Fig. 3

TABLE 2

Data	Assembly					
	1	2	3	4	5	6
$d$ , cm	0.06	0.06	0.08	0.1	0.06	0.12
$l$ , cm	0.03	0.15	0.03	0.08	0.08	0.08
$L$ , cm	0.05	0.2	0.05	0.08	0.08	0.08
$n$	100	80	100	50	40	40

The use of Curve 1, Fig. 3, can be illustrated by the following example. A throttle with  $d = 0.06$  cm,  $l = 0.5$  cm gave  $Q = 2.5$  cm<sup>3</sup>/sec, the kinematic viscosity of the working fluid being 0.3 stokes and the density 0.876 g/cm<sup>3</sup>. The pressure drop in the channel is to be calculated. We have

$$l_1 = 0.05 d \text{Re} = \frac{0.2Q}{\pi v}, = 0.568 \text{ cm};$$

$$l/l_1 = 0.855.$$



From the graph we find  $k = 4.05$ ; from (1), assuming  $v_{AV} = \frac{4Q}{\pi d^2}$ , we have  $\Delta P = 1.36 \text{ kg/cm}^2$ .

The graph can also be used for calculations on so-called throttle assemblies (Fig. 4) which are made up of a series of identical nozzles with chamfered ends. The hydraulic losses in each nozzle are independent of the total number of nozzles and determined as a function of  $\frac{l}{l_i}$ . As the internozzle resistances are identical the total hydraulic losses in each are increased by the amount of the additional losses caused by turbulent flow in the nozzle-separator gaps, viscous friction in the gaps, etc.

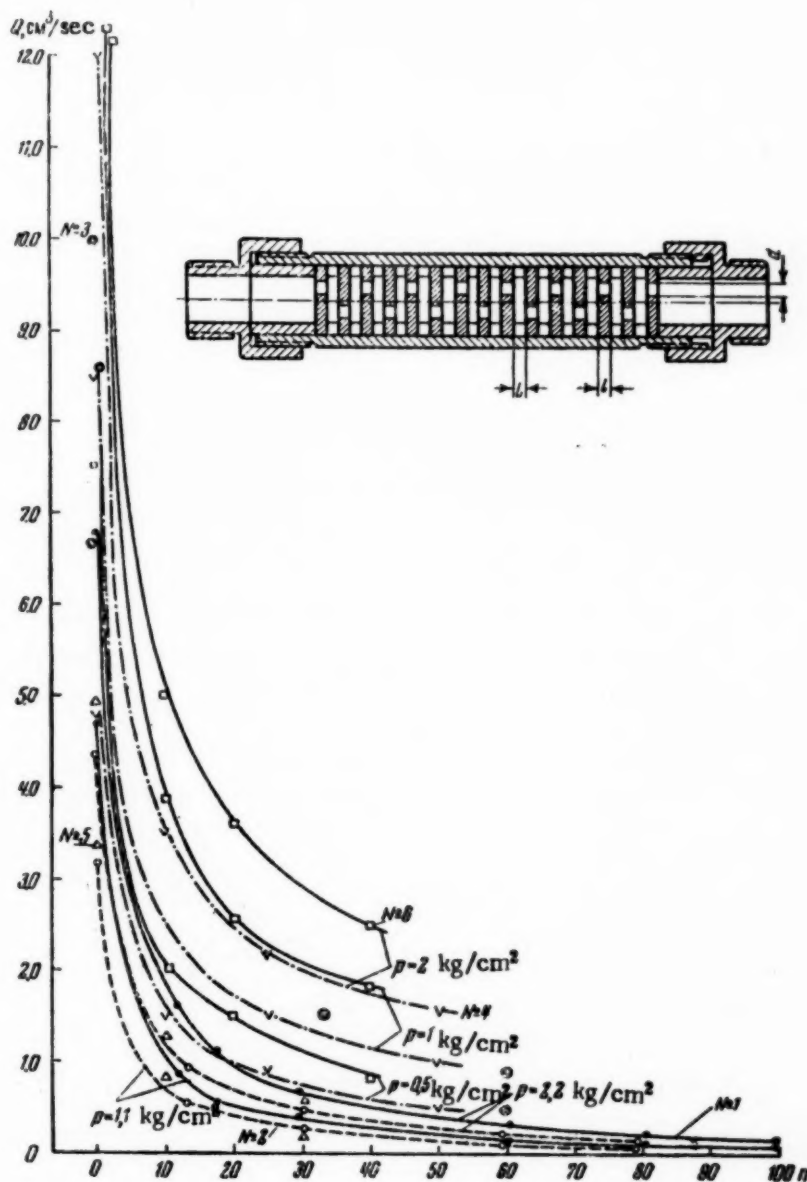


Fig. 4

The total hydraulic losses for a single nozzle can be found from (1), where  $\Delta P$  is taken as the pressure drop. The total loss in the assembly is equal to the sum of the individual losses.

Five assemblies were tested — the dimensions of these are given in Table 2.\*

Transformer oil was used ( $\nu = 27 \times 10^{-2}$  stokes,  $\gamma = 0.876$  g/cm<sup>3</sup>). The effluxes at pressure drops of 2.0-2.2, 1.0-1.1 and 0.5 kg/cm<sup>2</sup> were measured as a function of the number of nozzles used; the results are given in Fig. 4.

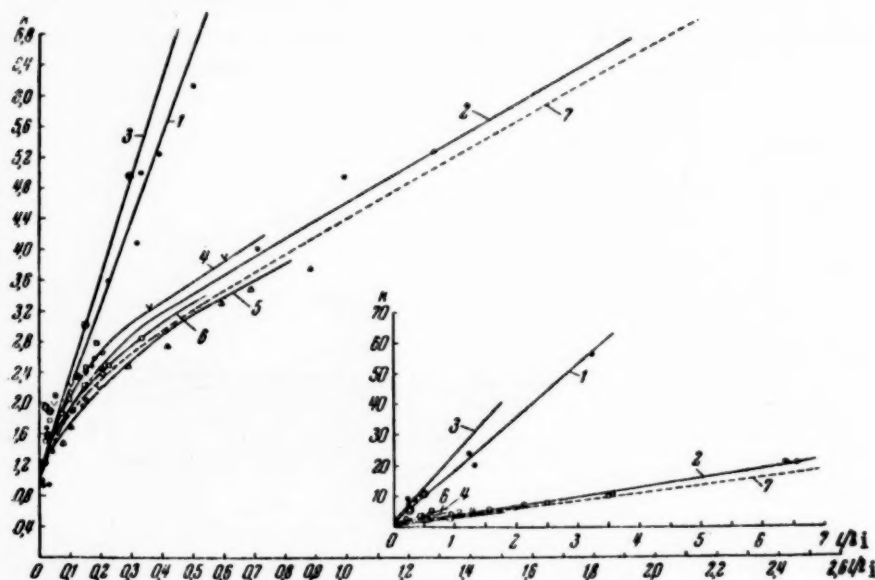


Fig. 5

The values of  $k$  and  $\frac{l}{l_i}$  were determined for a single hydraulic resistance in all assemblies using (1) and (2) for each test regime. The results are shown in Fig. 5. For each nozzle in an assembly of given geometry (Nos. 2, 4, 5, and 6) the resistance was independent of the number of nozzles under all conditions, giving a single curve (the individual curves being numbered 2, 4, 5, and 6, respectively) falling close to 7, which corresponds to Curve 1 of Fig. 4. The deviation of Curves 1 and 3 (corresponding to the resistances of assemblies (Nos. 1 and 3) from 7 is caused by the additional viscous losses occasioned by reducing the inter-nozzle distances  $L$  in these assemblies.

#### LITERATURE CITED

- [1] L. Prandtl, and O. Titens, Hydro- and Aerodynamics, ONTI, 1953.
- [2] N. Z. Frenkel, Hydraulics, Power Press, 1947.
- [3] A. G. Shashkov, Experimental and Theoretical Studies of Throttle Components and Hydraulic Relays of Nipple-Slide Type Operating on Oil, Dissertation, Institute of Automation and Remote Control, USSR Academy of Sciences, 1955.

Received March 5, 1956.

\* The test data for assembly No. 6 are reproduced from [3].

# SOME ASPECTS OF PNEUMATIC EXTREMUM CONTROLLER DESIGN

L. A. Zalmanzon

(Moscow)

Conditions are indicated under which it is desirable to supplement controllers of normal type by automatic adjustment to the maximum or minimum of some quantity dependent on the controlled parameter. One possible way of doing this, by means of pneumatic devices, is considered; automatic adjustment is performed by a pneumatic device consisting of a pneumatic divider coupled to a system of parallel and intersecting pipes, together with certain other units.

Very great attention has latterly been given to extremum controls which automatically maintain the value of  $x$  corresponding to an extremum of some quantity  $y$  related to  $x$  by the curve shown in Fig. 1, a and b. V. V. Kazakevich was the first to produce such a controller in this country [1]. A number of peak-holding controller designs have been described in recent years [2-7]. Electrical circuits have been used in such controls as have so far been described, but pneumatic and hydraulic principles can also be used.

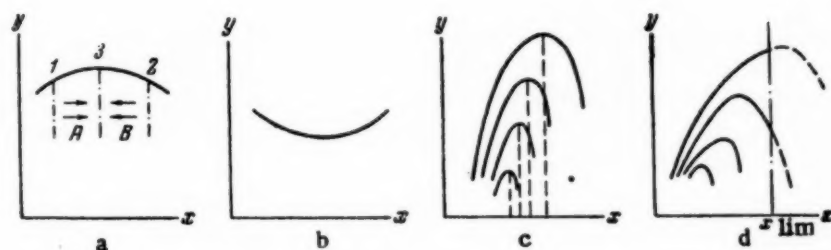


Fig. 1

In many cases no real difficulty is encountered in using extremum controllers. But great or insuperable difficulties are sometimes encountered. Then it is sometimes possible to use normal controllers (operating on  $x$ ) modified so as to maintain the extremum of  $y = f(x)$  automatically. Certain aspects of this problem are dealt with below.

1. In principle an extremum process controller involves self-maintained oscillations in the controlled object. The oscillation amplitude becomes larger the flatter the peak in  $y = f(x)$ . The conditions of operation frequently require that deviations from a steady-state mode must be of short duration, prolonged oscillation being impermissible. E. g., when internal combustion engines are controlled so as to maintain the minimum specific consumption  $c_{spec}$  it is not permissible to vary the speed  $n$  continually with an amplitude of several hundred rpm, which happens when the  $c_{spec} = f(n)$  characteristic is very flat.

2. An essential condition for using a peak-holding controller is that  $y = f(x)$  should show an extremum. The absolute values of  $y_{\max}$  or  $y_{\min}$ , and the corresponding values of  $x$  may alter (Fig. 1, c). But it may happen that some one of the family of curves may be monotonic, and that this is not known in advance. Extremum controllers cannot be used in such doubtful cases. This problem may arise, for instance, when one has to combine control of the extremum in  $y = f(x)$  with restriction of  $x$  to some limiting value  $x_{\lim}$  (Fig. 1, d).

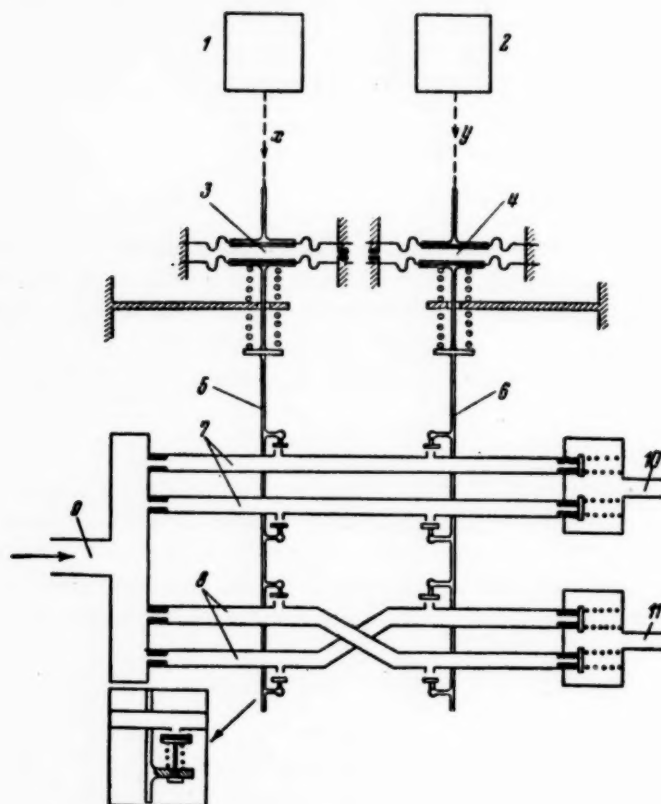


Fig. 2

3. One shortcoming inherent in extremum regulators is that the mean value of  $y$  during the control process is less than  $y_{\max}$  or greater than  $y_{\min}$ , i.e., it is in principle impossible to avoid deviations from the most favorable condition, and the losses associated with this.

4. In some cases the extremum controller is required to operate intermittently. In addition the position of the maximum in  $y = f(x)$  moves so slowly with time that one can work at  $y_{\max}$  or  $y_{\min}$  by using a normal controller set at a definite value of  $x$ , the setting being changed from time to time. The time intervals between resetting may range from seconds or minutes to hours or days. The latter is the case, for instance, for control of internal combustion engines, where the conditions change with atmospheric pressure or temperature, on replacing the fuel, etc.

5. If extremum controllers cannot be used for the reasons stated in 1 and 2 above, and when conditions such as were indicated in 4 prevail, normal controllers operating on  $x$  can advantageously be supplemented by automatic control of the value of  $x$  which gives a maximum or minimum value of  $y$ . When such an automatic controller is cut in accordance with a definite time cycle, or in some other way, the regulator operating on  $x$  must have its operating point shifted by a definite amount in the directions indicated by the arrows A and B in Fig. 1, a (from position 1 or 2 to 3).

A wider consideration must be given to the problem of accompanying peak-holding controllers operating on  $y = f(x)$  with controllers operating on  $\underline{x}$  as a way of improving the control speed, as opposed to the use of extreme controllers alone. In this way, we endeavor to eliminate sustained oscillations in the system, to reduce losses due to deviation from the most favorable mode, as noted in paragraph 3 above, and to approach the turning point from one side without ever passing to the other branch of the curve.

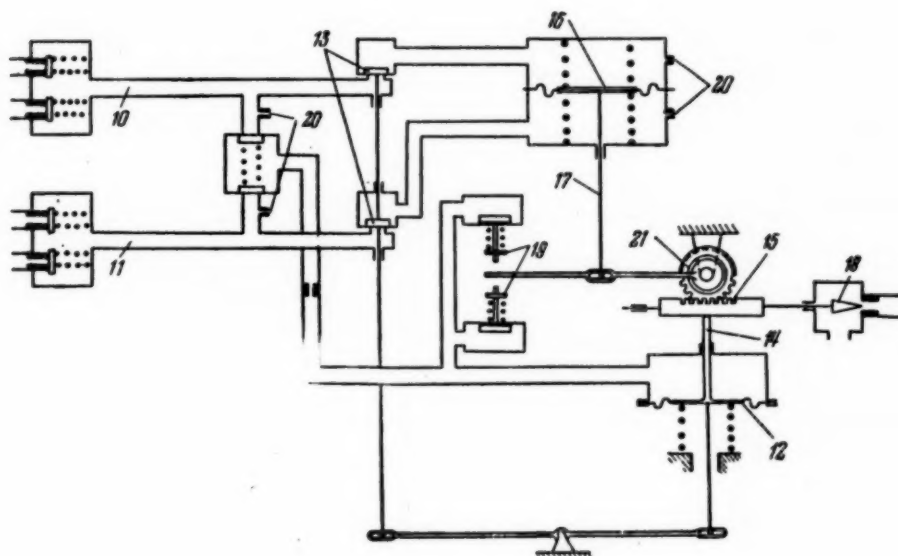


Fig. 3

6. One possible way of realizing the automatic adjustment envisaged in 5 above is to use the pneumatic divider with parallel and intersecting channels shown in Fig. 2. Each time the automatic adjuster is cut in,  $\underline{x}$  is altered (and hence  $\underline{y}$  also) for a short period. The sensing elements 1 and 2 are also cut in, these measuring the deviations from the initial values of  $\underline{x}$  and  $\underline{y}$  respectively. The movements of 1 and 2 are transmitted via the pneumatic dampers 3 and 4 to the rods 5 and 6. The rods carry caps which cover either the upper or the lower holes in the channels 7 and 8, depending on the direction of movement. If  $\underline{y}$  increases or decreases with  $\underline{x}$  (left branch in Fig. 1, *a*) the caps on the rods close the holes in one of the pair of channels 7, and pressure is transmitted from the feed tube 9 to channel 10, which causes the  $\underline{x}$  regulator to be displaced in a direction corresponding to A in Fig. 1, *a*. If  $\underline{y}$  falls as  $\underline{x}$  increases, or vice versa (right branch in Fig. 1, *a*) the caps close the holes in one of the pair of channels 8 and pressure is transmitted from 9 to 11, which causes the  $\underline{x}$  regulator to be displaced in a direction corresponding to B in Fig. 1, *a*. If the system is initially close to the extreme point the change in  $\underline{x}$  may be accompanied by changes in  $\underline{y}$  so small that they fall within the insensitive range of 2. This may occur, for instance, when  $f(x)$  is flat. The setting of the  $\underline{x}$  regulator will then be unaltered.

7. When resetting the  $\underline{x}$  regulator it may be important to move the reset device through a definite distance during each reset cycle. This can be done by means of the device shown in Fig. 3. When the pressure in 10 or 11 is raised (symbols as in Fig. 2) the pressure is transmitted to the membrane 12, thus lifting the valves 13 and releasing the clamp 14, and thereby the rack 15. The membrane 16 will displace the rod either downward or upward, depending on whether the pressure appears in 10 or 11, and the reset device will be displaced in the appropriate direction — in Fig. 3 this reset device is the throttle needle 18. The magnitude of the displacement is restricted by the release valves 19 in one channel. The pressure above the membrane 12 is thereby reduced, the clamp 14 operates and the valves 13 drop into place. As there are bleed holes 20, atmospheric pressure is restored until the next operating cycle. The rod 17 is returned to its initial position by the spring, the rack 15 being fixed due to the action of the friction plate 21.



8. The automatic setting unit can now be combined with a normal regulator in a simple fashion. Figure 4 shows the comparator element in a pneumatic regulator, in which air compressed to a pressure corresponding to the current magnitude of the regulated quantity is supplied to the chamber above the membrane 22 via channel 23, while the pressure from the setting unit is applied underneath the membrane. The cam 24 cuts in the automatic setting unit which removes the cover 25 for a short while, thus briefly altering the regulated quantity. The needle 18 is displaced one step by the operation of the automatic setter, this needle throttling the air flow from the output of the chamber under membrane 22.

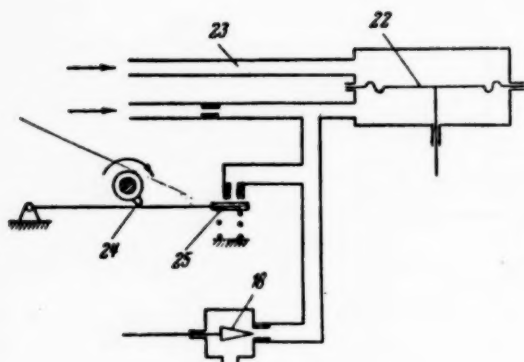


Fig. 4

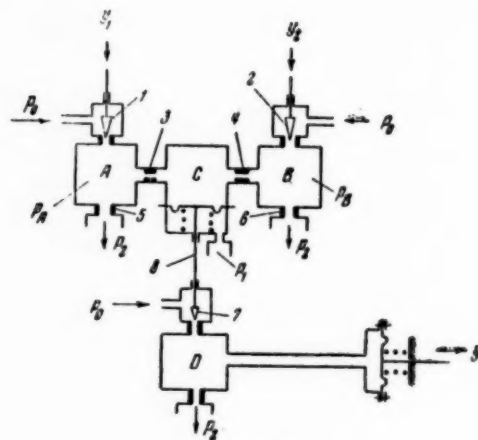


Fig. 5

If  $y_{\max}$  (Fig. 1, a) is maintained by the automatic regulator, and it is desired to use it to adjust  $y_{\min}$  (Fig. 1, b), we only need alter the points where the channels join at the output from the distributor. If  $y = f(x, u, v, \dots)$  and the parameters  $x, u, v, \dots$  are independently controlled, we may by successive operations set  $y$  as a maximum or minimum for all the parameters.

9. Technical difficulties may sometimes arise in using both extremum controllers and the automatic adjustment devices described above, due to the complexity involved in measuring  $y$ .  $y$  is frequently a derived quantity not susceptible of direct measurement, and is derived as products or ratios of simple quantities, or as powers (including fractional ones) of several primary quantities  $y_1, y_2, \dots, y_n$  which are susceptible of measurement. For instance, the power  $N = cMn$ , where  $M$  is the torque,  $n$  is the rpm, and  $c$  is a coefficient of proportionality; the specific fuel consumption is

$$C_{\text{spec}} = \frac{G}{N} = c \frac{G}{Mn},$$

where  $G$  is the fuel consumption in kg/hour; the flux of a gaseous product is  $G = c \sqrt{\Delta p \frac{p}{T}}$ , where  $\Delta p$  is the pressure drop across the measuring diaphragm,  $p$  and  $T$  are the pressure and temperature in front of the diaphragm, etc. One design of multiplication unit that can be used in such cases is shown in Fig. 5. It contains pneumatic (or hydraulic) chambers A, B, C, and D. A constant pressure  $p_0$  is supplied to the inputs of chambers A, B, and D. The pressure  $p_2$  at the outlets from these chambers is also constant, as well as  $p_1$  in the chamber under the membrane, all pressure being referred to this (in this particular case  $p_1$  can be atmospheric pressure). The needles 1 and 2 are displaced by the changes in  $y_1$  and  $y_2$  (primary parameters). The needles are so shaped that  $p_A$  is proportional to  $\log y_1$ , while  $p_B$  is proportional to  $\log y_2$ . The holes 3 and 4 are so small by comparison with 5 and 6 and with the annuli round 1 and 2 that the loss via C scarcely influences  $p_A$  and  $p_B$ . The pressure in C is then proportional to  $\log(y_1, y_2)$ , and the pressure in D, which is similarly throttled by the profile needle 7, is proportional to  $y = y_1 y_2$ .  $y_1$  and  $y_2$  can be included in the compound function when raised to any power (including fractional ones). If  $y$  is a function of more than two



parameters, several units similar to those shown in Fig. 5 are coupled as follows: D is absent in the first unit and the output rod 8 is coupled to needle 1 of the subsequent unit, etc. For example, to derive  $G = c \Delta p \frac{p}{T}$  two units are needed, since  $\log \frac{G}{c} = \frac{1}{2} \log \Delta p + \frac{1}{2} \log p - \frac{1}{2} \log T$ . With suitable needle profiles and appropriate choice of  $p_1$  (with respect to which all other pressures are reckoned) both positive and negative powers greater or less than unity can be accommodated.

#### LITERATURE CITED

- [1] V. V. Kazakevich, Extremum Control, Dissertation, Moscow Technical College, 1945.
- [2] Y. T. Li, Optimizing Systems for Process Control, Instruments, Vol. 25, Nos. 1-3, 1952.
- [3] H. S. Tsien, S. Serdengecti, Analysis of Peak - Holding Optimizing Control, JAS Vol. 22, No. 8 (1955).
- [4] H. S. Tsien, Engineering Cybernetics, New York McGraw-Hill, 1954.
- [5] R. Shull, An Automatic Cruise Control Computer for Long Range Aircraft, Trans. IRE, Professional Group of Electronic Computers, Dec. 1952.
- [6] O. G. Ivakhenko, Problems of Extremum Control, Automation (Acad. Sci. Ukrainian SSR) No. 3, 1956.
- [7] Yu. I. Ostrovsky and M. G. Eskin, An Extremum Control for Turbine Oil-Well Boring, Automation and Remote Control 17, 9 (1956).

Received March 12, 1956.



# COMMENTS ON A. V. MAIOROV'S ARTICLE "RAISING THE OPERATIONAL SAFETY OF AUTOMATIC CONTROLS"

(AUTOMATION AND REMOTE CONTROL, VOL. 16, NO. 5, 1955)

V. A. Andryushchenko

(Leningrad)

If the operational safety of automatic controls is to be increased then the most rational layout must be used, as well as consideration being given to the safety aspects of all major components.

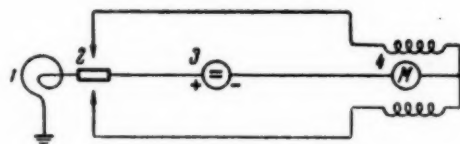


Fig. 1. 1) Bimetal; 2) contact system; 3) dc source; 4) effector mechanism.

Let us consider this question, following Maiorov, as regards electrical aircraft regulators.

Space restrictions in aircraft compel one to use compact units most advantageously arranged. Hence, Maiorov's block diagrams (Figs. 1-4) can be given several different layouts. We shall deal with one of these.

The circuit of Fig. 1 does not give type one consequences if damaged at any point. This circuit could be arranged as in Fig. 2. If a short-circuit

occurs at A, or a metal sheet  $a$  —  $a$  cuts the conductors and shorts the cut ends, the effector mechanism will receive a false signal, which results in type one consequences.

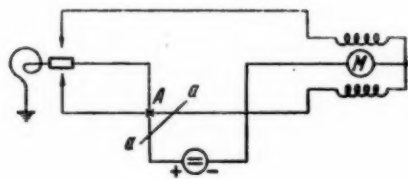


Fig. 2

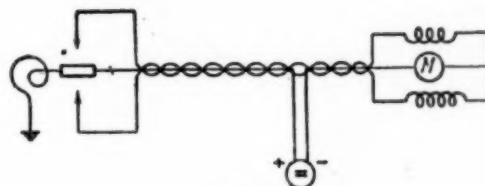


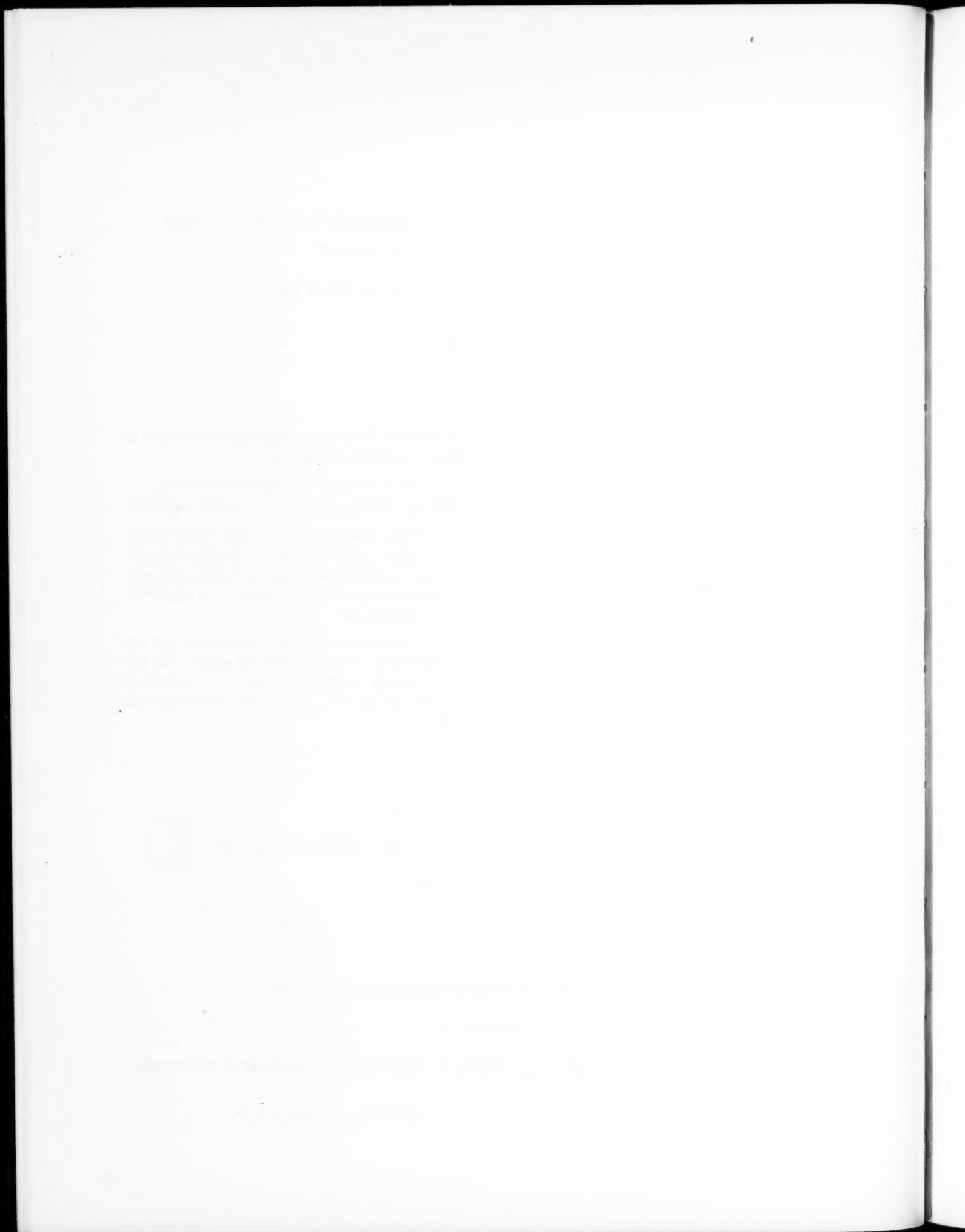
Fig. 3

The probability of this happening is still greater in the arrangement shown in Fig. 3.

## SUMMARY

Attention must be paid to circuit layout when seeking to increase the operational safety of automatic controls.

Received February 2, 1956.



## CHRONICLE

### AUTOMATIC CONTROL CONGRESS IN HEIDELBERG

#### 1. Congress Membership

An Automatic Control Congress took place from the 25th to the 29th of September, 1956 in Heidelberg. It was organized by an automatic control group (Fachgruppe Regelungstechnik - Dr. Grebe, President) which is a member of the German Union of Electrotechnicians and Engineers (VDE/VDI).

The Congress was international in character due to the number of participants and the countries represented.

Famous scientists in the field of automation were gathered at the Congress. Among them we can mention Tastin, Westkott (Great Britain), Oppelt, Oldenburg, Sartorius, Shuller, Magnus, Leonard, Sheffer, Grebe (Germany), Yansen (Holland), Shtein (Italy), Novatsky (Poland), Chestnut, Oldenburger (U.S.A.), Gerekke (Switzerland), Khamosh (Sweden), Skayashi, Isava (Japan), Shalomon (Czechoslovakia) and others.

The largest delegations (numbering over 10 members) were sent from Switzerland, Sweden, Great Britain, Holland, U.S.A., Czechoslovakia and Austria. It was natural that the majority of the Congress members were specialists from the Federated German Republic. Among them were practical engineers, representatives of various firms, and theoretical engineers from various scientific-research institutes, among them institutes concerned with aviation problems and other specialized types of automation.

Representatives from other countries came from the most outstanding scientific research centers, among which we can mention Massachusetts Institute of Technology, Columbia University (U.S.A.), Imperial College of Science and Technology (Great Britain), and others.

The number of reports presented by each country is given in the table below.

Country	Number of reports	Country	Number of reports
Austria	1	USSR	6
Great Britain	7	USA	14
Germany	26	Switzerland	4
Holland	1	Sweden	3
Italy	1	Japan	4

Our country was represented by a delegation from the Institute of Automation and Remote Control, Academy of Sciences of the USSR made up of Professor A. M. Letov (the head of the delegation), Professor Ya. Z. Tsypkin, Candidate of Technical Sciences, B. N. Naumov, Engineer V. A. Racheev. In addition to the reports of Professor A. M. Letov, Professor Ya. Z. Tsypkin and Candidate of Technical Sciences B. N. Naumov, reports were also given by the Corresponding Member of the Academy of Sciences of the USSR V. A. Trapeznikov and Candidate of Technical Sciences B. Ya. Kogan, Professor M. A. Aizerman, Professor V. V. Solodovnikov and Asp. A. M. Batkov. A report by Corresponding Member V. A. Trapeznikov and Candidate of Technical Sciences B. Ya. Kogan on problems of electronic models was included in the plenary reports; the other reports were given at the meetings of the various sections.

The basic tasks of our delegation were as follows: a) participation in the work of the present Congress; b) establishment of scientific contacts with foreign scientists and engineering and technical circles represented at the Congress; c) visiting of certain firms.

Our participation in the work of the Congress included: a) the presentation of our own reports, answering questions and participation in discussions; b) participation in the discussion of reports presented by members of other countries.

## 2. Organization and Work of the Congress

The actual organization of the Congress, well planned and carried out by the organizing committee of VDE/VDI under the direction of Dr. Grebe was particularly interesting. The Congress took place in a building of the Heidelberg University under the title "Contemporary theories and their Usefulness." Long before the meetings were held, the organizing committee of the Congress sent out invitations to various countries to attend the Congress on Automatic Control. Included with the invitation was a request for the names of members who would give papers, together with a text of the paper, to be sent to the organizing committee for preliminary publication.

Thus, approximately 70 original scientific reports were gathered together. These were preprinted and sent out to the participants a month and a half or two months before the opening of the Congress.

This enabled the participants to become acquainted with the content of the reports in all their details, (including the checking of calculations and results of experiments) and thus guaranteed their active participation in discussions. This greatly affected the content of the discussions and rendered them particularly fruitful.

The work of the Congress began on the 24th of September with an evening meeting of the speakers and the organizing committee.

The order of the plenary sessions and the sectional meetings were officially announced here. Unofficially the directors of the Congress, speakers and other guests had an opportunity to meet and discuss the scientific content of the reports. The work of our delegation was here fully discussed.

The Congress opened at 9 A. M. on Tuesday, September 25, 1956 in the conference hall of the University of Heidelberg.

Dr. Grebe and Professor Klaus Sheffer of the University of Heidelberg addressed the gathering and wished the Congress success in its work.

Professor Oldenburger (USA) read a message to the Congress on behalf of ASME. Then Professor A. M. Letov greeted the Congress in the name of the Institute of Automation and Remote Control of the Academy of Sciences of the USSR.

Following the preliminary remarks the plenary reports were read, which took up the first half of the day. After an intermission the section meetings were begun. Eleven sections were organized.

1. Technical means of automation - Chairman Dr. Oetker (5 reports).
2. Coupled control - Chairman Dr. Magnus (3 reports).
3. Linear methods in the theory of control - Chairman Dr. Oppelt (7 reports).
4. Automatic transmission - Chairman Dr. Gutarev (5 reports).
5. Determination of nonlinear processes by means of frequency methods - Chairman Dr. Pestel (5 reports).
6. Nonlinear and intermittent systems of control - Chairman Dr. Khan (5 reports).
7. Boiler control - Chairman Dr. Kuak (4 reports).
8. Optimal adjustment and quality control - Chairman Dr. Sartorius (8 reports).
9. Control in industry - Chairman Dr. Shturm (7 reports).
10. Statistical methods in control - Chairman Dr. Sheffer (7 reports).
11. Calculating machines in control techniques - Chairman Dr. Kremer (8 reports).

Thus, the sections covered a great number of questions in the field of contemporary control theory. Among the new problems discussed were: the use of nonlinear elements and calculating devices in control systems



(Matyushka, Ludwig); application of computers to the calculation of automatic systems (Khamosh, Bukovich); determination of dynamic characteristics under normal working conditions (Gudmen, Resvik, Chang, Westkott). A great number of the reports dealt with the analysis of specific automatic systems.

As a rule, several sections met simultaneously. Section No. 6 where the reports of the Soviet delegation to the Congress were read, met in the conference hall, so that all the Congress members had the opportunity to be present.

The sum total of all the reports presented by the Academy of Sciences, USSR and the high valuation given them in discussion by members of the Congress, enabled Dr. Grebe in his radio address to express the belief that the theory of automatic control had reached a high level of development in the Soviet Union. Dr. Grebe likewise emphasized the high level of the development of automatic control theory in the USA. Dr. Grebe also felt that country had more widely applied theoretical results to practice. He paid special attention to the introduction of calculating machines into automatic control.

In reference to the Federated German Republic, Dr. Grebe mentioned certain initial successes and stated that in the field of theory and technology it would soon join other leading countries. This is indicated by the large number of talented young people attracted to that field. In order to attract even more young people to the problems of automation Dr. Grebe suggested a higher level of instruction in the primary and middle schools in the natural science field. Under such conditions, young people finishing school would be better able to determine the future sphere of their scientific-technological activity.

This great interest in the theory and technology of automatic control, which is shown at the present time in the Federated German Republic, is due to a German effort toward industrial automation.

The work of the sections continued through the 29th of September. Our delegation took part in this work and in the discussions of the reports of foreign scientists.

Thus, Professor Ya. Z. Tsytkin took part in the discussions of the reports of Dr. Matyushka (Federated German Republic) "Application of Nonlinearity to the Improvement of Quality Control," Dr. West (England) "Application of Frequency Analysis to Nonlinear Systems," Professor Klotter (USA) "Application of a Descriptive Function to the Study of Nonlinear Closed Systems," Professor Nomoto (Japan) "Computation of Feedback Systems by Means of a Logarithmic Root Hodograph," Dr. Kühne (Federated German Republic) "Example of a Calculation of an Aperiodic Boundary Case in a Control Process."

Professor A. M. Letov took part in the discussion on the reports of Dr. Breto (USA) "Simplified Analysis of the Longitudinal Stability of Aircraft," Dr. Khamosh "Frequency Method for the Study of Nonlinear Systems."

Outside of the section work, scientists of various countries often met during intermissions between sessions for the discussion of various scientific problems. Such discussions were carried out with Professor Klotter, Professor Magnus, Dr. Bess (on the problems of nonlinear theory of control) with Professor Detch, Dr. Oldenburg, Dr. Sartorius (on the theory of pulse systems and the theory of differential equations), with Dr. Kalman and Dr. Bess (on the theory of nonlinear, and in particular, relay systems). These discussions greatly helped the formation of close scientific contacts with foreign scientists.

The two days following the close of the Congress, October 1 and 2, were given over to technical excursions to apparatus building firms. A special plan was worked out for our delegation by the organizing committee, taking into account our particular interests. We visited the Siemens works in Karlsruhe, the IBM factories in Stuttgart, the AEG in Berlin and others.

### 3. Proposal for an International Federation Organization

On Thursday, September 27, a special limited conference of the representatives of various countries was called for the discussion of a proposal made by the Vice-President of the American Society of Mechanical Engineers, Professor P. Oldenburger on the organization of an international federation of specialists on automatic control.

The aim of such a federation was formulated as follows:

1. To promote the exchange of scientific information in the field of automatic control between various countries, members of the federation.

2. To promote the organization of international congresses on automatic control every four years.

During the discussions on this proposal the points of view of the various conference members were gradually clarified. The general feeling was positive and the proposal of Professor Oldenburger was warmly seconded.

After the discussion Dr. Grebe introduced a resolution for consideration which was unanimously accepted.

#### Resolution

(Translated from the German)

The undersigned support the proposal to establish an international federation on automatic control and state that they are willing to publicize such in their country.

The federation should have the following aims:

- 1) to facilitate the exchange of information in the field of control and the development of that field;
- 2) to organize international congresses on control.

Heidelberg, September 27, 1956.

#### Signed:

O. Grebe (Germany)  
P. Oldenburger (USA)  
A. Tastin (Great Britain)  
Koels (Great Britain)  
Westkott (Great Britain)  
G. Mertsendorfer (Austria)  
M. Mesarovich (Yugoslavia)  
Yansen (Netherlands)  
Boes-Popper (Israel)  
M. Ainbinder (Belgium)  
F. Pass (Belgium)  
V. Broida (France)  
P. Profos (Switzerland)  
L. F. Khamosh (Sweden)

Balchen (Norway)  
Ieneen (Denmark)  
G. Muller (Germany)  
Novatsky (Poland)  
G. Kindler (Germany)  
G. Chestnut (USA)  
V. Polents (Germany)  
Evanpelisti (Italy)  
V. Streik (Czechoslovakia)  
B. Khanus (Czechoslovakia)  
A. M. Letov (USSR)  
Isava Keisuke (Japan)  
G. Rupel (Germany)

On the proposal of Dr. G. Chestnut (USA) the following committee was named at the meeting to prepare for the formation of an international federation: Dr. Broida (France) — temporary chairman of the committee, Professor A. M. Letov (USSR), Corresponding Member of the Academy of Sciences, P. Novatsky (Poland), Dr. Wilburn (Great Britain), Professor Oldenburger (USA), Dr. O. Grebe (Federated German Republic).

The committee is to canvass the points of view of the interested countries concerning the formation of an international federation of specialists in automatic control and is to select authorized persons able to make decisions on the final shaping of the federation.

We would like to mention here the warm and friendly attitude of the organizing committee and all members of the Congress toward our delegation.

A. M. Letov, B. N. Naumov, V. A. Racheev, Ya. Z. Tsyppkin

# DETERMINATION OF PERIODIC MODES IN SYSTEMS WITH PIECEWISE-LINEAR CHARACTERISTICS, COMPOSED OF SEGMENTS PARALLEL TO TWO SPECIFIED STRAIGHT LINES

M. A. Aizerman and F. R. Gantmakher

(Moscow)

Analysis of the problem of determining the periodic modes in systems with nonlinear characteristics, composed of segments of two straight lines. The periodic solutions of the differential equations are sought as complete Fourier series with no harmonics neglected. The solution of the problem reduces to setting up an equation for the periods, and the roots of the equation together with previously-derived equations yield the unknown periodic modes.

Unlike the fitting method, the proposed method does not require that the equations for the periods be derived from solutions of linear systems of equations, describing the process along each segment. The second part of the article, to be published in the next issue of the journal, will be devoted to the generalization of the method to include characteristics of a more general type.

## 1. Introduction

The following problem is frequently encountered in the investigation of automatic regulation systems. Given a system of  $n$  differential equations of the first order\*

$$\dot{x}_j = \sum_{k=1}^n a_{jk} x_k + \lambda_j f(x_1) + F_j(t) \quad (j=1, 2, \dots, n), \quad (1.1)$$

where  $a_{jk}$  and  $\lambda_j$  are numbers (some of which may be equal to zero),  $f(x_1)$  is a piecewise-linear function, and  $F_j(t)$  are specified sufficiently smooth\*\* periodic functions of time with a common period  $T$  (in particular,  $F_j(t)$  may be vanishing or nonvanishing constants).

The problem calls for the determination of the periodic solution of Equation (1.1). In the case when all the  $F_j(t)$ 's are identically constant (i.e., in the self-oscillation case), we seek all the periodic solutions of the system (1.1). If at least one of the  $F_j(t)$ 's is not constant, it is necessary to determine only those periodic solutions of Equations (1.1) that have a period  $T$ .

\*As is known, any system containing equations of higher order, algebraically solvable in terms of the higher-order derivatives, can be reduced to the form (1.1).

\*\*I. e., the functions  $F_j(t)$  are continuous and all the derivatives that may be of use in the development of the argument exist.

We shall seek the periodic solution of the system (1.1) in the form of Fourier series

$$x_j = \sum_{r=-\infty}^{r=\infty} \alpha_{jr} e^{i r \omega t} \quad (i = V-1, \omega = \frac{2\pi}{T}).$$

Expanding also the specified functions  $F_j(t)$  into Fourier series, substituting (1.2) into (1.1), and equating coefficients of like terms, we obtain a system consisting of an infinite number of equations, which are nonlinear with respect to the unknown Fourier coefficients  $\alpha_{jr}$ , and also nonlinear with respect to the unknown frequency  $\omega$  if  $F_j(t) = \text{const}$  ( $j = 1, 2, \dots, n$ ).

The difficulties involved in the solution of this problem have given rise to approximate methods, based on neglecting in the series (1.2) all the terms with  $|r| > 1$ . It is only recently that it became possible to overcome the difficulties caused by retaining all the terms in the series (1.2) and only for relay systems, in which  $f(x_1)$  consists of straight-line segments parallel to the  $x_1$  axis, and the transition from one straight line to the other is effected instantaneously when the coordinate  $x_1$  reaches certain fixed values (see [1, 2], which contain a list of earlier works). This is caused by the fact that in the case of a relay system all the unknowns are readily expressed in terms of  $t_0, t_1, \dots, t_N$  — the time intervals between the successive switchings of the relay during the time of the unknown periodic mode ( $T = t_N - t_0$ ). Elimination of all the unknown  $\alpha_{jr}$  reduces the problem to a solution of  $N$  equations (known as the equations of the periods) with unknowns  $t_1, t_2, \dots, t_N$ . If all the  $F_j(t)$ 's are constant,  $t_0$  can be put equal to zero (for in this case it is possible to select arbitrarily the instant of zero time), while  $t_0 = t_N - T$  if there is at least one  $F_j(t)$  that is not identically constant.

Attention was called in [3] to the fact that all the results obtained along these lines in the theory of relay systems can be extended also to the case when the segments of the characteristic  $f(x_1)$  are parallel not to the  $x_1$  axis, but to any nonvertical line.

The problem formulated above was solved in Section 5 of [4] for a symmetrical three-segment characteristic  $f(x_1)$  with outside segments that are parallel to each other. A method was proposed whereby all the  $\alpha_{jr}$ 's can be expressed in terms of the  $N$  unknowns  $t_1, t_2, \dots, t_N$ , also, in the case of the three-segment characteristics, when the periodic solutions are sought in the form (1.2).

The present article is devoted to a further development along these lines. The method used in [4] is generalized to the case when the piecewise-linear function  $f(x_1)$  in Equation (1.1) consists of any number of segments, each of which is parallel to any one of two specified lines.

The work consists of two parts. In the first part, the method proposed is explained in detail with the aid of an example dealing with the simplest type of periodic mode in a system having a characteristic composed of only two segments, subject to the simplest conditions of transition from one segment to another. The second part of the work (which will be published in the next issue of the journal) will show how this method for finding the periodic modes can be generalized to include systems having characteristics composed of any number of segments, parallel to two specified lines, and to more complicated transitions from one segment to the other.

## 2. Two-Segment Characteristic. Transformation of Equations

Let us eliminate all the unknowns, except  $x_1$  and  $y_1$ , from the system (1.1). As a result (see [4]) we obtain the following equation

$$D(p^*)x_1 = K(p^*)y_1 + \Phi(t), \quad y_1 = f(x_1), \quad (2.1)$$

where  $x_1$  and  $y_1$  can be looked upon as the output and input coordinates of the linear portion of the system;  $D(p^*)$  and  $K(p^*)$  are the following polynomials:

$$\begin{aligned} D(p^*) &= c_0 p^{*n} + c_1 p^{*n-1} + \dots + c_n, \\ K(p^*) &= d_0 p^{*m} + d_1 p^{*m-1} + \dots + d_m \quad (m < n). \end{aligned}$$



Hereinafter we shall call the Equation (2.1) the deriving equation.

The function  $\Phi(t)$  is derived from  $F_j(t)$  during the process of elimination of  $x_2, x_3, \dots, x_n$ , by differentiation multiplication by constants, and summation.  $\Phi(t)$  has therefore, the same period  $T$ ;  $\Phi(t)$  is identically constant if all the  $F_j(t)$ 's are constant, and generally speaking,  $\Phi(t)$  is not identically constant if at least one of the  $F_j(t)$ 's is not constant.

It was shown in [4] that in Equation (2.1) the operator  $p^*$  becomes the operator of ordinary differentiation only if  $x_1$  and  $y_1$  are sufficiently smooth functions. In the case of discontinuous functions,  $p^*$  must be considered as the "generalized derivative" operator, determined by the following equations

$$\begin{aligned} p^* F(t) &= pF(t) + \sum_q \xi_q \delta(t - t_q), \\ p^2 F(t) &= p^2 F(t) + \sum_q \xi_q \delta'(t - t_q) + \sum_q \xi_q^1 \delta(t - t_q), \\ p^3 F(t) &= p^3 F(t) + \sum_q \xi_q \delta''(t - t_q) + \sum_q \xi_q^1 \delta'(t - t_q) + \sum_q \xi_q^2 \delta(t - t_q) \quad \text{etc.} \end{aligned} \quad (2.2)$$

In these equations  $p = \frac{d}{dt}$  is the ordinary differentiation operator;  $\xi_q, \xi_q^1, \xi_q^2$ , etc., are the values of the discontinuities in the functions  $F(t)$  and their derivatives  $\frac{dF(t)}{dt}, \frac{d^2 F(t)}{dt^2}$ , etc., at the instant  $t = t_q$ ;  $\delta(t)$  is the Dirac impulse function, and  $\delta'(t), \delta''(t)$  etc., its derivatives. The summation is carried out over all the discontinuity points. \* Equating the terms in (2.1) that do not contain  $\delta$ , we obtain the equation

$$D(p)x_1 = K(p)y_1 + \Phi(t), \quad y_1 = f(x_1), \quad (2.3)$$

which relates the functions  $x_1, y_1$  and  $\Phi(t)$  everywhere except at the discontinuity points. Equating in addition the terms containing  $\delta, \delta', \delta''$ , etc., we obtain the "jump conditions," relating the values of  $x_1$  and  $y_1$  and of their derivatives before and after the discontinuities. \*\*

Considering only the solutions for  $x_1$ , the system of Equations (1.1) is equivalent to Equation (2.1), where the operator  $p^*$  is determined from (2.2), or else is equivalent to the derivation Equation (2.3), where  $p$  is the ordinary derivative operator, provided this equation is supplemented by the jump conditions.

Let us restrict ourselves for the time being to an analysis of a characteristic  $f(x_1)$  composed of two specified straight lines. With this, the coordinate  $x_1$  is continuous (since  $m < n$ ), and  $y_1$  can experience a jump discontinuity, since the transition from one straight segment of the characteristic to the other segment can occur not only at the point where the segments intersect, but through an instantaneous jump at all given values of  $x_1$  (Fig. 1).

\* Let us remark that if any periodic discontinuous function  $F(t)$  is represented by a Fourier series, then term by term differentiation of this series defines a Fourier series of the function  $p^* F(t)$  rather than of  $pF(t)$ .

In connection with this, when seeking a periodic solution of Equation (2.1) in the form of the Fourier series  $x_1 = \sum_{r=-\infty}^{\infty} \alpha_r e^{ir\omega t}$  it is possible by substituting the series into (2.1), to differentiate the series term by term.,

i.e., to use the identity

$$D(p^*) \sum_{r=-\infty}^{\infty} \alpha_r e^{ir\omega t} = \sum_{r=-\infty}^{\infty} D(ir\omega) \alpha_r e^{ir\omega t}.$$

\*\* These jump conditions are given in [4]. They are not given here, for they will not be used hereinafter.

In the particular case when both straight segments of the characteristic are parallel to the  $x_1$  axis, we obtain relay characteristics (Fig. 1 a).

We shall seek the simplest periodic solution, in which the transition between segments occurs at the beginning of the period ( $t = t_0$ ), at the end of the period ( $t = t_2$ ), and once only within the period ( $t = t_1$ ). In other words, with proper choice of the start of the period, the generating point travels during the time of the period first on

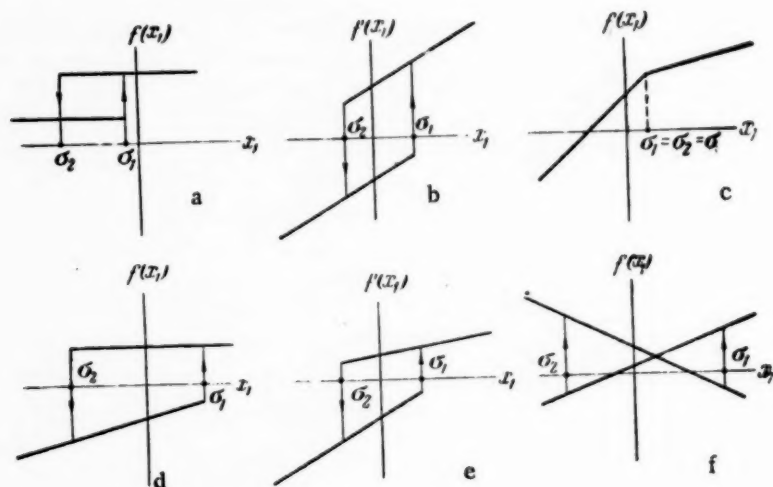


Fig. 1

one segment and then on the other segment of the characteristic.

Let us denote by  $\sigma_1$  and  $\sigma_2$  respectively the specified values of  $x_1$  at which the transition occurs from the first line to the second and from the second to the first.\*

It is furthermore assumed here that the transition between segments occurs at the instant when the coordinate  $x_1$ , moving along any one of the straight lines, first reaches the value  $\sigma_1$  or  $\sigma_2$  respectively.\*\*

If  $\Phi(t)$  is constant (and in particular, if  $\Phi(t) = 0$ ), the time origin  $t_0$  can be chosen arbitrarily. Hereinafter we shall choose  $t_0 = 0$ , and the problem, as will be shown later, reduces to determining the times  $t_1$  and  $t_2$  required to cover the segments of the characteristic.

If  $\Phi(t)$  is not constant, the time origin depends on the specified function  $\Phi(t)$  and cannot be chosen arbitrarily. The problem reduces again to the determination of two quantities, for example,  $t_1$  and  $t_2$ , since  $t_0$  can be determined from the relationship  $T = t_2 - t_0$ .

Let us return to Equation (2.1) and introduce a change of variables

$$\begin{aligned} x_1 &= \alpha x + \beta y + \lambda, \\ y_1 &= \gamma x + \delta y + \lambda, \\ \alpha\delta - \beta\gamma &\neq 0. \end{aligned} \quad (2.4)$$

\* In the particular case when  $\sigma_1 = \sigma_2 = \sigma$  (the abscissa of the point of intersection of the segments of the characteristic) the function  $y_1$  becomes continuous.

\*\* Hereinafter, as is done in the theory of relay systems, this supplementary condition is taken into account only at the very end. The periodic solutions are first sought without taking this condition into account, after which it is checked whether the resultant periodic modes satisfy this supplementary condition.



We then obtain in lieu of (2.1)

$$L(p^*)x = M(p^*)y + \Psi(t), \quad y = F(x), \quad (2.5)$$

where \*

$$\begin{aligned} L(p^*) &= \alpha D(p^*) - \gamma K(p^*) = a_0 p^{*n} + a_1 p^{*n-1} + \dots + a_n, \\ M(p^*) &= \delta K(p^*) - \beta D(p^*) = b_0 p^{*m} + b_1 p^{*m-1} + \dots + b_m, \\ \Psi(t) &= \Phi(t) + K(0)\lambda - D(0)\kappa = \sum_{r=-\infty}^{\infty} \varepsilon_r e^{ir\omega t} \quad (\varepsilon_r = \bar{\varepsilon}_{-r}). \end{aligned}$$

The function  $y = F(x)$  is specified implicitly by the relationship

$$\gamma x + \delta y + \lambda = f(\alpha x + \beta y + \kappa).$$

Equations (2.4) define a linear transformation of points on the  $(x_1, y_1)$  plane into points on the  $(x, y)$  plane and vice versa. In this transformation straight lines remain straight and parallel lines remain parallel. Let us choose the coefficients  $\alpha, \beta, \gamma, \delta, \kappa$  and  $\lambda$  of this transformation such that the first segment of the characteristic is transformed into the  $x$  axis of the  $(x, y)$  plane and the second segment is transformed into the  $y$  axis.

If the segments are not parallel to each other ( $k_1 \neq k_2$ ), it becomes necessary to put \*\* (Fig. 2)

$$\begin{aligned} \gamma &= k_1 \alpha, & \delta &= k_2 \beta, \\ \kappa &= \frac{h_1 - h_2}{k_2 - k_1}, & \lambda &= \frac{k_2 h_1 - k_1 h_2}{k_2 - k_1}. \end{aligned} \quad (2.6)$$

The values of  $\alpha, \beta, \gamma$  and  $\delta$  can be chosen arbitrarily, provided the first two relationships in (2.6) are satisfied.

As a result of this, the equation

$$D(p^*)x_1 = K(p^*)y_1 + \Phi(t)$$

becomes transformed into

$$L(p^*)x = M(p^*)y + \Psi(t),$$

\* If  $\Phi(t)$  is identically zero, then  $\Psi(t) = \text{const} = K(0)\lambda - D(0)\kappa$ .

\*\* The equations are written for the case when neither segment is parallel to the  $y_1$  axis. Otherwise, the form of the equations is changed.

and a characteristic composed of two straight segments is transformed into a characteristic composed of the coordinate axes.

Previously, in the  $(x_1, y_1)$  plane, the transition from the first segment to the second one was made from point  $P_1$  into point  $P'_1$ . Now, in the  $(x, y)$  plane, the corresponding points are  $Q_1$  and  $Q'_1$  (Fig. 3).

Analogously, the transition from the second segment to the first in the  $(x, y)$  plane is from the point  $Q_2$  into  $Q'_2$ . The coordinates of the points are indicated in Fig. 3.

If the "jumps" in the discontinuous modes occur in the  $(x_1, y_1)$  plane along lines parallel to the  $y_1$  axis, the jumps in the  $(x, y)$  plane will be along parallel but inclined lines having a slope  $\tan \varphi = \alpha/\beta$ .

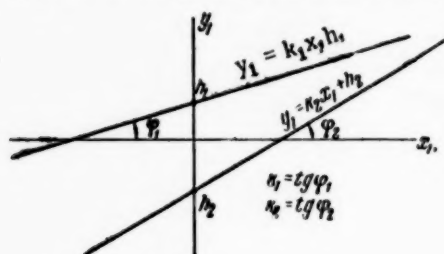


Fig. 2

All of this is true only if  $k_2 - k_1 \neq 0$ , i.e., if the segments of the characteristic are not parallel to each other. The case of parallel lines (relay characteristics and those that can be reduced to such characteristics) is not considered here, for as indicated above, methods of determining the periodic modes of relay systems are known from previously published works.

### 3. Derivation of the Equations of the Periods and Determination of the Periodic Mode

The variation of the coordinates  $x$  and  $y$  during the time of the simplest periodic mode (this concept was explained above) at  $t_0 < t < t_2$  is as shown in Fig. 4.

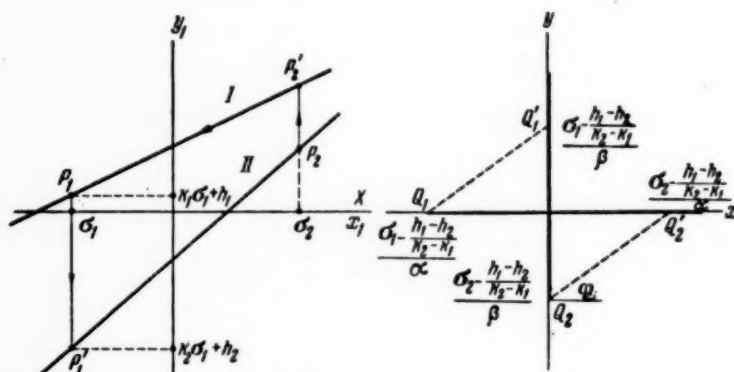


Fig. 3

We shall seek this periodic solution in the form of a Fourier series

$$x = \sum_{r=-\infty}^{+\infty} \alpha_r e^{ir\omega t}, \quad y = \sum_{r=-\infty}^{+\infty} \beta_r e^{ir\omega t}.$$

Substituting the series into the system of Equations (2.5), we get

$$L(ir\omega) \alpha_r = M(ir\omega) \beta_r + \varepsilon_r.$$

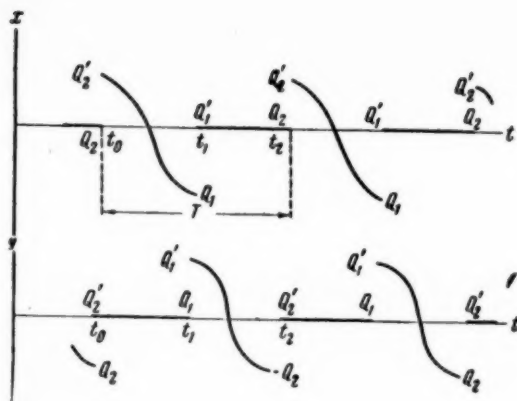


Fig. 4

number of discontinuities within the limits of the period, the following relationship\* exists between the Fourier coefficients  $\mu_r^*$  and  $\mu_r$ :

$$\mu_r^* = \mu_r + \frac{1}{T} \left[ e^{-ir\omega t_1} \sum_{k=0}^{n-1} \eta_k m_k(ir\omega) + e^{-ir\omega t_2} \sum_{k=0}^{n-1} \eta_k m_k(ir\omega) + \dots \right]. \quad (3.2)$$

Here  $\eta_k^1, \eta_k^2$  etc., are the values of the discontinuities of the  $k$ 'th derivative of the function  $y(t)$  at the instants  $t_1, t_2, \dots$ ,

$$m_k(S) = b_{n-k-1} + b_{n-k-2}S + \dots + b_0S^{n-k-1},$$

and the number of the sums—the terms in the square brackets—equals the number of discontinuity points within the period. In our case, there are two such points (for the instants  $t_1$  and  $t_2$ ) and the square bracket does not contain the terms represented by the dots.

The value of  $\mu_r$  is calculated from the following equation

$$\mu_r = \frac{1}{T} \int_{t_0}^{t_1} M(p) y e^{-ir\omega t} dt = \frac{1}{T} \left[ \int_{t_0}^{t_1} M(p) y e^{-ir\omega t} dt + \int_{t_1}^{t_2} M(p) y e^{-ir\omega t} dt \right]. \quad (3.3)$$

To calculate the integrals contained in this expression, let us insert the value of  $\psi(t)$  into (2.3) and replace  $p^*$  with  $p$ , bearing in mind only the sections that do not contain the discontinuity points; we then obtain

$$L(p)x = M(p)y + \Phi(t) + \lambda K(0) - xD(0). \quad (3.4)$$

In the periodic solution under consideration (Fig. 4), we have  $y=0$  at  $t_0 < t < t_1$ ;  $x=0$  at  $t_1 < t < t_2$ .

\*A proof of this relationship is given in Appendix I.

Let us denote by  $\mu_r^*$  the Fourier coefficients of the periodic function  $M(p^*)y$ , i.e.,  $\mu_r^* = M(ir\omega)\mu_r$ . Then

$$\alpha_r = \frac{\mu_r^* + \epsilon_r}{L(ir\omega)}, \quad \beta_r = \frac{\mu_r^*}{M(ir\omega)}. \quad (3.1)$$

Let us now consider in lieu of  $M(p^*)y$  the function  $M(p)y$ , where  $p$  is the ordinary derivative rather than the generalized one. In the case of periodic modes, when  $y$  is a periodic function of period  $T$ ,  $M(p)y$  is also a periodic function of the same period. Let us denote its Fourier coefficient by  $\mu_r$ .

In the general case, when the function  $y$  and its derivatives up to the  $(n-1)$ -th order are subject to any

The condition  $y = 0$  is equivalent to the condition

$$M(p)y = 0, \quad (3.5)$$

$$y(t_1 - 0) = y'(t_1 - 0) = \dots = y^{(n-1)}(t_1 - 0) = 0, \quad (3.6)$$

while the condition  $x = 0$  is equivalent to the condition

$$L(p)x = 0, \quad (3.7)$$

$$x(t_2 - 0) = x'(t_2 - 0) = \dots = x^{(n-1)}(t_2 - 0) = 0. \quad (3.8)$$

Equations (3.6) and (3.8) will be used later. For the time being, let us note that (3.5) leads to

$$\int_{t_0}^{t_1} M(p)y e^{-ir\omega t} dt = 0.$$

To use Condition (3.7), let us make use of Equation (3.4), which, by virtue of (3.7), reduces to the equation

$$M(p)y = -\Phi(t) - \lambda K(0) + xD(0) \quad (t_1 < t < t_2).$$

Equation (3.3) therefore, assumes the following form

$$\mu_r = -\frac{1}{T} \int_{t_1}^{t_2} [\Phi(t) + \lambda K(0) - xD(0)] e^{-ir\omega t} dt,$$

and the coefficients  $\mu_r$  can be readily calculated from the specified function  $\Phi(t)$ .

Taking (3.2) and (3.1) into account, we get

$$\begin{aligned} \alpha_r &= \frac{\mu_r + \varepsilon_r}{L(ir\omega)} + \frac{1}{TL(ir\omega)} \left[ e^{-ir\omega t_1} \sum_{k=0}^{n-1} \gamma_{lk} m_k(ir\omega) + e^{-ir\omega t_2} \sum_{k=0}^{n-1} \gamma_{lk} m_k(ir\omega) \right], \\ \beta_r &= \frac{\mu_r}{M(ir\omega)} + \frac{1}{TM(ir\omega)} \left[ e^{-ir\omega t_1} \sum_{k=0}^{n-1} \gamma_{lk} m_k(ir\omega) + e^{-ir\omega t_2} \sum_{k=0}^{n-1} \gamma_{lk} m_k(ir\omega) \right]. \end{aligned} \quad (3.9)$$

Substituting these expressions for  $\alpha_r$  and  $\beta_r$  into the Fourier series for  $x$  and  $y$ , and collecting terms with equal  $n$ , we get

$$x = \sum_{k=0}^{n-1} [R_k(t - t_1) \gamma_{lk}^1 + R_k(t - t_2) \gamma_{lk}^2] + R(t), \quad (3.10)$$

$$y = \sum_{k=0}^{n-1} [S_k(t - t_1) \gamma_{lk}^1 + S_k(t - t_2) \gamma_{lk}^2] + S(t), \quad (3.11)$$

where

$$\begin{aligned} R_k &= \frac{1}{T} \sum_{r=-\infty}^{\infty} \frac{m_k(i\omega)}{L(i\omega)} e^{i\omega t}, & S_k &= \frac{1}{T} \sum_{r=-\infty}^{\infty} \frac{m_k(i\omega)}{M(i\omega)} e^{i\omega t}, \\ R &= \sum_{r=-\infty}^{\infty} \frac{\mu_r + \varepsilon_r}{L(i\omega)} e^{i\omega t}, & S &= \sum_{r=-\infty}^{\infty} \frac{\mu_r}{M(i\omega)} e^{i\omega t}. \end{aligned} \quad (3.12)$$

Here  $R_k$ ,  $S_k$ ,  $R$ , and  $S$  are convergent Fourier series.

Let us now return to Conditions (3.6) and (3.8), and let us require that the functions  $\underline{x}$  and  $\underline{y}$ , defined by Equations (3.10) and (3.12), satisfy these conditions. These lead to the following equalities

$$\begin{aligned}
 & \sum_{k=0}^{n-1} [R_k(t_2 - t_1 - 0) \overset{1}{\gamma}_{lk} + R_k(-0) \overset{2}{\gamma}_{lk}] + R(t_2 - 0) = 0, \\
 & \sum_{k=0}^{n-1} [R'_k(t_2 - t_1 - 0) \overset{1}{\gamma}_{lk} + R'_k(-0) \overset{2}{\gamma}_{lk}] + R'(t_2 - 0) = 0, \\
 & \dots \dots \dots \\
 & \sum_{k=0}^{n-1} [R_k^{(n-1)}(t_2 - t_1 - 0) \overset{1}{\gamma}_{lk} + R_k^{(n-1)}(-0) \overset{2}{\gamma}_{lk}] + R^{(n-1)}(t_2 - 0) = 0, \\
 & \sum_{k=0}^{n-1} [S_k(-0) \overset{1}{\gamma}_{lk} + S_k(t_1 - t_2 - 0) \overset{2}{\gamma}_{lk}] + S(t_1 - 0) = 0, \\
 & \sum_{k=0}^{n-1} [S'_k(-0) \overset{1}{\gamma}_{lk} + S'_k(t_1 - t_2 - 0) \overset{2}{\gamma}_{lk}] + S'(t_1 - 0) = 0, \\
 & \dots \dots \dots \\
 & \sum_{k=0}^{n-1} [S_k^{(n-1)}(-0) \overset{1}{\gamma}_{lk} + S_k^{(n-1)}(t_1 - t_2 - 0) \overset{2}{\gamma}_{lk}] + S^{(n-1)}(t_1 - 0) = 0.
 \end{aligned}
 \tag{3.13}$$

Let us recall that  $\omega = 2\pi/t_2$  if  $\Phi(t)$  is constant, since  $t_0 = 0$ , and since  $\omega$  is specified in the case of forced oscillations. In any case, therefore, Equations (3.13) contain, in addition to the linearly dependent unknowns  $\eta$ , only the unknown values of time  $t_1$  and  $t_2$ .

If the values of  $t_1$  and  $t_2$  are assigned arbitrarily and substituted into the derived system of equations, the system yields\* all the values of the discontinuities  $\eta_k$  and  $\bar{\eta}_k$ . Substituting the resultant  $\eta_k$  and  $\bar{\eta}_k$  into the series (3.10) and (3.11) we obtain  $x(t)$  and  $y(t)$ . These values of  $x(t)$  and  $y(t)$  will satisfy the equation

$$L(p^*)x = M(p^*)y + \Psi(t).$$

Motion along the  $\underline{x}$  axis (i.e.,  $y = 0$ ) will be assured during the time  $t_0 < t < t_1$ , and motion along the  $\underline{y}$  axis (i.e.,  $x = 0$ ) will be assured during the time  $t_1 < t < t_2$ ; however, there is no assurance of the transition from the  $\underline{x}$  axis to the  $\underline{y}$  axis from point  $Q_1$  into  $Q'_1$ , or of the transition from the  $\underline{y}$  axis to the  $\underline{x}$  axis from the point  $Q_2$  into the point  $Q'_2$ . To insure this "joining condition" \*\* it is enough to require that

• It is assumed that the determinant of the system does not vanish for these values of  $t_1$  and  $t_2$ . The case when this determinant vanishes will be treated later.

•• In the theory of relay systems these conditions correspond to the condition of correct switching of the relay.

the following two conditions be satisfied (Fig. 3):

$$y(t_1 + 0) = y_1, \quad y(t_2 - 0) = y_2, \quad (3.14)$$

where

$$y_1 = \frac{\sigma_1 - \frac{h_1 - h_2}{k_2 - k_1}}{\beta}, \quad y_2 = \frac{\sigma_2 - \frac{h_1 - h_2}{k_2 - k_1}}{\beta}.$$

These conditions fix the position of points  $Q'_1$  and  $Q_2$ , consequently, also of points  $Q_1$  and  $Q'_2$ , since the directions of the jumps from  $Q_1$  into  $Q'_1$  and  $Q_2$  into  $Q'_2$  are specified by the selected linear transformation (2.2).

In connection with the fact that  $\eta_0^1 = y(t_1 + 0) - y(t_1 - 0)$  and  $\eta_0^2 = y(t_1 + 0) - y(t_2 - 0)$ , and that  $y(t_1 - 0) = y(t_2 + 0) = 0$  (motion along the  $x$  axis), Condition (3.14) can be rewritten as

$$\eta_0^1 = y_1, \quad \eta_0^2 = -y_2 \quad (3.15)$$

Assuming for the time being that the determinant  $\Delta(t_1, t_2)$  of the system (3.13) vanishes, let us solve it with respect to  $\eta_0^1$  and  $\eta_0^2$ . Let the solution be  $\eta_0^1 = f_1(t_1, t_2)$  and  $\eta_0^2 = f_2(t_1, t_2)$ . Then the conditions

$$f_1(t_1, t_2) = y_1, \quad f_2(t_1, t_2) = -y_2 \quad (3.16)$$

can be used to determine  $t_1$  and  $t_2$ .

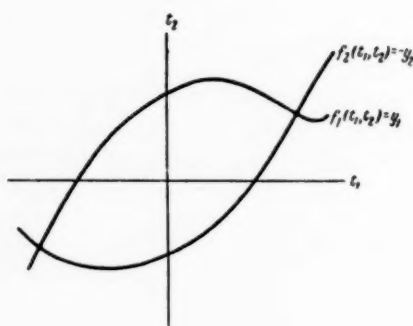


Fig. 5

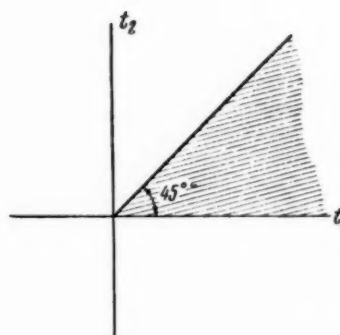


Fig. 6

For example, it is possible to plot the curves (3.16) in the  $(t_1, t_2)$  plane by usual methods and to find their intersection points (Fig. 5). The values of  $t_1$  and  $t_2$  corresponding to these points are "possible periodic solutions". Actually they determine the periodic solutions if the following conditions are satisfied:



a). One of the following inequalities holds:  $0 < t_1 < t_2$  (for self oscillations) or  $t_2 - T < t_1 < t_2$  (for forced oscillations).

b). There are no "switchings" within the period at  $t$ , other than  $t_1$  and  $t_2$ .

To check whether Condition "a" is satisfied, it is convenient to draw the angle between the  $t_2$  axis and the bisectrix of the first quadrant in the  $(t_1, t_2)$  plane in the case of the self-oscillating case (Fig. 6), or to draw the strip between the bisectrix and the line  $t_2 - t_1 = T$  in the forced oscillation case (Fig. 7). The intersection points of the plotted curves that lie in the crosshatched region (Fig. 6) in the self-oscillating case or in nonhatched region (Fig. 7) in the forced-oscillation case should be discarded. To check whether the remaining intersection points satisfy Conditions "b" it is necessary to use the system (3.13) to determine all values of  $\eta$  for the obtained  $t_1$  and  $t_2$ , substitute these values into (3.11), and plot the resultant periodic solution within the limits of the period.

Let  $x_1 = \frac{\sigma_1 - \frac{h_1 - h_2}{k_2 - k_1}}{\alpha}$  be the abscissa of point  $Q_1$ , and  $y_2 = \frac{\sigma_2 - \frac{h_1 - h_2}{k_2 - k_1}}{\beta}$  the ordinate of point  $Q_2$  (Fig-

ure 3).

If the plotted solution is such that the value of  $x_1$  is reached at any value of  $t$  other than  $t_1$ , or the value of  $y_2$  is reached at any value of  $t$  other than  $t_2$ , such a periodic solution does not satisfy Condition "b" and should be discarded.

All the pairs of numbers  $t_1$  and  $t_2$ , satisfying the equation of the periods (3.16) and satisfying Conditions "a" and "b", determine the periodic solutions that can be obtained from the derived equations. It may happen here that some periodic solutions are omitted, since we have assumed for the time being that  $\Delta(t_1, t_2) \neq 0$ .

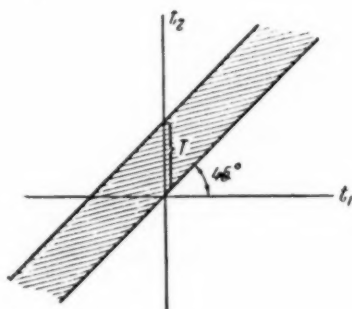


Fig. 7

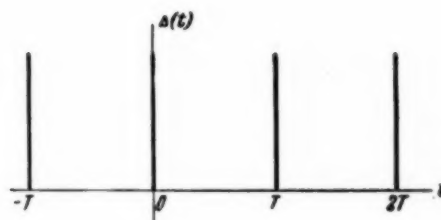


Fig. 8

If  $\Delta(t_1, t_2) = 0$ , the system (3.13) is generally speaking inconsistent and there are no periodic solutions. In exceptional cases, however, when the free terms are suitably chosen, the system (3.13) may be indeterminate and for some of its solution we may have  $\dot{\eta}_0 = y_1$ , and  $\dot{\eta}_0 = -y_2$ . These cases can be separated by employing the usual analysis of the system of algebraic equations (3.11).

#### 4. Calculation of the Coefficients of Equations (3.13)

It follows from the above that the determination of the periodic solution of Equation (2.1) reduces to a solution of a system of linear algebraic equations (3.13). The coefficients of these equations are the values of the functions  $R(t)$ ,  $S(t)$ ,  $R_k(t)$  and  $S_k(t)$  and their derivatives up to the  $(n-1)$ -th order inclusive at certain fixed values of time. The functions  $R$ ,  $S$ ,  $R_k$ , and  $S_k$  themselves can be evaluated by expanding them in Fourier series (3.12), for these series are convergent. However, certain difficulties arise when determining the values of the derivatives of these functions. If an attempt is made to determine these derivatives by differentiating the series (3.12) term by term, it must be borne in mind that the convergence of the series that results from the differentiation becomes considerably poorer with increasing  $\underline{r}$ , and these series may diverge, starting with a certain value  $\underline{r} \leq \underline{n} - 1$ .

To circumvent these difficulties, it is possible to employ the method developed by A. N. Krylov to improve the convergence of series, as was done in [4]. Let us explain the application of this method by using as an example the function

$$R_k = \frac{1}{T} \sum_{r=-\infty}^{\infty} \frac{m_k(ir\omega)}{L(ir\omega)} e^{ir\omega t},$$

where

$$m_k(S) = b_{n-k-1} + b_{n-k-2}S + \dots + b_0S^{n-k-1}.$$

Let  $l$  be any positive integer. Let us divide now the polynomial  $S^{k+l}m_k(S)$  by  $L(S)$ .

Let us denote the quotient by  $\gamma_0S^{l-1} + \gamma_1S^{l-2} + \dots + \gamma_{l-1}$ , and the residue as  $c_0S^{n-1} + c_1S^{n-2} + \dots + c_{n-1}$ . Then

$$S^{n+l}m_k(S) = (\gamma_0S^{l-1} + \gamma_1S^{l-2} + \dots + \gamma_{l-1})L(S) + c_0S^{n-1} + c_1S^{n-2} + \dots + c_{n-1}.$$

hence

$$\frac{m_k(S)}{L(S)} = \frac{\gamma_0}{S^{k+1}} + \frac{\gamma_1}{S^{k+2}} + \dots + \frac{\gamma_{l-1}}{S^{k+l}} + \frac{c_0S^{n-1} + c_1S^{n-2} + \dots + c_{n-1}}{S^{k+1}L(S)} \quad (4.1)$$

Using the identity (4.1), let us replace the Fourier series for  $R_k$  by the sum of the Fourier series \*

$$R_k = \frac{b_{n-k-1}}{a_n} + \gamma_0 H_{k+1}(t) + \gamma_1 H_{k+2}(t) + \dots + \gamma_{l-1} H_{k+l}(t) + R_k^*(t), \quad (4.2)$$

where

$$H_j(t) = \frac{1}{T} \sum_{r=-\infty}^{\infty} \frac{1}{(ir\omega)^j} e^{ir\omega t} \quad (j = k+1, k+2, \dots, k+l), \quad (4.3)$$

$$R_k^*(t) = \frac{1}{T} \sum_{r=-\infty}^{\infty} \frac{c_0(ir\omega)^{n-1} + c_1(ir\omega)^{n-2} + \dots + c_{n-1}}{(ir\omega)^{k+l}L(ir\omega)} e^{ir\omega t}, \quad (4.4)$$

and  $\Sigma^*$  denotes a sum from which the term  $r = 0$  is omitted.

\* The identity (4.1) holds at  $S = ir\omega$  for all values of  $r$  except  $r = 0$ . The constant term of the series (corresponding to  $r = 0$ ) is, therefore, deleted from the expression for  $R_k$ .

Unlike the series  $R_k(t)$ , the series  $R_k^*(t)$  has that property at  $\underline{l} \geq n - k - 1$  that all its term by term derivatives up to the  $(n-1)$ th inclusive are convergent. Furthermore, for greater  $\underline{l}$ , the better the convergence of the resultant series.

It is therefore possible to choose a value  $\underline{l}$  that is large enough to make the values  $R_k^*(t)$  and all its derivatives up to the  $(n-1)$ th inclusive readily calculable from the first few harmonics.

Let us now consider the function  $H_j(t)$ . Let us note that

$$H_j(t) = \frac{1}{\omega^j T} h_j(\omega t), \text{ where } h_j(z) = \sum_{r=-\infty}^{\infty} \frac{1}{(ir)^j} e^{irz}.$$

Differentiating  $h_j(z)$  term by term, we get

$$h_j'(z) = \sum_{r=-\infty}^{\infty} \frac{1}{(ir)^{j-1}} e^{irz} = h_{j-1}(z), \quad (4.5)$$

i.e.,

$$h_j(z) = \int h_{j-1}(z) dz + C. \quad (4.6)$$

In this recurrence equation, the integration constant is determined from the conditions:

a) if  $\underline{j}$  is even  $\int_0^{\pi} h_j(z) dz = 0;$

b) if  $\underline{j} > 1$  and is odd,  $h_j(0) = 0.$

The first condition follows from the fact that  $h_j$  (if  $\underline{j}$  is even) is an even function, the Fourier expansion of which has no free term; the second condition follows from the fact that if  $\underline{j}$  is odd and greater than unity,  $h_j$  is a continuous odd function.

Let us note that

$$h_1(z) = \sum_{r=-\infty}^{\infty} \frac{1}{(ir)} e^{irz} = 2 \sum_{n=1}^{\infty} \frac{\sin nz}{n}$$

is a periodic function with a period  $2\pi$ , which is given by the following equation at  $0 < z < 2\pi$ :

$$h_1(z) = \pi - z \quad (0 < z < 2\pi). \quad (4.7)$$

Substituting this value of  $h_1(z)$  into (4.6) we get

$$h_2(z) = \int (\pi - z) dz + C = \pi z - \frac{z^2}{2} + C$$

and C is determined from the condition

$$\int_0^\pi h_2(z) dz = \left( \pi \frac{z^2}{2} - \frac{z^3}{6} + Cz \right) \Big|_0^\pi = 0,$$

i.e.,

$$C = -\frac{\pi^2}{3} \text{ and } h_2(z) = \pi z - \frac{z^2}{2} - \frac{\pi^2}{3}.$$

Substituting now this value of  $h_2(z)$  into (4.6), we obtain  $h_3(z)$ , etc. Appendix II gives equations for the functions  $h_j(z)$  for  $j = 1$  to  $j = 11$ .

By virtue of (4.6) we have

$$\frac{d^s h_j}{dz^s} = h_{j-s}(z). \quad (4.8)$$

Using (4.8) and (4.2) we get

$$\begin{aligned} R_k(t) &= \frac{b_{n-k-1}}{a_n} + \frac{1}{2\pi} \left[ \frac{\gamma_0}{\omega^k} h_k(\omega t) + \frac{\gamma_1}{\omega^{k+1}} h_{k+2}(\omega t) + \dots \right. \\ &\quad \left. \dots + \frac{\gamma_{l-1}}{\omega^{l+k-1}} h_{k+l}(\omega t) \right] + R_k^*(t), \\ \frac{d^s R_k(t)}{dt^s} &= \frac{1}{2\pi} \left[ \frac{\gamma_0}{\omega^k} h_{k+1-s}(\omega t) + \frac{\gamma_1}{\omega^{k+1}} h_{k+2-s}(\omega t) + \dots \right. \\ &\quad \left. \dots + \frac{\gamma_{l-1}}{\omega^{l+k-1}} h_{k+l-1}(\omega t) \right] + \frac{d^s R_k^*(t)}{dt^s}, \end{aligned} \quad (4.9)$$

where  $h_g = 0$  if  $g < 0$ , and  $R_k^*(t)$  and its derivatives are determined from (4.4).

Thus, calculation of the values of  $R_k$  or  $R_k^{(s)}$  reduces to summing the first few harmonics of a rapidly converging series  $R_k^*(t)$  (or of  $\frac{d^s R_k^*(t)}{dt^s}$  respectively). The equations for the values of  $R$ ,  $S$ , and  $S_k$  and of their derivatives are derived in an exactly analogous manner.\*

\* Let us remark here that  $\gamma_0 = 1$  and  $\gamma_1 = \dots = \gamma_{n-k-1} = 0$  in the case of the functions  $S_k$ .

# APPENDIX I

## Derivation of the Relationship Between $\mu^*$ and $\mu$

Let us consider a periodic function  $\Delta(t) = \sum_{r=-\infty}^{\infty} \delta(t + rT)$  (Fig. 8). Its Fourier expansion is:

$$\Delta(t) = \frac{1}{T} \sum_{r=-\infty}^{\infty} e^{ir\omega t}.$$

Assuming that  $y$  is a periodic function and  $\eta_k, \eta_k', \dots$  are the values of the discontinuities of its  $k$ th derivatives ( $k = 0, 1, \dots, n-1$ ) within the limits of the period, it is possible to write down the following chain of equations by virtue of (1.4)

$$y = y,$$

$$p^*y = py + \sum_q \eta_0 \Delta(t - t_q),$$

$$p^{**}y = p^*y + \sum_q [\eta_0 \Delta'(t - t_q) + \eta_1 \Delta(t - t_q)],$$

$$p^{***}y = p^{**}y + \sum_q [\eta_0 \Delta''(t - t_q) + \eta_1 \Delta'(t - t_q) + \eta_2 \Delta(t - t_q)]$$

etc., up to  $p^{*n-1}y$ .

Multiplying the left and right halves of the first equation by  $b_n$ , that of the second equation by  $b_{n-1}$ , of the third by  $b_{n-2}$ , etc., and adding all the equations, we get

$$\begin{aligned} M(p^*)y &= M(p)y + \sum_q \Delta(t - t_q) (b_{n-1} \eta_0 + b_{n-2} \eta_1 + \dots) + \\ &+ \sum_q \Delta'(t - t_q) (b_{n-2} \eta_0 + b_{n-3} \eta_1 + \dots) + \dots \end{aligned}$$

But

$$\begin{aligned} M(p^*)y &= \sum_{r=-\infty}^{\infty} \mu_r^* e^{ir\omega t} d\omega, & M(p)y &= \sum_{r=-\infty}^{\infty} \mu_r e^{ir\omega t} d\omega, \\ \Delta(t) &= \frac{1}{T} \sum_{r=-\infty}^{\infty} e^{ir\omega t}, & \Delta'(t) &= \frac{1}{T} \sum_{r=-\infty}^{\infty} (ir\omega) e^{ir\omega t} \end{aligned}$$

etc.

Substituting the series into the resultant identity and equating terms with  $e^{ir\omega t}$  (for equal values of  $r$ ), we get

$$\mu_r^* = \mu_r + \frac{1}{T} \left[ e^{-ir\omega t_1} \sum_{k=0}^{n-1} \eta_k m_k(ir\omega) + e^{-ir\omega t_2} \sum_{k=0}^{n-1} \eta_k m_k(ir\omega) + \dots \right], \quad (k=0, 1, \dots, n-1, r=-\infty, \dots, 0, \dots, +\infty). \quad (3.2)$$

$$m_k(S) = b_{n-k-1} + b_{n-k-2}S + \dots + b_0 S^{n-k-1}.$$

## APPENDIX II

### Equations for Calculating $h_j$

$$\begin{aligned} h_1 &= -z + \pi, \\ h_2 &= -\frac{z^2}{2} + \pi z - \frac{\pi^2}{3}, \\ h_3 &= -\frac{z^3}{6} + \frac{\pi z^2}{2} - \frac{\pi^2 z}{3}, \\ h_4 &= -\frac{z^4}{24} + \frac{\pi z^3}{6} - \frac{\pi^2 z^2}{6} + \frac{\pi^3}{45}, \\ h_5 &= -\frac{z^5}{120} + \frac{\pi z^4}{24} - \frac{\pi^2 z^3}{18} + \frac{\pi^3 z}{45}, \\ h_6 &= -\frac{z^6}{720} + \frac{\pi z^5}{120} - \frac{\pi^2 z^4}{72} + \frac{\pi^3 z^2}{90} - \frac{2\pi^6}{945}, \\ h_7 &= -\frac{z^7}{5040} + \frac{\pi z^6}{720} - \frac{\pi^2 z^5}{360} + \frac{\pi^3 z^3}{270} - \frac{2\pi^6 z}{945}, \\ h_8 &= -\frac{z^8}{40320} + \frac{\pi z^7}{5040} - \frac{\pi^2 z^6}{2160} + \frac{\pi^3 z^4}{1080} - \frac{\pi^6 z^2}{945} + \frac{23\pi^9}{37800}, \\ h_9 &= -\frac{z^9}{362880} + \frac{\pi z^8}{40320} - \frac{\pi^2 z^7}{15120} + \frac{\pi^3 z^5}{5400} - \frac{\pi^6 z^3}{2835} + \frac{23\pi^9 z}{37800}, \\ h_{10} &= -\frac{z^{10}}{3628800} + \frac{\pi z^9}{362880} - \frac{\pi^2 z^8}{120960} + \frac{\pi^3 z^6}{32400} - \frac{\pi^6 z^4}{11340} + \frac{23\pi^9 z^2}{75600} - \frac{5813\pi^{10}}{19958400}, \\ h_{11} &= -\frac{z^{11}}{39916800} + \frac{\pi z^{10}}{3628800} - \frac{\pi^2 z^9}{1088640} + \frac{\pi^3 z^7}{226800} - \frac{\pi^6 z^5}{56700} + \frac{23\pi^9 z^3}{226800} - \frac{5813\pi^{10} z}{19958400}. \end{aligned}$$

Received June 20, 1956

## LITERATURE CITED

- [1] Ia. Z. Tsyarkin, Theory of Relay Systems, Gostekhizdat, 1955.
- [2] Iu. I. Neimark, "On Periodic Motion of Relay Systems," Collection "In Memory of A. A. Andronov" Published by Academy of Sciences, USSR, 1955.
- [3] M. A. Aizerman and F. R. Gantmakher, "On One Class of Dynamic Problems that are Reducible to the Theory of Relay Systems," Applied Mathematics and Mechanics, No. 2, 1955.
- [4] M. A. Aizerman and F. R. Gantmakher, "On the Determination of Periodic Modes in Nonlinear Dynamic Systems with Piecewise-Linear Characteristics," No. 5, 1956.



# CORRECTION OF PULSE REGULATION AND CONTROL SYSTEMS

Ia. Z. Tsypkin

(Moscow)

Analysis of continuous and pulsed methods for the correction of pulse (intermittent or sampled-data) systems. A procedure is given for the design of the correcting elements. A method of using digital computing devices as correcting elements is described.

## INTRODUCTION

The task of correcting pulse systems consists of so varying the structure of the system and determining the values of its parameters that the pulse systems acquire specified properties. The change in the structure of the system can take place either in the linear portion or in the pulse element. The first case corresponds to a continuous correction; it is analogous in some respect to the correction used in continuous systems.

The second case corresponds to pulse correction. Although this method of correction has no analogy in continuous systems, it can nevertheless be used for the correction of such systems.

### 1. Preliminary Remarks

Consider the pulse regulation or control system shown in Fig. 1. Let us denote the closed-loop transfer function of this uncorrected system by  $K_2^*(q)$ , so that

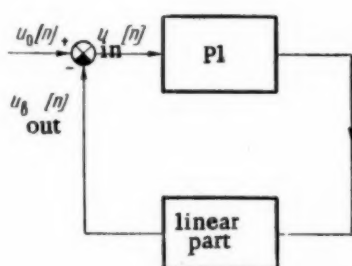


Fig. 1

$$\frac{U_{in}^*(q)}{U_0^*(q)} = K_2^*(q),$$

where  $U_{in}^*(q)$  is the transform of the error and  $U_0^*(q)$  is the transform of the driving force.

Let us denote by  $K_{2d}^*(q)$  the transfer function that is desirable from some particular point of view. The choice of  $K_{2d}^*(q)$  is connected with the requirements imposed on the pulse system. It is thus possible to require that the pulse system have a specified degree of astatic behavior or that it produce the so-called optimum effect. This will be discussed in greater detail in Section 4.

The task of correcting the pulse system consists of so changing the structure of the pulse system as to make the transfer function of this modified or corrected system equal to the desired one  $K_{2d}^*$ , i.e.,

\* One can also specify that  $K_{2c}^*(q)$  differ as little as possible from  $K_{2d}^*(q)$  in some respect.

$$K_{2c}^*(q) = K_{2d}^*(q). \quad (1.1)$$

Using the relationship between the closed-loop and open-loop transfer functions

$$K_2^*(q) = \frac{1}{1 + W^*(q)}, \quad (1.2)$$

we can write Condition (1.1) in the following term

$$W_0^*(q) = \frac{1}{K_{2d}^*(q)} - 1. \quad (1.3)$$

This relationship determines the open-loop transfer function, at which the closed-loop transfer function will be equal to the desired value.

The remainder of the problem consists of realizing  $W_0^*(q)$  by changing the linear portion or the pulse element. The former case corresponds to continuous correction, and the latter, to pulse correction. Let us consider these cases in greater detail.

## 2. Continuous Correction

The transfer function  $W_0^*(q)$ , obtained from the relationship (1.3), corresponds to the corrected system. From the transfer function it is possible to obtain the transfer function of the linear portion of the system  $W_c(q)$ . This can be done in various manners, some of which are described in the Appendix.

If the linear portion is modified so that the transfer function becomes equal to  $W_c(q)$ , then the closed corrected pulse system will have the desired properties. Such a modification is accomplished by introducing into the linear portion additional elements, which are connected with the elements of the linear portion in series (Fig. 2), in parallel (Fig. 3), or in the form of a feedback loop (Fig. 4)\*. For convenience, these diagrams show the linear portion in the form of two series-connected elements. The transfer functions of these

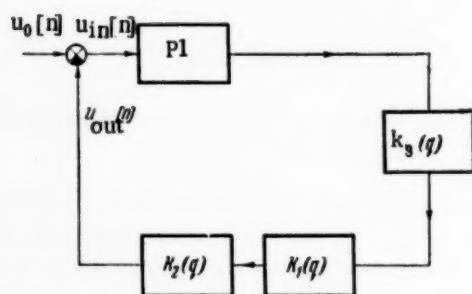


Fig. 2

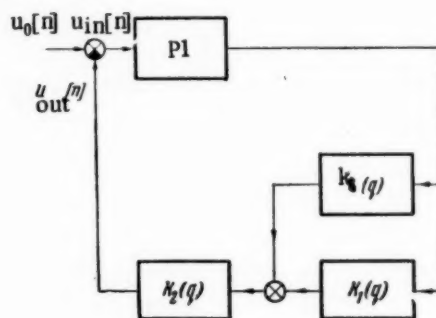


Fig. 3

\* Series continuous correction was treated in [1].

elements are  $K_1(q)$  and  $K_2(q)$  respectively, so that  $W(q) = K_1(q) K_2(q)$ . The transfer function of the supplementary correcting element will be denoted by  $K_s(q)$ . The transfer functions of the linear parts of these systems should equal  $W_c(q)$ . This condition is used to determine the transfer function of the supplementary or correcting element.

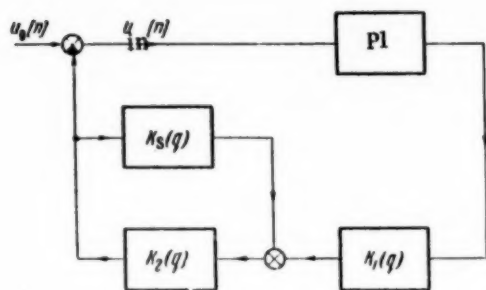


Fig. 4

For series correction (Fig. 2)

$$K_s(q) = \frac{W_c(q)}{K_1(q) K_2(q)}. \quad (2.1)$$

For parallel correction (Fig. 3)

$$K_s(q) = \frac{W_c(q)}{K_2(q)} - K_1(q). \quad (2.2)$$

For feedback correction (Fig. 4)

$$K_s(q) = \frac{K_1(q)}{W_c(q)} - \frac{1}{K_2(q)}, \quad (2.3)$$

From the resultant transfer functions it is possible to determine the structure and the parameter of the supplementary correcting elements, using methods known from the theory of continuous regulation and from network theory.

### 3. Pulse Correction

Pulse correction is unique to pulse systems. It involves modifying the pulse element either by introducing pulse networks as correcting elements or else by using digital computing elements as correcting elements.

The pulse correction can also be used in continuous-regulation systems.

Before proceeding to determine the design equations, let us recall the expressions for the transfer functions of interconnected pulse networks [2]:

For series connection (Fig. 5a)

$$K^*(q) = K_1^*(q) K_2^*(q); \quad (3.1)$$

For parallel connection (Fig. 5b)

$$K^*(q) = K_1^*(q) + K_2^*(q); \quad (3.2)$$

For feedback connection (Fig. 5c)

$$K^*(q) = \frac{K_1^*(q)}{1 + K_1^*(q) K_2^*(q)}. \quad (3.3)$$

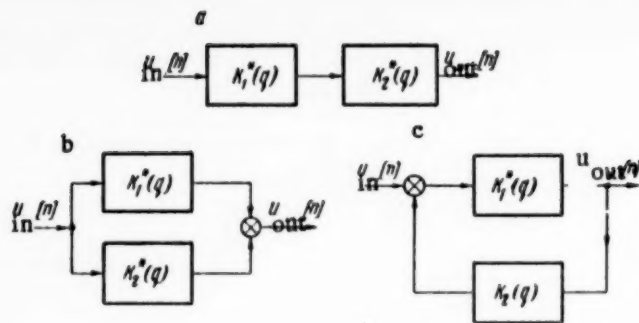


Fig. 5

It is assumed here that all the pulse networks operate in synchronism and in phase.

Pulse correction is realized by introducing into the pulse system a supplementary pulse network, and also by introducing a pulse network into the continuous system. We shall denote the transfer function of the supplementary pulse network by  $K_s^*(q)$ .

The structure of a system containing series or parallel pulse correction is shown in Fig. 6 or 7 respectively.\* We shall not consider the more complicated case of correction by means of a feedback network.

The transfer function of the supplementary pulse network  $K_s^*(q)$  must be so chosen that the open-loop transfer function of the corrected system equals the specified value, i.e.,  $W_c^*(q)$ .

Thus, we readily obtain for series correction (Fig. 6)

$$K_s^*(q) = \frac{W_c^*(q)}{W^*(q)}, \quad (3.4)$$

where  $W^*(q)$  is the open-loop transfer function of the initial system.

For parallel correction (Fig. 7) we have

$$K_s^*(q) = \frac{W_c^*(q) - W^*(q)}{K_1^*(q)}. \quad (3.5)$$

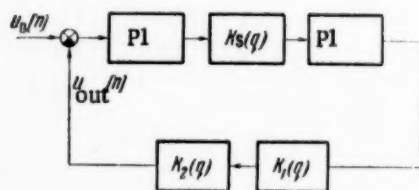


Fig. 6

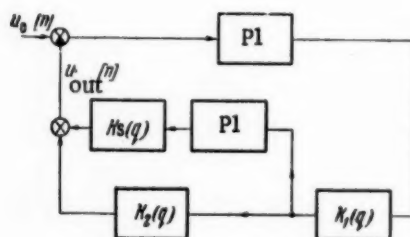


Fig. 7

\* Series pulse correction was discussed also in [3].

Knowing  $K_s^*(q)$ , it is possible to use the methods described in the Appendix to determine the transfer function of the linear portion  $K_s(q)$  of the supplementary pulse network;

Pulse correction can also be effected with a digital computing device, which is equivalent in its operating character to a certain pulse network.

The input quantity of the digital computing device represents equally-spaced discrete values  $u_1[n]$  of a certain function  $u_1(\tau)$ , and the output quantities are equally-spaced discrete values  $u_2[n]$  of a function  $u_2(\tau)$ , corresponding to the results of the calculation. The correspondence between these two values can be written in the following form:

$$\alpha_l u_2[n] = \sum_{v=0}^{l_1} \beta_{l_1-v} u_1[n-v] - \sum_{v=1}^l \alpha_{l-v} u_2[n-v]. \quad (3.6)$$

This difference equation defines a linear program (i.e., a sequence of actions) of the digital computing device [4, 5].

Subjecting (3.6) to a discrete Laplace transform

$$D\{u[n]\} = \sum_{n=0}^{\infty} u[n] e^{-qn} = U^*(q), \quad (3.7)$$

we get upon transformation

$$U_2^*(q) = \frac{\beta_0 + \beta_1 e^q + \dots + \beta_{l_1} e^{q l_1}}{1 + \alpha_1 e^q + \dots + \alpha_l e^{q l}} e^{q(l-l_1)} U_1^*(q). \quad (3.8)$$

The transfer function of the digital computing device will therefore be

$$K^*(q) = \frac{\beta_0 + \beta_1 e^q + \dots + \beta_{l_1} e^{q l_1}}{1 + \alpha_1 e^q + \dots + \alpha_l e^{q l}} e^{q(l-l_1)}; \quad (3.9)$$

and will not differ at all from the transfer function of a pulse network.

Thus, by choosing a suitable program for the digital computing device, it is possible to use the latter as an element for pulse correction.

The choice of correction elements can also be based on experimental characteristics of the linear portion of the system, provided the synthesis method described in [6] is used. The only difference here is that the transfer functions determined by Equations (3.4) and (3.5) will be represented as series in powers of  $e^{-q}$ .

In addition to using continuous or pulse correction, it is possible to employ a combination of the two. In this case a supplementary pulse network, or an equivalent digital computing device, is introduced in parallel to one of the continuous elements of the continuous (but not pulse) systems.

#### 4. Choice of the Transfer Function of the Corrected Pulse System

From the point of view of the steady-state processes, it is frequently desirable to have the  $r$  coefficients

of the errors of the pulse system vanish [7].

On the other hand, from the point of view of the transient process it is desirable that the transient in the pulse system terminate in a minimum time, for a given gain, or in other words, that the pulse system have an infinite degree of stability [2, 8].

A pulse system satisfying these conditions is called an optimum system. Let

$$W^*(q) = \frac{P^*(q)}{Q^*(q)}, \quad (4.1)$$

where  $P^*(q)$  and  $Q^*(q)$  are polynomials in  $e^q$  of degree  $l_1$  and  $l$  respectively, with  $l_1 \leq l$ .

Substituting  $W^*(q)$  from (4.1) into (1.2), let us represent the closed-loop transfer function as:

$$K_2^*(q) = \frac{Q^*(q)}{Q^*(q) + P^*(q)} = \frac{H_2^*(q)}{G^*(q)}. \quad (4.2)$$

Here  $H_2^*(q)$  and  $G^*(q)$  are polynomials in  $e^q$  of equal degree  $l$ , and

$$G^*(q) = a_0 + a_1 e^q + \dots + a_l e^{ql} = 0 \quad (4.3)$$

is the characteristic equation.

If the degree  $l_1$  of the polynomial  $P^*(q)$  is less than the degree  $l$  of the polynomial  $Q^*(q)$ , then, as can be seen from (4.2), the coefficients of the highest powers of  $H_2^*(q)$  and  $J^*(q)$  will equal each other.

The pulse system will have  $r$  vanishing error coefficients if  $H_2^*(q)$  can be represented as

$$H_2^*(q) = H_a^*(q) (e^q - 1)^r, \quad (4.4)$$

where

$$H_a^*(0) \neq 0. \quad (4.5)$$

The pulse system will have an infinite degree of stability, i.e., its transient will terminate in a minimum time, if it is possible to choose its parameters such that the characteristic equation is reduced to the form

$$G^*(q) = a_l e^{ql} = 0, \quad (4.6)$$

ie., if (see [8])



$$a_0 = a_1 = \dots = a_{l-1} = 0. \quad (4.7)$$

Consequently, the transfer function of the optimum pulse system can be represented as

$$K_{2\text{opt}}^*(q) = \frac{H_a(q)(e^q - 1)^r}{a_l e^{ql}}. \quad (4.8)$$

On the basis of Equation (1.3) we obtain an expression for the open-loop correction pulse-system transfer function for  $K_{2d}^*(q) = K_{2\text{opt}}^*(q)$ :

$$W_c^*(q) = \frac{1}{K_{2\text{opt}}^*(q)} - 1 = \frac{a_l e^{ql} - H_a^*(q)(e^q - 1)^r}{H_a^*(q)(e^q - 1)^r}. \quad (4.9)$$

This relationship can be used for the correction of pulse systems.

### 5. Examples of Corrections of Pulse Systems

By way of the first example, let us consider a system where discrete data are transformed into continuous ones, the diagram of the system being shown in Fig. 8. The transfer function of its linear part is

$$W(q) = \frac{k_l}{q}. \quad (5.1)$$

The open-loop transfer function of the system, in the case of a duty cycle  $\gamma = 1$ , is of the form

$$W^*(q) = \frac{k_0}{e^q - 1}. \quad (5.2)$$

According to (1.2) we obtain the transfer function of the closed-loop system

$$K_2^*(q) = \frac{e^q - 1}{e^q - 1 + k_0}. \quad (5.3)$$

The system will be stable if  $k_0 < 2$ .

The error coefficients, determined from equations given in [7], are

$$\begin{aligned} d_0 &= K_2^*(0) = 0, & d_1 &= -\frac{1}{k_0}, \\ d_r &= (-1)^r \frac{(k_0 - 1)^{r-1}}{k_0^r} & (r \geq 2). \end{aligned} \quad (5.4)$$

The static-error coefficient  $d_0$  of the system is 0. The velocity-error coefficient  $d_1$  has an absolute value that diminishes with increasing gain coefficient  $k_0$ .

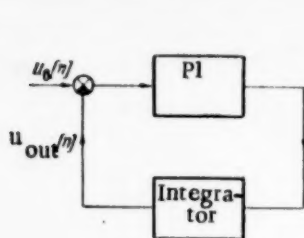


Fig. 8

However, since the stability condition requires that inequality  $k_0 < 2$  be satisfied, the absolute value of the velocity-error coefficient cannot be less than  $1/2$ .

An infinite degree of stability, corresponding to a minimum regulation time, is attained at  $k_0 = 1$ . In this case

$$K_2^*(q) = \frac{e^q - 1}{e^q} = 1 - e^{-q}. \quad (5.5)$$

The equation for the error will assume the following form:

$$U_{in}^*(q) = K_2^*(q) U_0^*(q) = (1 - e^{-q}) U_0^*(q).$$

Changing from the transform to the original, we obtain

$$u_{in}[n] = u_0[n] - u_0[n-1] = \Delta u_0[n-1].$$

If the driving function is constant,  $u_0[n] = c$ , we have

$$u_{in}[n] = \Delta u_0[n-1] = \begin{cases} c & \text{at } n = 0, \\ 0 & \text{at } n \geq 1, \end{cases} \quad (5.6)$$

i.e., starting with  $n = 1$  the system error will be zero (Fig. 9a). However, if the driving function varies linearly,  $u_0[n] = cn$ , then

$$u_{in}[n] = \Delta u_0[n-1] = \begin{cases} 0 & \text{at } n = 0, \\ c & \text{at } n \geq 1. \end{cases} \quad (5.7)$$

It follows from (5.7) that starting with  $n = 1$ , the error of the system will be constant and equal to  $c$  (Fig. 9b).

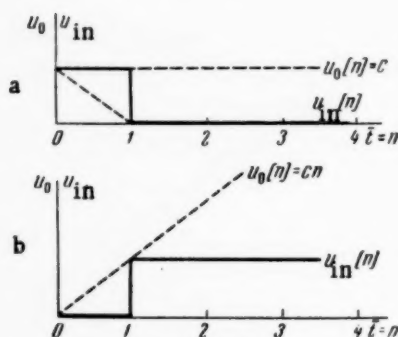


Fig. 9

Let us impose the requirement that the steady-state error be zero for a linearly-varying driving function and that the degree of stability be infinite.

To satisfy these conditions it is necessary that the closed-loop transfer function of the system be

$$K_2^* d(q) = \frac{(e^q - 1)^2}{e^{2q}} = (1 - e^{-q})^2. \quad (5.8)$$

The equation for the error will assume the form

$$\begin{aligned} U_{in}^*(q) &= K_2^* d(q) U_0^*(q) = \\ &= (1 - e^{-q})^2 U_0^*(q). \end{aligned} \quad (5.9)$$

After changing from the transform to the original we get

$$u_{in}[n] = u_0[n] - 2u_0[n-1] + u_0[n-2] = \Delta^2 u_0[n-1]. \quad (5.10)$$

In the case of a linearly-varying driving function

$$u_{in}[n] = \Delta^2 u_0[n-1] = \begin{cases} 0 & \text{at } n=0, \\ c & \text{at } n=1, \\ 0 & \text{at } n \geq 2, \end{cases} \quad (5.11)$$

from which it follows that in such a system, in the case of a linearly-varying driving function, the error will be zero starting with  $n=2$  (Fig. 10).

Substituting the resultant value of the closed-loop transfer function (5.8) into (1.3), we obtain the unknown open-loop transfer function

$$W_c^*(q) = \frac{e^{2q}}{(e^q - 1)^2} - 1 = \frac{2e^q - 1}{(e^q - 1)^2}. \quad (5.12)$$

Let us first consider the case of continuous correction. For this purpose, let us represent  $W_c^*(q)$  as

$$W_c^*(q) = \frac{e^q}{(e^q - 1)^2} + \frac{1}{e^q - 1}. \quad (5.13)$$

Using the table for  $W(q)$  vs.  $W^*(q)$ , given in the Appendix, we obtain the transfer function of the linear portion of the system ( $\gamma = 1$ )

$$W_c(q) = \frac{1}{q^2} + \frac{3}{2} \frac{1}{q}. \quad (5.14)$$

The transfer function of the uncorrected system is

$$W(q) = \frac{k_1}{q}.$$

Therefore, in the case of series correction, we obtain from (2.1) the transfer function of the correcting network in the form

$$K_s(q) = \frac{W_c(q)}{W(q)} = \frac{1}{k_1 q} + \frac{3}{2k_1}. \quad (5.15)$$

The correcting element consists of an integrating circuit with a relative gain coefficient  $1/k_I$  in parallel with an amplifying circuit with a relative gain coefficient  $3/2k_I$ . The block diagram of the corrected system is given in Fig. 11.

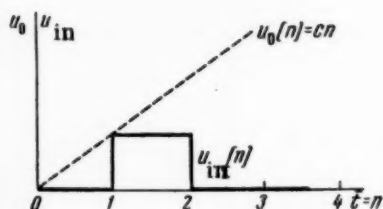


Fig. 10

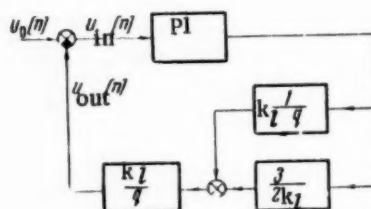


Fig. 11

In the case of parallel correction (see Fig. 3), assuming

$$K_1(q) = k_I \quad K_2(q) = \frac{1}{q}, \quad (5.16)$$

we obtain from (2.2)

$$K_3(q) = \frac{W_c(q)}{K_2(q)} - K_1(q) = \frac{1}{q} + \left(\frac{3}{2} - k_l\right). \quad (5.17)$$

As before, the correcting elements consist of a parallel junction of integrating and amplifying circuits, but the relative gain coefficients are respectively 1 and  $3/2 - k_I$ . The block diagram of the corrected system is shown in Fig. 12. If amplifying elements are combined, this circuit reduces to the previous one.

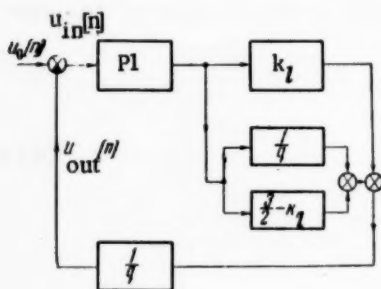


Fig. 12

In this case it is impossible to realize correction by means of a feedback element.

Let us consider now the case of pulse correction. The respective open-loop transfer functions of the corrected and uncorrected systems are, according to (5.12) and (5.2),

$$W_c^*(q) = \frac{2e^q - 1}{(e^q - 1)^2}, \quad W^*(q) = \frac{k_0}{e^q - 1}. \quad (5.18)$$

In the case of series correction, the transfer function of the correcting pulse network or of the digital computing device should be

$$K_L^*(q) = \frac{W_n^*(q)}{W^*(q)} = \frac{1}{k_0} \frac{2e^q - 1}{e^q - 1}. \quad (5.19)$$

A pulse correcting device having this transfer function can be realized in the form of a pulsed network, in the form of a system with delay lines or delay elements, and finally, in the form of a digital computing device with a suitable program.

Let us consider these possibilities briefly.

Representing  $K_s^*(q)$  of (5.19) in the form

$$K_s^*(q) = \frac{2}{k_0} + \frac{1}{k_0} \frac{1}{e^q - 1}. \quad (5.20)$$

and using the  $W(q)$  vs.  $W^*(q)$  table in the Appendix, we obtain the transfer function of the linear part of the correcting pulse network:

$$K_s(q) = \frac{2}{k_0} + \frac{1}{k_0} \frac{1}{q}. \quad (5.21)$$

Thus, the correcting pulse network consists of an integrating and an amplifying element with relative gain coefficients of  $1/k_0$  and  $2/k_0$  respectively.

A block diagram of the corrected system is shown in Fig. 13.

Let us now represent  $K_s^*(q)$  of (5.19) in the following form:

$$K_s^*(q) = \frac{1}{k_0} \frac{2 - e^{-q}}{1 - e^{-q}} = \frac{1}{k_0} \frac{1}{1 - e^{-q}} + \frac{1}{k_0}. \quad (5.22)$$

A device having a similar transfer function can be obtained using delay elements in the following manner.

Let us add to the feedback loop of a unity-gain amplifier a delay element with a relative delay time  $\bar{\tau} = \tau/T_r = 1$ , i.e., with a delay equal to the repetition period. Noting that the transfer function of such a delay

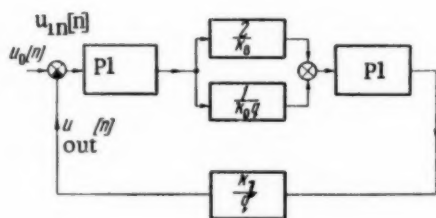


Fig. 13

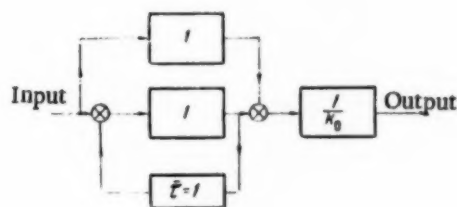


Fig. 14

element is  $e^{-q}$ , let us find the transfer function of such a combination (with positive feedback included) in the form

$$\frac{1}{1 - e^{-q}}. \quad (5.23)$$

Next, as seen from (5.22), it is necessary to parallel this combination with a unity-gain amplifier. The sum of the output signals is applied to the input of an amplifier with a gain  $1/k_0$  (Fig. 14). The device obtained in this manner should act on the pulse element. The block diagram of the corrected system is shown in Fig. 15.

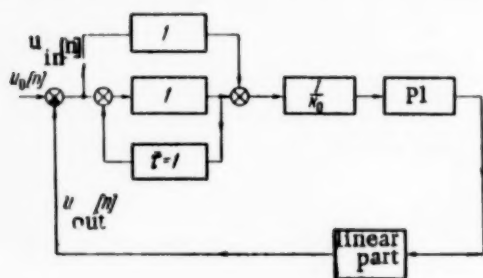


Fig. 15

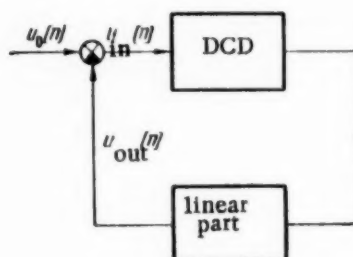


Fig. 16

Finally, a system having a transfer function of the form (5.22) can be realized by introducing a digital computing device (Fig. 16) in lieu of the pulse element. The input to this device should be the error, and the output the corresponding pulses representing the numbers. The program of the digital computing device can be obtained from the transfer function (5.22).

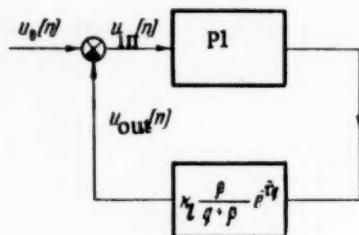


Fig. 17

According to (3.8) we have

$$U_2^*(q) = K_2^*(q) U_1^*(q) = \frac{1}{k_0} \frac{2 - e^{-q}}{1 - e^{-q}} U_1^*(q) \quad (5.24)$$

or

$$(1 - e^{-q}) U_2^*(q) = \frac{1}{k_0} (2 - e^{-q}) U_1^*(q). \quad (5.25)$$

Taking the inverse transform, we obtain an expression for the program of the correcting digital device in the form of a difference equation

$$u_2[n] - u_2[n-1] = \frac{1}{k_0} (2u_1[n] - u_1[n-1]) \quad (5.26)$$

or

$$\Delta u_2[n-1] = \frac{1}{k_0} (u_1[n] + \Delta u_1[n-1]). \quad (5.27)$$

By way of another example let us consider in automatic-regulation system with time delay, shown in Fig. 17.

The transfer function of the linear portion of the system, in relative parameters, is of the form



$$W(q) = k_t \frac{P(q)}{Q(q)} e^{-\tau q} = k_t \frac{\beta e^{-\tau q}}{q + \beta}, \quad (5.28)$$

where  $\beta = \frac{T_r}{T_a}$ ,  $\bar{\tau} = \frac{\tau}{T_r}$ ,  $T_a$  is the time constant,  $\tau$  is the delay time and  $T_r$  is the regulation interval.

Let us assume that  $\gamma = 1$ , i.e., we consider a pulse system of Type I, and that  $k > \bar{\tau} \geq k - 1$ , where  $k$  is an integer. The open-loop transfer function of the system, in accordance with the following equation

$$W^*(q) = k_0 e^{-qk} \left[ \frac{P(0)}{Q(0)} + \sum_{v=1}^l \frac{P(q_v)}{q_v Q'(q_v)} e^{qk(k-\bar{\tau})} \frac{e^q - e^{q_v(1-\gamma)}}{e^q - e^{q_v}} \right]$$

will then be

$$W^*(q) = k_0 e^{-qk} \left[ 1 - \frac{e^q - 1}{e^q - e^{-\beta}} e^{-\beta(k-\bar{\tau})} \right] \quad (5.29)$$

or

$$W^*(q) = \frac{b'_1 e^q + b'_0}{e^{qk} (e^q - e^{-\beta})}, \quad (5.30)$$

where

$$b'_1 = k_0 (1 - e^{-\beta(k-\bar{\tau})}), \quad b'_0 = k_0 (e^{-\beta(k-\bar{\tau})} - e^{-\beta}).$$

If  $\bar{\tau} = k$ , we obtain from (5.30)

$$W^*(q) = \frac{b'_0}{e^{qk} (e^q - e^{-\beta})}, \quad (5.31)$$

where  $b'_0 = k_0 (1 - e^{-\beta})$ .

Finally, if  $\bar{\tau} = 0$ , we have

$$W^*(q) = \frac{b'_0}{e^q - e^{-\beta}} \quad (5.32)$$

The closed-loop transfer function at  $\bar{\tau} = 0$  will be

$$K_2^*(q) = \frac{1}{1 + W^*(q)} = \frac{e^q - e^{-\beta}}{e^q - e^{-\beta} - b'_0}. \quad (5.33)$$

If we choose  $b'_0 = e^{-\beta}$  or, what is equivalent,  $k_0 = \frac{e^{-\beta}}{1 - e^{-\beta}}$ , we obtain from (5.33)

$$K_2^*(q) = \frac{e^q - e^{-\beta}}{e^q} = 1 - e^{-\beta} e^{-q}. \quad (5.34)$$

The equation for the error of the system will be

$$U_{in}^*(q) = K_2^*(q) U_0^*(q) = (1 - e^{-\beta} e^{-q}) U_0^*(q). \quad (5.35)$$

Taking the inverse transform, we get

$$u_{in}[n] = u_0[n] - e^{-\beta} u_0[n-1]. \quad (5.36)$$

In the case of a step driving function  $u_0[n] = c$  we get

$$u_{in}[n] = \begin{cases} c & \text{at } n = 0, \\ c(1 - e^{-\beta}) & \text{at } n \geq 1, \end{cases} \quad (5.37)$$

i.e., the process in the system terminates after the first interval (Fig. 18a), causing an infinite degree of stability.

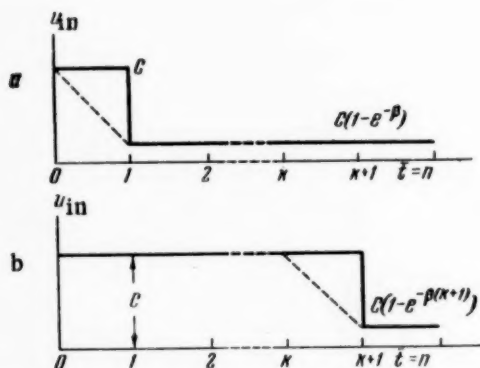


Fig. 18

We require that the system with delay behave like the system without delay, except for a time shift determined by the delay time. Under these conditions, the closed-loop transfer function of the system with delay should have been the form

$$K_{2d}^*(q) = 1 - ae^{-(k+1)q} = \frac{e^{(k+1)q} - a}{e^{(k+1)q}}. \quad (5.38)$$

In this case we obtain from the error equation

$$U_{in}^*(q) = K_{2c}^*(q) U_0^*(q) \quad (1 - ae^{-(k+1)q}) U_0^*(q); \quad (5.39)$$

we obtain by taking the inverse transform

$$u_{in}[n] = u_0[n] - au_0[n - k - 1]. \quad (5.40)$$

Consequently, in the case of a step driving function  $u_0[n] = c$

$$u_{in}[n] = \begin{cases} c & \text{at } n = 0, 1, \dots, k, \\ c(1-a) & \text{at } n \geq k+1, \end{cases} \quad (5.41)$$

i.e., the system transient terminates after the  $(k+1)$ -th interval, where  $k = \bar{\tau}$  is the relative delay time (Figure 18b). In other words, the output of the system with delay will have the same form as that of a system without delay, but will be shifted by an amount equal to the delay time.

Inserting (5.38) into (4.9) we obtain the open-loop transfer function of the system

$$W_c^*(q) = \frac{a}{e^{q(k+1)} - a}. \quad (5.42)$$

Choosing the series pulse-correction method, let us obtain the transfer function for the correcting device in accordance with Equation (3.4):

at  $k < \bar{\tau} < k+1$

$$K_s^*(q) = \frac{W_c^*(q)}{W^*(q)} = \frac{ae^{qk}(e^q - e^{-\beta})}{(e^{q(k+1)} - a)(b'_1 e^q + b'_0)}; \quad (5.43)$$

at  $k = \bar{\tau}$

$$K_s^*(q) = \frac{W_c^*(q)}{W^*(q)} = \frac{a}{b'_0} \frac{e^{qk}(e^q - e^{-\beta})}{e^{q(k+1)} - a}. \quad (5.44)$$

For simplicity, let us consider the case  $\bar{\tau} = k$ .

Let us represent the transfer function of the correcting device (5.44) in the form

$$K_s^*(q) = \frac{a}{b'_0} \frac{1 - e^{-\beta}e^{-q}}{1 - ae^{-q(k+1)}}. \quad (5.45)$$

The difference equation, corresponding to this transfer function, is of the form

$$u_2[n] - au_2[n-k-1] = \frac{a}{b'_0} [u_1[n] - e^{-\beta}u_1[n-1]]. \quad (5.46)$$

Thus, to correct the system it is necessary to introduce a correcting device with a transfer function as defined by Equation (5.43) or (5.44) (Fig. 19).

The correcting device can be realized with the aid of amplifying elements and delay elements connected in accordance with Equation (5.46) as shown in Fig. 20.

In particular, if we put  $a = e^{\beta(k+1)}$ , we obtain from (5.45)

$$K_s^*(q) = \frac{e^{-\beta(k+1)}}{b'_0} \frac{1}{1 + e^{-\beta}e^{-q} + e^{-2\beta}e^{-2q} + \dots + e^{-k\beta}e^{-kq}}. \quad (5.47)$$

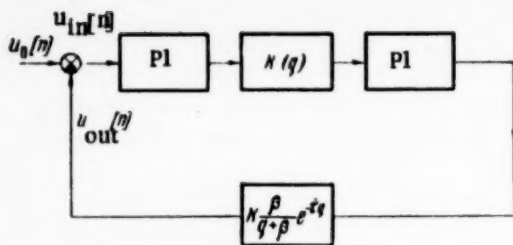


Fig. 19

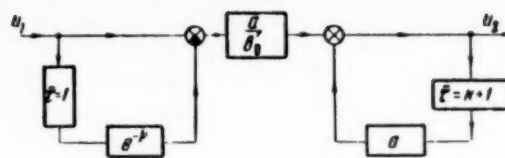


Fig. 20

The difference equation corresponding to this transfer function is

$$u_2[n] + e^{-\beta}u_2[n-1] + e^{-2\beta}u_2[n-2] + \dots + e^{-k\beta}u_2[n-k] = \frac{e^{-\beta(k+1)}}{k_0(1 - e^{-\beta})} u_1[n]. \quad (5.48)$$

The diagram of the correcting device must then be as shown in Fig. 21. It was obtained in a different manner in [10].

The correcting network can also be realized in the form of a digital computing device, the program of which is determined by the above difference Equation (5.40), (5.48), or which is equivalent, by transfer functions (5.38).

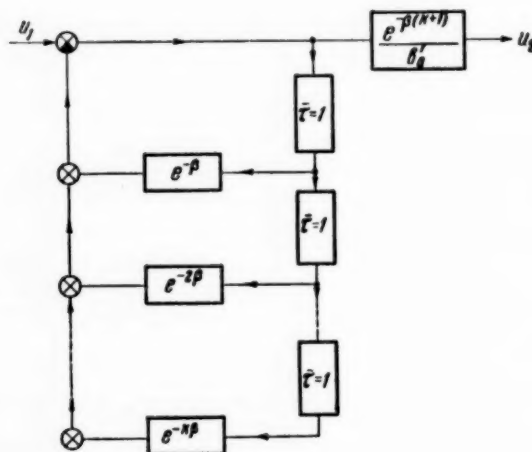


Fig. 21

If  $a = e^{-\beta(k+1)}$  we have according to (5.41)

$$u_{in}[n] = c(1 - e^{-\beta(k+1)}) \quad (n \geq k+1)$$

or, changing to absolute units

$$u_{in}[nT_r] = c \left( 1 - e^{-\frac{1}{T_a}(\tau + T_r)} \right) \quad (t \geq \tau + T_r).$$

It is seen from this that as  $T_r$  diminishes, the statistical error and the duration of the process decrease\*; the form of the transient remains the same (if  $\bar{\tau} = \tau/T_r = k$ ).

It follows from the above that introducing a pulse corrector in the form of a pulse network, delay element, or a digital computing device, into a continuous regulation system makes it possible to obtain optimum performance from the point of view of infinite degree of stability.

## APPENDIX

### Connection Between $W(q)$ and $W^*(q)$

Let

$$W(q) = \frac{P(q)}{Q(q)} = \sum_{v=1}^l \frac{P(q_v)}{Q'(q_v)} \frac{1}{q - q_v}, \quad (1)$$

where  $q_v$  are the poles of  $W(q)$ , which are assumed all different.

As was shown in [2], we have in this case

$$W^*(q) = k_p C + k_p \sum_{v=1}^l \frac{P(q_v)}{Q'(q_v)q_v} \frac{e^q - e^{q_v(1-\gamma)}}{e^q - e^{q_v}}, \quad (2)$$

where  $C = \lim_{q \rightarrow 0} \frac{P(q)}{Q(q)}$ .

Thus, if the expression derived for  $W^*(q)$  is represented in form (2) it is possible to obtain  $q_v$  and  $P(q_v)/Q(q_v)$ , and consequently also  $W(q)$ , using (1). It is useful to employ the following table

TABLE

$W(q)$	$W^*(q)$		
	$0 < \gamma \leq 1; k_p = 1$	$\gamma = 1, k_p = 1$	$\gamma < 1, k_p \gamma = 1$
$e^{-qk}$	$e^{-qk}$	$e^{-qk}$	$e^{-qk}$
$\frac{1}{q}$	$\frac{\gamma}{e^q - 1}$	$\frac{1}{e^q - 1}$	$\frac{1}{e^q - 1}$
$\frac{1}{q^2}$	$\gamma \frac{e^q}{(e^q - 1)^2} - \frac{\gamma^2}{2} \frac{1}{e^q - 1}$	$\frac{e^q}{(e^q - 1)^2} - \frac{1}{2} \frac{1}{(e^q - 1)}$	$\frac{e^q}{(e^q - 1)^2}$
$\frac{1}{q + \beta}$	$\frac{1}{\beta} \frac{e^{-\beta(1-\gamma)} - e^{-\beta}}{e^q - e^{-\beta}}$	$\frac{1}{\beta} \frac{1 - e^{-\beta}}{e^q - e^{-\beta}}$	$\frac{e^{-\beta}}{e^q - e^{-\beta}}$

\* In [11] it was indicated in error (Page 677, second line from the top) in the analysis of this system that the static error increases.

The Table gives the values of  $W^*(q)$  corresponding to  $W(q)$  for  $\gamma \ll 1$ , for  $0 < \gamma < 1$ , and for  $\gamma = 1$ . In the latter two cases we assume  $k_p \approx 1$ , and in the former case  $k_p \gamma = 1$ . If we do not restrict ourselves to the open-loop transfer function when  $\epsilon = 0$ , i.e., to  $W^*(q)$ , but consider  $W^*(q, \epsilon)$  (see [2]), the relationship between  $W(q)$  and  $W^*(q, \epsilon)$  is of the form

$$W(q) = \int_0^1 e^{q\epsilon} W^*(q, \epsilon) d\epsilon. \quad (3)$$

This relationship follows from the representation of  $W^*(q, \epsilon)$  in terms of  $W(q + m2\pi) e^{-q\epsilon}$  (see for example [9], [11]) in the form of a Fourier series:

$$W^*(q, \epsilon) = \sum_{m=-\infty}^{\infty} e^{(q+2\pi jm)\epsilon} W(q + 2\pi jm). \quad (4)$$

It represents the Fourier coefficient of series (4) at  $m = 0$ .

Received January 24, 1956

#### LITERATURE CITED

- [1] W. K. Linvill and R. W. Sittler, Extension of conventional techniques to the design of samples-data systems. Convention Record of the IRE, Part. 5, 1953.
- [2] Ia. Z. Tsypkin, Transient and Steady-State Processes in Pulse Circuits, Gosenergoizdat, (1951).
- [3] A. R. Bergen and J. R. Ragazzini, "Sampled data processing techniques for feedback control systems." Applications and Industry, 1954.
- [4] R. B. Conn, "Digital computers for linear, real-time control systems." Proceeding Joint Computer Conference, 1953.
- [5] J. M. Salzer, "Frequency analysis of digital computers operating in real time." Proc. of the IRE, Vol. 42, No. 2, 1954.
- [6] Ia. Z. Tsypkin, "On the Design of Nonlinear Intermittent (Pulsed) Regulation Systems," Transactions of Second All-Union Conference on the Theory of Regulation, Vol. II., Publ. by USSR Acad. Sci (1955).
- [7] Ia. Z. Tsypkin, "Investigation of Steady State Processes in Pulse Servo Systems," Automation and Remote Control, Vol. XVII, No. 12, (1956).
- [8] Ia. Z. Tsypkin, "Theory of Intermittent Regulation, III. " Automation and Remote Control, Vol. XI, No. 5, (1950).
- [9] Ia. Z. Tsypkin, "Frequency Method of Investigating Intermittent-Regulation Systems," Automation and Remote Control, Vol. XIV, No. 1 (1953).
- [10] R. H. Barker, "The pulse transfer function and its application to sampling servosystems. Proc. of the IEE, Part IV, No. 4, 1952.
- [11] Ia. Z. Tsypkin, "On Automatic-Regulation Systems Containing Digital Computing Devices," Automation and Remote Control, Vol. XVII, No. 8, 1956.
- [12] Ia. Z. Tsypkin, "Frequency method of Investigating the Periodic Modes of Automatic-Regulation Relay Systems," Collection "In Memory of A. A. Andronov," Publ. by USSR Acad. Sci (1955).



## TWO-CHANNEL AUTOMATIC REGULATION SYSTEMS WITH ANTISYMMETRIC CROSS CONNECTIONS

A. A. Krasovskii

(Moscow)

Linear systems, consisting of two identical channels and having antisymmetric cross connections are examined. The antisymmetric connections are classified and transfer functions with complex coefficients are derived. Possible antisymmetric connections of various types are analyzed with respect to their ability to increase the stability margin and the critical gain of a system.

It is shown that the possibilities of synthesizing correcting devices in two-channel systems are greater than in single-channel ones, and that introducing cross connections may extend the stability substantially.

A limited but important class of automatic-regulation systems is one containing two identical channels. This class includes radar tracking, servo systems, gyro verticals, and many other devices. Such systems are best investigated using complex coordinates and equations with complex coefficients.

This method was applied by many investigators to actual specific problems [1, 2, 3]. In the analysis of actual two-channel systems it was observed that introducing cross connections between each channel sometimes improves the response of the regulation process.

It is the purpose of this work to examine in a more general manner the properties of linear two-channel systems, using complex coordinates, and to exhibit the effect of cross connections on the stability of the above systems.

### 1. Complex Transfer Functions of Two-Channel Systems

Let us consider the block diagram of a conical-sweeptracking angle servo system, i.e. The servomechanism of a radar tracking antenna. The error signals are formed here with a phase network, which receives a voltage from the coordinate computer and a reference voltage.

The azimuth channel and the elevation angle channel of the servomechanism will be assumed identical and the drive will be assumed to be dc motors with reversible reduction gears and negligibly small friction.\* If the phase shift of the reference voltage is zero and the effect of the gyroscopic torque of the rotating parts of the servomechanism is small, the servo system channels are independent. The corresponding block diagram is shown in Fig. 1a, where  $W(p)$  denotes the transfer function of the amplifier with correcting networks, and the transfer function of the servo motor is represented as  $1/p(1 + Tp)$ ;  $p \equiv d/dt$ . In the presence of a phase shift  $\varphi$  in the reference voltage, the signals at the output of the phase network becomes

$$u'_h = u_h \cos \varphi - u_v \sin \varphi, \quad u'_v = u_h \sin \varphi + u_v \cos \varphi,$$

\*Reversible reduction gears are those in which the torque applied to the output shaft is transmitted in a definite ratio to the input shaft.

where  $u_h$  and  $u_v$  are signals entering the system channels in the absence of a phase shift.

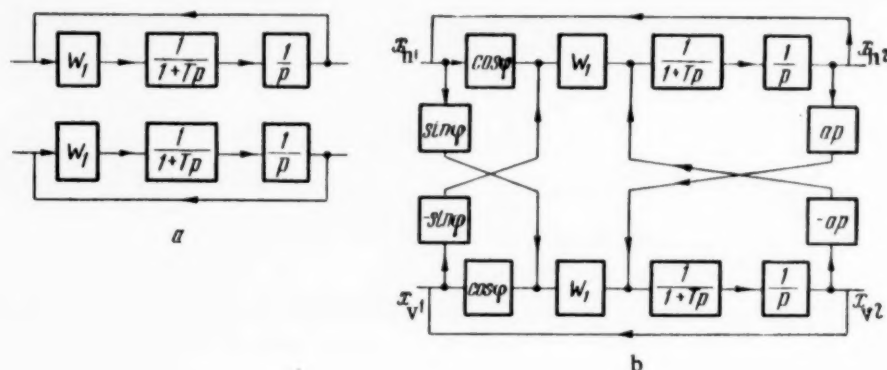


Fig. 1

Thus, if  $\varphi \neq 0$ , the channels of the servo system become interconnected. The gyroscopic torque produced by the rotating parts of the servo platform also causes a coupling between the channels, which can be characterized by the quantity  $a = HT/J$ , where  $H$  is the kinetic moment,  $J$  the equatorial moment of inertia of the servo system, and  $T$  the electromechanical time constant of the servo motors. The block diagram of the servo system in the presence of a phase shift in the reference voltage and in the presence of a kinetic moment is shown in Fig. 1b. It follows from this diagram that

$$\begin{aligned} \frac{1}{p(1+Tp)} \{W_1 [(x_{h1} - x_{h2}) \cos \varphi - (x_{v1} - x_{v2}) \sin \varphi] - apx_{v2}\} &= x_{h2}, \\ \frac{1}{p(1+Tp)} \{W_1 [(x_{v1} - x_{v2}) \cos \varphi + (x_{h1} - x_{h2}) \sin \varphi] + apx_{h2}\} &= x_{v2}. \end{aligned} \quad (1)$$

Let us introduce the complex variables

$$\bar{x}_1 = x_{h1} + jx_{v1}; \quad \bar{x}_2 = x_{h2} + jx_{v2}.$$

The imaginary unit  $j = \sqrt{-1}$ , which so to speak plays the role of a unit vector, is thus identified with the variable values of the elevation angle  $x_{v1}$  and  $x_{v2}$ .

Let us multiply the lower equation by  $j$  and add it to the upper. We then obtain

$$\frac{1}{p(1+Tp)} \{W_1 [(\bar{x}_1 - \bar{x}_2) \cos \varphi + j(\bar{x}_1 - \bar{x}_2) \sin \varphi] + jap\bar{x}_2\} = \bar{x}_2$$

or

$$We^{i\varphi} (\bar{x}_1 - \bar{x}_2) + \frac{ja}{1+Tp} \bar{x}_2 = \bar{x}_2, \quad (2)$$

where  $W = W_1/p(T+p)$  is the open-loop transfer function of the servo system in the absence of coupling between the channels. Equation (2) can be written as

$$x_2 = \frac{W}{\left(1 - \frac{ja}{1 + Tp}\right) e^{-j\varphi} + W} \bar{x}_1 \quad (3)$$

Let us now consider more general two-channel systems containing uni-directional links, and for this purpose let us classify the connections between the identical channels. Links of two identical channels will be called identical if they are equal and if they are located in equal positions on the path of the signals. A connection that transmits the signal from the output of any one link of one channel to the output of a following link of the second channel (the sequence being defined along the direction of propagation of the signal), will be called a direct cross connection. A connection that transmits the signal from the output of a link in one channel to the output of a preceding link of the second channel will be called a reverse cross connection.

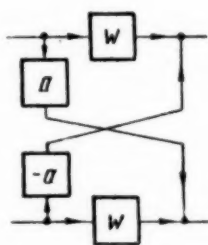


Fig. 2

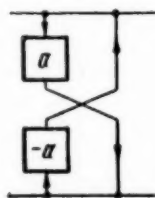


Fig. 3

A connection consisting of two crossing links, which have transfer functions of opposite signs and which carry the signal from the outputs of identical elements to the inputs of identical elements will be called antisymmetric. An antisymmetric connection is proportional if its transfer function equals a constant real value. According to the definitions introduced above, the servo system discussed here has antisymmetric connections of two types: a proportional direct connection, caused by the phase shift of the reference voltage, and a velocity feedback connection caused by the gyroscopic moment.

The direct antisymmetric connection contains the identical amplifying elements  $\cos \varphi$ , and the inverse antisymmetric connection contains the identical elements  $1/p(1 + Tp)$  (Fig. 1).

Figure 2 shows a direct antisymmetric connection with a transfer function  $a(p)$  containing the elements  $W$ . Such a connection will be called a two-channel link with direct antisymmetric connection. The output quantities of this link  $x_{out}$  and  $x'_{out}$  are related to the input quantities by the following equation

$$x_{out} = Wx_{in} - ax'_{in}, \quad x'_{out} = Wx'_{in} + ax_{in}.$$

Multiplying the second of these equations by  $j$ , adding, and introducing the complex quantities

$$\bar{x}_{in} = x_{in} + jx'_{in} \text{ and } \bar{x}_{out} = x_{out} + jx'_{out},$$

we get

$$\bar{x}_{out} = (W + ja) \bar{x}_{in}. \quad (4)$$

Thus, the complex transfer function of a two-channel link with a direct antisymmetric connection equals the transfer function  $W$  of the identical links plus the imaginary transfer function  $ja$  of the antisymmetrical connection. It is well worth mentioning that in single-channel systems, containing a link  $W$  with a direct connection  $a$  results in a transfer function of the form  $W + a$ . If the direct antisymmetric connection joins the outputs of identical links (Fig. 3), it can also be considered as a particular case of the just-described two-channel link (Fig. 2), in which  $W = 1$ . The transfer function of the two-channel link shown in Fig. 3 is therefore  $1 + ja$ .

A two-channel link with antisymmetric negative feedback is shown in Fig. 4. The input and output quantities of this link are related by the following equations:

$$x_{\text{out}} = Wx_{\text{in}} + aWx'_{\text{out}}, \quad x'_{\text{out}} = Wx'_{\text{in}} - aWx_{\text{out}}.$$

Changing to complex variables, we get

$$\bar{x}_{\text{out}} = \frac{W}{1 + jaW} \bar{x}_{\text{in}}. \quad (5)$$

In single-channel systems a link  $W$  encompassed by a negative feedback connection  $a$  has a transfer function  $W/(1 + aW)$ . The complex transfer function (5) of a two-channel link with an antisymmetric feedback connection differs from this function in the presence of a factor  $j$  in front of  $aW$ . In the particular case when  $W = 1$ , the transfer function of the two-channel link becomes  $1/(1 + ja)$ .

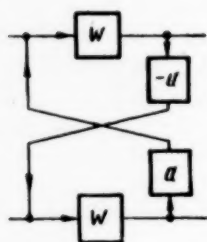


Fig. 4

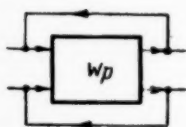


Fig. 5

It is evident that the complex transfer function of two directional two-channel links in series is the product of the transfer function of each of these links. It is also clear that if a two-channel system having a complex transfer function  $W_p$  is encompassed by proportional negative identical connections (Fig. 5), then  $x_{\text{out}} = W_p(x_{\text{in}} - x_{\text{out}})$  and the closed-loop transfer function is

$$\Phi = \frac{W_p}{1 + W_p}. \quad (6)$$

Using these rules and expressions for the transfer functions of the two-channel links, it is easy to obtain the complex transfer functions of systems containing any number of nonoverlapping\* antisymmetrical connections.

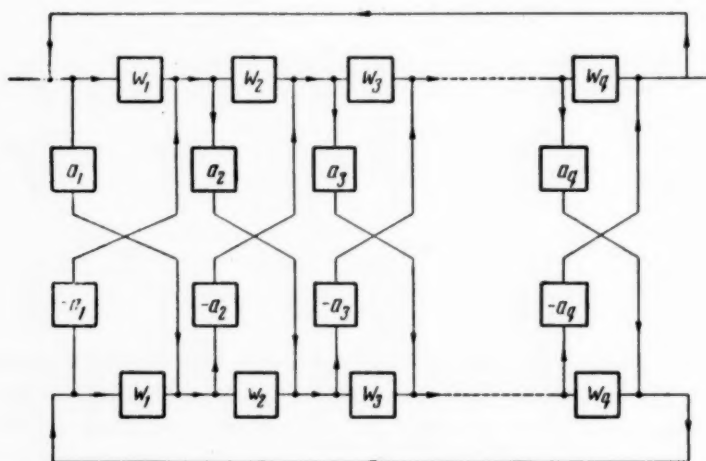


Fig. 6

\*If the connections overlap, i.e., the terminals of one connection are located between terminals of another connection, addition derivations are required to obtain the transfer function.

Thus, for example, if the system contains  $q$  direct non-overlapping antisymmetric connections (Fig. 6), its transfer function is

$$\Phi = \frac{(W_1 + ja_1)(W_2 + ja_2) \dots (W_q + ja_q)}{1 + (W_1 + ja_1)(W_2 + ja_2) \dots (W_q + ja_q)}.$$

The transfer function of a system with the same number of feedback connections (Fig. 7) is of the form

$$\Phi = \frac{\frac{W}{(1 + ja_1 W_1)(1 + ja_2 W_2) \dots (1 + ja_q W_q)}}{1 + \frac{W}{(1 + ja_1 W_1)(1 + ja_2 W_2) \dots (1 + ja_q W_q)}},$$

where  $W = W_1, W_2, \dots, W_q$  is the transfer function of the channel with both the crossing and the outside connections open.

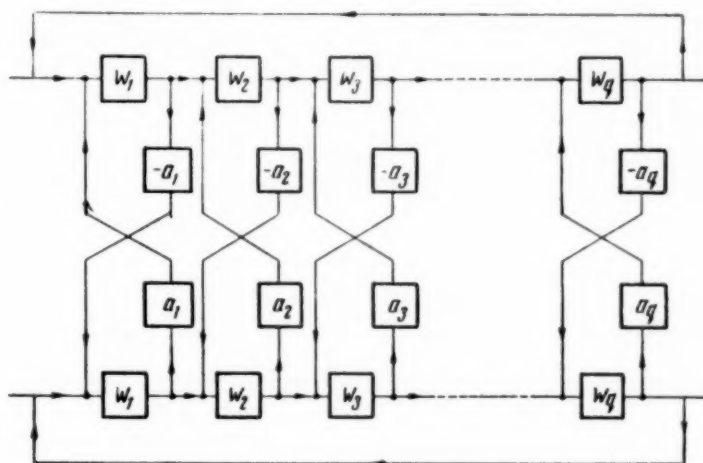


Fig. 7

## 2. Stability of Two-Channel Systems

To analyze the stability of the systems that are described above by linear differential equations with constant complex coefficients, one can employ both analytical as well as frequency stability criteria. An analytical criterion for equations with complex coefficients is the so-called Hermite-Hurwitz criterion [4].

However, the application of an analytical criterion to systems described by complex equations of the fourth order and above usually becomes difficult owing to the cumbersome determinants to be expanded. It is more convenient to employ the Nyquist or the Mikhailov criterion.

Thus, for example, if the complex closed-loop transfer function of the system is represented as

$$\Phi(p) = \frac{W_p(p)}{1 + W_p(p)},$$

where

$$W_p(p) = c \frac{(p - \beta_1)(p - \beta_2) \dots (p - \beta_m)}{(p - \alpha_1)(p - \alpha_2) \dots (p - \alpha_n)} \quad (m \leq n),$$

then a necessary and sufficient condition for stability is that the zeros of the function

$$\begin{aligned} 1 + W_p(p) &= \frac{(p - \alpha_1)(p - \alpha_2) \dots (p - \alpha_n) + c(p - \beta_1)(p - \beta_2) \dots (p - \beta_m)}{(p - \alpha_1)(p - \alpha_2) \dots (p - \alpha_n)} = \\ &= \frac{(p - \gamma_1)(p - \gamma_2) \dots (p - \gamma_n)}{(p - \alpha_1)(p - \alpha_2) \dots (p - \alpha_n)} \end{aligned}$$

have negative real parts. But for this, in turn, it is necessary and sufficient that the vector  $1 + W_p(j\omega)$  rotate by an angle  $2\pi d$  as  $\omega$  changes from  $-\infty$  to  $+\infty$ , where  $d$  is the number of poles of the open-loop transfer function  $W_p(p)$  of the system located to the right of the imaginary axis.

It therefore follows that if an open-loop system with a transfer function  $W_p(p)$  is stable, a necessary and sufficient condition for the stability of the closed-loop system is that the amplitude-phase characteristic  $W_p(j\omega)$  not contain the point  $-1$  as  $\omega$  varies from  $-\infty$  to  $+\infty$ .

The stability of two-channel systems can be conveniently studied by locus-of-roots method applied to the roots of the complex gain coefficient. If the gain is factored out of the open-loop transfer function  $W_p$ , i.e., if this function is represented in the form  $W_p = \bar{k}W$ , the characteristic equation becomes

$$1 + \bar{k}W = 0.$$

The equation for the locus of the roots of the complex gain is given by the equation

$$\bar{k} = -\frac{1}{W(j\omega)}, \quad (7)$$

i.e., except for the sign, the locus of the roots coincides with the reciprocal of the amplitude-phase characteristic of the open-loop system.

The stability region, if it exists, is found among those regions into which the curve (7) divides the  $\bar{k}$  plane in the same manner as in systems described by equations with real coefficients.

A distinguishing feature of two-channel systems with complex transfer functions is that the complex gain of such systems has a definite physical meaning and can be realized, while the gain of single-channel systems is a real quantity. Antisymmetric connections in two-channel systems may affect the stability both favorably and adversely.

Let, for example, a two-channel system have a direct antisymmetric connection, containing the link  $W_v$ . The transfer function of such a system, with the external connections open, will be

$$W_p = (W_v + ja)W_1W_2 \dots W_q,$$



where  $W_1, W_2, \dots, W_q$  are the transfer functions of the links that have no crossed connections.

The set of poles of this function can include only the poles of the functions  $W_1, W_2, \dots, W_q, W_p$ , and  $a$ .

Therefore, if the system is stable when fully open (at  $a = 0$ ), and if each connection in itself is stable, then the system with outside connections open will also be stable.

In other words, adding a stable antisymmetric direct connection does not affect the stability of the open-loop system, because the direct connections do not form closed loops in a system whose outside connections are open (see Fig. 6). If  $W_p = 1$ , we have

$$W_p(j\omega) = W(j\omega)[1 + ja(j\omega)],$$

where  $W = W_1 W_2 \dots W_q$ .

It follows from this expression that adding this direct antisymmetric connection is equivalent, from the point of view of stability, to adding a correcting device with an amplitude-phase characteristic  $1 + ja(j\omega)$  resulting from a rotation of the characteristic of the connection  $a(j\omega)$  by  $90^\circ$  and from a unity shift along the real axis. In particular, adding a connection having a transfer function of an inertia element is equivalent to adding the compensating network with an amplitude-phase characteristic shown in Fig. 8.

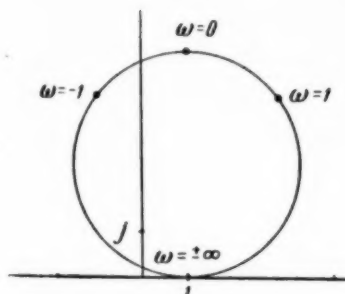


Fig. 8

If the connection is proportional, then  $a$  is a constant real quantity and the amplitude-phase characteristic can be represented as

$$W_p(j\omega) = W(j\omega)\eta e^{j\epsilon},$$

where  $\eta = \sqrt{1 + a^2} > 1$ ,  $\epsilon = \arctg a$ .

Thus, to judge the stability of a system with the above proportional direct antisymmetric connection it is enough to take the amplitude-phase characteristic of the fully-open system  $W(j\omega)$ , increase its scale by  $\eta$  times, and rotate it through an angle  $\epsilon$ .

An even simpler procedure can be used: locate the point  $-e^{-j\epsilon}/\eta$  on the complex plane on which the amplitude-phase characteristic  $W(j\omega)$  is drawn. The position of this point relative to the characteristic (Figure 9) will then determine the stability. It follows directly that adding one connection of the above type reduces the stability margin.

In fact, since  $1/\eta < 1$ , the point  $e^{-j\epsilon}/\eta$  is usually closer to the contour of the amplitude-phase characteristic than the point  $-1$ .

An exception is the rare case, when the open-loop amplitude characteristic  $A(\omega)$  has a rather sharply pronounced maximum at the frequency at which the phase  $\varphi = -180^\circ$  (Fig. 9,b).

Thus, generally speaking, proportional direct antisymmetric connections that contain transfer links do not, by themselves help the stability.

Antisymmetric reverse connections in conjunction with direct connections may produce a considerable increase in the stability. This will be illustrated with actual examples. Let us note here that in the presence of an antisymmetric reverse connection the boundary of the stability region, which coincides with a portion of the locus of the roots (7), is given by the following equation

$$\bar{k} = -\frac{1}{W} = -\frac{1}{W(j\omega)} - j\frac{a(j\omega)}{W_{-v}(j\omega)},$$

where  $W_v = W/W_v$  is the transfer function of elements not contained by the antisymmetric reverse connection.

By choosing the function  $a(j\omega)/W_v(j\omega)$  it is possible to expand the boundaries of the stability region.

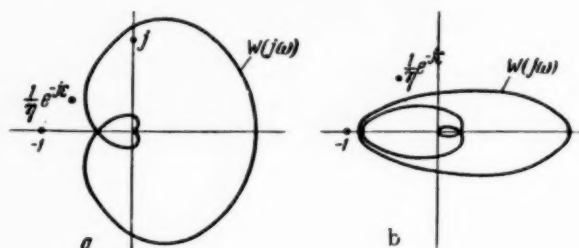


Fig. 9

### 3. Examples

Let us consider examples that illustrate some of the statements made above and show the possibility of using antisymmetric connections as stabilizing devices.

Let us first treat the angle-tracking servo system, the block diagram and transfer function of which were given above (Fig. 1b). The antisymmetric direct connection is produced in this system by the phase shift of

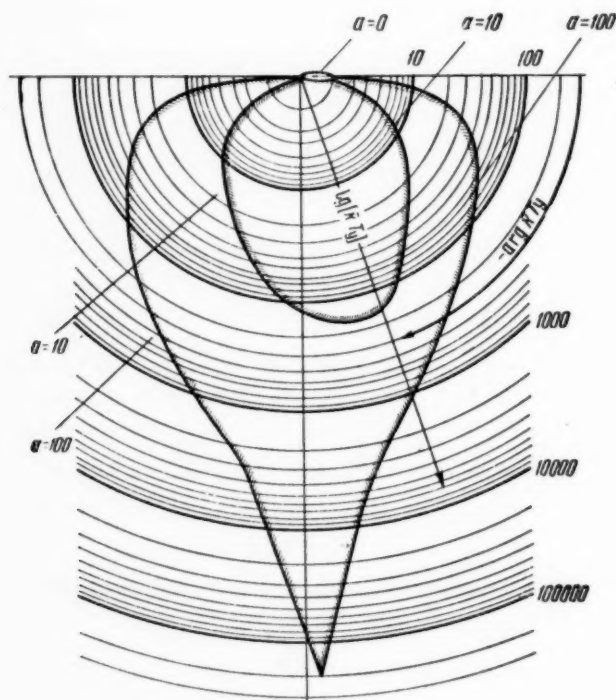


Fig. 10

the reference voltage, and the antisymmetric reverse connection is caused by the presence of a kinetic moment of the rotating portions of the following platform. For the sake of simplicity we shall assume that the amplifier is equivalent to an inertia element from the dynamic point of view, i.e.,  $W_1 = k/(1 + T_{ap})$ .

The transfer function (3) of the closed-loop servo system will then assume the following form:

$$\Phi(p) = \frac{\bar{k}}{\bar{k} + p(1 + T_a p)(1 + Tp) - j a p(1 + T_a p)}.$$

The transfer function of the error will be

$$\frac{1}{1 + W_p} = \frac{p(1 + T_a p)(1 + Tp) - j a p(1 + T_a p)}{\bar{k} + p(1 + T_a p)(1 + Tp) - j a p(1 + T_a p)}.$$

The coefficients of the expansion of this function in a power series in  $p$  are the error coefficients of the given servo system. The first three coefficients are

$$c_0 = 1, \quad c_1 = \frac{1 - ja}{\bar{k}}, \quad c_2 = \frac{T_a + T - jaT_a}{\bar{k}} - \frac{(1 - ja)^2}{\bar{k}^2}. \quad (8)$$

The loci of the roots of the complex gain  $\bar{k}$  are given by the equation

$$\bar{k} = -j\omega(1 + jT_a\omega)(1 + jT\omega) - a\omega(1 + jT_a\omega) \quad (9)$$

or

$$\bar{k}T_a = -j\omega_1(1 + j\omega_1)(1 + jd\omega_1) - a\omega_1(1 + j\omega_1),$$

where  $\omega_1 = T_a\omega$ ,  $d = T/T_a$ .

The part of the complex-gain plane, bounded by the curve (9) in the section from  $\omega_1 = 0$  to the point where this curve intersects itself, is the stability region. This can be readily seen by applying the analytical stability criterion to a characteristic equation having coefficients corresponding to any of the internal points of the above region.

Figure 10 shows the stability regions of this servo system at  $d = 1$  and at three values of  $a$ . These regions are plotted in polar semi-logarithmic coordinates,  $\log|\bar{k}T_a|$  and  $\tan^{-1}\bar{k}T_a$  being the radial and angular variables respectively. Figure 10 shows by how much the stability region can be extended with the aid of the antisymmetrical reverse connection that results from the kinetic moment. In spite of the logarithmic scale, it is impossible to show on the same drawing the stability regions for  $a = 0$  (no kinetic moment),  $a = 10$ , and particularly  $a = 100$ , so large is the latter.

The critical gain at  $a = 0$  is  $2/T_a$ ; at  $a = 10$  the maximum critical gain is  $320/T_a$ ; at  $a = 100$  this gain reaches the tremendous value  $4 \times 10^5/T_a$ . The quantity  $a = H/JT = (J_p/J)T\Omega$  where  $J_p$  is the polar moment of inertia of the parts rotating with a speed  $\Omega$ . It must be borne in mind here that while it is frequently difficult to obtain values of  $a$  on the order of 100, for it requires a high value of the ratio of the polar moment of inertia of the rotating parts to the equatorial moment of inertia  $J$  of the servo platform, it is comparatively easy to obtain  $a$  on the order of 10 in many cases. But this value of  $a$  makes it possible to increase the open-loop system gain by 160 times and to reduce the error coefficients (8) by approximately 15 times compared with a

servo system without crossed connections. It must be emphasized, as can be seen from Fig. 10, that such an increase in the gain and such an improvement in the dynamic properties of the system are accomplished only if the gain  $k$  is a complex quantity with properly chosen argument. In other words, a substantial improvement in the dynamic properties of the servo system is attainable only if the system contains, along with the antisymmetrical reverse connection, also an antisymmetrical direct connection caused by the phase shift of the reference voltage.

In order to insure maximum stability margin, the point corresponding to the complex gain of the system is best chosen near the center line of the stability region, i.e., near the line bisecting the arcs of circles corresponding to equal values of the modulus  $|\bar{k} T_a|$ . Therefore, at large values of  $a$ , the optimum phase shift approaches  $90^\circ$  (Fig. 10). In other words, for a servo system with so clearly pronounced gyroscopic properties it becomes advisable to use the so-called radial correction [1] instead of a direct distribution of the signals ( $\varphi = 0$ ), which is advisable in the absence of a kinetic moment ( $H = 0$ ).

The substantial increase in stability due to the kinetic moment suggests the idea of introducing an antisymmetric connection that imitates its action. As can be seen from Fig. 1, such a connection can be realized in a two-channel servo system with the aid of tachometer generators connected with the output shafts.

The tachometer generator signals can be fed either to the intermediate stages of the amplifiers or directly to the outputs of the servo system channels (past the points at which the signals of the external feedback loops are inserted). It is easy to see that a substantial increase in stability can be obtained when the signals of the tachometer generators are introduced in the intermediate stages of the amplifiers, or more accurately, when delay elements are placed between the points where the tachometer-generator signals are introduced and the inputs of the servo systems. An example of such a system is the two-channel servo system shown in Fig. 11.

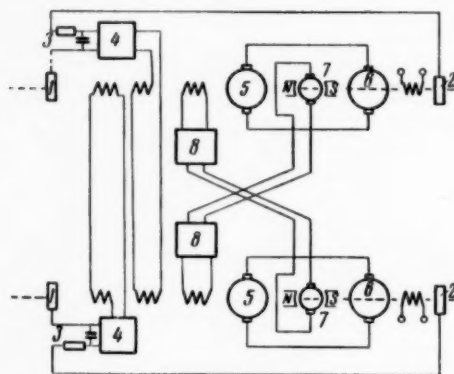


Fig. 11

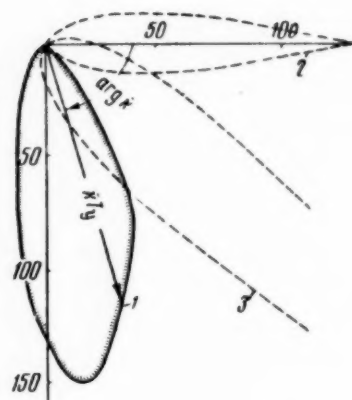


Fig. 12

In this servo system, the difference in the voltages of transducers 1 and 2, connected respectively to the input and output shafts, is applied to filters 3 and then to electronic amplifiers 4. The outputs of the electronic amplifiers are connected to the control windings of single-stage dynamoelectric amplifiers 5, and as a result of the crossed connection of the winding there is a proportional direct antisymmetric connection between the channels of the servo system.

The voltage from the dynamoelectric amplifiers is applied to the actuating motors 6, the shafts of which are coupled to the tachometer generator 7. The signals from the tachometer generators are fed through amplifiers 8 to supplementary windings of the dynamoelectric amplifiers, producing an antisymmetric velocity feedback connection.

If we assume that the transfer function of filter 3 and of amplifier 4 is  $k_f/(1 + T_f p)$ , then the complex transfer functions of the open-loop and closed-loop servo system will be

$$W_0 = \frac{\bar{k}}{(1 + T_f p) [(1 + T_a p) (1 + Tp) - ja] p},$$

$$F = \frac{\bar{k}}{\bar{k} + p (1 + T_f p) (1 + T_a p) (1 + Tp) - j a p (1 + T_f p)}.$$

The locus of the roots is given in this case by the equation

$$\bar{k} = -j\omega (1 + jT_f \omega) (1 + jT_a \omega) (1 + jT\omega) - a\omega (1 + jT_f \omega).$$

Figure 12 shows the stability region, plotted for  $T = T_f = 0.5$  seconds,  $T_a = 0.0025$  seconds,  $a = 10$  (boundary of region—Curve 1).

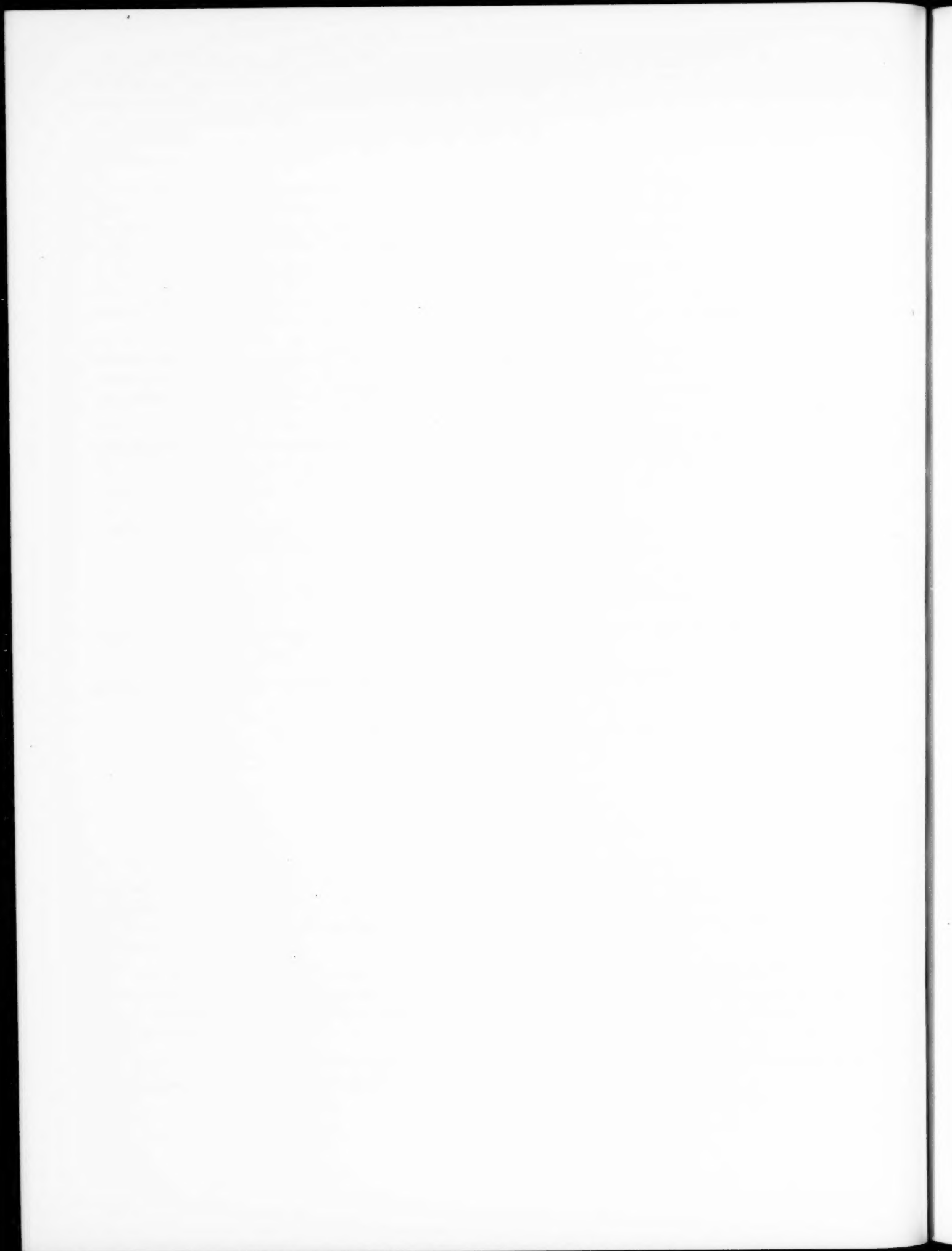
For the sake of comparison, the same drawing shows the boundaries of the stability regions in the case of the ordinary, uncrossed connection of the feedback loops (Curve 2), and in the presence of both antisymmetric as well as crossed connections (Curve 3). In all cases, the numerical values of the parameters are assumed to be the same.

This example shows that an artificially-produced antisymmetric connection may extend considerably the stability region of the system.

Received October 13, 1955

#### LITERATURE CITED

- [1] B. V. Bulgakov, Applied Theory of Gyroscopes, 1939.
- [2] R. A. Rankin, Mathematical Theory of Motion of Uncontrolled Rockets (Foreign Lit. Press, 1951), (Russ. Translation).
- [3] L. N. Obmorshev, "Oscillations and Stability in Machine-Building Problems" (Moscow Higher Technical School), Dissertation, 1952.
- [4] Iu. A. Neimark, Stability of Linearized Systems, LKVVIZ, 1949.





# SPEED REGULATION OF THREE PHASE INDUCTION MOTORS USING A BRIDGE-TYPE TRANSDUCER

V. S. Kulebakin and S. M. Domanitskii  
(Moscow)

A system using a bridge transducer is considered for regulating the speed of low-power three-phase induction motors. The theory of the proposed system is given for motors with ordinary squirrel-cage and wound-rotors, and also for motors with a heavy Shenfer rotor.

The use of both a-c and d-c automatized variable-speed electric drives, is continually on the increase in various branches of industry.

A closed-loop motor-speed regulation system is shown in Fig. 1. In this circuit, a feedback voltage  $U_f$ , which depends on  $\underline{n}$ , is picked off the transducer and compared with the set-point voltage  $U_s$ . The difference

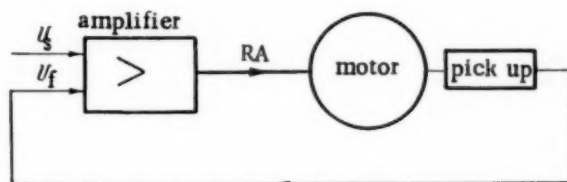


Fig. 1

$U_s - U_f$  is amplified and is used to vary the amount of regulating action RA. The regulating action, depending on the control circuit, can be the voltage applied to the motor, excitation current (for d-c motors), the frequency, or a change in the motor parameters. By changing  $U_s$  it is possible to regulate  $\underline{n}$ . Any automatic motor-control circuit must include a transducer for the feedback voltage  $U_f$ . This voltage can be obtained in various manners. For example, the  $U_f$  transducer may be a d-c or a-c tachometer generator, or else motor-voltage or motor-current feedback. In the case of d-c or single-phase induction motors, bridge circuits are also used to obtain the feedback voltage [1]. The output of such a network is a voltage proportional or almost proportional to  $\underline{n}$ .

We shall consider below a speed-measuring which is a further development of schemes based on the invariance principle [1]. This scheme can be used for nonreversing drives with three-phase induction motors. It can be used to regulate the speed of an induction motor by varying the applied voltage, in particularly in the case of reaction control (Fig. 2).

In the circuit shown in Fig. 2, the feedback voltage  $U_f$ , which depends on  $\underline{n}$ , is picked off the diagonal of a bridge consisting of four impedances  $Z_1, Z_2, Z_3$  and  $Z_m$  (Fig. 3).  $Z_m = r_m + jx_m$  is the impedance of any of the three phases of the motor. Whenever the operating conditions of the motor change, this impedance varies

nonlinearly.  $Z_3$ , which is connected in series with the phase winding of the motor, is usually a low active resistance  $r_3$ , which does not unbalance currents in the motor phases excessively. Impedances  $Z_1 = r_1$  and  $Z_2 = r_2 + jx_2$  are so chosen as to make  $r_1 \gg r_3$  and  $Z_2 \gg Z_m$ .  $Z_2$  can be a small choke with an impedance  $r + jx$ , working on the linear portion of its characteristic, connected in series with an additional active resistance  $r_{ad}$ .

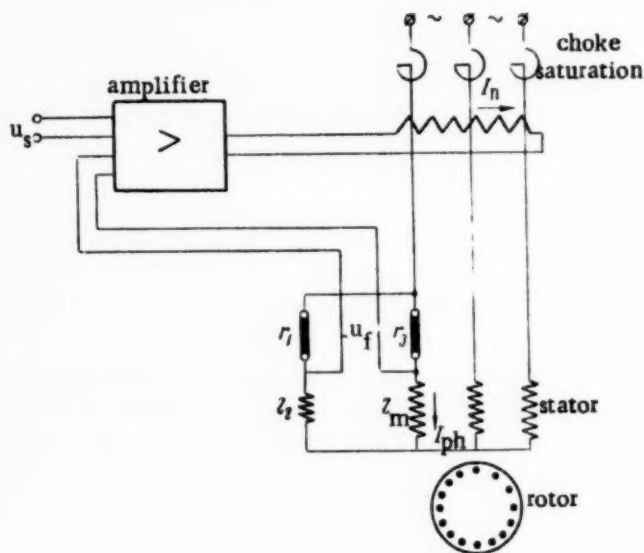


Fig. 2.

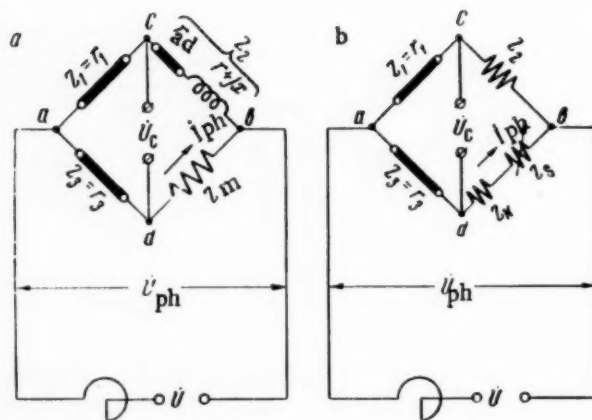


Fig. 3.

so that the sum has the required value  $r_2 + jx_2$ . Impedances  $Z_1, Z_2$  and  $Z_3$  are so chosen, that the bridge is balanced when the speed of the motor is zero, and when a definite voltage is applied on the motor, i.e., so that  $Z_1 Z_k = Z_2 Z_3$ . Here  $Z_k$  is the value of motor impedance  $Z_m$  at which the bridge is balanced.

An idea of the relative values of the bridge impedances can be obtained from the following data on a typical motor:  $Z_1 = r_1 = 200$  ohms,  $Z_2 = 4,000 + j4,000$  ohms,  $Z_3 = r_3 = 2$  ohms,  $Z_k = 40 + j40$  ohms.

As  $n$  increases, the impedance of the motor increases, the bridge becomes unbalanced, and an a-c voltage  $U_f$  is produced across its diagonal. This voltage can be applied to an a-c amplifier (Fig. 2) either directly or through a rectifier.

As will be shown below, the circuit of Fig. 2 can be used to obtain a voltage  $U_f(n)$  for squirrel-cage and wound-rotor induction motors, or for a motor with a heavy Shenfer rotor. Let us consider how the feedback voltage varies with the speed of such motors.

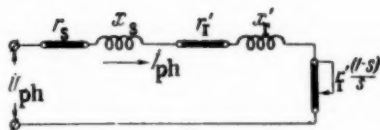


Fig. 4

### Theory of Proposed Scheme

a) Induction motor with squirrel-cage or wound rotor. The variation of the voltage  $U_f(n)$  picked off the bridge diagonal (Figure 3) can be obtained from the known equivalent circuit of an induction motor (Fig. 4). If we neglect the magnetizing-current branch, the impedance of the motor at any speed of rotation will be

$$Z_m = (r_s + r_r') + j(x_s + x_r') + r_r' \frac{(1-s)}{s}, \quad (1)$$

where  $r_s, x_s$  are the resistance and reactance of the stator,  $r_r'$  and  $x_r'$ , the resistance and reactance of the rotor, referred to the stator terminals;  $s = 1 - \nu$  is the slip of the motor,  $\nu = n/n_s$  the speed of the motor in relative units, and  $n_s$  is the synchronous speed of the motor.

Equation (1) can be rewritten as

$$Z_m = Z_k + Z_s, \quad (2)$$

where  $Z_k = r_k + jx_k = (r_s + r_r') + j(x_s + x_r') = \text{const}$  is the phase impedance of the motor at  $\underline{n} = 0$ .

Thus, the variable impedance  $Z_s = r_r' \left( \frac{1-s}{s} \right) = r_r' \frac{\nu}{1-\nu}$  (Fig. 3b) is a function of  $\underline{n}$ .

If the bridge is balanced at  $\nu = 0$  we have  $U_f = 0$ . Here

$$Z_s = r_r' \left( \frac{1-s}{s} \right) = r_r' \frac{\nu}{1-\nu} = 0.$$

If the motor rotates,  $Z_m = Z_k + Z_s$ , the bridge is unbalanced and the bridge diagonal (Fig. 3) feeds a feedback voltage  $\dot{U}_f(n)$  to an infinite resistance (grid circuit of a vacuum-tube amplifier):

$$\dot{U}_f = \dot{U}_{ac} - \dot{U}_{ad} = \left( \frac{Z_1}{Z_1 + Z_2} - \frac{Z_3}{Z_3 + Z_k + Z_s} \right) \dot{U}_{ph}. \quad (3)$$

Simplifying, we get

$$\dot{U}_f = \frac{Z_1 Z_s}{(Z_1 + Z_2)(Z_3 + Z_k + Z_s)} \dot{U}_{ph} = \frac{Z_1 Z_s}{Z_1 + Z_2} \dot{I}_{ph} \quad (4)$$

where  $\dot{U}_{ph}, \dot{I}_{ph}$  are the phase voltage and phase current vectors of the motor.

Eliminating  $Z_s$  we get

$$\dot{U}_f = \frac{Z_1}{Z_1 + Z_2} r_r' \frac{\nu}{1-\nu} \dot{I}_{ph} = cF(\nu) \dot{I}_{ph} \quad (5)$$

where

$$c = \frac{Z_1}{Z_1 + Z_2} r'_r = \text{const and } F(\nu) = \frac{\nu}{1-\nu}.$$

As can be seen from Fig. 5, where the Curve  $F(\nu) = \nu/(1-\nu)$  is shown solid,  $U_f(n)$  is nonlinear. Weak feedback is obtained at low values of  $n$ , and heavy feedback is obtained at large values of  $n$ . Nonlinear motor-speed feedback is now used extensively to improve the dynamic properties of systems.

The function  $F(\nu)$  obtained in the bridge circuit can be represented by the following series

$$F(\nu) = \frac{\nu}{1-\nu} = \sum_{k=1}^{\infty} \nu^k = \nu + \nu^2 + \dots + \nu^k + \dots \quad (\nu < 1), \quad (6)$$

An experimental investigation of a 250 watt squirrel-cage induction motor, using the circuit of Fig. 2, has shown that the experimental curve  $\nu/(1-\nu) = |U_f/cI_{ph}| = F(\nu)$ , shown dotted on Fig. 5, is in good agreement with the theoretical curve. The slight voltage  $U_f$  at  $n=0$  is caused by third harmonics in the voltage curve of the motor.

As can be seen (5), the voltage  $U_f$  depends not only on the speed, but also on the current of the motor. To exclude the influence of the motor current on the value of the feedback voltage, it is possible to use the ratio meter principle. For this purpose, a voltage given by Equation (5) is applied to one coil of the ratio meter, and the other coil carries the current  $I_{ph}$  of the motor. The deflection of the moving system of the ratio meter will then depend on the ratio of the currents flowing through the ratio meter coils, i.e., on the quantity  $U_f/I_{ph} = cF(\nu) = c\nu/(1-\nu)$ .

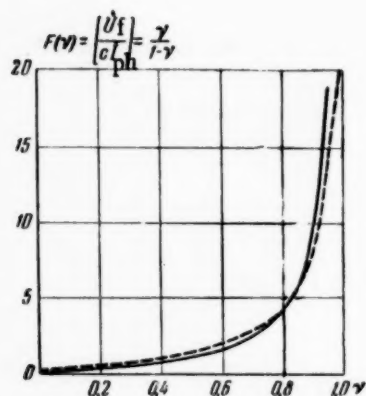


Fig. 5

The deflection of the moving system of the ratio meter can be converted with a rheostatic or inductive transducer into a voltage that can be applied to the amplifier of a closed-loop automatic motor regulation system. Since  $F(\nu)$  is independent of  $U_{ph}$ , the feedback voltage does not change with the fluctuations in the line voltage  $\dot{U}$ , if we disregard the saturation of the motor.

The proposed bridge speed-measuring circuit is easiest to use for those types of induction motors, in which the motor current  $I_{ph}$  varies relatively little with the speed of the motor and with a constant load torque.

One such motor is the Shenfer motor, which has a heavy steel rotor, and which will be discussed below.

**b) Shenfer Induction Motor with Heavy Rotor.** An induction motor with a Shenfer rotor is used in low-power automatized electric drives, intended for operation over a wide range of motor speeds and for prolonged operation at low speeds [3]. In such a motor, a change in speed causes a change not only in the active resistance but also in the inductance of the rotor. In addition, unlike a motor with the usual squirrel-cage rotor, the resistance and reactance of the rotor depend on the motor current.

Let us choose the resistances of the bridge shown in Fig. 3 in such a manner, that the bridge is balanced at  $s=1$  and at a certain current  $\dot{I}_{ph} = \dot{I}_k$  (at an impedance  $Z_m = Z_k$ ), i.e.,  $Z_1 Z_k = Z_2 Z_3$ . At any other value of slip or current, the motor impedance will then be

$$Z_m = Z_k + Z_s(s, I_k),$$

where  $Z_k = r_s + jx_s + r'_r + jx'_r$  is the motor impedance at which the bridge is balanced,  $Z_s$  is the variable impedance of the motor (a function of the motor current and slip),  $r_s$  and  $x_s$  the stator resistance and reactance,

$r'_r$  and  $x'_r$ , the rotor resistance and reactance referred to  $s=1$  and to  $I_{ph} = I_k$ ,  $I_k$ , the motor current with the bridge balanced and rotor locked,  $I_{phk} = I_{ph}/I_k$ , the relative phase current of the motor.

If we neglect the magnetizing component of the current, the equivalent circuit of the motor can be represented as shown in Fig. 6 [4].

The impedance of the motor for any value of slip can than be written as

$$Z_m = r_s + jx_s + r'_r + jx'_r + \frac{r'_r(1-\sqrt{I_{phk}^2 s})}{\sqrt{I_{phk}^2 s}} + j \frac{x'_r(1-\sqrt{I_{phk}^2 s})}{\sqrt{I_{phk}^2 s}} \quad (7)$$

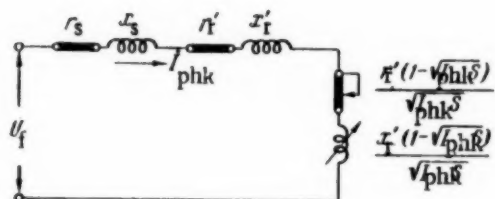


Fig. 6

Since the motor current at a definite value of slip depends on the torque, we have

$$Z_m = Z_k + Z_s(s, M) \quad \text{or} \quad Z_m = Z_k + Z_s(s, I_m),$$

where  $M$  is the torque of the motor corresponding to the selected values of  $s$  and  $I_{phk}$ , and  $I_m$  is the reactor magnetizing current, corresponding to the same values of  $s$  and  $I_{phk}$ .

Figure 7 shows the mechanical open-loop characteristics of a 250 watt motor, plotted at various reactor magnetizing currents, while Figure 8 shows a family of curves  $Z_m = f(n)$  for different values of  $I_m = \text{const.}$

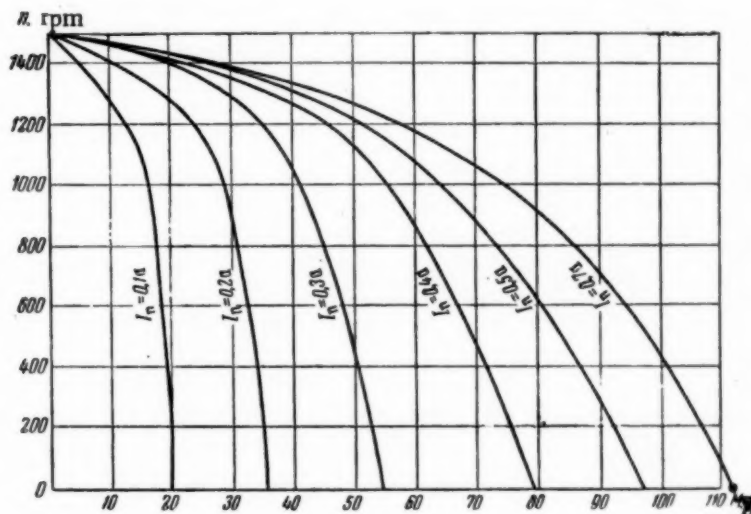


Fig. 7

The small circles on Figures 7 and 8 denote the balanced-bridge conditions  $n = 0$ ,  $M = 110$  grams,  $I_m = I_{mk} = 0.7$  amp.

The feedback voltage, picked off the diagonal of the bridge, can be determined from the motor characteristics. For this purpose, the value of  $I_m$  is determined from the curves  $n = f(M, I_m)$  for any pair of values of  $M$  and  $n$ , and the quantities  $Z_m$  and  $Z_s = Z_m - Z_k$  are then determined from the curves  $Z_m = f(n, I_m)$  and  $\cos \varphi_m = f(n, I_m)$ .



The feedback voltage will then be

$$\dot{U}_f = \frac{Z_1 Z_s}{Z_1 + Z_2} I_{ph}$$

where the absolute value of  $I_{ph}$  is found from the curves  $I_{ph} = f(\underline{n}, I_m)$ , and the phase of the current  $I_{ph}$  relative to the line voltage  $U$  can be determined from the vector diagrams.

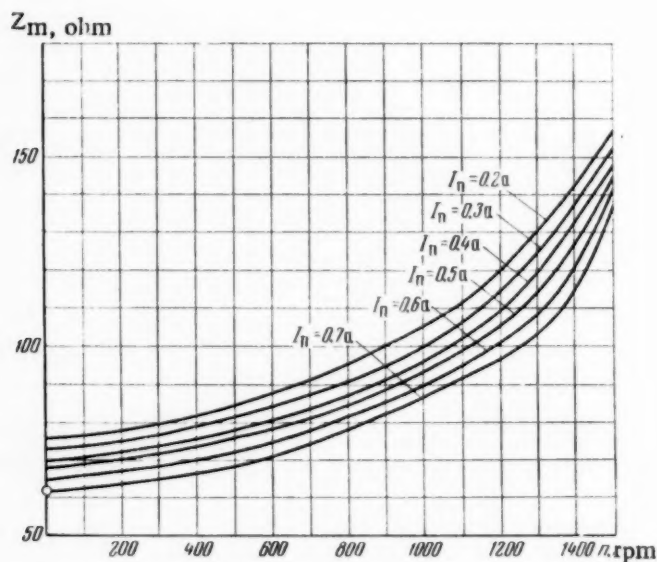


Fig. 8

Figure 9 shows experimental curves  $U_f = f(\underline{n})$ , plotted for two values of the reactor magnetization current.

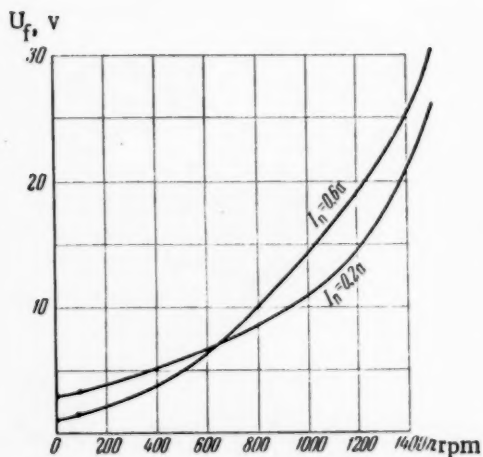


Fig. 9

The averaged curve is close to a quadratic parabola; the voltage is thus  $U_f \approx c \underline{n}^2$  and if the motor torque is limited, the transients due to command changes will be faster than when  $U_f = c \underline{n}$ . Since the motor current changes relatively little with  $\underline{n}$  for a constant torque, the voltage  $U_f$  depends basically on the variation of the impedance  $Z_s$  when  $M = \text{const.}$

In a motor with a Shenfer rotor one usually has  $r'_r \gg r_s$ ,  $x'_r \gg x_s$ , and in addition,  $r'_r/x'_r \approx \text{const.}$ , and therefore, the phase of the motor current changes relatively little over a wide range of torques and motor speeds. Calculations based on the characteristics of the motor as well as experimental investigations have shown that the phase of the feedback voltage in the case of reactor control changes only  $\pm 15^\circ$  relative to the line voltage at  $\underline{n} = 0 - 1200$  rpm. This makes it possible to apply the signal from the bridge speed-measuring circuit directly to the phase-sensitive a-c amplifier.

Figure 10 shows the mechanical characteristics of the motor, plotted for a closed-loop speed-regulation system with a bridge measuring circuit at various values of the set-point voltage  $U_s$ . A phase-sensitive vacuum-tube a-c amplifier with transformer input is used to amplify the signal applied from the measuring bridge. Magnetic or semiconductor amplifiers can be used as intermediate amplifiers. It follows from a comparison of Figures



7 and 10 that the addition of velocity feedback increases considerably the stiffness proportionality of the mechanical characteristics of the motor. The maximum relative stiffness of mechanical characteristics

$$\partial \left( \frac{M}{M_{\max}} \right) / \partial \left( \frac{n}{n_0} \right)$$

is obtained at low motor speeds, where it reaches 45. Here  $M_{\max}$  is the maximum motor torque at  $n=0$ . The circuit was so adjusted, that the value of the feedback voltage  $U_f$  diminished in the low-speed zone as the reactor magnetizing current changed from maximum to minimum, i.e., as the torque changed from maximum to minimum (Fig. 9). Correspondingly, if  $U_s$  is constant, it is necessary to have a lower droop in the motor speed characteristic to change the magnetizing current of the reactors within the same limits.

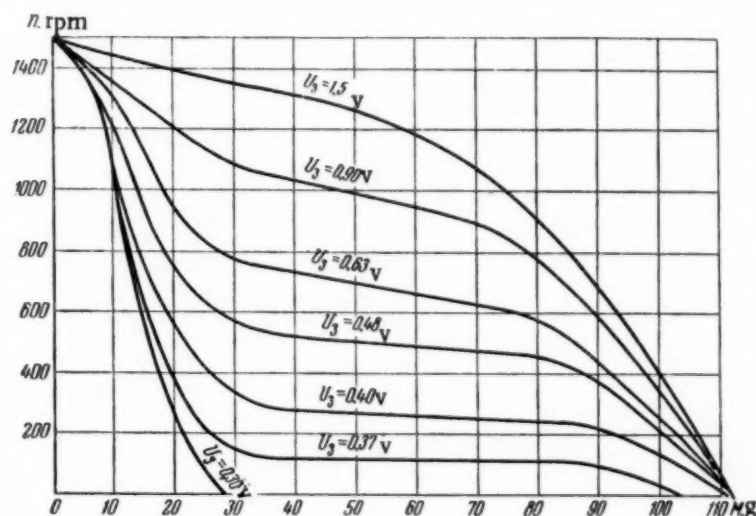


Fig. 10

A shortcoming of the bridge circuit is the dependence of the motor resistance, and consequently of the voltage  $U_f$ , on the temperature. A bridge balanced at a certain motor temperature may become unbalanced by motor heating. It is therefore necessary to tune the bridge to the most probable motor temperature.

This shortcoming can be reduced considerably by using a bridge resistance  $r_2$  that is dependent on the motor temperature. For example, it is possible to imbed an additional resistance  $r_{ad}$  (Fig. 3a), comprising the greater part of resistance  $r_2$ , into the front part of the motor stator winding. The effect of variation of line voltage  $\dot{U}$  on the magnitude of the feedback voltage  $\dot{U}_f = f(Z_s, \dot{I}_{ph})$  is relatively small, since at constant speed an increase in the voltage  $\dot{U}$  causes along with an increase in the current  $\dot{I}_{ph}$  also a decrease in  $Z_m$  and accordingly in  $Z_s = Z_m - Z_k$ .

Experience has shown that the proposed circuit is quite simple to adjust. The resistances and the reactance in the bridge arms are small in size.

The investigation of the bridge-type speed-regulation system for a three-phase induction motor results in the following conclusions:

1. In the case of a motor with an ordinary squirrel cage (or wound-rotor) rotor the feedback voltage, picked off the diagonal of the bridge circuit, depends on the motor current. The ratio-meter principle can be used to eliminate the effect of the motor current on the feedback voltage.

2. For a motor with a massive Shenfer rotor, where the current changes relatively little for constant torque and variable speed, the use of the circuit of Figure 3 makes it possible to obtain a considerable stiffness of the

mechanical characteristic, on the order of 40-50, over a certain range of speeds.

3. The curve showing the dependence of the feedback voltage on the speed of a motor with a Shenfer rotor has an approximately quadratic character.

4. The bridge circuit for speed measurement can be recommended for nonreversing adjustable-speed drives with induction motors having a Shenfer rotor.

Received January 23, 1956

#### LITERATURE CITED

[1] V. S. Kulebakin, "On the Application of the Principle of Absolute Invariance in Physical Real Systems" Dokl. An SSSR, New Series, Vol. LX, No. 2 (1948).

[2] A. Ia. Lerner, "Improving the Dynamic Properties of Automatic Compensators with the Aid of Non-linear Connections" Automation and Remote Control, Vol. XIII, No. 2 and 4 (1952).

[3] A. G. Ivakhnenko, "Automatic Regulation of Speed of Low Power Induction Motors" Publ. by Acad. Sci. Ukraine SSR, 1953.

[4] P. M. Postinkov, Design of Electric Machinery, Gostekhizdat Ukr. SSR, Kiev, 1952.

## A METHOD FOR THE SYNTHESIS OF COMPUTING AND CONTROL CONTACT CIRCUITS\*

G. N. Povarov  
(Moscow)

A method is given for the synthesis of computing and control contact circuits with a single input and  $k$  outputs, or with  $k$  inputs and a single output, with the conduction conditions between the inputs and outputs being arbitrary. In this method the circuit is built up in an unambiguous regular manner, employing bridge junctions and joining the circuits between different pole pairs. Except for a few exceptional cases, the method yields relatively — economical circuits (with respect to the number of contacts), without consuming too much time. The Appendix contains an extension of this method to include contactless switching circuits.

### 1. Introduction

Automatic computers and other modern automatic and remote-control installations make extensive use of contact circuits. Even high-speed electronic computers contain control contact circuits in some of their units.

The synthesis of contact circuits is changing at present from an art, based on experience and intuition, into a science, based on accurate calculations. Thanks to the work by P. S. Erenfest [1], V. I. Shestakov, [2], C. E. Shannon [3], M. A. Gavrilov [4, 5] and others it became clear that the basic mathematical discipline representing the laws of contact circuits is Boolean algebra ("Algebraic logic").

The use of Boolean algebra has made it relatively easy to synthesize parallel-series contact two-terminal networks, which can in turn be used to construct circuits having any number of poles. Matters are worse in the mathematical synthesis of contact-circuits containing bridge junctions or common contacts in the circuits between different pairs of poles. The known methods (see Ch. 11 and 13 of [5]) are for the most part not applicable for all conductance conditions \*\*, or else require a considerable number of circuit transformations.

As shown by M. A. Gavrilov [5, 6], contact circuits consist in general of multi-terminal networks connected either in parallel or in series. The way toward improving the methods for the synthesis of contact circuits containing bridge junctions or containing common contacts in the circuits between terminal pairs must

---

\* The contents of this article, with the exception of the Appendix, is part of the author's Candidate dissertation [7]. A preliminary report on the results cited is contained in [8, 9]. The method described was also reported at the Seminar on Relay Action and Algebraic Logic held at the Moscow State University on April 28, 1954, and at the Moscow City-Wide Seminar on Telemechanics at the Institute of Automation and Remote Control, Academy of Sciences, USSR, on February 8, 1956.

\*\* Conductance conditions are conditions that determine, for the required pole pairs, what combinations of operating and non-operating receiving elements will produce a closed path between the poles.

therefore be sought in a deeper study of the laws of multi-terminal connections. This path was chosen by C. E. Shannon [10], whose results were employed by this author, and by R. Righi [11]. The same path was chosen also by the author of [7-9]. Another noteworthy path is based on systematic evaluation of the "indeterminate" conductance in contact circuits [12-15].

The Appendix contains a brief report on the extension of the procedure used in the synthesis of contact circuits to include contactless circuits.

## 2. Contact 2 (p, q)-Terminal Networks

A contact multi-terminal network can be called oriented, if its terminal pairs are grouped by some feature into inputs and outputs, and unoriented otherwise. The rectangle of Fig. 1 may serve as a graphic symbol for an oriented multi-terminal network and the regular polygon of Fig. 2 can be used to represent an unoriented one.

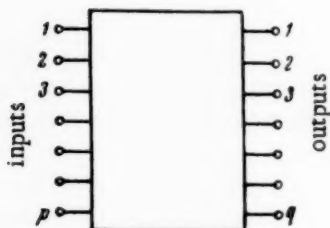


Fig. 1.

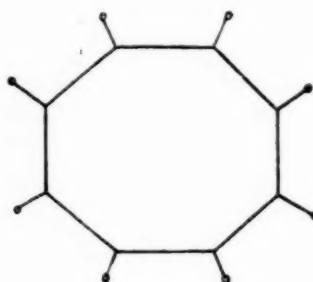


Fig. 2

An oriented multi-terminal network with  $p$  inputs and  $q$  outputs is called for short a (p,q)-terminal network. The inputs and outputs will be numbered separately 1, 2, 3,... (Fig. 1).

A contact (p,q)-terminal network is called isolating (in the direction from the inputs to the outputs) if the structural conductances  $h_{kl}$  of this (p,q)-terminal network between the outputs  $\underline{k}, \underline{l}$  where  $\underline{k}, \underline{l} = 1, 2, \dots, q$  and  $\underline{k} \neq \underline{l}$  vanish for some states of the receiving elements.\*

Assume we have a (p,q)-terminal network M and an (r,s)-terminal network N. Let us connect each output of M with one and one only input of N (Fig. 3). Certain inputs of N may remain free. The result is a certain (p,s)-terminal network, which we shall call a cascade connection or a cascade of multi-terminal networks M and N.

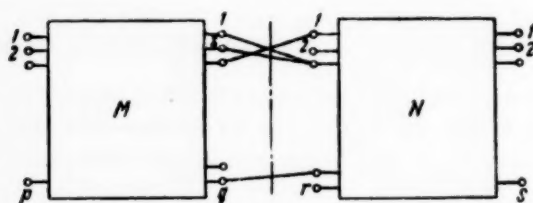


Fig. 3

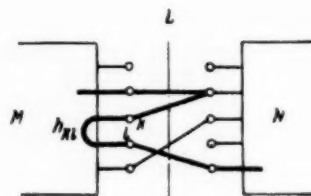


Fig. 4

Let  $\tau(\underline{k})$  denote the input of N to which the output  $\underline{k}$  of M is connected.

\* A structural conductance is one that equals either zero or unity. It equals zero if the circuit is open and unity if the circuit is closed.

Assume that multi-terminal network  $M$  is isolating and let us denote the structural conductance between input  $\underline{i}$  and output  $\underline{j}$  by  $f_{ij}^{(M)}$  in  $M$  and by  $f_{ij}^{(N)}$  in  $N$ . The structural conductance between input  $\underline{i}$  and output  $\underline{j}$  of the cascade will then be

$$f_{ij} = \sum_{k=1}^q f_{ik}^{(M)} f_{kj}^{(N)}, \quad (A)$$

where  $\underline{i} = 2, \dots, p$  and  $\underline{j} = 1, 2, \dots, s$ . In fact, the right half of the equation describes the current paths from the input  $\underline{i}$  to the output  $\underline{j}$ , crossing the line  $L$  only once, and there can be no other paths because  $M$  is isolating, since any other path would intersect  $L$  not less than three times (Fig. 4) and would contain a section inside the multi-terminal network  $M$  between any two of its outputs  $\underline{k}$  and  $\underline{l}$ . This means that at any one state of the receiving elements, the structural admittance  $h_{kl}$  of  $M$  between  $\underline{k}$  and  $\underline{l}$  would be unity, contradicting the assumption that it is isolating.

### 3. Synthesis of Contact $(k, 1)$ - and $(1, k)$ -Terminal Networks by the Cascade Method

A relay-contact circuit with  $\underline{k}$  operating elements can be realized in the form of a contact  $(k, 1)$ - or  $(1, k)$ -terminal network, having a source of voltage connected to its output (or input, respectively), and having operating elements connected to its inputs (or outputs, respectively) (Fig. 5). The latter operate if there is conductance between the output and the inputs of the  $(k, 1)$ -terminal network or between the input and the outputs of the  $(1, k)$ -terminal network. A relay-contact circuit of this type is called normal ([16], Sections 2, 6).

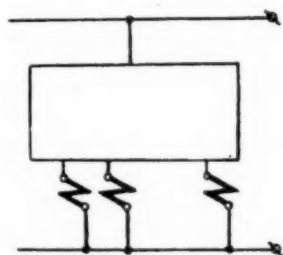


Fig. 5

Equation (A) affords a mathematical method for synthesizing contact  $(k, 1)$ -terminal networks. This method can be called the cascade method. It is suitable also for the synthesis of  $(1, k)$ -terminal networks, for the latter are obtainable from  $(k, 1)$ -terminal networks by interchanging inputs and outputs.

Let the synthesized  $(k, 1)$ -terminal network have  $\underline{n}$  receiving elements  $X_1, X_2, \dots, X_n$ . The state of receiving element  $X_i$  is algebraically represented by the variable  $x_i$ , which assumes a value 1 when the element  $X_i$  has operated (is connected) and a value 0 when  $X_i$  is at rest (disconnected). Using the correspondence between the words "or", "and", "no" and the addition, multiplication, and inversion operations of Boolean algebra any verbal specification of the conductance of the  $(k, 1)$ -terminal networks can be written in the form of Boolean functions of the variables  $x_1, x_2, \dots, x_n$ , i. e., in the form of equations made up of the letters  $x_1, x_2, \dots, x_n$ , with the aid of these three operations ([16], Sec. 2, 8). We shall therefore assume that the conductance conditions of a contact  $(k, 1)$ -terminal network with  $\underline{n}$  receiving elements  $X_1, X_2, \dots, X_n$ , can be specified in the form of  $\underline{k}$  Boolean functions of  $\underline{n}$  variables

$$f_1(x_1, x_2, \dots, x_n), f_2(x_1, x_2, \dots, x_n), \dots, f_k(x_1, x_2, \dots, x_n).$$

where the variable  $x_i$  represents the state of receiving element  $X_i$  and the function  $f_i$  specifies the conductance between the output and the  $\underline{i}$ -th input. For simplicity, we shall denote the function  $f_i$  by the symbol  $(i)$ .

The case when some of these functions are identical can be reduced to the case when they are all different, for each group of identical functions can be realized by a single contact circuit by placing together the corresponding inputs. We therefore, assume the functions  $(1), (2), \dots, (k)$  to be all different from each other. We also assume that they equal identically either zero or unity.

The cascade method consists of constructing a table for the expansion of functions  $(1), (2), \dots, (k)$  and a subsequent translation of the data of this table into graphic language.



Table 1 is an example of such an expansion. Here  $\underline{k} = \underline{n} = 3$ . The general case can be readily understood from this example.

Table 1	$(1) = x_1x_2 + x_1x_3 + x_2x_3$ $(2) = \bar{x}_1\bar{x}_2 + \bar{x}_1\bar{x}_3 + \bar{x}_2\bar{x}_3$ $(3) = x_1x_2x_3 + x_1\bar{x}_2\bar{x}_3 +$ $\quad + \bar{x}_1x_2x_3 + \bar{x}_1\bar{x}_2x_3$
$(1) = x_1(4) + \bar{x}_1(5)$ $(2) = x_1(6) + \bar{x}_1(7)$ $(3) = x_1(8) + \bar{x}_1(9)$	$(4) = x_2 + x_3, (5) = \bar{x}_2\bar{x}_3$ $(6) = \bar{x}_2\bar{x}_3, (7) = \bar{x}_2 + \bar{x}_3$ $(8) = x_2x_3 + \bar{x}_2\bar{x}_3$ $(9) = x_2x_3 + \bar{x}_2x_3$
$(4) = x_2 + \bar{x}_2(10)$ $(5) = x_2(10)$ $(6) = \bar{x}_2(11)$ $(7) = x_2(11) + \bar{x}_2$ $(8) = x_2(10) + \bar{x}_2(11)$ $(9) = x_2(11) + \bar{x}_2(10)$	$(10) = x_3, (11) = \bar{x}_3$

The expansion table consists of  $\underline{n}$  rows. The right half of the uppermost row contains the functions (1), (2), ..., (k). Thus, the right half of the first row of Table 1 contains the functions

$$\begin{aligned}
 (1) &= x_1x_2 + x_1x_3 + x_2x_3; \\
 (2) &= \bar{x}_1\bar{x}_2 + \bar{x}_1\bar{x}_3 + \bar{x}_2\bar{x}_3; \\
 (3) &= x_1x_2x_3 + x_1\bar{x}_2\bar{x}_3 + \bar{x}_1x_2\bar{x}_3 + \bar{x}_1\bar{x}_2x_3.
 \end{aligned}$$

To obtain the second row of the table, it is necessary to expand each function (1), (2), ..., (k) in terms of the variable  $x_1$  according to the known equation ([16], Sec. 2, 4)

$$f(x_1, x_2, \dots, x_n) = x_1f(1, x_2, \dots, x_n) + \bar{x}_1f(0, x_2, \dots, x_n) \quad (B)$$

and to compile a list of the expansion coefficients  $f(1, x_2, \dots, x_n)$  and  $f(0, x_2, \dots, x_n)$ . We obtain a total of  $2k$  expansion coefficients. They are functions of  $(n-1)$  variables. Some of these coefficients may equal zero or unity, and some may equal each other. Let us cross off the list all the zeros, all the ones, and all the functions that are encountered twice or more. Let us renumber the remaining functions as  $k+1, k+2$ , etc., and let us write them in the right half of Row 2 of the expansion table, denoting function No.  $j$  by  $(j)$ . In our example, the list of the coefficients of the expansion of the functions (1), (2), and (3) in terms of  $x_1$  will contain 6 coefficients:

$$x_2 + x_3, x_2x_3, \bar{x}_2\bar{x}_3, \bar{x}_2 + \bar{x}_3, x_2x_3 + \bar{x}_2\bar{x}_3, x_2\bar{x}_3 + \bar{x}_2x_3.$$



None is equal to zero or unity and all are different from each other. There is nothing to cross off, and all are therefore listed in the right half of the second row of Table 1. In the left part of the second row we write down the equations for the functions of the first row in terms of the functions of the second row.

To compare these coefficients with each other, and also to simplify the notation, the coefficients can be subjected to algebraic transformation. For example, writing unity in lieu of  $x_1$  in the function  $(1) = x_1x_2 + x_1x_3 + x_2x_3$  yields directly the coefficient  $x_2 + x_3 + x_2x_3$ . According to the rules of Boolean algebra ([16], Section 1.7)

$$x_2 + x_3 + x_2x_3 = x_2 + x_3.$$

The third row is obtained from the second in the same manner as the second from the first, but the functions of the second row are expanded in terms of  $x_2$  rather than of  $x_1$ , and the numbering of the coefficients that are not crossed off is started not with  $\underline{k} + 1$ , but with  $\underline{k}' + 1$ , where  $\underline{k}'$  is the number of the last function of the second row. In our example we obtain 12 expansion coefficients:

$$1, x_3, x_3, 0, 0, \bar{x}_3, \bar{x}_3, 1, x_3, x_3, \bar{x}_3, x_3.$$

This time the list of expansion coefficients contains zeros, ones and repeated terms. After crossing these off we obtain functions  $(10) = x_3$  and  $(11) = \bar{x}_3$ , which are written down in the right part of the third row. In the left part of the third row we write the equations expressing the functions of the second row in terms of the functions of the third row. The reader must pay attention to the manner in which these equations are influenced by the previously crossed-off ones and zeros. The effect of unity is seen in the equation for function (4), while the effect of the zeros is seen in the equations for functions (5) and (6).

If  $\underline{n} = 3$ , the third row is the last, and if  $\underline{n} > 3$  it is necessary to construct the fourth, fifth, ...,  $\underline{n}$ -th rows. The fourth row is obtained from the third, the fifth from the fourth, ..., and the  $\underline{n}$ -th from the  $(\underline{n}-1)$ -th in the same way as the second is obtained from the first or the third from the second, except that the  $i$ -th row is constructed by expanding the functions of the preceding  $(i-1)$ -th row in terms of  $x_{i-1}$  and the numbering of expansion coefficients not crossed off begins with  $\underline{k}^{(i-2)} + 1$ , where  $\underline{k}^{(i-2)}$  is the number of the last function in the  $(i-1)$ -th row.

It is easy to see that the  $i$ -th row of the table contains functions of  $\underline{n}-i+1$  variables  $x_1, x_{i+1}, \dots, x_{\underline{n}}$ , while the  $\underline{n}$ -th row contains functions of only one variable  $x_{\underline{n}}$ . Since there are only two functions of one variable that differ from zero or one, namely the functions  $x_{\underline{n}}$  and  $\bar{x}_{\underline{n}}$ , the  $\underline{n}$ -th row of the table contains only one or two terms, as is indeed the case with the third row of Table 1.

Once the expansion table is constructed, it remains to convert its left half into graphic language. The sequences of the functions in the rows of the table are replaced by parallel rows of circuit nodes. We shall draw these rows horizontally, but other directions are naturally also possible. The numbering of the functions is transferred to the nodes, and the equations in the right part of the table are replaced by junctions between the nodes through the contacts of the receiving elements. As is customary,  $x_i$  is replaced by the closing contact of element  $X_i$ , and  $\bar{x}_i$  by the opening contact of element  $X_i$ . Contacts  $x_{\underline{n}}$  and  $\bar{x}_{\underline{n}}$  are connected to the output node, to which are also connected the contacts representing the variables whose expansion coefficients equal one. For example, in the case of Equation (4)  $= x_2 + \bar{x}_2$  (10) of Table 1, Contact  $x_2$  is connected to the output. Nodes 1, 2, ...,  $\underline{k}$  are the inputs.

For example, Table 1 is represented by the circuit of Fig. 6.

The circuit obtained is a cascade connection of oriented multi-terminal networks  $M_1, M_2, \dots, M_{\underline{n}}$ , where  $M_1$  is made up only of contacts of element  $X_1$  and short-circuited terminals. Since  $x_1 \bar{x}_1 = 0$ , all these multi-terminal networks, with the exception of  $M_{\underline{n}}$ , are isolating ones (in the direction from the inputs to the output)\* and Equation (A) is therefore applicable. It is thus clear that the resulting circuit actually realizes the specified functions.

\*  $M_{\underline{n}}$  can be called isolating in the direction from the output to the inputs.

The results of the expansion of the conductance conditions can be represented directly in the form of a circuit, making the left part of the table superfluous.

Contacts  $x_i$  and  $\bar{x}_i$ , which are connected to the same node, can be unified into a single double-throw contact. The circuit of Fig. 6 becomes then the circuit of Fig. 7, where the contacts are represented by their

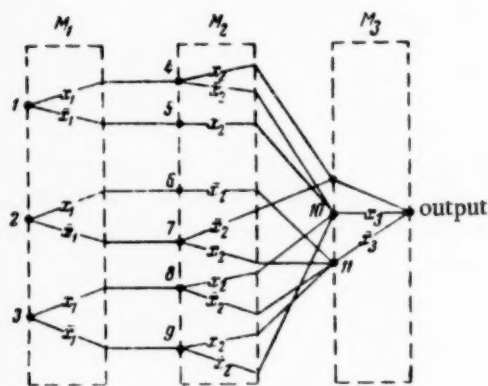


Fig. 6

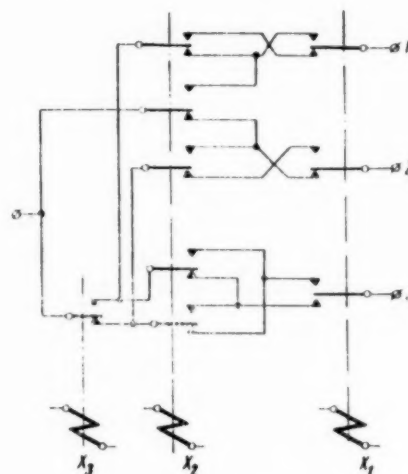


Fig. 7

traditional symbols.\* Let us remark that Equation (B) is indeed the equation for identifying a double-throw contact in element  $X_1$ . A circuit synthesized with the cascade method therefore consists, generally speaking, of double-throw contacts.

Since the contacts of the same receiving elements are always shown by us on a single line, it is easy to change over from the schematic to the wiring diagram.

With some practice it is possible to use the cascade method to construct directly the wiring diagram, using any of the traditional official symbols.

Let us note that D. Zeheb's and W. D. Caywood's synthesis method [21], which was developed independently of the cascade method, essentially duplicates the latter, but only as applied to two-terminal networks.

#### 4. Placement of the Receiving Elements in the Circuit

As is known,  $n$  receiving elements can be numbered in  $n!$  ways. Each method of numbering yields its own table for the expansion of the functions  $(1), (2), \dots, (k)$ , and determines in which order these variables will participate in the expansion of these functions. For specified conductance conditions of a  $(k, 1)$ -terminal network with  $n$  receiving elements, the cascade method yields  $n!$  circuits, differing from each other in the arrangement of the receiving elements. The number of contacts depends, in general, on the arrangement of the receiving elements, but so far there are no known methods of finding the best arrangement (except by surveying all  $n!$  circuits). An exception is the case of the so-called symmetrical circuits, the action of which is unaffected by any rearrangement of the receiving elements [5] (see Fig. 6 for an example). In the case of symmetrical circuits any arrangement is best. A method for recognizing a symmetrical circuit is described in [18].

#### 5. Effectiveness of the Cascade Method

The cascade method is applicable for all conductance conditions of  $(k, 1)$ - or  $(1, k)$ -terminal networks, and is universal in this sense. It usually results in bridge circuits, but parallel-series circuits are sometimes obtained. A characteristic feature of the cascade method is that bridge circuits can be constructed directly, without first constructing the parallel-series two-terminal networks. This feature is also shared by the combinatorial method of F. Svoboda [12, 13], based on the use of indeterminate Boolean functions.

\*According to [17].

The cascade method represents a single-valued regular process and makes it possible to construct complex circuits without excessive loss of time. Compared with other methods, the cascade method results frequently, although not always, in a smaller number of contacts. However, other methods of constructing circuits with bridges and for producing interconnections between terminal pairs are either not universal, or else require a large number of circuit transformations. The cascade method frequently results in a circuit that serves as the initial material for further simplification through the use of other methods. The cascade method can therefore be recommended for practical use (along with and in conjunction with other methods).

One can, in particular, propose the following considerations.

Let us define as irreducible a circuit in which (as in Fig. 6) not one of the contacts can be replaced by an open or solidly-closed connection. By testing the contacts of any circuit, it is possible to obtain an irreducible circuit that is equivalent to the initial one.\* If all the expansion coefficients of the realizable functions (1), (2), ..., (k) (with respect to  $x_1$ , with respect to  $x_1$  and  $x_2$ , with respect to  $x_1$ ,  $x_2$ , and  $x_3$ , etc.) are not equal to unity, the circuit constructed by the cascade method is irreducible. If certain coefficients are equal to unity, Equation (B) assumes the form:

$$f(x_i, x_{i+1}, \dots, x_n) = x_i f(1, x_{i+1}, \dots, x_n) + \bar{x}_i$$

or

$$f(x_i, x_{i+1}, \dots, x_n) = x_i + \bar{x}_i f(0, x_{i+1}, \dots, x_n).$$

Since  $x_i f + \bar{x}_i = f + \bar{x}_i$ ,  $x_i + \bar{x}_i f = x_i + f$ , the corresponding contacts  $x_i$  and  $\bar{x}_i$  can be eliminated, provided that this does not disturb the isolation properties of the multi-terminal networks  $M_1, M_2, \dots, M_k$ .

In the worse case, the function can be represented for any  $x_i$  in the form

$$f = x_i + f(0, \dots) \quad \text{or} \quad f = \bar{x}_i + f(1, \dots).$$

The circuit can then be built up of relays having either closing circuits only or opening circuits only. It is most convenient to employ here not the cascade method, but methods for the synthesis of bridge circuits by separating the initial and final elements, as developed by H. Piesch, A. M. Bryleev, and M. A. Gavrilov ([5], Ch. 11). In general, however, these methods are more complicated than the cascade method, since the presence of only open circuits makes the separation of the initial, final, and bridge elements quite complicated. In many cases the most convenient way is to construct parallel-series two-terminal networks by algebraic simplification of their equations [4, 5, 16] or by "mapping" methods [19, 20].

C. E. Shannon [10] proposed a method for the synthesis of bridge two-terminal networks, which this author extended to include  $(1, k)$ - and  $(k, 1)$ -terminal networks. This method can be called the method of universal multi-terminal networks. It is based on the same laws of the series multi-terminal network connection as the cascade method. It was shown [7, 9] that the method of cascades is more convenient than the method of universal multi-terminal networks and gives better circuits, and should therefore be given preference in practical synthesis. However, the method of universal multi-terminal networks retains a theoretical value, for it makes it possible to estimate the complexity of contact circuits.

The cascade method gives a better synthesis of symmetrical circuits than the method \*\* proposed in [5], Ch. 13.

\* A circuit with a minimum number of contacts is irreducible, but the converse is not necessarily true.

\*\* This method was proposed by C. E. Shannon [3].

## 6. Examples

We give below six examples of the synthesis of contact computing and control circuits by the cascade method. These examples merely illustrate the method and do not represent finished technical designs. The conditions of the problems were taken for the most part from other authors. With this reservation, we do not make reference to them. In some examples, the cascade method results in circuits already obtained by other methods or intuitively. In these cases, the advantages of the cascade method are simplicity and naturalness of the synthesis procedure.

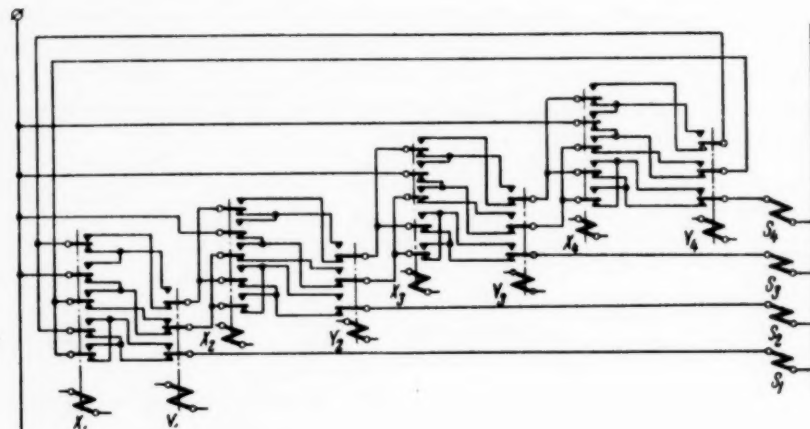


Fig. 8

**Example 1.** Order channel of single-stroke binary adder. Relay  $X_1$  represents the order of the augend, and relay  $X_2$ , the same order of the addend, and relay  $X_3$ , the carry from the preceding order; operation is denoted by 1 and nonoperation by 0. The channel represents a (3,1)- or (1,3)-terminal network, which represents by closing of its circuits the order of the sum, the carry to the next order, and the inversion of this carry. The

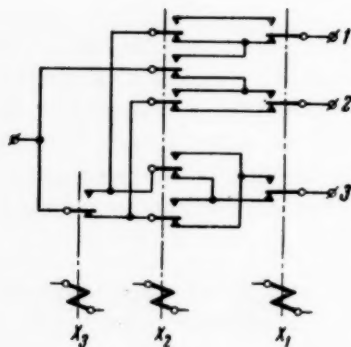


Fig. 9

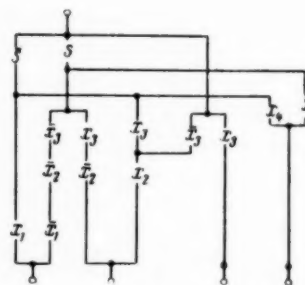


Fig. 10

algebraic conductance condition can be written as

$$f_1(x_1, x_2, x_3) = x_1x_2 + x_1x_3 + x_2x_3,$$

$$f_2(x_1, x_2, x_3) = \bar{x}_1\bar{x}_2 + \bar{x}_1\bar{x}_3 + \bar{x}_2\bar{x}_3,$$

$$f_3(x_1, x_2, x_3) = x_1x_2x_3 + x_1\bar{x}_2\bar{x}_3 + \bar{x}_1x_2\bar{x}_3 + \bar{x}_1\bar{x}_2x_3,$$

where  $f_1$  is the carry to the next order,  $f_2 = \bar{f}_1$ , and  $f_3$  is the order of the sum. The expansion is given in Table 1, and the circuit in Figures 6 and 7.

To construct the entire adder, it is enough to note that contacts  $x_3$  and  $\bar{x}_3$  can be replaced by circuits one and two of the channels of the preceding order. It is thus possible to connect any number of orders. By connecting the first channel to the last one it is possible to make the adder perform also subtraction of binary numbers with the aid of order by order complements and with the aid of cyclic transfer from the higher order to the lower.\* With this, an  $n$ -digit adder can add and subtract in modulo  $2^{n-1}$  and the number  $11\dots 1 = 2^{n-1} - 1$ , plays the part of zero. Figure 8 shows the compressed diagram of such an adder for  $n = 4$ . Here the relays  $X_1$ ,  $Y_1$ , and  $S_1$  represent respectively the orders of the augend, the addend, and of the sum.

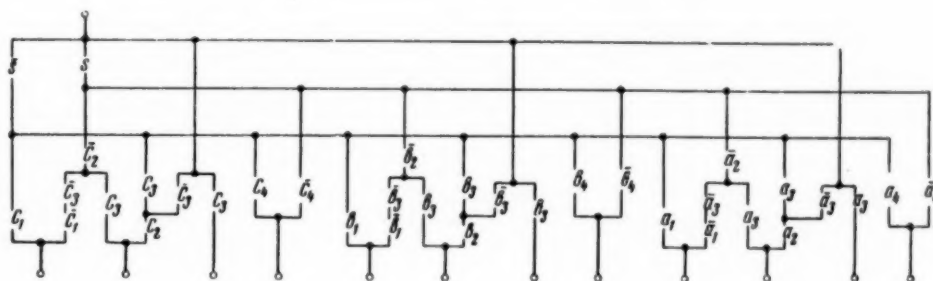


Fig. 11

This state is of interest since it comprises a ring circuit. The sign of a  $(n-1)$ -digit binary number can be considered as its  $n$ -th order, by representing the plus by zero and the minus by unity; a number  $11\dots 1$ , playing the role of zero, is considered negative. The adder of Fig. 8 will then work with positive and negative three-digit numbers.

**Example 2.** Order channel of one-stroke binary subtraction circuit. The relay  $X_1$  represents one order of the minuend and relay  $X_2$  the same order of the subtrahend, while relay  $X_3$  represents the "borrow" from the higher order; operation is denoted as before by the digit one, and nonoperation by zero. The channel is (3,1)

<p>Table 2</p>	<p>(1) = <math>\bar{x}_1 x_2 + \bar{x}_1 x_3 + x_2 x_3</math>  (2) = <math>x_1 \bar{x}_2 + x_1 \bar{x}_3 + \bar{x}_2 \bar{x}_3</math>  (3) = <math>\bar{x}_1 \bar{x}_2 x_3 + \bar{x}_1 x_2 \bar{x}_3 + x_1 \bar{x}_2 \bar{x}_3 + x_1 x_2 x_3</math></p>
<p>(4) = <math>x_1</math> (4) + <math>\bar{x}_1</math> (5)  (2) = <math>x_1</math> (6) + <math>\bar{x}_1</math> (7)  (3) = <math>x_1</math> (8) + <math>\bar{x}_1</math> (9)</p>	<p>(4) = <math>x_2 x_3</math>, (5) = <math>x_2 + x_3</math>  (6) = <math>\bar{x}_2 + \bar{x}_3</math>, (7) = <math>\bar{x}_2 \bar{x}_3</math>  (8) = <math>\bar{x}_2 \bar{x}_3 + x_2 x_3</math>  (9) = <math>\bar{x}_2 x_3 + x_2 \bar{x}_3</math></p>
<p>(4) = <math>x_2</math> (10)  (5) = <math>x_2 + \bar{x}_2</math> (10)  (6) = <math>x_2</math> (11) + <math>\bar{x}_2</math>  (7) = <math>\bar{x}_2</math> (11)  (8) = <math>x_2</math> (10) + <math>\bar{x}_2</math> (11)  (9) = <math>x_2</math> (11) + <math>\bar{x}_2</math> (10)</p>	<p>(10) = <math>x_3</math>, (11) = <math>\bar{x}_3</math></p>

\* See [22] Chapter VI, Section 8, for such subtraction.



or (1,3)-terminal network, which represents by closing of circuits the unknown order of the differences, the "borrow" from the next higher order, and the inversion of this "borrow." Algebraically, the conduction conditions are written in the following form:

$$\begin{aligned} f_1(x_1, x_2, x_3) &= \bar{x}_1 x_2 + \bar{x}_1 x_3 + x_2 x_3, \\ f_2(x_1, x_2, x_3) &= x_2 \bar{x}_3 + x_1 \bar{x}_3 + \bar{x}_2 x_3, \\ f_3(x_1, x_2, x_3) &= \bar{x}_1 x_1 x_3 + x_1 x_2 \bar{x}_3 + x_1 \bar{x}_2 x_3 + x_1 x_2 x_3, \end{aligned}$$

where  $f_1$  is the "borrow" from the next higher order,  $f_2 = \bar{f}_1$ , and  $f_3$  is the order of the difference. The expansion is given in Table 2, and the circuit in Fig. 9.

Replacing contacts  $x_3$  and  $\bar{x}_3$  by circuits 1 and 2 of the channel of the next higher order, we can construct the entire subtraction circuit.

Connecting the channel of the first order with the channel of the last order makes it possible to subtract larger numbers from smaller ones, and also operate with negative subtrahend and minuends. Negative numbers are represented in that case by the order complements, and the sign is considered to be senior order (see Example 1).

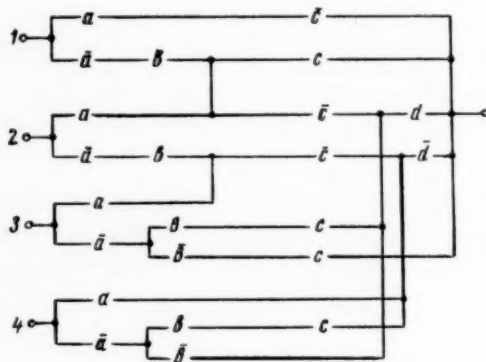


Fig. 12

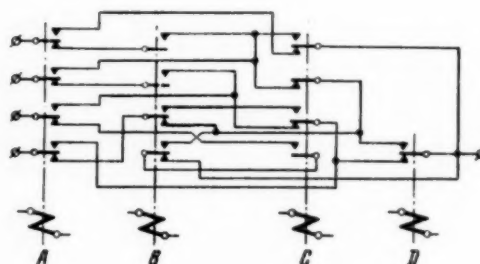


Fig. 13

**Example 3.** Order channel of decimal inverter (circuits translating negative decimal numbers into their order by order complements). The Relays  $X_1, X_2, X_3$  and  $X_4$  represent the order of a decimal number in accordance with Table 3. Relay  $S$  represents the sign of the decimal number (operation corresponds to minus).

TABLE 3

Decimal number	$x_1$	$x_2$	$x_3$	$x_4$
0	0	0	0	0
1	0	0	0	1
2	0	0	1	0
3	0	0	1	1
4	0	1	0	0
5	0	1	0	1
6	0	1	1	0
7	0	1	1	1
8	1	0	0	0
9	1	0	0	1

The channel is a (4,1)- or (1,4)-terminal network, and the closing of its circuit represents the order of the number formed by the inverter, in accordance with the same code. This number equals the initial number at  $s = 0$  and to its order complement at  $s = 1$ . Turning now to Table 3 and taking into account the unused states 1010, 1011, 1101, 1110, 1100 and 1111 ([16], Section 3.1), the conduction conditions can be written in the following form:

$$\begin{aligned} f_1(x_1, x_2, x_3, x_4) &= \bar{s} x_1 + s \bar{x}_1 \bar{x}_2 \bar{x}_3, \\ f_2(x_1, x_2, x_3, x_4) &= s x_2 + s (x_2 x_3 + x_3 \bar{x}_4), \\ f_3(x_1, x_2, x_3, x_4) &= x_3, \quad f_4(x_1, x_2, x_3, x_4) = \bar{s} x_4 + s \bar{x}_4. \end{aligned}$$

Let us employ the following arrangement of variables



$$x_1, x_2, x_3, x_4, s,$$

placing the variable  $\bar{s}$  in the last place, so that it becomes possible to connect the contacts of Relay S in all channels. The expansion is given in Table 4, the circuit in Fig. 10. It can be simplified somewhat. Figure 11 shows the entire inverter for three-digit decimal numbers, composed of simplified channels. Here the relays of the first channel are denoted by the letter A, the relays of the second channel by the letter B, and the relays of the third channel by the letter C.

This example shows how to apply the method of cascades to functions that depend on different arguments. Indeed, we write (2) = (7), (3) = (8), etc., because according to Equation (B)

$$\begin{aligned}(2) &= x_1(7) + \bar{x}_1(7) = (x_1 + \bar{x}_1)(7) = (7), \\ (3) &= x_1(8) + \bar{x}_1(8) = (x_1 + \bar{x}_1)(8) = (8)\end{aligned}$$

etc., (it must be borne in mind that  $x_1 + \bar{x}_1 = 1$ ).

Table 4	$(1) = \bar{s}x_1 + \bar{s}x_1\bar{x}_2\bar{x}_3$ $(2) = \bar{s}x_2 + s(\bar{x}_2x_3 + x_2\bar{x}_3)$ $(3) = x_3$ $(4) = \bar{s}x_4 + \bar{s}x_4$
$(1) = x_1(5) + \bar{x}_1(6)$ $(2) = (7)$ $(3) = (8)$ $(4) = (9)$	$(5) = \bar{s}, (6) = \bar{s}x_2\bar{x}_3$ $(7) = \bar{s}x_2 + s(\bar{x}_2x_3 + x_2\bar{x}_3)$ $(8) = x_3$ $(9) = \bar{s}x_4 + \bar{s}x_4$
$(5) = (10),$ $(6) = \bar{x}_2(11)$ $(7) = \bar{x}_2(12) + \bar{x}_2(13)$ $(8) = (14)$ $(9) = (15)$	$(10) = \bar{s}, (11) = \bar{s}x_3$ $(12) = \bar{s} + \bar{x}_3, (13) = \bar{s}x_3$ $(14) = x_3$ $(15) = \bar{s}x_4 + \bar{s}x_4$
$(10) = (16)$ $(11) = \bar{x}_3(17)$ $(12) = x_3(16) + \bar{x}_3$ $(13) = x_3(17)$ $(14) = x_3$ $(15) = (18)$	$(16) = \bar{s}, (17) = s$ $(18) = \bar{s}x_4 + \bar{s}x_4$
$(16) = (19), (17) = (20)$ $(18) = x_4(19) + \bar{x}_4(20)$	$(19) = \bar{s}, (20) = s$

**Example 4.** Circuit to convert decimal numbers (for example, subscriber pulses in automatic telephone stations) from the Code 1, 2, 4, 8 into the Code 1, 2, 4, 5. Relays A, B, C and D represent the digit in the Code 1, 2, 4, 8 and their circuits  $f_1, f_2, f_3$  and  $f_4$  represent the digit in the Code 1, 2, 4, 5 (see Table 5). Turning to Table 5 and taking into account the unused states 1011, 1100, 1101, 1110, 1111 ([16], Section 3.1),\* we can write

$$f_1 = \bar{a}b(c+d) + a\bar{c}, \quad f_2 = \bar{a}b\bar{c}d + a(c+d),$$

$$f_3 = \bar{a}bc + \bar{a}bcd + a\bar{c}\bar{d}, \quad f_4 = \bar{a}bd + \bar{a}bcd + a\bar{d}.$$

TABLE 5

Decimal number	ABCD	$f_1 f_2 f_3 f_4$	Decimal number	ABCD	$f_1 f_2 f_3 f_4$
1	0001	0001	6	0110	1001
2	0010	0010	7	0111	1010
3	0011	0011	8	1000	1011
4	0100	0100	9	1001	1100
5	0101	1000	0	1010	0101

Table 6	(1) = $f_1$ (2) = $f_2$ (3) = $f_3$ (4) = $f_4$
(1) = $a$ (5) + $\bar{a}$ (6) (2) = $a$ (7) + $\bar{a}$ (8) (3) = $a$ (9) + $\bar{a}$ (10) (4) = $a$ (11) + $\bar{a}$ (12)	(5) = $\bar{c}$ , (6) = $b(c+d)$ (7) = $c+d$ , (8) = $b\bar{c}\bar{d}$ (9) = $\bar{c}\bar{d}$ (10) = $\bar{b}c + bcd$ (11) = $\bar{d}$ , (12) = $\bar{b}d + b\bar{c}\bar{d}$
(5) = (13), (6) = $b$ (14) (7) = (14), (8) = $b$ (15) (9) = (15), (10) = $b$ (16) + $\bar{b}$ (17) (11) = (18) (12) = $b$ (19) + $\bar{b}$ (20)	(13) = $\bar{c}$ (14) = $c+d$ (15) = $\bar{c}\bar{d}$ (16) = $cd$ (17) = $c$ (18) = $\bar{d}$ (19) = $\bar{c}\bar{d}$ (20) = $d$
(13) = $\bar{c}$ (14) = $c + \bar{c}$ (21) (15) = $\bar{c}$ (22) (16) = $c$ (21) (17) = $c$ , (18) = (22) (19) = $c$ (22), (20) = (21)	(21) = $d$ (22) = $\bar{d}$

\* The Code 1, 2, 4, 8 was also used in Table 3, but with the code combination 0000 for the number 0. The combination 1010 was therefore unused. In our example the combination 0000 is not included in the code, but nevertheless it is included among those employed, since it denotes the nonoperative state of the circuits.

The expansion is given in Table 6 and the circuit in Figure 12. This circuit can be simplified somewhat. Figure 13 shows the final developed circuit using traditional symbols.

**Example 5. Order channel of circuit for comparison of binary numbers.** The Relay  $A_i$  represents the  $i$ -th order of a binary number  $\alpha = a_n a_{n-1} \dots a_1$ ; Relay  $B_i$  represents the  $i$ -th order of a binary number  $\beta = b_n b_{n-1} \dots b_1$ ; Relay  $C$  represents the result of comparison of the portions  $a_{i-1} a_{i-2} \dots a_1$  and  $b_{i-1} b_{i-2} \dots b_1$  of numbers  $\alpha$  and  $\beta$ . Relay  $C$  operates if  $a_{i-1} a_{i-2} \dots a_1 < b_{i-1} b_{i-2} \dots b_1$ . The channel is a two-terminal network, which closes when  $a_1 a_{i-1} \dots a_1 < b_1 b_{i-1} \dots b_1$ . Algebraically

$$f(a_i, b_i, c) = \bar{a}_i b_i + (a_i b_i + \bar{a}_i \bar{b}_i) c.$$

The expansion is given in Table 7, the diagram in Fig. 14. Replacing Contact  $c$  by the channel of the next-higher order, it is easy to construct the entire comparison circuit (see Fig. 15, where  $n = 4$ ).\*

Table 7	$(1) = f(a_i, b_i, c)$
$(1) = a_i (2) + \bar{a}_i (3)$	$(2) = b_i c$ $(3) = b_i + \bar{b}_i c$
$(2) = b_i (4)$ $(3) = b_i + \bar{b}_i (4)$	$(4) = c$

**Examples 6. Symmetrical lattice with three receiving elements.** This term is used to designate a (4,1)-terminal network, which represents by closing its circuits the number of receiving elements that have operated. Algebraically

$$\begin{aligned} f_1(x, y, z) &= \bar{x} \bar{y} \bar{z}, & f_2(x, y, z) &= x \bar{y} \bar{z} + \bar{x} y \bar{z} + \bar{x} \bar{y} z, \\ f_3(x, y, z) &= x y \bar{z} + x \bar{y} z + \bar{x} y z, & f_4(x, y, z) &= x y z, \end{aligned}$$

where  $f_1$  denotes the inoperative state of all the elements,  $f_2$  indicates operation of one element,  $f_3$  operation of two elements, and  $f_4$  operation of all three elements. The expansion is given in Table 8, the circuit, in Figure 16.

## APPENDIX

### On the Extension of the Cascade Method to Include Contactless Relay Circuits \*\*

1. When designing devices with contactless relay elements (electronic tubes, valves, etc.) one frequently encounters the following problem. Given  $k$  Boolean functions of  $n$  variables

$$f_1(x_1, x_2, \dots, x_n), f_2(x_1, x_2, \dots, x_n), \dots, f_k(x_1, x_2, \dots, x_n).$$

\* Examples 1, 2 and 4, employ the technique proposed by W. Zuehlisford, of introducing "conditional" relays into the circuit [23].

\*\* The main contents of this Appendix was reported at the seminar of the Laboratory on the Development of Scientific Problems in Wire Communication of the Academy of Sciences of the USSR on February 9, 1955.

It is required to construct a circuit, in which the voltage of the  $i$ -th output is a function  $f_i(x_1, x_2, \dots, x_n)$  of the input voltages  $x_1, x_2, \dots, x_n$  when the circuit is in a stationary state. All the input and output voltages are considered as quantities assuming only two values: 0, and 1. Physically this means classification of voltages into high or low, into negative or positives, or else as into on or off [24]. Such a circuit can be called a

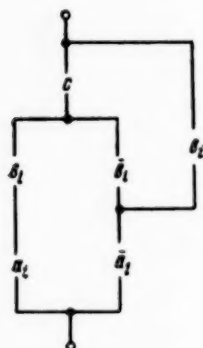


Fig. 14

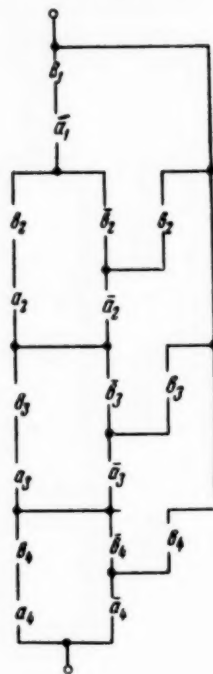


Fig. 15

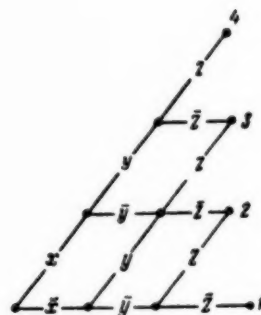


Fig 16

switching  $(n,k)$ -terminal network.\* Without loss of generality, one can assume that the functions  $f_1, f_2, \dots, f_k$  differ from zero and unity and are pairwise different.

Table 8	(1) = $f_1$ , (2) = $f_2$ (3) = $f_3$ , (4) = $f_4$
(1) = $\bar{x}$ (5) (2) = $x$ (5) + $\bar{x}$ (6) (3) = $x$ (6) + $\bar{x}$ (7) (4) = $x$ (7)	(5) = $\bar{y}\bar{z}$ (6) = $\bar{y}z + y\bar{z}$ (7) = $yz$
(5) = $\bar{y}$ (8) (6) = $y$ (8) + $\bar{y}$ (9) (7) = $y$ (9)	(8) = $\bar{z}$ (9) = $z$

\* In the foreign literature such circuits are frequently logical.

We shall start the construction of the circuit choosing its structure, i.e., the number and the composition of the elements of the circuit and the method of their interconnection. At the present time many algebraical methods are available for the description and synthesis of the structure of switching  $(n,k)$ -terminal networks with various contactless elements [24-29]. We shall show below on the basis of these developments how to apply the

TABLE 9

Values of $f', f''$	Operator for
$f' = 0 \begin{cases} f'' = 0 \\ f'' = 1 \\ 0 < f'' < 1 \end{cases}$	$f = 1$ $f = x_1$ $f = P_2(x_1, f'')$
$f' = 1 \begin{cases} f'' = 0 \\ f'' = 1 \\ 0 < f'' < 1 \end{cases}$	$f = \bar{x}_1$ $f = 0$ $f = T_2(x_1, f'')$
$0 < f' < 1 \begin{cases} f'' = 0 \\ f'' = 1 \\ 0 < f'' < 1 \end{cases}$	$f = P_2(x_1, f'')$ $f = T_2(\bar{x}_1, f'')$ $f = P_2(x_1, f'') P_2(\bar{x}_1, f'')$

basic ideas of the cascade methods to the structural synthesis of electronic, valve, and transformer switching  $(n,k)$ -terminal networks.

2. Let us start with electronic  $(n,k)$ -terminal networks. Their structure can be represented with the aid of the diagrams described in [24] under the designation of functional diagrams. Using the assumptions listed in [24], the algebraic solution of the problem of the structural synthesis of electronic  $(n,k)$ -terminal networks reduces directly or indirectly to the representation of each function  $f_i(x_1, x_2, \dots, x_n)$  in the form of a superposition of elementary functions, describing the operation of the individual vacuum tubes or their simplest connections. Such elementary functions are sums of functions of the form  $C_1(x) = x$  and products of functions of

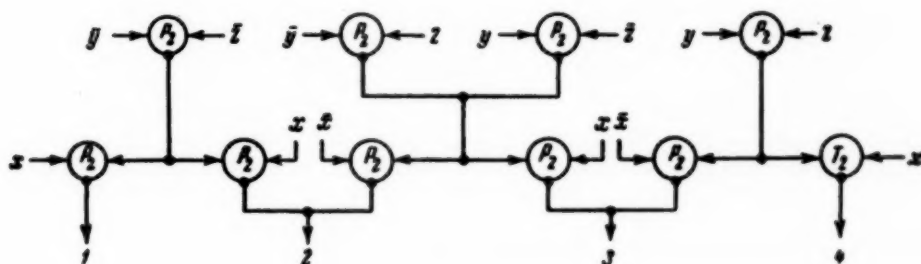


Fig. 17

the form  $T_1(x) = x$  and  $P_2(x,y) = x|y$ , where  $x|y = x + y$  is H. M. Sheffer's function [30]. The symbol  $C_1$  is the operator of cathode follower with one input, the symbols  $T_1$  and  $P_2$  denote tubes with plate loads. Here  $T_1$  is the triode operator (tube with single input) and  $P_2$  is the pentode operator (tube with two inputs).<sup>\*</sup> Addition

<sup>\*</sup> Concerning the arbitrariness of the terms "triode" and "pentode" in this sense, see [31].

represents the use of a common cathode resistor, multiplication, the use of a common plate resistance. For reasons indicated in [31], we use Boolean algebra and not its arithmetic equivalent used in [24].

For brevity we put

$$C_m(y_1, \dots, y_m) = \sum_{i=1}^m C_1(y_i), \quad T_m(y_1, \dots, y_m) = \prod_{i=1}^m T_1(y_i).$$

As in [24], it is assumed that the input voltage  $x_1$  is always accompanied by its inversion  $\bar{x}_1$ .

Depending on the method in which the signal is transmitted from the inputs to the outputs, electronic switching (n,k)-terminal networks are divided into (n,k)-terminal networks without feedback and (n,k)-terminal networks with feedback. An example of the latter is given in Figure 3 of [15]. We shall call a (n,k)-terminal network without feedback a converging one, if each of its tubes controls only one other tube, and a diverging one otherwise. Converging (n,1)-terminal networks are analogous to parallel-series contact two-terminal networks in that the structure of both can be represented algebraically in the form of a superposition of definite elementary functions. It is easy to see that converging (n,1)-terminal network can always be written in the form of a superposition of elementary vacuum-tube functions and that this representation specifies its structure uniquely. Converging (n,k)-terminal networks are divided into k (n,1)-terminal networks that are not connected with each other. Diverging (n,k)-terminal networks are analogous to contact (1,k)-terminal networks with bridge connections and with output circuits connected. The structure of a diverging (n,k)-terminal network cannot be represented in the form of a superposition of elementary functions.

Diverging (n,k)-terminal are used quite frequently in [24], but are not analyzed in a systematic manner. We shall use the ideas of the cascade methods to propose certain systematic methods for structural synthesis of diverging (n,k)-terminal networks.

Instead of Equation (B) we shall now use the equation

$$f(x_1, x_2, \dots, x_n) = [x_1 | \overline{f(1, x_2, \dots, x_n)}] [\bar{x}_1 | \overline{f(0, x_2, \dots, x_n)}]. \quad (C)$$

Expanding the functions  $f_1, f_2, \dots, f_k$  one after another in terms of the variables  $x_1, x_2, \dots, x_{n-1}$  in accordance with Equation (C) and using Table 9, where  $f' = f(1, x_2, \dots, x_n)$ ,  $f'' = f(0, x_2, \dots, x_n)$ , we shall represent these functions in the form of superpositions of elementary functions and thereby synthesize the converging (n,k)-terminal network. Here we shall consider that

$$P_2(y, 1) = T_2(y, 0) = \bar{y}, \quad P_2(y, 0) = 1, \quad T_2(y, 1) = 0$$

and that if  $m > 2$  a function of the form  $\sum_{i=1}^m y_i$  is realized by an operator  $C_m(y_1, \dots, y_m)$  and a function of the form  $\prod_{i=1}^m y_i$  by an operator  $T_m(y_1, \dots, y_m)$ . This process is the Boolean equivalent of the third principal method described in [24], Chapter IV, Page 44-50.

The cascade method consists essentially of interconnecting circuits that realize equal coefficients of the expansion. This idea can be used also in the case of expansion in accordance with Equation (C). It is possible to use (C) to compile an expansion table and to translate its left half into graphic language, obtaining a structural diagram (functional diagram). We shall illustrate how this is done with an example.

Let us synthesize a (3,4)-terminal network which realizes the following functions



$$f_1(x, y, z) = \bar{x}yz, \quad f_2(x, y, z) = x\bar{y}z + \bar{x}yz + \bar{x}y\bar{z},$$

$$f_3(x, y, z) = x\bar{y}\bar{z} + \bar{x}yz + \bar{x}y\bar{z}, \quad f_4(x, y, z) = xyz.$$

This is none other but an electronic symmetrical lattice, the electronic analogue of the circuit of Fig. 16. The expansion is given in Table 10, the diagram in Fig. 17. We obtain a diverging circuit.

Table 10	(1) = $f_1$ , (2) = $f_2$ (3) = $f_3$ , (4) = $f_4$
(1) = $T_1[x, (5)]$ (2) = $P_2[x, (5)] P_2[\bar{x}, (6)]$ (3) = $P_2[x, (6)] P_2[\bar{x}, (7)]$ (4) = $T_1[\bar{x}, (7)]$	(5) = $y + z$ (6) = $\bar{y}\bar{z} + yz$ (7) = $\bar{y} + \bar{z}$
(5) = $P_2(\bar{y}, \bar{z})$ (6) = $P_2(\bar{y}, z) P_2(y, \bar{z})$ (7) = $P_2(y, z)$	

For further economy in nets it is possible to discard from the list of coefficients of each expansion not only the functions that are encountered for a second time, but also the functions that are inversions of the preceding functions. In the circuit these inversions are realized with the aid of the operators  $T_1$ . For example, let us construct a circuit for binary summation  $w \oplus x \oplus y \oplus z$ . The expansion is given in Table 11 and the diagram in Fig. 18.

The method of cascades fills to some extent the gap in the procedure for selecting common elements for circuits with several outputs, referred to in [24], Chapter VII.

Table 11	(1) = $w \oplus x \oplus y \oplus z$
(1) = $P_2[w, (2)] P_2[\bar{w}, T_1[(2)]]$ (2) = $P_2[x, (3)] P_2[\bar{x}, T_1[(3)]]$ (3) = $P_2(y, z) P_2(\bar{y}, \bar{z})$	(2) = $x \oplus y \oplus z$ (3) = $y \oplus z$

3. Everything that was said in Section 2 concerning switching (n,k)-terminal networks composed of valve elements, such as vacuum-tube diodes, crystal diodes, selenium and copper oxide rectifiers, remains the same, except that the elementary functions will be different. In the case of valve (n,k)-terminal networks the elementary functions are

$$B_m(y_1, \dots, y_m) = \sum_{i=1}^m y_i \text{ and } F_m(y_1, \dots, y_m) = \prod_{i=1}^m y_i \quad (\text{for circuits of these functions see [24, 26-29]}).$$

Equation (C) is replaced here by Equation (B)

\* The possibility of applying the cascade method to the synthesis of diverging electronic (n,k)-terminal networks was first disclosed by the author in a report [32].

$$f(x_1, x_2, \dots, x_n) = x_1 f(1, x_2, \dots, x_n) + \bar{x}_1 f(0, x_2, \dots, x_n)$$

or by equation

$$f(x_1, x_2, \dots, x_n) = [x_1 + f(0, x_2, \dots, x_n)][\bar{x}_1 + f(1, x_2, \dots, x_n)].$$

It is possible to construct for each of these equations operator tables, analogous to Table 9. The cascade method makes it possible to construct diverging valve (n,k)-terminal networks and thereby effect an economy in the number of valves.

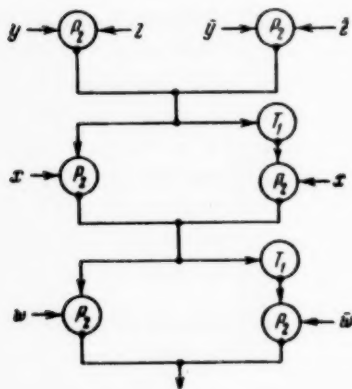


Fig. 18

Usual valve (n,k)-terminal networks are needed when intermediate amplifiers are needed in the connections of intermediate amplifiers between a definite number of their stages. Recently there have been developed methods for constructing multi-stage valve (n,k)-terminal networks with input circuits employing germanium transistors [27]. Such valve circuits do not require intermediate amplifiers. \*

The inversion operation is not realized directly with valve circuits. If triode tubes are introduced for this purpose, we obtain the set of elementary functions  $B_m, F_m, T_1$ , considered in [28]. In this case it is possible upon synthesis by the cascade method to invert the expansion coefficients as indicated in Section 2. The inversion can be obtained also with the aid of a transformer [29].

4. Ch. Raiskii [29] proposed a transformer circuit for binary summation of  $x \oplus y$ . Raiskii called this function a symmetrical difference and denotes it as  $x \dot{-} y$ . With the aid of this circuit and a valve circuit  $B_m$  it is possible to construct switching (n,k)-terminal networks, both converging and diverging, for any Boolean function. The method

is the same as in the preceding paragraphs, but (C) is replaced by the following equation

$$f(x_1, x_2, \dots, x_n) = [x_1 + \overline{f(0, x_2, \dots, x_n)}] \oplus [x_1 + \overline{f(1, x_2, \dots, x_n)}]. \quad (D)$$

The method of cascades makes it possible to construct diverging circuits by joining equal expansion coefficients.

The author thanks V. I. Ivanov, V. A. Khvoshchuk, A. A. Shavrov, Iu. L. Tomfel'd and G. K. Moskatov for reviewing this article. Their remarks improved considerably the presentation of the material.

Received April 16, 1956

#### LITERATURE CITED

- [1] P. Erenfest, Review of L. Kutiur's book "Algebra of Logic." ZhRfKhO (Jl. of Russian Phys. Chem. Soc.) Phys. Division, Vol. XLII, Div. 2, No. 10 (1910).
- [2] V. I. Shestakov, "Algebra of Two-Terminal Circuits Composed Exclusively of Two-Terminal Elements (Algebra of A-Circuits)." Automation and Remote Control, No. 2 (1941).
- [3] C. E. Shannon, A. Symbolic Analysis of Relay and Seitching Circuits, Trans. AIEE, Vol. XVII, 1938.
- [4] M. A. Gavrilov, "Methods of Synthesis of Relay-Contact Circuits." Electric Circuits. No. 2 (1946).
- [5] M. A. Gavrilov, Theory of Relay-Contact Circuits, Publ. by USSR Acad. Sci (1950).

- [6] M. A. Gavrilov, "Transformation of Relay-Contact Circuits of Class H," Dokl. AN SSSR, Vol. LIX, No. 9 (1948).
- [7] G. N. Povarov, "Investigation of Contact Circuits with Minimum Number of Contracts" Dissertation for scientific degree of Candidate of Technical Sciences, Inst. of Automation and Remote Control, Acad. Sci. USSR (1954).
- [8] G. N. Povarov, "On the Synthesis of Contact Multi-Terminal Networks" Dokl. AN SSSR, Vol. XCIV, No. 6 (1954).
- [9] G. N. Povarov, "Mathematical Theory of Synthesis of Contact (1,k)-Terminal Networks" Dokl. AN SSSR, Vol. C, No. 5 (1955).
- [10] C. E. Shannon, The Synthesis of Two-Terminal Switching Circuits. BSTJ, Vol. XXVIII, No. 1, 1949.
- [11] R. Righi, Latest development in communication Algebra: application to multiterminal circuits, Ingegneria ferroviaria 9, No. 4-5 (1954).
- [12] F. Svoboda, Neurcita dvouhodnotova Booleova funkce. Casopis pro pestovani matematiky (Undetermined bielemental Boolean function. Journal for the Cultivation of Mathematics) Vol. LXXCIII, No. 4, 1953.
- [13] F. Svoboda, F. Uziti neurcite dvouhodnotove Booleovy funkce na synthesu jednotaktnich hradlovych schemat. Stroje na zpracovani informaci, Sbornik II, 1954, (Application of the undetermined bielemental Boolean function in the synthesis of one terminal switching circuits. Machines For the Elaboration of Information, Symposium II, 1954).
- [14] A. Svoboda, Synthesa releovych siti. Stroje na zpracovani informaci, Sbornik II, 1954, (Synthesis of relay circuits. Machines for the Elaboration of Information, Symposium II, 1954).
- [15] H. Rohleder, Der dreiwertige Aussagenkalkul der theoretischen Logik und seine Anwendung zur Beschreibung von Schaltungen, die aus Elementen mit zwei stabilen Zustanden bestehen. ZAMM, Bd. XXXIV, Nr 8/9, 1954.
- [16] V. N. Reginskii and A. D. Kharkevich, Relay Circuits in Telephony, Sviaz'izdat (1955).
- [17] M. A. Anfimov, Synthesis of Electric Circuits, Oborongiz (1949).
- [18] G. N. Povarov, "On a Procedure for Analysis of Symmetric Contact Circuits," Automation and Remote Control, Vol. XVI, No. 4 (1955).
- [19] W. V. Quine, The Problem of Simplifying Truth Functions. Amer. Math. Monthly, Vol. LIX, No. 8 1952.
- [20] M. Karnaugh, The Map Method for Synthesis of Combinatorial Circuits. Trans. AIEE, Vol. LXXII, Part I, 1953.
- [21] D. Zeheb and W. P. Caywood, A Symbolic Method for Synthesis of 2-Terminal Switching Circuits. Communication and Electronics, No. 16, 1955.
- [22] High Speed Computing Machines, Translations Edited by D. Iu. Panov, (Foreign Lit. Press, 1952).
- [23] W. Zuhlsdorf, Methoden der theoretisch-mathematischen Behandlung von Aufgaben der Schaltungstechnik. Dtsch. Elektrotechnik, Jg. VIII, H. 2, 1954.
- [24] Synthesis of Electronic Computing and Control Circuits, Translations Edited by V. I. Shestakov, (Foreign Lit. Press, 1954).
- [25] S. H. Washburn, An Application of Boolean Algebra to the Design of Electronic Switching Circuits. Trans. AIEE, Vol. LXXII, Part I, 1953.

- [26] An Wang, Miniature Rectifier Computing and Controlling Circuits. Proc. IRE, Vol. XI, No. 8, 1952.
- [27] B. J. Yokelson and W. Ulrich, Engineering Multistage Diode Logic Circuits. Electr. Engng. Vol. LXXIV, No. 12, 1955.
- [28] H. Greniewski, K. Bochenek and R. Marczynski, Application of Bi-Elemental Boolean Algebra to Electronic Circuits. Studia Logica, t. II, 1955.
- [29] Cz. Rajski, Transformatorowa realizacja różnicy symetrycznej. Archiwum elektrotechniki, t. IV, zes. 3, 1955 (Transformative realization of symmetrical differences. Archives of Electrotechnics 4, 3 (1955)).
- [30] H. M. Sheffer, A Set of Five Independent Postulates for Boolean Algebras with Application to Logical Structures. Trans. Amer. Math. Soc., Vol. XIV, No. 4, 1913.
- [31] G. N. Povarov, "Review of book, Synthesis of Electronic Computing and Control Circuits." Automation and Remote Control, Vol. XV, No. 6 (1954).
- [32] G. N. Povarov, "Structural Theory of Electronic Relay-Action Circuits." Report No. 23-54 of Laboratory No. 3 of the Inst. of Automation and Remote Control, USSR Acad. of Sciences (1954).

## STABLE OPERATION OF TWO-PHASE INDUCTION MOTOR WITH NEGATIVE VELOCITY FEEDBACK

E. I. Slepushkin  
(Moscow)

The conditions of stable operation of a generally asymmetrical two-phase induction motor with negative-velocity feedback are considered for arbitrary machine parameters and for arbitrary supply parameters. Criteria for stable operation of the servo motor are established. It is recommended that the feedback parameters be determined from the parameters of the mechanical characteristic at the pull-out point. The design equations are expressed in terms of the so-called generalized parameters: rated critical slip of the equivalent circuits of the motor windings and the ratio of the resistances of the primary and secondary circuits.

The theoretical deductions are experimentally confirmed.

### INTRODUCTION

The customarily employed two-phase induction servo motors with critical slip  $s_c > 1$  have the property that they can be adjusted continuously from zero up to the maximum possible speed for a given load [1]. However, if the control winding of the motor is fed from an amplifier having a high internal impedance [for example, from a magnetic amplifier (Fig. 1)], the servo motor may lose its adjustable properties. The derivative  $d\mu/dv$  becomes positive in a certain range of speeds [2, 3]. In this case it is necessary to change artificially the mechanical characteristics of the motor, so as to make the derivative of the torque with respect to speed negative both in running and plugging operation for all values of  $v$ . Such a change in mechanical characteristics is effected in a squirrel cage rotor motor most simply by introducing negative velocity feedback.

The choice of feedback parameters for the case of zero phase shift between the phase voltages and for a zero static torque on the shaft of the motor was considered in [2]. In this work we shall derive equations for the choice of feedback parameters for the general case of asymmetry [4], in which the regulation is effected by changing the voltage and the phase shift. In this case the servo motor is treated as a link in an automatic regulation system in which the error frequency is considerably smaller than the frequency of the supply voltage [5]. The design equations are given with allowances for all the parameters of the equivalent circuits and of the supply circuit impedances [4], and for the load torque of the servo motor. The static torque is assumed constant in magnitude, corresponding to the operating conditions of the drive mechanisms of regulating devices used in the majority of automatic equipment.

The design equations are expressed in terms of the so-called generalized parameters [4]. When presented in this form, the design equations are suitable for both analysis and calculation.

---

\* The notation used in this article corresponds to that used in [3, 4, and 6].



# 1. Choice of Feedback Parameters for Stable Continuous Regulation

The two-phase servo motor used in a feedback circuit represents a closed system. When analyzing its operation it is necessary to investigate problems in its static [3] and dynamic stability.\* The determination of the criterion for dynamic stability for the most general case and for any speed  $\nu > 0$  is a rather complicated task. The connection between the input signal and the motor speed is given by an equation containing the gain  $K_m$  of the link and the time constant  $T_m$ . The values of  $K_m$  and  $T_m$  are variable, and depend on the speed of the motor and on the value of the input signal. No particular difficulty is involved in the investigation of the dynamic stability at low speeds, for in this case the coefficients  $K_m$  and  $T_m$  are rather easy to determine.

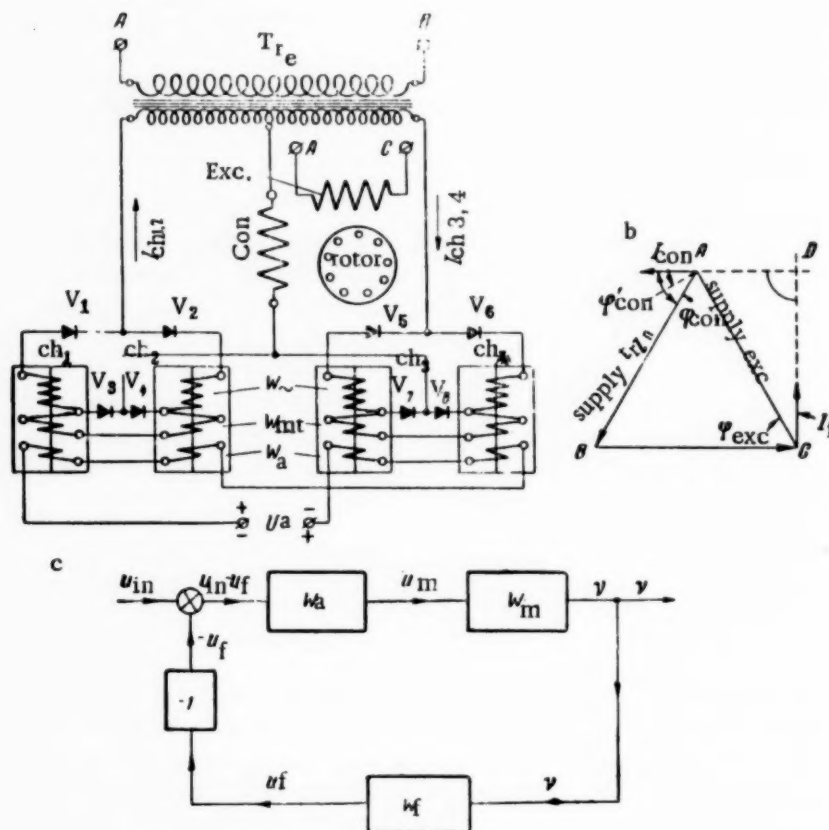


Fig. 1. Regulation of two-phase servo motor with the aid of a magnetic amplifier: a) electric circuit, b) vector diagram explaining the method of connecting the servo-motor windings, c) block diagram of the regulating circuit for a servo motor with velocity feedback.

Analysis of the criteria for dynamic and static stability at low speeds shows that this particular case is of greatest practical interest. In addition, study of this operating condition of the motor makes it possible to choose the feedback parameter with an accuracy that is also adequate for the general case.

Let us determine the stability criterion of a linearized system and let us see under what condition does the linearization of the system in the vicinity of  $\nu = 0$  make it possible to determine the feedback parameters; namely its gain  $K_f$  and time constant  $T_f$ .

The control circuit of a two-phase servo motor with negative velocity feedback consists in most practical cases of three elements: amplifier (magnetic or electronic) with a gain  $K_a$  and a time constant  $T_a$ , a motor, and the feedback loop. In magnetic amplifiers, as is known, it sometimes becomes necessary to determine separately the time constant of the control circuit and the time constant of the a-c circuit. The equations

\*An explanation of the concepts of static and dynamic stability is given below (see inequalities 6 and 8).



obtained in this work can also be used for the case when  $T_f$  is approximately zero.

The transfer function of a linearized system (Fig. 1c) in the vicinity of  $\nu \approx 0$  is

$$W = \frac{W_a W_m}{1 + W_a W_m W_f}, \quad (1)$$

where

$$W_a = \frac{K_a}{pT_a + 1}, \quad W_m = \frac{K_m}{pT_m - 1} \text{ and } W_f = \frac{K_f}{pT_f + 1} \quad (2)$$

are respectively the transfer functions of the amplifier, of the motor at  $d\mu/d\nu > 0$  (linearized [6, 7] unstable link), and of the feedback loop. If regulation is by varying the voltage and phase shift, the coefficients  $K_m$  will be respectively

$$K_m = \frac{\partial \mu}{\partial a_r} / \frac{\partial \mu}{\partial \nu}; \quad (3)$$

$$K_m = \frac{\partial \mu}{\partial \delta_r} / \frac{\partial \mu}{\partial \nu}. \quad (4)$$

The time constant of the motor will be

$$T_m = \frac{GD^2}{375} / \frac{d\mu}{d\nu}. \quad (5)$$

According to the Hurwitz criterion, the conditions for the stability of the servo motor with feedback will be

$$K'_f = K_a K_f > \frac{1}{K_m}; \quad (6)$$

$$T_a + T_f < T_m; \quad (7)$$

$$\left( \frac{1}{T_a} + \frac{1}{T_f} - \frac{1}{T_m} \right) (T_m - T_a - T_f) > K_f K_a K_m - 1. \quad (8)$$

For the sake of simplification, let us consider the system described by a second-order equation, assuming  $T_a = 0$ . The deductions obtained with such an assumption can be extended, as will be shown below, also to the case when  $T_a \neq 0$ . If  $T_a = 0$ , the static stability condition (6) does not change, and the dynamic stability condition assumes the form:

$$T_f < T_m. \quad (9)$$

It follows from inequalities (6) and (9) that the parameters of the feedback loop can be determined by linearizing the system in the vicinity of  $\nu = 0$ , provided the coefficient  $K_m$  and the time constant  $T_m$  are a minimum at speeds close to zero, for in this case the required gain  $K_f$  will have a maximum value and the permissible time constant  $T_f$  will be a minimum. The quantities  $K_m$  and  $T_m$  have minimum values at  $\nu = 0$

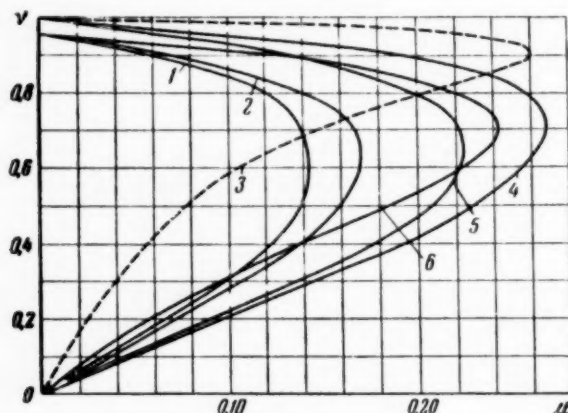


Fig. 2. Calculated mechanical characteristics of a servo motor operating in single phase at  $S_{cc} < 1$ .

if the positive value of the derivative  $\partial\mu/\partial\nu$  is a maximum at this point. It is therefore necessary to investigate the slope of the mechanical characteristics over a range of speeds  $\nu \geq 0$ , so as to show in what cases the calculation of the feedback parameters can be carried out using inequalities (6) and (9).

The mechanical characteristic has a maximum slope in the unstable region at  $\nu = 0$ , if it has no point of inflection at  $\nu > 0$ . Consequently, when designing the feedback loop it is first necessary to determine whether a point of inflection exists in the speed range  $\nu \geq 0$ . An analytical determination of the coordinates of the point of inflection of the mechanical characteristic is impossible for a motor having an asymmetrical impedance in general form, owing to the complexity of the expression for  $\partial^2\mu/\partial\nu^2$ . To solve the problem let us investigate the expression for the derivative [3]

$$\left. \frac{d\mu}{d\nu} \right|_{\nu=0} = \frac{1 - S_{cc}^2 + a_f^2 \frac{S_{cc}^2}{S_{ce}^2} (1 - S_{ce}^2)}{2 [S_{cc}^2 (2b_{cc} + 1) + 1]} \quad (10)$$

and let us calculate the mechanical characteristics of servo motors with different parameters.

As can be seen from Equation (10), if  $S_{cc}$  and  $S_{ce}$  are both less than unity, the value of the derivative

curve	values of quantities			
	$S_{cc}$	$S_{ce}$	$b_c$	$b_e$
1	0.3	2.0	1.0	0.2
2	0.3	1.0	1.0	0.5
3	0.1	0.1	1.0	1.0
4	0.1	1.0	1.0	0.5
5	0.1	2.0	1.0	0.2
6	0.3	0.3	1.0	1.0

Curve 3 torque values on 1:4 scale.

increases with the voltage gain  $a_f$  of the signal. Calculations show that at small values of  $S_{cc}$  and  $S_{ce}$ , the point of inflection may correspond to a speed greater than zero (Fig. 2). If  $S_{cc} < 1$  and  $S_{ce} > 1$ , the derivative  $d\mu/d\nu$  has a maximum at zero signal. The mechanical characteristics of motors operating in single-phase mode are shown in Fig. 2 (the values for the curves are given in the table).

It is seen from Fig. 2 that when a motor with  $S_{ce} > 1$  ( $S_c > 1$ ) is used the mechanical characteristic has no point of inflection at  $\nu > 0$  even at  $S_{cc} = 0.1$ . Consequently, one can assume under actual conditions that if  $S_{cc} < 1$ , the maximum value of  $d\mu/d\nu$  always corresponds to  $\nu = 0$ .

Calculation of the characteristics of a servo motor with a phase-shifting impedance in the excitation winding shows that if  $S_{cc} > 1$  and  $S_{ce} < 1$ , the maximum value of  $d\mu/d\nu$  for loads ranging up to the nominal torque can also be expected in practice at  $\nu = 0$ .

In the case when the impedances of the motor circuits are symmetrical the coordinates of the point of inflection vary slightly with the speed as a function of the regulating parameter (voltage, phase-shift angle). It is therefore enough to determine the coordinates of the points of inflection of the mechanical characteristic of the motor for a symmetrical supply, using the equation

$$(1 - \nu)^3 - 3S_c^2(1 - \nu) - 2bS_c^4 = 0, \quad (11)$$

obtained from the condition  $d^2\mu/d\nu^2 = 0$ . Putting  $\nu = 0$  in Equation (11) we find that the point of inflection of the mechanical characteristic at  $\nu = 0$  will occur if the following equation is satisfied

$$b = \frac{1 - 3S_c^2}{2S_c^4}. \quad (12)$$

It is possible to show that the point of inflection occurs at  $\nu < 0$  if the real value of  $b$  turns out to be greater than the value obtained from Equation (12). It also follows from Equation (12) that if  $S_c > 1/\sqrt{3}$ , the point of inflection of the mechanical characteristic of a motor with symmetrical impedances always occurs at  $\nu < 0$ .

Thus, if we take into consideration the fact that the two-phase induction motor, intended for use in asymmetrical regulation circuits, is usually manufactured with  $S_c > 1$  ( $S_c \approx 2$ ), as dictated by heating conditions and by the desire for obtaining optimum plugging properties in single-phase operation, it is possible to conclude that inequalities (6) and (9) are valid in the majority of cases.

Using inequalities (6) and (9) and taking Equations (3), (4), (5) and the expression for the starting torque of the motor [6] into account, we obtain the following expressions for the parameters of the feedback loop of an asymmetrical motor, regulated by voltage variation [Equation (13)] or regulated by phase-shift variation [Equation (14)]:

$$K'_f = K_c K_f > \frac{1}{2} \frac{S_{ce}}{S_{cc}} \frac{1 - S_{cc}^2 + a_r^2 (1 - S_{ce}^2) \frac{S_{cc}^2}{S_{ce}^2}}{K_{es} K_{cs} \sin(\delta_r \mp \varphi_{ecs})}. \quad (13)$$

$$K'_f = K_c K_f > \frac{1}{2} \frac{S_{ce}}{S_{cc}} \frac{1 - S_{cc}^2 + a_r^2 (1 - S_{ce}^2) \frac{S_{cc}^2}{S_{ce}^2}}{a_r K_{es} K_{cs} \cos(\delta_r \mp \varphi_{ecs})}. \quad (14)$$

$$T_f < \frac{GD^2}{375} \frac{2K_{cs}^2}{1 - S_{cc}^2 + a_r^2 (1 - S_{ce}^2) \frac{S_{cc}^2}{S_{ce}^2}}, \quad (15)$$

where

$$K_{es} = \sqrt{S_{ce}^2(2be + 1) + 1}, \quad (16)$$

$$K_{cs} = \sqrt{S_{ce}^2 (2b_c + 1) + 1}, \quad (17)$$

$$\varphi_{ecs} = \varphi_e - \varphi_{cs} = \tan^{-1} \frac{\sqrt{1 - b^2 S_{ce}^2}}{S_{ce} (1 + b_e)} - \tan^{-1} \frac{\sqrt{1 - b^2 S_{cc}^2}}{S_{cc} (1 + b_c)}. \quad (18)$$

When calculating the velocity feedback parameters of a voltage-regulated servo motor, the signal,  $a_r$ , must be assumed to equal a value at which the starting torque equals the static torque, i.e., [6]

$$a_r = a_{rs} = \frac{\mu_{st}}{\sin(\delta_r + \varphi_{ecs})} \frac{S_{ce} K_{cs}}{S_{cc} K_{es}}. \quad (19)$$

It is possible to show that with such a choice of feedback parameters it is possible to achieve continuous regulation over the entire range of speeds. An exception may be the case with  $S_{cc} < 1$  and  $S_{ce} > 1$ . Here it is necessary to determine the quantities  $K'_f$  and  $T_f$  from the parameters of the mechanical characteristics of the single-phase mode or from the parameters of the starting point ( $\mu_{stat} = \mu_{start}$ ) with subsequent verification of the static stability in the latter case by plotting the mechanical characteristic. When using Equations (13), (14), and (19) it is necessary to observe the following sign convention: the minus sign is used in front of  $\varphi_{ecs}$  if the phase of the control voltage lags the excitation voltage, while plus is used in the case of lead [4].

If the derivative  $d\mu/d\nu$  has a maximum value at  $\nu > 0$ , the value of the feedback gain can be determined in the following manner. The equation for the mechanical characteristic of a drive with feedback  $\mu_f = f(\nu)$  is derived by replacing the signal  $a_r$  in the usual equation of the mechanical characteristic with the quantity  $a_r - K'_f \nu$ . From the static-stability condition  $d\mu_f/d\nu \leq 0$  we obtain the dependence of the coefficient  $K'_f$  on motor parameters, on the signal amplitude, and on the speed  $\nu$ . Thus, for example, in the case of symmetry of the motor supply circuits with respect to impedance, this dependence assumes the following form if voltage regulation is used

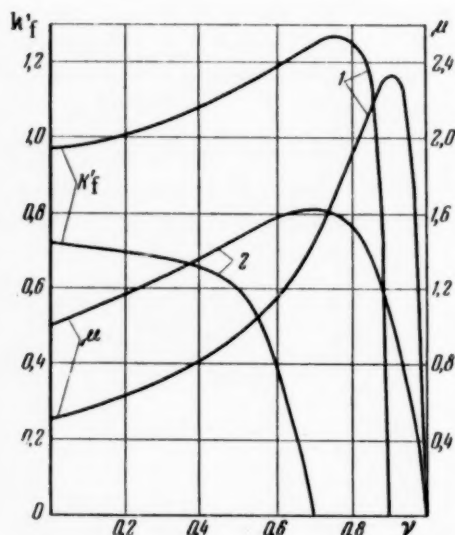


Fig. 3. Values of the function  $K'_f = f(\nu)$  for different mechanical characteristics of the servo motor. Curves 1:  $S_c = 0.1$ ,  $b = 1.0$ ,  $a = 1.0$ . Curves 2:  $S_c = 0.3$ ,  $b = 1.0$ ,  $a = 1.0$  (values of the torque are given for Curve 1 in a 1:2 scale).

$$K'_f = \frac{-B - \sqrt{B^2 - AC}}{A}, \quad (20)$$

where

$$A = \frac{[2\nu(1-\nu) - \nu^2] \{S_c^2 [2b(1-\nu) + 1] + (1-\nu)^2\} + 2\nu^2(1-\nu)[bS_c^2 + (1-\nu)]}{D_1} - \frac{[2\nu(1+\nu) + \nu^2] \{S_c^2 [2b(1+\nu) + 1] + (1+\nu)^2\} - 2\nu^2(1+\nu)[bS_c^2 + (1+\nu)]}{D_2},$$

$$B = (a + \sin \delta) \frac{(2\nu - 1) \{S_c^2 [2b(1-\nu) + 1] + (1-\nu)^2\} - 2\nu(1-\nu)[bS_c^2 + (1+\nu)]}{D_1} - (\sin \delta - a) \frac{(2\nu + 1) \{S_c^2 [2b(1+\nu) + 1] + (1+\nu)^2\} - 2\nu(1+\nu)[bS_c^2 + (1+\nu)]}{D_2},$$

$$C = (1 + a^2 + 2a \sin \delta) \frac{2(1 - \nu) [bS_c^2 + (1 - \nu)] - \{S_c^2 [2b(1 - \nu) + 1] + (1 - \nu)^2\}}{D_1} -$$

$$- (1 + a^2 - 2a \sin \delta) \frac{\{S_c^2 [2b(1 + \nu) + 1] + (1 + \nu)^2\} - 2(1 + \nu) [bS_c^2 + (1 + \nu)^2]}{D_2},$$

$$D_1 = \{S_c^2 [2b(1 - \nu) + 1] + (1 - \nu)^2\}^2$$

and

$$D_2 = \{S_c^2 [2b(1 + \nu) + 1] + (1 + \nu)^2\}^2.$$

It is next necessary to plot the curve  $K'_f = f(\nu)$  for the signal  $a_r = a_{rs}$  (Fig. 3). The gain of the feedback loop must be assumed to be the maximum value of the function  $K'_f = f(\nu)$ , if it corresponds to the speed  $\nu = 0$ ,

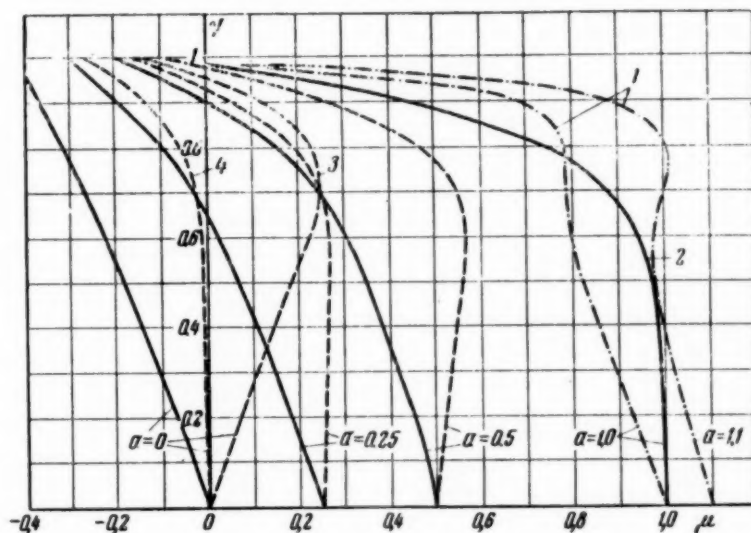


Fig. 4. Calculated mechanical characteristics of a servo motor in a feedback circuit: Curves 1:  $S_c = 0.1$ ,  $b = 1.0$ ,  $K_f = 1.27$  (corresponds to a maximum of the function  $F_f = f(\nu)$  at  $a_{rs} = 1$ ). Curve 2:

$$S_c = 0.3, \quad b = 1.0, \quad K_f = 0.72, \quad \left( \text{at } \frac{d\mu}{d\nu} \Big|_{\substack{a=1 \\ \nu=0}} \right); \quad \text{curve 3: } S_c =$$

$$= 0.3, \quad b = 1.0, \quad K_f = 0, \quad a_{rs} = 0; \quad \text{curve 4: } S_c = 0.3, \quad b = 1.0, \quad K_f =$$

$$= 0.36 \quad \left( \text{at } \frac{d\mu}{d\nu} \Big|_{\substack{a=0 \\ \nu=0}} \right)$$

or somewhat greater than this quantity, if  $K'_f = f(\nu)$  has a maximum value at  $\nu > 0$ . It is necessary to increase the value of the gain in the latter case because zones of discontinuous regulation (Fig. 4, Curves 1) may appear if the feedback gain is chosen to be equal to the maximum value of the function. In practice, however, the determination (estimate) of the feedback gain must be made using Equations (13) and (14), for calculations show that even if  $S_c = 0.1$ , the maximum value of the function  $K'_f = f(\nu)$  exceeds the value of the coefficient  $K'_f$  at the starting point by merely 30% (Fig. 3).



To estimate the value of the time constant  $T_f$  from inequality (9) in the case when the derivative  $d\mu/d\nu$  has a maximum value at  $\nu > 0$ , it is necessary to determine the time constant of the motor from the value of the derivative  $d\mu/d\nu$ , corresponding to the point of inflection.

The parameters of the feedback circuits are easy to determine by using experimental mechanical servo motor characteristics obtained for a circuit without feedback. For this purpose it is necessary to know the value of the stiffness of the mechanical characteristics without feedback  $\beta = \Delta\mu/\Delta\nu$  and  $K_\mu = \Delta\mu/\Delta a_r$  (or  $K_\mu = \Delta\mu/\Delta\delta_r$ ) and to determine the unknown parameters from Equations (6) and (9).

Thus, an analysis of a second-order system shows that the quantities  $K'_f$  and  $T_f$  should be calculated from the parameters of the starting-point of the mechanical characteristic. Comparing Equations (7) and (9), examining inequality (8) for  $|d\mu/d\nu| \nu \leq \nu_{cr} \geq 0^*$ , and examining an analogous condition for  $|d\mu/d\nu| \nu \geq \nu_{cr} \leq 0$ , it is possible to show that this deduction can be extended to include also the case when  $T_a \neq 0$ . Here the feedback parameters must first be determined from Expressions (6) and (7), followed by a check of Equation (8).

When choosing the supply circuit for the induction motor it is necessary to bear in mind that at low static torques a motor operating in a velocity feedback loop may operate with a negative net signal on the control winding, and consequently, the supply circuit should be reversible at  $\mu_{st} < \mu_{co}$  ( $\mu_{co}$  is the critical torque in single-phase operating mode). This can be deduced from an analysis of the calculated mechanical characteristics of a motor operating in a feedback loop, given in Fig. 4. At low signals the mechanical characteristics intersect the Curve 3. Thus, starting with a speed corresponding to the point of intersection of these curves, the signal  $(a_r - K'_f \rho)$  is negative.

## 2. Determination of the Value of the Feedback Coefficient for a Specified Stiffness or for a Specified Motor Gain

In practical cases it is frequently necessary to solve also the problem of determining the feedback coefficient so as to obtain a specified stiffness of mechanical characteristic  $\beta'$  or a gain coefficient  $K'_m$  at low speeds, or, conversely, it is necessary to estimate the value of  $K'_f$  at low speeds from the experimental mechanical and regulation characteristics of the motor operating in the feedback loop. The relationships between the feedback coefficient and the stiffness of the mechanical characteristic  $\beta'$  of a drive with feedback, which must be known to solve these problems, can be determined from the expression

$$K'_m = \frac{K_m}{K_m K'_f - 1} = \frac{K_\mu / \beta}{K'_f K_\mu / \beta - 1} = \frac{K_\mu}{\beta'}, \quad (21)$$

whence

$$K'_f = \frac{\beta + \beta'}{K_\mu} = \frac{1}{K_m} + \frac{1}{K'_m}.$$

## 3. Experimental Verification of Conclusions

Tests made on a regulator for a two-phase 50 watt induction motor using a magnetic amplifier (Fig. 1) confirms qualitatively the theoretical premises concerning the regulating properties of a motor used in a feedback circuit. Experiments have shown that such a system contains natural negative velocity feedback. The voltage induced in the control winding of the motor causes the same change in the parameters of the system as does a signal from a tachometer generator applied to the input of the amplifier. The effect of the control-winding voltage on the parameters of the amplifier is based on the sensitivity of a magnetic amplifier with heavy current feedback to changes in supply voltage. The voltage from the control winding reduces the supply

\*  $\nu_{cr}$  is the speed corresponding to the critical torque  $\mu_{cr} = \mu_{st}$ .



voltage of one arm of the amplifier (which becomes magnetized) and increases the voltage of the second arm. This change in the supply voltage causes the impedances of the arms of the magnetic amplifier to change at

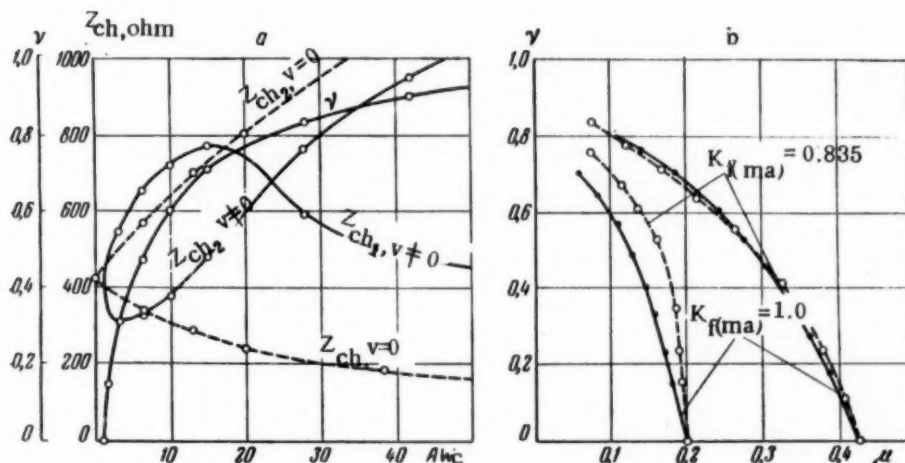


Fig. 5. Regulation and mechanical characteristics of a servo motor in a circuit with magnetic amplifier (Fig. 1): a) regulation characteristic at  $S_{cc} < 1$ ,  $S_{ce} > 1$ ,  $\mu_{st} = \Delta \mu_{no, load}$ ; b) mechanical characteristics of servo motor at various feedback coefficients of the amplifier.

low signals in such a manner as to produce at the output of the amplifier a voltage of a polarity opposed to the starting voltage (Fig. 5a; see the sign of the difference between the impedances of the amplifier arms for a stationary and for a moving servo motor).

The voltage produces a maximum action as velocity feedback, as expected, in the case when the phase angle between the motor winding voltages is  $90^\circ$  (Fig. 6). Such an angle can be obtained if a three-phase line is available (Fig. 1b). The same phenomenon is observed in differential and bridge magnetic-amplifier circuits with external current feedback.

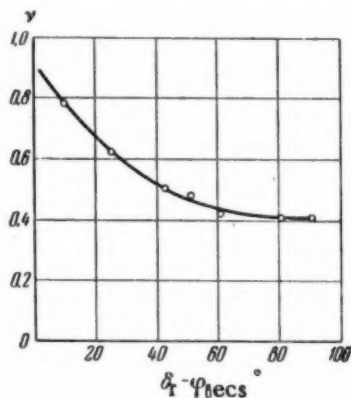


Fig. 6. Dependence of the speed of the servo motor in a circuit with magnetic amplifier (Fig. 1) on the angle  $\delta_T - \varphi_{ecs}$ :  $S_{ce} = 2.09$ ,  $b_c = b_e = 0.148$ ,  $S_{cc} < 1$ ,  $a_T = 0$ .

Experiments have shown that the motor can be continuously regulated at no load without introducing special velocity feedback even if  $S_{cc} = 0.32$  ( $S_{ce} = 2.09$ ,  $b_c \approx b_e = 0.148$ ). In this case the calculated value of the coefficient  $K'_f = K_a K_f$ , required to insure continuous regulation, is approximately unity. If the amplifier has different parameters and if a suitable bias is chosen, it is possible to obtain continuous regulation of the machine apparently also at smaller values of  $S_{cc}$ . Experiments have shown (Fig. 7) that the plugging times of the servo motor ( $S_{ce} = 2.09$ ,  $b = 0.148$ ) are approximately the same upon short circuiting the control winding of the motor as when removing the signal from the input of the amplifier ( $S_{cc} < 1$ ). Consequently, the internal negative velocity feedback is sufficiently effective.

Figure 5, b shows experimental mechanical characteristics of the motor at different amplifier current feedback coefficients, confirming the effect of the magnitude of this coefficient on the degree of velocity-feedback action of the voltage. Equation (22) was used to determine the coefficients  $K'_f$  for these characteristics at low speeds; the resultant values were 0.6 and 0.5 at amplifier current feedback coefficients of

1.0 and 0.835 respectively. The generalized parameters of the motor circuits at the starting point in the case of  $\mu_s = 0.2$  are:  $S_{ce} = 2.09$ ,  $S_{cc} = 0.5$ ,  $b_e = 0.148$  and  $b_c \approx b_e$ ; in the case when  $\mu_s = 0.45$ , the parameters are  $S_{ce} = 2.09$ ,  $S_{cc} = 0.56$ ,  $b_e = 0.148$ , and  $b_c \approx b_e$ .

When a capacitor is connected in parallel with the servo-motor control winding to obtain a phase shift of  $90^\circ$  between the currents in the motor windings, the reaction of the above circuit on the voltage of the control winding of the motor is opposite, analogous to the action of positive feedback. Therefore when the signal is removed from the input of the amplifier, the motor does not plug even at  $S_{cc} > 1$  (Fig. 8). Connecting the capacitor increases also the heating of the motor.

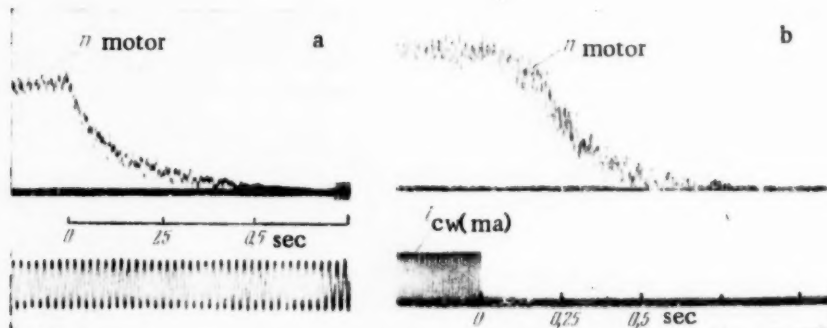


Fig. 7. Process of plugging a servo motor in single-phase operation: a) short circuiting the control winding of the motor, b) removing the signal at the input of the magnetic amplifier.

The information given here on the effect of the control-winding voltage on the operation of its supply circuit should be taken into account when choosing the amplifier circuit, when choosing the method for producing the phase shift between the motor winding voltages, and when choosing the parameters of the feedback loop.

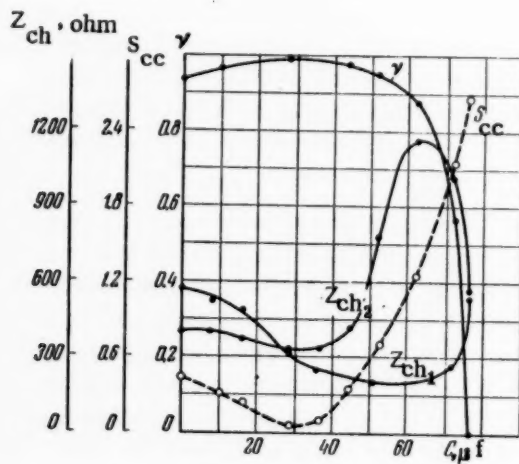


Fig. 8. Dependence of the speed of the servo motor in single-phase operation ( $a_r = 0$ ) on the size of the capacitor connected in parallel with the control winding (circuit of Fig. 1):  $S_{ce} = 2.09$ ,  $b_e = 0.148$ ,  $aw_a = 0$  ( $aw_a$  - control ampere turns of the magnetic amplifier).

## CONCLUSIONS

1. The negative velocity feedback parameters for a two-phase servo motor can be selected by linearizing the mechanical characteristics of the servo motor at low speeds.
2. The values of the gain  $K'_f$  and of the maximum permissible time constant  $T_f$  of the feedback loop, required to obtain stable continuous regulation of a two-phase servo motor, are determined in an overwhelming majority of practical cases by the parameters at the starting point of the mechanical characteristics for a specified static torque.
3. When regulating a two-phase servo motor with a circuit containing a full-wave magnetic amplifier, the natural velocity feedback can insure no-load stable operation of the servo motor at  $S_{cc} < 1$ .

Received May 12, 1955

## SUMMARY

The paper deals with the conditions of stable operation of a two-phase servomotor possessing any parameters of machine and supply system with negative speed feedback for general case of asymmetry.

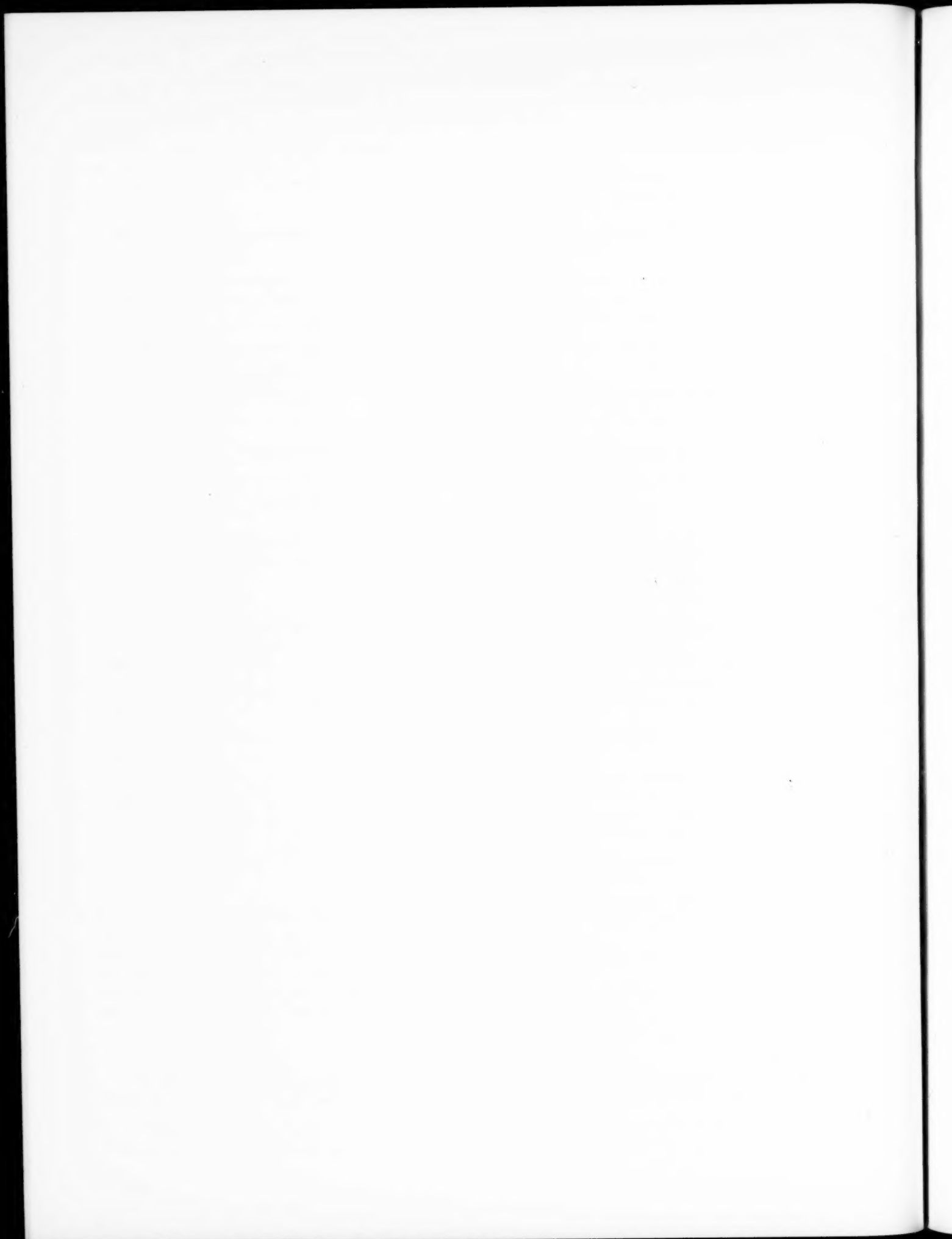
Criteria for stable operation of the servomotor are stated. The author recommends to define parameters of the negative feedback through parameters of mechanical characteristics at the starting point.

The expressions for the calculation are given in terms of generalized parameters.

Theoretical results are confirmed by experiments:

#### LITERATURE CITED

- [1] G. M. Kasprzhak, "Low Power Adjustable Induction Motor" *Electric Circuits*, No. 2, (1949).
- [2] E. K. Krug, "A. C. Actuating Mechanism" *Collection of Articles on Automation and Remote Control*, Institute of Automation and Remote Control, Acad. Sci. USSR (1953).
- [3] E. I. Slepushkin, "Criteria for Stable Operation of Two-Phase Induction Servomotor" *Automation and Remote Control*, Vol. XVII, No. 11 (1956).
- [4] G. M. Kasprzhak and E. I. Slepushkin, "Description and Determination of Initial Parameters and Quantities for the Calculation of the Characteristics of Two-Phase Minature Motors" *Automation and Remote Control*, Vol. XVII, No. 7 (1956).
- [5] I. M. Sadovskii, "Induction Servomotor as Element of Regulation Circuits" *Automation and Remote Control*, Vol. XII, No. 6 (1952).
- [6] G. M. Kasprzhak and E. I. Slepushkin, "Calculation of Operating Characteristics of Two-Phase Servomotors and Tachometer Generators" *Automation and Remote Control*, Vol. XVII, No. 7 (1956).
- [7] A. A. Voronov, *Elements of the Theory of Automatic Regulation*, Voenizdat (1954).



# REDUCING THE LAG OF MAGNETIC AMPLIFIERS BY INTRODUCING DERIVATIVE FEEDBACK

O. I. Aven

(Moscow)

Examination of methods for reducing the lag of magnetic amplifiers by introducing derivative feedback, and a proposed simplified method for determining its parameters. The effect of tuned accelerating networks on the gain of the magnetic amplifier is estimated. The experimental results are given.

In a magnetic amplifier, a new steady-state inductance of the a-c winding is attained after the d-c component of the magnetic induction stops changing. Consequently, whenever the input voltage experiences an abrupt change, the output current reaches a new steady-state value after a certain time lag, which is called the lag of the magnetic amplifier. In this article, this lag will be characterized by the transient time  $t_t$ .

The parameters of magnetic amplifiers should be such as to insure the fastest possible change in the d-c component of the magnetic flux, i.e., should insure a minimum possible value of  $t_t$ . The known methods for reducing the lag (introducing proportional feedback, use of multi-stage amplifiers, etc.) do not always produce the desired results. In addition, it is frequently necessary in practice to use a magnetic amplifier with excessive time delay simply because one is on hand. In this case the amplifier lag can be reduced by including tuned accelerating networks at the input of the magnetic amplifiers or else by introducing positive derivative feedback in the amplifier. Figures 1 and 2 show magnetic amplifiers with derivative feedback, produced by an RC network and an additional winding  $W_a$  wound in the same manner as a proportional feedback winding.

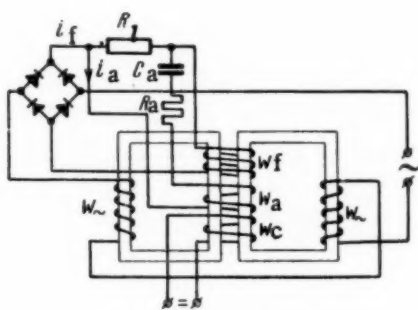


Fig. 1

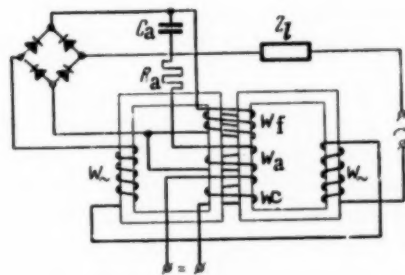


Fig. 2

Figure 3 shows a circuit where the derivative feedback is produced with the aid of a differentiating transformer.

Let us explain the action of the derivative feedback in a magnetic amplifier. In the steady state, the voltage drop across the load  $R_L$  (Fig. 1) is constant and no current flows in the derivative feedback winding. Whenever the signal changes, the value of the voltage drop across the load starts to change, the capacitor  $C_a$  starts

recharging and a current  $i_a$  begins to flow in winding  $W_a$ . This current produces an mmf in the same direction as the control mmf, and the d-c component of the flux will change faster. It is evident that the mmf of the derivative feedback can also act in opposition to the control mmf. In this case the derivative feedback will have a retarding action [1]. After the end of the transient the voltage across capacitor  $C_a$  again becomes constant and the velocity feedback (current  $i_a$ ) disappears.

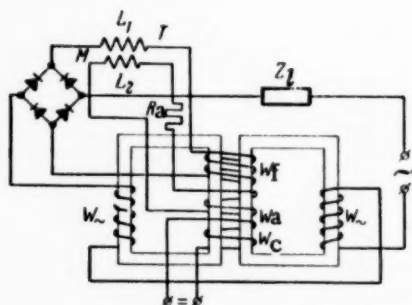


Fig. 3

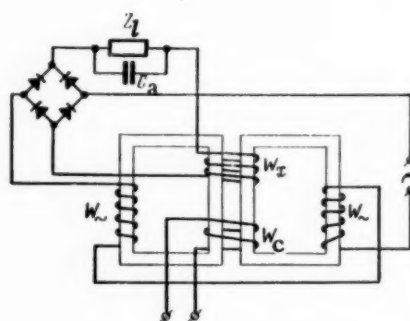


Fig. 4

In the circuit of Fig. 2, the input to the derivative feedback network is connected directly to the output of the rectifier.

In the circuit of Fig. 3, the primary winding of the derivative feedback transformer is connected in series with a proportional feedback network. The secondary winding of the transformer is connected across winding  $W_a$ . Whenever the load current changes, a current  $i_a$  appears in winding  $W_a$ , reducing the lag of the amplifier. The circuits in Figs. 1-3 have that shortcoming, that a special winding is needed to produce derivative feedback. If derivative feedback is to be produced in an already-built magnetic amplifier, it is not always possible to use a supplementary winding. To introduce derivative feedback it is possible to employ the control winding.

In the diagram of Fig. 4 the derivative feedback is produced by shunting the load with a capacitance.

The derivative feedback circuit is chosen in accordance with the type of magnetic amplifier, its power, operating conditions, and the points to which the load is connected (d-c or a-c).

The parameters of an accelerating network are chosen to make the d-c component of the flux rise as fast as possible. The core material and the amplifier-circuit parameters (without the accelerating network) are usually specified; the parameters of the accelerating network ( $C_a$ ,  $W_a$ ,  $R_a$ ) must be chosen. The freedom of choice of parameters of winding  $W_a$  is usually limited. When derivative feedback is added to an already-built magnetic amplifier, the winding  $W_a$  must be some available unused winding.

When a new amplifier is being constructed, the winding space is filled with other windings and as a rule it is possible to wind only a small number of additional turns for the winding  $W_a$ . Thus, the condition of maximum amplifier speed must be sought by properly choosing the values of  $C_a$  and  $R_a$ . The values of  $C_a$  and  $R_a$  are either chosen experimentally, or else are found by solving the differential equation that defines the variation of the d-c component of the magnetic flux  $\Phi_0$  with time after a change in the amplifier-input signal [2]. The transient behavior of the flux  $\Phi_0$  depends on many parameters, which in themselves do not remain constant during the transient. It is quite difficult to derive and solve the equations of the magnetic amplifier with allowance for all these factors. If the flux is assumed to be linearly dependent on the control ampere turns,  $\Phi_0 = \gamma AW_0$  [3], and if the losses in the steel are neglected, etc., the equation of the amplifier reduces to a linear differential equation of the second order. By way of an example, let us determine the parameters of derivative feedback circuit for the amplifier shown in Fig. 1. For this circuit, the following system of equations holds:

$$i_l R_l = i_a R_a + \frac{1}{C} \int i_a dt + W_a a \frac{d\Phi_0}{dt}, \quad (1)$$



$$U_f = i_{fc} R_{fc} + i_l R_l + W_f \frac{d\Phi_0}{dt}, \quad (2)$$

$$U_c = i_c R_c + W_c \frac{d\Phi_0}{dt}, \quad (3)$$

$$i_f = i_l + i_a, \quad (4)$$

$$AW_0 = i_c W_c + i_a W_a + i_f W_f, \quad (5)$$

$$\Phi_0 = \gamma AW_0. \quad (6)$$

Here  $i_l$ ,  $i_f$ , and  $i_a$  are respectively the currents flowing in the load, in the proportional feedback winding  $W_f$  and in the additional derivative feedback winding  $W_a$ , while  $U_f$  and  $U_c$  are the feedback and control voltages.

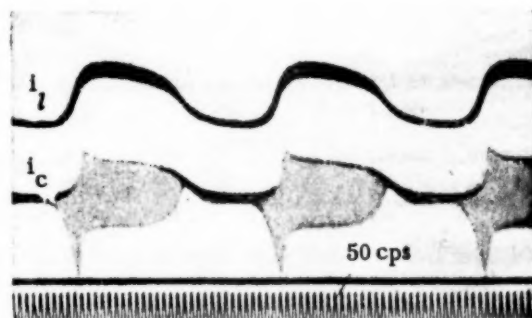


Fig. 5

Instead of using Equation (2) it is possible to make additional assumptions (absence of lag in the a-c circuit, absence of time intervals in which the rectifying bridge is short-circuited) it is possible to employ the ampere-turns balance law

$$i_{av} = i_f = i_l + \frac{AW_0}{W_{\sim}}, \quad (7)$$

where  $i_{nl}$  is the no-load current.

From Equations (1) and (3)–(7) we obtain an equation for  $\Phi_0$ :

$$\left[ \frac{W_c^2 (R_a + R_l)}{R_y} + W_a^2 \right] \frac{d^2 \Phi_0}{dt^2} + \left[ \frac{(W_{\sim} - W_f)(R_a + R_l)}{W_{\sim} \gamma} + \frac{W_c^2}{R_c C_a} - \frac{R_l W_a}{\gamma W_{\sim}} \right] \frac{d\Phi_0}{dt} + \frac{W_{\sim} - W_f}{\gamma W_{\sim} C_a} \Phi_0 = \frac{U_c W_c}{R_c C_a} + \frac{i_{nl} W_f}{C_a}. \quad (8)$$

Subject to the assumptions made, Equation (8) determines the variation of the d-c component of flux  $\Phi_0$  with time, after the control voltage  $U_c$  is connected to the input of the magnetic amplifier.

The capacitance  $C_a$  (for a chosen value of  $R_a$ ) is determined from the condition that a critical aperiodic transient to be obtained for the d-c component of the magnetic flux, i.e., from the condition that the roots of the characteristic equation be equal. We obtain the following equation for the capacitance:

$$C_a = \frac{\gamma W_{\sim} \times 10^{-8} (W_c^2 \beta_1 \beta_2 + R_l W_a W_c^2 + 2 W_c^2 R_c \beta_2)}{R_c (\beta_1 \beta_2 - R_a W_l)^2} -$$

$$- \frac{2 \gamma W_{\sim} \times 10^{-8}}{R_c (\beta_1 \beta_2 - R_l W_a)} V \frac{W_c^2 W_a^2 R_c \beta_2 (\beta_1 \beta_2 + W_c R_l) + W_c^4 \beta_1 \beta_2 R_l W_a + W_a^4 R_l^2 \beta_2^2}{\dots}$$

Here  $\beta_1 = R_a + R_l$ ,  $\beta_2 = W_{\sim} - W_l$ . As can be seen from the example, the value  $C_a$  depends on the winding data, on the operating conditions, and on the core material used in the magnetic amplifier. An experimental check shows that Equations (9) and (8) can be used for a qualitative investigation of the transient in magnetic

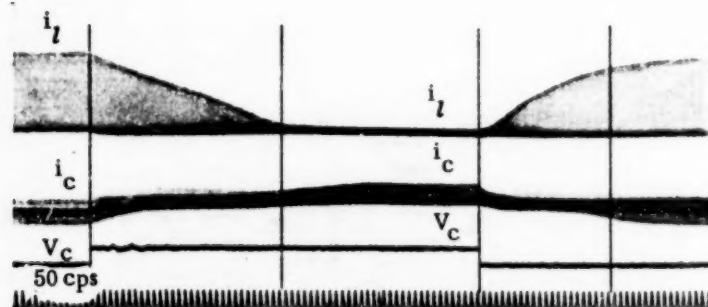


Fig. 6

amplifiers. The coefficient  $\gamma$  can be determined either experimentally, or by calculations [3]. Equation (9) can also be used for an approximate determination of the capacitance  $C_a$ . Analysis of the equations for the transients show that the most favorable conditions for accelerating the change in the d-c component of the magnetic flux in the amplifier cores can be obtained not in an aperiodic transient, but in an oscillatory one. In practice we are interested in those parameters of the accelerating network, which insure the necessary settling time of the transient, without permitting the current to deviate too widely during the oscillations.

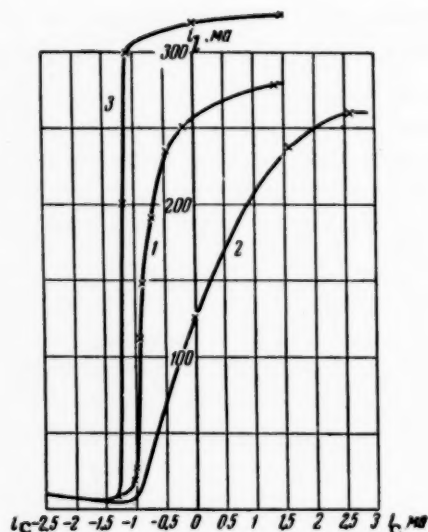


Fig. 7

In practice it is not always possible to assume a linear connection between the flux and the ampere turns, and consequently, the magnetic amplifier cannot always be assumed to be a linear element. Figure 5 shows an oscillogram of self-oscillations occurring in the magnetic amplifier at a certain value of capacitance.

Experiments have shown that sometimes it is possible to employ the self-oscillations in the amplifier to select experimentally the value of the capacitance  $C_a$ . For this purpose it is necessary to connect to the circuit a capacitance of such a size to produce self-oscillations in the circuit. The capacitance is then reduced until the self-oscillations cease. Equation (9) makes it possible to determine the order of magnitude of the capacitance necessary for the circuit to operate properly. As shown experimentally, connecting the accelerating circuit as shown in Fig. 1 gives best results. Figure 1 shows the diagram

of a magnetic amplifier with external proportional feedback. In the case of a magnetic amplifier with internal feedback, the derivative feedback network is also connected in parallel with the load (d-c load).

We give below the results of an investigation of an amplifier with internal proportional feedback. For this purpose we used a commercial model power amplifier UM-3, designed for a supply frequency of 400-500 cycles and intended to amplify d-c signals or slowly-varying a-c signals, as well as an amplifier with a core

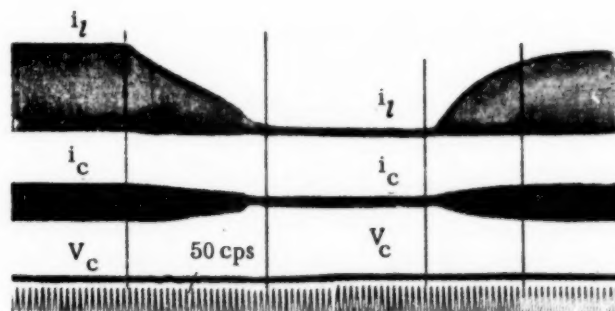


Fig. 8

made of transformer steel for  $f = 50$  cycles. The bias winding, having 50 turns, was used as the derivative feedback winding. Figure 6 shows an oscillogram of the transient process, plotted in the absence of an accelerating network (Amplifier UM-3). In Figure 7, this case is illustrated by Curve 1. Figures 8-10 show oscillograms of

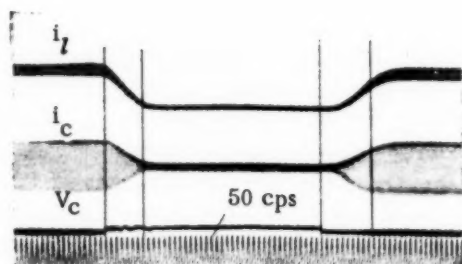


Fig. 9

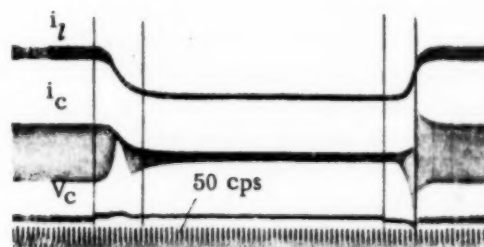


Fig. 10

the transient for the amplifier to which derivative feedback is added. The oscillograms differ in the size of the capacitor. The value of  $C_a$  for Figs. 8, 9, and 10 was 40, 370, and 1400 microfarads respectively.

When considering problems in lag and in the addition of accelerating networks to amplifiers, particular attention must be paid to the gain of the amplifier. It was shown in [4] that the even harmonics of the magnetic field intensity reinforce the magnetizing action of the d-c component of the magnetic field. The easier passage of even harmonics resulting from shunting the load with the derivative feedback network leads to an increase in the gain. Figure 11 shows the characteristic  $i_L = f(i_C)$ , plotted for the 50 cycle amplifier. The number 1 designates the characteristic of the amplifier without derivative feedback, and 2 the characteristic in the presence of a derivative feedback with a resistance of 306 ohms (load resistance 200 ohms), while 3 corresponds to a derivative feedback network resistance of 6 ohms. As can be seen from Fig. 6, the largest even-harmonic currents flow in the load circuit of the amplifier without derivative feedback. In the presence of derivative feedback, there are hardly any even-harmonics in the loads, but their magnitude increases in the control winding (Fig. 9).

The use of derivative feedback increases the gain of a magnetic amplifier and decreases its lag. If an increase in the gain is not required, it is possible to reduce the lag by a factor of several times by reducing the proportional feedback coefficient retaining the same power gain. The characteristics shown in Fig. 7 were obtained for the UM-3 amplifier. Curve 1 was obtained in the absence of derivative feedback and for a maximum proportional feedback coefficient. Curve 3 shows the effect of adding derivative feedback to the amplifier (the proportional feedback is the same as for Curve 1). The proportional feedback coefficient was then

reduced to such a value as to keep the total gain constant. Curve 2 (Fig. 7) was obtained at a reduced proportional feedback coefficient with a derivative feedback network added. When the derivative feedback network is added, Curve 2 becomes the same as Curve 1. Experimental and theoretical investigations show that increasing the resistance in the derivative feedback network affects both the speed and the power gain adversely.

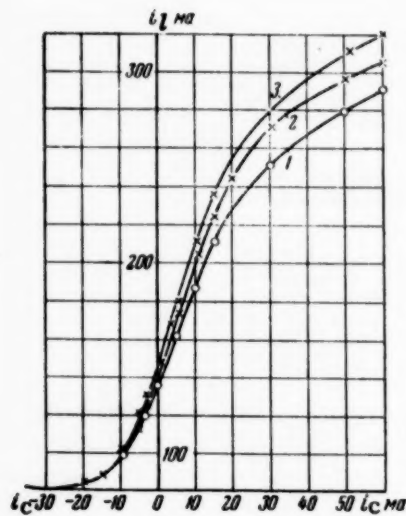


Fig. 11

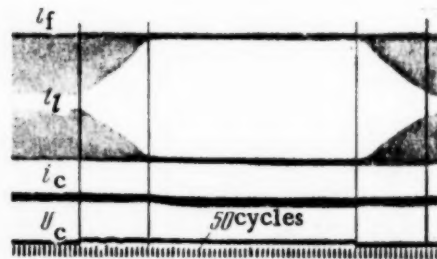


Fig. 12

also shows the change in the distribution of the even-harmonics as a function of the resistance  $R_a$ . Increasing the capacitance  $C_a$  (the other parameters of the amplifier circuit remaining constant) first increases the speed, and then causes a certain drawing out of the transient (Figs. 9 and 10). Attention must also be paid to the change in the slope of the rise and fall of the load current curve. The oscillograms of Figs. 9 and 10, for which the capacitance  $C_a$  is 370 and 1400 microfarads respectively, show that increasing  $C_a$  leads to a greater maximum slope of the current rise, but the total transient time increases because of the slower rise of the curve at the start of the process. It is evident that the problem of increasing the capacitance must be solved with allowances for practical requirements.

The curves given above were plotted for a purely-active load. The conclusions drawn can be extended to inductive loads. Figure 13 shows an oscillogram for an inductive load with a proportional feedback coefficient  $K_f = 1$  without derivative feedback, and Figure 14 shows one with the derivative feedback added.

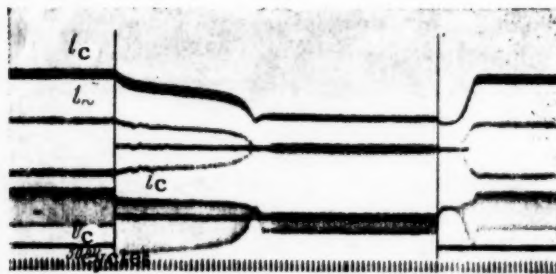


Fig. 13

Comparison of various derivative feedback networks has shown that best results are obtained with the circuit of Fig. 1. In the case of a d-c load it is always necessary to employ the circuit of Fig. 1. It must be noted that for the number of turns of winding  $W_a$  used it is necessary to employ considerable capacitors  $C_a$ . Figure 15 shows the character of the function  $C_a = f(W_a)$ . Figure 16 shows a theoretical curve for the dependence of the

transient time  $t_t = f(W_a)$  for  $C_a = \text{const}$ . It is clear from the curve that it is desirable to increase the number of turns of the winding  $W_a$ . This, however, is not always possible. In some cases it is possible to use for the derivative feedback winding some of the winding space intended for the control or proportional feedback windings, taking into account the increasing gain caused by introducing the latter into the magnetic amplifier.

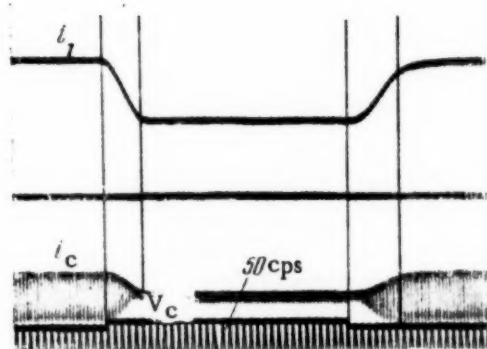


Fig. 14

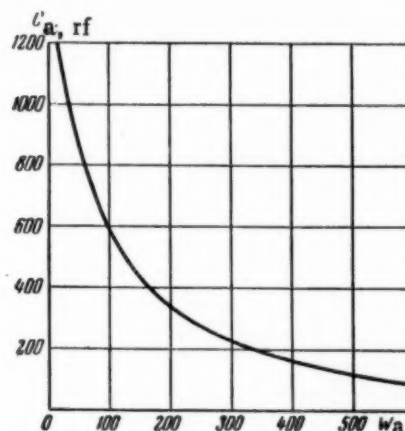


Fig. 15

The use of the circuit of Fig. 2 has many limitations. The circuit of Fig. 2 gives satisfactory results if  $W_a > W_f$ . If  $W_a < W_f$ , such a circuit leads in many cases not to an acceleration, but to retardation of the transient.

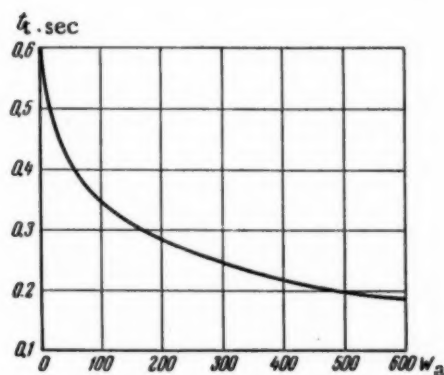


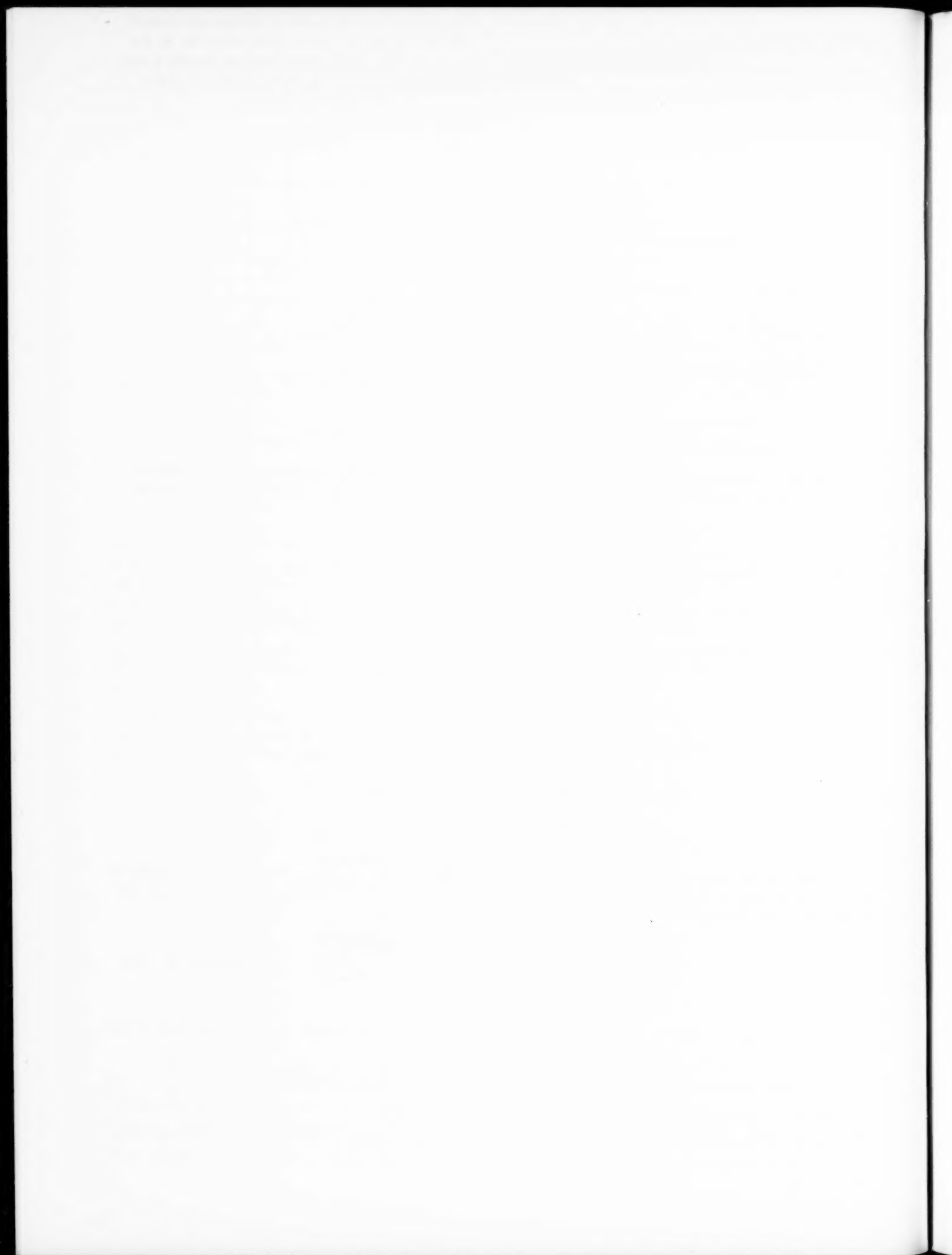
Fig. 16

Connecting the output of the derivative feedback to the input of the amplifier also gives poorer results, for the control winding is shunted by the transducer of the control signal, and in addition, it is not always permissible to have the current  $i_a$  flow through the transducer.

Received July 25, 1956

#### LITERATURE CITED

- [1] I. S. Mikadze and I. B. Negnevitskii, "Contactless Magnetic Time Relay" Trudy (Transaction) of Moscow Power Inst. In name of V. M. Molotov, No. XIV (1953).
- [2] L. A. Bessonov, Transients in Electric Circuits with Steel, Gosenergoizdat (1951).
- [3] M. A. Rozenblat, Magnetic Amplifiers, Gosenergoizdat (1949).
- [4] M. A. Rozenblat, "Effect of Even Harmonics on the Characteristics of Ferromagnetic Materials Subject to Simultaneous Magnetization with Alternating and Constant Magnetic Fields" J. Tech. Physics (USSR), XVIII, No. 6 (1948).





## NEWS

### SESSION OF THE ACADEMY OF SCIENCES OF THE USSR ON AUTOMATIZATION

A session of the Academy of Sciences of the USSR was held from October 15-20, 1956 at the Moscow State University and was devoted to problems of automation.

Participating in this session were approximately 2,000 scientists and engineering-technical workers of industry. The session summarized the accomplishments in the development of automation in the USSR and marked the future scientific trends in its development.

The problems of the technical sciences in the development of machines and the technological processes in connection with automatization were outlined in a joint article by Academician A. A. Vlagonravov, Academician I. I. Artobolevskii, Academician V. I. Dikushin and Academician V. S. Kulebakin; the problems of the technical sciences in the development of automatic control and technical means of automation were touched upon in a paper by Associate Member of the USSR Academy of Sciences, V. A. Trapenznikov.

The level of development of modern technology is characterized to a considerable extent by the development of computing machinery and its application to automatic control of production and for other specialized purposes. A large group of scientific problems, connected with the development and application of mathematical machines, was treated in a series of papers.

- 1) "Mathematical Problems of Machine Computation" by Academician M. V. Keldysh, Doctor of Physical-Mathematical Sciences A. A. Liapunov, and Doctor of Physical-Mathematical Sciences M. R. Shura-Bura;
- 2) "Electronic Computers" by Academician A. L. Lebedev;
- 3) "Prospect for Application of Controlling Machines in Automatization" by Associate Member of the USSR Academy of Sciences I. S. Bruk;
- 4) "Automatization of Translation from one Language Into Another" by Doctor of Technical Sciences D. Iu. Panov, Doctor of Physical-Mathematical Sciences A. A. Liapunov, and Candidate of Physical-Mathematical Sciences M. R. Muzin.

Partly belonging to this series of papers is also the paper by Academician A. N. Kolmogorov "Theory of Transmission of Information and Limits of Applicability." However, the contents of this paper is devoted to a considerable extent to the theoretical foundation of new scientific trends, which have recently been noted in automation, remote control, communication theory, etc.

The problems of economic sciences in the field of automatization of manufacturing processes were detailed in a paper by Academician S. G. Strumilin and Doctor of Economic Sciences G. D. Bakulev.

The sessions of the USSR Academy of Sciences were grouped into six sections, which concentrated their attention to the individual basic divisions of modern automation.

#### SECTION NO. 1. "FUNDAMENTAL PROBLEMS OF AUTOMATIC REGULATION AND CONTROL"

The work of the first section was devoted to problems of automatic regulation and control. The section paid attention to new principles of construction of automatic apparatus and to new scientific trends along with the development of paths already embarked on in the theory of automatic regulation.

The meetings of the section began on October 16 with a paper by Associate Member of the USSR Academy of Sciences V. N. Petrov "Fundamental Trends in the Development of the Theory of Automatic Regulation and Control." The lecturer noted that in recent time the theory of automatic regulation became enriched by many effective methods of design and construction of automatic regulation and control systems, that the accomplishments of Soviet scientists in this field are on a par with the accomplishments of foreign science and even surpass the latter in individual topics. However, thus far the accomplishments of the theory are being slowly adopted in the practice of engineering calculations and little attention is being paid to the development of new principles of construction of automatic regulation and control systems. Among the most important trends in the development of the theory of automatic regulation are the development of a theory of self-adaptive systems and of systems of extremal regulation, the development of the theory of optimum processes and of the theory of combined systems, and the application of computational techniques.

The problems of the development of one of the most important regions of the theory of regulation, namely the theory of stability of nonlinear systems of automatic regulation, were treated in a paper by Professor A. M. Letov and Professor A. I. Lur'e.

Doctor of Technical Sciences M. A. Aizerman lectured on the topic: "Problems Arising in Connection with the Theory of Self-Excited Oscillations in Systems of Automatic Regulation." The problem of calculating the self-oscillations, as noted by the lecturer, acquires particular significance in connection with the fact that recently it has been possible to employ self-oscillations in many cases to improve the regulation process.

A paper on the status and on the tasks in the study of the dynamics of nonlinear systems with the aid of phase space and on questions in dynamic accuracy was delivered by Candidates of Technical Sciences V. V. Petrov and G. N. Ulanov.

Problems in the theory of optimum automatic regulation systems, self-adaptive systems, systems of extremal regulation and also examples of their construction were given in the papers by Associate Member of the USSR Academy of Sciences L. S. Pontriagin, Professor Solodovnikov, and Doctor of Technical Sciences A. G. Ivakhnenko.

L. S. Pontriagin considered certain mathematical problems arising in connection with the theory of optimal automatic regulation processes.

V. V. Solodovnikov devoted his paper to the principles of construction and to problems in the theory of self-adaptive automatic-control systems. The paper gave rise to a discussion concerning the theory of self-adaptive systems, and also concerning the terminology used; the discussion raised also many objections. Participating in the discussion were Professor V. S. Pugachev, Doctor of Technical Sciences A. A. Fel'dbaum, Engineer A. M. Batkov and Professor V. V. Solodovnikov.

A paper by A. G. Ivakhnenko "Automatic Regulation Systems with Elements of Logical Action", considered several examples of extremal-regulation systems. The status and problems in the development of the theory of intermittent automatic regulation systems were the subject of a paper by Ya. Z. Tsytkin. Three basic types of intermittent automatic systems were considered in this paper: relay, pulse and digital.

The basic trends in the development of the theory of random processes as applied to problems of automatic regulation are illustrated in a paper by Professor V. S. Pugachev "Status and Problems in the Development of the Theory of Random Functions and Probability Methods of the Theory of Automatic Control."

Problems in information theory in systems of automatic-regulation, remote control, and telemetering were the subject of a paper by Professor A. A. Kharkevich.

The section participants heard also a paper by Professor M. A. Gavrilov on "Status and Problems in the Development of the Structural Theory of the Construction of Intermittent Automatic and Telemechanical Discrete-Action Apparatus."

Computing apparatus is of great significance in the construction and investigation of automatic regulation systems at the present time. Three lectures were devoted at the meetings of the section to problems in the development of computational techniques.

1. A. A. Fel'dbaum's "Fundamental Trends in the Development of Computing Devices for Automatic Systems," in which he considered the trends in the development of computing devices for automatic regulation

and self-adaptive systems, and also several problems in their theory.

2. A paper by Associate Member of the Academy of Sciences of the USSR V. A. Trapeznikov and by Candidate of Technical Sciences B. Ia. Kogan, "Electronic Analogues, the Prospect of Their Development, and of Their use in Automation." It is noted in the paper, that since 1946 the USSR has produced more than 18 modifications of simulating apparatus and many new elements distinguished for high precision and reliability were created. However, there is still a considerable lag in the field of manufacture of analogue devices compared with foreign countries. The greatest drag on the manufacture is the shortage of high-grade parts and components which should be supplied by the radio-industry factories. The paper indicated the prospective trends in the development of further work in the field of simulation.

3. A paper by Candidate of Technical Sciences V. B. Ushakov considered the principal paths of constructing the simulating elements in the SKB-245 of the MPSA. The lecturer cited as illustrations many new models of simulating apparatus, produced and developed at the SKB in recent times.

In addition to the lectures scheduled for the section, five additional reports were heard. Professor E. P. Popov reported on the use of the method of harmonic linearization in the investigation of transients in non-linear systems. G. P. Tartakovskii devoted his remarks to an investigation of intermittent automatic systems with variable parameters. Remarks were heard also from G. E. Pukhov, G. A. Bendrikov and S. A. Stebakov.

The last day of the sessions of the section was devoted to discussions and additional talks. In general, more than 20 persons participated in the discussions.

Comrades F. M. Kilin and O. P. Sitnikov remarked in their talks on the great significance of the method of canonical transformation for the calculation of systems that are subject to continuous random driving functions, and to the solution of radio-engineering problems. At the same time, they formulated many engineering problems, of importance to practical application, for which the methods of static dynamics do not give exhaustive solutions.

Many critical remarks concerning the status report contained in the lecture by A. M. Letov and A. I. Lur'e were made by Professor N. P. Erugin and by V. B. Astaurov, while Professor V. V. Solodovnikov made comments on the paper by V. S. Pugachev. Comments by I. K. Kiselev and S. A. Stebakov pointed out the great significance of phase-space methods for the solution of many practical problems.

A. A. Fel'dbaum, Professor B. A. Riabov, M. Sh. Shirin, Doctor of Technical Sciences M. V. Meerov, and G. A. Monastyrshin made critical remarks concerning the delivered lectures and raised many problems of practical significance in the field of extremal regulation, synthesis, theory of multi-loop systems, simulation, and remarked also concerning the working practices of academic and branch institutes, problems in information and publication of the work on the theory of automatic regulation and control.

## SECTION NO. 2. "SCIENTIFIC FOUNDATIONS OF THE DESIGN OF TECHNICAL MEANS OF AUTOMATION

The sessions of the section scheduled ten papers and three communications. More than 500 persons participated in the work of the section.

General problems in the theory of elements and devices of automation were the subject of papers by Professor B. S. Sotskov, Doctor of Technical Sciences N. N. Shumilovskii, and Candidate of Technical Sciences B. S. Sinitsyn.

In a paper "Principal Trends in the Development of the Theory and of the Principles of Construction of Automation Elements", B. S. Sotskov reported on general and fundamental theoretical problems, such as the development of theory of transformations in the elements and automatic control devices for automatic control, guidance, and regulation, as well as the development of theory of reliability of the building blocks and of their assemblies. No less important are the search for and the development of new principles of construction of these elements, and also further developments of methods of design and calculation of known types of elements and devices.



A paper by N. N. Shumilovskii and B. S. Sinitsyn, "Fundamental Problems of the Theory of Automatic Measurements," was devoted to the theory of automatic measurements.

Doctor of Physical-Mathematical Sciences B. T. Kolomiets reported in a paper "Semiconductors and Their Application in Automation" on the fundamental data on modern status of work on semiconductors and on the properties and parameters of the fundamental groups of semiconductor elements, such as photoresistors, photo-diodes, germanium and silicon rectifiers and amplifiers, varistors, thermistors, etc. The lecturer pointed out the fact that the industry has not yet sufficiently well mastered the developments of the scientific-research organizations, thus creating a lag in the application of semiconductors.

Doctor of Physical-Mathematical Sciences V. M. Tuchkevich, dwelled in his report on the need for a new approach to the design of semiconductor instruments taking into account their specific properties and the operating conditions of automation devices.

The prospects for the development of new types of electronic instruments for automatic and remote control devices were the topic of a lecture by Associate Member of the USSR Academy of Sciences D. V. Zernov, Candidate of Technical Sciences M. I. Elinson and Engineer A. M. Kharchenko. The paper contains an analysis of the present-day status and the prospects of the development of special types of electronic vacuum instruments: transducers for the measurement of the magnetic field, amplifiers, instruments of the commutator type, converters, etc. A general estimate is made of the development of special electronic instruments in our country.

A paper by Doctor of Technical Sciences L. I. Gutenmakher considers the prospects of employing contactless magnetic and capacitive blocks and elements in automatic systems. These elements and blocks can be used to produce memory devices, pulse transmission systems, etc. Many devices of such type were developed in the Laboratory of Electric Simulation of the Academy of Sciences of the USSR.

Many lectures were devoted to the prospect of employing radiations of various types (radioactive, electromagnetic, acoustic, etc.) in automation.

A paper by Candidate of Technical Sciences B. I. Verkhovskii, Professor N. N. Shumilovskii, and G. G. Jordan on the "Prospects of Employing Radioactive Radiations in Automation" considers the advantages of control methods based on the application of radioactive isotopes, and points out the fundamental trends in their application to instrument building and automation, and also discusses problems involving scientific-methods.

Engineer E. A. Nekhaevskii (Goznak) reported on the development of an instrument with a radioactive transducer for the measurement of the weight of paper tape.

Doctor of Technical Sciences A. A. Prokhorov lectured on "Radiospectroscopical Methods and Prospects of Their Application in Automation" in which he discussed briefly four groups of radiospectroscopic methods: gas radiospectroscopy, paramagnetic electronic resonance, nuclear paramagnetic resonance, and pure quadrupole transitions.

Devoted to mass-spectroscopic methods were paper by Candidate of Physical-Mathematical Sciences V. L. Tal'roze "The Mass Spectrometer as an Instrument for the Control of Manufacturing Processes" and the paper by Professor N. N. Shumilovskii and R. I. Stakhovskii "Automatic Gas Analyzers of the Mass-Spectroscopic Type."

Professor L. D. Rozenberg delivered a lecture on "Acoustic Methods of Measuring Non-Acoustic Quantities," in which he showed how acoustic measurements can be used for the measurement of geometrical dimensions of bodies and volumes, parameters of mechanical media, measurement of the states of media, determination of internal defects, and inhomogeneities of structure.

The work of the section has shown that the solution of the most important problems in the development of elements of automation and remote control requires large joint work on the part of mathematicians, physicists, chemists, and specialists in the field of technical means of automation and remote control.

### SECTION NO. 3. "SCIENTIFIC-TECHNICAL PROBLEMS IN AUTOMATIC ELECTRIC DRIVE"

Three sessions of the section were held (October 16, 17 and 18). At each session more than 200 persons were in attendance. Participating in the work of the section were workers in science, the ministries, represen-

tatives of the design-construction bureaus, supervising technical workers, and engineers from the industrial enterprises in various cities: Moscow, Leningrad, Kiev, Khar'kov, Riga, Sverdlovsk, Magnitogorsk, Cheliabinsk, Baku, Tbilisi and others.

A paper by Academician V. S. Kulebakin and Associate Member of the Academy of Sciences of the USSR A. N. Larionov was devoted to the scientific problems, connected with the development of systems of automatized electric drive. V. S. Kulebakin emphasized the great role of electric drive as a basic link in the mechanization and automatization of manufacturing processes in all branches of the national economy and in special branches of engineering. V. S. Kulebakin indicated that the modern tendency in the automatization to higher speeds, rapid operation, and the production of required response and type of motion of machines requires further scientific investigations and a search for methods of creating automatic systems that operate in response to a prescribed program.

This complex problem should be solved by simultaneous consideration of the entire system as a single complicated aggregate, acting in mutual relationship with the working machine, the power system, and the control system.

Further progress in the field of automatized electric drive requires an independent solution of problems in the creation of improved systems of automatized electric drive treated as a complex, multiply-related and complicated problem, which now is an independent field of the science of electrical engineering. The lecture by V. S. Kulebakin brought forward the fundamental problems and tasks in the field of automatized electric drive, including the following: development of theory and practice of automatized systems of electric drive using effective methods of control and regulation (combined methods, invariance methods, nonlinear feedback loops, semiconductor elements, computers, etc.). The lecture indicated the need for the development of theory and principles of construction of multi-motor electric drive systems with automatic synchronization of the motion of the individual motors at different speeds of rotation, power follow-up systems, and synchro-connection systems for all-out automatization of manufacturing processes and particularly for automatized units that are interrelated into shops and factories; attention was also paid for the need of further development and improvement of electric drive using d-c motors.

The choice of the most suitable frequency for commercial installations and for specialized purposes was the subject of a co-report by Associate Member of the Academy of Sciences of the USSR L. N. Larionov.

Noting the great range of frequencies used in practice without justification, the lecturer made some proposals concerning its reduction, indicating thereby that the changeover to higher speeds in electric-drive systems yields a substantial reduction in weight and dimensions, but requires the design of special machinery and converting devices.

The theory of operation of automatized electric drive as a complex multiply-connected system in which many parameters are controlled and regulated have not been adequately developed. Doctor of Technical Sciences M. V. Meerov reported on results in the investigation on the synthesis of structures comprising fundamental elements and stabilizing (correcting) devices, meeting specified requirements concerning the fundamental dynamic properties, used in conjunction with regulated and controlled dynamoelectric systems consisting of motors and converters.

Doctor of Technical Sciences V. D. Nagorski, considered in his paper the problems of the connection between the speed and the power of a motor. A paper and a communication by Engineer V. M. Terekhov, indicated ways towards further investigation of the power relationships in electric drives in response to various control and the driving signals.

Great attention was paid in the second session of the section to new methods and means of controlling automatized electric drive systems. Included among the progressive idea raised in this portion are frequency control, which makes it possible to extend considerably the range of adjustable speeds, and to increase the efficiency of the installation.

The papers by Academician M. P. Kostenko and Doctor of Technical Sciences D. A. Zavallishin presented the fundamental theoretical premises of frequency control and derived analytic relationships between the individual parameters, namely voltage, frequency, and torque, and presented some idea on how to choose these parameters correctly to insure high power output from the regulated apparatus. Their paper reported on new systems for high-power frequency conversion, proposed by M. P. Kostenko and V. P. Andreev. These systems

consist of single-phase slip-ring generators, connected into a two or three-phase group. For apparatus with limited power, a new system is proposed using dynamoelectric cross-field amplifiers, excited and controlled with a-c, using the method of M. P. Kostenko and V. V. Rudakov. The electron-ion frequency regulation circuits, based on the method by D. A. Zavalishin, with which the range of frequency regulation is extended, are of technical interest. This proposed method in the lecturer's opinion, makes it possible to solve practically the problem of frequency control of the electric drive.

Saturated reactor control was the subject of papers by Doctor of Technical Sciences A. G. Ivakhnenko, Candidate of Technical Sciences M. N. Gubanov, and Candidate of Technical Sciences Borisov, who considered the theory and methods of design of controllable reactors and systems of reactor control with a wide range of motor speed, at good stability and high proportionality of characteristics, both at low motor speeds and when plugging.

The lectures also contained a formulation of the fundamental problems pertaining to reactor control and to investigation of the dynamics of the processes occurring in the saturated reactors themselves.

Great interest was stimulated in the section by a paper by Doctor of Technical Sciences T. P. Gubenko on the use of the method of disturbing the symmetry of the stator winding and of the voltage to regulate and to brake induction motors. The lecturer set down a universal scheme he worked out for the connection of induction machines, and his recommendations on the choice of rational circuits for specified conditions and operating requirements of a manufacturing unit.

In the third session of the section Engineer V. I. Krupovich, remarked in his lecture "Prospects of Further Development of Automatized Commercial Electric Drive and Problems in the Electrical Industry" that the electrical engineers, jointly with the technologists and the machine designers, should produce a regulating system that responds continuously and simultaneously to many technological parameters including the quality of the ingot and the temperature of the metal during the continuous pouring process. The lecturer reported that the Khar'kov Division of the Institute "Tiazhprom elektropromekt" [Electric Design Office for Heavy Industry] has worked out a new instantaneous (electronic) circuit for grid control of mercury rectifiers in conjunction with a regulator for the regulation of continuous rolling mills.

The Ministry of Instrument Building and of Means of Automation must develop in the nearest future a whole series of reliable transducers for nonelectric quantities, for the lack of such transducers is a substantial hindrance to further automatization of manufacture. A paper by Candidates of Technical Sciences V. V. Petrov and N. S. Gorskaia set forth the principles of operation, the structural execution, and the results of a theoretical and experimental investigation on high speed electropneumatic servomechanism developed in the Institute of Automation and Remote Control of the USSR Academy of Sciences.

A paper by Candidate of Technical Sciences O. V. Slezhanovskii, was devoted to a survey of the status of the Russian electric industry and in particular of electric drive both in Russia and abroad. It is noted in the paper that at the present time Russia lags considerably in volume of manufacture of semiconductor and pumpless mercury rectifiers, of a complete line of magnetic amplifiers and of saturated reactors. Much work is being done in the Soviet Union at the present time on the creation of cheaper and lighter lines of d-c and a-c machinery using new brands of steels and new designs. In addition, lines of saturated reactors are being produced for use in reactor-control systems for automatized electric drives.

Docent Krechetovich reported in his communication on a circuit for pulse regulation of the speed of a high power induction motor, distinguished for simplicity and high economy. The remarks by L. A. Milovidov was devoted to a procedure for determining the parameters of a system of induction drive with choke control for specified limits of the variation of torque, slip of the motor and the stiffness of the artificial mechanical characteristic. Candidate of Technical Sciences A. G. Mekler, reported on controllable reactor systems for electric drive that were developed and introduced for high-power cranes and elevators and also on methods for the design of saturated reactors using nomograms.

L. A. Milovidov and A. G. Mekler remarked that reactor control systems for electric drives are sufficiently well developed at the present time and have been produced in practice, and that simple methods have been created for their design. These circuits should be introduced extensively in industry, for their regulating and economic indices are not inferior to systems employing d-c machinery and are considerably cheaper than the latter in those cases, when it is not necessary to regulate the speed over a long period of time.



Candidate of Technical Sciences G. V. Oreshkevich reported on a new system of control of synchronous motors with the aid of a reactive amplifier, which permits raising and lowering the line voltage.

Communications by Engineers V. Iu. Nevraev and Gul'mamedov reported on the results of investigations on the work of an induction electric drive fed from a power source of commensurate rating and discussed problems on the stabilization of the voltage for such electric drives when starting the motor; a procedure was proposed for the analysis of the transient and for the choice of the regulation system.

Candidate of Technical Sciences V. M. Bogoiavlenskii reported in his remarks that laboratory investigations have shown that the planetary-gear control system, developed at the Institute of Automation and Remote Control of the Academy of Sciences of the USSR makes possible a frequency transformation over a 1:2 range. In the lecturer's opinion, such a system can be used for high-power installations, particularly for mobile agricultural machines fed from a self-contained power source.

Work on ion-electronic drive was reported by Candidate of Technical Sciences M. Z. Khamudkhanov. He proposed a procedure designing the control system and suggested considerations concerning the choice of structural circuits.

Docent N. E. Kuvaev and Candidate of Technical Sciences A. M. Miroshnik used a slip-ring frequency converter to illustrate a circuit they developed for controlling a group of a-c motors for the power mechanisms of multi-bucket excavators and traveling bridges; this system offers considerable advantages over analogous d-c systems with respect to stability and simplicity of control.

An interesting investigation on the stabilization of d-c motor speeds are contained in the report by Candidates of Technical Sciences A. I. Bertinov and S. R. Miziurin. The lecturers report that the accuracy obtained in the circuit proposed by them is within  $\pm 0.05\%$ .

Candidates of Technical Sciences V. V. Petrov and G. M. Ulanov reported results of an investigation of combined automatic-regulation systems employing electro-hydraulic drives. It was shown that the use of error-proportional action effectively increases the accuracy and speed of the control systems.

Many of the comrades who addressed the session made demands on the scientific institutions that they develop engineering methods for the design of systems of electric-drive control.

The participants in the sessions of the section were given a list of problems and topics recommended for further attention. This list covers 60 individual problems and topics, pertaining to individual question in science and to methods of design and calculation in the field of automatized electric drive.

#### SECTION NO. 4. "THEORY AND METHODS OF CALCULATION AND DESIGN OF MECHANISMS FOR AUTOMATIC MACHINES AND AUTOMATIC LINES"

The section heard 11 papers and two communications, while seven persons participated in the discussion of the papers.

The paper by Academician I. I. Artobolevskii, showed the connection between problems in automatization of machines and methods for further improvement of labor productivity, and formulated the fundamental problems of the theory of mechanisms of machines in connection with the development of automatic machinery and automatic lines, particularly those using electronic control devices. The lecturer formulated the problems in the field of the theory of programming of technological processes, of the dynamics of actuating mechanisms of automatic control systems, of the synthesis of computing devices, and also in the field of development of the theory of design of mechanisms of complex type including hydraulic, pneumatic, electric, and electronic devices. The role of experimental methods in the study of the theory of automatic machinery was emphasized.

A paper by Professor F. S. Dem'ianiuk analyzed various methods of automatization technological processes in machine building, and showed the effectiveness of all-inclusive automatization based on strict sequence of the flow of the process of parts manufacture. The importance of work on standardization of technological processes was noted and a procedure for calculating the optimum output was given.

Candidate of Technical Sciences A. P. Vladzhevskii, reported on new automatic production lines, developed by the enterprises of the Machine-Construction and Tool-Construction Industry. The lecturer dwelled on the most important problems in the design of individual units of automatic lines and on the status of the theoretical problems, and also on the problem of insuring reliable operation of the production line.

A paper by Professor S. I. Artobolevskii was devoted to problems connected with the development of the general theory of automatic machinery as a base for the creation of a scientifically-founded method for their design, and for the organization of work on the analysis and exchange of experience in the field of production automatization between branches of industry. The lecturer indicated that particular attention must be paid to the development of methods of comparative technical-economical analysis of different models of automatic machinery and automatic production lines.

The lecture by Doctor of Technical Sciences N. I. Levitskii and Candidate of Technical Sciences S. A. Cherkudinov was devoted to an exposition of the basic problems in the design of mechanisms for automatic machinery. Particular attention was paid to the justification of the choice of the scheme of mechanisms that reproduce a given motion. The lecturers pointed out problems in the synthesis of mechanisms that remain to be solved and also paid attention to the need for systematizing the records of operating experiences with mechanisms and the development of handbook data.

The paper by Academician N. G. Bruevich considered the inputs to and outputs of the simplest devices that comprise the complicated mechanical and electrical systems used to realize implicit functional relationships. The lecturer formulated the conditions under which such systems can be assembled using simplest devices of directional or mixed action.

Reports by P. A. Metevosian (Institute of Machinery, Academy of Sciences, USSR) and A. K. Ganulich (VVA in the name of Zhukovskii) presented the result of experimental investigations of mechanical and electronic systems, which confirmed in principle the theoretical results indicated in the paper by Academician N. G. Bruevich.

The paper by Doctor of Technical Sciences M. L. Bykhovskii was devoted to problems in the dynamic accuracy of the automatic controllers of automatic assembly lines. The paper expounded on methods for the analysis of the dynamic accuracy of mechanical and electric circuits and formulated the most important problems occurring in connection with the development of systems for programmed digital control of machine tools, and also in connection with the development and improvement of control circuits for automatic machinery.

Doctor of Technical Sciences G. G. Baranov reported on research concerning technical conditions of bearings and the technology of their automatic manufacture. A prominent place in the lecture was devoted to problems of quality control of the shape of the bearing rings and, in connection with this, to a procedure for the investigating of the technological processes within the framework of correlation theory. The second part of the paper treated problems in dynamic investigation of the process of inside grinding of rings, carried out for the purpose of increasing their accuracy and to the development of methods of setting-up the automatic machine.

A paper by Doctor of Technical Sciences A. E. Kobrinskii was devoted to the analysis of program-control systems for metal-cutting machinery. He considered two groups of technological problems involved in program-control systems and pointed out the distinguishing features that make possible classification of the systems in accordance with the method used to convert the intermittent signals of the program, in accordance with the interpolation method, and in accordance with the number and type of controllable coordinates. In conclusion, the lecturer formulated the problems involved in the programming of technological processes of metal working, and also the problems involved in the design of automatic machines equipped with program-control systems.

Candidate of Technical Sciences B. N. Bezhanov indicated in his paper the fundamental trends in the development of research in the field of hydro-pneumatic automation, and the improvement in the construction of various devices used in hydraulic and pneumatic systems.

S. M. Kozhevnikov, Associate Member of the Academy of Sciences of the Ukraine SSR, lectured on problems in the automatization of an extensive class of machinery used in metallurgical production. The most

important problem in this field is the automatization of the auxiliary and finishing operations. Using as examples many specific technological processes, the lecturer pointed out the principal problems in the automatization of individual groups of machines and the topics in the theory of machines and mechanisms that are related to the solution of these problems.

Engineer V. A. Morozov commented on the contradictory premises contained in the paper by F. S. Dem'ianiuk. He noted that on the basis of experience of the automatic shop in the First State Bearing Plant, any further construction of automatic assembly lines in this plant should be based on all-out automatization of entire groups of machines.

Doctor of Technical Sciences N. A. Borodachev (Mathematics Institute, Academy of Sciences, USSR) who participated in the discussion of the papers, pointed out those characteristics of mechanisms that must be borne in mind when compiling handbook data and when designing and calculating automatic machinery; he also called attention to the need for correct evaluation of the economies of automatic machines and assembly lines.

Candidate of Technical Sciences V. F. Preis (Tula Mechanical Institute) devoted his comments to problems in the coordination of scientific-research work and the training of personnel in the field of automatization of manufacture.

Doctor of Technical Sciences A. P. Malyshev (Moscow Textile Institute) proposed that the higher technical schools engage in the training of specialists on automatic machinery, and that the study of automatic machinery occupy a suitable place in the teaching of the theory of mechanisms of machines. A. P. Malyshev dwelled further on problems in terminology and classification, touched upon in the lectures by A. P. Vladzhevskii, N. I. Levitskii, and S. A. Cherkudinov.

Candidate of Technical Sciences K. V. Tir remarked on the need of resolving problems in the compensation of dynamic forces, occurring in mechanisms, and also problems in optimum motion of their actuating devices. He also spoke of the need for developing simplified methods for the design of mechanisms.

Doctor of Technical Sciences V. A. Iudin noted the importance of publication of materials on the design of standard mechanisms, used in various branches of machine building. He indicated the extreme desirability of further development of the theory of synthesis of mechanisms particularly the development of dynamic synthesis.

Doctor of Technical Sciences S. I. Artobolevskii dwelled in his comments on shortcomings in the coordination of scientific work in the field of automatization and on the discrepancies in methods used to evaluate technical-economic indices.

#### SECTION NO. 5. "SCIENTIFIC PROBLEMS IN TELEMCHANIZATION OF MANUFACTURING PROCESSES"

The section of scientific problem of telemchanization of manufacturing processes held three sessions (October 16, 17 and 19). The first two were attended by approximately 130 persons, and the last by 80 persons. Seven papers and 15 reports were delivered at this section. Nineteen persons participated in the discussions.

The papers and reports were devoted to an analysis of three fundamental problems: the status of telemchanization in different branches of the national economy of the USSR, scientific problems in telemchanics, and new technical means used in this field.

Devoted to the status of telemchanization were papers by Engineer S. P. Krasivskii "Prospects of Development of Telemchanization in the National Economy," by Candidate of Technical Sciences V. N. Roginskii "Most Important Problems in the Development of Telemchanics in Communication," and by Candidate of Technical Sciences B. S. Riazantsev "Most Important Problems in the Development of Telemchanics in Transport."

The lecturers and those participating in the discussions after these lectures have noted that in spite of the great technical-economic effect, telemchanization is used in the USSR only in power systems and in transport. An obstacle to its wider adoption in the remaining branches of the national economy is the lack of production of telemchanical apparatus suitable for general industrial use.



It was noted that it is extremely important to organize such manufacture as soon as possible. It was indicated that the metallurgical, chemical and other combines, and also the petroleum industry, coal mining, and agricultural irrigation, etc., are in bad need for telemechanization. In the paper by V. N. Roginskii and in remarks made by many representatives of the organizations of the Ministry of Communication it was indicated that there is great need of employing telemechanical apparatus in communication installations for remote control of unattended substations of intertoll cable automatic telephone station lines, radio relay lines, etc. B. S. Riazantsev touched in his paper on the great prospects of employing telemechanics in railroad transport and on the fact that so far Russia lags in this field behind the level reached in the USA.

In a paper "Fundamental and Scientific Problems Involved in Telemechanization in the National Economy of the USSR," Doctor of Technical Sciences M. A. Gavrilov indicated that the national economy poses before telemechanics two fundamental technical problems: the problem of telemechanical centralization of control and regulation, and the problem of remote automatization. The solution of these problems creates in turn many scientific problems both in the field of construction of new telemechanized processes and in the development of the theory of telemechanics and new technical needs. Those participating in the discussions emphasized furthermore the great significance of the problem of remote automatization raised in the paper. As was already indicated in the paper, the most important theoretical divisions of telemechanics include the theory of design of telemechanical signals, the theory of the construction of relay-action apparatus, the theory of reliability and noise rejection, and the theory of telemetering converters. While certain success has been accomplished in the first two divisions, the work in the remaining two is still in its initial stage. It was indicated in the paper that it is exceedingly important to employ telemechanical devices with contactless elements, which increase considerably the reliability, accuracy, and speed of these devices. Experimental models of the first fully contactless remote-control devices, developed by the Institute of Automation and Remote Control of the Academy of Sciences of the USSR, were demonstrated.

Candidate of Technical Sciences O. A. Gorlainov (Moscow Power Institute in the name of Molotov), also discussed in his communication contactless remote-control systems. M. A. Gavrilov's paper mentioned also the scientific problems connected with the creation of new technical means for telemechanics. These means should be created on the basis of extensive unification, subdivision into standard units, and new more effective designs of telemechanical devices. The paper also raised the problem of producing a new type of all-purpose building-block telemechanical device of universal construction, unifying all the devices of the control point into a single unit. This idea was supported by many participants in the conference who participated in the discussion.

Owing to the great complexity of telemechanical devices, which frequently contain thousands and tens of thousands of elements, it is very important to develop automatic machines for their construction. The first such models, demonstrated at the sessions of the section, were machines for the analysis of relay devices, created by the Institute of Automation and Remote Control, and machines for synthesis developed by the Laboratory for Wire Communication Problems of the Academy of Sciences of the USSR.

More detailed scientific problems in the field of telemetering and remote control were considered in a joint paper by Doctor of Technical Sciences V. A. Il'in and Candidate of Technical Sciences V. S. Malov "Basic Problems in the Theory of Telemetering," and in a joint paper by Doctor of Technical Sciences M. A. Gavrilov and Candidate of Technical Sciences G. A. Shastova "Fundamental Problems in the Theory of Design of Signals and the Theory of Noise Rejection and Reliability." The latter considered also a new procedure for designing systems of signals that do not become converted into each other. The problem of constructing telemechanical signals, which is of great significance for the construction of telemechanical devices, was subjected to a detailed analysis in communications by Candidate of Technical Sciences R. I. Iurgenson, Candidate of Technical Sciences B. K. Shchukin, Scientific Worker V. M. Ostianu and D. Abdulaev, and in comments by many conferees.

Many theoretical questions, connected with the design of complicated telemechanical systems in telephone and telegraph communications, were raised in a paper by V. N. Roginskii. Problems of the application of telemechanics to communication were also the subject of reports by Candidate of Technical Sciences Iu. A. Grints and Engineer K. A. Kazarinov.

The status of manufacture of telemechanical apparatus was the subject of a joint paper by Engineers V. N. Chepurin and V. A. Ambrosovich. Outlining the status of the manufacture of telemechanical apparatus at the

"Elektropul't," plant, the lecturers touched upon many problems connected with the improvement of the telemechanical apparatus already produced and that under development. Questions were also raised concerning progress in many theoretical problems and new principles of construction of remote-control and telemetering devices, and many demands on industry were made concerning the production of many new elements for telemechanical devices.

Explanations of many new developments in the field of telemechanics were included in the reports by those attending the session and by representatives of the research and design organizations. They pointed out the need for considerable expansion of work in the field of telemechanics. It was indicated that the completed developments are very slow to be adopted and that it is necessary to do research on new principles of construction of telemechanical devices to develop criteria for their evaluation, etc. Shortcomings in the training of personnel to engage in the field of telemechanics were indicated. The need for better coordination was noted and it was emphasized that materials, specialists, physicists, physiologists, and economists must be enrolled in the coordination work and in work in the field of telemechanics.

The work of the section resulted in a summary of the present-day status of telemechanics. It was stated that in many branches of the national economy there is a great unfilled demand for telemechanization, requiring a rapid organization of the manufacture of technical means of telemechanics suitable for general commercial purposes. Note was made of the great promise of remote automatization as a new means for the transition to a greater extent of automatization and production of all-purpose remote-automation systems for apparatus that is still decentralized. The scientific problems involved in telemechanics were discussed and it was established that with the present day state of telemechanics it is possible to build telemechanical equipment employing contactless elements exclusively and that this trend in the development of the technical means of telemechanics is one of the most promising ones. Another important trend is the development of efficient telemechanical apparatus, particularly for complex telemechanical systems. In connection with this, the theoretical work that is carried out at the present time on a scale that is far from sufficient acquires particular significance. The fundamental trends of this work were approved, as were the tasks in the field of mathematics, physics, physiology, etc., formulated in the papers heard at the section.

#### SECTION NO. 6 (JOINT): "ALL-OUT AUTOMATIZATION OF MANUFACTURING PROCESSES"

The sessions of the sixth (joint) section on "All-Out Automatization of Manufacturing Processes" was held on October 17-19 of this year under the chairmanship of Associate Member of the Academy of Sciences of the USSR A. I. Tselikov and Professor N. N. Shumilovskii.

Sixteen papers and four reports were heard at the sessions of the section, and 24 persons participated in the discussion. In a paper by Doctor of Technical Sciences N. N. Shumilovskii and Doctor of Technical Sciences V. L. Lossievskii "Fundamental Problems in the Development of Science in the Field of All-Out Automatization of Manufacturing Processes" it was stated that the tasks of automation should encompass two sets of problems: problems in efficient construction of technological plans of manufacturing processes and of corresponding technological apparatus in various branches of industry, with allowances for further automatization of this equipment, and also problems of rational construction of the automatic control and regulation systems used for these processes.

Many factors impede the development of all-out automatization of manufacture: 1) The use of obsolescent technological aggregates, not amenable to automatization, in many branches of the industry, 2) an insufficiently developed instrument-building industry, 3) an insufficient number of specialists in the field of automation, 4) poor organization of scientific-research in the field of automatization of manufacture and the lack of scientifically-founded methods for the construction of equipment. The paper then went on to formulate the tasks of scientific research in the field of automatization.

A paper by Deputy Minister of Instrument Building and of Means of Automation of the USSR V. P. Lukin "Prospects of Development of Instrument Building and of Means of Automation and the Tasks of Science" dealt with equipment in various branches of industry, such as metallurgy, chemical, petroleum, food, and light industry, which should be the first to be automatized. The lecturer then turned to measures adopted by the

Ministry for the purpose of increasing the output of instruments and of means of automation by the end of 1960 by 5.3 times and the output of computing machines by 6 times, compared with the 1955 output. The increase in volume of manufacture should be accompanied by an expansion in the available types of new instruments. The lecturer noted many laggard fields of the technology of instrument building, such as the field of analytical instruments, etc.

A paper by Engineer A. M. Nekrasov "Prospects of the Development of Automation in the Power Industry and the Tasks of Science" described experience in the application of automation in the power systems of the USSR and the problems raised by the progress of the power industry.

Academician M. P. Kostenko in a paper "Problems of Automatic Control of Electric Power Systems Using Methods of Electrodynamical Models" threw light on the problems that can be studied with the aid of network analyzers. The paper considered the experience and the most important results obtained in the use of electrodynamic simulation in the USSR. He indicated the most important tasks of automatic regulation of power systems, which include the construction of new network analyzers, the development of excitation regulators for high power hydraulic generators, high speed excitation regulators, and the use of computing machinery.

A paper by Doctor of Technical Sciences V. A. Venikov like the paper by Academician M. P. Kostenko, was devoted to automatic regulation of electric power systems. It listed the basic tasks of the development of laboratory and analytical investigation of operating conditions of electric transmissions and electric systems, and stated in particular that the development of physical simulation should be carried along a different path, namely the simulation of fields and their affine similarity.

Doctor of Technical Sciences A. E. Khlebnikov delivered a paper on "New Metallurgical Processes and Problems in Their Automatization," in which he established the need and possibility of producing continuous technological processes in metallurgy.

Doctor of Technical Sciences V. G. Voskoboynikov and Engineer A. K. Adabash'ian delivered a paper "Prospects for the Development of Automatization of Blast Furnace, Steel Melting, and Steel-Rolling Manufacture, and the Tasks of Science."

Associate Member of the Academy of Sciences of the USSR A. I. Tselikov, in a paper "Automatization of Pressure Metal Working by using Continuous Processes" indicated the trends in the automatization of pressure metal working and cited the results of investigations on the production of new processes for transverse thread rolling.

Academician V. I. Dikushin delivered a paper "On the Results of Work of the Conference on Automatization in Machine Building Industry."

A paper by Doctor of Technical Sciences F. A. Trebina, "Prospects of the Development of Automation in the Petroleum Industry and the Tasks of Science," was devoted to the problems of the status of automation in the principal branches of petroleum manufacture: prospecting for oil deposits, drilling oil wells, industrial-geological investigations, oil extraction, oil refining, and storage of oil and oil products.

Engineer A. A. Matveev, in a paper "Level of Automation of the Petroleum Refining Plants with an Output of Six Million Tons of Crude Per Annum, Now Under Construction," described the control and automation equipment that is being used at the plant and named the problems that require the participation of the Academy of Sciences of the USSR and of the MPSA.

Engineer V. A. Nikitin, in a paper "On the All-Out Automatization of the Moscow Refining Plant," reported on experience in realizing all-out automatization in an already-operating petroleum refining plant.

It was shown in the paper how the adoption of automatization affects the scheme of the process and the entire production as a whole and what effect is produced by introducing automation.

Professor E. I. Tagiev, delivered a paper on the drilling of oil wells.

A paper by Engineer G. N. Kirikov, "Prospects of the Development of Automatization in the Chemical Industry and the Tasks of Science," indicated the obstacles to extensive use of automation and proved the need for all-out automatization of chemical manufacture. The lecturer cited data that described the economic effect of introducing automatization and increasing the productivity of the processes.



A paper by I. L. Farberov, "Problems of Automatization of Underground Gasification of coal," described the development of methods of underground gasification of coal in the USSR. The paper raised many problems on the control and running of the process of underground gasification of coal.

A paper by Doctor of Economic Sciences K. I. Klimenko, "Development of Methods of Estimating the Technical-Economic Indices of the Effectiveness of Automation," gave a comparison of the scales of manufacture of individual branches of industry in the USSR and in the capitalist countries. The paper considered problems of the recovery of expenditures for automation in many branches of industry, problems of the procedure of determining the effectiveness of automation, and problems in the application of automatic equipment and of computing machinery in new branches of technology. The paper raised problems of determining and achieving economic effectiveness in automation of manufacture.

Reports from the Republic Academies of Sciences were delivered by Vice President of the Academy of Science of the Ukraine SSR G. N. Savin, Associate Member of the Academy of Sciences of the Azerboidzhan SSR A. A. Efendizade, Academician of the Academy of Sciences of Estonian SSR I. G. Kheil, and Candidate of Chemical Sciences A. A. Zhukanskas (from the Academy of Sciences of the Lithuanian SSR).

G. N. Savin reported on the development of research work in the Institutes of the Academy of Sciences of the Ukraine SSR, noting in particular the need of creating within the Academy of Sciences of the Ukraine SSR an Institute of Automation that would be the principal center of the development of work on automatization in the Ukraine SSR.

Results of the investigation of the automation of objects in the oil industry and of the tasks faced by the Power Institute of the Academy of Sciences of the Azerboidzhan SSR in this field were reported by A. A. Efendizade.

I. G. Kheil dwelled on the causes that impede a wide introduction of automation in the industry of the Estonian SSR. The report described the work performed by the Academy of Sciences of the Estonian SSR in the field of automation of manufacturing processes and made suggestions on the topics to be covered by scientific research in the field of automation.

The development and organization of work on automation in the Lithuanian SSR was reported by A. A. Zhukauskas.

Associate Member of the Academy of Sciences of the USSR V. A. Trapeznikov devoted his remarks to problems of the economic effectiveness of introduction of automation in industry.

Professor Shaumian discussed automatization in machine building.

The remarks by Comrades Gutnikov, Vorob'ev, Kogan, Kuznitskii and Gruzinov, and others were devoted to the automatization of the metallurgical industry.

Comrade Fedorov commented after the lecture by I. L. Farberov on the automatization of underground gasification of coal.

Participating in the general discussion were Professor Borodachev, Engineer Malyi, Doctor of Technical Sciences Kapustin, Engineer Gal'rode, and others.



# DETERMINATION OF PERIODIC MODES IN SYSTEMS WITH PIECEWISE-LINEAR CHARACTERISTICS COMPOSED OF SEGMENTS PARALLEL TO TWO SPECIFIED LINES, II.

M. A. Aizerman and F. R. Gantmakher

(Moscow)

The method described in the first part of this article [1], whereby the periodic modes are determined in the form of a complete Fourier series, without neglecting any harmonics, is extended to include arbitrary piecewise-linear characteristics, composed of segments that are parallel to two specified straight lines, and to arbitrary types of periodic modes.

## 1. Generalization of the Problem

The method proposed for the determination of periodic modes was demonstrated in [1] using as an example the simplest periodic mode in the following system

$$\dot{x}_j = \sum_{i=1}^n a_{ji}x_i + \lambda_j f(x_1) + F_j(t) \quad (j = 1, 2, \dots, n) \quad (1.1)$$

subject to the following assumptions:

- a. The function  $f(x_1)$  is piecewise-linear and consists of two segments.
- b. The transition from the first segment to the second and from the second to the first is instantaneous, at the instant when  $x_1$  attains for the first time the specified values  $\sigma_1$  and  $\sigma_2$ .

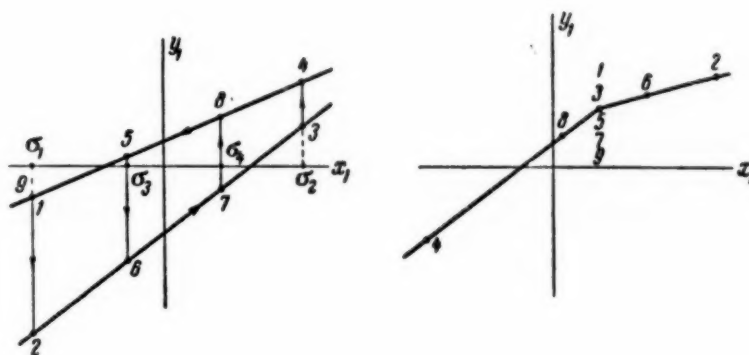


Fig. 1

c. We seek the simplest periodic mode, in which the first and second straight-line segments are each followed once during the period (see Fig. 3) [1].

The functions  $F_j(t)$  are sufficiently smooth, i.e., not only  $F_j(t)$ , but also all their derivatives that are encountered in the calculations are continuous and differentiable.

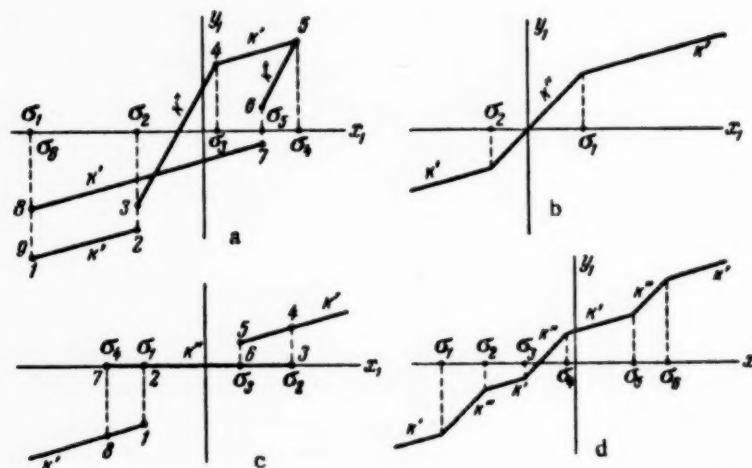


Fig. 2

The class of problems that can be solved with this method can now be generalized in four manners.

1. It is possible to consider characteristics that consist of more than two segments of the same two straight lines, i.e., one can specify not the simplest modes, but more complicated ones for systems with a two-piece characteristic curve. Examples of this kind are shown in Fig. 1, where the numbered points are passed-through in sequence during a single period.

2. It is possible to consider either continuous or discontinuous characteristics composed of any number of different straight segments, provided each segment is parallel to one of only two specified straight lines, i.e., provided the slopes of the straight lines assume only one of two values,  $k'$  or  $k''$ .

Figure 2 shows examples of such characteristics.

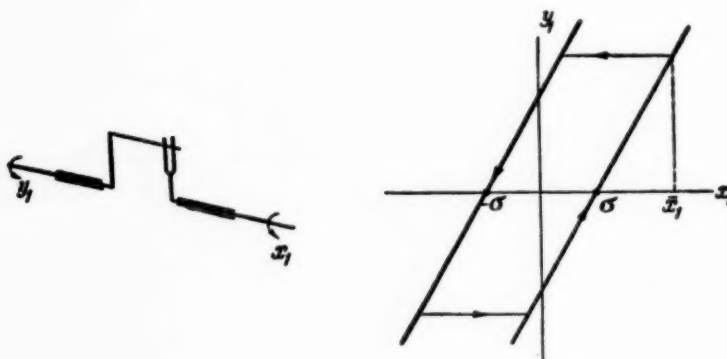


Fig. 3

3. One can consider more general transitions from one part of the characteristic to the other. Thus, for example, in the analysis of play or of dry friction in an inertialess element (Fig. 3), the coordinate  $y_1$  either varies with  $x_1$  ( $y_1 = x_1 + \text{const}$ ) if the play is taken up, or remains unchanged ( $y_1 = \text{const}$ ) if the play is not taken up. The characteristic consists of straight segments with slopes 1 or 0; the transition from the first segment to the second occurs the first time that  $\dot{x}_1$  vanishes, no matter what the value of  $x_1 = \bar{x}_1$  is at that instant, and the transition back to the sloping line occurs the first time that  $x_1$  differs from  $\bar{x}_1$  by a specified value. Other

examples can be cited, in which the characteristic consists of straight segments parallel to two specified lines, but the conditions under which the change from one segment to the other occurs are determined not by equations such as  $x_1 = \sigma_1$ , but by other (not necessarily linear) relationships between  $x_1$  and its derivative at various instants.

4. One can, finally, consider a more general class of driving functions, i.e., of the functions  $F_j(t)$ , assuming the latter to be piecewise-smooth and specified in terms of their own Fourier series. This generalization must be used in the analysis of stepwise and other discontinuous periodic driving functions.

Since it is our aim to generalize our class of problems in the above manners, let us turn to the derivation equation

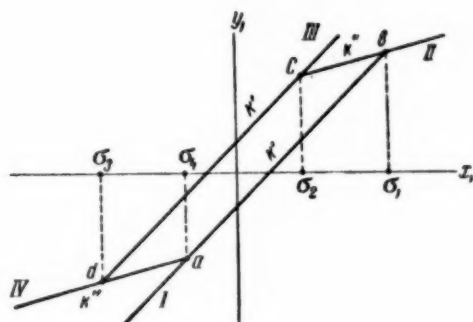


Fig. 4

$$\begin{aligned} D(p^*)x_1 &= K(p^*)y_1 + \Phi(t), \\ y_1 &= f(x_1), \end{aligned} \quad (1.2)$$

obtained by eliminating from the System (1.1) all the  $x_j$ 's except  $x_1$ , and let us assume now that the period  $T$  can be broken up into  $N$  stages, occurring at the instants  $t_1 - t_0, t_2 - t_1, \dots, t_N - t_{N-1}$  (here  $t_N - t_0 = T$ ), and that during each stage the point  $x_1, y_1$  moves along a straight line having one of the two specified directions, characterized by the slopes  $k^*$  and  $k^{**}$ .

We shall assume the following to be specified for each  $i$ 'th stage ( $i = 1, 2, \dots, N$ ):

a) the equation of the straight line along which the point  $x_1, y_1$  moves during this stage, is in the form

$$y_1 = k_i x_1 + \varphi_i x_{1,i-1} + \psi_i y_{1,i-1} + \theta_i, \quad (1.3)$$

where  $k_i$  is either  $k^*$  or  $k^{**}$ ,  $\varphi_i, \psi_i$ , and  $\theta_i$  are specified numbers, and  $x_{1,i-1}$  and  $y_{1,i-1}$  is the point at which the preceding  $(i-1)$ th stage terminated, i.e.,

$$x_{1,i-1} = x_1(t_{i-1} - 0), \quad y_{1,i-1} = y_1(t_{i-1} - 0);$$

b) the conditions under which the stage is terminated ("joining condition"), given in the form of a linear relationship between  $x_1(t)$  and its derivatives at the instants  $t_i$  and  $t_{i-1}$ :

$$\sum_{j=1}^n \zeta_j x_1^{(j-1)}(t_i) + \sum_{j=1}^n \pi_j x_1^{(j-1)}(t_{i-1}) + \zeta = 0; \quad (1.4)$$

the  $i$ -th stage terminates at the instant  $t_i$  when the Condition (1.4) is first satisfied.

Since the degree of  $K(p^*)$  in (1.2) is less than the degree of  $D(p^*)$ , the function  $x_1$  is continuous and there is no need for writing down the starting conditions for each stage — these are determined from the "joining conditions" by the continuity of  $x_1$ .

Let us illustrate the above with the following examples.

**Example 1.** The characteristic  $f(x_1)$  is broken, consisting of three parts, of which the outer two are parallel (Fig. 2, b). We seek the simplest continuous periodic mode.

In this case  $N = 4$ , and  $\varphi_1 = \psi_1 = 0$  at all stages;  $k = k'$  and  $\theta = 0$  for the middle part, and  $k = k''$  and  $\theta$  equals either  $(k'' - k') \sigma_1$  for the outer right part or  $(k'' - k') \sigma_2$  for the outer left part. The conditions for the termination of each stage are the equations  $x_1 = \sigma_1$  and  $x_2 = \sigma_2$ , respectively.

**Example 2.** The same characteristic, but comprising a loop. If the point is at a during the time  $t = t_0$ , it moves along line I (in particular, also down from a) until it first reaches point b, from where it follows line II until reaching point c, etc.

In this case, too,  $N = 4$ . The data for this stage are listed in Table 1.

TABLE 1

Таблица 1

Stage of motion of point	Equation of straight line	Joining condition
From a to b	$y = k'x + (h_1 - k'\sigma_1)$ , т.е. $k_1 = k'$ , $\varphi_1 = \psi_1 = 0$ , $\theta_1 = h_1 - k'\sigma_1$	$x_1 = \sigma_1$
From b to c	$y = k'x + (h_1 - k'\sigma_1)$ , т.е. $k_2 = k'$ , $\varphi_2 = \psi_2 = 0$ , $\theta_2 = h_1 - k'\sigma_1$	$x_1 = \sigma_2$
From c to d	$y = k'x + [h_1 + (k'' - k')\sigma_2 - k'\sigma_1]$ , т.е. $k_3 = k'$ , $\varphi_3 = \psi_3 = 0$ , $\theta_3 = h_1 + (k'' - k')\sigma_2 - k'\sigma_1$	$x_1 = \sigma_3$
From d to a	$y = k''x + [(k' - k'')\sigma_4 + h_1 - k'\sigma_1]$ , т.е. $k_4 = k''$ , $\varphi_4 = \psi_4 = 0$ , $\theta_4 = (k' - k'')\sigma_4 + h_1 - k'\sigma_1$	$x_1 = \sigma_4$

**Example 3.** The system differs from a linear one in that it contains an inertia-less element, subject to play or to dry (Coulomb) friction.

The values of  $k$ ,  $\varphi$ ,  $\psi$ ,  $\theta$ , and  $\xi$  for all stages of this example are given in Table 2.

TABLE 2

Stage	$k$	$\varphi$	$\psi$	$\theta$	Joining conditions
I	1	0	0	$-\sigma$	$\dot{x}(t_1) = 0$
II	0	0	1	0	$x(t_2) - x(t_1) = -2\sigma$
III	1	0	0	$\sigma$	$\dot{x}(t_3) = 0$
IV	0	0	1	0	$x(t_4) - x(t_3) = 2\sigma$

The derivation Equation (1.2) differs from the derivation equation in [1] not only in a different definition of the function  $f(x_1)$ , discussed above, but also in a different definition of the function  $\Phi(t)$ . The function  $\Phi(t)$  in (1.2) is a Fourier series obtained from the Fourier series for  $F_j(t)$  by eliminating from (1.1) all the  $x_j$ 's except  $x_1$ . Here the transformation from the  $F_j(t)$  series to the  $\Phi(t)$  series involves the use of a finite number of term-by-term differentiations, additions of series, and multiplication of the series by numbers.

It can be seen from this method of obtaining the series  $\Phi(t)$  from the series  $F_j(t)$  that



$$\Phi(t) = \Phi_0(t) + \sum_q [\kappa_q \delta(t - t_q) + \kappa'_q \delta'(t - t_q) + \dots], \quad (1.5)$$

where  $t_q$  are the instants at which  $\Phi(t)$  and its derivatives become discontinuous, coinciding with the instants at which the functions  $F_j(t)$  become discontinuous;  $\kappa_q, \kappa'_q$ , etc. are the values of these discontinuities,  $\delta(t)$  is the Dirac function, and  $\Phi_0(t)$  is a convergent Fourier series.

Inserting (1.5) into (1.2), recalling Equation (1.4) of [1], and equating the terms that do not contain  $\delta, \delta', \dots$ ,\* we get the equation

$$\begin{aligned} D(p)x_1 &= K(p)y_1 + \Phi_0(t), \\ y_1 &= f(x_1), \end{aligned} \quad (1.6)$$

which now replaces Equation (1.5) of [1] and describes the course of the process on the sections where  $x_1, y_1$ , their respective derivatives, and  $\Phi(t)$  are continuous functions.

## 2. Derivation of the Equation for the Periods in the Generalized Problem

Let us now make the same change in variables in Equation (1.2) (see Equation (2.2) of [1]), with the coefficients being determined from Equation (2.4) [1]. We shall take the values of  $h_1$  and  $h_2$ , which enter into (2.4) of [1], for any two arbitrary parts of the characteristic, having slopes  $k'$  and  $k''$ , respectively. The transformation will cause the first of these line segments to become the  $\underline{x}$  axis of the  $(x, y)$  plane, with the second segment becoming the  $\underline{y}$  axis. The linear transformation [Equations (2.2)] of [1] keeps the straight lines parallel. All lines with slope  $k'$  thus become parallel to the  $\underline{x}$  axis in the  $(x, y)$  plane, and all lines with slope  $k''$  become parallel to the  $\underline{y}$  axis.\*\*

As in [1], Equation (1.2) becomes

$$L(p^*)x = M(p^*)y + \Psi(t), \quad (2.1)$$

and (1.6) becomes

$$L(p)x = M(p)y + \Psi_0(t), \quad (2.2)$$

where  $\Psi(t)$  and  $\Psi_0(t)$  are Fourier series differing from  $\Phi(t)$  and  $\Phi_0(t)$ , respectively only by constant terms.

The joining Conditions (1.4) are changed by this transformation into

$$\begin{aligned} & \sum_{j=1}^n \zeta_j [\alpha x^{(j-1)}(t_i) + \beta y^{(j-1)}(t_i)] + \\ & + \sum_{j=1}^n \pi_j [\alpha x^{(j-1)}(t_{i-1}) + \beta y^{(j-1)}(t_{i-1})] + \zeta + \kappa(\zeta_1 + \pi_1) = 0 \quad (i = 1, 2, \dots, N). \end{aligned} \quad (2.3)$$

\* If the coefficients of  $\delta, \delta', \dots$  are also equated the results are the "jump conditions," which differ in this problem from the "jump conditions" mentioned in [1] in that the discontinuities of  $\Phi(t)$  must be allowed for. These jump conditions are of no use to us, and will not be written down here.

\*\* Indeed, the need for insuring this circumstance forces us to restrict ourselves to characteristics composed of segments parallel to specified straight lines. Were the characteristic to contain segments with more than two slopes, the affine-transformed system would contain segments not parallel to the  $\underline{x}$  and  $\underline{y}$  axes, and the entire subsequent argument (in particular, the calculation of  $\mu$ ), could no longer be made with this method.

The motion of the point in the  $(x, y)$  plane during the periodic mode can be represented as follows (example in Fig. 5). At the instant  $t_0$ , the point is on line I (for example, on the  $x$  axis), along which it moves until it reaches at the instant  $t_1$  the point 2, where the first of Conditions (2.3) is satisfied for the first time. If line II passes through this point 2, the motion will continue on this line; if it does not, the point will jump instantaneously onto line II along a line having a slope  $\tan \varphi = \beta/\alpha$ . The point moves then along line II until reaching, at the instant  $t_2$ , point 4, where the second condition of (2.3) is satisfied for the first time, etc. Since the motion in the  $(x, y)$  plane is only along lines parallel to the  $x$  or the  $y$  axis, either  $x$  or  $y$  are constant on each of the intervals. Figure 6 shows an example of the variation of  $x$  and  $y$ , corresponding to the periodic process of Fig. 5.

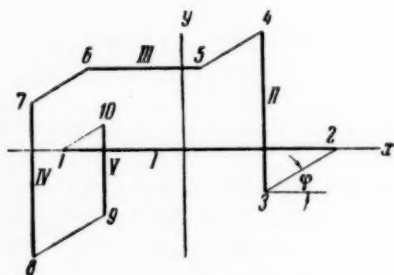


Fig. 5

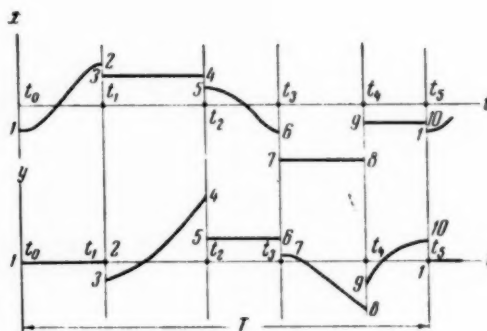


Fig. 6

If we retain the former symbols  $\epsilon_r$  for the Fourier coefficient of the series  $\psi(t)$ , and if we seek again periodic solutions in the form of Fourier series with Fourier coefficients  $\alpha_r$  and  $\beta_r$ , then Equations (3.1) of [1], which relate  $\alpha_r$  and  $\beta_r$  to the Fourier coefficients  $\mu_r^*$  of the function  $M(p^*)y$ , remain in force.

Let us retain the symbol  $\mu$  for the Fourier coefficients of the periodic function  $M(p)y$ . Equation (3.2) of [1]; relating  $\mu_r^*$  with  $\mu_r$ , can now be used also for the general case, but it becomes necessary to keep in this equation not two, but  $N$  terms — each term pertains to the instant  $t_1, t_2, \dots, t_N$ , respectively. Equation (3.2) of [1] therefore contains now  $Nn$  unknown quantities  $\eta_1$  — the discontinuities of the function  $y$ , and of its derivatives up to the  $(n-1)$ -th at these instants  $t_1, t_2, t_N$ . All these unknown discontinuities enter linearly into (3.2), while the unknown  $t_1, t_2, \dots, t_N$  are nonlinear.

The values of  $\mu_r$  are determined generally in the same manner as in the simplest case examined in [1] since the integral in the expression

$$\mu_r = \frac{1}{T} \int_{t_0}^{t_N} M(p) y e^{-ir\omega t} dt \quad (2.4)$$

can be expressed in terms of  $t_1, t_2, \dots, t_N$  if it is broken up into  $N$  integrals

$$\begin{aligned} \mu_r = \frac{1}{T} & \left[ \int_{t_0}^{t_1} M(p) y e^{-ir\omega t} dt + \right. \\ & \left. + \int_{t_1}^{t_2} M(p) y e^{-ir\omega t} dt + \dots + \int_{t_{N-1}}^{t_N} M(p) y e^{-ir\omega t} dt \right] \end{aligned} \quad (2.5)$$

and use is made of the fact that either  $x$  or  $y$  is constant between the integration limits of every one of these integrals.

In fact, if  $y = \text{const}_i$  in the interval  $t_{i-1} < t < t_i$ , this condition can be replaced with

$$M(p)y = b_n \text{const}_i,$$

$$y(t_i - 0) = \text{const}_i, y'(t_i - 0) = y''(t_i - 0) = \dots = y^{(n-1)}(t_i - 0) = 0. \quad (2.6)$$

$$(2.7)$$

Using (2.6), we can calculate the corresponding integral in (2.5)

$$\begin{aligned} \int_{t_{i-1}}^{t_i} M(p) y e^{-ir\omega t} dt &= b_n \text{const}_i \int_{t_{i-1}}^{t_i} e^{-ir\omega t} dt = \\ &= \frac{-b_n \text{const}_i}{ir\omega} [e^{-ir\omega t_i} - e^{-ir\omega t_{i-1}}]. \end{aligned}$$

If, on the other hand,  $x = \text{const}_j$  in the interval  $t_{j-1} < t < t_j$ , we get for this interval

$$L(p)x = a_n \text{const}_j,$$

$$x(t_j - 0) = \text{const}_j, x'(t_j - 0) = x''(t_j - 0) = \dots \quad (2.8)$$

$$\dots = x^{(n-1)}(t_j - 0) = 0. \quad (2.9)$$

It follows from (2.8) and (2.2) that

$$M(p)y = a_n \text{const}_j - \Psi_0(t)$$

and the corresponding integral in (6.11)

$$\begin{aligned} \int_{t_{j-1}}^{t_j} M(p) y e^{-ir\omega t} dt &= -\frac{a_n \text{const}_j}{ir\omega} [e^{-ir\omega t_j} - e^{-ir\omega t_{j-1}}] - \\ &- \int_{t_{j-1}}^{t_j} \Psi_0(t) e^{-ir\omega t} dt \end{aligned}$$

can be readily calculated, for the function  $\Psi_0(t)$  is specified.

We can thus compute all the integrals in (2.5), i.e., the values of  $\mu$ , but  $Nn$  initial conditions of the (2.7) or (2.9) type remain unused.

Substituting the found value of  $\mu_r$  into (3.2) of [1], we obtain  $\mu_r^*$ , which when substituted into (3.1) expresses all  $\alpha_r$  and  $\beta_r$  in terms of the  $Nn$  linearly related unknowns  $\eta_i^j$  and in terms of the  $N$  nonlinearly related unknowns  $t_1, t_2, \dots, t_N$ .

If we now require that the Fourier series  $x(t)$  and  $y(t)$ , obtained in this manner, satisfy all the  $Nn$  conditions of the (2.7) and (2.9) type, we obtain an inhomogeneous system of linear algebraic equations with respect to the  $Nn$  unknowns  $\eta_i^j$ . The coefficients of these linear algebraic equations depend upon the sought unknowns  $t_1, t_2, \dots, t_N$ .

Assuming for the time being the determinant of this system to be different from zero and solving this system, we obtain all the  $\eta_i^j$ 's as functions of  $t_1, t_2, \dots, t_N$ :

$$\eta_i^j = f_i^j(t_1, t_2, \dots, t_N) \quad \left( \begin{matrix} i = 0, 1, \dots, n-1, \\ j = 1, 2, \dots, N \end{matrix} \right). \quad (2.10)$$

Substituting now these  $\eta_i^j$ 's directly into the expressions for  $\alpha_r$  and  $\beta_r$  we obtain

$$x(t, t_1, t_2, \dots, t_N) \text{ and } y(t, t_1, t_2, \dots, t_N). \quad (2.11)$$

So far we did not use the "joining conditions" (2.3). Inserting now (2.11) into (2.3) we arrive at a system of  $N$  transcendental equations for the  $N$  unknowns  $t_1, t_2, \dots, t_N$ , i.e., at the equations for the periods.

The sought periodic modes are determined by the solutions of the equations for the periods, satisfying the following conditions:

a) the inequality

$$t_0 < t_1 < t_2 < \dots < t_N,$$

is satisfied, with  $t_0 = 0$  for self-oscillations and  $t_0 = T - t_N$  for forced oscillations;

b) there are no "switchovers" within the period, i.e., at instants  $t$  other than  $t_1, t_2, \dots, t_N$ .

Everything mentioned in [1] concerning the need for verifying whether the vanishing of the determinant of the system of the algebraic equations leads to additional solutions, and the entire contents of Section 4 of the first half of this work, concerning improvement to the convergence of the Fourier series, are equally in force for the more general case discussed here.

Let us remark in conclusion that the number of the unknown instants of time is reduced by one half if the mode is symmetrical, i.e., if it is known beforehand that

$$x(t) = -x\left(t + \frac{T}{2}\right), \quad y(t) = -y\left(t + \frac{T}{2}\right).$$

In this case one can consider only half the period  $\frac{T}{2}$  instead of the period  $T$ , as was done in [2].

#### LITERATURE CITED

- [1] M. A. Aizerman and F. R. Gantmakher, Determination of Periodic Modes in Systems with Piecewise Linear Characteristics Composed of Segments Parallel to Two Specified Lines, I. Automation and Remote Control, 18, 2 (1957).
- [2] M. A. Aizerman and F. R. Gantmakher, On the Determination of Periodic Modes in Nonlinear Dynamic Systems with Piecewise Linear Characteristics, Prikladnaia matematika i mekhanika, No. 5, 1956.

Received June 20, 1956.

# ON THE CALCULATION OF THE CORRELATION FUNCTION OF A STATIONARY RANDOM PROCESS FROM EXPERIMENTAL DATA

B. N. Kutin

(Moscow)

Discussion of the errors arising in the calculation of the correlation function of a stationary random process from experimental data and resulting from the fact that the process is observed during a finite time. The errors are estimated for the existing types of autocorrelation functions, which are determined approximately from the experimental data by various methods. Equations are derived for the mean-squared error in a so-obtained correlation function as a function of its argument.

To analyze the response of a dynamic system to a random action it is necessary to know the fundamental characteristic, namely the correlation function of the action or the related spectral density [1, 2].

In some cases the correlation function of the action can be calculated from theoretical probability considerations. In practice, however, this function must frequently be calculated from a set of curves that comprise the record of the random action  $x(t)$  ( $t$  is the running time) during a finite time interval. The correlation function so calculated is subject to errors, resulting from the finite time of observation of the random process  $x(t)$ . This article is devoted to an estimate of these errors.

The correlation function of a random process  $x(t)$  is defined as  $M[x(t)x(t+\tau)]$ , where  $M$  is the symbol for the mathematical expectation (mean value) [1-3].

The correlation function of the random process  $x(t)$  is sometimes defined somewhat differently [4, 5], for example, as  $M[\xi(t)\xi(t+\tau)]$ , where  $\xi(t) = x(t) - M[x(t)]$ .

For a stationary random process  $x(t)$ , the quantities  $M[x(t)x(t+\tau)]$  and  $M[\xi(t)\xi(t+\tau)]$  are functions of the variable  $\tau$  only and are independent of  $t$

$$R(\tau) = M[x(t)x(t+\tau)], \quad (0.1)$$

$$B(\tau) = M[\xi(t)\xi(t+\tau)], \quad (0.2)$$

and  $M[x(t)] = m = \text{const}$  and  $\xi(t) = x(t) - m$ .

One can obtain from (0.1) and (0.2) the following expression for  $B(\tau)$ :

$$B(\tau) = M[(x(t) - m)(x(t+\tau) - m)] = R(\tau) - m^2. \quad (0.3)$$

We shall call the function  $B(\tau)$  the middle correlation function to distinguish it from  $R(\tau)$ , thus emphasizing that  $B(\tau)$  is calculated for the random function  $x(t)$  taken with respect to its mean value  $m$ .

In the particular case when  $m = 0$  identically, the functions  $R(\tau)$  and  $B(\tau)$  become identical.

From the ergodic theorem, the function  $R(\tau)$  of a stationary random process with unity probability is expressed as:

$$R(\tau) = \lim_{T \rightarrow \infty} \frac{1}{T} \int_0^T x(t) x(t + \tau) dt. \quad (0.4)$$

Analogous relationships with unity probability hold also for the function  $B(\tau)$  and for the quantity  $m = M[x(t)]$ :

$$B(\tau) = \lim_{T \rightarrow \infty} \frac{1}{T} \int_0^T \xi(t) \xi(t + \tau) dt, \quad (0.5)$$

$$m = \lim_{T \rightarrow \infty} \frac{1}{T} \int_0^T x(t) dt. \quad (0.6)$$

The functions  $R(\tau)$  and  $B(\tau)$  can be calculated approximately from an experimentally-obtained record of the random function  $x(t)$ , using Equations (0.4) - (0.6).<sup>\*</sup> We shall denote the approximate values of the functions  $R(\tau)$  and  $B(\tau)$ , calculated from experimental data, by  $R_T(\tau)$  and  $B_T(\tau)$ , respectively. Owing to the finite time of observation  $T_{ob}$  of the random process  $x(t)$ , the quantities  $R_T(\tau)$  and  $B_T(\tau)$  are also random functions.

The degree to which the function  $R(\tau)$  is approximated by  $R_T(\tau)$  can be characterized by the mean-square  $\sigma_R^2(\tau)$  of the deviation of the function  $R_T(\tau)$  from  $R(\tau)$  [6, 7]

$$\sigma_R^2(\tau) = M[(R_T(\tau) - R(\tau))^2]. \quad (0.7)$$

Analogously, the degree of the approximation of  $B(\tau)$  by the function  $B_T(\tau)$  is given by the quantity

$$\sigma_B^2(\tau) = M[(B_T(\tau) - B(\tau))^2]. \quad (0.8)$$

References [6] and [7] give an expression for  $\sigma_R^2(\tau)$  only for  $\tau = 0$ , and for  $m$  identically equal to zero. In practice this is not enough.

One must bear in mind, in particular, that if  $\tau \neq 0$  the function  $R_T(\tau)$  can be calculated in various manners from the recorded random process  $x(t)$  during the time  $T_{ob}$ , and these will yield results that differ somewhat from each other. This, in turn results in different variations of  $\sigma_R^2(\tau)$  with  $\tau$ . The same can also be said of the quantities  $B_T(\tau)$  and  $\sigma_B^2(\tau)$ . Furthermore, the quantity  $m$  can in general not be assumed beforehand to vanish identically. It is therefore necessary to take into account, as will be shown below, the dependence of  $\sigma_R^2(\tau)$  on the quantity  $m$  and the dependence of  $\sigma_B^2(\tau)$  on the error that the finite time of observation  $T_{ob}$  introduces in the values of  $m$  calculated from the experimental data. This causes the quantities  $\sigma_R^2$  and  $\sigma_B^2$  to differ if  $m$  does not vanish identically.

It is also essential to know  $\sigma_R^2(\tau)$  and  $\sigma_B^2(\tau)$  to estimate the error in the calculation of the normalized correlation functions

$$\rho(\tau) = \frac{R(\tau)}{R(0)}, \quad (0.9)$$

\* Relationships (0.4) - (0.6) are subject to certain conditions (which are almost always satisfied), indicated, for example, in [3] and [4].



$$\beta(\tau) = \frac{B(\tau)}{B(0)}. \quad (0.10)$$

The purpose of this investigation is to fill the above-mentioned gaps.

### 1. Errors in Calculation of the Correlation Function $T(\tau)$

We shall estimate the errors in the calculation of the correlation function  $R(\tau)$  from the experimental data for several possible methods that can be used to calculate its approximate values  $R_T(\tau)$ .

Method 1. For a given  $T_{ob}$ , the maximum value of the time shift  $\tau$  ( $\tau_{max} > 0$ ) is chosen and used to determine the integration time

$$T = T_{ob} - \tau_{max} = \text{const}, \quad (1.1)$$

for all values of  $\tau$  satisfying the relationship

$$0 \leq \tau \leq \tau_{max} \quad (1.2)$$

The function  $R_T(\tau)$  is now calculated from the equation

$$R_T(\tau) = \frac{1}{T} \int_0^T x(t) x(t + \tau) dt, \quad (1.3)$$

where the quantity  $t + \tau$  turns out in this case to lie within the segment  $T_{ob}$  if  $0 \leq \tau \leq \tau_{max}$  and  $0 \leq t \leq T$ , i.e.,  $0 \leq t + \tau \leq T_{ob}$  (Fig. 1).

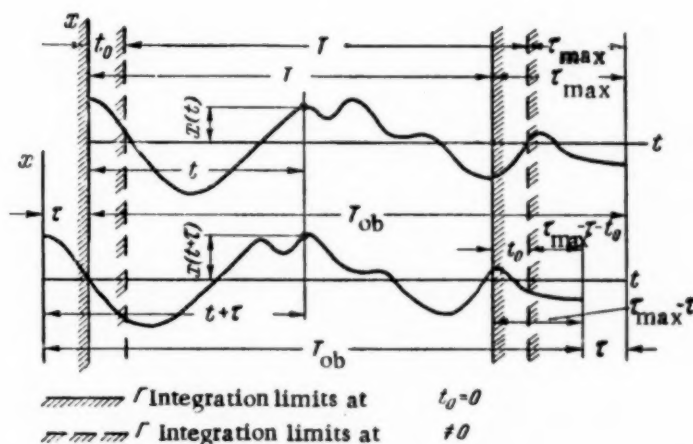


Fig. 1. Calculation of the function  $R_T(\tau)$  by Method 1.

The function  $R_T(\tau)$  can also be calculated by averaging the product  $x(t)x(t + \tau)$  over the same segment  $T$ , shifting the start and the end of the integration by an amount  $t_0$ :

$$R_T(\tau) = \frac{1}{T} \int_{t_0}^{T+t_0} x(t) x(t + \tau) dt, \quad (1.4)$$

where  $t_0 \geq 0$  must be chosen such as to make  $0 \leq t + \tau \leq T$ , i.e.,

$$0 \leq t_0 \leq \tau_{\max} - \tau. \quad (1.5)$$

**Method 2.** The integration time  $T$  is taken to vary with  $\tau$  and to equal

$$T = T_{\text{ob}} - \tau, \quad (1.6)$$

where  $\tau > 0$ , and the function  $R_T(\tau)$  is calculated from Equation (1.3), i.e.,

$$R_T(\tau) = \frac{1}{T_{\text{ob}} - \tau} \int_0^{T_{\text{ob}} - \tau} x(t) x(t + \tau) dt. \quad (1.7)$$

This method is illustrated graphically in Fig. 2.

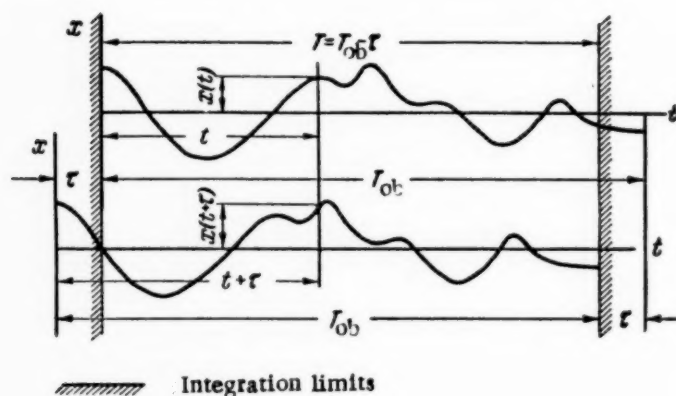


Fig. 2. Calculation of the function  $R_T(\tau)$  by Methods 2 and 3.

**Method 3.** The integration time  $T$  is chosen as in the preceding method, but the value of the integral of  $x(t)x(t + \tau)$  is referred to the time of observation  $T_{\text{ob}}$ , i.e.,

$$R_T(\tau) = \frac{1}{T_{\text{ob}}} \int_0^{T_{\text{ob}} - \tau} x(t) x(t + \tau) dt = \frac{1}{T_{\text{ob}}} \int_0^{T_{\text{ob}} - \tau} x(t) x(t + \tau) dt. \quad (1.8)$$

**Method 4.** The specified function  $x(t)$  is replaced over the segment  $T_{\text{ob}}$  by a periodic function  $x_p(t)$  having a period  $T_{\text{ob}}$  and identical with the specified function  $x(t)$  over the interval  $0 \leq t \leq T_{\text{ob}}$ . The value of  $R_T(\tau)$  is calculated from

$$R_T(\tau) = \frac{1}{T_{\text{ob}}} \int_0^{T_{\text{ob}}} x_p(t) x_p(t + \tau) dt = \frac{1}{T_{\text{ob}}} \int_0^{T_{\text{ob}} + t_0} x_p(t) x_p(t + \tau) dt, \quad (1.9)$$

where  $t_0$  is an arbitrary constant (Fig. 3).

The function  $R_T(\tau)$  is periodic with a period  $T_{\text{ob}}$ .

Let us proceed to calculate the mean-squared error  $\sigma_R(\tau)$  in the determination of the function  $R(\tau)$  from the experimental data.

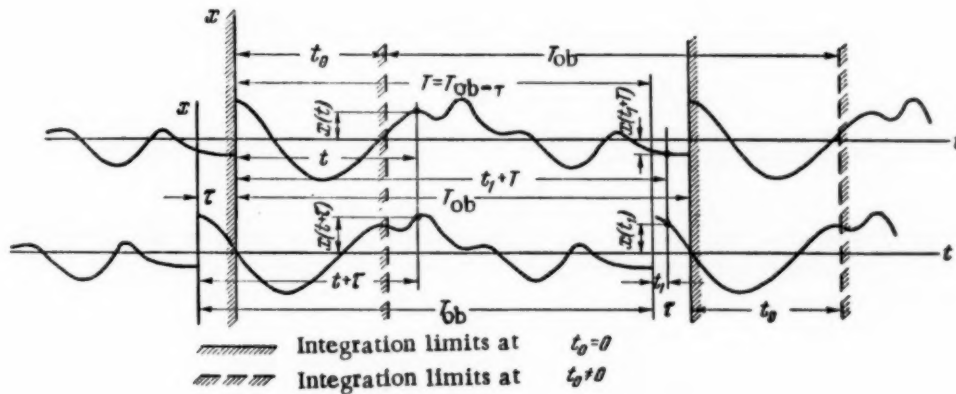


Fig. 3. Calculation of the function  $R_T(\tau)$  by Method 4.

Since  $R(\tau)$  is constant if  $\tau$  is constant, then, by virtue of the known properties of the mathematical expectation, Equation (0.7) can be rewritten as

$$\sigma_R^2(\tau) = M[R_T^2(\tau)] - 2R(\tau)M[R_T(\tau)] + R^2(\tau). \quad (1.10)$$

Equation (1.10) also yields an expression for  $\sigma_R(\tau)$  when  $R_T(\tau)$  is calculated by the above-mentioned methods.

Using Method 1. Inasmuch as the operation of the mathematical expectation and integration can be interchanged, we obtain from (0.1) and (1.3)

$$M[R_T(\tau)] = R(\tau) \quad (1.11)$$

and consequently

$$\sigma_R^2(\tau) = M[R_T^2(\tau)] - R^2(\tau). \quad (1.12)$$

$M[R_T^2(\tau)]$  becomes

$$M[R_T^2(\tau)] = \frac{1}{T^2} M \left[ \left( \int_0^T y(t) dt \right)^2 \right], \quad (1.13)$$

where  $y(t) = x(t)x(t+\tau)$ .

Assuming the probability distribution of the function  $x(t)$  to be normal, \* we obtain [see Equation (I.14) of Appendix I]

\* Such an assumption is valid in many practical cases.

$$R_y(\theta) = M[y(t)y(t+\theta)] = \\ = R^2(\tau) + R^2(0) + R(\theta+\tau)R(\theta-\tau) - 2m^4, \quad (1.14)$$

where  $R(\theta) = M[x(t)x(t+\theta)]$ , and  $m = M[x(t)]$ .

From (1.12), (1.13), (1.14), and (1.4) we get the following expression:

$$\sigma_R^2(\tau) = \frac{2}{T^2} \int_0^T (T-\theta) [R^2(\theta) + R(\theta+\tau)R(\theta-\tau)] d\theta - 2m^4. \quad (1.15)$$

As was already remarked, the function  $R_T(\tau)$  can be calculated for a chosen integration time  $T$  also with a certain shift in the start of the integration by an amount  $t_0$ , satisfying the Relationship (1.5), i.e.,  $R_T(\tau)$  can be calculated in two ways

$$R_{T[1]}(\tau) = \frac{1}{T} \int_0^T x(t)x(t+\tau) dt \quad (1.3)$$

and

$$R_{T[2]}(\tau) = \frac{1}{T} \int_{t_0}^{T+t_0} x(t)x(t+\tau) dt. \quad (1.4)$$

The quantity  $R_{T[2]}(\tau)$  represents an approximate value of the function  $R(\tau)$ , subject to the same mean-squared error  $R(\tau)$  as the approximation  $R_{T[1]}(\tau)$ . This is seen from (1.4), (1.11) - (1.14), and (1.6).

The quantity  $R_{T[2]}(\tau)$ , being a random function like  $R_{T[1]}(\tau)$ , may differ somewhat from  $R_{T[1]}(\tau)$ .

The distinction between the functions  $R_{T[1]}(\tau)$  and  $R_{T[2]}(\tau)$  can be estimated by the mean square of their difference:

$$\sigma_0^2(\tau) = M[(R_{T[1]}(\tau) - R_{T[2]}(\tau))^2]. \quad (1.16)$$

Using (1.3) and (1.4), we get

$$\sigma_0^2(\tau) = \frac{4}{T^2} \int_0^{t_0} (t_0-\theta) [R^2(\theta) + R(\theta+\tau)R(\theta-\tau)] d\theta - \\ - \frac{2}{T^2} \int_0^{t_0} (t_0-\theta) [R^2(\theta+T) + R(\theta+T+\tau)R(\theta+T-\tau)] d\theta - \\ - \frac{2}{T^2} \int_0^{t_0} (t_0-\theta) [R^2(\theta-T) + R(\theta-T+\tau)R(\theta-T-\tau)] d\theta. \quad (1.17)$$

Using Method 2. It is easy to see that in this case, as in Method 1:

$$M[R_T(\tau)] = R(\tau), \quad (1.18)$$

and the expression for  $\sigma_T^2(\tau)$  is

$$\sigma_R^2(\tau) = \frac{2}{(T_{ob} - \tau)^2} \int_0^{T_{ob} - \tau} (T_{ob} - \tau - \theta) [R^2(\theta) + R(\theta + \tau) R(\theta - \tau)] d\theta - 2m^4. \quad (1.19)$$

Let us determine, for example, the quantity  $\sigma_R^2(T_{ob})$  from (1.19). Denoting

$$F(\theta, T) = R^2(\theta) + R(\theta + T_{ob} - T) R(\theta - T_{ob} + T) \quad (1.20)$$

and assuming the function  $R(\theta)$  to be continuous, the well-known theorems on the mean value of an integral yield in the limit

$$\begin{aligned} \sigma_R^2(T_{ob}) &= 2 \lim_{T \rightarrow 0} F(\theta_1, T) \frac{1}{T} \int_0^T d\theta - \\ &- 2 \lim_{T \rightarrow 0} F(\theta_2, T) \frac{1}{T^2} \int_0^T \theta d\theta - 2m^4 = F(0, 0) - 2m^4, \end{aligned} \quad (1.21)$$

where  $0 \leq \theta_1 \leq T$  and  $0 \leq \theta_2 \leq T$ .

Hence

$$\sigma_R^2(T_{ob}) = R^2(0) + R^2(T_{ob}) - 2m^4. \quad (1.22)$$

Using Method 3. In the calculation of  $R_T(\tau)$  by Method 3, we obtain

$$M[R_T(\tau)] = \frac{T}{T_{ob}} R(\tau) = \left(1 - \frac{\tau}{T_{ob}}\right) R(\tau), \quad (1.23)$$

where

$$\lim_{T_{ob} \rightarrow \infty} M[R_T(\tau)] = R(\tau) \quad (1.24)$$

and

$$\begin{aligned} \sigma_R^2(\tau) &= \frac{2}{T_{ob}^2} \int_0^T (T - \theta) [R^2(\theta) + R(\theta + \tau) R(\theta - \tau)] d\theta + \\ &+ \frac{\tau^2}{T_{ob}^2} R^2(\tau) - 2m^4 \left(1 - \frac{\tau}{T_{ob}}\right)^2, \end{aligned} \quad (1.25)$$

where  $T = T_{ob} - \tau$ .

Equation (1.25) yields for  $\tau = T_{ob}$ , i.e., for  $T = T_{ob} - \tau = 0$ , the following obvious expression for  $\sigma_R^2(\tau)$ :

$$\sigma_R^2(T_{ob}) = R^2(T_{ob}), \quad (1.26)$$

which can be obtained also directly from (0.7) by recalling that  $R_T(T_{ob}) = 0$ .

Using Method 4. It is evident from Fig. 3 that

$$\int_0^{T_{ob}} x_p(t) x_p(t + \tau) dt = \int_0^T x(t) x(t + \tau) dt + \int_0^\tau x(t) x(t + T) dt, \quad (1.27)$$

and this means, from (1.9)

$$R_T(\tau) = \frac{1}{T_{ob}} \int_0^T x(t) x(t + \tau) dt + \frac{1}{T_{ob}} \int_0^\tau x(t) x(t + T) dt, \quad (1.28)$$

where  $T = T_{ob} - \tau$ .

It follows from the equations employed above that

$$M[R_T(\tau)] = \frac{T}{T_{ob}} R(\tau) + \frac{\tau}{T_{ob}} R(T) = \left(1 - \frac{\tau}{T_{ob}}\right) R(\tau) + \frac{\tau}{T_{ob}} R(T), \quad (1.29)$$

where

$$\lim_{T_{ob} \rightarrow \infty} M[R_T(\tau)] = R(\tau). \quad (1.30)$$

Using (1.3) and (1.14) we get

$$\begin{aligned} \sigma_R^2(\tau) = & \frac{2}{T_{ob}^2} \int_0^T (T - \theta) [R^2(\theta) + R(\theta + \tau) R(\theta - \tau)] d\theta + \\ & + 2 \frac{T}{T_{ob}^2} \int_0^\tau [R(\theta - T) R(\theta - \tau) + R(\theta) R(\theta - T - \tau)] d\theta - \\ & - \frac{2}{T_{ob}^2} \int_0^T \theta [R(\theta - T) R(\theta + \tau) + R(\theta) R(\theta - T + \tau)] d\theta + \\ & + \frac{2}{T_{ob}^2} \int_0^T \theta [R(\theta - T) R(\theta - \tau) + R(\theta) R(\theta - T - \tau)] d\theta + \\ & + \frac{2}{T_{ob}^2} \int_0^\tau (\tau - \theta) [R^2(\theta) + R(\theta + T) R(\theta - T)] d\theta + \\ & + \frac{\tau^2}{T_{ob}^2} [R(\tau) - R(T)]^2 - 2m^4, \end{aligned} \quad (1.31)$$

where  $T = T_{ob} - \tau$ .

Let us note the following corollary of (1.31):

$$\sigma_R^2(T_{ob}) = \sigma_R^2(0) + [R(T_{ob}) - R(0)]^2. \quad (1.32)$$

Equations (1.32) can be given a simple interpretation on the basis of (0.7), taking into account Equation (1.29) and the fact that the function  $R_T(\tau)$  is periodic.



## 2. Errors in Calculation of the Middle Correlation Function $B(\tau)$

One can calculate the function  $B(\tau)$  approximately from the experimental data by one of two ways:

Variant 1. The approximate value of  $B(\tau)$  is assumed to be, from (0.3),

$$B_T(\tau) = R_T(\tau) - m_T^2, \quad (2.1)$$

where  $R_T(\tau)$  is calculated for the random function  $x(t)$  by one of the methods considered above (see Section 1), and  $m_T$  is the approximate value of  $m = M[x(t)]$ . Here  $m_T$  is calculated from an Equation similar to (0.6):

$$m_T = \frac{1}{T_{ob}} \int_0^{T_{ob}} x(t) dt, \quad (2.2)$$

where  $T_{ob}$  is the time of observation of the random process  $x(t)$ .

The quantity  $m_T$ , like  $R_T(\tau)$ , is a random function, as a consequence of the finite time of observation  $T_{ob}$ .

Variant 2. The function  $B(\tau)$  is assumed approximately equal to

$$B_T(\tau) = R_{\eta T}(\tau), \quad (2.3)$$

where  $R_{\eta T}(\tau)$  is calculated from the value of  $m_T$  obtained from (2.2) for the random function  $\eta(t) = x(t) - m_T$ , using one of the methods of Section 1.

Let us examine the expressions for the mean-squared error  $\sigma_B(\tau)$ .

If  $B_T(\tau)$  is calculated by the first variant,  $\sigma_B^2(\tau)$  can be represented as

$$\sigma_B^2(\tau) = \sigma_R^2(\tau) - 2\mu(\tau) + \sigma_{m^2}, \quad (2.4)$$

where

$$\begin{aligned} \sigma_R^2(\tau) &= M[(R_T(\tau) - R(\tau))^2], \\ \mu(\tau) &= M[(R_T(\tau) - R(\tau))(m_T^2 - m^2)], \\ \sigma_{m^2} &= M[(m_T^2 - m^2)^2]. \end{aligned}$$

One can readily obtain a similar equation for  $\sigma_m^2$ :

$$\sigma_m^2 = (x_R - m^2)(3x_R + m^2); \quad (2.5)$$

where

$$x_R = \frac{2}{T_{ob}^2} \int_0^{T_{ob}} (T_{ob} - \theta) R(\theta) d\theta.$$

The quantities  $\sigma_R^2(\tau)$  and  $\mu(\tau)$  that enter into (2.4) in addition to  $\sigma_m^2$  depend on the method used to calculate the function  $R_T(\tau)$ . Equations for  $\sigma_R^2(\tau)$  were derived earlier. The four methods indicated for the calculation of the function  $R_T(\tau)$  yield:

$$\mu(\tau) = \frac{2}{T} \int_0^T P(t) P(t+\tau) dt - 2m^4, \quad T = T_{ob} - \tau_{\max} \quad (2.6)$$

$$\mu(\tau) = \frac{2}{T_{ob} - \tau} \int_0^{T_{ob} - \tau} P(t) P(t+\tau) dt - 2m^4, \quad (2.7)$$

$$\begin{aligned} \mu(\tau) &= \frac{2}{T_{ob}} \int_0^{T_{ob} - \tau} P(t) P(t+\tau) dt + \\ &+ \frac{\tau}{T_{ob}} R(\tau) (m^2 - x_R) - 2 \left(1 - \frac{\tau}{T_{ob}}\right) m^4, \end{aligned} \quad (2.8)$$

$$\begin{aligned} \mu(\tau) &= \frac{2}{T_{ob}} \int_0^T P(t) P(t+\tau) dt + \frac{2}{T_{ob}} \int_0^\tau P(t) P(t+T) dt + \\ &+ \frac{\tau}{T_{ob}} [R(\tau) - R(T)] (m^2 - x_R) - 2m^4 \\ &T = T_{ob} - \tau, \end{aligned} \quad (2.9)$$

where

$$P(t) = \frac{1}{T_{ob}} \int_0^{T_{ob}} R(\theta - t) dt.$$

In the calculation of  $\sigma_B^2(\tau)$  it may be more convenient to employ the function  $B(\theta)$  in the equations for  $\sigma_R^2(\tau)$ ,  $\sigma_m^2$ , and  $\mu(\tau)$  in lieu of  $R(\theta)$ ; this is readily done with the aid of (0.3).

If  $B_T(\tau)$  is calculated in the second of the two variants in the form of a function  $R_{\eta T}(\tau)$ , obtained in turn (by one of the methods discussed in Section 1, for the random function  $\eta(t) = x(t) - m_T$ , the function  $B_T(\tau)$  can be expressed in terms of  $R_T(\tau)$ :

$$B_T(\tau) = R_T(\tau) - E_T(\tau). \quad (2.10)$$

Here  $R_T(\tau)$  represents an approximate value of the function  $R(\tau)$ , which can be calculated for the random function  $x(t)$  as indicated in Section 1. Depending on the function used to calculate the function  $R_{\eta T}(\tau) = B_T(\tau)$ , the quantity  $E_T(\tau)$  is given by one of the following equations:

$$E_T(\tau) = \frac{m_T}{T} \int_0^T [x(t) + x(t+\tau)] dt - m_T^2, \quad T = T_{ob} - \tau_{\max} \quad (2.11)$$

$$E_T(\tau) = \frac{m_T}{T_{ob} - \tau} \int_0^{T_{ob} - \tau} [x(t) + x(t+\tau)] dt - m_T^2, \quad (2.12)$$

$$E_T(\tau) = \frac{m_T}{T_{ob}} \int_0^{T_{ob} - \tau} [x(t) + x(t+\tau)] dt - \left(1 - \frac{\tau}{T_{ob}}\right) m_T^2, \quad (2.13)$$

$$\begin{aligned}
E_T(\tau) &= \frac{m_T}{T_{ob0}} \int_0^T [x(t) + x(t + \tau)] dt + \\
&+ \frac{m_T}{T_{ob0}} \int_0^\tau [x(t) + x(t + T)] dt - m_T^2 = m_T^2, \\
T &= T_{ob} - \tau.
\end{aligned} \tag{2.14}$$

In this manner, taking (0.3) into account, we obtain for  $\sigma_B^2(\tau)$

$$\sigma_B^2(\tau) = \sigma_R(\tau) - 2\nu(\tau) + \sigma_E^2, \tag{2.15}$$

where

$$\begin{aligned}
\sigma_R^2(\tau) &= M[(R_T(\tau) - R(\tau))^2], \\
\nu(\tau) &= M[(R_T(\tau) - R(\tau))(E_T(\tau) - m^2)], \\
\sigma_E^2 &= M[(E_T(\tau) - m^2)^2].
\end{aligned}$$

Equations for  $\sigma_R^2(\tau)$ , in which  $R(\theta)$  is replaced by  $B(\theta)$  [according to (0.3)], as well as equations for  $\sigma_E^2$  and  $\nu(\tau)$ , all applying to the second variant for the calculation of  $B_T(\tau)$ , are given in Appendix II.

### 3. Errors in the Determination of the Normalized Correlation Function $\rho(\tau)$

An approximate expression for the function  $\rho(\tau) = \frac{R(\tau)}{R(0)}$  is given by

$$\rho_T(\tau) = \frac{R_T(\tau)}{R_T(0)}, \tag{3.1}$$

where  $R_T(\tau)$  and  $R_T(0)$  are calculated from experimental data (see Section 1).

It is evident that  $\rho_T(\tau)$ , like the functions  $R_T(\tau)$  and  $R_T(0)$ , is a random function.

In analogy with the above, the error in calculating  $\rho(\tau)$  from experimental data is estimated by means of the quantity

$$\sigma_\rho^2(\tau) = M[(\rho_T(\tau) - \rho(\tau))^2] = M\left[\left(\frac{R_T(\tau)}{R_T(0)} - \rho(\tau)\right)^2\right]. \tag{3.2}$$

Since we have  $\rho_T(0) = \rho(0) = 1$ , for  $\tau = 0$ , and consequently  $\sigma_\rho^2(0) = 0$ , the only values of  $\sigma_\rho^2(\tau)$  of interest are at  $\tau \neq 0$ . It will be shown below that  $\sigma_\rho^2(\tau)$  depends on the quantity  $\sigma_R^2(\tau)$  discussed above.

We shall merely approximate  $\sigma_\rho^2(\tau)$ , since the exact calculation is quite complicated. We shall assume here (as is frequently done; see, for example [8]) that the ratio  $\frac{R_T(\tau)}{R_T(0)} = f[R_T(\tau), R_T(0)]$  can be represented with an accuracy sufficient for practical purposes by the linear terms of a Taylor expansion of the function  $f[R_T(\tau), R_T(0)]$ :

$$\begin{aligned} \frac{R_T(\tau)}{R_T(0)} &= f(R_T(\tau), R_T(0)) = f(M[R_T(\tau)], M[R_T(0)]) + \\ &+ \frac{\partial f}{\partial R_T(\tau)} \Delta R_T(\tau) + \frac{\partial f}{\partial R_T(0)} \Delta R_T(0), \end{aligned} \quad (3.3)$$

where

$$\Delta R_T(\tau) = R_T(\tau) - M[R_T(\tau)], \quad \Delta R_T(0) = R_T(0) - M[R_T(0)],$$

and the partial derivatives of the function  $f[R_T(\tau), R_T(0)]$  are taken at the point  $M[R_T(\tau)], M[R_T(0)]$ .

Let us remark that the assumption made above concerning the possibility of using (3.3) to represent the ratio  $\frac{R_T(\tau)}{R_T(0)}$  follows from the assumption of a rather high probability that the quantities  $R_T(\tau)$  and  $R_T(0)$  deviate from their mathematical expectations in a sufficiently narrow range. We are essentially using here a device commonly employed in the theory of errors to calculate the error of a quantity that is a function of several directly-measured quantities (see, for example, [9]).

From (3.3), we get

$$\begin{aligned} \frac{R_T(\tau)}{R_T(0)} - \rho(\tau) &= \frac{R_T(\tau) - R(\tau)}{M[R_T(0)]} - \frac{M[R_T(\tau)]}{(M[R_T(0)])^2} (R_T(0) - R(0)) + \\ &+ \frac{(M[R_T(0)] - R(0))(R(0)M[R_T(\tau)] - R(\tau)M[R_T(0)])}{R(0)(M[R_T(0)])^2}. \end{aligned} \quad (3.4)$$

Taking into account that all the methods used above to calculate  $R_T(\tau)$  yield

$$M[R_T(0)] = R(0), \quad (3.5)$$

and bearing in mind only these methods for the calculation of  $R_T(\tau)$ , we obtain from (3.2) and (3.4) as a final result

$$\sigma_p^2(\tau) = \frac{1}{R^2(0)} \sigma_R^2(\tau) - 2 \frac{M[R_T(\tau)]}{R^3(0)} \lambda_R(\tau) + \frac{(M[R_T(\tau)])^2}{R^4(0)} \sigma_R^2(0), \quad (3.6)$$

where

$$\lambda_R(\tau) = M[(R_T(\tau) - R(\tau))(R_T(0) - R(0))]. \quad (3.7)$$

Let us incidentally remark that it follows from (3.7) that at  $\tau = 0$

$$\lambda_R(0) = \sigma_R^2(0), \quad (3.8)$$

and (3.5) and (3.6) yield the obvious expression  $\sigma_p^2(0) = 0$ .

With the aid of the above equations one can derive for  $\lambda_R(\tau)$  the following expressions for the four methods of calculating  $R_T(\tau)$ :

$$\lambda_R(\tau) = \frac{2}{T^2} \int_0^T (T-\theta) R(\theta) [R(\theta+\tau) + R(\theta-\tau)] d\theta - 2m^4, \quad (3.9)$$

$$\begin{aligned} T &= T_{ob} - \tau_{\max} \\ \lambda_R(\tau) &= \frac{4}{T_{ob}(T_{ob}-\tau)} \int_0^{T_{ob}-\tau} (T_{ob}-\tau-\theta) R(\theta) R(\theta+\tau) d\theta + \\ &+ \frac{2}{T_{ob}} \int_0^\tau R(\theta) R(\theta-\tau) d\theta - 2m^4, \end{aligned} \quad (3.10)$$

$$\begin{aligned} \lambda_R(\tau) &= \frac{4}{T_{ob}^2} \int_0^{T_{ob}-\tau} (T_{ob}-\tau-\theta) R(\theta) R(\theta+\tau) d\theta + \\ &+ \frac{2\left(1-\frac{\tau}{T_{ob}}\right)}{T_{ob}} \int_0^\tau R(\theta) R(\theta-\tau) d\theta - 2m^4 \left(1-\frac{\tau}{T_{ob}}\right), \end{aligned} \quad (3.11)$$

$$\begin{aligned} \lambda_R(\tau) &= \frac{4}{T_{ob}^2} \int_0^T (T-\theta) R(\theta) R(\theta+\tau) d\theta + \\ &+ 2 \frac{\tau}{T_{ob}^2} \int_0^T R(\theta) R(\theta-T) d\theta + \\ &+ \frac{4}{T_{ob}^2} \int_0^\tau (\tau-\theta) R(\theta) R(\theta+T) d\theta + \\ &+ 2 \frac{T}{T_{ob}^2} \int_0^\tau R(\theta) R(\theta-\tau) d\theta - 2m^4, \end{aligned} \quad (3.12)$$

$$T = T_{ob} - \tau.$$

#### 4. Errors in the Normalized Middle Correlation Function $\beta(\tau)$

Using the following approximate equation for the function  $\beta(\tau) = \frac{B(\tau)}{B(0)}$

$$\beta_T(\tau) = \frac{B_T(\tau)}{B_T(0)}, \quad (4.1)$$

we introduce the following estimate for the error resulting when  $\beta(\tau)$  is computed from experimental data:

$$\sigma_\beta^2(\tau) = M[(\beta_T(\tau) - \beta(\tau))^2] = M\left[\left(\frac{B_T(\tau)}{B_T(0)} - \beta(\tau)\right)^2\right], \quad (4.2)$$

with  $B_T(\tau)$  and  $B_T(0)$  calculated as shown in Section 2.

Reasoning exactly as in the derivation of Equation (3.4) for the difference  $\frac{B_T(\tau)}{B_T(0)} - \beta(\tau)$ , we obtain for  $\frac{B_T(\tau)}{B_T(0)} - \beta(\tau)$  an identical approximate equation

$$\frac{B_T(\tau)}{B_T(0)} - \beta(\tau) = \frac{B_T(\tau) - B(\tau)}{M[B_T(0)]} - \frac{M[B_T(\tau)]}{(M[B_T(0)])^2} (B_T(0) - B(0)) + \\ + \frac{(M[B_T(0)] - B(0)) (B(0) M[B_T(\tau)] - B(\tau) M[B_T(0)])}{B(0) (M[B_T(0)])^2} \quad (4.3)$$

From (4.2) and (4.3), we get

$$\sigma_B^2(\tau) = \frac{1}{(M[B_T(0)])^2} \sigma_B^2(\tau) - 2 \frac{M[B_T(\tau)]}{(M[B_T(0)])^2} \lambda_B(\tau) + \\ + \frac{(M[B_T(\tau)])^2}{(M[B_T(0)])^4} \sigma_B^2(0) + \gamma_B(\tau), \quad (4.4)$$

where

$$\lambda_B(\tau) = M[(B_T(\tau) - B(\tau))(B_T(0) - B(0))], \quad (4.5)$$

$$\gamma_B(\tau) = \frac{\{(M[B_T(0)])^2 - B^2(0)\} \{B(0) M[B_T(\tau)] - B(\tau) M[B_T(0)]\}^2}{B^2(0) (M[B_T(0)])^4}. \quad (4.6)$$

Appendix III gives the equations for  $\lambda_B(\tau)$  and  $\gamma_B(\tau)$  used in the calculation of the function  $B_T(\tau)$  in the first and second variants.

Let us also remark that the function  $\beta_T(\tau)$  can also be calculated directly from known values of  $\rho_T(\tau)$ :

$$\beta_T(\tau) = \frac{\rho_T(\tau) - \bar{m}_{TR}^2}{1 - \bar{m}_{TR}^2}, \quad (4.7)$$

where

$$\bar{m}_{TR} = \frac{m_T}{V R_T(0)}.$$

Equation (4.7) follows from the expression

$$\beta_T(\tau) = \frac{B_T(\tau)}{B_T(0)} = \frac{R_T(\tau) - m_R^2}{R_T(0) - m_R^2}.$$

\* An analogous equation, incidentally, also holds for the exact values of  $\beta(\tau)$  and  $\rho(\tau)$ :

$$\beta(\tau) = \frac{\rho(\tau) - \bar{m}_R^2}{1 - \bar{m}_R^2},$$

where

$$\bar{m}_R = \frac{m}{V R(0)}.$$



It is readily seen that Equation (4.7) gives for  $\beta_T(\tau)$  the same values that  $B_T(\tau)$  and  $B_T(0)$ , calculated by means of the first variant above, give for  $\beta_T(\tau) = \frac{B_T(\tau)}{B_T(0)}$ . Therefore, if  $\beta_T(\tau)$  is obtained from (4.7), it is necessary to estimate the error in the calculation of  $\beta(\tau)$  with the aid of Equations (4.4) - (4.6).

##### 5. Remarks on the Calculation of the Mean-Squared Errors $\sigma(\tau)$

It follows from the above that to obtain  $\sigma_T^2(\tau)$  it is necessary in general to know the true correlation function  $R(\tau)$  and the true value of  $m = M[x(t)]$ . On the other hand, the experimental data yield only the approximate quantities  $R_T(\tau)$  and  $m_T$ , from which it is possible to calculate  $\sigma_R^2(\tau)$  approximately. It is possible here to estimate whether the time of observation  $T_{ob}$  was correctly chosen and to calculate the maximum time shift, starting with the condition

$$\sigma_R(\tau) \leq \sigma_{R\text{ per}}, \quad (5.1)$$

where  $\sigma_{R\text{ per}}$  is the maximum permissible value of the mean-squared error  $\sigma_R(\tau)$ .

If  $\sigma_R(\tau)$  turns out to be greater than  $\sigma_{R\text{ per}}$  when  $\sigma_R(\tau)$  is calculated for the values of  $\tau$  of interest to us, it is obvious from the above that the time of observation  $T_{ob}$  must be increased. At the same time any analytic approximation of the function  $R_T(\tau)$  yields an analytic form for the function  $\sigma_R^2(\tau)$ , thus simplifying the calculation in many cases. Analogous remarks can be made also concerning the calculation of  $\sigma_B$ ,  $\sigma_\rho(\tau)$ , and  $\sigma_\beta(\tau)$ .

Let us remark further that instead of the mean-squared error  $\sigma_R(\tau)$ , it may be more convenient to calculate the error with respect to the correlation function at  $\tau = 0$ :

$$\bar{\sigma}_R(\tau) = \frac{\sigma_R(\tau)}{R(0)}. \quad (5.2)$$

Equations for  $\bar{\sigma}_R^2(\tau)$  are obtained from the expressions given above for  $\sigma_R^2(\tau)$ , by replacing the correlation function  $R(\tau)$  and the quantity  $\bar{m}$  in these expressions by the normalized correlation function  $\rho(\tau) = \frac{R(\tau)}{R(0)}$  and the quantity  $\bar{m}_R = \frac{m}{\sqrt{R(0)}}$  respectively.

For example, if the function  $R_T(\tau)$  is calculated by the first method, we obtain from (1.15) the following expression for  $\bar{\sigma}_R^2(\tau)$ :

$$\bar{\sigma}_R^2(\tau) = \frac{2}{T^2} \int_0^T (T - \theta) [\rho^2(\theta) + \rho(\theta + \tau)\rho(\theta - \tau)] d\theta - 2\bar{m}_R^4. \quad (5.3)$$

In exactly the same manner, one can consider instead of  $\sigma_B(\tau)$  the relative error

$$\bar{\sigma}_B(\tau) = \frac{\sigma_B(\tau)}{B(0)}. \quad (5.4)$$

The functions  $\bar{\sigma}_B^2(\tau)$  are calculated from the equations given above for  $\sigma_B^2(\tau)$ , in which the functions  $R(\tau)$  and  $B(\tau)$  are replaced by  $\frac{\rho(\tau)}{1 - \bar{m}_R^2}$  and  $\beta(\tau)$  respectively, where  $\bar{m}_R = \frac{m}{\sqrt{R(0)}}$ . With this, the quantity  $\bar{m}$  is replaced by either  $\frac{m}{\sqrt{1 - \bar{m}_R^2}}$  or  $\bar{m}_B = \frac{m}{\sqrt{B(0)}}$ . quantity  $\bar{m}$  is replaced by either  $\frac{m}{\sqrt{1 - \bar{m}_R^2}}$  or  $\bar{m}_B = \frac{m}{\sqrt{B(0)}}$ .

Let us also remark that  $\sigma_\rho^2(\tau)$  and  $\sigma_\beta^2(\tau)$  can be expressed in terms of  $\bar{\sigma}_R^2(\tau)$ ,  $\bar{\sigma}_B^2(\tau)$ , and the functions  $\rho(\tau)$  and  $\beta(\tau)$ .

By way of an illustration, if  $R_T(\tau)$  is calculated by Method 1, we obtain for  $\sigma_p^2(\tau)$  from (1.11), (3.6), and (3.9):

$$\sigma_p^2(\tau) = \bar{\sigma}_R^2(\tau) - 2\rho(\tau)\bar{\lambda}_R(\tau) + \rho^2(\tau)\bar{\sigma}_R^2(0), \quad (5.5)$$

where

$$\begin{aligned} \bar{\lambda}_R(\tau) = \frac{2}{T^2} \int_0^T (T-\theta)\rho(\theta)[\rho(\theta+\tau) + \\ + \rho(\theta-\tau)]d\theta - 2\bar{m}_R^4. \end{aligned} \quad (5.6)$$

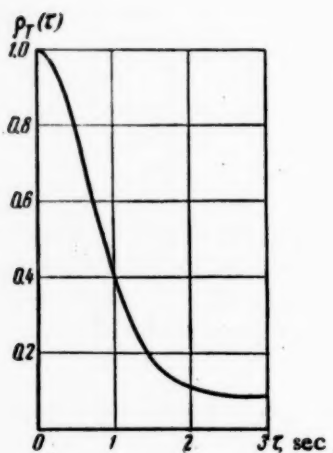


Fig. 4. Function  $\rho_T(\tau) = (1 - a^2)e^{-\alpha^2\tau^2} + a^2$  at  $\alpha = 1 \text{ sec}^{-1}$  and  $a = 0.3$ .

In conclusion, let us consider one example of the calculation of the mean-squared error.

Assume that the normalized correlation function  $\rho_T(\tau) = \frac{R_T(\tau)}{R_T(0)}$ , calculated from the experimental data, can be approximated by the expression

$$\rho_T(\tau) = (1 - a^2)e^{-\alpha^2\tau^2} + a^2,$$

where  $\alpha$  and  $a$  are constants. Let us also assume here

$$\bar{m}_{TR} = \frac{m_T}{V R(0)} = a.$$

Figure 4 shows the function  $\rho_T(\tau)$  for  $\alpha = 1 \text{ sec}^{-1}$  and  $a = 0.3$ .

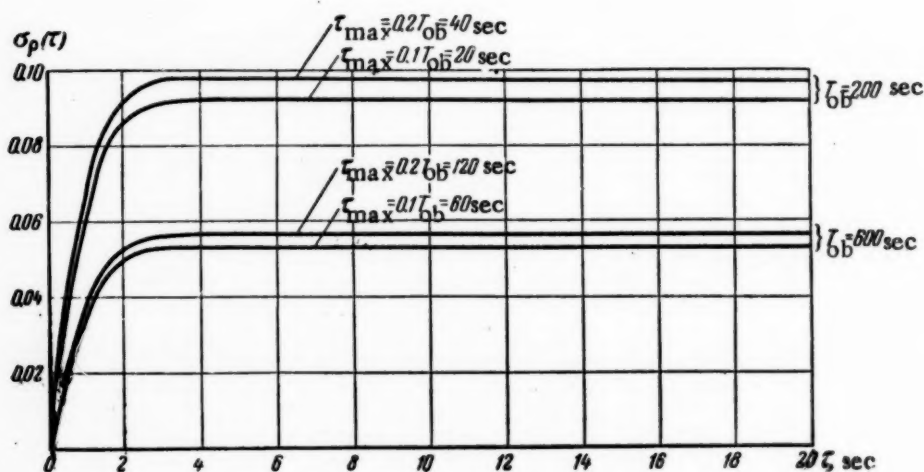


Fig. 5. Mean-squared error in the calculation of the normalized correlation function of the form shown in Fig. 4.

Assuming that the function  $R_T(\tau)$  was calculated by Method 1 for  $\sigma_\rho(\tau) = \sqrt{\sigma_\rho^2(\tau)}$  at  $\alpha = 1 \text{ sec}^{-1}$  and  $a = 0.3$ , we obtain the values shown in Fig. 5 for  $T_{\text{Ob}} = 200$  and  $600 \text{ sec}$ . From Fig. 5, incidentally, it is evident that  $\sigma_\rho(\tau)$  diminishes with increasing  $T_{\text{Ob}}$  and with diminishing  $\tau_{\text{max}}$ . With the aid of curves similar to those shown in Fig. 5 one can choose the time of observation  $T_{\text{Ob}}$  to suit a specified accuracy of the correlation function for the required values of the time shift  $\tau$ .

## APPENDIX I

### Derivation of Certain Equations

Let us consider the mathematical expectation of the product of two definite integrals of stationarily-related random functions  $y_1(t)$  and  $y_2(t)$ :

$$M \left[ \int_{a_1}^{b_1} y_1(t) dt \int_{a_2}^{b_2} y_2(t) dt \right] = M \left[ \int_{a_1}^{b_1} \int_{a_2}^{b_2} y_1(t) y_2(\theta) dt d\theta \right]. \quad (I.1)$$

By "stationarily-related functions" we mean here two functions  $y_1(t)$  and  $y_2(t)$  having a mutual correlation function

$$R_{y_1 y_2}(\theta) = M[y_1(t) y_2(t + \theta)] \quad (I.2)$$

that depends only on the time shift  $\theta$  [3].

Introducing in (I.1) a new variable  $\theta = \theta - t$  instead of  $\theta$ , and interchanging the operations of integration and mathematical expectation, we obtain with the aid of (I.2)

$$\begin{aligned} M \left[ \int_{a_1}^{b_1} y_1(t) dt \int_{a_2}^{b_2} y_2(t) dt \right] &= \int_{a_1}^{b_1} \int_{a_2-t}^{b_2-t} R_{y_1 y_2}(\theta) d\theta dt = \\ &= b_1 \int_{a_2-b_1}^{b_2-b_1} R_{y_1 y_2}(\theta) d\theta - a_1 \int_{a_2-a_1}^{b_2-a_1} R_{y_1 y_2}(\theta) d\theta - \\ &- \int_{b_2-a_1}^{b_2-b_1} (b_2 - \theta) R_{y_1 y_2}(\theta) d\theta + \int_{a_2-a_1}^{a_2-b_1} (a_2 - \theta) R_{y_1 y_2}(\theta) d\theta. \end{aligned} \quad (I.3)$$

In particular, if we put in (I.3)

$$y_1(t) = y_2(t) = y(t), \quad a_1 = a_2 = 0 \quad \text{и} \quad b_1 = b_2 = T,$$

we obtain (see also [7])

$$M \left[ \left( \int_0^T y(t) dt \right)^2 \right] = 2 \int_0^T (T - \theta) R_y(\theta) d\theta, \quad (I.4)$$

where

$$R_y(\theta) = M[y(t) y(t + \theta)].$$

For stationarily-related random functions  $y_1(t)$  and  $y_2(t)$  we have

$$M \left[ \int_{a_1+\alpha}^{b_1+\alpha} y_1(t) dt \int_{a_2+\alpha}^{b_2+\alpha} y_2(t) dt \right] = M \left[ \int_{a_1}^{b_1} y_1(t) dt \int_{a_2}^{b_2} y_2(t) dt \right] \quad (1.5)$$

where  $\alpha$  is constant but arbitrary.

To prove (1.5) it is enough to prove that the left half of (1.5) is independent of  $\alpha$ , i.e., that its derivative with respect to  $\alpha$  vanishes identically. This can be readily seen by differentiating the left half of (1.5) with respect to  $\alpha$ .

By way of illustration, we have from (1.5)

$$M \left[ \left( \int_{t_0}^{T+t_0} y(t) dt \right)^2 \right] = M \left[ \left( \int_0^T y(t) dt \right)^2 \right], \quad (1.6)$$

where  $t_0$  is an arbitrary constant.

Let us further consider the mathematical expectation of the product of four values of a stationary random function  $x(t)$  taken at four different instants of time, and the function  $\xi(t) = x(t) - m$ , where  $m = M[x(t)] = \text{const}$ . In other words, let us examine the quantities  $M[x(t_1)x(t_2)x(t_3)x(t_4)]$  and  $M[\xi(t_1)\xi(t_2)\xi(t_3)\xi(t_4)]$ , where  $t_1, t_2, t_3$ , and  $t_4$  are generally different.

Since  $x(t) = \xi(t) + m$ , we have

$$\begin{aligned} M[x_1x_2x_3x_4] = & M[\xi_1\xi_2\xi_3\xi_4] + (M[\xi_1\xi_2\xi_3] + M[\xi_1\xi_2\xi_4] + M[\xi_1\xi_3\xi_4] + M[\xi_2\xi_3\xi_4])m + \\ & + (M[\xi_1\xi_2] + M[\xi_1\xi_3] + M[\xi_1\xi_4] + M[\xi_2\xi_3] + M[\xi_2\xi_4] + \\ & + M[\xi_3\xi_4])m^2 + (M[\xi_1] + M[\xi_2] + M[\xi_3] + M[\xi_4])m^3 + m^4, \end{aligned} \quad (1.7)$$

where  $x_i = x(t_i)$  and  $\xi_i = \xi(t_i)$ , ( $i = 1, 2, 3, 4$ ).

In Expression (1.7)

$$M[\xi_i] \equiv 0 \quad (i = 1, 2, 3, 4) \quad (1.8)$$

Let us introduce the following designations for  $M[\xi_i\xi_k]$  ( $i, k = 1, 2, 3, 4; i \neq k$ )

$$B_{ik} = M[\xi_i\xi_k]. \quad (1.9)$$

Evidently  $B_{ik}$  is the middle correlation function:

$$B_{ik} = M[\xi(t_i)\xi(t_k)] = B(t_k - t_i). \quad (1.10)$$

In most practical cases the distribution of the probabilities of the stationary random functions is close to a normal (Gaussian) distribution. Therefore, considering the distribution of the probabilities of the stationary random function  $x(t)$ , and consequently that of the function  $\xi(t)$ , to be normal, we can obtain (see [4])

$$M[\xi_1\xi_2\xi_3] = M[\xi_1\xi_2\xi_4] = M[\xi_1\xi_3\xi_4] = M[\xi_2\xi_3\xi_4] = 0, \quad (1.11)$$

$$M[\xi_1\xi_2\xi_3\xi_4] = B_{12}B_{34} + B_{13}B_{24} + B_{14}B_{23}. \quad (1.12)$$

With the aid of the above equations, we get

$$M[x_1 x_2 x_3 x_4] = B_{12} B_{34} + B_{13} B_{24} + B_{14} B_{23} + (B_{12} + B_{13} + B_{14} + B_{23} + B_{24} + B_{34}) m^2 + m^4. \quad (I.13)$$

Since the middle correlation function  $B(\tau)$  can be expressed in terms of the correlation function  $R(\tau)$  by means of (0.3), we have

$$M[x_1 x_2 x_3 x_4] = R_{12} R_{34} + R_{13} R_{24} + R_{14} R_{23} - 2m^4, \quad (I.14)$$

where

$$R_{ik} = R(t_k - t_i). \quad (I.15)$$

## APPENDIX II

Equations for  $\sigma_R^2(\tau)$ ,  $\sigma_E^2$ , and  $\nu(\tau)$  to Determine  $\sigma_B^2(\tau)$  When  $B_T(\tau)$  Is Calculated by the Second Variant

Let us rewrite the equations given above for  $\sigma_R^2(\tau)$ , merely replacing  $R(\theta)$  by  $B(\theta)$  in accordance with (0.3):

Method 1:

$$\sigma_R^2(\tau) = \frac{2}{T^2} \int_0^T (T - \theta) [B^2(\theta) + B(\theta + \tau) B(\theta - \tau)] d\theta + 2m^2 \Phi_0, \quad (II.1)$$

where

$$\Phi_0 = \frac{1}{T^2} \left[ 2 \int_0^T (T - \theta) B(\theta) d\theta + \int_0^{T+\tau} (T + \tau - \theta) B(\theta) d\theta + \int_0^{T-\tau} (T - \tau - \theta) B(\theta) d\theta - 2 \int_0^\tau (\tau - \theta) B(\theta) d\theta \right], \quad T = T_H - \tau_{\max}$$

Method 2:

$$\sigma_R^2(\tau) = \frac{2}{(T_{ob} - \tau)^2} \int_0^{T_{ob} - \tau} (T_{ob} - \tau - \theta) [B^2(\theta) + B(\theta + \tau) B(\theta - \tau)] d\theta + 2m^2 \Psi_0, \quad (II.2)$$

where

$$\Psi_0 = \frac{1}{(T_{ob} - \tau)^2} \left[ \int_0^{T_{ob}} (T_{ob} - \theta) B(\theta) d\theta + 2 \int_0^{T_{ob} - \tau} (T_{ob} - \tau - \theta) B(\theta) d\theta + \int_0^{T_{ob} - 2\tau} (T_{ob} - 2\tau - \theta) B(\theta) d\theta - 2 \int_0^\tau (\tau - \theta) B(\theta) d\theta \right];$$

Method 3:

$$\sigma_R^2(\tau) = \frac{2}{T_{ob}^2} \int_0^{T_{ob}-\tau} (T_{ob}-\tau-\theta) [B^2(\theta) + B(\theta+\tau)B(\theta-\tau)] d\theta + \\ + 2m^2 \Omega_0 + [B(\tau) + m^2] \frac{\tau^2}{T_{ob}^2}, \quad (II.3)$$

where

$$\Omega_0 = \frac{1}{T_{ob}^2} \left[ \int_0^{T_{ob}} (T_{ob}-\theta) B(\theta) d\theta + 2 \int_0^{T_{ob}-\tau} (T_{ob}-\tau-\theta) B(\theta) d\theta + \right. \\ \left. + \int_0^{T_{ob}-2\tau} (T_{ob}-2\tau-\theta) B(\theta) d\theta - 2 \int_0^\tau (\tau-\theta) B(\theta) d\theta \right];$$

Method 4:

$$\sigma_R^2(\tau) = \frac{2}{T_{ob}^2} \int_0^T (T-\theta) [B^2(\theta) + B(\theta+\tau)B(\theta-\tau)] d\theta + \\ + \frac{T}{T_{ob}^2} \int_0^\tau [B(\theta-T)B(\theta-\tau) + B(\theta)B(\theta-T-\tau)] d\theta - \\ - \frac{2}{T_{ob}^2} \int_0^T \theta [B(\theta-T)B(\theta+\tau) + B(\theta)B(\theta-T+\tau)] d\theta + \\ + \frac{2}{T_{ob}^2} \int_0^T \theta [B(\theta-T)B(\theta-\tau) + B(\theta)B(\theta-T-\tau)] d\theta + \\ + \frac{2}{T_{ob}^2} \int_0^\tau (\tau-\theta) [B^2(\theta) + B(\theta+T)B(\theta-T)] d\theta + 4m^2 x_B, \quad (II.4)$$

where

$$x_B = \frac{2}{T_{ob}^2} \int_0^{T_{ob}} (T_{ob}-\theta) B(\theta) d\theta.$$

Using the already-known procedure and replacing  $R(\theta)$  by  $B(\theta)$  in the resulting equations, we obtain the following expression for  $\sigma_E^2$ :

Method 1:

$$\sigma_E^2 = 2(\Phi_1 + \Phi_2)^2 + 2m^2 \Phi_0 - 2x_B [3(\Phi_1 + \Phi_2) - \Phi_0] + 3x_B^2, \quad (II.5)$$



where

$$\begin{aligned}\Phi_1 &= \frac{1}{T T_{ob}} \left[ \int_0^{T_{ob}} (T_{ob} - \theta) B(\theta) d\theta + \int_0^T (T - \theta) B(\theta) d\theta - \int_0^{\tau_{max}} (\tau_{max} - \theta) B(\theta) d\theta \right], \\ \Phi_2 &= \frac{1}{T T_{ob}} \left[ \int_0^{T_{ob} - \tau} (T_{ob} - \tau - \theta) B(\theta) d\theta + \int_0^{T + \tau} (T + \tau - \theta) B(\theta) d\theta - \right. \\ &\quad \left. - \int_0^{\tau_{max} - \tau} (\tau_{max} - \tau - \theta) B(\theta) d\theta - \int_0^{\tau} (\tau - \theta) B(\theta) d\theta \right], \quad T = T_{ob} - \tau_{max}\end{aligned}$$

Method 2:

$$\sigma_E^2 = 8\Psi_1^2 + 2m^2\Psi_0 - 2\kappa_B [6\Psi_1 - \Psi_0] + 3\kappa_B^2, \quad (II.6)$$

where

$$\begin{aligned}\Psi_1 &= \frac{1}{T_{ob}(T_{ob} - \tau)} \left[ \int_0^{T_{ob}} (T_{ob} - \theta) B(\theta) d\theta + \int_0^{T_{ob} - \tau} (T_{ob} - \tau - \theta) B(\theta) d\theta - \right. \\ &\quad \left. - \int_0^{\tau} (\tau - \theta) B(\theta) d\theta \right];\end{aligned}$$

Method 3:

$$\begin{aligned}\sigma_E^2 &= 8\Omega_1^2 - 4m^2\Omega_1 \frac{\tau}{T_{ob}} + 2m^2\Omega_0 - 2\kappa_B \left[ 6\Omega_1 \left( 1 - \frac{\tau}{T_{ob}} \right) - \Omega_0 - m^2 \left( 1 - \frac{\tau}{T_{ob}} \right) \frac{\tau}{T_{ob}} \right] + \\ &\quad + 3\kappa_B^2 \left( 1 - \frac{\tau}{T_{ob}} \right)^2 + m^4 \frac{\tau^2}{T_{ob}^2}, \quad (II.7)\end{aligned}$$

where

$$\Omega_1 = \frac{1}{T_{ob}^2} \left[ \int_0^{T_{ob}} (T_{ob} - \theta) B(\theta) d\theta + \int_0^{T_{ob} - \tau} (T_{ob} - \tau - \theta) B(\theta) d\theta - \int_0^{\tau} (\tau - \theta) B(\theta) d\theta \right];$$

Method 4:

$$\sigma_E^2 = \kappa_B (3\kappa_B + 4m^2). \quad (II.8)$$

Analogously, we obtain for  $\nu(\tau)$ :

Method 1:

$$v(\tau) = \frac{1}{T} \int_0^T [G(t+\tau)H(t) + G(t)H(t+\tau) + G(t+\tau)H(t-\tau) + \\ + G(t)H(t) - 2G(t)G(t+\tau)] dt + 2m^2\Phi_0, \quad (II.9)$$

where

$$G(t) = \frac{1}{T_{ob}} \int_0^{T_{ob}} B(\theta-t) d\theta, \quad H(t) = \frac{1}{T} \int_0^T B(\theta-t) d\theta, \quad T = T_{ob} - \tau \max$$

Method 2:

$$v(\tau) = \frac{1}{T_{ob} - \tau} \int_0^{T_{ob} - \tau} [G(t+\tau)K(t) + G(t)K(t+\tau) + G(t+\tau)K(t-\tau) + \\ + G(t)K(t) - 2G(t)G(t+\tau)] dt + 2m^2\Psi_0, \quad (II.10)$$

where

$$K(t) = \frac{1}{T_{ob} - \tau} \int_0^{T_{ob} - \tau} B(\theta-t) d\theta;$$

Method 3:

$$v(\tau) = \frac{1}{T_{ob}} \int_0^{T_{ob} - \tau} [G(t+\tau)L(t) + G(t)L(t+\tau) + G(t+\tau)L(t-\tau) + G(t)L(t) - \\ - 2G(t)G(t+\tau) \left(1 - \frac{\tau}{T_{ob}}\right)] dt + 2m^2\Omega_0 + \\ + [B(\tau) + m^2] [\kappa_B - 2\Omega_1 + (m^2 - \kappa_B) \frac{\tau}{T_{ob}}] \frac{\tau}{T_{ob}}, \quad (II.11)$$

where

$$L(t) = \frac{1}{T_{ob}} \int_0^{T_{ob} - \tau} B(\theta-t) d\theta;$$

Method 4:

$$v(\tau) = \frac{2}{T_{ob}} \int_0^T G(t)G(t+\tau) dt + \frac{2}{T_{ob}} \int_0^\tau G(t)G(t+T) dt + \\ + \kappa_B \left[ (B(T) - B(\tau)) \frac{\tau}{T_{ob}} + 4m^2 \right], \quad (II.12) \\ T = T_{ob} - \tau.$$

# APPENDIX III

## Equations for $\lambda_B(\tau)$ and $\gamma_B(\tau)$ to Determine the Quantities $\sigma_B^2(\tau)$

Using the previous notation in the calculation of the function  $B_T(\tau)$  by the first variant, we obtain for the various calculation methods the following equations for the quantities  $M[B_T(\tau)]$ ,  $\lambda_B(\tau)$ , and  $\gamma_B(\tau)$ :

### Method 1:

$$M[B_T(\tau)] = B(\tau) - x_B, \quad (III.1)$$

$$\lambda_B(\tau) = \frac{2}{T^2} \int_0^T (T - \theta) B(\theta) [B(\theta + \tau) + B(\theta - \tau)] d\theta -$$

$$- \frac{2}{T} \int_0^T G(t) [G(t) + G(t + \tau)] dt - 2m^2 (3\Phi_1 + \Phi_2 - \Phi_0) + x_B (3x_B + 4m^2), \quad (III.2)$$

$$\gamma_B(\tau) = \frac{x_B^3 (x_B - 2B(0)) (B(\tau) - B(0))^2}{B^2(0) (B(0) - x_B)^4}, \quad (III.3)$$

$$T = T_{ob} - \tau_{\max}$$

### Method 2:

$$(III.4)$$

$$M[B_T(\tau)] = B_T(\tau) - x_B,$$

$$\lambda_B(\tau) = \frac{4}{T_{ob}(T_{ob} - \tau)} \int_0^{T_{ob} - \tau} (T_{ob} - \tau - \theta) B(\theta) B(\theta + \tau) d\theta + \frac{2}{T_{ob}} \int_0^{\tau} B(\theta) B(\theta - \tau) d\theta -$$

$$- \frac{2}{T_{ob}} \int_0^{T_{ob}} G^2(t) dt - \frac{2}{T_{ob} - \tau} \int_0^{T_{ob} - \tau} G(t) G(t + \tau) dt + 3x_B^2, \quad (III.5)$$

$$\gamma_B(\tau) = \frac{x_B^3 (x_B - 2B(0)) (B(\tau) - B(0))^2}{B^2(0) (B(0) - x_B)^4}; \quad (III.6)$$

### Method 3:

$$M[B_T(\tau)] = B(\tau) \left(1 - \frac{\tau}{T_{ob}}\right) - m^2 \frac{\tau}{T_{ob}} - x_B, \quad (III.7)$$

$$\lambda_B(\tau) = \frac{4}{T_{ob}^2} \int_0^{T_{ob} - \tau} (T_{ob} - \tau - \theta) B(\theta) B(\theta + \tau) d\theta +$$

$$+ \frac{2}{T_{ob}} \left(1 - \frac{\tau}{T_{ob}}\right) \int_0^{\tau} B(\theta) B(\theta - \tau) d\theta -$$

$$- \frac{2}{T_{ob}} \int_0^{T_{ob}} G^2(t) dt - \frac{2}{T_{ob}} \int_0^{T_{ob} - \tau} G(t) G(t + \tau) dt + x_B \left(3x_B + m^2 \frac{\tau}{T_{ob}}\right), \quad (III.8)$$

$$\gamma_B(\tau) = \frac{x_B (x_B - 2B(0)) \left[ x_B (B(\tau) - B(0)) - B(0) (B(\tau) + m^2 \frac{\tau}{T_{ob}}) \right]^2}{B^2(0) (B(0) - x_B)^4}; \quad (III.9)$$

Method 4:

$$M[B_T(\tau)] = B(\tau) \frac{T}{T_{ob}} + B(T) \frac{\tau}{T_{ob}} - x_B, \quad (III.10)$$

$$\begin{aligned} \lambda_B(\tau) = & \frac{4}{T_{ob}^2} \int_0^T (T-\theta) B(\theta) B(\theta+\tau) d\theta + 2 \frac{\tau}{T_{ob}^2} \int_0^T B(\theta) B(\theta-T) d\theta + \\ & + \frac{4}{T_{ob}^2} \int_0^\tau (\tau-\theta) B(\theta) B(\theta+T) d\theta + 2 \frac{T}{T_{ob}^2} \int_0^\tau B(\theta) B(\theta-\tau) d\theta - \\ & - \frac{2}{T_{ob}} \int_0^{T_{ob}} G^2(t) dt - \frac{2}{T_{ob}} \int_0^T G(t) G(t+\tau) dt - \frac{2}{T_{ob}} \int_0^\tau G(t) G(t+T) dt + \\ & + x_B \left[ 3x_B + (B(\tau) - B(T)) \frac{\tau}{T_{ob}} \right], \end{aligned}$$

(III.11)

$$\gamma_B(\tau) = \frac{x_B(x_B - 2B(0)) \left[ x_B(B(\tau) - B(0)) - B(0)(B(\tau) - B(T)) \frac{\tau}{T_{ob}} \right]^2}{B^2(0)(B(0) - x_B)^4}, \quad (III.12)$$

$$T = T_{ob} - \tau.$$

Bearing in mind the methods discussed above for the calculation of the function  $B_T(\tau)$  by the second variant, we obtain:

Method 1:

$$M[B_T(\tau)] = B(\tau) - (\Phi_1 + \Phi_2 - x_B),$$

$$\lambda_B(\tau) = \frac{2}{T^2} \int_0^T (T-\theta) B(\theta) [B(\theta+\tau) + B(\theta-\tau)] d\theta + \frac{2}{T} \int_0^T [G(t) + \quad (III.13)$$

$$+ G(t+\tau)] [G(t) - H(t)] dt - \frac{2}{T} \int_0^T G(t) [H(t-\tau) + H(t+\tau)] dt +$$

$$+ 2m^2(\Phi_1 - \Phi_2) + x_B(3x_B - 9\Phi_1 - 3\Phi_2 + 2\Phi_0) + 4\Phi_1(\Phi_1 + \Phi_2), \quad (III.14)$$

$$\gamma_B(\tau) = \frac{(2\Phi_1 - x_B)(2\Phi_1 - x_B - 2B(0)) [B(\tau)(2\Phi_1 - x_B) - B(0)(\Phi_1 + \Phi_2 - x_B)]^2}{B^2(0)(B(0) - 2\Phi_1 + x_B)^4},$$

$$T = T_{ob} - \tau_{\max} \quad (III.15)$$

Method 2:

(III.16)

$$M[B_T(\tau)] = B(\tau) - (2\Phi_1 - x_B),$$

$$\lambda_B(\tau) = \frac{4}{T_{ob}(T_{ob}-\tau)} \int_0^{T_{ob}-\tau} (T_{ob}-\tau-\theta) B(\theta) B(\theta+\tau) d\theta +$$

$$+ \frac{2}{T_{ob}} \int_0^\tau B(\theta) B(\theta-\tau) d\theta - \frac{2}{T_{ob}} \int_0^{T_{ob}} G(t) [K(t) + K(t-\tau) - G(t)] dt -$$

$$- \frac{2}{T_{ob}-\tau} \int_0^{T_{ob}-\tau} G(t) G(t+\tau) dt + 3x_B(2\Psi_1 - x_B), \quad (III.17)$$

$$\gamma_B(\tau) = \frac{x_B(x_B - 2B(0)) [B(\tau)x_B - B(0)(2\Psi_1 - x_B)]^2}{B^2(0)(B(0) - x_B)^4}; \quad (III.18)$$

Method 3:

$$M[B_T(\tau)] = B(\tau) \left(1 - \frac{\tau}{T_{ob}}\right) - \left[2\Omega_1 - x_B \left(1 - \frac{\tau}{T_{ob}}\right)\right], \quad (III.19)$$

$$\lambda_B(\tau) = \frac{4}{T_{ob}^2} \int_0^{T_{ob}-\tau} (T_{ob}-\tau-\theta) B(\theta) B(\theta+\tau) d\theta + \frac{2}{T_{ob}} \left(1 - \frac{\tau}{T_{ob}}\right) \int_0^\tau B(\theta) B(\theta-\tau) d\theta -$$

$$- \frac{2}{T_{ob}} \int_0^{T_{ob}} G(t) [L(t) + L(t-\tau)] dt + \frac{2}{T_{ob}} \left(1 - \frac{\tau}{T_{ob}}\right) \int_0^{T_{ob}} G^2(t) dt -$$

$$- \frac{2}{T_{ob}} \int_0^{T_{ob}-\tau} G(t) G(t+\tau) dt + 3x_B(2\Omega_1 - x_B) + [x_B(B(\tau) - 6m^2) + 3m^4] \frac{\tau}{T_{ob}}, \quad (III.20)$$

$$\gamma_B(\tau) = \frac{x_B(x_B - 2B(0)) \left\{ B(\tau)x_B - B(0) \left[ 2\Omega_1 - \left(1 - \frac{\tau}{T_{ob}}\right)x_B - B(\tau) \frac{\tau}{T_{ob}} \right] \right\}^2}{B^2(0)(B(0) - x_B)^4}. \quad (III.21)$$

The quantities  $M[B_T(\tau)]$ ,  $\lambda_B(\tau)$  and  $\gamma_B(\tau)$  are calculated for Method 4 from Equations (III.10) - (III.12), since the first and second variants for the function  $B_T(\tau)$  yield the same results in Method 4, because  $E_T(\tau) = m_T^2$  for this method.

#### SUMMARY

The results obtained make it possible to determine for a stationary random process  $x(t)$  the mean-squared errors  $\sigma(\tau)$  that result when the correlation function is calculated from experimental data; these errors are caused by the finite time during which the process  $x(t)$  is observed.

It is shown that in the calculation of these errors it is necessary to take into account the differences in the types of the correlation function and in the methods used to calculate its approximate values.

It is necessary here to distinguish between the following types of correlation functions:

The correlation function

$$R(\tau) = M[x(t)x(t+\tau)];$$

The middle correlation function

$$B(\tau) = M[(x(t) - m)(x(t + \tau) - m)], \text{ where } m = M[x(t)];$$

The normalized correlation function

$$\rho(\tau) = \frac{R(\tau)}{R(0)};$$

The normalized middle correlation function

$$\beta(\tau) = \frac{B(\tau)}{B(0)}.$$

The observation time  $T_{\text{ob}}$  of a random process  $x(t)$  should be chosen to suit the required accuracy of these functions for a specified value of the time shift  $\tau$ .

#### LITERATURE CITED

- [1] V. V. Solodovnikov, Introduction to the Statistical Dynamics of Automatic-Regulation Systems, Gostekhizdat, 1952.
- [2] V. V. Solodovnikov, (Edit.), Principles of Automatic Regulation, Mashgiz, 1954.
- [3] A. M. Iaglom, Introduction to the Theory of Stationary Random Functions, Usp. Matem. nauk, 7, 5, 51 (1952).
- [4] A. M. Obukhov, Statistical Description of Continuous Fields, Trudy Geofiz. in-ta AN SSSR, No. 24, 150, 1954.
- [5] V. S. Pugachov, Elements of the Theory of Random Functions, Izd. VVIA, 1954.
- [6] A. E. Kharybin, Analysis of Errors in the Determination of the Mean Value of a Random Quantity and of its Square, Resulting from the Finite Time of Observation, Report of Inst. of Automation and Remote Control, USSR, Acad. of Sci., 1953.
- [7] W. B. Davenport, R. A. Johnson, and D. Middleton, Statistical Errors in Measurements on Random Time Function, J. Appl. Phys., 23, 4 (1952).
- [8] N. Arleigh and K. R. Buch, Introduction to the Theory of Probability and Mathematical Statistics Russ. Tr. IL, 1951.
- [9] A. Worthing and D. Heffner, Mathematical Methods for the Processing of Observations, Russ. Tr., IL, 1953.

Received December 29, 1955.



# INVESTIGATION OF SIMPLEST RELAY SERVOSYSTEM

G. V. Gerkhen-Gubanov

(Leningrad)

The motion of a relay servosystem as it eliminates the initial error signal is considered for the case when the system contains a dead zone, a voltage ratio, a time lag in operation, and a time lag in relay dropout.

The fastest elimination of the initial error of a servosystem is attained by using a relay amplifier and nonlinear error-signal converters [1-5]. Less accurate, but simpler are relay servosystems employing a linear combination of error signals and feedback [5-9]. The least accurate is the servosystem shown in Fig. 1, but it is widely used along with other systems because of its simplicity.

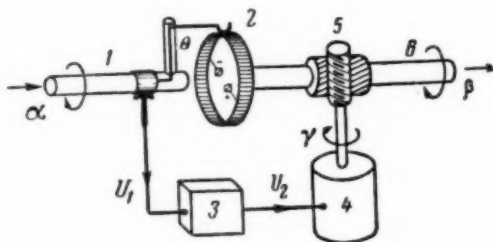


Fig. 1. Diagram of relay servosystem: 1) input shaft, 2) potentiometer transducer, 3) relay, 4) servomotor, 5) reduction gear, 6) output shaft.

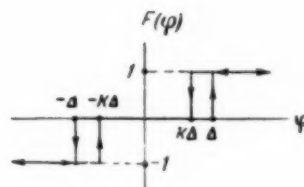


Fig. 2. Characteristic of a relay in dimensionless units:  $\Delta$ ) relative magnitude of dead zone of relay,  $k$ ) pull-in voltage ratio

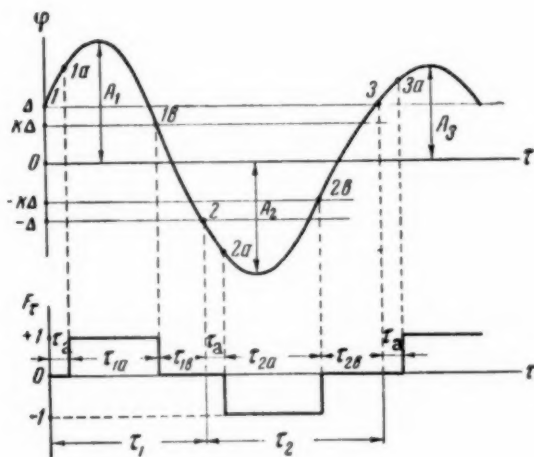


Fig. 3. Elimination of initial error in servosystem having a dead zone  $\Delta$ , a voltage pull-in ratio  $k$ , and a time delay  $\tau_a$  in the actuation of the relay.

To avoid unnecessary complication of the proposed servosystem it is necessary to know the capabilities of various types of systems, particularly the simplest systems.

An analysis of such a relay servosystem, from the point of view of stability and of the self-oscillation parameters, is found in [10-14]. These investigate the influence of the dead zone, of the relay pull-in voltage ratio, and the time delay of the system.

This communication considers the joint influence of these nonlinearities on the motion of a servosystem of the second kind as it reduces the initial error signal.

The conclusions obtained here are applicable also to a regulation system, the motion of which is described by equations analogous to those considered here.

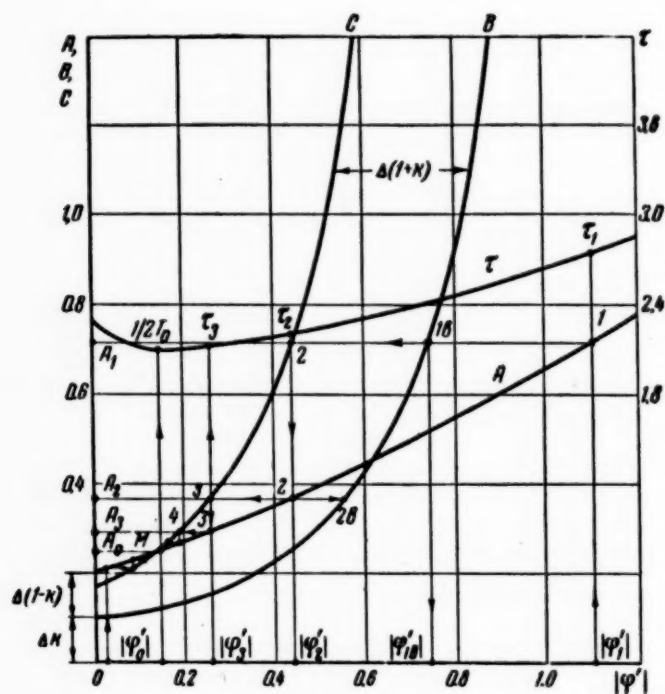


Fig. 4. Plot for determination of transient and of the self-oscillation parameters of the system:  $\Delta = 0.2$ ,  $k = 0.5$ ,  $\tau_a = 0.3$ .

Let us consider the motion of a relay servosystem (Fig. 1), describable by equation

$$T\ddot{\theta} + \dot{\theta} = -k_c F_t(k_1 \theta). \quad (1)$$

Here  $\theta$  is the error angle,  $F_t$  is the nonlinear function of the relay element, characterizing the presence of a time delay  $t_a$  in the relay actuation, a dead zone  $U_{10}$ , and a pull-in voltage ratio  $k$ . This function can be expressed by the following equations

$$F_t[U_1(t)] = \begin{cases} F[U_1(t)] & \text{at } |U_1| < U_{10}, \\ F[U_1(t - t_a)] & \text{at } |U_1| \geq U_{10}. \end{cases}$$

Let us introduce the dimensionless variables

$$\varphi = \frac{1}{k_a T} \theta, \quad \tau = \frac{1}{T} t, \quad \Delta = \frac{1}{k_1 k_a T} U_{10}, \quad \tau_a = \frac{1}{T} t_a; \quad (2)$$

We then obtain Equation (1) in dimensionless form

$$\varphi'' + \varphi' = \begin{cases} -F(\varphi) & \text{at } |\varphi| < \Delta \\ -F[\varphi(\tau - \tau_a)] & \text{at } |\varphi| \geq \Delta. \end{cases} \quad (3)$$

The function  $F(\varphi)$  involved here is shown in Fig. 2. Equations (3) are piecewise linear and can be integrated in segments. Figure 3 shows an approximate form of the curve  $\varphi(\tau)$  of the transient occurring under specified initial conditions.

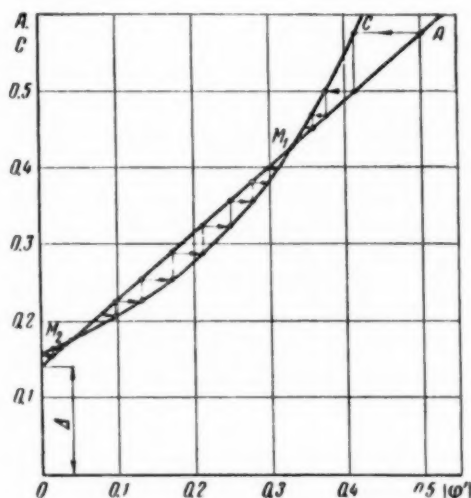


Fig. 5. Graph for determining the transient. The system is capable of two types of periodic motions — stable (point  $M_1$ ) and unstable (point  $M_2$ ).  $\Delta = 0.14$ ,  $k = 0.90$ ,  $\tau_a = 2.0$ .

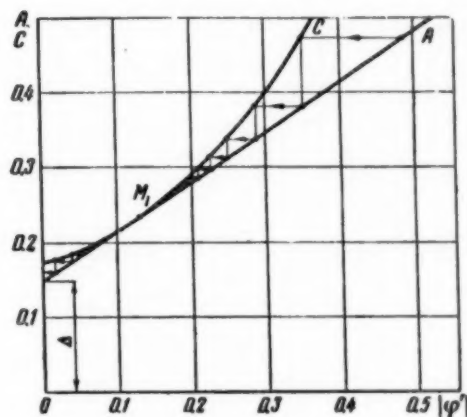


Fig. 6. Graph for determination of the transient process. The system is capable of semi-stable periodic motions (point  $M_1$ ).  $\Delta = 0.152$ ,  $k = 0.80$ ,  $\tau_a = 1.00$ .

Integrating Equations (3) along the individual segments of  $\varphi(\tau)$ , we get

$$A_n = \Delta + |\varphi'_n| - \ln(1 + |\varphi'_n| e^{-\tau_a}),$$

$$\tau_n = \tau_a + \ln \frac{1 + |\varphi'_n| e^{-\tau_a}}{1 - |\varphi'_{nb}|} + \ln \frac{|\varphi'_{nb}|}{|\varphi'_{n+1}|},$$

$$(4)$$

$$|\varphi'_{n+1}| = |\varphi'_{nb}| - \Delta(1 + k),$$

$$|\varphi'_n| - \ln(1 + |\varphi'_n| e^{-\tau_a}) + \Delta(1 - k) = -|\varphi'_{nb}| - \ln(1 - |\varphi'_{nb}|).$$

From Equations (4) it is possible to determine the basic characteristics of the motion of the system for specified initial conditions and the effects of the system parameters on its dynamics.

The simplest way to solve this problem is to use the following graphical method. Plot the functions  $A = \Delta + |\varphi'| - \ln(1 + |\varphi'| e^{-\tau_a})$ ,  $B = -|\varphi'| - \ln(1 - |\varphi'|) + k\Delta$ ,  $C(|\varphi'|) = B[|\varphi'| + \Delta(1 + k)]$ . Lay off the quantity  $|\varphi'|$  on the abscissa axis and draw the stepped line 1-2-2-3-3-4. According to Equations (4), the points 1, 1b, 2, 2b, 3, ... (Fig. 4) will determine the parameters of motion  $A_n$ ,  $|\varphi'_n|$ , and  $|\varphi'_{nb}|$ . Inserting these values into Equations (4) it is possible to find the values of  $\tau_n$ .

The point M where the Curves A and C intersect corresponds evidently to stable self-oscillations of the system, with a period  $T_0$  and an amplitude  $A_0$ . It is interesting to note that given the system parameters, the

minimum duration of the half wave, and consequently the maximum oscillation frequency occurs in the case of self-oscillation.

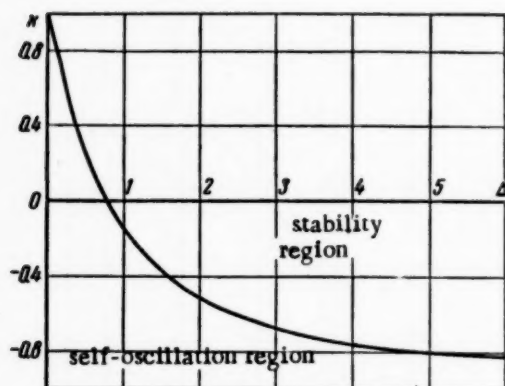


Fig. 7. Boundary of system stability region at  $\tau_a = 0$ .

either one intersection point (Fig. 4), two intersection points (Fig. 5), one point of tangency (Fig. 6), or no common point at all. Figure 4 represents a self-oscillating system with soft self oscillations, Figure 5 one with stiff self oscillations, and Fig. 6 corresponds to the limiting case of stability, with a semi-stable limit cycle.

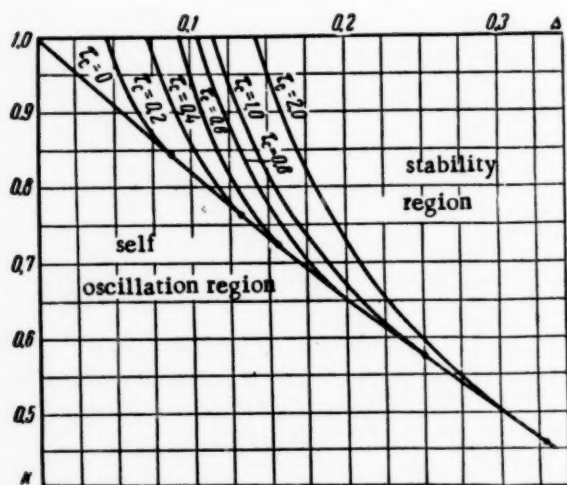


Fig. 8. Boundary of system stability region at  $\tau_a \neq 0$ .

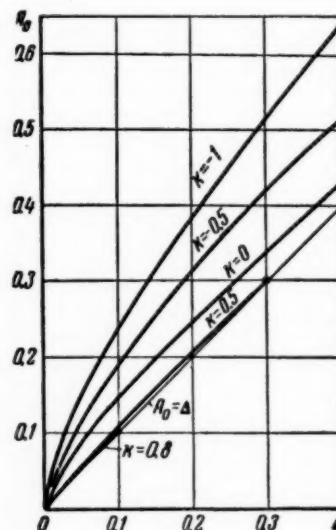


Fig. 9. Curve showing the dependence of the amplitude of the self oscillations on the system parameters at  $\tau_a = 0$ .

If  $\tau_a = 0$  and  $\Delta \neq 0$ , Curves A and C have either one point of intersection or no common points. Using the condition  $A \varphi^* = 0 = C \varphi^* = 0$  we get an equation for the boundary of the system stability region at  $\tau_a = 0$ :

$$k = \frac{1 - e^{-2\Delta}}{\Delta} - 1.$$

The curve for the boundary of the stability region is shown for this case in Fig. 7. For  $t_a \neq 0$  it is easiest to find the boundaries of the stability regions with the aid of templates of Curves A and B. This method was used, for example, to find the curves shown in Fig. 8.

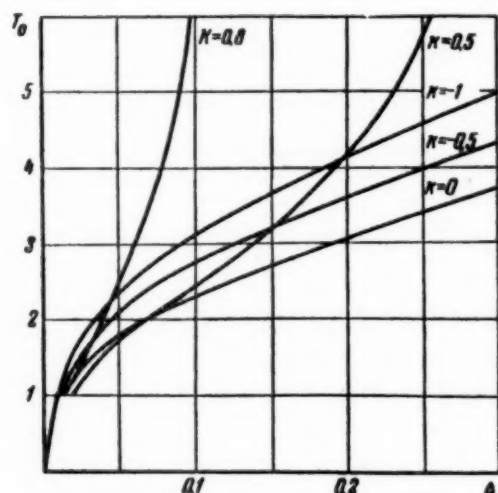


Fig. 10. Curves showing the dependence of the period of the self oscillations on the parameter of the system at  $\tau_a = 0$ .

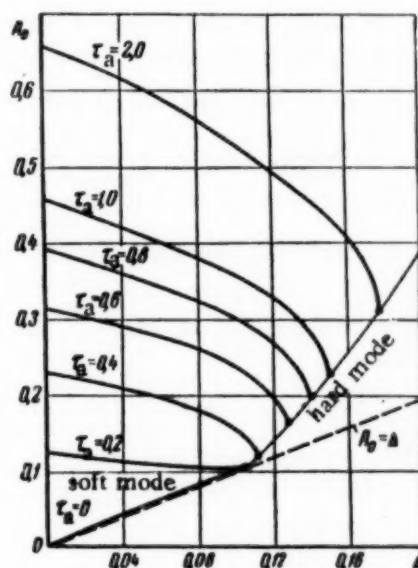


Fig. 11. Curves showing the dependence of the self oscillations amplitude on the system parameters at  $k = 0.8$ . At  $\tau_a \leq 0.25$  the mode of self oscillation is soft, at  $\tau_a > 0.25$  it is hard.

The parameters of the self oscillations can be found graphically from Equations (4) by substituting

$$|\varphi'_n| = |\varphi'_{n+1}| = \varphi'_0, \quad \tau_n = \frac{1}{2} T_0, \quad A_n = A_0.$$

The curves on Figs. 9, 10, and 11 were obtained in this manner.

To determine the effect of the system parameters on its motion, expressed in dimensional units, it is necessary to take Relationships (2) into account in the analysis of the graphs. This method was used to obtain the following conclusions.

1. Reducing the insensitivity  $U_{10}$  of the system increases the tendency of the system to self oscillations, reduces the amplitude of the self oscillations if the time delay  $t_a$  in relay actuation is small, and increases the amplitude if  $t_a$  is large; it also reduces the period of the self oscillations and the statistical error of the system.
2. Increasing the relay pull-in voltage ratio  $k$  reduces the tendency of the system to self oscillation, and reduces the amplitude of the self oscillation; it does not have a single-value effect on the period of the self oscillations.
3. Reducing the relay-operation time delay  $t_a$  and the relay release time delay  $t_r$  reduces the tendency of the system to self oscillations and reduces the amplitude of the self oscillations.
4. Reducing the electromechanical constant  $T$  of the motor reduces the tendency of the system to self oscillations and reduces the amplitude of the self oscillations at large values of  $t_a$  and at small values of  $k$ , but hardly affects the amplitude at small values of  $t_a$  and at large  $k$ ; it does not have a single-valued effect on the period of the self oscillations.

The velocity coefficient  $k_v$  has a similar effect on the stability of the system and on the amplitude of the self oscillations as the parameter  $T$ .

#### LITERATURE CITED

- [1] A. Ya. Lerner, Improvement of Dynamic Properties of Automatic Compensators with the Aid of Nonlinear Couplings, I, II. Automation and Remote Control 13, 2, 4 (1952).
- [2] E. K. Krug, Increasing the Speed of Actuating Devices, *ibid.*, 15, 4 (1954).
- [3] A. Ya. Lerner, On the Limiting Speed of Automatic-Regulation Systems, *ibid.*, 15, 6 (1954).
- [4] Ya. Z. Tsytkin, Theory of Relay Systems for Automatic Regulation, Tekhteorizdat, 1955.
- [5] A. A. Feldbaum, Simplest Relay Systems for Automatic Regulation, Automation and Remote Control 10, 4 (1949).
- [6] V. V. Petrov and G. M. Ulanov, Theory of Two Simplest Relay Systems for Automatic Regulation, *ibid.*, 11, 5 (1950).
- [7] V. V. Petrov, On Self Oscillations of Two-Stage Servomechanisms with Relay Control, *ibid.*, 12, 1 (1951).
- [8] V. V. Petrov and G. M. Ulanov, On the Stabilizing Effect of an Acceleration Pulse in the Feedback of a Relay Servosystem, *ibid.*, 12, 5 (1951).
- [9] V. V. Petrov and G. M. Ulanov, Use of Rigid and Velocity-Derived Feedback for the Suppression of Self Oscillation in a Two-Stage Servomechanism with Relay Control, *ibid.*, 13, 2 (1952).
- [10] L. S. Goldfarb, On Certain Nonlinearities in Regulating Systems, *ibid.*, 8, 5 (1957).
- [11] G. K. Veiss, Analysis of Relay Servomechanisms, 1947.
- [12] Ya. N. Nikolaev, Scientific Notes of the Gorky University, 13, 1947.
- [13] I. Ya. Lekhtman, On the Design of Relay Servosystems, Automation and Remote Control 12, 1 (1951).
- [14] Yu. V. Dolgolenko, Stability and Self Oscillations of a Relay System for Regulation, *ibid.*, 13, 2 (1952).

Received March 12, 1956.



# IMPROVING THE DYNAMIC PROPERTIES OF AUTOMATIC REGULATION SYSTEMS WITH THE AID OF APERIODIC FEEDBACK

S. Ya. Berezin

(Leningrad)

Analysis of the use of aperiodic feedback to improve the dynamic properties of automatic regulation systems. Practical methods are proposed for the design of aperiodic feedback circuits. The advantages of the use of aperiodic feedback are confirmed by the experimental results.

References [1-6] describe a method for improving the quality of an automatic-regulation system by introducing aperiodic feedback. References [1-4] contain a description and the characteristics of the VTI (All-Union Technical Institute) regulator with aperiodic feedback, introduce the equations for the conditions of the existence of the oscillations, and give the operational characteristics of the regulator. Reference [5] gives the theory of the direct-acting regulator with aperiodic feedback for speed regulation of Diesel engines. In these investigations the order of the equations did not exceed four. Reference [6] and earlier works of the author consider many automatic-regulation systems with aperiodic feedback.

The purpose of this article is to explain the influence of aperiodic feedback on the stability and response of automatic-regulation systems and to indicate practical methods of obtaining such feedback.

## 1. Use of Aperiodic Feedback in Servosystems

Let us assume that a servosystem employs instead of an external rigid feedback an aperiodic feedback with a transfer function

$$W_f(p) = \frac{k_f}{1 + T_f p} \quad (1)$$

The structural diagram of such a system is shown in Fig. 1. The transfer function of the closed-loop servosystem in the presence of aperiodic feedback has the form

$$\Phi(p) = \frac{x_n}{x_0} = \frac{W_0(p)}{1 + W_0(p) W_f(p)}, \quad (2)$$

where  $W_0(p)$  is the open-loop transfer function of the regulation system without the feedback.

The open-loop transfer function with aperiodic feedback is

$$W_{01}(p) = W_0(p) W_f(p). \quad (3)$$

Multiplying the vector  $W_0(j\omega)$  by the vector  $W_f(j\omega)$  will cause, as can be seen in Fig. 2, each vector  $W_{01}(j\omega)$  to be rotated relative to the vector  $W_0(j\omega)$  clockwise by a certain angle  $\beta$ . If  $k_f$  is chosen to be

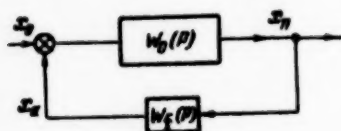


Fig. 1

less than unity, then the vectors  $W_0(j\omega)$  will not only be rotated, but be also reduced in modulus, and Curve 1 will assume a new position 2, and the system will be stable. If  $k_f > 1$ , the vectors  $W_0(j\omega)$  will increase in modulus, Curve 1 will occupy position 3, which in itself is unfavorable.

Thus, stability considerations make the use of  $k_f > 1$  in the servosystem undesirable.

Let us determine the effect of the aperiodic feedback on the response of the servosystem. It is easy to derive from (2) an expression for the error of the servosystem:

$$x_0 - x_n = e = \frac{[1 + W_0(p) W_f(p) - W_0(p)]}{1 + W_0(p) W_f(p)} x_0, \quad (4)$$

where

$$W_0(p) = \frac{R(p)}{Q(p)}. \quad (5)$$

Here  $Q$  and  $R$  are operator polynomials and the degree of the polynomial  $R$  is usually lower than the degree of the polynomial  $Q$  for all real systems. For servosystems with astatism of first order we have

$$\begin{aligned} Q(p) &= a_0 p^n + a_1 p^{n-1} + a_2 p^{n-2} + \dots + a_n p, \\ R(p) &= b_0 p^m + b_1 p^{m-1} + b_2 p^{m-2} + \dots + b_m. \end{aligned} \quad (6)$$

Let us substitute the values of  $W_0(p)$  and  $W_f(p)$  into (4):

$$\begin{aligned} e &= \frac{p(a_0 p^{n-1} + a_1 p^{n-2} + \dots + a_n)(1 + T_f p) +}{p(a_0 p^{n-1} + a_1 p^{n-2} + \dots + a_n)(1 + T_f p) +} \\ &\quad + \frac{(b_0 p^m + b_1 p^{m-1} + \dots + b_m)(k_f - 1 - T_f p)}{k_f(b_0 p^m + b_1 p^{m-1} + \dots + b_m)} x_0. \end{aligned} \quad (7)$$

If the ordinary rigid feedback is used

$$e = \frac{p(a_0 p^{n-1} + a_1 p^{n-2} + \dots + a_n) + (b_0 p^m + b_1 p^{m-1} + \dots + b_m)}{p(a_0 p^{n-1} + a_1 p^{n-2} + \dots + a_n) + (b_0 p^m + b_1 p^{m-1} + \dots + b_m)}. \quad (8)$$

If  $\omega_0 = p x_0 = \text{const}$ , we obtain from (7) the velocity error of the servosystem:

$$e_v = \frac{\omega_0(a_n - b_m T_f) + b_m(k_f - 1)}{k_f b_m}. \quad (9)$$

In servosystem where the response angle equals the error angle,  $k_f$  is always unity:\*

\* There exist servosystems (for example, those used for rudder control), in which the response angle should be greater than the error angle, i.e.,  $k_f < 1$ . An analysis of such systems is beyond the scope of this article.

$$e_v = \frac{\omega_0(a_n - b_m T_f)}{b_m}. \quad (10)$$

Expression (10) shows that if aperiodic feedback is used, the velocity error is decreased, and if  $T_f = \frac{a_n}{b_m}$ , the velocity error vanishes.

Let us ascertain the effect of the aperiodic feedback on the value of the steady-state error for harmonic disturbance at the input.

We obtain from (4) an expression for the relative steady-state error of the system for a harmonic driving function [9]:

$$\frac{e}{x_0} = \delta = \frac{[1 + W_0(j\omega)W_{oc}(j\omega) - W_0(j\omega)]}{1 + W_0(j\omega)W_{oc}(j\omega)} x_0 = \frac{Y_0(j\omega) + W_f(j\omega) - 1}{Y_0(j\omega) + W_{oc}(j\omega)} x_0, \quad (11)$$

where

$$Y_0(j\omega) = \frac{1}{W_0(j\omega)}.$$

Figure 3 shows the reciprocal amplitude-phase characteristics of the servosystem (Curve I) and the amplitude-phase characteristics of the aperiodic feedback (Curve II).

At a certain frequency  $\omega_i$ , the modulus of the steady-state relative error equals the ratio of the moduli of vectors DE and OD (Fig. 3):

$$|\delta| = \frac{|DE|}{|OD|}, \quad (12)$$

Since

$$DE = Y_0(j\omega_i) + W_f(j\omega_i) - 1, \quad OD = Y_0(j\omega_i) + W_f(j\omega_i).$$

In the case of rigid feedback,  $W_f(j\omega) = k_f - 1$ , and the modulus of the relative steady-state error is

$$|\delta| = \frac{|OA|}{|AB|}. \quad (13)$$

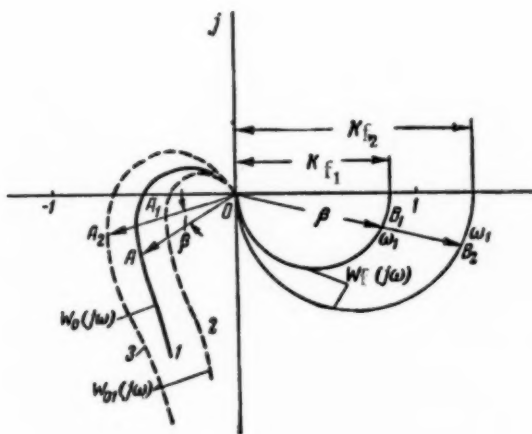


Fig. 2

It is clear from Fig. 3 that the length of the vector OA is always greater than zero if  $\omega_i \neq 0$ . The length of the vector DE can be made less than that of OA for a certain ratio of the parameters of the aperiodic feedback, and may even be reduced to zero. In fact, if the vector OD is parallel to the real axis, and its magnitude is unity, we have  $|DE| = 0$ , and  $|\delta| = 0$ .

Thus, for a specified value of  $|\delta|$  and a known value of  $Y_0(j\omega)$  at a definite working frequency, it is possible to use a graphical construction to select the parameters of the aperiodic feedback such as to make the ratio of the vectors DE and OD equal to  $|\delta|$ , i.e., to make the system under study operate with a specified error.

In the case of rigid external feedback, the steady-state phase error for a harmonic driving function with a frequency  $\omega_1$  will be equal to the angle ABO (Fig. 3) [9]; in the case of an aperiodic feedback, the error is determined from Equation (2):

$$\Phi(j\omega_1) = \frac{1}{Y_0(j\omega_1) + W_f(j\omega_1)}.$$

It is clear from Fig. 3 that  $\Phi(j\omega_1) = \frac{1}{OD}$ , and therefore the phase error for the latter case will be determined by the magnitude of the angle between the vector OD and the positive direction of the real axis — by the angle DOE (Fig. 3); by proper choice of the parameters of the aperiodic feedback this error can be reduced or made to vanish.

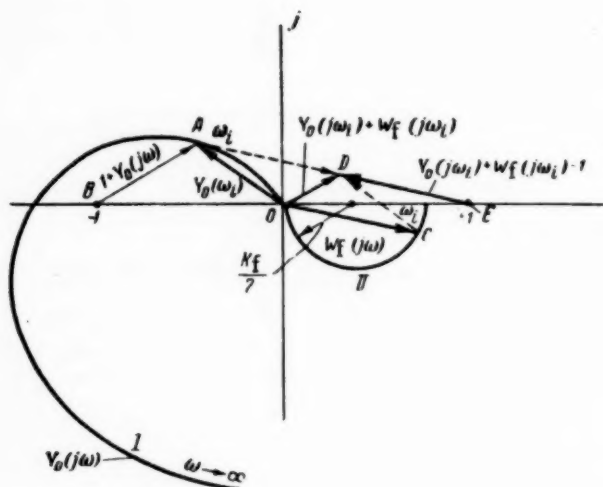


Fig. 3

If the steady-state system error vanishes, the phase error also vanishes, for in this case the vector OD is aligned with the positive direction of the real axis.

## 2. Use of Aperiodic Feedback in Automatic Regulation Systems

Let us examine the advisability of introducing aperiodic feedback in a multi-loop automatic-regulation system with internal rigid feedback and with driving forces applied to the regulation object.

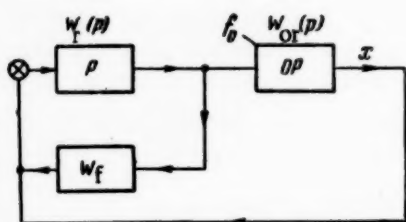


Fig. 4

Figure 4 shows the structural diagram of the system, containing the regulation object and an aperiodic feedback loop, including the regulator and replacing the rigid feedback.

Let the object of regulation have a transfer function of the following form: \*

$$W_{or}(p) = \frac{k_{or}}{p(1 + T_{or}p)}. \quad (14)$$

\* The regulation object may have a transfer function of another form, for example, in the regulation of thermal processes  $W_{or}(p) = k_{or} / (1 + T_{or}p)$ , and in the case of an automatic rudder system

$$W_{or}(p) = \frac{k_{or}(1 + a_1p)}{p(1 + a_2p + a_3p^2)}, \text{ etc.}$$

Assume that the transfer function of the regulator, without the feedback is:

$$W_r(p) = \frac{R(p)}{Q(p)}. \quad (15)$$

The over-all transfer function of the open system, in the case of an aperiodic internal feedback including the regulator, is [10]:

$$W_o(p) = \frac{W_r(p) W_{or}(p)}{1 + W_r(p) W_f(p)}$$

or

$$W_o(p) = \frac{k_{or}(1 + T_f p) R(p)}{Q(p) p (1 + T_{or} p) (1 + T_f p) + R(p) k_f p (1 + T_{or} p)}. \quad (16)$$

The reciprocal transfer function of the open system is

$$Y_o(p) = Y_{o1}(p) + \frac{k_f}{k_{or}} \frac{p(1 + T_{or} p)}{(1 + T_f p)}, \quad (17)$$

where

$$Y_{o1}(p) = \frac{1}{W_r(p) W_{or}(p)}.$$

Figure 5 shows part of the reciprocal amplitude-phase characteristics of the open regulation system,  $Y_{o1}(j\omega)$ , without internal feedback (Curve I) and shows the change of this characteristic resulting from introducing internal rigid feedback (Curve III) and an aperiodic feedback (Curve II) at  $T_f = T_{or}$ .

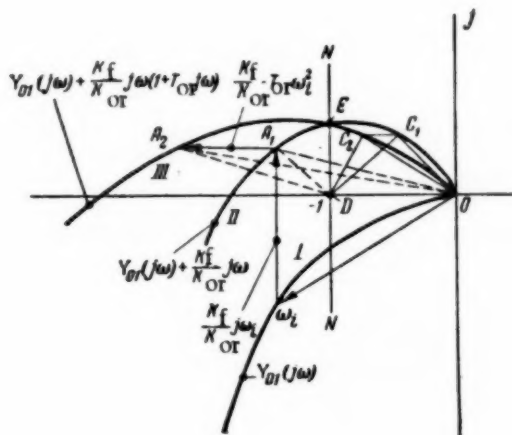


Fig. 5

If  $T_{or} > T_f$ , each of the vectors of characteristic II will be rotated clockwise by an angle equal to the difference of the arguments of the vectors,  $\overline{1 + T_{or} j\omega} - \overline{1 + T_f j\omega}$ . The moduli of the vectors of Curve II will increase, since the modulus of the vector  $\overline{1 + T_{or} j\omega}$  will be greater than the modulus of the vector  $\overline{1 + T_f j\omega}$ .

If  $T_{or} < T_f$ , the vectors of characteristic II will be turned counter-clockwise and their moduli will diminish.

Figure 5 shows that if rigid internal feedback is used, two vectors,  $\frac{k_f}{k_{or}} j\omega$  and  $-\frac{k_f}{k_{or}} T_f \omega^2$ , are added to each vector  $Y_{o1}(j\omega)$ . On the other hand, if aperiodic internal feedback is used (if  $T_{or} = T_f$ ) it is necessary to add to each vector  $Y_{o1}(j\omega)$  only one vector  $\frac{k_f}{k_{or}} j\omega$ .

This is why the modulus stability margin is less in the case of internal aperiodic feedback than in the case of internal rigid feedback.\* The regulation time will be less in the case of aperiodic internal feedback than

\* The term "modulus stability margin" denotes the value of the modulus of the vector of the reciprocal amplitude-phase characteristic at a  $180^\circ$  phase angle.

In the case of rigid feedback, since the frequency at the point E is greater for Curve II than for Curve III [8]. Let us study the effect of aperiodic feedback on the error of our system.

The closed-loop transfer function of the regulation system for a disturbance to the regulation object (Fig. 4) is

$$\Phi(p) = \frac{\Delta x}{f_0} = \frac{W_{or}(p)}{1 + W_0(p)} = \frac{W_{or}(p) Y_0(p)}{1 + Y_0(p)}, \quad (18)$$

where  $\Delta x$  is the deviation of the regulated quantity from the specified value.

The relative steady-state error in the case of a harmonic driving function will be

$$|e| = \frac{|\Delta x|}{|f_0|} = \frac{|W_{or}(j\omega)| |Y_0(j\omega)|}{|1 + Y_0(j\omega)|}. \quad (19)$$

The vector  $W_{or}(j\omega)$  remains constant for the specified frequency. We need therefore consider only the effect of the term  $\frac{|Y_0(j\omega)|}{|1 + Y_0(j\omega)|}$  on the quantity  $|e|$ . If the object of regulation has a sufficiently high inertia, then the working frequencies for which it is necessary to find error will obviously lie in a region close to the origin (Points  $C_1$  and  $C_2$ ). The errors will be equal for points  $C_1$  and  $C_2$ ; for Curve II,  $|e_1| = \frac{|OC_1|}{|DC_1|} |W_{or}(j\omega)|$ , and for Curve III,  $|e_2| = \frac{|OC_2|}{|DC_2|} |W_{or}(j\omega)|$ , where

$$OC_1 = Y_0(j\omega), \quad OC_2 = Y_0^*(j\omega), \quad DC_1 = 1 + Y_0(j\omega), \quad DC_2 = 1 + Y_0^*(j\omega).$$

It can be seen from Fig. 5 that the region lying to the right of the straight line NN, parallel to the imaginary axis and passing through the point  $(-1, j0)$  is where the following inequalities hold:  $|DC_1| > |DC_2|$ ,  $|DC_1| < 1$ , and  $|DC_2| < 1$ ,  $|OC_1| < |OC_2|$ .

Therefore,  $\frac{|OC_1|}{|DC_1|} < \frac{|OC_2|}{|DC_2|}$ , i.e., replacing the rigid internal feedback with an aperiodic feedback reduces the steady-state error. The bandwidth of the system increases. If  $T_{or}$  increases, the vector  $C_1C_2$  increases and so does the error  $e_2$ .

If the driving function frequency is sufficiently high, the operating frequencies of the system will be located away from the origin (for example, points  $A_1, A_2$ , in Fig. 5) and the steady-state error will not be reduced by substituting an aperiodic feedback for a rigid one. In fact, if we take  $OA_2 = k_1 OA_1$  and  $DA_2 = k_2 DA_1$ , one readily obtains  $|e_2| = \frac{k_1}{k_2} |e_1|$ . It is evident from Fig. 5 that  $k_1 < k_2$  and therefore  $|e_2| < |e_1|$ .

The substitution of aperiodic feedback for a rigid internal feedback is therefore advisable only in automatic-regulation systems with low operating frequencies, i.e., with frequencies that lie in a region close to the origin (to the right of straight line NN).

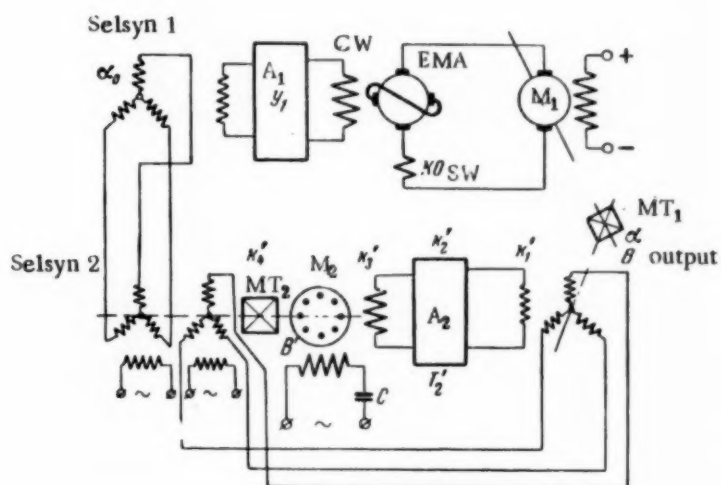
### 3. Practical Methods for Obtaining Aperiodic Feedback Loops

When used in practice, aperiodic feedback loops should introduce not only a delay in the operation, but also retain linear relationships between the output function of the system and the value of the signal at the output of the feedback loop.

Figure 6 shows the principal diagram of a servosystem in which the aperiodic feedback loop represents a low-power servo drive having an open-loop transfer function of the form



where  $T_2'$  is the time constant of amplifier  $A_2$ , and  $B'$  is the electromechanical time constant of motor  $M_2$ .



The closed-loop transfer function of the feedback loop is

$$W_f(p) = \frac{W_f(p)}{1 + W_f(p)}. \quad (20)$$

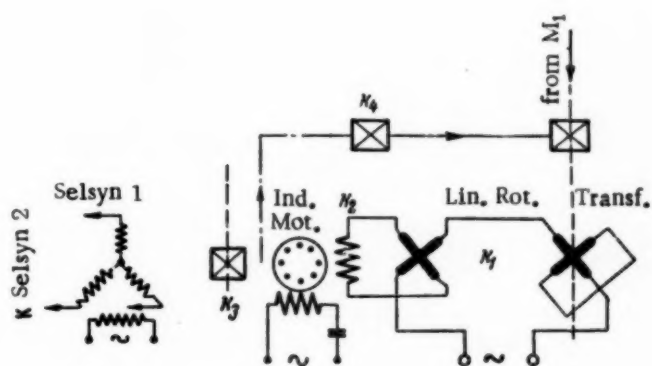


Fig. 7

Substituting the value of the transfer function  $W_f(p)$  into (20), we get

$$W_f(p) = \frac{k'_0}{p(1 + T'_2 p)(1 + B'p) + k'_0}.$$

If the feedback loop employs a vacuum tube amplifier and a two-phase induction motor of the ADP type one can assume  $T'_2 \approx 0$  and  $B' \approx 0$ , and use Equation (1) to obtain the transfer function, with

$$T_f = \frac{1}{k'_0}.$$

By varying  $k'_0$  we can vary the time constant  $T_f$  over a sufficiently wide range.

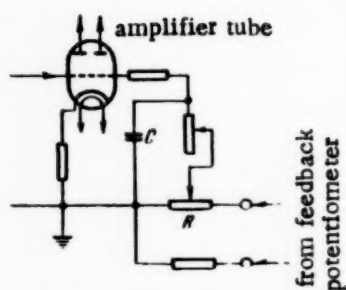


Fig. 8

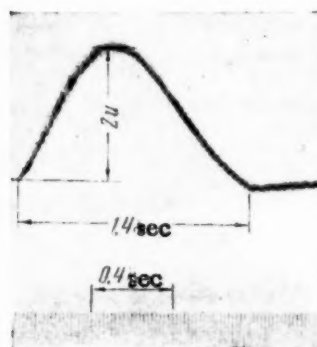


Fig. 9, a

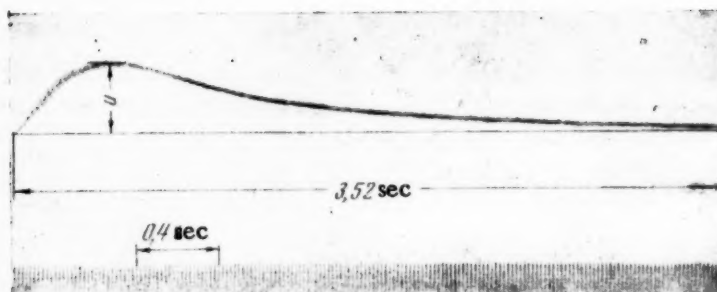


Fig. 9, b

The aperiodic feedback loop can be considerably simplified by replacing the selsyns with linear rotary transformers, feeding directly a type ADP two-phase induction motor with hollow rotor. The principal diagram of such a loop is shown in Fig. 7.\* The closed-loop transfer function can be obtained from Equation (1) by putting

$$k_f = \frac{k_3}{k_4}, \quad T_{oc} = \frac{1}{k_1 k_2 k_4}.$$

\* Such a feedback loop permits a limited (less than  $360^\circ$ ) rotation of the output shaft of the system.

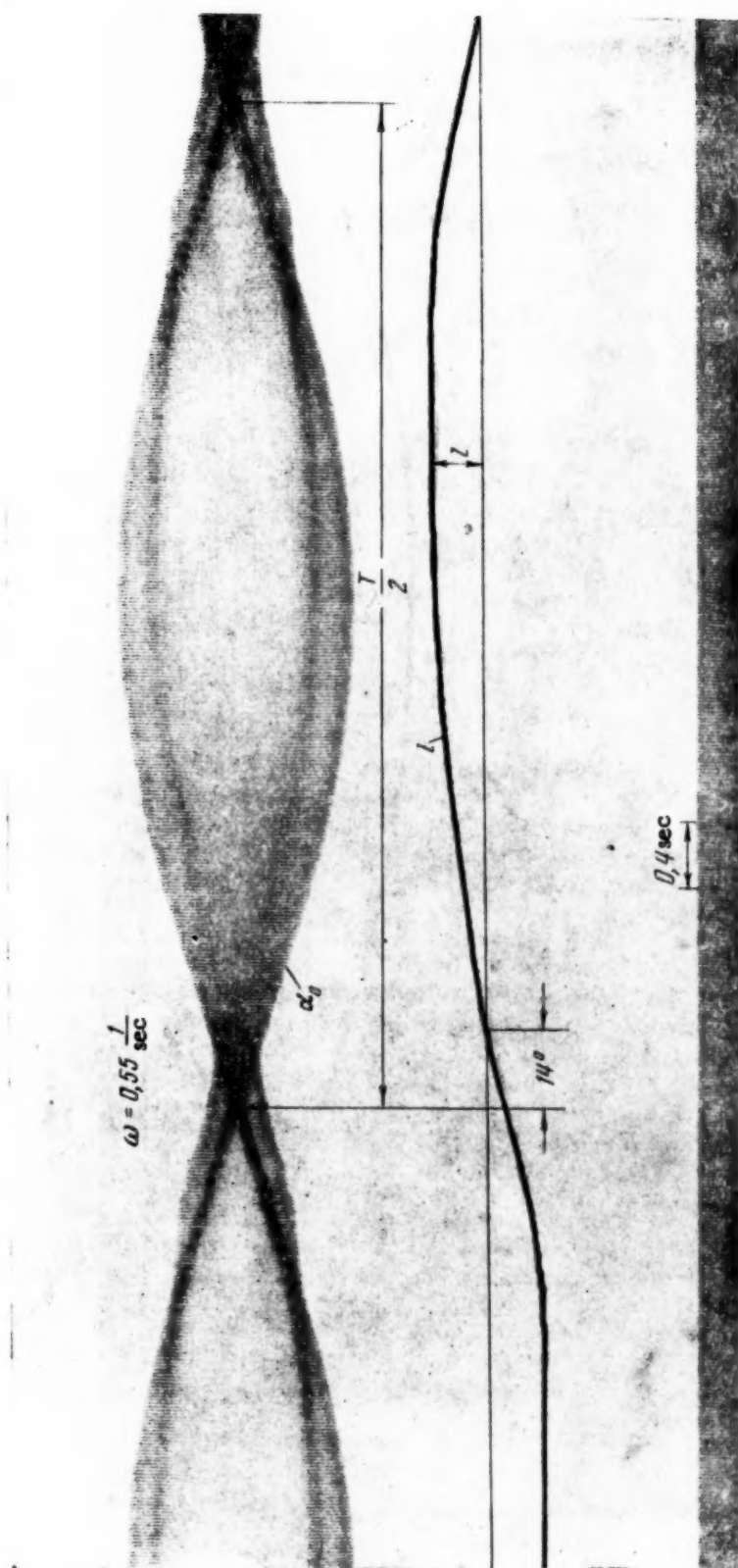


Fig. 10, a

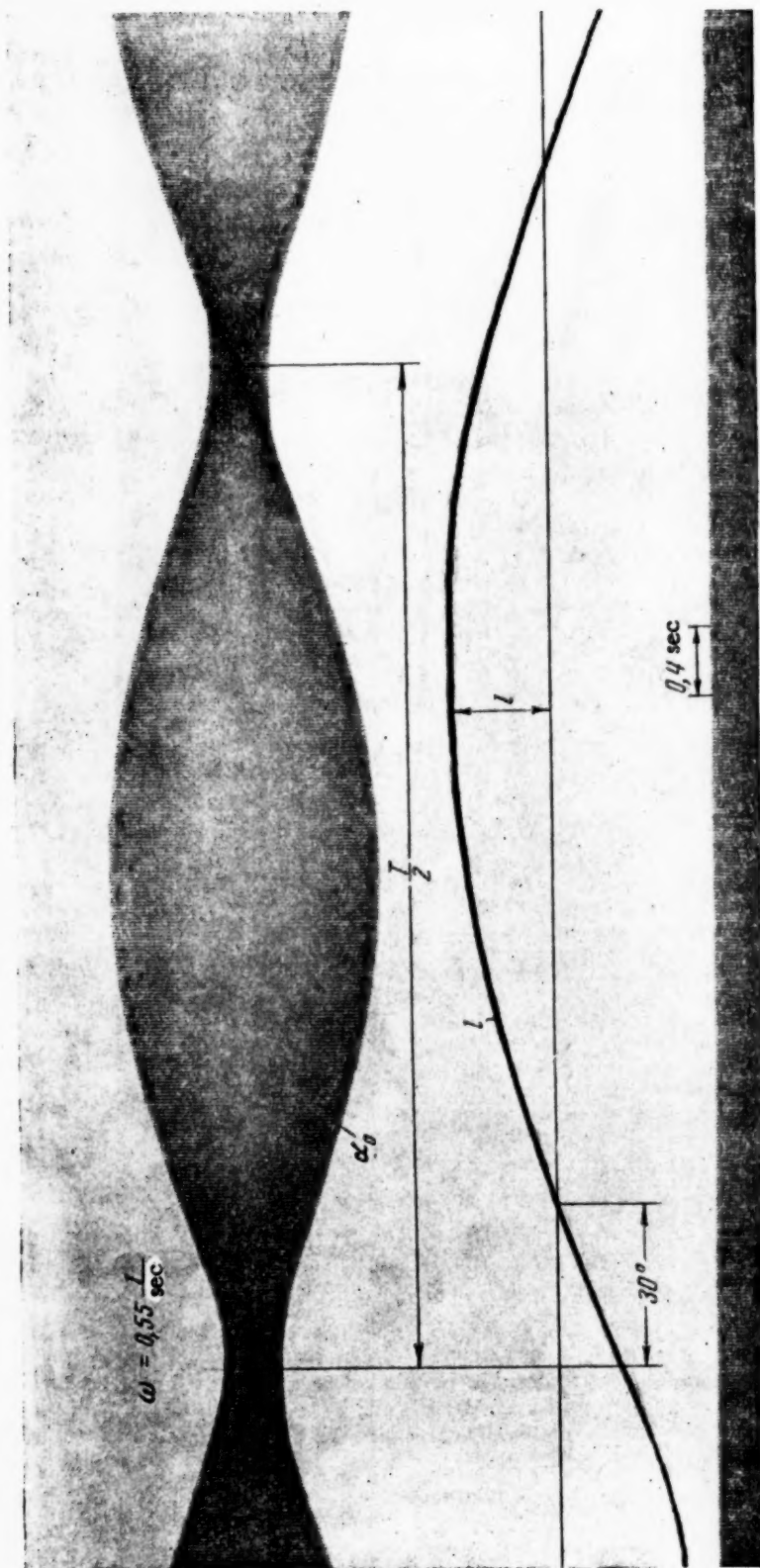


Fig. 10, b

The feedback coefficient ( $k_f$ ) can be regulated by changing the gear ratios of the mechanical transmissions  $k_3$  and  $k_4$ . Changing  $k_4$  will change simultaneously the time constant of the feedback loop.

If a vacuum tube or transistor amplifier is used as an intermediate amplifier, the aperiodic feedback loop can be formed by the RC circuit (Fig. 8) [4]. A regulating system, in which the regulating device is a servosystem (regulating systems for steam boilers, control system containing automatic rudders or automatic pilots, etc.) it is possible to employ aperiodic feedback loops of the form shown in Figs. 6 - 8. The loop must contain the regulator (servomotor) (Fig. 4).

#### 4. Experimental Investigation

A servosystem with aperiodic feedback was experimentally investigated to determine the effect of the aperiodic feedback on the response of the system.

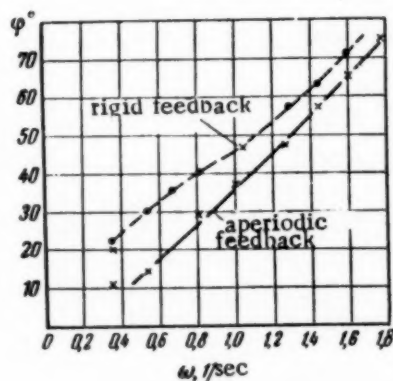


Fig. 11

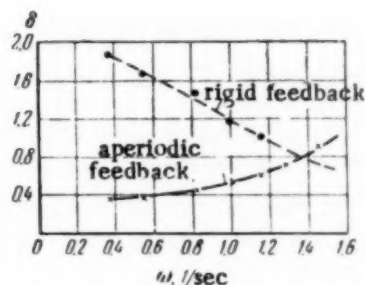


Fig. 12

The following investigation method was used: driving functions in the form of step functions or sinusoidal waves were applied to the input of the servosystem, the simplified circuit of which is shown in Fig. 6.\* An oscillograph was used to record the output and driving angles in the case of sinusoidal and step inputs. The investigations were repeated for the same conditions with the aperiodic feedback loop disconnected.

Figures 9 and 10 show oscillograms illustrating the transient in the servosystem for aperiodic (Figs. 9, a, 10, a) and rigid feedback (Figs. 9, b, 10, b) for a step function (Fig. 9) and harmonic driving function with a frequency  $\omega = 0.55 \text{ sec}^{-1}$  (Fig. 10).

Figure 11 shows the experimental curves for the variation of the phase error, and Fig. 12 shows the relative steady-state error of the system under investigation for various driving-force frequencies.

The time constant of the aperiodic feedback was approximately 0.15 sec. The experimental investigation of a servosystem with aperiodic feedback confirms the previously-made conclusion concerning the favorable effect of aperiodic feedback on transient response of the system and on the magnitude of its error.

\* Figure 6 does not show the stabilizing feedback loops.

## SUMMARY

The following conclusions can be drawn from the investigations:

1. Replacing rigid feedback loops in automatic-regulation systems with aperiodic ones reduces the velocity and the steady-state amplitude and phase errors.
2. The use of aperiodic feedback is recommended for automatic-regulation systems with slowly varying driving functions, for example, for harmonic signals with long periods.

## LITERATURE CITED

- [1] V. D. Mironov, On the Analysis of a Regulation Process with a Constant Speed and Flexible Feedback, *Izvestiya VTI*, No. 12, 1947.
- [2] V. D. Mironov, E. P. Stefani, and I. I. Davydov, The VTI Electronic Regulator, *Izv. VTI*, No. 3, 1949.
- [3] V. D. Mironov, Improved VTI Regulator, *Izv. VTI*, No. 7, 1952.
- [4] V. D. Mironov and E. P. Stefani, Electronic Automatic Regulators for Thermal Processes, Gosenergoizdat, 1955.
- [5] A. M. Kats, Theory and Application of Speed Regulators with Flexibly-Coupled Dashpot, *Automation and Remote Control* 12, 2 (1951).
- [6] W. Oppelt, *Kleines Handbuch technischer Regelvorgänge*, 1954.
- [7] A. A. Feldbaum, *Electric Automatic Regulation Systems*, Oborongiz, 1954.
- [8] V. V. Solodovnikov, Stability of Linear Servosystems and Regulation Systems, *Automation and Remote Control* 7, 1 (1946).
- [9] S. Ya. Berezin, On the Problem of Determination of Steady-State Operating Errors of Servo Drive in Response to Harmonic Signals, *ibid.*, 14, 4 (1953).
- [10] A. V. Fateev, *Fundamentals of Linear Theory of Automatic Regulation*, Gosenergoizdat, 1954.

Received January 23, 1956.



## SYNTHESIS OF RELAY CIRCUITS WITH THE AID OF MACHINES

F. Svoboda

(Prague)

Description of a semiautomatic experimental machine developed by the Institute of Mathematical Computers of the Czechoslovak Academy of Sciences for the synthesis and analysis of single-stroke relay circuits. The machine operates with indeterminate switching functions. The use of this machine in conjunction with the combinatorial method of synthesis expedites the circuit design by approximately 10 times.

### 1. Introduction

The theory of the design of relay machines or of their separate parts is still in the initial stages. The intuitive method is of little help in the solution of problems with a large number of input or output conditions, or for the solution of a large number of problems of any one definite type. The usual analysis methods become too cumbersome in this case, and become entirely useless for problems having a certain degree of complexity. The designers attempt therefore to cope with these more complex problems by introducing where possible a certain systematization in the process of the design of the relay circuits. It is interesting that one of the first to work along these lines was the Czech engineer Martin Boda [1].\* The works of the Austrians R. Edler and O. Plechl are based to some extent on Boda's work. Methods of this kind were slow to develop. Later, particularly after the second world war, many works were published on the design of relay circuits. The reader can gain an idea of the development of methods for design of relay circuits by reading, for example, the book by M. A. Gavrilov [2]. A very effective method was developed by A. Svoboda [3, 4].

Along with using graphic and graphite-mechanical methods, it is possible to synthesize relay circuits with machines, in which it is possible to insert the operating conditions of the circuit and which produce a definite solution in a predetermined form.

The results to date in the field of automatic synthesis of relay circuits are few in number. The feasibility of such a machine is mentioned in an article by C. E. Shannon, who lists in his introduction possible machines of this type, and who discusses later a method for the design of a automatic chess-playing machine.

In April 1953, A. Svoboda proposed the synthesis of a relay circuit by means of a machine that employs a model of the circuit. This procedure was used also by C. E. Shannon and E. F. More [7] in their relay-circuit analyzer.

By "model of the circuit" is meant a machine element containing directly those structural elements, of which the circuit is comprised, i.e., a relay with contacts in our case. The relay contacts are brought out to a plugboard (switching panel), where they can be interconnected at will with flexible cords.

The Shannon-More machine can also solve problems in the synthesis of relay-contact circuits. This is done by manually synthesizing any version of the circuits, which is then inserted into the machine and simplified

---

\* I am indebted to G. N. Povarov for calling this to my attention.

by eliminating "excess" contacts. It is clear that this method does not eliminate the fundamental work involved in the design of the circuit.

In dealing with this problem in the Institute of Mathematical Computers of the Czechoslovak Academy of Sciences, we observed that the automatic-synthesis problem is equivalent to a considerable extent to the problem of choosing an advantageous synthesis method that lends itself to automatization. The author of this article developed the so-called combinatorial method, which satisfies the principal requirements imposed on such a method, namely simplicity and generality.

We know that the principal theoretical tool for the synthesis of relay circuits is Boolean algebra, which is widely used at the present time. As already explained, this algebra is not suitable for mechanical synthesis of relay circuits.

The use of the combinatorial method expedites substantially the entire circuit-design process. At the present stage of development, the machine of the Institute of Mathematical Computers of the Czechoslovak Academy of Sciences can be used to synthesize combinatorial relay circuits having  $n$  switching variables,  $p$  inputs, and  $m$  outputs, provided  $n + p + m \leq 12$  and  $n_{\max} = 6$ . This limitation is imposed by the fact that the model contains six relays with eight switching contacts each. The input variables and the output functions can be specified for a maximum of 32 independent variables, i.e., for 32 different states of the circuits.

The machine has been in operation a relatively short time. The work required to design the circuits is expedited by approximately 10 times. In addition, it is possible to set up with the machine more complicated circuits than could be obtained with ordinary "manual" methods.

The machine is semiautomatic in the sense that the attendant must perform the switching manually, with the aid of flexible cords, in the particular unit in which we wish to form the circuits. This is done on the basis of information obtained by means of the machine. For each elementary synthesis operation one can read at the output of the machine the type of contacts that is to be used for the given operation and the method of connecting these contacts.

## 2. Combinatorial Method \*

The combinatorial method for the synthesis of contact circuits was described elsewhere [6]. The circuit is built up in the sequence illustrated in Fig. 1. Each section of the diagram denotes several parallel contacts of different relays. These elements are called  $\Sigma$ -branches, representing the maximal two-terminal network of the circuit. This network contains only two nodes and cannot contain along with contact  $\tilde{x}_i$  other contacts  $\tilde{x}_i$  or  $\bar{\tilde{x}}_i$  of the same relay. The  $\Sigma$ -branch contains the maximum  $n$  contacts. The points on Fig. 1 denote the nodes, the output terminals are shown to the right, and the input terminal is shown to the left in the figure. One section is added in each elementary increment of the circuit. One can see from the individual stages shown in the illustration that the circuit is alternately built up by two methods; we shall therefore speak of two operations,  $\omega_1$  (stages 3, 4, 5, 6, 7, and 8) and  $\omega_2$  (stages 1, 2, 9, and 10).

The elementary operations  $\omega_1$  and  $\omega_2$  are carried out, with the aid of functions to be described below, at the nodes (poles) of the circuit.

In the analysis of the completed circuit, it is possible to define the switching functions in its internal nodes and poles. We shall denote these by  $F(x_1, x_2, \dots, x_n)$  and  $X_k(x_1, x_2, \dots, x_n)$ , respectively, where  $k = 1, 2, \dots, m$ ;  $x_1, x_2, \dots, x_n$  are the independent input variables.

At any given node  $U$ , the functions  $F$  or  $X_k$  assume the values 0 or 1 for the given combination of arguments, depending on whether or not the node  $U$  is connected to the input pole.

In the gradual synthesis of the circuit by the combinatorial method we shall employ four values of the functions at the nodes or poles: 0, 1,  $\bar{1}$ , and  $\sim$ . We shall now explain the meaning of these values, which differs somewhat from the meaning of the values 0 and 1 used in the analysis.

\* It will be assumed hereinafter that the relay has an unlimited number of contacts. In practice this assumed relay may consist of several parallel relays, each having a finite number of contacts (3 - 5), depending on its construction.

Let us imagine an incomplete circuit, obtained either by removing certain elements from a complete circuit, or to the contrary, during the gradual synthesis process. However, let, the function at the output poles  $P_k$  be completely known. Let us again analyze this circuit and, given a combination of the values of the independent variables  $x_1, x_2, \dots, x_n$ , let us assume the following values for the switching function at the node or at the pole:

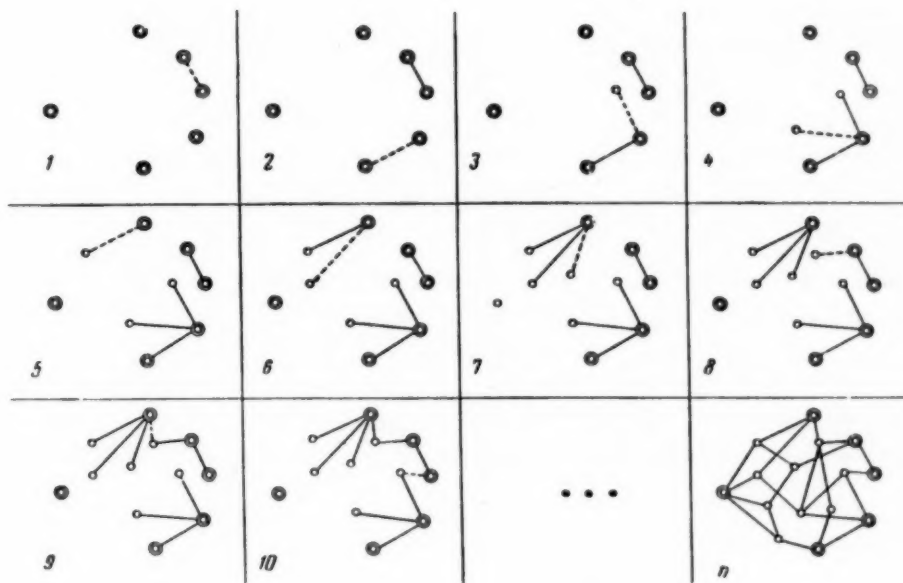


Fig. 1. Process of formation of the circuit with the aid of the combinatorial method.

the value 0, if the node  $U$  is connected to at least one output pole, the functions of which are specified by the operating conditions of the circuit to have a value 0;

the value 1, if the node  $U$  is connected to at least one output pole, the function of which is specified by the operating conditions of the circuit to have a value 1;

the value  $\bar{1}$ , if the node  $U$  is connected to an input pole;

the value  $\sim$  ("indeterminacy"), if the node  $U$  is connected to no pole or if it is connected to one or several output poles, for which the functional values were not specified, and can consequently be chosen arbitrarily\* (compare with the concept of the indeterminate switching function in [7, 8, and 9]).

All nodes or poles are accordingly assigned functions  $F$  and  $X_k$  in tabular form; these functions assume four values. The solution is not yet complete, and the work must be continued by using the operation  $\omega_1$  or  $\omega_2$ .

Using the functions at the node, we first determine the so-called auxiliary indeterminate switching functions  $\varphi$  for operation  $\omega_1$  and  $\psi$  for operation  $\omega_2$ :

$$\varphi[F(x_1, x_2, \dots, x_n)], \psi[F_1(x_1, x_2, \dots, x_n), F_j(x_1, x_2, \dots, x_n)],$$

which assume the values 0, 1, and  $\sim$ . These functions are used to select the contacts with which the operations  $\omega_1$  and  $\omega_2$  are performed.

\* According to this method of designation, the function at the node can assume simultaneously both values  $\bar{1}$  and 1. It is readily seen that this leads to no contradiction, signifying only that the node  $U$  is connected to at least one output, the function of which is assigned a value 1, and is also connected to the input.

Before considering all the possible cases occurring in the determination of the functions  $\varphi$  and  $\psi$ , let us study the general meaning of the values 0, 1, and  $\sim$ .

These functions assume the value 0 if it is desired that the function  $f(x_1, x_2, \dots, x_n)$  of the  $\Sigma$ -branch be equal to zero.

The functions assume the value 1 if it is desired that the function  $f(x_1, x_2, \dots, x_n)$  of the  $\Sigma$ -branch be equal to 1.

The functions assume the value  $\sim$  if it is immaterial whether the function  $f(x_1, x_2, \dots, x_n)$  assumes the value 0 or 1.

Let us now consider the two operations in sequence.

The left side of Fig. 2 shows a table for the determination of the functions  $\psi [F_i(x_1, x_2, \dots, x_n), F_j(x_1, x_2, \dots, x_n)]$  for operation  $\omega_2$ .

Recalling the meaning of the values 0, 1,  $\sim$ , and  $\sim$  just defined, we can readily determine the functional values of  $\psi$ . Let us consider the fundamental cases.

Fig. 2. Table for finding the auxiliary indeterminate functions  $\varphi$  and  $\psi$ .

$F_i$	$F_j$	$\psi$	$F$	$\varphi$
0	0	$\sim$	0	0
1	0	0	1	1
1	0	0	1	$\sim$
$\sim$	0	$\sim$	$\sim$	$\sim$
1	1	1, $\sim$		
1	1	1		
$\sim$	1	$\sim$		
1	1	$\sim$		
$\sim$	1	$\sim$		
$\sim$	$\sim$	$\sim$		

A value of 0 is indicated in the second and third lines. The fact is that connecting the nodes  $U_i$  and  $U_j$  in this state, would result in spurious circuits. For this reason, most  $\omega_2$  operations will not be realized, for in most cases one cannot connect a pair of nodes through a nonempty\*  $\Sigma$ -branch.

$x_3$	$x_2$	$x_1$	$F_i$	$F_j$	$\psi$	$x_3$	$\bar{x}_3$	$x_2$	$\bar{x}_2$	$x_1$	$\bar{x}_1$
0	0	0	1	$\sim$	$\sim$	0	1	0	1	0	1
0	0	1	1	1	1	0	1	0	1	1	0
0	1	0	0	1	0	0	1	1	0	0	1
0	1	1	$\sim$	0	$\sim$	0	1	1	0	1	0
1	0	0	1	1	1, $\sim$	1	0	0	1	0	1
1	0	1	0	1	0	1	0	0	1	1	0
1	1	0	1	1	1	1	0	1	0	0	1
1	1	1	1	0	0	1	0	1	0	1	0

Fig. 3. Simple examples of the determination of the function  $\psi$ .

The value 1 is indicated in the 5th and 6th lines. Let us consider the sixth line first. The node  $U_i$  is connected to the input pole, and the unit  $U_j$  is connected to some output pole, the function of which can be assigned a value 1 in this state. It is therefore desirable to join these two nodes, for this effects also the connection between the input pole and the corresponding output pole. This is clearly not essential, but if it is desirable to bring the solution to its conclusion, we will have to effect this connection in some other manner.

The fifth line is somewhat more complicated for it is impossible to determine from the values of the functions whether these two nodes are joined. We must therefore determine this fact somehow and choose a solution accordingly. If the nodes are already joined, there is no sense in joining them again, and consequently,  $\psi = \sim$ , but if the nodes are not joined, it may be useful in the solution to join them. As soon as one of the nodes is joined to the input pole, the other node is simultaneously joined with the same pole.

A value of  $\sim$  is indicated in the remaining cases. Let us call attention to the fact that in such cases it is either impossible to decide whether nodes  $U_i$  and  $U_j$  should be joined (lines 4, 7, and 9) or else it is immaterial whether the junction is effected or not (lines 1, 8, 10).

Figure 3 shows a simple example.

\* This is, one containing at least one contact.



The table for the determination of the functions  $\varphi[F(x_1, x_2, \dots, x_n)]$  for the operation  $\omega_1$  is shown to the right of Fig. 2.

A value of 0 is indicated in the first line. This signifies that upon choosing the  $\Sigma$ -branch  $f(x_1, x_2, \dots, x_n)$  for the operation, the functional value can be chosen in the new mode at will; it therefore has a value  $\sim$ .

A value 1 is indicated in the second line. This means that after choosing the  $\Sigma$ -branch  $f(x_1, x_2, \dots, x_n)$  for the operation, the given node can be joined with the input pole by means of a new node. The function in the node is usually still "less determinate" and affords therefore a wider choice for the operation  $\omega_2$ .

$x_3$	$x_2$	$x_1$	$F$	$\varphi$
0	0	0	1	$\sim$
0	0	1	$\sim$	$\sim$
0	1	0	0	0
0	1	1	1	1
1	0	0	1	1
1	0	1	0	0
1	1	0	$\sim$	$\sim$
1	1	1	1	$\sim$

Fig. 4. Simple example of the determination of the function  $\varphi$ .

Values  $\sim$  are indicated in the third and fourth lines, and their meaning is the same as in the preceding operation. An example is shown in Fig. 4. Assume that a circuit must be synthesized with one input pole  $P_0$  and with  $m$  output poles,  $P_1, P_2, \dots, P_k, \dots, P_m$ , specified in tabular form, as shown in Fig. 5, where the  $?$  sign stands for either 0, 1, or  $\sim$ . (Figure 18 shows an example of such a table).

Let us take one pair of functions after another, a total of  $\frac{m+1}{2}$  pairs (all poles are accordingly assigned certain functions), and let us determine the function  $\psi$  for each pair. This serves as the basis for the performance of operation  $\omega_2$ , i.e., for finding the function  $\psi$  and for connecting the

contacts, if possible. This is the beginning of the combinatorial method. We thus begin with the output terminals, a great convenience, as already mentioned.\* We shall call methods employing this initial step "direct methods."

$x_1$	$x_2$		$x_l$		$x_n$	$X_1$	$X_2$		$X_k$		$X_m$
0	0	.	0	.	0	?	?	.	?	.	?
0	0	.	0	.	1	?	?	.	?	.	?
.	.	.	.	.	.	.	.	.	.	.	.
.	.	.	.	.	.	.	.	.	.	.	.
.	.	.	.	.	.	.	.	.	.	.	.
1	1	.	1	.	1	?	?	.	?	.	?

Fig. 5. Operating condition table.

Assume we succeeded in connecting certain  $\Sigma$ -branches. Sometimes this may complete the solution, but in most cases, particularly in our case, the solution is not completed and a method different from the one used thus far must be followed.

Let us employ the other method, i.e., operation  $\omega_1$ . Let us take any pole  $P_k$ , at which not all specified conditions have been satisfied so far, so that at least one combination of the values of the input variables is encountered, while  $X_k = 1$  was specified for  $P_k$  and so far there is no 1.\*\* Wishing to complete the solution, we should, consequently, connect at least one more  $\Sigma$ -branch to the selected node. We thus connect one end of any  $\Sigma$ -branch to  $P_k$ , and the second end of this branch forms the first intermediate node  $U_1$ . We shall attempt

\* This, too, was noted by G. N. Povarov [8].

\*\* The poles (or nodes) at which the operation described here is performed, were called "leading" in [6]. These nodes make up part of all the nodes to which the operation  $\omega_1$  is applicable in this simplified form of the method.

to produce here  $f = 1$  for the states in which  $X_k = 1$ , i.e., we shall make the  $\Sigma$ -branch conducting. It is equally suitable (as will be shown below) to take  $f = 0$  for  $X_k = 0$ . It is clear that if the  $\Sigma$ -branch conducts,  $f = 1$  and  $F_1 = X_k$ , and where  $f = 0$ ,  $F_1 = \sim$ . We thus added new contacts to the circuit as a result of this operation. We also call this operation the expansion of the function  $X_k$  with the aid of the  $\Sigma$ -branch  $f$ .

It does not follow yet from the above description that we can complete the solution with the aid of these operations at all, and it is equally unclear what  $\Sigma$ -branches are to be used for the operations and what the next step is. But it is already clear that introducing the new node increased the number of possibilities of performing operation  $\omega_2$ . In some problems it may happen again that one or few such operations are enough to complete the solution, but if the solution is not completed, it is necessary to introduce another node, etc. Unless operations that are clearly unsuitable are introduced, the solution will come to an end after a certain time lapse, which increases with the complexity of the problem. This simplified form of the method makes no use of the value 1 for functions of the poles or of the nodes, in spite of the definite role that this value plays in the complete method [6].

Let us see now how the two operations can be performed most economically, economy being taken in the sense of minimum contacts.

Let us analyze operation  $\omega_2$ . In this operation we choose the  $\Sigma$  branch after determining the function  $\psi$  and comparing it with the functions of the contacts. The comparison is made only at those contacts  $\tilde{x}_i$ , at which  $\tilde{x}_i = 0$  when  $\psi = 0$ .

In comparison we shall count the states in which  $\psi = 1$  simultaneously with  $x_i = 1$ . The number of the states, if these relationships do take place, we shall denote by  $\check{\tilde{x}}_1$ . We next count the states in which  $\psi = 1$  simultaneously with  $\bar{x}_1 = 1$ , and set their number equal to  $\check{\bar{x}}_1$ . The number of states for which  $\psi = 1$  simultaneously with  $x_2 = 1$  we shall denote by  $\check{x}_2$ , etc. Finally, the number of states for which  $\psi = 1$  simultaneously with  $x_n = 1$  will be denoted  $\check{x}_n$ . We thus obtain the numbers  $\check{\tilde{x}}_i$  and  $\check{\bar{x}}_i$ . We choose for the operation  $\omega_2$  those permissible contacts, for which  $\check{\tilde{x}}_i$  is a maximum.

We gave an example of a simple operating hypothesis. It can be employed in the following manner. Let us assume that some arbitrary number  $\check{\tilde{x}}_i = 0$ . Were the operation to be performed only with this contact, it would serve no use in the solution, in spite of the fact that the operation is correct.\* If one must choose one of the  $\check{\tilde{x}}_i$ 's, the solution is expedited by choosing the largest of these numbers, for this would satisfy a greater number of cases in which the connection is desirable. If all the nonzero  $\check{\tilde{x}}_i$ 's are equal to each other, the result is symmetrical functions. It is then immaterial which of the contacts is used. But once some of these contacts are used, the "balance" is destroyed, and all these  $\check{\tilde{x}}_i$ 's will no longer be equal in the subsequent operations.

In spite of this "shortcoming" of the working hypothesis, this method does yield solutions with a rather small number of contacts. We can disregard the states in which  $\psi = 0$  and  $x_i$  (or respectively  $\bar{x}_i$ ) = 0, for such states make no substantial contribution to the solution. Even these, however, are of some interest, for they isolate neighboring nodes (otherwise the circuit may operate incorrectly). Experience helps in the correct performance of the operation in each individual case. States in which  $\psi = \sim$  do not play an important role.

The situation is analogous for operation  $\omega_1$ . In the performance of this operation it is forbidden to use a  $\Sigma$  branch to connect the employed node with the input pole, as explained earlier in the definition of the function  $\psi$ . This indicates, at the same time, that one cannot perform the operation  $\omega_1$  in such a manner as to make  $x_i = 0$  every time  $\varphi = 0$  and to make  $x_i = 1$  when  $\varphi = 1$ . This, however, is to some extent an ideal case, which need merely be approached. The fact is that one could attempt in that case to connect the second node, introduced with the aid of the  $\Sigma$  branch, directly to the input pole. The operation is therefore performed with the aid of those contacts  $\tilde{x}_i$ , at which the simultaneous combinations of  $\varphi = 0$  and  $\tilde{x}_i = 0$  or  $\varphi = 1$  and  $\tilde{x}_i = 1$  occur for the maximum number of cases.

\* This is used by certain enterprises to prevent copying of their developments. Excess operating elements are added to a normally-operating device to complicate the analysis of the product.



The selection is made in the same way as in the preceding case, with great attention being paid to the coincidence of the ones. For example, there would be no sense in performing the operation with the aid of  $\Sigma$  branch which satisfies the "zeros" of the function at the node, but does not satisfy the "ones" at the node at all. \*

### 3. Principal Arrangement of Machine

The machine employs the following blocks: model of the circuit, generator of switching functions, decoder, and function comparator (see Fig. 6, where the arrows indicate the logical direction of the information flow along the signal channels).

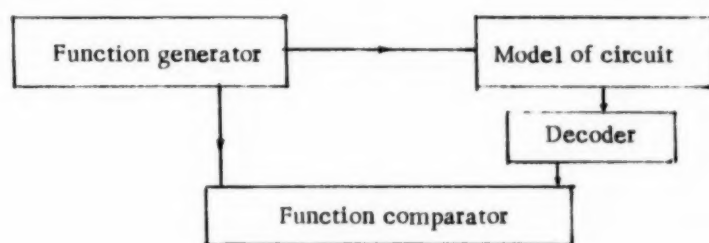


Fig. 6. Block diagram of machine.

The circuit model can be formed in two manners - "parallel" or "series" (see Figs. 7, a and 7, b, respectively).

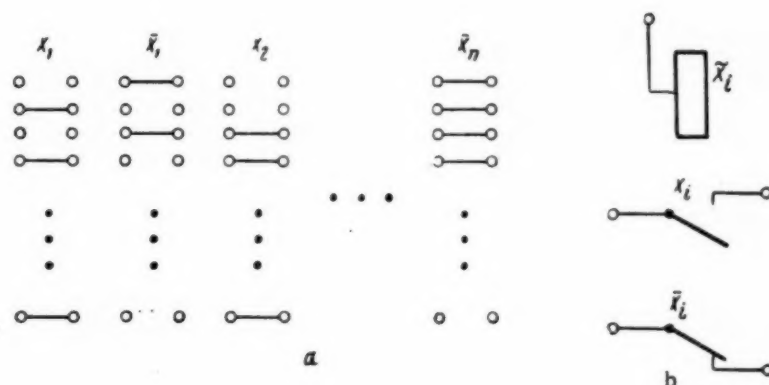


Fig. 7. Possibility of realization of the model of the circuit: a) "parallel" model; b) "series" model.

In the parallel model we employ  $2 \times 2^n$  terminals for each contact, say in the form of plug-in jacks. As can be seen, this model does not use contact relays; instead, the conduction states of contact  $x_i$  or  $\bar{x}_i$  are realized here for all the possible states of the circuit (see table on the right side of Fig. 3). If  $\tilde{x}_i = 1$  for any

\* If this comparison of the functions  $\varphi$  with the functions  $x_i$  or  $\bar{x}_i$ , is examined from the point of view of the functors of the mathematical logic [11], we can say that we define thereby a certain "measure of equivalence" of the functions  $\varphi$  and  $x_i$  or  $\bar{x}_i$ . In fact, it is correct to state that the functor of logical equivalence, which assumes two values, equals 1 if both predictions are (1, 1) or (0, 0), and equals 0 in all other cases. This measure varies over a range  $(2^n, 0)$ .

particular state, the neighboring terminals are connected (see terminals connected with heavy lines in Fig. 7, a). If, however,  $\tilde{x}_1 = 0$ , the terminals are not connected. In the series model (Fig. 7, b), relay contacts are used and are placed in sequence in  $2^n$  states. In each of these states, the contact either conducts or does not. Both types of models have their advantages and disadvantages.

The parallel model has the great advantage, that the information on the switching functions is obtained in a "global" manner and we have a clear idea of all the functional values. This model has, on the other hand, the important shortcoming that the operations are laborious, particularly for large  $n$ ; in addition, it cannot be extended readily to include a large number of variables. The opposite holds for the series model. We obtain the information on the functional values in sequence, and thus have no "global" view of them. However, this model is substantially briefer, and can be readily extended to include a large number of variables.

The series model employed in our machine is fed from output terminals having various voltages for the cases when  $X_k = 0$  or  $1$ , as is required for the combinatorial method.

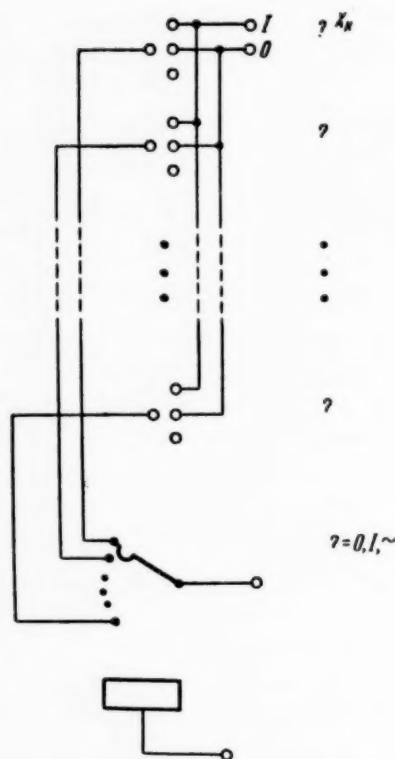


Fig. 8. Method of presentation of switching function in the function generator, and method of switching-function pick-off.

The switching-function generator contains one three-position element, such as a three-position switch, for each value of the input variable and for each value of the output function. Each of these elements can be independently placed in a position marked  $0$ ,  $1$ , and  $\sim$ , and thereby permits inserting into the machine the functional values specified in the operating-conditions table. The meaning of these values are described in Section 2. The generator contains also a device (telephone selector switch) which picks off the functional values and transmits them through the signal channel to the model of the circuit and to the function-comparator (Fig. 8). This may be effected in parallel or in series. This machine employs serial pick-off. If one of the values  $0$ ,  $1$ , or  $\sim$  is picked off, a voltage corresponding to this value is transmitted to the signal channel. One bar of the telephone selector is earmarked in the generator for each value of the input variable (relay)  $x_i$  and for each output  $X_k$ .

The above-mentioned series model contains relays with contacts. The terminals of these contacts are brought out to the plugboard. The terminals can be connected at will with flexible cord, thus making up the circuit. The control terminals of the relays and the input and output poles of the circuit are placed in the state specified by the table with the aid of the signal channel, which connects this block with the function generator. The auxiliary operation  $\omega_3$  [6] is thus performed automatically, and this is why we did not include this operation in the description of the combinatorial method given in Section 2. If a circuit is synthesized by

the combinatorial method without using a machine, this operation consists of setting  $\sim \rightarrow 0, 1, 1, 1$  or  $1, 1 \rightarrow 1, 1, 1$  after the operations  $\omega_1$  and  $\omega_2$ , so as to prevent formation of a wrong circuit. Flexible cords can be used to connect two probes to any two nodes and to determine the switching functions at these nodes. This information is transmitted to the decoder over the signal channel.

The next block is the decoder. Its input receives from the signal channel information on the functional values of the switching functions of the poles and of the nodes, and its output delivers information on the indeterminate function  $\varphi$  or  $\psi$ , depending upon the number of the functions (one or two). This information flows over the signal channel to the function comparator. The decoder performs still another function, which will be discussed in Section 4.

The function comparator is a block in which the values of the auxiliary indeterminate functions  $\varphi$  and  $\psi$  are compared with the functional values of the elementary structural elements, which are formed automatically in the machine, namely contacts  $x_1, \bar{x}_1; x_2, \bar{x}_2; \dots; x_n, \bar{x}_n$ . The coincidences of the functional values are counted as in Section 2. The results of this comparison are converted into information that expresses the measure of the suitability of each contact for operation  $\omega_1$  or  $\omega_2$ . The estimate obtained in this manner is both qualitative and quantitative. The qualitative estimate is performed only for the operation  $\omega_2$ , where we must determine what contacts will be used at all for the operation. A quantitative estimate is made for the contacts that are suitable for use in operation  $\omega_2$  and for all contacts in the case of operation  $\omega_1$ . Elements of the "on-off" type are used for the qualitative estimate, such as an optical signalling device (blinker), and counters are used for the quantitative estimate.

The blocks operate as follows. During the synthesis, the values of the operating-condition table are inserted into the function generator. A pick-off device is used to transmit these values over the signal channel first to the model of the circuit and second to the function comparator. The blocks are therefore placed in sequence in all the states specified by the operating-condition tables. The information on the auxiliary indeterminate function  $\varphi$  or  $\psi$  is formed in the following manner for the function comparator. Let, for example, the signal channel from the circuit model to the decoder be connected to some node  $U$  in the case of the function  $\varphi$  or to two nodes  $U_i, U_j$ , in the case of the function  $\psi$ . As the control terminals of the model and its input and output terminals are placed in the states specified by the tables, the nodes  $U$  or  $U_i$  and  $U_j$  are placed in definite voltage states, which serve as the basis for the formation of the functions  $\varphi$  or  $\psi$ . The function comparator thus receives simultaneous information on the auxiliary indeterminate functions  $\varphi$  and  $\psi$  as well as on the contact functions  $x_1, \bar{x}_1; x_2, \bar{x}_2; \dots; x_n, \bar{x}_n$ . The "required" connections are thus compared with the "available" connections, and as a result we obtain at the output of the comparator the exact qualitative and quantitative information which serve as the basis for the elementary operations  $\omega_1$  and  $\omega_2$ .

#### 4. Description of Machine

The machine is constructed with conventional units and parts: relays, selectors, counters, etc. Figure 9 shows the principal diagram of the machine. The blocks are shown in this diagram in the same order as in the block diagram in Fig. 6. The function generator is to the upper left, and the function comparator is beneath.

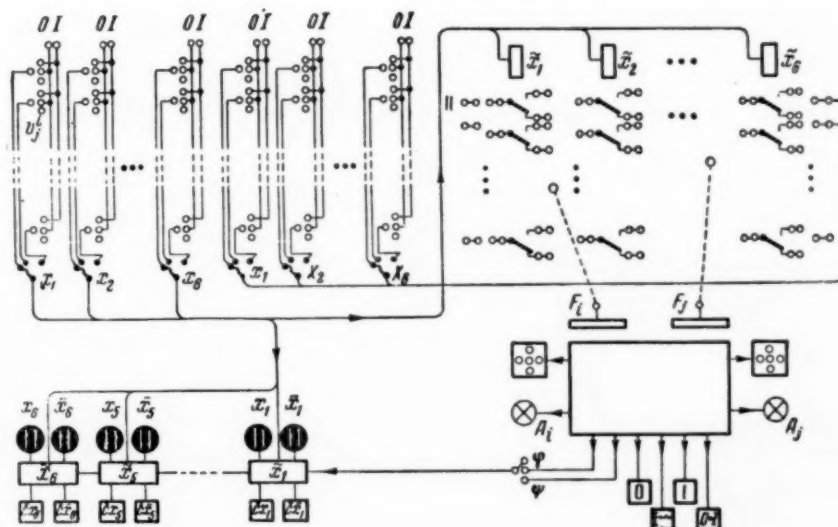


Fig. 9. Principal diagram of machine.

To the right of the generator is the circuit model, and beneath it is the decoder. The over-all view of the model and of the entire machine, built at the Institute of Mathematical Computers of the Czechoslovak Academy of Sciences, are shown in Figs. 10 and 11, respectively.

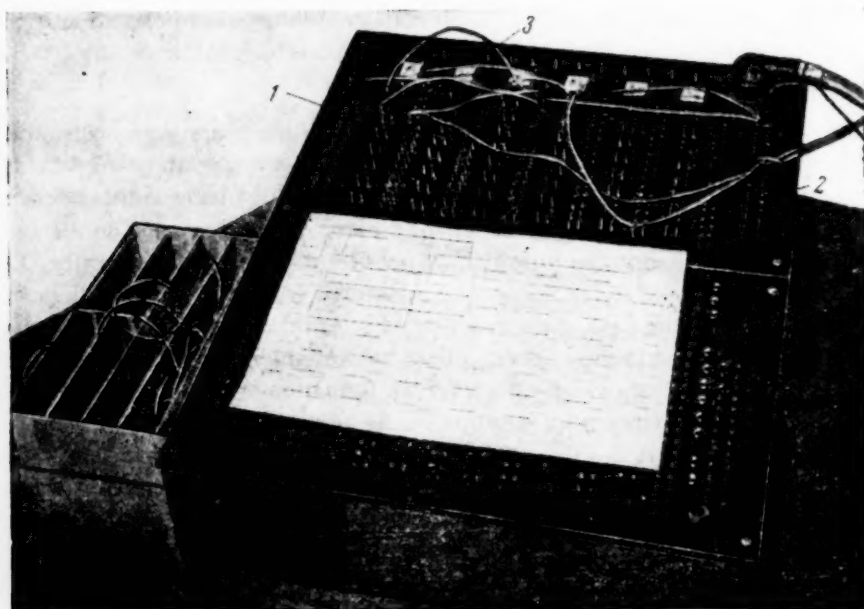


Fig. 10. External view of circuit model with log sheet for recording the circuit.

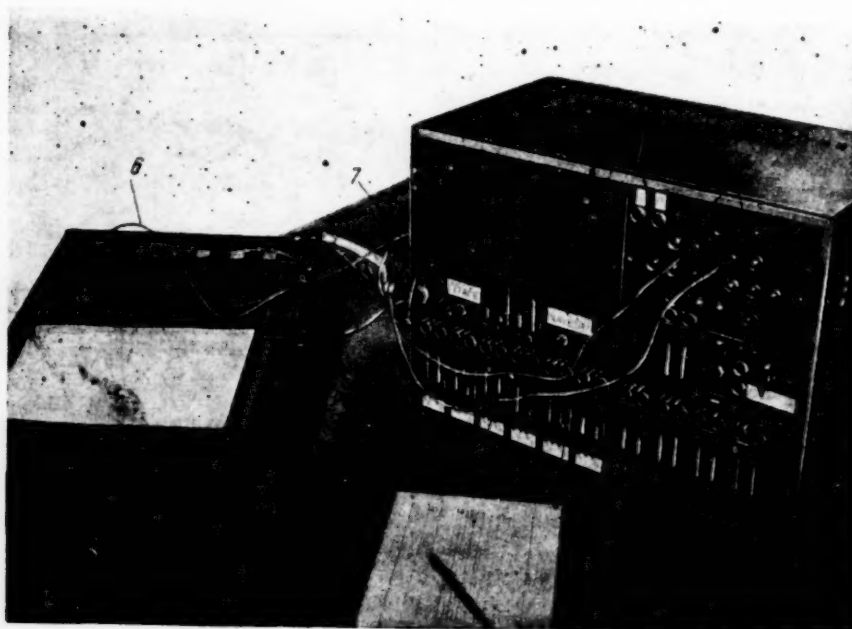


Fig. 11. Over-all view of the machine.

The three-position element used in the function generator is a plug receptacle and a plug (Fig. 12). The central positions of all the switches  $v_j^i$ , where  $i = 1, 2, \dots, n + m$  (in this case  $n = m = 6$  and  $j = 1, 2, \dots, 2^n$ ) denote 0, the upper position denotes 1, and the lower position  $\sim$  is produced by not inserting the plug. Terminals 0 and 1 are connected in parallel and are fed with three voltages:  $e_4 \sim 1$  for the input variables,  $e_2 \sim 1$  for the output functions, and  $e_3 \sim 0$ .  $e_2$  passes through rectifiers to distinguish whether two nodes with values 1 are connected directly in the model.

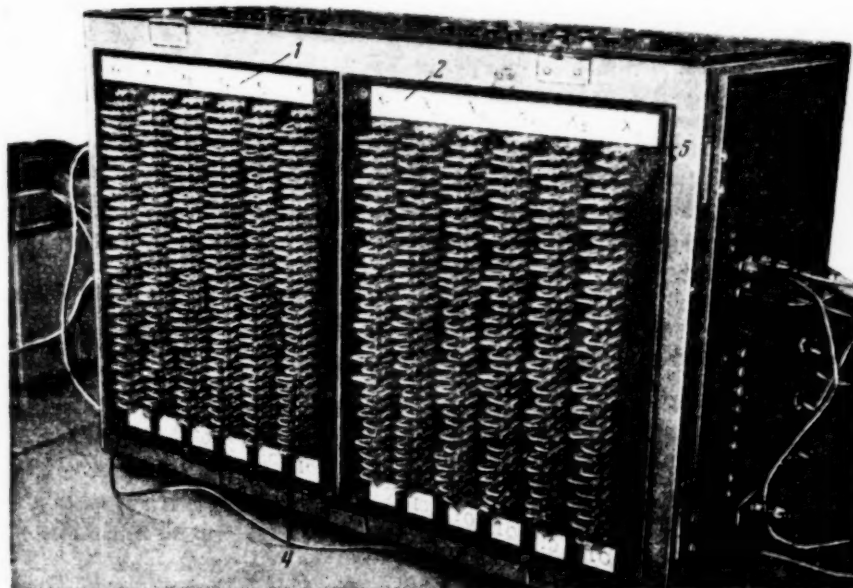


Fig. 12

The terminals of the switches are connected to the bars of the pickoff devices (Fig. 9). The generator is thus fed through three terminals and has 12 output terminals.

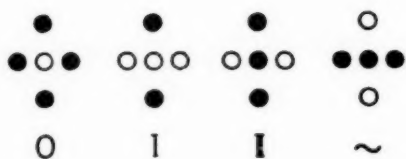


Fig. 13. Presentation of functional values with neon bulbs.

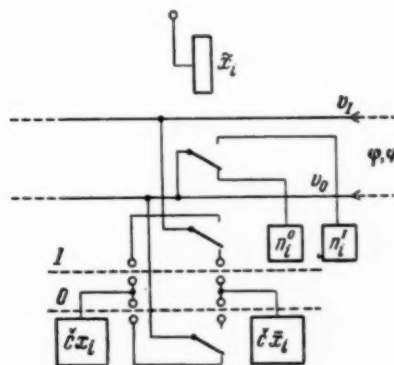


Fig. 14. Section of function comparator.

The model of the circuit contains  $2 \times 6$  relays with four double-throw contacts each. Each terminal of the double-throw contact is brought out with two leads to the plugboard so that any number of other terminals can be connected through it with the aid of a flexible cord. The dotted lines indicate cords for the probes, with which the voltage is applied to the decoder. The input terminals of the model are to the right, the output terminals are to the left.



The decoder contains, first, the circuits which generate the information on the auxiliary indeterminate functions  $\varphi$  and  $\psi$  and the information needed for the representation of the functions  $F_i$  and  $F_j$ . It contains in addition information on whether the circuit operates correctly, i.e., whether any value of a function is simultaneously equal to 0 and 1 at a node ( $A_{ij}$ ). The fact that at least one value of the function is 0 is denoted by 0, and analogous information concerning 1 is denoted by 1. It contains finally also information that is of significance to the possible simplification of the circuit, namely knowledge of whenever the value of the function  $F_i$  is 1 and the value of the function  $F_j$  is  $\sim$ , denoted by  $1 \rightarrow \sim$ , and knowledge of whether the value of the function  $F_i$  is 0 and the value of the function  $F_j$  is 1, denoted by  $0 \rightarrow 1$ . Figure 13 shows the method used to denote the functional values 0, 1,  $\sim$ .

The function comparator has two inputs (Fig. 9), one for the indeterminate functions  $\varphi$  and  $\psi$ , and one for the contact-switching functions  $x_1, \bar{x}_1; x_2, \bar{x}_2; \dots; x_n, \bar{x}_n$ . Optical signal devices (blinkers) marked with the symbols  $x_1, \bar{x}_1; x_2, \bar{x}_2; \dots$  indicate which contacts can be used for operation  $\omega_2$  (the contacts with unlit blinkers can be used). The counters  $\check{x}_1, \check{\bar{x}}_1; \check{x}_2, \check{\bar{x}}_2; \dots$  are shown under the individual sections of the comparator.

One of the comparator sections is shown in more detail in Fig. 14. It contains a relay  $\tilde{x}_1$ , two blinkers  $n_1^0$  and  $n_1^1$ , and two counters  $\check{x}_1$  and  $\check{\bar{x}}_1$ . The terminals marked 1 and 0 are connected together when the zero and one coincidences of the functions are counted. It is naturally possible to count both types of coincidences simultaneously. Let us explain the operation of the block. Assume relay  $\tilde{x}_1$  to be at rest. This state can be stated in terms of the contact function as follows:  $x_1 = 0$  and  $\bar{x}_1 = 1$ .

Let us examine now the values of the auxiliary functions  $\varphi$  or  $\psi$ . If these functions are 0, the conductor  $v_0$  is energized; if they are 1,  $v_1$  is energized; if they are  $\sim$ , neither is energized.

If  $\varphi$  and  $\psi$  are 0, the blinker  $n_1^0$  is not energized, and in the case of operation  $\omega_2$  this signifies that the contact  $\bar{x}_1$  cannot be connected between nodes  $U_i$  and  $U_j$ , lest a spurious circuit be formed. The blinkers serve no other purpose. A third contact and the connected 0 terminals on the left energize the counter  $\check{x}_1$ , which records the information that  $\varphi$  or  $\psi = x_1 = 0$ . The same situation prevails for  $\varphi$  or  $\psi = 1$ , the only difference being that the blinker is unnecessary for operation  $\omega_2$ , for no spurious circuits can be formed for  $\varphi$  or  $\psi = 1$  and  $x_1 = 0$  or 1. Neither the counter nor the blinker is energized if  $\varphi$  or  $\psi = \sim$ .

If the relay is in its operating state, the information is formed in the function comparator in an analogous manner.

## 5. Solution of Problems With the Machine

The circuit to be analyzed is made up with the aid of flexible cords in the circuit-model block. The circuit is then placed in all possible states with the function generator and with the control terminals of the model. The supply is fed through the input terminal. The probe is used to determine the values of the functions of the output poles for each state corresponding to each line of the sheet (Fig. 15). These values can be counted on a separate indicator. The sheet is thus gradually filled-in and the symbol ? is gradually replaced by 0 or 1.

$x_1$	$x_2$	$x_i$			$x_n$	$X_1$	$X_2$	$X_k$			$X_m$
0	0	.	.	0	.	0	?	?	.	.	?
0	0	.	.	0	.	1	?	?	.	.	?
.	.	.	.	.	.	.	.	.	.	.	.
.	.	.	.	.	.	.	.	.	.	.	.
.	.	.	.	.	.	.	.	.	.	.	.
1	1	.	.	1	.	1	?	?	.	.	?

Fig. 15

In the synthesis of the circuit, one first inserts the table of the operating conditions of the circuit manually into the machine. This is followed by operations  $\omega_1$  and  $\omega_2$  in sequence. The progress of the solution is entered in the sheets shown in Figs. 16 and 17. The former is used to record the operations, the latter to sketch the



connections. We shall illustrate the use of the log sheets with examples. We shall use  $k$  for  $U_k$  and  $l$  for  $\omega_l$  in the log sheet and in the verbal description of the course of the solution.

Let the operation considered be  $\omega_2$ . We connect the probes to nodes  $U_1$  and  $U_j$ , thereby connecting these nodes to the decoder. We now start the machine; let the pick-off devices pass once over the operating-condition tables. The "signal device" (blinker) switch is now on, and the "counter" switch is off. The contacts corresponding to the blinkers that remain at rest, say,  $\bar{x}_2$ ,  $\bar{x}_3$ , and  $x_5$ , can be employed in the operation. To make

Operation	Nodes	Units derived	$x_4 \bar{x}_5$	$x_5 \bar{x}_4$	$x_4 \bar{x}_3$	$x_5 \bar{x}_3$	$x_3 \bar{x}_2$	$x_2 \bar{x}_1$	New nodes	Remarks
2	0 1	I					⊗ 4			
	0 2									
	0 3									
	0 4									
	0 5									
	1 2									
	1 3	I				⊗ 2				
	1 4									
	1 5									
	2 3	I						⊗ 2		
	2 4									
	2 5	I				⊗ 3				
	3 4									
	3 5									
	4 5									
1	1	I				1	1	1	3	
	2	I				1	3	1	1	
	3	I				2	2	1	1	
	4	I				1	1	2	1	
	5	I				2	3	2	3	
2	6 0	I				0	0	⊗ 2	6	
						2	0	0		
2	6 1									
	6 2									
	6 3								0	
	6 4									
1	2	I				1	2	1	3	
						2	1	2	⊗	
2	7 0	I				⊗ 2	⊗ 1	⊗ 0	7	
								0	function2	compiled
1	7 1,3,4,5	I				⊗ 2	0	0	8	
2	8 0					0	0		⊗ 1	
2	8 7	I				0	0		0	
						⊗ 1	0	0	0	
1	3	I					0	0	0	
							0	0	⊗ 1	
2	9 6	I				0	0	0	1	
						0	0	0		
2	9 1						⊗ 1		0	
1	5	I				0			0	
						0			0	
2	10 1						0		⊗ 1	
									1	
1	1	I						⊗ 1	11	
2	11 7	I				⊗ 1	0		0	
							0		0	

Fig. 16

a note of this, we place circles in the columns  $\bar{x}_2$ ,  $\bar{x}_3$ , and  $x_5$  of the operations log sheet. If there are no inoperative blinkers, we proceed to another pair of nodes or to another operation. We next disconnect the "signal device," connect the "counters," and again start the pick-off device. We then count the coincidences of the ones. Let the counters read, for example, 3, 14, and 1. These figures are copied in the operations log sheet. In this case it will not be advisable to use  $x_3$  for the operation. We denote this in the log sheet by a cross placed inside the corresponding circuit. Let us now join in the model node 14, say, with node 6 through  $\bar{x}_3$ . This is also marked graphically on connections in the log sheet (Fig. 16). In this case we adhere to the following principle: a line on the log sheet for each connecting cord. The log sheet makes it also possible to find the nodes in the model by number. It is thus possible to monitor constantly the correct connection of the contacts. For a more detailed example see Section 6.

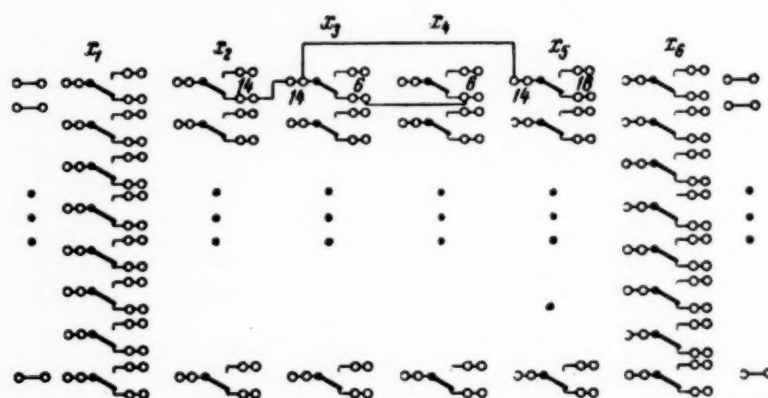


Fig. 17

The operation is analogous in the case of operation  $\omega_1$ , except that the information furnished by the blinker is lacking. Assume that two more lines of the log sheets were established with the aid of the counters. It is now important to choose the correct working hypothesis. Assume that we prefer a smaller number of contacts per operation, rather than a greater one. We therefore perform the operation with the aid of contact  $\bar{x}_5$ , which appears to be the most suitable. We thus obtain a new node, 16.

The operations  $\omega_2$  are always monitored, and for this purpose the probes remain at the nodes after the elements are connected, and the machine is started again. In this case both the "signal device" and the "counters" are disconnected and the signalization mentioned in the detailed description of the circuit is connected. If an erroneous contact, leading to spurious circuits, was connected during the operation, or some other error leading to spurious circuits was made, a signal lamp will light. It is also necessary to check from time to time the progress of the solution by analyzing the synthesized circuit; the I units that change into I are recorded in the log sheet.

## 6. Example

Let us build a decoder to convert from the binary code into the teletype code. The operating-conditions table of the decoder is shown in Fig. 18. Let us make the first attempt at a solution.

We first use operation  $\omega_2$ . Of the 15 possible operations, four are realizable. Let us perform all four. The circuit diagram is shown in Fig. 19, and the course of the solution is shown in Fig. 16. The first operation makes it possible to construct almost the entire function 1 with the aid of contact  $x_2$ , a very convenient circumstance. In the remaining operations, part of the values I of functions 2 and 3 will change into I thus increasing the number of alternatives for the construction of other values I (i.e., for their change into the value I).

It is next necessary to employ operation  $\omega_1$ . It is very convenient to expand either function 2 or function 5 with the aid of contacts  $\bar{x}_3$ ,  $\bar{x}_2$ , and  $\bar{x}_1$ . Let us expand the function 5 with the aid of contact  $\bar{x}_2$ . We obtain the first intermediate node 6. We now attempt operation  $\omega_2$  again. Of the five possibilities of the operation, three are realizable. The first possible operation connects the input to node 6 through contacts  $\bar{x}_3$ ,  $x_2$ , or  $x_1$ . But there is no sense in using contact  $x_2$ , for this does not help the solution. Of the two remaining possibilities, we choose  $x_1$ . Operations with nodes 6 - 1 and 6 - 3 are also of no help, and are also meaningless.

$x_3$	$x_2$	$x_1$	$X_1$	$X_2$	$X_3$	$X_4$	$X_5$
0	0	0	0	1	1	0	1
0	0	1	1	1	1	0	1
0	1	0	1	1	0	0	1
0	1	1	1	0	0	0	0
1	0	0	0	1	0	1	0
1	0	1	0	0	0	0	1
1	1	0	1	0	1	0	1
1	1	1	1	1	1	0	0

Fig. 18

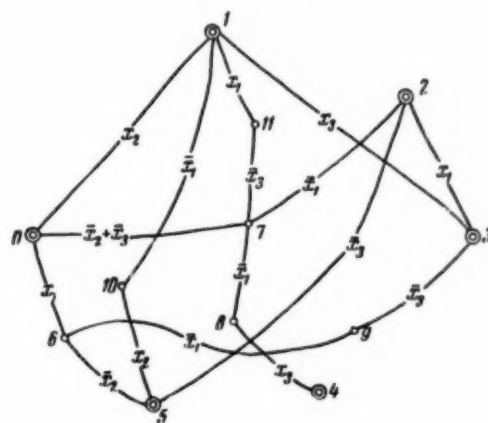


Fig. 19

We attempt to expand function 2 and choose contact  $\bar{x}_1$  for the purpose. This produces a new node, 7.

We attempt operation  $\omega_2$  again. Nodes 7 and 0 we connect through contacts  $\bar{x}_2$  and  $\bar{x}_3$ ; contact  $x_1$  is useless. This completes function 2. Operation  $\omega_2$

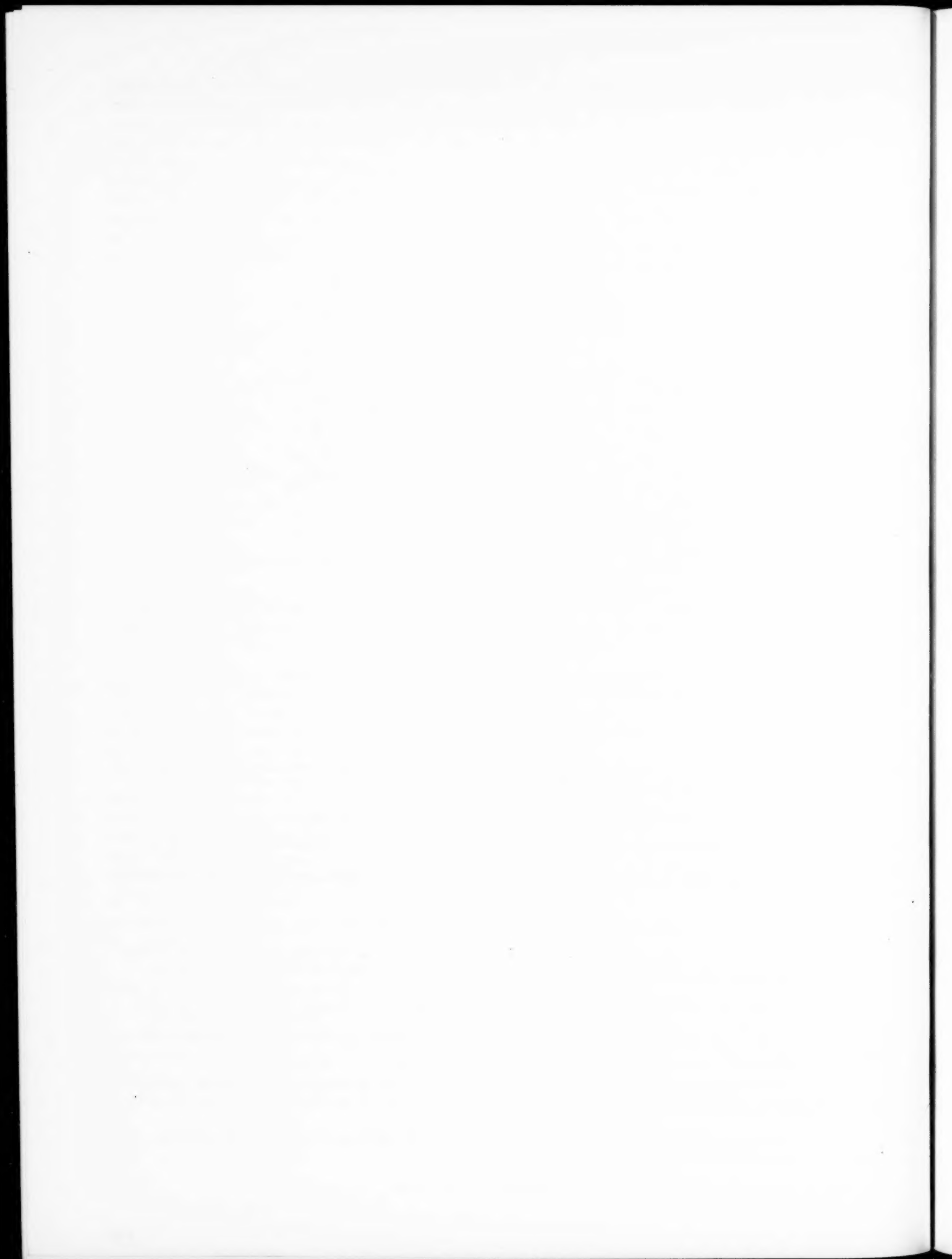
cannot be applied to node pairs 7 - 1, 7 - 2, 7 - 3, 7 - 4, and 7 - 5. We expand function 4 with the aid of contact  $x_3$ . We realize operations  $\omega_2$  for nodes 8 - 7 with the aid of contact  $\bar{x}_1$ ; the other two contacts are useless.

We proceed in the same manner. The solution can be traced on Figs. 19 and 16.

#### LITERATURE CITED

- [1] M. Boda, Stromlauf-Formeln und Ihre Anwendung zur Schaltung Siemenscher Blockwerke, Zeitschrift des Oesterr. Ingenieur und Architekten-Vereines, 1897, 49, 620, 634, 647, 664, 33.
- [2] M. A. Gavrilov, Theory of Relay Contact Circuits, Izd. AN SSSR, 1950.
- [3] A. Svoboda, Synthesis of relay circuits. Machines for the evaluation of information, v. 2, 1954.
- [4] A. Svoboda, Graphic-mechanical aids used for the synthesis of circuits. Machines for the evaluation of information, v. 4, 1956.
- [5] C. E. Shannon, Programming a Computer for Playing Chess, The Phil. Mag., t. 41, No. 314, March, 1950.
- [6] F. Svoboda, The application of the indeterminate bivalent Boolean function for the synthesis of one-stage degree schemes. Machines for the evaluation of information, v. 2, 1954.
- [7] C. E. Shannon and E. F. More, Machine Aid for Switching Circuit Design, Proc. IRE, No. 41, 1953.
- [8] G. N. Povarov, Mathematical Theory of the Synthesis of Contact (1, k)-Pole Networks, Dokl. AN SSR, Vol. C, No. 5 (1955).
- [9] F. Svoboda, The indeterminate bivalent Boolean function. The Czechoslovak Journal for the Cultivation of Mathematics, v. 79, 1953.
- [10] V. Roginsky, The calculation of unutilized states during the synthesis of relay-contact schemes. Automatic and Telemechanics, V. XV, No. 3, 1954.
- [11] A. Mostowski, Mathematical Logic. Warsaw-Wroclaw, 1948.

Received July 20, 1956



# CRITERIA FOR EVALUATION OF ELECTROMAGNETIC RELAYS

B. S. Sotskov

(Moscow)

Discussion of a method of evaluating the basic properties of electromagnetic relays. The method permits a rational selection of a relay to meet specified operating conditions.

The sensitive elements of an electromagnetic relay can be evaluated completely and clearly in terms of their work capacity, i.e., the work that can be realized when the armature passes from one extremal ("rest") position to the other ("working") position, the ampere turns (or power) in the winding circuit remaining constant.

The work produced by armature travel with  $IW_a \approx IW = \text{const}$ , where  $IW_a$  are the ampere turns needed to produce the flux across the working air gap, is given by the expression

$$\begin{aligned} A &= \int_{\delta_0}^{\delta'} P_e d\delta = \int_{G_0}^{G'_a} \frac{(0.4\pi IW_a)^2}{8\pi} dG = \frac{(0.4\pi)^2}{8\pi} (IW_a)^2 (G'_a - G_0) = \\ &= \frac{(0.4\pi W)^2}{8\pi} \frac{U^2}{R} \frac{G_0}{R} \left( \frac{G'_a}{G_0} - 1 \right) = 0.05 \times 10^{-8} P \tau \left( \frac{G'_a}{G_0} - 1 \right). \end{aligned} \quad (1)$$

The time constant  $\tau$  of the relay operation can be calculated as follows:

$$\begin{aligned} \tau &= \frac{0.4\pi 10^{-8} W^2}{R_{m0} R} = \frac{0.4\pi 10^{-8} W^2}{R} G_0 = \frac{0.4\pi 10^{-8} W^2}{\frac{\rho l_{av} W}{q}} \frac{S_a}{\delta_0} = \\ &= \frac{0.4\pi 10^{-8} f_0 Q S_a}{\rho l_{av} \delta_0} = \frac{0.4\pi 10^{-8} f_0}{\rho} \frac{1}{\delta_0} \frac{L (D_{ex} - D_0) \pi D_0^2}{\pi (D_{ex} + D_0) \frac{4}{4}} = \\ &= \frac{0.4\pi 10^{-8} f_0}{\rho} \frac{1}{\delta_0} \frac{k^2 (1 - k)}{1 + k} \left( \frac{\pi D_{ex}^2 L}{4} \right). \end{aligned} \quad (2)$$

Here  $k = \frac{D_0}{D_{ex}}$ , where  $D_0$  and  $D_{ex}$  are the internal and external diameters of the winding, respectively.

The following notation is used in (1) and (2):  $P$  is the power supplied to the relay,  $I$  is the current in the winding,  $U$  is the voltage,  $R = \frac{\rho l_{av} W}{q}$  is the relay winding resistance,  $W$  is the number of turns,

$\rho$  is the specific resistivity,  $l_{av}$  is the average length of turn,  $q$  is the copper cross section of conductor,  $G_0 = \frac{1}{R_{mra}}$  and  $G_0' = \frac{1}{R_{ma}}$  are the values of the magnetic permeance (and  $R_{mra}$  and  $R_{ma}$  are the values of the magnetic reluctance of the air gap) with the armature released and pulled-in, respectively,  $Q$  is the area of the winding form,  $f_0$  is the filling factor,  $\delta$  and  $S_a$  are the length ( $\delta_0$  with the armature released and  $\delta'$  with the armature pulled-in) and the cross section of the working air gap,  $L$  is the length of the winding,  $P_e$  is the mechanical pulling force, and  $R_{mo}$  is the total magnetic reluctance.

Remark. If we consider that the ampere turns needed to produce the flux across the air gap are

$$IW_a = \frac{IWR_{ma}}{R_{mc} + R_{ma}} = \frac{IW}{\frac{R_{mc}}{R_{ma}} + 1} = \frac{IW}{\frac{G_a}{G_m} + 1},$$

where  $IW = \frac{U}{R}$   $W$  are the total ampere turns of the winding,  $R_{mc}$  is the magnetic reluctance of the magnetic core,  $G_{mc} = \frac{1}{R_{mc}}$ , and  $R_{ma}$  is the magnetic reluctance of the air gap, and  $G_a = \frac{1}{R_{ma}}$ , we get

$$A = \int_{G_0}^{G_a'} \frac{(0.4\pi)^2}{8\pi} \frac{(IW)^2}{\left[ \frac{G_a}{G_m} + 1 \right]} dG_a \text{ ergs.}$$

Assuming the magnetic permeability  $\mu$  of the magnetic core material and  $G_m$  to be nearly constant, we get

$$\begin{aligned} A &= 0.02\pi (IW)^2 G_0 \frac{\frac{G_a'}{G_0} - 1}{\left[ \frac{G_a'}{G_m} + 1 \right] \left[ \frac{G_0}{G_m} + 1 \right]} = \\ &= 0.02\pi \left( \frac{U^2}{R} \right) \frac{G_0}{R} W^2 \frac{\frac{G_a'}{G_0} - 1}{\left[ \frac{G_a'}{G_m} + 1 \right] \left[ \frac{G_0}{G_m} + 1 \right]} = \\ &= 0.02\pi \frac{f_0}{\rho} P \frac{1}{\delta_0} \frac{L(D_{ex} - D_0)}{\pi(D_{ex} + D_0)} \frac{\pi D_0^2}{4} \frac{\frac{G_a'}{G_0} - 1}{\left[ \frac{G_a'}{G_m} + 1 \right] \left[ \frac{G_0}{G_m} + 1 \right]} \end{aligned}$$

or

$$A = 0.02 \frac{f_0}{\rho} \frac{k^2(1-k)}{1+k} P \frac{1}{\delta_0} \left( \frac{\pi L D_{ex}^2}{4} \right) \frac{\frac{G_a'}{G_0} - 1}{\left[ \frac{G_a'}{G_m} + 1 \right] \left[ \frac{G_0}{G_m} + 1 \right]}.$$



If, however, we take

$$G'_a = \frac{S_a}{\delta'}, \quad G_0 = \frac{S_a}{\delta_0}, \quad G_m = \frac{S_m \mu}{l_m} \text{ and } S_a \approx S_m,$$

where  $l_m$  and  $S_m$  are the length and cross section of the magnetic core, we get

$$A = 0.02 \frac{f_0}{\rho} \frac{k^2 (1-k)}{1+k} \frac{P}{\delta_0} \left( \frac{\pi L D_{ex}^2}{4} \right) \frac{\frac{\delta_0}{\delta'} - 1}{\left( \frac{l_m}{\mu \delta'} + 1 \right) \left( \frac{l_m}{\mu \delta_0} + 1 \right)}. \quad (3)$$

On the other hand,

$$\begin{aligned} P &= I^2 R = (jq)^2 \frac{\rho l_{av} W}{q} = j^2 \rho l_{av} W q = j^2 \rho l_{av} f_0 Q = \\ &= j^2 \rho f_0 \frac{\pi}{2} (D_{ex} + D_0) \frac{L(D_{ex} - D_0)}{2} = j^2 \rho f_0 \left( \frac{\pi L D_{ex}^2}{4} \right) (1 - k^2), \end{aligned}$$

where  $j$  is the current density in the winding conductor.

Thus,

$$A = 0.02 \frac{f_0^2}{\rho} \frac{\rho}{\delta_0} j^2 k^2 (1 - k)^2 \left( \frac{\pi L D_{ex}^2}{4} \right)^2 \frac{\frac{\delta_0}{\delta'} - 1}{\left[ \frac{l_m}{\delta' \mu} + 1 \right] \left[ \frac{l_m}{\delta_0 \mu} + 1 \right]}.$$

Introducing the symbol  $V_p = \frac{\pi L D_{ex}^2}{4}$ , we get

$$A = 0.02 \frac{f_0^2}{\delta_0} j^2 k^2 (1 - k)^2 V_p^2 \frac{\frac{\delta_0}{\delta'} - 1}{\left[ \frac{l_m}{\delta' \mu} + 1 \right] \left[ \frac{l_m}{\delta_0 \mu} + 1 \right]}.$$

Expressions (1) - (4) give the connection between the work capacity of the relay and its design data, and can be used to select the relay dimensions during the design process.

As to the operating parts of the relay contacts, we know that the energy required to wear away the contact under the most severe operating condition - that of closing the load circuit with accompanying arc formation, is

$$A_k = N \int_0^{t_a} v_{oa} i dt = N v_{oa} q = N v_{oa} I_0 t_0,$$

where  $t_0 = q/I_0$ .\*

\* The value of  $q$  can be determined from [2]

$$\begin{aligned} \int_0^{t_a} i dt &= \int_0^{t_a} \left\{ I_0 - \frac{kt}{R} - \left( \frac{v_{oa} - k\tau}{R} \right) \left( 1 - e^{-\frac{t}{\tau}} \right) \right\} dt = \\ &= I_0 \left\{ \left( 1 - \frac{v_{oa} - k\tau}{E} \right) t_a - \frac{kt_a^2}{2E} - \frac{v_{oa} - k\tau}{E} \tau e^{-\frac{t_a}{\tau}} \right\} = I_0 t_0, \end{aligned}$$

where  $I_0 = E/R$ .

If the permissible volume that can be eroded from the contact is  $V_0$ , we have

$$V_0 = \gamma_v q N$$

or

$$\frac{V_0}{\gamma_v} = q N = N I_0 t_0.$$

The above leads to the expression

$$A_k = v_{0a} \frac{V_0}{\gamma_v} = N v_{0a} I_0 t_0 = N E I_0 \left( \frac{v_{0a}}{E} t_0 \right) = N E I_0 t_{0E}.$$

The symbols used in the above equations are:  $E$  and  $I$  - current and voltage in the circuit controlled by the contacts,  $q = \int_0^{t_a} i dt$  - the quantity of electricity passing through the arc into the contact during the switching of the controlled circuit,  $t_a$  - time of arc glow,  $v_{0a}$  - cathode voltage drop in the arc,  $t_{0E} = \frac{v_{0a} t_a}{E}$ ,  $t_0$  - hypothetical duration of arc glow, corresponding to the same quantity of electricity  $q$  at a constant flow of current  $I$  through the contact circuit,  $N$  - number of contact-operation cycles (closing and opening), and  $\gamma_v$  - volume of contact material eroded for each coulomb passing through the contact during the duration of the arc.

The ratio  $k_0 = \frac{A_k}{A}$ , which can be represented as

$$k_0 = \frac{N E I_0 t_{0E}}{0.05 P \tau \left( \frac{G'}{G_0} - 1 \right) 10^{-8}},$$

or else as

$$k_0 = \frac{v_{0a} \frac{V_0}{\gamma_v}}{0.05 \times 10^{-8} P \tau \left( \frac{G'}{G_0} - 1 \right)},$$

is a general criterion, characterizing the properties of the operating and sensitive elements of the relay. One can use instead of  $k_0$  a simpler criterion

$$k'_0 = \frac{N E I_0 t_{0E}}{P \tau},$$

since  $0.05 \left( \frac{G'}{G_0} - 1 \right) 10^{-8}$  is approximately constant for relays of the same type.

In addition to the general criterion considered above, the following are important indices of relay performance:

1. Operating reliability of the relay, defined as

$$k_n = \frac{N - n}{N} = 1 - \frac{n}{N},$$

where  $N$  is the number of operating cycles, and  $n$  the number of failures. The ratio  $\frac{n}{N}$  is the probability of operating failures in each  $N$  cycle of operation.

The value  $\frac{n}{N}$  of an electromagnetic relay can be expressed as  $\frac{n}{N} = \left(\frac{n}{N}\right)_c + \left(\frac{n}{N}\right)_{se}$ . Here  $\left(\frac{n}{N}\right)_c$  is the probability of contact failure in the controlled circuit, having an approximate logarithmic dependence on the force  $P_c$  on the contacts, namely  $\log\left(\frac{n}{N}\right)_c = \left(\frac{n}{N}\right)_{c0} - cP_c$ .  $\left(\frac{n}{N}\right)_{se}$  is the probability of failure of the electromagnetic (sensing) system of the relay,

$$\left(\frac{n}{N}\right)_{se} \ll \left(\frac{n}{N}\right)_c.$$

2. Weight and volume occupied by the relay.

3. Parameters of relay operation ( $P_{op}$  - operating power or  $I_{op}$  - operating current,  $U_{op}$  - operating voltage) and of relay release ( $P_{rel}$ ,  $I_{rel}$ ,  $U_{rel}$ ).

4. Dependence of the relay operating and release parameters on various factors. The relay-operating and release power depend on the mechanical forces that must be overcome in the operation of the relay. These forces, and consequently the operating and release power, can vary because of effects of temperature, humidity, acceleration, vibration, and orientation in space, on the relay or on its parts. One can assume

$$P_{op} = P_{op0} + \frac{\partial P_{op}}{\partial \alpha} \Delta \alpha + \frac{\partial P_{op}}{\partial \theta} \Delta \theta + \frac{\partial P_{op}}{\partial f} \Delta f + \frac{\partial P_{op}}{\partial a} \Delta a$$

and

$$P_{rel} = P_{rel0} + \frac{\partial P_{rel}}{\partial \alpha} \Delta \alpha + \frac{\partial P_{rel}}{\partial \theta} \Delta \theta + \frac{\partial P_{rel}}{\partial f} \Delta f + \frac{\partial P_{rel}}{\partial a} \Delta a.$$

The change in the relay operation and release parameters, resulting from different factors, can therefore be characterized by the partial derivatives of the operation and release parameters:

with respect to the position (orientation) of the relay axis in space

$$\frac{\partial P_{op}}{\partial \alpha} \text{ and } \frac{\partial P_{rel}}{\partial \alpha},$$

with respect to the change in the ambient temperature

$$\frac{\partial P_{op}}{\partial \theta} \text{ and } \frac{\partial P_{rel}}{\partial \theta};$$

with respect to the relative humidity

$$\frac{\partial P_{op}}{\partial f} \text{ and } \frac{\partial P_{rel}}{\partial f};$$

with respect to the acceleration

$$\frac{\partial P_{op}}{\partial a} \text{ and } \frac{\partial P_{rel}}{\partial a}.$$

The relays having the lowest values of partial derivatives are of the best design.

5. Endurance of the relay, determined by the following factors:

- a) thermal endurance – maximum temperature to which the relay can be exposed without causing irreversible changes in the relay operation and release parameters;
- b) electric endurance – maximum voltage that can be applied between any relay terminals without causing irreversible changes in the relay operation and release parameters;
- c) mechanical endurance – maximum permissible acceleration at which no irreversible changes occur in the relay operation and release parameters;
- d) chemical endurance – maximum permissible concentration of corrosive impurities that can be tolerated in the relay ambient for a specified service period without causing irreversible changes in the relay operation and release parameters.

6. Relay temporal parameters and characteristics:

- a)  $\tau$  – time constant of relay upon operation (i.e., with armature released), and  $\tau^*$  – time constant of relay upon release (i.e., with relay armature pulled in);

b) relay operating time  $t_{op} = f_1 \frac{P}{P_{op}}$  .

c) relay release time  $t_{rel} = f_2 \frac{P}{P_{op}}$  .

7. Limiting parameters for the sensing elements of the relay:

$P_{per}$  – maximum permissible power (determined by heat-rise conditions), that can be delivered to the sensing part (for example, the relay winding).

8. Limiting parameters for the operating parts (contacts of the relay):

- a)  $P_{perc}$  – maximum switchable power in the contact circuits, determined by the conditions under which a stable arc is formed;
- b)  $I_{lim}$  – maximum current in the contacts, determined by the heat rise in the closed contacts;
- c)  $U_{br}$  – maximum voltage limit in the contact circuit, imposed by breakdown conditions in the gap between the contacts.

The values of  $P_{perc}$  and  $U_{br}$  depend upon the gas pressure in the medium.

Knowledge of the above parameters permits accurate selection of a relay with assurance that the required operating reliability will be attained for specified operating conditions without wear of the circuit elements.

LITERATURE CITED

- [1] B. S. Sostkov, Elements of Automatic and Remote Control Apparatus, Gosenergoizdat, 1950.
- [2] B. S. Sostkov, Problems in the Engineering Theory of Relay Circuits, Automation and Remote Control 13, 6 (1952).

Received August 6, 1956.

# SIMPLIFIED CALCULATIONS FOR MAGNETIC AMPLIFIERS WITH IRON-NICKEL ALLOY CORES

N. A. Kaluzhnikov

(Kharkov)

The optimization (determination of minimum volume of steel, maximum gain, etc.) of magnetic amplifiers operating in the middle power range ( $P_{in} > 10^{-5} \text{ w}$ ,  $P_L < 10-100 \text{ w}$ ) is seldom justified.

Such amplifiers are of relatively small size (the volume of the steel averages  $1-100 \text{ cm}^3$ ) and no special difficulties are involved in the amplification of the input signals; the designer is therefore most interested under these conditions in a simple design method for the determination of the magnetic-amplifier parameters. None of this applies, naturally, either to high-power magnetic amplifiers, for which minimum dimensions are of decisive importance, or to low-power amplifiers operating near the sensitivity threshold, where the amplifying ability of the magnetic amplifier is substantially reduced and design for maximum gain becomes essential.

In the intermediate cases it is enough to obtain medium figures for the dimensions and for the gain of magnetic amplifiers.

The method discussed here is based on the use of experimental magnetizing curves of the core material,  $B = f(H_{\sim}, H_{\pm})$  for a certain "model" core, subsequently recalculated for new values of power, current and voltage, and hence for new dimensions and winding data.

The design of magnetic amplifiers, as is known, comprises the choice of the operating conditions in the magnetic circuits and of the calculations of the ac circuit, of the core, and of the winding data.

## 1. Determination of the Operating Conditions of the Magnetic Circuit

An "ideal" magnetic amplifier obeys the relationship  $AW_{\sim av} = AW_{\pm}$ , where  $AW_{\sim av}$  are the ac ampere turns averaged over the half cycle, and  $AW_{\pm}$  are the total dc ampere turns.

In the case of magnetic amplifiers with iron-nickel-alloy cores, this relationship holds, with an accuracy to several percent, over a sufficient range of currents and voltages.

The above circumstance leads to a simplification in the design of such amplifiers.

Let us examine the curves  $H_{\sim} = f(H_{\pm})$  for variable  $B_{\sim}$  (Fig. 1). In these curves

$$H_{\sim} = \frac{I_{\sim} w_{\sim}}{l_{\mu}}, \quad H_{\pm} = \frac{I_{\pm} w_{\pm}}{l_{\mu}}, \quad B_{\sim} = \frac{u_{ch}}{4w_{\sim} S_{st} f},$$

$u_{ch}$  is the ac voltage of the magnetic amplifier,  $w$  is the number of its turns,  $l_{\mu}$  and  $S_{st}$  are the average lengths of the flux line and the cross-section area of the steel stack. Let us draw two lines at a  $45^\circ$  angle, with intercepts  $H_k$  on the coordinate axes, where  $H_k$  (Fig. 2) corresponds to the field intensity at the knee of the magnetizing curve (at  $I_{\pm} = 0$ ). Within the "transformer" zone bounded by these lines,  $H_{\sim} = H_{\pm} \pm H_k$  at all

points. Let us specify as a design condition that  $H_{\sim}$  and  $H_{=}$  remain within this zone under all possible operating conditions, for it is exactly in this case that the magnetic amplifier is capable of developing its full amplifying capabilities.

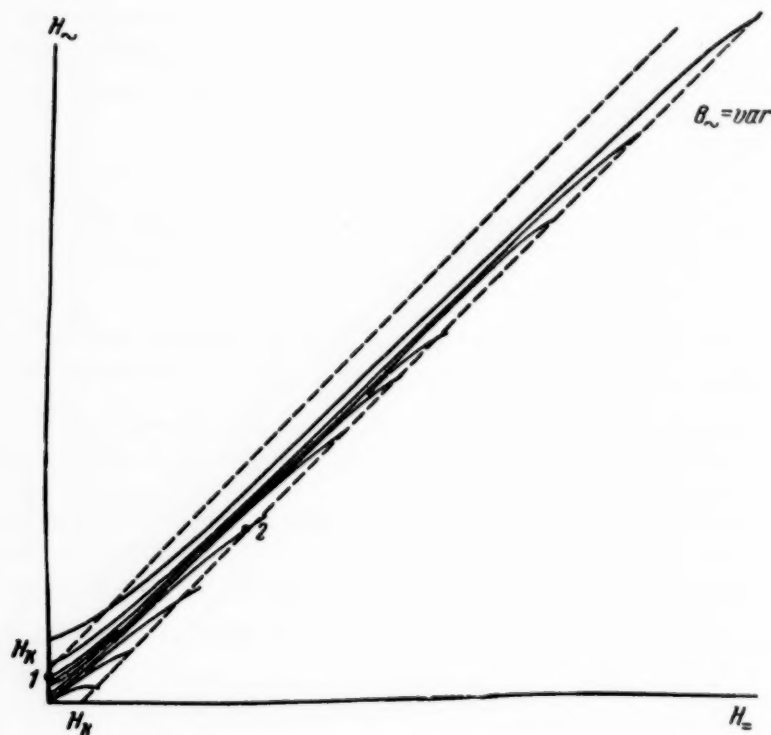


Fig. 1. Characteristics of a magnetic amplifier  $H_{\sim} = f(H_{=})$ , when  $B_{\sim} = \text{var}$ .

For this purpose let us choose two points (1 and 2) with coordinates  $B_{\text{max}}$ ,  $H_{\sim \text{min}}$ , and  $B_{\text{min}}$ ,  $H_{\sim \text{max}}$ , defining the two extreme operating conditions of the magnetic circuit of the amplifiers. The first point corresponds to a total absence of magnetization or to its minimum value, the second to the maximum value of the dc magnetizing field. Let us introduce the following design coefficients to characterize the operating conditions of the magnetic circuit:

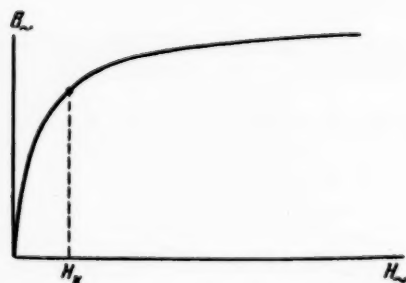


Fig. 2. No-load characteristic of a magnetic amplifier.

$$k_B = \frac{B_{\text{max}}}{B_{\text{min}}}$$

and

$$k_H = \frac{H_{\sim \text{max}}}{H_{\sim \text{min}}}.$$

We shall return to the selection of points 1 and 2 at the close of the article, after the necessary analysis is completed, for the choice of these points determines the weight of the magnetic amplifier. Let points 1 and 2 be inside the "transformer" zone. This means that  $H_{\sim \text{min}} \leq H_k$  and  $H_{\sim \text{max}} \geq H_{\text{max}} - H_k$ . The second inequality for the boundary of the transformer zone



can be transformed into equation  $H_{\sim \max} = H_{\sim \max} + H_k$ , which yields the maximum value of the magnetizing field intensity for the specified conditions.

In the presence of control and bias windings, the necessary values of the control and bias intensities  $H_C$  and  $H_B$  can be obtained from the following equations.

a) For an "unpolarized" magnetic amplifier without self-magnetization (with a control signal of one polarity)

$$H_C = H_{\sim \max} + H_k, \quad H_B = 0. \quad (1a)$$

b) For a "polarized" magnetic amplifier without self-magnetization (with a sign-reversing control signal)

$$H_V = \pm \frac{H_{\sim \max} + H_k}{2}, \quad H_B = \frac{H_{\sim \max} + H_k}{2}. \quad (1b)$$

c) For an "unpolarized" magnetic amplifier with compensated feedback ( $w_f = w_{\sim}$ ).

$$H_V = 2H_k, \quad H_B = -H_k. \quad (1c)$$

d) For a "polarized" magnetic amplifier with compensated feedback

$$H_V = \pm H_k, \quad H_B = 0. \quad (1d)$$

Equations (1c) and (1d) can be used in a first approximation for a magnetic amplifier with internal feedback.

## 2. Design of the ac Circuit

The theory of the "ideal" magnetic amplifier yields for the design of the ac circuit an equation that is independent of the load power factor

$$u_{ch} = u_s - u_L, \quad (2)$$

where  $u_s$  is the supply voltage, and  $u_L$  is the magnetic-amplifier load voltage.

The above equation is simpler than the usually-employed equations containing effective values (for example  $u_{ch} = \sqrt{u_s^2 - u_L^2}$  for a choke magnetic amplifier with active load). In addition, this equation has still another advantage in that it yields values of  $u_{ch}$  and  $B_{min}$  that are lower than the experimental values. This means that the actual magnetic amplifier will require less control ampere turns to produce the same output current than called for by the design calculations (Fig. 1).

The design of the ac circuit of the magnetic amplifiers reduces to establishing the following relationships:

$$\begin{aligned} P_{ch} &= \varphi_{1ckt} P_L, & u_{ch} &= \varphi_{2ckt} u_L, \\ P_s &= \psi_{1ckt} P_L, & u_s &= \psi_{2ckt} u_L. \end{aligned} \quad (3)$$

Here  $P_{ch}$ ,  $P_L$ , and  $P_s$  are the apparent (no-load) choke power, the maximum load power and the maximum power drawn from the supply line, and  $u_{ch}$ ,  $u_L$ , and  $u_s$  are the maximum choke, load, and common-supply voltages.

The coefficients in Equations (3) are functions of  $k_B$ , of  $k_H$ , and of the magnetic amplifier circuit. They can be readily calculated from Equation (2) and have the following form.

a) For choke-type magnetic amplifiers:

$$\begin{aligned}\varphi_{1\text{ckt}} &= \frac{k_H - 1}{k_H^2} \frac{k_B}{k_B - 1}, & \psi_{1\text{ckt}} = \psi_{2\text{ckt}} &= \frac{k_B k_H - 1}{k_H (k_B - 1)}, \\ \varphi_{2\text{ckt}} &= \frac{k_H - 1}{k_H} \frac{k_B}{k_B - 1}.\end{aligned}$$

b) For push-pull bridge-type and differential magnetic amplifiers (see [1]):\*

$$\begin{aligned}\varphi_{1\text{ckt}} &= \frac{2k_B}{k_B - 1} \frac{1}{k_H - 1}, & \psi_{1\text{ckt}} &= \frac{k_B + 1}{k_B - 1} \frac{k_H + 1}{k_H - 1}, \\ \varphi_{2\text{ckt}} &= \frac{2k_B}{k_B - 1}, & \psi_{2\text{ckt}} &= \frac{k_B + 1}{k_B - 1}.\end{aligned}$$

### 3. Design of Core

a) For specified  $P_L$ . From the well-known relationships, we have

$$V_{\text{st}} = S_{\text{st}} l_{\mu} = \frac{\varphi_{1\text{ckt}} P_L}{4B_{\text{max}} H_{\sim \text{min}} f}.$$

It is convenient in practical computations to express the volume of the steel in terms of one of its linear dimensions (for example, the width  $a$  of the center member of a shell-type core):

$$V_{\text{st}} = \varphi_{1\text{sh}} a^3.$$

where  $\varphi_{1\text{sh}}$  is calculated for the model core.

Then

$$a = \sqrt[3]{\frac{\varphi_{1\text{ckt}} P_L}{4\varphi_{1\text{sh}} \beta B_{\text{max}} H_{\sim \text{min}}}}. \quad (4)$$

b) For specified  $P_C$ . Based on the known equation  $P_C = n \frac{H_c^2 l_{\mu}^2}{\beta S_C} l_w \rho$ , where  $S_C$  is the shell area occupied by the control winding,  $l_w$  is the average turn length,  $\beta$  is the filling factor, and  $\rho$  is the specific resistivity and  $n$  is the number of control windings, and based on the ratio  $\frac{l_{\mu}^2 l_w}{S_C} = (\varphi_{2\text{sh}})a$ , where  $\varphi_{2\text{sh}}$  is determined for the model core, we obtain

$$a = \frac{\beta P_C}{n \rho \varphi_{2\text{sh}} H_c^2}. \quad (5)$$

\* For a transformer-type magnetic amplifier these equations become

$$\varphi_{2\text{ckt}} = \frac{1}{c} \frac{k_B}{k_B - 1} \quad \text{and} \quad \psi_{2\text{ckt}} = \frac{1}{c} \frac{k_B + 1}{k_B - 1},$$

where  $c = \frac{w_2}{w_1}$  are the turns ratio of the primary and secondary ac windings.

#### 4. Design of Windings

The number of ac turns is determined from the equation

$$w_{\sim} = \frac{u_{ch}}{4B_{\max} f S_{st}}, \quad (6)$$

and the wire diameter is determined from the permissible current density. The number of turns and the diameter of the wire of the compensated feedback winding are taken to be equal to number of turns and to the diameter of the ac winding.

The bias and control windings are calculated from the intensities  $H_B$  and  $H_C$ , the former on the basis of the permissible current density, and the latter on the basis of filling all the remaining winding space.

#### 5. Determination of the Gain of the Magnetic Amplifier

The gain of the magnetic amplifier is  $k_C = \frac{P_L}{P_C}$ .

Using this expression, we obtain from Equations (4) and (5)

$$k_C = K A P_y^2 \quad \text{or} \quad k_C = \sqrt[3]{K A P_L^2}, \quad (7)$$

where

$$K = 4f\varphi_{1sh} \left( \frac{\beta}{n\rho\varphi_{2sh}} \right)^3 \quad \text{and} \quad A = \frac{B_{\max} H_{\sim\min}}{\varphi_{1ckt} H_C^6}.$$

These expressions make possible the design of a magnetic amplifier for a specified gain. For this purpose one determines  $A = \frac{k_C}{K P_C^2}$  and chooses points 1 and 2 on the simultaneous magnetization curves to obtain the required value of  $A$ .

In practice it is advisable to assume point 1 first and to vary the position of point 2.

Let us return now to the choice of points 1 and 2. In most cases it is possible to place point 1 on the curve of the magnetizing curve. The choice of point 2 is dictated by the features of each actual design.

If the gain is specified, the problem can be solved uniquely, but this requires more cumbersome calculations. It is necessary to choose for this purpose from among the points having a specified value of  $A$  the particular point for which  $\varphi_{1ckt}$  has a minimum value and  $H_C$  has a maximum value. This insures minimum dimensions for a specified  $k_C$ .

If  $P_L$  is specified, for example in the design of the output stage of a multistage magnetic amplifier, two cases may be encountered. If  $P_L$  is considerable, it is necessary to choose point 2 on the boundary of the transformer zone such as to get a minimum value for  $\varphi_{1ckt}$ . Such calculations consume little time and yield small magnetic-amplifier dimensions. For lower powers it is enough to choose point 2 inside the transformer zone so as to make  $k_H$  not less than 4-5 and make  $k_B$  1.25-1.5. This insures sufficiently small dimensions with adequate gain.

Let us indicate the procedure for magnetic-amplifier design.

1. The family of current-voltage characteristics of the magnetic amplifier is recalculated in terms of the relative quantities  $H_{\sim}$ ,  $H_{\pm}$ , and  $B_{\sim}$ , and  $\varphi_{1sh}$  and  $\varphi_{2sh}$  are calculated for the "model" magnetic amplifiers.
2. Operating points 1 and 2 are chosen, and  $k_B$ ,  $k_H$ ,  $H_C$ , and  $H_B$  are calculated.

\* This equation is only approximately true for a choke magnetic amplifier.

3. Equations (3) are used to design the ac circuit.
4. Equations (4) or (5) are used to determine the basic linear dimension of the core. The remaining dimensions are calculated by similarity with the model core.
5. The magnetic-amplifier windings are designed.
6.  $k_c$  is calculated from Equations (7).

#### SUMMARY

The proposed method features simplicity and reliability and can be recommended for magnetic amplifiers of medium power with iron-nickel-alloy cores for those cases, when the designer is not faced with an optimization problem.

#### LITERATURE CITED

- [1] M. A. Rozenblat, *Magnitnye usiliteli* (Magnetic Amplifiers), Gosenergoizdat, 1949.

Received April 10, 1956.

# ANALYTIC EXPRESSION FOR THE STATIC CHARACTERISTIC OF THE MEASURING ELEMENT OF A CHOKE REGULATOR

E. A. Yakubaitis

(Riga)

Piecewise approximation of the magnetization curve of a saturated reactor and the voltage-current characteristics of a semiconductor valve are used to derive an analytic expression for the static characteristic of the measuring element of a choke regulator.

There are several known types of choke-regulator measuring elements, the operating principle of which is based on the comparison of currents, voltages or magnetizing forces in a linear and nonlinear circuit [1-6]. The most common circuit contains a measuring element based on the comparison of two voltages (Fig. 1).

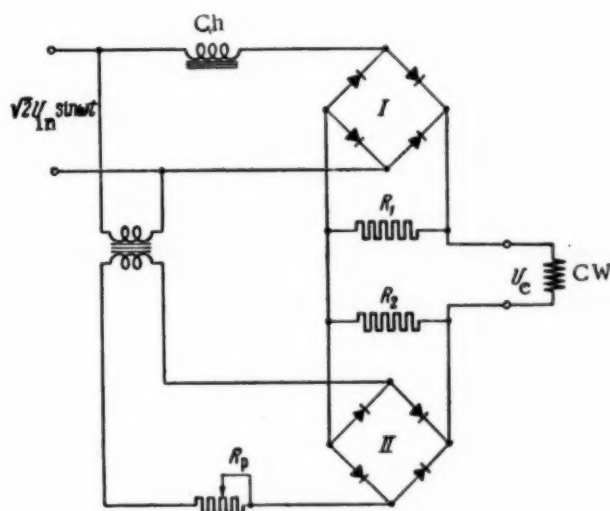


Fig. 1 \*

This device consists of a nonlinear network comprising choke  $Ch$  with saturated core, rectifier  $I$ , and resistance  $R_1$  and of a linear element consisting of a regulating resistor  $R_p$ , rectifier  $II$ , and resistor  $R_2$ . The rectifier bridges are so connected that the output voltage of one produces in the control winding  $CW$  a current opposing the current produced in the same winding by the output voltage of the second rectifier. Regulating resistor  $R_p$  is so chosen that when the voltage  $U_{in}$  at the input of the device is at its nominal value, the algebraic sum of the currents (of the dc components) in the control winding is zero.

\* [Here and elsewhere ' $R_p$ '  $\equiv$  ' $R_{reg}$ ' - editor's note].

The output of the measuring element (Fig. 1) is a voltage  $U_C$  proportional to the deviation of its input voltage from the nominal value  $U_{in}$ .

The voltage  $U_{in}$  applied to the input of the element is proportional to the regulated parameter. The output of the element is connected to the control winding CW of the amplifier.

Suitable simplification of this circuit leads to other types of measuring elements. The design procedure for the measuring element assembled as shown in Fig. 1 can be readily extended to other types of measuring elements.

The method proposed for the analytic determination of the static characteristic of the element (the steady-state dependence of the voltage  $U_C$  or of the output current  $I_C$  on the input voltage  $U_{in}$ ) is based on the following assumptions.

1. The magnetic characteristic of the choke is approximated to some extent by two straight lines (Fig. 2), one of which corresponds to the initial high-permeability portion, and the second to the saturated state ( $B_s$  is the saturation induction).

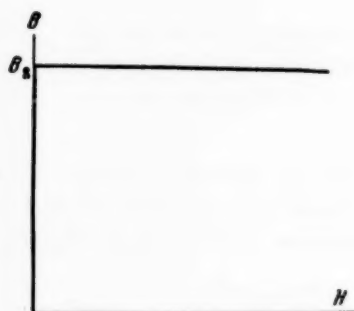


Fig. 2. Idealized magnetization curve of choke core.

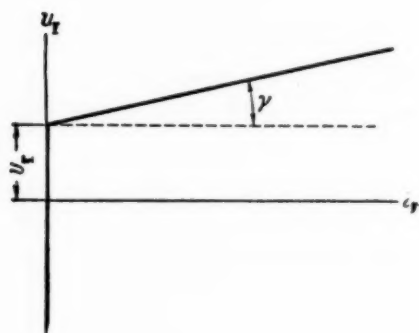


Fig. 3

2. The actual voltage-current characteristic of the valve is replaced with an idealized one, consisting of two straight lines, one parallel to the ordinate (voltage) axis, the other coinciding as much as possible with the real characteristic.

3. The control winding is represented in the equivalent circuit by a pure resistance  $R_C$ .
4. The effect of the isolating transformer is disregarded.

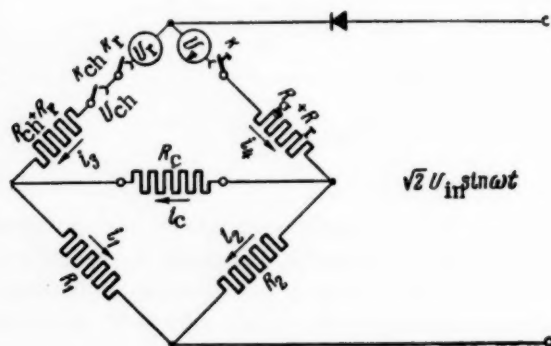


Fig. 4. Equivalent circuit of measuring element.



Under these assumptions it is possible to replace the measuring element (Fig. 1) during one half of the input-voltage cycle with the circuit shown in Fig. 4. All the processes occurring in the element during the second half cycle (Fig. 4) are analogous.

In the latter circuit the choke is replaced by contactor  $k_{ch}$  and resistor  $R_{ch}$ , equal to the pure resistance of the choke. Each rectifying bridge is replaced by contactor  $k_r$ , voltage  $u_r$ , and resistance  $R_r$ . The control winding of the amplifier is represented by pure resistance  $R_c$ .

Depending on the voltage at the input of the measuring element, the static characteristic of the circuit of Fig. 4 can be broken up into three parts (Fig. 5), in accordance with the operation of contactors  $k_{ch}$  and  $k_r$ .

During each half cycle of the input voltage  $U_{in}$ , the contactors  $k_r$  close at the instant (angle  $\beta$ ) when the instantaneous voltage drop across the rectifier rises to a value  $u_r$  (Fig. 3):

$$\beta = \arcsin \frac{u_r}{\sqrt{2} U_{in}}. \quad (1)$$

At the angle  $(\pi - \beta)$ , when the rectifier voltage drop diminishes to the value  $u_r$ , contactors  $k_r$  open. Consequently, when the input voltage to the measuring element is

$$U_{in} \leq \frac{u_r}{\sqrt{2}},$$

the contactors  $k_r$  are open during the entire half period, and the equation of the first part of the static characteristic becomes

$$J_c = 0 \quad \left( U_{in} \leq \frac{u_r}{\sqrt{2}} \right). \quad (2)$$

If the input voltage to the measuring element is greater than  $\frac{u_r}{\sqrt{2}}$ , but too small to saturate the choke, the contactor  $k_{ch}$  is open during the entire half-cycle, and the contactors  $k_r$  are closed during the part of the half-cycle when  $\beta \leq \omega t \leq \pi - \beta$ . The second portion of the static characteristic is therefore determined from the equation

$$J_c = \frac{1}{\pi} \int_{\beta}^{\pi-\beta} i_{cI} d(\omega t) \quad \left( \frac{u_r}{\sqrt{2}} \leq U_{in} \leq U_{in_{cr}} \right), \quad (3)$$

where  $i_{cI}$  is the instantaneous value of the current flowing through the amplifier control winding when the contactor  $k_{ch}$  is open (choke is unsaturated), and  $U_{in_{cr}}$  is the maximum voltage at the input of the measuring element, at which the choke is unsaturated during the entire half period.

Once the input voltage of the measuring element exceeds the value  $U_{in_{cr}}$ , the contactor  $k_{ch}$  is closed during that part of the half cycle when the choke is saturated. During the time when  $\beta \leq \omega t \leq \pi - \beta$ , the contactors  $k_r$  are also closed. The static characteristic becomes in this case

$$J_c = \frac{1}{\pi} \int_{\beta}^{\alpha} i_{OI} d(\omega t) + \frac{1}{\pi} \int_{\alpha}^{\pi-\beta} i_{cI} d(\omega t), \quad (U_{in} \geq U_{in_{cr}}), \quad (4)$$

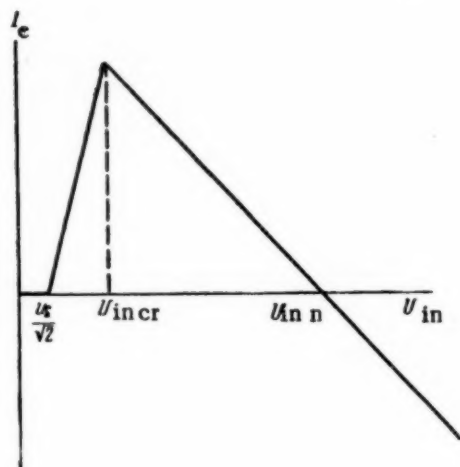


Fig. 5. Calculated static characteristic of measuring element.

where  $i_{cII}$  is the instantaneous current flowing through the amplifier control winding when contactor  $k_{ch}$  is closed (choke saturated), and  $\alpha$  is the angle at which the choke becomes saturated.

The static characteristic of the measuring element is thus described by three equations corresponding to the three regions of input-voltage variation.

Equation (4) determines the working portion of the characteristic. Equations (2) and (3) pertain to the nonworking portions of the characteristic, resulting from the fact that the choke is not saturated if it carries a low current.

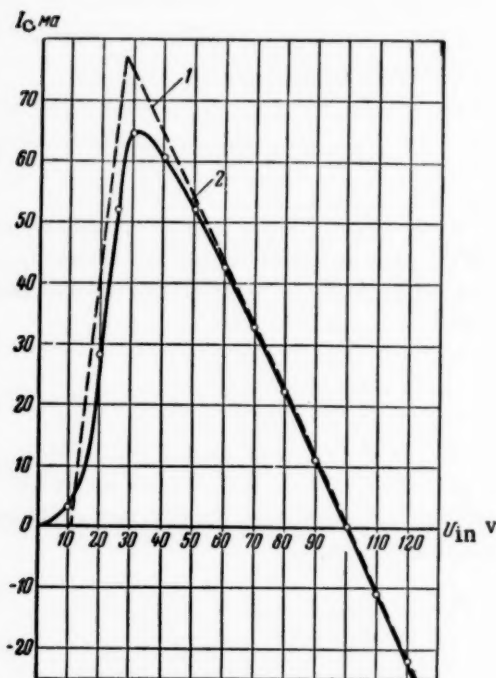


Fig. 6. Static characteristic of measuring element used with a dynamoelectric amplifier.

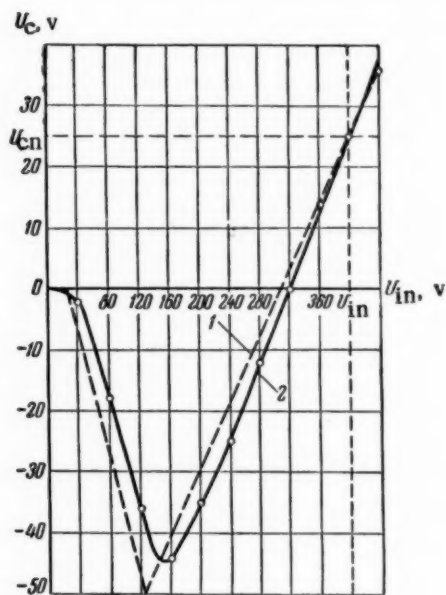


Fig. 7. Static characteristic of a measuring element used with a thyatron amplifier.

Let us determine currents  $i_{cI}$  and  $i_{cII}$  entering into Equation (3) and (4), and the angle  $\alpha$  at which the choke induction  $B_s$  reaches saturation.

For that part of the half cycle in which  $\beta \leq \omega t \leq \alpha$ , i.e., when the contactor  $k_{ch}$  is open, it is possible to write for the circuit of Fig. 4

$$\begin{aligned} \sqrt{2} U_{in} \sin \omega t &= u_r + u_{ch} + i_{1I} R_1, \\ \sqrt{2} U_{in} \sin \omega t &= u_r + i_{4I} (R_p + R_t) + i_{2I} R_2, \\ i_{eI} P_c + i_{1I} R_1 &= i_{2I} R_2, \quad i_{cI} = i_{1I}, \quad i_{4I} = i_{cI} + i_{2I}. \end{aligned} \quad (5)$$

In the absence of saturation it is possible to determine the voltage  $u_{ch}$  on contactor  $k_{ch}$ , which replaces a choke with an ideal magnetization curve (Fig. 2), using the following equation:

$$u_{ch} = w s \frac{dB}{dt} 10^{-8}.$$

Therefore, solving Equations (5) simultaneously, we get

$$i_{0I} = k_I (\sqrt{2} U_{in} \sin \omega t - u_r), \quad (6)$$

$$(1 - k_I R_1) (\sqrt{2} U_{in} \sin \omega t - u_r) = ws \frac{dB}{dt} 10^{-8}, \quad (7)$$

where

$$k_I = \frac{R_2}{R_2(R_c + R_1) + (R_p + R_r)(R_c + R_1 + R_2)}. \quad (8)$$

During the time when the voltage vector at the input of the measuring element rotates through an angle  $\alpha - \beta$  after contactors  $k_r$  are closed, the induction in the choke core increases from a value  $-B_s$  to  $+B_s$ . It therefore follows from (7) [7] that

$$(1 - k_I R_1) \int_{\beta}^{\alpha} (\sqrt{2} U_{in} \sin \omega t - u_r) d(\omega t) = ws 10^{-8} \int_{-B_s}^{+B_s} dB.$$

Integrating the last expression we get the angle  $\alpha$  at which the choke becomes saturated:

$$\cos \alpha = \cos \beta - \frac{\sqrt{2} ws \omega B_s 10^{-8}}{(1 - k_I R_1) U_{in}} - \sin \beta (\alpha - \beta) \quad (\alpha \leq \pi - \beta). \quad (9)$$

For the second half cycle, when the choke is saturated, i.e., when contactor  $k_{ch}$  is closed [ $\alpha \leq \omega t \leq (\pi - \beta)$ ] one can write for the circuit of Fig. 4

$$\begin{aligned} i_{3II} + i_{cII} &= i_{1II}, \quad i_{4II} = i_{cII} + i_{2II}, \\ i_{4II}(R_p + R_r) + i_{cII} R_c &= i_{3II}(R_{ch} + R_r), \\ \sqrt{2} U_{in} \sin \omega t &= u_r + i_{4II}(R_p + R_r) + i_{2II} R_2, \\ i_{cII} R_c + i_{1II} R_1 &= i_{2II} R_2. \end{aligned}$$

Solving these equations simultaneously we get

$$i_{cII} = -k_{II} (\sqrt{2} U_{in} \sin \omega t - u_r), \quad (10)$$

where

$$k_{II} = \frac{(R_p + R_r) R_1 - (R_{ch} + R_{in}) R_2}{R_1 R_2 R_c + R_2 (R_{ch} + R_r)(R_c + R_1) + [R_1(R_c + R_2) + (R_{ch} + R_r)(R_c + R_1 + R_2)](R_{reg} + R_r)}. \quad (11)$$

Inserting into Equation (4) the values of the currents  $i_{cI}$  from (6) and  $i_{cII}$  from (10) and integrating we obtain the equation for the working portion of the static characteristic of the measuring element

$$\begin{aligned} J_c = \frac{\sqrt{2}}{\pi} [(k_I - k_{II}) \cos \beta - (k_I + k_{II}) \cos \alpha] U_{in} - [(k_I + k_{II}) \frac{\alpha}{\pi} - \\ - (k_I - k_{II}) \frac{\beta}{\pi} - k_{II}] u_r \quad (U_{in} \geq U_{in cr}). \end{aligned} \quad (12)$$

Analogously we obtain for the nonworking portion of the static characteristic, by integrating Equation (3)

$$J_c = k_I \left[ \frac{2\sqrt{2}}{\pi} \cos \beta U_{in} - \left( 1 - \frac{2\beta}{\pi} \right) u_r \right] \quad \left( \frac{u_r}{\sqrt{2}} \leq U_{in} \leq U_{in_{cr}} \right). \quad (13)$$

#### SUMMARY

Piecewise linear approximation of the magnetization curve of the choke and of the voltage-current characteristics of the semiconductor rectifiers makes it possible to arrive at an approximate design of a measuring element with two nonlinear sections.

This design procedure can be extended to other types of measuring elements of choke regulators, and also to certain circuits used for other purposes, containing a saturated reactor and a semiconductor valve.

Figures 6 and 7 show the discrepancies between the calculated results and the experimental data.

#### LITERATURE CITED

- [1] E. A. Yakubaitis, Measuring Elements of Choke Regulators, Izv. AN Latv. SSR, No. 6, 1954.
- [2] D. Bolton, Current-Regulating Reactor for Electrolytic Processes, Power and Works Engineering, December, 1952.
- [3] W. A. Hunter, Static Magnetic Regulators in the Power Generation Field, Power Engineering, December, 1950.
- [4] U. Krabbe, Spannungsregulator vo transduktortip for mindre Vāxelstromgeneratoren, ASEA Thidning, No. 5, 1945.
- [5] C. Lynn and C. E. Valentine, Rototrol Provides Generator Excitation, Westinghouse Engineer, Vol. 8, March, 1948.
- [6] C. P. West and J. D. Applegate, A Generator Voltage Regulator Without Moving Parts, The Electric J. April, 1936.
- [7] Yu. G. Tolstov, Contact-Making Converters, Izd. AN SSR, 1953.

Received April 7, 1956.

## TRANSIENTS IN A TRANSISTOR SWITCHING CIRCUIT

N. I. Brodovich

(Moscow)

Treatment of the transients in a grounded-base switching circuit employing one point-contact transistor.

Equations are derived for the currents and curves are plotted for the variation of the current in a standard circuit for various transistor parameters  $\alpha$  and  $\tau$  in the active operating region, in response to a rectangular voltage pulse that throws the transistor into the closed state.

The operating speed of the circuit is estimated and the basic requirements that must be met by point-contact transistors intended for high-speed switching circuits are formulated.

### INTRODUCTION

Problems in the dynamics of switching circuits employing point-contact transistors for the active element are directly related to the research and development of high-speed electronic automation circuits.

The principal works published to date on the dynamics of such circuits are those by B. G. Farley [1], I. L. Lebow and R. H. Baker [2], and T. R. Bashkow [3]. Reference [1] gives the differential equation of a grounded-base starting circuit and gives the form of the output signal, plotted by the integral-curve method. Reference [2] examines the task of determining the connection between the duration and the emitter voltage pulse required to actuate the switching circuit. Reference [3] analyzes the stability of a starting circuit that has an equilibrium position in the active region.

The references cited do not cover all the problems in the dynamics of starting circuits. In the development and in the research one must be able to calculate the transient curves, to estimate the capabilities of the circuit, and, what is particularly important, to determine the time at which the circuit changes from one state to the other. It is also important to estimate the effect of the transistor parameters on this time and to formulate the requirements that must be met by transistors chosen for such a circuit.

We shall consider these problems below as applied to a grounded-base starting circuit, taking the input capacitance into account.

#### Initial Equations

Let us consider a typical starting circuit with one point-contact transistor, connected in a grounded-base circuit (Fig. 1). The operation of such a circuit is based on using the negative portion of the current-voltage characteristic of a two-terminal network containing a transistor with current gain (Fig. 2).

As is known, the static mode of the circuit of Fig. 1 is conveniently analyzed and calculated by using a voltage-current characteristic (Fig. 2, a) which can be plotted [4] or computed [5] from the static characteristics

of the transistors. Once the parameters of the two-terminal network are selected, the voltage-current curve can be plotted point by point or obtained on an oscillograph screen by introducing in the emitter circuit a resistance exceeding the negative slope of the curve.

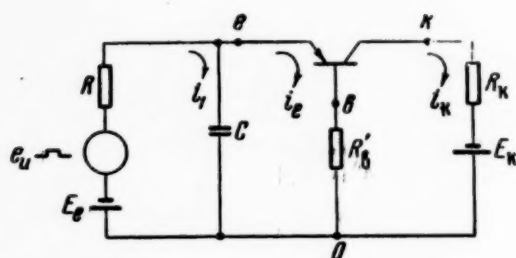


Fig. 1. Typical switching circuit with point-contact transistor: R) external resistor in emitter circuit, including the fixed-bias and pulse sources; C) total capacity in the emitter circuit;  $R_b$ ) external resistance in base circuit,  $R_k$ ) external resistance in the collector circuit.

The static voltage-current characteristic is not sufficient for the calculation of currents flowing in the switching circuit when the transistor tumbles through the active region, for this curve, naturally, does not take into account the influence of inertia phenomena in the transistor itself (diffusion character of the minority-carrier distribution) and in other circuit elements.

To determine the transient currents, let us write down the Kirchoff equations for the circuits of Fig. 1, replacing the transistor with an equivalent current generator, called the Adler circuit [6] (Fig. 3):

$$i_1 - C \frac{dv_c}{dt} - i_e = 0, \quad (1)$$

$$Ri_1 + v_c = E_e + e_u, \quad (2)$$

$$v_c - (r_e + R_b)i_e + R_b i_k = 0, \quad (3)$$

$$-R_b i_e + (R_b + r_k + R_k)i_k - \alpha r_k i_g = E_k, \quad (4)$$

$$i_e - i_g = C_g \frac{dv_g}{dt}, \quad (5)$$

$$v_g = R_g i_g. \quad (6)$$

Equations (1) - (6) can be reduced to a nonlinear second-order differential equation. The nonlinearity is due to the dependence of  $r_e$ ,  $r_k$ , and  $\alpha$  on the currents  $i_e$ ,  $i_g$ , and  $i_k$ . Using a piecewise-linear approximation for the static characteristics of the transistors, the system of Equations (1) - (6) can be considered as linear within each segment for which  $r_e$ ,  $r_k$ , and  $\alpha$  are assumed constant, and the system can be solved for each region, matching the solutions in the individual regions to the initial conditions.

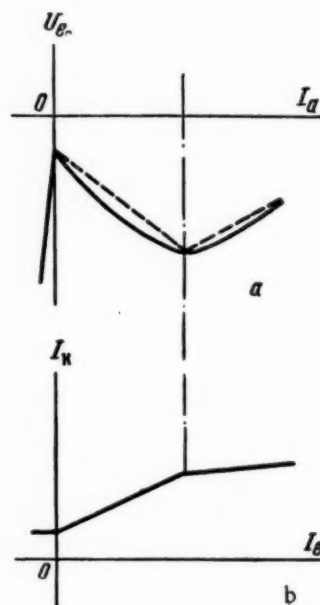


Fig. 2. a) Form of static voltage-current characteristic,  $U_{e0} = \Psi(I_e)$  of a section of the circuit of Fig. 1, containing the transistor (the dotted lines show the rectified characteristics); b) form of static rectified curve  $I_k = F(I_e)$ .



### Equations for the Currents

Solving the System (1) - (6) with Laplace transforms we obtain the following expressions for currents  $i_e$  and  $i_g$ :

$$i_e|_{t < t_0} = i_e^* = \left(i_{e0} + \frac{E_u}{R + R_N}\right) \left\{ 1 + e^{at} \left[ \left( \frac{a}{b} + \frac{a^2 - b^2}{b} \tau \right) \text{sh } bt - \text{ch } bt \right] \right\} +$$

$$+ i_{e0} \left[ \left( a + \frac{1}{\tau} \right) \frac{1}{b} \text{sh } bt + \text{ch } bt \right] e^{at} + i_{g0} \left( 1 - \frac{R_N}{R_p} \right) \left[ \left( \frac{1}{\tau_1} - \frac{1}{\tau} \right) \frac{1}{b} \text{sh } bt \right] e^{at}, \quad (7)$$

$$i_e|_{t > t_0} = i_e^* - \frac{E_u}{R + R_N} \left\{ 1 + e^{a(t-t_0)} \left[ \frac{a}{b} \text{sh } b(t-t_0) - \text{ch } b(t-t_0) + \frac{a^2 - b^2}{b} \tau \text{sh } bt \right] \right\}, \quad (8)$$

$$i_g|_{t < t_0} = i_g^* = \left(i_{g0} + \frac{E_u}{R + R_N}\right) \left[ 1 + e^{at} \left( \frac{a}{b} \text{sh } bt - \text{ch } bt \right) \right] +$$

$$+ i_{e0} \frac{\text{sh } bt}{b\tau} e^{at} + i_{g0} e^{at} \left[ \frac{\text{sh } bt}{b} \left( -a - \frac{1}{\tau} \right) + \text{ch } bt \right], \quad (9)$$

$$i_g|_{t > t_0} = i_g^* - \frac{E_u}{R + R_N} \left\{ 1 + e^{a(t-t_0)} \left[ \frac{a}{b} \text{sh } b(t-t_0) - \text{ch } b(t-t_0) \right] \right\}. \quad (10)$$

Here  $\tau = C_g R_g$ ,  $\tau_1 = CR$ ,  $\tau_2 = CR_p$ ,  $i_{e0}$  and  $i_{g0}$  are the initial values of currents  $i_e$  and  $i_g$ ,  $t_0$  is the duration of the pulse (in the given region), and

$$i_{e0} = \frac{E_e + E_k \frac{R_b}{R_b + r_k + R_k}}{R + R_N}$$

is the current that would flow in the emitter circuit were only constant-bias sources in the circuit at a value of  $R_N$  corresponding to the given region,  $E_u$  is the magnitude of the voltage step, and

$$a = \frac{p_1 + p_2}{2}, \quad b = \frac{p_1 - p_2}{2},$$

where  $p_1$  and  $p_2$  are the roots of the characteristic equation

$$p^2 + p \left( \frac{R_p}{\tau} + \frac{1}{\tau_1} + \frac{1}{\tau_2} \right) + \left( \frac{R_N}{\tau} \frac{1}{\tau_1} + \frac{1}{\tau} \frac{1}{\tau_2} \right) = 0. \quad (11)$$

In the coefficients of the equations

$$R_N = r_e + \frac{R_b [(1 - \alpha) r_k + R_k]}{R_b + r_k + R_k} \quad (12)$$

is the active resistance of the two-terminal network and

\* [Here and elsewhere, 'sh'  $\equiv$  'sinh'; 'ch'  $\equiv$  'cosh' - editor's note].

$$R_p = r_e + \frac{R_b(r_k + R_k)}{R_b + r_k + R_k} \quad (13)$$

is the passive resistance of the two-terminal network,

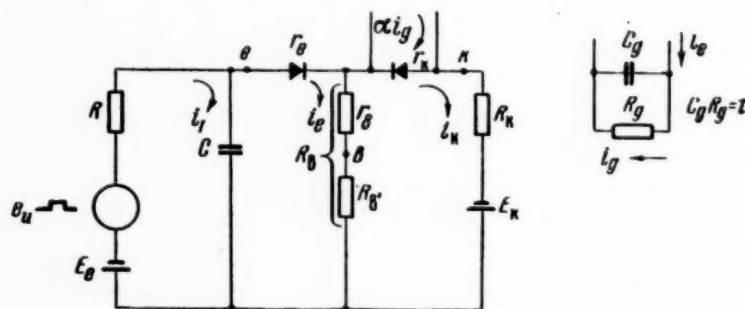


Fig. 3. Equivalent circuit for Fig. 1 (the current  $i_g$  is related to the current  $i_e$  as shown in the circuit to the right).

Having determined  $i_g$  and  $i_e$  from (7) and (9) and from (8) and (10) it is possible to use (4) to determine  $i_k$ :

$$i_k = \frac{R_b}{R_b + r_k + R_k} i_e + \frac{\alpha r_k}{R_b + r_k + R_k} i_g + \frac{E_k}{R_b + r_k + R_k}, \quad (14)$$

#### Transition from the Cutoff Region to the Active Region

Expressions (7) - (10) can be simplified considerably in the individual regions by taking into account the initial values of the currents  $i_e$  and  $i_g$  (designated  $i_{e0}$  and  $i_{g0}$ ) and also the values of the parameters  $\alpha$ ,  $r_k$ , and  $r_e$ .

**a) Cutoff region.** The solution of the problem assumes the simplest form in the cutoff region. It is possible to disregard here the current generator ( $\alpha = 0$ ) and the equivalent circuit reduces to a passive network having a single capacitance  $C$ . This leads to a first-order equation, and the expression for the emitter current becomes \*

$$i_e = \frac{E_u}{R + R_p} (1 - e^{-\frac{t}{\tau_3}}) + i_{e0}, \quad (15)$$

where  $\frac{1}{\tau_3} = \frac{1}{\tau_1} + \frac{1}{\tau_2}$ .

Equation (15) leads to an expression for the time the emitter current takes to assume a zero value after application of a voltage step  $E_u$

$$t = -\tau_3 \ln(1 - k), \quad (16)$$

\* In the cutoff region we have  $R_N = R_p$ , since  $\alpha = 0$ .

where

$$k = - \frac{E_e + E_k \frac{R_b}{R_b + r_k + R_k}}{E_u}$$

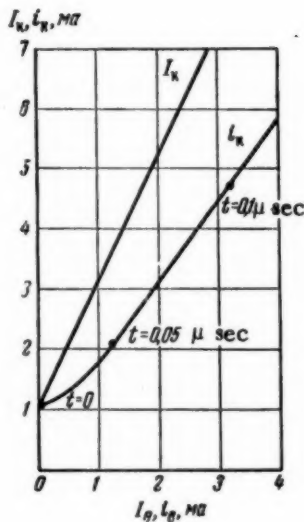


Fig. 4. Active portion of static rectified curve  $I_k = F(I_e)$  and of the curve  $i_k = f(i_e)$ .

b) Active region. Putting  $i_{e0} = 0$  and  $i_{g0} = 0$  in Equations (7) - (10) for the transition through the active region, from the transistor off to the transistor on position, we get

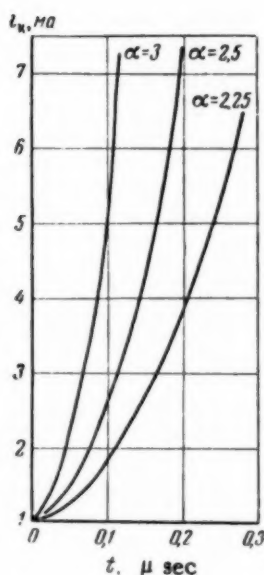


Fig. 5. Curve showing buildup of collector current in the active region for the circuit of Fig. 1 having the following parameters:  $R = 2.5$  kilohm,  $R_b^* = 4.9$  kilohm,  $R_k = 4$  kilohm,  $C = 25$   $\mu$ f,  $\tau = 0.075$   $\mu$ sec,  $r_k = 30$  kilohm,  $E_k = 40$  v,  $E_e = 8.5$  v,  $E_u = 7$  v.

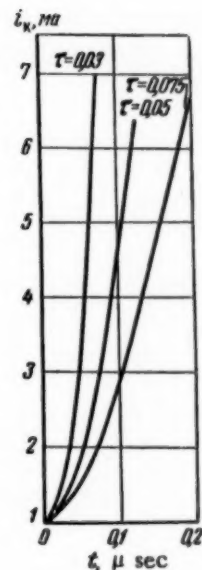


Fig. 6. Curve showing buildup of collector current in the active region for the circuit of Fig. 1 having the following parameters:  $R = 2.5$  kilohm,  $R_b^* = 4.9$  kilohm,  $R_k = 4$  kilohm,  $C = 15$   $\mu$ f,  $\tau = 0.075$   $\mu$ sec,  $r_k = 30$  kilohm,  $E_k = 40$  v,  $E_e = 8.5$  v,  $E_u = 7$  v,  $\alpha = 2.5$ .

$$\tilde{i}_e|_{t < t_0} = i_{e0}^{**} = \left( i_{e0I} + \frac{E_u}{R + R_N} \right) \left\{ 1 + e^{at} \left[ \left( \frac{a}{b} + \frac{a^2 - b^2}{b} \tau \right) \text{sh } bt - \text{ch } bt \right] \right\}, \quad (17)$$

$$i_e|_{t > t_0} = i_e^{**} - \frac{E_u}{R + R_N} \left\{ 1 + e^{a(t-t_0)} \left[ \frac{a}{b} \text{sh } b(t-t_0) + \frac{a^2 - b^2}{b} \tau \text{sh } b(t-t_0) - \text{ch } b(t-t_0) \right] \right\}. \quad (18)$$

$$i_g|_{t < t_0} = i_g^{**} = \left( i_{g0I} + \frac{E_u}{R + R_N} \right) \left[ 1 + e^{at} \left( \frac{a}{b} \text{sh } bt - \text{ch } bt \right) \right], \quad (19)$$

$$i_g|_{t > t_0} = i_g^{**} - \frac{E_u}{R + R_N} \left\{ 1 + e^{a(t-t_0)} \left[ \frac{a}{b} \text{sh } b(t-t_0) - \text{ch } b(t-t_0) \right] \right\}. \quad (20)$$

Figure 4 shows the curve  $i_k = f(i_e)$ , calculated from (17), (19), and (14) for a specific case, as well as the corresponding portion of the rectified static characteristic  $I_k = F(I_e)$ . It is seen from Fig. 4 that the slope of the curve  $i_k = f(i_e)$  is much less than the slope of the static curve  $I_k = F(I_e)$ . Comparison of the two curves shows at a glance the error introduced by plotting the waveform of the output signal on the basis of the static characteristic.

#### Effect of Transistor Parameters

The effect of the transistor parameters  $\tau$  and  $\alpha$  on the operating speed of the circuit is illustrated by the curves of Figs. 5 and 6 and by Table 1, which is compiled from these curves. Table 1 lists the buildup time  $t_a$  of the collector current from a value corresponding to  $i_e = 0$  to a value  $i_k = \alpha i_g$ , which determines the instant at which the transition to the saturated state occurs.

TABLE 1

	$C = 15 \text{ } \mu\mu\text{f}$			$C = 25 \text{ } \mu\mu\text{f}$		
$\tau, \text{ } \mu\text{ sec}$	0.03	0.05	0.075	0.075	0.075	0.075
$\alpha$	2.5	2.5	2.5	2.25	2.5	3
$t_a, \text{ } \mu\text{ sec}$	0.07	0.13	0.19	0.3	0.2	0.12

**Remark.** The values of the transistor limiting frequency  $F_{lim}$ , corresponding to time constants 0.03, 0.05, and 0.075  $\mu\text{ sec}$ , are approximately 5.3, 3.2, and 2.1 Mc, respectively, since  $\tau =$

$$= \frac{1}{2\pi F_{lim}}.$$

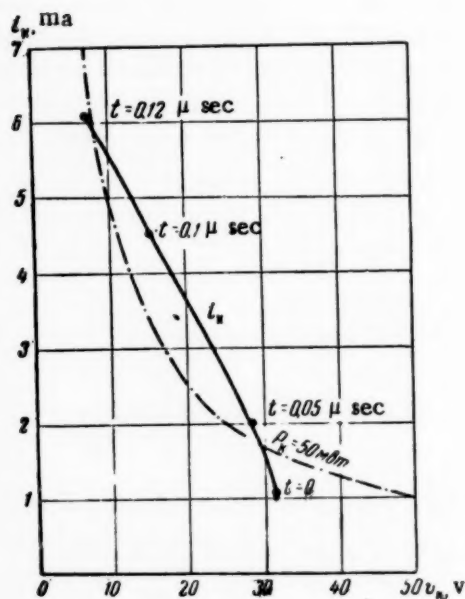


Fig. 7. Curve  $i_k = f_1(v_k)$ .

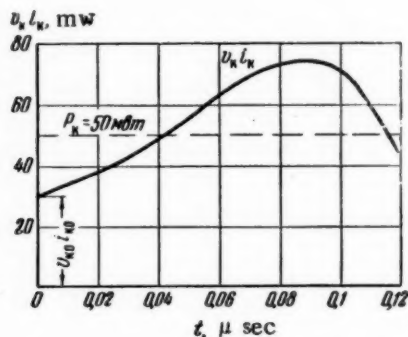


Fig. 8. Curve  $i_k v_k = f(t)$ .

The time  $t_a$  is thus seen to depend substantially on  $\tau$  and  $\alpha$ . To clarify the effect of other transistor parameters on the operation of the circuit, let us plot the curves  $i_k = f(v_k)$  and  $i_k v_k = f(t)$  for the transition from the cutoff region into the active region, using calculated data (Fig. 8). These curves show at a glance that the value of the collector

current,  $i_{k0}$ , with no current in the emitter and the value of the transistor saturation voltage limit the possibility of using the transistor under pulse conditions to the maximum power  $P_K$  that can be dissipated by the collector.

## SUMMARY

On the basis of the above analysis, let us formulate the requirements imposed on point-contact transistors for high-speed switching circuits.

1. The current gain of the transistor must not be less than 2.
2. The value of the current gain must not diminish noticeably over the active region of transistor operation.
3. The transistors must have low values of  $\tau$ ; if the circuit calls for a maximum time of  $0.1 \mu \text{ sec}$  to pass through the active region, the transistor time constant must be less than  $0.05 \mu \text{ sec}$ .
4. The transistors should have a low value of  $i_{k0}$ ; the collector resistance of pulse transistors should not be less than 25 kilohm.
5. The collector static characteristic should have its bend at a low voltage value.

## LITERATURE CITED

- [1] B. G. Farley, Dynamics of Transistor Negative-Resistance Circuits, Proc. IRE 40, 11 (1952).
- [2] I. L. Lebow and R. H. Baker, The Transient Response of Transistor Switching Circuits, Proc. IRE 42, 6 (1954).
- [3] T. R. Bashkow, Stability Analysis of a Basic Transistor Switching Circuit, Proc. of the National Electronic Conference, Vol. 9, 1954.
- [4] N. I. Brodovich, Grapho-Analytic Method of Plotting the Voltage-Current Characteristic of a Two-Terminal Network Containing a Transistor, Automation and Remote Control 17, 4 (1956).
- [5] Ch. A. Krause, Transistor Negative Resistance Characteristics Radio-Electronic Eng. May, 1954.
- [6] A. Lo, R. O. Endres, J. Zawels, F. D. Waldhauer and Ch. Ch. Cheng, Transistor Electronic, New York, 1955.

Received June 22, 1956.

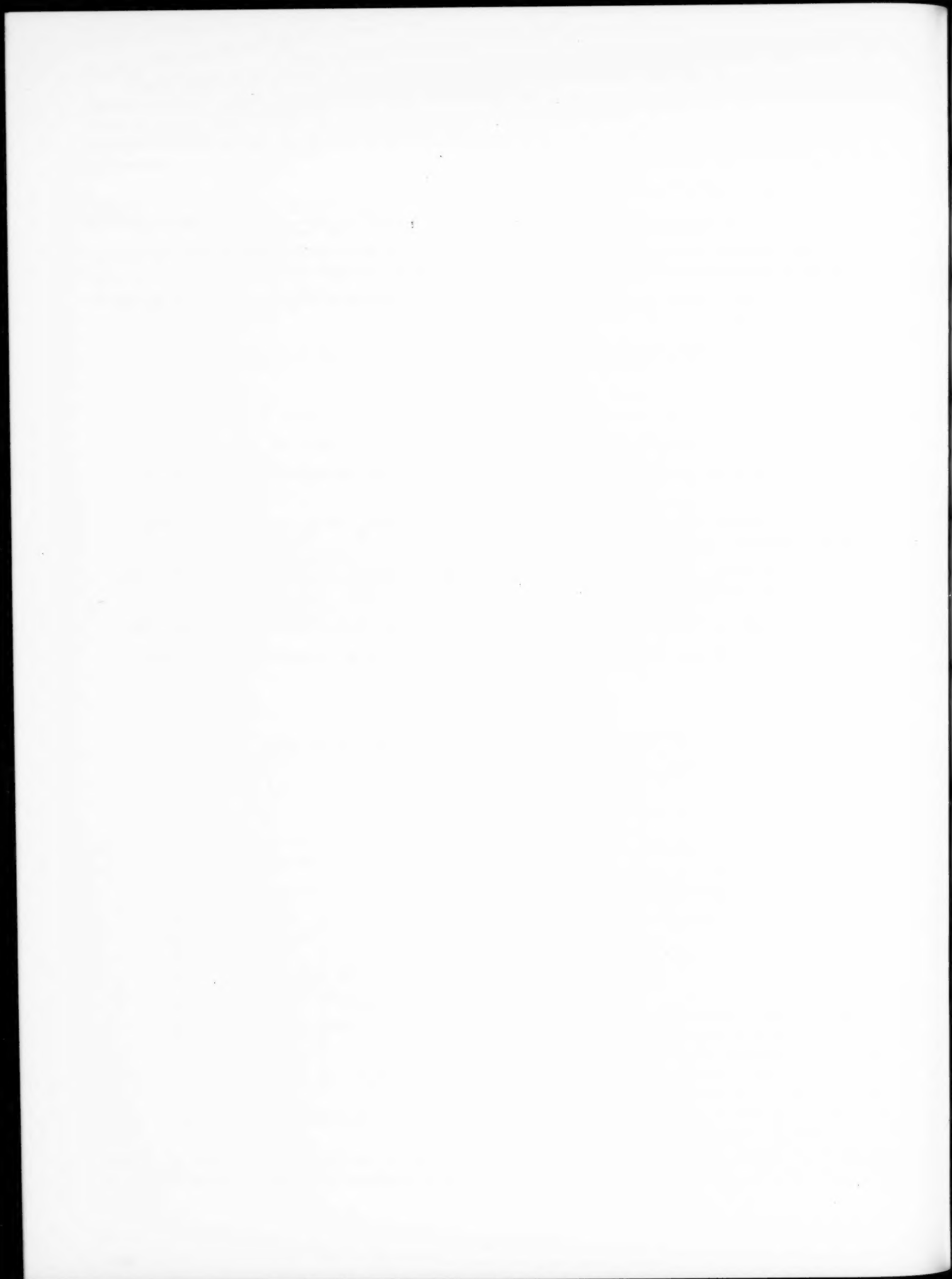




# DIAGRAM FOR DETERMINING THE REAL FREQUENCY CHARACTERISTIC FROM OPEN-LOOP LOGARITHMIC CHARACTERISTIC OF AN AUTOMATIC-REGULATION SYSTEM

Yu. M. Astapov

(Moscow)

To determine the transient behavior from trapezoidal or triangular characteristics it is necessary first to prepare a plot of the real frequency characteristic of the automatic-regulation system. The method proposed here makes the preparation of this plot possible from available plots of the amplitude-frequency and phase-frequency characteristics of the automatic-regulation system, which are required for the stability analysis. Stability is best investigated in logarithmic coordinates, for the plotting of logarithmic frequency characteristic presents no difficulties.

Extensive use is made at the present time of the circle diagram, with which one can readily obtain the real and imaginary closed-loop characteristics by plotting the open-loop hodograph  $W(j\omega)$ .

The real grid of the circle diagram is constructed according to the known equation

$$P(\omega) = \frac{U(\omega)[1 + U(\omega)] + V^2(\omega)}{[1 + U(\omega)]^2 + V^2(\omega)}.$$

Here  $U(\omega)$  and  $V(\omega)$  are respectively the real and imaginary open-loop frequency characteristic of the automatic-regulation system, so that

$$W(j\omega) = U(\omega) + jV(\omega).$$

The circle diagram is used by plotting the hodograph  $V(j\omega)$  in rectangular coordinates  $U$  and  $V$ , and the values of  $P(\omega)$  are obtained from the curvilinear grid by reading the indices of the circles intersected by the hodograph  $W(j\omega)$ .

To simplify the plotting of the hodograph  $W(j\omega)$ , let us put

$$W(j\omega) = H(\omega) e^{j\theta(\omega)},$$

where  $H(\omega)$  is the open-loop amplitude-frequency characteristic and  $\theta(\omega)$  the open-loop phase-frequency characteristic of the system. Furthermore

$$H(\omega) = \sqrt{U^2(\omega) + V^2(\omega)} \text{ и } \theta(\omega) = \arctg \frac{V(\omega)}{U(\omega)},$$

i.e., the lines  $H = \text{const}$  are concentric circles with centers at the origin of the  $U, V$  coordinates, and the lines  $\theta(\omega) = \text{const}$  are straight lines passing through the origin.

In this case it is necessary to plot  $W(j\omega)$  on the circle diagram in polar coordinates.



## DISCUSSIONS

### REMARKS ON THE ARTICLE BY V. L. INOSOV\*

V. L. Inosov's work is devoted to an exceedingly urgent problem.

None of the presently-available methods permit the calculation of the static stability limit of complicated power systems based on the "self-rocking" conditions, without requiring the development of characteristic determinants of very high orders, and consequently practically useless for the analysis of the parallel operation of more than three units. The simple stability conditions, proposed by V. L. Inosov for a system of any complexity and considered by the author to be sufficient, would find wide use in the design of regulating apparatus.

Unfortunately, the deductions of this work cannot be considered reliable, for they are based on many fundamentally-erroneous premises.

1. In the discussion of several known facts from the theory of small oscillations of dynamic systems (§ 1 of the article), it is indicated that the system of Equations (1) of the type

$$\sum_{k=1}^n (a_{ik}\ddot{q}_k + b_{ik}\dot{q}_k + c_{ik}q_k) = 0 \quad (i = 1, 2, \dots, n)$$

can be used to describe "the general case of interaction of material bodies" (p. 302) provided the matrix coefficients are symmetrical,  $a_{ik} = a_{ki}$ ,  $b_{ik} = b_{ki}$ , and  $c_{ik} = c_{ki}$ ; this would permit the study of the motion in this "general case" with the aid of three quadratic forms:

$$T = \sum_{i=1}^n \sum_{k=1}^n a_{ik} \dot{q}_i \dot{q}_k, \quad \Pi = \sum_{i=1}^n \sum_{k=1}^n c_{ik} q_i q_k, \quad \Phi = \sum_{i=1}^n \sum_{k=1}^n b_{ik} \dot{q}_i q_k,$$

expressing respectively the kinetic energy, the potential energy, and the dissipation function of the system, and to write down the equations for the free oscillations in the classic form:

$$\frac{d}{dt} \frac{\partial T}{\partial \dot{q}_i} + \frac{\partial \Pi}{\partial q_i} + \frac{\partial \Phi}{\partial \dot{q}_i} = 0 \quad (i = 1, 2, \dots, n).$$

The author's statements that these relationships are applicable is in general not true.

When the equations for small oscillations are written in Form (1), it is necessary in general to assume the matrix coefficient to be asymmetric [1, 2], and the equations in term of the energy functions assumes in principle a different form.

Following B. V. Bulgakov [2], we can present these equations in the following form:

$$\frac{d}{dt} \frac{\partial A}{\partial \dot{q}_i} + \frac{\partial}{\partial \dot{q}_i} (N + 2I) + \frac{\partial}{\partial q_i} (H + 2G) = 0 \quad (i = 1, 2, \dots, n),$$

\* Automation and Remote Control 15, 4 (1954).

in which the description of the system already calls for five forms, A, H, N, G, and I, of which only the three quadratic forms A, H, and N, which correspond to the kinetic, potential, and dissipative functions in the case of oscillations about the equilibrium position, have a symmetrical coefficient matrix, while the bilinear forms have a skew-symmetric matrix, i.e.,  $g_{jk} = -g_{kj}$  and  $i_{jk} = -i_{kj}$ .

Let us call particular attention to the physical meaning of the function I, which appears in the case of a sufficient asymmetry in the coefficients  $C_{ik}$ .<sup>\*</sup> This function is determined by the action of forces of a non-conservative character, and its appearance presupposes the presence of a certain theoretically unlimited energy source [2]. It is evident even from physical considerations that automatic-regulation systems (more accurately, indirect-regulation systems) are essentially dynamic systems of a general type, for they are indeed characterized by the presence of a certain controllable source of external energy. This generally well-known premise can be readily confirmed by analysis of any system. For example, the equations of a system for the regulation of the excitation of a unit feeding a network of infinite power through a transmission line have the following form (using the symbols employed by V. L. Inosov):

$$\begin{aligned} (Mp^2 + Dp + \frac{UE_d}{X_d} \cos \delta_0) \Delta \delta + \frac{U}{X_d} \sin \delta_0 \Delta E_d &= 0; \\ -\frac{X_d - X'_d}{X_d} T_0 U \sin \delta_0 p \Delta \delta + (T_0 \frac{X'_d}{X_d} p + 1) \Delta E_d - \Delta E_{de} &= 0, \\ F_\delta(p) \Delta \delta + F_{iE}(p) \Delta E_d - \Delta E_{de} &= 0. \end{aligned}$$

It is quite obvious here that the coefficient matrix is quite asymmetric.

One can assume in general that automatic-regulation systems for which the function I of the "artificial forces" vanishes, are usually nonexistent. But then the energy stability criteria assumed in V. L. Inosov's work become insufficient, as already shown by Routh [2].

Thus, the general theorems developed in §1 of the article are not applicable to the investigation of the stability of power systems with their automatic-regulation apparatus.

2. Without attempting at all to use the energy functions directly, the author builds up his subsequent arguments on the well-known premise [2, 3] that a well-known connection exists between the frequency characteristic of a system and the power dissipated per cycle in forced oscillations caused by an external harmonic force.

However, by treating this premise wrongly, namely by identifying the condition that the power dissipated in the forced oscillations be positive,  $-\int_0^T P dt > 0$ , with the condition that the dissipation function  $\Phi$  must be

positive, the author reaches the conclusion that if the first condition (or a corresponding condition imposed on the frequency characteristic) is satisfied for any element of the system, the element assumes the properties of an ordinary passive element in the sense used in network theory. \*\*

No clear definition is given here for the concept "system element" or "link," and in the absence of any requirements imposed on the coupling the use of the above conditions becomes unclear in principle.

3. The application of the proposed analysis method to power systems, made in §3 of the article, clearly shows that it is incorrect.

\* Let us note that if the line losses are accounted for, even the equations of an over-regulated system become asymmetric, depending on whether one of the angular coordinates, assumed as a general starting point for the computation, is ignored.

\*\* Let us note that the condition  $-\int_0^T P dt > 0$  subject to certain limitations, can actually be used to in-

vestigate the stability of a system, for it is identical with the condition that follows from the usual frequency criterion.

The element (link) of the power system is taken to be a generator equipped with an excitation regulator.

The unit operates into the remaining system, replaced here by an equivalent voltage of variable magnitude and phase, through an external reactance. The investigation reduces in final analysis to the imposition of conditions on the characteristic Equation (9) of the article, which is none other than the characteristic equation of a unit feeding an infinite-power network through a transmission line, the reactance of which remains undetermined [ $X_d$  and  $X_d'$  in Equations (4) and (6) of the article stand obviously for the total machine and line reactances].

Yet it is clear to any engineer engaging in the calculation of the parallel operation of the units that the value of these reactances is the decisive factor in the determination of the stability.

It is also evident that if all the units connected to an infinite bus satisfy the stability conditions, this does not necessarily mean the stability of the power system as a whole, if it is not "ruggedized" by superposition of such buses.

The above leads to the conclusion that V. L. Inosov's work is based on false theoretical premises and leads to technically nonrational conclusions.

#### LITERATURE CITED

- [1] L. G. Loitsiansky and A. I. Lurye, *Theoretical Mechanics*, Vol. 3, 1934.
- [2] B. V. Bulgakov, *Oscillations*, GITTL, 1954.
- [3] H. Bode, *Network Theory and Feedback Amplifier Design*, IL, 1948, (Russian translation).

A. A. Pervozvansky



# ANSWER TO REMARKS BY A. A. PERVOZVANSKY

1. The article did take into account the asymmetry of the coefficients,  $c_{ik}$ , although not in the form given in B. V. Bulgakov's book "Oscillations," for this book was published after the article. In particular, the expression

$$2 \frac{1}{\beta} \sum \sum \Delta c_{ik} P_i Q_k$$

in the equation for  $\alpha$  on p. 303 reflects the fact that the quadratic form  $I$  in Bulgakov's book differs from zero. Since the quadratic form  $G$  does not enter into the equation for the dissipation of the total energy

$$\frac{d(A+H)}{dt} = -2(I+N)$$

(the symbols are Bulgakov's, see p. 405), it cannot affect the sign of the damping coefficient and the case  $G \neq 0$  is not different in principle from the case  $G = 0$ .

The sum of the quadratic forms  $*(A+N)*$  which determines the total energy stored in the system satisfies the conditions of the Liapunov function, and therefore the sign of the derivative  $\frac{d(A+H)}{dt}$  becomes decisive for the system stability.

The article is based on the idea that if energy must be supplied to the system to maintain its oscillations, then the sign of the above derivative will be negative in the free process, and the system will be stable.

Naturally, the case when the coefficients are not symmetrical will be more general, and the paragraph at the end of p. 302 should therefore be corrected, but this naturally does not affect the applicability of my further development of the method.

As indicated in the article, I do not use the quadratic form, and the method I propose presupposes that the couplings between the links obey the reciprocity rule. This is why the simple conditions I propose, guaranteeing the absence of self-rocking in a complicated power system, cannot be extended, for example, to closed regulation systems, in which there is a directed flow of action from link to link (measuring elements, amplifiers, servomotors).

2. The average power, needed to maintain the forced oscillations of the system, is (Bulgakov, p. 499)

$$P_{av} = \frac{1}{2} \zeta^T (N - \frac{J}{i\omega}) \bar{\zeta}.$$

In a passive system  $I = 0$  and  $N > 0$ . This is why we always have for a passive system (Bode's theorem)  $P_{av} = \frac{1}{2} \zeta^T N \bar{\zeta} > 0$ . A condition is imposed on the links in the article that  $P_{av}$  be positive for all frequencies. One can therefore put  $\frac{1}{2} \zeta^T (N - \frac{J}{i\omega}) \bar{\zeta} = \frac{1}{2} \zeta^T N_{eq} \bar{\zeta}$ .

It follows therefore that the above link can be replaced by an equivalent passive link with a positive dissipative function. We are therefore right in assuming, without loss to the rigor of the analysis (particularly



if the structure of the system is unknown) that the system is passive if the energy of the external disturbances is positive at all frequencies, even if the system does contain controllable energy sources.

As to the fact, raised by A. A. Pervozvansky, that no clear definition was given to the "concept of a "system element" or "link," and in the absence of any requirements imposed on the coupling the use of the above conditions becomes unclear in principle," I must say that the limitations I imposed on the couplings are indicated in the footnote of p. 305. By link is meant any two-terminal network with a positive pure input resistance. As applied to a power system, the term "link" in the article refers to a generator with a section of the network, as was clearly indicated there.

3. The logic of the third remark is unclear to me. Actually, the parameters  $X_d$  and  $X'_d$  are decisive in the determination of the stability, but they also enter in the expression given to us, and are determined when the system is subdivided into elements. Where does A. A. Pervozvansky see any falsity in the method here?

The aperiodic stability of the system, dependent on the real roots, actually depends on whether the common buses will be solid or not, but the possibility of self-rocking is eliminated if each element has a positive disturbance power at all frequencies, or a positive dissipation in the sense indicated above. (As A. A. Pervozvansky would state it, under all conditions when operating into an infinite bus).

#### SUMMARY

Taking the above into account, it must be stated that A. A. Pervozvansky had no grounds for stating that the method treated in the article "is based on false theoretical premises and leads to technically nonrational conclusions."

V. L. Inosov

## CHRONICLE

### SCIENTIFIC SEMINAR HELD IN KIEV ON THE THEORY OF AUTOMATIC REGULATION

In accordance with the resolution of the Second All-Union Conference on the Theory of Automatic Regulation, held in Moscow in November, 1953, a Scientific Seminar on the Theory of Automatic Regulation was organized in Kiev in February, 1954, by scientific workers and engineers engaged in automation.

Detailed information on the first stage of the work of the Scientific Seminar was published in "Automation and Remote Control," No. 4, 1954, and in "Automation" No. 1, 1956 (published by the Academy of Sciences of the Ukraine SSR).

In 1955-56 the Scientific Seminar examined many urgent problems.

Several papers were devoted to the application of statistical methods to the theory of automatic regulation.

On January 10 and 24, 1955, Candidate of Technical Sciences, N. I. Kuznetsov (Kiev Higher Engineering Aviation School) explained in two seminars the basic premises of the method for the investigation of automatic-regulation systems under the influence of disturbances that are random functions of time.

The paper pointed out the extensive potentialities of the mathematical disciplines of probability theory and of the theory of random functions in the investigation of automatic-regulation systems that are acted upon by disturbances that are random functions of time (external noise, measurement errors of the control signal, etc.); the principles of this method were given.

In the discussions, Doctor of Technical Sciences A. G. Ivakhnenko (Electrical Engineering Institute of the Academy of Sciences of the Ukraine SSR), Doctor of Technical Sciences, A. I. Kukhtenko (Institute of Mining Affairs of the Academy of Sciences of the Ukraine SSR), Candidate of Technical Sciences, O. M. Kryzhanovsky (Institute of Mining Affairs of the Academy of Sciences of the Ukraine SSR) and Candidate of Technical Sciences L. N. Dashevsky (Institute of Mathematics, of the Academy of Sciences of the Ukraine SSR) cited many practical examples to show the effectiveness of the use of the theory of random functions in the investigation of individual problems in automatic-regulation systems.

A. G. Ivakhnenko and O. M. Kryzhanovsky indicated the need for the scientific workers and engineers engaged in automation to master the theory of random function and the need for developing methods for the investigation of the automatic regulation of systems under the influence of disturbances that are random functions of time.

On February 21, Doctor of Technical Sciences, A. I. Kukhtenko read a paper on "Statistical Methods in the Investigation of the Regulation of Mining Machinery." The first part of the paper indicated that the dynamics of automatic regulation systems for coal cutters and for coal combines can be described in terms of linear differential equations with a delayed argument.

The second part of the paper was devoted to the investigation of the response of the system to continuously-acting disturbances of random nature (for example, coal of differing strength). The lecturer suggested that the real diagram be replaced by an ideal one (in which the coal is assumed homogenous), and to have a random quantity  $k$  allow for the variable strength of the coal.

A. I. Kukhtenko showed how it is possible to synthesize automatic regulation systems for mining machines on the basis of the least-squared error requirement.

Participating in the discussion after the paper were Candidate of Technical Sciences L. A. Shoykhet (Institute of Mining Affairs of the Academy of Sciences of the Ukraine, SSR), Candidate of Technical Sciences N. I. Kuznetsov and others. N. I. Kuznetsov raised doubts concerning the statement of the problem and concerning the use of the theory of random functions for its solution. In his opinion it is more correct to consider the limiting strength of the coal not as a random quantity  $k$ , but as a random function  $k(t)$ , for the machine is in motion; the use of random-function theory will then become valid.

On February 7, A. G. Ivakhnenko indicated in his communication that the invariance conditions, derived by him previously to show ways of eliminating errors in linear combined-regulation systems subject to disturbances is applicable also for statistically-specified disturbances.

Two lectures: "The Passage of Random Functions Through a Linear Dynamic System," and "The Synthesis of Automatic Regulation Systems Subject to Random Action" were delivered by Candidate of Technical Sciences V. I. Ushankin (Kiev Higher Engineering Aviation School).

In the discussions after the lecture A. G. Ivakhnenko, A. I. Kukhtenko, O. M. Kryzhanovsky and N. M. Chumakov (Kiev Higher Engineering Aviation School) made many critical comments on the nature of the problem investigated.

Two seminars held on October 3 and 17 were devoted to lectures by Doctor of Technical Sciences Yu. A. Mitropolsky (Institute of Mathematics of the Academy of Sciences of the Ukraine SSR) on the "Application of the Small Parameter Method to the Theory of Automatic Regulation." Along with presenting the classical foundations of this method, developed by N. M. Krylov and N. N. Bogoliubov, the lecturer reported on new results obtained by using the small-parameter method for equations with variable coefficients.

Discussions by Active Member of the Academy of Sciences of the Ukraine SSR, A. Yu. Ishlinsky, A. G. Ivakhnenko, and O. M. Kryzhanovsky praised the paper highly and recommended that the methods developed by Yu. A. Mitropolsky be applied to actual automatic-regulation systems.

Candidate of Technical Sciences N. M. Chumakov raised doubts concerning the proposed mathematical theory, for the estimate of the small parameter appeared to him to be purely intuitive.

Candidate of Technical Sciences I. I. Krinetskiy (Kiev Institute of Civilian Fleet Engineers) remarked that the method presented is intended for engineering calculations. Such approximate methods, when used jointly with experiments, are very valuable in practice.

Toward the end of 1955 the Bureau of the Seminar resolved to invite wide participation in the work of the Seminar on the part of scientific workers and engineers in the Ukraine SSR, engaged in automation.

The scientific organizations of Lvov, Stalino, Dnepropetrovsk, and other cities, responded to this resolution. The Kiev Municipal Seminar thus became a Republic Seminar.

Great interest was created at the Seminar of October 31 by A. G. Ivakhnenko's paper "New Method for Design of Magnetic Amplifiers." At the same time, N. M. Chumakov explained a method for the design of magnetic amplifiers, developed by N. P. Vasilyeva and O. A. Sedykh (Institute of Automation and Remote Control of the Academy of Sciences, USSR).

On November 28, Engineer D. P. Avrinsky (Institute of Mining Affairs of the Academy of Sciences of the Ukraine SSR) delivered a survey lecture, based on materials in the foreign literature, on "Circuits and Operating Principles of New Types of Magnetic Amplifiers."

The lecturer's data were supplemented after the lecture by Doctor of Technical Sciences, A. G. Ivakhnenko and Candidate of Technical Sciences, A. D. Riabinin (Kiev Higher Engineering Aviation School).

On December 28, Engineer K. B. Shulgin (Donets Industrial Institute, Stalino), delivered a lecture on "Automatic Regulation of a Closed-Cycle Hydro-Compressor." The lecture threw light on the results of theoretical and experimental investigations obtained by him for a new system of automatic regulation.

In the discussions, A. Yu. Ishlinsky, A. I. Kukhtenko, P. I. Chinaev, N. M. Chumakov and others made many critical comments and at the same time praised this new work highly. In particular, A. I. Kukhtenko remarked on the correct statement of the problem and on the clever combination of theoretical and experimental

investigation. K. B. Shulgin employed mathematical theories of the investigation of pulse systems. It is a valuable engineering-computation procedure that K. B. Shulgin first developed and applied to the automatic-regulation system of a closed-cycle hydro-compressor. In the discussions N. M. Chumakov raised doubts concerning the correctness of the simulation of the object under laboratory conditions. The actual pressure ratio and change in level, occurring in the mines, is different than that obtainable in a laboratory setup. The failure to obtain similitude may lead to incorrect conclusions concerning the operation of the system. P. I. Chinaev supported the lecturer, stating that to simulate hydraulic object it is necessary to have equal Froude number, and this was done by the lecturer; consequently, the results can be of practical value.

Attention was paid in the program of the Seminar for 1956 to computation techniques and their application to automatic-regulation systems. A prominent place was given also to the analysis of the results of independent investigations performed by the participants in the Seminar during 1955-1956.

## WORK OF THE SEMINAR IN 1956

On January 9, Engineer V. I. Ivanenko (Institute of Electrical Engineering of the Academy of Sciences of the Ukraine SSR) lectured on his dissertation work, "Investigation of Automatic Speed-Regulation Systems for Mining Hoists." The lecturer embarked on finding a rational structural diagram for the regulator, so as to insure that the motion of the regulating system would not differ from the specified value. The inverse circuit-synthesis method was employed for this purpose.

To clarify the dynamic problems, the lecturer used electronic computers to determine the transients in the nonlinear systems. The investigations led to specific recommendations. Those participating in the seminar rated the dissertation work highly.

On February 6, Reader E. A. Papernyi (Lvov Polytechnic Institute) lectured on the "Use of Computers in Automatic Regulation Systems." The lecturer showed that a computer, based on a mathematical simulation of the object, can be used to regulate processes in blast furnaces. Such a computer was developed by a group headed by Professor K. B. Karandaev. A large commercial model has been in experimental operation in conjunction with Blast Furnace No. 2 at the "Azovstal" plant.

The data of the computer are used so far as "counsel" in the choice of the optimum operating conditions. It will be used in the near future as a master control for an automatic blast-furnace regulation system.

O. M. Kryzhanovsky remarked after the lecture that the lecturer refers only to a measuring element, and not to a computer as a whole. It would be more correct to build a computer with a memory device to permit analysis of the preceding processes and to employ this analysis for optimum adjustment of the system.

A. G. Ivakhnenko remarked that the fundamental shortcoming of the work reported is that it was performed without the participation of specialists in automatic regulation.

Candidate of Technical Sciences, L. N. Dashevsky indicated that discrete-action circuits extend considerably the field of computer application in automatic-regulation systems.

A series of survey articles on electronic computers was arranged by the Seminar.

On December 26, 1955 and January 16, 1956, Candidate of Technical Sciences, Yu. V. Blagoveshchensky (Institute of Mathematics of the Academy of Sciences of the Ukraine SSR) lectured on computer programming.

On February 13, Candidate of Technical Sciences, G. K. Nechaev (Institute of Electrical Engineering of the Academy of Sciences of the Ukraine SSR) lectured on "Techniques of High-Speed Computing Machinery."

On February 27, L. D. Dashevsky lectured on "Principles of Construction of Electronic Computers."

On March 12, L. A. Shoikhet lectured on "Guided Motion of Drifting Combines."

The lecture treated the question of automatic control of the guided motion of a drifting combine and derived the automatic-regulation system required for the purpose, using a computer device to determine the setting of the regulator as a function of the path covered by the combine. Experiments performed under laboratory conditions have shown that the operation of the basic units of the computer device will operate accurately.

On March 26, P. I. Chinaev lectured on "Graphoanalytic Methods for the Analysis of Automatic Regulation Systems." The lecturer dwelled in great detail on D. A. Bashkirov's graphoanalytic method, noting its principal advantage, namely its applicability to various automatic-regulation problems.



In the discussions, V. I. Ivenenko and O. M. Kryzhanovsky supplemented the survey of the numerical-integration methods made by the lecturer and expressed their disagreement with his views on the universality of the Bashkirov method. O. M. Kryzhanovsky claimed that the invention of electronic computer has reduced the value of approximate methods for numerical integration.

On April 2, N. P. Chumakov reported on methods developed under his leadership for experimental determination of phase frequency characteristics of servosystems and of stabilization systems with a real-frequency range from 0 to 5 cycles. He presented the principal diagrams and the structural drawings of breadboard models of instruments for the measurement of the phase shift. The lecturer reported that the breadboard models gave satisfactory results.

After the lecture A. G. Ivakhnenko, A. Yu. Ishlinsky, and A. I. Kukhtenko remarked on the value of this work and recommended that the possible accuracy of the developed instruments be theoretically determined.

At the same session of the Seminar, A. Yu. Ishlinsky reported on a new instrument for the measurement of the angular velocity of a moving object, or more accurately, of its component on a certain line tied to the object.

The instrument is called a "gyrotron" and comprises a vibrating tuning fork attached on a stand that can be twisted. Flexural vibration, maintained by an electromagnetic device, causes the moment of inertia of the tuning fork about its symmetry axis to vary. This, in turn results in a variation of the angular momentum about the same axis; in the absence of torsional vibration this angular momentum is the product of the moment of inertia by the component of the unknown angular velocity along the symmetry axis of the tuning fork. Since the twist stiffness is not zero, torsional vibrations will be produced, having an amplitude that is proportional to the measured angular velocity.

The sensitivity of the gyrotron is quite high, but the useful signal, usually picked-off electromagnetically, contains many parasitic signals which are difficult to eliminate. This report was heard with great interest.

On April 23-24 a coordination conference of the scientific-research institutions, higher institutes of learning, and manufacturing organizations of the Ukraine SSR was held to discuss plans for scientific work in the field of automatic regulation and automation during the sixth five-year plan. Detailed information on this conference was published in "Automation" No. 3, 1956 (published by the Academy of Sciences of the Ukraine SSR) and in "Automation and Remote Control," No. 12, 1956.

On May 7 Candidate of Technical Sciences L. V. Tsukernik (Institute of Electrical Engineering of the Academy of Sciences of the Ukraine SSR), in a lecture on "New Automatic-Regulation Systems for the Excitation of Synchronous Machinery," presented a survey of new work in this field, pertaining to large power systems and to generators of relatively low capacity.

Using as an example the automatic excitation regulator for the generators of the Kuibyshev Hydroelectric Station, developed by the All-Union Electric Institute of the Ministry of Electric Industry, by the Central Scientific Research Experimental Laboratory of the Ministry of Electric Stations, and by the Institute of Automation and Remote Control of the Academy of Sciences of the USSR, the lecturer demonstrated the effectiveness of introducing the first and second derivatives of the deviations from the terminal parameters into the regulation law, and also the value of introducing relay and logical control elements. Using as an example the voltage regulator for marine electric generators, developed by the Institute of Electrical Engineering of the Academy of Sciences of the Ukraine SSR, the lecturer examined the features involved in the regulation of low and medium power generators. The advantages of negative statism for voltage regulation were shown, and it is pointed out that this insures stable operation of parallel generators connected to common buses by using equalizing connections in the excitation circuits. An automatic regulator, based on a controllable compounding phase circuit in conjunction with compounding of parallel generators according to the average current, and developed at the Institute of Electrical Engineering of the Academy of Sciences of the Ukraine SSR (L. V. Tsukernik, O. M. Kostyuk, and V. E. Rybinsky) provides good operating characteristics, particularly with respect to high speed and quality of regulation. The regulator, furthermore, is relatively small in size.

The lecture was followed with great interest by representative of plants, design organizations, the Kiev Power System, and scientific-research institutes, who attended the seminar. The lecturer was asked many questions.



On May 21, Instructor A. I. Sud-Zlochevsky (Kiev Higher Engineering Aviation School) lectured on his dissertation work on the improvement of the quality of coupled regulation by introducing artificial couplings. The lecturer analyzed the effect of the coupling on the regulation quality of systems with two and three regulated parameters. The lecturer's conclusion that it is possible to improve the quality of system regulation by  $n$  times by introducing artificial couplings was verified with a voltage regulator and a frequency regulator for an aircraft generator converter.

After the lecture, Doctor of Technical Sciences, Yu. G. Kornilov, A. G. Ivakhnenko, A. I. Kukhtenko, and V. L. Inosov remarked on the urgency of the topic selected by A. I. Sud-Zlochevsky and offered many useful recommendations.

At the same Seminar session, the Chief of Setup Operations of the Kiev Power System, Yu. M. Bulavitsky, reported on experience in extending the use of thermal automation to the electric station of the Glaviuzhenergo (Main Southern Power System). The lecture was based on material on the monitoring of 15 electric stations in the Glaviuzhenergo system, carried out at the instigation of the USSR Ministry of Electric Stations by a brigade of operating personnel, which included the lecturer.

On June 4, 1956, Doctor of Technical Sciences A. N. Miliakh (Institute of Electrical Engineering of the Academy of Sciences of the Ukraine SSR) lectured on "The Inductive-Capacitive Transformer as an Automation Element." The inductive-capacitive transformer installation is based on the use of the phenomenon of electromagnetic induction occurring when both the magnetic and the electric fields are varied simultaneously in the transformer core. Ferrites, which have a good magnetic permeability and high electric properties, make the construction of an inductive-capacitive transformer possible. The inductive-capacitive transformer can be realized by cascade or parallel connection of an inductive transformer with a capacitive transformer, tuned to resonance at the operating frequency. Inductive-capacitive devices are used in high-frequency engineering.

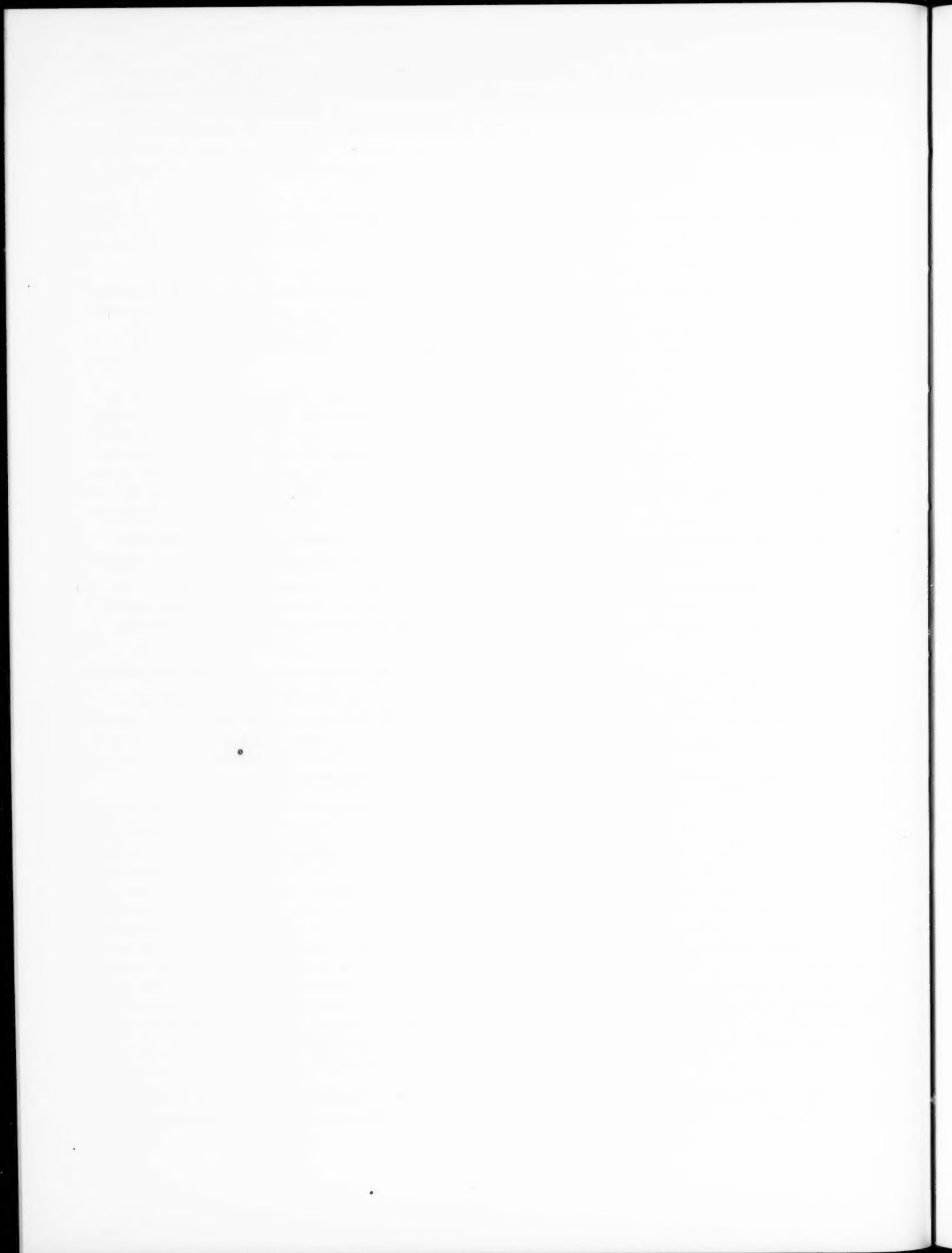
On June 18, P. I. Chinaev reported on his experimental and theoretical investigations of a relay system for automatic temperature regulation. The regulation object employed was a model of a ventilated airplane cabin. The regulator was of the RGVK-45 type. The system was investigated by the phase-trajectory method and by D. A. Bashkirov's graphoanalytic method. New operating properties were obtained by modifying the regulator.

In the discussions, I. I. Krinetsky remarked that the main problem in the cabin is the air ventilation. Maintenance of air temperature is a side issue. The practical value of this investigation is that a new type of regulation object was considered and that possible methods were found to improve the regulation.

At the same Seminar session, N. M. Chumakov reported on "Phenomena in Biology."

With this, the Seminar concluded its activities for the 1955-1956 academic year.

N. A. Kachanova and P. I. Chinaev



# USE OF MEMORY DEVICE TO IMPROVE THE STABILIZATION OF AUTOMATIC-REGULATION SYSTEMS WITH LIMITED SERVO MOTOR SPEED

V. A. Kotel'nikov

(Moscow)

The problem of designing a stable automatic-regulation system is considered under conditions of limited drive speed and unlimited initial errors.

A memory and switching device, satisfying the above requirements in the presence of a regulator with proportional feedback, is developed. The stability limits, which serve as a basis for determining the permissible values of regulator parameters, are determined for automatic-regulation systems with such a memory device. Analogue methods are used to determine the transients in the automatic-regulation systems when the errors exceed the linear speed range of the regulator drive.

## INTRODUCTION

To stabilize automatic regulation systems (ARS), extensive use is made of regulators with proportional feedback, which produces a deviation of the controlling device that is proportional to the signal if the drive of the regulator has a sufficiently high speed. A real regulator, however, always has a drive of limited speed, since its power is limited. The limitation imposed on the speed of the drive with high rate of change of the control signal leads in certain systems to poor transient response or even to loss of stability.

It is the purpose of this work to develop a device which makes possible an improvement of the stabilization of the object with the aid of a regulator having a limited drive speed.

We shall consider problems of guaranteeing the stability of and improving the static accuracy of an ARS, consisting of an object and a regulator with a proportional feedback in the presence of unlimited initial errors.

It is assumed that the regulator has:

- 1) A limited maximum of speed, power, and sensitivity in the drive;
- 2) A feedback gain that is limited by the time delay in the elements.

Under the above conditions and under the above limitations, the system is stabilized with the aid of a memory device developed by the author. The article will consist essentially of a description of the principle of operation and an analysis of the operation of this device.

### 1. Description of Circuit and of the Principle of Operation of the Memory and Switching Devices

The circuitry of the memory and switching devices (Fig. 1) incorporates six high-gain operational amplifiers [1].

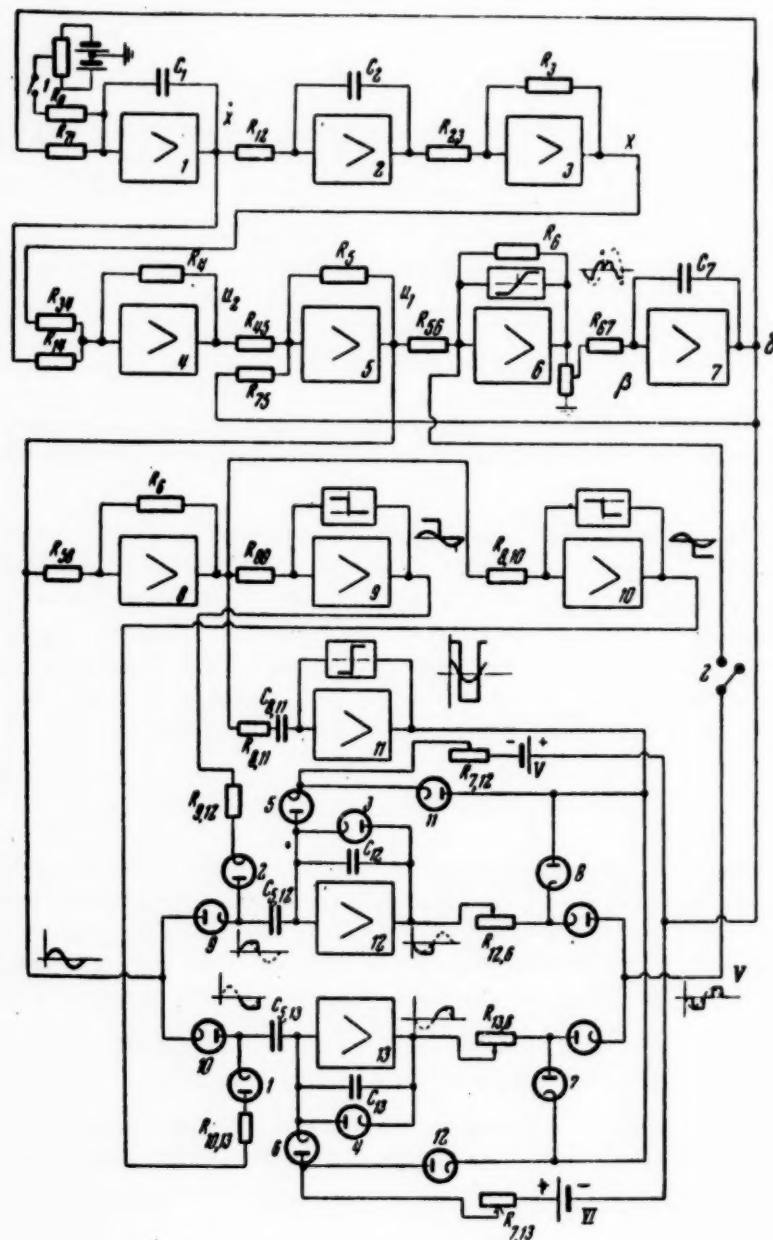


Fig. 1.

Amplifiers 12 and 13 are used for the memory. Amplifier 8 serves as a phase inverter. Amplifiers 9, 10, and 11 act as triggers, with amplifiers 9 and 10 operating when the signal is zero, and amplifier 11 operating when the derivative of the signal is zero. Amplifier 6 simulates the amplifier of the servo mechanism system of the regulator, while amplifier 7 simulates the drive mechanism of the regulator.

Operation of amplifiers 9, 10, and 11 in the trigger mode is guaranteed by the use of diodes connected in the feedback circuit. Diodes 1 and 2 serve to discharge capacitors connected at the input of amplifiers 12 and 13 after each memory cycle. Diode 3 prevents positive voltage from appearing at the input of amplifier 12, and diode 4 prevents negative voltage at the output of amplifier 13. If accidentally there appears at the

output of amplifier 12 an additional negative voltage on top of the signal voltage, diode 5 will remove this voltage during the non-operating half cycle of amplifier 12, with the aid of diode 3. Diode 6 operates in the second amplifier analogously with diode 5.

Forced discharging of memory capacitors  $C_{12}$  and  $C_{13}$  is produced by batteries V, VI through resistances  $R_{7, 12}$  and  $R_{7, 13}$ .

Capacitor  $C_{12}$  discharges when the voltage corresponding to the coordinate  $\delta$  is less than the voltage of the battery V and the voltage at the output of amplifier 11 is negative. Capacitor  $C_{13}$  discharges when the voltage corresponding to the coordinate  $\delta$  is greater than that of the battery VI and the voltage at the output of amplifier 11 is positive.

Diodes 7 and 8, operated by amplifier 11, block the voltage fixed by the capacitors at the input of amplifier 6 during the first quarter of the working half cycle, and diodes 11 and 12 permit the discharge of the memory capacitors only during the second quarter of the working half cycle.

Let us trace the variation of the voltage at various points of the circuit when a sinusoidal input signal is applied.

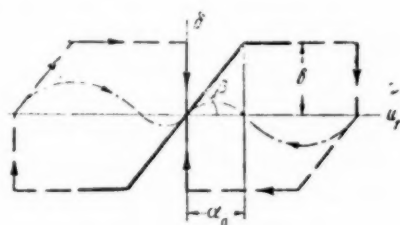


Fig. 2.

During the first quarter cycle, the voltage at the output of amplifier 12, the transfer coefficient of which is unity, will have the same absolute value as the signal voltage. During the second quarter, when the signal voltage diminishes, the output voltage of amplifier 12 remains constant, since diode 9 opens the input circuit of this amplifier. During the third and fourth quarters of the cycle, the trigger (amplifier 9) operates, and consequently the voltage at the output of amplifier 12 is zero.

The voltage established at the output of amplifier 12 by the operation of diode 8 is applied to the input of amplifier 6 only during the second quarter of the cycle.

The operation of the second half of the memory device with amplifier 13 is analogous, and amplifier 13 applies to amplifier 6 the voltage fixed at the output of amplifier 13 during the fourth quarter of the period. Since the input signal and the rectangular wave forms from amplifiers 12 and 13 are summed in amplifier 6, we obtain at the output of amplifier 6 a lead relative to the input signal  $u_1$ .

The solid line of Fig. 2 shows the variation of the speed as a function of the signal  $u_1$  for an ordinary regulator, the dotted line shows it for a regulator with a memory device without forced discharge of the memory capacitors, while the dash-dot line shows it for a regulator with a memory device and forced discharge of the memory capacitors.

The symbols on Fig. 2 are:  $\beta$  -- angle determining the velocity coefficient of the drive,  $\eta = \tan \beta$ ,  $b$  -- maximum value of speed,  $\alpha_1$  -- signal amplitude corresponding to the linear portion of the speed characteristic.

A device based on an idea similar to above is employed in [2].

## 2. Linearization of the Nonlinear Dependence of the Speed on the Input Signal

For approximate replacement of the nonlinear dependences (Fig. 2) with linear ones we shall employ the equivalent-linearization method. For this purpose we shall expand in a Fourier series the functions  $\delta = f_1(u_1)$  (solid line) and  $\delta = f_2(u_2)$  (dotted line).

In the expansion we neglect all harmonics except the first, i.e., we shall assume that  $f(u) = a_0 + a^* \cos x + b^* \sin x$ .

For the function  $f_1$ , the Fourier series coefficients will be

$$a_0 = 0, \quad a^* = 0, \quad b^* = \frac{2}{\pi} \left( \eta \alpha \arcsin \frac{b}{\eta \alpha} + b \cos \arcsin \frac{b}{\eta \alpha} \right).$$

The curve showing the dependence of the quantity  $b^*/\alpha$  on  $\alpha$ , calculated from the above equation is shown dotted in Fig. 3.

For the function  $f_2$ , the Fourier series coefficients will be

$$a_0 = 0, \quad a^* = \frac{2b}{\pi} \left(2 - \frac{b}{\eta a}\right), \quad b^* = \frac{\eta a}{\pi} \arcsin \frac{b}{\eta a} - \frac{\eta a}{2\pi} \sin 2 \arcsin \frac{b}{\eta a} + \\ + \frac{2b}{\pi} \cos \arcsin \frac{b}{\eta a} + 2 \frac{\eta a}{\pi} \cos \arcsin \left(1 - \frac{b}{\eta a}\right) + \frac{\eta a}{\pi} \arcsin \left(1 - \frac{b}{\eta a}\right) - \\ - \frac{\eta a}{2\pi} \sin 2 \arcsin \left(1 - \frac{b}{\eta a}\right) - \frac{\eta a}{2} - \frac{2b}{\pi} - \frac{2b}{\pi} \cos \arcsin \left(1 - \frac{b}{\eta a}\right).$$

The curves showing the dependence of the coefficients  $a^*/\alpha$  and  $b^*/\alpha$  on  $\alpha$ , corresponding to the above equations, are shown in Fig. 3. In both cases the unit of amplitude is taken to be the amplitude of the linear portion  $\alpha_1$ , and the unit of  $a^*/\alpha$  and  $b^*/\alpha$  is taken to be the quantity  $\eta = \tan \beta$ .

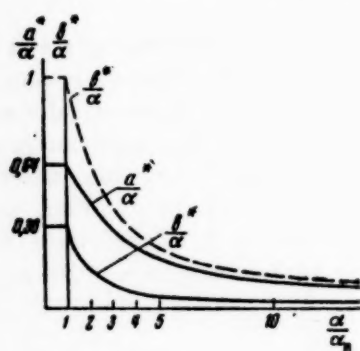


Fig. 3.

Thus, after performing the linear approximation, the equation for the drive will be  $\dot{\delta} = (b^*/\alpha) u$  for the nonlinear dependence  $f_1$ , while for the nonlinear dependence  $f_2$  we have

$$\dot{\delta} = (a^*/\alpha i + b^*/\alpha) u_1, \quad \text{where } i = \sqrt{-1}.$$

In the first averaging formula the velocity coefficient depends on the amplitude of the signal  $u_1$ , and the phase of the velocity coincides with the phase of the signal for all frequencies and amplitudes. In the second formula, the velocity coefficient and the phase shift between the velocity  $\dot{\delta}$  and the signal  $u_1$  depend on the amplitude of the signal, but are independent of the frequency.

### 3. Equations and Parameters of System Employed for the Investigation of the Stability of the ASR and for Simulation

The advisability of using a memory device will be considered using as an example the stabilization of an object, the motion of which is described by the following equation.

$$\ddot{X} = -p\delta, \quad (1)$$

where  $X$  is the regulated coordinate,  $\delta$  is the coordinate of the controlling device of the regulator, and  $p$  is the coefficient of effectiveness of the regulating device.

Let us use for stabilization a regulator with proportional feedback. The equation of the regulator in operational form, with allowance for the time lag, will be

$$D\delta = e^{-D\tau} f(Da_1 X + a_2 X - a\delta),$$

where  $\tau$  is the time delay of the drive,  $f$  is the nonlinear dependence (see Fig. 2), and  $a$ ,  $a_1$ ,  $a_2$  are constant coefficients, and  $D = d/dt$ .

For a regulation system consisting of an object, described by Eq. (1) and a linear regulator with proportional feedback without time delay, we obtain the following characteristic equation:

$$D^3 + \eta a D^2 + \eta a \frac{a_1}{a_2} p \frac{a_2}{a} D + \eta a p \frac{a_2}{a} = 0,$$



where  $\eta$  is the velocity coefficient of the drive of the regulator, obtained as a result of linearization of function  $f$ . The resultant equation contains three combinations of the parameters:  $a_1/a_2$ ,  $\eta a$ , and  $pa_2/a$ .

The ratio  $a_1/a_2$  is stable and varies little with random variations of the regulator parameters.

The product  $\eta a$  characterizes the total gain over the feedback loop. In the product  $\eta a$  the quantity  $\eta$  can change spontaneously by a factor of 2-3 owing to variation in the velocity characteristic of the drive.

In the presence of a backlash zone in the drive, the accuracy of the operation of the servo system of the regulator increases with increasing coefficient  $a$ .

The product  $pa_2/a$  characterizes the total gain in the regulator-object loop.

The value of the effectiveness of the regulating device can vary over a wide range, since the quantity  $p$  depends on the mode in which the stabilized system is operated, for example, for such an object of regulation as an airplane, the quantity  $p$  is proportional to the square of the flight speed.

We shall consider the gain of the servo system of the regulator and the total gain of the regulator-object system to be the principal parameters of the system, which characterize its properties. We shall use these coordinates to compare the results of the calculation of the periodic modes for various methods of regulation.

#### 4. Periodic Modes of an ASR with a Regulator Without Lag, but with Limited Speed of the Regulator Drive

To illustrate the advantages of system stabilization by means of a regulator with a memory device, let us compare three versions of stabilization: 1) with ordinary regulators, 2) with a regulator responding to the signal and its derivative, and 3) with a regulator having a memory device.

The first version is described by the following equation:

$$\begin{aligned} D^2X &= -p\delta, \\ D\delta &= f_1(a_1DX + a_2X - a\delta). \end{aligned} \quad (2)$$

The periodic modes that are possible in the linearized system corresponding to system (2) are determined from the following relationships

$$\frac{a_1}{a} p = \omega^2, \quad \eta a \frac{b^*}{a} = \frac{1}{a_1/a_2},$$

where  $\omega$  is the oscillation frequency.

The calculated results obtained from the formulas derived are given in Fig. 4. Using the Hurwitz criterion, it was established that the system is stable to the right of the curve corresponding to the periodic mode, and unstable to the left of this curve. The location of the stability regions are confirmed by simulation.

The results obtained show that when the amplitude increases above a certain value, the stability is destroyed, for the averaged velocity coefficient drops below the permissible value. The loss of stability at large amplitudes limits the permissible value of the disturbances that can act on the system.

The second version is described by the equation

$$\begin{aligned} D^2X &= -p\delta, \\ D\delta &= f_1(kD + 1)(a_1DX + a_2X - a\delta), \end{aligned} \quad (3)$$

where  $k$  is the factor in front of the derivative of the control signal.

The equations for the periodic mode of the linearized system (3) will be

$$\frac{a_2}{a} p = \frac{\omega^2}{1 - k \frac{a_1}{a_2} \omega^2}, \quad \eta a \frac{b^*}{a} = \frac{1 - k \frac{a_1}{a_2} \omega^2}{\frac{a_1}{a_2} (1 + \omega^2 k^2)}.$$

Figure 4 shows the results of calculations with the above equations for  $k = 1.75$  and  $a_1/a_2 = 0.5$ . According to Hurwitz criterion, the system is stable to the right of the boundary of the periodic mode.

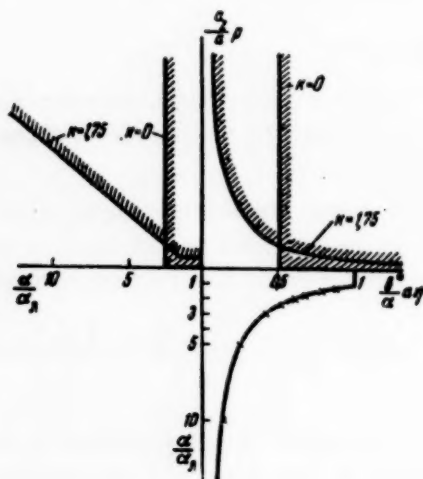


Fig. 4.

As in the first version of stabilization, the stability of the ASR is destroyed when the amplitude  $\alpha$  increases for a specified value of  $a_2 p/a$ .

Increasing the action of the derivative of the control signal (increasing the coefficient  $k$ ) makes it possible to increase the permissible amplitude. However, the permissible value of the coefficient  $k$  is limited if the system contains a regulator with time delay.

The third version is described by the following equation:

$$D^2 X = -p\delta, \\ D\delta = f_2(a_1 DX + a_2 X - a\delta). \quad (4)$$

The equations for periodic modes of the linearized system (4) will be

$$\frac{a_2}{a} p = \frac{\omega^2}{1 - \frac{a^*}{b^*} \frac{a_1}{a_2} \omega^2}, \quad \eta a \frac{b^*}{a} = \frac{\left(1 - \frac{a^*}{b^*} \frac{a_1}{a_2} \omega^2\right)}{\frac{a_1}{a_2} \left[1 - \left(\frac{a^*}{b^*}\right)^2\right]}.$$

Figure 5 gives the results of the calculation of the periodic modes for various amplitudes  $\alpha$ .

The location of the stability regions is analogous to that of the first case. When the periodic modes are redrawn from the initial coordinates  $a_2 p/a$  and  $\eta b^* a/\alpha$  into coordinates  $a_2 p/a$  and  $\alpha/\alpha_1$ , a single point on the curve  $\eta a b^*/\alpha$  vs.  $\alpha/\alpha_1$  corresponds to each amplitude.

Figure 5 shows this latter curve for a regulator servo system with a gain  $\eta a = 1$ .

For any other value of gain, the values of  $b^*/\alpha$  (Fig. 3) should be multiplied by  $\eta a$ .

If  $\eta a > 1.5$ , the stability is retained for all values of the parameter  $a_2 p/a$  and for all amplitudes  $\alpha$ . However, in the presence of a time delay, one can increase the gain  $\eta a$  to extend the stability region only within a narrow range (see below for the stability boundaries in the case of time delay). The stability region obtained differs from the stability region as plotted in coordinates  $a_2 p/a$ ,  $\alpha$ , shown in Fig. 4, since in the latter case the system stability is not affected by an increase in the amplitude, starting with a certain value of  $a_2 p/a$ . This permits the system to operate stably in the presence of disturbances of all amplitudes. In such a regulation system, the minimum speed of the regulating device is determined by the permissible deviation of the system due to action of random disturbances and by the value of the mode rate of change that is adequate for the control purposes.

Many automatic regulation systems do not require a high control-device speed to satisfy these conditions. This makes it possible to use a step-down gear reduction between the drive and the regulating device.

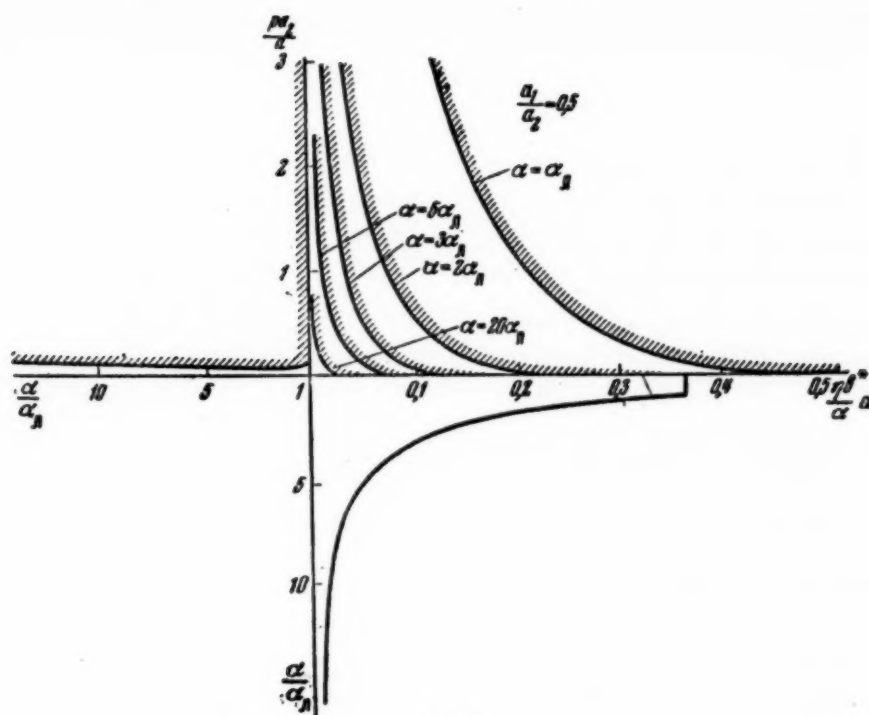


Fig. 5.

Introducing a gear reduction makes it possible to increase the load acting on the control device, and to increase the coefficient  $a_1$  of the position feedback.\* Increasing the position feedback while retaining constant the transfer factor from the sensitive elements to the control device (the ratio  $a_2/a_1$ ) makes it possible to increase the coefficient  $a_2$  by the same amount.

In the presence of an insensitivity zone in the drive mechanism of the regulator, an increase in the feedback coefficient and in the coefficient  $a_2$  leads automatically to a corresponding reduction in the insensitivity zone. Along with increasing  $a_2$  and  $a_1$ , the deviation of the regulated coordinate, at which a maximum speed of the regulator control device is attained, is diminished. This makes the characteristic of the servo drive of the regulator approximate that of a relay. The relay characteristic makes it possible to obtain maximum action on the part of the regulator on the regulation object within the limits of the maximum velocity of the regulating device. Optimization of the regulation processes [3-7] becomes little effective in such systems.

Comparing the above three methods of stabilization, we see that stabilization with the aid of memory and switching is preferred.

## 5. Simulation of an ASR with a Memory and Switching Device

The simulation was carried out for the purpose of comparing the transients in a linear system and in a system with a regulator having a drive of limited speed.

A system with limited speed was stabilized with a proportional feedback regulator and with a regulator having proportional feedback and a memory device (Fig. 1).

Two memory devices were tested in the simulation.

In the first circuit, the resistances  $R_{7, 12}$  and  $R_{7, 13}$  (Fig. 1) were not used and the memory capacitors were not discharged forcibly, and in the second system, the memory capacitors were forcibly discharged through resistances  $R_{7, 12}$  and  $R_{7, 13}$ .

\* In a real regulator the feedback coefficient and the transfer coefficient from the object to the regulator are limited by time delay; they can be increased by reducing the velocity coefficient of the drive.

The speed of the drive was limited by diode limiters, connected in the feedback circuit of amplifier 6. The voltage  $u_2$  of the error coordinate (Figs. 6-12), corresponding to the linear range of speed, was 4.6 volts in the simulating device. The parameters of the memory and switching circuit remain constant for all cases of simulation.

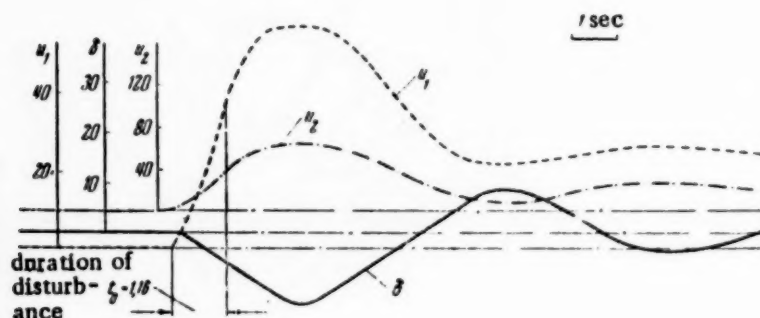


Fig. 6.

The disturbing action in the system was produced in the form of a constant torque in the right half of Eq. (1).

In the analogue of the system this was effected by means of a voltage connected by switch 1 at the input of the first amplifier (Fig. 1). The duration  $t_0$  of the voltage was so chosen as to keep the circuits from saturating.

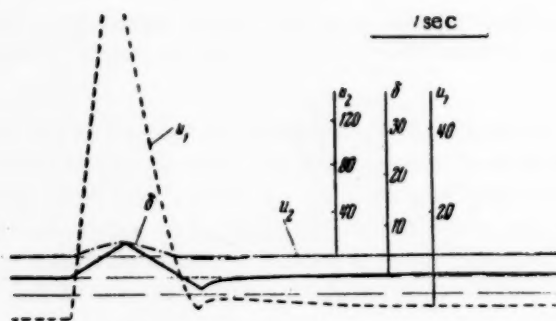


Fig. 7.

The simulation was carried out under the following combinations of system parameters:  $a_1/a_2 = 0.5$ ,  $\eta a = 2$ ,  $a_2 p/a = 0.1, 1, 100$ , and  $500$ .

Resistances  $R_{12,6}$  and  $R_{13,6}$  were used to adjust the transfer coefficients of the signal passing through resistance  $R_{5,6}$  and through the memory device to an equal value.

For all values of regulator effectiveness  $a_2 p/a$  and for values  $a_1/a_2 = 0.5$  and  $\eta a = 2$ , the linear system was at the stability limit when the speed was unlimited.

When the speed of the drive of the regulator was limited, the system became rapidly swinging if

the disturbance caused an amplitude deviation exceeding the linear range of the drive speed.

Figures 6, 7 and 8 show oscillograms of the motion of a system, stabilized by a switching device with "memory," for various values of regulator effectiveness,  $a_2 p/a = 1, 100$  and  $500$  respectively. The oscillogram illustrates the stability of the system for disturbances causing a large deviation of the coordinate  $u_2$ , exceeding by many times the linear range of speed. The oscillograms given here show that a switching device with "memory" ensures phase agreement between the coordinate  $\delta$  and the control signal.

If the speed of the drive is limited, the maximum attenuation is observed when the regulator effectiveness is high. A characteristic feature of the oscillograms shown is the shift of the zero position of the system after the disturbance.

The value of the shift remaining after the damping of the system approaches zero very slowly. The shift is caused by the charging of the memory capacitors  $C_{12}$  or  $C_{13}$  during the action of the disturbance. A reduction in the shift is the result of a slow discharge due to leakage through the memory capacitors.

Figures 9, 10, 11 and 12 show oscillograms of a system stabilized with a switching device having a "van-

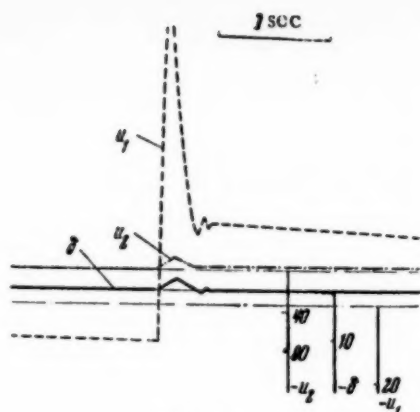


Fig. 8.

ishing memory" for the following values of regulator effectiveness:  $a_2 p/a = 0.1, 1, 100$  and  $500$  respectively. These oscillograms illustrate the stability of the system under disturbances exceeding the linear range of speed, and the return of the system to the initial state.

However, the use of a "vanishing memory" combined with a small regulator effectiveness has been shown by analog simulation to reduce somewhat the stability of the system.

At low effectiveness, the stability is reduced owing to the change in the sign of the variation of coordinate  $\delta$ .

The sign of the variation of the coordinate  $\delta$  is determined by the sign of the control signal, which in turn is determined by the difference of the coordinate  $u_2$  and the voltage fixed by capacitors  $C_{12}$  and  $C_{13}$ . The above difference is shown dotted in Figures 9 and 10. Starting with an instant  $t^*$ , when  $\delta$  becomes smaller

than the voltage of the charging batteries, the memory capacitor discharges and the difference decreases rapidly. The change in the sign of the difference, caused by the discharge, leads to a change in the sign of  $\delta$ .

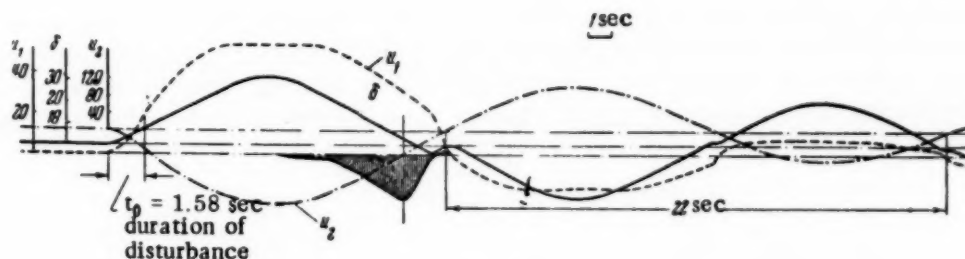


Fig. 9.

The delay in the change of the system coordinates when the regulator effectiveness is high, over a time period  $\Delta t$  (Figure 12), is due to the charge of the memory capacitor. To illustrate this statement, let us examine Figure 13, where  $u_1$  stands for the coordinate of the object,  $\delta$ , for the coordinate of the control device,  $V$ , for the voltage of the output of the memory device, and  $\epsilon$ , for the signal acting at the input of the amplifier of the regulator drive mechanism.

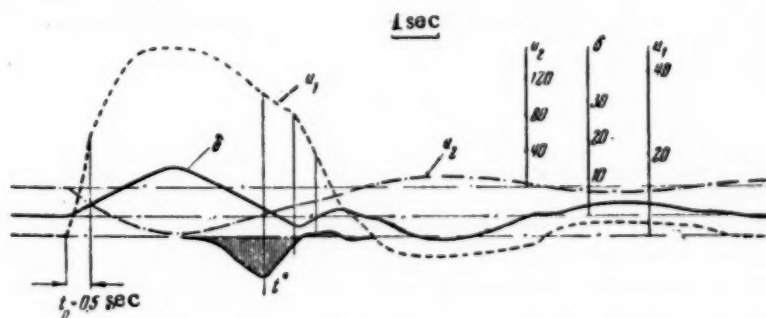


Fig. 10.

When the fixed voltage is applied to the input of the amplifier of the drive mechanism, we have  $\epsilon = u_1 - \delta - V$ , and when the voltage is not applied,  $\epsilon = u_1 - \delta$ . The coordinate  $\epsilon$  is shown dotted in Figure 13.

The disturbance causes a change in  $u_1$ , which produces a motion of the regulating device. The difference between  $u_1$  and  $\delta$  is memorized.

At the instant that the sign of the motion of coordinate  $u_1$  changes, the signal  $\epsilon$  becomes  $u_1 - \delta - V$ , which



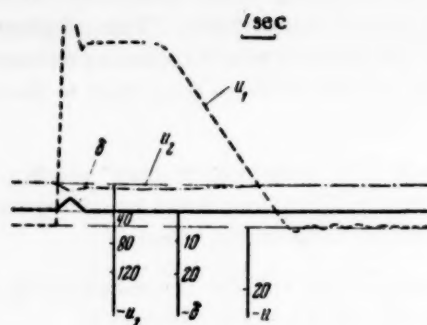


Fig. 11.

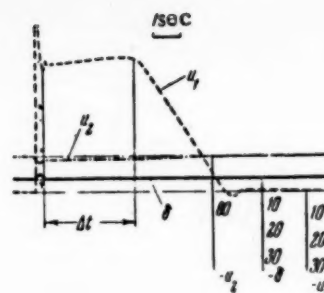


Fig. 12.

causes a reduction in  $\delta$ . When  $\delta$  becomes less than the value at which the capacitors start discharging (at the instant  $t^*$ ), the fixed voltage  $V$  starts diminishing. During the discharge process, the system oscillates at a high frequency (approximately 50 cycles). These oscillations are due to the periodic variations in the sign of the control signal  $\epsilon$ , which occurs every time the sign of  $\dot{u}_1$  changes. Actually, as  $u_1$  increases, a positive voltage appears at the output of amplifier 11 (Figure 1), and this voltage is applied to diodes 7 and 8, preventing the voltage  $V$  from being applied to the input of amplifier 6. This changes the sign of the control signal, since it is determined principally by the value of  $u_1$  ( $\delta$  is a small quantity). The change in the sign of the control signal causes a change in the sign of  $\dot{\delta}$ , which changes the sign of  $\dot{u}_1$ . The change in the sign of the derivative produces a negative voltage at the output of amplifier 11, and diodes 7 and 8 start transmitting the signal to the input of amplifier 6. The control signal changes its sign and causes a change in the sign of  $\delta$ , and consequently the coordinate  $u_1$  increases.

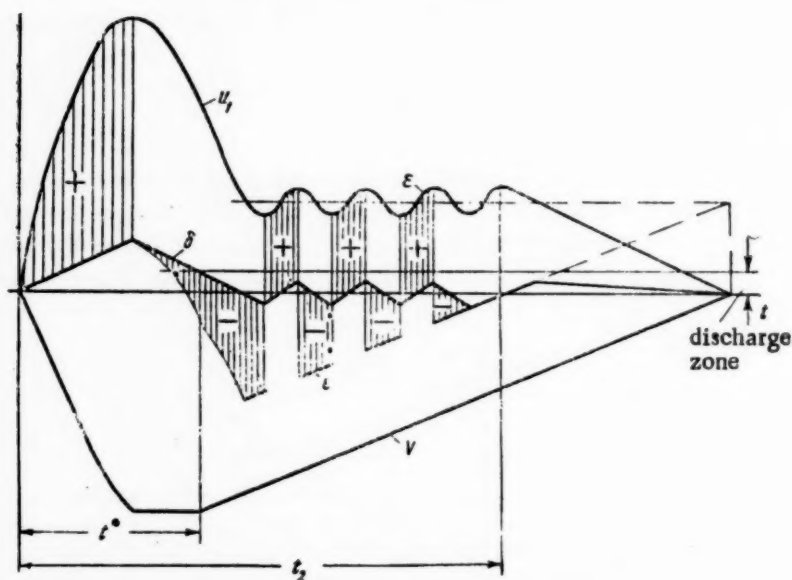


Fig. 13.

The above oscillations will continue until the memory capacitor is discharged to a voltage  $V$ , equal to the voltage  $u_1$ . Actually, if  $V \leq u_1$ , the summation signal will have the same sign for both positive and negative voltages at the output of amplifier 11, and the coordinate  $\delta$  will be positive, causing the coordinate  $u_1$  to diminish to zero.

The increase in the discharge speed past the instant  $t_2$  is explained by the fact that periodic disconnecting of diodes 5 and 6 stops, and the charging process is continuous.

To accelerate the return of the system to the initial state after the disturbance it is necessary to increase the speed of the discharge of the memory capacitors. However, increasing the discharge speed reduces the sta-



bility at low regulator effectiveness. To eliminate this shortcoming it is necessary to make the capacitor discharge rate depend not only on the deviation of the control device of the regulator, but also on the speed of variation of the coordinate  $u_1$ . When the derivative  $\dot{u}_1$  is large, the rate of discharge should be small and vice versa. The correctness of this conclusion can be checked by simulation.

#### 6. Periodic Modes in an ASR with a Regulator Having a Time Delay and a Limited Drive Speed

To evaluate the advisability of using a regulator with a memory device in the presence of a time delay in the regulator, let us calculate and compare the values of the parameters of a linearized system, in which periodic modes are possible. We shall calculate the parameters for the three above laws of regulation (2), (3) and (4) mentioned above. The best result will be assumed to be that at which the periodic modes are missing from the greatest range of amplitude  $\alpha$  and from the greatest range of the parameters  $\eta a \tau$  and  $p a_2 \tau^2 / a$ .

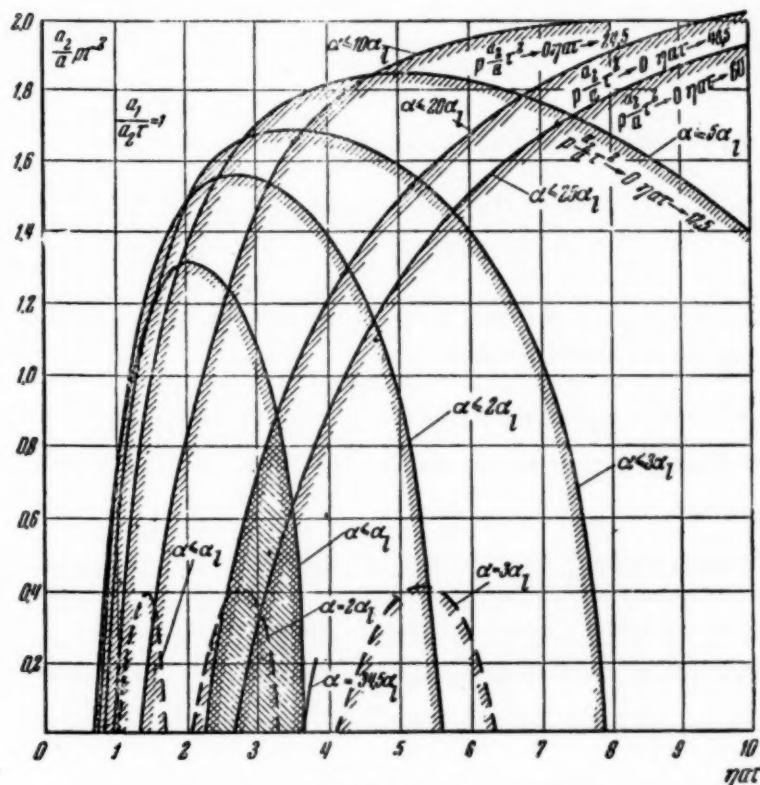


Fig. 14.

Let us list the following ideas concerning the location of the region of stable motion relative to the curves of the periodic modes.

It is known that increasing the feedback coefficient in the above regulator versions produces an oscillation with an equivalent frequency  $\omega \tau = \Omega \leq \pi/2$ . This makes it possible to state that to the right of the curves corresponding to the periodic modes at these frequencies there is an instability region, and that to the left of these curves there is a stability region. At low frequencies,  $\Omega < 0.05 \frac{\pi}{2}$ , it is possible to neglect the delay; in this case the stability is determined with the Hurwitz criterion. In accordance with the above statement, the stability region is shown cross hatched in Figures 14 and 15, where the solid lines indicate the curves corresponding to the periodic modes in a system with a memory device, and the dotted lines indicate the curves for a system without such a device.

The equations of System (2), in the presence of delay, will be

$$D^2 x = -p \delta, \quad D \delta = e^{-D\tau} f_1(a_1 D x + a_2 x - a \delta).$$

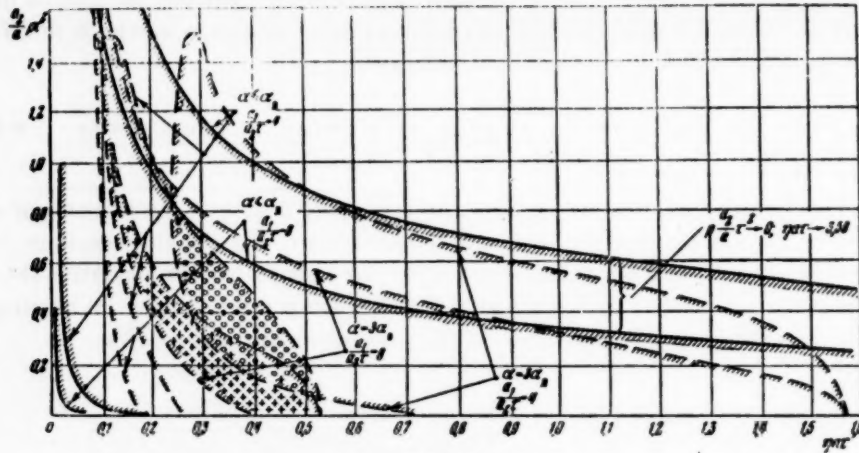


Fig. 15.

The equations of the periodic modes of this linearized system will be

$$p\tau^2 \frac{a_2}{a} = \frac{\Omega^2 \cos \Omega}{\frac{a_1}{a_2\tau} \Omega \sin \Omega + \cos \Omega}, \quad \eta a \frac{b^*}{a} \tau = \frac{\frac{a_1}{a_2\tau} \Omega \sin \Omega + \cos \Omega}{\frac{a_1}{a_2\tau}}.$$

Figure 14 shows dotted the curves corresponding to the periodic modes for the amplitudes  $\alpha \leq \alpha_l$ ,  $\alpha = 2\alpha_l$ , and  $\alpha = 3\alpha_l$ , bounding the stability regions.

The curves of the periodic modes for the amplitudes  $\alpha > \alpha_l$  are calculated by dividing the parameter  $\eta a \tau \frac{b^*}{a}$ , obtained for the linear portion of the speed characteristic, by the value of  $b^*/a$ , calculated for the required amplitude  $\alpha$  (Figure 3).

The amplitude increases, the curves corresponding to the periodic modes shift to the right. As a result, an increase in the range of amplitudes  $\alpha$  decreases the region that is common to the curve  $\alpha \leq \alpha_l$  and the curve  $\alpha = \alpha_m$  ( $\alpha_m$  is the maximum amplitude within the specified range of amplitudes).

Actually, for the example given, the stability region vanishes for  $\alpha_m \geq 1.57 \alpha_l$ .

In the presence of delay, the equations of the System (3) become

$$D^2x = -\rho\delta, \quad D\delta = e^{-D\tau} f_1(kD + 1)(a_1Dx + a_2x - a\delta).$$

The equations of the periodic modes of this linearized system will be

$$\frac{a_2}{a} p\tau^2 = \frac{\Omega^2 \cos \Omega + \Omega^3 \frac{k}{\tau} \sin \Omega}{\Omega \left( \frac{k}{\tau} + \frac{a_1}{a_2\tau} \right) \sin \Omega + \left( 1 - \frac{k}{\tau} \frac{a_1}{a_2\tau} \Omega^2 \right) \cos \Omega},$$

$$\eta a \frac{b^*}{a} \tau = \frac{\left( \frac{k}{\tau} + \frac{a_1}{a_2\tau} \right) \Omega \sin \Omega + \left( 1 - \frac{k}{\tau} \frac{a_1}{a_2\tau} \Omega^2 \right) \cos \Omega}{\frac{a_1}{a_2\tau} \left[ 1 + \left( \frac{k}{\tau} \right)^2 \Omega^2 \right]}.$$

The calculated curves corresponding to the periodic modes for  $k/\tau = 1.75$  and for  $a_1/a_2\tau = 4$  and  $a_1/a_2\tau = 8$  are shown dotted in Figure 15.

Increasing the signal amplitude above the linear range decreases the quantity  $\eta a \tau$  in proportion to the value of  $(b^*/\alpha)^{-1}$  (Figure 3). The stability region for the amplitude range from  $\alpha \leq \alpha_l$  to  $\alpha = 3\alpha_l$  at  $a_1/a_2\tau = 4$

is limited to a region marked by the small circles, while the stable region for the same range of amplitudes at  $a_1/a_2\tau = 8$  is marked by the crosses.

To estimate the effect of the derivative of the control signal let us compare the stability boundaries shown in Figures 14 and 15.

In the linear speed range,  $0 < \alpha < \alpha_1$ , adding a signal proportional to the derivative of the control signal decreases the permissible value of  $\eta a\tau$ , but makes it possible to increase the gain  $a_2 p\tau^2/a$ .

The decrease in  $\eta a\tau$  signifies a reduction in the gain of the servo system of the regulator, meaning also a reduction in its accuracy.

An analogous result is obtained also for large amplitudes.

The fundamental adverse property of the ASR, namely the loss of stability by increase of the amplitude of the control signal, owing to the limited speed of the drive, is not eliminated by introducing the derivative of the signal.

The equations of the System (4) with a "memory" and switching network in the presence of a time delay will be

$$D^2x = -p\delta, \quad D\delta = e^{-D\tau}/2 (a_1 Dx + a_2 x - a\delta).$$

The equations of the periodic modes of this linearized system will be

$$\begin{aligned} \frac{a_2}{a} p\tau^2 &= \frac{\Omega^2 \cos \Omega + \Omega^2 \frac{a^*}{b^*} \sin \Omega}{\left(\frac{a^*}{b^*} + \frac{a_1}{a_2\tau} \Omega\right) \sin \Omega + \left(1 - \frac{a^*}{b^*} \frac{a_1}{a_2\tau} \Omega\right) \cos \Omega}, \\ \gamma_1 a\tau \frac{b^*}{a} &= \frac{\left(\frac{a^*}{b^*} + \frac{a_1}{a_2\tau} \Omega\right) \sin \Omega + \left(1 - \frac{a^*}{b^*} \frac{a_1}{a_2\tau} \Omega\right) \cos \Omega}{\frac{a_1}{a_2} \tau \left[1 + \left(\frac{a^*}{b^*}\right)^2\right]}. \end{aligned}$$

The calculated periodic modes are represented by solid lines in Figures 14 and 15. Figure 15 shows the periodic modes for the amplitude  $\alpha = \alpha_1$ .

At large amplitudes, the region bounded by the curves of the periodic modes increases rapidly. The periodic modes shift to the right and upwards with increasing frequency  $\Omega \geq \pi/2$ , and shift to the left with decreasing frequency.

An analysis of the calculation results shows that when  $a_1/a_2\tau = 1$  the stability region of Figure 14 vanishes only at an amplitude  $\alpha \approx 34\alpha_1$ , and if  $a_1/a_2\tau = 4$  and  $a_1/a_2\tau = 8$ , the stability region expands with increasing amplitude (Figure 15). In addition, the use of the developed apparatus makes it possible to assign larger values of  $\eta a\tau$  for all values of  $a_1/a_2\tau$  and makes it possible to increase the permissible value of  $a_2 p\tau^2/a$  for  $\alpha \leq \alpha_1$  at  $a_1/a_2\tau = 1$  (Figure 14).

The use of a memory device makes it possible to increase the permissible disturbance, even in the presence of a time delay, leading to deviations exceeding by many times the linear range of the drive speed.

The conclusions arrived at on the basis of an analysis of the stability boundaries remain valid also in the presence of a "vanishing memory."

Actually, the vanishing of the memory does not affect the change in the stability boundaries at high frequencies and high regulator effectiveness, since the process will terminate earlier than the required to produce a considerable change in voltage across the memory capacitors (see oscillograms of Figures 11 and 12). If the regulator has low effectiveness, when the period of the system is large and its speed is low, the time delay  $\tau$  can be neglected and the stability region is determined with sufficient accuracy by the equations that disregard the delay.

## SUMMARY

As a result of the use of a memory device, the phase of the coordinate of the drive mechanism of the regulator, having a limited speed, coincides with the phase of the control signal. The phase lead reached even in the presence of time delay in the regulator makes it possible to: 1) increase the gain of the system by a factor of three and 2) increase practically without limit the amplitude of the control signal without disturbing the stability of the ASR.

This latter property makes it possible to choose a maximum speed for the drive mechanism, without regard to stability requirements. This permits in many cases to reduce the maximum speed of the drive mechanism, and consequently, to decrease the power and weight of the drive mechanism or to increase its permissible load.

## LITERATURE CITED

- [1] G. Korn and T. Korn, *Electronic Analog Computers* (Russian translation) (Foreign Lit. Press, Moscow, 1955).
- [2] V.A. Maslennikov, "High Quality Regulation of a Neutral Object by Means of an Astatic Regulator," *Avtomatika i Telemekhanika* 17, No. 2 (1956).\*
- [3] A.Ia. Lerner, "Improving the Dynamic Properties of Automatic Compensators with the Aid of Nonlinear Links. I," *Avtomatika i Telemekhanika* 13, No. 2 (1952).
- [4] A.Ia. Lerner, "Improving the Dynamic Properties of Automatic Compensators with the Aid of Nonlinear Links. II," *Avtomatika i Telemekhanika* 13, No. 4 (1952).
- [5] A.Ia. Lerner, "On the Limiting Speed of Automatic Control Systems," *Avtomatika i Telemekhanika* 15, No. 6 (1954).
- [6] A.A. Fel'dbaum, "Optimum Processes in Automatic Regulation Systems," *Avtomatika i Telemekhanika* 15, No. 6 (1954).
- [7] A.A. Fel'dbaum, "On the Synthesis of Optimum Systems with the Aid of Phase Space," *Avtomatika i Telemekhanika* 16, No. 2 (1955).

Received June 20, 1956

\*[See C.B. translation, *Automation and Remote Control*.]

# ANALYSIS OF ERRORS IN THE DETERMINATION OF THE AVERAGE VALUE OF A RANDOM QUANTITY AND OF ITS SQUARE, DUE TO FINITE TIME OF OBSERVATION

A. E. Kharybin

(Moscow)

The errors in the determination of the average value of a random quantity and of its dispersion, due to the finite time of observation, are analyzed.

The formulas obtained are used to calculate nomograms, which show whether the interval used to observe the random quantity chosen for the static reduction is long enough. The nomograms also give the assumed mean-squared errors in the determination of the average value of the random quantity and of its dispersion for a chosen observation interval for the most typical case, when the correlation function of the random process can be represented in the form

$$R(\tau) = Ce^{-\alpha|\tau|} \cos \beta\tau.$$

## 1. Statement of Problem

In accordance with the ergodic theorem, in the calculation of the basic statistical characteristic of stationary random processes, namely the mathematical expectation (mean value)  $\underline{m}$  and the correlation function  $R(\tau)$ , it becomes necessary to determine the time-averaged values of the random functions  $z(t)$  and  $z(t)z(t+\tau)$ . By definition we have

$$\lim_{T \rightarrow \infty} M \left\{ \frac{1}{T} \int_0^T z(t) dt - \underline{m} \right\} = 0, \quad (1)$$

$$\lim_{T \rightarrow \infty} M \left\{ \frac{1}{T} \int_0^T z(t) z(t+\tau) dt - R(\tau) \right\} = 0, \quad (2)$$

where the symbol  $M$  denotes the mathematical expectation of the random quantity, indicated in the braces. It follows from (1) and (2) that the time of observation  $T$  should be infinitely large for accurate determination of  $\underline{m}$  and  $R(\tau)$ .

Under real conditions the time of observation  $T$  is always finite. Moreover, it is always desired to restrict oneself to a minimum possible observation time, since the error in integration increases with time, owing to the imperfections in the integrator.

It is evident that the average value  $m(T)$  of the random function  $z(t)$  ( $0 \leq t \leq T$ ), determined for finite  $T$ , will differ from the mathematical expectation  $\underline{m}$ , while the deviation  $[m(T) - \underline{m}]$  will increase with diminishing  $T$ .



Actually, as  $T$  approaches infinity, the deviation  $[m(T) - m]$  approaches zero, and when  $T$  approaches zero we have  $[m(T) - m] \rightarrow z(t) - m$ , i.e., at a very small observation time  $T$ , the absolute error in the determination of  $m$  will equal the pulsation of the random process  $z(t)$ .

In connection with the above, the problem becomes that of finding such a value of the observation time  $T$ , at which the relative mean-squared error  $\sigma$ , defined as

$$\sigma = \left[ \frac{M[m(t)]^2 - m^2}{m^2} \right]^{1/2} = \left\{ \frac{M[m(T)]^2 - [Mz(t)]^2}{[Mz(t)]^2} \right\}^{1/2}, \quad (3)$$

does not exceed a certain value  $\sigma_{\max}$ .

## 2. Assumed Mean-Squared Error and its Connection with the Correlation Function

To determine the assumed mean-squared error in accordance with (3) it is necessary to find the mathematical expectation of the square of the random quantity

$$m(T) = \frac{1}{T} \int_0^T z(t) dt. \quad (4)$$

The mathematical expectation of the square of  $m(T)$ , as is known,\* equals

$$\begin{aligned} M[m(T)]^2 &= \frac{1}{T^2} \int_0^T \int_0^T M[m(T_1)m(T_2)] dT_1 dT_2 = \\ &= \frac{1}{T^2} \int_0^T \int_0^T R(T_2 - T_1) dT_1 dT_2 = \frac{2}{T^2} \int_0^T (T - \tau) R(\tau) d\tau. \end{aligned} \quad (5)$$

Equation (5) can be represented as

$$M[m(T)]^2 = \frac{2}{T} \int_0^T \left(1 - \frac{\tau}{T}\right) R(\tau) d\tau. \quad (6)$$

For sufficiently large  $T$ , when  $\tau/T \ll 1$ , we have

$$M[m(T)]^2 \approx \frac{2}{T} \int_0^T R(\tau) d\tau. \quad (7)$$

The mathematical expectation of the square of a random quantity, and consequently also the assumed relative mean-squared error incurred in the determination of the mean value, will thus diminish linearly with increasing observation interval  $T$ .

It is evident from (6) and (7) that the error in the determination of the mean value of the random quantity  $z(t)$ , caused by the finite observation time, depends only on the duration of the observation interval  $T$  and on the form of the correlation function  $R(\tau)$ . To determine the assumed relative mean-squared error while determining the ordinates of the correlation function  $R(\tau)$  it is possible to employ the formulas given above, putting  $z(t) = z_1(t)z_1(t + \tau)$ , where  $z_1(t)$  is the initial stationary random process that is to be investigated.

Thus, to determine the assumed error it is necessary to know not only the form of the correlation function of the investigated process  $z_1(t)$ , but also the correlation function of the more complicated random process:

\*See, for example, the work by W.B. Davenport, R.A. Johnson and D. Middleton, J. Appl. Phys. 23, No. 4 (1952).



$$z(t) \equiv z_1(t) z_1(t + \tau). \quad (8)$$

In the particular case when  $\tau = 0$ ,  $z(t) \equiv z_1^2(t)$ , the correlation function  $R(\tau)$  of a random process  $z(t)$  can be expressed in terms of the correlation function  $R_1(\tau)$  of the primary random process  $z_1(t)$ .

It can be shown that if

$$R_1(\tau) = ce^{-\alpha|\tau|},$$

then

$$R(\tau) = c^2(1 + 2e^{-2\alpha|\tau|}). \quad (9)$$

If

$$R_1(\tau) = ce^{-\alpha|\tau|} \cos \beta\tau,$$

then

$$R_1(\tau) = c^2(1 + e^{-2\alpha|\tau|} + e^{-2\alpha|\tau|} \cos 2\beta\tau). \quad (10)$$

### 3. Determination of the Observation Interval from a Specified Error $\sigma_{\max}$ and the Assumed Correlation Functions

In practice, the experimentally-obtained correlation functions  $R(\tau)$  are approximated more frequently in the form of a polynomial:

$$R(\tau) = a_0^2 + \sum_{v=1}^n \frac{a_v^2}{2} \cos \omega_v \tau + ce^{-\alpha|\tau|} \cos \beta\tau. \quad (11)$$

In the particular case when  $a_0 = 0$ ;  $a_v = 0$  ( $v = 1, 2, \dots, n$ ),  $\beta = 0$ , we have

$$R(\tau) = ce^{-\alpha|\tau|} \quad (12)$$

and if  $\beta \neq 0$

$$R(\tau) = ce^{-\alpha|\tau|} \cos \beta\tau. \quad (13)$$

$R(\tau)$  is represented very frequently in form (12) or (13) particularly in the investigation of automatic control systems operating in the presence of noise.

If (11) is inserted in (5) we get

$$M[m(T)]^2 = \frac{2}{T^2} \int_0^T \left\{ (T - \tau) \left[ a_0^2 + \sum_{v=1}^n \frac{a_v^2}{2} \cos \omega_v \tau + ce^{-\alpha|\tau|} \cos \beta\tau \right] \right\} d\tau. \quad (14)$$

Carrying the multiplication under the integral sign in (14), we arrive at

$$\begin{aligned} M[m(T)]^2 &= \frac{2}{T} \int_0^T \left[ a_0^2 + \sum_{v=1}^n \frac{a_v^2}{2} \cos \omega_v \tau + ce^{-\alpha|\tau|} \cos \beta\tau \right] d\tau - \\ &- \frac{2}{T^2} \int_0^T \tau \left[ a_0^2 + \sum_{v=1}^n \frac{a_v^2}{2} \cos \omega_v \tau + ce^{-\alpha|\tau|} \cos \beta\tau \right] d\tau. \end{aligned} \quad (15)$$

The first integral  $I_1$  in the right half of (15) is broken up into three integrals

$$\begin{aligned}
I_1 &= \frac{2}{T} \int_0^T a_0^2 d\tau = 2a_0^2, \\
I_2 &= \frac{2}{T} \int_0^T \sum_{v=1}^n \frac{a_v^2}{2} \cos \omega_v \tau d\tau = \frac{1}{T} \sum_{v=1}^n \frac{a_v^2}{\omega_v} \sin \omega_v T, \\
I_3 &= \frac{2}{T} \int_0^T c e^{-\alpha |\tau|} \cos \beta \tau = \frac{2c}{T(\alpha^2 + \beta^2)} [e^{-\alpha T} (\beta \sin \beta T - \alpha \cos \beta T) + \alpha].
\end{aligned} \quad (16)$$

The second integral  $I_2$  in the right half of (15) breaks up into three integrals

$$\begin{aligned}
I'_1 &= \frac{2}{T^2} \int_0^T \tau a_0^2 d\tau = a_0^2, \\
I'_2 &= \frac{2}{T^2} \int_0^T \tau \left[ \sum_{v=1}^n \frac{a_v^2}{2} \cos \omega_v \tau \right] d\tau = \frac{1}{T^2} \sum_{v=1}^n \frac{a_v^2}{\omega_v^2} (\cos \omega_v T + T \omega_v \sin \omega_v T - 1), \\
I'_3 &= \frac{1}{T^2} \int_0^T \tau c e^{-\alpha |\tau|} \cos \beta \tau = \\
&= \frac{2c}{T^2 \alpha^3 \left(1 + \frac{\beta^2}{\alpha^2}\right)} \left[ e^{-\alpha T} \left\{ \frac{\beta}{\alpha} \left[ 2 + \alpha T \left(1 + \frac{\beta^2}{\alpha^2}\right) \right] \sin \beta T + \left(1 - \frac{\beta^2}{\alpha^2}\right) - \right. \right. \\
&\quad \left. \left. - \left[ (1 + \alpha T) - \frac{\beta^2}{\alpha^2} (1 - \alpha T) \right] \cos \beta T \right\} \right].
\end{aligned} \quad (17)$$

The right half of (15) will be  $I_1 - I_2$ . Calculating term by term, we get

$$\begin{aligned}
I_1 - I'_1 &= a_0^2, \quad I_2 - I'_2 = \frac{2}{T^2} \sum_{v=1}^n \frac{a_v^2}{\omega_v^2} \sin^2 \frac{\omega_v}{2} T, \\
I_3 - I'_3 &= \frac{2c}{T^2 \alpha^3 \left(1 + \frac{\beta^2}{\alpha^2}\right)^2} \left\{ e^{-\alpha T} \left[ \left(1 - \frac{\beta^2}{\alpha^2}\right) \cos \beta T - 2 \frac{\beta}{\alpha} \sin \beta T \right] + \right. \\
&\quad \left. + \alpha T \left(1 + \frac{\beta^2}{\alpha^2}\right) - \left(1 - \frac{\beta^2}{\alpha^2}\right) \right\}.
\end{aligned} \quad (18)$$

Finally

$$\begin{aligned}
M[m(T)]^2 &= a_0^2 + \frac{2}{T} \sum_{v=1}^n \frac{a_v^2}{2} \sin^2 \frac{\omega_v}{2} T + \frac{2c}{\alpha^2 T^2 \left(1 + \frac{\beta^2}{\alpha^2}\right)^2} \times \\
&\times \left\{ e^{-\alpha T} \left[ \left(1 - \frac{\beta^2}{\alpha^2}\right) \cos \beta T - 2 \frac{\beta}{\alpha} \sin \beta T \right] + \alpha T \left(1 + \frac{\beta^2}{\alpha^2}\right) - \left(1 - \frac{\beta^2}{\alpha^2}\right) \right\}.
\end{aligned} \quad (19)$$

The maximum value of the mathematical expectation of the square of the random quantity  $m(T)$  will be

$$M[m(T)]^2_{\max} = a_0^2 + \frac{2}{T} \sum_{v=1}^n \frac{a_v^2}{\omega_v^2} \frac{2c}{\alpha^2 T^2 \left(1 + \frac{\beta^2}{\alpha^2}\right)} \left\{ e^{-\alpha T} + \alpha T - \frac{1 - \frac{\beta^2}{\alpha^2}}{1 + \frac{\beta^2}{\alpha^2}} \right\}. \quad (20)$$

If we substitute (20) in (3) and consider that

$$[M\{z(t)\}]^2 = m^2 = a_0^2,$$

we get

$$\sigma_{\max} = \left[ \frac{2}{a_0^2 T} \sum_{v=1}^n \frac{a_v^2}{\omega_v^2} + \frac{2c}{a_0^2 \alpha^2 T^2 \left(1 + \frac{\beta^2}{\alpha^2}\right)} \left\{ e^{-\alpha T} + \alpha T - \frac{1 - \frac{\beta^2}{\alpha^2}}{1 + \frac{\beta^2}{\alpha^2}} \right\} \right]^{1/2}. \quad (21)$$

The proposed maximum relative mean-squared error  $\sigma_{\max}$  can be represented, according to (21), in the form of a sum

$$\sigma_{\max}^2 = \sigma_{I \max}^2 + \sigma_{II \max}^2, \quad (22)$$

where  $\sigma_I$  is the error in the determination of the mean value due to the presence of hidden periodicities in the investigated random process  $z(t)$ , and  $\sigma_{II}$  represents the error due to the properties of the random process itself.

In the case when the process  $z(t)$  has a constant component  $m = 0$  ( $a_0 = 0$ ), it is necessary to consider instead of the maximum relative mean square error  $\sigma_{\max}$  the assumed maximum mean squared deviation  $\sigma_{\max}^0$ , which will be

$$\sigma_{\max}^0 = \{M[m(T)]^2\}^{1/2}.$$

Taking (20) into account, we obtain for  $\sigma_{\max}^0$

$$\sigma_{\max}^0 = \left[ \frac{2}{T} \sum_{v=1}^n \frac{a_v^2}{\omega_v^2} + \frac{2c}{\alpha^2 T^2 \left(1 + \frac{\beta^2}{\alpha^2}\right)} \left\{ e^{-\alpha T} + \alpha T - \frac{1 - \frac{\beta^2}{\alpha^2}}{1 + \frac{\beta^2}{\alpha^2}} \right\} \right]^{1/2}. \quad (23)$$

The assumed maximum mean squared deviation  $\sigma_{\max}^0$  can also be represented in the form of a sum

$$\sigma_{\max}^{02} = \sigma_{I \max}^{02} + \sigma_{II \max}^{02}. \quad (24)$$

It is seen from (21-24) that if  $m \neq 0$

$$\sigma_{\max}^{02} = a_0^2 \sigma_{\max}^2 = a_0^2 (\sigma_{I \max}^2 + \sigma_{II \max}^2), \quad (25)$$

where

$$\begin{aligned} \sigma_{I \max}^2 &= \frac{2}{a_0^2 T} \sum_{v=1}^n \frac{a_v^2}{\omega_v^2}, \\ \sigma_{II \max}^2 &= \frac{2c}{a_0^2 \alpha^2 T^2 \left(1 + \frac{\beta^2}{\alpha^2}\right)} \left\{ e^{-\alpha T} + \alpha T - \frac{1 - \frac{\beta^2}{\alpha^2}}{1 + \frac{\beta^2}{\alpha^2}} \right\}. \end{aligned} \quad (26)$$

Taking (24) and (25) into account, we get

$$\begin{aligned} \sigma_{I \max}^{02} &= \frac{2}{T} \sum_{v=1}^n \frac{a_v^2}{\omega_v^2}, \\ \sigma_{II \max}^{02} &= \frac{2c}{\alpha^2 T^2 \left(1 + \frac{\beta^2}{\alpha^2}\right)} \left\{ e^{-\alpha T} + \alpha T - \frac{1 - \frac{\beta^2}{\alpha^2}}{1 + \frac{\beta^2}{\alpha^2}} \right\}. \end{aligned} \quad (27)$$

Formulas (26) and (27) can be used for the calculations.

From the analysis of these formulas it follows that:

1) the error and the determination of the mean value of the random quantities  $z(t)$  for a fixed observation time  $T$  will increase: a) with diminishing frequency  $\omega_\nu$  and increasing amplitude  $a_\nu$  of the hidden periodicities, b) with diminishing attenuation of the correlation function, as characterized by the quantity  $\alpha$ , and with diminishing frequency of this function  $\beta$ ;

2) the error diminishes with increasing time of observation  $T$ .

#### 4. Nomograms for Determining the Observation Interval

The derived Formulas (26) and (27) make it possible to find the assumed maximum mean squared error in the determination of the mean value of the random process  $z(t)$  or the error in the determination of the initial ordinate of the correlation function  $R(\tau)$ , provided the correlation function itself  $R(\tau)$ , the mean value of the random variable  $z(t)$ , and the amplitude and frequency of the hidden periodicities  $a_\nu$  and  $\omega_\nu$  are all known.

Naturally, we do not have these data when determining the mean value  $m$  or the initial ordinate of the correlation function  $R(\tau)$ , but certain assumptions concerning the quantities of interest to us can always be made either on the basis of statistical processing of analogous random processes, or else from the character of the record obtained for the random process  $z(t)$ .

Under these conditions, it is desirable to have nomograms for rapid determination of the assumed error.

It was indicated above that the error in the determination of the mean value, due to the finite observation time, occurs as a result of the presence of hidden periodicities in the investigated process and depends on the character of the process.

The error due to the presence of hidden periodicities can be determined from the expression

$$\sigma_{I \max}^2 = \frac{2}{T} \sum_{\nu=1}^n \frac{a_\nu^2}{\omega_\nu^2} = \frac{2a_1^2}{T\omega_1^2} + \frac{2a_2^2}{T\omega_2^2} + \dots + \frac{2a_n^2}{T\omega_n^2} = \sigma_{1 \max}^2 + \sigma_{2 \max}^2 + \dots + \sigma_{n \max}^2 \quad (28)$$

and

$$\sigma_{I \max}^0 = [\sigma_{1 \max}^2 + \sigma_{2 \max}^2 + \dots + \sigma_{n \max}^2]^{1/2}.$$

Thus, the determination of  $\sigma_{I \max}^0$  reduces to the determination of

$$\sigma_{\nu \max}^2 = \frac{2a_\nu^2}{T\omega_\nu^2} \quad (\nu = 1, 2, \dots, n). \quad (29)$$

Introducing a new variable

$$n_\nu^2 = \omega_\nu^2 T, \quad (30)$$

we can rewrite (29) as

$$\sigma_{\nu \max}^2 = \frac{2a_\nu^2}{n_\nu^2}. \quad (31)$$

Taking the logarithm of (31) and multiplying both sides by 20, we get

$$20 \lg \sigma_{\nu \max}^2 = 20 \lg 2 + 20 \lg a_\nu^2 - 20 \lg n_\nu^2 \quad (32)$$

or, in decibels:

$$\sigma_{\nu \max}^2 \text{ db} - a_\nu^2 \text{ db} = 6 \text{ db} - 20 \lg n_\nu^2. \quad (33)$$

If we plot on semilogarithmic paper the values of the variable  $n$  along the logarithmic axis, and the dependence of  $\sigma_{\nu \max}^2 - a_{\nu}^2$  on  $n$  in decibels, this dependence will be a straight line passing through the point (+ 6 db,  $n = 1$ ) and having a slope of -40 db per decade.

An analogous procedure is used to change from the variable  $n$  to  $\omega$ .

In fact,  $T = n^2/\omega^2$  and  $20 \log T = 20 \log n^2 - 20 \log \omega^2$

$$T \text{ db} = 20 \lg n^2 - 20 \lg \omega^2. \quad (34)$$

If we choose a certain value of  $\omega$ , for example  $\omega = 1$ , the dependence of the time of observation  $T$  in decibels on  $n$  will be represented by a straight line passing through the point ( $n = 1$ ,  $T = 0$ ) and having a slope + 40 db/decade.

For other values of  $\omega$ , this dependence will be represented by straight lines, having a slope + 40 db/decade and intercepting the ordinate axis at a distance  $-20 \log \omega$  from the line representing  $\omega = 1$ .

The nomogram for determination of the observation time  $T$  in the averaging of stationary random signals from known values of the amplitude and frequency of the hidden periodic components is shown in Figure 1.

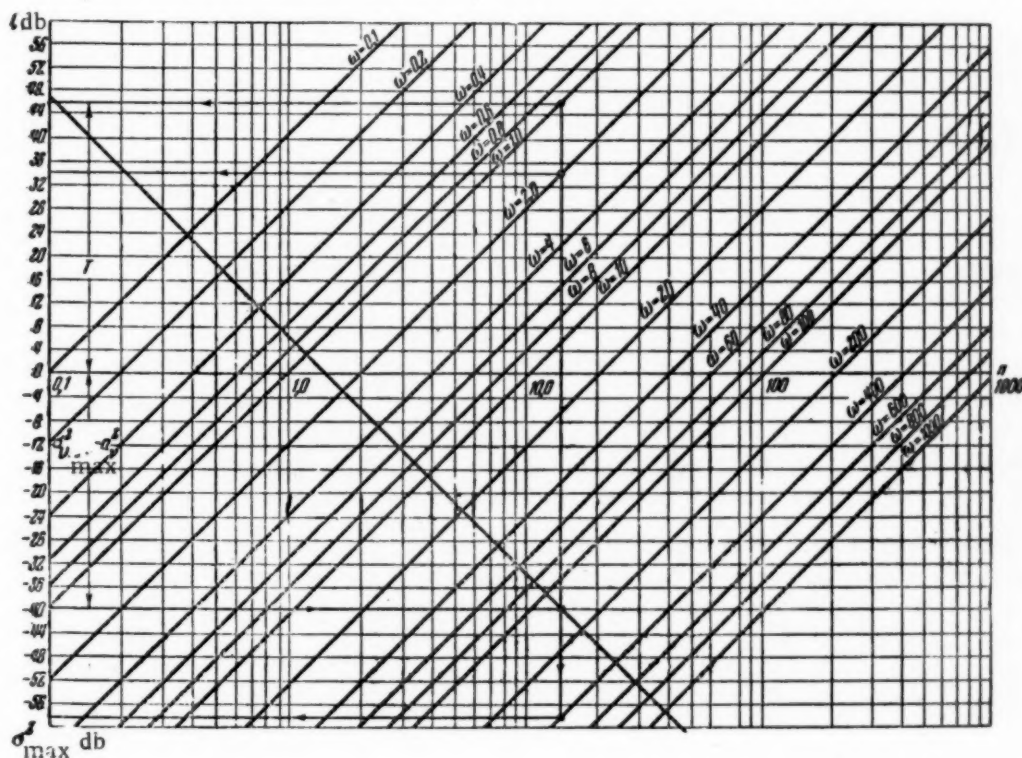


Fig. 1. Nomogram for determining the time of observation when averaging stationary random signals from known values of the amplitude and frequency of the hidden periodic components.

Let us indicate a method for using this nomogram. The point corresponding to  $\sigma_{\nu \max}^2 - a_{\nu}^2$  in decibels is marked on the ordinate axis, and a line parallel to the abscissa axis is drawn through this point. This line intersects the auxiliary line, which has a slope -40 db/decade. From the point of intersection we draw an auxiliary line parallel to the ordinate axis until it intersects the line marked  $\omega_{\nu}$ . The projection of the latter intersection on the ordinate axis determines the necessary observation time  $T$  in decibels, at which the error and the determination of the mean value does not exceed  $\sigma_{\nu \max}^2$ . The change from the values of  $\sigma_{\nu}$  or  $T$  in decibels to the ordinary numbers and vice versa is carried out with the aid of a logarithmic slide rule.

The figure shows the auxiliary lines necessary to determine the observation time  $T$  for three values of the

frequency of the hidden periodic components ( $\omega_1 = 1 \text{ sec}^{-1}$ ,  $\omega_2 = 2 \text{ sec}^{-1}$ , and  $\omega_3 = 400 \text{ sec}^{-1}$ ) and for a relative mean square error  $\sigma_{\text{II max}}^2 = 0.01$ . The necessary time of observation is 200, 50 and 1.26 seconds respectively.

The nomogram for determining the error as a function of the type of the correlation function is plotted in an analogous manner.

Introducing new variables

$$x = \alpha T \quad (35)$$

and

$$y = \frac{\beta}{\alpha}, \quad (36)$$

then

$$\sigma_{\text{II max}}^2 = \frac{2c}{x^2(1+y^2)} \left\{ e^{-x} + x - \frac{1-y^2}{1+y^2} \right\}. \quad (37)$$

If  $x \gg 1$ , and considering that  $\left| \frac{1-y^2}{1+y^2} \right| \leq 1$  for  $0 \leq |y| \leq \infty$ , one can write

$$\sigma_{\text{II max}}^2 \approx \frac{2c}{x(1+y^2)}. \quad (38)$$

The latter yields

$$20 \lg \sigma_{\text{II max}}^2 - 20 \lg c = 20 \lg 2 - 20 \lg x - 20 \lg (1+y^2) \quad (39)$$

or, in decibels

$$(\sigma_{\text{II max}}^2 - c) \text{ db} = 6 \text{ db} - 20 \lg x - 20 \lg (1+y^2). \quad (40)$$

If a certain value of  $y$  is chosen, say  $y = 0$ , then  $\sigma_{\text{II max}}^2 - c$  will be represented by a straight line having a slope  $-20 \text{ db/decade}$ . To plot the straight line it is enough to put  $x = 10^3$ ; then  $\sigma_{\text{II max}}^2 - c = 6 \text{ db} - 20 \lg 10^3 = -54 \text{ db}$ , and a line is drawn through the point ( $x = 10^3$ ,  $y = -54 \text{ db}$ ) at a slope of  $-20 \text{ db/decade}$ . For all other values of  $y$ , this straight line will be positioned lower at a distance  $20 \lg (1+y^2) \text{ db}$ .

At small values of  $x$  it is necessary to take into account the expression contained in the braces in Equation (37). The values of the polynomial in the braces were calculated for two decades of  $x$  from 0.1 to 10 and for  $y = n$  ( $n = 0, 1, 2, \dots, 5$ ). The exact values of the polynomial in numbers and in decibels are given in Tables 1 and 2.

TABLE 1

Values of  $e^{-x} + x - \frac{1-y^2}{1+y^2}$  for  $y = n$  ( $n = 0, 1, \dots, 5$ )

y	x										
	0.1	0.2	0.4	0.6	0.8	1.0	2.0	4.0	6.0	8.0	10.0
0	0.005	0.019	0.070	0.149	0.249	0.368	1.135	3.018	5.002	7.000	9.000
1	1.005	1.019	1.070	1.149	1.249	1.368	2.135	4.018	6.002	8.000	10.000
2	1.605	1.619	1.670	1.749	1.849	1.968	2.735	4.618	6.602	8.600	10.000
3	1.805	1.819	1.870	1.949	2.049	2.168	2.935	4.818	6.802	8.800	10.800
4	1.888	1.902	1.953	2.032	2.132	2.251	3.018	4.901	6.885	8.883	10.883
5	1.928	1.942	1.993	2.072	2.172	2.291	3.058	4.941	6.925	8.923	10.923



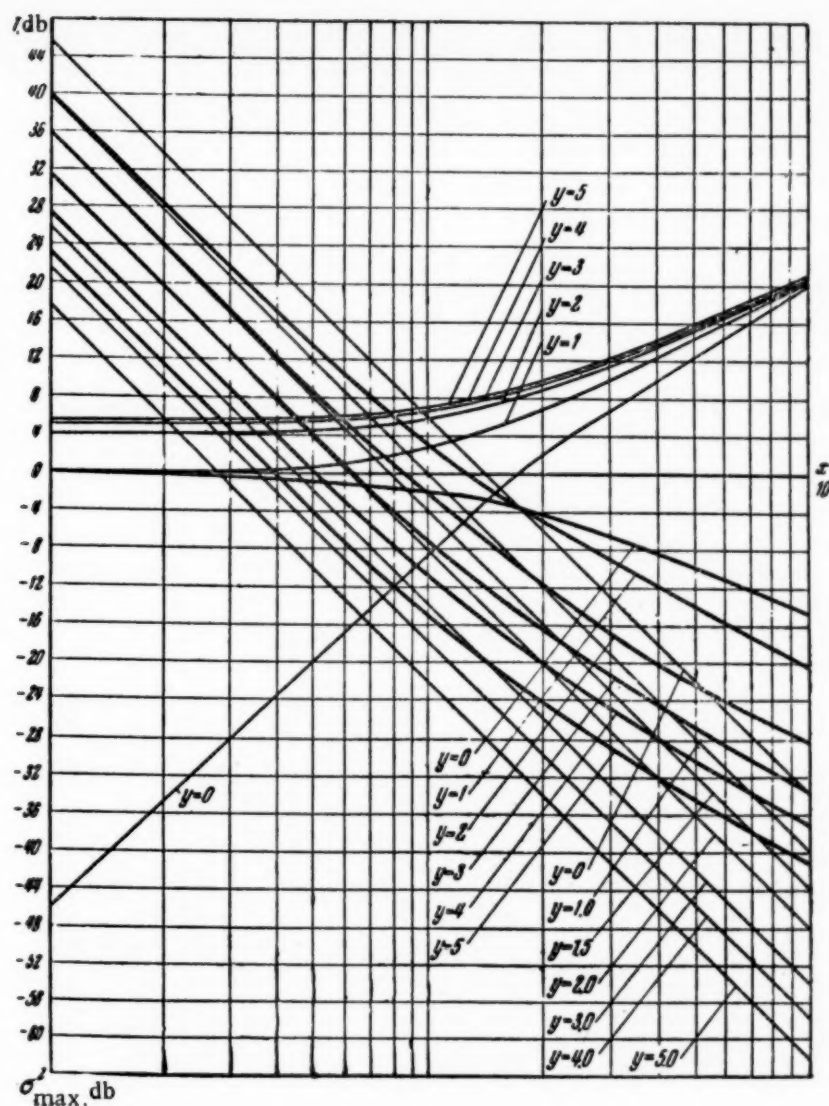


Fig. 2. Auxiliary curves.

TABLE 2

Values of  $e^{-x} + x - \frac{1-y^2}{1+y^2}$  in decibels for  $y = n$  ( $n = 0, 1, \dots, 5$ ).

y	x										
	0.1	0.2	0.4	0.6	0.8	1.0	2.0	4.0	6.0	8.0	10.0
0	-46	-34.4	-23.1	-16.54	-12.08	-8.68	2.6	9.6	14.0	16.9	19.08
1	0.00	0.08	0.6	1.2	1.94	2.71	6.58	12.2	15.54	18.06	20.0
2	4.1	4.16	4.46	4.86	5.34	5.88	8.74	13.28	16.4	18.7	20.5
3	5.14	5.20	5.44	5.80	6.24	6.74	9.34	13.66	16.66	18.88	20.68
4	6.5	5.58	5.82	6.16	6.58	7.06	9.60	13.80	16.74	18.92	20.74
5	5.7	5.76	6.0	6.3	6.72	7.20	9.72	13.86	16.80	19.00	20.76

It follows from (37) that for small values of  $x$

$$20 \lg \sigma_{II \max}^{02} - 20 \lg c = 20 \lg 2 + 20 \lg \{ \quad \} - 20 \lg x^2 - 20 \lg (1 + y^2)$$

or

$$\sigma_{II \max}^2 \text{ db} - c \text{ db} = 6 \text{ db} + 20 \lg \{ \} - 20 \lg x^2 - 20 \lg(1 + y^2). \quad (41)$$

The sum  $[6 \text{ db} - 20 \lg x^2 - 20 \lg(1 + y^2)]$  will be represented on the logarithmic characteristics by a family of straight lines having a slope  $-40 \text{ db/decade}$ . If  $x = 1$  and  $y = 0$ , the line will pass through the point  $(x = 1, y = 6 \text{ db})$ . If  $y = 0$ , the line will pass lower at a distance  $-20 \lg \{ \} \text{ db}$ . The curves corresponding to  $20 \lg \{ \}$  can be plotted from the data of Table 2.

Thus, to calculate  $\sigma_{II \max}^2 - c$  it is necessary to add the ordinates of the straight line with a slope  $-40 \text{ db/decade}$  and the curve for  $-20 \lg \{ \}$  for equal values of  $y$ . The curves corresponding to  $-20 \lg \{ \}$  and the lines corresponding to the sum  $[6 - 20 \lg x^2 - 20 \lg(1 + y^2)]$  for  $y = 0, 1, 2, \dots, 5$  are shown in Figure 2. The heavy lines represent their sum.

To change from the variable  $x$  to  $T$  it is necessary to use the Relationship (35), from which it follows that  $T = x/\alpha$  and  $20 \lg T = 20 \lg x - 20 \lg \alpha$ , or

$$T \text{ db} = 20 \lg x - 20 \lg \alpha. \quad (42)$$

If we choose  $\alpha$ , for example  $\alpha = 1$ , then the dependence of  $T$  on  $x$  will be represented by straight lines having a slope  $20 \text{ db/decade}$  and passing through the point  $(T = 0, x = 1)$ . If  $\alpha \neq 1$ , the straight line will pass parallel to the line for  $\alpha = 0$  at a vertical distance of  $20 \lg \alpha \text{ db}$ .

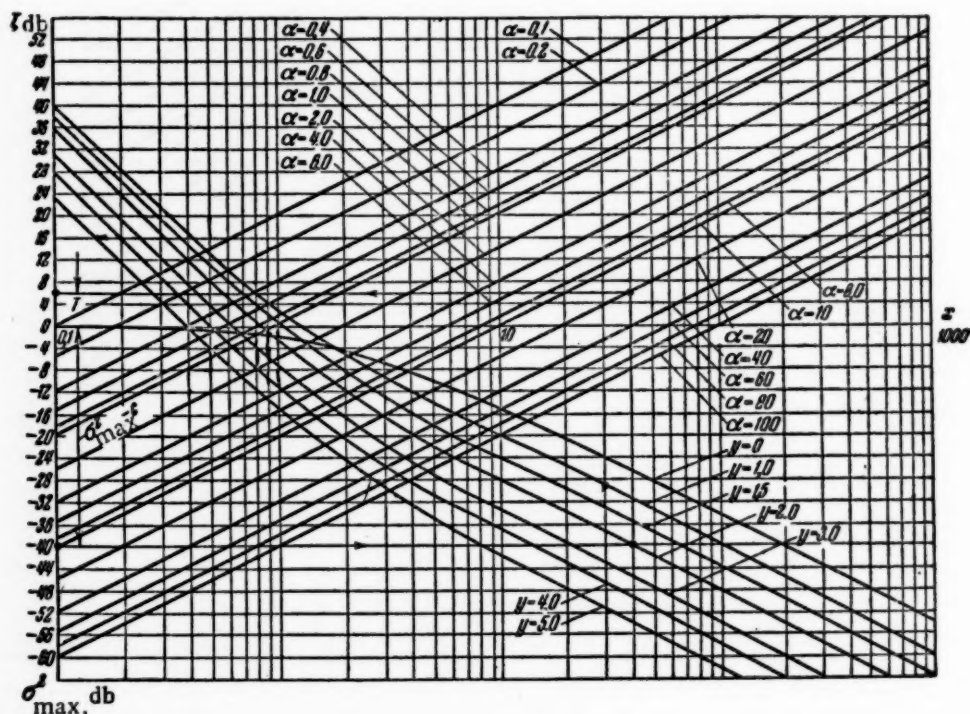


Fig. 3. Nomogram for determining the time of observation in the averaging of stationary random signals from the assumed correlation function.

The nomogram for determining the observation time  $T$  in the averaging of stationary random signals from the assumed correlation function is shown in Figure 3.

By way of an example, the nomogram shows the auxiliary lines for the determination of the necessary observation time  $T$  for the case of a process  $z(t)$ , having the following assumed correlation functions

$$R(\tau) = ce^{-\alpha|\tau|} \cos \beta\tau,$$

where

$$c = 10^{-2} \text{ or } -40 \text{ db, } \alpha = 20, \beta = 40, y = \frac{\beta}{\alpha} = 2.$$

Let the assumed mean-squared error be limited to 1%, then  $\sigma_{II \max}^2 = 10^{-4}$  or -80 db and  $\sigma_{II \max}^2 - c = -80 + 40 = -40$  db.

The point corresponding to -40 db is marked on the ordinate axis and a straight line parallel to the abscissa is drawn until it intersects the curve  $y = 2$ . A line is drawn from the point of intersection parallel to the ordinate axis until it intersects the line marked  $\alpha = 20$ . The projection of the latter point of intersection on the ordinate axis determines the necessary time of observation. In our example, this time is 6 db or two seconds.

To determine the time of observation from the assumed maximum relative mean-squared error  $\sigma_{II \max}^2$  in the case when the investigated process  $z(t)$  has a dc component  $m = a_0 \neq 0$ , it is necessary to mark on the ordinate the point corresponding to  $(20 \log \sigma_{II \max}^2 - 20 \log c + 20 \log a_0^2)$  db.

The above nomograms are suitable for the solution of the reverse problem, for example, to find the error in the determination of the initial ordinates of the experimentally-obtained correlation function  $R(\tau)$ . In this case we know the observation interval and the type of the correlation function  $R(\tau)$ . From the simple geometric constructions indicated above, performed in the reverse order, we obtain the value of  $\sigma_{II \max}^2$ .

It must be noted that

$$(\sigma_{II \max}^2 - c) \text{ db} = 20 \lg \frac{\sigma_{II \max}^2}{c} = 20 \lg \frac{\sigma_{II \max}^2}{R(0)} = 20 \lg \frac{\sigma_{II \max}^2}{M[z(t)]^2}.$$

If the process does not contain hidden periodicities and has a zero dc component, we have

$$\frac{\sigma_{II \max}^2}{M[z(t)]^2} = \frac{D[m(T)]}{D[z(t)]}, \quad (43)$$

i.e., the value of  $\sigma_{II \max}^2 - c$  obtained from the nomogram will characterize the ratio of the dispersion of the random quantity  $m(T)$  to the dispersion of the random  $z(t)$ . In the determination of the error of the initial ordinate of the correlation function  $R(\tau)$  it is necessary to take into account the Relationships (9) and (10), from which it follows that the attenuation coefficient of the correlation function and its frequency are doubled for the random variable  $z^2(t)$ . Consequently, the necessary time of observation may be considerably smaller than that in the determination of the mean value.

Received March 13, 1956



# ANALYTICAL INVESTIGATION OF THE STABILITY OF AN ELECTROMECHANICAL CONVERTING DEVICE

I. M. Makarov

(Moscow)

The operating principle of an electromechanical converting device used for simulation is given. The equations of motion of the device are derived. Its stability is investigated.

## INTRODUCTION

In the simulation of automatically-regulated systems, the analog of the object is usually connected to the actual regulator with the aid of special devices, which convert certain electrical quantities into corresponding mechanical quantities.

We shall consider in this article one such device, converting the dc voltage from an electronic simulator into an angle of rotation, and derive the equations of motion and solve the stability problem. The device is an electromechanical servo system driven through an electrodynamic clutch (EDC) [1].

### 1. Description of the Principal Diagram and of the Individual Elements of the Converting Device

The principal diagram of the converting device comprises the following basic elements (Figure 1): control amplifier 1, drive mechanism (EDC) 2, reduction gear 3, proportional feedback potentiometer 4, and derivative feedback tachometer generator 5.

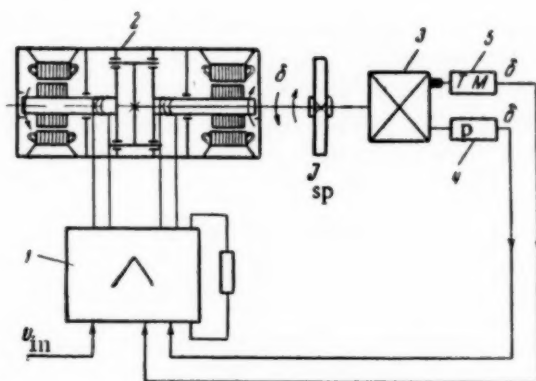


Fig. 1.

When the system is in operation, amplifier 1 receives signals from an electronic analog as well as feedback signals. The output stage of the amplifier incorporates the control windings of the EDC, one of which receives the amplified signal in accordance with the polarity of the error signal. As a result, the output shaft of the EDC rotates until the signal from the analog is balanced by the proportional feedback signal. This motion is transmitted through the reduction gear to a platform carrying the sensitive elements of the regulator. This is how the control error signal applied to the input of the device is eliminated.

### 2. Principle of Operation and Equations of Motion of Elements of Converting Device

The power amplifier chosen for this circuit was a dc amplifier with deep negative feedback (Figure 2). All the impedances shown in the diagram of the amplifier are purely resistive,  $L_l$  represents the inductances of the electromagnet windings, and  $R_l$  the active resistances of these windings. Such an amplifier can conveniently

couple the converter with the electronic analogs operating on dc. In addition, such an amplifier can perform relatively simply and with sufficient accuracy the operations of summation, scale increase, and integration. Its gain can vary over a wide range and may reach  $k = 200$  at an output rating of 30 va.

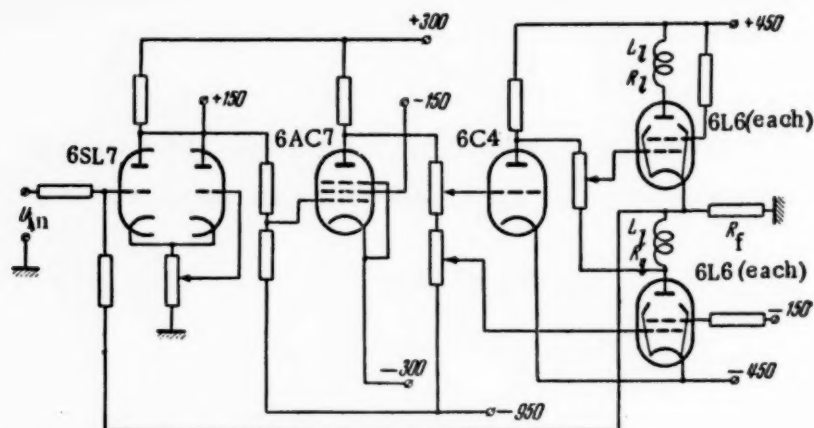


Fig. 2.

The equation determining the change in the output signal of the amplifier feeding inductive loads at the output, without allowances for the internal capacitances of the tubes and other small parameters, can be written as

$$T \frac{dI}{dt} + I = \eta V_{in}, \quad (2.1)$$

where  $T = L/R_n$  is the time constant of the control winding,  $R_n = R_l + R_f + R_i$  is the total resistance,  $L$  the inductance of the control coil,  $\eta$  is a proportionality factor,  $I$  is the current in the control windings, and  $V_{in}$  is the error signal, which in turn is determined by the equation

$$V_{in} = kU_{in} - a\delta - m\dot{\delta}, \quad (2.2)$$

where  $U_{in}$  is the control signal,  $\delta$  the proportional feedback signal,  $\dot{\delta}$  the derivative feedback signal, and  $k$ ,  $m$  and  $a$  are the gain coefficients.

The principle of operation of the drive mechanism of the device is as follows. The EDC has two electromagnets, rotating at a constant speed in opposite directions. The windings of the electromagnets are connected to the output of the power amplifier. Placed in the air gap of the electromagnet is a hollow rotor, comprising a duraluminum cup attached to the output shaft of the EDC. The rotating field of the electromagnet induces in the rotor eddy currents. The interaction between these currents and the magnetic flux that causes them produces a counter force, determined by the following equation [1]:

$$F = \frac{d}{\rho_0} \frac{\alpha^2 L_1}{4\pi} \dot{\delta}_1 B^2, \quad (2.3)$$

where  $d$  is the thickness of the cup wall,  $\alpha$ , the length of the pole of the magnet,  $\rho_0$ , the specific resistivity of the cup material,  $L_1$ , the inductance of the current loop per unit length,  $\dot{\delta}_1$ , the relative angular speed of the electromagnet relative to the cup:  $\dot{\delta}_1 = \dot{\delta}_2 - \dot{\delta}$  (where  $\dot{\delta}$  is the speed of the cup,  $\dot{\delta}_2$ , the constant speed of rotation of the electromagnets), and  $B$  is the flux density in the gap.

The torque on the output shaft of the EDC can be determined from the equation

$$M = k_1 (\dot{\delta}_2 - \dot{\delta}) B^2, \quad (2.4)$$

where  $k_1$  is a proportionality coefficient.



To determine the character of the variation of the torque as a function of the current in the control coils, we employ the relationship  $B = f(I)$ . If the gaps between the rotor-cup and the magnets of the EDC are small, it is possible, upon suitable choice of material and of the cross section of the electromagnetic core, to make the following assumptions: 1) the leakage flux of the magnetic field is small; 2) there is practically no hysteresis in the electromagnet cores; and 3) the electromagnet core does not saturate. The unknown relationship is then determined from the following equation

$$B = \bar{b}I, \quad (2.5)$$

where  $\bar{b}$  is a proportionality coefficient, determined from the magnetization curve of the core material by measuring the slope of the characteristic.

Taking (2.4) and (2.5) into account, we obtain the following equation of motion for the EDC

$$J\ddot{\delta} + b_1 I^2 \dot{\delta} = b_2 I^2 \text{sign } I, \quad (2.6)$$

where  $b_1 = k_1 \bar{b}^2 \dot{\delta}_2$ ,  $b_2 = k_1 \bar{b}^2$ , and  $J$  is the moment of inertia of the moving parts, referred to the shaft of the clutch.

If the ratios of the gear reduction and of the feedback proportional potentiometer are included in the coefficient  $\bar{a}$ , and if the gain of the tachometer generator is included in the coefficient  $\underline{m}$  (2.2), the equations of motion of the converting device are as follows:

$$J\ddot{\delta} + b_1 \dot{\delta} I^2 = b_2 I^2 \text{sign } I, \quad T\dot{I} + I = \eta(kU_{in} - \bar{a}\delta - m\dot{\delta}). \quad (2.7)$$

### 3. Investigation of the Equations of Motion (2.7)

The most important characteristic of a servo system is the accuracy with which it reproduces the control action. The accuracy of reproduction depends to a considerable extent on the value of the gain coefficient, and the system accuracy increases with the latter. However, an excessive gain may lead to loss of stability. The investigation of the stability of the system for specified equations of motion is therefore of certain interest.

The Equations of Motion (2.7) are nonlinear, and the corresponding first-approximation equations have a double zero root. Our attempts to use known methods [2, 3, 4] to determine the stability of the System (2.7) were unsuccessful. On the other hand, using the methods of qualitative theory of differential equations, to which attention was called in Ref. [5], and the use of the direct Liapunov method, have made it possible to obtain the desired result.

Let us assume that all the constants contained in Equation (2.7) are positive quantities. The specified steady state of the servo system, which the system must maintain, is determined by the equation

$$\delta^* = \frac{kU_{in}}{\bar{a}} = \text{const.} \quad (3.1)$$

Let us introduce new variables

$$x = \delta - \delta^*, \quad y = \dot{\delta}, \quad z = I. \quad (3.2)$$

Put

$$\frac{b_1}{J} = a_2, \quad \frac{b_2}{J} = a_1, \quad \frac{\bar{a}\eta}{T} = a, \quad \frac{m}{T}\eta = b, \quad \frac{1}{T} = c \quad (3.3)$$

and reduce the initial Equations (2.7) to the Cauchy normal form:

$$\begin{aligned} \dot{x} &= y, \\ \dot{y} &= (a_1 \text{sign } z - a_2 y) z^2, \\ \dot{z} &= -ax - by - cz. \end{aligned} \quad (3.4)$$

Taking into account the sign of the variable  $z$ , the given system of Equations (2.7) transforms in the following manner:

$$\begin{aligned}
 1) \ z > 0 \quad & \begin{aligned} \dot{x} &= y, \\ \dot{y} &= (a_1 - a_2 y) z^2, \\ \dot{z} &= -ax - by - cz; \end{aligned} \\
 2) \ z < 0 \quad & \begin{aligned} \dot{x} &= y, \\ \dot{y} &= -(a_1 + a_2 y) z^2, \\ \dot{z} &= -ax - by - cz; \end{aligned} \\
 3) \ z = 0 \quad & \begin{aligned} \dot{x} &= y, \\ \dot{y} &= 0, \\ \dot{z} &= -ax - by. \end{aligned}
 \end{aligned} \tag{3.5}$$

The steady state of the system is determined by the equation

$$x^* = y^* = z^* = 0. \tag{3.6}$$

and the phase space of the system is symmetrical with respect to the origin.

Let us consider a right-handed coordinate system  $x, y, z$ . Let us construct the planes determined by the equations

$$(A) \ y_1 = \frac{a_1}{a_2}, \quad (B) \ ax + by + cz = 0, \tag{3.7}$$

$$(A') \ y_1 = -\frac{a_1}{a_2}, \quad ax + by + cz = 0. \tag{3.8}$$

Let us consider the space outside the planes (A) and (A') (Figure 3). Since according to Equation (3.5) we have  $\dot{y} > 0$  to the left of (A') and  $\dot{y} < 0$  to the right of (A), the generating point will pass over one of the above planes for all values of  $x_0, z_0, |y_0| > a_1/a_2$ . It can be said that these planes are elements of attraction for all the trajectories that begin at any point  $x_0, z_0, |y_0| > a_1/a_2$  in space.

For a further study of the trajectory, let us consider the motion of the generating point along the plane (A). For this purpose, let us construct the solutions of Equation (3.5) for the initial conditions  $x = x_0, y_0 = a_1/a_2, z = z_0 > 0$ .

Using the method of successive approximations we get:  
first approximation

$$\begin{aligned}
 x_1 &= x_0 + y_0 t, \\
 y_1 &= y_0, \\
 z_1 &= z_1^* + (z_0 - z_1^*) e^{-ct}, \quad z_1^* = -\frac{ax_0 + \left(b - \frac{a}{c}\right)y_0}{c} - \frac{a}{c} y_0 t
 \end{aligned}$$

second approximation

$$\begin{aligned}
 x_2 &= x_0 + y_1 t, \\
 y_2 &= y_1, \\
 z_2 &= z_2^* + (z_0 - z_2^*) e^{-ct}, \quad z_2^* = z_1^* \\
 &\dots \dots \dots
 \end{aligned}$$

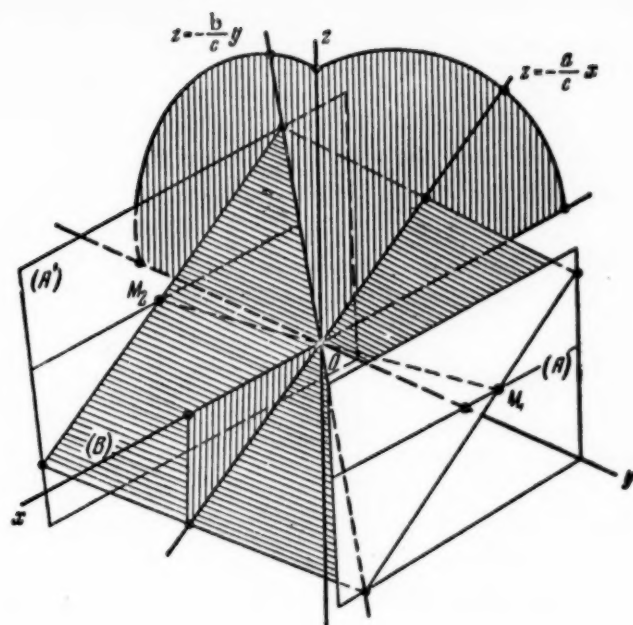


Fig. 3.

n-th approximation

$$\begin{aligned} x_n &= x_0 + y_{n-1}t, \\ y_n &= y_{n-1}, \\ z_n &= z_n^* + (z_0 - z_n^*)e^{-ct}, \quad z_n^* = z_{n-1}^*. \end{aligned}$$

The resultant sequence of functions will have a limit

$$\begin{aligned} x &= x_0 + y_0 t, \\ y &= y_0, \\ z &= z^* + (z_0 - z^*)e^{-ct}, \end{aligned} \quad (3.9)$$

which serves as the solution\* of System (3.5) for the given choice of initial conditions.

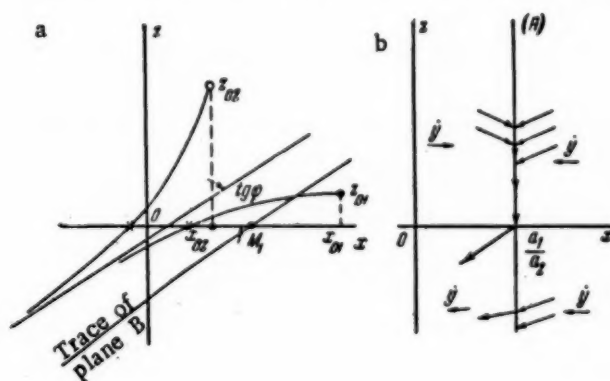


Fig. 4.

\*N.P. Erugin called attention to the fact that for the given initial conditions, this solution follows from the uniqueness theorem.

To determine the type of trajectory, let us eliminate from Solution (3.9) the independent variable  $t$  and get

$$z = z^{**} + (z_0 - z^{**}) e^{-\frac{c}{y_0}(x-x_0)} - \frac{a}{c}(x - x_0),$$

$$z^{**} = \frac{ax_0 + \left(b - \frac{a}{c}\right)y_0}{c}. \quad (3.10)$$

It is clear from the above that all the trajectories to the right of (A) continue on a plane (A). To investigate them on the plane (A), let us draw the straight line (Figure 4a)

$$z = -\frac{a}{c}x - \frac{y_0}{c}\left(b - \frac{a}{c}\right). \quad (3.11)$$

The equation of the line (3.11) can be otherwise written as

$$z = z^{**} - \frac{a}{c}(x - x_0). \quad (3.12)$$

It is clear from the last equation that all points  $z^{**}$  are located on a straight line (3.12) which is the asymptote of the trajectory (3.10). The latter follows from the fact that

$$\lim_{x \rightarrow \infty} \frac{dz}{dx} = \lim_{x \rightarrow \infty} \left[ -\frac{c}{y_0}(z_0 - z^{**}) e^{-\frac{c}{y_0}(x-x_0)} - \frac{a}{c} \right] = -\frac{a}{c}. \quad (3.13)$$

One can therefore state that on the plane (A), for all trajectories originating at arbitrary values  $x_0$  and  $z_0 > 0$ , the intersection between the plane (A) and the plane  $z = 0$  is an element of attraction. From this line, all these lines become continuous in the portion of space included between the planes (A) and (A') (Figure 4b). The trajectories that intersect plane (A) at  $z < 0$ , simply pierce through it and enter the space between (A) and (A'). If an analogous investigation is made of the trajectories on the plane (A'), it can be shown that their character will be as shown in Figure 5. The latter also follows from the symmetry of the system pointed out earlier.

It can be concluded from the above that all the space of the trajectories to the left and to the right of planes (A) and (A') contracts into a strip contained between them.

A study of the behavior of this system in the region between planes (A) and (A'), to which all the trajectories contract, will be made using Liapunov's method. For this purpose let us consider the quadratic form

$$2V = a_{11}x^2 + a_{22}y^2 + 2a_{13}xz + a_{33}z^2 + 2a_{23}yz, \quad (3.14)$$

all the coefficients of which are positive numbers  $a_{k_0} > 0$ . It will certainly be of definite sign and everywhere positive if the following condition is satisfied

$$\begin{vmatrix} a_{11} & 0 & a_{13} \\ 0 & a_{22} & a_{23} \\ a_{33} & a_{23} & a_{33} \end{vmatrix} = a_{22}(a_{11}a_{33} - a_{13}^2) > a_{11}a_{23}^2. \quad (3.15)$$

Let us assume that

$$a_{11}a_{33} > a_{13}^2. \quad (3.16)$$

Then, for arbitrary values  $a_{11}$ ,  $a_{23}$ . Condition (3.15) is readily satisfied if  $a_{22}$  is sufficiently large.

The total derivative function  $2V$ , calculated on the basis of Equation (3.4) will be

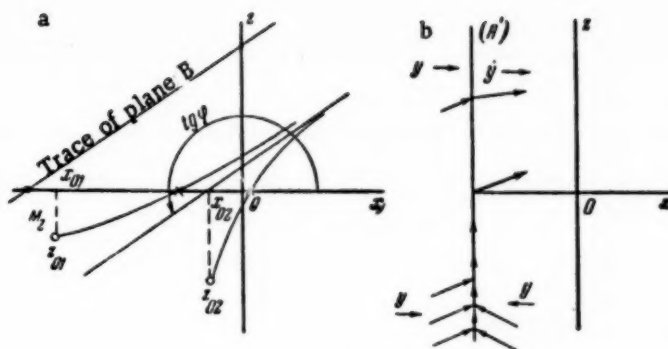


Fig. 5.

$$\begin{aligned} \dot{V} = & -aa_{13}x^2 - (-a_{11} + ba_{13} + aa_{23})xy - ba_{23}y^2 - \\ & -(-a_{13} + ca_{23} + ba_{33})yz - ca_{33}z^2 - (aa_{23} + ca_{13})xz + \\ & + (a_1 \operatorname{sign} z - a_2 y) z^2 [a_{22}y + a_{23}z]. \end{aligned} \quad (3.17)$$

Let us consider the quadratic form

$$\begin{aligned} W = & aa_{13}x^2 + (aa_{23} + ba_{13} - a_{11})xy + ba_{23}y^2 + (ba_{33} + ca_{23} - a_{13})yz + \\ & + (aa_{23} + ca_{13})xz + ca_{33}z^2. \end{aligned} \quad (3.18)$$

To draw conclusions concerning the sign of the form (3.18), let us consider the determinant

$$\Delta = \begin{vmatrix} aa_{13} & \frac{aa_{23} + ba_{13} - a_{11}}{2} & \frac{aa_{23} + ca_{13}}{2} \\ \frac{aa_{23} + ba_{13} - a_{11}}{2} & ba_{23} & ba_{33} + ca_{23} - a_{13} \\ \frac{aa_{23} + ca_{13}}{2} & \frac{ba_{33} + ca_{23} - a_{13}}{2} & ca_{33} \end{vmatrix}. \quad (3.19)$$

By virtue of the assumptions made above, the form of  $W$  will be positive definite, if the determinant (3.19) and its principal diagonal second-order minor are positive. Whether this minor is positive depends on the existence of an inequality

$$4aba_{13}a_{23} > (aa_{23} + ba_{13} - a_{11})^2 \quad (3.20)$$

or an inequality

$$0 > (aa_{23} - ba_{13})^2 - 2(aa_{23} + ba_{13})a_{11} + a_{11}^2. \quad (3.21)$$

Let

$$x_1, x_2 = aa_{23} + ba_{13} \pm 2\sqrt{aba_{13}a_{23}} \quad (3.22)$$

be the roots of the equation

$$x^2 - 2(aa_{23} + ba_{13})x + (aa_{23} - ba_{13})^2 = 0, \quad (3.23)$$

Evidently  $x_1 > 0, x_2 > 0$ .

Inequality (3.21) is then satisfied if the number  $a_{11}$  lies within the range

$$x_2 < a_{11} < x_1 \quad (3.24)$$

of the equality

$$a_{11} = \frac{aa_{23} + b_1 a_{13}}{2}. \quad (3.25)$$

To determine the conditions under which the inequality  $\Delta > 0$  is satisfied, let us expand the Determinant (3.19).

Introducing the symbols  $a_{13} = x$ ,  $a_{23} = y$ , and  $a_{33} = z$  and carrying elementary algebraic transformations, we obtain the inequality

$$\varphi z^2 + \psi z + \chi > 0, \quad (3.26)$$

where

$$\begin{aligned} \varphi &= -ab(ay + bx), \\ \psi &= \left(3ab + \frac{b^2c}{2}\right)x^2 + a(bc - a)xy + \frac{a^2c}{2}y^2, \\ \chi &= x[(bc + 3a)cxy - ac^2y^2 - (bc + 2a)x^2] = -xU(x, y). \end{aligned} \quad (3.27)$$

It now remains to establish that there exists in the first quadrant  $Q$  of the space  $x, y, z$  a region of values of  $x, y$  and  $z$  in which Inequality (3.26) is satisfied. It is evident that everywhere in  $Q$  we have  $\varphi z^2 < 0$ .

To establish the sign of  $\psi z$  let us consider the discriminant of the quadratic form  $\psi$ :

$$\Delta_\psi = \begin{vmatrix} 3ab + \frac{b^2c}{2} & \frac{a(bc - a)}{2} \\ \frac{a(bc - a)}{2} & \frac{a^2c}{2} \end{vmatrix} = \frac{a^3}{4}(8bc - a). \quad (3.28)$$

We see that the form  $\psi$  is everywhere positive if the following inequality is satisfied

$$8bc > a. \quad (3.29)$$

The sign of  $\chi$  can be established by considering a discriminant of the form  $U(x, y)$ :

$$\Delta_x = \begin{vmatrix} bc + 2a & -\frac{bc^2 + 3ac}{2} \\ -\frac{bc^2 + 3ac}{2} & ac^2 \end{vmatrix} = -\frac{a(a + 2bc) + b^2c^2}{4}c^2. \quad (3.30)$$

It is evident that when  $\Delta_x < 0$ , it is possible to separate in the quadrant  $Q$  a wedge formed by the planes

$$y = \frac{(bc + 3a)c \pm 2\sqrt{-\Delta_x}}{2ac^2}x, \quad (3.31)$$

in which  $\chi > 0$  everywhere (Figure 6).

Upon further study of Inequality (3.26), we can determine the values of  $z_1$  and  $z_2$  by the aid of equation

$$z_1, z_2 = \frac{-\psi \pm \sqrt{\psi^2 - 4\varphi\chi}}{\varphi}. \quad (3.32)$$

Inequality (3.26) can then be rewritten as  $(z - z_1)(z - z_2) < 0$ .

It is evident that if Inequality (3.29) is satisfied  $z_1 < 0$ ,  $z_2 > 0$ , and Inequality (3.26) is satisfied by all values  $z < z_2$ . On the other hand, it is also necessary to satisfy Inequality (3.16). Using the above symbols, the inequality becomes

$$z > \frac{2x^2}{ay + bx}. \quad (3.33)$$



$$\frac{2x^2}{ay+bx} < z < \frac{\psi + \sqrt{\psi^2 - 4\varphi\chi}}{-\varphi}.$$
$$2abx^2 < \psi + \sqrt{\psi^2 - 4\varphi\chi}. \quad (3.34)$$

From the definitions in (3.27) it is obvious that this is true.

$$\dot{V} = -W + (a_1 \operatorname{sign} z - a_2 y) (a_{22} y + a_{23} z) z^2. \quad (3.35)$$

Thus, we have proved that Inequality (3.29) is the only condition that must be satisfied to guarantee the stability of the above servo system for all disturbances except zero and for sufficiently small disturbances  $y_0$  and  $z_0$ . For a specified time constant  $T$  of the control windings, this condition makes it possible to choose the coefficients  $\bar{a}$  and  $m$  of the feedback loops of the servo system.

[1] I.M. Makarov, "Choice of Geometrical Dimensions of the Magnetic Circuit and the Structural Scheme of an Electrodynamical Clutch," *Avtomatika i Telemekhanika* 17, No. 10 (1956).\*

[2] A.M. Liapunov, Obshchaia zadach ob ustoičivosti dvizheniia (General Problem of Stability of Motion) (Gostekhizdat, 1950).

[3] G.V. Kamenkov, "On the Stability of Motion," Transactions (Trudy) of the Kazan' Aviation Institute No. 9 (Kazan' 1939).

[4] I.G. Malkin, *Teoriia ustoičivosti dvizheniia* (Theory of Stability of Motion) (Gostekhlizdat, 1952).

[5] N.P. Erugin, "On Certain Problems in the Stability of Motion and a Qualitative Theory of Differential Equations as a Whole," PMM (Applied Mathematics and Mechanics) Vol. 14, No. 5 (1950).

Received December 28, 1956

355



## CERTAIN PROBLEMS IN THE CONSTRUCTION OF MULTICHANNEL AUTOMATIC REGULATION SYSTEMS

V. P. Kazakov

(Moscow)

Examination of the circuitry and of methods used to construct basic multichannel (multiple-point) automatic regulation systems with time sharing of the channels, using contactless elements.

### INTRODUCTION

One of the ways of reducing the quantity of apparatus necessary in the automatization of objects with a large number of controlled and regulated quantities, and to facilitate the use of the apparatus, is to use multi-channel (multiple-point) control and regulation systems. In general, a multichannel regulation system (MRS) is a device comprising many transducers and drive mechanisms (as many as there are objects) and a so-called common section, which contains the remaining functional units of the regulation systems together with devices that make possible the distribution of the signals among the individual channels.

In the automatization of modern technological units, the use of multichannel regulators would be quite effective in many cases. Thus, for example, steel is heat treated with electric dome furnaces, whose temperature is regulated by means of contactors that switch heaters in and out. Each production line usually contains dozens of such furnaces, each requiring from two to four temperature regulators. The replacement of so large a number of regulators with a multichannel regulation system would facilitate considerably the problem of maintaining the proper temperature in the furnaces. It is evident that remote control of groups of objects, located at great distances from the points where the quantities used for the regulation are measured, is possible only with the aid of a MRS, which makes possible the use of a single communication channel (wire or radio) for the transmission of the control signals to the actuating mechanisms of the objects.

In connection with the development of work on the application of computers to the automatic control of manufacturing processes, problems of multichannel regulation become even more urgent. The unification of objects into several groups, each of which is regulated by a single multichannel regulator, would simplify substantially the system used to gather the information, since any multichannel regulator already contains devices for the production of data on the course of the process in each object served (measuring and scanning devices), and if necessary it can convert these data into digital form.

The need for multichannel regulators arose quite a while ago. Thus, several MRS's were designed in the Thirties, for example, the 8-point temperature regulator for air dust, designed by Iu. G. Kornilov and E. P. Fel'dman [1] and the 12-point TF-12-SP thermal regulator by G. A. Fil'tser [2]. However, these systems did not find wide application owing to serious shortcomings, particularly their low reliability, short life, and low speed. This was caused by the fact that the principal devices of the common portion of the system were electromechanical devices (contact switches, relays, galvanometers, etc.). At the present time, when we have such highly reliable elements as crystal diodes and transistors, magnetic elements with rectangular hysteresis loops, cold-cathode thyratrons, etc., the problem of constructing MRS's can be satisfactorily solved.

## 1. General MRS Scheme

In multichannel regulation systems it is possible to employ two principles of channel sharing: frequency and time. Frequency sharing, however, not only requires complicated circuitry and constructions, but imposes a limitation in principle on the possible maximum number of regulation channels. The time-sharing principle is widely used in multichannel systems for pulse communication and for remote control; all the known MRS's also employ this principle. In time sharing, the error and control signals are transmitted sequentially in time with a definite repetition rate. Sequential switching is effected by means of a commutator, which becomes one of the principal elements in such systems.

A suitable method for producing a pulse error signal in a high speed MRS is to close periodically, for a short instant of time, the circuit of the output signal. This makes it possible, with a minimum closed-state time,  $t_c$ , to transmit all the information concerning the signal at discrete instants of time and no special device for shaping the pulses is necessary, for the pulses are shaped by the commutator itself. In this case the pulse signals are formed in the measuring devices of each channel or else directly past these devices.

For a given time  $t_c$  in the closed state and for a given duration of regulation cycle  $T_r$ , the maximum number of channels which the MRS can contain is

$$K_{\max} = T_r/t_c = 1/\gamma,$$

where  $1/\gamma$  is the duty cycle of the pulse signals in the system. The number of channels is usually chosen less than  $K_{\max}$ , to prevent mutual interference, i.e., influence of one channel on another due to the finite bandwidth of the common regulator elements. The capacity of the MRS, i.e.,  $K_{\max}$  for a given  $T_r$ , is determined by the required closed time  $t_c$ , the value of which depends on the time necessary to form the error signal and control signal, and also on the speed of the drive devices, for the latter must have time to operate in response to the arriving pulse.

The dependence of the choice of the required value of  $t_c$  on the speed of the drive mechanism can be eliminated by increasing with the aid of memory devices the duration of the control pulses acting on each channel past the commutator. In such devices, which will be called henceforth forming devices, the duration of the control pulses can be increased from  $t_c$  to the value of the regulation cycle  $T_r$ . The action of the forming device is illustrated in Figure 1. Here  $U_d$  is the control signal (signal past the distributor) in one of the channels,

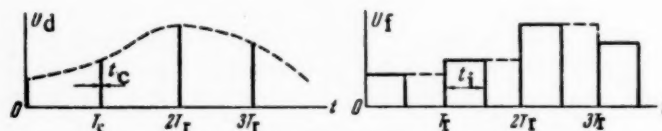


Fig. 1.

and  $U_f$  is the same signal, prolonged with the aid of the forming device. The duration of the pulse that now acts on the actuating mechanism is determined by the following inequality:

$$t_c < t_i \leq T_r.$$

Let us note that the forming device can also transform the amplitude modulation of pulses into time modulation or into polarity modulation, thus converting the regulation system in each channel into a pulse system with broad-band pulse modulation or into a relay-pulsed system.

The functional scheme of a multichannel regulator, in which time sharing of the channel is used along with the conversion of the duration of the pulse control signals, is shown in Figure 2, where the following designations are used: 1) measuring devices of the channels, 2 and  $\bar{2}$ ) switches for the commutation of the error and control signals, 3) circuit for the control of the operation of switches 2 and  $\bar{2}$  (devices 2,  $\bar{2}$ , and 3 comprise the commutator of the system), 4) electronic pulse amplifier, 5) correcting (control) device, 6) forming devices, 7) drive mechanisms, 8) power supply, and 9) generator for the sinusoidal voltage required to modulate the error

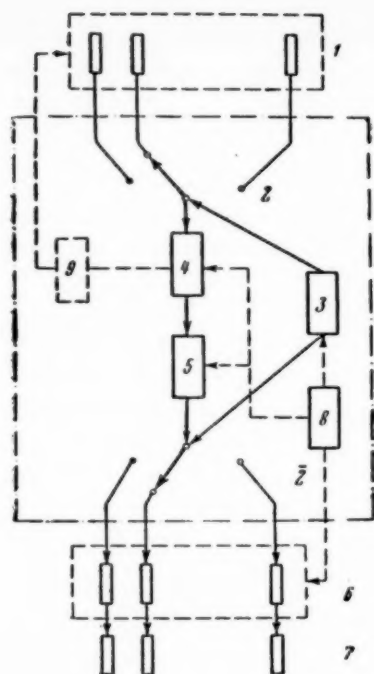


Fig. 2.

We shall consider below certain of the possible solutions to these problems, principally in the case of regulation of a large number of channels (on the order of 100), in which the processes can occur at frequencies up to 0.5-1 cycle.

## 2. Measuring Devices

The use of automatically balanced circuits as measuring devices in the MRS (self-balancing circuit) would result in the maximum measurement accuracy. However, this method requires that each channel be closed for a considerable time  $t_c$ , and consequently this reduces sharply the possible number of channels in the system. To form the error signals in the MRS, it is most convenient therefore to employ the method of unbalanced circuits (bridges), in which one measures the voltage or the current between specified points of the circuits, which is proportional, if the unbalance is not excessive, to the error in the regulated quantities. The measuring devices of the MRS can be subdivided into two groups, depending on the method used to form the pulse error signals.

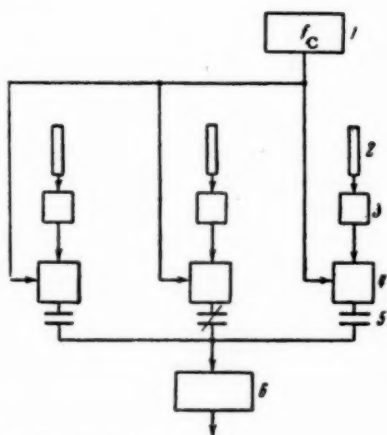


Fig. 3. 1) Generator;

signals. The dot-dash line border contains the section of the regulator that is common to all the channels.

The regulator operates in the following manner. The commutator closes in sequence each regulation circuit for a short time  $t_c$ , applying to the input of the common amplifier 4 discrete values of the error signals from the outputs of the measuring devices. The sequence of pulses so formed is amplified and is converted with the aid of correcting device 5 into a second sequence, which differs from the first by the manner in which the pulse amplitudes are modulated; as a result, the action on the operating mechanisms will incorporate the necessary law of regulation.

The output sequence of the pulse signals of the correcting device is distributed by switch  $\bar{2}$ , which operates in synchronism and in phase with switch 2, in accordance with the forming devices 6, in which the durations of the control pulses are amplified, and if necessary, in which the amplitude modulation is converted into a different type of pulse modulation.

The development of a multichannel regulation system involves problems in the formation and commutation of pulse error signals through each channel, the commutation of the channels with the aid of a contactless high speed and long-lived commutator, increasing the duration of action of the pulse control signals, and the correction of the regulation processes in the MRS.

The devices of the first group, used principally in the case when active transducers are used, produce a continuous measurement signal, which is subjected to subsequent commutation. To use contactless commutators, the switching of the signals is carried out by means of "time-selectors," which can be based on vacuum tubes or transistors, as well as on magnetic elements. In this case it is necessary to switch not the transducers, but the signals directly from the measuring devices, i.e., after the comparison with the set point has been made. This is necessary because of the considerable inherent instability of the keying circuits, which may reach the order of millivolts and even tenths of millivolts. Therefore, for contactless commutation of small signals, the latter must be represented in the form of modulated ac voltages with a frequency exceeding the commutation frequency by at least one order of magnitude. If the modulated signals flow directly from the transducers, they must be com-



pared with the set values at ac, and this, as is known, involves considerable difficulties. Figure 3 shows a block diagram of the measuring device of a MRS, using modulation of the error signal. The modulators employed may be contact-making vibrators, but if the commutation frequency exceeds 5-10 cycles, it becomes necessary to employ magnetic modulators with increased supply frequency. At the present time there exist already magnetic modulators with a voltage sensitivity approximately  $10^{-5}$  volts, and with a voltage gain of  $10-10^2$ . The continuously acting voltage from the outputs of the modulators is applied in sequence for a time  $t_c$  by the input keys of the commutator to the common amplifier and are thus transformed into pulse error signals.

In the second group of the measuring devices for MRS, the pulse error signals are produced directly in the measuring device itself. This is done by supplying the measuring device with pulsed current rather than with continuous current.

The idea of a pulse method of measurement as used in multichannel control systems, and the method of realizing such a method, are discussed in [3].

The simplest way of realizing such a measuring device is to use parametric transducers. If a rectangular pulse is applied to the terminals of a bridge, consisting of ohmic resistances and parasitic reactances in the form of shunt capacitances or series inductances, the output voltage will have the form of the pulse shown in Figure 4. The amplitude of the flat portion,  $U_0$ , depends on the unbalance with respect to the ohmic resistances, i.e., it is proportional to the deviation of the measured quantity from the specified value. The overshoots at the start and

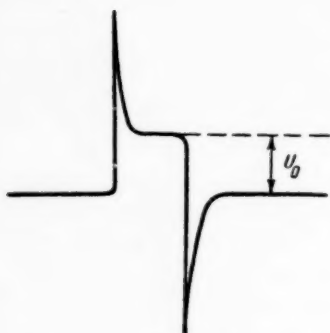


Fig. 4.

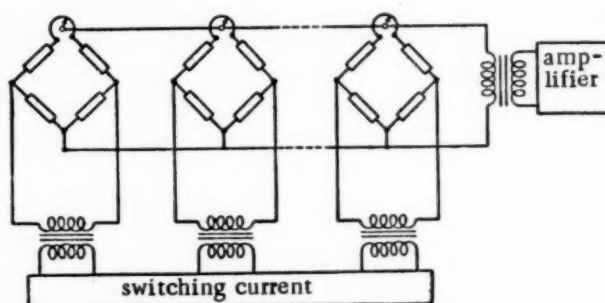


Fig. 5.

at the end of the pulse are due to the unbalance of the parasitic reactive parameters of the bridge. By suitable choice of the duration of the supply pulse it is possible to make the duration of the flat portion of the pulse, i.e., its useful part, many times greater than the duration of the overshoots. If for some reason it is impossible to reduce substantially the relative duration of the overshoots, it is still possible to employ a strobing circuit to transmit only the flat portion of the pulse through the common amplifier, owing to the fact that the action of the overshoots and of the flat portion are separated in time. The pulse method for exciting bridges (let us note that this pertains not only to resistive but also to inductive bridges) makes it possible to realize relatively simply the measuring unit of a MRS. For this purpose, a special switching circuit is used to excite in sequence each bridge by means of a supply pulse, and the outputs of all the bridges are connected in parallel and through a step-up transformer to the common amplifier (Figure 5). What is switched here is not the error signal, but a supply pulse of dc or ac of large and constant amplitude, thus reducing considerably the difficulties involved in the switching of the channels because of the presence of unbalance and drift in the keying circuits. Such a measuring device makes use of still another advantage of pulse supply for bridges, namely that in pulse excitation the heat dissipated in the transducer is reduced in inverse proportion to the duty cycle ( $1/\gamma$ ) and consequently, it is possible to increase the current in the transducer by  $1/\sqrt{\gamma}$  without exceeding the maximum permissible heating.

The advantages of the null methods of measurement can be realized in a MRS if the measuring devices are constructed on the basis of dynamic balance. However, the use of this principle in MRS is limited owing to the considerable reduction in the possible number of channels in the system and owing to the complexity in the use of contactless commutators. The first circumstance is connected with the fact that the use of dynamic balance presupposes the presence of time-pulse error-signal modulation and therefore requires larger values of  $t_c$  than in the cases considered above. The second circumstance is connected with the need for comparing ac input



and sweep voltages. To obtain the maximum possible measurement accuracy, it is necessary to ensure in this case that the phases of these voltages are strictly constant.

### 3. Commutator

Depending on the type of the measuring device, the contactless high speed commutator of the MRS can be constructed in accordance with one of two general schemes shown in Figure 6a and 6b. It is seen from these diagrams that the commutator consists of two parts - a switching circuit and groups of identical selector devices, namely keying circuits.

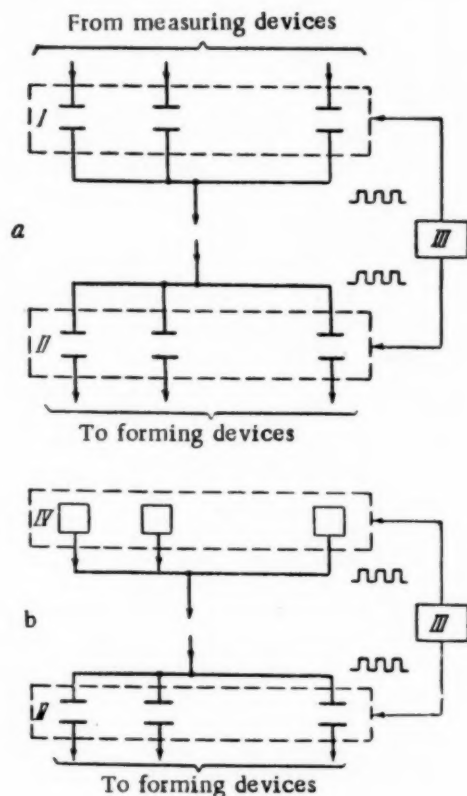


Fig. 6. I - input keys; II - output keys; III - switching circuit; IV - measuring devices.

and long life. However, this circuit does not permit a ready variation of the switching speed over a wide range, thus reducing its value for use as an MRS commutator. This is explained by the fact that the choice of the repetition period for each channel,  $T_r$ , depends principally on the dynamic properties of the objects of regulation and is one of the tuning parameters of any pulse regulation system.

Switching circuits employing cold-cathode thyratrons have many of the advantages of circuits employing magnetic amplifiers, and at the same time make it possible to change the switching speed of the commutator over a wide range. Recently, a Russian small-size cold-cathode thyatron, MTKh-90, has been used to construct many remote-control devices and pulse circuits [6, 7].

The simplest switching circuit that can be used is the counting ring circuit, in which the number of tubes should equal the number of channels. If the number of channels in the MRS is large, the number of tubes in the switching circuit can be reduced considerably by using a matrix commutator, in which the switching function is partly assumed by a circuit consisting of semiconductor diodes and resistances.

The keying circuits of the commutator are time-sharing devices, the task of which is to separate out portions of the signal that coincides with specified instants of time. The time selectors can be built using diodes, triodes and multigrid tubes, and also saturated reactors. Circuits employing semiconductors and magnetic elements have high reliability and long service life. By way of an example, let us illustrate the input key circuits

It is the task of the switching circuit to generate pulses that are distributed in time and that are of constant amplitude. The keying circuit should change from the cut-off to the conducting state whenever pulses are received from the switching circuit, with good linearity and with a transfer coefficient nearly equal to unity. The commutator shown in Figure 6a is used in those cases, when the measuring devices modulate an ac voltage with the error signal and subsequently distribute the modulated signal ahead of the common amplifier. In this case each channel consists of two keys - input and output.

If the measuring devices of the MRS are constructed on the pulse excitation principle, the commutator used is that shown in Figure 6b. Unlike the preceding one, the commutator does not contain input keys, and the pulses from the switching circuit arrive directly at the measuring devices, and thus exciting them in sequence. In all other respects the circuits are identical. When commutator circuits employing vacuum tube and cathode-ray tubes are used in the MRS, the result is a device of high speed, but the need for using a large number of such tubes reduces substantially the reliability and life of the equipment, owing to the fact that there is no guaranteed minimum tube life.

The use of magnetic elements for the construction of switching and selector circuits for the multichannel system commutators is quite promising. References [4] and [5] report an investigation of a switching circuit made of magnetic elements with rectangular hysteresis loops, operating at high switching speed and high reliability, high parameter stability,

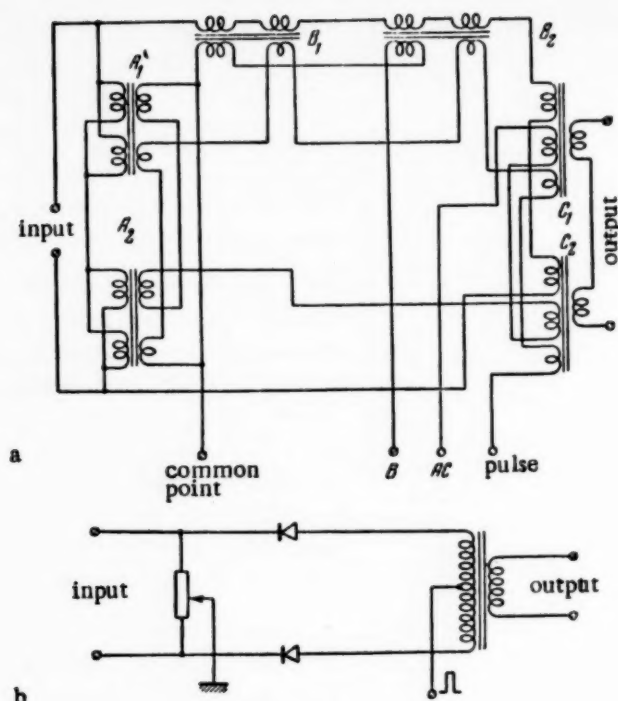


Fig. 7.

used in the commutation of error signals in the form of small ac voltages (Figure 7a and 7b).

The first circuit, discussed in Ref. [8], employs as the basic elements saturated reactors and toroidal-section transformers. If cores  $B_1$  and  $B_2$  are saturated (terminal B is under voltage), and the four cores A and C are not saturated, the key conducts and the input signal, with an attenuation of approximately 10%, passes through the output. If, on the other hand, cores A and C are saturated (terminal AC under voltage) and  $B_1$  and  $B_2$  remain unsaturated, the signal cannot reach the output owing to the shunting action of chokes A, the large resistance of chokes B, and the weak coupling between the primary and secondary windings of transformers C.

The additional winding on each toroid is used to apply a demagnetizing pulse every time after the control voltage is removed.

Such a device makes it possible to distribute reliably ac signals from a level of 1 millivolt up with good linearity and with a power of less than 20 milliwatts consumed for control. A shortcoming of the circuit is the relatively high weight, dimensions, and cost.

The second output-key scheme is considerably simpler than the first and employs as distributing elements two semiconductor diodes. When a positive pulse, greater than the constantly-applied blocking voltage, is applied through the center tap of the transformer the diodes conduct and the signal passes through the key with almost no attenuation.

This circuit calls for control pulses of high amplitude, so that the operating point of the conducting diodes falls on the linear portion of their voltage-current characteristic. In this case instability in the amplitude of the distributing pulse will not affect the output voltage of the key. The strong dependence of the voltage-current characteristic of a semiconductor diode on the variation in temperature may cause a considerable drift in the initial level of the above circuit. The key will not become unbalanced whenever the ambient temperature changes, provided the change in the slope of the linear portion of the voltage-current characteristic of both diodes is the same. Suitable choice of the diodes makes it possible to construct a key that has low sensitivity to temperature variations. The use of silicon diodes simplifies this problem owing to the considerably lower temperature dependence of their parameter than in the case of the germanium diodes. An experimental verification of the above input-key circuit has shown that it is capable of commutation of error signals at a carrier frequency of 500-5000 cycles, starting with a level of 1 mv.

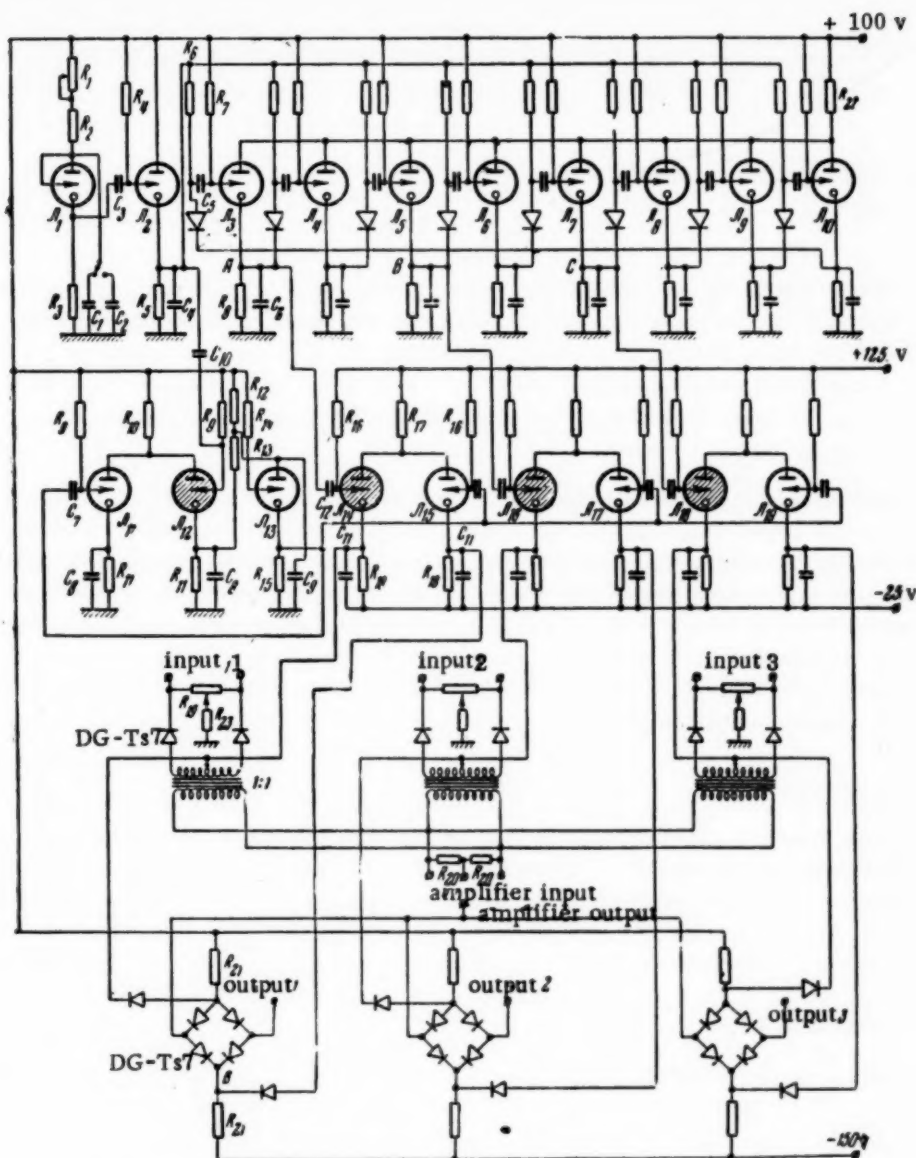


Fig. 8.\*

If it is necessary to distribute pulse control signals of high amplitude, the output keys can be assembled, for example, using one of the circuits investigated in Ref. [9] and shown in Figure 8, which represents the complete diagram of a three-channel MRS distributor. The principal parameters of the circuit are as follows:  $R_1 = 1.5$  megohm,  $R_2 = 140$  kilohm,  $R_3 = 1.1$  kilohm,  $R_4 = 43$  megohm,  $R_5 = 1.2$  megohm,  $R_6 = 2$  megohm,  $R_7 = 43$  megohm,  $R_8 = 47$  kilohm,  $R_9 = 10$  megohm,  $R_{10} = 12$  kilohm,  $R_{11} = 20$  kilohm,  $R_{12} = 720$  kilohm,  $R_{13} = 780$  kilohm,  $R_{14} = 4$  megohm,  $R_{15} = 2$  kilohm,  $R_{16} = 10$  megohm,  $R_{17} = 3$  kilohm,  $R_{18} = 5.1$  kilohm,

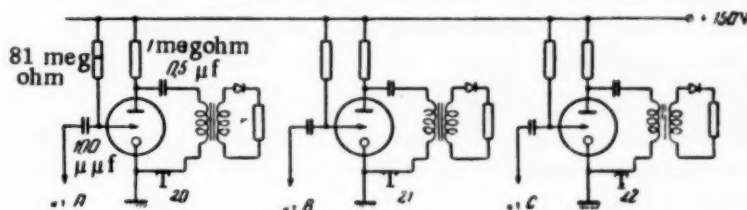


Fig. 9.

\*[Here  $\pi$  = 'tube'.]

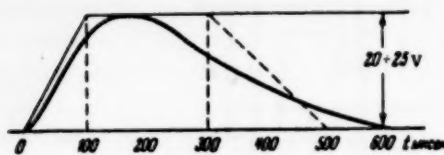


Fig. 10.

$R_{19} = 22$  kilohm,  $R_{20} = 3.3$  kilohm,  $R_{21} = 180$  kilohm,  $R_{22} = 39$  kilohm,  $R_{23} = 31$  kilohm,  $C_1 = 0.16$  microfarad,  $C_2 = 1$  microfarad,  $C_3 = 48$  micromicrofarad,  $C_4 = 1000$  micro-microfarad,  $C_5 = 91$  micromicrofarad,  $C_6 = 0.04$  microfarad,  $C_7 = 91$  micromicrofarad,  $C_8 = 0.02$  microfarad,  $C_9 = 0.004$  microfarad,  $C_{10} = 116$  micromicrofarad,  $C_{11} = 0.015$  microfarad,  $C_{12} = 110$  micromicrofarad. The switching circuit  $V_1 - V_{19}$  is assembled using cold-cathode MTKh-90 thyratrons and consists of the following units:  $V_1$  and  $V_2$  - master gene-

erator,  $V_3 - V_{10}$  - commutator in the form of a closed counting ring,  $V_{11} - V_{13}$  - Kipp relay, which normalizes the duration of the commutation pulses, and  $V_{14} - V_{19}$  - triggers for the control of the keys. An experimental verification of this circuit has shown it to operate reliably over a switching frequency range from 0.1 to 200 cycles. The output keys are capable of switching signals from 0 to  $\pm 25$  volts. The duration of the pulse signals in the system is determined by the delay time of the Kipp relay and can be made greater than or equal to 1 millisecond. The power consumed by the circuit is approximately 3.5 watts.

If pulse-excited measuring devices are used, the commutator is constructed in accordance with the same scheme, but without input keys. The pulses occurring at points A, B and C of the commutator are applied both to the triggers, as well as the circuits comprising tubes  $V_{20} - V_{22}$  (Figure 9), which excite the measuring bridges. In each such circuit, the thyatron plays the role of a controlled discharge switch. At the instant that the control electrode receives the pulse from the commutator circuit, the thyatron ignites, its resistance decreases sharply, and the capacitor discharges to the primary winding of the transformer. The resistances  $r$  are the equivalent input resistances of the measuring bridges. Figure 10 shows an approximate form of the excitation pulse, occurring across a resistance  $r = 200$  ohms.

#### 4. Forming Devices

Depending on the type and structure of the system, on the desirable character of the regulation process, etc., the forming devices should be capable of producing pulse and relay-pulse action signals that can vary with amplitude or duration.

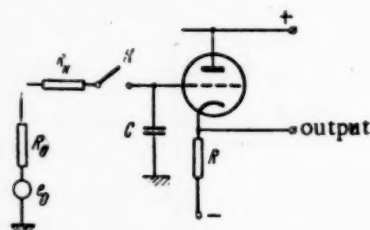


Fig. 11.

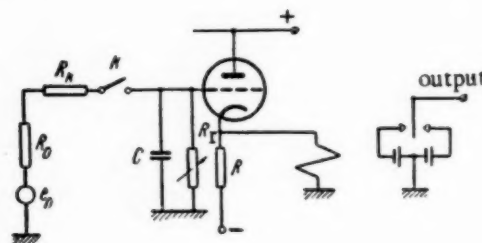


Fig. 12.

Figure 11 shows the diagram of a forming device, capable of producing stepped or amplitude-modulated pulse signals of required duration. In this diagram  $R_0$  and  $e_0$  are the resistance and amplitude of the signals at the output of the common section of the system respectively,  $K$ , the output key of the commutator, and  $R_C$ , its forward resistance. The value of the capacitor  $C$  is chosen to satisfy the condition  $(3-5)C(R_0 + R_C) = t_C$ . If one replaces in the key circuit the two output semiconducting diodes by vacuum diodes and if special cathode follower circuits (doubled) are used, the fixing capacitance is capable of holding a charge without substantial leakage for a considerable length of time. Experimental verification of such a forming circuit has shown that it is possible to obtain a charge leakage rate of approximately 0.3 volts/min at  $C = 0.05$  microfarad.

If the output keys of the commutators are made exclusively of semiconductor diodes, the above circuit will form amplitude-modulated pulse signals of exponential waveform. The time constant of the trailing edge of the pulse depends on the backward resistance of the semiconductor diodes and on the value of the fixing capacitor.



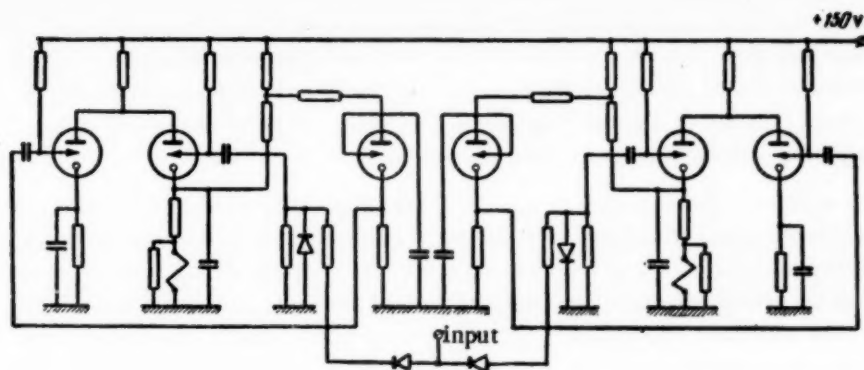


Fig. 13.

A forming circuit, which converts the amplitude-pulse modulation of the control signal into time-duration modulation, is shown in Figure 12. Using regulating resistor  $R_r$  it is possible to change the rate of capacitor discharge, over a certain range, up to the drop-out voltage of the relay. Such a circuit produces a logarithmic dependence of the duration of the output pulses on the amplitude of the input pulses; at small signals, however, not exceeding the sensitivity of the relay by more than a factor 8-10, this dependence may be considered linear. Instead of a contact-making polarized relay it is possible to employ other relay-action devices, such as contactless magnetic relays, to serve as forming and power-amplifying elements. The conversion of the pulse control signal into a relay-pulse signal can be effected without using vacuum tubes in the forming devices and in the output keys.

Figure 13 shows the diagram of such a forming device, made up of cold-cathode MTKh-90 thyatrons. It contains two Kipp relays, one of which is triggered by a positive control pulse, the other by a negative one. Two identical windings of the polarized relay are connected in opposition in the cathode circuits of the first tubes of each Kipp relay. The output signal of the device is pulsed. It differs from the input pulse in the duration of the pulses and in the fact that their amplitude is constant. The duration of the output pulses equals the delay time of the Kipp relay and is established in accordance with the requirement of the dynamics of the regulation system.

### 5. Correcting Device

The known methods for correcting the regulation process, based on converting the error signals, cannot be used in a MRS owing to the fact that the signals from the measuring circuits represent in this case amplitude-modulated pulses of small duration, and the ordinary correcting devices can convert only continuous signals.

The method of correcting with the aid of feedback, which is quite effective, has limited capabilities in the MRS, and if the number of channels is large it is difficult to realize, for it requires a considerable increase in the number of lines between the objects and the regulator.

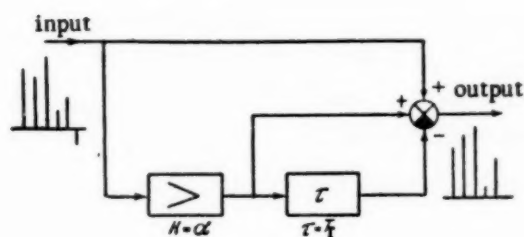


Fig. 14.

It was shown in Reference [10] that correction can be effected in pulse systems by choosing the shapes of the control pulses (in the MRS circuit under consideration here, these pulses are obtained from the forming devices). However, it is not always possible to realize the required form of control pulses such as to insure variation of the dynamic properties of the system in the desired direction.

It is therefore necessary to employ in MRS's special pulse correction methods, the nature of which consists of converting a single pulse sequence, acting in the common section of the system, into another sequence, so as to insure the required properties of the system in each channel.

The pulse method of correction involves connecting a certain pulse network into the common section of the multichannel regulation system so as to change the character of the modulation of the pulse sequence.

That such correction is possible is readily illustrated with a simple example whereby a signal proportional to the first derivative of the error is introduced into the regulation loop. Since discrete values of signals are employed in the MRS, the derivative can be approximated by the first difference, which at values of  $T_r$  which are small compared with the period of the regulation process, correspond to the speed of variation of the error signals. Figure 14 shows the block diagram of a correcting device for a MRS, performing the above function. It represents a pulse network, comprising a delay element with a time delay  $\tau = T_r$ .

Delay elements with  $\tau = T_r$  can be used to create correcting devices for the MRS that introduce into the regulation loop second and higher derivatives, so as to ensure infinite stability in proportional systems and reduce to a minimum the steady-state errors, or to increase the self-oscillation frequency in relay-pulse systems. The method of determining the transfer functions and the structure of the pulse correcting networks is discussed in Ref. [11]. Since the most characteristic values of  $T_r$  range from 1 to 60 seconds, the delay elements are designed at such a time with the aid of magnetic recording on a drum or a continuous tape, or else using memory circuits comprising capacitors or ferrites.

The use of a pulse correcting device in the MRS makes it possible to regulate groups of objects, whose dynamic properties differ greatly. In this case, it is necessary to switch, during each cycle, the various parameters of the correcting device immediately after the circuit around the group of channels, corresponding to regulation objects of the same type, is completed. Thus, in the example given here (Figure 14) it is necessary to switch the gain of the amplifier, the value of which affects the degree of the first-derivative action.

It is possible to use as a universal correcting device for the MRS a digital computer, the operating characteristics of which are determined by suitable choice of its program.

#### LITERATURE CITED

- [1] Iu.G. Kornilov and E.P. Fel'dman, "Multiple-Point Temperature Regulator," *Tochnaia Industria* No. 12 (1940).
- [2] V.U. Kaganov, "Automatic Thermal Regulator of the G.A. Fil'tser System," *TsLA NKChM* (Moscow, 1941).
- [3] D.G. Eitz, D.H. Lukas and D.D. Johnson, "Method of Multichannel Measurement of Physical Quantities with the Aid of Pulse Measurement Methods as Applied to the Investigation of Stresses," *Prikladnaia Mekhanika i Mashinostroenie* No. 4 (1952).
- [4] V.N. Tutevich and V.A. Zhozhikashvili, "Distributor Comprising Magnetic Elements with Rectangular Hysteresis Loops," *Avtomatika i Telemekhanika* 15, No. 1 (1954).
- [5] V.A. Zhozhikashvili and K.G. Mitiushkin, "On the Operation of Computing-Switching Network Employing Magnetic Elements with Rectangular Hysteresis Loops in Remote-Control Devices," *Avtomatika i Telemekhanika* 16, No. 14 (1955).
- [6] L.N. Korablev, "Computing Circuits Operating with Neon Bulbs," *Doklady Akad. Nauk SSSR* 75, No. 3 (1950).
- [7] I.A. Nabiev, "Development and Investigation of Remote Control Devices Using Cold-Cathode Thyatrons," *Candidate's Dissertation* (MEI, 1954).
- [8] L.P. Gieseler, "Magnetic Switching Network for Data Handling Systems," *Proceedings of the National Electronics Conference* Vol. 10 (1953).
- [9] J. Millman and T.H. Puckett, "Accurate Linear Bi-Directional Diode Gates," *Proc. IRE* 43 (Nov., 1955).
- [10] Ia.Z. Tsyarkin, "Calculating the Shapes of Pulses in Continuous-Regulation Systems," *Avtomatika i Telemekhanika* 16, No. 5 (1955).
- [11] Ia.Z. Tsyarkin, "Correction of Pulse Regulation and Control Systems," *Avtomatika i Telemekhanika* 18, No. 2 (1957).\*

Received November 21, 1956

[\* See C.B. translation, *Automation and Remote Control*.]



## MULTIPLYING AND DIVIDING DEVICE EMPLOYING THYRITES

A. A. Maslov

(Moscow)

A new analytic method is proposed for determining the parameters of quadratic elements employing thyrites. A new multiplier circuit employing thyrite quadrators requiring only two operational amplifiers is described. Experimental data on the multiplier are given.

### INTRODUCTION

Multiplying devices employing diode quadrators have been widely used in dc analog devices and in other computers.

While they have sufficiently high accuracy and other good properties, these devices have, at the same time, shortcomings, such as a ragged variation of the output quantity, considerable power consumption in the filament circuit of the diodes, the need for a stabilized reference voltage, high cost, and limited service life.

Multiplying devices constructed of nonlinear quadratic elements (vacuum tubes, semiconductor rectifiers, etc.) are free of these shortcomings, but the latter are unstable in operation and do not provide sufficient accuracy. Accordingly, there is a great interest in the possibility of constructing a multiplying device employing nonlinear resistances, which have stable voltage-current characteristics that can be artificially trimmed to become quadratic. Such, for example, are the carborundum resistances (thyrite, or wilite) [1].

Many articles are devoted to the problem of design of multiplying devices based on carborundum resistances [2-5].

The circuits proposed in [4] and [5] can be used directly in analog equipment, for these circuits incorporate operational dc amplifiers (the former circuit contains five amplifiers, the latter three).

However, the complexity in designing the squaring elements limits the application of the proposed multiplying devices with thyrites. Thus, to design a single quadrator, using the procedure developed by B.L. Benin [3], it is necessary to solve for each thyrite, using the method of successive approximation, a system of four nonlinear equations with four unknowns.

We propose in this work a method for designing the thyrite quadrators, whereby the circuit parameters are determined by substituting into the equations data obtained experimentally when plotting the static characteristics of the thyrite resistances. We also propose a new multiplying-dividing circuit, differing from those proposed earlier [5] in using the minimum number of operational amplifiers (two only), and will give the experimental results on such a circuit.

#### 1. Procedure for Designing Thyrite Quadrators

The characteristics of thyrite resistances differ from quadratic characteristics even in a narrow range. However, by deforming the voltage-current characteristics of the thyrite with the aid of suitably designed linear resistances, it is possible to obtain a characteristic that is nearly quadratic or that approximates any other curve. It is possible to devise many circuits that insure thyrite characteristics that approximate a specified characteristic with any desired degree of accuracy.

Two versions of such circuits are shown in Figures 1 and 2. To determine the values of the resistances of these circuits, let us find out what should be the characteristic of each circuit in order to make the required quadratic dependence ideally accurate. Let us find the required characteristic of the thyrite for the circuit shown in Figure 1.

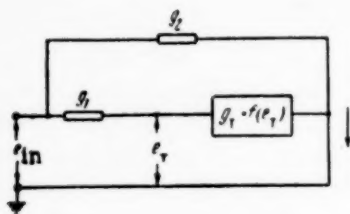


Fig. 1.

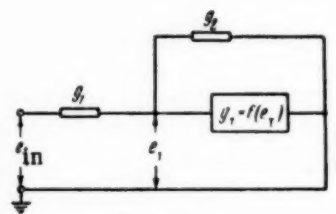


Fig. 2.

To obtain the dependence of  $i = me_{in}^2$  it is necessary that the total conductance of the circuit vary in accordance with the following law

$$g(e_{in}) = \frac{i(e_{in})}{e_{in}} = me_{in} \quad (1)$$

Here  $g(e_{in})$  is the conductance of the circuit as a function of the voltage of the argument, and  $m$  is a scale coefficient.

Expressing  $g(e_{in})$  in terms of the parameters of the circuit and equating the results to Equation (1) we obtain

$$me_{in} = g_2 + \frac{g_1 g_T(e_{in})}{g_1 + g_T(e_{in})} \quad (2)$$

Putting for convenience  $g_2 = g_1(k+1)$ , we obtain from Equation (2)

$$g_T(e_{in}) = \frac{g_1 [me_{in} - g_1(k-1)]}{kg_1 - me_{in}} \quad (3)$$

The voltage on the thyrite resistor should vary as a function of  $e_{in}$  in accordance with the following law:

$$e_T(e_{in}) = e_{in} - \frac{me_{in}^2 - g_1(k-1)e_{in}}{g_1} \quad (4)$$

Solving Equation (4) with respect to  $e_{in}$  and substituting the positive root in Expression (3), we get

$$g_T(e_T) = \frac{\left[ \frac{kg_1^2}{2} - \sqrt{\frac{k^2 g_1^4}{4} - g_1^3 me_T - mg_1 e_T} \right]}{me_T} \quad (5)$$

Hence

$$i = \frac{kg_1^2}{2m} - \sqrt{\frac{k^2 g_1^4}{4m^2} - \frac{g_1^3 e_T}{m} - g_1 e_T} \quad (6)$$

Performing similar operations for the circuit shown in Figure 2, we get

$$i = \frac{g_1^2}{2m} - \sqrt{\frac{g_1^4}{4m^2} - \frac{g_1^3 e_T}{m} - kg_1 e_T} \quad (7)$$

\*[Here, and in subsequent equations, subscript 'T' should be read 't' - editor's note.]

Let us now approximate the characteristic of a thyrite by means of

$$i = a - \sqrt{a^2 - be_T} - ce_T \quad (8)$$

and compare the latter with Equations (6) and (7). We find that to obtain a quadratic dependence the parameters of the circuit of Figure 2 should be

$$r_1 = \frac{1}{g_1} = \frac{2a}{b}, \quad r_2 = \frac{1}{g_1(k-1)} = \frac{1}{g_2} = \frac{2a}{2ac-b}, \quad m = \frac{b^2}{8a^3}, \quad (9)$$

and the parameters of the circuit of Figure 1 should be

$$r_1 = \frac{1}{g_1} = \frac{1}{c}, \quad r_2 = \frac{b}{(2ac-b)c}, \quad m = \frac{c^3}{b}. \quad (10)$$

The coefficients a, b and c are determined from three points of an experimentally-plotted thyrite characteristic.

To obtain the design formulas for coefficients a, b and c, let us solve simultaneously the following system of equations

$$\begin{aligned} i_1 &= a - \sqrt{a^2 - be_{T_1}} - ce_{T_1}, \\ i_2 &= a - \sqrt{a^2 - be_{T_2}} - ce_{T_2}, \\ i_3 &= a - \sqrt{a^2 - be_{T_3}} - ce_{T_3}. \end{aligned} \quad (11)$$

The currents  $i_1$ ,  $i_2$  and  $i_3$  of the thyrite resistor can be measured respectively at voltages  $e_{T_1}$ ,  $e_{T_2}$  and  $e_{T_3}$ .

After separating the square root in each equation and squaring, this system transforms into

$$\begin{aligned} (i_1 + ce_{T_1})^2 - 2a(i_1 + ce_{T_1}) + be_{T_1} &= 0, \\ (i_2 + ce_{T_2})^2 - 2a(i_2 + ce_{T_2}) + be_{T_2} &= 0, \\ (i_3 + ce_{T_3})^2 - 2a(i_3 + ce_{T_3}) + be_{T_3} &= 0. \end{aligned} \quad (12)$$

Eliminating first b and then a from these equations and solving the resultant quadratic equation, we get\*

$$c_{1,2} = \frac{\beta \pm \sqrt{\beta^2 + \alpha\gamma}}{\alpha},$$

where

$$\begin{aligned} \alpha &= [e_{T_1}e_{T_3}i_3(e_{T_3} - e_{T_1}) - e_{T_1}e_{T_2}i_2(e_{T_2} - e_{T_1}) + e_{T_2}e_{T_3}i_1(e_{T_3} - e_{T_1})], \\ \beta &= [i_1i_2e_{T_1}(e_{T_3} - e_{T_1}) - i_1i_3e_{T_3}(e_{T_2} - e_{T_1}) + e_{T_1}i_2i_3(e_{T_3} - e_{T_2})], \\ \gamma &= [i_1i_2e_{T_1}(i_3 - i_1) - i_1e_{T_1}i_3(i_3 - i_1) + e_{T_1}i_2i_3(i_{T_3} - i_{T_1})]. \end{aligned} \quad (13)$$

Using the obtained value of c, we determine the coefficients a and b from the equations

$$a = \frac{e_{T_1}(i_3 + ce_{T_3})^2 - e_{T_3}(i_3 + ce_{T_3})^2}{2(e_{T_1}i_2 - e_{T_3}i_3)}, \quad (14)$$

\*In the calculation it is necessary to employ the positive root

$$c = \frac{\beta + \sqrt{\beta^2 + \alpha\gamma}}{\alpha}.$$

$$b = \frac{2a(i_3 + ce_T) - (i_3 + ce_T)^2}{e_{T_1}} \quad (15)$$

The formulas obtained in this manner make it possible to compute the parameters of the quadrator circuits in Figures 1 and 2 such that their characteristics coincide with the ideal characteristic in three points.

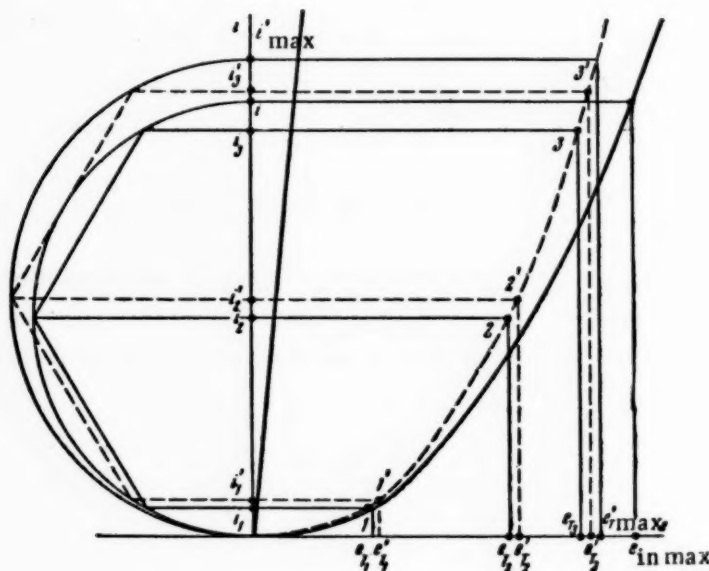


Fig. 3.

The remaining points are subject to a certain error, the maximum value of which depends considerably on the choice of the points on the voltage-current characteristics of the thyrite.

A rational choice of these points, ensuring optimum approximation of the curve described by Equation (18) to the specified voltage-current characteristics, is carried out graphically using the P.L. Chebyshev polygon [6, 7]. For this the following range of variation of the voltage, namely  $0 < e_t < e'_{tmax}$ , was chosen on the experimentally-plotted voltage-current characteristic of the thyrite (Figure 3).\*

The value of  $e'_{tmax}$  was chosen in the first approximation as

$$e'_{tmax} = 0.9 e_{inmax}.$$

A circle of radius  $i'_{max}/2$  was then drawn about the center of the projection of the selection portion of the characteristic on the ordinate axis. A regular hexagon was inscribed in the circle such that two of its sides are perpendicular to the ordinate axis.

From the projections of the vertices of the resultant polygon on the specified voltage-current characteristics one obtains in first approximation the desired points (1', 2' and 3' on Figure 3).

For a more accurate determination of the design points it is necessary to refine the magnitude of the working interval of the thyrite characteristics. For this purpose, the points 1', 2' and 3' are used to calculate the values of the conductances  $g_1$  (Figures 1 and 2). The characteristic of the conductance  $g_1$  is superimposed on the characteristic of the thyrite\* and the maximum value of the input voltage  $e_{inmax}$  is used to determine the maximum values of the thyrite current  $i_{max}$ , after which one finds finally points 1, 2 and 3 (Figure 3).

As a result of calculations performed on several specimens of thyrites, it became clear that the conduct-

\*The characteristic of the thyrite is shown dotted on the graph.

\*\*The total characteristic is shown solid in Figure 3.

ances  $g_2$  of both circuits (Figures 1 and 2) have in most cases negative values. This circumstance imposes a limitation on the use of the circuit of Figure 2, for in this case it is necessary to add to the circuit an additional sign-reversing amplifier, as shown in Figure 4.

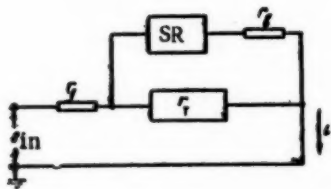


Fig. 4.

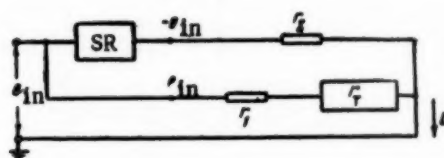


Fig. 5.

The circuit of Figure 1 is more convenient, for to produce a negative value of  $r_2$  it is possible to employ the inverting amplifier, which is usually contained in the functional converters to obtain a negative voltage of the argument (Figure 5). In connection with this, circuit 5 was therefore chosen to construct the multiplying device.

Graphic verification of several quadrators, built in accordance with this diagram and calculated in the above manner, has shown that they can insure the reproduction of a quadratic dependence with a maximum error not exceeding 0.5%.\*

## 2. Summing Quadrator Employing Thyrites

To perform the operation of squaring a sum of several voltages, i.e., to reproduce the function

$$e_{out} = -v \left( \sum_{i=1}^n \zeta_i e_i \right)^2 \quad (16)$$

(where  $\zeta_i$  is the scale coefficient of the  $i$ -th component, and  $v$  the scale coefficient of the function), it is possible to employ the circuit of Figure 6.\*\*

The resistances  $r_{1i}$  and  $r_{2i}$  of the circuit will be chosen to be

$$r_{1i} = \frac{r_1}{\zeta_i}, \quad r_{2i} = \frac{r_2}{\zeta_i}. \quad (17)$$

To determine the resistances  $r_1$  and  $r_2$ , we shall use the circuit shown in Figure 7. The latter is equivalent to the circuit of Figure 6 if

$$\sum_{i=1}^n \frac{(e_i - e_d) \zeta_i}{r_1} = \frac{\sum_{i=1}^n \frac{\zeta_i e_i r_{2i}}{r_1} - e_d}{r_{1e}}, \quad (18)$$

$$\sum_{i=1}^n \frac{\zeta_i e_i r_{2i}}{r_2} = \sum_{i=1}^n \frac{\zeta_i e_i r_{1i}}{r_1}, \quad (19)$$

\*The error is relative to a full scale value of 100 volts.

\*\*It is assumed that  $\sum_{i=1}^n \zeta_i e_i$  is always positive. If the sum of the input voltages changes sign, the function reproduced will be

$$e_{out} = -v \left( \sum_{i=1}^n \zeta_i e_i \right)^2 \text{sign} \sum_{i=1}^n \zeta_i e_i.$$

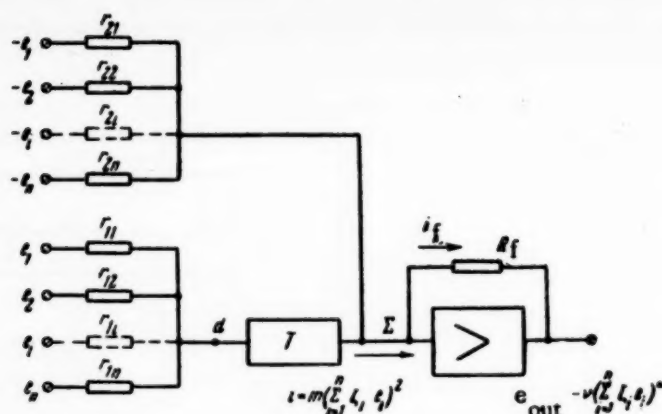


Fig. 6.  $\Sigma$  - summing point of amplifier;  $m$  - scale coefficient of the function (with respect to the current); T - thyrite.

where  $r_{1e}$  and  $r_{2e}$  are the total equivalent resistances.

Solving Equation (18) with respect to  $r_{1e}$ , we get

$$r_{1e} = \frac{r_1}{\sum_{i=1}^n \zeta_i} \quad (20)$$

Condition (19) is satisfied if

$$r_{1e}/r_1 = r_{2e}/r_2 \quad (21)$$

To calculate the parameters of the summing quadrator (Figure 6), it is necessary first to find the maximum value of the input voltage of its equivalent circuit (Figure 7). Eliminating from the expression for  $e_{ine}$  (Figure 7) the resistance  $r_{1e}$ , determined by Equation (20) we get

$$e_{ine} = \frac{\sum_{i=1}^n \zeta_i e_i}{\sum_{i=1}^n \zeta_i} \quad (22)$$

$$e_{ine\max} = \frac{\left(\sum_{i=1}^n \zeta_i e_i\right)_{\max}}{\sum_{i=1}^n \zeta_i} \quad (23)$$

After determining  $e_{ine\max}$ , we determine the resistances  $r_{1e}$  and  $r_{2e}$  and the scale coefficient  $m_e$  of the current characteristic of the quadrator, as described in the preceding section.

The values of  $r_{1i}$  and  $r_{2i}$  are determined from Equations (17), (20) and (21) and amount to

$$r_{1i} = \frac{r_{1e} \sum_{i=1}^n \zeta_i}{\zeta_i}, \quad r_{2i} = \frac{r_{2e} \sum_{i=1}^n \zeta_i}{\zeta_i} \quad (24)$$



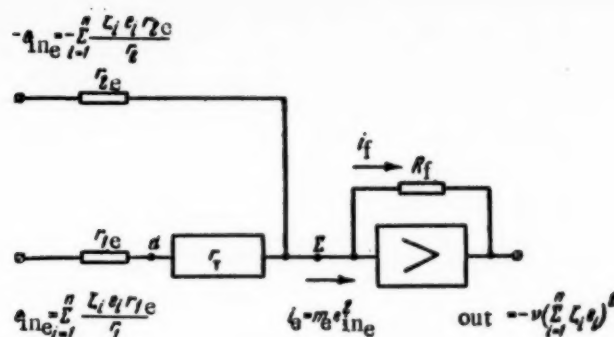


Fig. 7.  $e_{ine}$  - input voltage of equivalent circuit;  $m_e$  - scale of current characteristic of equivalent circuit of the summing thyrite quadrator.

The scale coefficient  $\underline{m}$  of the voltage-current characteristic of the summing quadrator is determined from the equation

$$i = i_e = m_e e_{ine}^2. \quad (25)$$

Using Expressions (16) and (22), we get

$$m = \frac{m_e}{\left(\sum_{i=1}^n \zeta_i\right)^2}. \quad (26)$$

The feedback resistance  $R_f$  of the operational amplifier is determined from the coefficient  $\nu$  using the condition that the currents  $\underline{i}$  and  $i_f$  must be equal, i.e.,

$$\frac{\nu \left(\sum_{i=1}^n \zeta_i e_i\right)^2}{R_{fc}} = m \left(\sum_{i=1}^n \zeta_i e_i\right)^2. \quad (27)$$

Hence

$$R_f = \nu / m. \quad (28)$$

### 3. Thyrite Squaring Circuits for Sign-Reversing Voltages

The squaring circuits given above are suitable only in those cases when the voltage of the argument or the sum of the voltages of the arguments does not change sign.

Squaring a voltage that changes sign (or a sum of such voltages) can be carried out with the circuit of Figure 5 by separating the positive and negative moduli of this voltage, using for example the circuit of Figure 8.

When squaring the sum of several voltages with this circuit, it is necessary to use an additional amplifier for the summation of the input voltages. It is possible to avoid increasing the number of amplifiers in this case if the modulus of the sum of the arguments is separated in accordance with the following formulas:

$$\left| \sum_{i=1}^n \zeta_i e_i \right| = \begin{cases} \sum_{i=1}^n \zeta_i e_i, & \sum_{i=1}^n \zeta_i e_i > 0, \\ \sum_{i=1}^n \zeta_i e_i - 2 \sum_{i=1}^n \zeta_i e_i, & \sum_{i=1}^n \zeta_i e_i < 0 \end{cases} \quad (29)$$

or

$$-\left|\sum_{i=1}^n \zeta_i e_i\right| = \begin{cases} \sum_{i=1}^n \zeta_i e_i - 2 \sum_{i=1}^n \zeta_i e_i, & \sum_{i=1}^n \zeta_i e_i > 0, \\ \sum_{i=1}^n \zeta_i e_i, & \sum_{i=1}^n \zeta_i e_i < 0. \end{cases}$$

By way of an example, let us consider a circuit for squaring the sum of two voltages, intended for a multiplying device (Figure 9).

The voltage  $(-e_x - e_y)/2$ , obtained with the aid of a summing amplifier, is resolved by means of a diode key  $g_1, R_2, g_2, g_3, R_2', g_4$  into two components:

$$e_1 = \begin{cases} 0, & \frac{-e_x - e_y}{2} < 0, \\ \frac{-e_x - e_y}{2}, & \frac{-e_x - e_y}{2} > 0 \end{cases} \quad (30)$$

and

$$e_2 = \begin{cases} \frac{-e_x - e_y}{2}, & \frac{-e_x - e_y}{2} < 0, \\ 0, & \frac{-e_x - e_y}{2} > 0. \end{cases}$$

Resistances  $R_2$  and  $R_2'$  of the diode key are equal and are intended to maintain the diodes  $g_2$  or  $g_4$  in open state for closed  $g_1$  or  $g_3$ . Their value is chosen in accordance with the condition

$$\frac{e_d}{r_{12}} \leq \frac{-e_x - e_y}{2R_2}. \quad (31)$$

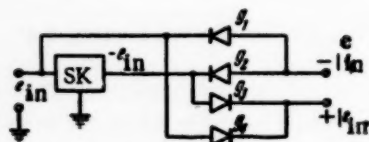


Fig. 8.

The voltages  $e_x, e_y$  and  $4e_1, 4e_2$  are combined in the summing quadrator as shown in Figure 9.

Since  $e_x + e_y + 4e_1 = |e_x + e_y|$  and  $e_x + e_y + 4e_2 = |e_x + e_y|$ , when the switch is placed in the "plus" position, the current flowing into the summing point of the amplifier  $\Sigma$  (the amplifier is not shown in the diagram) is

$$i = m(e_x + e_y + 4e_1)^2 = m(e_x + e_y)^2.$$

When the switch is changed to the "minus" position, the current  $i$  changes sign

$$i = -m(e_x + e_y)^2.$$

At the end of this section we shall consider a circuit for squaring the difference of two voltages, as shown in Figure 10. The circuit employs the principle proposed in [8] for obtaining the difference of two voltages

$$\frac{e_x - e_y}{2} = \frac{-e_x - e_y}{2} + e_x \quad (32)$$

and

$$-\frac{e_x - e_y}{2} = \frac{-e_x - e_y}{2} + e_y. \quad (33)$$

The modulus of half the difference between  $e_x$  and  $e_y$  is separated in this case by adding to the voltage  $(-e_x - e_y)/2$  a large initial voltage,  $e'_1 = \max(e_x, e_y)$ , i.e.,

$$|e_x - e_y| = 2 \left[ \left( \frac{-e_x - e_y}{2} \right) + \max(e_x, e_y) \right]. \quad (34)$$

The negative modulus of the difference of voltages  $e_x$  and  $e_y$  is formed by adding to the voltage  $(-e_x - e_y)/2$  the smaller input voltage

$$-|e_x - e_y| = 2 \left[ \frac{-e_x - e_y}{2} + \min(e_x, e_y) \right]. \quad (35)$$

The largest and smallest voltages  $e'_1 = \max(e_x, e_y)$  and  $e'_2 = \min(e_x, e_y)$  are obtained with the aid of diode keys  $g_5, g_6, R_3$ , and  $g_7, g_8, R'_3$ .

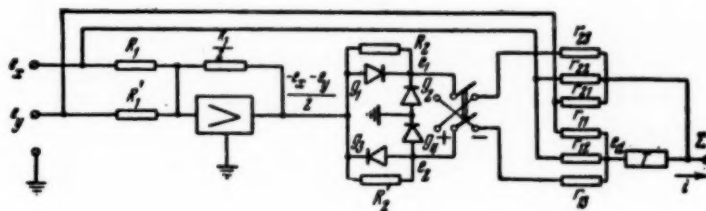


Fig. 9.

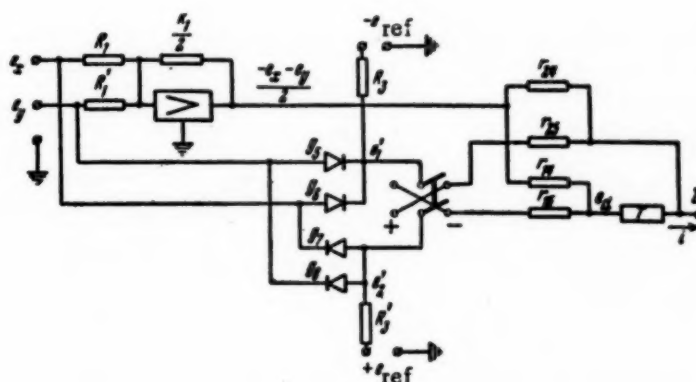


Fig. 10.

The principle of operation of one of these keys is explained in Figure 11.

If both input voltages (or one of these) are positive, the diode conducting will be the one having the higher plate voltage, and therefore the voltage passing through point a will be the one that happens to be larger at the given instant. For the key to work also at negative values of  $e_x$  and  $e_y$ , the potential of the point a is reduced by voltage  $e_{ref}$ . Here it is necessary that the following inequalities be observed

$$\left| \frac{e_{ref} R_{ref}}{R + R_n} \right| > |e_{y \max}| \quad \text{and} \quad \left| \frac{e_{ref} R_{ref}}{R + R_l} \right| > |e_{x \max}|. \quad (36)$$

For given values of  $e_{ref}$  and  $R_l$ , this condition is satisfied by choosing resistance  $R$  in accordance with

$$R \leq R_l \frac{e_{ref} - e_{\max}}{e_{\max}}, \quad (37)$$

where  $e_{\max} = e_{x \max} = e_{y \max}$ .

To separate the smaller of the two voltages it is enough to change the connections of the diodes, making the anodes of the diodes common, and to change the sign of the reference voltage  $e_{ref}$ .

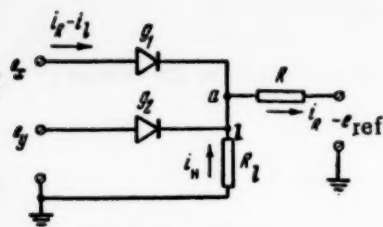


Fig. 11.

If an unstabilized source of supply is used to provide the voltage  $e_{ref}$ , it is necessary to substitute into (37) the minimum value of  $e_{ref}$ .

In the diode keys of the circuit of Figure 10, the role of the resistance  $R$  is played by resistances  $R_3$  and  $R'_3$ . To calculate their value it is necessary to replace in Equation (37) the resistance  $r_{15}$  in lieu of  $R_1$ , since  $e_d$  of the thyristor (Figure 10) is zero for the maximum input voltages.

In all other respects the circuit of Figure 10 operates in the same manner as that shown in Figure 9.

The current flowing through the summing point is obtained from the equation  $i = m(e_x - e_y)^2$ . The sign of the current is changed by means of the switch.

#### 4. Principal Diagram of Multiplying-Dividing Network

The multiplication circuit shown in Figure 12, as in the case of the majority of networks employing quadrators, is based on the relationship

$$e_z = \frac{1}{400} [(e_x + e_y)^2 - (e_x - e_y)^2] = \frac{1}{100} e_x e_y.$$

The circuit was designed for input and output voltages ranging from  $-100$  to  $+100$ .

The division circuit is based on the multiplication network as is done in the multiplying-dividing network used in the EMU-5 electronic analog apparatus [9]. The sum and difference of voltages  $e_x$  and  $e_y$  are squared with the aid of the circuit shown in Figure 9. The current scale factors of the two circuits is made equal by using thyrites with identical characteristics, adding to the circuit used to square the difference of the voltages  $e_x$  and  $e_y$ , a resistance  $r_{16}$  (Figure 12), the value of which is chosen in accordance with Equation (26).

It follows from (26) that to make the scales of each of the circuits equal for equal values of  $m_e$  it is necessary that the sums of the coefficients of the individual components be equal. For this purpose, the value of the resistance  $r_{16}$  is chosen to be

$$r_{16} = \frac{r_1}{2} = 3r_{1e}.$$

The resistances  $r_{21}$ ,  $r_{22}$  and  $r_{24}$  of the circuits of Figures 9 and 10 and in the complete principal diagram of a multiplying-dividing network (Figure 12) have been eliminated, since the sum of the currents sent by these resistances into the summing points of the amplifier  $\Sigma$  is always zero.

The voltage-current characteristics of the thyrites are made equal in the realized circuits of the multiplication-division network in two ways:

1. If the available thyrites have characteristics that do not differ from each other by more than  $\pm 10\%$ , one connects in parallel to the thyrite with the smaller current level a resistance  $r$  (Figure 12), the value of which is chosen to satisfy the condition that the approximated characteristics must coincide at the terminal points of the working range. This method ensures similarity of the characteristic with an accuracy of approximately 0.2% of the maximum current.
2. By placing on the same specimen of thyrite three electrodes in such a way, that it becomes possible to obtain both characteristics. Here it is necessary to place the electrodes in such a way that the electrode connected to the summing point of the amplifier is between the two others, for example, as shown in Figure 13. The potential of the center electrodes remains unchanged, and therefore in addition to serving its principal function, this electrode eliminates also the leakage between the outside electrodes.

When we checked the multiplying-dividing network constructed in accordance with the circuit discussed in this article, we employed thyrites in the form of a disc 50 mm in diameter and 10 mm in height. The placement of the electrodes is shown in Figure 14.

The characteristics of each half of the thyrite were trimmed by applying to them equal voltages of opposite polarities (Figure 14). If the current  $i_\Sigma$  was positive, the left electrode was reduced, and vice versa.

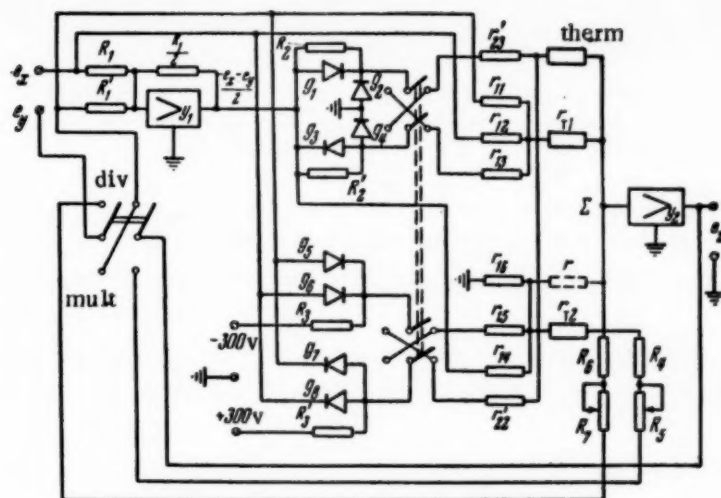


Fig. 12.  $g_1, g_2, g_3, g_4$  - DG-Ts25;  $R_5, R_7$  - potentiometers of the Omega type;  $g_5, g_6, g_7, g_8$  - DG-Ts27;  $r_{t1}$  and  $r_{t2}$  - thyrites;  $r_{th}$  - type MMT thermistor;  $R_1$  to  $R_4, R_6$  - type VS and NLT resistors.

When  $i_\Sigma = 0$ , and for equal current-characteristic scale factors, the maximum error for both halves of the thyrite did not exceed 0.2% in this case.

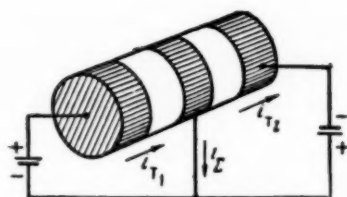


Fig. 13.

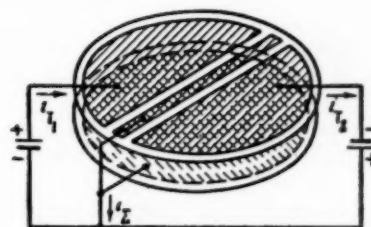


Fig. 14.

The temperature error of the multiplying-dividing network, resulting from the negative temperature coefficient of the thyrite discs [1], was compensated for with the aid of a thermistor  $r_{th}$  (Figure 12). The values of resistances  $r_{23}$  and  $r_{22}$  of the circuits of Figures 9 and 10 were replaced when connected to the thermistor by  $r'_{23}$  and  $r'_{22}$  so that the current flowing through these resistances into the summing point of the amplifier remain constant. For this purpose it was necessary to satisfy the relation

$$\frac{1}{r_{23}} = \frac{1}{r'_{23} \left( \frac{r_T}{r'_{23}} + 1 \right) + r_T}, \quad \frac{1}{r_{22}} = \frac{1}{r'_{22} \left( \frac{r_T}{r'_{22}} + 1 \right) + r_T}. \quad (38)$$

The calculated value of resistance  $r_{23}$  is always half the calculated value of resistance  $r_{22}$ , and therefore the resistances  $r'_{23}$  and  $r'_{22}$ , obtained from Equation (38), should equal

$$r'_{23} = r_{23} - 1.5r_T, \quad r'_{22} = r_{22} - 3r_T. \quad (39)$$

In the multiplication-division networks realized in this work, we employed type MMT thermistors which had a negative temperature coefficient ranging from 2.8 to 3%/°C [10].



The value of the resistance of the thermistor was chosen from the condition that the temperature error be compensated for at the maximum value of the output voltage  $e_{z\max} = 100$  volts.

For this purpose, the temperature coefficient of resistances  $r_{22}$  and  $r_{23}$  should be

$$\eta_{r_{22}} = \eta_{r_{23}} = \eta_e \frac{i_{t\max}}{i_{(r_{22}+r_{23})\max}} \quad (40)$$

Here  $\eta_{r_{22}}$  and  $\eta_{r_{23}}$  are the temperature coefficients of resistances  $r_{22}$  and  $r_{23}$ ,  $\eta_e$  is the equivalent temperature coefficient of the thyrite and of the resistances connected in series with it,  $i_{t\max}$  is the maximum current flowing through each of the thyrites, and  $i_{(r_{22}+r_{23})\max}$  is the maximum total current through resistances  $r_{22}$  and  $r_{23}$ .

The coefficient  $\eta_e$  is negative and ranges from 0.3-0.4%/°C for various thyrite discs. The ratio  $i_{t\max}/i_{(r_{22}+r_{23})\max}$  ranges from 3 to 4, and therefore the coefficients  $\eta_{r_{22}}$  and  $\eta_{r_{23}}$  were approximately taken to be 1%/°C.

The resistance of the thermistor is determined from Equation (39), rewritten to allow for the temperature variation:

$$(r_{23} - 1.5r_T)(1 + \eta_r \Delta\theta) = r_{23}(1 - \eta_{r_{22}} \Delta\theta) - 1.5r_T(1 - \eta_r \Delta\theta),$$

where  $\eta_r$  is the temperature coefficient of types VS and MLT resistors, and  $\eta_{th}$  is the temperature coefficient of the thermistor, and  $\Delta\theta$ , the increment in the temperature.

Hence

$$r_T = r_{23} \frac{\eta_{r_{22}} + \eta_r}{1.5(\eta_r + \eta)} \approx 0.25r_{23} \quad (41)$$

## 5. Results of Experimental Verification of the Multiplying-Dividing Network

When checking the experimental models of the multiplying-dividing networks, the following results were obtained.

1. The maximum static error of each of the models in the multiplication of two voltages did not exceed 0.6% of the full scale of 100 volts at room temperature. The maximum error in division did not exceed 2%.
2. The temperature error without compensation amounted to 0.3-0.4%/°C. After compensation, the maximum temperature error did not exceed 0.5% with the unit heated to +50°C.
3. The frequency characteristic was plotted while multiplying and dividing a constant sinusoidal voltage. In both cases, the frequency characteristic remained flat within the passed band of the operational amplifiers used, i.e., 100 cycles at an output voltage amplitude of 100 volts.

## SUMMARY

1. The methods proposed in this work for separating the moduli of the sums and differences of two voltages made it possible to develop a multiplication network using quadrators with a minimum number of operational amplifiers (two amplifiers) compared with the previously-proposed versions.
2. The procedure detailed for the design of quadrators employing nonlinear resistances makes it possible to calculate the circuit parameters by means of formulas given in closed form.
3. The multiplication network using thyrites are not inferior in accuracy and stability to diode networks, and at the same time have many new valuable properties. Among the advantages of such networks are: a) simplicity of circuit and low cost; b) reliability and long service life; c) absence of reference voltage; d) smooth variation of the output voltage and of its derivatives.

The circuit developed differs from the thyrite multiplication networks proposed earlier in that they employ a new quadrator circuit, use a new method for separating the moduli of sums of differences of the input quantities,



and are able to perform the division operation.

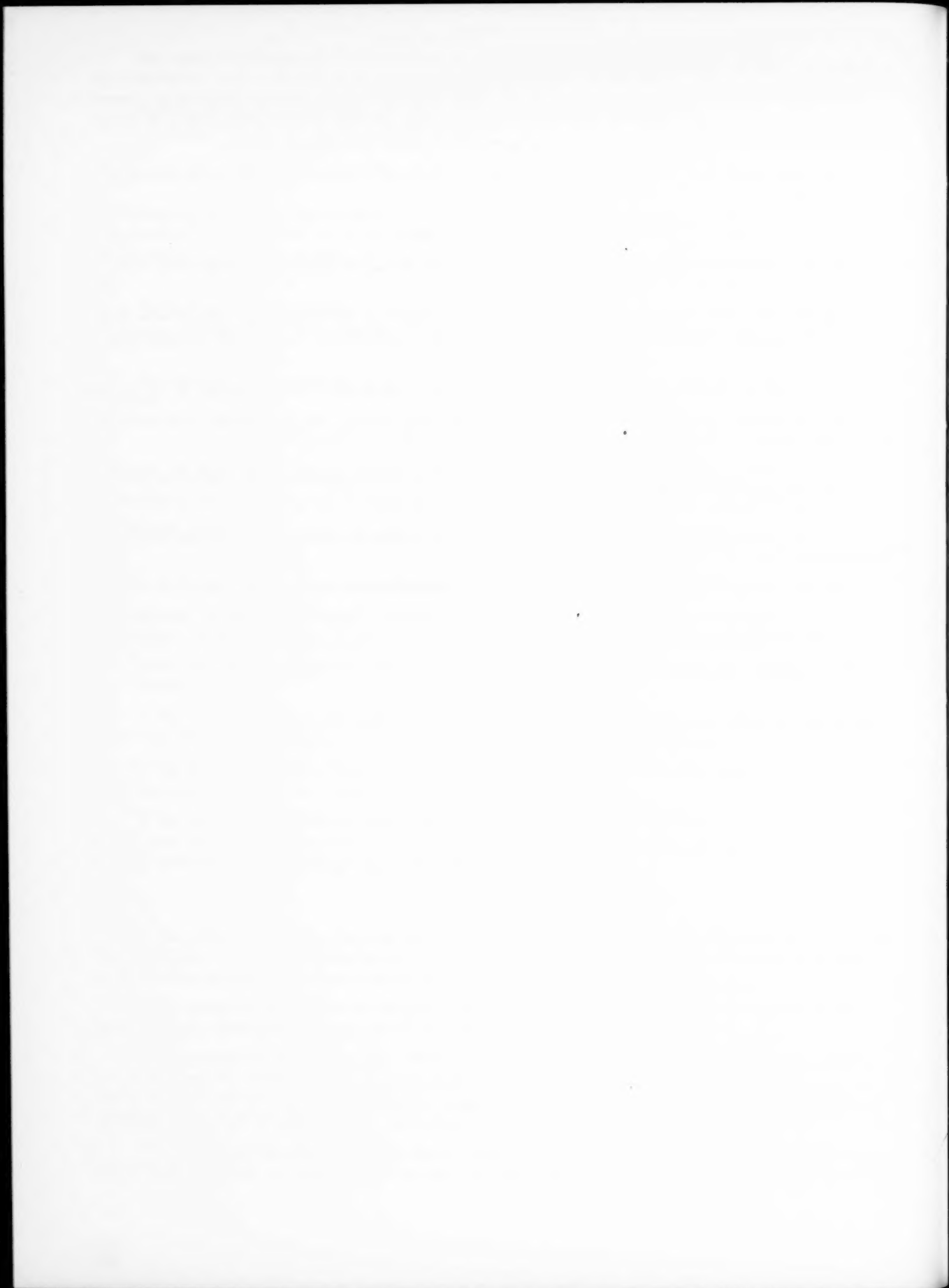
A general shortcoming of multiplication networks using thyrites is the need for determining the parameters of the circuit for each model. However, the above shortcoming does not limit the possibility of using the above circuit, which can be recommended for use in analog computers and other computing devices.

The author thanks B.Ia. Kogan for help and valuable advice in the development of the circuit considered in this article.

#### LITERATURE CITED

- [1] M.A. Rozenblat and O.A. Sedykh, "Electrical Properties and use of Carborundum Resistances," *Avtomatika i Telemekhanika* 12, No. 4 (1951).
- [2] G.N. Balasanov, "Theoretical and Experimental Investigation of Static Power Transformers with Semi-conducting Resistances," Dissertation, Institute of Automation and Telemekhanics, Academy of Sciences, USSR (Moscow, 1954).
- [3] V.L. Benin, "Wattmeter Using Carborundum Resistances," *Avtomatika i Telemekhanika* 16, No. 2 (1955).
- [4] L.D. Kovach and V. Comley, "An Analog Multiplier Using Thyrite," *IRE Transactions - Electronic Computers* (June, 1954).
- [5] L.N. Fitsner, "Multiplication Unit Using Thyrites," *Priborostroenie (Instrument Building)* No. 4 (1956).
- [6] P.L. Chebyshev, "Collected Works," Volume 2 (1947), pp. 23-51.
- [7] N.E. Kobrinskii, *Matematicheskie mashiny nepreryvnogo deistviia (Mathematical Analog Computers)*, Gostekhizdat, 1954.
- [8] G.A. Korn and T.M. Korn, "Electronic Analog Computers," (McGraw Hill Book Co., New York, 1952).
- [9] V.A. Trapeznikov, B.Ia. Kogan, V.V. Gurov and A.A. Maslov, "Type EMU-5 Electronic Analog Apparatus," ITEIN, Academy of Sciences, USSR (1956).
- [10] I. Petrov, "Thermistors," *Radio* No. 7 (1955).

Received June 11, 1956



# ON THE THEORY OF HALF-WAVE MAGNETIC AMPLIFIERS. • I.

R.A. Lipman and I.B. Negnevitskii

(Moscow)

In 1951 R. Ramey [1, 2] described a new circuit of magnetic amplifier, differing from the usual circuits in its high speed. Such amplifiers were called half-wave amplifiers in the literature. Thereafter, many magnetic amplifier circuits, based on the simple Ramey circuit, have appeared. The descriptions of the physical processes and the calculation of the characteristics of the Ramey amplifier, contained in the available literature [1-5], are inadequate. In addition, there is no detailed analysis of the transients or of the cases where control is effected by various types of signals.

The published reference containing the most detailed theoretical analysis of the Ramey circuit is [3]. However, [3] considers only control by means of rectified half-wave sinusoidal voltage, while in practice it is no less interesting to investigate the control by alternating sinusoidal or by dc voltages. Reference [3] does not analyze the change in the current in the control circuit, does not show the range of applicability of the derived equation for the load current and for the voltage gain coefficient, and does not consider the problem of the power gain.

This article is devoted to an analysis of all these problems.

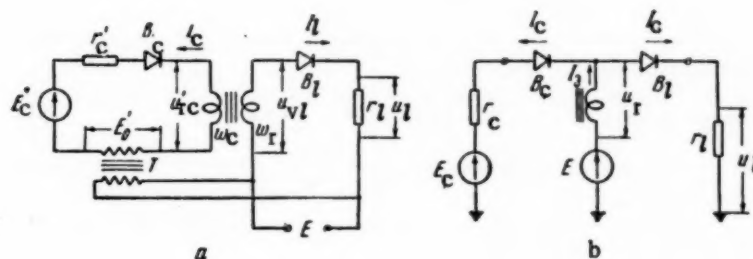


Fig. 1.

The principal circuit of the amplifier is shown in Figure 1a. The right half of the diagram shows the load circuit, and the left one the control circuit. The voltage  $E_0$  and the control circuit will be called the reference voltage. The transformer  $T$  serves to decouple the load and control circuits.

The supply voltage  $E$  of the amplifier and the reference voltage  $E_0$  are sinusoidal, have the same frequency, and are in phase.

In the steady state, it is advisable to distinguish between the so-called control half cycle, when rectifier  $V_c$  conducts and the core is demagnetized (is magnetized in the negative direction), and the working half cycle, when rectifier  $V_l$  conducts, the load carries a current, and the core is magnetized in the positive direction.

•Delivered at the Seminar on Magnetic Amplifiers at the Institute of Automation and Remote Control, Academy of Sciences, USSR, April 4, 1956.

During some instant of time in the working half-cycle, the core saturates and the supply voltage is applied to the load. The instant of saturation, and consequently, also the voltage across the load, is determined by the degree of demagnetization of the core during the control half cycle, which in turn depends on the control voltage. This indeed is the principle on which the operation of this magnetic amplifier is based.

### Basic Assumptions

We shall analyze this amplifier subject to the following assumptions.

1. The core of the amplifier reactor is made of a material with an ideal rectangular hysteresis loop.

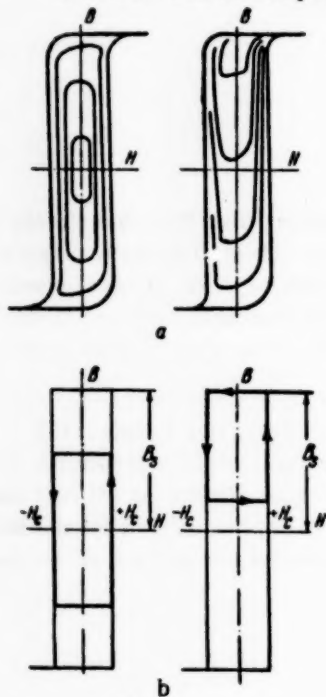


Fig. 2.

Figure 2a shows the type of real dynamic hysteresis loops and several particular cycles with constant demagnetization and without it, while Figure 2b shows the idealization assumed for the dynamic loops and particular cycles.

That it is possible to employ such an idealization for a qualitative analysis of the processes on the amplifier is obvious. As will be shown below, even the quantitative agreement with the experimental data will be good if high grade magnetic materials with rectangular hysteresis loop (type N50-P and N65-P) are used. A magnetic material with an ideal rectangular hysteresis loop is characterized by two parameters - the saturation flux density  $B_s$  and the coercive force  $H_{c0}$ . A reactor with a core made of such a material, having a cross section  $S$ , an average length of flux line  $l$ , and a winding with  $w$  turns supplied by a sinusoidal voltage, can also be characterized by two parameters: the saturation voltage and the "arbitrary coercive" current:

$$E_{sm} = \omega w S B_s 10^{-8}, \quad I_{co} = \frac{H_{c0} l}{w}. \quad (1)$$

2. The inverse current of the rectifiers is in all cases small compared with the current  $I_{co}$ .

Here it is possible to neglect the inverse currents and to assume backward resistance of the rectifiers to be infinite.

3. The control and load circuits are purely resistive.
4. The resistances of the reactor windings and the forward resistance of the rectifiers is contained in resistances  $r_l$  and  $r'_c$  respectively (Figure 1a).
5. The resistances  $r_l$  and  $r'_c$  are related by

$$r'_c (w_l/w_c)^2 > r_l. \quad (2)$$

Otherwise, as will be seen from the discussion that follows, the control and load circuits so to speak interchange places in the absence of the signal, saturation will occur during the control half cycle, and demagnetization will occur during the operating half cycle.

If all the quantities of the control circuit are referred to the load circuit, we have

$$r_c = r'_c \left( \frac{w_l}{w_c} \right)^2, \quad I_{co} = \frac{H_{c0} l}{w_l}, \quad e_c = e'_c \frac{w_l}{w_c}, \quad e_0 = e'_0 \frac{w_l}{w_c}, \quad i_c = i'_c \frac{w_c}{w_l} \quad (3)$$

and if we take into account that the operation of the amplifier is usually considered at

$$\frac{E'_0}{w_c} = \frac{E}{w_l},$$

$$E_m \leq \omega w B_s S 10^{-8} \quad \text{or} \quad \varepsilon = \frac{E_m}{E_{sm}} \leq 1, \quad (4)$$

it becomes evident that the amplifier circuit of Figure 1a can be replaced by an equivalent circuit of Figure 1b, where the arrows indicate the chosen positive directions.

The processes in the amplifiers will be analyzed subject to the Supplementary Conditions (4), although the first of these two conditions, as will be shown below, is not obligatory. The analysis will be carried out using the circuit of Figure 1b, but the end results will be given also for the initial circuit.

The quantities referred to the load circuit will be unprimed, and the principal ones primed.

### Steady-State Operation

An analysis of the processes in the steady state is carried out for control with: a) rectified half-wave voltage; b) alternating sinusoidal voltage; and c) dc voltage.

In all cases the supply voltage is

$$e = E_m \sin \omega t = E_m \sin \theta. \quad (5)$$

#### a) Control with Half-Wave Rectified Voltage

A "positive signal" is applied to the input of the amplifier

$$\begin{aligned} e_c &= E_{cm} \sin \theta & \text{at} & \quad -\pi \leq \theta \leq 0, \\ e_c &= 0 & \text{at} & \quad 0 \leq \theta \leq \pi. \end{aligned} \quad (6)$$

Control half-cycle ( $-\pi \leq \theta \leq 0$ ). We shall assume that during the control half cycle, the current in the load circuit is zero.

Let us assume that at the start of the half cycle ( $\theta = \theta_0 = -\pi$ ) the core is saturated and its state is determined by the point 0 on the hysteresis loop (Figure 3a). With this, the reactor voltage  $u_r$  is zero and the current flowing through the control circuit is

$$i_c = \frac{e - e_c}{r_c} = \frac{E_m - E_{cm}}{r_c} \sin \theta. \quad (7)$$

During the instant when  $\theta = \theta_1$ , the current  $i_c$  becomes equal to  $-I_{c0}$ . The state of the core is now determined by point 1. The core then begins to demagnetize, and the control current remains unchanged:

$$i_c = -I_{c0}. \quad (8)$$

The demagnetization takes place under the influence of the following voltage applied to the reactor

$$u_r = e - e_c - i_c r_c = e - e_c + I_{c0} r_c. \quad (9)$$

When the reactor voltage becomes zero, the demagnetization terminates ( $\theta = \theta_2$ ). The magnetic state of the core is now determined by point 2.

It follows from (7) that the angle  $\theta_1$  can be determined from the expression

$$\theta_1 = \arcsin \left( \frac{I_{c0} r_c}{E_m - E_{cm}} \right) - \pi, \quad (10)$$

and the angle  $\theta_2$  is

$$\theta_2 = -\pi - \theta_1. \quad (11)$$

Starting with the instant of time when  $\theta = \theta_2$ , the current  $i_c$  attempts to assume an absolute value that is less than  $I_{c0}$ , and as a result the magnetic state of the core goes through a minor cycle. Under the assumptions

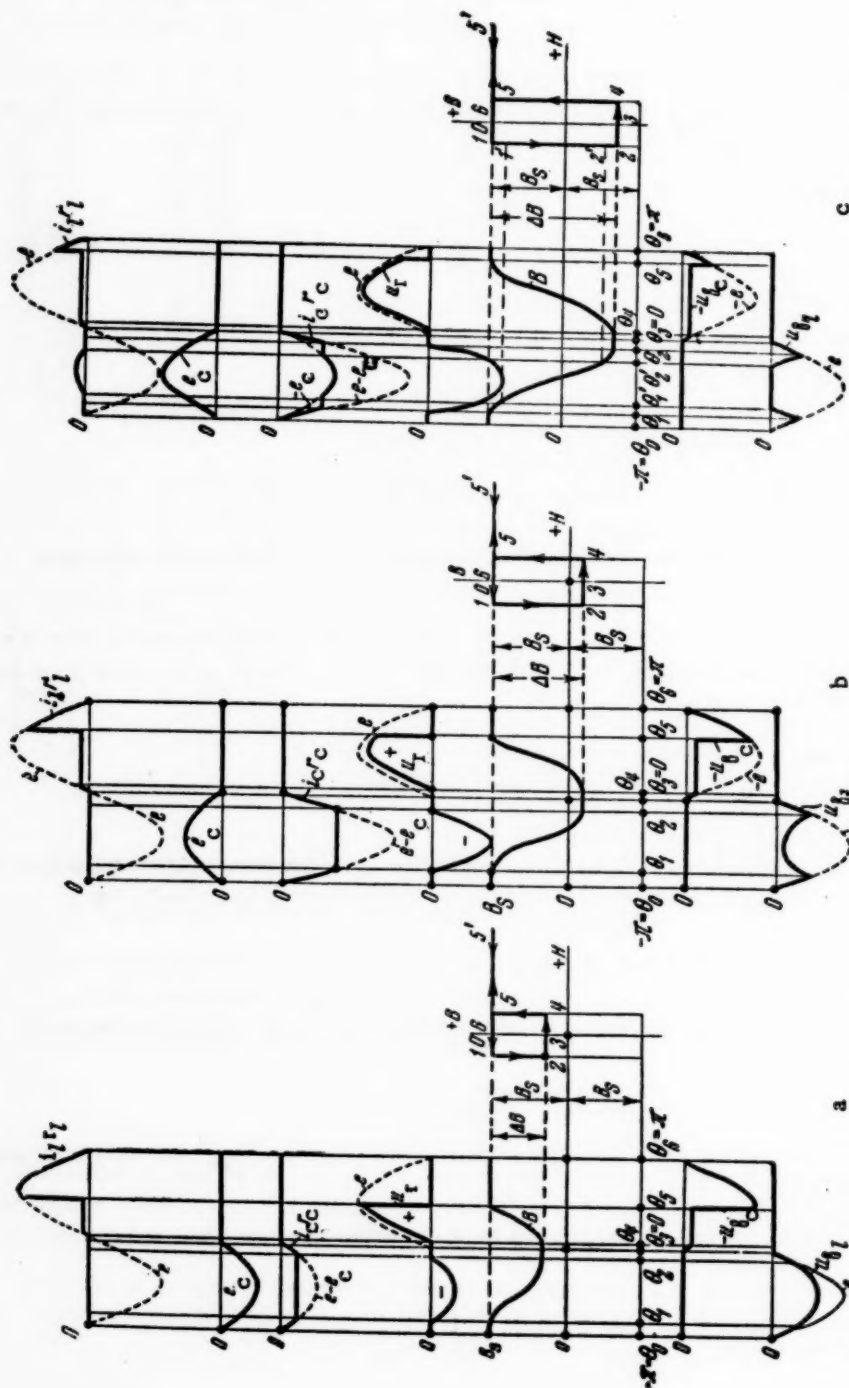


Fig. 3. Theoretical curves for the variation of the supply voltage, control voltage across the reactor, voltage across the rectifiers, as well as of the currents and induction in the core, occurring when a rectified half wave control voltage is used: a) for "positive" signal  $e_c = E_{cm} \sin \theta$ ; b) for "negative" signal  $e_c = -E_{cm} \sin \theta$ ; c) for large "negative" signal, when  $E_{cm} > I_{0f} \omega L$ .



made above, this change occurs at a constant flux density (portion 2-3 on the loop, Figure 3a), and consequently the voltage across the reactor remains zero, and the control current again is determined by Equation (7).

When  $\theta = \theta_3 = 0$ , the current  $i_c$  becomes equal to zero, the state of the core corresponds to point 3 on the loop (Figure 3). This terminates the control half cycle.

In this case, the condition that no current flow through the load during the control half cycle is satisfied. Actually, the current  $i_l = 0$  if rectifier  $V_l$  is blocked, i.e., if

$$u_{vl} = e - u_r < 0. \quad (12)$$

Since  $e < 0$ , Condition (12) is satisfied during the entire control half cycle, because  $u_r$  is either zero or else satisfies Equation (9).

Figure 3a shows graphs for the variation of the supply and control voltages across the reactor, the valves, and also on the currents and flux density in the core.

Let us consider the case where the "sign" of the control voltage changes - a "negative" signal:

$$\begin{aligned} e_c &= -E_{cm} \sin \theta & \text{at } -\pi \leq \theta \leq 0, \\ e_c &= 0 & \text{at } 0 \leq \theta \leq \pi. \end{aligned} \quad (13)$$

If we assume also, in this case, that the load current is zero during the control half cycle, the processes described above remain the same in the amplifier, and it is necessary to reverse the sign of  $E_{cm}$  in the equations. Now, however, Condition (12) will be satisfied only if

$$E_{cm} \leq I_{co} r_c. \quad (14)$$

The corresponding graphs for the variations of the voltages, currents, and flux density are given in Figure 3b.

Let us follow the course of the process in the case when Condition (14) is not satisfied, i.e., if the control signal is too large (Figure 3c).

The initial conditions being the same in the interval from  $\theta = \theta_0 = -\pi$  to  $\theta = \theta_1$ , the core is saturated, the reactor voltage is zero, and the current flowing in the control winding is

$$i_c = \frac{e - e_c}{r_c} = \frac{E_m + E_{cm}}{r_c} \sin \theta. \quad (15)$$

During the instant corresponding to  $\theta_1$ , we have  $i_c = I_{co}$  and

$$\theta_1 = \arcsin \left( \frac{I_{co} r_c}{E_m + E_{cm}} \right) - \pi. \quad (16)$$

Rectifier  $V_l$  is blocked ( $u_{vl} = e < 0$ ). After  $\theta = \theta_1$ , the core begins to demagnetize under the influence of the voltage across reactor (9).

The voltage across rectifier  $V_l$  is now

$$u_{vl} = e - u_r = e_c - I_{co} r_c = -E_{cm} \sin \theta - I_{co} r_c. \quad (17)$$

If Condition (14) is not satisfied, then the voltage  $u_{vl}$  becomes zero at  $\theta = \theta'_1$ , and will then tend to become positive, and rectifier  $V_l$  will start conducting. It is obvious that

$$\theta'_1 = \arcsin \left( \frac{I_{co} r_c}{E_{cm}} \right) - \pi. \quad (18)$$

With rectifier  $V_l$  conducting, and bearing in mind that the current flowing in the reactor is  $i_e = -I_{co}$  (the

operating point shifts on the hysteresis loop along section 1-2), we can write

$$e_c = -i_c r_c + i_l r_l, \quad i_l = i_l - i_c = -I_{co} - i_c, \quad (19)$$

hence

$$i_c = -\frac{e_c + I_{co} r_l}{r_l + r_c}, \quad i_l = \frac{e_c - I_{co} r_c}{r_c + r_l}. \quad (20)$$

The demagnetization of the core continues under the influence of the following voltage

$$u_r = e - e_c \frac{r_l}{r_l + r_c} + I_{co} \frac{r_c r_l}{r_c + r_l}. \quad (21)$$

Rectifier  $V_l$  remains conducting until  $\theta = \theta'_2$  ( $\theta'_2 = -\pi - \theta'_1$ ) when the current  $i_l$  becomes zero (Figure 3c), because after this time  $u_{Vl} < 0$  and rectifier  $V_l$  is cut off. Here the current is  $i_c = -I_{co}$ , and the voltage across the reactor is given by (9). The demagnetization continues until  $\theta = \theta_2$  ( $\theta_2 = -\pi - \theta_1$ ), when  $u_r = 0$ . Starting with  $\theta_2$ , the voltage  $u_r$  remains zero, and the control current varies in accordance with (15).

When  $\theta = \theta_3 = 0$ , the current  $i_c = 0$  and the magnetic state of the core corresponds to the point 3 (Figure 3c). This concludes the control half cycle.

Working Half Cycle ( $0 \leq \theta \leq \pi$ ). In the interval from  $\theta = \theta_3 = 0$  to  $\theta = \theta_4$  the flux density in the core remains constant, the voltage across the reactor is zero, and the load current varies as

$$i_l = \frac{e}{r_l} = \frac{E_m}{r_l} \sin \theta. \quad (22)$$

When  $\theta = \theta_4$  (the magnetic state of the core is determined by point 4 on the loop, Figure 3), the load current becomes  $+I_{co}$ , and

$$\theta_4 = \arcsin \frac{I_{co} r_l}{E_m}. \quad (23)$$

A positive voltage appears across the reactor, and the core begins to demagnetize (the operating point shifts along section 4-5 of the loop).

Since the load current remains constant

$$i_l = I_{co}, \quad (24)$$

the magnetization occurs under the influence of the following voltage:

$$u_r = e - i_l r_l = e - I_{co} r_l. \quad (25)$$

When  $\theta = \theta_5$ , the core saturates (point 5 on the hysteresis loop), the voltage is  $u_r = 0$ , and all the supply voltage is applied to the load

$$u_l = i_l r_l = e = E_m \sin \theta. \quad (26)$$

The angle  $\theta_5$  can be calculated from the condition that the voltage across the loop, averaged over the cycle, should be zero

$$\int_{-\pi}^{\pi} u_r d\theta = \int_{\theta_1}^{\theta_2} u_r d\theta + \int_{\theta_4}^{\theta_5} u_r d\theta = 0. \quad (27)$$

After  $\theta_5$ , the core remains saturated, the operating points on the hysteresis loop passes through positions 5-5'-5, and at  $\theta_6 = \pi$ , when the load current vanishes, the core returns to its initial state, determined by the point 6 (or 0) on the loop.

This completes the operating half cycle. During the entire operating half cycle the rectifier  $V_C$  is cut off, since the inverse voltage across it (considering that  $e_C = 0$ ) is

$$u_{VC} = u_L = i_L r_L. \quad (28)$$

Plots showing the variations of the voltages, currents, and flux during the working half cycle are shown in Figures 3 and 4.

#### b) Control with Alternating Sinusoidal Voltage

A "positive" signal  $e_C = E_{cm} \sin \theta$  is applied to the input of the amplifier.

It is obvious that during the control half cycle the circuit will operate in exactly the same manner as in the case considered above, where control is by half-wave voltage. The only difference occurs during the working half cycle, which will be considered below.

At the end of the control half cycle, the state of the core is determined by point 3 on the hysteresis loop (Figure 4). Starting with  $\theta_3 = 0$  to  $\theta_4$  (23), the flux density remains constant, the voltage  $u_r = 0$ , and the load current is determined by Equation (22). In this case the rectifier  $V_C$  blocked by the inverse voltage  $u_{VC} = e -$

$-e_C$ .

During the instant  $\theta = \theta_4$  (point 4 on the hysteresis loop), the current is  $i_L = I_{co}$ , a positive voltage appears across the reactor, and the core is magnetized. The value of  $u_r$  is now determined by Equation (25).

The inverse voltage across rectifier  $V_C$  becomes

$$u_{VC} = I_{co} r_L - e_C. \quad (29)$$

When  $\theta = \theta'_4$ , where

$$\theta'_4 = \arcsin \frac{I_{co} r_L}{E_{cm}}, \quad (30)$$

the inverse voltage  $u_{VC}$  is zero and rectifier  $V_C$  becomes conducting (Figure 4). Now the following equations hold

$$\begin{aligned} e_C &= i_L r_L - i_C r_C, \quad i_L = i_L + i_C \\ \text{or} \quad i_L &= I_{co} - i_C \end{aligned} \quad (31)$$

and

$$\begin{aligned} i_C &= -\frac{e_C - I_{co} r_L}{r_L + r_C}, \\ i_L &= \frac{e_C + I_{co} r_C}{r_L + r_C}. \end{aligned} \quad (32)$$

The core continues to magnetize under the influence of the voltage

$$u_r = e - i_L r_L. \quad (33)$$

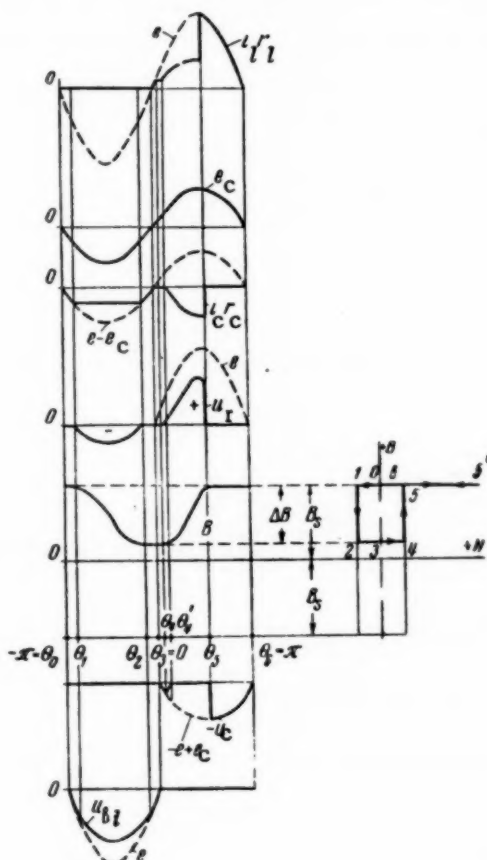


Fig. 4. Supply voltages, currents, and induction when sinusoidal alternating control voltage is used.

and during the instant  $\theta_5$ , where  $\theta_5$  is determined from (27), the core saturates (point 5 on the loop), the voltage  $u_r = 0$ , the entire supply voltage is applied to the load, and rectifier  $V_C$  is again blocked ( $u_{VC} = e - e_C$ ).

At  $\theta_6 = \pi$ , the working half cycle is completed and the subsequent control half cycle begins.

Thus, during control with alternating voltage, a characteristic feature is the fact that current flows through the control circuit during the working half cycle. At the same time, a corresponding "addition" appears in the load current. With this, as will be shown below, the average value of the load current, for equal values of  $E_{cm}$  and other conditions being equal, will remain the same as during half-wave voltage control. This can be explained by the fact that the presence of the current  $i_C$  during the working half cycle causes the saturation of the reactor to take place later, thus reducing the average value of the current  $i_L$ , compensating for the "addition" indicated above.

The processes occurring when the phase of the control signal is changed - for a "negative" signal - can be analyzed in a similar manner.

### c) DC Control

A "positive" signal is applied to the input of the amplifier

$$e_C = -E_C. \quad (34)$$

The curves for the current, voltage, and flux density are shown in Figure 5a.

Control half cycle. When  $\theta = \theta_0 = -\pi$ , the core is saturated and its state is determined by point 0 on the hysteresis loop. With this,  $u_r = 0$ , the control current is zero, because rectifier  $V_C$  is blocked by the inverse voltage

$$u_{VC} = e - e_C = E_m \sin \theta + E_C. \quad (35)$$

When  $\theta = \theta_1$ , where

$$\theta_1 = \arcsin \frac{E_C}{E_m} - \pi, \quad (36)$$

the voltage  $u_{VC} = 0$  and rectifier  $V_C$  conducts. The core is still saturated, the control current varies in accordance with

$$i_C = \frac{e - e_C}{r_C} = \frac{E_m \sin \theta + E_C}{r_C}. \quad (37)$$

When  $\theta = \theta_2$ , the current is  $i_C = -I_{CO}$  (point 2 on the hysteresis loop). The core begins to demagnetize, and the current  $i_C$  remains constant;  $i_C = -I_{CO}$ .

The demagnetization is effected under the influence of the following voltage

$$u_r = e - e_C - i_C r_C = e + E_C + I_{CO} r_C. \quad (38)$$

When  $\theta = \theta_3$ , the demagnetization terminates ( $u_r = 0$ ) - point 3 on the loop.

The angle  $\theta_2$  is determined from (37):

$$\theta_2 = \arcsin \left( \frac{E_C + I_{CO} r_C}{E_m} \right) - \pi, \quad (39)$$

and the angle  $\theta_3$  is

$$\theta_3 = -\pi - \theta_2. \quad (40)$$

The magnetic state of the core varies next over the minor cycle at  $B = \text{const}$  (section 3-4 on the loop), and the current  $i_C$  is determined from (37). At  $\theta_4$  the current  $i_C = 0$  ( $\theta_4 = -\pi - \theta_1$ ). After this the current  $i_C$  remains zero until the end of the control half cycle ( $\theta_5 = 0$ ), and the rectifier  $V_C$  is cut off.

The load current is zero during the control half cycle, and the rectifier  $V_L$  is blocked by the voltage

$$u_{VL} = e - u_L. \quad (41)$$

When the polarity of the control voltage is reversed - when the signal is "negative" - we have

$$e_C = E_C \quad (42)$$

The voltage, current, and flux density curves are as shown in Figure 5b.

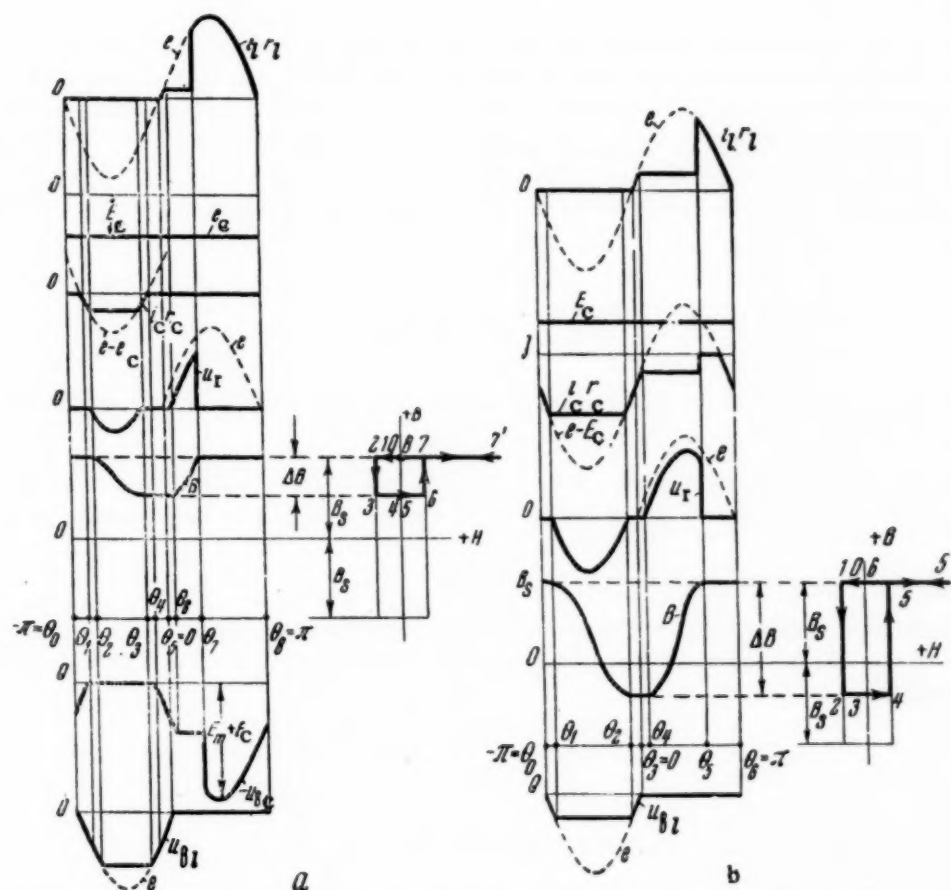


Fig. 5. The same as in Figure 3, but when dc voltage is used for control: a) for "positive" signal  $e_C = -E_C$ ; b) for "negative" signal  $e_C = E_C$ .

During the control half cycle, as long as the reactor is saturated, the current  $i_C$  varies as

$$i_C = \frac{e - E_C}{r_C}. \quad (43)$$

Over the section  $\theta_1 - \theta_2$ , the current is  $i_C = -I_{CO}$ . In the interval  $\theta_2 - \theta_3$ , the current  $i_C$  again varies as in (43). The load current is  $i_L = 0$ , since rectifier  $V_L$  is blocked.

**Working half cycle.** If the control voltage is as given in (34), the working half cycle is the same as obtained by control with rectified half-wave voltage. It is necessary only to note the increased inverse voltage across rectifier  $V_C$ .



Let us examine the working half cycle when the polarity of the control voltage is reversed, as given in (42).

In the interval  $\theta_3 - \theta_4$  (Figure 5b), the current  $i_c$  continues to vary as in (43), and its absolute value diminishes. The load current is  $i_l = e/r_l$ , and now the current in the reactor

$$i_e = i_l + i_c \quad (44)$$

increases, and becomes equal to  $+I_{CO}$  when  $\theta = \theta_4$ . Following this, a voltage appears across the reactance and the core magnetizes to saturation ( $\theta = \theta_5$ ), and  $i_e = I_{CO}$ .

Inasmuch as current flows in both the control and load circuits during the interval  $\theta_4 - \theta_5$ , we can use equations analogous to (19) to obtain

$$i_l = \frac{I_{CO} r_c + E_c}{r_l + r_c} = \text{const}, \quad i_c = \frac{I_c r_l - E_c}{r_l + r_c} = \text{const}. \quad (45)$$

At  $\theta = \theta_5$  the core saturates and until the end of the working half cycle we have  $i_l = e/r_l$ , and  $i_c$  is as given by (43). It should be noted that the process will follow this course only until the value of  $E_c$ , for a signal as given in (42) exceeds a certain critical value. Actually, as  $E_c$  increases, the core will become demagnetized more strongly during the control half cycle, and a condition will be reached where it will be impossible to saturate the core during the working half cycle. The critical condition occurs when the "limiting" state of the core during the working half cycle corresponds to the point 5 of Figure 5b. It is possible to show that the critical value  $E_{c\text{cr}}$  is

$$E_{c\text{cr}} = I_{CO} r_c \frac{r_c}{r_c + 2r_l} \quad (46)$$

At  $E_c = E_{c\text{cr}}$ , the value of the load current is a minimum. If  $r_c$  is substantially greater than  $r_l$  (2), then  $E_{c\text{cr}} \approx I_{CO} r_c$ , as in (14).

The equations obtained above for the various operating modes make it possible to calculate, for the assumptions made above, by relatively simple means the various relationships in the amplifier for the steady state.

### "Input-Output" Characteristics

Let us agree to call the principal "input-output" characteristic of the amplifier the dependence of the average value of the voltage across the load (during the cycle) on the control voltage and on the resistance in the control circuit:

$$U_{l\text{av}} = f(E_c, m, r_c).$$

#### a) Control with Rectified Half Wave and Alternating Sinusoidal Voltages

For both cases, with the exception of a mode in which the load current flows partially during the control half cycle, i.e., with the exception of the case when a signal  $e_c = -E_{cm} \sin \theta$  is applied and  $E_{cm} > I_{CO} r_c$ , it is possible to write for  $U_{l\text{av}}$

$$2\pi U_{l\text{av}} = \int_0^\pi u_l d\theta = \int_0^\pi (e - u_r) d\theta. \quad (47)$$

Next, taking (27) into account

$$\int_0^\pi u_r d\theta = \int_0^{\theta_4} u_r d\theta = - \int_{\theta_1}^{\theta_2} u_r d\theta. \quad (48)$$



Using (48) and (9) we obtain from (47)

$$2\pi U_{l\text{ av}} = \int_0^\pi e d\theta + \int_{\theta_1}^{\theta_2} u_r d\theta = \int_0^\pi e d\theta + \int_{\theta_1}^{\theta_2} (e - e_c + I_{co} r_c) d\theta. \quad (49)$$

Integrating (49), bearing (5), (6), (10) and (11) in mind, we obtain an equation for a family of "input-output" characteristics in the following form

$$\frac{\pi U_{l\text{ av}}}{E_m} = 1 - \frac{I_{co} r_c}{E_m} \left( \cot \alpha - \frac{\pi}{2} + \alpha \right), \quad (50)$$

where

$$\sin \alpha = \frac{I_{co} r_c}{E_m - E_{cm}}. \quad (51)$$

If the signal is  $e_c = -E_{cm} \sin \theta$ , it is necessary to reverse the sign of  $E_{cm}$  in the equations.

In the particular case when  $I_{co} r_c = 0$ ,\* we obtain from (50) and (51)

$$\pi U_{l\text{ av}} = E_{cm}. \quad (52)$$

In the absence of a signal at no load ( $E_{cm} = 0$ ) we have

$$\frac{\pi U_{l\text{ av}}}{E_m} = \sin \alpha \left( \frac{\pi}{2} - \alpha \right) + 1 - \cos \alpha, \quad \sin \alpha = \frac{I_{co} r_c}{E_m}. \quad (53)$$

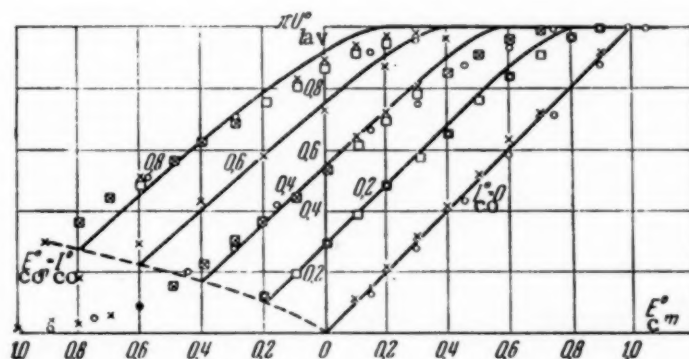


Fig. 6. "Input-output" characteristics when half-wave rectified or alternating sinusoidal control voltage is used. Experimental points: O) control with half-wave rectified voltage; x) control with alternating sinusoidal voltage; □) control with alternating sinusoidal voltage in the absence of rectifier  $V_c$ .

It is advantageous to introduce the following relative quantities

$$\frac{U_{l\text{ av}}}{E_m} = U^0, \quad \frac{E_{cm}}{E_m} = E_{cm}^0, \quad \frac{I_{co} r_c}{E_m} = I_{co}^0 \quad (54)$$

\* This equality is possible only in the absence of hysteresis, when  $I_{co} = 0$ , since  $r_c \neq 0$  in accordance with Condition (2).

Equations (50) and (51) will now assume the following form in relative units

$$\begin{aligned} \pi U_{lav}^0 &= 1 - I_{co}^0 \left( \operatorname{ctg} \alpha - \frac{\pi}{2} + \alpha \right), \\ \sin \alpha &= \frac{I_{co}^0}{1 - E_{cm}^0}, \end{aligned} \quad (55)$$

and Condition (14) becomes

$$E_{cm}^0 \leq I_{co}^0. \quad (56)$$

The family of "input-output" characteristics, calculated in accordance with (55), is plotted in Figure 6. The characteristics shown to the right of the ordinate axis correspond to signals (6), which we called "positive" signals, while those to the left of the ordinate axis correspond to "negative" signals (13).

The characteristics for "negative" signals are calculated for those values of  $E_{cm}^0$ , at which the Condition (56) is satisfied. The characteristics can naturally be calculated by the same procedure also for  $E_{cm}^0 > I_{co}^0$ , but the calculations are more cumbersome and are not cited here, particularly since these sections of the characteristics are of considerably smaller practical interest.

Since  $U_{lav} = I_{lav} r_l$ , the same characteristics represent the dependence of the average current in the load on the control voltage.

Strictly speaking, the characteristics are nonlinear over the entire working range, with the exception of  $I_{co}^0 = 0$ .

Let us note that the characteristics of the amplifier are quite identical for half wave rectified and alternating sinusoidal control voltages.

#### b) Control with DC Voltage

The equation for the family of "input-output" characteristics for dc control are obtained in a manner analogous to that given above, and are of the form

$$\frac{\pi U_{lav}}{E_m} = 1 - \cos \alpha + \left( \frac{\pi}{2} - \alpha \right) \sin \alpha, \quad (57)$$

where

$$\sin \alpha = \frac{I_{co}^0 + E_c}{E_m}. \quad (58)$$

In relative units (54), Equation (57) can be written as

$$\pi U_{lav}^0 = 1 - \cos \alpha + \left( \frac{\pi}{2} - \alpha \right) \sin \alpha, \quad (59)$$

where  $\sin \alpha = I_{co}^0 + E_c$ .

If the signal is  $e_c = E_c$ , it is necessary to reverse the sign of  $E_c$  in Equations (58) and (59).

A family of "input-output" characteristics, calculated from (59), is shown in Figure 7. For negative signals (42), the characteristics of Figure 7 are correct up to  $E_c \leq E_{c\text{cr}}$  (46).

Comparing Figures 6 and 7, it can be seen that the nonlinearity of the characteristics is more clearly pronounced for dc control. The characteristics of Figure 7, unlike those of Figure 6, are parallel to each other; in other words, a change in  $I_{co}^0$  merely represents a shift of the characteristic without changing its slope.

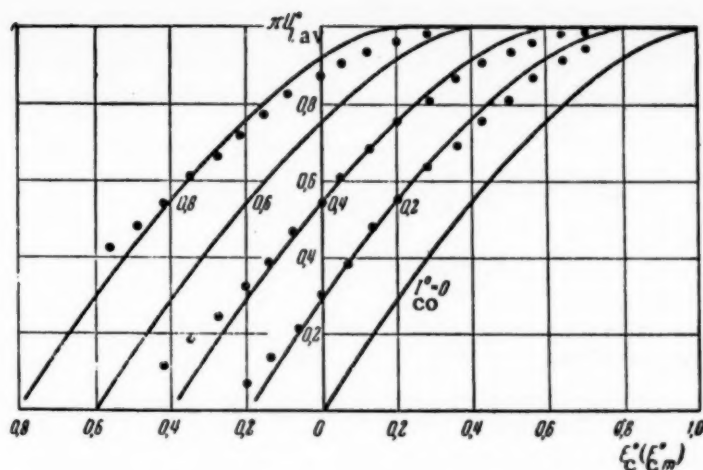


Fig. 7. "Input-output" characteristics for control with dc voltage. The points indicate the experimental data.

#### c) Control with the Aid of a Resistance in the Control Circuit

From an examination of the processes in the amplifier and from the equations obtained for the amplifier characteristics, it follows naturally that it is possible to effect control by varying the resistance in the control circuit. The amplifier characteristics for a variation in  $r_c$  can be calculated from Equation (53) subject to the condition

$$r_c \leq E_m / I_{CO}. \quad (60)$$

#### Voltage Gain Coefficient

Let us agree to call the voltage gain coefficient of the amplifier of Figure 1a the following quantity:

$$k_u = \frac{\partial U_{lav}}{\partial E'_{cav}}, \quad (61)$$

where  $E'_{cav}$  is the average value of the voltage from the source of the control signal at the input of the amplifier, averaged over the half cycle.

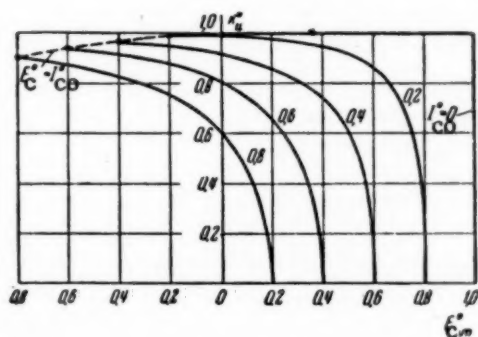


Fig. 8. Dependence of the relative voltage gain coefficient when half wave rectified or alternating sinusoidal voltage is used.

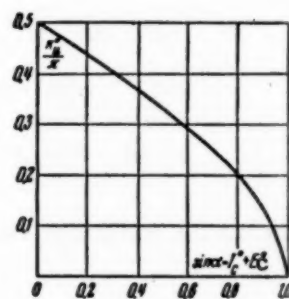


Fig. 9. The same as Figure 8, but with dc control.

We shall call the average voltage gain coefficient the quantity

$$k_u^0 = \frac{\partial U_{l \text{ av}}}{\partial E_{c \text{ m}}} \pi. \quad (62)$$

Then, in the case of control by half-wave rectified and sinusoidal voltages, we obtain from (55)

$$k_u^0 = \cos \alpha = \sqrt{1 - \left( \frac{I_{co}^0}{1 - E_{cm}^0} \right)^2}, \quad (63)$$

$$k_u = 0,5 k_u^0 \frac{w_l}{w_c}. \quad (64)$$

In the case of dc control, we obtain from (59)

$$k_u^0 = \frac{\pi}{2} - \alpha = \frac{\pi}{2} - \arcsin(I_{co}^0 + E_c^0), \quad (65)$$

$$k_u = \frac{k_u^0}{\pi} \frac{w_l}{w_o}. \quad (66)$$

Figure 8 shows a family of curves for  $k_u^0$ , calculated from (63), and Figure 9 shows the corresponding curve calculated from (65).

The voltage gain coefficient depends on the position of the working point on the characteristic of the amplifier (on the value of the input signal), and reaches a maximum for negative signals.

#### Current in the Control Circuit, and Power Gain

The equations given above for the current in the control circuit can be used to calculate the average or effective value of the control current. We shall restrict ourselves only, by way of an example, to a calculation of the average value of the current  $i_c$  in the case of control by rectified half-wave voltage.

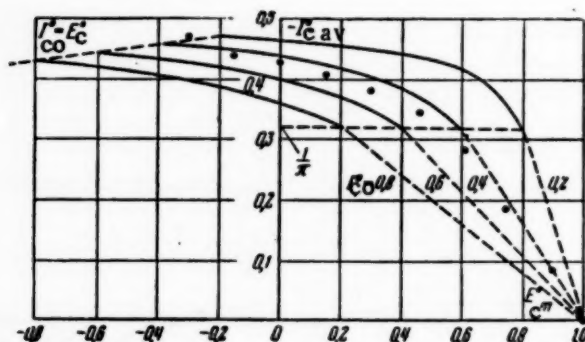


Fig. 10. Average value of current in the control circuit when half-wave rectified control voltage is used. The points represent the experimental data.

For positive signals (6), integrating Equations (7) and (8) over the cycle with allowance for (10), (11) and (51), we obtain

$$I_{c \text{ av}} = - \left[ \frac{E_m - E_{cm}}{\pi r_c} (1 - \cos \alpha) + I_{co} \left( 0,5 - \frac{\alpha}{\pi} \right) \right] \quad (67)$$

or in relative units

$$I_{c \text{ av}}^0 = \frac{I_{c \text{ av}}}{I_{co}} = - \left[ \frac{1 - E_{cm}^0}{\pi I_{co}^0} (1 - \cos \alpha) + 0,5 - \frac{\alpha}{\pi} \right]. \quad (68)$$

In the case of negative signals it is necessary to reverse the sign of  $E_{cm}$  in (67), (68) and (51).

Figure 10 shows the variation of the control current as a function of the control voltage.

When  $E_c = 0$ , the current  $I_c \neq 0$ . For positive signals, the control current and voltage do not agree in direction - when  $E_c$  increases,  $I_{cav}$  diminishes in value. When  $E_{cm}^0 = 1 - I_{c0}^0$ , the current  $I_c$  in control half cycle is sinusoidal with an amplitude equal to  $I_{c0}$ , and beyond that, as  $E_{cm}$  increases, the control current remains sinusoidal (up to  $E_{cm} = E_m$ ); from there on the current  $I_{cav}$  diminishes linearly with increasing  $E_{cm}$ . For negative signals, the direction of the current  $I_c$  agrees with that of  $E_c$ , and when  $E_c$  increases  $I_{cav}$  increases.

Analogous phenomena occur for all types of control voltages.

Naturally, one cannot employ in this case the usual definition of the control power (input power), for example in the form  $P_c = I_{cr}^2 r_c$ . It is equally inadvisable to employ the definition of the power gain coefficient, usually used for magnetic amplifiers. In addition, although in an ordinary magnetic amplifier one can speak of the power gain of the amplifier proper, without reference to the parameters of the transducer used at the input of the amplifier (with accuracy up to the influence of the even harmonics in the control circuit), in our case the internal resistance of the transducer (which enters into  $r_c$ ) determines the operating condition of the amplifier and affects directly the gain coefficient  $k_u$ . This amplifier must therefore be analyzed in conjunction with the actual transducer.

To estimate the power gain of a Ramey amplifier and to compare it with other types of magnetic amplifiers, particularly those characterized by the ratio of the power gain to the time constant, it is necessary to introduce such a definition of the power gain, that would be equally valid for all types of amplifiers.

Under these conditions, it is advisable to determine the input power by starting with the "potential" power that the transducer can deliver to the input of the amplifier. Actually, it makes no difference to us whether the particular transducer delivers power or not, but it is important to know what its power rating should be.

The maximum power that can be delivered to a load by a transducer with an emf  $E'_c$  and an internal resistance  $r'_l$  (under our assumptions, a pure resistance), is

$$P_c = \frac{(E'_c)^2}{4r'_l}. \quad (63)$$

Since we are interested in the average value of the current at the output of the amplifier (or voltage), the input and output power will be calculated from the average values. Here the power gain coefficient will be defined in the following manner:

$$k_p = \left( \frac{\Delta U_{l \text{ av}}}{\Delta E'_{c \text{ av}}} \right)^2 \frac{4r'_l}{r_l} = k_u^2 \frac{4r'_l}{r_l}. \quad (64)$$

In the case of half-wave or sinusoidal control, we obtain with allowance for (64)

$$k_p = \left( 0,5 k_u^0 \frac{w_l}{w_c} \right)^2 \frac{4r'_l}{r_l} = \frac{r'_l w_l^2}{r_l w_c^2} (k_u^0)^2, \quad (71)$$

and in the case of dc control, considering (66), we get

$$k_p = \frac{4r'_l w_l^2}{\pi^2 r_l w_c^2} (k_u^0)^2. \quad (72)$$

Let us recall that the quantities  $I_c$ ,  $E_{cm}$ , and  $r_c$  which enter into the expression for  $k_u^0$  are all referred to the load circuit (3).

It follows from the above that the amplifier will act as a power amplifier only if Condition (2) is satisfied:

$$r_c > r_l \quad \text{or} \quad r'_c \frac{w_l^2}{w_c^2} > r_l \quad (73)$$



Since the steady state is essentially determined by the position and magnitude of the minor cycle, which in turn, subject to the assumptions made, is determined by the value of the constant component of the flux density  $B_0$ , it is evident that in this amplifier the transients will be fully characterized by the manner in which the dc flux component will vary in the core.

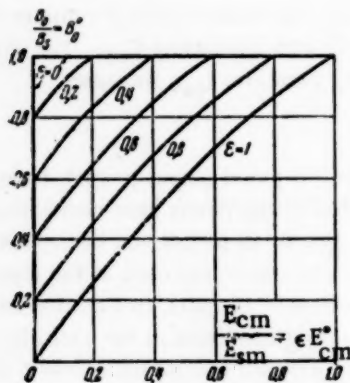


Fig. 11. Dependence of the relative value of the dc component of induction  $B_0^0$  on the relative values of the supply voltage  $\epsilon$  and of the signal voltage  $E_{cm}^0$  when the control voltage is sinusoidal or half wave rectified and  $I_{CO}^0 = 0$ .

We shall show that for the assumed idealization of the hysteresis loop, the appearance of an arbitrarily small dc component of field intensity in the core causes the steady state to exhibit such a dc flux density component  $B_0$ , at which the resultant asymmetrical minor cycle passes through the saturation point  $+B_s$  (or  $-B_s$ ), regardless of the value of

$$\epsilon = \frac{E_m}{E_{sm}}. \quad (74)$$

Actually, since the width of the minor cycles is  $2H_{CO}$  independently of  $\epsilon$  and  $B_0$ , the dc component of the intensity can occur only if during some part of the cycle the instantaneous value of the intensity exceeds the value  $H_{CO}$ , which, in turn, is possible only in a saturated core.

Let us consider now the quantitative dependence of  $B_0$  on  $\epsilon$ , assuming for the sake of simplicity

$$I_{CO} r_L \ll E_m, \quad (75)$$

which always holds in practice.

In the steady state, the value  $B_0$  in relative units is

$$B_0^0 = \frac{B_0}{B_s} = 1 - \epsilon \left[ 0.25 + \frac{1}{2\pi} \sin \beta - \left( 0.25 + \frac{\beta}{2\pi} \right) \cos \beta \right], \quad (76)$$

where

$$\beta = \arccos(2\pi U_{LAV}^0 - 1).$$

The angle  $\beta$  can be called the "saturation angle" and corresponds, for example, to the angle  $\theta_5$  of Figure 3.

Equation (76) is valid for any of the types of control considered above. The value of  $U_{LAV}^0$  as a function of  $E_{cm}^0$  and  $I_{CO}^0$  (control by means of an alternating voltage and resistance  $r_C$ ) or as a function of  $E_C^0$  and  $I_{CO}^0$  (control by means of a dc voltage and resistance  $r_C$ ) can be determined from (55) and (57) respectively, or else directly from the curves of Figures 6 and 7.

Figure 11 shows the dependence of  $B_0^0$  on  $E_{cm}^0$  for various values of  $\epsilon = \text{const}$ , for the particular case  $I_{CO}^0 = 0$  (in practice, this case corresponds to  $I_{CO} r_C \ll E_m$ ). It follows from Figure 11 and from (75) that when the control signal is constant, decreasing  $\epsilon$  (decreasing the ac component of the flux density) causes an increase in the dc component of the flux density (the same as in ordinary magnetic amplifiers). In particular, an increase in the value of  $U_{LAV}^0$  from zero (more accurately, from the value  $\frac{\pi I_{CO} r_L}{2E_m}$ , no matter how small, resulting from turning on  $E_C$  or varying  $r_C$ , causes the dc component of the flux density to increase in a "jump" (the dynamics of this jump will be considered below) by an amount

$$\Delta B_0^0 = 1 - \epsilon. \quad (78)$$

If  $\epsilon = 0$  ( $E_m = 0$ ), the flux density, naturally, increases abruptly to  $V_s$ .



It is evident that the instantaneous value of the relative flux density will be, for this case,

$$B^0(\theta) = 1 - \varepsilon - \varepsilon \cos \theta. \quad (79)$$

Consequently,

$$B^0(-\pi) = B^0(+\pi) = 1; \quad (80)$$

thus proving the assumption proposed above.

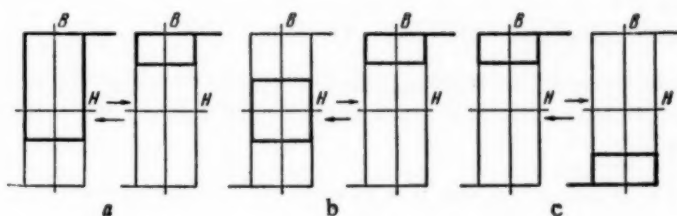


Fig. 12.

The amplifier can operate in two possible modes. The first, which can be called symmetrical, is characterized by the absence of a dc flux-density component; in this case the magnetization of the core is reversed through a symmetrical minor cycle, and the load current is a minimum.

A symmetrical mode is possible only if the equivalent load and control circuits are absolutely identical, i.e.,

$$r_c = r_l, e = e_0 + e_c. \quad (81)$$

The second mode — the asymmetric one — is characterized by the presence of  $B_0$ . The reversal of core magnetization takes place through an asymmetric minor cycle, which must pass through the saturation point of the extreme hysteresis loop, regardless of the value of the supply voltage. The asymmetric mode takes place when Equations (81) are violated by any amount, no matter how small.

It follows from the above that the transients in the amplifier can be divided into three types:

- transient produced upon changing from one asymmetric mode to another (also asymmetric) with the flux density  $B_0$  having a constant sign (Figure 12a);
- transient due to change from a symmetric mode to an asymmetric one and vice versa (Figure 12b);
- transient due to change from one asymmetric mode to another, with a change in the sign of the flux density  $B_0$  (Figure 12c).

Let us examine the transients occurring upon an abrupt change in the amplitude of the control voltage and resistance of the control circuit. We shall call henceforth the change in the above quantities (individually or together) as the change in the control signal.

Transient of the first type. Assume that the circuit operates in a certain stationary asymmetric mode. If the control signal assumes a new value at the instant  $\theta = \theta_0 = -\pi$ , when  $B = B_s$  and  $i_c = 0$ , it is evident that the change in the induction during the interval  $-\pi \leq \theta \leq 0$  (controlling half cycle) will be determined already by the new value of the control signal, whereby

$$\frac{\Delta B_c}{B_s} = \frac{1}{E_s} \int_{-\pi}^0 u_1 d\theta. \quad (82)$$

During the next working half cycle the core must reach saturation, and consequently

$$\int_0^{\pi} u_r d\theta = - \int_{-\pi}^0 u_r d\theta. \quad (83)$$

Since

$$2\pi U_{lav} = \int_0^{\pi} u_l d\theta = \int_0^{\pi} e d\theta - \int_0^{\pi} u_r d\theta = \int_0^{\pi} e d\theta + \int_{-\pi}^0 u_r d\theta, \quad (84)$$

the value of  $U_{lav}$  during the very first working half cycle after the change in the control signal will correspond to the new value of the control signal, i.e., there is no transient.

If, however, the control signal changed during any instant of time within the given cycle ( $-\pi < \theta < \pi$ ), the conditions considered above will occur only at the beginning of the next cycle and the steady state will take place during this next cycle.

Thus, the time of the transient of the first type of transient does not exceed one cycle of the amplifier supply frequency.

Transient of the second type. Let us consider this transient, for example, for a sinusoidal half-wave or alternating control voltage at  $I_{co}^0 = 0$  (Figure 13). Assume that at  $\theta < \theta_0$  the symmetrical steady-state mode corresponded to  $E_{cm}^0 = 0$ ,  $I_{co}^0 = 0$ , and  $\epsilon < 1$ . The induction in the core varied through a symmetrical minor cycle with an amplitude  $B_m^0 = \epsilon < 1$ . Let at the instant  $\theta_0 = -\pi$  a signal

$$\frac{e_c}{E_{sm}} = \epsilon E_{cm}^0 \sin \theta. \quad (85)$$

be applied to the input of the amplifier.

Let us trace the variation of the induction, starting with this instant. At  $\theta = \theta_0$

$$B^0(\theta_0) = \epsilon. \quad (86)$$

During the first control half cycle, the core demagnetizes under the influence of the voltage

$$\frac{u_r}{E_{sm}} = \frac{e - e_c}{E_{sm}} = \epsilon (1 - E_{cm}^0) \sin \theta, \quad (87)$$

and during the first subsequent working half cycle the core is magnetized under the influence of the voltage

$$\frac{u_r}{E_{sm}} = \frac{e}{E_{sm}} = \epsilon \sin \theta. \quad (88)$$

The corresponding total change in induction during the first cycle is

$$\Delta B^0 = 2\epsilon - 2\epsilon (1 - E_{cm}^0) = 2\epsilon E_{cm}^0, \quad (89)$$

and towards the end of the first cycle the induction is

$$B^0(\theta_0 + 2\pi) = B^0(\theta_0) + \Delta B^0 = \epsilon (1 + 2E_{cm}^0). \quad (90)$$

At the end of the  $n$ -th cycle, assuming that saturation has not yet been reached, we have

$$B^0(\theta_0 + n2\pi) = B^0(\theta_0) + n\Delta B^0 = \epsilon (1 + 2nE_{cm}^0). \quad (91)$$

The transient terminates when saturation occurs, i.e.,

$$B^0(\theta_0 + 2n_k\pi) = \epsilon(1 + 2n_k E_{cm}^0) = 1. \quad (92)$$

From (92) we get

$$n_k = \frac{1 - \epsilon}{2\epsilon E_{cm}^0}. \quad (93)$$

When  $n_k$  is calculated from (93) it is necessary to take the nearest highest integral value of  $n_k$ .\*

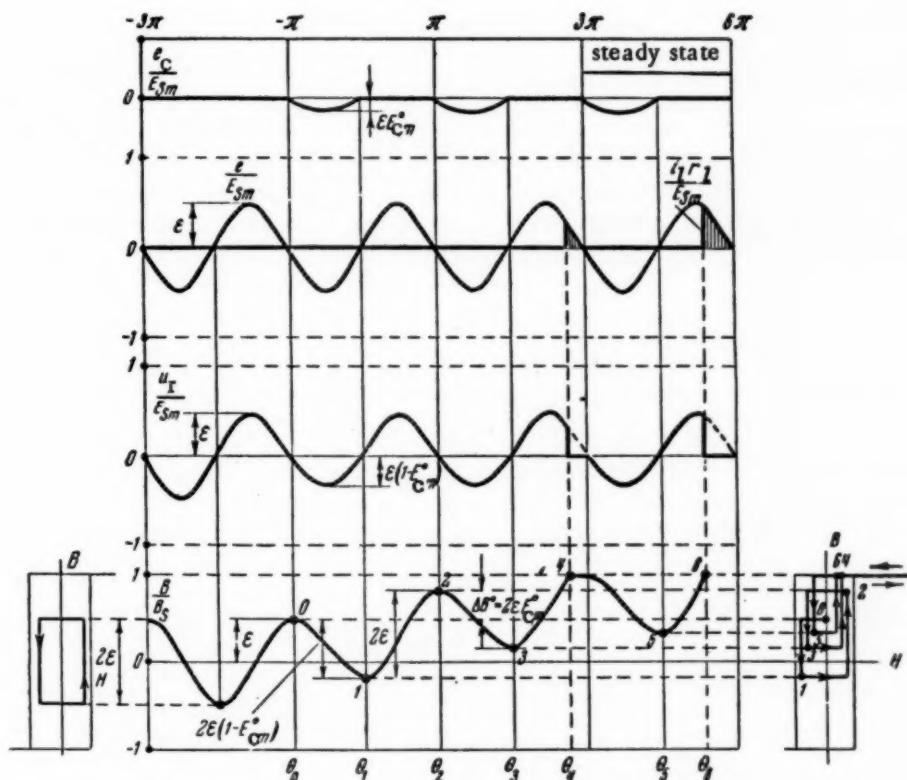


Fig. 13. Transient of the second type occurring when half wave rectified control voltage is turned on. For the sake of illustration, the minor cycles are shown in the drawing as having different widths. Actually their widths are the same and amount to  $-2H_{co}$ .

Taking into account the arbitrariness of the instant at which the control signal is switched on, the duration of the transient will be

$$t = (n_k + 1)T, \quad (94)$$

where  $T$  is the period of the supply frequency.

The transient of the second type follows a similar course in the case of dc control, and also if the resistance  $r_c$  is changed (increased).

The transient of the third type can be investigated in an analogous manner, but modes of this type are of less interest in practice and will not be considered here.

\*When  $\epsilon = 1$  we have  $n_k = 0$ , meaning that the transient of the second type follows the same course as the transient of the first type, since the induction is  $B = B_s$  when  $\theta = \pm\pi$ .

It is important to note that the duration of the transients of the second and third type depend on the values of  $\epsilon$  and of the control signal, and can be made theoretically as large as desired. Thus, if  $E_{cm}^0 \rightarrow 0$ ,  $n_k \rightarrow \infty$ , corresponding to an infinite value of  $dB_0^0/dE_{cm}^0$  as  $E_{cm}^0 \rightarrow 0$  (Figure 11).

It must be emphasized, however, that normally the amplifier should operate in an asymmetrical mode with a constant sign of the dc component of induction. Actually, since in a power amplifier we always have  $r_c > r_l$  (73), the symmetrical mode does not occur even if the control voltage is zero.

Consequently, in the normal mode of the power amplifier, the transient time in an abrupt change in the control signal does not exceed one cycle of the supply frequency (regardless of the value of the supply voltage  $-\epsilon$ ).

Thus, the circuit considered above provides maximum possible operating speed for an amplifier operating with a carrier frequency and detection.

### Results of Experimental Verification

A quantitative verification of the results obtained in this article was carried out with several amplifiers, built in accordance with the circuit of Figure 1. The reactor of one of the amplifiers had the following parameters: toroidal core 31 mm inside diameter, 46 mm outside diameter, wound of N65P tape 0.15 mm thick and 3.5 mm wide, the length of the tape being 6 m ( $l = 12$  cm,  $S = 0.247$  cm<sup>2</sup>); the number of turns in the windings were  $w_c = w_l = 700$ , the wire being 0.38 mm in diameter.

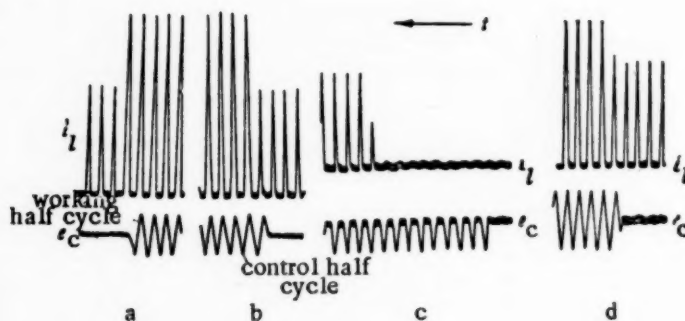


Fig. 14. Oscillograms of transients. Transient of the first type: a) signal off; b) signal on; d) signal on and rectifier  $V_c$  removed from control circuit. Transient of second type: c) signal on.

Measurements in a dc field have shown that  $B_s = 12,100$  gauss (in a field of 60 oersted),  $B_r = 10,900$ , the squareness coefficient of the loop  $B_r/B_s = 0.9$ , and  $H_{co} = 0.12$  oersted.

The coercive force, corresponding to the extreme dynamic hysteresis loop at a frequency  $f = 500$  cycles, measured with the aid of a cathode-ray oscillograph, was 0.28 oersted. The nominal coercive force was taken to be  $H_{co} = 0.25$  oersted, corresponding to a minor cycle with  $\Delta B \approx 0.5 B_m$ .<sup>\*</sup> With this, the parameters characterizing the reactor (1) were:  $I_c = 3.4$  ma,  $E_{sm} = 59$  v (according to  $B_r$ ).

The rectifiers  $V_c$  and  $V_l$  used were germanium diodes DG-Ts24, the inverse current of which did not exceed 0.1 ma ( $\ll I_{co}$ ) in the operating mode.

The static characteristics were plotted for  $f = 500$  cycles,  $E_m = 30\sqrt{2}$  volts,  $E_{0m} = 30\sqrt{2}$  volts,  $r_l = 54$  ohms ( $E_m/\pi r_l = 250$  ma). The total active resistance of the control circuit was set at  $r'_c = 50, 2500, 5000, 7500$  and  $10,000$  ohms; the corresponding values of  $I_{co}^0$  were 0.004, 0.2, 0.4, 0.6 and 0.8.

The measurement results were recalculated in relative units; the corresponding experimental points are shown in Figures 6, 7 and 10.

The agreement between the calculated characteristics and the experimental ones can be considered to be

<sup>\*</sup>The change in induction  $\Delta B$  is shown, for example, in Figure 3.

fully satisfactory. The experimental "input-output" characteristics in the case of control with half-wave and sinusoidal voltages actually overlap.

It is seen from Figures 6 and 7 that the slope of the experimental "input-output" characteristics is somewhat smaller than the calculated value, particularly at large values of  $I_{CO}^0$ . This discrepancy is principally explained by the fact that the equivalent width of the minor cycle (consequently also of  $I_{CO}^0$ ) does not remain constant, and diminishes somewhat with increasing load current (increasing dc component of the induction).

Figure 14 shows oscillograms of the transient of the first type when a sinusoidal control voltage is turned on and off: a) signal disconnected; b) connected. The lower half wave of the control voltage corresponds to the control half cycle. In Figure 14a the signal was disconnected at the end of the control half cycle; in Figure 14b it was disconnected at the start of the working half cycle.

In both cases, the instant at which the signal changed was the most unfavorable one and the transient time equaled one cycle.

The oscillogram of Figure 14c shows the transient for a symmetrical initial mode where a half wave rectified signal is switched on. The transient lasts nine cycles. The calculated duration of the transient for the given case ( $\epsilon = 0.35$ ,  $E_{cm}^0 = 0.16$ ) with Equation (94) is seven cycles. This discrepancy between the value calculated from (94) and the experimental value results from the assumptions made and has no practical significance, for in practice one should not operate in the symmetrical mode.

### SUMMARY

The Ramey circuit was analyzed in this article in the same simple form in which it was presented by its inventor.

The results obtained, represented in the form of equations and curves in relative units, can be considered as generalized. They can be used to obtain readily the necessary characteristics of an actual amplifier. The generalized characteristics are calculated only once, and there is no need whatever to repeat these calculations. The basic characteristics are cited in this article.

The experimental values are in good agreement with the calculated ones if good magnetic materials with rectangular hysteresis loop are used.

The results obtained can be generalized to include the more common type of "single-core" magnetic amplifiers with internal feedback.

Thus, it is seen at a glance from the analysis performed that the reference voltage need be considered only as an ordinary bias voltage. It may also be absent. Changing the reference voltage does not change the generalized "input-output" characteristics if the control signal is rectified or alternating; they merely shift with respect to the ordinate axis (if dc is used for control, the characteristics, as shown in Figure 7, change somewhat).

A significant problem is the role and necessity of rectifier  $V_C$  in the control circuit, which in the Ramey circuit exerts a harmful influence in the amplification of small voltages. It can be shown that the "input-output" characteristics of Figure 6 do not change even in the absence of rectifier  $V_C$ . Actually, since rectifier  $V_C$  conducts in all cases when there is a change in the induction in the control half cycle, its absence does not affect the change in induction ( $\Delta B$ , Figure 3), during the control half cycle. On the other hand, the average value of the load current is determined fully by the change in the induction during the control half cycle. Consequently, for a given value of  $E_{cm}$  and other conditions being equal, the elimination of rectifier  $V_C$  does not change  $I_{lav}$ .

A theoretical analysis and experimental verification (see Figure 6 and oscillograms Figure 14) have fully confirmed these premises for both the steady state and the transient modes.

Thus, the Ramey circuit does not offer to a certain extent anything new compared with the ac controlled single-core magnetic amplifier with internal feedback. To the contrary, the presence of a rectifier in the control circuit of the Ramey circuit can only affect adversely the operation of the amplifier.

Problems connected with the elimination of rectifier  $V_C$  and changing the reference voltage, as well as allowance for the slope of the "vertical" sides of the hysteresis loops and elements of amplifier design will be considered in the second part of this article.



#### LITERATURE CITED

- [1] R. Ramey, "On the Mechanics of Magnetic Amplifier Operation," Trans. AIEE Vol. 70, Part II (1951).
- [2] R. Ramey, "On the Control of Magnetic Amplifiers," Trans. AIEE Vol. 70, Part II (1951).
- [3] G. Hughes and H. Miller, "Fast-Response Magnetic Amplifiers," Trans. AIEE Vol. 73, Part I (1954).
- [4] C. House, "Flux Preset High-Speed Magnetic Amplifiers," Trans. AIEE Vol. 72, Part I (1953).
- [5] D. Scorgie, "Fast Response with Magnetic Amplifiers," Trans. AIEE Vol. 72, Part I (1953).

Received April 18, 1956



## INFORMATION CRITERIA FOR EVALUATING TELEMETERING SYSTEMS

M.M. Bakhmet'ev and E.R. Vasil'ev

(Moscow)

Information criteria are proposed for the determination of the quality of operation of telemetering systems.

### INTRODUCTION

Information theory which has received a comparatively complete formulation in Shannon's work [1] has made it possible to compare the effectiveness of the operation of existing telemetering systems (TS) and to find in principle a new approach to their design. This article is devoted to an examination of the first of these possibilities. To be able to make a correct choice of the method of designing a TS, it is necessary to have an objective estimate of the operation of various systems. Attempts to make such an estimate are already available in the literature (see, for example, [2]). However, all the known criteria have that shortcoming that they are arbitrary to a certain extent.

The use of information theory for the analysis of the operation of a TS can be more successful than in the field of telephony or television, where the information loop contains such information-converting "devices" as human sensory organs. The insufficient knowledge of their operation causes the parameters that characterize the transmission of information to be determined only approximately.

In telemetering, the channel used to transmit the information has parameters that are sufficiently well-known or that can be determined with sufficient accuracy even in the present state of the art.\* The only field that has not been sufficiently studied in the case of transmission of information over a TS is the subject of noise.\*\* For all its complexity, this problem does not apparently present any theoretical difficulties.

#### 1. Speed of Message Production as the Most Rational Criterion for Evaluating Telemetering Systems

Telemetering systems serve to transmit information concerning processes that occur at places where the transducers are installed. The information that is received at the receiving end of the TS determines the degree of acquaintance with the actual state of the objects. The aggregate of parameters used to accomplish a transmission of this information depends on the technical capabilities and on the effectiveness with which the TS is constructed. In any case, however, the best system is one which, other conditions being equal, can produce at the output a larger amount of information. This amount of information can be measured in certain units, most frequently binary, and can serve as the basis for the establishment of a variety of criteria that characterize the operation of the TS.

One of the important criteria of the quality of a TS is the number of information units transmitted per unit of total frequency bandwidth of the communication line.

\*For example, the speed of transmission of information is determined by the character of the distortion introduced by the communication channel, along with other factors.

\*\*The concept "noise" includes in this article both noise in the communication line, as well as apparatus instability and other factors that disturb the information.

The degree of complexity of the TS can be judged from the ratio of the number of information units transmitted by the system to the number of definite elements of the system, and its reliability can be judged from the ratio to the number of nonreliable elements. In those cases when the volume or weight of the system is limited, its quality can be judged from the number of information units per unit volume or weight of the system, etc.

The amount of information at the output of the system can be calculated if many parameters, characterizing the TS, are known. These parameters include the bandwidth of the signal, the average power of the system, the average power of the noise, etc.

All TS can be divided into two large classes: systems of discrete action and systems of continuous action. In the case of a discrete TS, and also in the case of a continuous TS having a finite accuracy of transmission of the measured quantities, the amount of information at the output represents a finite quantity. Accurate computation of this quantity may be a complicated matter in some cases. However, under certain assumptions, the speed of creation of information at the output of the TS can be determined in a relatively simple manner.

When a TS operates under actual conditions, the amount of information at its output depends both on the characteristics of the TS itself, as well as on the statistical laws that determine the variation of the transmitted quantities, which are considered to be random functions of time. When estimating the quality of a TS it is necessary to determine the maximum amount of information that can be obtained with its aid. It is known [1] that the maximum amount of information corresponds to the case of uniform distribution of the values of the transmitted quantities in the specified limits (in the absence of limitations on the average power) and corresponds to statistical independence of all values of the transmitted quantities.

## 2. Examples of the Determination of the Criterion for Estimating the Operation of a TS

Let us first consider discrete systems and let us assume that all the values of the transmitted quantity in the  $i$ -th channel of a multi-channel TS have equal probability and are bounded within the limits  $(-a_i, a_i)$ , and that the quantization interval of the signal  $\delta_i$  was chosen sufficiently large, so that the probability that the signal will become distorted by the noise can be neglected. Evidently, under such limitations the amount of information transmitted in each message is

$$\log_2 \left( \frac{2a_i}{\delta_i} + 1 \right) \text{ binary units}$$

If the TS has  $M$  channels and the readings are transmitted over each channel in  $\tau_i$  seconds, the speed of message formation at the receiving end (speed of information transmission) in such a system is

$$R = \sum_{i=1}^M \frac{1}{\tau_i} \log_2 \left( \frac{2a_i}{\delta_i} + 1 \right) \frac{\text{binary units}}{\text{sec}} \quad (1)$$

In the case when all the channels are identical

$$R = \frac{M}{\tau} \log_2 \left( \frac{2a}{\delta} + 1 \right) \frac{\text{binary units}}{\text{sec}} \quad (2)$$

As indicated above, one of the basic criteria for estimating the quality of a TS is the quantity that shows the speed at which information is transmitted per unit bandwidth of the communication channel of the system

$$\frac{R}{\Delta W_c} = \frac{M}{\tau \Delta W_c} \log_2 \left( \frac{2a}{\delta} + 1 \right) \text{ binary units} \quad (3)$$

where  $\Delta W_c$  is the frequency bandwidth of the communication channel.

In many cases the TS contains time-delay elements (for example, output pointer-type instruments, in which the time  $\tau_{ss}$  required to produce steady-state indications amounts to 3-4 seconds). Such elements reduce

the actual speed of message formation at the output of the system, since the transmission of the individual independent readings can be effected only after approximately the time  $\tau_{ss}$  (independently of the cycle frequency of the system). It is therefore necessary in such cases to insert in Equations (1-3)  $\tau_{ss}$  in lieu of  $\tau_1$  (or  $\tau$ ).

In TS with continuous transmission, in which the input and output quantities are continuous functions of time, the action of the noise and the limit on the bandwidth of the communication channel make it impossible to obtain absolutely accurate transmission of the values of the measured quantities. To estimate the quality of the transmission of the continuous functions it is necessary to introduce criteria for the fidelity of the transmission. One of the possible criteria is one in which the fidelity of transmission is determined through the average value of the square of the deviation of the received quantity  $[y(t)]$  from the transmitted one  $[x(t)]$ , namely  $v = [x(t) - y(t)]^2$ .

This criterion is widely used and is mathematically convenient, provided the error at the receiving end follows the normal distribution law.

The speed of message formation  $R$  at the output of the TS, under the assumptions made and subject to uniform distribution of the measured parameter within a range  $(-a, a)$  is bounded by the following quantities\*

$$W \log_2 \frac{2}{\pi e} \frac{a^2}{\sigma^2} \leq R \leq W \log_2 \frac{a^2}{3\sigma^2}, \quad (4)$$

where  $W$  is the frequency bandwidth of the signal, and  $\sigma$  is the mean squared value of the error.

For a numerical estimate of the accuracy of the work of the TS one employs frequently the value of the limiting relative error, which in the case of a normal distribution of the error amounts to

$$\gamma = \frac{3\sigma}{2a} 100\%, \quad (5)$$

where  $3\sigma$  is the maximum error and  $2a$  the interval of parameter variation.

It follows from (4) and (5) that the quantity  $R$  lies between the following limits

$$W (12,363 - 2 \log_2 \gamma) \leq R \leq W (12,873 - 2 \log_2 \gamma). \quad (6)$$

It is evident from (6) that since the difference between limits is half a binary unit, one can assume with sufficient practical accuracy that

$$R = W (12,5 - 2 \log_2 \gamma) \frac{\text{binary units}}{\text{sec}}. \quad (7)$$

All the above pertains obviously to a single channel of a multichannel telemetering system. In the case of  $M$  channels the speed of message formation at the output of the TS is

$$R = \sum_{i=1}^M W_i (12,5 - 2 \log_2 \gamma_i) \frac{\text{binary units}}{\text{sec}}. \quad (8)$$

If all the channels are identical, we have

$$R = MW (12,5 - 2 \log_2 \gamma) \frac{\text{binary units}}{\text{sec}}. \quad (9)$$

As in the case of discrete systems, an important criterion for estimating the quality of a TS is the quantity

$$\frac{R}{\Delta W_c} = \frac{MW}{\Delta W_c} (12,5 - 2 \log_2 \gamma) \text{ binary units} \quad (10)$$

\*This inequality follows from Shannon's 23rd theorem [1].

where  $\Delta W_c$  is the bandwidth of the communication channel.

In the case when the TS contains time-delay elements, that have a settling time  $\tau_{ss}$ , it is necessary to employ the quantity  $\tau_{ss}/2$  instead of the quantity  $W_1$  (or  $W$ ) in Formulas (7-10).

Formulas (7-10) can be used to evaluate TS also without account of the limitations imposed by the normal character of the distribution of the error. The results obtained will be approximate. For example, let us give an informational estimate of three commercial telemetering systems (Table 1). The parameters of these systems are taken from [2].

TABLE 1

Name of TS and type of modulation	Number of channels M	Bandwidth $\Delta W_c$ , cycles	Accuracy, $\gamma$ , %	Speed $\tau$ , seconds	Speed of information R, binary units/sec	Criterion $R/\Delta W_c$ , binary units
"Brown-Boveri" (time-frequency-pulse-modulation)	8	120	2	$\frac{0.1}{3-4}$	$\frac{415}{13.8-10.4}$	$\frac{3.46}{0.115-0.086}$
British System (code-pulse-modulation, amplitude-modulation)	10	120	1	4	15.4	0.128
System of the Institute of Automation and Remote Control (IAT), USSR Academy of Sciences (amplitude-pulse modulation, frequency modulation).	7	250	1.5	$\frac{0.2}{3-4}$	$\frac{206}{13-9.8}$	$\frac{0.83}{0.052-0.039}$

Remarks: 1. The table should be considered as a purely illustrative material, explaining the procedure for calculation, since there is no knowledge of the conditions under which the errors are determined, nor are there accurate data on the settling time of the output recording instruments used in these systems.

2. In the "Brown-Boveri" and the IAT systems there are two values of speed. The first value corresponds to the frequency of operating cycles of the system, and the second to the actual speed in the case of indication of data produced by pointer instruments with a settling time of approximately 3-4 seconds.

It follows from Table 1 that the best system from the point of view of utilization of the bandwidth of the communication channel in the case of indication of data received from pointer instruments is the English code system.

For different noise levels, the accuracy can vary in different systems in a different manner, for example, owing to the different methods used to modulate the signal in the transmission over the communication line. It may therefore turn out to be that at low noise level the greatest ratio  $R/\Delta W_c$  will be exhibited by some systems, and at high noise level by others. This should be taken into account when deciding the comparative estimate of the quality of various TS's, i.e., the comparison should be carried out under noise conditions that are customary for the given operating conditions of a TS.

If additional limitations are imposed on the statistics of the signal, the optimum distribution will not be uniform, but of some other type. The Appendix contains a determination of the optimum distribution of a parameter when the value of the mean square of the parameter and its maximum value are limited.

#### APPENDIX

The determination of the distribution of probabilities  $\rho(x)$ , insuring maximum information  $H = -$

$$-\int_{-a}^a \rho(x) \log \rho(x) dx, \text{ subject to limitations imposed on the possible values of the measured quantity } -a \leq x \leq a$$



$\leq a$  and the average power  $Q = \int_{-a}^a x^2 \rho(x) dx$ , reduces to solving the isoperimetric problem of variational calculus. Adding the normalization conditions to these limitations and solving the Euler equation, we get

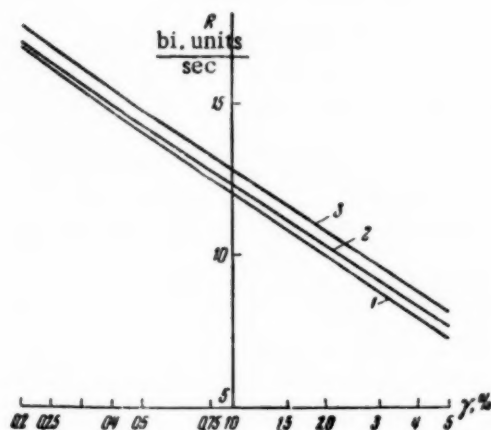


Fig. 1. 1) Truncated normal distribution; 2 and 3) lower and upper limits for uniform distribution.

$$\rho(x) = \begin{cases} e^{\lambda_1 - 1} e^{\lambda_2 x^2} & \text{at } -a \leq x \leq a, \\ 0 & \text{at } |x| > a. \end{cases}$$

The above equation shows that the unknown probability distribution will be analogous to the normal one. Taken as the initial distribution

$$\rho(x) = \begin{cases} \frac{a}{V 2\pi\sigma} e^{-\frac{x^2}{2\sigma^2}} & \text{at } -a \leq x \leq a, \\ 0 & \text{at } |x| > a, \end{cases}$$

we obtain the dependence of the parameters  $\alpha$  and  $\sigma$  on  $Q$ . This dependence is given implicitly by the equations  $a = u\sigma$ ,

$$Q = \sigma^2 \left( 1 - \frac{2au}{V 2\pi} e^{-\frac{u^2}{2}} \right) = \sigma^2 k^2(u),$$

$$a = \left( \frac{1}{V 2\pi} \int_{-u}^u e^{-\frac{u^2}{2}} du \right)^{-1}$$

The difference between the amounts of information for the normal and truncated normal laws, having equal average powers  $Q$ , is

$$\Delta H = H - H_{tr} = \ln V 2\pi e Q - \ln \frac{V 2\pi e k^2 Q}{a k} = \ln k + \ln a + \frac{1}{2} (1 - k^2).$$

To solve the problem, we assume that the speed of information transmission at a specified accuracy  $\gamma$  should differ from the maximum possible by 1%. Mathematically this is written as:

$$R_{tr} = 2W (H - H_n - \Delta H) = 0.99 \times 2W (H - H_n).$$

Inserting the values for  $H_n$ ,  $H$  and  $\Delta H$ , we obtain the dependence of  $R_{tr}$  on  $\gamma$  (see Table 2 and Figure 1).

TABLE 2

$\gamma, \%$	5.08	4.38	3.95	3.55	3.18	2.84	2.55	2.25
$R, \frac{\text{binary units}}{\text{sec}}$	7.24	7.67	8.00	8.31	8.64	8.98	9.30	9.68
$\gamma, \%$	1.87	1.55	1.11	0.78	0.54	0.366	0.244	0.62
$R, \frac{\text{binary units}}{\text{sec}}$	10.23	10.79	11.78	12.82	13.91	15.05	16.23	17.44

Figure 1 shows the speed of information creation at the output of the TS for uniform and truncated normal distribution, as a function of the accuracy  $\gamma$ . The fact that the uniform distribution gives a greater speed is not surprising, for with equal measurement limit  $a$  and equal noise, i.e., with equal accuracies, the uniform distribution corresponds to a greater average signal power.

#### LITERATURE CITED

- [1] C.E. Shannon, "Mathematical Theory of Communication," Collection edited by N.A. Zhelezov; "Theory of Transmission of Electrical Signals in the Presence of Noise" (Foreign Lit. Press, 1953).

[2] V.A. Il'in and A.N. Novikov, "Survey of Multi-Channel Pulse Telemetering Systems," Automation and Remote Control 16, 4 (1955).

Received March 9, 1956



## LETTER TO THE EDITOR

The journal "Automation and Remote Control" (Volume 15, No. 6, 1954) contains an article by A.S. Sadovskii "Through-Type Inductive Transducer."

The article is devoted to the important problem of the theory of the inductive transducer, which is used in the "coordinate-boring" machine model 2430. The article becomes even more timely because of the lack of any literature on the theory of the operation of through-type inductive transducers. The need for theory that would permit the design and calculation of the above type of transducer is sharply felt by engineers who design machine tools with inductive determination of coordinates.

During our work we encountered the need for selecting the optimum parameters for an inductive through-type transducer (ampere turns, configuration, and dimensions of the magnetic core and of the air gap). We hoped to find answers to some of our problems in the above article.

Attempts at a practical application of the deductions obtained by the author have not led to the desired results. A closer acquaintanceship with the article has shown that it cannot help persons engaged in the design of through-type inductive transducers. The theoretical arguments on which the investigation is based contain many principal errors, which practically nullify all the conclusions reached by A.S. Sadovskii. It is therefore no wonder that the theoretical conclusions obtained by the author of the article are in disagreement with the experimental data given in the article.

The basic principal errors of the article are as follows.

1. The magnetic circuit of the through-type inductive transducer consists of a ferromagnetic portion and an air gap. In real transducers the sensitivity is increased by making the air gap so small, that its magnetic reluctance becomes commensurate with the reluctance of the ferromagnetic portion. Consequently, one cannot agree with the author of the article, who disregards the reluctance of the ferromagnetic portion of the magnetic circuit.

How important the design and correct construction of the ferromagnetic portion is can be seen from the fact that only thanks to the use of the particular shape of the ferromagnetic circuit it became possible to produce the "precision armored transducer" (I.Iu. Klugman, V.S. Mozakerin and M.P. Rashkovich, Patent Application No. 6961), which has a sensitivity that exceeds by a factor of eight the sensitivity of any transducer with a different shape of magnetic circuit having the same number of teeth and having the same size of air gap.

2. No allowance is made for the density of the magnetic flux lines in the air gap, as a result, if the derivations given are followed, the tooth surface of the transducer is not an equipotential surface. Considering that in the above transducer the length of the magnetic flux lines in case of "covering" (Figure 5) changes from 0.1 to 5 mm, i.e., by a factor of 50, the intensity of the magnetic field along the surface of the tube also changes by a factor of 50, which is quite absurd.

3. The author assumes that the flux lines of the magnetic field are in the form of ellipses (Page 514) (since  $p \approx q$  and  $x \gg \delta$ , these lines become circular arcs). This assumption does not agree with reality, for the actual shape of the magnetic flux lines varies in accordance with the position of the teeth and is represented by equations of higher order.

4. In the article the area of the teeth "pierced" by the magnetic flux lines (Figure 8) varies whenever the mutual placement of the teeth changes (?). Thus, the author does not take into account the actual dimensions of the teeth, and operates with teeth of variable height equal to  $\underline{x}$ .

In addition, the article contains mathematical errors and inaccuracies.

1. Instead of Expression (22) he should have obtained

$$\Delta G = \frac{2\mu_0 b}{\pi} \left( \frac{1}{2l_m + \delta + \lambda} + \frac{1}{2l_y + \delta + \lambda} - \frac{2}{\lambda + \delta} \right) \Delta \lambda.$$

2. The author assumes without any foundation that "the maximum value  $\Delta G$  will occur when  $\lambda = 0$ " (Page 519), but when Expressions (10), (13), (22) and (23) are tested for their maximum entirely different results are obtained (and Expression (15) does not contain  $\lambda$  at all).

3. The simplifications assumed in the article are suitable only for the case  $x_1 \gg \delta$ , while the author many times assumes  $x_1 > \delta$ .

We cannot understand why the author of the article, who gave preference to transducers having the configuration shown in Figures 3e and f, considers only the theory of the transducer shown in Figure 3d, which he does not recommend for use.

The author does not compare the theoretical results he obtained with the experimental curves given in the article (Figure 4). Not one of the expressions obtained can explain the shape of the curve  $I_n = f(\Delta \lambda)$ : for large armature displacement - the sharp increase (to 10 ma at  $\Delta \lambda = 0.1$  mm), and then a smooth decrease (to 4 ma at  $\Delta \lambda = 1.5$  mm), followed by an asymptotic approach to the ordinate (4 ma).

I.Iu. Klugman and Ia.L. Litmanov

## A METHOD OF DETERMINING THE OPTIMUM CHARACTERISTICS FOR ONE CLASS OF SELF-ADAPTING SYSTEMS

A. M. Batkov and V. V. Solodnikov

(Moscow)

The problem of optimizing a system, in the sense of reducing the sum of the squares of the dynamic and mean-square deviations to a minimum, is considered for one class of linear systems with variable parameters when a stationary level of random noise is present. This method gives systems which are optimal in that they are self-adapting to the nature of the signal input.

### INTRODUCTION

One of the main obstacles to further improvement in the dynamic accuracies of automatic control systems is that they are inflexible and have invariant dynamic responses, which are built in during design and fabrication to correspond with certain typical conditions of operation. It is thus of considerable interest to produce systems which can automatically adapt their responses to external conditions, or which are, in other words, self-adapting to give optimal properties in response to the continually changing circumstances in their environment.

The importance of self-adaptation to automatic control is obvious. Firstly, real systems always differ from the ideal ones used in design on account of theoretical difficulties, and secondly, not only do the properties of the system itself change with time, mainly in an unpredictable fashion, but so also do the external circumstances.

Self-adaptation principles, as they develop, can be used to overcome these difficulties, e.g., by using computers in automatic control systems. One may assume that in the future automatic control systems will be designed as follows. They will be designed approximately for some typical operating mode and supplemented by a self-adaptation unit, which will seek out the optimum mode of operation and tend to maintain this under all possible circumstances.

At present only the very first attempts to develop the theory and to produce self-adapting systems have appeared; e. g., in Ashby's [1] homeostat, the self-adapting system is one which is initially unstable and which tends automatically to a stable state by adjusting its responses and rejecting the unstable elements in its behavior. A self-adapting servo system has been described [2] which was designed to reproduce discrete input data. The system operated in two ways: an averaging mode when there is no acceleration input, and a following mode when an acceleration input appears. The system switches from one mode of operation to another automatically. A method of designing systems with variable parameters and indications as to certain ways of making them have been given [3], these leading to the minimal mean-square error between any wanted signal and the output on the assumption that the 'current' (see [3]) spectral density of the wanted signal changes unpredictably with time and that the spectral density of the superimposed noise is either constant in time or else changes in a known fashion.

The present paper gives a method of deriving the pulse transfer function for a system with variable parameters which change to correspond with the current values of the wanted signal and noise correlation functions in such a way as to ensure that the sum of the squares of the dynamic and mean-square errors, suitably weighed, is a minimum at any instant.

An integral equation is obtained which defines the optimum condition in the above sense; a method is given for solving this equation for a noise type important in practice, and examples of calculations of pulse transfer functions are presented.

### 1. Setting-Up the Problem

A system will be termed self-adapting if it automatically seeks an optimum or demanded mode of operation and carries out 'experiments' to this end, and if it continually alters its internal responses so as to remain close to the demanded mode when the external circumstances and other perturbing factors alter.

The above definition shows clearly that self-adapting control systems must contain the following basic elements: 1) an assembly of sensing elements to analyze the surroundings; 2) a computer unit which determines the optimum operating conditions from the information supplied by the sensing elements, and which produces the appropriate control signals; 3) an effector unit which creates the optimum conditions of operation by altering the structure, responses or parameters to correspond with the control signals; 4) a comparator unit, which compares the actual and optimum operating conditions and which produces additional control signals if there is any discrepancy.

We shall in the future consider that class of self-adapting systems in which the surroundings act via the system input, and we will restrict the problem to that of deriving the pulse transfer function appropriate to the optimum operating condition as regards dynamic accuracy in the sense explained above.

So we suppose that a perturbation or noise  $n(t)$  acts on the system and that at some instant a control or useful signal  $g(t)$  appears at the input. Then the input is

$$y(t) = g(t) + n(t). \quad (1)$$

The system must reproduce\* the wanted  $g(t)$  and suppress the noise  $n(t)$  in the best possible fashion.

By best possible we mean a reproduction in which the sum of the squares of  $\epsilon_d(t)$  (dynamic) and  $\epsilon_{ms}(t)$  (mean-square) errors [ $\epsilon_{ms}(t)$  being assigned some weight  $\lambda(t)$ ] is at all times minimal. In other words we take the dynamic accuracy index to be

$$E^2(t) = \epsilon_d^2(t) + \lambda^2(t) \epsilon_{ms}^2(t). \quad (2)$$

$g(t)$  will be taken as being a certain function of time, known from its analytic expression.

As regards  $n(t)$  we will assume that it is a random function of time of average value zero having a known correlation  $R(t, \tau)$ .

We then have to find a method of deriving the pulse transfer function for the system,  $k(t, \tau)$ , which ensures (2) is a minimum and which simultaneously satisfies the physical feasibility condition

$$k(t, \tau) = 0, \quad t < \tau, \quad (3)$$

where  $\tau$  is the instant at which the action is applied.

We shall now make certain comments on this way of setting up the problem and of selecting the dynamic accuracy index.

\* For simplicity we here restrict consideration to reproducing  $g(t)$ , this being a particular case of transforming it with the operator  $H(p)$  (see, e.g., [4]).

1. Since the requirement is that  $E^2$  be a minimum the pulse transfer function must clearly depend on the instantaneous values of input signal and noise correlation function.

2. The solution shows that this index leads to optimal systems with variable parameters even with stationary random noise, unlike results that have been given [5, 6] which lead to systems with constant parameters under these conditions. This more complex system (see below) is justified by its providing a more accurate reproduction of the wanted signal than does one with constant parameters.

3. The above way of setting up the problem, unlike the ways adopted in other papers [5, 6], imposes no requirement that  $k(t, \tau)$  return to zero outside a finite interval  $(0, T)$ . In other words we obtain systems with infinite memories which are somewhat more readily producible than those with finite ones [5].

4. (2) specifies the system response in both transient and steady-state modes arising directly from the application of a control signal. The factor  $\lambda$  appearing in (2), which is in general a function of time, enables one to a) alter the weighting assigned to dynamic and mean-square errors (if  $\lambda = 1$ , the weightings are equal at all times); b) to obtain a set of dynamic error at a definite instant.

## 2. The Integral Equation Defining the Minimum Condition

We shall first pause over the expression relating the input  $y(t) = g(t) + n(t)$  and output  $x(t)$ .

Results that have been published [5] show that the usual formula

$$x(t) = \int_0^T y(t - \tau) k(\tau) d\tau, \quad (4)$$

gives an expression for  $k(t)$  with second-order discontinuities at the ends of the integration range  $(0, T)$  in most cases of practical interest. These results [5] cannot be taken as completely rigorous if no special conditions are applied to the range of integration (see Appendix I). We therefore suppose that the correlation function for  $n(t)$  has  $2q$  continuous derivatives, and so  $y(t)$  may be differentiated  $q$  times\*, thereby using (see [17]) another formula

$$x(t) = \sum_{i=0}^q \int_{-\infty}^t y^{(i)}(\tau) d_i W_i(t, \tau), \quad (5)$$

where  $W_i(t, \tau)$  is a function with a restricted range which is characteristic of the optimal system. We assume it continuous in the range  $(-\infty, t)$  and to have possibly a step at  $\tau = t$ , so the Stieltjes integral in (5) exist.

In the simplest case of practical importance  $q = 0$  and

$$x(t) = \int_{-\infty}^t y(\tau) d_i W(t, \tau). \quad (6)$$

Then  $W(t, \tau)$  is simply the integral of the pulse transfer function in the range  $(-\infty, t)$ , i.e., the response to a unit step function.

It is readily seen that by integrating (5) by parts, subject to the initial conditions being zero, we get the form

$$x(t) = \int_{-\infty}^t y(\tau) k(t, \tau) d\tau + \left[ \sum_{i=0}^q \frac{d^i y(\sigma)}{d\sigma^i} k_i^0(t, \sigma) \right]_{\sigma=t}, \quad (7)$$

\*  $g(t)$  is assumed at least as 'smooth' as  $n(t)$ .



where  $k(t, \tau)$  is the pulse transfer function for  $t > \tau$ .

(7) shows that the necessary and sufficient conditions for  $\epsilon_d^2(t) + \lambda^2(t)\epsilon_{ms}^2(t)$  to have a minimum is that  $k(t, \tau)$  should satisfy the integral equation

$$\int_{-\infty}^t [\lambda^2(t) R(\tau, \theta) + g(\tau) g(\theta)] k(t, \theta) d\theta + \sum_{i=0}^n \left\{ \left[ \lambda^2(t) \frac{\partial^i R(\tau, \sigma)}{\partial \sigma^i} + g(\tau) g^{(i)}(\sigma) \right] k_i^0(t, \sigma) \right\}_{\sigma=t} = g(t) g(\tau) \quad (8)$$

(see Appendix II) when  $t > \tau$ .

### 3. Solution of the Integral Equation

Let us consider a method of solving the integral equation (11) for a class of noise  $n(t)$  which has a correlation function  $R(t, \tau)$  bearing a known relation to the function in Green's self-conjugate differential system.

A stationary  $n(t)$  with a rational-fraction spectral density of the form

$$S_n(\omega) = |\psi_n(j\omega)|^2 = N^2 \frac{b_0 \omega^{2m} + b_1 \omega^{2m-2} + \dots + b_m}{a_0 \omega^{2n} + a_1 \omega^{2n-2} + \dots + a_n}, \quad (9)$$

in particular, belongs to this class, where  $\psi_n(s)$  has no poles or zeros in the right half-plane of  $s$ .

If we introduce the linear self-conjugate differential operators with constant coefficients

$$\begin{aligned} M_\tau &= (-1)^m b_0 p^{2m} + (-1)^{m-1} b_1 p^{2m-2} + \dots - b_{m-1} p^2 + b_m, \\ L_\tau &= (-1)^n a_0 p^{2n} + (-1)^{n-1} a_1 p^{2n-2} + \dots - a_{n-1} p^2 + a_n, \end{aligned} \quad (10)$$

where  $p \equiv \frac{d}{d\tau}$ , then we can show that

$$R(\tau, \theta) = N^2 M_\tau G(\tau, \theta), \quad (11)$$

where  $G(\tau, \theta)$  is Green's function for the self-conjugate differential system

$$\begin{aligned} L_\tau(z) &= 0, \\ \lim_{\tau \rightarrow \infty} z^{(k)}(\tau) &= \lim_{\tau \rightarrow -\infty} z^{(k)}(\tau) = 0, \quad k = 0, 1, \dots, n-1. \end{aligned} \quad (12)$$

The class of stationary random noise distributions considered in [7] which have spectral densities of rational-fraction form with constant numerators is a subdivision of the class considered here, which latter includes most cases of practical interest.

And so we shall solve the integral equation for random processes with spectral density forms as of (9)\*.

\* This method of solution can readily be generalized to nonstationary processes occurring at the outputs of linear systems with variable parameters when white noise is applied to the inputs, since the correlation functions are the results of integro-differential transformations of the pulse transfer function [as distinct from (11)].



(8), taken together with (11), may be rewritten as

$$\begin{aligned} & \lambda^2(t) N^2 \int_{-\infty}^t M_\tau G(\tau, \theta) k(t, \theta) d\theta + \lambda^2(t) N^2 M_\tau \left[ \sum_{i=0}^q \frac{\partial^i G(\tau, \sigma)}{\partial \sigma^i} k_i^0(t, \sigma) \right]_{\sigma=t} = \\ & = g(t) g(\tau) - \sum_{i=0}^q [g(\tau) g^{(i)}(\sigma) k_i^0(t, \sigma)]_{\sigma=t} - \int_{-\infty}^t g(\tau) g(\theta) k(t, \theta) d\theta, \end{aligned} \quad (13)$$

since  $\tau, \theta, \sigma, t$  are independent variables, so

$$\begin{aligned} & \lambda^2(t) N^2 M_\tau \left[ \int_{-\infty}^t G(\tau, \theta) k(t, \theta) d\theta + \sum_{i=0}^q \left( \frac{\partial^i G(\tau, \sigma)}{\partial \sigma^i} k_i^0(t, \sigma) \right) \right]_{\sigma=t} = \\ & = g(\tau) \left[ g(t) - \sum_{i=0}^q (g^{(i)}(\sigma) k_i^0(t, \sigma))_{\sigma=t} - \int_{-\infty}^t g(\theta) k(t, \theta) d\theta \right]. \end{aligned} \quad (14)$$

To reduce the lengths of the expression  $D(\tau)$  will be used to denote the quantity in square brackets on the right side of (14), and then we clearly get a linear nonhomogenous differential equation of order  $2m$  with constant coefficients:

$$M_\tau [D(\tau)] = g(\tau). \quad (15)$$

Its general solution can be written as

$$D(\tau) = \sum_{\mu=0}^{2m-1} C_\mu e^{\lambda_\mu \tau} + M_\tau^{-1} [g(\tau)], \quad (16)$$

where  $\lambda_\mu$  are the roots of the characteristic equation

$$M(\lambda_\mu) = 0 \quad (17)$$

and  $M_\tau^{-1} [g(\tau)]$  denotes a particular solution of (15)

To the general solution (16) we apply the condition\*

$$\lim_{\tau \rightarrow -\infty} D^{(\mu)}(\tau) = 0 \quad (\mu = 0, 1, 2, \dots, m-1), \quad (16')$$

\* (20) shows that these conditions are those necessary and sufficient for  $k(t, \tau)$  to be finite when  $\tau \rightarrow -\infty$ .

from which we can determine the  $m$  arbitrary constants  $C_\mu$ . Further, (14) and (16) give

$$\int_{-\infty}^t G(\tau, \theta) k(t, \theta) d\theta = \frac{D(\tau)}{\lambda^2(t) N^2} \left\{ g(t) - \sum_{i=0}^q [g^{(i)}(\sigma) k_i^0(t, \sigma)]_{\sigma=t} - \right. \\ \left. - \int_{-\infty}^t g(\theta) k(t, \theta) d\theta \right\} - \sum_{i=0}^q \left[ \frac{\partial^i G(\tau, \sigma)}{\partial \tau^i} k_i^0(t, \sigma) \right]_{\sigma=t}. \quad (18)$$

But since  $G(\tau, \theta)$  is Green's function and the operations of differentiating with respect to  $\tau$  and  $\sigma$  are commutative we can rewrite (18) as

$$k(t, \tau) = \frac{1}{\lambda^2(t) N^2} \left\{ g(t) - \sum_{i=0}^q [g^{(i)}(\sigma) k_i^0(t, \sigma)]_{\sigma=t} \right\} L_\tau [D(\tau)] - \\ - \frac{1}{\lambda^2(t) N^2} \int_{-\infty}^t L_\tau [D(\tau)] g(\theta) k(t, \theta) d\theta. \quad (19)$$

Thus we get a nonhomogeneous Fredholm integral equation of order two in  $k(t, \tau)$  having a degenerate nucleus.

By normal methods it may be shown that the solution of this takes the form

$$k(t, \tau) = \frac{L_\tau [D(\tau)] A(t)}{\lambda^2(t) N^2 + \int_{-\infty}^t L_\theta [D(\theta)] g(\theta) d\theta}, \quad (20)$$

where

$$A(t) = g(t) - \sum_{i=0}^q [g^{(i)}(\sigma) k_i^0(t, \sigma)]_{\sigma=t} \quad (20')$$

and  $L_\tau, D(\tau)$  are defined by (10) and (16).

From (16), (16') and (17) it is clear that the solution contains  $m + q + 1$  arbitrary constants. These can be determined from the  $m + q + 1$  algebraic equations obtained by substituting the expression found for  $k(t, \tau)$  into the initial Equation (8).

In fact if we substitute  $k(t, \tau)$  into (8) and use Green's formula it can be shown by direct calculation that when the conditions imposed on the operators  $R(t, \tau)$ ,  $D(\tau)$  and the input  $g(t)$  are fulfilled the  $C_\mu$  and the steps  $k_i^0(t)$  are defined from the conditions

$$\left\{ \left[ g(t) - \sum_{i=0}^q g^{(i)}(\sigma) k_i^0(t, \sigma) \right] \left[ \sum_{v=1}^n a_{n-v} \sum_{k=0}^{2v-1} (-1)^{k-v} \frac{\partial^k R(\tau, \sigma)}{\partial \sigma^k} D^{(2v-k-1)}(\sigma) \right] + \right. \\ \left. + \left[ \lambda^2(t) N^2 + \int_{-\infty}^t L_\theta [D(\theta)] g(\theta) d\theta \right] \left[ \sum_{i=0}^q \frac{\partial^i R(\tau, \sigma)}{\partial \sigma^i} k_i^0(t, \sigma) \right]_{\sigma=t} \right\} = 0, \\ \text{где } q = n - m - 1. \quad (21)$$

where  $q = n - m - 1$ .

Let us consider certain particular cases of these solutions.

1. If  $g(t)$  can appear at the input only when  $t \geq 0$ , then

$$k(t, \tau) = \frac{L_{\tau}[D(\tau)] [g(t) - \sum_{\sigma=0}^q (g^{(i)}(\sigma) k_1^0(t, \sigma))_{\sigma=t}]}{\lambda^2(t) N^2 + \int_0^t L_{\theta}[D(\theta)] g(\theta) d\theta} \quad (22)$$

(21) remains in force, the lower limit in the integral changing to zero.

2. With white noise having a correlation function  $N^2 \delta(\tau - \theta)$  (20) takes the form

$$k(t, \tau) = \frac{g(t) g(\tau)}{\lambda^2(t) N^2 + \int_0^t g^2(\theta) d\theta} \quad (t \geq \tau). \quad (23)$$

Then all the  $k_1^0(t)$  are zero, i.e., the pulse transfer function has only steps and no second-order discontinuities at  $t = \tau$ . The angular points in the transient correspond to these steps, and (21) is automatically fulfilled.

3. When the noise has a rational-fraction spectral density, as in (9), subject to the condition  $m = n - 1$ , [The correlation function being, e.g.,  $N^2 e^{-\alpha|\tau-\theta|}$ ,  $N^2 e^{-\alpha|\tau-\theta|} \cos \omega_0(\tau - \theta)$ , ], the pulse transfer function

$$k(t, \tau) = \frac{L_{\tau}[D(\tau)] g(t) [1 - k^0(t)]}{\lambda^2(t) N^2 + \int_0^t L_{\theta}[D(\theta)] g(\theta) d\theta} \quad (t > \tau \geq 0) \quad (24)$$

has only one discontinuity at  $t = \tau$ , which is determined from the condition

$$g(t) [1 - k^0(t)] \left[ \sum_{v=1}^n a_{n-v} \sum_{k=0}^{2v-1} (-1)^{k+v} \frac{\partial^k R(\tau, \sigma)}{\partial \sigma^k} D^{(2v-k-1)}(\sigma) \right]_{\sigma=t} + \\ + [\lambda^2(t) N^2 + \int_0^t L_{\theta}[D(\theta)] g(\theta) d\theta] R(\tau, t) k^0(t) = 0. \quad (25)$$

#### 4. Preliminary Remarks on the Production of Systems Falling in this Class

The present paper does not describe the possible ways of making the adaptive systems falling in this class. We only intend to relate the results to various more or less evident physical concepts, so we only present one of the simplest possible designs. This design is adaptive (self-adjusting) in response to the type of input signal.

We suppose that  $y(t) = g(t) + n(t)$  is applied to the inputs both of the system and of a special computer (Fig. 1). We assume that although the characteristics of both components are not known in advance, certain preliminary information is nevertheless available; E.g., a case of practical interest is where  $g(t)$  depends on the parameters  $a_1, a_2, \dots, a_n$ , concerning which there is no prior information, while the noise has known statistical aspects.

Published results [9] enable one to devise a computer unit 3 (Fig. 1) which will compute these parameters. Then the system will operate as follows. Over some time interval 3 estimates the parameters of the wanted input signal, and 5 uses these data to determine  $k_{opt}(t, \tau)$  (the optimum pulse transfer function), this being compared with the current pulse transfer function for system 1, i.e.,  $k(t, \tau)$ . This latter is fed continuously to unit 6. Comparison of these functions in 7 gives rise to changes in the parameters of the corrector unit 2 such as to cause the pulse transfer function of the whole system to approach the optimum one, defined by (20).

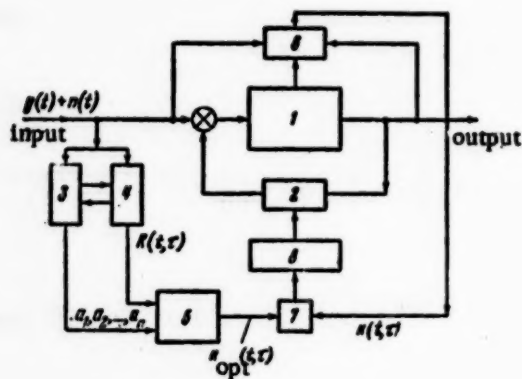


Fig. 1

But in the general case both noise and signal parameters may not be known in advance. Then the computer must contain both the parameter calculator 3 and the correlator 4. Under definite conditions these units will correlate against one another and will provide the required information about the input signal. The accuracy of such parallel operation of the two units is a subject for separate study.

The way in which the accuracy of the computer affects the accurate operation of the whole system is also of interest here.

The complete consideration of this problem is a separate task. Only a particular case is considered here: that where the computer of Fig. 1 determines the instantaneous values of  $g(t)$ , with a maximum error  $\alpha$ , together with  $N^2$ , the noise per unit band-width (for simplicity the noise is assumed 'white'), with maximum error  $\beta^2$ , i.e. we suppose  $g_1(t) = \alpha g(t)$  and  $N_1^2 = \beta^2 N^2$ .

when  $\lambda(t) = 1$ , (23) gives

$$k(t, \tau) = \frac{g_1(t) g_1(\tau)}{N_1^2 + \int_0^t g_1^2(\theta) d\theta}.$$

If a signal  $g(t)$  and a noise  $N^2$  appear at the input of such a system the total error in the reproduction will be

$$E_1^2 = e_d^2 + e_{ms}^2 = g^2(t) \frac{\rho^2(t) \left[ \left( \frac{\beta^2}{\alpha^2} \right)^2 \rho^2(t) + 1 \right]}{\left[ \frac{\beta^2}{\alpha^2} \rho^2(t) + 1 \right]^2}, \quad (26)$$

where

$$\rho^2(t) = \frac{N^2}{\int_0^t g^2(\theta) d\theta}. \quad (27)$$

Since when the system is exactly adapted to the input signal characteristics the error is

$$E^2 = g^2(t) \frac{\rho^2(t)}{1 + \rho(t)}, \quad (28)$$

the relative error due to inexact control of the system may be represented as

$$\frac{E_1^2}{E^2} = \frac{[1 + \rho^2(t)] \left[ \left( \frac{\beta^2}{\alpha^2} \right)^2 \rho^2(t) + 1 \right]}{\left[ \frac{\beta^2}{\alpha^2} \rho^2(t) + 1 \right]^2}. \quad (29)$$

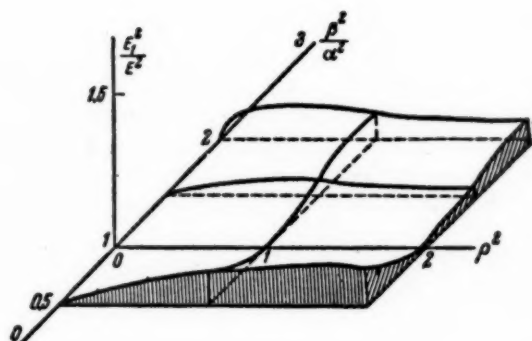


Fig. 2. Relative error when an optimum system is inexact control.

The relations between  $E_1^2/E^2$  and the parameters  $\rho^2(t)$  and  $\beta^2/\alpha^2$  are shown in Fig. 2. It is readily seen that  $E_1^2/E^2$  is always greater than one (when  $\beta^2/\alpha^2 \neq 1$ ), which must be so, since the error is increased by the system being inexact control. It is interesting that, according to (29), the error is optimal when  $\alpha^2 = \beta^2$ . Also Fig. 2 shows that (29) is maximal when  $\alpha^2/\beta^2 = \rho^2$ , having a region in the  $(\beta^2/\alpha^2, \rho^2)$  plane where  $E_1^2$  is close to  $E^2$  for large  $\alpha^2$  and  $\beta^2$ .

The possibility of using such a control method in principle indicates that the increase in total error,  $E_1^2 - E^2$ , produced by the inexact control, is always less than the permitted error in the computer determining the signal.

In fact if  $\epsilon^2 = [g_1(t) - g(t)]^2 = g^2(t) (1 - \alpha)^2$ , then when  $\beta^2 = 1$  we have

$$[E_1^2 - E^2]_{\max} - \epsilon^2 = \frac{g^2(t) (\alpha - 1)^2}{4(1 + \alpha^2)} (2\alpha - 3\alpha^2 - 3) < 0$$

for all  $\alpha$ , i.e.,  $[E_1^2 - E^2]_{\max} < \epsilon^2$ . For example if  $\alpha = 0.5$ , then  $[E_1^2 - E^2]_{\max} = 0.11 g^2(t)$ , since  $\epsilon^2 = 0.25 g^2(t)$ .

## 5. Examples

Let us consider certain examples of the use of (22) to illustrate these results.

**Example 1.** Let the wanted signal be a unit step-function  $1(t)$ , while  $n(t)$  represents white noise.

(23), with  $\lambda^2 = 1$ , gives

$$k(t, \tau) = \frac{1}{N^2 + t}, \quad t \geq 0. \quad (30)$$

$x(t)$ , which appears at the output of the system [the latter having a pulse transfer function of the type of (30) when the input is  $1(t)$ ], is given by  $x(t) = \frac{t}{N^2 + t}$ .

Figure 3 clearly shows that the transient  $x(t)$  will rise more slowly the greater  $N^2$ .

**Example 2.** Let the wanted signal be  $g(t) = at$ , while the noise, as before, is white. Then (23), with  $\lambda^2 = 1$ , gives

$$k(t, \tau) = \frac{a^2 t \tau}{N^2 + \frac{a^2 t^3}{3}} \quad (t \geq \tau) \quad (31)$$

(Fig. 4) and the total error is

$$E^2 = \frac{N^2}{\frac{t}{3} + \frac{N^2}{a^2 t^3}}. \quad (32)$$

The optimal system with constant parameters considered in [5] for zero dynamic error gives a mean-square error  $\epsilon_{ms}^2 = \frac{4N^2}{T}$  for all  $t \geq T$ .

Comparison of  $E^2$  and  $\epsilon_{ms}^2$  gives

$$\frac{\epsilon_{ms}^2}{E^2} = \frac{4N^2}{a^2 t^3 S} + \frac{4}{3} \frac{t}{T}. \quad (33)$$

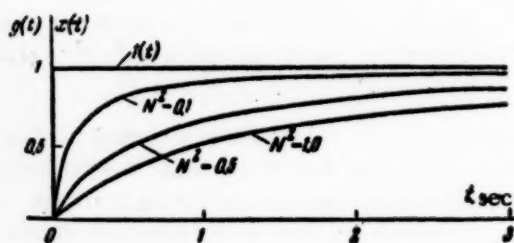


Fig. 3. Response of the optimal system to a unit function.

This shows that

$$1) E^2 < \epsilon_{ms}^2 \text{ for all } t \geq T;$$

2) the use of a system with variable parameters enables one to obtain errors equal to  $\epsilon_{ms}^2$  when  $t < T$ ; e.g., when  $a^2 = N^2$  and  $T = 1.41$  sec.  $E^2 = \epsilon_{ms}^2$  when  $t = 0.72$  sec.

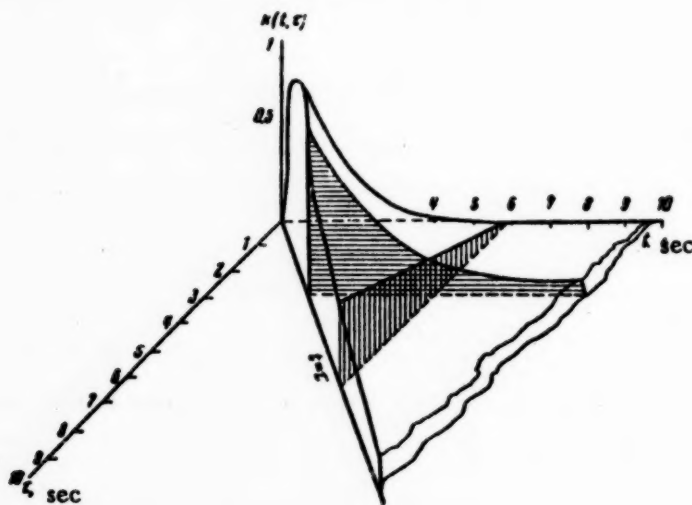


Fig. 4. The optimum pulse transfer functions for the signal  $g(t) = at$  ( $t \geq 0$ ), when the noise has  $R(\tau) = N^2 \delta(\tau)$ , ( $a^2 = N^2$ ).



3)  $E^2 < \epsilon_{ms}^2$  becomes stronger when the noise level rises and  $E^2 \rightarrow 0$  when  $t \rightarrow \infty$ , since  $\epsilon_{ms}^2 = \text{const}$ ; this is one of the fundamental properties of this class of systems.

Example 3. We suppose the wanted signal is given by a function  $g(t)$ , ( $t \geq 0$ ), while the correlation function and spectral density of the noise are given by

$$R(\tau, 0) = N^2 e^{-a|\tau-0|}, \quad S_n(\omega) = \frac{2aN^2}{\omega^2 + a^2}, \quad (34)$$

i.e.,

$$L_\tau = -p^2 + a^2, \quad M_\tau = 2a = \text{const}, \quad q = 0.$$

Then  $D(\tau) = \frac{g(\tau)}{2a}$  and when  $\lambda^2 = 1$ , (24) gives

$$k(t, \tau) = \frac{[a^2 g(\tau) - g''(\tau)] g(t) [1 - k^0(t)]}{2aN^2 + \int_0^t [a^2 g(\theta) - g''(\theta)] g(\theta) d\theta} \quad (t > \tau \geq 0). \quad (35)$$

Further (25) gives

$$k^0(t) = \frac{g(t) [ag(t) + g'(t)]}{g(t) [ag(t) + g'(t)] + 2aN^2 + \int_0^t [a^2 g(\theta) - g''(\theta)] g(\theta) d\theta} \quad (36)$$

and so the optimum pulse transfer function takes the form

$$k(t, \tau) = \frac{g(t) [a^2 g(\tau) - g''(\tau)]}{g(t) [ag(t) + g'(t)] + 2aN^2 + \int_0^t [a^2 g(\theta) - g''(\theta)] g(\theta) d\theta} \quad (t > \tau \geq 0). \quad (37)$$

In particular, if

$$g(t) = \begin{cases} \sum_{\alpha=0}^p b_\alpha t^\alpha, & t \geq 0, \\ 0, & t < 0, \end{cases} \quad (38)$$

then

$$k(t, \tau) = \frac{\sum_{\alpha=0}^p \sum_{\beta=0}^p b_\alpha b_\beta t^{\alpha+\beta} \left[ a^2 - \frac{\beta(\beta-1)}{\tau^2} \right]}{2aN^2 + \sum_{\alpha=0}^p \sum_{\beta=0}^p b_\alpha b_\beta t^{\alpha+\beta-1} \frac{[(\alpha+\beta)^2-1](\alpha t + \beta) + a^2 t^2 (\alpha+\beta-1) - \alpha(\alpha-1)(\alpha+\beta+1)}{(\alpha+\beta)^2-1}}, \quad (39)$$

$$t > \tau \geq 0,$$

$$k^0(t) = \frac{\sum_{\alpha=0}^p \sum_{\beta=0}^p b_{\alpha} b_{\beta} t^{\alpha+\beta-1} (at + \beta)}{2aN^2 + \sum_{\alpha=0}^p \sum_{\beta=0}^p b_{\alpha} b_{\beta} t^{\alpha+\beta-1} \frac{[(\alpha+\beta)^2-1] [at+\beta] + a^2 t^2 (\alpha+\beta-1) - \alpha(\alpha-1)(\alpha+\beta+1)}{(\alpha+\beta)^2-1}} \quad (40)$$

If

$$g(t) = \begin{cases} b \sin \omega_0 t, & t \geq 0, \\ 0 & t < 0, \end{cases}$$

then

$$k(t, \tau) = \frac{b^2 (a^2 + \omega_0^2) \sin \omega_0 t \sin \omega_0 \tau}{2aN^2 + ab^2 \sin^2 \omega_0 t + \frac{b^2}{2} \left[ (a^2 + \omega_0^2) t + \frac{\omega_0^2 - a^2}{2\omega_0} \sin 2\omega_0 t \right]} \quad (t > \tau \geq 0) \quad (41)$$

and

$$k^0(t) = \frac{b^2 (a \sin \omega_0 t + \omega_0 \cos \omega_0 t) \sin \omega_0 t}{2aN^2 + ab^2 \sin^2 \omega_0 t + \frac{b^2}{2} \left[ (a^2 + \omega_0^2) t + \frac{\omega_0^2 - a^2}{2\omega_0} \sin 2\omega_0 t \right]} \quad (42)$$

Example 4. Suppose  $g(t) = at$ ,  $t \geq 0$ , while for the noise

$$R_n(\tau, \theta) = N^2 e^{-a|\tau-\theta|} \cos \omega_0 (\tau - \theta) \quad (43)$$

the spectral density of the noise being

$$S_n(\omega) = N^2 \frac{2a(\omega^2 + a^2 + \omega_0^2)}{\omega^4 + 2(a^2 - \omega_0^2)\omega^2 + (a^2 + \omega_0^2)^2} \quad (44)$$

then

$$\begin{aligned} L_{\tau}(p) &= p^4 - 2(a^2 - \omega_0^2)p^2 + (a^2 + \omega_0^2)^2, \\ M_{\tau}(p) &= (-p^2 + a^2 + \omega_0^2)2a. \end{aligned} \quad (45)$$

The solution to  $M_{\tau}[D(\tau)] = \frac{g(\tau)}{2a}$  is

$$D(\tau) = Ce^{\beta\tau} + C_1e^{-\beta\tau} + \frac{b\tau}{2a\beta^2} \quad (46)$$

Imposing the condition  $\lim_{\tau \rightarrow -\infty} D(\tau) = 0$  and remembering that  $g(\tau) = 0$  when  $\tau = -\infty$ , we get

$$D(\tau) = Ce^{\beta\tau} + \frac{b\tau}{2a\beta^2} \quad (47)$$

where  $\beta = a^2 + \omega_0^2$  is the root of the characteristic equation  $M(\lambda_\mu) = 0$ .

Further

$$L_\tau[D(\tau)] = \beta^2 \left[ 4\omega_0^2 Ce^{\beta\tau} + \frac{b\tau}{2a} \right] \quad (48)$$

Substituting (43), (47) and (48) into (25) when  $\lambda^2 = 1$ , equating the coefficients to the linearly-independent functions  $\sin \omega_0(t - \tau)$  and  $\cos \omega_0(t - \tau)$  to zero, and solving the resulting pair of algebraic equations for  $k^0(t)$  and  $C$ , we get

$$k_0(t) = \left\{ 1 + 2aN^2 + \frac{1}{3} b^2 \beta^2 t^3 - \frac{2b^2 \omega_0^2 (b^2 t + 2a\omega_0)}{\beta^2 (a + \beta)} [3t - 1 - e^{-\beta t}] + \right. \\ \left. + \frac{b^2 t}{\beta^2} \left[ \frac{\omega_0^2 (3^2 + 2a\omega_0)}{\beta + a} + \beta^2 (at + 1) - 2\omega_0^2 \right] \right\}^{-1} \quad (49)$$

$$C = - \frac{b [3^2 t + 2a\omega_0]}{4a\beta^2 (\beta + a)} \quad (50)$$

Substituting (48), (49) and (50) into (24) we get the final expression for the optimum pulse transfer function as

$$k(t, \tau) = \frac{\beta^2 b^2 t \left[ \frac{\tau}{2a} - \frac{\omega_0^2 (\beta^2 t + 2a\omega_0)}{a\beta^2 (a + \beta)} e^{-\beta(t-\tau)} \right]}{\frac{b^2 t}{\beta^2} [\beta^2 (at + 1) - 2\omega_0^2] + 2aN^2 + b^2 \beta^2 \frac{t^3}{3} + \frac{2b^2 \omega_0^2 (\beta^2 t + 2a\omega_0)}{\beta^2 (a + \beta)} (1 + e^{-\beta t})} \quad (51)$$

$(t > \tau \geq 0).$

A partial test that these results are correct is obtained by putting  $\omega_0 = 0$  and comparing (52) and (54) with the results from example 3 with  $g(t) = bt$ .

## CONCLUSIONS

1. The theory of self-adapting systems which automatically alter their responses in such a way as to keep the operating mode near optimal as the surrounding conditions change is an important current problem in the theory of automatic control.

2. (2) may be chosen as an index of optimum operation in this class of dynamic systems, as regards dynamic accuracy; i.e.,  $E^2 = c_{ms}^2(t) + \lambda^2(t) \epsilon_d^2(t) = \min$  at any time  $t$ .

In order to satisfy the optimum condition (2) and the physical feasibility condition (3) for stationary random noise  $n(t)$  as well as for a fairly wide class of nonstationary noise spectra it is both necessary and sufficient that the pulse transfer function should satisfy the integral equation (8), this latter having a solution of the form of (20) when the random noise is stationary.

4. The above approach to the problem leads to systems with variable parameters and an 'infinite memory' even with random stationary noise; and the criteria of dynamic accuracy proposed above specify the system response during transients as well as in the steady state, provide a known relation between the dynamic and random errors at different times, and ensure that the error during the response is reduced.

5. One possible way of producing adaptive systems which fall in this class is to use computers to determine approximately the instantaneous signal values and noise correlation functions.

6. These examples show that the proposed method of computing the optimum pulse transfer functions encounters no difficulty in many practical instances.

#### APPENDIX I

In [5] [formula (64)] the optimum pulse transfer function  $k(t)$  contained terms of the type  $\delta^{(i)}(t)$  and  $\delta^{(i)}(t-T)$ . When  $k(t)$  takes these forms the output signal, strictly speaking, does not exist, since the values of  $t$  at which the derivatives of the  $\delta$ -function are taken, fall at the end of the range of integration in (4).

This fact was not allowed for in [5] since it was assumed that

$$\int_0^T y(t-\tau) \delta^{(i)}(\tau) d\tau = y^{(i)}(t).$$

and

$$\int_0^T y(t-\tau) \delta^{(i)}(T-\tau) d\tau = y^{(i)}(t-T), \quad (52)$$

but these integrals diverge to infinity (the first when  $\tau = 0$ , the second when  $\tau = T$ ). Let us consider for instance the expression

$$x_{\delta'}(t) + \int_0^T y(t-\tau) \delta'(\tau) d\tau. \quad (53)$$

By taking the  $\delta$ -function and its derivative  $\delta'(\tau)$  as being limits (see [8]) e.g.,

$$\delta(\tau) = \lim_{\lambda \rightarrow \infty} \frac{\lambda}{\pi(\lambda^2 \tau^2 + 1)}, \quad (54)$$

$$\delta'(\tau) = - \lim_{\lambda \rightarrow \infty} \frac{2}{\pi} \frac{\lambda^3 \tau}{(\lambda^2 \tau^2 + 1)^2} \quad (55)$$

it is readily seen that

$$\int \delta'(\tau) d\tau = \delta(\tau). \quad (56)$$

So by integrating (53) by parts we get

$$x_{\delta'}(t) = [y(t-\tau)\delta(\tau)]_0^T + y'(t) \quad (57)$$

and so  $x_{\delta'}(t)$  does not exist when  $y(t) \neq 0$ , since according to (57),  $\delta(\tau) = \infty$  when  $\tau = 0$ .

The discussion shows that (52), strictly speaking, is only correct over the range of integration  $0 < \tau < T$  or  $0 \leq \tau \leq T^+$ , and not in the range  $0 \leq \tau \leq T$ .

## APPENDIX II

In accordance with (7) the expression for the dynamic error may be put in the form

$$\epsilon_d(t) = g(t) - \int_{-\infty}^t g(\tau) k(t, \tau) d\tau - Q(t), \quad (58)$$

where

$$Q(t) = \left[ \sum_{i=0}^q g^{(i)}(\sigma) k_i^0(t, \sigma) \right]_{\sigma=t}, \quad (59)$$

and the random error expression in the form

$$\epsilon_r = \int_{-\infty}^t n(\tau) k(t, \tau) d\tau + p(t), \quad (60)$$

where

$$p(t) = \left[ \sum_{i=0}^p n^{(i)}(\sigma) k_i^0(t, \sigma) \right]_{\sigma=t}, \quad (61)$$

so

$$\begin{aligned} E^2 &= \epsilon_d^2(t) + \lambda^2(t) \epsilon_{ms}^2(t) = \\ &= g^2(t) - 2[g(t) - Q(t)] \int_{-\infty}^t g(\tau) k(t, \tau) d\tau + Q^2(t) - 2g(t)Q(t) + \\ &+ \int_{-\infty}^t \int_{-\infty}^t [\lambda^2(t) R(\tau, \theta) + g(\tau)g(\theta)] k(t, \tau) k(t, \theta) d\tau d\theta + \lambda^2(t) \overline{p^2(t)} + \\ &+ 2 \int_{-\infty}^t \lambda^2(t) \overline{p(t)n(\tau)} k(t, \tau) d\tau. \end{aligned}$$

Let us find a  $k(t, \tau)$  such that  $E^2$  is a minimum. Assume that  $k(t, \tau)$  is varied by  $\Delta k(t, \tau)$ . Then we get

$$\begin{aligned} E_{\Delta}^2 = E^2 - 2\Delta [g(t) - Q(t)] \int_{-\infty}^t g(\tau) k(t, \tau) d\tau + 2\Delta \lambda^2(t) \int_{-\infty}^t \overline{p(t)n(\tau)} k(t, \tau) d\tau + \\ + 2\Delta \int_{-\infty}^t \int_{-\infty}^t [\lambda^2(t) R(\tau, \theta) + g(\tau) g(\theta)] k(t, \tau) k(t, \theta) d\tau d\theta + \\ + \Delta^2 \int_{-\infty}^t \int_{-\infty}^t [\lambda^2(t) R(\tau, \theta) + g(\tau) g(\theta)] k(t, \tau) k(t, \theta) d\tau d\theta. \end{aligned}$$

Differentiating  $E_{\Delta}^2$  with respect to  $\Delta$ , equating the result to 0 and then putting  $\Delta = 0$  (as usual) we get

$$\begin{aligned} [g(t) - Q(t)] \int_{-\infty}^t g(\tau) k(t, \tau) d\tau - \lambda^2(t) \int_{-\infty}^t \overline{p(t)n(\tau)} k(t, \tau) d\tau = \\ = \int_{-\infty}^t \int_{-\infty}^t [\lambda^2(t) R(\tau, \theta) + g(\tau) g(\theta)] k(t, \tau) k(t, \theta) d\tau d\theta. \end{aligned} \quad (62)$$

Since (62) must be satisfied for all  $k(t, \tau)$  we have

$$g(t) g(\tau) = \int_{-\infty}^t [\lambda^2(t) R(\tau, \theta) + g(\tau) g(\theta)] k(t, \theta) d\theta + \lambda^2(t) \overline{p(t)n(\tau)} + Q(t) g(\tau). \quad (63)$$

but

$$Q(t) g(\tau) = \left[ \sum_{i=0}^q g(\tau) g^{(i)}(\sigma) k_i^0(t, \sigma) \right]_{\sigma=t} \quad (64)$$

and

$$\overline{p(t)n(\tau)} = \overline{\left[ \sum_{i=0}^q n(\tau) n^{(i)}(\sigma) k_i^0(t, \sigma) \right]_{\sigma=t}} = \left[ \sum_{i=0}^q \frac{\partial^i R(\tau, \sigma)}{\partial \sigma^i} k_i^0(t, \sigma) \right]_{\sigma=t}.$$

Substituting (64) and (65) into (63) we get (8).

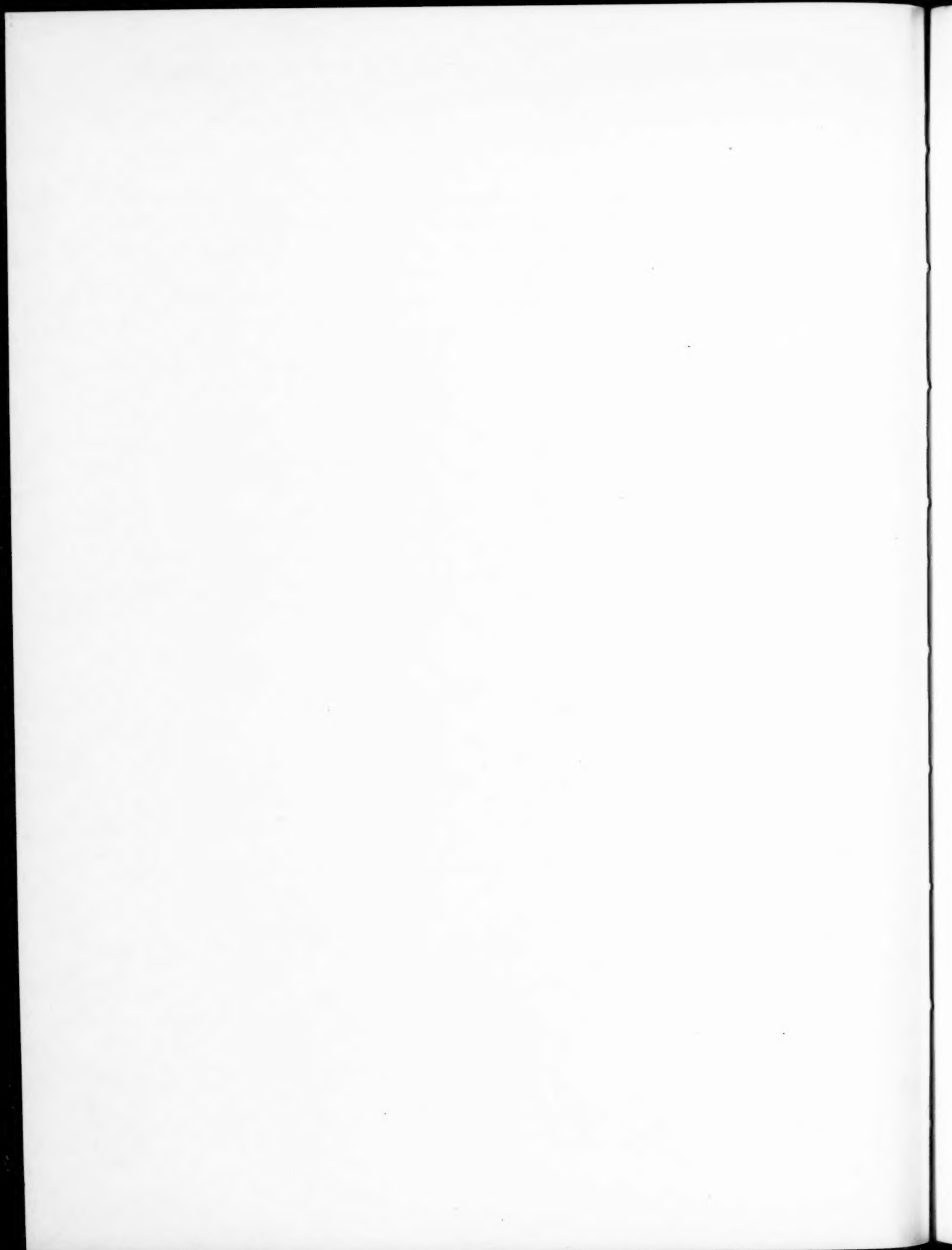
Received July 3, 1956

#### LITERATURE CITED

- [1] Ashby, W. R. Design for a brain. Wiley, 1952.
- [2] Benner, A. H., Drenick R. An adaptive Servo System. IRE Convention Record, part 4, March, 1955.
- [3] Keiser, B. E. The linear Input-Controlled Variable-Pass Network. Trans IRE on Information theory, No. 1, March, 1955.



- [4] Solodnikov, V. V. Introduction to the statistical dynamics of automatic control systems. State Technical Press, 1952.
- [5] Zadeh, L., Ragazzini, J. An Extension of Wiener's Theory of Prediction. Journ. Appl. Ph., July, 1950.
- [6] Solodnikov, V. V. and Matveev, P. S. Design of corrector units for servos to satisfy set demands for dynamic accuracy where noise is present. Automation and Remote Control, 16, No. 3, 1955.
- [7] Dolph, Woodbury M. On the relation between Green's functions and covariances of certain stochastic processes and its application to unbiased linear prediction. Trans. Amer. Math. Soc., vol. 72, No. 3, 1952.
- [8] Van der Pol, Bremer. Operational calculus using the bilateral Laplace transform, ch. V. Foreign Literature Press, 1952.
- [9] Slepian, D. Estimation of signal parameters in the presence of noise. Trans. IRE, PGIT-3, March, 1954.



## STABILIZING CONTROL SYSTEMS WITH A SPECIAL SIGNAL

R. Oldenburger  
(Lafayette, Ind., U.S.A.)

Linear automatic control systems with two or more main delay links\* may be stabilized by injecting noise or a signal of sufficiently high frequency subject to the condition that system hunt is not too severe.\*\* The signal amplitude must be sufficient to drive a bounded element to its limits, e.g., must correspond to the control range of an auxiliary control valve in the regulator. Optimal nonlinear control systems with one or more delay links can also be stabilized by injecting a suitable signal. If the stabilizing signal is not very great the responses to the larger perturbations will only be slightly affected.

### 1. Stabilizing with Signals

Early automatic control systems were stabilized about their equilibrium positions using stable linear links.

Automatic control systems, which in the vast majority are nonlinear at large deviations, are considered as linear on the assumption that the errors in the controlled variable and its derivatives are sufficiently small and that the roots of the characteristic equation are satisfactory.\*\*\*

Here the stability is produced by nonlinear methods. The results given here were obtained in work on the frequency-response of a regulator-turbine system programmed on a Philbrick electronic computer. The system showed hunting, but when a sinusoidal signal of appropriate amplitude and frequency was applied the hunting ceased. These results are due to the changes in the gains of the nonlinear links.

MacColl and Minorsky have derived certain results in the general theory of stability.

MacColl [1] considered servomechanisms operating on the all-or-none principle, in which the output was  $-A, 0$  or  $A$  for positive, zero and negative inputs respectively. Thus the output was always either zero or one of the limiting values  $\pm A$ . When a sinusoidal signal was applied the system operated linearly for small inputs.

This approach differs from that used here in that here the output from the nonlinear element is taken as proportional to the input.

Minorsky [2] studied the use of signals for exciting or damping oscillations in physical systems described by second-order differential equations in the variable  $x(t)$ , while the coefficient of the damping term, which contains  $dx/dt$ , was an even polynomial in  $x$ .

Minorsky's method of stabilization depends on the properties of the asymptotic solution to the differential equation and its adequacy is different from that of the method given here.

The piston speed is bounded in any hydraulic servomechanism. In Fig. 1 the variable  $\dot{m}$  is the controlled

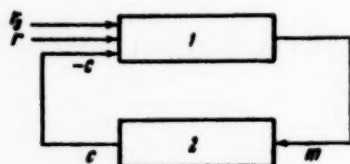
\* This evidently implies systems containing two or more time-constants. (Trans. editor, A. M. Letov).

\*\* Having in mind periodic oscillations which may change in amplitude but do not differ greatly from a set constant value. (Ed.)

\*\*\* Meaning roots with negative real parts. (Ed.)

variable, being, for instance, the position of the throttle in an internal combustion engine. The output variable from the controlled system is denoted by  $c$ . In an engine + controller system  $c$  can be the r.p.m. The input to the controller is  $r - c + r_s$ , where  $r$  is the set value of the controlled variable (set angular velocity when the engine speed is controlled), and  $r_s$  is an extra input designed to stabilize the system,  $r$ ,  $c$  and  $r_s$  represent deviations from equilibrium, where  $r = r_s = c = 0$ .

On account of physical restrictions we have



$$|m'| \leq K, \quad (1)$$

where  $|m'|$  is the absolute value of  $m' = dm/dt$ ;  $K = \text{const.}$

Real systems always have delay links. Systems to which the method of stabilization described here is applicable have two or more such links, none of which predominates. The controller is based on a linear control law, i.e., on a normal combination of integral, proportional and derivative control.

This method is also applicable to physical systems with one or more delay links in which the control function contains the products  $|m''| m'$  [3] or analogous products of higher derivatives.

Let us now suppose that the system of Fig. 1 hunts at a low frequency  $f$  when  $r_s = r = 0$ , i.e., when the input signal is zero, and  $r = 0$ . The method described here is usually used in systems which hunt over less than 10% of the total range in the controlled variable, e.g., 10% of the nominal engine speed.

If we inject a sinusoidal signal  $r_s$ , of frequency not less than  $10f$  and of amplitude slightly greater than is needed to cause  $m'$  to reach its limiting value in the absence of a disturbance, the amplitude of the system hunt will be much reduced and will tend to zero. The amplitude of the signal  $r_s$ , for example, can be 1.2 and even 4 times (but not 20 times) the value needed to make  $m'$  reach its limits. In systems with linear control laws  $r_s$  may be injected into the controller at any point up to the output. Random noise can be used instead of a sinusoidal signal. In addition  $r_s$  can take the form of triangular pulses or waves, or any other convenient repetitive signal of frequency not less than  $10f$ , or with components of such frequency. The amplitudes of such signals must be sufficient to giving limiting values of  $m'$ . The bounded element must be unsaturated over a certain time interval. So rectangular waves will not produce stability ( $r$  and  $c$  must be in a 1:1 ratio).

If  $r_s$ , present as rectangular waves, is insufficiently large to produce a saturation zone in the bounded element when  $r$  is fairly small, the gain in the system will not change. If on the other hand rectangular waves produce a saturated zone at sufficiently small  $r$  the output  $c$  will remain unchanged, independently of  $r$ . Thus the relation between  $c$  and  $r$  will be destroyed. The bounded element will then be continually saturated by such signals.

The stabilization of a signal with  $r_s$  we shall term signal stabilization. The frequency of the stabilizing signal must not be a multiple of  $f$ . This method of stabilization enables one to use higher gains and thus to improve the transient response.

Other quantities than speed may be bounded in a servomechanism e.g., the torque on the rotor of an electric motor or the current producing the torque.

## 2. Advantages of the Signal Stabilization Method

Signal stabilization changes the gain of a channel. The presence of a convenient 50 cycle or 400 cycle supply, or some other convenient high frequency supply, simplifies the injection of a stabilizing signal with electrical equipment.

Let us now consider a simple hydraulic servomechanism comprised of a normal valve and piston assembly.

Speed restriction in a servo is equivalent to restricted valve range here. The characteristic of a bounded element, such as a valve, is shown in Fig. 2. The gain curve for such an element is shown in Fig. 3\* (cf. [4]).

\* The so-called 'equivalent admittance' is here implied.

As the input amplitude increases the gain falls. The equation for the servomechanism takes the form

$$m' = kx, \quad (2)$$

where  $x$  is the valve opening,  $m'$  the servo speed, and  $k = \text{const}$ .

Consider a regulator with the control law

$$\Sigma = c_1 + \alpha c_1', \quad (3)$$

where  $c_1'$  is the derivative of  $c_1$  ( $c_1 = r - c + r_s$ ),  $\alpha = \text{const}$ .

The valve opening will be

$$x = -K_1 \Sigma, \quad (4)$$

where  $K_1 = \text{const}$ .

Injection of a stabilizing signal reduces the gains for deviations in  $c_1$  and  $c_1'$ , which gain reductions are transferred to the bounding element and corresponding increase the stability.

Suppose  $\psi = c_1$  or  $\psi = c_1 + Tc_1'$  when  $T = \text{const}$ . If the control function is

$$\Sigma = \psi + \beta |\psi'| \psi' \quad (\beta = \text{const}) \quad (5)$$

or

$$\Sigma = c_1 + \gamma c_1' + \lambda |c_1'| c_1' \quad \left( \begin{array}{l} \gamma = \text{const} \\ \lambda = \text{const} \end{array} \right), \quad (6)$$

then the injection of a stabilizing signal reduces the gains of the linear elements (corresponding to reductions in the terms  $\psi$ ,  $c_1$  and  $\gamma c_1'$ ) but raises the gain of the multiplier channel ( $\beta |\psi'| \psi'$ ). The gain of the channel in (5) which corresponds to  $|\psi'| \psi'$  will be zero when  $\psi' = 0$ . To render the loop stable we should increase the gain. This can be done by injecting a stabilizing signal provided the signal is injected before the multiplying element. The desired result is not obtained if the signal is injected after the multiplying element. Similar remarks apply to the nonlinear control system described by (6).

In general if the curvature of the characteristic curve for the nonlinear element (in which curve the ordinate is the output and the abscissa the input), which passes through the origin (output zero when input is zero), increases numerically, the injection of a sinusoidal signal at the input of this element will increase the gain as compared with the pre-signal value. Similarly, if the curvature drops numerically the injection of a sinusoidal signal will reduce the gain as from the instant of injection.

### 3. Experimental Results

Consider a system containing machine and controller. The engine is described by the equation

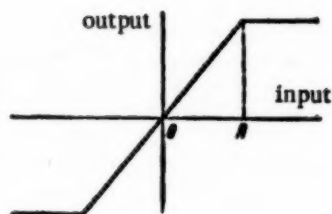


Fig. 2. Characteristic of a bounded element.

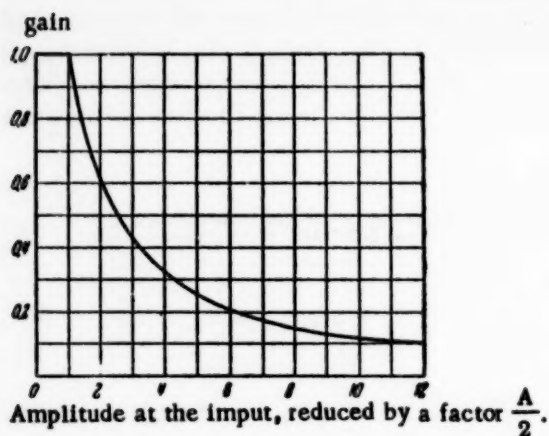


Fig. 3. Horizontal axis: Amplitude at the input, reduced by a factor  $\frac{1}{2} A$ . Gain curve for a bounded element.

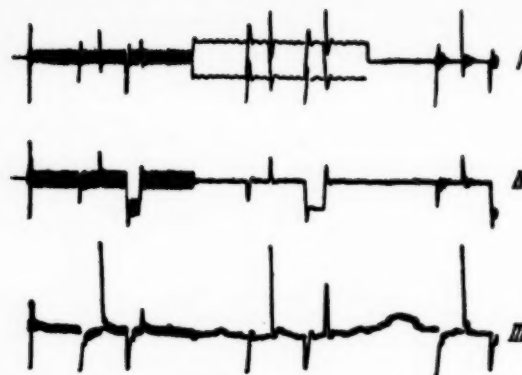


Fig. 4. Signal stabilization of a system acted on by a stepwise perturbation

$$e' = \frac{m}{(0.1D + 1)^2} + L, \quad (7)$$

where  $D$  represents the derivative with respect to time  $t$  and  $L$  is a load term.

The denominator in (7) corresponds to there being two first-order delay links with time-constants of 0.1 sec. The controller equation takes the form

$$\begin{aligned} m' &= 100\Sigma, \\ \Sigma &= 0.8c_1 + \frac{|c'_1|c'_1}{5}, \quad c_1 = r - c + r_s, \end{aligned} \quad (8)$$

where  $\Sigma$  is the control law. Also

$$|m'| \leq 10 \quad (9)$$

this being the restriction on the servo piston speed.

Fig. 4 shows the data for the servosystem with a bounded speed. Curve I denotes the speed  $m'$ , while II denotes the position  $m$ , III indicating the rpm of the engine  $c$ . The system has two delay links with identical time-constants of 0.1 sec. The left side of the oscillogram shows the inherent hunting in the system, while the right side shows the stabilizing signal applied (30 cycles/sec). The engine is described by (7). The controller laws took the form

$$\begin{aligned} m' &= 50\Sigma, \\ \Sigma &= c_1 + 0.8c'_1, \\ c_1 &= r - c + r_s, \end{aligned} \quad (10)$$

\* The stabilizing action of the signal is evidently due to its suppressing the servomotor hunting while the engine speed remains unchanged (Ed.).



subject to the condition  $|m'| \leq 10$ .

Fig. 4 shows that the response to a perturbation is only slightly affected by injecting the stabilizing signal.

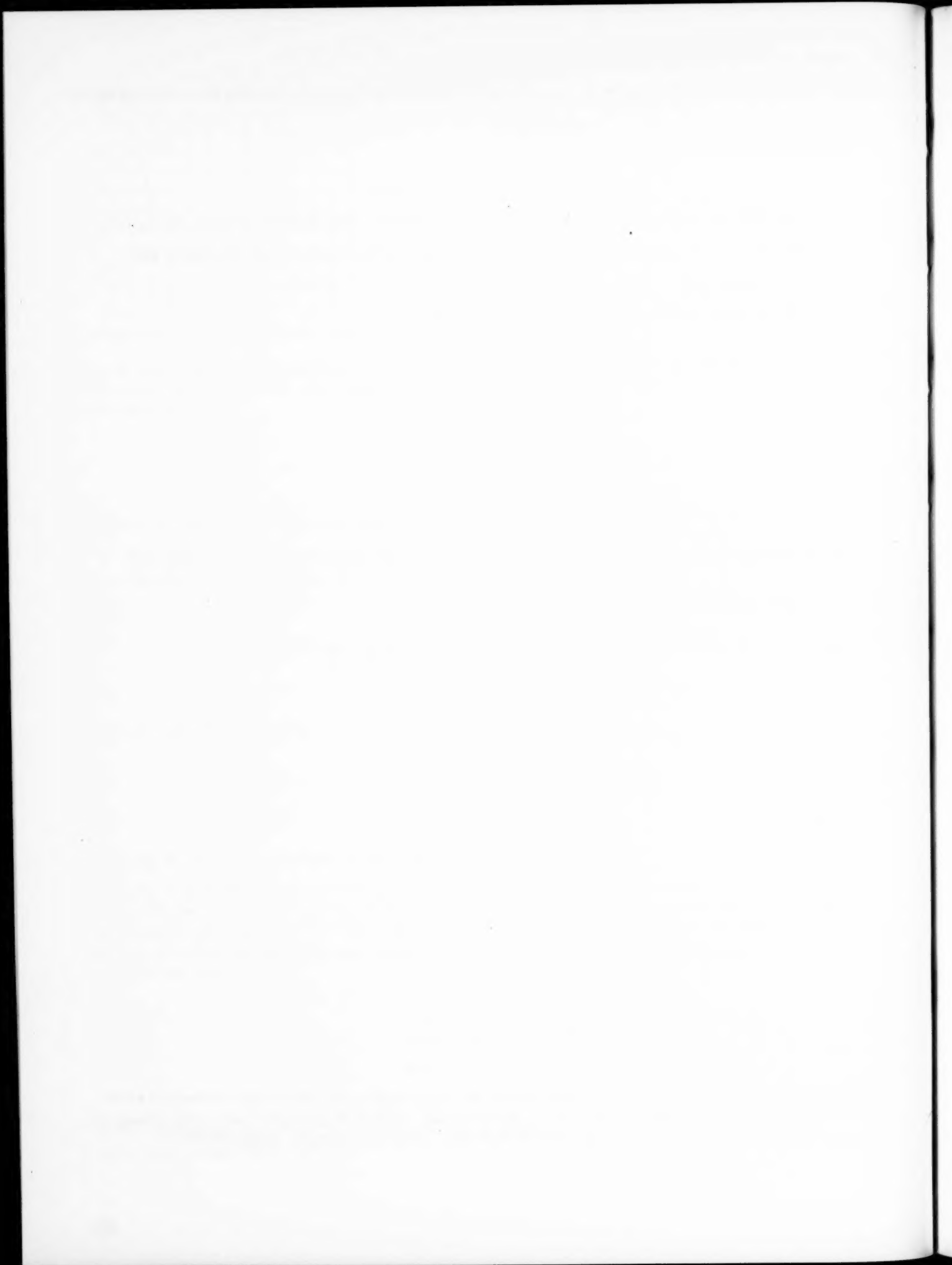
Received October 24, 1956

#### LITERATURE CITED

- [1] MacColl, LeRoy, Fundamental theory of servomechanisms. Van Nostrand Company, N. Y., 1946.
- [2] Minorsky, N. On asynchronous action. Journ. of the Franklin Institute, Vol. 259, No. 3, 1955.
- [3] Oldenburger, R. Optimum nonlinear control.
- [4] Frequency Response. Macmillan Co., 1956, p. 242.

---

Note: The above is a translation of a Russian version of a paper by Dr. Rufus Oldenburger, Professor of Mechanical Engineering and Engineering Sciences, Purdue University, entitled "Signal Stabilization of a Control System." Dr. Oldenburger's paper appeared in the November, 1957 issue of Trans. ASME.



# PULSE STABILIZATION OF AUTOMATIC CONTROL RELAY SYSTEMS

N. A. Korolev

(Moscow)

A pulse method of increasing the self-oscillation frequency in automatic control relay systems is described, together with some ways of designing stabilizing circuits.

## INTRODUCTION

Some relay systems (e.g., Figure 1a) operate in a self-excited oscillatory mode. Typical examples are vibration controllers, bistable servos etc. Relay units with characteristics as shown in Figures 1b and 1c are usually used. One problem in designing and using these systems is that of increasing the frequency and decreasing the amplitude of self-oscillation. This is sometimes termed the stabilization problem. It can be solved by using accelerator (forcing) elements in the controller circuit or by using additional loops (other than feedback) in parallel with the controlled object and with the inertial links. The transfer function for the linear link is then altered (see, e.g., [1-3]). But it is sometimes difficult to use the normal methods, and others have to be sought; e.g., the brush B (Figure 2) has to be kept in contact with the contact strip C by the follower system in a predictor without the brush being mechanically loaded. The strip oscillates continuously with respect to the end of the brush.

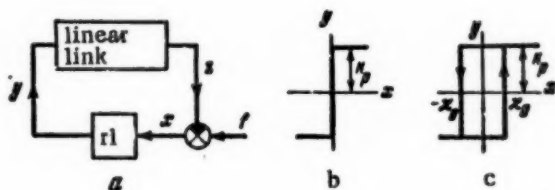


Fig. 1\*

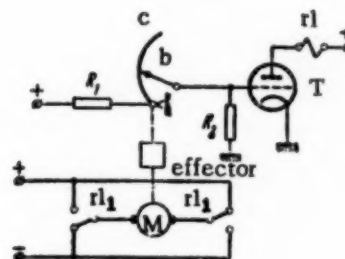


Fig. 2

The static motor voltage characteristic as a function of the B-C distance is the same as for an ideal relay system (Figure 1,b).

The accuracy of this follower system is improved by increasing the frequency and diminishing the amplitude of oscillation. Derivatives with respect to error are difficult to derive as the error itself is not measured in this arrangement. Applying internal feedback to the relay is also ineffective because this cannot be done in such a way as to ensure relay oscillation when the B-C contact is both open and closed. At high feedback the relay system acquires the properties of a linear link (vibrational linearization). This is impossible here because the sign alone, and not the magnitude of the error, is determined.

Any method of stabilizing automatic control systems can be considered as equivalent to performing the requisite change in the operation of the effector. But control in relay systems is not only exerted by altering

\* ["rl" ≡ "relay" - editor's note.]

the linear link by the use of derivative feedback in the control characteristic, and so on. A similar effect can be produced by pulse methods. Pulse stabilization of relay systems has been briefly described [4]. The pulses form ( $y$  in Figure 1,a) is changed by altering the linear link (effector). The self-oscillation frequency is changed by altering  $y$ . The problem is then to give  $y$  a form such as to increase the self-oscillation frequency and to derive a relation between this latter and the pulse shape.

Only stepwise changes in  $y$  are considered here: two types of pulse stabilization using auxiliary circuits to correct the pulse shape are described, and methods of designing the circuits are given. Transients are not considered.

#### Stabilization by Pulses of Arbitrary Duration

Suppose an automatic control or servo system using an ideal relay unit (Figure 1,b) self oscillates at a frequency  $\omega'_0$ . The linear link has the transfer function

$$W(p) = \frac{P(p)}{Q(p)}. \quad (1)$$

The control signal  $\tilde{y}(t)$  at the relay output will be a train of rectangular pulses.\* The self-oscillation frequency is independent of the steady-state gain when the control pulses are rectangular if the loop in the relay characteristic is of zero width [1]. The self-oscillation frequency is to be increased.

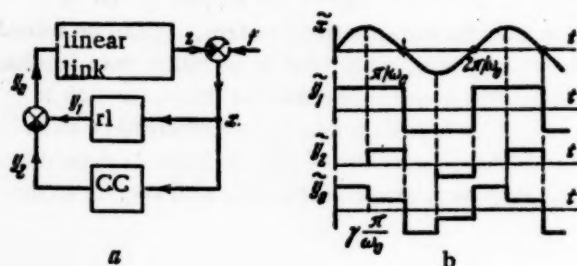


Fig. 3

Let us alter the form of  $\tilde{y}_0(t)$  with the correcting circuit CC (Figure 3,a) which subtracts from the primary pulse train  $\tilde{y}_1(t)$  a train  $\tilde{y}_2(t)$ , as in Figure 3,b, i.e., the extra pulse is displaced in time by  $\gamma\pi/\omega_0$ . The extra pulses are of length  $(1-\gamma)\pi/\omega_0$ , where  $\gamma < 1$ . We shall show that with this type of control signal,  $\tilde{y}_0(t) = \tilde{y}_1(t) - \tilde{y}_2(t)$ , the self-frequency is raised.

In an uncorrected relay system  $\omega'_0$  is defined by the solution to [1]:

$$\tilde{x}_1\left(\frac{\pi}{\omega}\right) = 0 \quad (2)$$

if

$$\dot{\tilde{x}}_1\left(\frac{\pi}{\omega_0}\right) < 0. \quad (3)$$

(2) and (3) assume that the self-oscillation is simple, i.e., the relay switches over once per half-period:

$$\tilde{x}(t) > 0 \quad \left(0 < t < \frac{\pi}{\omega}\right).$$

\* The sign  $\sim$  over a symbol denotes that it changes periodically.

This may be verified on drawing the waveforms.\*

Using Tsyarkin's method [1] we have to determine the self-frequency by constructing the characteristic  $J_1(\omega)$  for the relay system:

$$J_1(\omega) = \operatorname{Re} J_1(\omega) + j \operatorname{Im} J_1(\omega) = -\frac{1}{\omega} \dot{z}_1\left(\frac{\pi}{\omega}\right) - j \tilde{z}_1\left(\frac{\pi}{\omega}\right). \quad (4)$$

If the system is closed in the absence of an external disturbance

$$x(t) \equiv -z(t),$$

this frequency is given by the point where  $J_1(\omega)$  intersects the negative real axis.\*\*

We now turn to the derivation of the self-frequency for a corrected relay system.  $\tilde{y}_0(t)$ , applied to the linear link, produces the response  $\tilde{z}_0(t)$ . The principle of superposition enables us to represent  $\tilde{z}_0(t)$  as the difference  $\tilde{z}_0(t) = \tilde{z}_1(t) - \tilde{z}_2(t)$ .

Determination of  $\omega_0$  obviously amounts to solving

$$-\tilde{z}_0\left(\frac{\pi}{\omega}\right) = \operatorname{Im} J_0(\omega, \gamma) = \operatorname{Im} J_1(\omega) - \operatorname{Im} J_2(\omega, \gamma) = 0 \quad (5)$$

if

$$-\frac{1}{\omega_0} \dot{z}_0\left(\frac{\pi}{\omega_0}\right) = \operatorname{Re} J_0(\omega_0, \gamma) = \operatorname{Re} J_1(\omega_0) - \operatorname{Re} J_2(\omega_0, \gamma) < 0, \quad (6)$$

i.e.,  $\omega_0$  is defined by the point where the hodograph  $J_0(\omega, \gamma)$  intersects the negative real axis.  $J_1(\omega)$  and  $J_2(\omega, \gamma)$  can only be constructed when expressed explicitly in terms of the system parameters.

At  $t = \pi / \omega$  the component response  $\tilde{z}_1(t)$  may be computed (see Appendix) from (A) if we suppose  $\gamma = 0$  and remember that  $h(0) = 0$ :

\* If on relay switch-over (i.e., at the instant  $t = \pi / \omega'_0$ ) the rate of change of the control signal shows a break we should subtract  $\tilde{x}_1$  on the left in (3) from the step when the relay has a loop characteristic (Figure 1,c), i.e., subtract  $\tilde{x}_1(\pi / \omega'_0 - 0)$ . If the relay characteristic is single-valued (Figure 1,b)  $\tilde{x}_1$  should be subtracted from the step on the right, i.e.,  $\tilde{x}_1(\pi / \omega'_0 + 0)$  (see [5]). We shall in future assume that (1) shows the property

$$\lim_{p \rightarrow \infty} pW(p) = h(0) = 0.$$

Then

$$\dot{x}\left(\frac{\pi}{\omega} - 0\right) = \dot{x}\left(\frac{\pi}{\omega} + 0\right) = \dot{x}\left(\frac{\pi}{\omega}\right).$$

\*\* For the stability of self-oscillation see [1].

$$-\tilde{z}_1\left(\frac{\pi}{\omega}\right) = k_{p1} \sum_{v=1}^n c_{v0} \frac{1 - e^{\frac{\pi}{\omega} p_v}}{1 + e^{\frac{\pi}{\omega} p_v}} = \operatorname{Im} J_1(\omega). \quad (7)$$

$\tilde{z}_2(t)$  at  $t = \pi/\omega$  is also determined from (A):

$$-\tilde{z}_2\left(\frac{\pi}{\omega}\right) = k_{p2} \sum_{v=1}^n c_{v0} \frac{1 - e^{(1-\gamma)\frac{\pi}{\omega} p_v}}{1 + e^{\frac{\pi}{\omega} p_v}} = \operatorname{Im} J_2(\omega, \gamma). \quad (8)$$

$k_{p1}$  and  $k_{p2}$  are the gains of relay and corrector respectively,  $n$  being the number of poles  $p_v$  of  $W(p)$ ,  $c_{v0}$  being a coefficient defined by  $c_{v0} = \frac{P(p_v)}{p_v Q'(p_v)}$ ,  $J_1(\omega)$  is the uncorrected relay system characteristic, and  $J_2(\omega, \gamma)$  is the characteristic of the linear link plus corrector.

The real part of the relay system characteristic is determined from (C) by analogy with the above (on the condition that  $\dot{h}(0) = 0$ ):

$$\operatorname{Re} J_1(\omega) = \frac{k_{p1}}{\omega} \sum_{v=1}^n p_v c_{v0} \frac{1 - e^{\frac{\pi}{\omega} p_v}}{1 + e^{\frac{\pi}{\omega} p_v}}, \quad (9)$$

$$\operatorname{Re} J_2(\omega, \gamma) = \frac{k_{p2}}{\omega} \sum_{v=1}^n p_v c_{v0} \frac{1 - e^{(1-\gamma)\frac{\pi}{\omega} p_v}}{1 + e^{\frac{\pi}{\omega} p_v}}. \quad (10)$$

If the poles of (1) are difficult to determine the relay characteristic can be derived by using the partial characteristic  $W(j\omega) = U(\omega) + jV(\omega)$ :

$$\begin{aligned} J_1(\omega) &= \frac{4k_{p1}}{\pi} \sum_{m=1}^{\infty} \left\{ U[(2m-1)\omega] + j \frac{V[(2m-1)\omega]}{2m-1} \right\}, \\ \operatorname{Im} J_2(\omega, \gamma) &= -\frac{2k_{p2}}{\pi} \sum_{m=1}^{\infty} \left\{ \frac{\sin(2m-1)\gamma\pi}{2m-1} U[(2m-1)\omega] - \right. \\ &\quad \left. - \frac{1 + \cos(2m-1)\gamma\pi}{2m-1} V[(2m-1)\omega] \right\}, \\ \operatorname{Re} J_2(\omega, \gamma) &= \frac{2k_{p2}}{\pi} \sum_{m=1}^{\infty} \{ [1 + \cos(2m-1)\gamma\pi] U[(2m-1)\omega] + \\ &\quad + \sin(2m-1)\gamma\pi V[(2m-1)\omega] \}. \end{aligned} \quad (11)^*$$

\* The first formula in (11) is given in [1]. The second and third may be derived from those in [1] by replacing  $\gamma$  with  $(1-\gamma_1)$ , followed by displacing the origin of coordinates by  $\gamma_1\pi/\omega$ , to the left along the time axis, i.e., by the substitution  $t = t_1 - \gamma_1\pi/\omega$ .



If  $k_{p2}$  is given a family of  $J_2(\omega, \gamma)$  curves for different values of  $\gamma$  ( $0 < \gamma < 1$ ), may be drawn up. From

$$J_0(\omega, \gamma) = J_1(\omega) - J_2(\omega, \gamma), \quad (12)$$

the  $J_0(\omega, \gamma)$  family can readily be derived and the self-oscillation frequency determined at any given  $\gamma$ . Figures 4a and c show the  $J_2(\omega, \gamma)$

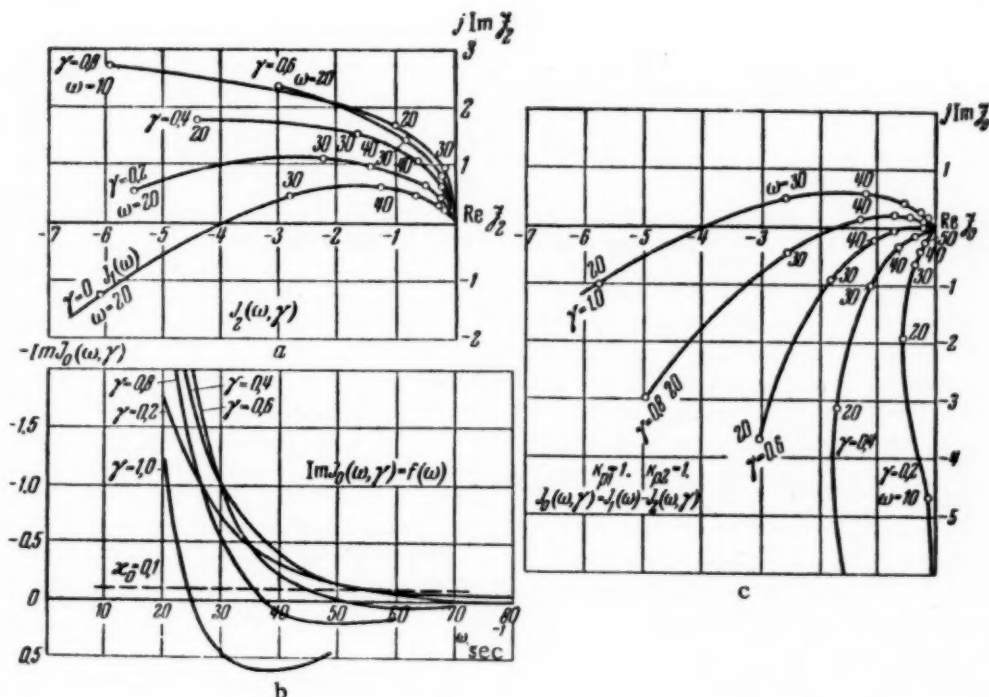


Fig. 4

and  $J_0(\omega, \gamma)$  families drawn for a particular system. The transfer function for its linear link was

$$W(p) = \frac{75}{p(0.05p + 1)(0.03p + 1)}. \quad (13)$$

$k_{p2}$  was assumed equal to one.

The self-frequency is in practice more conveniently determined from  $J_0(\omega, \gamma)$ . Figure 4,b shows this. When the self-frequency for each value of  $\gamma$  has been determined from (5) we can draw up the relation

$$\omega_0 = f(\gamma). \quad (14)$$

Figure 5a shows a group of these relations for varying  $k_{p2}$ . The effect of the extra pulse train (from the corrector circuit) on the self-frequency is clear from the graph. When  $k_{p2} < k_{p1}$  the curves  $\omega_0 = f(\gamma)$  have maxima, the optimum  $\gamma$  falling as  $k_{p2}$  increases. When  $k_{p2} \geq k_{p1}$ , (14) becomes monotonic: as  $\gamma$  falls,  $\omega_0$

(in theory) increases without limit. It may be shown that in the high-frequency range  $J_0(\omega, \gamma)$  in (13) can be approximated with adequate accuracy by the first term in its trigonometric expansion. From (5) and (11) we get

$$\operatorname{Im} J_0(\omega, \gamma) = \frac{2}{\pi} \{k_{p2} \sin \gamma \pi U(\omega) + [2k_{p1} - k_{p2}(1 + \cos \gamma \pi)] V(\omega)\} = 0, \quad (15)$$

and hence directly

$$\tan \theta(\omega_0) = \frac{V(\omega_0)}{U(\omega_0)} = - \frac{\sin \gamma \pi}{2 \frac{k_{p1}}{k_{p2}} - 1 - \cos \gamma \pi}. \quad (16)$$

But if we put  $p = j\omega$  in (13) and separate the real and imaginary parts we get

$$\tan \theta(\omega_0) = \frac{1 - T_1 T_2 \omega_0^2}{(T_1 + T_2) \omega_0}, \quad (17)$$

where  $T_1 = 0.05$  sec,  $T_2 = 0.03$  sec.

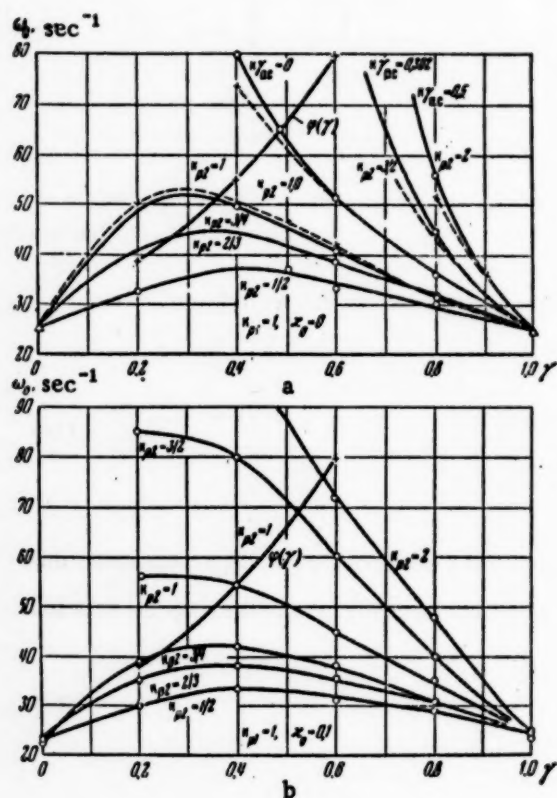


Fig. 5

Simultaneous solution of (16) and (17) shows that  $\omega_0 \rightarrow \infty$  when

$$2 \frac{k_{p1}}{k_{p2}} - 1 - \cos \gamma \pi = 0, \quad \sin \gamma \pi \neq 0. \quad (18)$$

The asymptotic curves  $\omega_0 = f(\gamma)$  for various  $k_{p2} \geq k_{p2}^*$  are determined from (18); these are the vertical straight lines  $\gamma_{as}$ . The  $\gamma_{as}$  values for various  $k_{p2}$  are shown in Figure 5,a. This also shows (dashes) the  $\omega_0 = f(\gamma)$  curves computed from the first harmonic of  $J_0(\omega, \gamma)$ . The Figure shows that the curves computed exactly and approximately are in good agreement.

This pulse stabilization method can be used in systems with  $\kappa_0$  hysteresis in the relay. Then the left of (5) (equations for the periods) must be equated to  $-\kappa_0$ , and the line  $\operatorname{Im} J_0(\omega, \gamma) = -\kappa_0$  (dashed) must be produced. The  $\omega_0$  are defined by the points where the line  $-\kappa_0$  intersects  $\operatorname{Im} J_0(\omega, \gamma)$ . Figure 5,b shows  $\omega_0 = f(\gamma)$  when  $\kappa_0 = 0.1$  for various  $k_{p2}$  in system (13). The relay hysteresis clearly lowers the self-oscillation frequencies in the original and in the pulse-stabilized systems.

\* When  $k_{p2} = k_{p1}$  the indeterminacy is dealt with in the usual way.

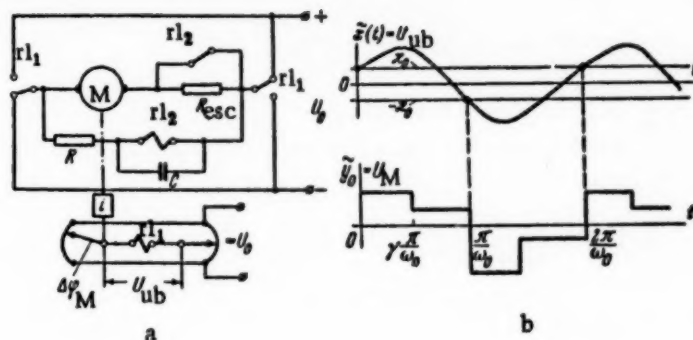


Fig. 6\*

Figure 6a shows a circuit illustrating the principles of pulse stabilization. The contacts of the main relay  $rl_1$  connect the motor to a d.c. supply. After a certain time  $\tau = \gamma\pi/\omega_0$ , relay  $rl_2$  operates and cuts in the resistance  $R_{ex}$ .  $\tau$  is determined by  $R$  and  $C$  in the circuit  $rl_2$ . At the instant when  $rl_1$  changes over  $C$  is discharged via the low resistance of  $rl_2$ ; the process then repeats. The requisite  $\gamma$  is obtained by choice of  $R$  and  $C$ .  $k_{p2}$  is varied from 0 to 1 by appropriate choice of  $R_{ex}$ . The requisite values of  $\gamma$  and  $k_{p2}$  are determined from graphs analogous to those of Figure 5 in accordance with the chosen  $\omega_0$  and  $\kappa_0$  for  $rl_1$ . Figure 6,b shows the self-oscillation in the system. Here  $\pm y_1(t) = U_0$  is the supply voltage,  $y_2(t) = U_R$  is the voltage drop in  $R_{ex}$ ,  $y_0(t) = U_M$  is the motor voltage,  $z_0(t) = \varphi_M$  is the motor shaft rotation,  $x(t) = k\Delta\varphi_M = U_{ub}$  is the bridge unbalance voltage,  $\kappa_0 = U_t$  is the relay switch-over threshold voltage.

The additional pulses can also be shaped with a delay line. If the delay is fixed to be  $\tau = \gamma\pi/\omega_0$  and the extra pulse drops to zero at the same time as the main one the delay line system will in no way differ in its mode of operation from the one above. The use of delay-lines for correcting signals in open-loop (effector) and closed-loop linear systems has been described (e.g., [6, 7]). In this case the shape of the extra pulse is predetermined and there is no need to repeat the shape of the main pulse; the delay line can then be replaced by a normal RC circuit, as in Figure 6,a.

#### Dependent Pulse Stabilization

This stabilization method can also be used for raising the self-oscillation frequency: it differs from the previous method in that the start of the extra pulse is not arbitrarily defined, being the moment when the control signal  $\tilde{x}(t)$  is maximal. The extra and main pulses end at the same time. The resultant action on the linear link  $\tilde{y}_0(t)$  is primarily that of the difference between the main and extra pulses (Figure 3,b).

We here have to determine both  $\omega_0$  and  $\gamma$ , and this is more complex than the previous case: the first equation for the periods

$$\text{Im } J_0(\omega, \gamma) = 0$$

or, where the relay link shows hysteresis

$$\text{Im } J_0(\omega, \gamma) = -\kappa_0 \quad (19)$$

is supplemented by a second

\* ["1"  $\equiv$  "effector" - editor's note.]

$$\operatorname{Re} J_{0\gamma}(\omega, \gamma) = -\frac{1}{\omega} \tilde{z}_0 \left( \gamma \frac{\pi}{\omega} \right) = 0. \quad (20) *$$

The sought frequency  $\omega_0$  and the relative duration  $\gamma$  are determined by simultaneous solution of (19) and (20), on the condition that (20) and

$$\operatorname{Im} J_{0\gamma}(\omega_0, \gamma) = -\tilde{z}_0 \left( \gamma \frac{\pi}{\omega_0} \right) > 0. \quad (21)$$

are fulfilled.

To determine  $\operatorname{Re} J_{0\gamma}(\omega, \gamma)$  we need to know  $\tilde{z}_1 \left( \gamma \frac{\pi}{\omega} \right)$  and  $\tilde{z}_2 \left( \gamma \frac{\pi}{\omega} \right)$ .

$\tilde{z}_2(\gamma\pi/\omega)$  is determined from (C) by substituting  $t = \gamma\pi/\omega$ . Since  $H(0) = \sum_{\nu=1}^n c_{\nu 0} p_{\nu} = 0$ , we get

$$\operatorname{Re} J_{2\gamma}(\omega, \gamma) = -\frac{1}{\omega} \tilde{z}_2 \left( \gamma \frac{\pi}{\omega} \right) = -\frac{k_{p2}}{\omega} \sum_{\nu=1}^n c_{\nu 0} p_{\nu} \frac{e^{\frac{\pi}{\omega} p_{\nu}} - e^{\frac{\gamma\pi}{\omega} p_{\nu}}}{1 + e^{\frac{\pi}{\omega} p_{\nu}}}. \quad (22)$$

$\tilde{z}_1(\gamma\pi/\omega)$  is also determined from (C). First of all we must put  $\gamma = 0$ , and then  $t = \gamma\pi/\omega$  in the formula found. Then

$$\operatorname{Re} J_{1\gamma}(\omega, \gamma) = -\frac{1}{\omega} \tilde{z}_1 \left( \gamma \frac{\pi}{\omega} \right) = -\frac{k_{p1}}{\omega} \sum_{\nu=1}^n c_{\nu 0} p_{\nu} \frac{2e^{\frac{\gamma\pi}{\omega} p_{\nu}}}{1 + e^{\frac{\pi}{\omega} p_{\nu}}}. \quad (23)$$

The family  $\operatorname{Re} J_{0\gamma}(\omega, \gamma)$  may now be drawn up for various  $\gamma$ . Figure 7 shows this family of curves when  $k_{p1} = k_{p2} = 1$ , for the relay example above with the linear link of (13). Each  $\gamma_1$  has its own  $\omega_0$ , given by the point where  $\operatorname{Re} J_{0\gamma}(\omega, \gamma)$  cuts the  $\omega$  axis.

The curve  $\omega_0 = \varphi(\gamma)$  shown in Figure 5 was drawn up from Figure 7. At the points where the curves for the  $k_{p2}$  intersect,  $\omega_0, \gamma_0$  are determined; these will be the required self-oscillation parameters, since both (19) and (20) are then satisfied simultaneously. The required frequencies can be obtained by varying  $k_{p2}$  for the correcting circuit.

The frequency is determined approximately (from the first harmonic) from Figure 5 with  $\gamma = 0.5$ . An exact calculation for  $\kappa_0 = 0$  gives  $\gamma_0 = 0.485$  which is close to this (see Figure 5,a) but when  $\kappa_0 = 0.1$  the difference is already important ( $\gamma_0 = 0.4$ ), although the error in determining the frequency is less than 10% (Figure 5,b).

Figure 8 shows the application of dependent pulse stabilization to Figure 2. The tachometer Tach, Relay 2 and the resistance  $R_{ex}$  in the armature circuit form the correcting circuit. Relay 1 operates when C touches B, its contact in the armature circuit changing over. At the same time its other contact shunts  $R_{ex}$ . The motor slows down, its armature current being reversed. The tach output passes through zero and changes sign at the moment when the motor stops. Relay 2 then switches over and its contact cuts in  $R_{ex}$ . When the C-B contact

\* The index  $\gamma$  in  $J_{0\gamma}$  denotes that the characteristic is taken at the instant  $\gamma\pi/\omega$ .

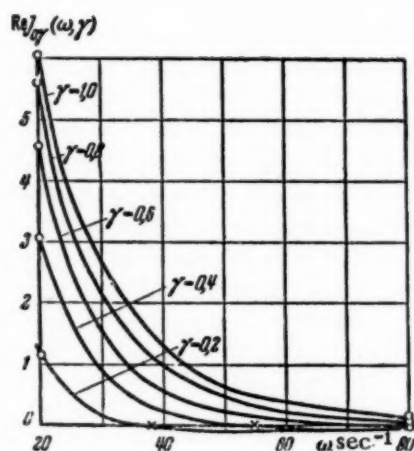


Fig. 7

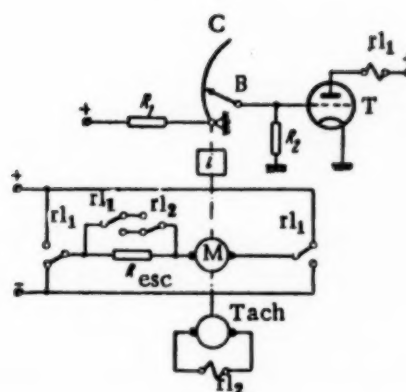


Fig. 8

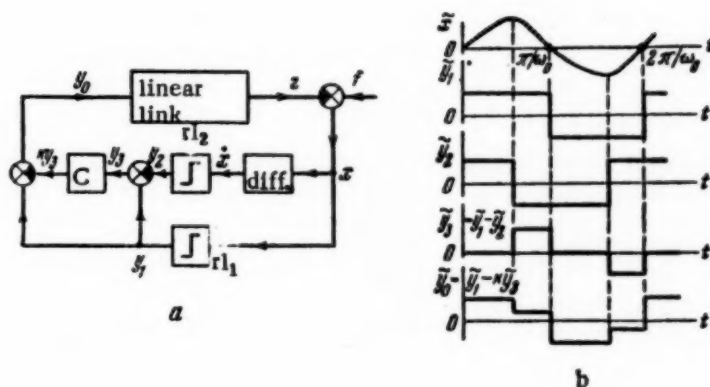


Fig. 9

opens Relay 1 again changes the supply polarity and also reshunts  $R_{ex}$ . This cycle is periodically repeated at a frequency  $\omega_0$ .

The effects of dependent pulse stabilization were verified on an EMU electronic analog unit. The linear part of the system had the transfer function of (13) and was built up from analog equipment units; the relay unit, having a characteristic as in Figure 1,b, and the correcting circuit were simulated with nonlinear circuits (using diode limiter circuits). Figure 9,a shows the block diagram. Figure 9,b shows the signal waveforms in various parts of the circuit. The oscillograms of Figure 10,a show the self-oscillation in the uncorrected system ( $y_2 = 0$ ). Those of 10,b illustrate the working of pulse stabilization when  $k_{p2} = k_{p1}$ . We see that the correcting circuit raises the self-oscillation frequency from  $25.2 \text{ sec}^{-1}$  to  $52.3 \text{ sec}^{-1}$ . The amplitude drops by a factor of 6.7.\*

\* I am deeply indebted to Engineer I. V. Pyshkin who carried out the experimental work in the Automation and Remote Control Laboratory of the Academy of Sciences of the USSR.



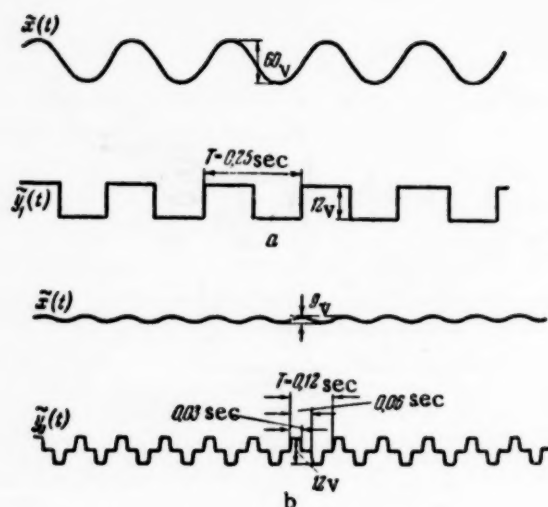


Fig. 10

cal upper limit of the self-oscillation frequency is dependent on the hysteresis and time delay in the relay.

When  $k_{p2} < k_{p1}$  there is an optimum  $\gamma$  ( $\gamma$  being the relative duration of the corrector circuit pulse) the self-oscillation frequency then being maximal.

3. Both types of pulse stabilization — arbitrary and dependent pulse-length stabilization — are equally efficient. Dependent stabilization is preferable as being simpler in design and more reliable.

## APPENDIX

§ 41 of [1] gives equations (10.16) and (10.17) which define the form of the hunting mode  $\tilde{z}(t)$  for the case where the origin of time coincides with the beginning of  $\tilde{y}(t)$ :

$$\tilde{z}(t) = k_p \left\{ c_{00} + \sum_{v=1}^n c_{v0} \frac{1 + e^{\frac{(1-\gamma)\pi}{\omega} p_v}}{1 + e^{\frac{\pi}{\omega} p_v}} e^{p_v t} \right\} \quad \left( 0 \leq t < \gamma \frac{\pi}{\omega} \right);$$

$$\tilde{z}(t) = k_p \sum_{v=1}^n c_{v0} \frac{1 - e^{-\frac{\gamma\pi}{\omega} p_v}}{1 + e^{\frac{\pi}{\omega} p_v}} e^{p_v t} \quad \left( \gamma \frac{\pi}{\omega} \leq t < \frac{\pi}{\omega} \right),$$

where  $\gamma$  is the relative pulse length in  $\tilde{y}(t)$ ,  $k_p$  being the relay gain.

To determine  $\tilde{z}(t)$  for  $\tilde{y}_2(t)$  (Figure 3,b)  $\gamma$  must be replaced by  $1-\gamma$  in these formulae, the zero of time being displaced  $\gamma\pi/\omega$  to the left, i.e., we put  $t - \gamma\pi/\omega$  for  $t$ . Performing this substitution in (10.16) we get

$$\tilde{z}(t) = k_p \left\{ c_{00} + \sum_{v=1}^n c_{v0} \frac{1 + e^{\frac{\gamma\pi}{\omega} p_v}}{1 + e^{\frac{\pi}{\omega} p_v}} e^{p_v (t - \frac{\gamma\pi}{\omega})} \right\},$$

$$\left( 0 \leq t - \gamma \frac{\pi}{\omega} < (1 - \gamma) \frac{\pi}{\omega} \right)$$

Finally we observe that the stepwise control action  $\tilde{y}_0(t)$  can be produced by adding the main pulse train  $\tilde{y}_1(t)$  from the relay and an extra train  $\tilde{y}_2(t)$  from the corrector circuit (instead of subtracting, as in Figure 3,b). The main and extra pulses must then begin together. The instant when the extra pulse terminates can either be selected from Figure 5, or can be superimposed on the maximum of  $x(t)$ . This latter method demands a larger overall gain, which normally implies a higher supply voltage and effector overloading. The self-oscillations also become of larger amplitude at the same frequency since the power input to the system as a whole is larger than when subtraction is used on  $\tilde{y}_0(t)$ , as above.

## SUMMARY

1. Pulse stabilization of automatic control relay systems consists in altering the form of the signal from the relay to the linear link.
2. When  $k_{p2} > k_{p1}$  ( $k_{p1}$  being the relay coefficient and  $k_{p2}$  the corrector coefficient) the practical upper limit of the self-oscillation frequency is dependent on the hysteresis and time delay in the relay.



or

$$\tilde{z}(t) = k_p \left\{ c_{00} + \sum_{v=1}^n c_{v0} \frac{1 + e^{-\gamma \frac{\pi}{\omega} p_v}}{1 + e^{\frac{\pi}{\omega} p_v}} e^{p_v t} \right\} \left( \gamma \frac{\pi}{\omega} \leq t < \frac{\pi}{\omega} \right). \quad (\text{A})$$

From (10.17)

$$\begin{aligned} \tilde{z}(t) &= k_p \sum_{v=1}^n c_{v0} \frac{1 - e^{-(1-\gamma) \frac{\pi}{\omega} p_v}}{1 + e^{\frac{\pi}{\omega} p_v}} e^{p_v \left( t - \gamma \frac{\pi}{\omega} \right)} = \\ &= k_p \sum_{v=1}^n c_{v0} \frac{e^{-\gamma \frac{\pi}{\omega} p_v} - e^{-\frac{\pi}{\omega} p_v}}{1 + e^{\frac{\pi}{\omega} p_v}} e^{p_v t} \\ &\left( \frac{\pi}{\omega} (1 - \gamma) \leq t - \gamma \frac{\pi}{\omega} < \frac{\pi}{\omega} \right) \text{ or } \left( -\frac{\pi}{\omega} \leq t < (1 + \gamma) \frac{\pi}{\omega} \right). \end{aligned}$$

Since  $\tilde{z}(t)$  is of interest in the first half-period we replace  $t$  by  $t + \pi/\omega$ . Since  $\tilde{z}(t) = -\tilde{z}(t + \pi/\omega)$ , we get

$$\tilde{z}(t) = k_p \sum_{v=1}^n c_{v0} \frac{1 - e^{(1-\gamma) \frac{\pi}{\omega} p_v}}{1 + e^{\frac{\pi}{\omega} p_v}} e^{p_v t} \left( 0 \leq t < \gamma \frac{\pi}{\omega} \right). \quad (\text{B})$$

Differentiating  $\tilde{z}(t)$  we have

$$\dot{\tilde{z}}(t) = k_p \sum_{v=1}^n c_{v0} p_v \frac{1 + e^{-\gamma \frac{\pi}{\omega} p_v}}{1 + e^{\frac{\pi}{\omega} p_v}} e^{p_v t} \left( \gamma \frac{\pi}{\omega} \leq t < \frac{\pi}{\omega} \right), \quad (\text{C})$$

$$\dot{\tilde{z}}(t) = k_p \sum_{v=1}^n c_{v0} p_v \frac{1 - e^{(1-\gamma) \frac{\pi}{\omega} p_v}}{1 + e^{\frac{\pi}{\omega} p_v}} e^{p_v t} \left( 0 \leq t < \gamma \frac{\pi}{\omega} \right). \quad (\text{D})$$

The poles  $p_v$  of the transfer function for the linear link  $W(p)$  are supposed simple and nonzero; but when  $p_1 = 0$  the result can be derived by the usual method of passing to the limit.

Received October 16, 1956

#### LITERATURE CITED

- [1] Tsyppkin, Ya. Z. Theory of automatic control relay systems. State Tech. Press, 1955.
- [2] Ivakhenko, A. G. Electrical automation, ch. 2. State Tech. Press, Ukrain. SSR, 1954.
- [3] Davydov, N. I. The dynamic characteristics of an electronic regulator using delayed a.c. feedback. Bull. All-Union Tech. Institute, No. 7, 1952.
- [4] Tsyppkin, Ya. Z. Stabilization of automatic control relay systems. Symposium on problems of automation, Milan, 1956.
- [5] Korolev, N. A. Hunting modes in relay systems using internal feedback. Automation and Remote Control, 17, No. 11, 1956.
- [6] Gukov, V. I. Correction methods using delay links. Symp. of papers on Automation and Remote Control. (Trans. 2nd and 3rd research conferences of young specialists at the Institute of Automation and Remote Control, Academy of Sciences of the USSR) Acad. Sci. USSR Press, 1956.
- [7] Yu-Chi Ho and Ronald E. Scott, Delay-line method for compensating closed-loop systems in the time domain. IRE Convention Record, part IV, 1955.

# THE DESIGN OF LINEAR FOLLOWER SYSTEMS FROM THE CRITERION OF MINIMUM PRACTICAL LIMITING REPRODUCTION ERROR

K. I. Kurakin

(Moscow)

The optimum transfer function of a servo system is determined for the case where the input to be reproduced is a known slowly-varying function of time and the noise spectrum is uniform over the working frequency range. The follower design is based on the criterion of minimum practical follow-up error given in [1]. Methods of producing an optimum servo transfer function are described which employ a corrector unit operating on d.c.

## INTRODUCTION

In some practical cases the input quantity to be reproduced changes according to a completely defined law during one cycle of servo operation while the main parameters in the law change from cycle to cycle but the character of the law remains the same. Such real slowly-varying time functions can be represented approximately by  $n$ th-order polynomials or by harmonic functions. In the latter case the function period is hundreds of times greater than the inherent period of self-oscillation in the system. When the problem is approached in this way the input is considered as an assembly of functions which is in general not ergodic. The results of [2] are known to be then inapplicable. It has been shown [3] that the optimum system for nonstationary input functions (determined from the means of the assemblies) is a linear one with parameters variable in time. This paper presents a method of deriving the optimum transfer function for a servosystem with parameters constant in time from the means of the assembly of input functions when the noise at the input is white.

### 1. Derivation of Optimum Transfer Functions which provide Minimum Practical Limiting Follow-Up Error.

Consider a stable linear servo system denoted by the following symbols:  $\beta_1(t)$  is the input to be reproduced,  $\beta_0(t)$  the output produced,  $\delta\beta(t) = \beta_1(t) - \beta_0(t)$  the reproduction error,  $\beta_n(t)$  the total noise, referred to the servo system input, having a spectral power density  $G\beta_n(\omega) = \epsilon^2 = \text{const}$ . For simplicity we assume that there is no correlation between the input to be reproduced and  $\beta_n(t)$ .  $Y(p)$  denotes the optimum transfer function for the open-loop condition, the closed-loop one then being

$$K(p) = \frac{Y(p)}{1 + Y(p)}.$$

Here  $p \equiv d/dt$  and is an operator. The follow-up error of the servo system will be assumed to be

$$\delta\beta(t) = |\delta\beta_{\text{st}}(t)| + \delta\beta_{\text{ms}} \quad (1)$$

$\delta\beta_{is}(t)$  is the dynamic or systematic error due to the input  $\beta_i(t)$ , and  $\delta\beta_{ms}$  is a mean-square error due to the noise operating at the input.

Case 1.  $\beta_i(t)$  is a monotonic function of time, being zero when  $t < 0$ , which can be represented approximately by a polynomial of degree  $\underline{n}$ . Then

$$\delta\beta_{is}(t) = c_0\beta_i(t) + c_1\dot{\beta}_i(t) + \frac{c_2}{2!}\ddot{\beta}_i(t) + \frac{c_3}{3!}\dddot{\beta}_i(t) + \dots + \frac{c_n}{n!}\beta_i^{(n)}(t). \quad (2)$$

Applying the Laplace transform to both parts of (2) gives

$$\frac{\delta\beta_{is}(p)}{\beta_i(p)} = c_0 + c_1 p + \frac{c_2}{2!} p^2 + \frac{c_3}{3!} p^3 + \dots + \frac{c_n}{n!} p^n, \quad (3)$$

whence

$$\begin{aligned} c_0 &= \lim_{p \rightarrow 0} \left[ \frac{\delta\beta_{is}(p)}{\beta_i(p)} \right], \\ c_1 &= \lim_{p \rightarrow 0} \frac{1}{p} \left[ \frac{\delta\beta_{is}(p)}{\beta_i(p)} - c_0 \right], \\ &\dots \dots \dots \\ c_n &= n! \lim_{p \rightarrow 0} \frac{1}{p^n} \left[ \frac{\delta\beta_{is}(p)}{\beta_i(p)} - \sum_{k=0}^{n-1} \frac{c_k}{k!} p^k \right]. \end{aligned} \quad (4)$$

We will now look for the optimum transfer function for servo systems showing first-order astatic properties.  $Y(p)$  (open loop) for such systems takes the general form

$$Y(p) = \frac{k_v \prod_{i=1}^m (1 + p\tau_i)}{p \prod_{i=1}^n (1 + pT_i)}. \quad (5)$$

In general it is complicated to find the optimum values of  $k_v$ ,  $\tau_1$  and  $T_1$ . But the problem can be simplified [4] if we look for a  $Y(p)$  of the form

$$Y(p) = \frac{k_v}{p} \frac{1 + p\tau_1}{1 + pT_1}, \quad (6)$$

i.e., put  $m = n = 1$  in (5). The optimum parameters sought then become  $k_v$ , the velocity gain in the system,  $\tau_1$ , a time-constant characteristic of the 'forcing' properties (acceleration) of the system, and  $T_1$ , a time-constant specifying the integrating properties. The closed-loop  $K(p)$  will then take the form

$$K(p) = \frac{Y(p)}{1 + Y(p)} = \omega_n^2 \frac{\tau_1 p + 1}{p^2 + 2\zeta\omega_n p + \omega_n^2}, \quad (7)$$

where  $\omega_n = \sqrt{\frac{k_v}{T_1}}$  is the natural frequency of undamped oscillation in the system, and  $\zeta = \frac{1 + k_v\tau_1}{2\sqrt{k_v T_1}}$  is the relative damping coefficient.

(3) and (7) imply that

$$\frac{\delta\beta_{is}(p)}{\beta_i(p)} = 1 - K(p) = \frac{p[p + \omega_n(2\zeta - \omega_n\tau_1)]}{p^2 + 2\zeta\omega_n p + \omega_n^2}. \quad (8)$$

The error coefficients  $c_0, c_1, c_2, c_3, \dots, c_n$  are readily determined from the system of equations in (4) and (8), being

$$\begin{aligned} c_0 &= 0, \\ c_1 &= \frac{2\zeta - \omega_n\tau_1}{\omega_n} = \frac{1}{k_v}, \\ c_2 &= \frac{2(1 + 2\zeta\omega_n\tau_1 - 4\zeta^2)}{\omega_n^2} = \frac{2[(T_1 - \tau_1)k_v - 1]}{k_v^2}, \\ c_3 &= \frac{6[\omega_n\tau_1(1 - 4\zeta^2) - 4\zeta(1 - 2\zeta^2)]}{\omega_n^3} = \frac{6[1 - k_v(2 + k_v\tau_1)(T_1 - \tau_1)]}{k_v^3} \text{ etc.} \end{aligned}$$

Let the averaged  $\beta_i(t)$  be defined by the polynomial

$$\beta_i(t) = \sum_{v=1}^n \gamma_v t^v. \quad (9)$$

Then, having formed the derivatives  $\dot{\beta}_i(t), \ddot{\beta}_i(t), \dots, \beta_i^{(n)}(t)$  from (9) and utilized (2) we get a general expression for  $\delta\beta_{is}(t)$  (the systematic error):

$$\begin{aligned} \delta\beta_{is}(t) &= \sum_{v=1}^n \gamma_v c_v + t \sum_{v=1}^{n-1} (v+1) \gamma_{v+1} c_v + t^2 \sum_{v=1}^{n-2} \frac{(v+2)!}{2! v!} \gamma_{v+2} c_v + \\ &+ t^3 \sum_{v=1}^{n-3} \frac{(v+3)!}{3! v!} \gamma_{v+3} c_v + \dots + t^{n-2} \sum_{v=1}^2 \frac{(n-2+v)!}{(n-2)! v!} \gamma_{n-2+v} c_v + t^{n-1} n \gamma_n c_1. \end{aligned} \quad (10)$$

When  $\gamma_v > 0$  for  $v = 1, 2, \dots, n$   $\delta\beta_{is}(t)$  will be an increasing function of time, so if we bear in mind that any real servo has an effector motor with bounded angular velocity and acceleration, and is nonlinear on account of saturation, we see that at some value of  $t$  the normal follow-up is disorganized and the system becomes in general uncontrollable if the control response range is restricted. We shall in future suppose that the steady-state design for the system has already been drawn up and an effector motor selected such that when the gear reduction ratio between motor shaft and load is optimal, for a given input law  $\beta_i(t)$  and cycle time  $t_c$   $\delta\beta_{is}(t)$  does not fall outside the linear section of the control response.

The component  $\delta\beta_{ms}$ , due to the noise, is given by

$$\delta\beta_{ms}^2 = \frac{1}{2\pi} \int_0^\infty |K(j\omega)|^2 G_{\beta_n}(\omega) d\omega. \quad (11)$$

Using (7), (11) gives

$$\delta\beta_{ms}^2 = \frac{\varepsilon^2}{2\pi} \int_0^\infty \omega_n^4 \frac{|\tau_1 j\omega + 1|^2}{|\omega_n^2 + 2\zeta\omega_n j\omega - \omega^2|^2} d\omega. \quad (12)$$

Supposing the servo system stable, and using the tables for  $I_n$  [5,6] we have

$$\delta\beta_{ms} = \frac{1}{2} \sqrt{\varepsilon^2} \sqrt{\frac{\omega_n^2 (\tau_1^2 \omega_n^2 + 1)}{2\zeta\omega_n}} = \frac{1}{2} \sqrt{\varepsilon^2} \sqrt{\frac{k_v T_1 + k_v^2 \tau_1^2}{T_1 + k_v T_1 \tau_1}}. \quad (13)$$

Inserting  $t = t_c$  and the expressions for  $c_1, c_2, \dots, c_n$ , into (10) we get  $\delta\beta_{is}(t_c, k_v, T_1, \tau_1)$ .

Hence we may take the following expression as representing the practical limiting follow-up error.

$$\delta\beta = |\delta\beta_{is}(t_c, k_v, T_1, \tau_1)| + \delta\beta_{ms}(k_v, T_1, \tau_1). \quad (14)$$

Further, we have to seek values of  $k_v, T_1$  and  $\tau_1$  for a given  $t_c$  at which  $\delta\beta$  will be minimal.

Practical cases are encountered where  $\beta_i(t)$  (Fig. 1) can be represented sufficiently accurately by a second-degree equation

$$\beta_i(t) = \gamma_0 + \gamma_1 t + \gamma_2 t^2, \quad (15)$$

where  $\gamma_0, \gamma_1, \gamma_2$  are positive constants. (10) and the expressions for  $c_1$  and  $c_2$  then imply that

$$\delta\beta_{is}(t_c) = (\gamma_1 + 2\gamma_2 t_c) \frac{1}{k_v} + 2\gamma_2 \frac{(T_1 - \tau_1) k_v - 1}{k_v^2}$$

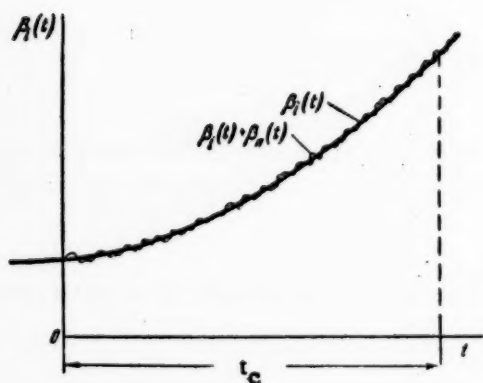


Fig. 1. Graph of the input function to be reproduced  $\beta_i(t)$



Remembering that  $T_1 \gg \tau_1$  and  $(T_1 - \tau_1) k_v \gg 1$ , in an optimal system, we can, to an adequate degree of accuracy, put

$$\delta_{\beta_{is}}(t_c) = \frac{\gamma_1 + 2\gamma_2(t_c + T_1)}{k_v} \quad (16)$$

(13) shows that  $\delta_{\beta_{ms}}$  depends materially on both  $T_1$  and  $\tau_1$ . Since, according to (16),  $\delta_{\beta_{is}}(t_c)$  is independent of  $\tau_1$ , the optimum  $\tau_1$  can be expressed in terms of  $k_v$  and  $T_1$  using the condition that  $\delta_{\beta_{ms}}$  be a minimum. The optimum  $\tau_1$  and  $k_v$  are given by

$$\tau_1 = \frac{1}{k_v} (\sqrt{1 + k_v T_1} - 1), \quad (17)$$

$$k_v = 4 \sqrt[5]{\frac{T_1(\gamma_1 + 2\gamma_2(t_c + T_1))^4}{\epsilon^4}} \quad (18)$$

Further, having substituted for  $T_1$  and  $k_v$  in (17) we get the optimum  $\tau_1$ .

Study of (14) at an extremum shows that  $\delta_{\beta}$  is reached when  $T_1 = \infty$  and  $k_v = \infty$ . According to (6)  $Y(p)$  is then determined for a servo with second order astatic properties.

Case 2.  $\beta_i(t)$  is a harmonic function of time,

$$\beta_i(t) = \beta_{i0} \sin \omega_0 t. \quad (19)$$

The maximum systematic error  $\delta_{\beta_{is} \max}$  is found from

$$\begin{aligned} \delta_{\beta_{is} \max} &= \beta_{i0} |1 - K(j\omega_0)| = \frac{\beta_{i0} \omega_0 \sqrt{\omega_0^2 + \omega_n^2 (2\zeta - \omega_n \tau_1)^2}}{\sqrt{(\omega_n^2 - \omega_0^2)^2 + 4\zeta^2 \omega_n^2 \omega_0^2}} = \\ &= \frac{\beta_{i0} \omega_0 \sqrt{1 + T_1^2 \omega_0^2}}{\sqrt{(k_v + T_1 \omega_0^2)^2 + \omega_0^2 (1 + k_v \tau_1)^2}}. \end{aligned} \quad (20)$$

The following form is then given to  $\delta_{\beta}$ :

$$\delta_{\beta} = \frac{\beta_{i0} \omega_0 \sqrt{1 + T_1^2 \omega_0^2}}{\sqrt{(k_v + T_1 \omega_0^2)^2 + \omega_0^2 (1 + k_v \tau_1)^2}} + \frac{1}{2} \sqrt{\frac{\epsilon^2}{T_1}} \sqrt{\frac{k_v T_1 + k_v^2 \tau_1^2}{T_1 + k_v T_1 \tau_1}}.$$

In most practical cases  $\omega_0 < 1$  so the previous equation can to an adequate accuracy be written as

$$\delta_{\beta} = \frac{\beta_{i0} \omega_0 \sqrt{1 + T_1^2 \omega_0^2}}{k_v} + \frac{1}{2} \sqrt{\frac{\epsilon^2}{T_1}} \sqrt{\frac{k_v T_1 + k_v^2 \tau_1^2}{1 + k_v \tau_1}}. \quad (21)$$

(21) shows, by analogy with the previous case, that the optimum  $\tau_1$  is defined by (17). Then having substituted  $\tau_1$  from (17) into (21) we get

$$\delta_\beta = \frac{\beta_{i0} \omega_0 \sqrt{1 + T_1^2 \omega_0^2}}{k_v} + \sqrt{\frac{\epsilon^2}{2T_1}} \sqrt{1 + k_1 T_1 - 1}. \quad (22)$$

Also since  $\sqrt{k_v T_1} \gg 1$ ,

$$\delta_\beta = \frac{\beta_{i0} \omega_0 \sqrt{1 + T_1^2 \omega_0^2}}{k_v} + \sqrt{\frac{\epsilon^2}{2T_1}} T_1^{1/4} k_v^{-1/4}. \quad (23)$$

As previously we suppose  $T_1$  given. Then differentiating  $\delta_\beta$  with respect to  $k_v$  and equating the derivative to zero, we have

$$\frac{\partial \delta_\beta}{\partial k_v} = -\frac{\beta_{i0} \omega_0 \sqrt{1 + T_1^2 \omega_0^2}}{k_v^2} + \frac{1}{4} \sqrt{\frac{\epsilon^2}{2T_1}} T_1^{1/4} k_v^{-5/4} = 0.$$

The optimum  $k_v$  is found as

$$k_v = 4 \sqrt[5]{\frac{T_1}{\epsilon^4} \beta_{i0}^4 \omega_0^4 (1 + T_1^2 \omega_0^2)^2}. \quad (24)$$

## 2. Relation Between $\delta_{\beta i}$ and $\delta_{\beta ms}$

In the case of the  $\beta_i(t)$  defined by (15), we have

$$\delta_{\beta is} \max = \frac{\gamma_1 + 2\gamma_2(t_c + T_1)}{k_v}$$

and

$$\delta_{\beta ms} = \sqrt{\frac{\epsilon^2}{2T_1}} T_1^{1/4} k_v^{-1/4}.$$

Substituting the optimum of  $k_v$  found from (18) into the expressions for  $\delta_{\beta is} \max$  and  $\delta_{\beta ms}$  we get a relation between these errors in the optimum servo which satisfies the minimum practical reproduction error:

$$\delta_{\beta is} \max = \frac{1}{4} \delta_{\beta ms} \quad (25)$$

With the  $\beta_i(t)$  defined by (19) we have

$$\delta_{\beta_{is}} \max = \frac{\beta_{i0} \omega_0 \sqrt{1 + T_1^2 \omega_0^2}}{k_v}$$

and

$$\delta_{\beta_{ms}} = \sqrt{\frac{\epsilon^2}{2T_1}} T_1^{1/4} k_v^{1/4}.$$

Substituting the optimum  $k_v$  from (24) into the expressions for  $\delta_{\beta_{is}} \max$  and  $\delta_{\beta_{ms}}$  we get (25) after some simple manipulations.

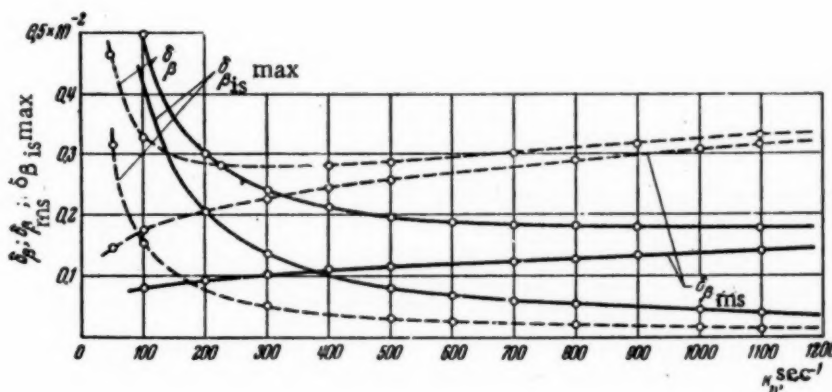


Fig. 2. Curves relating  $\delta_{\beta}$ ,  $\delta_{\beta_{ms}}$  and  $\delta_{\beta_{is}} \max$  to  $k_v$  when  $T_1 = 1$  sec and 25 sec.

If the  $k_v$  differs from the optimum value the relation between  $\delta_{\beta_{is}} \max$  and  $\delta_{\beta_{ms}}$  changes in this case, and is defined in general by the equation

$$\alpha = \frac{\delta_{\beta_{is}} \max}{\delta_{\beta_{ms}}} = \frac{\beta_{i0} \omega_0 \sqrt{1 + T_1^2 \omega_0^2}}{T_1^{1/4} \sqrt{\frac{\epsilon^2}{2T_1}}} k_v^{-1/4}. \quad (25)$$

(26) shows that as  $k_v$  falls,  $\alpha$  increases. Then  $\delta_{\beta}$  remains approximately constant as  $k_v$  varies in some range around the optimum. These assertions are illustrated in Fig. 2, which shows  $\delta_{\beta}$ ,  $\delta_{\beta_{ms}}$  and  $\delta_{\beta_{is}} \max$  as functions of  $k_v$  when  $T_1 = 1$  sec (dashed lines) and 25 sec (full lines). It is here assumed that  $\epsilon^2 = 0.612 \times 10^{-6}$  sec,  $\omega_0 = 0.1$  sec and  $\beta_{i0} = \frac{\pi}{2}$ . The curves in Figure 2 were computed using a  $\tau_1$  computed from (17). A study of (26) leads one to conclude: a) the optimum  $k_v$  for a given  $\epsilon^2$  falls with  $T_1$ ; b) the optimum  $k$  becomes more critical the smaller  $T_1$ ; c) the optimum  $k_v$  for a given  $T_1$  is larger the smaller  $\epsilon^2$ .

### 3. Amplitude and Phase Frequency Characteristics of the Optimum Closed-Loop Servo.

The optimum amplitude characteristic for the closed-loop servo, from (7), takes the form

$$|K(j\omega)| = \omega_n^2 \sqrt{\frac{\tau_1^2 \omega^2 + 1}{\omega^4 + 2\omega_n^2 (2\tau_1^2 - 1) \omega^2 + \omega_n^4}}. \quad (27)$$

The phase characteristic with the loop closed  $\varphi(\omega)$  is from (7) defined by

$$\varphi(\omega) = \arctg \left\{ -\frac{\omega [\tau_1 \omega^2 + \omega_n (2\zeta - \tau_1 \omega_n)]}{(2\zeta \omega_n \tau_1 - 1) \omega^2 + \omega_n^2} \right\}. \quad (28)$$

A servo with transfer function  $Y(j\omega)$  is, according to (6), absolutely stable with an infinite modulus of reserve stability. The reserve stability in phase in such a system is defined by

$$\Delta\varphi(\omega_0) = \frac{\pi}{2} + \arctg \omega_0 \tau_1 - \arctg \omega_0 T_1, \quad (29)$$

where  $\omega_0$  is found from

$$Y(j\omega_0) = 1. \quad (30)$$

Substituting (6) into (30) we get the biquadratic

$$\omega_0^4 T_1^2 - (k_v^2 \tau_1^2 - 1) \omega_0^2 - k_v^2 = 0,$$

whence

$$\omega_0 = \sqrt{\frac{k_v^2 \tau_1^2 - 1}{2T_1^2}} + \sqrt{\frac{(k_v^2 \tau_1^2 - 1)^2}{4T_1^4} + \frac{k_v^2}{T_1^2}}. \quad (31)$$

The allowances for the separate elements in the servo show that the reserve phase stability must not be less than 40°.

#### 4. Normal Response of the Optimum Servo to a Step Input

Certain requirements as to transient response are imposed on the usable servos, as well as those relating to steady-state behavior. The servo must respond in a set fashion to an input which is either a step or its time-derivative.

If a signal in the form of a unit function  $\beta_{i1}(p) = \frac{1}{p}$ , is applied to the optimum servo input, then from (7) the response at the output takes the form

$$\beta_{01}(p) = \frac{\tau_1 \omega_n^2 p + \omega_n^2}{p(p^2 + 2\zeta \omega_n p + \omega_n^2)}. \quad (32)$$

Expanding the explicit form of  $\beta_{01}(p)$  into components of which the originals are known we get the output  $\beta_{01}(t)$  as a function of time

$$\beta_{01}(t) = 1 - e^{-\zeta \omega_n t} \left( \cos \omega_n \sqrt{1 - \zeta^2} t - \frac{\omega_n \tau_1 - \zeta}{\sqrt{1 - \zeta^2}} \sin \omega_n \sqrt{1 - \zeta^2} t \right). \quad (33)$$

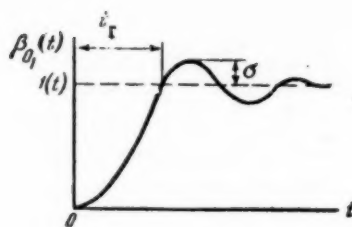


Fig. 3. Transient response rise time.

Then, if we need to determine the rise time  $t_r$  at the output, i.e., the time  $\beta_0(t)$  takes to rise from zero to unity (Fig. 3), we can use (33). Then equating the expression in parentheses in (33) to zero we get

$$t_r = \frac{1}{\omega_n \sqrt{1-\zeta^2}} \arctg \frac{\sqrt{1-\zeta^2}}{\omega_n \tau_1 - \zeta}. \quad (34)$$

If a set response speed, specified by  $t_r$ , is required in addition to the minimum limiting practical reproduction error the choice of an optimum  $T_1$  becomes restricted. Supposing that the condition  $T_1 \gg \tau_1$  is satisfied the optimum  $k_v$  is from (17) determined in the form

$$k_v = \frac{T_1 - 2\tau_1}{\tau_1^2}. \quad (35)$$

Further, substituting for  $\omega_n$ ,  $\zeta$  and  $k_v$  from (35) into (34) and bearing in mind that  $T_1 \gg \tau_1$ , we get

$$\tau_1 = 0.83 t_r \quad (36)$$

In future we shall use the curve  $\tau_1 = f(T_1)$ , which defined the relation between  $\tau_1$  and  $T_1$  which satisfies the minimum practical limiting error criterion to determine the  $T_1$  which corresponds to the  $\tau_1$  given by (36). It then frequently happens that large values of  $T_1$  are not compatible with (36) being satisfied or with the use of servos with second-order astatism for which  $T_1 = \infty$ .

As regards a number of other dynamic indices for the system we must firstly consider the overshoot  $\sigma\%$  upon a step input and the first four error coefficients  $c_1$ ,  $c_2$ ,  $c_3$  and  $c_4$ . Then if the servo has a  $Y(p)$  of the form of (6), i.e., belongs to the class of absolutely stable systems, then when  $T_1 \gg \tau_1$  it is easily shown from (4) and (8) that  $c_1 > 0$ ,  $c_2 > 0$ ,  $c_3 > 0$  and  $c_4 > 0$  at all times. Comparison of the error coefficients for various values of  $T_1$  shows that at small values the systematic error is mainly determined by  $c_1$ , while at large  $T_1$  by  $c_2$ .  $c_3$  is negative in both cases, so when the signs of the first and third derivatives of  $\beta_0(t)$  are the same the error components due to  $c_1$  and  $c_3$ , may to some extent balance out.

##### 5. Production of the Optimum Transfer Function for the Open-Loop Servo

Correcting links are frequently used in practice to produce servos with given responses: these links may be inserted in the circuit where the error signal is amplified directly or in the feedback circuit. The transfer function of power amplifier and effector motor plus object,  $Y_0(p)$ , is usually given.

When the signal to noise ratio is fairly unfavorable it becomes difficult to perform corrections using passive four-terminal networks in the signal amplification circuit because the output from the amplification circuit is greatly overloaded by the high-frequency components in the noise. It is then convenient to use a.c. feedback, the correction then being effected on the output  $\beta_0(t)$ , which is less overloaded with noise than is the error signal  $\delta\beta(t)$ . The block diagram of a servo using the correction of the type which is most frequently employed in practice is shown in Fig. 4.

The following symbolism is used here:  $Y_t(p)$  is the transfer function of the transforming and amplifying unit,  $Y_c(p)$  is the desired corrector unit transfer function.

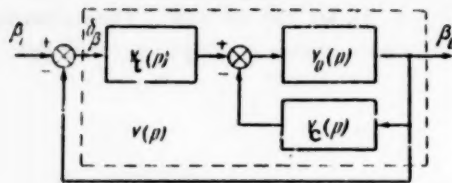


Fig. 4. Servo design using a corrector in the feedback circuit.

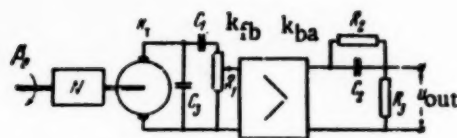


Fig. 5. Corrector unit satisfying (39)

It follows directly from Fig. 4 that

$$\frac{Y(p)}{Y_t(p)} = \frac{Y_0(p)}{1 + Y_c(p) Y_0(p)},$$

whence

$$Y_c(p) = \frac{Y_0(p) Y_t(p) - Y(p)}{Y_0(p) Y(p)}. \quad (38)$$

Let us consider the possible ways of producing the optimum transfer function for different given  $Y_t(p)$  and  $Y_0(p)$ .

#### Case 1.

$$Y(p) = \frac{k_v}{p} \frac{1 + p\tau_1}{1 + pT_m}, \quad T_m \gg \tau_1,$$

$$Y_t(p) = k_a, \quad Y_0(p) = \frac{k_{v_1}}{p(1 + pT_m)},$$

where  $T_m$  is the electromechanical time-constant of the electric motor — power amplifier — object assembly,  $k_a$  the gain of the amplifying and transforming unit,  $k_{v_1}$  the velocity gain of the power amplifier plus motor.

Using (37) simple manipulations then give

$$Y_c(p) = -\frac{1}{k_{v_1}} p \frac{p^2 \tau_1 T_m - p \left( \frac{k_a k_{v_1}}{k_v} T_1 - T_m - \tau_1 \right) - \left( \frac{k_a k_{v_1}}{k_v} - 1 \right)}{1 + p\tau_1}. \quad (38)$$

Several different ways of realizing (38) are available, depending how we choose  $\frac{k_a k_{v_1}}{k_v}$ .

a)  $\frac{k_a k_{v_1}}{k_v} = 1$ , then we have

$$Y_c(p) = -\frac{T_m + \tau_1 - T_1}{\tau_1 k_{v_1}} p \frac{p\tau_1}{1 + p\tau_1} \left( 1 + p\tau_1 \frac{T_m}{T_m + \tau_1 - T_1} \right). \quad (39)$$



The condition for (39) to be physically possible implies that the following inequality must be fulfilled.

$$T_m + \tau_1 > T_1. \quad (40)$$

To get sufficiently large  $T_1$  values we must increase the electro-mechanical time-constant of the motor by using, for instance, a power amplifier with an internal resistance equal to or somewhat greater than the input resistance of the effector motor, as well as by using an increased moment of inertia in the rotor. Then we can thus obtain  $T_m = 1-2$  sec.

From (39) the transfer function for the corrector can be produced e.g., with the design of Fig. 5. This design is comprised of: reduction gear of ratio  $N$ , a d.c. tachometer and a phase-advance circuit.  $C_3$  is intended to eliminate the brush noise, etc., load in the feedback circuit amplifiers.

The transfer function for the design of Fig. 5 takes the form

$$Y_{k_1}(p) = \frac{u_{out}(p)}{\beta_a(p)} = -(Nk_T k_{fb} k_{ba} G_0) p \frac{p\tau_1}{1+p\tau_1} \frac{1+p\tau_1 S}{1+p\tau_1 S G_0}, \quad (41)$$

where  $k_T$  is the tachometer constant in volts/radian/sec,  $k_{fb}$  is the feedback coefficient;  $k_{fb} < 1$ ,  $k_{ba}$  is the buffer amplifier gain,

$$G_0 = \frac{R_3}{R_2 + R_3}, \quad S = \frac{T_m}{T_m + \tau_1 - T_1} > 1.$$

A comparison of (39) and (41) shows that the following inequalities from which the corrector unit parameters are readily determined, must be satisfied:

$$Nk_T k_{fb} k_{ba} G_0 = \frac{T_m + \tau_1 - T_1}{\tau_1 k_{v_1}},$$

$$\tau_1 = R_1 C_1, \quad \tau_1 S = R_2 C_2 \text{ and } S G_0 \leq 0.1.$$

The time constant ( $\tau_1 S G_0$ ) must be small enough for the agreement between  $Y_C(p)$  and  $Y_{k_1}(p)$  to be sufficiently close.

b)  $\frac{k_a k_{v1}}{k_v} < 1$ . Here (38) implies the inequality

$$T_m + \tau_1 > \frac{k_a k_{v1}}{k_v} T_1. \quad (42)$$

(42) leads us to conclude that we can here produce larger  $T_1$  values than in the previous case. We rewrite (38) in the form

$$Y_c(p) = - \left( \frac{T_m + \tau_1 - \frac{k_a k_{v1}}{k_v} T_1}{\tau_1 k_{v1}} \right) p \frac{p \tau_1}{1 + p \tau_1} \times \\ \times \left( 1 + p \tau_1 \frac{T_m}{T_m + \tau_1 - \frac{k_a k_{v1}}{k_v} T_1} \right) - \frac{1 - \frac{k_a k_{v1}}{k_v}}{k_{v1}} p \frac{1}{1 + p \tau_1}. \quad (43)$$

In accordance with (43) the transfer function for the corrector unit can be realized via the circuit shown in Fig. 6. Here the corrector has two branches, the first being identical with the circuit of Fig. 5, the second involving positive feedback via  $R_4$  and  $R_5$ . High frequencies are shunted off by  $C_4$ . The corrector and error control signal  $U_{\delta\beta}$  are combined in a mixer, a multigrid tube being used for the purpose. The transfer function for the circuit of Fig. 6 takes the form

$$Y_{k_1}(p) = \frac{u_{out}(p)}{\beta_0(p)} = - (N k_{\tau} k_{fb1} k_{ba} G_0 k_{m1}) p \frac{p \tau_1}{1 + p \tau_1} \frac{1 + p \tau_1 T}{1 + p \tau_1 S G_0} - \\ - (N k_{\tau} G_1 k_{fb2} k_{m2}) p \frac{1}{1 + p \tau_1}, \quad (44)$$

where  $k_{fb1}$  and  $k_{fb2}$  are feedback coefficients, and  $k_{m1}$  and  $k_{m2}$  the amplification factors of the mixer,

$$G_1 = \frac{R_5}{R_4 + R_5} \text{ and } S = \frac{T_m}{T_m + \tau_1 + \frac{k_a k_{v1}}{k_v} T_1} > 1.$$

(43) and (44) imply that the following equalities must be satisfied:

$$N k_{\tau} k_{fb1} k_{ba} G_0 k_{c1} = \frac{T_m + \tau_1 - \frac{k_a k_{v1}}{k_v} T_1}{\tau_1 k_{v1}}, \\ \tau_1 = R_1 C_1 = C_4 R_4 G_1, \quad N k_{\tau} G_1 k_{fb2} k_{m2} = \frac{1 - \frac{k_a k_{v1}}{k_v}}{k_{v1}}.$$

In this case also  $\tau_1 S G_0$  must be negligibly small.

c)  $\frac{k_a k_{v1}}{k_v} > 1$ . In accordance with (38) the condition for  $Y_c(p)$  to be physically feasible is defined by (42).

Hence systems with  $T_1$  values less than  $T_m$  (the electromechanical time-constant of the motor) can be realized. The circuit of Fig. 6 can be used in the corrector unit, except that the feedback in the second branch is made negative instead of positive.

#### Case 2.

$$Y(p) = \frac{k_v}{p} \frac{1 + p\tau_1}{1 + pT_1}, \quad T_1 \gg \tau_1,$$

$$Y_t(p) = \frac{k_y}{1 + pT_a}, \quad Y_o(p) = \frac{k_{v1}}{p(1 + pT_m)},$$

where  $T_m$  is the amplifier unit time-constant.

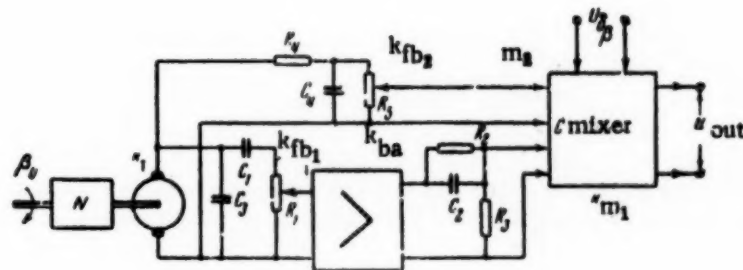


Fig. 6. Corrector unit satisfying (43).

Using (37) we get the corrector unit transfer function as

$$Y_c(p) = -\frac{1}{k_{v1}} p \frac{a_0 p^2 + a_1 p + a_2}{(1 + p\tau_1)(1 + pT_a)}, \quad (45)$$

where

$$a_0 = \tau_1 T_a T_m, \quad a_1 = T_m \tau_1 + T_m T_a + \tau_1 T_a,$$

$$a_2 = \tau_1 + T_a + T_m - T_1 \frac{k_a k_{v1}}{k_v}, \quad a_3 = 1 - \frac{k_a k_{v1}}{k_v}.$$

We shall restrict our consideration to the simplest form in which (45) can be realized, i.e., where  $\frac{k_a k_{v1}}{k_v} = 1$ . Then (45) may be written as

$$Y_c(p) = -\left( \frac{T_m \tau_1 + T_m T_a + \tau_1 T_a}{k_{v1} \tau_1 T_a} \right) p \frac{\tau_1 T_a p^2}{(1 + p\tau_1)(1 + pT_a)} \times$$

$$\times \left( 1 + p \frac{\tau_1 T_a T_m}{T_m \tau_1 + T_m T_a + \tau_1 T_a} \right) - \left( \frac{T_m + T_a + \tau_1 - T_1}{k_v \tau_1} \right) p \frac{p \tau_1}{1 + p \tau_1} \frac{1}{1 + p T_a}. \quad (46)$$

The transfer function  $\frac{\tau_1 T_a p^2}{(1 + p \tau_1)(1 + p T_a)}$  can be realized with an R-L-C filter, using the circuit shown in Fig. 7a. In fact the transfer function of such a filter takes the form

$$\frac{u_{out}(p)}{u_{in}(p)} = \frac{R_1 C_1 R_2 C_2 p^2}{R_1 C_1 R_2 C_2 p^2 + (R_1 C_1 + R_1 C_2) p + \frac{R_2 C_2 p + 1}{\frac{L_1}{R_1} p + 1}}.$$

If we put  $R_1 C_1 = \tau_1$ ,  $R_2 C_2 = T_a$ ,  $R_2 C_2 = \frac{L_1}{R_1}$  and  $R_1 = R_2$ , we get

$$\frac{u_{out}(p)}{u_{in}(p)} = \frac{\tau_1 T_a p^2}{(1 + p \tau_1)(1 + p T_a)}. \quad (47)$$

The link transfer function of (47) can to a first approximation be realized with a two-stage R-C filter using the circuit of Fig. 7b. The transfer function of such a filter takes a form which differs somewhat from that of (47):

$$\frac{u_{out}(p)}{u_{in}(p)} = \frac{R_1 C_1 R_2 C_2 p^2}{R_1 C_1 R_2 C_2 p^2 + (R_1 C_1 + R_2 C_2 + R_1 C_2) p + 1}.$$

But if we put  $R_1 C_1 = \tau_1$ ,  $R_2 C_2 = T_a$ ,  $C_2 \ll C_1$  and  $R_1 \ll R_2$  then, in view of the smallness of  $R_1 C_2$  as compared with  $\tau_1$  and  $T_a$ , we may to a sufficient accuracy assume that in some cases the transfer function

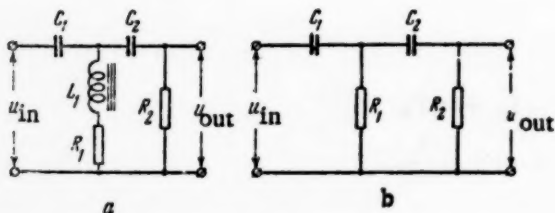


Fig. 7. R-L-C and R-C type filters in the feedback circuit.

of a two-stage R-C filter is described by (47).  $Y_c(p)$  for the corrector is defined by (46), the design and basic parameters of this unit being derived directly from this. Fig. 8 gives the corrector unit circuit. The first branch contains an R-L-C filter, a d.c. amplifier of gain  $k_{ba1}$ , and a phase-advance circuit. The second branch consists of a differentiating circuit  $R_5-C_5$ , an amplifying stage of gain  $k_{ba2}$ , and the voltage divider  $R_6-R_7$ . The transfer function for the circuit of Fig. 8 takes the form

$$Y_c(p) = \frac{u_{out}(p)}{\beta_o(p)} = - (N k_{\tau} k_{fb1} k_{ba1} G_0 k_{m1}) p \frac{\tau_1 T_a p^2}{(1 + p \tau_1)(1 + p T_a)} \frac{1 + p \tau_1 S}{1 + p \tau_1 S G_0} - (N k_{\tau} k_{fb2} k_{ba2} G_1 k_{m2}) p \frac{p \tau_1}{1 + p \tau_1} \frac{1}{1 + p T_a}. \quad (48)$$

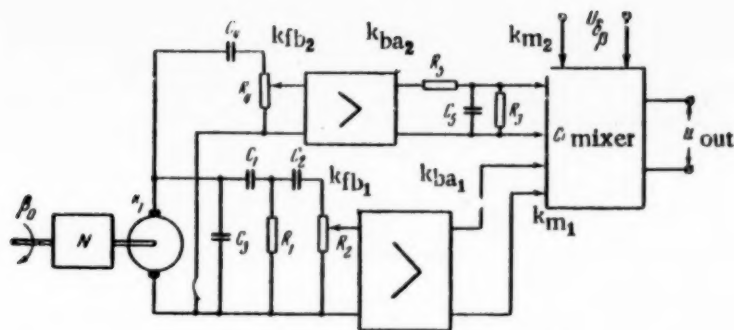


Fig. 8. Corrector unit satisfying (46).

Here

$$G_0 = \frac{R_7}{R_6 + R_7}, \quad G_1 = \frac{R_9}{R_8 + R_4}, \quad S = \frac{T_a T_m}{T_m \tau_1 + T_a T_m + \tau_1 T_a} < 1.$$

(46) and (48) imply that the following equalities must be satisfied:

$$\begin{aligned} N k_{fb1} k_{ba1} G_0 k_{m1} &= \frac{T_m \tau_1 + T_m T_a + \tau_1 T_a}{k_{v1} \tau_1 T_a}, \\ \tau_1 &= R_1 C_1 = \frac{C_4 R_4}{S} = C_8 R_8, \\ N k_{fb2} k_{ba2} G_1 k_{m2} &= \frac{T_m + T_a + \tau_1 - T_1}{k_{v1} \tau_1}. \end{aligned}$$

The other corrector circuit parameters are selected as in the previous cases.

Case 3.

$$\begin{aligned} Y(p) &= \frac{k_v}{p} \frac{1 + p\tau_1}{1 + pT_1}, \quad T_1 \gg \tau_1, \\ Y_t(p) &= \frac{k_a}{1 + pT_a}, \quad Y_0(p) = \frac{k_{v1}}{p(1 + pT_p)(1 + pT_m)}, \end{aligned}$$

where  $T_p$  is the time constant of the power amplifier. In accordance with Equation (37) the transfer of the corrector unit has the form:

$$\begin{aligned} Y_c(p) &= -\frac{1}{k_{v1}} p \frac{a_0 p^4 + a_1 p^3 + a_2 p^2 + a_3 p + a_4}{(1 + p\tau_1)(1 + pT_a)}, \\ a_0 &= \tau_1 T_m T_p T_a, \\ a_1 &= T_m T_p T_a + \tau_1 T_p T_a + \tau_1 T_m T_a + \tau_1 T_m T_p, \\ a_2 &= T_p T_a + T_a T_m + \tau_1 T_a + T_m T_p + \tau_1 T_p + \tau_1 T_m, \\ a_3 &= T_a + T_p + T_m + \tau_1 - T_1 \frac{k_{v1} k_y}{k_v}, \\ a_4 &= 1 - \frac{k_a k_{v1}}{k_v}. \end{aligned}$$

It is fairly difficult to realize (49) in a general form. But this equation may frequently be simplified if terms in  $p^3$  and  $p^4$  are neglected in the numerator, since these only influence the result at high frequencies. If the servo cutoff frequency is less than  $10 \text{ sec}^{-1}$  and the frequency range in which stability is in hazard is  $0 < \omega < 10 \text{ sec}^{-1}$  then the above simplification is quite permissible. In addition one should remember that  $T_p$  and  $T_a$  are in the several hundreds of a second range in a servo. Assuming  $\frac{k_a k_{v1}}{k_v} \approx 1$ , we get

$$Y_c(p) \approx - \frac{T_p T_a + T_a T_m + \tau_1 T_a + T_m T_p + \tau_1 T_p + \tau_1 T_m}{k_{v_1} \tau_1 T_a} p \frac{p^2 \tau_1 T_a}{(1 + p \tau_1)(1 + p T_a)} - \frac{T_m + T_p + T_a + \tau_1 - T_1}{k_{v_1} \tau_1} p \frac{p \tau_1}{1 + p \tau_1} \frac{1}{1 + p T_a}. \quad (50)$$

Fig. 9 gives the corrector circuit which can be used to realize (50). Its transfer function takes the form

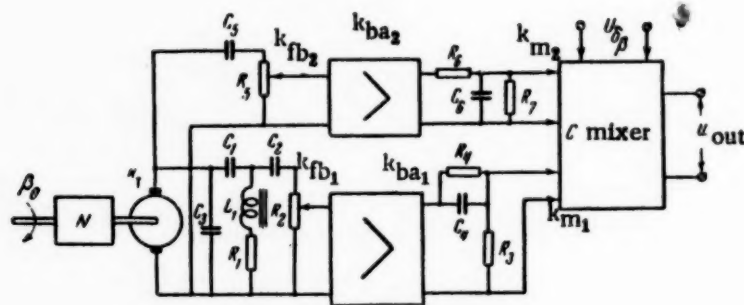


Fig. 9. Corrector unit satisfying (50).

$$Y_{c_1}(p) = \frac{u_{out}(p)}{\beta_0(p)} = - (N k_{\tau} k_{fb_1} k_{ba_1} k_{m_1}) p \frac{\tau_1 T_a p^2}{(1 + p \tau_1)(1 + p T_a)} - (N k_{\tau} k_{fb_2} k_{ba_2} G_1 k_{m_2}) p \frac{p \tau_1}{1 + p \tau_1} \frac{1}{1 + p T_a}, \quad (51)$$

where  $G_1 = \frac{R_1}{R_3 + R_5}$ ,  $\tau_1 = R_1 C_1$  and  $T_a = R_2 C_2$ , with  $C_2 \ll C_1$  and  $R_1 \ll R_2$ .

(50) and (51) imply that

$$N k_{\tau} k_{fb_1} k_{ba_1} k_{m_1} = \frac{T_p T_a + T_a T_m + \tau_1 T_a + T_m T_p + \tau_1 T_p + \tau_1 T_m}{k_{v_1} \tau_1 T_a}$$

and

$$N k_{\tau} k_{fb_2} k_{ba_2} G_1 k_{m_2} = \frac{T_m + T_p + T_a + \tau_1 - T_1}{k_{v_1} \tau_1}.$$

If we can assume  $T_1 = T_m + T_p + T_a + \tau_1$  here, then the corrector can be simplified considerably and can be reduced to a single feedback link comprised of a d.c. tachometer, a two-stage R-C filter and an amplifying state. Such circuits are frequently used in practice. It is of course inconvenient to produce complicated corrector units in practice in some cases because of technical complexities, unreliability and expense. So approximate solutions must always be studied and deviations from the optimum transfer function caused by using simpler correcting units estimated.



## 6. An Example of the Use of these Results

Suppose we have to determine the optimum transfer function for a servo system which satisfies the criterion of minimum practically limiting reproduction error in two instances: a)  $t_r$  (rise time) must not be more than 0.03 sec; and b)  $t_r$  is unrestricted. The input takes the form

$$\beta_i(t) = \frac{\pi}{2} \sin 0.25t,$$

$$\text{i. e. } \beta_{i0} = \frac{\pi}{2}, \omega_0 = 0.25 \text{ sec}^{-1}, \left(\frac{d\beta_i}{dt}\right)_{\max} = 22.5^\circ \text{sec}^{-1} \text{ and } \left(\frac{d^2\beta_i}{dt^2}\right)_{\max} = 5.6^\circ \text{sec}^{-2}$$

The spectral density of noise is  $\epsilon^2 = 0.612 \times 10^{-6} \text{ sec}$ . From (24) we construct a graph of  $k_v$  as a function of the same integrating time  $T_1$ . Then when  $T_1 \rightarrow \infty$

$$k_v = 4 \sqrt{\frac{\beta_{i0}^4 \omega_0^8}{\epsilon^4}} T_1 = 220 T_1.$$

Further, curves for  $\tau_1$  and  $\delta_\beta$  as functions of  $T_1$  are drawn from (17) and (22). Then when  $T_1 = \infty$  we get

$$\tau_1 = \frac{1}{\omega_n} = \frac{1}{2 \sqrt{\frac{10}{\beta_{i0}^4 \omega_0^8} \frac{\epsilon^4}{\epsilon^4}}} = 0.0675 \text{ sec}.$$

The minimum  $\delta_\beta$  corresponds to  $T_1 = \infty$ , being  $2.526 \times 10^{-3}$ . The curves for  $k_v$ ,  $\tau_1$  and  $\delta_\beta$  are given in Fig. 10. To get  $t_r = 0.03 \text{ sec}$  we must have from (36)

$$\tau_1 = 0.83 \times 0.03 = 0.025 \text{ sec}.$$

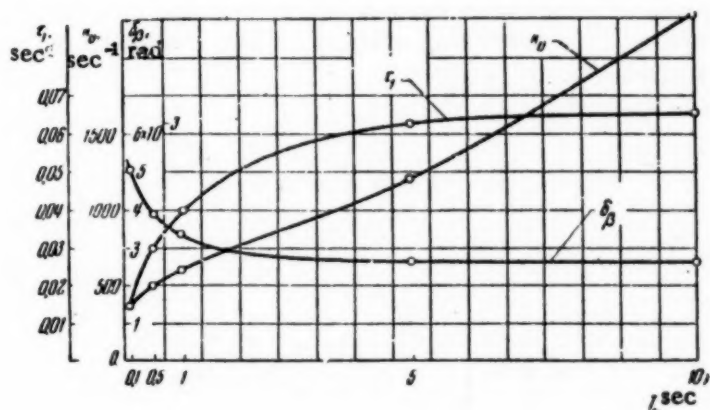


Fig. 10. Curves relating  $k_v$ ,  $\tau_1$  and  $\delta_\beta$  to  $T_1$  (integrating time-constant).

The curves of Fig. 10 show  $\tau_1 = 0.025 \text{ sec}$  correlated with  $k_v = 450 \text{ sec}^{-1}$  and  $T_1 = 0.3 \text{ sec}$ . Thus for case a) above the optimum open-loop transfer function is

$$Y(p) = \frac{450}{p} \left( \frac{0.025p + 1}{0.3p + 1} \right).$$

Then the practical limiting reproduction error is  $4.33 \times 10^{-3}$ , i.e., 1.7 times greater than when  $T_1 = \infty$ . The error coefficients are  $c_1 = 0.003 \text{ sec}$  and  $c_2 = 0.0017 \text{ sec}^2$ . Other dynamic parameters, e.g.,  $\omega_n = 38.8 \text{ sec}^{-1}$  and  $\zeta = 0.528$ , may be computed.

The cutoff frequency  $\omega_1$ , the resonant frequency  $\omega_m$  and the resonant peak on the amplitude curve for the closed-loop system are also easily determined. By solving  $|K(j\omega_1)| = 1$ , we get the cutoff frequency:

$$\omega_1 = \omega_n \sqrt{\omega_n^2 \tau_1^2 + 2 - 4\zeta^2}. \quad (52)$$

In the above example  $\omega_1 = 52.4 \text{ sec}^{-1}$ .

$\omega_m$  is determined from the solution to  $\frac{\partial |K(j\omega)|^2}{\partial \omega} = 0$ , taking the form

$$\omega_m = \frac{1}{\tau_1} \sqrt{-1 + \sqrt{1 + \tau_1^2 \omega_n^2}}. \quad (53)$$

So  $\omega_m = 32.4 \text{ sec}^{-1}$  and the resonance peak has  $|K(j\omega_m)| = 1.38$ . In case b) we take  $T_1 = \infty$  to minimize the practical limiting reproduction error. The optimum open-loop transfer function is then

$$Y(p) = \frac{220}{p^2} (0.0675p + 1).$$

The optimum servo system has second-order astatism, the acceleration gain being  $k_a = 220 \text{ sec}^{-2}$ . The error coefficients are  $c_1 = 0$  and  $c_2 = \frac{1}{k_a} = 0.0091 \text{ sec}^2$ , while  $\omega_n = k_a = 14.85 \text{ sec}^{-1}$  and  $\zeta = 0.5$ .  $\omega_1 = \omega_n \sqrt{2} = 21 \text{ sec}^{-1}$ , while the peak frequency in  $|K(j\omega)|$  is

$$\omega_m = \omega_n \sqrt{-1 + \sqrt{3}} = 12.7 \text{ sec}^{-1}$$

The peak height is

$$|K(j\omega_m)| = \sqrt{\frac{1}{\sqrt{3}(2 - \sqrt{3})}} = 1.46. \quad (54)$$

The rise-time  $t_r = \frac{\tau_1}{0.83} = \frac{0.0675}{0.83} = 0.08 \text{ sec}$ , i.e., is 2.67 times greater than in the preceding case

### CONCLUSIONS

1. The method of determining the optimum transfer function of a servo given in [4] has been extended for the case where the function to be reproduced is a given slowly varying one, while the noise is uniformly distributed over the whole working frequency range. The extension involves the concept of minimum practical limiting reproduction error introduced in [1].
2. General formulae for the error coefficients and amplitude and phase responses are derived, as well as for the stability reserve, the normal response to a step input and for other dynamic parameters of the optimum servo system.
3. Methods of realizing the optimum transfer function using corrector units operating on d.c. are presented.

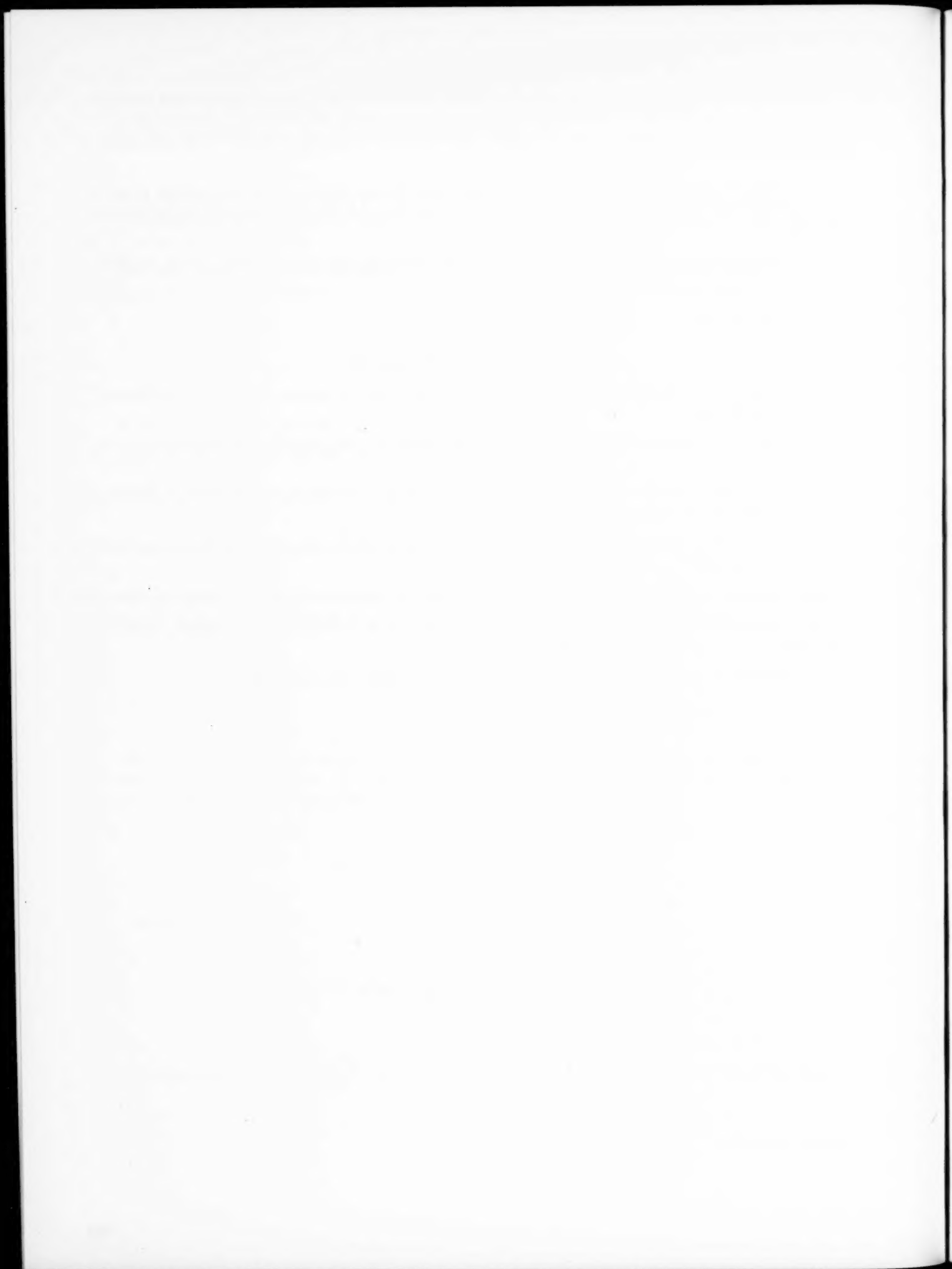
Received April 13, 1955

### LITERATURE CITED

- [1] Kurakin, K. I. On the responses of servos and automatic control systems. *Automation and Remote Control*, 12, No. 2, 1951.
- [2] Wiener, N. *Extrapolation, Interpolation and Smoothing of Stationary Time Series*. John Wiley, N. Y., 1949. \*
- [3] Booton, R. C. An Optimization Theory for Time-Varying Linear Systems with nonstationary Statistical Inputs. *Proc. IRE*, vol. 40, No. 8, 1952.
- [4] Kurakin, K. I. The choice of optimum characteristics for linear servo systems. I. *Automation and Remote Control*, 14, No. 4, 1953.
- [5] James, H. M., Nichols, N. B. and Phillips, R. S. *Theory of servo-mechanisms*. Foreign Lit. Press, 1951. \*
- [6] Solodnikov, V. V. *Introduction to the statistical dynamics of automatic control systems*. State Tech. Press, 1952.
- [7] Smirnov, V. I. *Course in higher mathematics*, vol. 1. State Tech. Press, 1945.

---

\* Russian Translation.



## AN OPERATIONAL AMPLIFIER WITHOUT STABILIZED POWER SUPPLIES\*

V. M. Evseev

(Moscow)

A new design for an operational amplifier without stabilized power supplies is considered, and the results of theoretical and experimental studies are presented.

### INTRODUCTION

The operational amplifiers used in current analog equipment which are designed around electronic tubes are highly reliable in operation. The strong negative feedback allows the tube parameters to vary within wide limits.

Analysis of electronic analogs shows that their sizes are not determined by those of the operational amplifiers but by those of the control units, of the feedback loop components and of the power supplies. The need to use stabilized power supplies with electronic analogs reduces the reliability considerably and presents a substantial obstacle to the use of operational amplifiers in automatic control systems, particularly when few such amplifiers are needed.

Two ways of designing amplifiers which do not require stabilized power supplies are available. The first consists in designing the amplifiers for carrier frequencies and is adopted when high-quality modulators requiring high carrier frequencies (10 kc or more) at very low modulation levels (from 30  $\mu$ v) are not used. The second method is based on extending the use of parallel channels for low and high frequencies, this mainly involving the design of operational amplifiers with automatic zero stabilization.

This paper deals with an operational amplifier using parallel amplifying channels.

#### 1. Operative Principals of an Amplifier with Parallel Amplifying Channels. Choice of Time-Constants.

Each channel in an amplifier with parallel amplifying channels (Figure 1) amplifies the input signal over a definite frequency range and shows no drift or change in output voltage caused by circuit parameter or power supply changes [1].

An operational amplifier of this type contains a summing amplifier  $A_2$  and feedback elements  $Z_1$  and  $Z_2$ , as well as the two amplifying channels connected in parallel. The upper channel (Figure 1) contains a d.c. amplifier  $A_1$ , connected to the summing point  $\Sigma$  and to the amplifier  $A_2$  via capacitors  $C_1$  and  $C_3$ , and amplifies a.c. signals. The lower channel operates via modulation-demodulation and amplifies constant or slowly varying signals.

With certain definite relations between the time-constants  $T_1 = C_1 R_1$  and  $T_2 = C_2 R_2$  in the upper channel and the filter time-constants  $T_2 = C_2 R_2$  and  $T_3 = C_3 R_3$  in the lower channel it can be arranged that the trough

\* Work carried out under the direction of B. Ya. Kogan.

in the total gain-frequency curve for the parallel channels does not exceed 30%. The circuit design is such that the channels have gains considerably greater than that of  $A_2$ . Hence as the negative feedback is strong the drift in  $A_2$  can in practice be neglected.

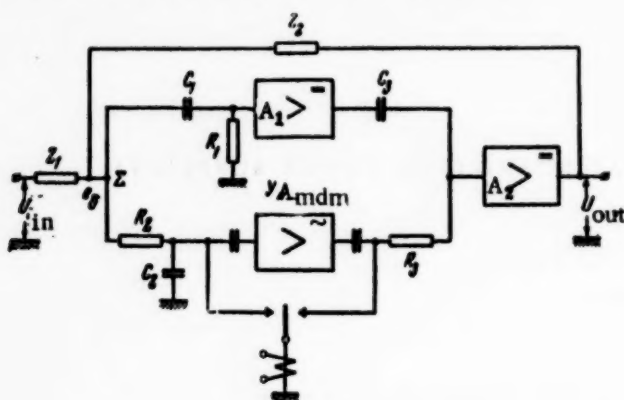


Fig. 1

The parallel channels can be considered as a special double T-filter made up of two isolated amplifiers  $A_1$  and  $A_{mdm}$  separated from  $C_3R_3$  by  $C_1R_1$  and  $C_2R_2$ . If  $A_1$  and  $A_{mdm}$  introduce no phase and amplitude distortions the transfer function of such a filter will be defined as the ratio of the image voltage at the input of  $A_2$  to that at the summation point  $Z$ :

$$W(p) = \frac{k_1 T_1 T_3 p^3}{(1 + T_1 p)(1 + T_3 p)} + \frac{k_{mdm}}{(1 + T_2 p)(1 + T_3 p)} = \quad (1)$$

$$= \frac{k_1 T_1 T_3 T_3 p^3 + k_1 T_1 T_3 p^3 + k_{mdm} T_1 p + k_{mdm}}{T_1 T_2 T_3 p^3 + (T_1 T_3 + T_2 T_3 + T_1 T_2) p^2 + (T_1 + T_2 + T_3) p + 1}.$$

Here  $k_1$  is the gain of  $A_1$ ,  $k_{mdm}$  the gain of  $A_{mdm}$ .

Replacing  $p$  in (1) by  $W(j\omega)$  and considering the modulus of the amplitude-phase characteristic  $T_1 \gg T_2$ ,  $T_1 \gg T_3$ ,  $T_3 \gg T_2$ , subject to the conditions  $\omega$ , we find that this modulus approximates to  $k_{mdm}$  when  $W$  is small, and to  $k_1$  when it is large. The modulus has a minimum value  $W(\omega_0)$  when its phase angle is zero.

Three equations are needed to determine  $T_1$ ,  $T_2$  and  $T_3$ . The relation used to determine  $T_3$  is obtained from the condition of minimum carrier-frequency pulsance described below. The phase-shifts in the parallel channels equated to zero and the permissible trough in the amplitude-phase curve at  $\omega_0$  are used as conditions for defining  $T_1$  and  $T_2$ . The relations given by these conditions yield a system of nonlinear algebraic equations from which a solution cannot be obtained in an explicit form.

When the phase shift in the differentiating circuit at the upper channel input is compensated by that in the integrating circuit in the lower channel input, while the phase shifts in the differentiating and integrating circuits at the outputs of the upper and lower channels likewise compensate, the following relation holds:

$$\omega_0 T_3 = 1, \quad \alpha = \frac{T_1}{T_2} = \frac{T_3}{T_2}.$$

$\alpha$ , which satisfies a given value of  $\bar{W}(\omega_0)$  is found from

$$\alpha = \frac{1 + \sqrt{1 + 4[1 - \bar{W}(\omega_0)] \bar{W}(\omega_0)}}{2(1 - \bar{W}(\omega_0))},$$

where

$$\bar{W}(\omega_0) = \frac{W(\omega_0)}{k}, \quad k = k_1 = k_{mdm}$$

For practical purposes it is more convenient to use the approximate equations



$$\bar{W}(\omega_0) \approx \frac{T_1}{T_1 + T_2 + T_3} \cdot \quad \bar{W}(\omega_0) \approx \frac{T_3}{T_3 + T_2} \cdot$$

These equations apply when  $T_1 \gg T_3$ ,  $T_1 \gg T_2$ , which is usually so in an amplifier.

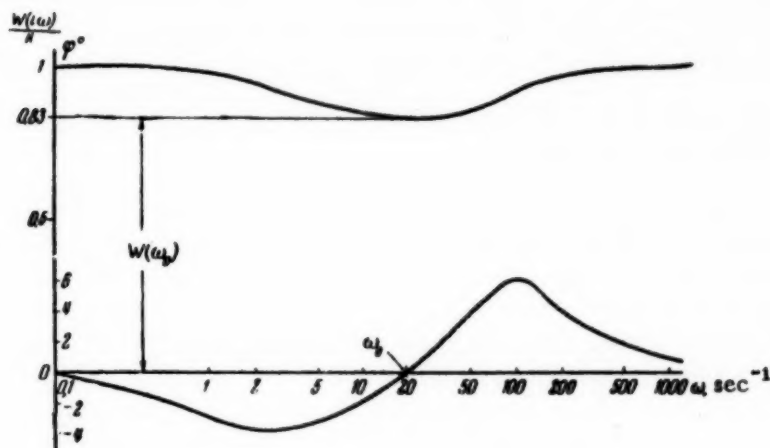


Fig. 2

Solution of these equations gives the following inequality, usable in practice:

$$T_2 \frac{\bar{W}(\omega_0)}{1 - \bar{W}(\omega_0)} \leq T_3 \leq [1 - \bar{W}(\omega_0)] T_1. \quad (2)$$

$T_3$  is defined by the modulation frequency, by the permissible amplitude output at this frequency and by the gains  $k_1$  and  $k_{\sim}$  (where  $k_{\sim}$  is the a.c. gain of  $A_{mdm}$ ).  $T_3$  can be determined from the approximate formula by assuming that a constant voltage  $e_0 = -\frac{U_{out \max}}{k_{mdm} k_3}$  is applied to the summation point (where  $k_3$  is the gain of  $A_2$ ) and that the transfer coefficients of the coupling circuits in the upper channel at the commutation frequency are unity:

$$T_3 \approx \frac{0.5 k U_{out \max} \left( 1 + \left| \frac{Z_2}{Z_1} \right| \right) k_{\sim}}{k_{mdm} k_1 k_3 \omega \Delta U_{out}}.$$

Here  $\Delta U_{out}$  is the permissible output from the amplifier at the modulation frequency of the commutator,  $\omega$ .  $T_3$  having been determined and a value assigned to  $\bar{W}(\omega_0)$ ,  $T_2$  and  $T_1$  are determined from (2). For the amplifier considered here the values of  $T_1 = 0.5$ ,  $T_2 = 0.01$ ,  $T_3 = 0.06$ , the d.c. gains being  $k_1 = k_{mdm} \approx 2500$ .

Figure 2 shows the amplitude and phase responses corresponding to (1) drawn up from the above data. The maximum dip in the amplitude curve is not greater than 17%, while the maximum phase shift does not exceed 6°. When the negative feedback is coupled in, the dip in the amplitude curve practically vanishes, and the phase shift becomes negligible.

## 2. The Main Properties and Peculiarities of the Amplifier.

If several amplifiers are connected to an unstabilized power supply the voltage changes at the output of one amplifier, caused by input voltage changes, cause voltage changes at the outputs of the other amplifiers although their input signals may be unchanged. The amplifiers are linked via the power supply, which has an output impedance much higher than that of a stabilized supply.

Let us investigate how the voltage at the output of the first amplifier  $\Delta U_{out 1}$ , varies if the output from the second amplifier,  $U_{out 2}$ , is an a.c. voltage of different frequency and amplitude. The second amplifier can be considered as a load which will cause changes in the power supply voltage at the frequency with which the load changes. Since  $\Delta U_{out 1} \ll U_{out 2}$  when the amplifier loads are equal we can consider the first amplifier as a constant load on the power supply. The power supply voltage changes are equivalent to injecting certain emfs into the grids of the second stages in the upper channel and in the summing amplifier  $A_2$ .

The voltage at the output of the first amplifier may be determined from the parameters of the amplifier itself and of the power supply, using the equation

$$\Delta U_{out 1}(\omega) = M_1(\omega) Z_t(\omega) I_0 \sin \omega t. \quad (3)$$

Here  $Z_t(\omega)$  is the total internal impedance of the power source, defined by

$$Z_t(\omega) = \frac{\sqrt{(R_t - R_t C L \omega^2)^2 + \omega^2 L^2}}{\sqrt{(1 - L C \omega^2)^2 + \omega^2 (2 R_t C - R_t L C^2 \omega^2)^2}},$$

where  $R_t$  is the rectifier resistance,  $L$  and  $C$  the smoothing circuit parameters,  $I_0$  the change in current drawn from the source by the load,  $M_1(\omega)$  a coefficient of proportionality, dependent on frequency and defined by

$$M_1(\omega) = k' \frac{\sqrt{A^2 + \omega^2 B^2}}{\sqrt{C^2 + \omega^2 D^2}},$$

where  $k' = 0.5 k_2 k_3 T_3$ ,  $k_2$  and  $k_3$  being the gains in the second stages of  $A_1$  and  $A_2$ ,

$$A = (T_1 + T_2) \omega^2, \quad B = 1 - T_1 T_2 \omega^2, \quad C = \frac{k}{1 + \left| \frac{Z_2}{Z_1} \right|} - \frac{k T_1 T_3 \omega^2}{1 + \left| \frac{Z_2}{Z_1} \right|},$$

$$D = \frac{k T_1}{1 + \left| \frac{Z_2}{Z_1} \right|} - \frac{k T_1 T_2 T_3 \omega^2}{1 + \left| \frac{Z_2}{Z_1} \right|}.$$

$k$  in these expressions is the open-loop gain of the whole amplifier.

(3) shows that  $\Delta U_{out 1}$  depends on  $T_1$ ,  $T_2$ ,  $T_3$ , on the supply impedance  $Z_t(\omega)$  and  $I_0$ , the load current change. This equation also implies that  $\Delta U_{out 1}$  can be reduced by changing  $T_1$ ,  $T_2$ ,  $T_3$ , reducing the supply impedance, and also reducing  $I_0$ . If the output stage is a cathode follower and supplied from a separate source,  $I_0$  will be changed by very little and  $\Delta U_{out 1}$  will not depend on the load from the second amplifier.

Figure 3 shows  $M_1(\omega)$  and  $Z_t(\omega)$  for the amplifier parameters given above when  $\left| \frac{Z_2}{Z_1} \right| = 100$ . The power supply smoothing circuit parameters were  $L = 10$  henries,  $C = 20 \mu f$ ,  $R_t = 200$  ohms. The output from the second amplifier was an alternating voltage of amplitude 100 v produced across a load  $R_v$  10 kohm

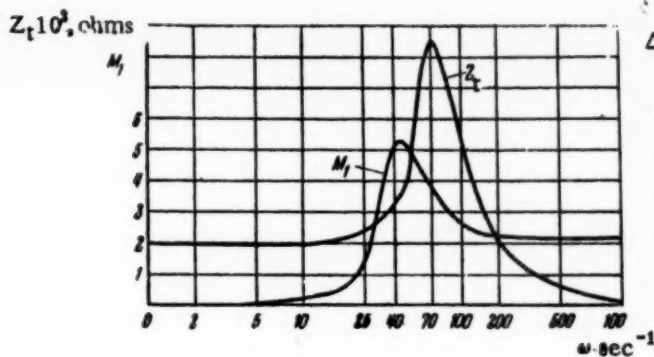


Fig. 3

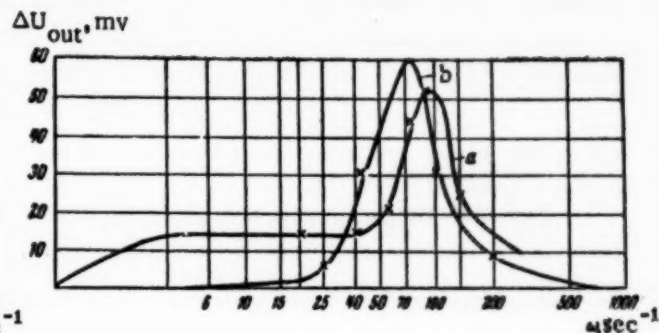


Fig. 4

Figure 3 shows that the resonant frequencies of  $M_1(\omega)$  and  $Z_t(\omega)$  almost coincide. If  $\Delta U_{out 1}$  is to be reduced the resonance peak in  $M_1(\omega)$  must be displaced towards higher frequencies by reducing  $T_3$ , while that in  $Z_t(\omega)$  must be displaced towards lower frequencies.  $T_3$  cannot be changed over a wide range since if  $T_3$  is to be greatly reduced the carrier frequency used in  $A_{mdm}$  must be raised. It is therefore practical to reduce  $\Delta U_{out 1}$  by increasing  $C$  and  $L$  in the power supply, this displacing the resonance to lower frequencies, and to use a semiconductor rectifier to reduce  $R_1$ . Figure 4 shows curves: (a) — experimental; (b) — computed, for  $Z_2/Z_1 = 100$ . The divergence between these at frequencies below 3 cycles/sec is due to neglect of a component in  $\Delta U_{out 1}$  dependent on changes in the supply voltage of the the cathode follower.

The filtration requirements for rectified power supplies are defined by the permissible 'hum' amplitude at the amplifier output. The amplitude of this output,  $\Delta U_s$ , may be found from

$$\Delta U_s \approx 0,5 k_2 k_3 T_3 \frac{V \sqrt{A^2 + \omega^2 R^2}}{\sqrt{C^2 + \omega^2 D^2}} \Delta E_a,$$

where  $\Delta E_a$  is the amplitude of the 'hum' from the rectified supply voltage applied to the grid of the second stage in  $A_1$ . The formula can be simplified if we remember that when  $\omega = 628 \text{ sec}^{-1}$  (full-wave rectification)  $A^2 \ll B^2 \omega^2$  and  $C^2 \ll D^2 \omega^2$ . Then we get

$$\Delta U_s \approx 0,5 \frac{\Delta E_a}{k_1'} \left( 1 + \left| \frac{Z_2}{Z_1} \right| \right),$$

where  $k_1'$  is the gain in the first stage of  $A_1$ .

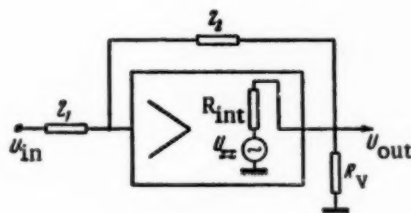


Fig. 5

If we assume the 'hum' due to the power supply to be 1 mv when  $\left| \frac{Z_2}{Z_1} \right| = 1$ , then  $\Delta E_a = 40 \text{ mv}$  when  $k_1' = 40$ . It is fairly simple to produce this degree of smoothing with rectified voltages from low-power sources.

The output and input impedances of an operational amplifier are important. The input resistance, defined as  $R_{in} = U_{in}/I_{in}$ , is determined by  $Z_1$ , as in all operational amplifiers with large gains and strong negative feedback.

From the output side an operational amplifier can be considered as a generator producing an amplified signal which has a certain internal resistance  $R_{int}$  (Figure 5). This internal resistance is the amplifier output impedance and depends on the output stage circuit, the open-

loop amplifier gain and on the type and circuit parameters of the feedback loop. The output impedance of an amplifier can be determined from Tevenen's formula, which gives

$$R_{int} = R_{out} = \frac{U_{xx}}{I_{kz}}.$$

Here the voltage  $U_{xx}$  and the current  $I_{kz}$  are defined by the equations

$$U_{xx} = \frac{k\mu R_c Z_2 U_{in}}{[R_i + (\mu + 1) R_c] (Z_1 + Z_2) + Z_1 k\mu R_c}, \quad I_{kz} = \frac{Z_2 \mu k U_{in}}{R_i (Z_1 + Z_2)},$$

where  $R_i$ ,  $\mu$ ,  $R_c$  are the cathode follower parameters.

Substituting for  $U_{xx}$  and  $I_{kz}$  in the expression for  $R_{out}$  we get

$$R_{out} = \frac{R_i R_c \left(1 + \left|\frac{Z_2}{Z_1}\right|\right)}{[R_i + (\mu + 1) R_c] \left(1 + \left|\frac{Z_2}{Z_1}\right|\right) + k\mu R_c}$$

or

$$R_{out} \approx \frac{\left(1 + \left|\frac{Z_2}{Z_1}\right|\right)}{Sk} \text{ when } \left|\frac{Z_2}{Z_1}\right| \ll k,$$

where  $S$  is the curvature of the tube output curve.

When a 6P1P tube is used in the output stage (this having  $\mu \approx 8$ ,  $R_i \approx 3 \text{ k}\Omega$ ) and when  $R_c = 15 \text{ k}\Omega$ ,  $\left|\frac{Z_2}{Z_1}\right| = 100$ , the output impedance of the amplifier will be  $0.35 \text{ k}\Omega$  i.e., approximately a factor 10 less than the output impedance of a plate-load output stage.

### 3. Basic Amplifier Circuit

Figure 6 shows the basic amplifier circuit. The amplifier is so designed that the open-loop gain is as large as possible. All stages are designed round 6N2P double triodes which have high amplification factors ( $\mu = 80 - 110$ ). The output stage, operating as a cathode follower, uses a 6P1P tube.

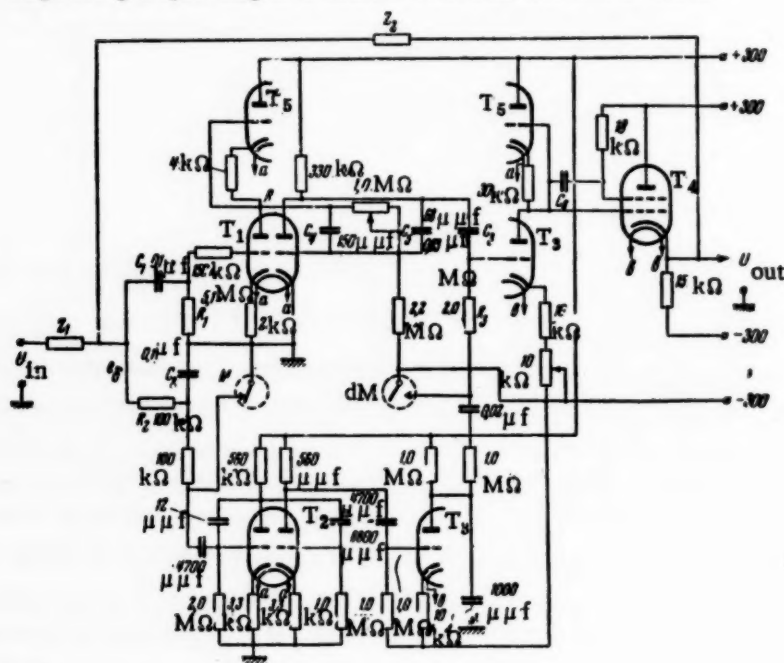


Fig. 6

The parallel high-frequency amplifier channel  $A_1$  is a two-stage d.c. amplifier (tube  $T_1$  plus one-half of  $T_3$ ). If the first stage in  $A_1$  has a normal plate load then when the plate and heater potentials alter, the operation of the second stage is disturbed. To maintain the correct operating condition in the second stage when the line voltage alters, the first stage is designed as a series degenerative balance circuit.

The working point in the second stage is set by adjusting the divider chain resistance. If the gain of the first stage is  $k_1 = 40$ , and of the second  $k_2 = 80$ , the overall gain in  $A_1$ , the effect of the divider being allowed for, will be  $k_1 \approx 2500$ . Negative feedback for slowly varying signals and a gain of  $k_1$  imply that  $A_{mdm}$  must have three stages of gain (tube  $T_2$  and one-half of  $T_3$ ) since the input modulator reverses the sign of the signal.

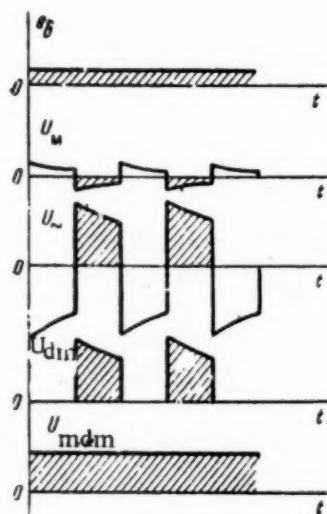


Fig 7.  $e\delta$  is the voltage at the summation point,  $U_M$  the voltage at the modulator contact,  $U_~$  the voltage at the amplifier output,  $U_{dm}$  the voltage at the demodulator contact,  $U_{mdm}$  the voltage at the  $A_{mdm}$  channel output.

The linear range is extended by cutting out the load. The pass-band, which defines the amplifier frequency response, is 600-700 cycles/sec at 100 v output and 7-8 kc/sec at 10 v output.

The d.c. gain, being about 2500, is fairly easily obtained in three stages. The  $A_{mdm}$  channel uses reversed-phase commutation as the number of a.c. amplifying stages is odd. The idealized waveforms shown in Figure 7 illustrate the operation of this channel. A vibrator with two separate armatures must be used, since the potential applied to the demodulator armature is -300 v, while the modulator armature is at zero potential. The adding stage is a series balance circuit with a gain  $k_3 = 40$ . The gain of the cathode follower output is close to unity. If the amplifier layout, using the above circuit parameters, is such that there is no current leakage from the high-voltage side to the summation point and no interference is present at the modulator input the amplifier output in the steady state is almost zero. The output zero is set exactly by adjusting the cathode resistance of  $T_3$  in the summing stage.

High-frequency parasitics are suppressed by the capacitors  $C_4, C_5, C_6$  (Figure 6).  $T_1, T_2$  and  $T_5$ , and  $T_3$  and  $T_4$ , are fed from separate heater supplies (a and b in Figure 6).

To utilize a 64P relay completely two amplifiers are mounted on one chassis, one relay serving as modulator  $\underline{m}$  and the other as demodulator  $\underline{dm}$ . Figure 8 shows the duplicated operational amplifier.

#### 4. Test Results for the Operational Amplifier

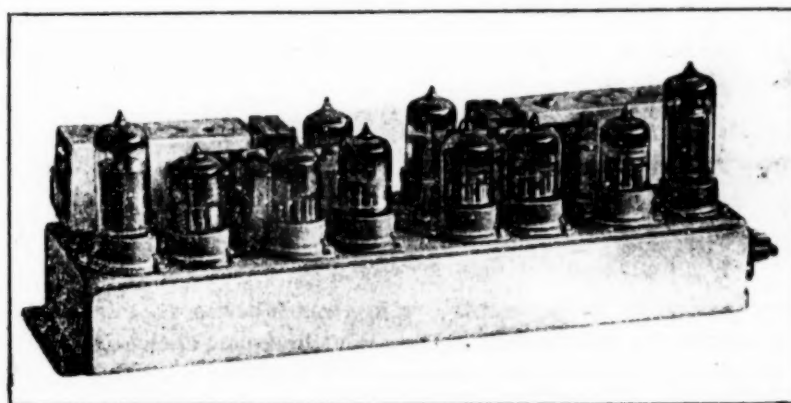


Fig. 8



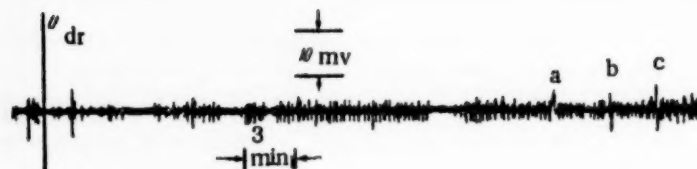


Fig. 9

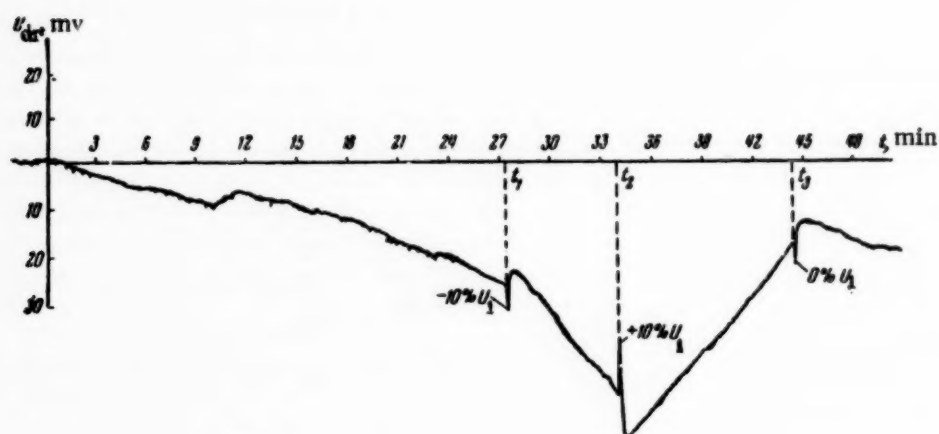


Fig. 10

Figure 9 shows the amplifier drift curve taken when it is working as a scalar amplifier with  $k = 1$  using an automatic self-balancing potentiometer recorder over a period of 50 min. This curve also shows the changes in output voltage when a  $\pm 10\%$  stepwise change in line voltage  $U_1$  is applied. From a to b  $U_1$  is below nominal by 10%, while from b to c it is nominal, and from c onwards 10% above nominal. The output voltage drift when operating as an integrator was basically determined from the inexact zero setting at the output. Figure 10 shows the drift curve when operating as an integrator with a transfer coefficient  $k = 1$  ( $R = 1$  meg,  $C = 1\mu f$ ). The effects of line voltage changes on the drift are clear from this curve. The line voltage was 10% below nominal from  $t_1$  to  $t_2$ , 10% above nominal from  $t_2$  to  $t_3$ , and nominal from  $t_3$  on.

The output voltage changes by 16 mv in 6 min when the line voltage change is  $\pm 10\%$ , i.e., the drift rate referred to the input is  $45 \mu v$  per sec.

The power drain is mostly that of the output stage since all other stages operate at low currents. The power drain from the low-power supplies is 1 watt per amplifier, the output stage taking about 12 watts from its supply.

#### SUMMARY

These data on the design of an operational amplifier which does not require stabilized power supplies show that the circuit satisfies the requirements applicable to electronic analog amplifiers. As compared with certain designs for operational amplifiers with automatically stabilized zeros [2], this design is much more reliable and economical, while providing the same technical performance because the power supply contains

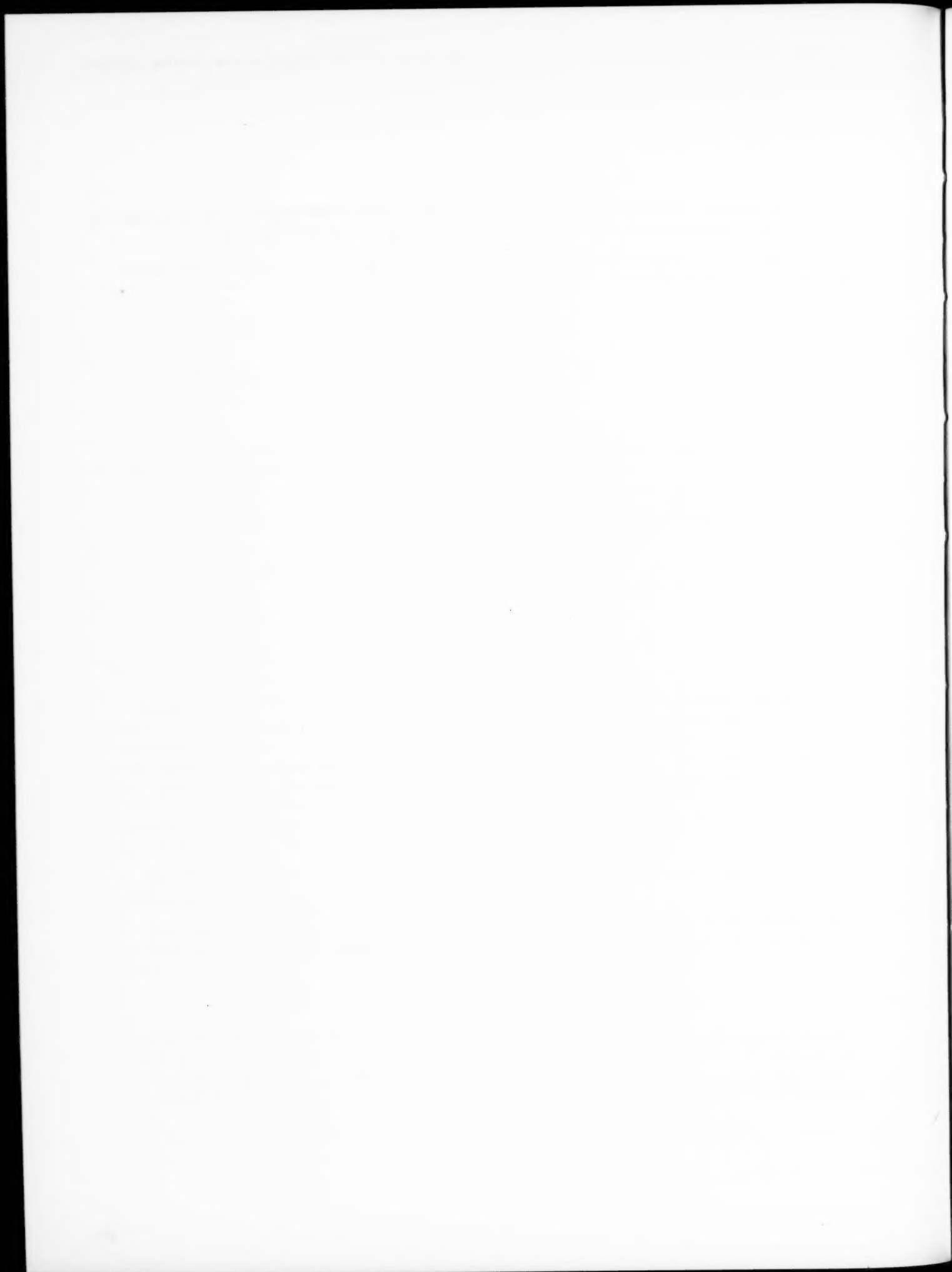


no tubes. Hence such amplifiers may be recommended for use in electronic analogs and in complex automatic control systems.

Received August 14, 1956

#### LITERATURE CITED

- [1] Buckerfield P. S. T. The parallel - T. D. C. Amplifier: A low drift amplifier with wide frequency response. The Proceedings of the Institution of Electrical Engineers, part II, October, 1952.
- [2] Gurov, V. V., Kogan, B. Ya., Talantsev, A. D. and Trapeznikov, V. A. New electronic analog equipment. Automation and Remote Control, 17, No. 1, 1956.



## AN ELECTRONIC ANALYZER FOR CONTACTOR CIRCUITS

V. I. RODIN

(Moscow)

Means of analyzing contactor circuits and of solving some design problems using a special high-speed device are dealt with.

The electronic contactor circuit analyzer is designed to facilitate and expedite the design of relay contact circuits.

The function of the device is to determine the possible combinations of states in six relays in which the contacts of a two-terminal network are either open or closed. In the same way the technical conditions in such two-terminal circuits can be established and checked on the device.

The circuit can also solve certain design problems, in particular in simplifying circuits by short-circuiting or eliminating excess contacts.

The analyzer block diagram is given in Fig. 1. Let us consider its operation when analyzing a two-terminal contact network.

The operation of the device is synchronized by the pulse-generator 3, which feeds combination program unit 4 and the pulse distributor 5. The number of different possible relay state combinations is  $2^6 = 64$ . When a pulse passes from the pulse generator to unit 4 a signal is passed on to the relay unit 2 and to the combination recording unit 6, this signal corresponding to a definite combination of relay states. When 64 signals have been transmitted the program unit reacts no further to generator pulses.

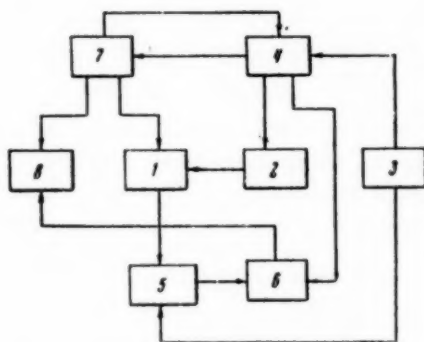


Fig. 1

When the signal is received in relay unit 2 the set combinations of relay states are produced, corresponding changes being produced in the contact unit 1. The circuit to be analyzed, being a two-terminal network, may be either open or closed in any combination of relay states. The pulse distributor 5 differentiates these two states in the two-terminal network and, depending on which state is present, distributes generator pulses along the two channels leading to the combination recorder unit 6. Depending on the channel by which a generator pulse arrives which coincides in time with the signal from the combination program unit 4, the open or closed-circuit state in the two-terminal network is recorded, for each relay state combination.

If the device is to solve design problems the projected circuit must have its technical details set up in unit 6 before commencing work. The contact testing unit 7 short-circuits

or eliminates a contact on the relay at the expense of which the circuit is being simplified.

So when unit 1 has taken up its 64 states one contact in it will remain unchanged since it will be eliminated or short-circuited by the contact testing unit 7. On starting the device the operations of the units will remain the same as during the circuit analysis, but the combination recorder unit 6 will as it were compare the set technical parameters and those actually obtaining on removing or short-circuiting the contact.

If one such technical condition is not complied with a signal passes from the combination recorder unit 6 to the contact recorder unit 8 which indicates that under the set conditions the short-circuited or eliminated contact is not superfluous.

When unit 4 has passed 64 signals to unit 2 and to unit 6 a signal is passed to the contact testing unit 7, which then causes a second contact of the same type (making or breaking) on the same relay to be eliminated or short-circuited. Then the 64 signals are again supplied from 4. This cycle is repeated until all such contacts on that relay have been tested. Then unit 7 passes a signal to unit 4, this latter then responding no further to generator pulses and thus bringing the operation to an end.

If there are several surplus contacts of the same type on the relay tested it may occur that on removing (or short-circuiting) one of them the others become necessary. Hence only one contact in the projected circuit is altered, and on restarting the device the need for the other contacts of this type on the relay is rechecked. The contacts in all relays in the circuit can be checked in this way.

Fig. 2 show the front panel of the device. The circuit under test is connected to the commutation panel with flexible leads. When the circuit is under test the commutator keys are put in positions appropriate to the technical conditions, the central positions corresponding to conditions where the circuits can be either open or closed. The right-hand rotary switch cuts in the number of relays present in the circuit being tested. The tumbler switch and commutator key are set in their 'technical conditions' positions, while the tumbler switch on the technical conditions panel is turned 'on'. On pressing the start button operation commences. If a thyatron above a key lights up this indicates that the technical condition is not satisfied. If it is desired to determine the technical conditions in the circuit the commutator keys are turned either to the upper or lower positions. If a thyatron above a key strikes it indicates that the given technical is the reverse of that shown by the key. When a circuit is being tested the keys are put in positions corresponding to the technical conditions in the circuit. The tumbler is switched over to 'simplify circuit', while the tumbler on the technical conditions key panel is turned to 'off'. The center rotary switch indicates the type of circuit simplification introduced, and the type of contact at the expense of which it is desired to simplify the circuit is set by the left-hand rotary switch. After introducing an appropriate circuit change on the commutation panel further attempts at simplifying the circuits are made. The left-hand tumbler serves to cut out the commutation panel, which is to be recommended on setting up the circuit to be analyzed.

Let us consider the bridge circuit of Fig. 3 as an example.

Set up the circuit on the commutation panel and set the right-hand rotary switch to the position where four relays (ABCD) operate.

The right-hand tumbler and key are set at 'technical conditions', while the tumbler on the key panel is set at 'on'.

In the relay states brought into action by the 'technical conditions' keys, a nonenergized relay is indicated by a line over the relay symbol. All the keys in which relays E and F are indicated without a line are placed in the center position because no contacts on E and F appear in the circuit under analysis.

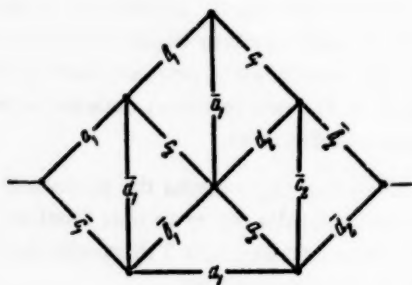


Fig. 3

When no technical conditions are applied the rest of the keys remain in the lower positions. On pressing the start button the device is set up in the initial condition, and when it is released the device begins to operate: in this case the cycle lasts 0.08 sec.

The thyatrons above the keys relating to  $\overline{A}\overline{B}\overline{C}\overline{D}$  ( $\overline{E}\overline{F}$  not being considered)  $\overline{A}\overline{B}\overline{C}D$ ,  $\overline{A}\overline{B}C\overline{D}$ ,  $\overline{A}B\overline{C}\overline{D}$  and  $\overline{A}B\overline{C}D$  strike. This means that these technical conditions (open-circuit in the system) are reversed, i.e., the circuit under analysis is closed when these relay states are combined.

With the other combinations of relay states ( $\overline{A}\overline{B}\overline{C}D$ ,  $\overline{A}\overline{B}C\overline{D}$ ,  $\overline{A}B\overline{C}\overline{D}$ ,  $\overline{A}B\overline{C}D$ ,  $\overline{A}\overline{B}\overline{C}D$ ,  $\overline{A}\overline{B}C\overline{D}$ ,  $\overline{A}B\overline{C}\overline{D}$ ,  $\overline{A}B\overline{C}D$ ) the system presents an open circuit.

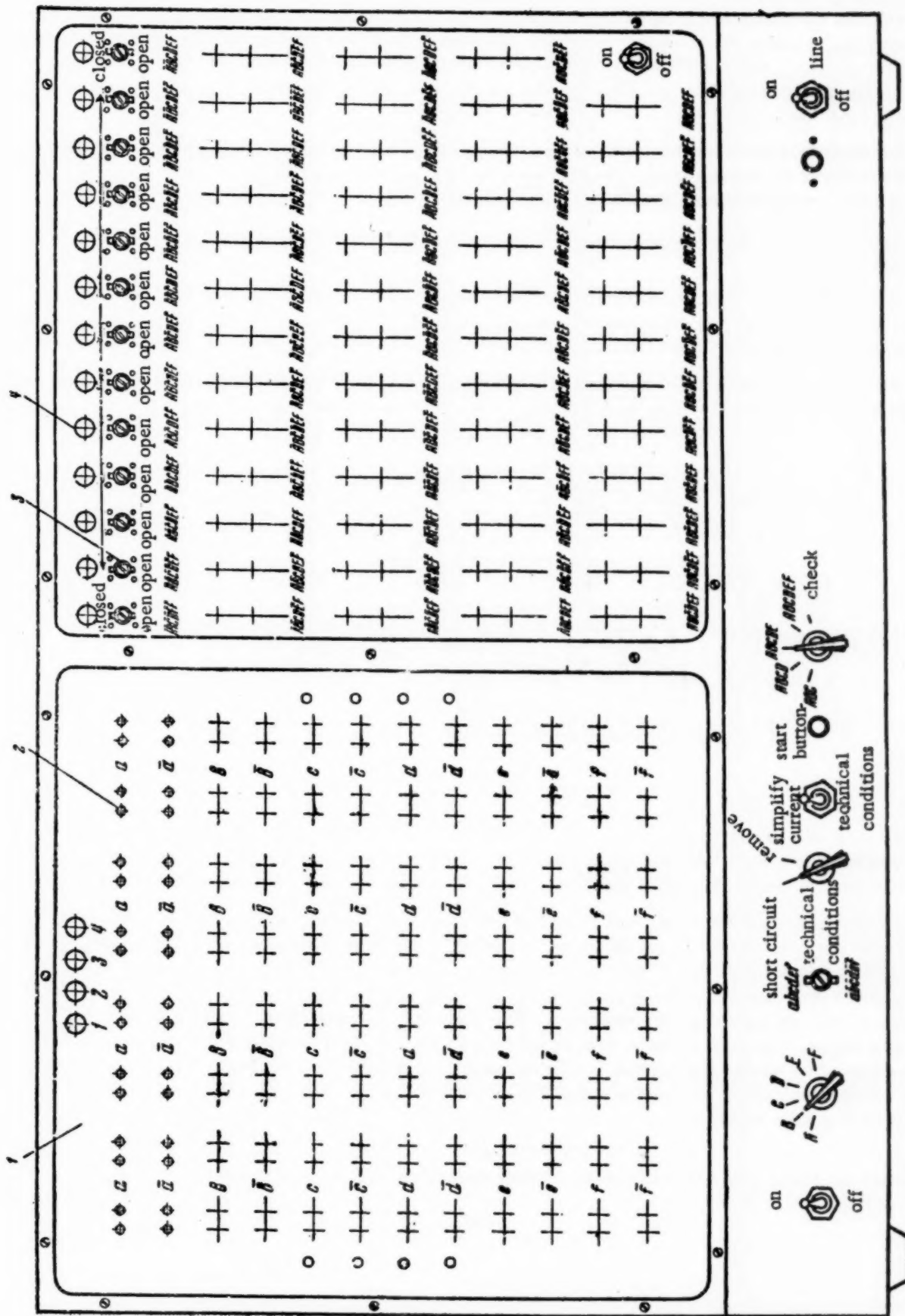


Fig. 2. Front panel of device: 1) commutator panel, 2) plug-in socket, 3) commutator keys for technical conditions, 4) thyatron type MTKh-90



Let us attempt to simplify the circuit. The tumbler switch is tuned to the 'simplify circuit' position, while that on the key panel is turned to 'off'. The keys remain in the positions corresponding to the technical conditions applying in the circuit. Let us attempt to simplify the circuit by removing contacts from relay A. The left rotary switch remains in position A, the key in position abcdef, and the next rotary switch remains at 'remove'. Let contacts  $a_1$  and  $\bar{a}_1$  appear in the first column of contacts on the commutation panel and  $a_2$  in the second ( $a_1$ ,  $\bar{a}_1$  and  $a_2$  are all on the same relay). Thyatrons 1 and 2 on the commutation panel strike when the device operates. This implies that neither  $a_1$  nor  $a_2$  can be removed. Turning the key to abcdef, let us again operate the device.. The first thyatron does not fire, so  $\bar{a}_1$  can be removed from the circuit under these technical conditions.

Let us verify whether it is impossible to short-circuit  $\bar{a}_1$ ; for this purpose the center rotary switch is set at 'short-circuit' and the device started. The first thyatron fires, which implies that this cannot be done. It is also not possible to short-circuit  $a_1$  or  $a_2$ .

The need for all other contacts in the circuit can similarly be checked, all possible prior simplifications having been made.

Of the equipment of this type at present in existence we must take note of Shannon and Moore's relay contact circuit analyzer,\* which was designed around electromagnetic relays and stepping switches (uniselectors), and which can be used to study two terminal contact networks containing at most 16 contacts and 4 relays [1].

Such devices can possibly be combined with other units: to this end they must operate rapidly. The need for high speed is particularly evident when studying circuits with many contacts and telephone relays.

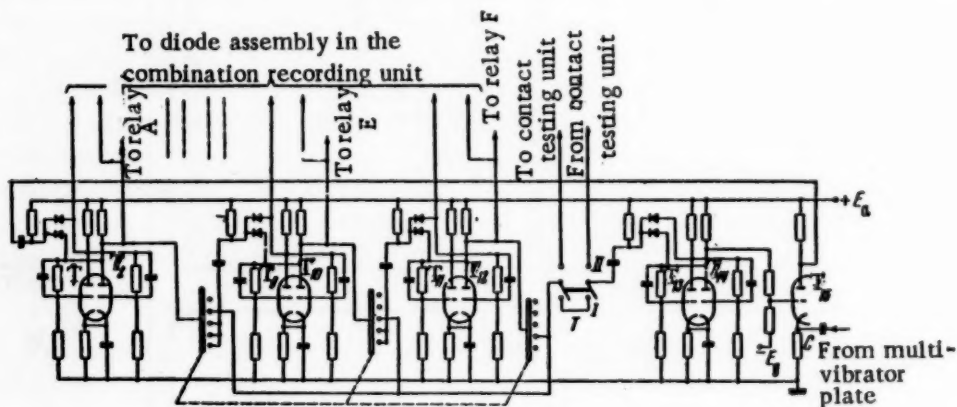


Fig. 4

By using tube circuits in this device the time taken was about 0.3 sec (when two-terminal networks employing telephone relays were used). Only slight changes in the circuit are required in dealing with two-terminal contact networks using many telephone relays and contacts; the size can be reduced by using transistors.

The combination programming unit consists of seven trigger circuits in series, each of which operates the next one (Fig. 4). Each of the six relays can take up two states, so in all there can be  $2^6 = 64$  combinations of relay states, which are produced by applying the potentials from the plates of the first six triggers operating in sequence. Pulses from the multivibrator plate are passed to the cathode of  $T_{15}$ , which is initially cut off by its negative grid voltage, and cause it to conduct. The negative-going pulses from the plate of  $T_{15}$  are passed to the first trigger. Operation of the seventh trigger shuts  $T_{15}$  off completely and the multivibrator pulses are not passed on. The combinations cannot then be repeated, i.e., the analysis is finished. When attempts are made to simplify the circuit the tumbler switch T is thrown over to position II. Then the seventh trigger operates when a pulse arrives from the contact testing unit.

\* Shannon and Moore give a brief description of their device, but omit the circuit and calculations.



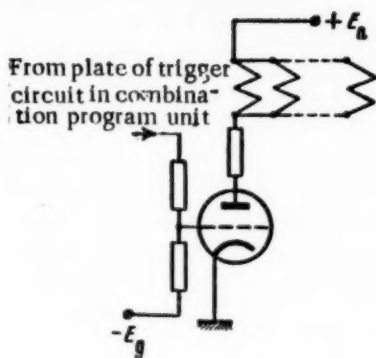


Fig. 5

The contact unit contains the polarized relay contacts from which the circuit to be analyzed is set up.

The pulse distributor unit (Fig. 6) differentiates between the two states in the two terminal network. If the contact unit circuit is open  $T_1$  conducts while  $T_2$ ,  $T_3$  and  $T_4$  are cut off by  $-E_g$ .  $T_3$  is given a large negative grid bias, so even the large negative pulses at its cathode do not cause it to conduct while  $T_4$  does. If the contact unit circuit is closed  $T_3$  and  $T_4$  change their conducting states.  $T_5$  and  $T_6$  coordinate the pulse distributor and combination recorder units. Thus the multivibrator pulses are distributed to the two channels in accordance with conditions in the contact unit. The multivibrator pulses from different plates pass to the combination program and distributor units, so the contact unit can first be operated and then the pulse applied to the distributor.

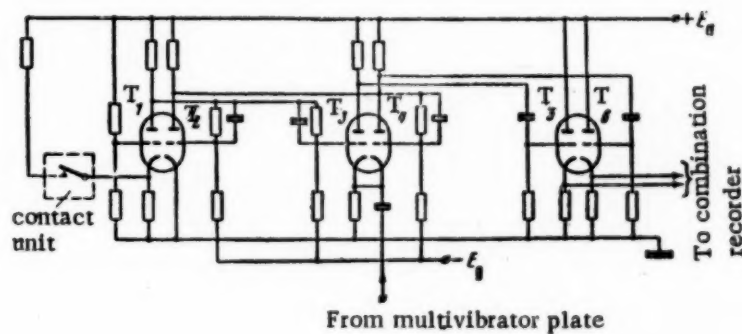


Fig. 6

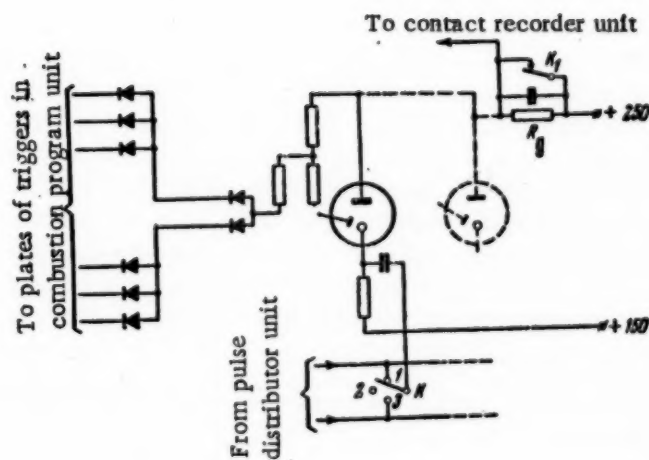


Fig. 7

The combination recorder unit consists of a square diode grid [2], the 64 MTKh-90 thyratrons and the commutator keys (sufficient for the number of combinations). Figure 7 shows a thyatron circuit. For each combination of trigger plate voltages only one thyatron will have a high potential on its control electrode, thereby preparing it to strike. If a negative-going pulse is now applied to the cathode of this thyatron it will strike and burn no matter how the central electrode voltage changes. The position of key K is set from the technical condition in that particular combination in such a way that when the condition applied to the contactor circuit is fulfilled no pulse passes to the thyatron cathode.  $K_1$  is opened when circuit simplification is attempted, and if a thyatron fires  $R_d$  passes a pulse to the contact recorder unit.

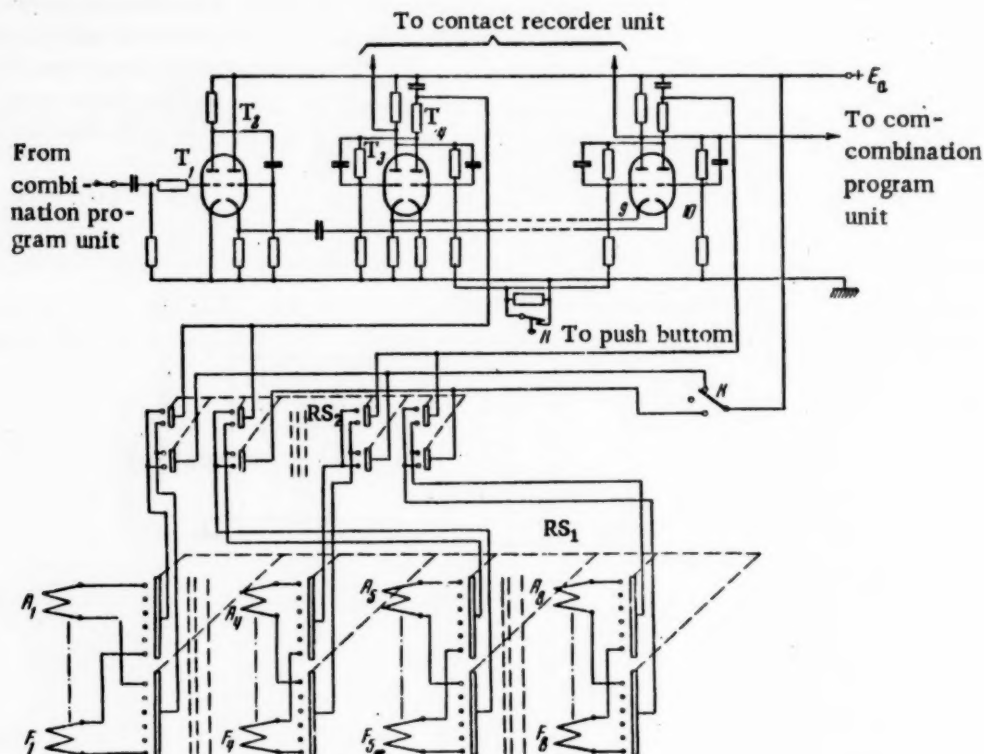


Fig. 8

The contact testing unit is used in seeking to simplify the circuit and contains a scaling circuit, two rotary switches and a commutator key (Fig. 8). The plate circuits of  $T_4$ ,  $T_6$ ,  $T_8$  and  $T_{10}$  contain the second coils on the RP-7 polarized relays in series with the plate loads. Hence a polarized relay can be put in the operated or nonoperated state, depending on the sense of the second coil, no matter what the action of the first coil, which is fed from the relay unit. The rotary switch  $RS_1$  selects the coils of the relay on which one is attempting to eliminate or short-circuit contacts (A, B, C, D, E, or F).  $RS_2$  alters the coil senses to correspond with removing or short-circuiting a contact. The polarized relay coils ( $A_5, \dots, F_5 - A_8, \dots, F_8$ ) which give open-circuited contacts are cut in the reverse sense to those of the polarized relays ( $A_1, \dots, F_1 - A_4, \dots, F_4$ ) which give closed contacts. K connects the plate voltage to the polarized relay coils which give either open-circuit or closed contacts. This corresponds to inserting the appropriate coils in the plate circuits. The center position on the key corresponds to cutting out these coils, which is required when analyzing a circuit in order to avoid accidental operation of the contact testing unit.

The contact recording unit (Fig. 9) consist of a shaper unit plus MTKh-90 thyratrons, which latter operate as in the combination recorder unit.

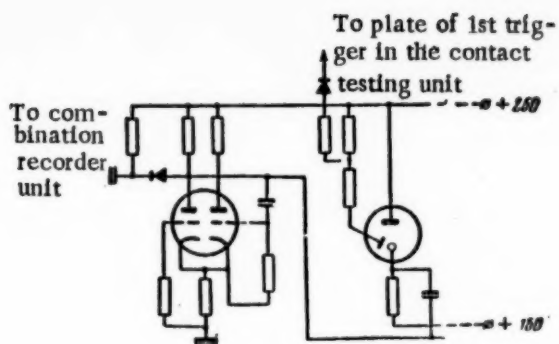


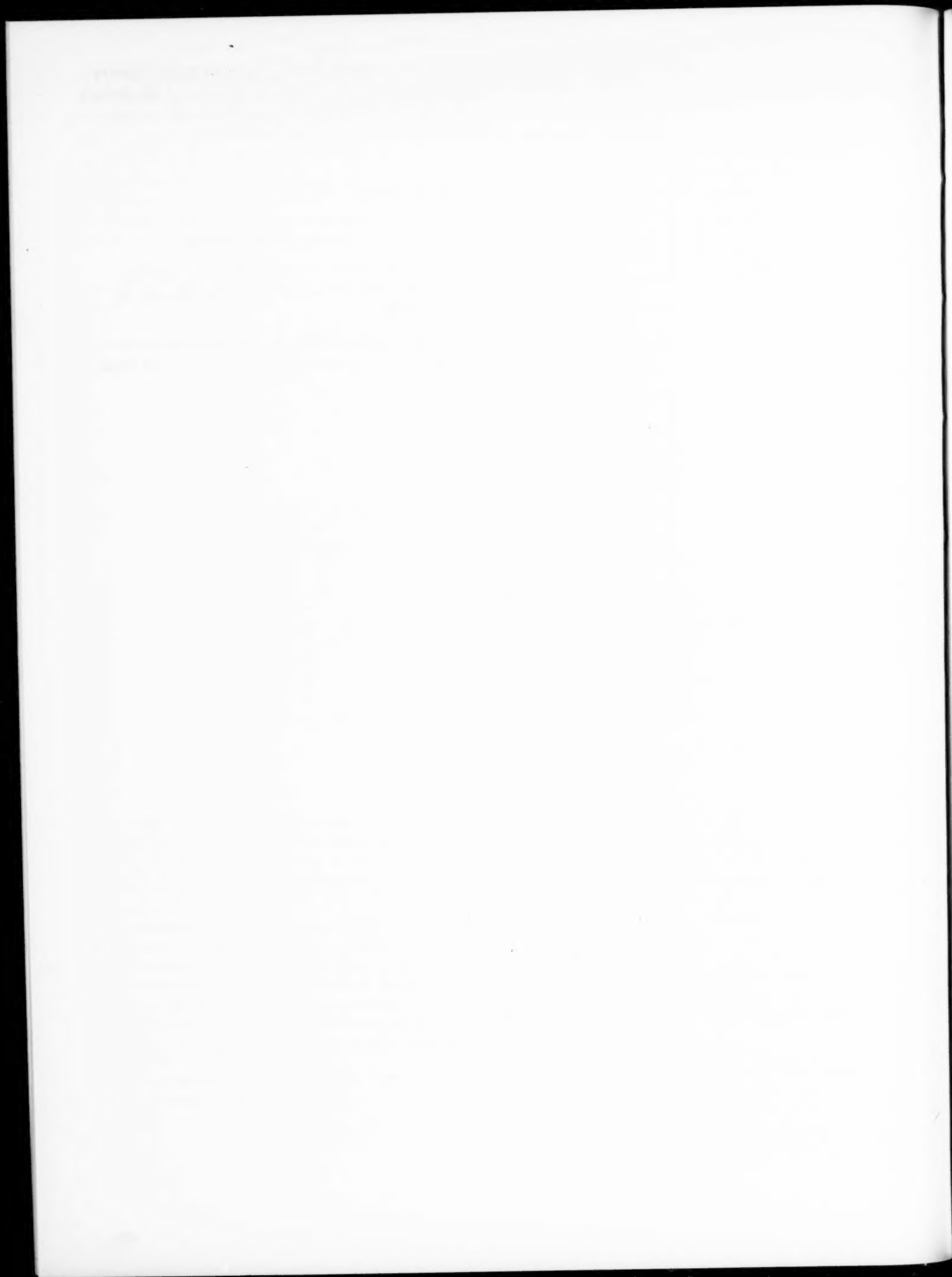
Fig. 9

The problems of design and automation in relay-contact circuits are extremely complex and this device, like that of Shannon and Moore, should only be considered a first step in this direction.

Received June 25, 1956

#### LITERATURE CITED

- [1] Shannon C. E. and Moore E. F. Machine Aid for Switching Circuit Design, Proc. IRE, vol. 41, No. 10, 1953.
- [2] Design of electronic computer and control circuits (Ed. V. I. Shestakov), Foreign Literature Press, 1954.



## A STATIC TRANSMITTER UNIT FOR PULSE-FREQUENCY TELEMETERING SYSTEMS

A. M. Pschenichnikov

A static balancing transmitting unit for pulse-frequency telemetering developed at TsLEM (Central Laboratory and Experimental Workshops) is briefly described and compared with existing devices.

Pulse-frequency telemetering systems have been widely used in Union power systems since the late 30's because of their simplicity and relatively high accuracy. In future, when pulse-frequency units are replaced, the motorized and contactor elements typical of former designs will be replaced by contactor-free frequency systems.

Even so the contactor units used in pulse-frequency systems have the advantages of simplicity and higher accuracy than uncompensated frequency systems. For instance the Moscow power grid, which has used the most telemetering equipment, has so far successfully employed contactor pulse-frequency systems.

Much work on improving pulse-frequency telemetering systems has been done at the Central Laboratory and Experimental Workshops of Moscow Power (TsLEM). Thermoelectric and magnetic power transducers were developed in 1951-3 (see [1-2]); in 1954 a static amplifier to replace the generator-compensator in the KKS adding unit, and in 1955 a static transfer device for pulse-frequency telemetering systems was developed [3].

The development of a combined static pulse-frequency telemetering system was carried out at TsLEM in conjunction with the Institute of Automation and Remote Control, Academy of Sciences of the USSR. The transmitting and receiving units were developed at TsLEM, while the units for keying the communication channels were developed in No. 4 Laboratory at the Institute.

Contactor and motorized units have now been completely eliminated from the check-points in pulse-frequency systems thanks to this work. The receivers are either contactor-free electronic units or else relay capacitor frequency meters with transformer filters. All the receivers at a sending point are normally supplied from an electronic voltage stabilizer. It is sometimes reasonable to use relay-capacitor frequency meters at sending points because they are exceptionally simple, small and cheap. Long use of these in the Moscow system has proved them reliable.

The static balancing transmitter unit developed at TsLEM for pulse-frequency telemetering is described briefly below, and is compared with current devices for frequency telemetering.

Figure 1 shows the theoretical circuit of the device. A direct current  $I_M$  flows from the output to the control coil of the magnetic null-detector [4]. The magnetization produces a first-harmonic voltage at the null-detector output, this being amplified by an electronic amplifier and fed to the grid of the phase stage. The phase stage amplifies and rectifies this voltage. The d.c. output voltage (across  $R_d$ ) from this stage is fed to the grid of a multivibrator. This alters the grid bias and hence the pulse frequency generated. The plate circuit contains the primary coils of the balanced transformer generator (coils on  $T_3$  and  $T_4$ ). The secondaries are connected in such a way that when the current in one triode increases stepwise and decreases similarly in the other triode the voltages induced in the secondaries add. The total voltage is proportional to the pulse frequency and independent of the multivibrator supply voltages within fairly wide limits; it is rectified by the copper-oxide bridge rectifier  $B_1$ , the rectified current  $I_R$  is passed through a balancing coil

on the null-detector, thereby establishing negative feedback at the output frequency.  $I_R$  is made independent of the multivibrator supply voltage by the cores of  $T_3$  and  $T_4$  being saturated by the plate current pulses. The stability of operation can be specified by a quantity  $\eta$ :

$$\eta = \frac{\Delta k}{k} / \frac{\Delta \mu}{\mu} \approx \frac{dk}{d\mu} / \frac{k}{\mu} = \frac{1}{1 + \mu\beta} = \delta, \quad (1)$$

where  $k$  is the closed-loop gain,  $\mu$  the open-loop gain,  $\Delta k$  and  $\Delta \mu$  being changes in these gains,  $\delta$  being the circuit stability and  $\beta$  the feedback coefficient.

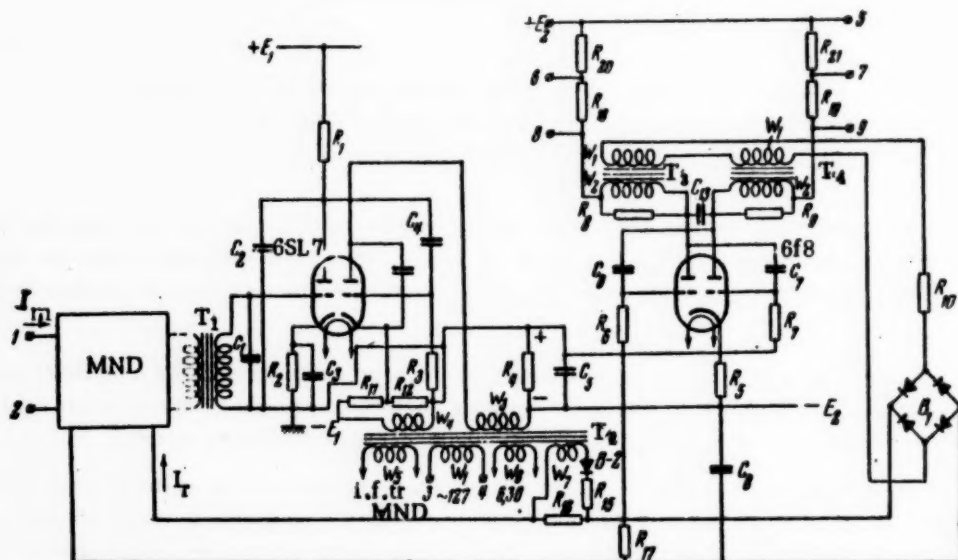


Fig. 1. Theoretical circuit of the static balancing transmitter unit for pulse-frequency telemetering systems.

The current flowing in the measuring coil of the null-detector, which produces a nominal frequency of 10 cycles/sec with the loop open, is  $5 \mu\text{a}$ , and  $150 \mu\text{a}$  with the loop closed. Then  $\delta = \frac{k}{\mu}$  i.e., 3.3%, and the closed-loop gain is 30 times less than the open-loop one.

The circuit stability is increased by employing a.c. feedback via  $C_6$  in addition to the d.c. feedback. The voltage drop across  $R_4$  is to a first approximation proportional to the generated frequency: when this changes  $C_6$  alters its state of charge. The current produced is  $i = C_6 \frac{du}{dt}$ ; it flows through the balancing coil on the null-detector and tends to reduce the change in voltage drop across  $R_4$ . This prevents hunting in the pulse frequency generated.

There are two methods of transmitting the readings.

1. Transmission via telephone line using pulses of alternating polarity. The lines can then be connected directly at the junctions between  $R_{18}$  and  $R_{20}$  and between  $R_{19}$  and  $R_{21}$  (terminals 6 and 7 of Fig. 1).

2. Transmission by audio-frequency pulses. Here the voltage drop in the plate resistors  $R_{18}$  and  $R_{20}$  is supplied either to a generator used for telephone line transmission (cf [6]) or to a subcarrier frequency generator in a high-frequency transmitter for power-cable transmission. When the distances are particularly large (thousands of kilometers) and important data have to be sent via overhead cables the 'active pause' method can be used to advantage, two generators of differing frequency being used which in turn receive the voltage drops across  $R_{18} + R_{20}$  and  $R_{19} + R_{21}$ .



The zero of the measured quantity is assigned the frequency  $f_0 = 1$  cycle/sec. The zero frequency is adjusted by applying a biasing d.c. voltage  $U_b$  to the balancing circuit, this being performed by applying the half-wave rectified voltage from  $W_7$  on  $T_2$  to  $R_{16}$ . The nominal frequency of the unit is 10 cycles/sec. This choice of transmission frequency makes telemetering of small values of the input easy. The pass-band required to transmit the signals along telephone wires is extremely narrow, so if the appropriate filters are used the immunity to noise interference can be made much higher than with frequency methods, and extra channels can sometimes be made available. As  $f_{max}/f_0$  is high the operational accuracy is improved.

Changes in  $U_b$  due to line voltage changes cause additional errors some ten times smaller than would be produced directly by the line voltage change. This is because the m.m.f. produced by  $U_b$  is:  $i_b W_T = U_b W_T / (R_{16} + R_{17} + R_T)$  where  $W_T$  is the number of turns on the balancing winding and  $R_T$  ensures that the m.m.f. is only 10% of that produced by the measurement winding. Since the error due to the transformer generator current being dependent on line voltage changes has the opposite sign to the error due to changes in  $U_b$  the two tend to balance out. When the line voltage changes by 10% the transformer generator current changes by 1.5%. Thus the additional error due to line voltage change  $\delta_{add}$  occasioned by elements not included in the negative feedback loop is

$$\delta_{add}\% = 0,1 \frac{\Delta U}{U_n} 100\% - 0,15 \frac{\Delta U}{U_n} \left[ 0,1 + 0,9 \frac{i_m}{i_{mn}} \right] 100\%,$$

where  $\Delta U$  is the line voltage deviation from nominal (in volts),  $U_n$  the nominal line voltage,  $C_M$  the measured current and  $i_{Mn}$  the nominal measured current.

Figure 2 shows the calculated straight line for the additional errors on a line voltage change of 15% (solid line) and the experimental curve for this (dashed). The deviations are due to displacement of the null-detector zero by line voltage changes.



Fig. 2

Two d.c. sources of 200v each ( $E_1$  and  $E_2$ ) are required to feed the plates in the transmitter unit. The current drawn from  $E_1$  is less than 1 ma. That drawn from  $E_2$  is not more than 20 ma. Semiconductor diodes are used as rectifiers. Laboratory tests of two transmitting units showed that the main error in the unit (deviation from linearity in the characteristic passing through  $f_0 = 1$  cycle/sec when the measured current is zero and through  $f_n = 10$  cycles/sec at

the nominal current) was not greater than  $\pm 0,4\%$ . The additional errors due to line voltage changes of  $\pm 15\%$ , when the frequency changed from 45 to 52 cycles/sec and the temperature  $\pm 15^\circ\text{C}$ , did not exceed 1%.

The table gives data for comparing the GChB-1 and GChB-2 units produced by 'Electropult' [7] with the ChIS-1-D static transmitter unit for pulse-frequency systems.

The tabulated data clearly demonstrate the comparative simplicity and high quality of the static transmitter unit for pulse-frequency systems.

The use of this unit, due to the absence of contactor elements at the check-point, provides simpler and therefore more reliable and cheaper telemetering.

The narrow pass-band required ensures high immunity to noise interference and makes it possible to utilize telephone lines efficiently. As the circuit is simple and contains few tubes it is not difficult to replace the tubes by transistors. Taken all in all this shows that pulse-frequency telemetering is the most promising for industrial use in a number of ways.

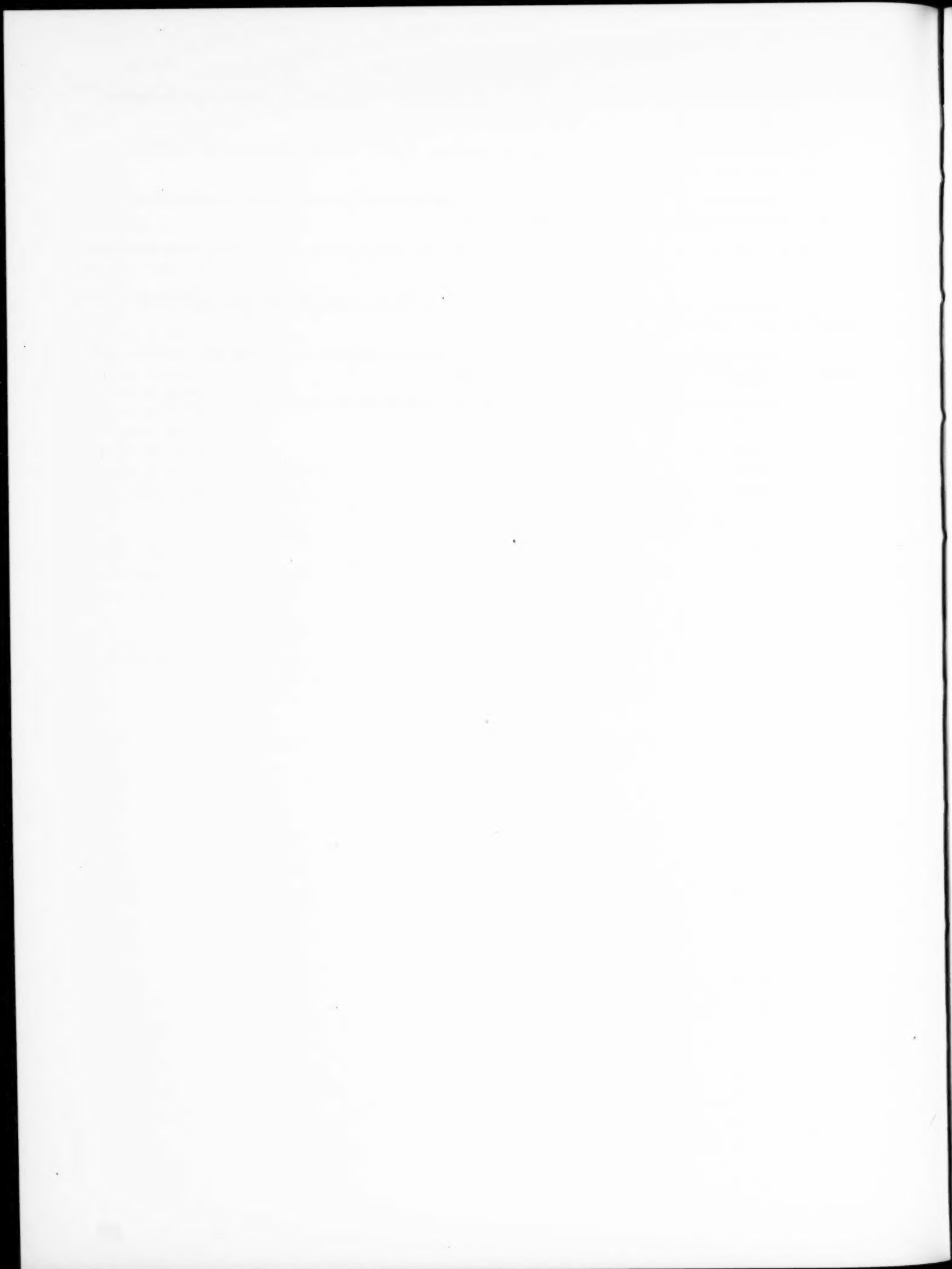
Received April 10, 1956

Parameters	Type of Input			Remarks
	GChB-1	GChB-2	ChIS-1-D	
Accuracy, %	2.5	2.5	2.5	Together with receiver
Type of circuit	Static	Astatic	Static	
Statism coefficient, %	5	-	4	
Minimum nominal input current, ma	-	1.5	0.15	Together with power supply
Output frequency limits, cycles/sec	27 x 44	27 x 44	1 x 10	
Number of tubes	7	6	2	
Number of magnetic amplifiers	-	1	1	Together with power supply
Number of transformers	5	6	4	
Number of chokes	2	3	-	
Number of motors	-	1	-	Ditto
Number of resistors	37	32	26	
Number of capacitors	29	28	14	
Number of semiconductor rectifiers	1	-	5	Ditto
External dimensions, mm	Two units	Two units	One unit	
	308 x 408 x	308 x 408 x	255 x 320 x	
	x 204	x 204	x 220	Ditto
Weight, kg	~30	37	9	
Power drain, watts	120	120	15	
Cost, roubles	-	5400	4100*	

\* Cost quoted for one-off

#### LITERATURE CITED

- [1] Pshenichnikov, A. M. A thermoelectric power transducer. Symp. 'Remote control of power systems', Acad. Sci. USSR Press, 1954.
- [2] Ginzburg, S. A. A magnetic static power transducer. Symp. 'Remote control of power systems' Acad. Sci. USSR Press, 1954.
- [3] Pshenichnikov, A. M. A static contactless self-balancing unit for pulse-frequency telemetering systems. Author's affidavit No. 102438 at 30 January 1956.
- [4] Pshenichnikov, A. M. Use of magnetic null-detectors in telemetering and recording units. Electricity, No. 1, 1956.
- [5] Ginzburg, S. A., Lekhtman, T. Ya. and Malov, V. S. Fundamentals of Automation and Remote Control. State Power Press, 1953.
- [6] Geronimus, Ts. E. A simplified equipment for combining telephone line circuits with transmission of remote control signals. Information data. State Power Press.
- [7] Telemetering units using a low-frequency system. Brief technical data 'Electropult' works.



## THEORY OF THE HALF WAVE MAGNETIC AMPLIFIER. II\*

R. A. Lipman and I. B. Negnevitsky

(Moscow)

The theory of the halfwave magnetic amplifier is considered, the finite dynamic permeability of the core material being allowed for when the  $R_{con}$  rectifier is absent. The practical and theoretical amplifier parameters are related to one another.

This paper extends the analysis of a halfwave magnetic amplifier working into an active load (Fig. 1,a). In part I [1] the circuit was analyzed with a rectifier  $R_{con}$  in the control circuit on the assumption that the hysteresis loop for the core was of ideal rectangular form (Fig. 2,a), with an infinitely great dynamic permeability in the vertical sections of the loop. In spite of this assumption the computed and experimental character-

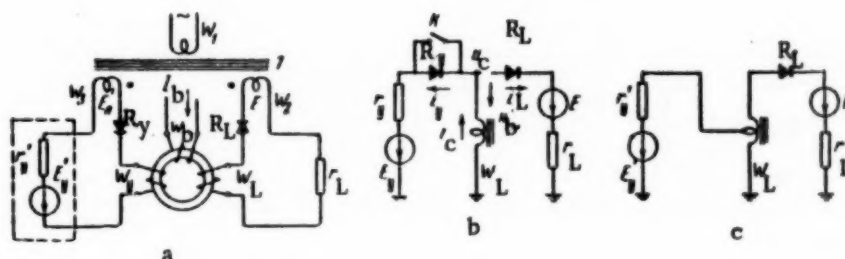


Fig. 1. a) theoretical circuit of amplifier; b) equivalent reduced circuit; c) equivalent amplifier circuit with an autotransformer series coil ( $R_{con}$  absent).\*

istics were extremely similar. But if an initial biasing field equal to  $-H_c$  is produced with the biasing winding  $w_b$  (Fig. 1a) fed with d.c. this assumption gives that the amplifier gain is infinite. This naturally cannot be so in practical conditions and so when bias is applied the finite dynamic permeability in the 'vertical' loop sections must be allowed for.

It is also of interest to relate the amplifier parameters to the component dimensions (coil sizes etc.).

The supporting voltage (e.m.f.)  $E_0$  (Fig. 1a) is in essence a bias voltage which is selected from the required position of the input-output characteristic relative to the control signal zero; it may be absent.

The control e.m.f. will be considered as sinusoidal and as being of the same frequency as the amplifier supply and either of the same phase or of the reverse phase to the supporting e.m.f. The question of whether the results are correct when the control is applied via a single or full-wave rectifier or by a constant voltage

\* From a paper at the seminar on magnetic amplifiers at the Institute of Automation and Remote Control, Academy of Sciences of the USSR, 25 April, 1956.

will be dealt with separately.

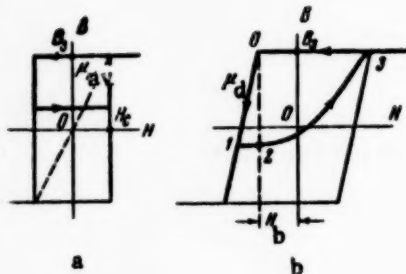


Fig. 2. Idealized hysteresis loops and parts of cycles. a) when a steady bias is not used; b) when  $H_b$  is used.

$e_{con}$  will be written as  $e_{con} = E_{con,m} \sin \theta$ .

Control half-wave ( $-\pi \leq \theta \leq 0$ ): this is unaffected by  $R_{con}$  since the control current is unchanged in direction during this time.

Figure 3 shows the supply, control, coil and rectifier voltages, the currents and the induction in the core.

Let us assume that the core is saturated at the beginning of the half wave, ( $\theta = \theta_0 = -\pi$ ), and the magnetic state is that of a point 0 on the hysteresis loop. The coil voltage is then zero ( $u_c = 0$ ) and the control circuit current is

$$i_y = \frac{e_y}{r_y} = \frac{E_{ym}}{r_y} \sin \theta. \quad \dots \quad (1)$$

When  $\theta = \theta_1$ , the instantaneous value of  $i_{con}$  is  $-I_c$ .\*\* The core begins to demagnetize but the control current is unchanged:

$$i_y = -I_c. \quad (2)$$

Demagnetization is produced by the coil voltage

$$u_c = e_y - i_y r_y = E_{ym} \sin \theta + I_c r_y. \quad (3)$$

When the coil voltage becomes zero at  $\theta_2$  demagnetization ceases (point 2 on the hysteresis curve).

(1) - (3) imply that

\* To simplify the notation the reduced quantities are undashed while the basic ones are dashed - the reverse of normal notation.

\*\* Remembering [1] that  $I_c = \frac{H_c I_c}{W_L}$

\*\*\* [Here and elsewhere subscript 'y'  $\equiv$  'con' where 'con'  $\equiv$  'control' - editor's note.]



$$\theta_1 = \arcsin \frac{I_{c,r,y}}{E_{ym}} - \pi, \quad \theta_2 = -\pi - \theta_1. \quad (4)$$

From time  $\theta = \theta_2$ ,  $i_{con}$  tends to become less in absolute value than  $I_c$ , and the magnetic state of the core begins to change over part of the cycle. With these assumptions the changes occur at constant induction (parts 2-3 on the hysteresis curve); so the coil voltage remains zero, and the control current changes are again defined by (1).

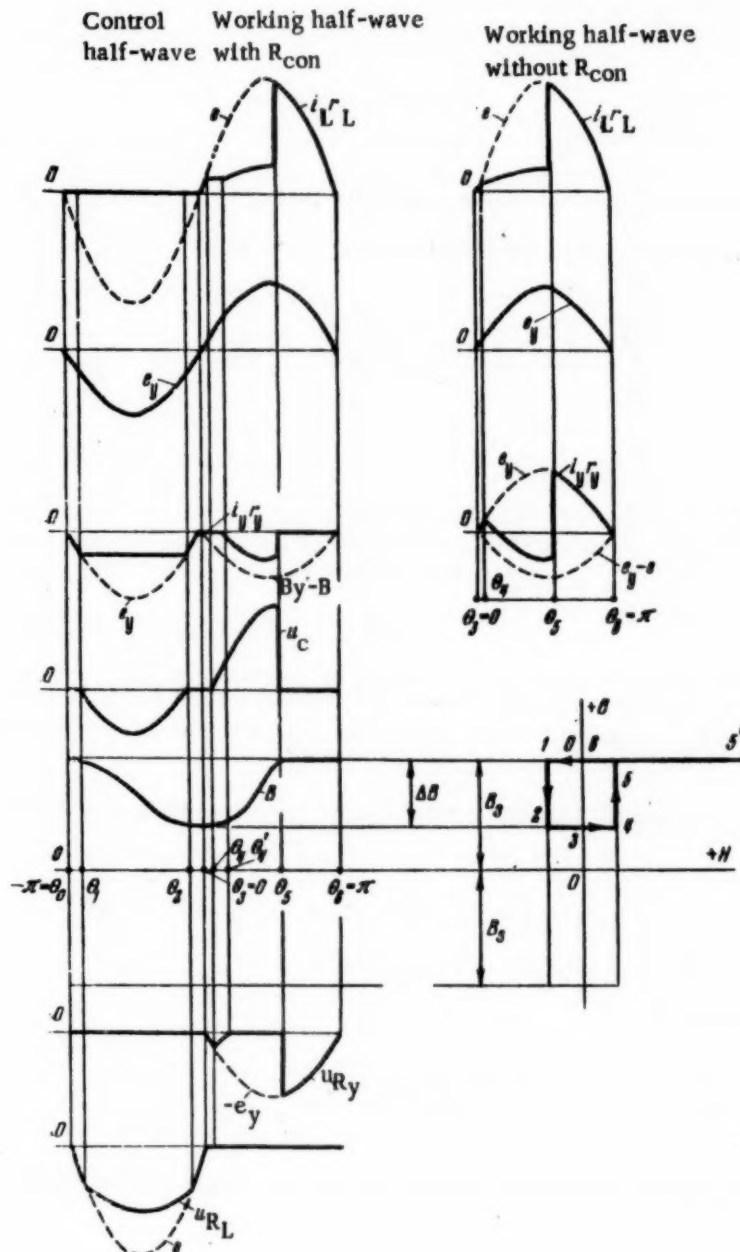


Fig. 3. Computed curves for the supply, control coil and rectifier voltages, for the currents in control and load, and for the core induction when control is by a.c., when  $R_{con}$  is both present and absent and when the idealized hysteresis loop of Fig. 2a is used.

When  $\theta_3 = 0$ ,  $i_{\text{con}} = 0$  (point 3 on loop). The control half-wave ends at this point.

The control half-wave will take the above course if  $R_L$  is nonconducting throughout ( $u_{tL} < 0$ ,  $i_L = 0$ ). The voltage on  $R_L$  is

$$u_{tL} = e - u_c \quad (5)$$

(3) and (5) imply that  $u_{tL} < 0$  when

$$E_{ym} < E_m + I_c r_y \quad (6)$$

Only modes in which (6) is fulfilled will be considered here.

The induction changes during the control half-wave are defined by

$$\int_{\theta_1}^{\theta_2} u_c d\theta = -2E_{ym} \cos \alpha + I_c r_y (\pi - 2\alpha), \quad (7)$$

where

$$\alpha = \arcsin \frac{I_c r_y}{E_{ym}}.$$

Working half-wave ( $0 \leq \theta \leq \pi$ ). Figure 3 shows the voltage, current and induction curves. This half-wave has been considered when  $R_{\text{con}}$  is present in [1]. Only these aspects due to  $R_{\text{con}}$  being absent are considered here.

Along  $\theta_3 - \theta_4$ ,  $u_c = 0$ , and the load and control circuit currents when  $R_{\text{con}}$  is absent follow the laws

$$i_L r_L = e = E_m \sin \theta, \quad i_y r_y = e_y = E_{ym} \sin \theta. \quad (8)$$

When  $\theta = \theta_4$ ,  $i_c$  given by

$$i_c = i_L + i_y \quad (9)$$

becomes equal to  $+I_c$ , a positive coil voltage appears and the core begins to be magnetized.

$\theta_4$  is defined by

$$\theta_4 = \arcsin \left[ I_c / \left( \frac{E_{ym}}{r_y} + \frac{E_m}{r_L} \right) \right]. \quad (10)$$

Along  $\theta_4 - \theta_5$  the core is magnetized by the voltage

$$u_c = e - u_L = e - i_L r_L \quad (11)$$

The coil current remains unchanged:  $i_c = I_c$ , while the load and control circuit currents follow the laws

$$i_L = \frac{e - e_y + I_c r_y}{r_y + r_L}, \quad i_y = \frac{e_y - e + I_c r_L}{r_y + r_L}. \quad (12)$$

From  $\theta = \theta_5$ , the core is saturated,  $u_c = 0$  and so  $i_{con}$  and  $i_L$  correspond to (8) - i.e., section 5-5'-6 on the hysteresis loop.

$\theta_5$  can be found from

$$\int_{\theta_1}^{\theta_2} u_c d\theta + \int_{\theta_2}^{\theta_3} u_c d\theta = 0. \quad (13)$$

The working half-wave ends when  $\theta = \theta_5$ .

Comparison of the working half-waves with and without  $R_{con}$  (Fig. 3) shows that in the latter case an additional current flows in the control circuit and that the 'angle of incidence' at  $\theta_5$  and the shape of the load current curve change somewhat.

#### Input-output transfer characteristics of the amplifier.

At all times during the working half-wave, no matter whether  $R_{con}$  is present or absent, we have

$$u_L = e - u_c \quad (14)$$

Since  $i_L \neq 0$  only during the working half-wave

$$2\pi U_{L,av} = \int_0^\pi u_L d\theta = \int_0^\pi e d\theta - \int_0^\pi u_c d\theta. \quad (15)$$

The second integral on the right in (15) determines the change in induction  $\Delta B$  after the working half-wave, and in the steady state it must equal the induction change after the control half-wave with the sign reversed. Thus,

$$2\pi U_{L,av} = 2E_m + \int_{\theta_1}^{\theta_2} u_c d\theta. \quad (16)$$

So the mean load voltage (current) is solely determined by the control circuit operation during the control period and is independent of what happens in the working period.

(7) and (16) give an expression for the static input-output transfer characteristic which is correct whether  $R_{con}$  is present or absent:

$$2\pi U_{L.av} = 2E_m - 2 \cos \alpha E_{ym} + I_c r_y (\pi - 2\alpha). \quad (17)$$

In relative units

$$U_{L.av}^0 = 1 - I_c^0 \left( \cot \alpha - \frac{\pi}{2} + \alpha \right), \quad (18)$$

where

$$U_{L.av}^0 = \frac{\pi U_{L.av}}{E_m}, \quad I_c^0 = \frac{I_c r_y}{E_m}, \quad E_{ym}^0 = \frac{E_{ym}}{E_m}, \quad \sin \alpha = \frac{I_c^0}{E_{ym}^0}. \quad (19)$$

In relative units (6) takes the form

$$E_{ym}^0 < 1 + I_c^0. \quad (20)$$

The relative voltage gain [1] is

$$k_u^0 = \pi \frac{\partial U_{L.av}}{\partial E_{ym}} = \cos \alpha = \sqrt{1 - \left( \frac{I_c^0}{E_{ym}^0} \right)^2}. \quad (21)$$

(19) - (21) are the same as the analogous expressions (55), (56) and (63) in [1] if we replace  $1 - E_{con,m}^0$  by  $E_{con,m}^0$  in the latter. The curves for the transfer characteristics and voltage gain given in Figs. 6 and 8 of [1] are also correct if the vertical axis is displaced one unit to the right. The input-output curve as a function of the total control-circuit voltage is shown in Fig. 4. The choice of bias (maintenance) voltage may be made from the desired position of the curve relative to the zero signal position.

So the control-circuit rectifier does not alter the basic amplifier characteristics. When small voltages are to be amplified it may be undesirable, however.

Eliminating  $R_{con}$  also has no effect on the transient response, since it does not affect the operation in the working half-wave.

The rise in control-circuit current on removing  $R_{con}$  in most practical cases is unimportant, since the basic characteristics are unaffected. But the current rise may overload the signal source (pickup) or overheat the control winding. The expressions given above for the instantaneous control current enable one to compute the control current in any concrete case and to determine the power dissipation in the control coil. The power dissipation may be estimated in advance since the maximum effective control current (referred) approximately satisfies.

$$I_y < \frac{E_y - E}{\sqrt{2} (r_y + r_L)}. \quad (22)$$

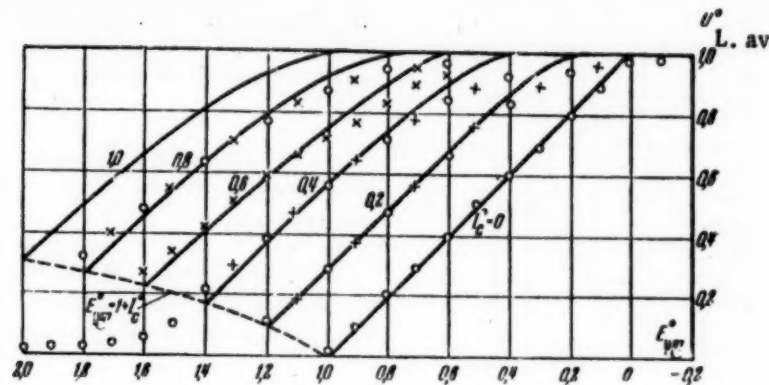


Fig. 4. Input-output curves with ideal hysteresis loop as in Fig. 2a, with no biasing (maintenance) voltage present. The curves are correct for control by sinusoidal a.c. and by half- or full-wave rectified voltages whether  $R_{con}$  is present or absent. The experimental points are for a.c. control: O)  $R_{con}$  present; X)  $R_{con}$  absent.

Experimental data given in the Appendix completely confirm the theoretical deductions.

In [1] the power gain in the circuit was defined as the ratio of the output power to the maximum power that the control signal source can provide (when working into a matched load):

$$k_p = \left( \frac{\Delta U_{L,av}}{\Delta E_{Y,av}} \right)^2 \frac{4r_s}{r_L} = k_u^2 \frac{4r_s}{r_L} \quad (23)$$

When control is by a sinusoidal voltage, and as in normal conditions  $r_s \approx r'_{con}$ , an expression was derived in [1], which is

$$k_p = \left( 0.5 \frac{W_L}{W_Y} \right)^2 (k_u^0)^2 \frac{4r'_y}{r_L} \approx 0.25 (k_u^0)^2 \frac{4r_c}{r_L} \quad (23a)$$

which, bearing in mind (19), may be put as

$$k_p = 0.25 \frac{E_m}{I_c r_L} 4I_c^0 (k_u^0)^2 \quad (23b)$$

The relative power gain is defined as

$$k_p^0 = 4I_c^0 (k_u^0)^2 \quad (24)$$

\* (23) is quite general and convenient. It also applies to transistor amplifiers. A formula frequently used for normal magnetic amplifiers controlled by d.c. is  $k_p = \frac{\Delta I_L^2 r_L}{\Delta I_{con}^2 r_{con}}$ , which is the same as (23) when the control winding resistance  $r_{con}$  is equal to the signal source resistance  $r_s$ .

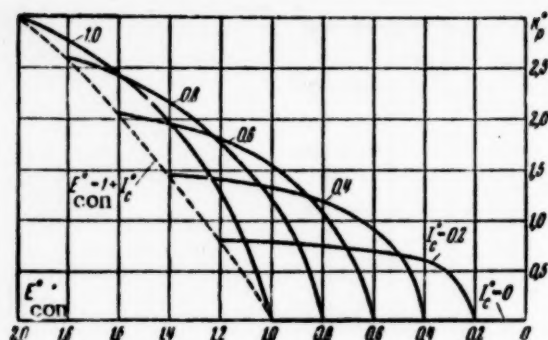


Fig. 5. Dependence of the relative power gain on the transfer characteristic of Fig. 4.

Figure 5 shows how  $k_p^0$  varies with  $I_c^0$  and  $E_{con,m}^0$ , the curves being computed from (21) and (24) for the range in which (20) applies. We can only get  $I_c^0 = 0$  under our conditions when  $r_{con} = 0$ , and then, of course,  $k_p = 0$ .

The  $k_p^0$  curves facilitate the choice of working parameters to give the highest power gain in a given working region.

When control is by half- or full-wave rectified voltages the removal of  $R_{con}$  does not affect the main input-output characteristics.

When d.c. control is used a change in bias (maintenance) voltage changes the transfer characteristic somewhat, while removal of  $R_{con}$  has no effect within certain ranges of  $E_{con}$ .

## 2. Operation of the Biassed Amplifier, the Finite Dynamic Magnetic Permeability Being Taken Into Account.

Figure 2b shows the approximate hysteresis loop and partial cycles assumed here. The induction changes over section 2-3 are shown qualitatively; the nature of these changes does not affect the basic characteristics. Section 1-2 is taken as horizontal, which substantially facilitates analysis without introducing impermissible quantitative or qualitative errors.

The bias field  $H_b$  is selected to be as in Fig. 2b. The bias coil  $W_b$  (Fig. 1a) is fed from the current source  $I_b$  (the a.c. impedance of the bias being taken as infinite). The basic assumptions are as previously.

Control half-wave ( $-\pi \leq \theta \leq 0$ ).  $i_L$  (load current) is assumed zero in this period. We assume that at the beginning ( $\theta = -\pi$ ) the coil current  $i_c$  is zero (Fig. 1b) and that the magnetic state of the core is therefore set at point 0 on the hysteresis curve (Fig. 6) by the bias.

As of  $\theta_0$ ,  $i_{con} = i_c$ , and so as this control current demagnetizes the core it will follow the law

$$e_y = i_y r_y + x_c \frac{di_y}{d\theta}, \quad (25)$$

where  $x_c$  is the dynamic inductive impedance of the coil dependent on  $\mu_d$ , the dynamic permeability on a vertical side of the hysteresis loop:

$$x_c = \omega \frac{S_c W_L^2}{l_c} \mu_d 10^{-8}. \quad (26)$$

Here  $S_c$  is the core cross section,  $l_{av}$  is the mean length of a line of force,  $\omega = 2\pi f$ .

When  $\theta = \theta_1$ , the coil voltage is

$$u_c = x_c \frac{di_y}{d\theta} = 0, \quad (27)$$

\* The above equations for the input-output characteristic and the corresponding curves are correct if the load voltage (current) is not down to the minimum value  $I_c r_L / E_m$ . But if  $r_{con} / r_L$  is sufficiently large (in practice  $> 5$ ) the minimum lies below the limit defined by (20).



and the control current is maximal (in modulus):  $i_{\text{con}}(\theta_1) = I_{\text{con.M}}$  (Fig. 6). The core state will then be determined by point 1 on the hysteresis loop.

Later  $i_{\text{con}}$  begins to drop, and the core state changes over part of the cycle. On the above assumption this change will occur at constant induction (section 1-2 on the cycle); so the coil voltage remains zero, and  $i_{\text{con}}$  varies as

$$i_y r_y = e_y. \quad (28)$$

When  $\theta = \theta_2 = 0$ ,  $i_{\text{con}} = 0$  (point 2 on cycle) and the control period ends.

The above discussion shows that the total induction change  $\Delta B$  (Fig. 6) is of greatest interest in the control half-wave.

The induction change is proportional to

$$\int_{\theta_0}^{\theta_1} u_c d\theta = x_c I_{ym} \quad (29)$$

(remembering that initially  $i_{\text{con}}(\theta_0) = 0$ ).

$I_{\text{con.M}}$  is found from (26) and (27):

$$I_{ym} = -\frac{E_{ym}}{r_y} \sin \psi, \quad (30)$$

Fig. 6. Computed curves for the variables of Fig. 1,b, using the idealized hysteresis loop of Fig. 2b with  $E_{\text{con.m}}^0 < 1$ .

where

$$\psi = \theta_1 - \theta_0 = \psi(\varphi_y), \quad (31)$$

and

$$\varphi_y = \tan^{-1} \frac{x_c}{r_c}. \quad (32)$$

The relation of  $\psi$  to  $\varphi_{\text{con}}$  is given in Fig. 7.

Thus  $\Delta B$  is proportional to

$$-E_{ym} \frac{x_c}{r_y} \sin \psi = -E_{ym} \tan \varphi_y \sin \psi. \quad (33)$$

Hence  $\Delta B$  varies linearly with  $E_{\text{con.m}}$ .

The control half-wave takes the above course if the load current is zero. This condition is readily shown to be fulfilled if

$$E_{ym} \leq E_m \quad \text{or} \quad E_{ym}^0 \leq 1. \quad (34)$$

If (34) is not fulfilled  $R_L$  will conduct during part of the period and a load current will flow. Figure 8 shows the corresponding graphs. A detailed analysis of this case is not given here. In essence,  $\Delta B$  will then not vary linearly with  $E_{con,m}$ .

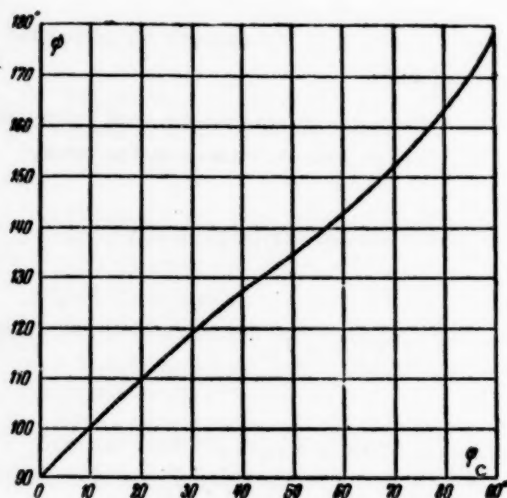


Fig. 7

**Working half-wave ( $0 \leq \theta \leq \pi$ ).** The type of changes in the load current and other quantities here depends on the shape of the part cycle 2-3 (Figs 2b, 6 and 8). But on our assumptions the basic input-output characteristics do not depend on the shape of this section.

So we shall only consider the voltage, current and induction curves during the working half-wave (Figs. 6 and 8) qualitatively.

**Input-output characteristic.** Normally  $r_{con} \gg r_L$  in an amplifier, and when  $E_{con,m} > E_m$  the load current flowing in the control half-wave can be neglected. In addition, as experiment has shown, the rectifier  $R_L$  also remains practically cut off for  $E_{con,m} > E_m$  due to the nonlinearity of the rectifier characteristic at small currents.

Below we shall show that the operating sector of the input-output characteristic lies in the range  $E_{con,m} \approx 0-2E_m$ . We will thus assume, approximately, that load current only flows in the working half-wave, and that (33) is also correct when  $E_{con,m} > E_m$ .\*

No matter what the control circuit condition, throughout the working half-wave

$$u_L = e - u_c \quad (14)$$

(15) remains true under our conditions, and since the total induction change must be zero we have

$$\int_0^\pi u_c d\theta = - \int_{\theta_1}^{\theta_2} u_c d\theta. \quad (35)$$

Thus

$$2\pi U_{L,av} = 2E_m + \int_{\theta_1}^{\theta_2} u_c d\theta. \quad (36)$$

\* If in some particular case  $r_{con}$  is close to  $r_L$ , then, as will be clear from what follows, there is no need to consider the state  $E_{con,m} > E_m$ .

(36), (29) and (33) taken together give the static input-output characteristic as

$$2\pi U_{L,av} = 2E_m - E_{ym} \tan \varphi_y \sin \psi \quad (37)$$

or in relative units

$$U_{L,av}^0 = 1 - 0.5 \tan \varphi \sin \psi E_{ym}^0. \quad (38)$$

The family of input-output characteristics drawn up in relative units from (38) in the parameter  $\varphi$  of (32) is shown in Fig. 9. These curves also relate the mean load current to the total voltage in the control circuit.

The computed characteristics are linear over the whole working range if the above assumptions hold, unlike the nonlinear transfer characteristics obtained with zero bias (Fig. 4).

If we take account of the load current drawn during the control half-wave when  $E_{con m}^0 > 1$  in (34) then, as of  $E_{con m}^0 = 1$ , the curves will be nonlinear. The dashed curves of Fig. 9 show (for three values of  $\varphi_{con}$ ) computed sections of the curves when  $E_{con m}^0 > 1$ , allowing for  $R_L$  conducting during the control period. As has been stated above, and will appear from the experimental results, this more exact and complex calculation with  $E_{con m}^0 > 1$  is not justified.

Voltage and power gains. An expression for the relative voltage gain is derived from (38):

$$k_u^0 = \pi \frac{\partial U_{L,av}}{\partial E_{ym}} = 0.5 \tan \varphi_y \sin \psi, \quad (39)$$

while the voltage gain when a sinusoidal a.c. control voltage is used is [1]

$$k_u = 0.5 k_u^0 \frac{W_L}{W_y} \quad (40)$$

Since  $\psi$  depends only on  $\varphi_{con}$ ,  $k_u^0$  also depends on  $\varphi_{con}$ . As the ratio of  $x_c$  to  $r_{con}$  falls the relative voltage gain also falls.

But, on the other hand, when the signal source internal resistance increases its maximum possible power output diminishes. Evidently only when there is some definite relation between  $r_{con}$  and  $x_c$  will the maximum possible power output be utilized and hence the power gain be maximal.

Let us consider this question, which is of great practical importance, in more detail. (23a) can be put as

$$k_p = 0.25 \frac{x_c}{r_L} 4 (k_u^0)^2 \frac{r_y}{x_c}. \quad (41)$$

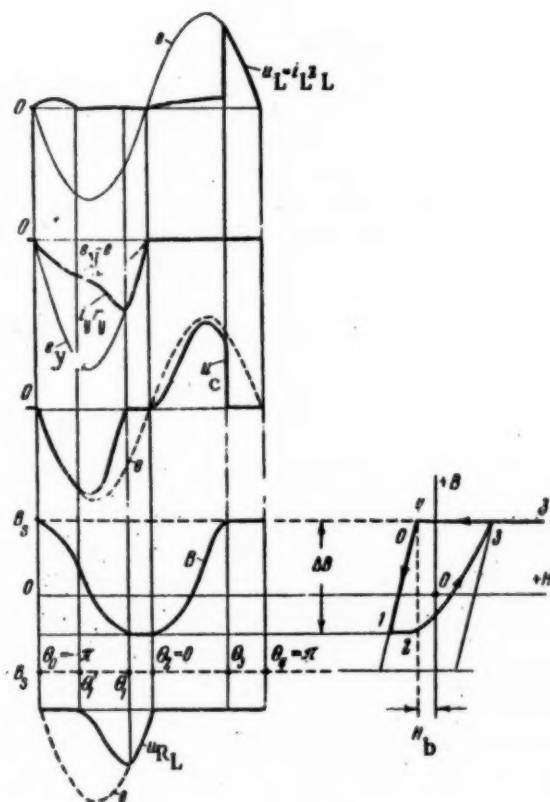


Fig. 8. As in Fig. 6, but with  $E_{con m}^0 > 1$ .

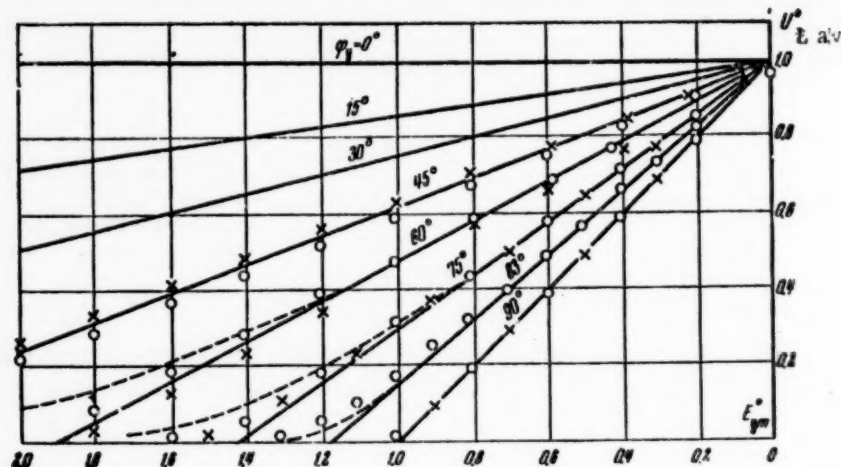


Fig. 9. As in Fig. 4, but with the idealized hysteresis loop of Fig. 2b and with a constant bias. The experimental points are: O)  $f = 500$  cycles/sec, x)  $f = 50$  cycles/sec.

The "relative power gain" is

$$k_p^0 = 4 (k_u^0)^2 \frac{r_y}{x_c} = \frac{4 (k_u^0)^2}{\tan \varphi_y}, \quad (42)$$

and it depends only on  $\varphi_{con}$ .

Figure 11 shows the relation of  $k_p^0$  to  $\varphi_{con}$ , whence it is clear that the optimum relation between  $r_{con}$  and  $x_c$  (from the point of view of power gain) occurs when  $\varphi_{con} \approx 60^\circ$ . Or in other words it occurs when

$$r_y \approx 0.6 x_c \quad (43)$$

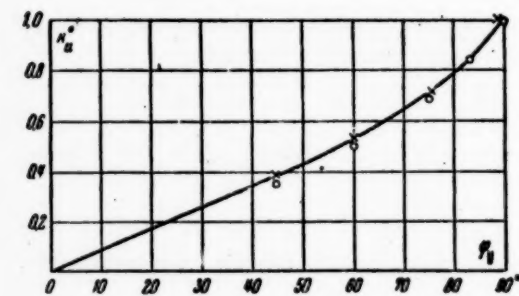


Fig. 10. Relation of the relative voltage gain to  $\varphi_{con}$  for the characteristic of Fig. 9. Experimental points: O)  $f = 500$  cycles/sec, x)  $f = 50$  cycles/sec.

and then

$$(k_p^0)_{max} \approx 0.63. \quad (44)$$

Correspondingly the optimum transfer characteristic (in the power gain sense) occurs when  $\varphi_{con} = 60^\circ$  (Fig. 9). The working range of  $E_{con,m}$  is from 0 -  $1.9 E_{mr}$ .

Thus  $x_c$  in (26) appears as it were an amplifier input impedance (referred). The optimum use of the signal source power will only occur when the source internal impedance matches the amplifier "input" impedance. (43) is the matching condition.

\* It will be shown below that (42) and (24) are completely analogous under definite conditions.

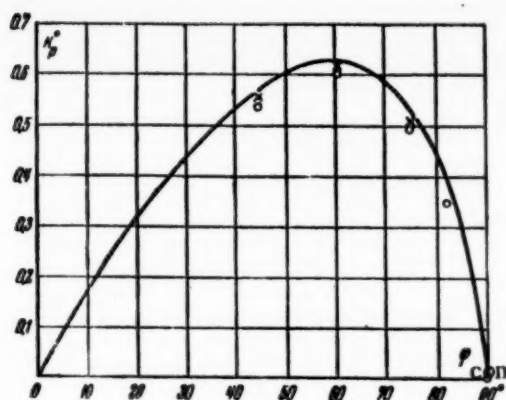


Fig. 11. Relation of the relative power gain to  $\varphi_{con}$  for the characteristics of Fig. 9. Experimental points; O)  $f = 500$  cycles/sec; x)  $f = 50$  cycles/sec.

and the power gain is

$$k_p = 0.25 (k_u^0)^2 \frac{4ry}{R_L} r^2 = 0.25 (k_u^0)^2 \frac{4ry}{r} \eta (1 - \eta). \quad (46)$$

The factor 0.25 corresponds to a half-wave output amplifier.

We now introduce the quality factor  $Q$  of the amplifier coil, defined as

$$Q = \frac{x_c}{r}. \quad (47)$$

$x_c$  and  $r$  are as before. When the hysteresis loop is rectangular (no bias used)  $x_c$  is determined by the averaged permeability

$$\mu_{av} = \frac{B_s}{H_c}, \quad (48)$$

corresponding to the magnetization curve for the core material shown dashed in Fig. 2a. When bias is used (Fig. 2b)  $x_c$  is defined by (26).

If no constant bias is used and  $E_m$  is made equal to the so-called saturation e.m.f.  $E_{sm}$  of the coil [1], then

$$I_c^0 = \frac{I_c r_y}{E_m} = \frac{I_c r_y}{E_{sm}} = \frac{r_y}{x_c} \quad (49)$$

and for  $k_p^0$  in (24) and  $k_p$  in (23b) we get, allowing for the potential drop coefficient,

$$k_p^0 = 4 (k_u^0)^2 \frac{r_y}{x_c}, \quad (50)$$

\* [Here and subsequently the 'R' has a line under it to distinguish it from the 'R' used earlier for the rectifier - editor's note.]

It can be shown that the static transfer characteristic remains unchanged when bias is used,  $\mu_d \neq \infty$  and  $R_{con}$  is absent.

The experimental data, which confirm the theoretical deductions completely, are given in the Appendix.

### 3. Relation Between the Amplifier Parameters, the Coil Dimensions and the Magnetic Properties of the Core.

So far when considering  $k_u$  and  $k_p$  we have taken  $r_L$  to be the resistance of the whole load circuit. We now assume that the load winding  $W_L$  has a resistance  $r$ , while the true load has a resistance  $R_L$ .\*

Then the potential drop coefficient is

$$\eta = \frac{R_L}{r_L} = \frac{R_L}{r + R_L}, \quad (45)$$



$$k_p = 0.25 k_p^0 \eta (1 - \eta) Q. \quad (51)$$

Thus when bias is used with the hysteresis loop of Fig. 2b (50) is the same as (42 and (51) as (46).

In practice the winding area available for the control coil is much less than that for the load coil. Also when the control and load windings do not need to be separate a separate control coil can usually be omitted, the necessary voltage gain being provided by autotransformer connection of the coil (Fig. 1c). So to an adequate accuracy we can assume that the whole winding area  $S_{cu}$  (copper cross section) is occupied by load winding. Then  $Q$  in (47) is that of the coil as a whole. On this assumption it is easy to derive an expression for  $Q$ :

$$Q = \omega \mu \gamma \frac{S_{st} S_{cu}}{l_{av} l_m} 10^{-8}, \quad (52)$$

where  $S_{st}$  and  $S_{cu}$  are the steel and copper cross-sections in  $\text{cm}^2$ ,  $l_{av}$  and  $l_m$  being the mean lengths in cm of a line of force and a turn on the coil respectively,  $\mu$  being the permeability  $\mu_{av}$  or  $\mu_d$  in gauss  $\text{cm a}^{-1}$ ,  $\gamma$  the specific conductivity of copper in  $\text{ohm}^{-1} \text{cm}^{-1}$ ,  $\omega$  the line frequency in  $\text{sec}^{-1}$ .

Substituting (52) into (51) the desired expression for the power gain in terms of the coil dimensions and magnetic properties of the core is obtained.

$k_p^0$  is defined by (24) or by (42) and (50), depending on the hysteresis loop approximation used when  $H_b$  is constant. In the first case  $k_p^0 \approx 1 - 3$  (Fig. 5) while in the second the maximum is  $k_p^0 \approx 0.63$  (Fig. 11).

$\eta (1 - \eta)$  has a maximum value of 0.25 when  $\eta = 0.5$ ; in other words  $k_p$  will be largest when the load winding resistance equals the load resistance. This evidently also corresponds to the maximum possible power output if we neglect the forward resistance of  $R_{con}$  and the inductive impedance of the saturated coil which are present in any real case. But when germanium plate rectifiers are used and the coefficient of rectangularity for the hysteresis loop is 0.85 or greater these factors have little effect. The inductance of the saturated coil may in any case be neglected at comparatively small coil sizes and low line frequencies, the  $Q$  of the coil being then much less than one.

With large coil sizes and high line frequencies, or, in other words, quite high potential power outputs it would seem impossible to fulfill the condition  $r = R_L$  ( $\eta = 50\%$ ) as a rule because of overheating  $W_L$  and also for reasons of economy. The potential drop factor is then about 0.75 - 0.9 and so  $\eta (1 - \eta) \approx 0.1 - 0.2$ .

The reason why power gain is determined by the  $Q$  of the coil from (51) can be explained as follows.  $x_c$  for an unsaturated coil is defined as the referred input impedance of the amplifier. The output impedance is determined by the resistance of  $W_L$ . So when input and output are matched  $k_p$  depends solely on  $Q$ .

The relation between the signal source internal impedance and the input impedance determines  $k_p^0$ . The relation between the output and load impedances determines  $\eta (1 - \eta)$ .

When bias is not used the nonlinearity of the transfer characteristic of Fig. 4 increases with the referred internal impedance of the signal source, more exactly with  $I_c^0 = r_{con}^0 / x_c$ . Thus it is difficult to assign a theoretical optimum value to  $I_c^0$ . In practice we can assume  $I_c^0$  to be between 0.6 and 1.0. The latter value implies that the referred internal impedance of the source must be about equal to  $x_c$  in (49).

(43) must be fulfilled when bias is used.\*

\* If  $r_{con} \approx r_L$  then in power amplification we must have  $r_{con} \ll x_c$ . But then  $\varphi_{con} \approx 90^\circ$  and the working section of the transfer characteristic scarcely goes beyond  $E_{conm}^0 \approx 1$ .



(51) and (52) are the starting-points for designing an amplifier of set power gain.

We must emphasize that  $k_p$  is proportional to the supply frequency, core permeability and the square of the linear dimensions of the coil. Other things being equal, the best coil design is one in which  $Q_{st} Q_{Cu} I_{av}^2 M$  is the largest ( $Q$  largest). But the shape of the core may influence its mean magnetic properties. Thus, for instance, if the ratio of the external to the internal diameter is increased in the toroidal core the magnetic properties may on the whole become poorer.

In conclusion, in relation to [2], we consider it useful to pause briefly on a comparative evaluation of the proposed amplifier.

#### 4. Comparison of the Proposed Amplifier with a Normal Magnetic Amplifier Containing an Internal Feedback Loop

One of the most important characteristics of a magnetic amplifier is its dynamic response  $D$  — the ratio of the power gain to some other parameter which uniquely defines the time-lag in the amplifier. When the amplifier can be considered as a first-order inertial link (with normal magnetic amplifier circuits working into a resistive load this is quite permissible) this parameter can be the time-constant, expressed in seconds or in cycles of the line frequency.

A certain expression for the dynamic response of a magnetic amplifier using internal feedback has been given [3], which can be put as

$$D = \frac{k_p}{\tau} \approx 2f \frac{x_c}{R_L} \eta^2. \quad (53)$$

This is true for a resistive load, an idealized hysteresis loop as in Fig. 2a, and the point on the transfer characteristic which is of maximum curvature if  $x_c \gg R_L$ .

The following expression has been given for  $D$  [4] for the case where the magnetization curve is approximated by sections of three straight lines without allowing for hysteresis (Fig. 2a, dashed), using an averaged transfer characteristic curvature for an amplifier with external feedback and with  $k_{fb} = 1$ , and for an amplifier with internal feedback:

$$D = 0,78 \times 2f \frac{x_c}{R_L} \eta^2. \quad (54)$$

In both expressions for  $D$  it must be emphasized that  $\tau$  only means the control-circuit time-constant, and the transient response in the a.c. circuit, which involves a time about equal to that of one cycle of supply\* is completely neglected.

In the amplifier considered here the transient duration is not greater than one half-wave when signal and supply voltages are in phase. In addition the transient response is quite different — the output does not rise exponentially (or approximately so) but merely shows a 'pure' half-cycle delay.

This makes it very difficult to compare the dynamic responses of this amplifier with those of normal ones.

None the less they can be evaluated roughly by comparing their power gains, supposing (extremely arbitrarily!) that in all cases the time-constants equal one quarter-period.

On this condition (53) and (54) give, after simple manipulations, the following expressions, in which the source impedance is assumed equal to that of the amplifier input;

\* It has been shown [5] that an amplifier with internal feedback may have a much longer transient duration because the a.c. winding is short-circuited in relation to the control circuit during part of the cycle.

$$k_p = \eta(1 - \eta) Q, \quad (53a)$$

$$k_p = 0,78 \eta(1 - \eta) Q. \quad (54a)$$

It is noteworthy that (53a) and (54a) have exactly the same form as (51).

(51) and (53a) were obtained, subject to condition that  $k_p^0$  is defined by (24), using identical approximations for the hysteresis loop and other identical assumptions, and so are quantitatively comparable.

As above,  $k_p^0$  is about 1-3. Taking the largest  $k_p^0$  as in (53a) we find that  $k_p$  for the present half-wave amplifier and the dynamic quality of an amplifier with internal feedback in practice do not differ.

But the complete arbitrariness of the comparison must be emphasized.

We must emphasize that the comparatively good dynamic response of this amplifier by no means exhausts its prominent advantages. Some of these latter are as follows.

1. The short rise-time is not dependent on the gain, mode of operation, etc. (in normal magnetic amplifiers inexact design and changes in the external conditions can materially alter the response time).
2. When supply and control voltages are in phase the delay is fixed at one-half-cycle of the supply. Thus this circuit can be used to produce various units for discrete counting and control [6].
3. The amplifier can be controlled with either d.c. or a.c. with no practical loss in gain.

It is thus naturally possible to amplify an amplitude-modulated signal which has a frequency and phase unrelated to those of the supply (with the usual restrictions applying to any amplifier operating at carrier frequency).\*

4. The design and layout of a half-wave amplifier are considerably simpler than those of a normal one.

A shortcoming in this design is that in some cases a half-wave rectified current passes through the load. But this can be obviated by combining two units as of Fig. 1 in various full-wave or two-phase circuits. This makes the design and layout more complex.

## 5. Conclusions

The results derived here, which are confirmed by experiment, establish practically important relations between signal source impedance and the inductive and resistive impedances of coil and load. These relations make it possible to match these quantities during design. It is shown that the coil inductance has to be determined in different ways depending on whether bias is used or not. It is also shown that the power gain in this amplifier can only be raised by increasing the core size and supply frequency (while maintaining the response time) unlike in ordinary amplifiers.

## APPENDIX

The experimental work was performed with a number of amplifiers designed in accordance with the circuits of Figs. 1a, b and c. In all cases the amplifier coil had a toroidal core made of N65P 0.15 mm strip, the saturation induction being  $B_s = 12,000$  gauss (in a field of to amp cm<sup>-1</sup>), the rectangularity coefficient being 0.85-0.9 and the coercive force (in a d.c. field) being  $H_c = 0.1$  amp cm<sup>-1</sup>. DG-Ts24 germanium diodes were used for  $R_{con}$  and  $R_L$ . The line frequencies used were 50 and 500 cycles/sec.

Figure 4 gives the experimental points on the transfer characteristic taken with zero bias and a.c. control for two cases:  $R_{con}$  absent and present.  $H_c$  was determined by experiment for one point of Fig. 4 (roughly the point  $I_c^0 = 0.4$ ,  $E_{con,m}^0 = 1$  - the central point in the family) in order to recompute the experimental data in relative units; subsequently this coercive force was assumed as theoretical for all other points in the family. This value of  $H_c$  was close to the  $H_c$  for the limiting dynamic hysteresis loop measured with an oscillograph;

\* In [2] it is erroneously asserted that this amplifier can only amplify signals of the same frequency as the supply.

e.g., for a core of outside diameter 46 mm, inside diameter 31 mm and radial width of 7 mm ( $l_{av} = 12$  cm,  $S_{st} = 0.5$  cm<sup>2</sup>) the computed  $H_C$  at 500 cycles/sec is 0.2 amp cm<sup>-1</sup>, while  $H_C$  measured on a cathode-ray oscillograph was 0.23 amp cm<sup>-1</sup>. The corresponding permeability value derived from (48) at  $B_s = B_r = 10^4$  gauss was  $\mu_C = 5 \times 10^4$  gauss amp<sup>-1</sup> cm.

The supply voltage was made close to  $E_{sm}$ . The internal impedance of the signal source was varied from  $r_{con\ min} \ll x_C$  to  $r_{con\ max} \sim x_C$ .

The experiments showed satisfactory agreement with theory. Removing  $R_{con}$  had practically no effect on the transfer characteristic.

Figure 9 gives the experimental points on the transfer characteristic when bias is used.  $H_b$  was chosen in accordance with Fig. 2, being  $H_b = 0.13$  amp cm<sup>-1</sup> when  $f = 500$  cycles/sec and  $H_b = 0.08$  amp cm<sup>-1</sup> when  $f = 50$  cycles/sec. The dynamic permeability was also determined at one point on the family of curves in Fig. 9 (at  $\varphi_{con} = 60^\circ$ ,  $E_{con.m}^0 = 1$ , the 'central' point) after which that value of  $\mu_d$  was taken as theoretical for all the other points. The theoretical  $\mu_d$  did not correspond with the slope of the 'vertical' sections of the limiting dynamic hysteresis loop observed on the oscillograph, e.g., for the core detailed above the 'theoretical'  $\mu_d$  was  $8 \times 10^4$  gauss amp<sup>-1</sup> cm when  $f = 500$  cycles/sec and  $21 \times 10^4$  gauss amp<sup>-1</sup> when  $f = 50$  cycles/sec. The slope of the 'vertical' sections gave in this case  $\mu_d = 14 \times 10^4$  gauss amp<sup>-1</sup> cm when  $f = 500$  cycles/sec, and  $40 \times 10^4$  gauss amp<sup>-1</sup> cm when  $f = 50$  cycles/sec.

The problem of the most rational method of determining  $\mu_C$ ,  $\mu_d$ ,  $H_C$  and  $B_s$  in order to approximate the loop in the cases dealt with here demands detailed study of the family of dynamic loops when d.c. and a.c. magnetization are used together, and forms the subject of a separate paper.

The experimental points in Figs. 9, 10 and 11 show quite good agreement with theory. As in the previous cases short-circuiting  $R_{con}$  left the output current (voltage) practically unchanged.

Received July 27, 1956

#### LITERATURE CITED

- [1] Lipman, R. A. and Negnevitsky, I. B. Theory of the half-wave magnetic amplifier. I. Automation and Remote Control, 18, No. 4, 1957. \*
- [2] Gorodetsky, A. B. Comparison of certain typical magnetic amplifier circuits using feedback. Automation and Remote Control, 17, No. 2, 1956. \*
- [3] Storm H. F. Theory of Magnetic Amplifiers with Square Loop Core Materials. Trans. AIEE, vol. 72, part I, 1953.
- [4] Rozenblat, M. A. Magnetic amplifiers. Radio technique, Vol. 8, No. 2, 1953.
- [5] Krabbe, U. The Residual Time-Constant of Self-Saturating Auto-Excited Transducers. Proc. Inst. Electr. Engrs., No. 3, 1956.
- [6] Ramey, R. A. The Single-Core Magnetic Amplifier as a Computer Element. Trans. AIEE, vol. 72, part I, 1953.

[See C. B. Translation].



# GRAPHICAL DETERMINATION OF THE ROTATION-INDUCED EMF IN SELSYN SYSTEMS

E. M. Sadovsky  
(Moscow)

The determination of the extra emfs induced in selsyn transformer circuits when the selsyns rotate at constant speed is considered. A nomogram which simplifies the graphical determination of this EMF and of the shift it produces in the zero position of selyn is presented.

The selsyns used in automatic control systems in most cases operate in transformer circuits such as of Fig. 1, in which selsyn 1 is a.c. excited, while the single-phase winding of selsyn 2 receives a voltage dependent on the mutual orientation of the selsyn rotors. This voltage  $E$  is reduced to zero in stationary selsyns of adequate accuracy when the difference between the rotor angles computed from the axis of the single-phase coil to the axis of phase I of the three-phase winding on the corresponding selsyn,  $\alpha_2 - \alpha_1 = 90^\circ$ . The position  $\alpha_2 - \alpha_1 = 90^\circ$  is therefore taken as 'zero' in Fig. 1, and the error angle  $\delta = (\alpha_2 - 90^\circ) - \alpha_1$  is computed with respect to this.

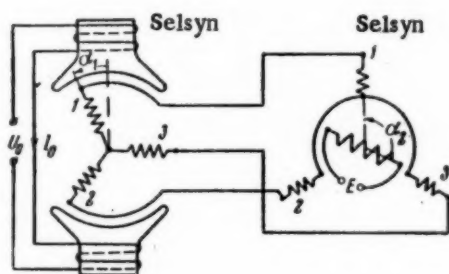


Fig. 1

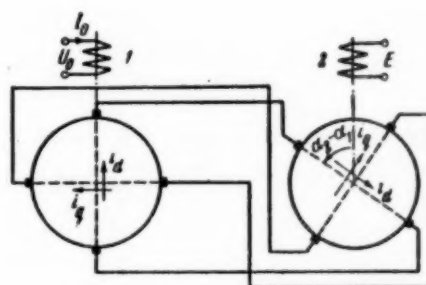


Fig. 2

When the selsyns rotate at the same speed a certain emf appears across the single-phase coil of selsyn 2 even when  $\delta = 0$ . This emf causes an undesirable displacement of the point of minimum  $E$  from the zero found with stationary selsyns [1-3]. This paper deals with a simplified graphical determination of this rotation-induced emf which demands the minimum amount of prior information.

In general, selsyns 1 and 2 of Fig. 1 are assumed nonidentical. Selsyn 1 can either have a uniform air-gap or a salient-pole single-phase winding, while the second can have a uniform air-gap and can frequently be of smaller size than the first. The single-phase coil current in selsyn 2 is taken as negligibly small, as is usually the case when the circuit works into the input of an electronic amplifier, etc.

To simplify the circuit analysis when salient-pole and nonidentical selsyns are used it is convenient to employ transforms of the currents in the three-phase windings which are known from the theory of synchronous machines, e.g., transformation of these currents to the direct and quadrature axes of the single-phase winding on selsyn 1 (cf [4, 5] etc), which corresponds to passing from Fig. 1 to the equivalent circuit of Fig. 2.



The equations for the  $d$  and  $q$  circuits in the equivalent scheme and for the circuits of the single-phase coils on selsyns 1 and 2 are quite simple. For steady-state modes using a.c. of angular frequency  $\omega_0$  the equations may be derived, for instance, directly from Fig. 2 by a published [6] method, in the form

$$\begin{aligned} U_0 &= (R + jx) I_0 + j \frac{3}{2} x_{01} i_d, \\ [(r_1 + r_2) + j(x_d + x_2)] i_d + \nu(x_q + x_2) i_q + jx_{01} I_0 &= 0, \\ [(r_1 + r_2) + j(x_q + x_2)] i_q - \nu(x_d + x_2) i_d - \nu x_{01} I_0 &= 0, \\ E &= -j \frac{3}{2} x_{02} [i_d \cos(\alpha_2 - \alpha_1) - i_q \sin(\alpha_2 - \alpha_1)], \end{aligned} \quad (1)$$

where  $j = \sqrt{-1}$ ,  $r_1$ ,  $x_d$ , and  $x_q$  are the phase resistances and the direct and quadrature inductive impedances of the three-phase winding on selsyn 1 (if selsyn 1 has a uniform air-gap  $x_q = x_d$ ),  $r_2$  and  $x_2$  being the resistance and inductive impedance of the three-phase winding on selsyn 2 (allowing for mutual coupling of phases),  $U_0$  and  $I_0$  are the voltage and current in the single-phase winding of selsyn 1,  $R$  and  $x$  being the resistance and inductive impedance of this winding,  $\nu = \omega/\omega_0$  being the relative angular velocity of the selsyns as a fraction of the synchronous speed,  $\omega_0$ ,  $x_{01}$  and  $x_{02}$  being the maximum mutual inductance impedances as between the single-phase and three-phase windings on selsyns 1 and 2 respectively.

Eliminating  $I_0$ ,  $i_d$  and  $i_q$  from (1), remembering that  $\alpha_2 - \alpha_1 = \delta + 90^\circ$ , we get the output emf  $E$  as

$$E = \frac{\frac{3}{2} x_{01} x_{02} U_0 [(a + jbc) \sin \delta + jva \cos \delta]}{\{a^2 + ja(x_d + x_q + 2x_2) - bc(x_d + x_2)\}(R + jx) + \frac{3}{2} x_{01}^2 (a + jbc)} \quad (2)$$

where

$$a = (r_1 + r_2), \quad b = x_q + x_2, \quad c = 1 - \nu^2.$$

With stationary selsyns ( $\nu = 0$ ) and  $\delta = 90^\circ$  this gives, in particular, the maximum emf:

$$E_m = \frac{3}{2} \frac{x_{01} x_{02} U_0}{[(r_1 + r_2) + j(x_d + x_2)](R + jx) + \frac{3}{2} x_{01}^2} \quad (3)$$

$E_m$  is most readily determined on the circuit of Fig. 1, and  $E$  in (2) is conveniently expressed in terms of  $E_m$ . As the selsyn speed does not usually exceed a few hundred rpm and even at 500 rpm ( $\omega = 52.5$  radians/sec) with a line frequency of 50 cycles/sec ( $\omega_0 = 314$  radians/sec)  $\nu^2 = \left(\frac{\omega}{\omega_0}\right)^2$  is only 0.028 and is negligible compared with unity in (2).  $\delta$  is also extremely small in a follow-up mode so to a high accuracy we may put  $\sin \delta \approx \delta$  and  $\cos \delta \approx 1$ .

Putting  $1 - \nu^2 \approx 1$ ,  $\sin \delta \approx \delta$ ,  $\cos \delta \approx 1$  in (2) and dividing the resultant expression by (3), elementary manipulations give

$$E = E_m \delta + \nu E_m \frac{j(r_1 + r_2)}{(r_1 + r_2) + j(x_q + x_2)} \quad (4)$$



The first term in (4) gives the normal 'transformer' emf for the circuit of Fig. 1, which is proportional to  $\delta$  when this is small, while the second gives the rotational emf which is proportional to  $\nu = \omega/\omega_0$ . At a given  $\omega$  the rotational emf decreases with  $r_1 + r_2$  (circuit of three-place windings in Fig. 1) and decreases as the line frequency  $f = \omega_0/2\pi$  increases.

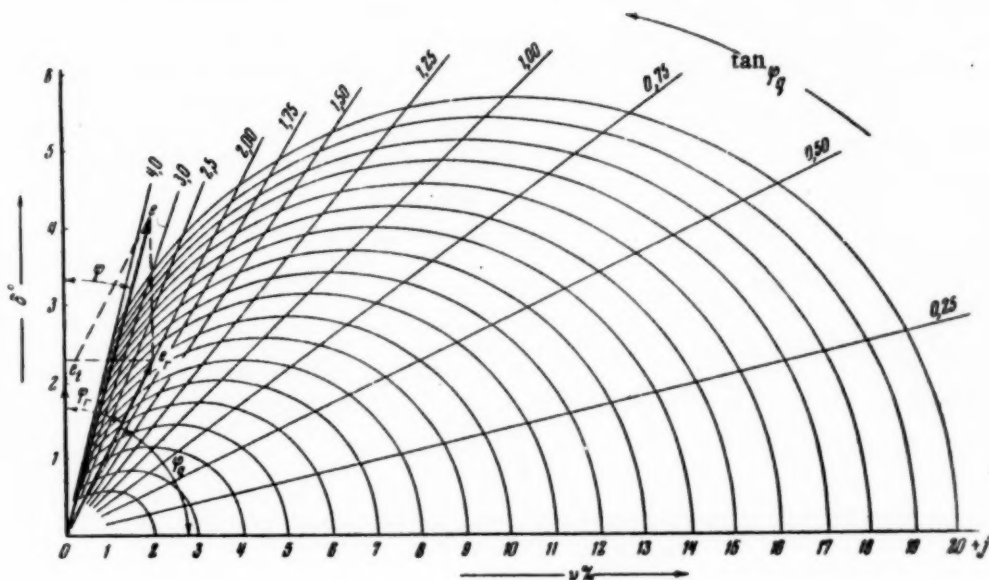


Fig. 3

By introducing the relative emf  $e = E/E_m$  and denoting the phase displacement of the quadrature selsyn currents by  $\varphi_q$ , such that

$$\tan \varphi_q = \frac{x_q + x_2}{r_1 + r_2}, \quad (5)$$

we get from (4) the simple relation

$$e = \delta + \frac{\nu}{\tan \varphi_q - j}, \quad (6)$$

in which only one selsyn circuit parameter  $\varphi_q$  enters, this being given by (5).

(6) enables us to draw up a simple nomogram for determining  $\underline{e}$ , and its components  $e_t = \delta$  and the rotational emf.

$$e_r = \frac{\nu}{\tan \varphi_q - j}. \quad (7)$$

The theory of loci (cf. [7], etc.) shows that when  $\varphi_q = \text{const}$  and  $\nu$  changes, the tip of the vector (7) moves along a straight line in the complex plane which passes through the origin at an angle  $\varphi_q$  to the imaginary axis, while when  $\tan \varphi_q$  changes and  $\nu = \text{const}$  it describes an arc of a circle of radius  $1/2 \nu$  with its center on the imaginary axis at the point  $1/2 j \nu$ . By drawing up a family of semicircles for various  $\nu$  (expressed and in per cent) and a family of straight lines for various values of  $\tan \varphi_q$ , we get the nomogram shown in Fig. 3. The vector

$e_r$  is then determined from the point where the circle of a given  $\nu$  intersects the corresponding line of given  $\tan \varphi_q$ . Figure 3 shows an example where  $\nu = 10\%$  and  $\tan \varphi_q = 2$ . Compounding vectors  $e_r$  and  $e_t = \delta$ , given by the vertical scale for the angle  $\delta^\circ$ , we get the total relative emf  $\underline{e}$  (In Fig. 3 this construction is shown for  $\delta = 2^\circ$ ). The angles  $\varphi_r$  and  $\varphi$  between  $e_r$  and  $\underline{e}$  and the real axis are then equal to the corresponding phase shifts of the emfs relative to  $E_m$ . In order to pass from  $e_r$  and  $\underline{e}$  to the actual emfs we need only multiply them by  $E_m$ .

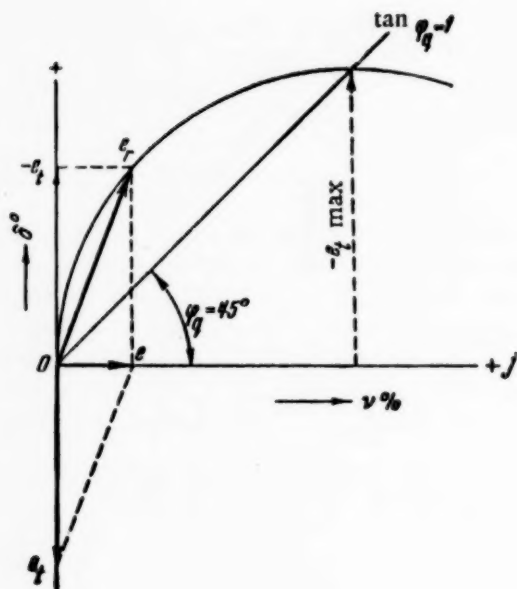


Fig. 4

Figure 3 shows, in particular, that with rotating selsyns ( $\nu \neq 0$ )  $\underline{e}$  is nonzero at all  $\delta$ . If solely the component  $E$ , in phase with  $E_m$ , is used for control purposes, as is frequently done, the selsyn zero corresponds to  $\underline{e}$  being directed exactly along the imaginary axis in the complex plane. Transforming (6) to the form

$$e = \delta + jv \cos \varphi_a e^{-j\varphi_a} \quad (8)$$

and equating the real part of  $\underline{e}$  to zero, to obtain a purely imaginary  $\underline{e}$ , we get

$$\delta + v \cos \varphi_g \sin \varphi_g = 0.$$

Hence since  $2 \sin \varphi_q \cos \varphi_q = \sin 2\varphi_q$ , we find that

$$\delta = -\frac{v}{2} \sin 2\varphi_q, \quad (9)$$

the zero of the circuit in Fig. 1 being displaced relative to that for nonrotating selsyns when the relative selsyn speeds are  $\nu$ . This velocity error is also computed from Fig. 3 — being the projection of  $e_r$  on the  $\delta^\circ$  axis with the sign reversed, and being read directly in degrees (when  $\nu = 10\%$  and  $\tan \varphi_q = 2$  the error is about  $-2.3^\circ$ , for instance). In fact if  $\underline{e}$  is to be made purely imaginary we must, as Fig. 4 shows, add to  $e_r$  a component  $e_t$  equal to the projection of  $e_r$  on the vertical axis but with the sign reversed. The zero shift at any given  $\nu$  is greater when  $\varphi_q = 45^\circ$ , i.e., when  $r_1 + r_2 = x_q + x_2$  (Fig. 4).

Figure 3 also enables one to determine the amplitudes and phases of the selsyn outputs at different angular errors and rotational speeds. Only  $E_m$  and  $\varphi_q$  need be known in order to carry out calculations with Fig. 3.  $E_m$  is measured directly and is known for normal types of selsyn, while  $\varphi_q$  can be determined in the usual way by current and power measurements made when two phases of the three-phase winding are fed from a known alternating voltage with both magnetic axes at  $90^\circ$  to the excitation axis (i.e., in the arrangement which gives the maximum current).  $E_m$  and  $\varphi_q$  can be determined once for each type of selsyn; the values found are suitable for all calculations. The resistances of the wires connecting the three-phase windings are included  $r_1 + r_2$ .

Received April 10, 1956

## LITERATURE CITED

- [1] Iosifyan, A.G. Theory of transformer operation of selsyns in thyatron synchronous power control circuits. Bulletin of the All-Union Power Institute, No. 9, 1940.

[2] Chestnut, H. Electrical Accuracy of Selsyn Generator-Control Transformer System. Electrical Engineering, August-September, 1946.

[3] Galteev, F. F. Study of the operation of transformer selsyns as relating to their use in servos. Trans. Moscow Power Inst. No. 15, State Power Press, 1955.

[4] Iosifyan, A. G. Linear transforms of currents in electrical machines. Bull. All-Union Power Inst., No. 8, 1940.

[5] Gruzov, L. N. Design of circuit characteristics for synchronous links using salient-pole single-phase selsyns. Trans VKAS, No. 21, 1949.

[6] Sadovsky, I. M. Simplified transforms in the theory of electrical machines. Bulletin of the Electrical Industry, No. 1, 1949.

[7] Gauffe, G. Loci in high-current engineering, ONTI, 1935.

THE UNIVERSITY OF CHICAGO PRESS

CHICAGO, ILLINOIS 60607

1997

1998

1999

2000

2001

2002

2003

2004

2005

2006

2007

2008

2009

2010

2011

2012

2013

2014

2015

2016

2017

# THE THEORY OF DERIVATIVE CONTROL IN THIRD-ORDER LINEAR SYSTEMS

G. A. Bendrikov and K. F. Teodorchik

(Moscow)

Control employing derivatives of a function of the error sometimes results in an increase in reserve stability and an improvement in servo properties. The mechanisms of these effects can be explained by tracing out the movements of the roots of the characteristic equation for the closed-loop system in the complex plane (of  $p$ ) as the coefficient to the first power of  $p$  changes continuously. This is carried out for a linear third-order equation below.

The characteristic equation for a linear third-order servo system is conveniently studied by reducing it to the 'normal' form [1, 2]:

$$p^3 + p^2 + \sigma p + \sigma_1 = 0. \quad (1)$$

This equation relates to a stable system if

$$\sigma - \sigma_1 > 0 \quad (2)$$

(condition of oscillatory stability) and

$$\sigma_1 > 0 \quad (3)$$

(condition of aperiodic stability).

When derivative control is used  $\sigma_1$  may be constant while  $\sigma$  varies continuously. The system remains stable while  $\sigma$  falls within the limits.

$$\sigma_1 \leq \sigma < \infty. \quad (4)$$

(2) shows that the beginning of this range corresponds to a pair of purely imaginary roots leaving the right semiplane of  $p$  for the imaginary axis. The roots of (1) with  $\sigma = \sigma_1$  will be

$$p_1 = -1 \text{ and } p_{2,3} = \pm i \sqrt{\sigma_1}. \quad (5)$$

Let us now determine what occurs at the ends of the range in (4). When  $\sigma \rightarrow \infty$  (1) may be written as

$$\left(p + \frac{\sigma_1}{\sigma}\right) \left\{ p^2 + \left(1 - \frac{\sigma_1}{\sigma}\right) p + \left[\sigma - \frac{\sigma_1}{\sigma} \left(1 - \frac{\sigma_1}{\sigma}\right)\right] \right\} + \left(\frac{\sigma_1}{\sigma}\right)^2 \left(1 - \frac{\sigma_1}{\sigma}\right) = 0. \quad (6)$$

This shows that as  $\sigma$  increases without limit the real root of (1) approaches zero as  $\frac{\sigma_1}{\sigma}$ . The other two roots are obtained from the quadratic derived from the expression in braces in (6).

So when  $\sigma \rightarrow \infty$  the roots of (1), no matter what the value of  $\sigma_1$  tend to

$$p_1 = 0, \quad p_{2,3} = -\frac{1}{2} \pm i\infty. \quad (7)$$

Hence the upper bound to the  $\sigma$  permitted by (4) corresponds to the system tending asymptotically to the boundary of aperiodic stability.

This shows that each value of  $\sigma_1$  and  $\sigma$  defined by the stability boundaries of (4) corresponds to a group of root trajectories in the  $p$ -plane, the system passing from the boundary of oscillatory stability to that of aperiodic stability.

To elucidate the possible trajectory types let us consider the case  $\sigma_1 = \frac{1}{27}$ , when (1) becomes

$$p^3 + p^2 + \sigma p + \frac{1}{27} = 0 \quad (8)$$

and within the stability limits  $\sigma$  can vary over the range

$$\frac{1}{27} \leq \sigma < \infty. \quad (9)$$

When  $\sigma = \frac{1}{27}$ , (8) has three roots:  $p_{1,2,3} = -\frac{1}{3}$ . Bearing in mind also the roots of (8) at the stability boundaries of (9) we get the following table

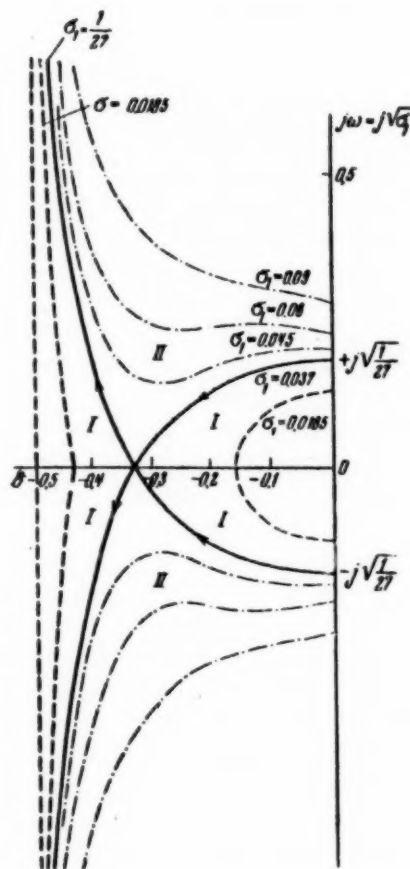
$$\begin{array}{l} \sigma_1 = \frac{1}{27} \\ \sigma = \frac{1}{27}, \quad p_1 = -1, \quad p_2 = +i\sqrt{\frac{1}{27}}, \quad p_3 = -i\sqrt{\frac{1}{27}} \\ \sigma = \frac{1}{3}, \quad p_1 = -\frac{1}{3}, \quad p_2 = -\frac{1}{3}, \quad p_3 = -\frac{1}{3} \\ \sigma = \infty, \quad p_1 = 0, \quad p_2 = -\frac{1}{2} + i\infty, \quad p_3 = -\frac{1}{2} - i\infty \end{array}$$

This table defines the way the roots vary in this case.

As  $\sigma$  increases within the limits set by (9) the real root moves to the right of the point  $-1$ . The complex conjugate root pair moves away from the imaginary axis to the left, approaching the real axis. All three coalesce into a triple root at the point  $-\frac{1}{3}$ . Subsequently one root continues to move to the right towards the origin, the others going over to a complex conjugate pair and approaching the values  $p_{2,3} = -\frac{1}{2} \pm i\infty$  asymptotically. The full lines in the Figure show the root trajectories for this case. It is readily seen that the trajectories of the complex roots of a third-order equation can only intersect with trajectories falling on the real axis. Bearing



this in mind we see that the trajectories for  $\sigma_1 = \frac{1}{27}$  divide the whole stable-state band [the  $(-1, 0)$  band] into two parts. Region I (see Figure) corresponds to  $0 < \sigma_1 < \frac{1}{27}$ , this being filled with type one trajectories. As  $\sigma$  increases in this region, within the limits set by (4), the complex root pair moves to the left and these two roots coalesce into a real double root (between 0 and  $-\frac{1}{3}$ ) on the real axis. Hence one real root moves to the origin while the other moves to the left, approaching the third real root which is moving to the right. These two roots meet at some point in the section  $(-\frac{1}{3}, -\frac{1}{2})$ , coalescing into a double root and then passing outwards as a complex conjugate pair along trajectories which approach the line  $\delta = -\frac{1}{2}$  asymptotically (dashed trajectories in Figure).



Trajectories of the roots of  $p^3 + p^2 + \sigma p + \sigma_1 = 0$  as  $\sigma$  changes continuously. The maximum stability  $S = \frac{1}{3}$  is found when  $\sigma = \frac{1}{3} + 3(\sigma_1 - \frac{1}{27})$ .

[2] Teodorchik, K. The trajectories of the roots of the characteristic equation of a third-order system as the free term changes continuously, and the maximum attainable stability in the system. *J. Tech. Phys.*, **18**, p. 1394, 1948.

[3] Bendrikov, G. and Teodorchik, K. The laws of root migration for third- and fourth-power linear algebraic equations as the free term changes continuously. *Automation and Remote Control*, **16**, No. 3, 1955.

Region II is filled by type two trajectories corresponding to  $\sigma_1 < \frac{1}{27}$ . In this region the complex conjugate roots move to the left and approach the line  $\delta = -\frac{1}{2}$  asymptotically without passing through the real axis. The real root moves continuously to the right from  $-1$  to the origin (see Figure, dot and dash trajectories).

This picture of the root motions clearly shows that the stabilizing action exerted by the derivatives in the control law in third-order systems exists when the complex-conjugate root-pair is closest to the real axis. The reserve in  $S$  is greatest when the complex-conjugate root-pair coalesces into a double root. In region I this reserve stability  $S < \frac{1}{3}$ , at all times and is lower the lower  $\sigma_1$ . In region II the maximum reserve,  $S = \frac{1}{3}$ , can always be attained.

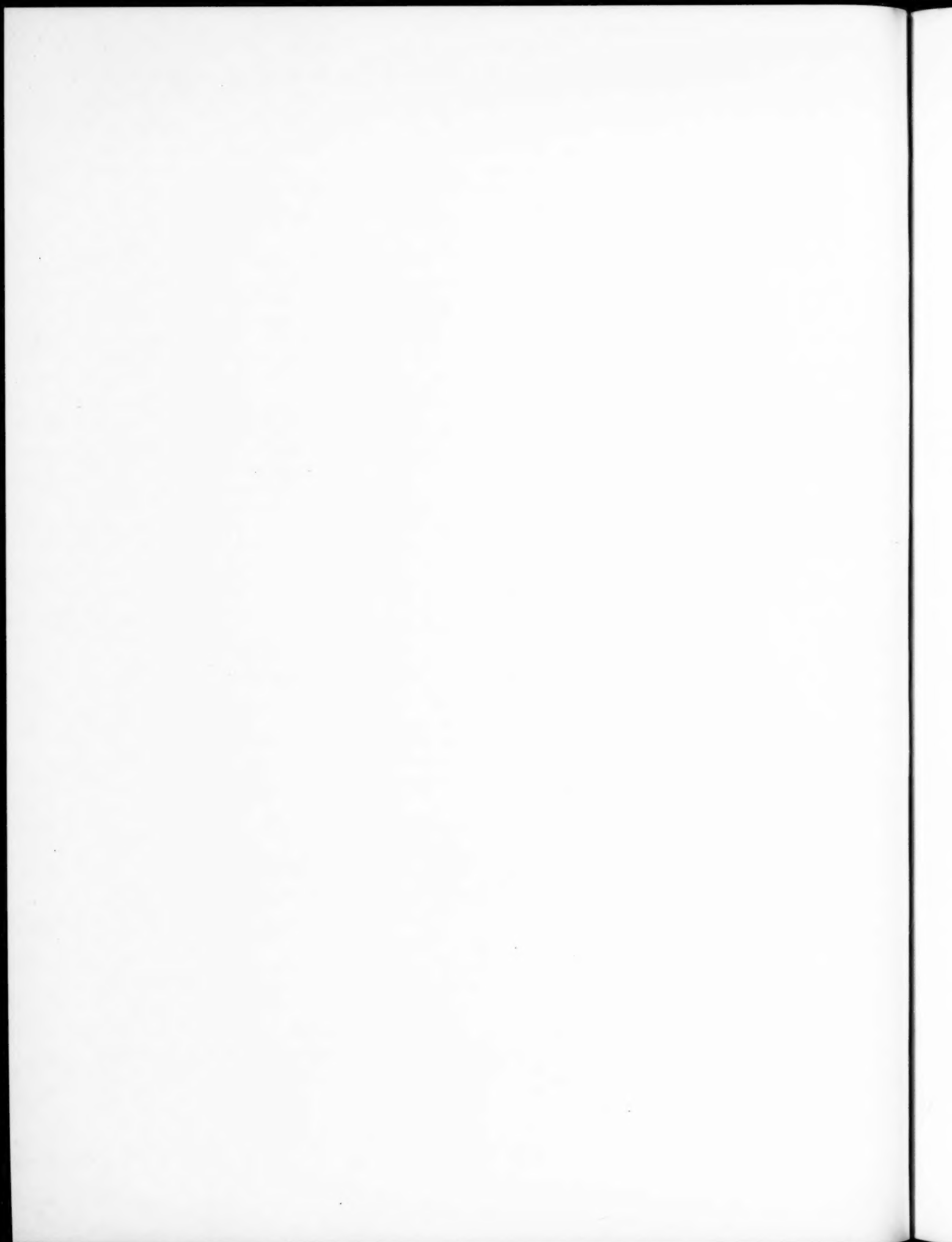
Also the stability region is left asymptotically when  $\sigma \rightarrow \infty$  if derivative control is used.

Comparison of our laws of root motion on  $\sigma$  varying with those derived earlier [2, 3] for  $\sigma_1$  variable shows that the directions of motion of all roots obtained with derivative control are always contrary to that with error control, and that control via error plus derivative enables one always to ensure any preset root arrangement for a closed third-order system.

Received February 16, 1956

#### LITERATURE CITED

[1] Teodorchik, K. An iteration method for solving the characteristic equation of a third-order system. *J. Tech. Phys.*, **19**, p. 231, 1949.



## BIBLIOGRAPHY

### TITLES OF SOVIET AND FOREIGN PAPERS ON AUTOMATIC CONTROL AND RELATED TOPICS IN 1955

#### I. GENERAL TOPICS

##### A. Cybernetics. Information Theory. General Communication Theory

- Vudvord, F. M. The theory of probability and information theory as applied to radar. Moscow, 'Soviet Radio', pp 128, Bibliography, p. 126.
- Kitov, A. Technical cybernetics. Radio, 1955, No. 11, pp. 42-44.
- Kolman, E. What is this cybernetics? Questions of philosophy, 1955, No. 4, pp. 148-160.
- Sigorskii, V. P. General four-terminal network theory. Kiev, Acad. Sci. Ukrain SSR Press, 1955, 315 pp. 209 figs., 297 references.
- Sobolev, S. L., Kitov, A. I. and Lyapunov, A. A. The basic features of cybernetics. Questions of philosophy, 1955, No. 4, pp. 136-148.
- Broida V. Un enseignement d'ensemble, de l'Automatisme et de la Regulation automatique est-il une nécessité? Mesures et controle industr., 1955, Fevr., 20 année, No. 213, p. 75-88, 9 fig.
- Grebe O. Die Bedeutung der Elektrotechnik für die Regelungstechnik. AEG Mitt., 1955, Bd. 45, Nr. 1-2, S. 3-11. 4 Abb. Bibliogr. 17.
- Harwood E. H. Introduction to Communication theory. Trans. South African Inst. Electr. Engrs., 1955, Aug., vol. 44, part. 8, p. 241-252.
- Herschberger W. D. Principles of Communications Systems. - N. Y., Prentice-Hall, 1955, 253 pp.
- Information theory. Widening Fields of Application Discussed at London Conference. Wireless World, 1955, Vol. 61, No. 11, p. 545-546.
- King, R. W. P. Transmission-line theory - N. Y., Mc Graw-Hill Book Co., 1955, 509 p.p.
- Luce R. D. Macy J., Christie L. S. Information flow in Task-Oriented Groups. - Mass. Inst. Technology - Research Laboratory of Electronics. Techn. Report, No. 264, 1955, Aug. 31, 95 p.p.
- McMillan Brockway. The Mathematics of Information Theory. JRE Convent. Rec., 1955, part 4, p. 48-51.
- Meyer-Eppler W. Grundlagen und Anwendungen der Informationstheorie. Berlin-Göttingen-Heidelberg, Springer, 1955.
- Rogge G. O. Personality Factors and Their Influence in Group Behaviours Questionnaire studies. Mass. Inst. Technology. Research Laboratory of Electronics. Tech. Report, No. 265, 1955, 31 Aug., 35 p.p.
- Tustin A. Cybernetics and all that. J. Instn. Electr. Engrs, 1955, Oct. vol. 1, No. 10, p. 634-635.
- Vickers G. Cybernetics and the management of men. Process Control and Automation, 1955, Nov., No. 11, p. 423-424.

##### B. History of Automation

- Aizerman, M. A. A review of the work of A. A. Andronov on automatic control. In the symposium in honor of A. A. Andronov, Moscow. Acad. Sci. USSR, 1955, pp 20-32.
- Gorelik, G. S. The work of A. A. Andronov on the theory of automatic control. In "Trans. 2nd All-Union conf. on the theory of automatic control", 1955, Vol. 1, pp. 51-62.
- Petrov, B. N., Popov, E. P., Voronov, A. A. and Khramoi, A. V. Development of the theory of automatic control in the USSR. In "Trans. 2nd All-Union Conf. on the theory of Automatic Control", 1955, Vol. 1, pp 12-50. Bibliography pp. 39-50.

- Piven, V. D. The work of I. N. Voznensky (corresponding member of the USSR Academy of Sciences) on automatic control. In "Trans. 2nd All-Union Conf. on the theory of automatic control, 1955", Vol. I, pp. 63-67.
- Roitenberg, Ya. N. The work of B. V. Bulgakov (corresponding member of the USSR Academy of Sciences) on the theory of automatic control. In "Trans. 2nd All-Union Conf. on the Theory of Automatic Control", 1955, Vol. I, pp. 68-75.
- Hrones J. A. A survey of some Recent Developments in the Automatic Control Field. Applied Mechanics Review, 1955, Dec., Vol. 8, No. 12, p. 501-504, Bibliogr. 10.
- Takahashi Y. and Oshima J. Der gegenwärtige Stand der selbsttätigen Regelung in Japan. Regelungstechnik, 1955, 3 Jg., H. 7, S. 161-166, 10 Abb. Bibliogr. 7.

### C. Terminology

- Blaum O. H. und Demlow R. Begriffe und Bezeichnungen der Regelungstechnik. AEG Mitt., 1955, Jg. 45, Nr 1-2, S. 22-33.
- Bönnhoff H. Begriffe der Regelungstechnik nach DIN 19226 und Systematik der Regler. Gaswärme, 1955, Jg. 4, Nr 3, S. 78-84.
- Mandelbrot B. Théorie du comportement. Une définition de la cybernétique, application linguistique. Revue générale des sciences pures et appliquées, 1955, t. 62, No. 9-10, p. 278-294. Bibliogr. p. 294.
- Wörterverzeichnisse der British Standards Institution. Regelungstechnik, 1955, 3 Jg. Nr 2, S. 49.

### D. Education

- Broida V., Demarles T. et Vivie J. La situation actuelle de l'enseignement de l'automatisme et de la régulation automatique en France et à l'étranger. Mesures et Contrôle Industr., 1955, Mars 20 année, No. 214, p. 171-178.

## II. CONFERENCE DATA

- Voronov, A. A. All-Leningrad seminar on the theory of automatic control (1953-4). Automation and remote control, 1955, 16, No. 3, pp. 300-305, 2 figs.
- All-Union Conf. on the Theory of Automatic Control, Trans. of 2nd. Moscow-Leningrad, USSR Acad. Sci., 1955, Vol. 1. Stability and hunt problems in the Theory of Automatic Control, 604 pp. Vol. 2. Problems of quality and dynamic accuracy in the Theory of Automatic Control, 536 pp. Vol. 3. Methods and apparatus for the experimental study of automatic control systems. Bibliography on the theory of automatic control and related topics, 352 pp.
- Resolution of the 2nd. All-Union Conf. on the Theory of Automatic Control, adopted. December 4th, 1953. In "Trans. 2nd. All-Union Conf. on the Theory of Automatic Control", 1955, Vol. 3, pp. 183-190.
- Conference on the theory of motional stability and of oscillations in mechanical systems, held by the Mechanics Institute of the USSR Acad. Sci., 24-28 May, 1955. Bull. Acad. Sci. USSR, Tech. Sci. Section, 1955, No. 7, pp. 151-152.
- Trapeznikov, V.A. The tasks of the 2nd All-Union Conf. on the Theory of Automatic Control. In "Trans. 2nd All-Union Conf. on the Theory of Automatic Control", 1955, Vol. 1, pp. 7-9.
- Fischbeck K. Internationale Ausstellung der Mess- und Regeltechnik in Philadelphia, 1954. Chemikerzeitung, 1955, Jg. 79, Nr 7, S. 223-226.
- Information Theory. Third London Symposium. (London, Sept. 1955). Nature, 1955, Oct. 22, vol. 176, No. 4486, p. 773-774.
- International Symposium on Modern Network Synthesis, April 13, 14, 15, 1955. N.Y. Trans IRE, 1955, vol. CT-2, No. 1, p. 106.
- Joint Conference on Automatic Control in the Process Industries. (London, Oct. 1955.) Instrument Practice, 1955, vol. 9, p. 870-889.
- Oetker R. Bericht über die 14. Tagung der Normen - Arbeitsgemeinschaft für Mess und Regeltechnik in der Chemischen Industrie. Regelungstechnik, 1955, Jg 3. Nr 6, S. 153-158.
- Sartorius H. Sitzung der VDJ-VDE - Fachausschusses "Regelungstechnik". Regelungstechnik, 1955, 3. Jg., Nr 4, S. 101.
- Sitzung des Beirates der VDJ-BDE - Fachgruppe Regelungstechnik. Regelungstechnik, 1955, Jg. 3, Nr 12, S. 313.

### III. BIBLIOGRAPHIES

- Vildt, E. O. and Lundsberg, R. S. Titles of Soviet and Foreign papers on automatic control and related control and related topics in 1954, *Automation and Remote Control*, 1956, 16, No. 3, pp. 306-316.
- Khramoi, A. V. Bibliography of papers on automatic control and related topics. In "Trans. 2nd All-Union Conf. on the Theory of Automatic Control", 1955, vol. 3, pp. 193-349.
- Behmenburg H. und Gressler H. Beispiel für den Aufbau eine. Dokumentationsstelle für die Mess-und Regelungs-technik. *Regelungstechnik*, 1955, 3 Jg., Nr. 1, S. 2-4, 2 Abb.
- Hunsinger W. *Regelungstechnik*. Z. Vereines dtsh. Ingr., 1955, Bd. 97, Nr 19-20, S. 657-662. Bibliogr. 243.
- Macmillan R. H. The Literature of Control Engineering. *Engineering*, 1955, June 3, No. 4662, p. 687, Bibliogr. 35.
- Regelungstechnik*. Ein universeller Wegweiser zur internationalen Buch-und Zeitschriften-literatur der Jahre 1952-54. München, Verlag Documentation der Technik, 1955, 243 Seiten.
- Veröffentlichungen der AEG aus dem Gebiet der Regelungstechnik. *AEG Mitt.*, 1955, Jan.-Feb., Jg., 45, Nr 1-2, S. 224-226.

### IV. THEORY OF AUTOMATIC CONTROL

- Abdullaev, A. A., Vaiser, I. V. and Nadzhafov, E. M. The equation of an 04 pneumatic regulator. *Automation and Remote Control*, 1955, 16, No. 5, pp. 431-453, 13 figs.
- Abramyan, Sh. G. Effect of automatic excitation control applied to synchronous generators on the dynamic stabilities of long-distance transmission lines. Author's abstract of dissertation for the degree of Candidate in Technical Sciences. Leningrad, 1955, 19 pp., (Leningrad Pedology Institute, USSR Ministry of Higher Education).
- Aizerman, M. A. and Smirnova, I. M. The use of 'small parameter' methods in studying hunting in automatic control systems. In the symposium in honor of A. A. Andronov. Moscow, USSR Acad. Sci., 1955, pp. 77-92.
- Aizerman, M. A. The determination of periodic modes in automatic control systems. In "Trans. 2nd. All-Union Conf. on the Theory of Automatic Control", 1955, vol. 1, pp. 105-130.
- Akselrod, Z. M. Study of the effects of parameter changes on the period and amplitude of balance oscillations for a discharge regulator with obstructed input. In "Precision Mechanics Equipment", Moscow-Leningrad, State Machine Press, 1955, pp. 49-63, 10 figs., 1 tabl., 3 references.
- Alekseev, A. S. A bistable temperature controller using anticipation. Author's abstract of dissertation for the degree of candidate in physico-mathematical sciences, Gorky, 1955, 4 pp. (Gorky State University, Faculty of Radiophysics).
- Aminov, M. Sh. One method of deriving the sufficient conditions for non-steady-state motion to be stable. *Appl. Math. and Mech.*, 1955, 19, No. 5, pp. 621-622. 3 references.
- Andronov, A. A. and Bautin, N. N. Effect of coulomb friction in the slide valve on an indirect control process. *Bull. Acad. Sci. USSR, Tech. Sci. Section*, 1955, No. 7, pp. 34-48. 11 figs., 1 reference.
- Anisimov, I. V. Determination of the dynamic characteristics of automatic control systems using production units and regulators. *Chemical Industry*, 1955, No. 7, pp. 24-30, 8 figs., 10 references.
- Artemenko, V. I. Control of commutator servomotor speeds using magnetic amplifiers. Author's abstract of dissertation for the degree of candidate in technical sciences. Moscow, 1955, 16 pp. (Moscow Power Institute).
- Arkhangelsky, B. I. Rise in generator voltage on switching on the excitation, voltage regulator action allowed for. *Bull. Leningrad Electrical Engineering Institute*, 1955, No. 27, pp. 50-55.
- Afanasyev, K. I. Theory of tractor motor control by varying the cycling. Author's abstract of dissertation for the degree of candidate in technical sciences. Tashkent, 1955, 15 pp. (Ministry of Higher Technical Education).
- Baranchuk, E. I. The theory of multivariable servo systems. In "Trans. 2nd All-Union Conf. on the Theory of Automatic Control", 1955, vol. 1, pp. 501-520. 9 figs., 22 references.
- Barbashin, A. V. A method of computing the transient responses of synchronous propulsion motors fed from synchronous generators of comparable power where frequency control is used. In "Bull. Leningrad Electrical Engineering Institute", 1955, No. 27, pp. 55-56, 9 figs.
- Bashkirov, D. A. A method of deriving the transient responses in nonlinear automatic control systems. In "Trans. 2nd. All-Union Conf. on the Theory of Automatic Control", 1955, vol. 2, pp. 82-95, 5 figs., 4 references.
- Beirakh, Z. Ya. Theory of control of boiler units. In "Trans. 2nd. All-Union Conf. on the Theory of Automatic Control", 1955, vol. 1, pp. 521-542, 18 figs.



- Beirakh, Z. Ya. Some problems in the theory and technology of self-regulating boiler units. In "Jubilee scientific research session (Bauman Higher Technical, Moscow - 1830-1955). Summaries of reports. Moscow, State Machine Press, 1955, pp. 10-11.
- Berezkin, E. N. Some problems of stability in the theory of automatic control. Author's abstract of dissertation for the degree of candidate in Physico mathematical sciences. Moscow, 1955, 4 pp., (Lomonosov State University).
- Bernett, J. R. and Keprall, P. E. Linear correcting unit for saturating servo mechanisms. In "Machine design", 1955, No. 10, pp. 3-12, 12 figs, 3 references.
- Bernshtein, S. I. Theory of vibration regulators for electric machines. In "Trans. 2nd. All-Union Conf. on the Theory of Automatic Control", 1955, vol. 1, pp. 439-458, 19 figs., 17 references.
- Burford, T. M., Rideout, V. C. and Sather, D. S. Use of correlation functions for studying servomechanisms. In "Machine design", 1955, No. 11, pp. 3-14, 8 figs. 25 references.
- Biernson, G. A way of rapidly deriving the poles in the closed-loop transfer function for an automatic control system. In "Machine design", 1955, No. 1, pp. 5-44, 20 figs. 6 references.
- Blekhman, I. P. and Dzhanelidze, G. Yu. Dynamics of the Buass-Sardu regulator. Bull. Acad. Sci. USSR, Tech. Sci. Section, 1955, No. 10, pp. 48-59, 3 figs., 5 references.
- Blokh, Z. Sh. Some calculations of control quality from frequency responses, Automation and Remote Control, 1955, 16, No. 3, pp. 258-268, 6 figs., 8 references.
- Blokh, Z. Sh. Computation of controller parameters to meet set control requirements. In "Trans. 2nd. All-Union Conf. on the Theory of Automatic Control", 1955, vol. 2, pp. 117-144, 5 figs., 6 references.
- Bogolyubov, V. E. and Dyatlov, V. L. A method of multiple phase planes for dealing with processes in non-linear systems. In "Trans. All-Union Concealed Energy Institute", No. 5. Electrical Engineering. Moscow, 1955, pp. 16-34, 5 figs., 4 references.
- Bogolyubov, V. E. Transients in premagnetized ferroresonant circuits. Author's abstract of dissertation for the degree of doctor of technical sciences. Moscow, 1955, 31 pp. (Molotov Power Institute, Moscow).
- Bodner, V. A., Ryazanov, Yu. A. and Kalpin, V. M. Theoretical and experimental dynamic studies on (Tachometer-rectifier motor) (TVD) control systems employing differential reduction gear. In "Symp. No. 20 on the control of aircraft engines (No. 3)". Moscow, State Defense Press, 1955, pp. 5-58, 33 figs., 4 references.
- Bolotin, V. V. The errors in certain papers on dynamic stability. Bull. Acad. Sci. Section, 1955, No. 11, pp. 144-147, 1 fig., 10 references.
- Bulgakov, A. A. Frequency control of asynchronous motors. Moscow, USSR Acad. Sci., 1955, 216 pps. plus illustrations (Institute of Automatic and Remote Control USSR Academy of Sciences).
- Bulgakov, N. G. Oscillations in Quasilinear automatic systems with many degrees of freedom and the non-analytic character of the nonlinearity. Appl. Math. and Mech., 1955, 19, pp. 265-272.
- Bulgakov, N. G. Periodic Oscillations in quasilinear automatic systems with many degrees of freedom. Author's abstract of dissertation for the degree of candidate in physicomathematical sciences. Sverdlovsk, 1955, 8 pp. (Gorky State University, Urals).
- Vaiser, I. V. Remarks on the use of the concept 'degree of stability' for designing control processes. Automation and Remote Control, 1955, 16, No. 5, pp. 481-482. 1 reference.
- Venikov, V. A. Transient analysis in electrical systems using the Gorev-Park equation, Moscow, 1955, 71 pp. (All-Union Concealed Energy Institute, No. 1).
- Vitenberg, I. M. Methods of designing functional units for nonlinear electrical analogs developed by the Design Office of the USSR Ministry of Machine and Equipment Construction. In "Trans. 2nd. All-Union Conf. on the theory of Automatic Control", 1955, vol. 3, pp. 75-84, 16 figs.
- Voronov, A. A. Methods of deriving transients from frequency characteristics and vice versa. In "Trans. 2nd. All-Union Conf. on the Theory of Automatic Control", 1955, vol. 2, pp. 41-52, 2 figs. References pp. 51-2.
- Galteev, F. F. Study of telemetering and servo systems in the electrical equipment of aircraft and guided missiles. Chapter 1. Moscow, Molotov Power Institute, 1955, 68 pp.
- Galteev, F. F. Study of the operating modes of selsyn transformers as applied to their use in servo systems. Trans. Moscow Power Inst., 1955, No. 15, pp. 76-102.
- Galperin, I. I. Development of the theory of structural stability and of structural design. In "Trans. 2nd. All-Union Conf. on the Theory of Automatic Control", 1955, vol. 1, pp. 313-314, 4 references.



- Gantmakher, F. R. The structural stability of a single-loop automatic control system using derivative control. In "Trans. 2nd. All-Union Conf. on the Theory of Automatic Control", 1955, vol. 1, pp. 315-323, 5 references.
- Getsov, L. N. The control stability of a turbine-propeller motor using differential reduction gear. In "Symp. of papers No. 20 on the control of aircraft engines (No. 30". Moscow, State Defense Press, 1955, pp. 59-96, 7 figs.
- Ginzburg, A. A. Electromechanical units reproducing the functions of a complex variable (applied to automatic control systems). In "Trans. 2nd. All-Union Conf. on the Theory of Automatic Control", 1955, vol. 3, pp. 130-139, 9 figs.
- Goldich, Yu. L. Some problems of self-oscillation in relay automatic control systems. Author's abstract of dissertation for the degree of candidate in technical sciences, Leningrad, 1955. 9 pp. (Leningrad Polytechnical Institute).
- Goldfarb, L. S. A method of studying nonlinear control systems based on the principle of harmonic balance. In "Trans. 2nd. All-Union Conf. on the Theory of Automatic Control", 1955, vol. 1, pp. 177-192, 9 figs, 7 references.
- Gornshtein, V. M. Some ways of increasing the stabilities of power systems with 'weak' links. Electricity, 1955, No. 5, pp. 27-31, 4 figs., 5 references.
- Goryainov, F. A. and Tokarev, B. F. Effect of magnetic assymetry on the operation of a three-step electromagnetic amplifier, Electricity, 1955, No. 11, pp. 43-46, 5 figs.
- Goryainov, F. A. and Gusev, B. Ya. Study of a two-step amplidyne longitudinal field regulator. Trans. Moscow Power Institute, 1955, No. 15, pp. 55-66.
- Gritskov, V. I. and Kozuychenko, Yu. V. The dynamic characteristics of the IR-130 isodrome regulator. Papers from the student scientific society, Moscow Power Institute, Moscow 1955, pp. 3-18.
- Guzenko, A. I. Study of the stabilities and performance of certain automatic control systems using parallel correcting units. In 'some problems in the theory of automatic control. A collection of papers', Moscow, State Defence Press, 1955, pp. 52-62, 7 figs., 2 references.
- Guzenko, A. I. Derivation of circuit parameters for local feedback using single-stage RC circuits. In 'Some problems in the theory of automatic control. A collection of papers'. Moscow, State Defense Press, 1955, pp. 63-86, 11 figs.
- Demchenko, O. N. Derivation of frequency characteristics for automatic control systems using Mikhailov's curves. Proc. Acad. Sci. USSR, 100, No. 4, pp. 693-696, 1 fig., 3 references.
- Dmitriev, V. N. Experimental and theoretical study of nozzle-piston pneumatic relays. Author's abstract of dissertation for the degree of candidate in technical sciences, Moscow, 1955, 10 pp.
- Dogolenko, Yu. V. 'Sliding' modes in relay indirect control systems. Author's abstract of dissertation for the degree of doctor of technical sciences. Leningrad, 1955, 19 pp. (Kalinin Polytechnical Institute, Leningrad).
- Dogolenko, Yu. V. 'Sliding' modes in relay indirect control systems. In 'Trans. 2nd. All-Union Conf. on the Theory of Automatic Control' 1955, vol. 1, pp. 421-438, 7 references.
- Drozdof, Yu. M. Forced vibrations in nonlinear almost conservative systems with one degree of freedom. Appl. Mathem. and Mech., 1955, 19, No. 1, pp. 33-40.
- Dub, Ya. T. The automatic metering and control of water efflux from small irrigation canal systems. Author's abstract of dissertation for the degree of candidate in technical sciences. Lvov, 1956, 18 pp. (Lvov Polytechnical Institute).
- Dudnikov, E. G. Study of control performance from the experimental dynamic characteristics of system elements. Trans. 2nd. All-Union Conf. on the Theory of Automatic Control, 1956, vol. 2, pp. 500-513, references pp. 512-513.
- Dudnikov, E. G. Methods of determining the optimum settings for industrial control systems from the experimental dynamic characteristics. In 'Automation of production processes'. Moscow, USSR Acad. Sci., 1955, pp. 13-28, 14 figs., 7 references. (Institute of Automation and Remote Control).
- Dudnikova, I. P. A graphical analytic method of determining regulator settings from the frequency characteristics of the controlled sections. Thermal Power, 1955, No. 6, pp. 28-32, 4 figs., 4 references.
- Egorov, K. V. Fundamentals of automatic control (Students manuals on electrical and power engineering) Moscow-Leningrad, State Power Press, 1955, 456 pp. 355 figs., 74 references.
- Ergin, N. P. Qualitative methods in stability theory. Appl. Mathem. and Mech., 1955, 19, No. 5, pp. 599-616, 35 references.
- Ergin, N. P. A general method of solving stability problems. In 'Trans. 2nd. All-Union Conf. on the Theory of Automatic Control' 1955, vol. 1, pp. 133-141, Bibliography pp. 140-141.

- Zalmanzon, L. A. Self-oscillations in pneumatic regulator systems containing closed chambers. In 'Trans. 2nd. All-Union Conf. on the Theory of Automatic Control', 1955, vol. 1, pp. 266-298, 24 figs., 9 refs.
- Zalmanzon, L. A. Allowing for the effects on the control processes of nonlinear characteristics in closed chambers in pneumatic control systems. *Automation and Remote Control*, 1955, 16, No. 6, 454-461, 5 figs., 4 refs.
- Zubov, V. I. The theory of Lyapunov's second method: derivation of a general solution in the region of asymptotic stability. *Appl. Mathem. and Mech.*, 1955, No. 2, pp. 179-210.
- Ivanenko, A. G. Determination of optimum values for the adjustable parameters in combined control systems by an inverse method (calculation by parts). In 'Trans. 2nd. All-Union Conf. on the Theory of Automatic Control', 1955, vol. 2, pp. 208-232, 7 figs., 12 refs.
- Ivanenko, A. G. The use of invariance conditions in automatic control systems having limited effector powers. *Proc. Acad. Sci. Ukrain. SSR*, 1955, No. 5, pp. 429-434, 3 figs., 3 refs.
- Idelson, I. I. A method of investigating servo systems subject to noise in the sensing elements. *Trans. 2nd. All-Union Conf. on the Theory of Automatic Control*, 1955, vol. 2, pp. 457-471, 2 figs., 2 refs.
- Kagan, B. M. A frequency method of deriving and studying transients in nonlinear automatic control systems. In 'Trans. 2nd. All-Union Conf. on the Theory of Automatic Control', 1955, vol. 2, pp. 62-81, 16 figs., 7 refs.
- Kazakevich, V. V. Theory of multistage dynamic systems: its application to automatic control systems. In 'Trans. 2nd. All-Union Conf. on the Theory of Automatic Control', 1955, vol. 1, p. 386.
- Kalish, G. G. Quantitative calculation of process convergence and resonance phenomena in the automatic control of internal combustion engines from Vyshnegradsky's diagram. In 'Trans. 2nd. All-Union Conf. on the Theory of Automatic Control', 1955, vol. 1, pp. 567-573, 3 figs., 5 refs.
- Kampe-Nemm, A. A. Dynamic of two-position control. Moscow-Leningrad State Power Press, 1955, 935 pp. plus graphs, 33 refs.
- Kampe-Nemm, A. A. Dynamics of a three-position temperature control. *Thermal Power*, 1955, No. 6, pp. 33-37, 8 figs.
- Karabanov, V. A. Some ways of using the frequency method for analyzing linear dynamic system with variable parameters. In 'Some problems in the theory of automatic control systems', Moscow, State Defense Press, 1955, pp. 37-51, 9 refs.
- Karandeev, K. B. and Sinitsky, L. A. One method of deriving the transients in circuits containing conditionally nonlinear elements. *Automation and Remote Control*, 1955, 15, No. 5, pp. 483-487, 3 refs.
- Karandeev, K. B. and Sinitsky, L. A. Derivation of transients in d.c. circuits containing conditionally nonlinear elements. *Proc. Lvov Polytech. Inst.*, 1955, 1, No. 1, pp. 108-111.
- Karnyushin, L. V. The equations and methods of study for the stabilities of systems which control oil-well drilling automatically. Scientific reports of Lvov Polytech. Inst., No. 34, Electrical Engineering series, No. 8. Lvov. University, 1955, pp. 205-232, 4 figs., 16 refs.
- Kats, A. M. Forced oscillations in nonlinear almost conservative systems with one degree of freedom. *Appl. Mathem. and Mech.*, 1955, 19, No. 1, pp. 13-32.
- Kats, A. M. Derivation of the regulator parameters from the characteristic equation of the control system. *Automation and Remote Control*, 1955, 16, No. 13, pp. 269-272, 1 fig., 1 ref.
- Kacherovsky, V. M. Automatic speed control of a skip hoist during skip emptying using an asynchronous motor. Author's abstract of dissertation for the degree of candidate in technical sciences. Kharkov, 1955, 18 pp. (Kharkov Mining Institute).
- Kislov, B. P. Derivation of the stability region and lines of equal reserve in phase and amplitude for automatic control systems using nomogram methods. *Automation and Remote Control*, 1955, 16, No. 6, pp. 508-529, 3 refs.
- Kitsev, B. I., Lomankin, L. M. and Madison, V. G. Stability conditions for fast automatic control systems. In 'Trans. Urals Polytech. Inst.' 1955, Symp. 53, pp. 61-64, 5 figs.
- Klovsky, D. D. An approximate graphical method of deriving the frequency characteristics of linear systems from their transient characteristics. *J. Tech. Phys.*, 1955, 25, No. 2, pp. 333-338, 5 figs., 2 refs.
- Kozhevnikov, K. I. Selection of characteristics for an automatic excitation regulator for use with synchronous motors subject to variable load. In 'Trans. All-Union Power Institute', 1955, No. 6, pp. 66-80, 5 figs.
- Kononenko, V. O. Oscillation in nonlinear systems with many degrees of freedom. *Proc. Acad. Sci. USSR*, 105, No. 4, pp. 664-667, 4 refs.

- Kornilov, Yu. G. Automatic control systems for boiler assemblies. Author's abstract of dissertation for the degree of doctor in technical sciences, Kiev, 1955, 24 pp. (Kiev Polytech. Inst.).
- Kornilov, Yu. G. Theory of 'sliding' modes in relay automatic control systems. In 'Trans. 2nd. All-Union Conf. on the Theory of Automatic Control', 1955, vol. 1, p. 459.
- Korobochkin, B. L. Study of the hydraulic follower systems on copying machines. Author's abstract of dissertation for the degree of candidate in technical sciences, Moscow, 1955, 11 pp. (Stalin machine-tool Institute, Moscow).
- Krassov, I. M. and Barkalov, P. T. Determination of the dynamic responses of regulators and loads to slowly changing actions. In "Automation of production processes", Moscow, Acad. Sci., Moscow, 1955, pp. 68-80. 16 figs., 4 refs. (Institute of Automation and Remote Control).
- Krassovsky, A. A. Some problems in the design of automatic control systems via the transient function method. In 'Trans. 2nd. All-Union Conf. on the Theory of Automatic Control', 1955, vol. 2, pp. 105-116, 8 figs., 2 refs.
- Krassovsky, N. N. Stability in a first approximation. Appl. Mathem. and Mechan., 1955, 19, No. 5, pp. 516-530, 1 fig., 11 refs.
- Krinetsky, I. I. Simplified computations for certain nonlinear systems. In 'Trans. 2nd. All-Union Conf. on the Theory of Automatic Control', 1955, vol. 1, pp. 299-308, 6 figs., 2 refs.
- Kryzhanovsky, O. M. The selection of parameters for a control system described by a linear differential equation with constant coefficients. Proc. Acad. Sci. Ukrain. SSR, 1955, No. 1, pp. 26-31, 2 refs.
- Kryzhanovsky, O. M. Derivations of the regions for the coefficient values in the differential equation at the boundary of the maximum natural frequencies in a control system. Proc. Acad. Sci. Ukrain. SSR, 1955, No. 4, pp. 328-332, 2 figs., 12 refs.
- Krug, G. K. The influence of nonlinearities on the response of a servo unit. In 'Trans. 2nd. All-Union Conf. on the Theory of Automatic Control', 1955, vol. 1, pp. 251-265, 14 figs., 3 refs.
- Krug, E. K. and Minina, O. M. Studies of the dynamic properties of nonlinear systems each with an unstable link. Automation and Remote Control, 1955, 16, No. 1, pp. 43-46, 4 figs., 3 refs.
- Kuzovkov (reviewer), Bruns, R. A. and Saunders, R. M. Analysis of feedback control systems, N. Y., McGraw Hill, 1955, 383 pp. 'New Books from Abroad', 1955, No. 12, pp. 34-37.
- Kuzmichev, G. M. Electrical analog studies of electromechanical servo systems. Papers from the student scientific society (Penza industrial Institute). Penza, 1955, pp. 29-66, 36 refs.
- Kulagen, A. V. Analysis of general throttle-controlled hydraulic transmission designs, and selection of the most rational design. Author's abstract of dissertation for the degree of candidate in technical sciences, Moscow, 1955, 7 pp. (Moscow Higher Technical College).
- Kulebakin, K. I. Fundamental problems and basic methods in improving response in automatic control systems. In 'Trans. 2nd. All-Union Conf. on the Theory of Automatic Control', 1955, vol. 2, pp. 184-207, 13 figs., bibliography p. 207.
- Kurakin, K. I. Response criteria and their use in choosing optimum response in linear automatic control systems. In 'Trans. 2nd. All-Union Conf. on the Theory of Automatic Control', 1955, vol. 2, pp. 442-456, 11 figs., 10 refs.
- Kurakin, K. I. The choice of optimum differentiator characteristics for automatic control systems. Automation and Remote Control, 1955, 16, No. 3, pp. 293-299, 8 refs.
- Kukhtenko, A. I. Analysis of nonholonomic control system dynamics as regards the automatic controls of boring machines and combines. In 'Trans. 2nd. All-Union Conf. on the Theory of Automatic Control', 1955, vol. 2, pp. 487-499, 6 figs. Bibliography p. 499.
- Kukhtenko, A. I. One type of mechanism with nonholonomic linkages. Trans. Inst. Machine Design. Seminar on the theory of machines and mechanisms, 1955, vol. 15, No. 58, pp. 46-71, 11 figs., 22 refs.
- Kyunapp, E. Yu. Automatic control of shale-burning in the furnaces of steam boilers. Author's abstract of dissertation for the degree of candidate in technical sciences, Leningrad 1955, 14 pp. (Polzunov Central Steam Turbine Institute).
- Lebedev, I. K. The design of automatic controls for boiler assemblies operated in parallel. Bull. Tomsk Polytech. Inst., 1955, vol. 80, pp. 48-53, 3 figs.
- Leonard, A. Determination of transient responses from the frequency response. In 'Symp. on Machine design', 1955, No. 5, pp. 3-13, No. 6, pp. 3-31, 36 figs., 11 refs.



- Lerner, A. Ya. Design of fast automatic control systems when the controlled coordinate has a limited range. In 'Trans. 2nd. All-Union Conf. on the Theory of Automatic Control', 1955, vol. 2, pp. 305-324, 17 figs., 7 refs.
- Letov, A. M. The state of stability problems in the theory of automatic control. In 'Trans. 2nd. All-Union Conf. on the Theory of Automatic Control', 1955, vol. 1, pp. 79-101, bibliography pp. 101-104.
- Letov, A. M. Stability in nonlinear controlled systems. Moscow, State Press for Tech.-Theor. Literature, 1955, 313 pp., 12 figs.
- Letov, A. M. Stability of non-steady-state motion in controlled systems. Appl. Mathem. and Mech., 1955, 19, No. 3, pp. 257-264, 1 fig., 7 refs.
- Lekhtman, I. Ya. A graphical method of designing magnetic circuits in the case where d.c. and a.c. fields act simultaneously. Automation and Remote Control, 1955, 16, No. 5, pp. 476-480, 5 figs.
- Lidsly, V. B. and Neigauz, M. G. Stability criteria in a system of differential equations with periodic coefficients. Appl. Mathem. and Mech., 1955, 19, No. 5, pp. 625-627, 7 refs.
- Litvin-Sedoi, M. Z. The problem of steady-state mode existence in nonlinear automatic control systems. In 'Trans. 2nd. All-Union Conf. on the Theory of Automatic Control', 1955, vol. 2, pp. 523-530, 3 figs.
- Lukashov, E. S. On the stability of excitation control using an electromagnetic voltage corrector. Electric Power Stations, 1955, No. 5, pp. 31-33.
- Lurye, A. I. Lyapunov's direct method and its use in the theory of automatic control. In 'Trans. 2nd. All-Union Conf. on the Theory of Automatic Control', 1955, vol. 1, pp. 142-148, bibliography pp. 146-148.
- Lyukov, M. G. Study of the dynamic properties of automatic control systems for arcs in steel-melting furnaces. Scientific reports of Lvov Polytech. Inst., No. 34, Electrical Engineering Series No. 8, Lvov University Press, 1955, pp. 177-196, 7 figs., 5 refs.
- Mavromati, G. S. and Baiko, V. F. Calculation of voltage rise rate on field-forcing in electromagnetically excited hydroelectric generators using two-stage magnetic amplifiers. In 'Bull. Leningrad Electrical Engineering Inst.', 1955, No. 27, pp. 40-49, 6 figs., 1 ref.
- Maierov, A. V. Increasing the operational safety of automatic controls. Automation and Remote Control, 1955, 16, No. 5, pp. 476-480, 5 figs., 2 refs.
- McGuire, D. T. and Halliday, R. G. A method of analyzing and designing closed-loop automatic control systems containing a small nonlinearity (step in the response). In 'Machine Design', 1955, No. 3, pp. 3-18, 20 figs.
- Malkin, I. G. The current state of Poincare's method and the ways of using it. In 'Trans. 2nd. All-Union Conf. on the Theory of Automatic Control', 1955, vol. 1, pp. 169-176, bibliography p. 176.
- Markovich, I. M. and Solalov, S. A. An experimental study of generator resynchronization. Electricity, 1955, No. 4, pp. 24-29, 8 figs., 4 refs.
- Maryanovsky, D. I. Stabilities of multistage amplifiers using negative feedback. In 'Trans. 2nd. All-Union Conf. on the Theory of Automatic Control', 1955, vol. 1, pp. 514-586, 14 figs., 2 refs.
- Matulevich, D. Yu. A gas-drying system as controlled object. In 'Automation in the chemical industry', Moscow, Acad. Sci., USSR, 1955, pp. 97-106, 5 figs., 4 tables, 4 refs.
- Meerov, M. V. Study and design of multiloop systems having many controlled parameters and high degree of steady-state accuracy. In 'Symposium in honor of A. A. Andronov'. Moscow Acad. Sci., USSR, 1955, pp. 230-241.
- Meerov, M. V. Study of automatic control system response from the D-curve picture. In 'Trans. 2nd. All-Union Conf. on the Theory of Automatic Control', 1955, vol. 2, pp. 145-162, 14 figs., 9 refs.
- Meerov, M. V. Some design principles for multiloop systems having many controlled parameters and high degrees of steady-state accuracy. In 'Trans. 2nd. All-Union Conf. on the Theory of Automatic Control', 1955, vol. 1, pp. 479-500, 9 figs., 6 refs.
- Mikirtichev, A. L. Effect of excitation control in synchronous machines on their dynamic stabilities. Author's abstract of dissertation for the degree of candidate in technical sciences. Leningrad, 1955, 13 pp. (Leningrad Polytech. Inst.).
- Mikhailov, N. N. Apparatus for determining the roots of characteristic equations. In 'Trans. 2nd. All-Union Conf. on the Theory of Automatic Control', 1955, vol. 3, pp. 117-129, 9 figs., 7 refs.
- Mikhailov, F. A. Choice of regular parameters for an automatic stabilizer. Trans. Moscow Aviation Inst., 1955, No. 41, pp. 80-116, 9 refs.
- Mikhailov, F. A. The limiting values of squared errors and their use in the selection of automatic control system parameters. In 'Trans. 2nd. All-Union Conf. on the Theory of Automatic Control', 1955, vol. 2, pp. 424-441, 2 figs., 16 refs.

- Moskvin, D. A. A matrix method of deriving transient responses. In 'Trans. 2nd. All-Union Conf. on the Theory of Automatic Control', 1955, vol. 2, pp. 53-61, appendix. 2 refs.
- Myasnikov, N. N. The effect of delays on the stabilities of self-regulating systems. In 'Trans. 2nd. All-Union Conf. on the Theory of Automatic Control', 1955, vol. 1, pp. 587-601, 21 figs., 5 refs.
- Nadzhzhatov, F. M. Approximate derivation of the periodic solutions in automatic control systems containing several nonlinearities. In 'Trans. 2nd. All-Union Conf. on the Theory of Automatic Control', 1955, vol. 1, pp. 204-218, 14 figs., 16 refs.
- Nadzhzhatov, E. M., Abdullaev, A. A. and Krementulo, Yu. A. An experimental study of self-oscillations in the internal loop of a pneumatic regulator. Automation and Remote Control, 1955, 16, No. 1, pp. 27-42, 17 figs., 3 refs.
- Naumov, B. N. An approximate method of dealing with automatic control systems containing nonlinear elements. Author's abstract of dissertation for the degree of candidate in technical sciences, Moscow, 1955, 12 pp. Acad. Sci., USSR, Institute of Automation and Remote Control).
- Nedoves, N. P. Automatic control of cutting processes. Author's abstract of dissertation for the degree of candidate in technical sciences, Lvov, 1955, 15 pp. (Lvov Polytechnical Institute).
- Some problems in the theory of automatic control. Collection of papers. Moscow, State Defense Press, 1955, 100 pp., 30 figs., 19 refs.
- Nechaev, G. K. Design of circuits with thermistors operating as relay elements. Automation and Remote Control, 1955, 16, No. 3, pp. 273-277.
- Olesevich, K. V. Calculation of control responses. Scientific reports of Odessa Polytech. Inst., 1955, vol. 4, No. 2, pp. 73-105, 11 figs., 17 refs.
- Orlov, K. V. Choice of control program for compound gas-turbine units. Trans. Leningrad Polytech. Inst., 1955, No. 177, Power Unit design, pp. 57-67, 1 fig., 1 ref.
- Ostrovsky, G. M. The derivation of stability regions. Automation and Remote Control, 1955, 16, No. 6, pp. 501-507, 6 figs., 2 refs.
- In honor of Aleksandr Aleksandrovich Andronov. Collection of papers. Moscow, Acad. Sci., USSR, 1955, 719 pp. Bibliography pp. 33-42.
- Paperny, E. A. An apparatus for studying transients in automatic control. Proc. Lvov Polytech. Inst., 1955, vol. 1, No. 1, pp. 104-107, 3 refs.
- Pelegren, M. J. Analysis of servomechanism and regulator performance on systematic perturbation. In 'Machine Design', 1955, No. 7, pp. 3-21, 12 figs., 9 refs.
- Petrov, V. V. Dynamics of one- and two-stage servomechanisms with certain nonlinear characteristics. In 'Trans. 2nd. All-Union Conf. on the Theory of Automatic Control', 1955, vol. 1, pp. 387-409, 22 figs., 9 refs.
- Petrov, V. V. and Ulanov, G. M. The theory of indirect control, coulomb friction in the sensing element being allowed for. Proc. Acad. Sci. USSR, 1955, 101, No. 4, pp. 611-614, 2 figs., 2 refs.
- Plishkin, Yu. M. The computation of integral criteria for the control responses of nonlinear systems. Automation and Remote Control, 1955, 16, No. 1, pp. 19-26, 5 refs.
- Popkov, S. L. Fundamentals of servo drives. Moscow, State Defense Press, 1955, 972 pp. illus., 27 refs.
- Popov, E. P. The small parameter in the harmonic linearization method. Bull. Acad. Sci. USSR, Tech. Sci. Section, 1955, No. 2, pp. 41-59, 10 figs., 19 refs.
- Popov, E. P. Approximate derivation of self- and forced-oscillations in automatic control systems. In 'Trans. 2nd. All-Union Conf. on the Theory of Automatic Control', 1955, vol. 1, pp. 219-248, 25 figs., 17 refs.
- Popovsky, A. M. Derivation of the working range for control systems involving mutually dependent variables. In 'Automation of production processes', Moscow, USSR Acad. Sci., 1955, pp. 34-61, 12 figs., 31 refs. (Institute of Automation and Remote Control).
- Popovsky, A. M. A solution to one case of Vovnesenky's problem for a control system with high-order mutually dependent variables. In 'Trans. 2nd. All-Union Conf. on the Theory of Automatic Control', 1955, vol. 1, pp. 465-478, 4 figs., 7 refs.
- Pospelov, G. S. Vibrational linearization of relay automatic control systems: responses of relay systems to slowly varying perturbations. In 'Trans. 2nd. All-Union Conference on the Theory of Automatic Control', 1955, vol. 1, pp. 363-385, 15 figs., 10 refs.
- Presnukhin, L. N. Methods of studying semiautomatic servo and control systems. In 'Computer-controlled equipment', a collection of papers. Moscow, State Defense Press, 1955, pp. 6-12.
- Puyachev, V. S. The general theory of random functions and its application in the theory of automatic control. In 'Trans. 2nd. All-Union Conf. on the Theory of Automatic Control', 1955, vol. 2, pp. 403-424, bibliography pp. 423-424.

- Pfalfer, P. E. Maximum signal rates in linear automatic control systems. In 'Machine Design', 1955, No. 12, pp. 3-12, 2 figs., 1 table.
- Rabkin, G. L. Mitrofanov, B. A. and Shterenberg, Yu. O. Determination of the numerical values of coefficients in transient functions from the experimental response curves. Automation and Remote Control, 1955, 16, No. 5, pp. 488-494, 8 refs.
- Razumikhin, B. S. The stability of a trivial solution for a second-order system. Appl. Mathem. and Mech., 19, No. 2, pp. 279-286.
- Rasulov, M. M. Development and theoretical and experimental study of excitation control circuits for synchronous generators. Author's abstract of dissertation for the degree of candidate in technical sciences. Moscow, 1955, 12 pp. (Acad. Sci., USSR, Krizhanovsky Power Institute).
- Rozanov, M. N. Analysis of static stability in complex systems when selecting optimum methods of automatic excitation control. Author's abstract of dissertation for the degree of candidate in technical sciences. (Acad. Sci. USSR Krizhanovsky Power Institute).
- Rozonoer, L. I. Some problems in the theory of linked control. Collection of papers from the student scientific society at the Moscow Power Institute, Moscow, 1955, pp. 35-72, 17 refs.
- Rotach, V. Ya. Design of a.c. and d.c. feedback industrial regulators from experimental response curves for closed-loop control systems, Moscow, 1955, pp. 15-16 (USSR Ministry of Higher Education, Moscow Power Institute).
- Rushchinsky, V. M. Dynamic response of a series direct-fired 67SP boiler, and control system selection. Jubilee scientific research conference. Summaries of reports, Moscow, 1955, pp. 17-18. (USSR Ministry of Higher Education, Moscow Power Institute).
- Rushchinsky, V. M. Study of the automatic control system on a 67SP direct-fired boiler. Author's abstract of dissertation for the degree of candidate in technical sciences, Moscow, 1955, 15 pp. (Acad. Sci. USSR, Institute of Automation and Remote Control).
- Rudenberg, R. Transients in electrical power systems. Moscow, Foreign Literature Press, 1955, 715 pp. McGraw Hill 1952. (Russian translation).
- Ryabov, B. A. The self-oscillation mode parameter changes in some nonlinear servo systems. Trans. Moscow Aviation Inst., 1955, No. 41, pp. 134-140, 4 figs.
- Ryabov, B. A. Stability of self-oscillation in some nonlinear systems. Trans. Moscow Aviation Inst., 1955, No. 50, pp. 138-141, 2 refs.
- Sarkisyan, E. P. Speed control of an a.c. drive using a pulse-controlled magnetic clutch. Proc. Acad. Sci. Armenian SSR, 1955, 21, No. 2, pp. 73-76.
- Simonov, N. A. Derivation of element response in self-regulating systems from the structural stabilities. Symp. of papers from the State Scientific Research Institute of the USSR Ministry of Communications, 1955, No. 2, (4), pp. 26-38, 3 figs., 3 refs.
- Sirotinsky, E. L. Improvements to the magnetic voltage regulator circuit of a compounded generator. Electric Power Stations, 1955, pp. 25-28, 3 figs.
- Slezhansky, O. V. Analysis of reversible rolling-mill control systems. Electricity, 1955, No. 5, pp. 1-9, 9 figs., 2 refs.
- Slutskovsky, A. I. Automatic gain control in seismic amplifiers. In 'Applied Geophysics', a collection of papers, No. 12, Moscow, State Exp. -Tech. Press, 1955, pp. 210-216, 6 figs., 1 ref.
- Smelnitsky, S. G. Development of control systems using the MEP regulator. Jubilee scientific research conf. Summaries of reports. Moscow, 1955, p. 11, (USSR Ministry of Higher Education, Moscow Power Inst.).
- Smirnov, I. M. The stabilities of periodic modes derived by approximation for automatic control systems. In 'Trans. 2nd. All-Union Conf. on the Theory of Automatic Control', 1955, vol. 1, pp. 193-203, 8 figs., 5 refs.
- Sokolov, T. N. and Goryachenko, A. T. Response indices for servo systems. Trans. Leningrad Polytech. Inst., 1955, No. 181, Radiophysics, pp. 131-148, 1 table, 3 refs.
- Sokolov, T. N. The problems of design and physical feasibility in electromechanical servo systems. 'Trans. 2nd. All-Union Conf. on the Theory of Automatic Control', 1955, vol. 2, pp. 163-183, 16 figs., 4 refs.
- Solodovnikov, V. V. Response and dynamic error problems in the theory of automatic control. 'Trans. 2nd. All-Union Conf. on the Theory of Automatic Control', 1955, vol. 2, pp. 7-37, bibliography pp. 36-37.
- Solodovnikov, V. V. Design of correction units for automatic control systems. 'Trans. 2nd. All-Union Conf. on the Theory of Automatic Control', 1955, vol. 2, pp. 253-263, 6 figs., 6 refs.



- Solodovnikov, V. V. and Matveev, P. S. Design of correction units for follower systems in which noise is present, to set limits of dynamic error. *Automation and Remote Control*, 1955, 16, No. 3, pp. 233-257, 20 figs., 4 tables, 12 refs.
- Solodovnikov, V. V., Topcheev, Yu. I. and Krutikova, G. V. A frequency response method of deriving transients (Appendix - tables and nomograms) Information manual. Moscow, State Power Press, 1955, 195 pp., 56 figs., 15 tables.
- Static and dynamic characteristics of TsKTI electromechanical regulators. Scientific papers from the Ivanov Power Institute, 1955, No. 6, pp. 86-93, 11 figs., 7 refs.
- Stebakov, S. A. Use of phase-space concepts in studying automatic control systems. In 'Trans. 2nd. All-Union Conf. on the Theory of Automatic Control', 1955, vol. 1, pp. 149-165, 10 figs., 2 refs.
- Sterpinson, L. D. Automatic frequency control in large power systems. *Electric Power Stations*, 1955, No. 10, pp. 22-28.
- Syromyatnikov, V. F. Study of automatic fuel burning control dynamics in the fuel layers of ships' boilers. Author's abstract of dissertation for the degree of candidate in technical sciences, Leningrad, 1955, 17 pp., (Leningrad Ship-Building Institute).
- Tal, A. A. Effect of self-regulation and derivative feedback on direct control processes. In the symposium in honor of A. A. Andronov, Moscow, Acad. Sci. USSR, 1955, pp. 282-299.
- Trapeznikov, V. A. and Kogan, B. Ya. Current experimental methods of studying automatic control systems. In 'Trans. 2nd. All-Union Conf. on the Theory of Automatic Control', 1955, vol. 3, pp. 7-36, 20 figs., 28 refs.
- Tuzov, A. P. Stability problems in one control system. *Bull. Leningrad Univ.*, 1955, No. 2, pp. 43-70, 6 refs.
- Westcott, J. G. Design of optimal automatic control systems subject to power restrictions. In 'Machine Design', 1955, No. 8, pp. 3-23, 4 refs.
- Ulanov, G. M. Theory of dynamic accuracy in nonlinear indirect control systems. *Proc. Acad. Sci. USSR*, 1955, 102, No. 3, pp. 465-467, 1 fig., 11 refs.
- Ulanov, G. M. Some problems of dynamic accuracy in nonlinear automatic control systems and servomechanisms subject to disturbances of restricted modulus. In 'Trans. 2nd. All-Union Conf. on the Theory of Automatic Control', 1955, vol. 2, pp. 472-483, 5 figs., bibliography pp. 482-483.
- Ulanov, G. M. The maximum deviations in nonlinear automatic control systems using a single relay. *Proc. Acad. Sci. USSR*, 1955, 102, pp. 741-742, 1 fig. 11 refs.
- A unit for automatic excitation control in a synchronized asynchronous motor. In 'Collection of rationalization proposals', No. 49, Moscow 1955, pp. 37-39. (Ministry of the Electrical Engineering Industry, Central Bulletin of Technical information).
- West, J. C. and Leonard, J. L. The torque required of the servomotor in a follower system. In 'Machine Design', 1955, No. 9, pp. 9-14, 1 table, 3 refs.
- Fateev, A. V. A graphical method of selecting the parameters of correcting feedbacks in automatic units. In 'Trans. 2nd. All-Union Conf. on the Theory of Automatic Control', 1955, vol. 2, pp. 266-279, 22 figs., 4 refs.
- Fedorov, M. M. Control theory for pit hoist gear. *Coal*, 1955, No. 9, pp. 25-30, 3 figs., 2 tables, 4 refs.
- Feldbaum, A. A. The design of optimal automatic control systems. In 'Trans. 2nd. All-Union Conf. on the Theory of Automatic Control', 1955, vol. 2, pp. 325-360, 21 figs., 14 refs.
- Fialko, G. M. and Milman, D. I. The optimum parameters of isodrome regulators for static and astatic controlled objects. *Trans Urals Chemical Research Institute*, 1955, No. 3, pp. 221-228, 6 figs., 3 refs.
- Fuller, A. T. Automatic control systems with quasicritical damping, In 'Machine Design', 1955, No. 2, pp. 3-15, 10 refs.
- Fufaev, N. A. Theory of a vibration link operated via the electromagnetic interrupter principle. In 'Trans. 2nd. All-Union Conf. on the Theory of Automatic Control', 1955, vol. 1, pp. 410-420, 6 figs., 3 refs.
- Khamovich, E. M. Some problems in the theory and design of hydraulic follower units for metal-cutting machines. *Trans. Inst. Machine Operation, Seminar on the Theory of Machines and Mechanisms*, 1955, vol. 14, No. 56, pp. 48-58, 10 figs., 9 refs.
- Khoklov, V. A. Hydraulic loss and liquid leakage coefficients for the slide valves of hydraulic effector mechanisms. *Automation and Remote Control*, 1955, 16, No. 1, pp. 64-70, 5 figs., 6 refs.
- Taypkin, Ya. Z. The design of sampled-data nonlinear control systems. In 'Trans. 2nd. All-Union Conf. on the Theory of Automatic Control' 1955, vol. 2, pp. 367-385, 17 figs., 3 tables, 8 refs.

- Tsyarkin, Ya. Z. The theory of relay automatic control systems. In 'Trans. 2nd. All-Union Conf. on the Theory of Automatic Control', 1955, vol., 1, pp. 329-362, 35 figs., 24 refs.
- Tsyarkin, Ya. Z. Lectures on the theory of automatic control, 2nd. edition, revised and enlarged, Moscow, 1955, 96 pp. 81 figs., (All-Union Power Correspondence Inst. Dept. of automatic checking and control).
- Tsyarkin, Ya. Z. The asymptotic properties of certain multiloop automatic control systems. In 'Trans. All-Union Power Correspondence Inst. 1955, No. 6, pp. 10-16, 4 figs., 9 refs.
- Tsyarkin, Ya. Z. Allowing for pulse shape in pulsed control systems. Automation and Remote Control, 1955, 16, No. 5, pp. 462-466, 5 figs., 6 refs.
- Tsyarkin, Ya. Z. Determination of the dynamic responses of systems described by linear differential equations of order not greater than two from oscillograms of transients. In 'Trans. (All-Union Power Correspondence Inst., 1955, No. 6, Electrical Engineering, pp. 3-9, 10 figs.
- Tsyarkin, Ya. Z. The theory of relay automatic control systems. Moscow, State Tech.-Theor. Press, 1955, 456 pp., 249 figs., 16 tables., bibliography pp. 437-450.
- Tsyarkin, Ya. Z. A frequency method of studying periodic modes in relay automatic control systems. In 'Symp. in honor of A. A. Andronov, Moscos Acad. Sci. USSR, 1955, pp. 383-412.
- Chernov, E. I. The uses of configuration theorems in analyzing automatic control systems with variable coefficients. In 'Trans. 2nd. All-Union Conf. on the Theory of Automatic Control', 1955, vol. 2, pp. 386-398, 1 circuit, 8 refs.
- Chetaev, N. G. Stability of motion. 2nd. edition, revised. Moscow, State Press for Tech.-Theor. Lit., 1955, 207 pp. Bibliography in footnotes.
- Chistyakov, S. V. Use of the systematic responses of controlled objects for deriving their dynamic properties. Trans. Moscow Power Inst., 1955, No. 25, pp. 197-222, 21 figs., 2 refs.
- Chikhladze, G. A. Automatic control of hydroelectric station output from the water flow. Author's abstract of dissertation for the degree of candidate in technical sciences. Tbilisi, 1955, 16 pp. (Gruz Kirov Polytech. Inst.)
- Chichinadze, V. K. One method of improving the dynamic properties of certain automatic control systems. Automation and Remote Control, 1955, 16, No. 2, pp. 150-157, 5 figs., 7 refs.
- Shangin, Yu. A. Analysis of steam-engine automatic control equipment. Author's abstract of dissertation for the degree of candidate in technical sciences, Leningrad, 1955, 13 pp. (Obraztsov Inst. of Railway Transport Engineers, Leningrad).
- Shashkov, A. G. An experimental and theoretical study of throttle units and hydraulic relays of nipple-piston type operating on oil. Author's abstract of dissertation for the degree of candidate in technical sciences. Moscow, 1955, 10 pp. Acad. Sci., USSR, Institute of Automation and Remote Control).
- Shefter, Ya. I. and Orlov, V. A. Some problems of statics and dynamics of the D-18 centrifugal windmill governor. Agricultural Machines, 1955, No. 5, pp. 17-28, 5 figs., 7 refs.
- Shoikhet, L. A. On A. I. Kukhtenko's paper "An automatic load controller for borers and coal combines" (Coal, 1953, No. 4) and on B. N. Lyubimov's "Readers' replies to A. I. Kukhtenko's paper" (Coal, 1953, No. 12). Coal, 1955, No. 1, pp. 42-43, 6 refs.
- Shchulhin, A. I. Generalization of the transfer function formula and block designs for multiloop servo and controlled systems. Trans. All-Union Power Correspondence Inst., 1955, No. 6, pp. 27-35.
- Efendizade, A. A. Theory of a controlled asynchronous electric drive. Baku, Academy of Sciences of the Azerb. SSR, 1955, 187 pp., 5 tables, 89 refs. (Esman Power Institute).
- Yakubaitis, E. A. Optimum parameter relations for the measuring head of a choke controller. In 'Power problems', vol. 3, Riga, Academy of Sciences of the Latvian SSR, 1955, pp. 65-74, 9 figs.
- Yakubaitis, E. A. Static characteristics of the measuring head of a choke controller. In 'Power problems', vol. 3. Riga Academy of Sciences of the Latvian SSR, 1955, pp. 43-61, 15 figs., 5 tables, 8 refs.
- Yakubaitis, E. A. Generator voltage control stability using chokes and magnetic amplifiers when there is a load fault. Bull. Acad. Sci. Latvian SSR, 1955, No. 9, pp. 87-95, 8 figs., 17 refs.
- Adler, F. P. Information required for missile guidance J. Appl. Physics, 1955, April, vol 26, No. 4, p. 492.
- Alle G. and Fortpied G. The Regulation of Ward-Leonard Systems by Magnetic Amplifiers., - Engrs' Digest., 1955, Nov., vol. 16, No. 11, p. 527-529, 6 fig., ACEC Rev., 1955, No. 1, p. 27-35.
- Amile T h. S. and Higgins Th. J. A general theory for determination of the stability of linear limped-parameter multiloop servomechanisms (and other feedback). Applic. and Ind., 1955, No. 19, p. 134-147.

- Anger, A. G. and Pettit, D. L. Accurate control of relative speed and cut in a continuous process line. *Applic. and Ind.*, 1955, No. 16, p. 485-493.
- Anke K. Eine neue Berechnungsmethode der quadratischen Regelfläche. *Z. angew. Mathe. u. Phys.*, 1955, Bd., 6, Nr. 4, S. 327-331.
- Armstrong, H. L. An approximate Treatment of Cascaded Four-Terminal Networks. *Electronic Engng*, 1955, March, vol. 27, No. 325, p. 130-131, 2 figs., Bibliogr. 7.
- Arthurs, E. and Martin, L. H. Closed expansion of the convolution integral (a generalization of servomechanism error coefficients). *J. appl. Phys.*, 1955, Jan., vol. 26, No. 1, p. 58-60. Bibliogr. 6.
- An automatically Adjusted Live Centre with Fluid Pressure Regulator. *Machinery, L.*, 1955, Febr., vol. 86, No. 2206, p. 408, 1 fig.
- Baker, W. L. A New Approach to the Approximation Problem. *JRE Convent. Rec.*, 1955, part. 2, Circuit Theory, p. 35-39, 6 figs.
- Baillie, T. L. Effects of system components in process control - *Trend. Engng. Univ. Wach.*, 1955, Apr., vol. 7, No. 2, p. 10-14.
- Beintker W. Gleichlaufregelung hoher Genauigkeit. *Elektrotechn. Z. B.*, 1955, 7 Jg, Nr 4, S. 98-100, 8 Abb. Bibliogr. 2.
- Benes J. a Trnka Z. Analytic and graphic methods of solving regulation problems. *Praha, Ceskoslovenské Akad. Ved.*, 1955, p. 73-178, 57 figs., Bibliogr. 38.
- Bennett, W. R. Steady-State transmission through networks containing periodically operated switches. *Trans. IRE*, 1955, vol. CT-2, N. 1, p. 17-21.
- Benson, F. A. and Lusher, G. V. Effects of heater-voltage variation of valves in certain stabilizer circuits. *Electronic Engng*, 1955, Nov., vol. 27, No. 11, p. 502-503.
- Bertram, J. E. and Franklin G. Sampled-data feedback improves system response. *Control Engng.*, 1955, Sept., vol. 2, No. 9, p. 107-111. 8 figs. Bibliogr. 3.
- Bhalla, M. S. An a.c. Voltage Stabilizer. *J. Scient. and Industr. Res.*, 1955, Oct., vol. 14, No. 10, p. 467-468, 1 fig.
- Biernsen, G. A. A simple method for calculating the time response of a system to an arbitrary input. *Applic. and Ind.*, 1955, No. 20, p. 227-245.
- Blase W. und Dietze R. Die Regelung der Übergabewirkleistung im Verbundbetrieb mit dem Impulseleistungsregler. *AEG Mitt.*, 1955, Bd. 45, Nr 1-2, S. 104-106, 4 Abb. Bibliogr. 1.
- Blase W. Spannungsregler mit magnetischem Verstärker und Störgrössenaufschaltung für Wechsel- und Drehstromgeneratoren mit Erregermaschine. *AEG Mitt.*, 1955, Jg. 45, Nr 1-2, S. 63-69, 7 Abb.
- Bock, H. Toleranz geregelter Grössen. *Regelungstechnik*, 1955, Jg. 3, Nr 11, S. 272-275, 2 Abb. Bibliogr. 3.
- Bonnet, P. Etude du comportement dynamique des asservissements comportant des thyristors. *L'Onde électrique*, 1955, Fevr., 35 année, No. 335, p. 97-104, 15 figs.,
- Bönnhoff, H. Selbsttätige Spannungsregelung von Transformatoren mit Stufenschaltwerken. *Elektrizitätswirtschaft*, 1955, Jg. 54, Nr 12, S. 395-398.
- Bradford, T. M., Rideout, V. C. and Sather, D. J. The use of correlation techniques in the study of servomechanisms. *J. Brit. Instn. Radio Engrs.*, 1955, May, vol. 15, No. 5, p. 249-257, 8 figs., Bibliogr. 25.
- Braae R. Tensor analysis and linear networks theory. *Trans. S. Afric. Inst. Electr. Engrs.*, 1955, March, vol. 46, Pt, 3, p. 67-95 with Discussion, 15 figs. Bibliogr. 3.
- Braun, H. Stetige Regelungsvorgänge mit Zweipunktregler System Tirrill. *AEG - Mitt.*, 1955, Bd. 45, Nr 1-2, S. 180-185, 13 abb. Bibliogr. 11.
- Brodin, J. Analysis of time-dependent linear networks. *Trans. IRE*, 1955, vol. GT-2, No. 1, p. 12-16. Bibliogr. 14.
- Bronzi, G. Della regolazione automatica di frequenza nella radiotelegrafia e spostamento di frequenza. *Alta frequenza*, 1955, June, vol. 24, No. 3, p. 284-287, 4 figs.,
- Bruus, R. A. and Scunders, R. M. Analysis of feedback control systems: Servomechanisms and Automatic Regulators. London, McGraw-Hill, 1955, 383 p., fig. Appendix.
- Brunschweiler, K. Leistung und Empfindlichkeit thermostatischer Expansionsventile. *Kältetechnik*, 1955, Jg. 7, Nr 1, S. 2-4.
- Burford, T. M., Rideout, V. C. and Sather, D. S. The use of correlation techniques in the study of servomechanisms. - *J. Brit. Instn. Radio Engrs.*, 1955, vol. 15, No. 5, p. 249-257. 7 figs. Bibliogr. 25.
- Cahen, F. Load-phase tie-line energy control of interconnected power systems. *Trans. Amer. Inst. Electr. Engrs*, 1955, vol. 74, part. 3, p. 1-5. (Power Apparatus System, No. 17, April 1955).



- Carniol, B., Dykast, K. Choice of bandwidth in servosystems to minimize transient and fluctuation errors. Slaboprondy Obzor, 1955, N 4, str. 187-198, 20 obr. Bibliogr. 9.
- Caryotokis, G. A., Demuth, H. B. and Moore, A. D. Iterative Network Synthesis. - IRE Convent. R c., 1955, part 2, Circuit Theory, p. 9-16, 14 figs., Bibliogr. 5.
- "Cathode Ray" - The Nyquist Diagram at Work. (Dealing with feedback over more than one stage). - Wireless World, 1956, Jan., vol. 62, No. 1, p. 43-48, 9 figs.
- Chang, S. S. L. Optimum switching criteria for higher order contractor servo with interrupted circuits. - Applic. and Ind., 1955, No. 21, p. 273-276.
- Chang, S. S. L. Transient analysis of a.c. servomechanisms. Applic. and Ind. 1955, No. 17, p. 30-37.
- Chang, Sh. S. J. On the separability of Laplace transform variable and its applications in carrier systems. IRE Convent. Rec., 1955, part. 2, Circuit Theory, p. 27-33. Bibliogr. 6.
- Chow, F. F. and Stern, A. P. Automatic gain control of transistor amplifiers. Trans. IRE, 1955, vol. BTR-1, No. 2, p. 1-15, 18 figs. Bibliogr. 6.
- Coales, J. F. Automatic Control. J. Instn. Electr. Engrs, 1955, May, No. 5, p. 278-279.
- The control of liquid levels with electronic relays. Philips Serv. Sci. and Ind., 1955, vol. 2, No. 3, p. 17-20.
- Cosgriff, R. L. Servos that use logic can optimize. Control Engng., 1955, Sept., vol. 2, No. 9, p. 133-135, 5 figs.
- Critchlow, D. L. Oscillographic techniques for the evaluation of magnetic amplifier response. Commun. Electronics, 1955, Nov., No. 21, p. 607-610, 5 figs., 1 table, Bibliogr. 2.
- Cuénod, M. La répartition de la charge entre les groupes asservis à un réglage puissance-fréquence. Bull. Assoc. suisse Electriciens, 1955, t. 46, No. 21, p. 1019-1025, 14 figs. Bibliogr. 17.
- Czalkowski, S. A harmonic response plotter. Electronic Engng, 1955, May, vol. 27, No. 327, p. 207-211, 7 figs.
- Davidson, G. M. and Nashman, L. How stabilization improves closed-loop operation. Control Engng., 1955, Dec., vol. 2, No. 12, p. 67-74, 10 figs.
- De Claris, N. A method of rational function approximation for network synthesis. IRE Convent. R c., 1955, part 2, circuit theory, p. 51-58, 6 figs. Bibliogr. 10.
- Dickey, F. E. Servo-analyzer for wide-range testing. Electronics, 1955, April, vol. 28, No. 4, p. 172-175.
- Diehl, B. Temperatur-Messung und Regelung mit Thermistoren. Industriekurier, Techn. u. Forschung, 1955, Jg. 8, Nr 42, S. 106.
- Discussion on "The use of correlation technique in the study of servomechanisms". J. Brit. Instn. Radio Engrs., 1955, Oct., vol. 15, No. 10, p. 526.
- Dumur, P. et Comtat R. Le réglage des puissances de la fréquence des usines hydroélectriques et des lignes d'interconnexions de la S. A. l'Energie de l'Ouest - Suisse. (EOS) - Bull. Assoc. Suisse, Electriciens, 1955, 30, April, vol. 46, No. 9, p. 425-437. 8 figs.
- Eggers, H. R. Anwendung und Theorie der Proportionalregelung für Temperaturen. AEG Mitt., 1955, Bd. 45, Nr 1-2, S. 45-57, 11 Abb.
- Erwiderung zur Diskussionsbemerkung des Herrn Hanny zum Aufsatz C. Kessler. "Über die Vorausberechnung optimal abgestimmter Regelkreise, Teil III". Regelungstechnik, 1955, 3 Jg., Nr 4, S. 102.
- Evans, W. R. Control system dynamics. N. Y., London, McGraw-Hill, 1955, 282 pp.
- Fatur, J. Ein Planimeterverfahren zur Bestimmung der statischen Moments und der Momente höherer Ordnung ebener Kurven. Techn. Rundschau, 1955, Jg. 47, Nr 3, S. 10-13.
- Ferner, V. Die graphische Ermittlung des Übergangsverhaltens von Regelstrecken. Feingerätetechnik, 1955, 4 Jg., Mai, Nr 5, S. 195-200, 200 Abb.
- Ferner, V. Über das Verhalten geschlossener Regelkreise. Feingerätetechnik, 1955, Juni, 4 Jg. Nr 6, S. 259-264, 11 Abb. Nr 8, S. 361-365, 9 Abb.
- Fersohl, L. Neue Selbststeuergeräte für die Schnellsynchronisierung von Synchronmaschinen. Elektrotechnik und Maschinenbau, 1955, Bd. 72, Nr 10, S. 217-222.
- Fiebigler, H. und Bosch, J. Flächengewichts-Regelung von Papier mit Hilfe von Beta-Strahlen. Wochenbl. Papierfabr., 1955, Jg. 83, Nr 7, S. 271-274; Nr 8, S. 317-320.
- Friedrich, H. R. A method for investigating the influence of flexibility of the mounting structure of hydraulic servosystems on the dynamic stability quality of control system. J. Aeronaut. Sci., 1955, Febr., vol. 22, No. 2, p. 101-106, 123, 6 figs.
- Fuller, A. T. The adjustment of control system for quick transient response. Proc. Instn. Electr. Engrs, 1955, Pt. B, Sept., vol. 102, No. 5, p. 596-601, 2 figs. Bibliogr. 13.

- Göller, E. Regelungen mit vorgegebenen Wurzeln der Stammgleichung. Regelungstechnik, 1955, 3 Jg. Nr 11, S. 268-272, 9 Abb.
- Hahn, W. Stabilitätsuntersuchungen in der neueren Sowjetischen Literatur. Regelungstechnik, 1955, Jg 3, Nr. 9, S. 229-231, 1 fig.
- Hahn, W. Über Stabilität bei nichtlinearen Systemen. Z. angew. Math. und Mech., 1955, Dec., Bd. 35, Nr 12, S. 459-462.
- Haier, U. Gesichtspunkte für den Aufbau von Gleichstromregelantriebe. Regelungstechni., 1955, July, 3 Jg., H. 7, S. 167-172. 8 Abb.
- Hallen, K. Eine elektronische Synchronsteueranlage hoher Winkelgenauigkeit. Regelungstechnik, 1955, 3 Jg. Nr. 2, S. 70-71, 4 Abb.
- Hanny, J. Stellungnahme zum Aufsatz C. Kessler "Über die Vorausberechnung optimal abgestimmter Regelkreise", Teil III. Die optimal Einstellung des Reglers nach dem Betragsoptimum. Regelungstechnik, 1955, 3 Jg., Nr. 3, S. 74-75.
- Heinrich, R. Selbsttätige Regeleinrichtung zum Symmetrieren eines unsymmetrischen Drehstromnetzes. ETZ - A, 1955, Mai, Bd. 76, Nr. 9, S. 315-320, 16 Abb. Bibliogr. 4.
- Heinz, R. Spannungsregelung von Transformatoren mit Stufenschaltwerken. AEG, Mitt., 1955, Bd. 45, Nr 1-2, S. 106-115, 12 Abb.
- Henning, H. Stellungnahme zum Aufsatz von K. Seidl: Die Dynamik der Synchronmaschine als Masstab ihrer regeltechnischen Bemessung. Regelungstechnik, 1955, Jg. 3, Nr 7, S 183-184.
- Higgins, Th. J. A new simple general criterion for determining the stability of servomechanisms. Proc. Nat. Electronics Conference, vol. 10. Chicago, 1955, p. 748-757, 3 figs., 2 tables, Bibliogr. 8.
- Hoberman, M. A design philosophy for man-machine control system. Proc. IRE, 1955, vol. 43, No. 5, p. 623.
- Hochrainer, A. Die Grundbegriffe der Regelungstechnik, erläutert am Beispiel der Spannungsregelung. AEG-Mitt., 1955, Bd. 45, Nr 1/2, S. 12-21, 26 Abb. Bibliogr. 5.
- Holzbock, W. G. Basic principles of pneumatic control mechanism. Air Condit., Heating and V ntilation, 1955, vol. 52, No. 1, p. 101-109.
- Hovius, R. L. Jitter in instrument servos. Applic. and Ind., 1955, No. 16, p. 393-398.
- Jaskula, H. W. Röhrengeregelter Netzgleichrichter mit extrem hoher Spannungs Konstanz: AEG Mitt., 1955, Bd. 45, Nr 1/2, S. 82-84, 4 Abb. Bibliogr. 9.
- Janssen, J. M. L. Die Deutung des Verhaltens eines Regelsystems aus dem Abweichungsverhältnis. Regelungstechnik, 1955, 3 Jg., Nr 12, S. 303-309. 10 Abb. Bibliogr. 13.
- Janssen, J. M. L. A practical guide to plant controllability. Control Engng., 1955, Nov., vol. 2, No. 11, p. 58-63, 4 figs., Bibliogr. 3.
- Johnson, G. W., Lindorff, D. P. and Nordling, C. G. A. Extension of continuous data system design techniques to sampled data control systems. Appl. and Ind., 1955, No. 20, p. 252-263.
- Jung, S. Die Prüfung und Beurteilung von Temperaturwächtern für Kühlgeräte - Kältetechnik, 1955, 7 Jg, Nr. 1, S. 9-11.
- Junker, B. Das Verhalten idealisierter stetiger Regler an regelstrecken mit Ausgleich. Regelungstechnik, 1955, 3 Jg, Nr 3, p. 54-58; Nr 4, S. 80-84, 26 Abb.
- Jury, E. J. The effect of pole and zero locations on the transient response of sampled-data systems. Applic. and Ind., 1955, No. 17, p. 41-48.
- Kalman, R. E. Analysis and design principles of second and higher order saturating servomechanisms. Applic. and Ind., 1955, No. 21, p. 294-310.
- Kalman, R. E. Phase-plane analysis of automatic control systems with nonlinear gain elements. Appl. and Ind., 1955, No. 16, p. 383-390.
- Kaufman, W. M. and Woodford, J. B. A new series representation for correlation functions. IRE Convent. Rec., 1955, part 2, circuit theory, p. 40-44, 6 figs.
- Kessler, C. Über die Vorausberechnung optimal abgestimmter Regelkreise. Regelungstechnik, 1955, 3 Jg., Nr 1, S. 16-23, 40 Abb.; Nr 2, S. 40-49, 30 Abb.
- Keve, Th. Regelung eines Leonardkreises auf konstanten Strom., ETZ - A, 1955, Bd. 76, Nr 6, S. 213-216, 5 Abb. Bibliogr.
- Kotek, Z. Nonlinear regulators - Souhrn Praci o Automatizaci. - Praha, Ceskosl.
- Ku, Y. H. Analysis of nonlinear systems with more than one degree of freedom by means of space trajectories. J. Franklin Inst., 1955, Febr., vol. 259, No. 22, p. 115-131. Bibliogr. 14.

- Kundt, W. Mess- und regelungstechnische Probleme bei der Qualitätsregelung des Endproduktes in der Verfahrenstechnik. Chem. Technik, 1955, Bd. 7, Nr 8, S. 473-479, 13 Abb Bibliogr. 30.
- Kundt, W. Die Regelung von Destillationskolonnen nach der Produktqualität. Regelungstechnik, 1955, Jg. 3, Nr 8, S. 194-197, 8 Abb. Bibliogr. 13.
- Lago, G. V. Additions to sampled-data theory. Proc. Nat. Electronics Conference, vol. 10 - Chicago, 1955, p. 758-766, 4 figs. Bibliogr. 4.
- Lago, G. V. Addition to Z-transformation theory for sampled-data systems. Applic. and Ind., 1955, No. 16, p. 403-408.
- Lajoy, M. H. and Beillif, E. A. Process control analysis. Instrument and Automat., 1955, vol. 28, No. 4, 617-619; No. 5, p. 794-797; No. 7, p. 1114-1118.
- Lampard, D. G. The response of linear networks to suddenly applied stationary random noise. Trans. IRE, 1955, vol., CT-2, No. 1, p. 49-57, 6 figs.
- Lang, G. and Ham, J. M. Conditional feedback systems - a new approach to feedback control. Appl. and Ind., 1955, No. 19, p. 152-161.
- Le Boiteux, H et Moreau, R. Les idées fondamentales de la théorie des servo mécanismes. La Recherche Aéronautique, 1955, Sept./Okt., No. 47, p. 47-54.
- Leonard A. Stellungnahme zum Aufsatz, L. Merz.: Die Begriffe Schwierigkeit, Leistungsfähigkeit und Durchführbarkeit in der Regelungstechnik. Regelungstechnik, 1955, 3, Jg., Nr 1, S. 24.
- Lühr, W. Graphische Ermittlung der Kennlinien von Regelkreisen im Beharrungszustand aus den Übertragungsfunktionen. AEG Mitt., 1955, Bd. 45, Nr 1/2, S. 45-49, 6 Abb. Bibliogr. 3.
- Lang, A. Kennzeichnung von Regelkreisgliedern und Regelkreisen durch Blockschaltbilder. AEG Mitt., 1955, Bd. 45, Nr 1/2, S. 33-34, 13 Abb.
- McDonald, D. C. An appraisal of nonlinearities in servomechanisms. Proc. Nat. Electronics Conference, vol. 10 - Chicago, 1955, p. 732-747. Bibliogr. 48.
- McDonald, D. C. Backlash compensation improves servo-system operation. Instruments and Automat., 1955, Oct., No. 10, p. 1728-30.
- Magnus, K. Eigenschwingungen hydraulischer Stellmotore. Regelungstechnik, 1955, Jg. 3, Nr 11, S. 276-281; Nr 12, S. 293-296, 20 Abb. Bibliogr. 4.
- Magnus, K. Über ein Verfahren zur Untersuchung nichtlinearer Schwingungs - und Regelungs-Systeme. Düsseldorf, VDJ - Verlag, 1955, 32 Seiten, 41 Abb. VDJ - Forschungsheft, Nr 451).
- Mahewson, C. E. Advantage of electronic control - Trans. IRE, 1955, PGJE-2, p. 40-50; Instruments and Automat., 1955, vol. 28, No. 2, p. 258-265.
- Mandel, L. The square wave response method of analyzing process control systems. Brit. J. Appl. Phys., 1955, vol. 6, No. 8, p. 291-296. 6 figs. Bibliogr. 12.
- Mathews, M. V. A method for evaluating nonlinear servomechanisms. Applic. and Ind., 1955, No. 18, p. 114-123.
- Merrit, S. Y. An adjustable speed power selsyn system. Trans. Amer. Inst. Electr. Engrs., 1955, Pt. 11, vol. 74, p. 71-75 (Applic. and Ind., No. 18, May, 1955).
- Merz, L. Entgegnung zur Diskussionsbemerkung Professor Leonhards zum Aufsatz L. Merz: Die Begriffe Schwierigkeit, Leistungsfähigkeit und Durchführbarkeit in der Regelungstechnik. Regelungstechnik, 1955, 3 Jg., Nr 3, S. 75-76.
- Miller, K. S. Properties of impulsive responses and Green's functions. Trans. IRE, 1955, vol. CT-2, No. 1, p. 26-31.
- Mohr, O. und Rehm, H. Aufbau und Wirkungsweise von Steuerketten und Regelkreisen. Elektrotechnische Z. 1955, Nr 1, S. 753-765, 15 Abb. Bibliogr. 58.
- Morris, J., Gouriet, G. G. and Head, J. W. Servomechanism performance. Aircraft Engng., 1955, July, vol. 27, No. 317, p. 220-222.
- Muzzey, B. C. and Sims, V. A wider choice of missile control instrument functional characteristics. Aeron. Eng. Rev., 1955, No. 5, p. 73-76, 8 figs.
- Nashman, L., Davidson, G. M., Savet, P. H. and Kaszerman, Ph. Effects of Carrier Frequency Drift on performance of Notch Networks in A.C. Servo Systems. Aeron. Eng. R v., 1955, Febr., vol. 14, No. 2, p. 61-66, 11 figs. Bibliogr. 1.
- Neuse, W. und Schneider, E. Eine neue thermische Rückführung für Zweipunkt-regelungen. Siemens S., 1955, Jan., Bd. 29, Nr 1, S. 20-25.
- Newton, G. C. Design of control systems for minimum bandwidth. Appl. and Ind., 1955, No. 19, p. 161-168.



- Nikiforuk, P. N. A technique for nonlinear function generation. *Electric. Engng.*, 1955, March, vol. 27, No. 325, p. 118-119.
- Pacax, M. The normal degenerative stabilizer: possibilities of overcompensation. *Slaboproudý Obzor*, 1955, No. 1, str. 562-568.
- Paul, S. Die thermische Rückführung als Ergänzung zum Zweipunktregler. *Regelungstechnik*, 1955, 3 Jg., H. 12, S. 296 - 302, 15 Abb.
- Pek, W. Fundamentals of amplidyne theory. *Electrotech. Obz.*, 1955, vol. 44, No. 3, p. 130, 136, 3 obr. Bibliogr. 5.
- Peters, C. J. and Woodford, J. B. Application of Time Series to the Calculation of the Transient Response of Band-Pass Systems. *IRE - Convent. Rec.*, 1955, part. 2, circuit theory, p. 65-70, 3 figs.
- Pfeiffer, P. E. The maximum response ratio of linear systems. *Applic. and Ind.*, 1955, No. 16, p. 480-484.
- Philippov, E. An approximate method of determining the parameters of voltage stabilizers using saturated chokes. *Nachrichtentechnik*, 1955, March, vol. 5, No. 3, p. 108-112.
- Povejsil, D. J. and Fuchs, A. M. A method for the preliminary synthesis of a complex multiple-loop control system. *Applic. and Ind.* 1955, No. 19, p. 129-134.
- Pun, Lucas. Regulation de vitesse des groupes hydroelectriques. Analyse et recherche d'une constitution optimum. *Bull. Societe Francaise des Electriciens*, 1955, Oct., t. 5, No. 58, p. 727-748, fig., Bibliogr. 72.
- Quick Response of Control Systems. *J. Instn. Electr. Engrs.*, 1955, Nov., vol. 1., No. 11, p. 698, 1 fig.
- Reissig, R. Über die Stabilität gedämpfter erzwungener Bewegungen mit linearer Rückstellkraft. *Math. Nachrichten*, 1955, Bd. 14, Nr. 1, Juli, S. 17-20. Bibliogr. 2.
- Reza, F. M. A Generalization of Foster's and Cauer's Theorems. - *IRE Convent. Rec.*, 1955, part. 2, circuit theory, p. 22, 5 figs.
- Richards, H. H. C. Carbon-pile regulator theory: calibration adjustment and factors affecting its operation. *Applic. and Ind.*, 1955, No. 16, p. 357-363.
- Rock, H. Toleranz geregelter Größen. *Regelungstechnik*, 1955, 3 Jg., Nr 11, S. 272-275, 2 Abb. Bibliogr. 3.
- Rosenbrock, H. H. An approximate method for obtaining transient response from frequency response. *Proc. Instn. Electr. Engrs.*, 1955, Nov., Pt. B, vol. 102, No. 6, p. 744-752, 16 figs., 4 tables.
- Rosenbrock, H. H. The integral of Error-Squared-Criterion for Servo Mechanisms. *Proc. Instn. Electr. Engrs.*, part B., 1955, Sept., vol. 102, No. 5, p. 602-607, 9 figs.,
- Salamon, M. Self-regulators. *Souhrn Práci o Automatizaci. Praha, Ceskoslovenska Akad. Ved.*, 1955, p. 343-404, 36 figs., Bibliogr. 5.
- Savant, Ch A. and Savant C. J. Electromechanical networks for a.c. servosystems. *Electronics*, 1955, vol. 28, No. 2, p. 190, 192, 194, 196.
- Saxe, R. F. Automatic control and display in impulse testing. *Proc. Instn. Electr. Engrs.*, 1955, May, vol. 102, part B, No. 2, p. 371-374, 7 figs.
- Schäffer, O. und Feissel W. Ein verbessertes Verfahren zur Frequenzgang - Analyse industrieller Regelstrecken. *Regelungstechnik*, 1955, Jg 3, Nr 9, S. 225-229, 8 Abb. Bibliogr. 8.
- Schmidt, S. F. and Triplett, W. C. Use of nonlinearities to compensate for the effects of a rate-limited servo on the response of an automatically controlled aircraft. *NACA, Techn. Note 3387*, 1955, Jan., 27 pages.
- Schöne, E. Spannungs- und frequenzgeregelter Prüffeldgeneratoren. *AEG Mitt.* 1955, Bd., 45, Nr 1/2., S. 69-78, 17 Abb. Bibliogr. 5.
- Schottländer, S. Über gemischte Regelungen. - *Z. angew. Math. und Mech.*, 1955, Nr 9-10, S. 334-336.
- Seidl, K. Dynamik der Synchronmaschine als Maßstab ihrer regeltechnischen Bemessung, Teil II. *Regelungstechnik*, 1955, 3 Jg., Nr 10, S. 248-254, 22 Abb.
- Silva, L. M. Predictor control optimizes control-system performance. - *Trans. ASME*, 1955, vol. 77, No. 8, p. 1317-1323, 10 figs., Bibliogr. 6.
- Singer, Dionys. Theoretical aspects of optimum controller operation. *Slaboproudý Obzor*, 1955, No. 3, Str. 120-125, 7 obr., 2 tables. Bibliogr. 4.
- Sklansky, J. and Ragazzini, J. R. Analysis of errors in sampled-data feedback systems. *Applic. and Ind.*, 1955, No. 18, p. 65-71.
- Smith, P. E. Design regulating systems by error coefficients. *Control Engng.*, 1955, Nov., vol. 2, No. 11, p. 69-74, 11 figs. Bibliogr. 2.
- Stabilité des Installations de regulation automatique. *Mesures et controle industr.*, 1955, Fevr., 20 année, No. 213, p. 99-103, 111.

- Stallard, D. V. A series method of calculating control-system transient response from the frequency response. *Applic. and Ind.*, 1955, No. 17, p. 61-64.
- Stein, W. A. and Thaler, G. J. Evaluating the effect of nonlinearity in a 2-phase motor. *Electr. Engng.*, 1955, Febr., vol. 74, No. 2, p. 142, 2 figs., *Applic. and Ind.*, 1955, No. 16, p. 518-521.
- Stephens, R. B. Main-Voltage Stabilizers. *Philips Techn. Rev.*, 1955, July, vol. 17, No. 1, p. 1-9.
- Die stetige Durchflussregelung zähiger Stoffe. *Regelungstechnik*, 1955, Jg. 3, Nr 5, S. 117, 1 Abb. 116
- Ströle, D. Messung von Frequenzgängen. *Regelungstechnik*, 1955, Jg. 3, Nr 8, S. 197-200, 5 Abb.
- Stubbs, G. S. A new method for designing the compensation of feedback control systems. *IRE Convent. Rec.*, 1955, part. 10, p. 66-77, 7 figs., Bibliogr. 9.
- Sze, T. W. and Calvert, J. F. Short-time memory devices in closed-loop system-steady state response. *Applic. and Ind.*, 1955, No. 21, p. 340-344.
- Thal-Larsen, H. Frequency response from experimental nonoscillatory transient response data. *Applic. and Ind.*, 1955, No. 18, p. 109-114.
- Thaler, G. J. Elements of servomechanism theory. N.Y., McGraw Hill Book Co., 1955, 282 p.
- Thomson, J. G. Linear feedback analysis. - N. Y., McGraw Hill Book Co., 1955, 255 pages.
- Török, V. Measurement and Automatics, 1955, t. 3, N 3, cmp. 66-80.
- Truxal, J. G. Automatic feedback control system synthesis. N.Y., McGraw-Hill, 1955, 675 pages.
- Tsien, H. S. and Serdengeci, S. Analysis of Peak-Holding Optimizing Control. *J. Aeronaut. Sci.*, 1955, Aug., vol. 22, No. 8, p. 561-570, 11 figs. Bibliogr. 3.
- Uebersax, H. Fernmesskanäle für Regelzwecke. *BBC - Mitteilungen*, 1955, Bd. 42, Nr 7-8, S. 271-274.
- Vallese, L. M. Analysis of backlash in feedback control system with one degree of freedom. *Applic. and Ind.*, 1955, No. 17, p. 1-4.
- Vazaca, Chr. Fundamental design principles in servomechanisms. *Electrotechnika*, 1955, Oct., vol. 3, N 10, p. 429-441, 13 figs.
- Veltman, B. P., Delft und Westcott, J. H. Bestimmung der Parameter eines Reglers durch ein einfaches Frequenzgangverfahren. *Regelungstechnik*, 1955, 3 Jg., H. 4, S. 95-100, 6 Abb. Bibliogr. 4.
- Vomstein, C. Neues Verfahren zur Zentralen Regelung der Dampfheizung. *Heizg. Lüftg. Haustechnik*, 1955, Bd. 6, Nr 1, S. 1-6.
- Walther, L. Die praktische Auswahl von Regelgeneräten. *Regelungstechnik*, 1955, 3 Jg., H. 12, p. 309-312, 4 Abb.
- Ward, J. E. Better synchro repeaters from damper-stabilized feedback. *Control Engng.*, 1955, July, vol. 2, No. 7, p. 90.
- West, J. C. and Douce, J. L. The mechanism of sub-harmonic generation in a feedback system. *Proc. Instn. Electr. Engrs.*, part. B., 1955, Sept., vol. 102, No. 5, p. 569-574, 8 figs. Bibliogr. 10.
- West, J. C. and Leonard, J. L. The necessary torque requirements for a servomotor. *J. Scient. Instrum.*, 1955, vol. 32, No. 1, p. 30-32.
- West, J. C. and Nikiforuk, P. N. The response of remote-position-control systems with hard-spring nonlinear characteristics to step-function and random inputs. *Proc. Instn. Electr. Engrs.*, 1955, Sept., part B, No. 5, p. 575-593, Discuss. Bibliogr. 20.
- Westburg, R. Powered control systems. *Aeronautics*, 1955, June, p. 54-59.
- Wünsch, G. Das Verhalten technischer Regelkreise in experimenteller Darstellung. *Konstruktion.*, 1955, Bd. 7, Nr 3, S. 85-91, 21 Abb. Bibliogr. 18.
- Zemanek, H. Die Universal - Relairechenmaschine (URRI) des Institute für Niederfrequenztechnik an der technischen Hochschule Wien. *Elektrotechnik und Maschinenbau*, 1955, Bd. 72, Nr 1, S. 6-12.
- Zwanziger, F. Speicherwerk und Grenzzeitwerk zur Auswertung von Impulsen für Überwachungs- und Regelaufgaben. *Elektrizitätswirtschaft*, 1955, Jg. 54, Nr 14, S. 462-463.

## V. ANALOGS TO CONTROL AND ADJUSTMENT SYSTEMS

- Benikov, V. A. and Ivanov-Smolensky, A. V. Development of physical analogs for electrical systems. *Electricity*, 1955, No. 8, pp. 1-10.
- Golubxhin, Yu. E. Typical nonlinearity units for automatic control analogs. Collection of papers from the student scientific society, Moscow Power Institute, Moscow, 1955, pp. 173-190.
- Kogan, B. Ya. Analogs to automatic control systems. *Trans. Acad. Defense Industry*, 1955, No. 2, pp. 80-124, 28 figs., 9 refs.

- Kogan, B. Ya. Analogs to automatic control systems when typical nonlinearities are present. *Automation and Remote Control*, 1955, 16, No. 2, pp. 113-128, 12 figs., 10 refs.
- Kogan, B. Ya. The electronic analog equipment of the Institute of Automation and Remote Control, Academy of Sciences, USSR. In 'Trans. 2nd. All-Union Conf. on the Theory of Automatic Control', 1955, vol. 3, pp. 47-69, 25 figs., 10 refs.
- Kostenko, M. P. and Urusov, I. D. Electrodynanic analogs to the hydroelectric generators at the Kuibyshev Hydroelectric Power Station. *Electricity*, 1955, No. 8, pp. 11-19, 10 figs., 7 refs.
- Kuzmichev, G. M. Study of electromechanical relay servos by electrical analog methods. In 'Collection of papers from the student scientific society, Penza Industrial Institute', 1955, pp. 24-66, 36 refs.
- Levitan, S. A. and Kaganov, V. Yu. An electromechanical analog to a hot object for studying automatic control systems. Moscow, 30 pp. Academy of Sciences USSR. Institute of Technico-Economic Information on Equipment and Test Facilities, Topic No./Fo, No-55-493.
- Malmin, A. A. Study of the behavior of a relay system via an electronic analog. *Automation and Remote Control*, 1955, 16, No. 6, pp. 542-547.
- Petrov, G. M. Linear electronic analogs produced by the Ministry of Machine and Equipment Production: experiments on their utilization. In 'Trans. 2nd. All-Union Conf. on the Theory of Automatic Control', 1955, vol. 3, pp. 39-46, 5 figs., 4 refs.
- Petrovsky, A. M. A review of methods of generating subacoustic random emfs. In 'Trans. 2nd. All-Union Conf. on the Theory of Automatic Control', 1955, vol. 3, pp. 105-107, 2 figs., 3 refs.
- Ushakov, V. B. Ultralow frequency apparatus for recording dynamic responses of automatic control systems. In 'Trans. 2nd. All-Union Conf. on the Theory of Automatic Control', 1955, vol. 3, pp. 147-162, 14 figs.
- Fialko, G. M. Producing analogs and calculating optimum parameters for automatic controls used in the chemical industry. In 'Trans. 2nd. All-Union Conf. on the Theory of Automatic Control', 1955, vol. 2, pp. 514-522, 11 figs.; bibliography pp. 521-522.
- Eterman, I. I. and Obuvalin, M. I. A method of solving characteristic equations on electronic analog equipment. *Automation and Remote Control*, 1955, 16, No. 6, pp. 554-555.
- Bühler, H. Modell zur Darstellung und Ausmessung der Reguliervhältnisse von Synchrongeneratoren, zwecks Bestimmung der günstigsten Spannungsregelung. *Bull. Oerlikon.*, 1955, Febr., Nr 308, S. 9-14, 18 Abb.
- Computer analysis of industrial control regulating systems. *Product Engng.*, 1955, June, vol. 26, No. 6, p. 314-315.
- Ferner, V. Über die Darstellung und Untersuchung von Regelungsvorgängen mit Hilfe von Modellregelstrecken. *Bergakademie, Z. Bergbau*, 1955, Bd. 7, Nr 4, S. 171-181.
- Johnson, E. F. and Bay, T. Application of pneumatic analog. *Industr. and Engng. Chem.*, 1955, vol. 47, No. 3, part. 1, p. 403-408.
- Klein, R. C. Analog simulation of sampled data systems. *Trans. IRE*, 1955 TRC-1, No. 2, p. 2-7.
- Singer, D. Use of analogs for solving control problems. *Souhrn Praci o Automatizaci. Praha, Ceskoslovenska Akad. Ved.*, 1955, p. 244-266, 20 figs. Bibliogr. 12.
- Wheeler, H. A. The potential analog applied to the synthesis of stagger-tuned filters. *Trans. IRE*, 1955, vol. CT-2, No. 1, p. 86-96. Bibliogr. 35.
- Winkler, H. Über eine elektronische Analogiemaschine zur Lösung von Differentialgleichungen höherer Ordnung und zur Untersuchung von Problemen der Regelungstechnik. *Wiss. Z. Hochschule für Electrotechnik, Ilmenau*, 1954-55, Nr 1, S. 15-27, 21 Abb. Bibliogr. 16.

(Continued in next issue)



## ON OPTIMUM TRANSIENT RESPONSE IN POWER-SATURATING SYSTEMS\*

E. A. Rozenman

(Moscow)

The paper solves the problem of determining the nature of the shortest transient response in power-saturating (heat saturating) systems. It is demonstrated that the optimum law for the variation of the actuating-motor current is almost linear for large heating time constants. A family of isochrone regions is plotted, and a comparison is made between the optimum transient response for power saturation and the optimum transient response for current saturation. It is demonstrated that in the case where the derived optimum law is utilized the transient response time can be substantially diminished for the same rated power.

Power saturation of elements in automatic control systems is one of the basic factors (along with other limitations, such as limitations with respect to the coordinates of a system with respect to their derivatives and with respect to their linear combinations) which determine the limiting speed of response of the system. Power saturation should be understood first of all as the bounding of the rated power which is determined by the amount of energy which can be dissipated in one or another element. In an actual automatic control system power saturation is germane to all elements of the system. However, in properly designed control systems the control elements must not limit the degree to which the rated power of the power element in the system can be utilized. Therefore it is of interest to examine systems in which power saturation is primarily germane to one element of the system — the power element. In order to be specific we shall assume that this element is an electric motor. In such a case power saturation means the bounding of the nominal rated power which is determined by the maximum allowable temperature to which the windings of the motor can be heated.

In this paper we shall examine the first part of the extensive problem of designing optimum (in the sense of their speed of response) automatic control systems with power saturation, namely: determining the shape of the shortest transient response. This problem is especially important with regard to systems which use drive machines to a high degree. Such systems include, for example, the main drive and auxiliary mechanisms in rolling mills, mine hoists, firing control systems, etc.

The methods for determining the nature of the optimum transient response for systems which are governed by specified conditions and are bounded with respect to their coordinates (in particular, with respect to the torque and speed of the actuating motor) were examined in a number of other papers [1-5]. Taking the heating limitations into account requires the use of other methods for the reasons indicated below.

The problem of determining the shape of the shortest transient response for a power saturating system consists of the following: for a given production operation (for example, for a given input-variation law) it is necessary to find a law for the time variation of the controlling quantity (for example, the current of a drive

\* Read at the All-Moscow Seminar on the Theory of Automatic Control in the Institute of Automation and Remote Control of the Acad. Sci. USSR on April 6, 1955.



rotor) which is such that it matches the power saturation requirement and at the same time guarantees that the operation will be completed in the minimum amount of time.

If we find that the allowable values of the system coordinates are exceeded for an optimum response which is determined in the above manner (for example, the values of the maximum torque or maximum speed of the motor), then still another problem arises in addition to the one indicated above — the problem of determining the optimum law for the variation of the controlling quantity while taking the indicated limitations into account.

### 1. Posing and Bounding the Problem

Let the power-saturating element be an electric motor whose torque is proportional to the current (for example, a dc motor with separate excitation). When the armature circuit inductance is neglected the motion of the motor can be described by the system of equations:

$$\frac{d\omega}{dt} = a_2(i - i_{\text{load}}), \quad \frac{d\varphi}{dt} = \omega, \quad (1)$$

where  $i$  is the armature current,  $i_{\text{load}}$  is the load current,  $\omega$  is the angular velocity,  $\varphi$  is the angular displacement. We should add the heating equation to System (1), this equation is of the following form if we assume that the motor is a homogeneous body:

$$\frac{d\tau}{dt} = a_1 i^2 - a_0 \tau, \quad (2)$$

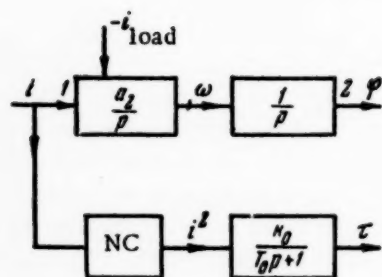


Fig. 1. Block diagram of the power section of the system:  $k_0 = a_1/a_0$ ,  $T_0 = 1/a_0$ ; NC is a quadrature converter.

where  $1/a_0 = T_0$  is the heating time constant, and  $\tau$  is the overheating (the motor temperature referred to the ambient temperature). These equations describe the motion of the power saturating section of the system without considering the inertia of the elements which belong to the control system and the supply sources of the motor. Figure 1 shows the block diagram of the indicated section of the system. The input coordinate is the armature current of the motor  $i$ , and the output coordinates are the angular velocity  $\omega$ , the angular displacement  $\varphi$  and the overheating of the winding  $\tau$ . The peculiar feature of the system being analyzed is that the relationship between the current and the overheating is quadratic; this fact substantially differentiates this problem from the problems examined in [1-5].

In a control system all coordinates are bounded. In this paper we shall examine the case where only one limitation is essential:  $\tau \leq \tau_m$ .

The formulation of the problem being examined depends substantially upon the nature of the controller input variation. If the input varies cyclically, then the conditions for which the shape of the optimum transient response is determined are limited to the confines of one cycle. When the input varies in a random non-cyclic manner a probability approach to the problem is necessary in order to establish the nature of the optimum transient response; this is true because the conditions which are used as a basis for determining the optimum response must include a prognosis of the possible nature of the input variation. In this paper we examine systems with a cyclic input-variation law which is characteristic for many units (mine hoists, the mechanisms used in rolling mills, etc.). For the indicated limitations the problem can be mathematically formulated in the following manner: It is required to find a time variation law  $i(t)$  which is such that the time  $t_{tr}$  for the system to shift from its initial state  $\varphi(0) = \varphi_0$ ,  $\omega(0) = \omega_0$  to the specified state  $\varphi(t_{tr}) = \varphi_f$ ,  $\omega(t_{tr}) = \omega_f$  is minimum. Under these conditions  $\tau(0) = \tau_0$ , and during the period  $t_{tr}$  the overheating  $\tau$  must not exceed the quantity  $\tau_m$ .



(i.e.,  $\tau \leq \tau_m$  for  $0 < t < t_{tr}$ ). It can be easily be shown that it is practical to choose  $\tau(t_{tr}) = \tau_m$ ,\* but this does not eliminate the possibility of  $\tau = \tau_m$  for  $t < t_{tr}$ .

Posing the problem in such a manner is tantamount to postulating a repetitive brief mode of operation during which the overheating that takes place during the motion of the system does not exceed the steady-state value (which is greater than  $\tau_m$ ); during the pause the overheating cannot diminish to zero but attains the value  $\tau_0$ . Without diminishing the generality of the results, it is possible to assume that  $\varphi_0 = 0$ ,  $\omega_0 = 0$  and  $\tau_0 = 0$ ; this corresponds to a parallel shift of the coordinate axes in the phase space ( $\varphi$ ,  $\omega$ ,  $\tau$ ). Initially let us assume that the duration of the working cycle is so small in comparison to the heating time constant that the heat transferred from the motor to the ambient medium can be neglected. Under these conditions  $a_0 = 0$ , and the motion of the system must be accompanied by a continuous increase in the overheating. If for  $t = t_{tr}$  we assume that  $\tau = \tau_m$ , then for  $t < t_{tr}$  it must be true that  $\tau < \tau_m$ . Thus, when the indicated assumptions are made the problem can be mathematically formulated as follows: It is necessary to find a function  $i(t)$  which is such that  $t_{tr}$  will be a minimum under the following conditions:

$$\begin{aligned} \varphi(0) &= 0, \quad \omega(0) = 0, \quad \tau(0) = 0, \\ \varphi(t_{tr}) &= \varphi_f, \quad \omega(t_{tr}) = \omega_f, \quad \tau(t_{tr}) = \tau_m. \end{aligned} \quad (3)$$

Here we should assume that  $a_0 = 0$  in Equation (2).

In [1-5] methods are given for plotting optimum transient responses for systems which can be described by equations of the type

$$\frac{dx_i}{dt} = f_i(x_i, x_{i+1}),$$

where  $x_{i+1}$  is the input coordinate of the  $i$ -th element and  $x_i$  is its output coordinate.

The functions  $f_i$  must satisfy the condition which requires that the derivative  $\partial f_i / \partial x_{i+1}$  maintain the same sign for any of the allowable values of the coordinates  $x_i$  and  $x_{i+1}$ . The optimum response in systems of this type consists of a definite number of intervals during which one of the bounded coordinates is maintained at the limiting level. This is due to the fact that when the condition requiring that the derivative  $\partial f_i / \partial x_{i+1}$  maintain the same sign is fulfilled, the monotonic increase of  $\partial x_i / \partial t$  is guaranteed when the input coordinate increases monotonically.

In the problem under discussion this condition is not fulfilled for one member. In fact, for the heating equation we have

$$f(i, \tau) = a_1 i^2 - a_0 \tau; \quad x_{i+1} = i.$$

The derivative  $\partial f / \partial x_{i+1} = 2a_1 i$  changes sign when the coordinate  $i$  varies.

## 2. The Optimum Transient Response

For the purposes of further investigation it is more practical to convert the equations to relative coordinates. Let us select the following quantities as base quantities:  $\omega_b$  is the angular velocity under ideal no-load conditions for the nominal applied voltage,  $\theta = I\omega_b / M_{s.c.}$  is the electromechanical time constant,  $\varphi_b = \omega_b \theta$  is the path which is traversed at the angular velocity  $\omega_b$  during a time  $\theta$ ,  $i_{s.c.}$  is the short-circuit current,  $\tau_m$

\* In fact,

$$\tau = \tau_0 + a_1 e^{-a_0 t} \int_0^t i^2(t) e^{a_0 t} dt$$

is the integral function of the current  $i(t)$ . It is evident that for  $\tau = \tau_m$  it is possible to select greater values of the current  $i(t)$  than for  $\tau < \tau_m$ , and therefore it is possible to reduce the transient response time.

is the limiting value of the overheating; the following definitions are used:  $t/\theta = \beta$  is the relative time,  $i/i_{s.c.} = z$  is the relative current,  $i_{load}/i_{s.c.} = z_{load}$  is the relative load current,  $\omega/\omega_b = y$  is the relative angular velocity,  $\varphi/\varphi_b = x$  is the relative displacement,  $\tau/\tau_m = \vartheta$  is the relative overheating.

Let us introduce the following additional relative parameters:  $\gamma = T_0/\theta$  is the relative heating time constant,  $\beta_h = t_h/\theta$  is a relative parameter which characterizes the specific heat of the motor (here  $t_h = \tau_m/a_1 i_{s.c.}^2$  is the time required for the short-circuit current to heat the motor up to an overheating value of  $\tau_m$  when there is no heat exchange).

Then the original system of equations will be written in the form

$$\frac{dy}{d\beta} = z - z_{load}, \quad \frac{dx}{d\beta} = y, \quad \frac{d\vartheta}{d\beta} = \frac{1}{\beta_h} z^2 - \frac{1}{\gamma} \vartheta, \quad (4)$$

where  $\vartheta \leq 1$ .

Let us first examine the case where  $z_{load} = 0$ . The problem formulated above is an Euler variational problem with a conditional extremum. In order to solve this problem the System (4) can be written more conveniently in integral form. For the case  $a_0 = 0$  ( $\gamma = \infty$ ) we have

$$y(\beta) = \int_0^\beta z(\zeta) d\zeta, \quad x(\beta) = \int_0^\beta (\beta - \zeta) z(\zeta) d\zeta, \\ \vartheta(\beta) = \frac{1}{\beta_h} \int_0^\beta z^2(\zeta) d\zeta. \quad (5)$$

Correspondingly, the bounding equations will be

$$\int_0^{\beta_{tr}} z(\zeta) d\zeta = y_f, \quad \int_0^{\beta_{tr}} (\beta - \zeta) z(\zeta) d\zeta = x_f, \\ \frac{1}{\beta_h} \int_0^{\beta_{tr}} z^2(\zeta) d\zeta = 1. \quad (5a)$$

The unknown function  $z(\beta)$  is found from the condition requiring that the functional

$$v = \beta_{tr} + \int_0^{\beta_{tr}} [\lambda_1 (\beta - \zeta) z(\zeta) + \lambda_2 z^2(\zeta) + \lambda_3 z(\zeta)] d\zeta, \quad (6)$$

must be a minimum (here  $\lambda_i$  are Lagrange multipliers).

The first variation of  $v$  is equal to

$$\delta v = \delta v(\beta_{tr}) + \delta v(z). \quad (7)$$

The extremal is found from the condition

$$\delta v = 0, \quad (8)$$

which subdivides into two:

$$\delta v(z) = 0 \text{ and } \delta v(\beta_{tr}) = 0. \quad (9)$$

The first of these equations determines the equation of the extremal (i.e., it determines the unknown law for the current variation). The second equation yields an auxiliary condition for determining the multipliers  $\lambda_1$ . From Equation (9) we find that

$$\lambda_1(\beta - \zeta) + 2\lambda_2 z + \lambda_3 = 0.$$

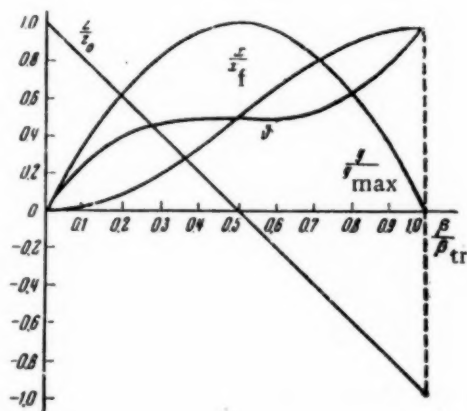
Replacing the variable of integration  $\zeta$  by the variable  $\beta$ , and assuming that  $z = z_0$  for  $\beta = 0$ , we find

$$z(\beta) = z_0 \left(1 - \frac{\beta}{\beta_a}\right), \quad (10)$$

where  $z_0$  and  $\beta_a$  are parameters of the response and are functionally associated with the Lagrange multipliers. It can easily be shown that the law  $z(\beta)$  which we have found for the current variation corresponds precisely to the minimum time  $\beta_{tr}$ . By integrating Equation (10) it is easy to find the laws governing the velocity variation, the path variation and the time variation of the overheating when the transient response is optimum:

$$\begin{aligned} y &= z_0 \beta \left(1 - \frac{\beta}{2\beta_a}\right), & x &= \frac{1}{2} z_0 \beta^2 \left(1 - \frac{\beta}{3\beta_a}\right), \\ \vartheta &= \frac{1}{\beta_{tr}} z_0^2 \left(\beta - \frac{\beta^2}{\beta_a} + \frac{\beta^3}{3\beta_a^2}\right). \end{aligned} \quad (11)$$

A characteristic feature of the optimum response which we have determined is the fact that it is depicted by smooth curves (with no angular vertices); this is in contrast to the optimum responses examined in [1-5].



The constants  $z_0$  and  $\beta_a$  (as well as the transient response time  $\beta_{tr}$ ) are determined from the boundary conditions and are found by substituting  $\beta = \beta_{tr}$  into the System (11):

$$\begin{aligned} z_0 \beta_{tr} \left(1 - \frac{\beta_{tr}}{2\beta_a}\right) &= y_f, & \frac{1}{2} z_0 \beta_{tr}^2 \left(1 - \frac{\beta_{tr}}{3\beta_a}\right) &= x_f, \\ \frac{1}{\beta_{tr}} z_0^2 \left(\beta_{tr} - \frac{\beta_{tr}^2}{\beta_a} + \frac{\beta_{tr}^3}{3\beta_a^2}\right) &= 1. \end{aligned} \quad (12)$$

For the particular case of  $y_f = 0$ , we find

$$\beta_a = \frac{1}{2} \beta_{tr}, \quad \beta_{tr} = \sqrt[3]{12 \frac{x_f^2}{\beta_h}}, \quad z_0 = \sqrt[3]{\frac{3}{2} \frac{\beta_h^2}{x_f}}. \quad (13)$$

Fig. 2. The optimum transient response.

In this case the transient response is symmetrical with respect to the instant  $\beta_{tr}/2$  (Incidentally, this is evident from the physical concepts involved; Figure 2).•

It is of interest to formulate and solve this problem in the phase space. Let us examine the system

$$\frac{dx}{d\beta} = y, \quad \frac{dy}{d\beta} = z, \quad \frac{d\vartheta}{d\beta} = \frac{1}{\beta_{tr}} z^2. \quad (14)$$

Let the phase trajectory of a symmetrical (for the sake of simplicity) optimum response be depicted upon

• In issue No. 6, 1956, of the journal "Electricity" a paper by K. I. Kozhevnikov was published in which this particular problem was evidently solved independently of the author.

the phase plane ( $y, z$ ) (Fig. 3). It is easy to show that the area  $S_{y,z}$ , which is bounded by this phase trajectory is proportional to the bounded value of the overheating.

In fact,

$$S_{y,z} = 2 \int_0^{y_{\max}} z dy = 2 \int_0^{\beta_{tr}} z^2 d\beta = 2\beta_h \int_0^{\frac{1}{2}} d\beta = \beta_h. \quad (15)$$

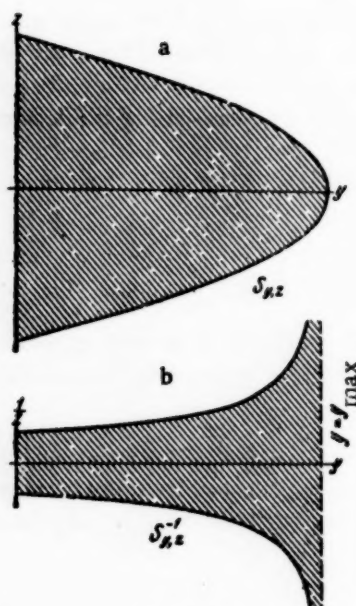


Fig. 3.

In addition,

$$2 \int_0^{y_{\max}} \frac{y}{z} dy = x_f. \quad (17)$$

Now the problem of determining the optimum response can be formulated thus: it is required to find a function  $z(y)$  which is such that the area  $S_{y,z}^{-1}$  is minimal under the following conditions:

$$S_{y,z} = \beta_h, \quad 2 \int_0^{y_{\max}} \frac{y}{z} dy = x_f.$$

The solution of this variational problem leads to the equation for the phase trajectory of the optimum process in the coordinates ( $y, z$ ):

$$z = \pm z_0 \sqrt{1 - \frac{y}{y_{\max}}}. \quad (18)$$

Here  $z_0$  and  $y_{\max}$  are functions of  $\beta_h$  and  $x_f$  and are determined from the bounding equation:

$$z = \sqrt{\frac{3}{2} \frac{\beta_h^2}{x_f}}, \quad y_{\max} = \sqrt[3]{\frac{9}{32} \beta_h x_f}. \quad (19)$$

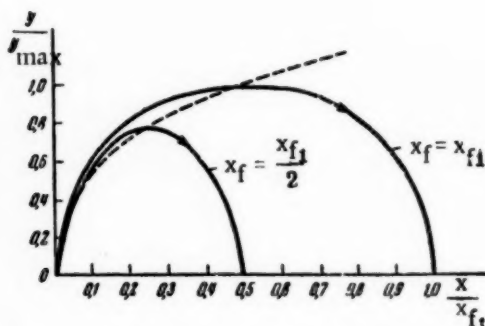


Fig. 4. Phase trajectories of the optimum responses.

The area  $S_{y,z}^{-1}$ , which is bounded by the inverse curve and the straight lines  $y = 0$  and  $y = y_{\max}$  is proportional to the transient response time:

$$S_{y,z}^{-1} = 2 \int_0^{y_{\max}} \frac{dy}{z} = 2 \int_0^{\beta_{tr}} d\beta = \beta_{tr}. \quad (16)$$

On the basis of Equations (18) it is possible to find the phase trajectory in the coordinates  $(x, y)$ :

$$x = \frac{x_f}{4} \left[ 2 \pm \left( 2 + \frac{y}{y_{\max}} \right) \sqrt{1 - \frac{y}{y_{\max}}} \right]. \quad (20)$$

It is depicted by a third-order curve (Fig. 4). Actually the curve does not intersect itself at the point  $\left( \frac{x}{x_f} = \frac{1}{2}; \frac{y}{y_{\max}} = -2 \right)$ . This becomes evident if we add a third coordinate  $\beta$  to the examined phase plane.

### 3. The Family of Isochrone Regions and its Structure

If we eliminate  $z_0$  and  $\beta_a$  from the System (12) and specify the values of  $\beta_h$  and  $\beta_{tr}$ , then we obtain one equation which provides the relationship between the coordinates  $x_f$  and  $y_f$  which represents the final state of the system; this equation is written in canonical form:

$$12x^2 - 12\beta xy + 4\beta^2 y^2 - \beta_h \beta^3 = 0 \quad (21)$$

(the subscripts for  $x_f$ ,  $y_f$  and  $\beta_{tr}$  are omitted in order to simplify the notation).

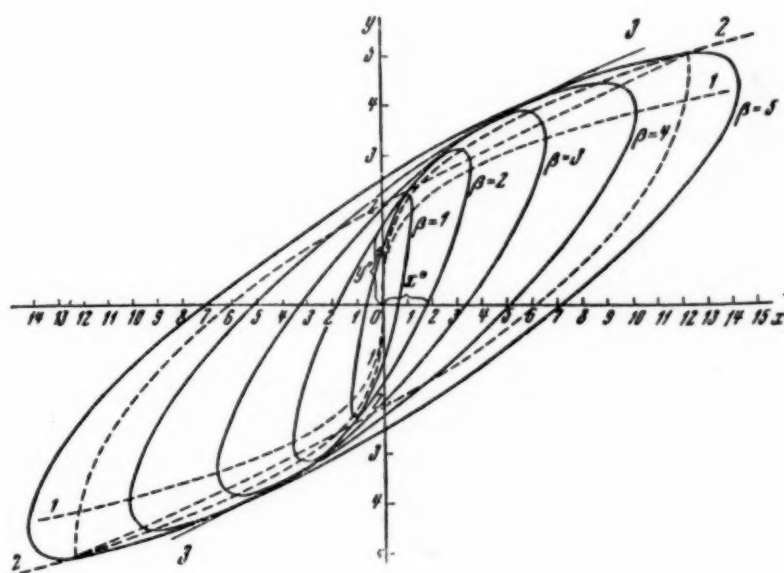


Fig. 5. a) Family of isochrone regions for the case  $a_0 = 0$ ,  $z_{\text{load}} = 0$ ,  $\beta_h = 5$ ; b) family of isochrone regions in the coordinates  $(x, y, \beta)$ .

This equation describes a single-parameter (with respect to the parameter  $\beta$ ) family of boundaries for the isochrone regions [2, 6] with a pole at the point  $(x = 0, y = 0)$ . For each value of the parameter  $\beta$  this equation determines the geometric locus of the points in the phase plane which are furthest from the initial state (pole); it takes a time equal to  $\beta$  for the system to arrive at these points for an optimum transient response which matches the limitations. A state which is described by a point which lies outside of the specified isochrone can be attained only during a time which is greater than the isochrone time. It can easily be seen that the curve defined by Equation (21) is an ellipse for a specified value of  $\beta$ ; the center of this ellipse is located at the origin, and the main axes are rotated through a certain angle with respect to the coordinate axes (Fig. 5, a). The sectors which are intercepted by the isochrone boundary on the coordinate axes are equal to

$$x^0 = \pm \sqrt{\frac{1}{12} \beta_h \beta^3} \quad y^0 = \pm \sqrt{\frac{1}{4} \beta_h \beta}. \quad (22)$$



When  $\beta \rightarrow \infty$ ,  $x^0$  and  $y^0$  increase monotonically.

In order to obtain a fuller characteristic of the structure of the isochrone family let us examine this family at certain points. We are interested first of all in points which are furthest from the coordinate axes, since they characterize the dimensions of the isochrone region. At points which are furthest from the  $y$  axis we have

$$\frac{dy}{dx} = \infty.$$

These points are disposed on the curve

$$y = \sqrt[3]{\frac{9}{8} \beta_h^3 x}, \quad (23)$$

which is the isocline of the family for  $\partial y / \partial x = \infty$  (Curve 1, Figure 5,a). The coordinates of these points are equal to

$$x^{(y)} = \pm \sqrt{\frac{1}{3} \beta_h^3} = 2x^0, \quad y^{(y)} = \pm \sqrt{\frac{3}{4} \beta_h^3}. \quad (24)$$

Correspondingly, points which are furthest from the  $x$  axis are disposed on the curve

$$y = \sqrt[3]{2 \beta_h^3 x}, \quad (25)$$

which is the isocline of the family for  $\partial y / \partial x = 0$  (Curve 2, Figure 5a). The coordinates of these points are equal to

$$x^{(x)} = \pm \sqrt{\frac{1}{4} \beta_h^3}, \quad y^{(x)} = \pm \sqrt{\beta_h^3}. \quad (26)$$

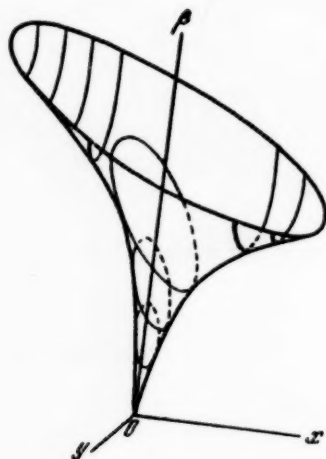


Fig. 5 b.

On the phase plane ( $x, y$ ) the above-mentioned points are disposed on Curve 3 (Fig. 5a) which is described by the equation

$$y = \sqrt[3]{\frac{4}{9} \beta_h^3 x}. \quad (27)$$

The family of boundary curves shown in Fig. 5a for the Isochrone Regions (21) consists of a series of ellipses which fit one inside the other; each of these ellipses is turned through a certain angle with respect to the neighboring one. Ellipses which are infinitely close have tangent points which are located on the curve mentioned above. These ellipses fill the entire phase plane ( $x, y$ ).

For convenience we shall add a third coordinate  $\beta_{tr}$  to the phase plane ( $x, y$ ). Then the family of isochrone regions will be depicted in the form of a twisted elliptical cone (Fig. 5, b) with its vertex at the origin. The region which corresponds to the specified values of  $\beta_{tr}$  is the cross-section of the cone which is produced by a plane that is a distance  $\beta_{tr}$  away from the plane ( $x, y$ ).



#### 4. Comparison with the Response Which Obtained for Constant Current

In order to perform a quantitative evaluation of the increase in the speed of response when the transient response is optimum, it is convenient to compare the response with the response which obtains for the case of constant current. We shall perform the comparison by comparing the boundaries of the isochrone regions while assuming that in both cases the bounded value of the overheating  $\tau_m$  is attained at the end of the transient response. Let us find the isochrone equation for the constant-current case. Let us assume that the system has passed from the state  $(x = 0, y = 0)$  to the state  $(x = x_f, y = y_f)$ . In the general case such a transition can occur over two intervals, where  $z = +z_m = \text{const}$  over one interval and  $z = -z_m = \text{const}$  over the other interval. We shall examine the duration of the first interval as an independent variable which varies within the limits of from 0 to  $\beta_{tr}$ . Then

$$y_f = z_m \beta_{tr} \left( 2 \frac{\beta_1}{\beta_{tr}} - 1 \right), \quad x_f = \frac{1}{2} z_m \beta_{tr}^2 \left( 4 \frac{\beta_1}{\beta_{tr}} - 2 \frac{\beta_1^2}{\beta_{tr}^2} - 1 \right), \quad (28)$$

where  $0 \leq \beta_1 / \beta_{tr} \leq 1$ .

Expression (28) determines the equation for the boundary of the isochrone region in parametric form. After  $\beta_1 / \beta_{tr}$  has been eliminated, we find

$$y_f = z_m \beta_{tr} \left[ 1 + \sqrt{2 \left( 1 - \frac{2x_f}{z_m \beta_{tr}^2} \right)} \right]. \quad (29)$$

Equation (29) describes two intersecting parabolic segments on the phase plane; these parabolas bound the closed space represented by the isochrone region.

Let  $z_m$  be selected in such a way that at the end of the transient response (when  $\beta = \beta_{tr}$ ) an overheating which is equal to  $\tau = \tau_m$  is attained. Then

$$\frac{1}{\beta_h} z_m^2 \beta_{tr} = 1, \quad (30)$$

$$y = \sqrt{\beta_h \beta_{tr}} \left[ 1 \pm \sqrt{2 \left( 1 - \frac{2x}{\beta_{tr} \sqrt{\beta_h \beta_{tr}}} \right)} \right]. \quad (31)$$

It is not difficult to see that the Isochrones (21) and (31) have solitary common points with the coordinates:  $x = \frac{1}{2} \sqrt{\beta_h \beta^3}$ ,  $y = \sqrt{\beta_h \beta}$  and  $x = -\frac{1}{2} \sqrt{\beta_h \beta^3}$ ,  $y = -\sqrt{\beta_h \beta}$ .

These points correspond to the case where the transient response consists of only one interval. By substituting the values of the coordinates for the points where Isochrones (21) and (31) meet into System (12), and by taking Equation (30) into account, we find the values for the parameters  $\beta_a$  and  $z_0$  of the transient response at these points:  $\beta_a = \infty$ ,  $z_0 = z_m$ .

This means that the straight line which determines the current-variation law at these points is parallel to the axis of abscissas, and thus the optimum transient response which is determined on the basis of the heating limitation coincides with the optimum transient response which obtains for constant current:  $|z| = z_m$ .

In Fig. 5, a the isochrone for  $\beta = 5$  is given for the purposes of illustration; it has been plotted on the basis of Equation (31). The figure shows that it meets the corresponding Isochrone (21) at the two points mentioned above.

From Figure 5, a it follows, for example, that a linear law of current variation for the case  $y_f = 0$  yields up to a 15% advantage in path, as compared to the transient response which obtains for  $|z| = \text{const}$ ; when the values of the specified paths are identical, such a law makes it possible correspondingly to lower the power rating of the installation. Let us find the relationship between the initial value  $z_0$  for an optimum transient response and the current  $z_m$ . It is evident that when  $\tau_m$  is identical for both cases it is always true that

$z_0 \geq z_m$ . On the basis of Equations (13) and (30) we find that  $z_0 = \sqrt{3z_m}$  for the case where  $y = 0$  at the end of the response.

Thus, for an optimum transient response where  $y_f = 0$ , the starting current which is required is approximately 70% greater; however, this current decreases rapidly. The increased starting current occurs only when the speed of the motor is small. For a dc motor this is essential, since at small speeds the commutation conditions, as we know, are more favorable.

### 5. Structure of the Family of Isochrone Regions when a Load is Present

Let us examine the problem of the optimum transient response when the motor is loaded; we shall assume that  $z_{load} = z_{load}(\beta)$  in Equation (4). Over the sector 1-2 (Fig. 1) the examined system is linear. Applying the principle of superposition, it is possible to represent the coordinates  $\underline{x}$  and  $\underline{y}$  in the form of two components:

$$x = x_z + x_{z_{load}}, \quad y = y_z + y_{z_{load}}. \quad (32)$$

Here  $x_z$  and  $y_z$  are components which depend upon the optimum motor-current variation law  $z(\beta)$ ;  $x_{z_{load}}$  and  $y_{z_{load}}$  are components which depend upon the law governing the load variation  $z_{load}(\beta)$ . Let us compute each of the components independently.

It is evident that there is a relationship between the components  $x_z$  and  $y_z$  which is determined by Equation (21) for the isochrone boundary in the case  $z_{load} = 0$ . In fact, the nature of the optimum law of variation  $z(\beta)$  cannot depend upon the load because of the linearity of the sector 1-2 of the system. This can easily be proven by repeating the derivations of Section 2 in the case being examined here. For the assumptions which we have made ( $a_0 = 0$ ) the optimum current-variation law is still linear when a load is present.

The components  $x_{z_{load}}$  and  $y_{z_{load}}$  can be computed by integrating the System (4) independently of  $\underline{z}$  (i.e., for  $z = 0$ ):

$$y_{z_{load}} = - \int_0^\beta z_{load}(\beta) d\beta, \quad x_{z_{load}} = \int_0^\beta y_{z_{load}} d\beta. \quad (33)$$

For the particular case  $z_{load} = \text{const}$ , we have

$$y_{z_{load}} = -z_{load}\beta, \quad x_{z_{load}} = -\frac{1}{2} z_{load}\beta^2. \quad (34)$$

Let us find the equation for the boundary of the isochrone region in the case  $z_{load} = \text{const}$ . For this purpose we shall substitute the following quantities for the variables  $\underline{x}$  and  $\underline{y}$  in Equation (21):

$$x_z = x - x_{load} \quad \text{and} \quad y_z = y - y_{load}. \quad (35)$$

Then the isochrone equation in canonical form is written as

$$12x^2 - 12\beta xy + 4\beta^2 y^2 + 2\beta^3 z_{load} y + \beta^3 (\beta z_{load}^2 - \beta_h) = 0. \quad (36)$$

When  $z_{load} = 0$  it reduces to (21).

For a fixed value ( $z_{load} = \text{const}$ ) Equation (36) describes a single-parameter family of ellipses just as in the case of Equation (21). However, in contrast to (21), the centers of the ellipses are not concentrated at the origin but are disposed along the curve:

$$y_c = \mp \sqrt{2z_{load}} x_c \quad (37)$$

(the "-" sign corresponds to the case  $z_{load} > 0$ , and the "+" sign corresponds to the case  $z_{load} < 0$ .)

For a specified value of  $\beta$  the coordinates of the center are respectively equal to

$$x_c = x_{z_{load}}, \quad y_c = y_{z_{load}} \quad (38)$$

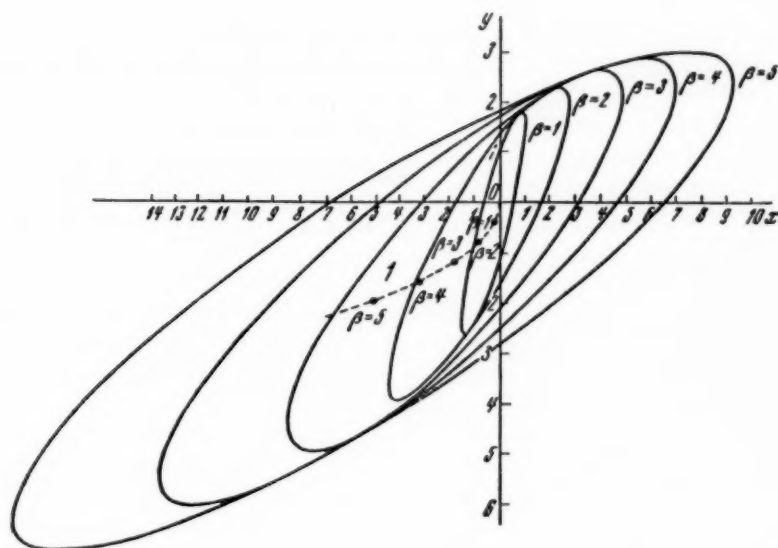


Fig. 6.

The coordinates of the center therefore determine the point on the phase plane at which the system arrives after a time  $\beta$  due to the effect of the load alone when the motor current is equal to zero (the load is assumed to be resistive). It is also evident that if the origin is placed at the center of the Ellipse (36) by a parallel shift of the axes, the equation for this ellipse will be identical to Equation (21). This means that for each value of  $\beta$  and  $z_{load} \neq 0$  the isochrone regions are constant in shape and are oriented in the same manner as the isochrone regions which obtain for  $z_{load} = 0$ . The difference consists solely in the fact that the center of the isochrones which obtain for  $z_{load} \neq 0$  is located at the point  $(x = x_{z_{load}}, y = y_{z_{load}})$ . Figure 6 shows the family of isochrone regions when the following parameters obtain:  $a_0 = 0$ ;  $z_{load} = 0.4$ ;  $\beta_h = 5.0$ . Curve 1 is the geometric locus of their centers.

## 6. The Region of Attainable States

As we have indicated, when  $z_{load} = 0$  the isochrones fill the entire phase plane densely. Therefore for a sufficiently large  $\beta$  any state can be attained by this system. When  $z_{load} \neq 0$ , the "growth" of the isochrone regions with an increase of  $\beta$  is accompanied by a simultaneous displacement of their centers in a corresponding direction: when  $z_{load} > 0$ , the displacement is into the III quadrant of the plane  $(x, y)$ , and when  $z_{load} < 0$ , the displacement is into the I quadrant.

Let us draw a beam of vectors in various directions from the origin (the initial state of the system, or the pole of the isochrone). When the isochrone time  $\beta$  increases, the moduli of the vectors which are pointed in the direction of the displacement of the isochrone centers will also increase. The moduli of the vectors which are pointed in other directions will at first increase when  $\beta$  increases (due to the "growth" of the isochrone regions) and will then decrease (due to the displacement of the centers). For specified values of  $\beta$  the moduli of the corresponding vectors attain a maximum. The geometric locus of the ends of vectors with maximum moduli limits the region (on the phase plane) of states which are in general attainable for the system when the value of the load is specified and there is no heat exchange. This region is evidently open-ended, and this can easily be clarified by means of Fig. 6.

On the plane  $(x, y)$  the curve which bounds the region of attainable states is the envelope of a family of

isochrones which can be found by eliminating the parameter  $\beta$  from the system

$$\psi(x, y, \beta) = 0, \quad \frac{\partial \psi}{\partial \beta} = 0, \quad (39)$$

where  $\psi(x, y, \beta) = 0$  is the equation for the isochrone boundary.

The computation of the curve is substantially simplified when the substitution  $x = c\beta y$  is made. Figure 7 shows the region of attainable states for  $\beta_h = 5$  and  $z_{load} = 0.2$ . The corresponding values of  $\beta$  are noted on the curve.

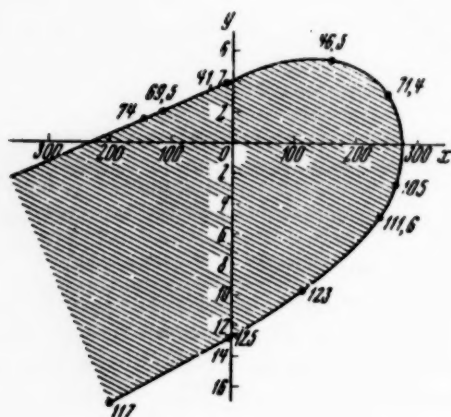


Fig. 7.

sector over which  $|z| = z_a = \text{const}$ , and during which the overheating no longer varies (i.e.,  $\Phi = 1 = \text{const}$ ). The conditions under which such a response can occur are found by means of the family of isochrone region boundaries.

Let the system be required to pass from its initial state  $(x_0, y_0)$  to the specified state  $(x_f, y_f)$  in the shortest time. The optimum transient response will be fully determined if we find the coordinates  $(x_m, y_m)$  of the bounding state of the system, which separates these sectors. For this purpose the following is necessary.

a) We must determine the shape of the optimum transient response for the first sector when  $a_0 = 0$  by assuming that the bounded value of the overheating  $\Phi = 1$  is attained at the end of this sector. The problem of finding the shape of the optimum transient response for this case is solved in a manner analogous to the case where  $a_0 = 0$  (Appendix I). The optimum current variation law is described by the equation

$$z = z_0 \left(1 - \frac{\beta}{\beta_a}\right) e^{\frac{-\beta}{\gamma}} \quad (41)$$

and its deviation from the Rectilinear Law (10) is the greater, the smaller the heating time constant.

b) We must determine the shape of the optimum transient response for the second sector by assuming that the bounded value of current is constant in absolute magnitude and equal to  $|z| = z_a$ .

c) We must plot two families of isochrone region boundaries that correspond to the two current-variation laws  $z(\beta)$  over the first and second sectors. The structure of the family of isochrone regions for the first sector is analogous to the families shown above (Fig. 5,a) (see Appendix I). Figure 8 shows the family of isochrone regions for the first sector where  $\beta_h = 1$ ,  $\gamma = 5$ ,  $z_{load} = 0$ .

The family of isochrone regions for the second sector is analogously described in [2] (see Appendix II).

Let us place the pole of the isochrone family of the first sector at the point representing the initial state of the system; we place the pole of the isochrone family of the second sector at the point representing the final state.

## 7. The Method for Determining the Optimum Transient Response when Heat Exchange is Taken into Account

When heat exchange is present we may have prolonged operation without the accumulation of overheating (i.e., with  $\tau = \tau_m = \text{const}$ ). For this to be true the current must not exceed the value

$$z_a = \sqrt{\frac{\beta_h}{\gamma}}; \quad (40)$$

this can easily be seen from the third equation of the System (4). From this it follows that the optimum transient response for  $a_0 \neq 0$  may consist of two sectors: 1) the sector over which  $z = z(\beta)$  and during which the overheating monotonically attains the limiting value ( $\Phi = 1$ ), and 2) a



Of all the possible combinations between isochrones of the first and second families, only such pairs of isochrones as have one common point (see Appendix III) can correspond to the optimum transient response.

Practically, the problem of finding the pair of tangent isochrone region boundaries with the minimum (or close to minimum) transient response time  $\beta_{tr} = \beta_1 + \beta_2$  can be solved in the following manner. The family of isochrones for the second sector (for  $\Phi = 1$ ) is copied on tracing paper. The pole of this family is superimposed upon the point which depicts the specified final state of the system on the graph which depicts the family of isochrone regions of the first sector. When the network of isochrone regions is sufficiently dense it is no problem to select that pair of tangent isochrones for which the time  $\beta_{tr} = \beta_1 + \beta_2$  is minimum. The conditions for the existence of an optimum transient response that consists of two sectors are given in Appendix IV in analytical form. By means of the method described here the author solved a large number of problems involving the determination of the optimum transient response in the presence of heat exchange within the framework of the assumptions which have been made (when only heating saturation is taken into account). Systems were examined that had various parameters which were of practical interest; the systems were subjected to various loads.

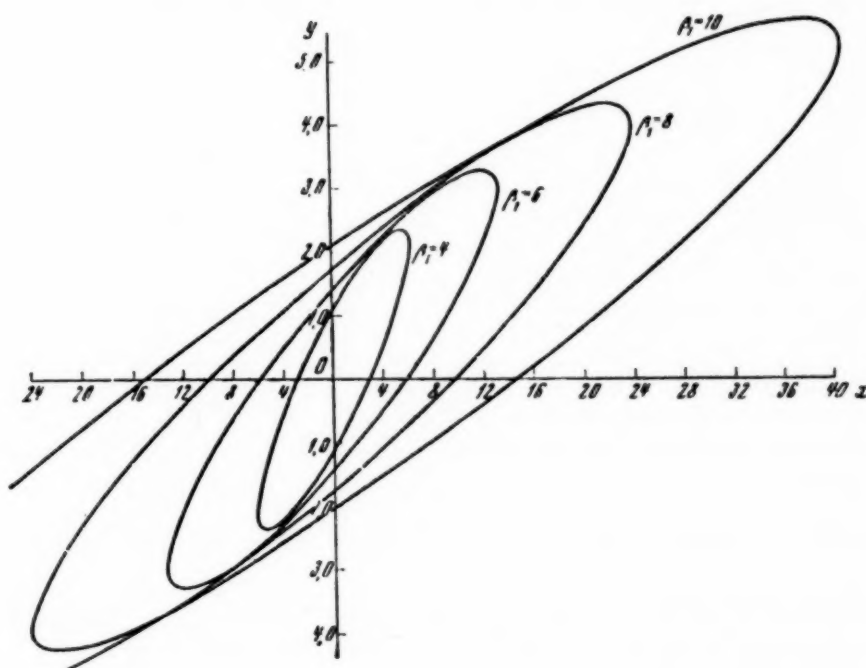


Fig. 8.

In all cases the optimum response proved to consist only of the first sector defined by Equation (41).

The author expresses his appreciation to A. Ia. Lerner for the valuable advice which he accorded during the preparation of this paper.

#### APPENDIX I

##### Shape of the Optimum Response for the First Sector

The problem of finding the optimum response for the first sector is analogous to the problem examined earlier as far as its mathematical formulation is concerned. It is necessary to find the law  $z(\beta)$  which guarantees a minimum time  $\beta_1$  for the transition of a system whose motion is described by the system of Equations (4) from its initial state  $x(0) = 0$ ,  $y(0) = 0$ ,  $\Phi(0) = 0$  to a specified state  $x(\beta_1) = x_m$ ,  $y(\beta_1) = y_m$ ,  $\Phi(\beta_1) = 1$  when the following conditions obtain:

$$\int_0^{\beta_1} z(\zeta) d\zeta = y_m, \quad \int_0^{\beta_1} (\beta_1 - \zeta) z(\zeta) d\zeta = x_m, \quad \frac{1}{\beta_h} e^{-\frac{\beta_1}{\gamma}} \int_0^{\beta_1} z^2(\zeta) e^{\frac{\zeta}{\gamma}} d\zeta = 1. \quad (I.1)$$

The optimum current-variation law  $z(\beta)$  is found from the condition governing the minimum of a functional which is composed in a manner analogous to Equation (6):

$$v = \beta_1 + \lambda_1 \int_0^{\beta_1} (\beta_1 - \zeta) i(\zeta) d\zeta + \lambda_2 \int_0^{\beta_1} i(\zeta) d\zeta + \lambda_3 e^{-\frac{\beta_1}{\gamma}} \int_0^{\beta_1} i^2(\zeta) e^{\frac{\zeta}{\gamma}} d\zeta. \quad (I.2)$$

When  $z(0) = z_0$ , the optimum current-variation law is written in the form

$$z = z_0 \left( 1 - \frac{\beta}{\beta_a} \right) e^{-\frac{\beta}{\gamma}}. \quad (I.3)$$

The values of  $z_0$ ,  $\beta_a$  and the response time  $\beta_1$  are found from the bounding conditions (I.1). Then by eliminating  $z_0$  and  $\beta_a$  from the system of algebraic equations which is obtained as a result of integration, we find the equation for the family of isochrone boundaries which can be written in the form

$$x^2 - Axy + By^2 - C = 0, \quad (I.4)$$

where

$$A = -2\gamma \frac{1 - q - \frac{\beta_1}{\gamma}}{1 - q}, \quad B = 2\gamma^2 \frac{1 - q - \frac{\beta_1}{\gamma} + \frac{\beta_1^2}{2\gamma^2}}{1 - q},$$

$$C = \beta_h \gamma^2 \frac{(1 - q)^2 - \frac{\beta_1^2}{\gamma^2} q}{q(1 - q)} \quad (q = e^{-\frac{\beta_1}{\gamma}}).$$

Structurally this equation does not differ from (21). For each value of  $\gamma$  it describes a family of ellipses which fit one inside the other and whose axes are mutually rotated with respect to one another; these ellipses fill the entire phase plane ( $x, y$ ).

When  $\gamma \rightarrow \infty$  ( $a_0 \rightarrow 0$ ), Equation (I.4) reduces to (21), and the optimum current-variation law  $z(\beta)$  becomes linear.

When a load is present ( $z_{load} \neq 0$ ) the nature of the transient response does not change (this is the same as before). Only the parameters  $z_0$  and  $\beta_a$  have other values. The center of the isochrone region (just as in the case of  $a_0 = 0$ ) is shifted to the point  $(x_{zload}, y_{zload})$ .

When  $z_{load} = \text{const}$ , the equation for the isochrone region is of the form:

$$x^2 - Axy + By^2 - C + ax + by + d = 0, \quad (I.5)$$

where

$$a = z_{load} \beta_1 \left( 2\gamma - \beta_1 \frac{1 + q}{1 - q} \right),$$

$$b = z_{load} \beta_1 \left( 4\gamma^2 + \frac{\beta_1^2}{1 - q} - \beta_1 \gamma \frac{3 + q}{1 - q} \right),$$

$$d = z_{load}^2 \beta_1^2 \left( \frac{\beta_1^2}{4} + 2\gamma^2 - \beta_1 \gamma \frac{1 + q}{1 - q} \right).$$



## APPENDIX II

### The Shape of the Optimum Transient Response for the Second Sector

Over the second sector the transient response occurs for a constant current. The equation of the family of isochrone regions for this sector is analogous to (29), but the quantity  $z_m$  should be replaced by  $z_a = \sqrt{\beta_h/\gamma}$ , and the coordinate  $x$  should be replaced by  $x_f - x$ . Then we obtain

$$y^2 + 4z_a(x_f - x) - 2z_a\beta_2y - z_a^2\beta_2^2 = 0, \quad (II.1)$$

When a load is present the center of the region (just as in the cases examined above) is shifted to the point  $(x_{z_{load}}, y_{z_{load}})$ , where for the case under investigation we have

$$x_{z_{load}} = \frac{1}{2} z_{load} \beta_2^2, \quad y_{z_{load}} = z_{load} \beta_2.$$

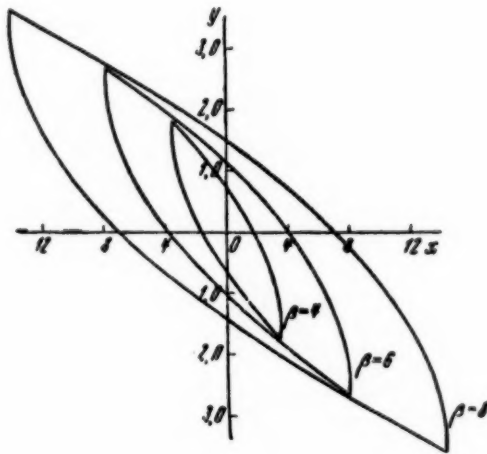


Fig. 9.

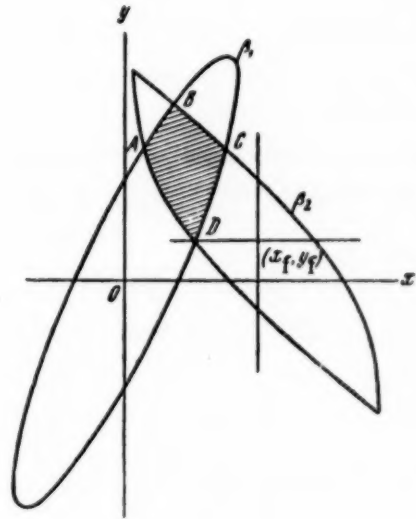


Fig. 10. Intersection of the isochrone regions.

When  $z_{load} = \text{const}$ , the equation for the family of isochrone regions is of the form:

$$y^2 + 4z_a(x_f - x) - 2z_a\beta_2y - z_a^2\beta_2^2 - 2z_{load}\beta_2y + \beta_2^2 z_{load}^2 = 0. \quad (II.2)$$

The points of the Family (II.2) which are furthest from the straight line  $x = x_f$  are disposed along the parabola

$$y = \pm \sqrt{2(z_a + z_{load})(x_f - x)}, \quad (II.3)$$

where the "+" sign corresponds to  $x_f - x > 0$ , and the "-" sign corresponds to  $x_f - x < 0$ .

Figure 9 shows the family of isochrone regions for the second sector when the following parameters obtain:  $\beta_h = 1.0$ ,  $\gamma = 5$ ,  $z_{load} = 0$ .

## APPENDIX III

In the general case two isochrones which belong to different families can intersect in the manner shown in Fig. 10. Let the process involved in the transition of the system from its initial state  $(0,0)$  to the specified

state  $(x_f, y_f)$  consist of the above-mentioned two sectors. We shall prove the following postulates: if a pair of isochrone regions from Families I and II having isochrone times of  $\beta_1$  and  $\beta_2$ , respectively, have sections of area which belong to both isochrone regions, then the optimum transient response time is  $\beta_{tr} < \beta_1 + \beta_2$ .

In fact, a transient response with the duration  $\beta_{tr} = \beta_1 + \beta_2$  can only occur in a case where the points A, B, C and D are chosen as boundary points (these points represent the boundary intersections of the isochrone regions). However, in such a case the transient response will not be optimum, since for any point which lies inside the region ABCD and has been chosen as a boundary point the time taken up by the first sector is  $\beta_I < \beta_1$ , and the time taken up by the second sector is  $\beta_{II} < \beta_2$ . This is true because for a specified transient response the time required for the system to make the transition from its initial state to the point which lies inside the region is always less than the time required for the system to shift to a point which lies on the boundary of the region. For the segments AB and DC we have:  $\beta_I = \beta_1$ ,  $\beta_{II} < \beta_2$ ; for the sectors AD and BC we have  $\beta_I < \beta_1$ ,  $\beta_{II} = \beta_2$ .

Thus the postulate is proven.

#### APPENDIX IV

##### On the Conditions Required for the Existence of an Optimum Transient Response Which Consists of Two Sectors

As we have indicated, only a pair of isochrones which have one common point can correspond to an optimum transient response.

Let us draw the tangent to the boundary of the region representing the first sector at the point  $M(x_m, y_m)$  where the isochrone regions touch (Fig. 11). Let us examine two cases of tangency between the two isochrone regions.

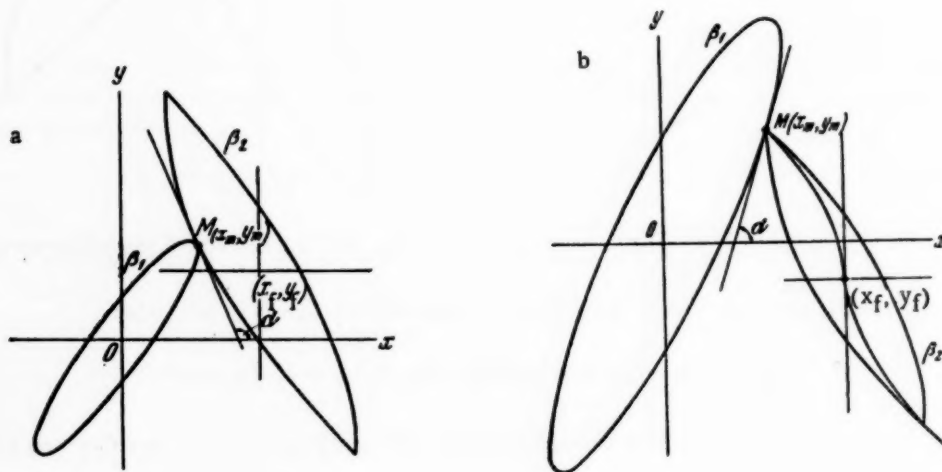


Fig. 11.

1) If the angle  $\alpha$  which is formed by this tangent line with the  $x$  axis is greater than  $90^\circ$ , then the isochrone of the first sector is tangent to the lower branch of the isochrone of the second sector (this is shown in Fig. 11, a). Here the tangent which is drawn to the point  $M$  will be simultaneously tangent to the isochrone of the second sector. Let  $\psi(x, y, \beta_1) = 0$  and  $\varphi(x, y, \beta_2) = 0$  be the equations for the boundaries of the isochrone regions of the first and second sectors respectively. Therefore at the point  $M$  with the coordinates  $(x_m, y_m)$  we have

$$\psi(x_m, y_m, \beta_1) = 0, \quad \varphi(x_m, y_m, \beta_2) = 0, \quad \left(\frac{\partial y}{\partial x}\right)_M^\psi = \left(\frac{\partial y}{\partial x}\right)_M^\varphi < 0. \quad (\text{IV.1})$$

If we do not impose any additional conditions, then the System (IV.1) determines the entire ensemble of points  $M(x_m, y_m)$  at which corresponding isochrones are tangent. From among all of these points it is necessary to select a point which is such that the response time  $\beta_{tr} = \beta_1 + \beta_2$  is minimum.

After we have eliminated  $x_m$  and  $y_m$  from the System (IV.1), let us assume that we obtain one equation which has been solved with respect to  $\beta_1$ :  $\beta_1 = f(\beta_2)$ . This equation can be rewritten in the form  $\beta_{tr} = \beta_1 + \beta_2 = \beta_2 + f(\beta_2)$ .

The condition for the minimum  $\beta_{tr}$  will be

$$\frac{\partial \beta_{tr}}{\partial \beta_2} = 0 \quad \text{or} \quad \frac{\partial f(\beta_2)}{\partial \beta_2} = -1. \quad (\text{IV.2})$$

The resulting condition can be used together with (IV.1) to determine the coordinates of the point M and the values of  $\beta_1$  and  $\beta_2$  for which  $\beta_{tr}$  will be a minimum.

2) If the angle  $\alpha < 90^\circ$ , then the isochrone of the II family can be tangent to the isochrone of the I family only at the vertices of family II; this is true since these points are furthest from the vertical straight line  $x = x_f$  (Fig. 11,b). In that case all of the points  $M(x_m, y_m)$  at which the isochrones are tangent are disposed on a second-order parabola  $U(x_m, y_m) = 0$ , which is the geometric locus of the points which are furthest from the straight line  $x = x_f$ . The coordinates of the points of tangency for pairs of isochrones are determined by the system of equations

$$\psi(x_m, y_m, \beta_1) = 0, \quad U(x_m, y_m) = 0. \quad (\text{IV.3})$$

Augmenting (IV.3) by the equation for the isochrone of the second sector  $\varphi(x_m, y_m, \beta_2) = 0$ , we again find  $\beta_1 = f(\beta_2)$  and then determine the condition for the minimum  $\beta_{tr}$  (IV.2).

Received September 25, 1956

#### LITERATURE CITED

- [1] A. Ia. Lerner, Improving the Dynamic Properties of Automatic Compensators by means of Nonlinear Loops. I. Automation and Remote Control, Vol. XIII, No. 2, 1952.
- [2] A. Ia. Lerner, The Limiting Speed of Response of Automatic Control Systems. Automation and Remote Control, Vol. XV, No. 6, 1954.
- [3] A. A. Fel'dbaum, Optimum Responses in Automatic Control Systems. Automation and Remote Control, Vol. XIV, No. 6, 1953.
- [4] V. V. Solodovnikov, Synthesis of Corrective Networks for Servosystems by Means of Optimum and Typical Logarithmic Frequency Responses. Automation and Remote Control, Vol. XIV, No. 5, 1953.
- [5] A. M. Hopkin, A Phase-Plane Approach to the Compensation of Saturating Servomechanisms. Trans. AIEE, Vol. 70, No. 1, 1951.
- [6] A. B. Naishul' and V. A. Svetlitsky, Determining the Configuration of the Region of Possible Solutions for Systems of Linear Differential Equations. Applied Math. and Mech., Vol. XX, No. 1, 1956.

# DETERMINING THE COEFFICIENTS OF TRANSFER FUNCTIONS FOR LINEARIZED AUTOMATIC CONTROL ELEMENTS AND SYSTEMS

M. P. Simoiu

(Moscow)

A method is given for determining the coefficients of transfer functions from experimental curves which are plotted for the transient responses of linearized automatic control elements and systems. A method for applying this procedure to the problem of approximating of complex transfer functions by means of simpler ones is given. The theory is clarified by means of an example.

In performing an analytical investigation of an automatic control system the derivation of the differential equation for the controlled object is often associated with appreciable difficulties. In a number of cases the complexity of the resulting equations makes its practical utilization inconvenient. At the same time it is usually possible to make an experimental determination of the response of the system to a specified perturbation; thus we are confronted with the problem of determining the transfer function of the system according to these experimental curves. A number of papers [1-4] have been devoted to the methods of determining the coefficients of the differential equations and of the transfer functions from experimental dynamic characteristics. These methods either have a limited applicability or suffer from organic shortcomings.

In this paper we develop a method for using the experimental curve of the transient response to determine the coefficients of a transfer function which approximates the actual transfer function of the system to the desired degree of accuracy. In addition, we provide a method for utilizing this procedure in order to approximate complex transfer functions by means of simpler ones.

## 1. Approximation of the Transient Function

Let us prove that any transient function can be approximated to the desired degree of accuracy by the transient function of a system whose transfer function is fractionally rational (this is the same as solving a differential equation with constant coefficients). Let us assume that

$$\overline{\varphi(t)} = \frac{k}{W(p)} \frac{1}{p}, \quad (1)$$

where  $\varphi(t) = \int_0^{\infty} \varphi(t) e^{-pt} dt$  is the Laplace transform of the transient function  $\varphi(t)$ ,  $k$  is the gain coefficient, and  $k/W(p)$  is the transfer function.

In the case of a system with lumped constants\*

$$W(p) = \frac{\overline{a}_n p^n + \overline{a}_{n-1} p^{n-1} + \dots + \overline{a}_1 p + 1}{b_n p^n + b_{n-1} p^{n-1} + \dots + b_1 p + 1}. \quad (2)$$

\* Certain of the higher-order coefficients  $b_n, \dots, b_m$  may be equal to zero.

Without violating the generality of our analysis, we shall henceforth assume that  $W(p)$  has no singularities at the point  $p = 0$ . Keeping this in mind, we expand  $W(p)$  into a power series with respect to  $p$ :

$$W(p) = 1 + \sum_{i=1}^{\infty} a_i p^i. \quad (3)$$

Limiting ourselves to the first  $n$  terms in the Expansion (3), we obtain an approximating function  $\varphi_n$  for which

$$\overline{\varphi_n} = \frac{k}{W_n(p)} \frac{1}{p}, \quad (4)$$

where  $W_n(p) = 1 + \sum_{i=1}^n a_i p^i$ .

Subtracting (1) from (4), we obtain

$$\overline{\varphi_n} - \overline{\varphi} = \frac{W(p) - W_n(p)}{W_n(p) W(p)} \frac{k}{p} = \frac{R_n(p)}{W_n(p) W(p)} \frac{k}{p}, \quad (5)$$

where  $R_n(p)$  is the remainder term of the expansion of  $W(p)$ .

But  $R_n(p) \rightarrow 0$  for  $n \rightarrow \infty$ , and therefore  $\varphi_n \rightarrow \varphi$  for  $n \rightarrow \infty$ .

Thus, the transient function  $\varphi(t)$  can be approximated to a definite degree of accuracy by the function  $\varphi_n(t)$ . The corresponding approximate transient function is of the form (4) under these conditions.

When the original function  $\varphi(t)$  or its first derivatives have values at the point  $t = 0^+$  which are not equal to zero, an expansion of  $W(p)$  of the form (3) can diverge for certain  $p \neq 0$ . This means that in such cases the response which is defined by the function  $\varphi_n$  will be unstable (for example, if certain of the expansion coefficients are negative). In addition, for values of  $t$  which are close to zero the approximating function may coincide poorly with the original one.

In that case we should not use an approximating function of the type (4). We can obtain good results for this case as well if we define the approximating function as one which satisfies the operator equation

$$\overline{\psi_n(t)} = \frac{k}{V(p)} \frac{1}{p}, \quad (6)$$

where  $V(p)$  is a fractionally rational function:

$$V(p) = \frac{1 + \sum_{i=1}^n q_i p^i}{1 + \sum_{i=1}^n c_i p^i}, \quad (7)$$

which is selected in such a way that the first  $2n-1$  terms of its expansion into a power series with respect to  $p$  coincide with the first  $2n-1$  terms of the expansion of  $W(p)$ , and, in addition, the values of the approximating

\* If there are such singularities, then  $W(p)$  can be represented in the form  $W(p) = W_1(p)/p^m$  or  $W(p) = p^m W_2(p)$ , where  $m$  is a multiple of the singularities and  $W_1(p)$  and  $W_2(p)$  no longer have any singularities at the point  $p = 0$ .

Therefore the results given below all refer to  $\overline{\varphi(t)}/p^m$  or  $p^m \overline{\varphi(t)}$ .



and original functions at the point  $t = 0$  are equal:\*

$$\psi_n(0^+) = \varphi(0^+). \quad (8)$$

If we now subtract (1) from (6), we obtain

$$\begin{aligned} \overline{\psi_n - \varphi} &= \frac{W(p) - V(p)}{V(p)W(p)} \frac{k}{p} = \frac{W_{2n-1}(p) + R_{2n-1}(p) - V_{2n-1}(p) - r_{2n-1}(p)}{V(p)W(p)} \frac{k}{p} = \\ &= \frac{R_{2n-1}(p) - r_{2n-1}(p)}{V(p)W(p)} \frac{k}{p}. \end{aligned} \quad (9)$$

Here  $V_{2n-1}(p)$  and  $W_{2n-1}(p)$  are the first  $2n-1$  terms of the expansions of  $V(p)$  and  $W(p)$  respectively into series with respect to powers of  $p$ , and  $r_{2n-1} = V(p) - V_{2n-1}(p)$  and  $R_{2n-1} = W(p) - W_{2n-1}(p)$  are the remainder terms of these expansions; here  $V_{2n-1}(p) = W_{2n-1}(p)$ , according to the conditions which we have assumed.

Keeping in mind that according to (5)  $R_{2n-1}(p)$  and  $r_{2n-1}(p)$  go to zero when  $n \rightarrow \infty$ , we find that  $\psi_n \rightarrow \varphi$  when  $n \rightarrow \infty$ .

Therefore any transient function  $\varphi(t)$  can be approximated with a definite degree of accuracy by the function  $\psi_n(t)$ .\*\* Under these conditions the corresponding transfer function will be a fractionally rational function.

## 2. Determining the Expansion Coefficients from the Experimental Transient Functions

Let  $\varphi(t)$  correspond to (1) and (3). Then

$$\overline{k - \varphi} = \frac{k}{p} \frac{1}{W(p)} \frac{k}{p} = \frac{W(p) - 1}{W(p)} \frac{k}{p}. \quad (10)$$

Substituting the value of  $W(p)$  from Equation (3) into Equation (10), we obtain

$$\overline{k - \varphi} = \frac{\sum_{i=1}^{\infty} a_i p^{i-1}}{1 - \sum_{i=1}^{\infty} a_i p^i} k. \quad (11)$$

We find the area under the curve  $k - \varphi$ :

$$S_1 = \int_0^{\infty} (k - \varphi) dt = \lim_{p \rightarrow 0} \int_0^{\infty} e^{-pt} (k - \varphi) dt = \lim_{p \rightarrow 0} \overline{k - \varphi}. \quad (12)$$

Substituting  $\overline{k - \varphi}$  from Equation (11) into Equation (12) and making  $p$  go to zero, we obtain

$$S_1 = ka_1, \quad (13)$$

since the terms of Equation (11) which contain  $p$  go to zero together with  $p$ , and  $W(p) \rightarrow 1$  for  $p \rightarrow 0$  according to Equation (3).

Therefore the area  $S_1$  (we shall call it the first-order area) is equal to a first expansion coefficient of

\* This condition improves the convergence for small  $t$ .

\*\* Here the necessary condition is merely the stability of the response defined by the resulting function.



$W(p)$  with respect to powers of  $p$ , multiplied by a factor of  $k$  [5].

Let us call the first approximating function a function  $\varphi_1$  which has the same values for its first-order area  $S_1$  and its gain coefficient  $k$  as does the original function  $\varphi$ ; here the transfer function which corresponds to  $\varphi_1$  will be

$$\frac{k}{W(p)} = \frac{k'}{a_1'p + 1} \quad (14)$$

By definition and in accordance with Equation (13),  $a_1' = a_1$  and  $k' = k$ . Then

$$\overline{\varphi_1} = \frac{1}{a_1p + 1} \frac{k}{p} \quad (15)$$

We find the Laplace transform of the difference between the first approximating function and the original function:

$$\overline{\varphi_1 - \varphi} = \frac{W(p) - a_1p - 1}{(a_1p + 1)W(p)} \frac{k}{p} = k \frac{\sum_{i=2}^{\infty} a_i p^{i-1}}{(a_1p + 1)W(p)}$$

Then

$$\frac{\overline{\varphi_1 - \varphi}}{p} = k \frac{\sum_{i=2}^{\infty} a_i p^{i-2}}{(a_1p + 1)W(p)}$$

and therefore

$$S_2 = \int_0^{\infty} \int_0^t (\varphi_1 - \varphi) dt dt = \lim_{p \rightarrow 0} \frac{\overline{\varphi_1 - \varphi}}{p} = ka_2, \quad (16)$$

i.e.,  $S_2$  (we shall call this quantity the second-order area) is equal to the second expansion coefficient of  $W(p)$  multiplied by  $k$ .

Let us call the second approximating function a function  $\varphi_2$  which has the same values of first-order ( $S_1$ ) and second-order ( $S_2$ ) areas (for the same gain  $k$ ) as does the original function  $\varphi$ ; here the transfer function which corresponds to  $\varphi_2$  will be

$$\frac{k}{W(p)} = \frac{k''}{a_2''p^2 + a_1''p + 1} \quad (17)$$

By definition,  $a_2'' = a_2$ ,  $a_1'' = a_1$ ,  $k'' = k$ ; therefore

$$\overline{\varphi_2} = \frac{1}{a_2p^2 + a_1p + 1} \frac{k}{p} \quad (18)$$

Let us find the difference:

$$\overline{\varphi_2 - \varphi} = k \frac{\sum_{i=3}^{\infty} a_i p^{i-1}}{(a_2p^2 + a_1p + 1)W(p)}$$

\* Let us first examine the functions  $\varphi(t)$  for which the response determined by the resulting function  $\varphi_n(t)$  will be stable when the higher-order terms in  $W(p)$  are discarded.

Then

$$\frac{\overline{p_2 - p}}{p^3} = k \frac{\sum_{i=3}^{\infty} a_i p^{i-3}}{(a_2 p^2 + a_1 p + 1) W(p)}.$$

Therefore the third-order area is (in a manner analogous to the procedure used above):

$$S_3 = \int_0^{\infty} \int_0^t \int_0^{\tau} (p_2 - p) dt^3 = \lim_{p \rightarrow 0} \frac{\overline{p_2 - p}}{p^3} = k a_3 \quad (19)$$

and in general,

$$S_i = \int_0^{\infty} \int_0^t \cdots \int_0^{\tau} (p_{i-1} - p) dt^i = k a_i. \quad (20)$$

Thus the geometric interpretation of the expansion coefficients consists of considering them as integral deviations (areas of a definite order) from the corresponding approximating functions (divided by the factor  $k$ ).

A determination of the expansion coefficients from the experimental transient functions by means of computing the areas of corresponding order from Formulas (20) requires cumbersome computation, since multiple integration is necessary here. In addition, as we have already indicated, certain approximating functions of the type (15), (18) may correspond to an unstable response, and therefore in such a case we cannot perform the computation according to Formula (20).

It is possible to reduce all computations to a single integration. Here we must define a more general concept of the areas which is also valid for the case when the approximating functions of the type (15), (18) correspond to an unstable response.

Substituting the values of  $M_i$  from (I.4) into (I.7) (see Appendix I), we obtain

$$S_i = \int_0^{\infty} (k - p) \left[ \frac{(-t)^{i-1}}{(i-1)!} + \sum_{j=0}^{i-2} S_{i-1-j} \frac{(-t)^j}{j!} \right] dt. \quad (21)$$

Let us pass over to the relative times  $\tau = \frac{t}{S_1}$ ; then

$$S_i = S_1^i \int_0^{\infty} (k - p) \left[ \frac{(-\tau)^{i-1}}{(i-1)!} + \frac{(-\tau)^{i-2}}{(i-2)!} + \sum_{j=0}^{i-3} \frac{S_{i-1-j}}{S_1^{i-1-j}} \frac{(-\tau)^j}{j!} \right] d\tau. \quad (22)$$

Thus we obtain the following recursion formulas for determining the areas:

$$S_1 = \int_0^{\infty} (k - p) dt, \quad (22a)$$

$$S_2 = S_1^2 \int_0^{\infty} (k - p) (1 - \tau) d\tau, \quad (22b)$$

$$S_3 = S_1^3 \int_0^{\infty} (k - p) \left[ \frac{\tau^2}{2} - \tau + \frac{S_2}{S_1^2} \right] d\tau = S_1^3 \int_0^{\infty} (k - p) \left( 1 - 2\tau + \frac{\tau^2}{2} \right) d\tau, \quad (22c)$$

$$S_4 = S_1^4 \int_0^{\infty} (k - p) \left( \frac{S_3}{S_1^3} - \frac{S_2}{S_1^2} \tau + \frac{\tau^3}{2} - \frac{\tau^2}{6} \right) d\tau. \quad (22d)$$

etc., in accordance with Equation (22).

Table 1 (Appendix III) provides values of the corresponding integrands. Therefore the expansion coefficients of the transfer functions can be determined according to Formulas (22) by numerical integration with an accuracy which is determined by the accuracy of this integration and by the accuracy to which the function  $k - \varphi$  can be detected.

The areas which are determined according to Formulas (22) exist for all functions  $k - \varphi$  for which Laplace transforms are possible.\*

### 3. Determining the Coefficients of Transfer Functions According to the Known Areas and the Value of the Function at the Point $0^+$

The formula (for the derivation see Appendix II)

$$a_j = \frac{S_j}{k} + b_j + \sum_{i=1}^{j-1} b_i \frac{S_{j-i}}{k} \quad (23)$$

establishes the relationship between the coefficients of the differential equations and the areas of corresponding orders. In addition, we make use of the known formula (from the theory of operational calculus):

$$\frac{b_n}{a_n} = \frac{\psi_n(0^+)}{k}. \quad (24)$$

In accordance with the general theory developed in Section 1, we shall approximate the original transient function  $\varphi(t)$  by the function  $\psi_n(t)$  in which the first  $2n - 1$  terms of the expansion of  $W(p)$  coincide with the first  $2n - 1$  terms of the expansion of  $V(p)$  (II.1); the values of the approximating and original functions coincide at the point  $\psi_n(0^+) = \varphi(0^+)$ . Then in order to determine the  $2n$  unknown coefficients  $a_i, b_i$  of the approximating function we have  $2n - 1$  Equations (23) and one Equation (24).

In the case where  $\varphi(0^+) = 0$ , but  $\varphi'(0^+) \neq 0$ , we assume (in accordance with the theory) that  $b_n = 0$ , and  $b_{n-1} \neq 0$ ; then the  $2n - 1$  unknown coefficients are determined from Equation (23).

When  $\varphi(0^+) = \varphi'(0^+) = 0$ , and  $\varphi''(0^+) \neq 0$ , then  $b_n = b_{n-1} = 0$ , and  $b_{n-2} \neq 0$ ; thus the  $2n - 2$  unknowns are determined from  $2n - 2$  Equations (23).

In practice it is very difficult to use the experimental transient functions to determine whether or not  $\varphi''(0^+)$  and the other higher-order derivatives are equal to zero. In such a case it is convenient (as a rule it proves possible) to approximate the experimental curve by a curve having the values  $\psi_n(0^+) = \psi'_n(0^+) = \dots = \psi^{n-1}(0^+) = 0$ , then  $b_1 = 0$ , and the coefficients of the differential equation are determined from Equation (20) (i.e., they are simply equal to the areas of corresponding orders, diminished by a factor of  $k$ ).

An example of such a computation is given in Appendix IV.

### 4. Certain Other Cases of Applying the Method Which has Been Developed Here.

For high-order experimental curves a successive determination of all the coefficients is extremely cumbersome. Often it is possible to diminish the amount of computation by introducing lag. By shifting the origin to the point  $\theta$  we determine the coefficients of the transfer function for the displaced curve.

Then the Laplace transform of the transient function will be

$$\bar{\varphi} = \frac{1}{D(p)} e^{-p\theta} \frac{k}{p}, \quad (25)$$

\* We have in mind the fact that the transfer functions which correspond to the functions  $\varphi(t)$  do not have singularities at point  $p = 0$ .

where the coefficients  $D(p)$  are determined for the displaced curves. Expanding  $e^{p^0} = \sum_{i=0}^{\infty} \frac{(p^0)^i}{i!}$  into a series and multiplying the result by  $D(p)$ , we obtain the coefficients for the original curve.

In the case where the perturbation is not a step function but is an aperiodic function or a decaying periodic function, it is necessary to determine the coefficients of the transfer functions separately for the output and input functions; the ratio of these coefficients determines the transfer function of the investigated object.

It is also evident that (in accordance with what has been said above) systems in which

$$\bar{\varphi} = \frac{b_n p^n + \dots + b_m p^m}{a_n p^n + \dots + a_1 p + 1} \bar{\mu}, \quad (26)$$

and systems in which

$$\bar{\varphi} = \frac{b_n p^n + \dots + b_1 p + 1}{a_n p^n + \dots + a_m p^m} \bar{\mu}, \quad (27)$$

can be reduced [by integration in Equation (26) and by differentiation in Equation (27)] to the system examined previously.

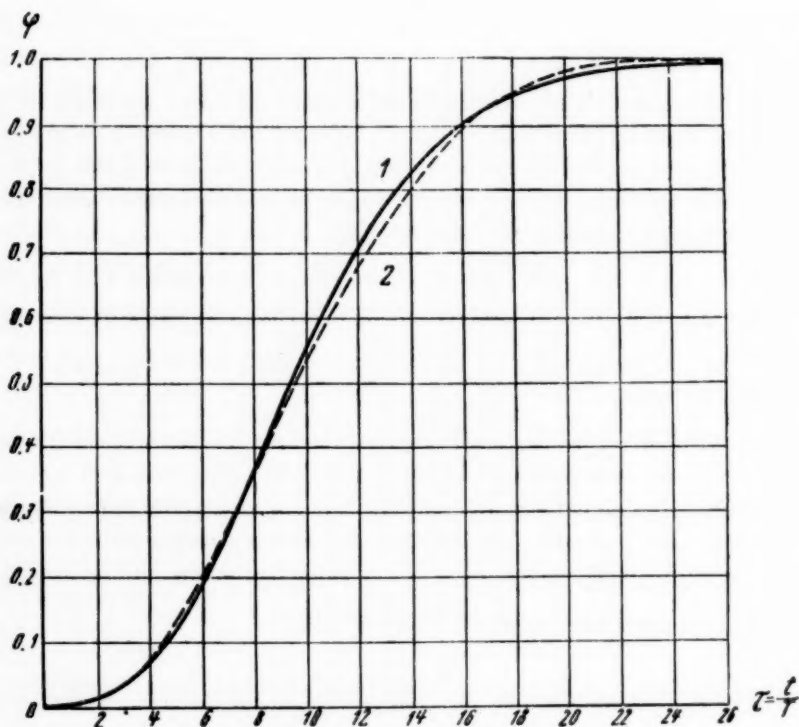


Fig. 1.

The method which is developed here can also be utilized in order to simplify complex equations. Figure 1 shows the solution of a complex system of differential equations (the equation for a section of a steam superheater when the temperature at the input varies step-wise) which has the form:

$$\frac{\partial \varphi}{\partial x} + k\varphi = k\varphi_s, \quad T \frac{\partial \varphi_s}{\partial t} + \varphi_s = \varphi, \quad (28)$$

for the initial conditions  $t = 0$ ,  $\varphi = \varphi_s = 0$  and the boundary conditions  $x = 0$ ,  $\varphi = 1$ . Figure 1 also shows the approximation of this solution by an integral of the third-order differential equation:

$$(a_3 p^3 + a_2 p^2 + a_1 p + 1) \bar{\varphi}_3 = \bar{1}. \quad (29)$$

This example is given in Appendix V.

### 5. The Method of Moments

In this paper we have proposed that the coefficients of the approximating differential equation be determined from the expansion coefficients of  $W(p)$  into powers of  $p$  (i.e., according to areas).

The Burmese scientist Ba-Hli [4] has proposed that the coefficients of the approximating differential equation be determined from the Expansion (I.5) of the transfer function  $1/W(p)$  with respect to  $p$  (i.e., according to moments). Here Ba-Hli took the presence of a step variation in the function or in any of its derivatives at the point  $t = 0^+$  into account in addition to the moments; however, he did not take the magnitude of the variation into account. In our opinion, such a method (the method of moments) is considerably inferior in accuracy and convenience to the method of areas.

In fact, the expansion coefficients of (I.5)

$$M_t = \int_0^{\infty} (k - \varphi) \frac{(-t)^i}{i!} dt$$

(see Appendix I) can be determined from the experimental transient function  $\varphi$ .

The decrease in the reliability of determining the coefficients of the experimental curve can be explained by the fact that the moments have a "weight"  $t^i$  in the integrand. Because of this "weight" the magnitudes of the values of the original function increase artificially at large  $t$  (Incidentally, these values of  $t$  are determined much less accurately), and therefore the corresponding coefficient is determined not as an average over the entire curve but only as an average over the final values of that curve. It is evident that the

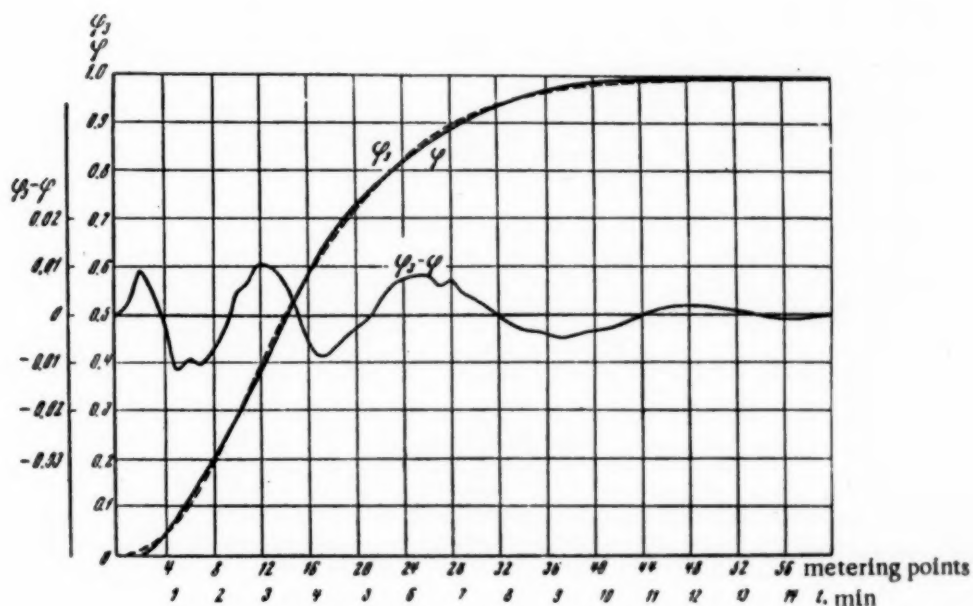


Fig. 2.

higher the order of the coefficient being determined, the less the accuracy with which it is found, since in such a case the points which are furthest from the origin have the greatest effect. Because of this shortcoming the



process of determining approximating functions for experimental curves may diverge. In contrast to this the method of areas determines the average coefficient for all the points on the curve. The process of approximation always converges.

Figures 2 and 3 show the results of computing third-order approximating functions by the method of areas and by the method of moments ( $\varphi$  is the accurate function,  $\varphi_3$  is the approximating function). In Figure 3 the solid curve corresponds to the method of areas, and the broken-line curve corresponds to the method of moments determines the coefficient  $a_2$  with an accuracy of 1% and the coefficient  $a_3$  with an accuracy of 60%. Here the actual points (beginning with  $\varphi = 0.193$ ) were used to determine the second moment, and the points beginning with  $\varphi = 0.538$  were used to determine the third moment. In addition, the equality between the approximating and original functions at the point  $t = 0^+$  is of essential importance for the convergence of the approximating and original functions at small values of  $t$ . As we have already noted, Ba-Hil did not take the value of the function at the point  $t = 0^+$  into account in his paper (he only took into account the fact that it was not equal to zero).

Figure 4 shows an approximation of the function

$$\varphi = \begin{cases} 0, & t < 0, \\ 1, & 0 < t < 0.5, \\ -1, & 0.5 < t < 1, \\ 0, & t > 1. \end{cases}$$

When the magnitude of the step variation in the function at the initial point was not taken into account (the Ba-Hil method) an error which amounted to a factor of 2.7 at that point resulted, in addition to large overshoots in the initial section of the curve (solid curve). The dashed line in Fig. 4 represents the curve computed according to the method of areas.

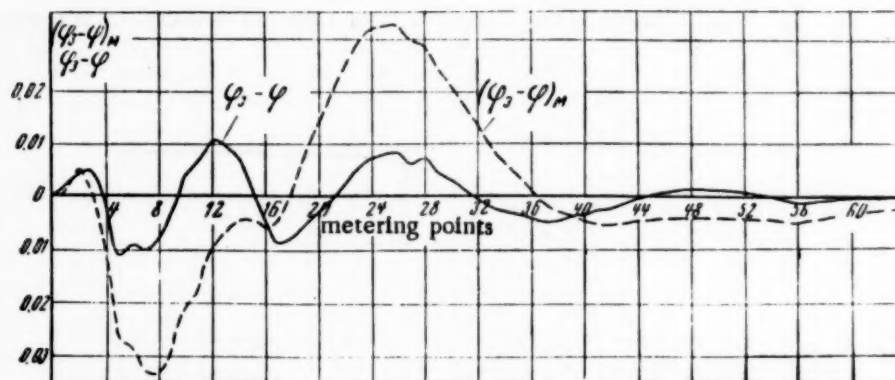


Fig. 3.

## APPENDIX I

### The Relationship Between Areas and Moments

By definition the operator

$$\overline{k - \varphi} = \int_0^{\infty} (k - \varphi) e^{-pt} dt, \quad (I.1)$$

where  $\varphi$  is the transient function which is defined by Equations (1) and (3).



We shall determine the area of  $i$ -th order in accordance with (21). Then

$$W(p) = 1 + \sum_{i=1}^{\infty} \frac{S_i}{k} p^i. \quad (1.2)$$

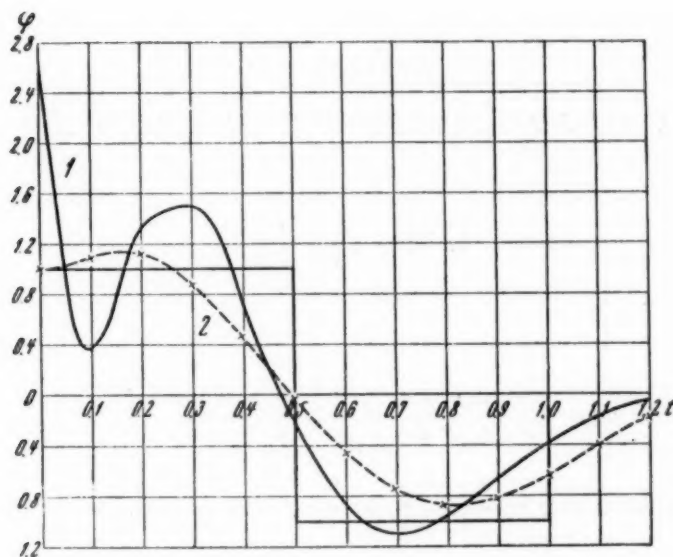


Fig. 4.

We shall expand  $e^{-pt}$  in Equation (I.1) into a series with respect to  $pt$ . Then

$$\begin{aligned} \overline{k - \varphi} &= \int_0^{\infty} (k - \varphi) dt + p \int_0^{\infty} (k - \varphi) \frac{(-t)}{1!} dt + p^2 \int_0^{\infty} (k - \varphi) \frac{(-t)^2}{2!} dt + \dots \\ &\dots + p^i \int_0^{\infty} (k - \varphi) \frac{(-t)^i}{i!} dt + \dots = \sum_{i=0}^{\infty} M_i p^i. \end{aligned} \quad (1.3)$$

where the expression

$$M_i = \int_0^{\infty} (k - \varphi) \frac{(-t)^i}{i!} dt \quad (1.4)$$

shall be called the  $i$ -th-order moment. Comparing Equations (10) and (1.3), we obtain

$$\frac{1}{W(p)} = 1 - \sum_{i=0}^{\infty} \frac{M_i}{k} p^{i+1}. \quad (1.5)$$

Let us substitute the value  $W(p)$  from Equation (1.2) into Equation (1.5):

$$\frac{1}{1 + \sum_{i=1}^{\infty} \frac{S_i}{k} p^i} = 1 - \sum_{i=0}^{\infty} \frac{M_i}{k} p^{i+1}. \quad (1.6)$$

Equation (1.6) is fulfilled for any  $p$  if



# APPENDIX III

TABLE 1  
Table of Integrands

$\tau$	$1 - \tau$	$1 - 2\tau + \frac{\tau^2}{2}$	$\frac{\tau^2}{2}$	$\frac{\tau^3}{6}$	$\frac{\tau^4}{24}$
0	1	1	0	0	0
0.1	0.9	0.805	0.005	0.0001667	0.00000417
0.2	0.8	0.620	0.020	0.00133	0.0000667
0.3	0.7	0.445	0.045	0.00450	0.00034
0.4	0.6	0.280	0.080	0.0107	0.00107
0.5	0.5	0.125	0.125	0.0208	0.0026
0.6	0.4	-0.020	0.180	0.0360	0.0054
0.7	0.3	-0.155	0.245	0.0572	0.0100
0.8	0.2	-0.280	0.320	0.0854	0.0170
0.9	0.1	-0.395	0.405	0.122	0.0273
1.0	0	-0.500	0.500	0.167	0.0417
1.1	-0.1	-0.595	0.605	0.222	0.061
1.2	-0.2	-0.680	0.720	0.288	0.086
1.3	-0.3	-0.755	0.845	0.366	0.119
1.4	-0.4	-0.820	0.980	0.457	0.160
1.5	-0.5	-0.875	1.125	0.563	0.211
1.6	-0.6	-0.920	1.280	0.683	0.273
1.7	-0.7	-0.955	1.445	0.819	0.348
1.8	-0.8	-0.980	1.620	0.972	0.438
1.9	-0.9	-0.995	1.805	1.143	0.543
2.0	-1.0	-1.000	2.000	1.334	0.667
2.1	-1.1	-0.995	2.205	1.544	0.810
2.2	-1.2	-0.980	2.420	1.775	0.976
2.3	-1.3	-0.955	2.645	2.028	1.166
2.4	-1.4	-0.920	2.880	2.304	1.383
2.5	-1.5	-0.875	3.125	2.605	1.628
2.6	-1.6	-0.820	3.380	2.930	1.904
2.7	-1.7	-0.755	3.645	3.281	2.214
2.8	-1.8	-0.680	3.920	3.659	2.561
2.9	-1.9	-0.595	4.205	4.066	2.947
3.0	-2.0	-0.500	4.500	4.501	3.375
4.0	-3.0	1.00	8	10.67	10.67
5.0	-4.0	3.50	12.5	20.84	26.04
6.0	-5.0	7.00	18.0	36.01	54.00
7.0	-6.0	11.5	24.5	57.18	100.1
8.0	-7.0	17.0	32.0	85.35	170.7
9.0	-8.0	23.5	40.5	121.5	273.4
10.0	-9.0	31.0	50.0	166.7	416.7
11.0	-10.0	39.5	60.5	221.9	610.1
12.0	-11.0	49.0	72.0	288.1	864.1
13.0	-12.0	59.5	84.5	366.2	1190
14.0	-13.0	71.0	98.0	457.4	1601
15.0	-14.0	83.5	112.5	562.6	2110

# APPENDIX IV

## Recommended Method of Computing the Transfer Function Coefficients From the Experimental Transient Function

1) We determine the first-order ares ( $S_1$ ) in accordance with Equation (22a) by numerical integration according to the trapezoid formula:

$$\int_0^{\infty} y dt \approx \Delta t \left( \frac{1}{2} y_1 + y_2 + \dots + y_{n-1} + \frac{1}{2} y_n \right) = \Delta t \left[ \sum_{i=1}^n y_i - 0.5 (y_1 + y_n) \right]. \quad (\text{IV.1})$$

For Equation (22a),  $y = k - \varphi$ ,  $y_1 = k - \varphi(0^+)$  and  $y_n = 0$ . Then

$$S_1 = \Delta t \left[ \sum_{i=1}^n (k - \varphi_i) - 0,5 k + 0,5 \varphi(0^+) \right]. \quad (\text{IV.2})$$

Let us make up a computing Table A.

2) We determine the second-order area ( $S_2$ ). We change the time scale of the function  $\varphi$  by a factor of  $S_1$ , thus converting to the relative coordinates  $\tau = t/S_1$ .

We perform the numerical integration of  $S_2$  in accordance with Equation (22b) and (IV.1), keeping in mind that  $y = (k - \varphi)(1 - \tau)$ ,  $y\tau = k - \varphi(0^+)$  and  $y_n = 0$ . Then

$$S_2 = \Delta \tau \left[ \sum_{i=1}^n (k - \varphi_i)(1 - \tau_i) - 0,5 k + 0,5 \varphi(0^+) \right] S_1^2. \quad (\text{IV.3})$$

Let us make up the Table B.

3) In an analogous manner we determine the areas  $S_3$ ,  $S_4$  etc., for which it is evident that

$$S_3 = \Delta \tau \left[ \sum_{i=1}^n (k - \varphi_i) \left( 1 - 2\tau_i + \frac{\tau_i^2}{2} \right) - 0,5 k + 0,5 \varphi(0^+) \right] S_1^3 \quad (\text{IV.4})$$

and in general

$$S_l = \Delta \tau \left\{ \sum_{i=1}^n (k - \varphi_i) \left[ \frac{(-\tau)^{l-1}}{(l-1)!} + \frac{(-\tau)^{l-2}}{(l-2)!} + \sum_{j=0}^{l-3} \frac{S_{l-1-j}}{S_1^{l-1-j}} \frac{(-\tau)^j}{j!} \right] - 0,5 [k - \varphi(0^+)] \frac{S_{l-1}}{S_1^{l-1}} \right\} S_1^l. \quad (\text{IV.5})$$

In order to carry out the computation according to Formulas (IV.4) and (IV.5) we continue Table B by writing out the values of the corresponding integrands obtained from Table 1.

TABLE A

1	2	3
$\frac{t}{\Delta t}$	$\varphi(0^+)$	$k - \varphi(0^+)$
$n\Delta t$	...	...
		$\sum_{i=1}^n (k - \varphi_i)$

4) We now determine the coefficients of the transfer function according to the known values of  $S_l$ .

a) If  $\varphi(0^+) \neq 0$ , then all  $2n$  coefficients of the transfer function

$$W_n(p) = \frac{b_n p^n + \dots + b_1 p + 1}{a_n p^n + \dots + a_1 p + 1}$$

are determined from the system comprising Equation (24) and  $2n-1$  Equations (23).

b) If  $\varphi(0^+) = 0$ , and  $\varphi'(0^+) \neq 0$ , then  $b_n = 0$ ; thus the coefficients are determined from the  $2n-1$  Equations (23).

c) If  $\varphi(0^+) = \varphi'(0^+) = 0$ , then we recommend the procedure of assuming that  $b_1 = 0$ ; thus  $a_1 = S_1/k$ .

If under these conditions certain of the coefficients  $a_i$  prove to be negative or determine a transfer function which corresponds to an unstable response (this occurs very rarely), we should assume that  $b_n = b_{n-1} = 0$  and then obtain the remaining  $2n-2$  coefficients from the  $2n-2$  Equations (23).

According to this method we determine the coefficients of the transfer function for the experimental curve shown in Fig. 2 by the solid line; the computation is given in Table 2 (which corresponds to Table A) and in Table 3 (which corresponds to Table B).

TABLE B

1	2	3	4	5	6	7	8
$\tau$	$t = S_1 \tau$	$\varphi$	$k - \varphi$	$1 - \tau$	$(k - \varphi)(1 - \tau)$	$1 - 2\tau + \frac{\tau^2}{2}$	$(k - \varphi)(1 - 2\tau + \frac{\tau^2}{2})$
0	0	$\varphi(0^+)$	$k - \varphi(0^+)$	1	$k - \varphi(0^+)$	1	$k - \varphi(0^+)$
$\Delta\tau$	...	...	...	...	...	...	...
$2\Delta\tau$	...	...	...	...	...	...	...
$n\Delta\tau$	...	...	...	...	...	...	...
					$\sum_{i=1}^n (k - \varphi_i) \times$ $\times (1 - \tau_i)$		$\sum_{i=1}^n (k - \varphi_i) \times$ $\times (1 - 2\tau_i + \frac{\tau_i^2}{2})$

TABLE 2  
Determining the Coefficient  $a_1$ 

$t$	$\varphi$	$1 - \varphi$	$t$	$\varphi$	$1 - \varphi$	$t$	$\varphi$	$1 - \varphi$
0	0	1	330	0.772	0.228	660	0.991	0.009
30	0	1	360	0.815	0.185	690	0.992	0.008
60	0.040	0.960	390	0.853	0.147	720	0.994	0.006
90	0.113	0.887	420	0.887	0.113	750	0.995	0.005
120	0.198	0.802	450	0.915	0.085	780	0.997	0.003
150	0.282	0.718	480	0.938	0.062	810	0.998	0.002
180	0.375	0.625	510	0.956	0.044	840	1	0
210	0.475	0.525	540	0.969	0.031	870	1	0
240	0.575	0.425	570	0.979	0.021	$\sum_{i=1}^n (1 - \varphi_i) = 8.54$		
270	0.657	0.343	600	0.985	0.015			
300	0.720	0.280	630	0.989	0.011			

$$a_1 = \Delta t \left[ \sum_{i=1}^n (1 - \varphi_i) - 0.5 \right] = 30 (8.54 - 0.5) = 30 \times 8.04 = 241 \text{ sec.}$$

In accordance with Table 3, the coefficients  $a_2$  and  $a_3$  are equal to

$$\Delta\tau \left[ \sum_{i=1}^n (1 - \varphi_i)(1 - \tau_i) - 0.5 \right] = 0.1 (3.939 - 0.5) = 0.3439,$$

$$\Delta\tau \left[ \sum_{i=1}^n (1 - \varphi_i) \left( 1 - 2\tau_i + \frac{\tau_i^2}{2} \right) - 0.5 \right] = 0.1 (0.882 - 0.5) = 0.0382.$$

$$a_2 = 0.3439 \times 241^2 = 19974 \text{ sec}^2, \quad a_3 = 0.0382 \times 241^2 = 534705 \text{ sec}^3.$$

Remarks on Points 1, 2 and 3. It is not necessary to use a constant interval in the formula. It is possible to subdivide the curve into sections in such a manner that the interval within any one section is identical but the interval in different sections is different. This is especially advantageous for extended curves where integration with a small interval leads to excessively cumbersome computations.

The integration interval should be selected in such a way that the integrand  $\gamma$  (IV.1) remains as linear as possible within each interval.

It is also possible to use comparatively large integration intervals, but then it is necessary to use more accurate numerical integration formulas than that given by (IV.1).

In determining the coefficients from the experimental curves, the latter must first be manipulated in order to eliminate the point spread which is usually present.

TABLE 3  
Determining the Coefficients  $a_2$  and  $a_3$

$\tau$	$\varphi$	$1 - \varphi$	$1 - \tau$	$(1 - \varphi)(1 - \tau)$	$1 - 2\tau + \frac{\tau^2}{2}$	$(1 - \varphi)(1 - 2\tau + \frac{\tau^2}{2})$
0	0	1	1	1	1	1
0.1	0	1	0.9	0.90	0.805	0.805
0.2	0.015	0.985	0.8	0.788	0.620	0.611
0.3	0.065	0.935	0.7	0.655	0.445	0.416
0.4	0.130	0.870	0.6	0.522	0.280	0.244
0.5	0.195	0.805	0.5	0.403	0.125	0.101
0.6	0.265	0.735	0.4	0.294	-0.02	-0.015
0.7	0.335	0.665	0.3	0.200	-0.155	-0.103
0.8	0.415	0.585	0.2	0.117	-0.280	-0.164
0.9	0.500	0.500	0.1	0.050	-0.395	-0.198
1.0	0.576	0.424	0	0	-0.500	-0.212
1.1	0.644	0.356	-0.1	-0.036	-0.595	-0.212
1.2	0.700	0.300	-0.2	-0.060	-0.680	-0.204
1.3	0.745	0.255	-0.3	-0.077	-0.755	-0.193
1.4	0.784	0.216	-0.4	-0.086	-0.820	-0.177
1.5	0.817	0.183	-0.5	-0.092	-0.875	-0.160
1.6	0.847	0.153	-0.6	-0.082	-0.920	-0.141
1.7	0.875	0.125	-0.7	-0.088	-0.955	-0.119
1.8	0.900	0.100	-0.8	-0.080	-0.980	-0.098
1.9	0.922	0.078	-0.9	-0.070	-0.995	-0.078
2.0	0.940	0.060	-1	-0.060	-1.000	-0.060
2.1	0.955	0.045	-1.1	-0.050	-0.995	-0.045
2.2	0.965	0.035	-1.2	-0.042	-0.980	-0.034
2.3	0.975	0.025	-1.3	-0.033	-0.995	-0.024
2.4	0.980	0.020	-1.4	-0.028	-0.920	-0.018
2.5	0.985	0.015	-1.5	-0.023	-0.875	-0.013
2.6	0.990	0.010	-1.6	-0.016	-0.820	-0.008
2.7	0.992	0.008	-1.7	-0.014	-0.755	-0.006
2.8	0.994	0.006	-1.8	-0.011	-0.680	-0.004
2.9	0.995	0.005	-1.9	-0.010	-0.595	-0.003
3.0	0.996	0.004	-2.0	-0.008	-0.500	-0.002
3.1	0.997	0.003	-2.1	-0.006	-0.395	-0.001
3.2	0.998	0.002	-2.2	-0.004	-0.280	-0.001
3.3	0.999	0.001	-2.3	-0.002	-0.155	0
3.4	0.999	0.001	-2.4	-0.002	-0.02	0
3.5	1	0.000	-2.5	0		0
3.6	1	0.000	-2.6			
				0.882		3.939

## APPENDIX V

### An Example of Approximating the Transfer Function

Figure 1 shows the solution of Equation (18) and the approximation of that solution.

In fact, if we convert to relative coordinates  $\tau = t/T$  and  $y = kx$ , in the System (28), then its solution will be

$$\varphi(\tau) = e^{-\nu} \left[ 1 + \int_0^\tau e^{-\theta} \frac{1}{\sqrt{\frac{\theta}{y}}} I_1(2\sqrt{y\theta}) d\theta \right], \quad (V.1)$$

where  $I_1$  is a Bessel function of the first kind; in operator form we have

$$\overline{\varphi(\tau)} = e^{-\nu \frac{p}{p+1}} \frac{1}{p}. \quad (V.2)$$



From Equation (V.1) it follows that the gain in this case is equal to unity, and  $\varphi(0^+) = e^{-y}$ .

For our case let us substitute  $y = 10$ ; then we obtain a value of  $\varphi(0^+)$  which is so small that it can be neglected.

Let us expand  $W(p) = e^{\frac{y}{p+1}}$  into a series with respect to  $p$ ; then we obtain

$$a_1 = W'(0) = y, \quad a_2 = \frac{W''(0)}{2!} = y \left( \frac{1}{2} y - 1 \right), \quad a_3 = \frac{W'''(0)}{3!} = y \left( -\frac{1}{6} y^2 - y + 1 \right). \quad (V.3)$$

Keeping in mind the fact that in our case  $y = 10$ , we obtain  $a_1 = 10$ ,  $a_2 = 40$  and  $a_3 = 76.7$ .

The results of the computation are shown in Fig. 1, where Curve 1 is the accurate value of the function  $\varphi(\tau)$  which was computed according to Equation (V.1), and Curve 2 is the approximating function  $\varphi_3$ .

#### SUMMARY

1) A method is proposed for determining the coefficients of transfer functions for linearized automatic control elements or systems from the experimental transient response curve.

2) The indicated method also makes it possible to simplify Equations of complex elements. Elements with distributed parameters, which are described by partial differential equations, can be approximated by means of elements with lumped parameters.

In conclusion the author expresses his deep appreciation to Prof. Ia. Z. Tsypkin and Professor M. I. Vishik for their valuable advice.

Received October 23, 1956

#### LITERATURE CITED

- [1] R. Ol'denburg and G. Sartorius, The Dynamics of Automatic Control. State Power Press, 1949. (Russian book).
- [2] E. P. Popov, The Dynamics of Automatic Control Systems. State Tech. Press, 1954. (Russian book).
- [3] G. L. Rabkin, B. A. Mitrofanov and Iu. O. Shterenberg, Determining the Numerical Values of Transfer Function Coefficients for Elements and Systems from Experimental Frequency-Response Curves. Automation and Remote Control, Vol. XVI, No. 5, 1955.
- [4] Freddy Ba-Hli, A General Method for Time Domain Network Synthesis. Trans. IRE, 1954.
- [5] A. A. Voronov, Elements of Automatic Control Theory. Military Press, 1950. (Russian book).

# NOISE STABILITY OF FREQUENCY MODULATED SYSTEMS

V. A. Kashirin

(Moscow)

The paper examines the ideal noise stability of multi-channel frequency modulated telemetering systems when weak fluctuating noise is present. The noise stability which obtains for frequency and time division of the channels is compared.

The noise stability of any system which transmits information depends both upon the method of transmission and upon the perfection of the equipment which is utilized. In investigating noise stability it is convenient to make a separate evaluation of the possibilities of increasing it by the selection of a rational method for transmitting signals, and by perfecting the equipment. In the case of fluctuating noise such a separation makes it possible to make use of the theory of ideal noise stability developed by V. A. Kotel'nikov [1]. This theory makes it possible to determine the potential (i.e., the ideal possible) noise stability of any transmission method. By comparing the ideal noise stability of a specified method of transmission with the actual noise stability of the specific system, it is possible to make a quantitative evaluation of the possibility of increasing the noise stability by way of perfecting the receiver. By determining the ideal noise stability of various transmission methods it is possible to select the one which offers the highest noise stability. As a criterion for evaluating noise stability we use the magnitude of the mean-square error at the output of the receiver

$$\delta_{\text{min. m. s.}}^2 = \frac{\sigma^2}{2TA_{\lambda}^2(\lambda, t)}, \quad (1)$$

where  $\sigma$  is the specific noise voltage (in cps<sup>-1/2</sup>),  $\lambda$  is the transmitted parameter,  $T$  is the time during which the transmitted parameter cannot be metered,  $A(\lambda, t)$  is the signal which is a function of time and of the transmitted parameter.

In Formula (1),

$$A'_{\lambda}(\lambda, t) = \left[ \frac{\partial A(\lambda, t)}{\partial \lambda} \right] \text{ and } TA_{\lambda}^2(\lambda, t) = \int_{-\frac{T}{2}}^{\frac{T}{2}} A_{\lambda}^2(\lambda, t) dt. \quad (2)$$

For an ideal receiver this error is the minimum possible one and will characterize the ideal noise stability for a signal  $A(\lambda, t)$  and a fluctuating noise of low intensity. The ideal noise stability is determined by the specific energy  $TA_{\lambda}^2(\lambda, t)$  of the wave  $A_{\lambda}(\lambda, t)$ .

## 1. Frequency Division of the Channels

Frequency division of the channels is widely utilized in power systems when telemetering signals are

transmitted over the high frequency channel of power lines and over telephone lines. Let us note the characteristic features of frequency division.

a) The time required for multi-channel transmission is equal to the time required for transmission over one channel, since all the channels in the system operate simultaneously.

b) The frequency band occupied by a N-channel system is equal to the sum of the individual channel bands and the guard bands between them.

For identical channels this can be expressed by the formula\*

$$\Delta\omega = \sum_{k=1}^N \Delta\omega_{ch} \alpha_f = 2\omega_d N \alpha_f. \quad (3)$$

Here  $\alpha_f$  is a dimensionless coefficient:

$$\alpha_f = \frac{\Delta\omega_{ch} + \Delta\omega_{int}}{\Delta\omega_{ch}}, \quad (4)$$

$\Delta\omega_{ch}$  is the frequency band of one channel,  $\omega_{dev}$  is the frequency deviation of the transmitter,  $\Delta\omega_{int}$  is the guard band between adjacent channels.

c) The maximum signal voltage is equal to the sum of the individual channel signal voltages.

If all channels in the system are identical, then for a maximum voltage  $U_m$  and a resultant band width  $\Delta\omega$  the signal from each of the channels can be represented in the following form when transmission without secondary modulation obtains:

$$A(\lambda_{ch}) = \frac{U_m}{N} \cos \left[ \left( \omega_0 + \frac{\Delta\omega \lambda_{ch}}{2N\alpha_f} \right) t + \varphi_0 \right]. \quad (5)$$

As was shown in [1], it can be assumed that the wave  $U_m^2 t^2$  does not contain the frequency  $2 \left[ \left( \omega_0 + \Delta\omega \lambda_{ch} / 2N\alpha_f \right) t \right]$ . Taking into account the fact that the average value of the product of two functions which do not have identical frequencies is equal to the product of the average values of the two factors, and that when  $T \gg 2\pi / \omega_0$ ,

$$\overline{\sin^2 \left[ \left( \omega_0 + \frac{\Delta\omega \lambda_{ch}}{2N\alpha_f} t + \varphi_0 \right) \right]} = \frac{1}{2},$$

we obtain

$$\overline{TA_{\lambda_{ch}}'^2(\lambda_{ch})} = \frac{U_m^2 \Delta\omega^2 T^2}{96\alpha_f^2 N^4}. \quad (6)$$

Substituting Equation (6) into Equation (1), we find

$$\delta_{\min, m.s.}^2 = \frac{48\sigma^2 N^4 \alpha_f^2}{U_m^2 T^2 \Delta\omega^2}. \quad (7)$$

It is evident from (7) that for constant T and  $\Delta\omega$  the error increases in proportion to the square of the number of channels.

Let us determine the ideal noise stability of a multi-channel system which is frequency and amplitude modulated (FM-AM). In such a system a high carrier frequency  $\omega_0$  is amplitude modulated by a sum of tonal (subcarrier) frequencies

\*[In the display equations  $\omega_{dev} \equiv \omega_d$  - Editor's note.]

$$\sum_{k=1}^N U_{ch} \cos [(\omega_{ch} + \omega_{dch} \lambda_{ch})t + \varphi_0], \quad (8)$$

each of which is independently controlled by the signal  $\lambda_{ch}$  of the primary transmitter. When the carrier and two side-band frequencies are transmitted, we shall have

$$\Delta\omega = 4\omega_{dev} N\alpha_f. \quad (9)$$

Assuming that all  $N$  channels of the system are identical, we determine the ideal noise stability of one channel while the other channels of the system are operated simultaneously.

In order to eliminate interaction between the channels it is necessary that the resultant voltage from all the channels at the output of the modulator be limited to the linear sector of the transmitter modulating characteristic. Then if the power is uniformly distributed over all  $N$  channels the modulation depth in one channel will comprise  $M_1 = M_{\max}/N$ . The signal in one of the channels can be written in the form

$$A(\lambda_{ch}, t) = \left\{ 1 + \frac{M_{\max}}{N} \left[ \cos \left( \omega_{ch} + \frac{\Delta\omega\lambda_{ch}}{4\alpha_f N} \right) t + \varphi_0 \right] \right\} U_{car} \cos(\omega_0 t + \varphi), \quad (10)$$

where  $U_{car}$  is the amplitude of the carrier-frequency voltage,  $M_{\max}$  is the maximum resultant linear modulation coefficient.

The derivative with respect to  $\lambda_{ch}$  of (10) will be

$$A'_{\lambda_{ch}}(\lambda_{ch}, t) = -\frac{M_{\max} U_{car} \Delta\omega}{4\alpha_f N^2} \cos(\omega_0 t + \varphi) \sin \left[ \left( \omega_{ch} + \frac{\Delta\omega\lambda_{ch}}{4\alpha_f N} \right) t + \varphi_0 \right]. \quad (11)$$

By determining the specific energy of the wave  $A'_{\lambda_{ch}}(\lambda, t)$ , we obtain the minimum mean-square error in one of the channels of a multi-channel FM-AM system:

$$\delta^2_{\min, m.s.} = \frac{384\alpha_f^2 N^4 \sigma^2}{M_{\max}^2 U_{car}^2 T^3 \Delta\omega^2}. \quad (12)$$

If the maximum amplitude of the resulting signal in the channel is specified as  $U_{\max}$ , then

$$\delta^2_{\min, m.s.} = \frac{1536\alpha_f^2 N^4 \sigma^2}{U_{\max}^2 \Delta\omega^2 T^3}. \quad (13)$$

The latter expression characterizes the ideal noise stability of the specified method of transmission.

Let us determine the ideal noise stability for FM-AM transmission when frequency division of the channels obtains; we shall consider the case where transmission is performed by means of a single-side-band system (SSB). The expression for the signal is of the form:

$$A(\lambda_{ch}, t) = \frac{U_m}{N} \cos \left[ \left( \omega_0 + \omega_{ch} + \frac{\Delta\omega\lambda_{ch}}{2N\alpha_f} \right) t + \varphi \right]. \quad (14)$$

As a result of analogous transformations we obtain

$$T A_{\lambda_{ch}}'^2(\lambda_{ch}, t) = \frac{U_m^2 \Delta\omega^2 T^3}{96N^4 \alpha_f^2}, \delta^2_{\min, m.s.} = \frac{48\alpha_f^2 N^4 \sigma^2}{U_m^2 \Delta\omega^2 T^3}. \quad (15)$$

From (15) it follows that a system with SSB transmission has the same noise stability as a system with frequency division and no secondary modulation.

The noise stability of a FM-AM system which transmits the carrier and two side-bands is several times as low as the noise stability of a SSB system. For identical values of  $U_m$  and  $\Delta\omega$  we have

$$\frac{\delta_{\min, \text{m.s. FM-AM}}}{\delta_{\min, \text{m.s. SSB}}} \approx 5.$$

As an example, let us determine the ideal noise stability of a frequency modulated multi-channel tele-metering system which has the following specification:  $N = 6$ ,  $\Delta f_N = 120$  cps,  $U_m = 0.1$  v,  $\alpha_f = 1.4$ ,  $T \leq 1/2\Omega_{\max} = 0.6$  sec, where  $\Omega_{\max}$  is the highest modulating frequency.

Let this system operate over the high-frequency channels of a 220 kv power line. In such lines the noise level in the 5 kc band comprises approximately 2.0-2.5 nepers under normal conditions; here the noise is predominantly of a fluctuating nature [3] in the frequency band which is of interest to us. Let us determine the specific noise voltage (in cps<sup>-1/2</sup>):

$$\sigma = \frac{U_n \Delta f}{V \Delta f} = 1.5 \times 10^{-3}. \quad (16)$$

From (15) we find

$$\delta_{\min, \text{m.s.}}^2 = \frac{\sqrt{48} \alpha_f N^2 \sigma}{U_m T V T \Delta \omega_N} = \frac{\sqrt{48} \times 1.4 \times 36 \times 1.5 \times 10^{-3}}{0.1 \times 0.5 \times 2\pi \times 1200} = 0.13\%. \quad (17)$$

## 2. Time Division of the Channels

Let us note the characteristic features which obtain when time division of the channels is realized.

a) The resultant time required to transmit a cycle of measurements over  $N$  channels depends upon the number of channels, since the transmission is performed in time sequence. This time can be determined from the formula

$$T = \sum_N T_{ch} \alpha_t, \quad (18)$$

where  $T_{ch}$  is the time required for transmission over one channel,  $\alpha_t$  is a coefficient which characterizes the utilization of the time  $T_{ch}$  ( $\alpha_t = T_{ch}/\tau$ ).

b) The frequency band occupied by a time division system is

$$\Delta\omega = 2\omega_{dev} + \frac{2}{\tau}, \quad (19)$$

where  $\tau$  is the duration of a pulse,  $\omega_{dev}$  is the frequency deviation of the transmitter.

c) The maximum voltage is equal to the maximum voltage in a channel.

For a frequency modulated system with time division of the channels the signal can be represented in the form

$$A(\lambda, t) = \sum_{k=0}^q f[(t - t_{ch} \lambda) \lambda], \quad (20)$$

where

$$f(\lambda, t) = \begin{cases} U_0 \cos [(\omega_0 + \omega_d \lambda) t + \varphi_0] & \text{for } -\frac{\tau}{2} < t < \frac{\tau}{2}, \\ 0 & \text{for } \frac{\tau}{2} < t < -\frac{\tau}{2}, \end{cases}$$

$t_{ch} = kT_{rep}$  ( $k$  is a whole number,  $T_{rep}$  is the repetition of the pulses in one channel,  $q = T/T_{rep}$ ).

In order to determine the minimum mean-square error we find the expression for  $\overline{TA_{\lambda}^2}(\lambda, t)$ .

We have

$$A_{\lambda}^2(\lambda, t) = \left[ \sum_{k=0}^q \{f'_{\lambda}[(t - t_{ch})\lambda]\} \right]^2. \quad (21)$$

The pulses do not overlap, and therefore it is possible to write

$$A_{\lambda}^2(\lambda, t) = \sum_{k=0}^q \{f'_{\lambda}[(t - t_{ch})\lambda]\}^2, \quad (22)$$

where

$$[f'_{\lambda}(\lambda, t)]^2 = \begin{cases} U_0^2 \omega_d^2 \tau^2 \sin^2 [(\omega_0 + \omega_d \lambda) t + \varphi_0] & \text{for } -\frac{\tau}{2} < t < \frac{\tau}{2}, \\ 0 & \text{for } \frac{\tau}{2} < t < -\frac{\tau}{2}. \end{cases}$$

The average value of  $A_{\lambda}^2(\lambda, t)$  over the time  $T$  will be

$$\overline{TA_{\lambda}^2}(\lambda, t) = \int_{-\frac{T}{2}}^{\frac{T}{2}} \sum_{k=0}^q \{f'_{\lambda}[(t - t_{ch})\lambda]\}^2 dt = \sum_{k=0}^q \int_{-\frac{\tau}{2}}^{\frac{\tau}{2}} \{f'_{\lambda}[(t - t_{ch})\lambda]\}^2 dt. \quad (23)$$

Expression (23) represents a sum (from 0 to  $q$ ) of identical integrals, since during the time  $T$  the magnitude of the measured parameter is considered constant. Using the method developed above, we find

$$\overline{TA_{\lambda}^2}(\lambda, t) = \frac{1}{24} q U_0^2 \omega_d^2 \tau^3. \quad (24)$$

Expressing  $\tau$  in terms of  $T$ , the number of channels  $N$  and the coefficient of division  $q$ , we obtain

$$\tau = \frac{T}{Nq\alpha_t} \text{ and } \delta_{\min. m.s.}^2 = \frac{12q^2 N^3 \alpha_t^3 \sigma^2}{U_0^2 \omega_d^2 T^3}. \quad (25)$$

As we can see from the resulting formula, the maximum noise stability will correspond to a value  $q = 1$  (i.e.,  $T_{rep} = T$ ) and will diminish with an increase in  $q$ . A decrease in the duration  $\tau$  of the pulses is associated with a decrease in  $T_{rep}$  and an increase in  $q$  (for a constant value of  $T$ ). As a result, the error is proportional to the  $3/2$ 's power of the number of channels for constant  $U_0$  and  $\omega_{dev}$ .

### 3. A Comparison Between Frequency Division and Time Division of the Channels

A comparison between the noise stabilities of multi-channel systems with frequency division and time division of the channels must be performed when identical frequency bands are occupied by the systems in the communications channels, and when the number of channels and the speed of response are identical. In the case of an identical transmission-frequency band the frequency deviation per one channel will be different for frequency division and time division. In telemetering systems which operate with large modulation indices the frequency band for  $N$  channels will be  $\Delta\omega = 2\omega_{dev} N\alpha_f$  for frequency division of the channels, and will be  $\Delta\omega = 2\omega_{dev} + 2/\tau$  for time division.

The mean-square error for a multi-channel system with frequency division of the channels [see (7)] can be found from the expression



$$\delta_{\min, m.s.f}^2 = \frac{12\sigma^2 N^4 \alpha_f^2}{U^2 T^3 \left(\frac{\Delta\omega}{2}\right)^2} \quad (26)$$

For time division of the channels the mean-square error will be [taking Equation (25) into account]:

$$\delta_{\min, m.s.t}^2 = \frac{12\alpha_t^2 q^2 N^3 \sigma^2}{U^2 T^3 \left(\frac{\Delta\omega}{2} - \frac{Nq}{T}\right)^2} \quad (27)$$

Let us denote the ratio of the errors which obtain for frequency division and time division of the channels by  $\delta_0$  (for identical  $T$ ,  $U$ ,  $\Delta\omega$  and  $N$ ):

$$\delta_0 = \frac{\delta_{\min, m.s.f}^2}{\delta_{\min, m.s.t}^2} = \frac{\alpha_f^2 N \left(\frac{\Delta\omega}{2} - \frac{Nq}{T}\right)^2}{\alpha_t^2 q^2 \left(\frac{\Delta\omega}{2}\right)^2} \quad (28)$$

If  $q = 1$  and  $N/T \ll \Delta\omega/2$ , then

$$\delta_0 \approx \frac{\alpha_f V \bar{N}}{\alpha_t V a_t} \quad (29)$$

From this formula it is evident that for  $\alpha_f = \alpha_t$ ,  $q = 1$  and  $N/T \ll \Delta\omega/2$  the ideal noise stability for time division of the channels is  $(N/\alpha_t)^{1/2}$  times as great as the noise stability which obtains for frequency division. Figure 1 shows the function  $\delta_0 = f(N)$  for  $\alpha_f = \alpha_t$ ,  $q = 1$  and various values of  $\Delta FT$  and  $\Delta FT/N$  computed according to Formula (28).

From Fig. 1 it follows that for  $\alpha_f = \alpha_t$ ,  $q = 1$  and a number of channels which are equal to 2-4 and greater, time division can guarantee a greater noise stability than that which obtains for frequency division. However, for  $\Delta FT = \text{const}$ , (beginning at a definite value of  $N$ ) the noise stability which obtains for time division again becomes less than it is for frequency division. The boundary representing equal noise stabilities depends upon the magnitude of  $\Delta FT$ .

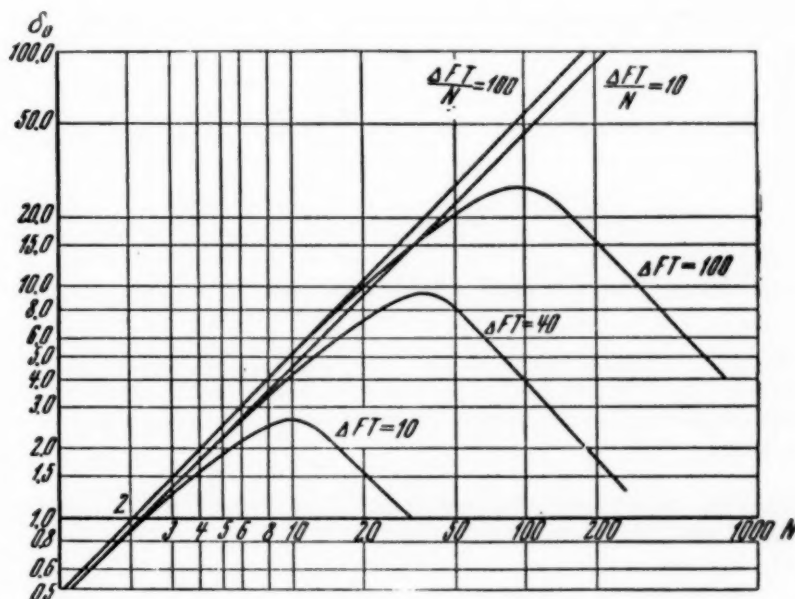


Fig. 1.

The sectors of the curves which coincide correspond to an abnormal mode of operation (the system becomes a narrow-band one). Usually, in systems where the number of channels is increased the magnitude of  $\Delta F T$  also increases, and  $\Delta F T / N$  remains constant. For such a condition  $\delta_0$  depends linearly upon  $N$ . Time division guarantees better noise stability for large  $N$ .

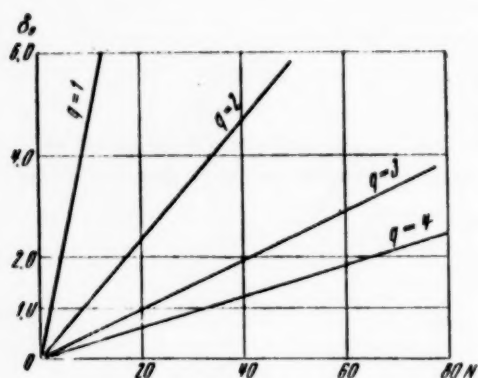


Fig. 2.

If the amplitude of the signal in one channel is equal to the resultant signal divided by the number of channels, then the dependence of the mean-square error upon the number of channels  $N$  will be more abrupt for frequency division (the error is proportional to  $N^4$ ) than for time division of the channels (the error is proportional to  $N^3$ ).

When the number of channels is large the probability that all of the signals will simultaneously attain a maximum amplitude is small. Therefore in frequency division it is possible in a number of cases to select the signal amplitude in each channel so that it is somewhat greater than  $U_{\text{tot}}/N$  (see [4]). In that case the advantages of time division may diminish considerably.

#### SUMMARY

A comparison of time division and frequency division of the channels shows that for a small number of channels a better noise stability can be obtained when frequency division of the channels is utilized; for a large number of channels, time division is superior. The limiting number of channels  $N_{\text{lim}}$  depends upon  $q$  and upon the relationship between the coefficients  $\alpha_f$  and  $\alpha_t$ . When  $q = 1$ ,  $N_{\text{lim}} = 2$  to 3; when  $q$  increases,  $N_{\text{lim}}$  increases.

Received October 22, 1956

#### LITERATURE CITED

- [1] V. A. Kotelnikov, Theory of Ideal Noise Stability when Fluctuating Noise is Present. Dissertation, 1946.
- [2] I. S. Gonorovsky, Frequency Modulation and Its Application. Communications Press, 1948.
- [3] Informational Material on Electrical Communications. Ministry of Electrical Communications, State Power Press, 1953.
- [4] McCarthy Brok, On the modulation Levels in a Frequency Multiplied Communication System by Statistical Methods. Trans. IRE, Information Theory, No. 1, pp. 54-59, 1955.

## ELECTRICAL ANGULAR ERRORS AND RESIDUAL VOLTAGES IN INDUCTIVE COMPUTER ELEMENTS

Iu. M. Pul'er

(Moscow)

The paper examines the basic errors which arise in the metering (detecting) systems of inductive computer units while taking into account the manner in which these units are manufactured. Relationships are obtained for determining the angular and amplitude-phase errors (as well as the residual voltages) of sine-cosine transformers as a function of the nonuniformity of the air gap while taking the losses in the steel into account. The residual voltages which are caused in inductive tachometer-generators by the variable wall thickness of the rotor are evaluated. The mathematical method analyzed here makes it possible to provide a more general analysis of the effect which structural and technological errors in the mechanical section, as well as the characteristics of the magnetic materials, have upon the electrical errors of inductive computer elements.

Modern automatic equipment makes broad use of inductive computer elements; heading the list of such elements are: a) sine-cosine rotary transformers which are widely used (with various coil arrangements) as vector function generators in automatic units and as selsyn-transformers in automatic tracking systems; b) inductive tachometer-generators with thin-walled rotors, which have found wide application in the capacity of ac electromechanical differentiating elements.

Due to the high accuracy requirements which are imposed upon inductive computer elements and due to the fact that in many fields of modern automation it is necessary to use small elements, the investigation of errors which are caused by technological factors are of especial importance. As practice has demonstrated, technological factors (especially in small units) cause the largest error components since to a considerable degree they determine the deviation (from the design law) of the actual law which governs the variation of the flux linkage between the windings of the system. The basic technological factors which cause errors in induction computer elements include the inaccuracy of the shape and dimensions of system parts (within the limits of the engineering tolerances), the magnetic nonuniformity and the nonlinearity of the various types of steel which are used, the presence of parasitic inductive and capacitive couplings between sections of the windings, shielding layers which appear on the surfaces of the lamination packets when they are ground and assembled, etc.

A special part is played by the phenomenon of dissymmetry in the indicated engineering errors; this phenomenon reflects the most probable state in manufactured inductive systems. A consequence of the structural dissymmetry (which leads to electromagnetic dissymmetry as well) is the appearance of residual voltages (or an intrinsic "noise") in the inductive system; this is a specific feature of all inductive computer elements and induction-type transmitters. In sine-cosine transformers the residual voltages (as we know from practical

experience) are evidenced in terms of the fact that their output voltage almost never becomes zero (with the accompanying sharp phase reversal) when the rotor passes through the zero angular position; the output voltage merely acquires a certain minimum or residual value.

It is also well known from practical experience that in inductive tachometer-generators residual voltages appear which are evidenced in the form of a certain output voltage that appears when the rotor is stationary. In the latter case this residual voltage usually depends upon the position of the rotor shell. In modern inductive elements the phenomena of residual voltages can be ascribed to one of the basic shortcomings of such elements; these shortcomings are due first of all to: a) the harmful heating of the booster (and sometimes the saturation of the booster) at large values of gain, and the harmful heating of the control windings of the adjusting motor in systems with automatic adjustment; b) the restriction of the static accuracy when several signals are summed, and also the restriction of the drive-mechanism sensitivity in automatic tracking systems of the transformer type due to the restrictions which must be imposed upon the booster gain on the basis of what was said in "a".

The problem of analyzing the electrical and angular errors and the residual voltages reduces to the necessity of obtaining an analytical expression for the output voltage (and, in particular, the expression for this voltage in the zero zone) as a function of those structural factors which are essential and can be mathematically expressed. Below we provide the solution of two problems which are important in practice.

1) Finding the electrical errors, the angular errors and the residual voltages in sine-cosine transformers as functions of the air-gap nonuniformity caused by the eccentricity and beats of the rotor magnetic circuit with respect to the stator and rotor blocks in the case where the steel has hysteresis losses (Fig. 1.).

2) Finding the residual voltage in inductive tachometer-generators with thin-walled rotors as a function of the nonuniform thickness of the latter (Fig. 2).

First it should be said that the known mathematical methods for investigating such dynamoelectric systems — the longitudinal and transverse field method and the method of symmetrical components [1, 2, 3] — cannot be used to solve the indicated problem, since these methods are based upon representing the actual systems (which are basically distributed electromagnetic systems) by certain simplified transformer circuits with lumped constants. In problems which involve the accuracy of a dynamoelectric system these circuits are valid only when they are highly idealized. When a dynamoelectric system is idealized in such a way that it is represented by known simplified transformer circuits, the above-indicated important practical spatial technological factors (which cause the electromagnetic dissymmetry and therefore the errors in the system) are eliminated from consideration.

A rigorous solution of the problems which have been posed must be accomplished by the methods of field theory. The latter, however, are associated with mathematical difficulties and lead to final functions which are difficult to use in a practical sense. We can expect especially great difficulties in solving the problems we have posed by the method of field theory when a complex inductive system with a thin-walled rotor is involved; for such a system this method leads to relatively complex relationships even in the case of a rotor which is completely uniform.

An approximate and at the same time sufficiently accurate and convenient practical solution of the problems which we have posed can be attained by the methods of magnetic and electric circuit theory [5], using an iterative spatial distributed equivalent circuit which has been proposed by the author and used for practical computations [6]. In this method a dynamoelectric system with a thin-walled rotor (Fig. 3) is represented as a spatial system made up of the distributed magnetic network of the outer and inner magnetic circuits and the distributed electrical network of the thin-walled rotor which is flux-linked with it (Figs. 4 and 5). Thus this equivalent circuit represents a closed magnetic transmission line with sinusoidally distributed resistive and reactive coil mmf's and a resistive electrical transmission line which is linked with it and simulates the reaction of the thin-walled rotor. The indicated equivalent circuit is based upon rational assumptions concerning the configuration of the reactive current circuits of the rotor (Fig. 6) and upon a linear approximation of the current density distribution in the rotor and the air-gap induction in the axial direction (this is shown in Fig. 7).

Here it is true that for the case of an ideally constructed system which has rigorous magnetic symmetry the indicated equivalent circuit produces a uniform magnetic transmission line (when  $\mu = \text{const}$ ) that has top and bottom rungs consisting of the per-unit longitudinal reluctance  $Z_{\mu 0}$  and has side rungs which consist of the



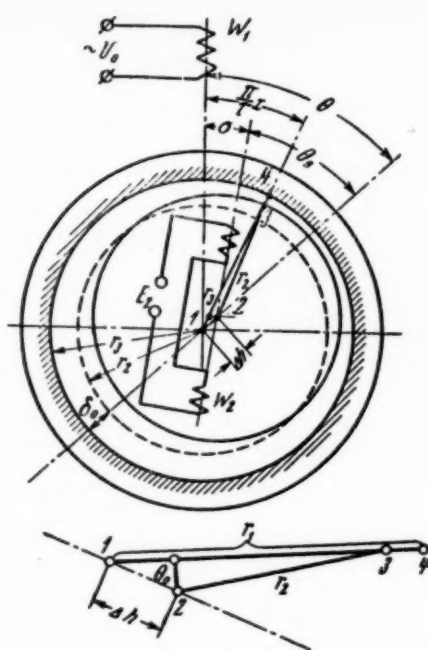


Fig. 1. Nonuniformity of the air gap in a sine-cosine transformer; this nonuniformity is caused by the eccentricity and the beats of the inner magnetic circuit with respect to the outer ones: 1) center of the stator circle and center of rotation of the rotor, 2) center of the rotor circle.

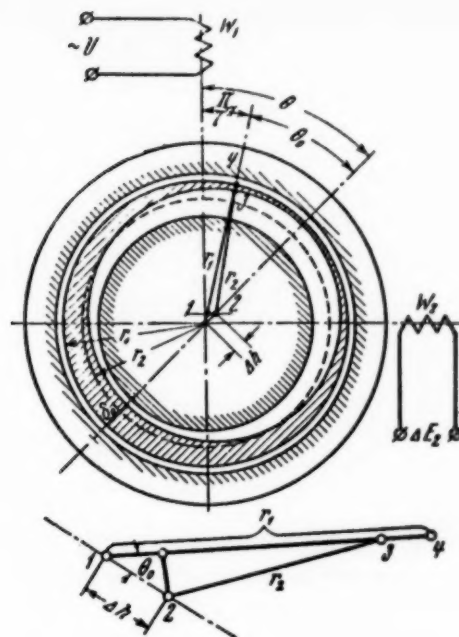


Fig. 2. Variation in rotor wall thickness in an inductive tachometer-generator; this variation is caused by the eccentricity of the inside and outside circumferences of the rotor shell.

per-unit air-gap permeance  $G_0$ , and a uniform electrical transmission line which is linked with the magnetic line and represents a rotor with a longitudinal per-unit impedance  $Z_{or}$  and a transverse per-unit conductance (along the generant of the rotor)  $g_{or}$  [6].

The parameters of the magnetic and electric transmission lines will in this case have the following values (on the basis of Figs. 4, 5 and 6) for a steady-state mode of operation:

For the magnetic line,

$$Z_{\mu 0} = \frac{1}{\mu \mu_0 l} \left( \frac{1}{b_1} + \frac{1}{b_2} \right), \quad G_0 = \frac{\mu_0 l}{\delta};$$

for the electrical line,

$$Z_{or} = \frac{2\rho_{or}}{a_2 \delta_r}, \quad g_{or} = \frac{\delta_r}{\rho_r l}, \quad (1)$$

where  $\mu$  is the relative magnetic permeability of the steel in the magnetic circuits,  $\mu_0$  is the magnetic permeability of the air,  $\delta$  is the air gap,  $\delta_r$  is the thickness of the rotor,  $\rho_r$  is the resistivity of the rotor material; the dimensions  $l$ ,  $b_1$ ,  $b_2$ ,  $a_2$  are indicated in Fig. 3.

Here  $Z_{or}$  is due to the parts which project beyond the limits of the block (basically, all of the paths for the rotor currents close through these parts),  $g_{or}$  is caused by the galvanic conductivity of the rotor along its generant.

We must keep in mind the fact that each elementary path of the magnetic circuit includes elementary

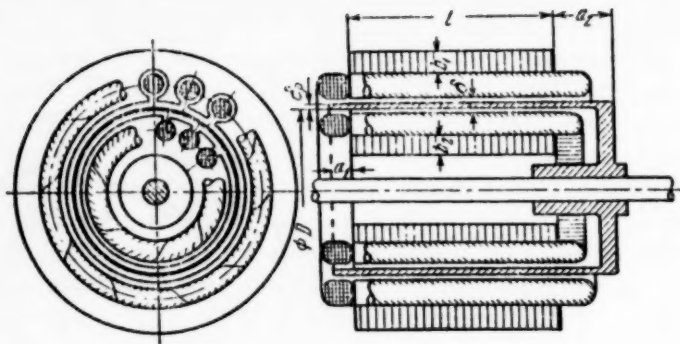


Fig. 3. Inductive dynamoelectric system with a thin-walled rotor and windings wound upon the outer and inner cores.

mmf's of the primary winding  $dM_1$  and the sum of the elementary reactive mmf's from the secondary winding  $d\Sigma M_{2k}$ , as well as the mmf's from the rotor  $dM_r = i_r(x)$  (Fig. 4).

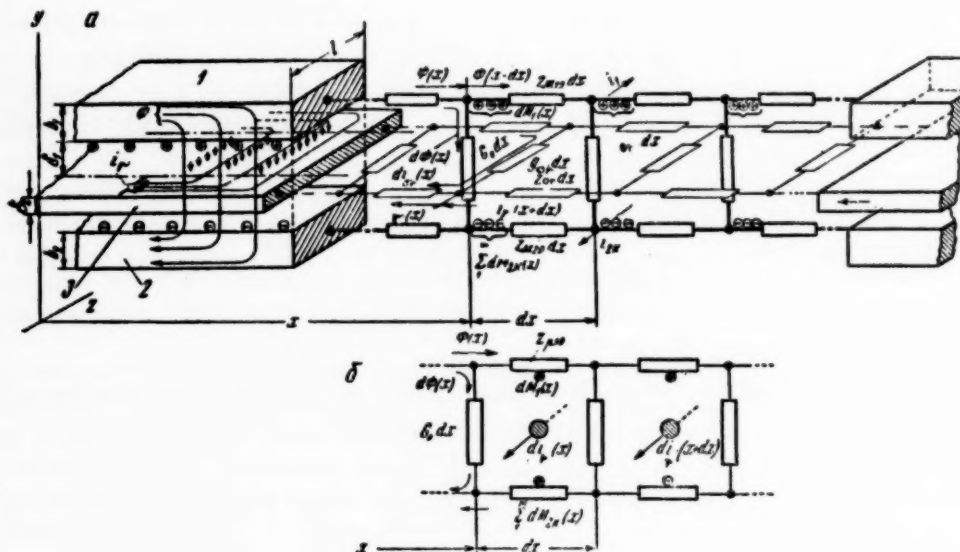


Fig. 4. Development of the spatial distributed circuit. a: 1) magnetic circuit of the outer stator, 2) magnetic circuit of the inner core, 3) thin-walled rotor shell; b) an element of the equivalent circuit.

A solution of the problem for the case of uniform lines ( $Z_{\mu 0} = \text{const}$ ,  $G_0 = \text{const}$ ,  $Z_{or} = \text{const}$ ,  $g_{or} = \text{const}$ ; these assumptions are valid for ideally accurate systems) leads very rapidly to functions which are analogous to those which can be obtained by the above-mentioned known methods; this was shown in [6].

In examining actual systems, where we must take into account the technological errors involved in manufacture and the characteristics of the steel, the magnetic and electric lines will be nonuniform.



# 1. The Joint Effect of Eccentricity, Beats and Hysteresis Losses in the Steel of the Magnetic Circuit Upon the Electrical Errors, the Angular Errors and the Residual Voltages in Sine-Cosine Rotary Transformers (the Case of "No-Load" Operation)

On the basis of the assumed equivalent network for the magnetic circuit (Fig. 4), we obtain the following steady-state equations for the magnetic circuit when there is no thin-walled rotor ( $g_{or} = 0$ ,  $Z_{or} = \infty$  and  $M_r = 0$ ) and where the stator has only one excitation winding  $W_1$  and one secondary winding  $W_2$  which is wound upon an inner repeating core (Fig. 1); here we assume that  $\mu = \text{const}$  (complex  $\mu$ ) and take into account the sinusoidal distribution law  $M_1 = I_1 W_1 \sin(\pi/\tau) x$  of the primary-winding mmf:

$$\begin{aligned} \dot{U}_L G_{0x} dx &= -d\dot{\Phi}, \\ -d\dot{U}_L &= \dot{\Phi} Z_{\mu 0} dx - I_1 W_1 \frac{\pi}{\tau} \cos \frac{\pi}{\tau} x dx. \end{aligned} \quad (2)$$

Here  $\dot{U}_L$  is the magnetic potential drop,  $G_{0x}$  is the current value of the per-unit magnetic permeance of the air gap,  $\dot{\Phi}$  is the magnetic flux in the rung of the magnetic conductor that has the current coordinate  $x$ ,  $I_1$  is the exciter winding current,  $\tau$  is the length of a pole division.

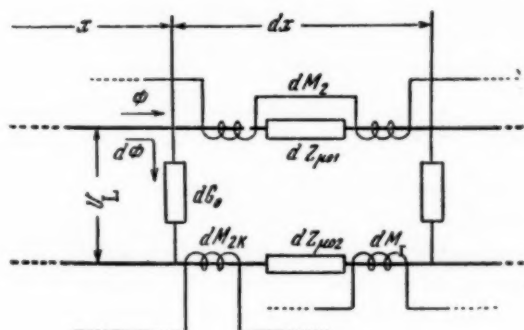


Fig. 5. Plane view of the elements of the complete equivalent circuit.

beat tolerance),  $\theta$  is the displacement between the axis of the primary winding (the origin) and the axis of geometric symmetry,  $\pi/\tau, x$  is the current angular coordinate along the gap.

If the nonuniformity of the gap is caused solely by the eccentricity of the rotor axis (Point 2 in Fig. 1) when the rotor is accurately centered with respect to this axis, then the field pattern will not vary as a function of the rotor rotation and  $\theta = \text{const}$ . Here the axis of rotation of the rotor will be located at point 2. If beats

The magnetic line of the examined system is nonuniform with respect to the quantity  $G_{0x}$  which depends upon the coordinate  $x$  [ $x$  is measured along the circumference of the stator boring from an origin which is located at the zero-density point of the stator-winding mmf (Fig. 1)].

It can easily be seen from Fig. 1 that the air gap  $\delta$  can be represented in the following form when eccentricity and beats are present:

$$\delta = \delta(x) = \delta_0 - \Delta h \cos\left(\theta - \frac{\pi}{\tau} x\right), \quad (3)$$

where  $\delta_0$  is the average air gap in an accurate system,  $\Delta h$  is the displacement of the center of the rotor along the axis of symmetry (or the eccentricity or

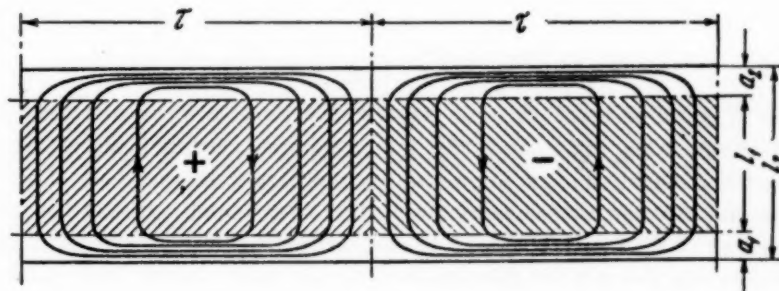


Fig. 6. The assumed pattern of current distribution in the conducting layer of a rotor which is located in the magnetic field of a two-pole electromagnetic system:  $L_1$  is the length of the steel block,  $L_2$  is the length of the rotor shell,  $a_1$  and  $a_2$  are the sections of the shell which are outside of the zone of the magnetic circuits.

are present [for which the axis of rotation of the rotor does not coincide with its geometric axis; in particular, when the axis of rotation passes through Point 1 (Fig. 1)], then it should be assumed that  $\theta = \theta_0 + \sigma$ , where  $\theta_0$  is the angular displacement between the axis of the secondary winding and the axis of geometric symmetry,  $\sigma$  is the angle of rotation of the rotor (the angle between the axes of the windings).

When the gap is nonuniform,  $Z_{\mu_0}$  will also be determined in accordance with (1), and the permeance  $G_{0x}$  will be determined on the basis of the general Expression (3) into which the specified law governing the air gap variation is substituted. In that case,

$$G_{0x} = \frac{\mu_0 l}{\delta(x)} = \frac{\mu_0 l}{\delta_0 - \Delta h \cos\left(\theta - \frac{\pi}{\tau} x\right)}. \quad (4)$$

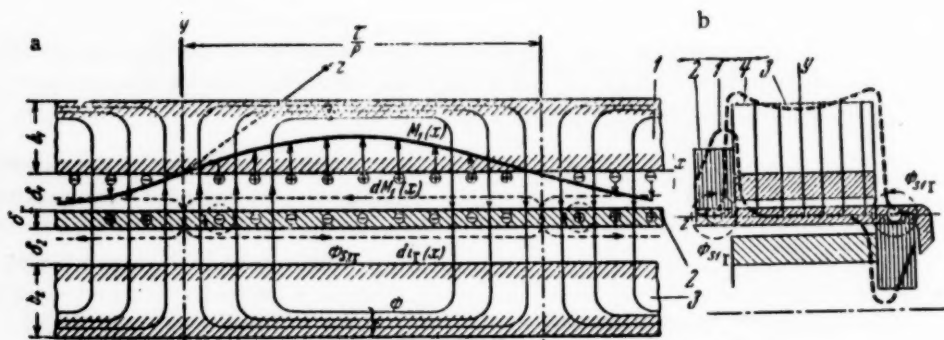


Fig. 7. Approximate pattern for the fields in an actual and idealized system, plotted in accordance with the assumed equivalent circuit: a) development along the axis: 1) outer stator, 2) conducting layer of the rotor, 3) inner core,  $\Phi_{s2r}$  ) rotor flux which corresponds to "slot" leakage; b) current density distribution in the rotor, and the induction in the gap along the generant: 1, 2) actual and approximated (by means of the equivalent circuit) current density distribution in the rotor, 3, 4) the actual and approximated distribution of the induction,  $\Phi_{s1r}$  ) the rotor flux which corresponds to "head-on" leakage.

Substituting Equation (4) into Equation (2), we obtain the following differential equation for the magnetic network as a function of the resultant flux (after elementary transformations):

$$\left[1 - q \cos\left(\theta - \frac{\pi}{\tau} x\right)\right] \frac{d^2 \Phi}{dx^2} - \frac{\pi}{\tau} q \sin\left(\theta - \frac{\pi}{\tau} x\right) \frac{d\Phi}{dx} - Z_{\mu_0} G_0 \Phi = I_1 W_1 \frac{\pi}{\tau} G_0 \cos \frac{\pi}{\tau} x, \quad (5)$$

where

$$G_0 = \frac{\mu_0 l}{\delta}, \quad q = \frac{\Delta h}{\delta_0}.$$

The differential equation which we have obtained is a linear differential equation of the second order with variable coefficients in the right-hand side, and its rigorous solution is associated with mathematical difficulties. The solution of Equation (5) is substantially simplified if we make use of the specific conditions governing the particular problem under examination. Due to the small value of the ratio  $\Delta h/\delta_0 = q$  (this is always the case because of the relatively small tolerances) we should expect little difference between the unknown flux distribution function and the distribution function which obtains for an accurate idealized system. This makes it possible to write the solution of Equation (5) in the form

$$\Phi = \Phi_0 + \Delta \Phi. \quad (6)$$

Here  $\dot{\Phi}_0$  is the flux distribution function for an ideal system [6]:

$$\dot{\Phi}_0 = \frac{U Z_0 \cos \frac{\pi}{\tau} x}{2\pi W_1 j \omega 10^{-8} (Z_0 + Z_{1s})}, \quad (7)$$

where

$$Z_0 = \frac{2j\omega 10^{-8} W_1^2 G_0 \tau}{1 + Z_{\mu 0} G_0 \left(\frac{\tau}{\pi}\right)^2} \approx 2j\omega 10^{-8} W_1^2 G_0 \tau = jX_0$$

is the magnetization input impedance,  $Z_{1s}$  is the leakage impedance of the primary winding;  $\Delta\dot{\Phi}$  is an unknown function which is small in comparison to  $\dot{\Phi}_0$  and is caused by the deformation of the magnetic field which is a consequence of the indicated deformation of the air gap. Substituting Equation (6) into Equation (5), neglecting relatively small quantities and transposing the known functions into the right-hand side, we obtain

$$\begin{aligned} & \left[1 - q \cos\left(\theta - \frac{\pi}{\tau} x\right)\right] \Delta\dot{\Phi}'' - q \frac{\pi}{\tau} \sin\left(\theta - \frac{\pi}{\tau} x\right) \Delta\dot{\Phi}' - Z_{\mu 0} G_0 \Delta\dot{\Phi} = \\ & = I_1 W_1 G_0 \frac{\pi}{\tau} \cos \frac{\pi}{\tau} x - \left[1 - q \cos\left(\theta - \frac{\pi}{\tau} x\right)\right] \dot{\Phi}_0'' + q + \frac{\pi}{\tau} \sin\left(\theta - \frac{\pi}{\tau} x\right) \dot{\Phi}_0' + Z_{\mu 0} G_0 \dot{\Phi}_0. \end{aligned} \quad (8)$$

On the basis of a known relationship [6], we have the following expression for the primary no-load current in the specified ideal accurate system:

$$\dot{I}_{10} = \frac{\dot{U}}{Z_0 + Z_{1s}}. \quad (9)$$

A variation  $\Delta Z$  in the input impedance will cause the primary currents to become equal to

$$\dot{I}_1 = \frac{\dot{U}}{Z_0 + Z_{1s} + \Delta Z}, \quad (10)$$

where  $\Delta Z$  is the unknown variation in the magnetization impedance which is caused by the nonuniformity of the air gap.

Here  $\dot{I}_1 = \dot{I}_{10} + \Delta\dot{I}_1$ , where  $\Delta\dot{I}_1$  is the variation caused in the primary current by  $\Delta Z$ .

Comparing Equations (9) and (10), we obtain

$$\Delta\dot{I}_1 = \dot{U} \frac{\Delta Z}{(Z_0 + Z_{1s})(Z_0 + Z_{1s} + \Delta Z)} \approx \dot{U} \frac{\Delta Z}{(Z_0 + Z_{1s})^2}. \quad (11)$$

From (8) [taking Equations (7) and (9)-(11) into account] we finally obtain a differential equation of the following form after elementary transformations:

$$\begin{aligned} & \left[1 - q \cos\left(\theta - \frac{\pi}{\tau} x\right)\right] \Delta\dot{\Phi}'' - q \frac{\pi}{\tau} \sin\left(\theta - \frac{\pi}{\tau} x\right) \Delta\dot{\Phi}' - Z_{\mu 0} G_0 \Delta\dot{\Phi} = \\ & = -\gamma \delta Z_0 \cos \frac{\pi}{\tau} x - \gamma q \left[ \sin \theta \sin \frac{2\pi}{\tau} x - \cos \theta \cos \frac{2\pi}{\tau} x \right], \end{aligned} \quad (12)$$

where we have introduced the notation

$$\gamma = \frac{\pi}{\tau} \frac{\dot{U} G_0 W_1}{Z_0 + Z_{1s}}, \quad \delta Z_0 = \frac{\Delta Z}{Z_0 + Z_{1s}}$$

for the sake of brevity.

It is important to underscore the fact that the equation we have obtained is an equation which is not written in terms of the unknown function  $\dot{\Phi}$  itself but in terms of its variation (error)  $\Delta\dot{\Phi}$ ; in view of this, the solution of this equation is governed by considerably lower accuracy requirements than that of the original Equation (5). This substantially simplifies the solution, since it can be performed approximately by the method of indeterminate coefficients [7, 8].

We shall seek a solution in the form

$$\Delta\dot{\Phi} = \Delta\dot{\Phi}_1 + \sum_1^m \left( \Delta\dot{\Phi}_{1k} \sin k \frac{\pi}{\tau} x + \Delta\dot{\Phi}_{2k} \cos k \frac{\pi}{\tau} x \right). \quad (13)$$

Here the expression for the error in the secondary voltage (which determines the flux linkage between the secondary sine winding and the flux  $\Delta\dot{\Phi}$  in accordance with Figure 1) will be

$$\Delta\dot{E}_2 = j\omega 10^{-8} W_2 \frac{\pi}{\tau} \int_{\alpha}^{\alpha+\tau} \cos \frac{\pi}{\tau} (x - \alpha) [\Delta\dot{\Phi}]_{x+\tau}^x dx. \quad (14)$$

Substituting the function  $\Delta\dot{\Phi}$  into the integrand in accordance with the indicated limits, we then perform the integration and obtain

$$\Delta\dot{E}_2 = -2j\omega 10^{-8} W_2 \pi \left( \Delta\dot{\Phi}_{11} \sin \frac{\pi}{\tau} \alpha + \Delta\dot{\Phi}_{21} \cos \frac{\pi}{\tau} \alpha \right). \quad (15)$$

Expression (15) shows that only the amplitudes of the fundamental flux harmonics affect the magnitude of  $\Delta\dot{E}_2$ .

Since the supply voltage  $\dot{U}$  is constant, the variation in the primary flux linkage is equal to zero. Here we do not take into account the effect of primary-winding leakage upon the variation in its flux linkages (this is done because  $\Delta Z$  is small), i.e.,

$$\Delta\dot{U}_0 = j\omega 10^{-8} W_1 \frac{\pi}{\tau} \int_0^{\tau} \cos \frac{\pi}{\tau} x [\Delta\dot{\Phi}]_{x+\tau}^x dx = 0. \quad (16)$$

Substituting the value of  $\Delta\dot{\Phi}$  into Equation (16) and performing the integration, we obtain  $j\omega 10^{-8} W_1 \pi \Delta\dot{\Phi}_{21} = 0$  for  $\Delta\dot{\Phi}_{21} = 0$ . Therefore the equation for  $\Delta\dot{E}_2$  will be

$$\Delta\dot{E}_2 = -2j\omega 10^{-8} W_2 \pi \Delta\dot{\Phi}_{11} \sin \frac{\pi}{\tau} \alpha. \quad (17)$$

On the basis of Equation (17) we conclude that in order to segregate the error in the secondary voltage from the entire spatial spectrum of flux harmonics only  $\Delta\dot{\Phi}_{11}$  must be taken into account. Setting the terms of equal periodicity in the right- and left-hand sides of Equation (12) equal to one another and limiting ourselves solely to the second harmonic in the left-hand side, we obtain a system of four algebraic equations whose solution yields the following result for the second harmonics:

$$\Delta\dot{\Phi}_{21} = -\frac{\gamma q \cos \theta}{\left(\frac{2\pi}{\tau}\right)^2 + Z_{\mu 0} G_0}, \quad \Delta\dot{\Phi}_{12} = \frac{\gamma q \sin \theta}{\left(\frac{2\pi}{\tau}\right)^2 + Z_{\mu 0} G_0} \quad (18)$$

and for the first harmonic

$$\Delta\dot{\Phi}_{11} = \frac{1}{2} q^2 \left(\frac{\pi}{\tau}\right)^3 \frac{\dot{U} G_0 W_1}{(Z_0 + Z_{10})} \frac{\sin 2\theta}{\left[\left(\frac{\pi}{\tau}\right)^2 + Z_{\mu 0} G_0\right] \left[\left(\frac{2\pi}{\tau}\right)^2 + Z_{\mu 0} G_0\right]}. \quad (19)$$

Keeping in mind the fact that  $\delta Z_0 = \Delta Z / Z_0 + Z_s$ , we obtain the following expression for the increment of input impedance:

$$\Delta Z = -\frac{1}{2} q^2 \frac{\cos 2\theta}{4 + Z_{\mu 0} G_0 \left(\frac{\tau}{\pi}\right)^2} (Z_0 + Z_{1s}). \quad (20)$$

It is essential to underscore the fact that in the examined case of a nonuniform air gap the variation in the flux distribution arises chiefly because of the appearance of second-harmonic flux components ( $\Delta \dot{\Phi}_{21}$  and  $\Delta \dot{\Phi}_{12}$ ), which contain  $q$  to a power which is one greater than the power of  $q$  in the first-harmonic increment  $\Delta \dot{\Phi}_{11}$ .

From Equations (19) and (7) we obtain the final expression for  $\Delta \dot{E}_2$  when eccentricity and beats are taken into account for  $\theta = \theta_0 + \sigma$ :

$$\Delta \dot{E}_2 = \frac{1}{2} \left(\frac{\Delta h}{\delta_0}\right)^2 \frac{\dot{U}_j X_0}{i X_0 + Z_{1s}} \frac{\sin 2(\theta_0 - \sigma) \sin \sigma}{\left[1 + Z_{\mu 0} G_0 \left(\frac{\tau}{\pi}\right)^2\right] \left[4 + Z_{\mu 0} G_0 \left(\frac{\tau}{\pi}\right)^2\right]}. \quad (21)$$

Now the resultant magnitude of the secondary no-load voltage is found as the sum of two terms — the no-load voltage for the ideal accurate system [6] and the increment  $\Delta \dot{E}_2$  which we have found:

$$\dot{E}_2 = \frac{\dot{U}_j X_0}{i X_0 + Z_{1s}} \frac{W_2}{W_1} \left[ \cos \alpha + \frac{1}{2} \left(\frac{\Delta h}{\delta_0}\right)^2 \frac{\sin^2(\theta_0 + \sigma) \sin \sigma}{\left[1 + Z_{\mu 0} G_0 \left(\frac{\tau}{\pi}\right)^2\right] \left[4 + Z_{\mu 0} G_0 \left(\frac{\tau}{\pi}\right)^2\right]} \right]. \quad (22)$$

In order to take the steel losses into account in a first approximation we shall examine  $Z_{\mu 0}$  as a complex quantity:

$$Z_{\mu 0} = R_{\mu 0} + jX_{\mu 0}, \quad (23)$$

where  $X_{\mu 0} = R_{\mu 0} \operatorname{tg} \varphi_{\text{loss}} = |Z_{\mu 0}| \sin \varphi_{\text{loss}}$ , and  $\varphi_{\text{loss}}$  is the loss angle which is experimentally determined for the particular magnetic material.

Keeping Equation (23) in mind, we obtain the following final expression for  $\dot{E}_2$  after a series of simplifications:

$$\dot{E}_2 = \frac{\dot{U}_j X_0}{i X_0 + Z_{1s}} \frac{W_2}{W_1} \left\{ \cos \sigma + \frac{1}{32} \left(\frac{\Delta h}{\delta_0}\right)^2 \sin 2(\theta_0 + \sigma) \sin \sigma \times \left[4 + j5 \left(\frac{\tau}{\pi}\right)^2 G_0 |Z_{\mu 0}| \sin \varphi_{1s}\right] \right\}, \quad (24)$$

We should turn our attention to a number of consequences which are of practical importance and which flow from the relationships which we have found for the secondary voltage  $\dot{E}_2$ . We shall give the most basic of these consequences below:

1) From Equation (24) we conclude that  $\dot{E}_2$  does not become zero for any values of the rotor angle of rotation  $\sigma$ . The same expression shows that in the case under examination the system has an elliptic field with semi-axes that are respectively proportional to the maximum and minimum (residual) secondary voltages  $|\dot{E}_{2\text{max}}|$  and  $|\dot{E}_{2\text{min}}|$ . From this latter fact it follows, in particular, that when such elements are utilized in compensating networks which contain an automatic phase-detecting drive the adjustment must be performed solely according to the real portion of the output voltages  $\dot{E}_2$  (i.e., according to  $\operatorname{Re}[\dot{E}_2]$ ). Here it is useful to introduce the concept of an error voltage in the zero zones for two rotor positions of a sine-cosine transformer.

a) For the position  $\sigma = 90^\circ$ , when there is a "zero" voltage:

$$\Delta \dot{E}_{20} = \dot{E}_2|_{\sigma=90^\circ} = \frac{1}{4} \left(\frac{\Delta h}{\delta_0}\right)^2 \frac{W_2}{W_1} \frac{\dot{U}}{1 + \frac{Z_{1s}}{i X_0}} \sin 2(\theta_0 + 90^\circ). \quad (25)$$



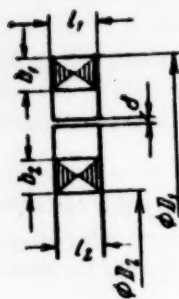


Fig. 8.

Here  $\dot{\Delta E}_{20}$  is called "zero" voltage because at the position  $\sigma = 90^\circ$   $\dot{E}_2$  must be equal to zero (when the errors are zero).

b) At the position  $\sigma = 90^\circ + \Delta\sigma$ , where  $\Delta\sigma$  corresponds to the rotor position for which

$$\operatorname{Re}[\dot{E}_2] = 0. \quad (26)$$

Here the secondary winding will contain a residual voltage (or the intrinsic "noise" of an inductive system operating on the fundamental time harmonic):

$$\Delta \dot{E}_{\text{res}} = \operatorname{Im}[\dot{E}_2]_{\sigma=90+\Delta\sigma} = j \left( \frac{\Delta h}{\delta_0} \right)^2 5 |Z_{\mu 0}| \sin \varphi_{1s} \left( \frac{\tau}{\pi} \right)^2 G_0 \frac{U \frac{W_2}{W_1}}{1 + \frac{Z_{1s}}{jX_0}} \times (\sin 2\theta_0 + 2\Delta\sigma \cos \theta_0). \quad (27)$$

The angle  $\Delta\sigma$  is determined on the basis of Equation (26), and this angle in turn determines the shift of the magnetic axis of the excitation flux (or, more precisely, the shift of the major axis of the magnetic-field ellipse). Substituting the value of  $E_2$  from (24) into (26), we obtain the equation for determining the angular displacement

$$\cos(90 + \Delta\sigma) + \frac{1}{8} \left( \frac{\Delta h}{\delta_0} \right)^2 \sin 2(\theta_0 + 90 + \Delta\sigma) \times \sin(90 + \Delta\sigma) = 0.$$

Taking the smallness of  $\Delta\sigma$  into account, we finally obtain

$$\Delta\sigma \approx -\frac{1}{8} \left( \frac{\Delta h}{\delta_0} \right)^2 \sin 2\theta_0.$$

2) It is evident from Equation (27) that the residual voltages are phase-shifted by  $90^\circ$  with respect to the phase of the nominal secondary voltage  $E_{2\max}$  which phases the actuating motor so that the torque at its shaft is produced by a control voltage whose phase coincides with the phase of the reference voltage  $E_{2\max}$ . Thus when the indicated phasing is applied to a servo-drive with automatic adjustment and when there is no nonlinear distortion or phase distortion in the booster, the residual signal  $\Delta E_{2\text{res}}$  does not produce any torque in the adjusting motor. Here, however, the above-indicated harmful effect of the residual voltages is not diminished.

3) The second term in the outer parentheses of Equation (24) determines the amplitude and phase errors for all rotor positions  $\sigma$  and also makes it possible to determine easily the angular errors. Let us examine the example of a plane sine-cosine transformer-selsyn (Fig. 8) which has the following parameters:

$b_1 = l_1 = 4.5$  mm,  $b_2 = l_2 = 5$  mm,  $D_1 = 44.5$  mm,  $D_2 = 24$  mm,  $\delta = 0.5$  mm,  $G_0 = 12$  h/cm,  $Z_{\mu 0} \approx 1.38 \times 10^{-3}$ ,  $\sin \varphi_{1\text{loss}} \approx 0.3$  for  $B_m \approx 3000$  gauss,  $W_2 = 1920$ ,  $W_1 = 500$ ,  $X_0 = 1020$  ohm,  $Z_{1s} = (1180 + j1950)$  ohms,  $U = 36$  v,  $f = 400$  cps.

For an eccentricity and beat tolerance of  $\Delta h = 0.05$  mm and for a nominal gap  $\delta_0 = 0.5$  mm we determine the maximum possible displacement of the magnetic axis:

$$\Delta\sigma_{\max} = \frac{1}{8} \left( \frac{0.05}{0.5} \right)^2 \approx 4.3 \text{ ang. min.}$$

Further, on the basis of Equation (27) we determine that  $(\Delta \dot{E}_{2\text{res}})_{\max} \approx 5$  mv; this comprises approximately 0.005% of the maximum secondary no-load voltage  $|\dot{U}_{2\max}| = \left| \dot{U} \frac{W_2}{W_1} \frac{1}{1 + \frac{Z_{1s}}{jX_0}} \right| \approx 100$  v. When  $\Delta h = 0.1$  mm



and  $\delta_0 = 0.5$  mm we have  $\Delta\sigma_{\max} \approx 17'$ ;  $(\Delta E_{\text{res}})_{\max} \approx 20$  mv, which comprises  $\sim 0.02\%$  of the maximum.

## 2. The Effect of the Structural Variation of the Rotor Wall Thickness of an Inductive Tachometer-Generator Upon Its Residual Voltages

In manufacturing the units of the mechanical section of an inductive tachometer-generator appreciable difficulties are associated with the accurate manufacture of thin-walled rotors with a uniform wall thickness. The difficulties arise at small diameters (10-15 mm) and wall thicknesses (0.15-0.12 mm) which are characteristic in fast-response small units. In this regard the problem of an approximate computation of the effect produced by the nonuniformity in the rotor wall thickness (this nonuniformity is caused by the tolerances in the eccentricity of the inner and outer circumferences of the shell boring) upon the residual voltages of the tachometer-generator are not only of theoretical but also of practical interest. The solution of this problem lays the basis for a rational choice of the tolerance for the wall-thickness variation; this tolerance plays an appreciable part in determining the requirements which govern the engineering fittings of the unit and affects the productivity as far as mass production is concerned. In addition, a solution of the indicated problem makes it possible approximately to evaluate the limiting possibilities of decreasing the rotor wall thickness and of lowering the over-all dimensions of the tachometer-generator's inductive system.

On the basis of the general equivalent circuit which was described above for a dynamoelectric system with a thin-walled rotor (Figs. 4 and 5), we have the following system of differential equations for the distributed electrical network of the rotor and the distributed magnetic network of the stator\* when the secondary stator winding is open-circuited and the rotor is stationary ( $U_r = 0$ ; see Fig. 2), provided the rotor leakage fluxes  $\dot{\Phi}_{s1r}$  and  $\dot{\Phi}_{s2r}$  are neglected:

$$\begin{aligned} \dot{U}_r g_{0x} &= -\dot{I}_r', \\ -\dot{U}_r' &= \dot{I}_r Z_{orx} - \dot{e}', \\ \dot{\Phi}' &= \dot{\Phi} Z_{\mu 0} G_0 - \dot{I}_r' G_0 = -\dot{I}_1 W_1 \frac{\pi}{\tau} G_0 \cos \frac{\pi}{\tau} x, \end{aligned} \quad (28)$$

where, in addition to the functions which we have indicated previously,  $\dot{U}_r$  is the voltage along the rotor generator which has the coordinate  $x$ ,  $\dot{I}_r$  is the rotor current in the part of the rotor which projects beyond the limits of the blocks in the cross-section that has the coordinate  $x$ ,  $\dot{e}$  is the elementary transformer emf in the elementary path that has the coordinate  $x$ .

Due to the variation in wall thickness the electrical line of the rotor in the system under examination is nonuniform with respect to the magnitude of the current per-unit conductance  $g_{0x}$  and impedance  $Z_{orx}$  which are functions of the coordinate  $x$ . Under these conditions the variation in  $Z_{orx}$  can be neglected because it is so small; thus it can be assumed that  $Z_{orx} \approx Z_{or}$  for which we obtained a solution above according to (1).

From Fig. 2 we find the dependence of the wall thickness of the shell upon the coordinate  $x$ :

$$\delta_{or}(x) = \delta_{or} - \Delta h \cos\left(\theta - \frac{\pi}{\tau} x\right), \quad (29)$$

where  $\delta_{or} = r_1 - r_2$  is the difference between the inner and outer radii of the rotor,  $\Delta h$  is the eccentricity of the inner and outer circumferences of the rotor,  $\theta$  is the position of the axis of symmetry of the rotor. Then

$$g_{0x} = g_{or} \left[ 1 - q \cos\left(\theta - \frac{\pi}{\tau} x\right) \right], \quad (30)$$

where

$$q = \frac{\Delta h}{\delta_{or}}.$$

\* In System (28) the primes denote derivatives with respect to the coordinate  $x$ .

Based on the fact that the system is not being examined while it is rotating but only at different rotor positions ( $\theta = \text{var}$ ), the expression for the elementary emf  $de$  in the elementary rotor-circuit path (Figs. 4 and 5) [6] will be

$$de = -j\omega 10^{-8} \dot{\Phi}' dx \quad \text{or} \quad e' = -j\omega 10^{-8} \dot{\Phi}'. \quad (31)$$

Taking Equations (30) and (31) into account, we obtain the equation for the distributed rotor circuit with respect to the current  $I_r$ ; together with the equation for the magnetic network, this equation provides a system of differential equations:

$$\begin{aligned} \dot{I}_p + \dot{I}_r \frac{g_{or}}{g_{ox}} q \frac{\pi}{\tau} \sin\left(\theta - \frac{\pi}{\tau} x\right) - \dot{I}_r Z_{or} q_{or} \left[1 - q \cos\left(\theta - \frac{\pi}{\tau} x\right)\right] = \\ = -j\omega 10^{-8} \dot{\Phi}' g_{or} \left[1 - q \cos\left(\theta - \frac{\pi}{\tau} x\right)\right], \\ \dot{\Phi}'' - \dot{\Phi} Z_{\mu 0} G_0 - \dot{I}_r' G_0 - \dot{I}_1 W_1 \frac{\pi}{\tau} G_0 \cos \frac{\pi}{\tau} x. \end{aligned} \quad (32)$$

Thus the problem we have posed reduces to solving a linear differential equation with respect to the unknowns  $\dot{I}_r$  and  $\dot{\Phi}$ ; here the first equation contains variable coefficients. As in the preceding case, the solution of the resulting equations can be realized in a simplified manner if we take into account the smallness of the quantity  $q$  which in such systems is always small because of the high accuracy with which the parts are manufactured.

This leads to a situation where the unknown functions  $\dot{I}$  and  $\dot{\Phi}$  differ little from the analogous functions for an ideal accurate system ( $q = 0$ ). Therefore the unknown functions can be represented in the form

$$\dot{I}_r = \dot{I}_{r0} + \Delta \dot{I}_r, \quad \dot{\Phi} = \dot{\Phi}_0 + \Delta \dot{\Phi}, \quad (33)$$

where  $\dot{I}_{r0}$  and  $\dot{\Phi}_0$  are the known functions for the ideal tachometer-generator system (for  $q = 0$ ). These functions are of the following form for a tachometer-generator with an open-circuited secondary winding [6] when the leakage in the secondary winding is neglected:

$$\dot{I}_{r0} = \frac{\dot{U} Z_0 \sin \frac{\pi}{\tau} x}{(Z_0 + Z_{1s}) 2 W_1 Z_r}, \quad \dot{\Phi}_0 = j \frac{\dot{U} Z_0 \cos \frac{\pi}{\tau} x}{2 \pi \omega 10^{-8} W_1 (Z_0 + Z_{1s})}, \quad (34)$$

where  $Z_r$  is determined in [6] and is of the following form for a two-pole system:

$$Z_r = \frac{\pi^2}{\tau g_{or}} + Z_{or} \tau.$$

Making use of Equations (33) and (34), we obtain the following system of equations with respect to the increments  $\Delta \dot{I}_r$  and  $\Delta \dot{\Phi}_1$  (which are the unknown functions) on the basis of the System (32) after transposing the known functions into the right-hand sides:

$$\begin{aligned} \Delta \dot{I}_r' + \Delta \dot{I}_r' q \frac{\pi}{\tau} \sin\left(\theta - \frac{\pi}{\tau} x\right) - \Delta \dot{I}_r Z_{or} g_{or} \left[1 - q \cos\left(\theta - \frac{\pi}{\tau} x\right)\right] - \\ - j\omega 10^{-8} \Delta \dot{\Phi}' g_{or} \left[1 - q \cos\left(\theta - \frac{\pi}{\tau} x\right)\right] = q \frac{\dot{U} Z_0}{2 W_1 Z_r (Z_0 + Z_{1s})} \times \\ \times \left(\frac{\pi}{\tau}\right)^2 \left[\cos \theta \sin \frac{2\pi}{\tau} x - \sin \theta \cos \frac{2\pi}{\tau} x\right], \\ \Delta \dot{\Phi}'' - \Delta \dot{\Phi} Z_{\mu 0} G_0 - \Delta \dot{I}_r' G_0 = \frac{\pi}{\tau} G_0 W_1 \frac{U \Delta Z}{(Z_0 + Z_{1s})^2} \cos \frac{\pi}{\tau} x, \end{aligned} \quad (35)$$

where  $\Delta Z$  is the increment of the input magnetization impedance and is also an unknown function.

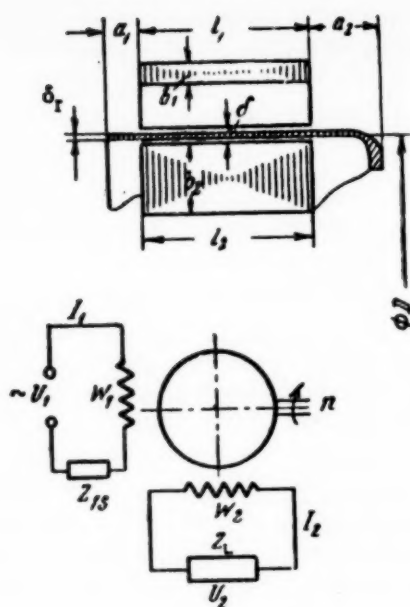


Fig. 9.

As in the preceding case, it is most convenient to seek solutions for the functions  $\Delta\dot{\Phi}$  and  $\Delta\dot{I}_r$  in the form of trigonometric series. This is one method of obtaining an approximate solution of the resulting System (35). Representing the solutions in the form of a trigonometric series is also useful because a flux linkage with the secondary winding that is different from zero yields only the fundamental harmonic of the unknown function  $\Delta\dot{\Phi}$  [this follows from Equation (15)]. Thus if we have the approximate solution in the form of a trigonometric series, it is sufficient to know the value of the fundamental space harmonic of  $\Delta\dot{\Phi}$  (15) in order to obtain the residual voltage.

Limiting ourselves to the second harmonic in the series for the unknown functions, we obtain

$$\begin{aligned}\Delta\dot{I}_r &= \Delta\dot{I}_{or} - \Delta\dot{I}_{11} \sin \frac{\pi}{\tau} x + \\ &+ \Delta\dot{I}_{21} \cos \frac{\pi}{\tau} x + \Delta\dot{I}_{12} \sin \frac{2\pi}{\tau} x + \Delta\dot{I}_{22} \cos \frac{2\pi}{\tau} x, \\ \Delta\dot{\Phi} &= \Delta\dot{\Phi}_0 + \Delta\dot{\Phi}_{11} \sin \frac{\pi}{\tau} x + 0 + \\ &+ \Delta\dot{\Phi}_{12} \sin \frac{2\pi}{\tau} x + \Delta\dot{\Phi}_{22} \cos \frac{2\pi}{\tau} x.\end{aligned}\quad (36)$$

Let us note that on the basis of the preceding discussion,  $\Delta\Phi_{21} = 0$ . After substituting Equation (36) into Equation (35) and setting terms in the left- and right-hand sides which are of identical periodicity equal to one another, we obtain a system of algebraic equations from which we determine the spatial harmonic components of the unknown rotor-current and flux increments. Here we obtain the following expression for the first flux harmonic when the magnetic reluctance of the steel is neglected ( $Z_{\mu 0} = 0$ ):

$$\begin{aligned}\Delta\dot{\Phi}_{11} &= -q^4 \frac{\frac{\pi}{\tau} \dot{U} Z_0 G_0}{32 W_1 Z_r (Z_0 + Z_{1s})} \times \\ &\times \frac{\sin 2\theta \left\{ \frac{1}{2} \left[ 2 \left( \frac{\pi}{\tau} \right)^2 + Z_{or} g_{or} \right] + 2j\omega 10^{-8} g_{or} G_0 \right\}}{\left[ \left( \frac{2\pi}{\tau} \right)^2 + Z_{or} g_{or} + j\omega 10^{-8} g_{or} G_0 \right] \left[ \left( \frac{\pi}{\tau} \right)^2 + Z_{or} g_{or} + j\omega 10^{-8} g_{or} G_0 \right]}.\end{aligned}\quad (37)$$

Making use of Equations (37) and (17), we obtain an expression for the residual voltage  $\Delta E_{2res}$  across the secondary quadrature winding  $W_2$  in the following form (for  $\sigma = 90^\circ = \text{const}$ ):

$$\Delta\dot{E}_{2res} = -\frac{q^4}{16} \frac{\dot{U} j X_0}{Z_r (j X_0 + Z_{1s})} \frac{W_2}{W_1} \frac{\frac{\pi}{\tau} \frac{j X_0}{W_1^2} \sin 2\theta \left( \frac{2\pi^2}{\tau g_{or}} + Z_{or} \tau + \frac{1}{2} \frac{j X_0}{W_1^2} \right)}{g_{or} \left[ \left( \frac{2\pi}{\tau} \right)^2 + Z_{or} \tau + \frac{1}{2} \frac{j X_0}{W_1^2} \right] \left( \frac{\pi}{\tau} Z_r + \frac{1}{2} \frac{j X_0}{W_1^2} \right)}.\quad (38)$$

Equation (38) can be simplified in order to obtain a first approximation which is sufficient for practical use. In simplified form the maximum value of  $\Delta\dot{E}_{2res}$  will be

$$\Delta\dot{E}_{20max} = -\frac{q^4}{8} \frac{\dot{U} j X_0}{Z_r (j X_0 + Z_{1s})} \frac{W_2}{W_1} \frac{\pi^2}{\tau g_{or}}.\quad (39)$$

From Formula (38) it follows that the residual voltage which is caused by the examined variation in the wall-thickness of the rotor changes according to the sine of twice the angle  $\theta$  while retaining an approximately

Identical phase  $\varphi_{20} = \arg(\Delta \dot{E}_{2res})$  which is different from the phase of the useful signal  $\dot{E}_{2max}$ . The quantitative result of the relationship which we obtained for  $\Delta E_{2res}$  can be illustrated by using the example of a small two-pole tachometer-generator with an aluminum rotor whose design parameters (these are shown in Fig. 9) have the following values:  $W_1 = 240$ ,  $W_2 = 825$ ,  $X_0 = 540$  ohm,  $Z_r \approx 11.4 \times 10^{-3}$  ohm;  $g_{or} \approx 7.37 \times 10^2$  (1/ohm cm),  $Z_{or} \approx 24 \times 10^{-4}$  (ohm/cm),  $Z_{1s} = (135 + j78)$  ohm,  $U = 36$  v,  $f = 400$  cps,  $U_2 = 1.4$  v, for  $n = 1000$  rpm.

When  $\delta = 0.15$  mm,  $\Delta h = 0.02$  mm and  $\Delta h = 0.05$  mm we have  $q^4 = 3 \times 10^{-4}$  and  $q^4 = 12 \times 10^{-4}$  respectively. Substituting the values of  $q$  into Equation (39), we obtain  $\Delta \dot{E}_{20 max} \approx 5e^{j45}$  mv,  $\Delta \dot{E}_{20 max} \approx 200e^{j45}$  mv respectively.

#### SUMMARY

1) The analysis of the effects which technological errors have upon the amplitude and phase errors (and, in particular, upon the zero and residual voltages) of sine-cosine transformers shows that the probability of realizing such dynamoelectric systems with a pure pulsating field is practically zero when such units are constructed from magnetic materials which have hysteresis losses. In actual units of the indicated type the examined technological factors will (when only one exciting winding is energized) give rise to magnetic fields (which are elliptical) that have a ratio between semi-axes that is approximately proportional to the ratio between the residual voltage across the secondary winding and the maximum secondary voltage. From what we have said above, it also follows that the residual voltages in sine-cosine transformers can be reduced to a minimum by utilizing magnetic materials with small hysteresis losses (in addition to increasing the accuracy with which the mechanical parts are manufactured).

2) The practical importance of the results we have obtained is based on the fact that they make it possible to segregate the accuracy of manufacturing the mechanical section of the system from the entire aggregate of technological factors. The formulas which have been derived here make it possible analytically to determine the effect of these factors upon the amplitude-phase errors and, in particular, upon the magnitude of the zero and residual voltages and angular errors of sine-cosine transformers and selsyns, as well as upon the magnitudes of the residual voltages of inductive tachometer-generators with thin-walled rotors.

3) The indicated method of analyzing inductive computer elements is based upon representing them by distributed iterative circuits and makes it possible to introduce many other technological and design factors into the analysis after determining their effect upon the functions  $Z_{\mu 0}(x)$ ,  $G_0(x)$ ,  $g_{or}(x)$  and  $Z_{or}(x)$ .

Received July 26, 1956

#### LITERATURE CITED

- [1] L. N. Gruzov, Methods for the Mathematical Investigation of Electrical Machines.\*
- [2] B. I. Stanislavsky, Fundamentals of the Theory of Electrical Computer Units. Defense Press, 1948.\*
- [3] S. H. Frazier, Analysis of the Drag-Cup AC - Tachometer by means of two phase symmetrical components, Trans. AIEE, Vol. 70, Part II, 1951, p. 1894.
- [4] E. M. Lopukhina, Analysis of a Hollow-Rotor Motor. Electricity, No. 5, 1950.
- [5] V. I. Kovalenkov, Fundamentals of Magnetic Circuit Theory. Acad. Sci. USSR Press, 1940.\*
- [6] Iu. M. Pul'er, Theory of Calculating Inductive Computer Elements of the Dynamoelectric type by Considering them as Systems with Distributed Magnetic and Electric Parameters. Precision of Mechanisms and Machines, No. 7, Acad. Sci. USSR Press, 1954.
- [7] I. N. Bronshtein and K. A. Semendiaev, Mathematics Handbook, State Tech. Press, 1954.\*
- [8] E. Kamke, Handbook on Ordinary Differential Equations. Foreign Lit. Press, 1951. (Foreign book).

\* In Russian.



## THE PROBLEM OF MATCHING MAGNETIC AMPLIFIERS OF THE "SECOND HARMONIC" TYPE TO A LOAD

V. N. Mikhailovsky and Iu. I. Spektor

(Lvov)

The paper examines the operation of a second-harmonic magnetic amplifier when it is loaded. The effect of the nature of the load upon the stability of the magnetic amplifier is clarified, and the region of unstable operation is delineated. Relationships are obtained which make it possible to match the magnetic amplifier to a resistive load on the basis of the conditions governing the achievement of maximum power sensitivity for specified excitation conditions. The paper clarifies the dependence of the power sensitivity of a resistance-loaded magnetic amplifier upon the amplitude of the exciting field when optimum matching obtains.

Recently magnetic amplifiers and pick-up elements (magnetic probes) which operate on the principle of frequency doubling have become widely utilized. The indicated type of unit has a number of advantages, the foremost of which are a low sensitivity threshold and high stability.

Extensive literature [1-7] et al. has been devoted to analyzing the operation of magnetic amplifiers and pick-up elements.

However, the overwhelming majority of the authors limit their analysis to the no-load operation of magnetic amplifiers [1-7].

In fact, magnetic amplifiers operate into some load (in the general case this load is complex). Because of this it is of interest to match the amplifier to the load. It can be asserted that in practically all cases (even when the operating conditions of the amplifier are close to no-load conditions) it is useful to match the load with respect to power output. In the latter case the utilization of a matching step-up transformer provides a considerable reserve as far as increasing the sensitivity is concerned.

The problem of matching a "second harmonic" amplifier to a resistive load for a particular case of excitation was first solved by M. A. Rozenblat. This paper represents an attempt at a further investigation of the problem of matching an amplifier to a load; the analysis is based upon the condition which requires a maximum power sensitivity.

We shall examine the power sensitivity of the amplifier for small input signals when the amplifier can be assumed linear. Such an operating mode is characteristic of the operation of an amplifier in a circuit which provides automatic compensation of the measured signal.

### 1. The Effect of the Nature of the Load Upon the Stability.

Let us examine a widely used magnetic amplifier circuit which has series-connected excitation windings (Fig. 1).

Let us make the following assumptions:

- a) The excitation of the amplifier is achieved by means of a pure sinusoidal current,  $i_1 = I_{1m} \cos \omega t$ ;
- b) the magnetic state of the cores is determined by the exciting field (i.e.,  $H_0 + H_{2m} \ll H_{1m}$ ;
- c) we neglect the hysteresis loss in the cores, the leakage fluxes, the eddy currents and the effects of current harmonics (higher than the second harmonic) in the load;
- d) the cores and excitation windings of the amplifier are completely symmetrical (i.e., when there is no control signal the emf of the detector winding of the amplifier is equal to zero)).

The magnetic field intensity in each of the cores (Fig. 1) consists of the sum of three components:

$$H_I = H_1 + H_2 + H_0, \quad H_{II} = H_1 - H_2 - H_0$$

where  $H_1 = H_{1m} \cos \omega t$  is the instantaneous value of the magnetic field intensity produced by the excitation windings,  $H_2 = H_{2m} \cos (2 \omega t + \varphi)$  is the instantaneous value of the magnetic field intensity created by the load current,  $H_0$  is the magnetic field intensity created by the control current.

Correspondingly, the magnetic induction in each of the cores will be equal to

$$B_I = B(H_1 + H_2 + H_0), \quad B_{II} = B(H_1 - H_2 - H_0). \quad (1)$$

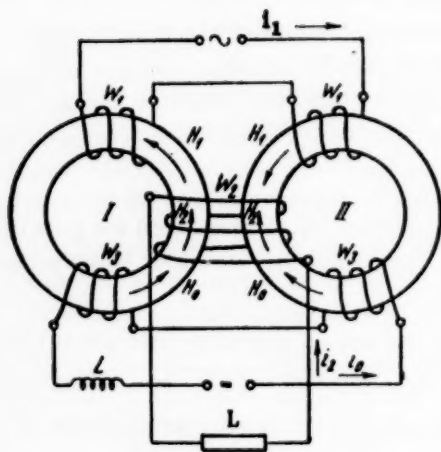


Fig. 1

The resultant magnetic flux which links the detection winding  $W_2$  (Fig. 1) will be proportional to the difference between the values of magnetic induction in the cores. Limiting ourselves to the linear term of the expansion of Function (1) into a Taylor series based upon powers of  $(H_0 + H_2)$  we obtain

$$\begin{aligned} \Delta B &= B_I - B_{II} = \\ &= 2(H_2 + H_0) \left( \frac{dB}{dH_1} \right) = 2(H_2 + H_0) \mu_d, \end{aligned} \quad (2)$$

where  $\mu_d$  is the differential magnetic permeability which characterizes the magnetic state of the cores.

Neglecting the initial rising sector of the curve  $\mu_d = f(H)$ , we approximate it by means of the comparatively simple function

$$\mu_d = \frac{\mu_0}{1 + \beta^2 H_1^2}, \quad (3)$$

where  $\mu_0$  is the value of the maximum magnetic permeability which will correspond to the zero value of field intensity in the approximating function.

The values of  $\beta^2$  and  $\mu_0$  are determined from the experimentally determined curve  $\mu_d = f(H)$  according to the formulas

$$\beta^2 = \frac{\mu_0 - \mu_d}{\mu_d H_1^2}, \quad \mu_0 = \mu_{\max}. \quad (4)$$

The values of  $\mu_d$  and  $H$  should be selected in the region of the maximum curvature of the falling sector of the experimental curve  $\mu_d = f(H)$ .

As an example, Fig. 2 shows the function  $\mu_d = f(H)$  as computed according to Formula (3) for the values  $\mu_0 = 160 \times 10^3$  gauss/oerst. and  $\beta^2 = 1180$  1/oerst. [obtained from the experimental curve for Mo-permalloy;



see (Fig. 2) ] by means of a broken line. It is evident from Fig. 2 that the computed curve agrees sufficiently closely with the experimentally-obtained curve.

In accordance with what has been said above,

$$\Delta B = 2\mu_0 \frac{H_0 + H_{2m} \cos(2\omega t + \varphi)}{1 + \beta^2 H_{1m}^2 \cos^2 \omega t}. \quad (5)$$

We determine the second harmonic of the difference between the magnetic inductions in the cores (i.e., the second term of the expansion of Expression (5) into a Fourier series).

The expansion term which is of interest to us can be written in the form

$$B_2 = B_{2a} \cos 2\omega t + B_{2b} \sin 2\omega t, \quad (6)$$

where

$$B_{2a} = \frac{2\mu_0}{T} \int_{-T/2}^{T/2} \frac{H_0 + H_{2m} \cos(2\omega t + \varphi)}{1 + \beta^2 H_{1m}^2 \cos^2 \omega t} \cos 2\omega t dt, \\ B_{2b} = \frac{2\mu_0}{T} \int_{-T/2}^{T/2} \frac{H_0 + H_{2m} \cos(2\omega t + \varphi)}{1 + \beta^2 H_{1m}^2 \cos^2 \omega t} \sin 2\omega t dt. \quad (7)$$

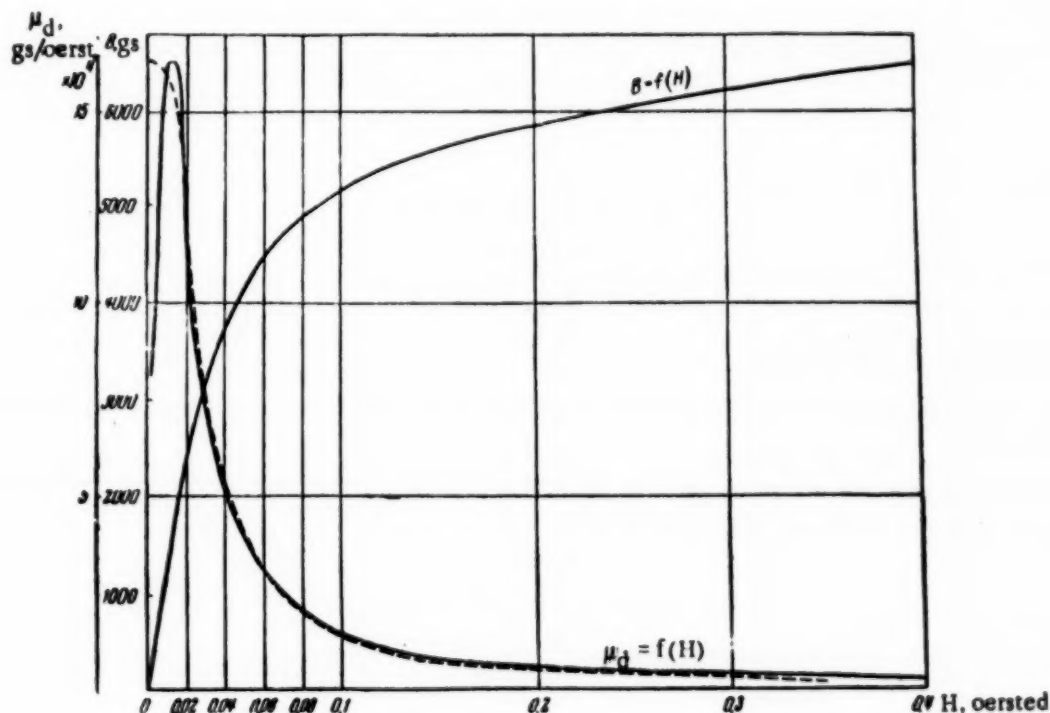


Fig. 2

The solution of these integrals can be represented in the following form:

$$B_{2a} = -A\mu_0 H_0 + B\mu_0 H_{2m} \cos \varphi, \quad B_{2b} = -D\mu_0 H_{2m} \sin \varphi, \quad (8)$$

where

$$A = \frac{2(1 - \sqrt{1 + \beta^2 H_{1m}^2})^3}{\beta^2 H_{1m}^2 \sqrt{1 + \beta^2 H_{1m}^2}}, \quad (9a)$$

$$-E = \frac{2(1 - \sqrt{1 + \beta^2 H_{1m}^2})^2 (2 + \beta^2 H_{1m}^2)}{\beta^4 H_{1m}^4 \sqrt{1 + \beta^2 H_{1m}^2}}, \quad (9b)$$

$$H = \frac{(1 - \sqrt{1 + \beta^2 H_{1m}^2})^3 (3\beta^2 H_{1m}^2 + 2\sqrt{1 + \beta^2 H_{1m}^2} + 6)}{\beta^4 H_{1m}^4 \sqrt{1 + \beta^2 H_{1m}^2}}. \quad (9c)$$

Substituting (7) into (6), we obtain an expression for the second harmonic of the difference between the magnetic inductions in the cores:

$$B_2 = -A\mu_0 H_0 \cos 2\omega t + E\mu_0 H_{2m} \cos \varphi \cos 2\omega t - H\mu_0 H_{2m} \sin \varphi \sin 2\omega t. \quad (10)$$

Let the load  $Z$  which is connected to the output of the amplifier consist of a resistance  $R$ , a capacitance  $C$  and an inductance  $L$  connected in series. The Kirchhoff equation for the load circuit is

$$2SW_2 10^{-8} \frac{dB_2}{dt} - i_2 Z = 0, \quad (11)$$

or, substituting the expressions for  $B_2$  and  $Z$ , we obtain

$$E - 2\omega L_0 I_{2m} (B \cos \varphi - jH \sin \varphi) + \left[ (R + r)j - 2\omega L + \frac{1}{2\omega C} \right] \times I_{2m} (\cos \varphi + j \sin \varphi) = 0,$$

where

$$E = 4\omega W_2 S \mu_0 A H_0 10^{-8}, \quad (12a)$$

$$L_0 = \frac{2SW_2^2 0.4\pi \mu_0 10^{-8}}{l}, \quad (12b)$$

$r$  is the resistance of the detection coil  $W_2$ .

In Expressions (12a) and (12b)  $S$  is the cross-section of the amplifier cores,  $l$  is the mean length of the magnetic circuit.

Setting the real and imaginary portions of (11) equal to zero and solving the resulting equations with respect to the unknowns which are of interest to us, we obtain

$$\varphi = \arctg \frac{R + r}{2\omega L + 2\omega L_0 H - \frac{1}{2\omega C}}, \quad (13)$$

$$I_{2m} = \frac{E}{(R + r) \sin \varphi + \left( 2\omega L + 2\omega L_0 H - \frac{1}{2\omega C} \right) \cos \varphi}. \quad (14)$$

Solving Equations (13) and (14) simultaneously and introducing the quantities

$$\varepsilon = \frac{I_{2m}(R + r)}{E}, \quad \eta = \frac{2\omega L + 2\omega L_0 H - \frac{1}{2\omega C}}{R + r}, \quad \zeta = \frac{\omega L_0 (B - H)}{R + r},$$

we obtain

$$\epsilon = \frac{\sqrt{1 + \eta^2}}{1 + 2\zeta\eta + \eta^2} \quad (15)$$

Analyzing Expression (15), we find that the quantity  $\epsilon$  which represents the ratio between the voltage drop across the resultant resistive load of the amplifier and the no-load emf can go to infinity at definite values of  $\zeta$  and  $\eta$  (i.e., the operation of the amplifier becomes unstable). The possibility of such an operating mode ( $\epsilon \rightarrow \infty$ ) is governed by the criterion that  $\eta$  must fall in a region where  $\eta \rightarrow -\zeta \pm \sqrt{\zeta^2 - 1}$ ; this follows from Equation (15). Here  $\eta$  will always have a negative value. The condition  $\zeta = 1$  and  $\eta = -1$  corresponds to resonance. For  $\zeta > 1$ ,  $\eta$  corresponds to the presence of two negative roots which characterize the operating mode  $\epsilon \rightarrow \infty$  for which it is possible to have a step-wise phase reversal of the output voltage.

Figure 3, which shows the dependence of the quantity  $\epsilon$  upon  $\eta$  for various values of  $\zeta$ , very clearly shows the special operating features of the magnetic amplifier when it works into various types of loads.

In the region of values  $\eta = 0$  to  $+\infty$  and  $\zeta = 0$  to  $+\infty$  (i.e., for resistive and resistive-inductive loads)  $\epsilon$  varies from 1 to 0. Here the (relatively) greatest voltage across a resistive load and the small dependence of this voltage upon the variation of the circuit parameters is realized for the case  $\zeta \rightarrow 0$  and  $\eta \rightarrow 0$ , i.e., for a relatively large circuit (load) resistance. In the region of values  $\eta = 0$  to  $-\infty$  and  $\varphi = 0$  to 1 (i.e., for a capacitive load)  $\epsilon$  can acquire values from 0 to  $+\infty$  according to the assumptions that we have made.

Here it is true that the greater the values of  $\epsilon$  and  $\zeta$ , the more heavily  $\epsilon$  depends upon the variation of the circuit parameters (i.e., the less stable the operation of the magnetic amplifier when other conditions remain the same). However, even when a capacitance  $C$  is present in the load, the stability of the amplifier remains relatively high when  $\zeta = 0$  to 0.1.

For a capacitive load ( $\eta < 0$  and  $\zeta > 1$ ) phase reversal is possible. Thus, increasing the voltage across the load resistance by introducing a capacitance into the circuit is inescapably associated with a lowering of the stability. Since the stability usually plays an essential part, we should choose  $\zeta \leq 0.1$  and  $|\eta| < 1$  (i.e., we should strive to achieve a relative increase of the resistance in the load circuit).

## 2. The Conditions Which Govern the Achievement of Maximum Power Sensitivity for a Resistive Load.

In the majority of cases which are of practical importance magnetic amplifiers work into a load which is almost resistive. Let us establish the output conditions of the amplifier when it is supplying such a load with the maximum useful power (i.e., the conditions which govern the matching of the amplifier to a resistive load when maximum power sensitivity is desired. In order to obtain these conditions we shall express the power delivered to the load in terms of the magnitude of the load and the parameters of the amplifier.

Assuming that  $L \rightarrow 0$ ,  $C \rightarrow \infty$  and  $r \ll R$  in Expressions (13) and (14), we obtain

$$I_{2m} = \frac{4\omega W_2 S A \mu_0 H_0 10^{-8} V \sqrt{R^2 + (2\omega L_0 I)^2}}{R^2 + (2\omega L_0 I)^2 B I} \quad (16)$$

The resistive second-harmonic power in the load acquires the following form according to Equations (16) and (12b):

$$P_2 = \frac{1}{2} I_{2m}^2 R = 5fV A^2 \mu_0 H_0^2 \frac{m(1 + m^2 I^2)}{(1 + m^2 I B)^2} \quad (17)$$

The power sensitivity (with respect to the second harmonic) of the amplifier is

$$S_{P_2} = \frac{\partial P_2}{\partial (H_0^2)} = 5fV A^2 \mu_0 \frac{m(1 + m^2 I^2)}{(1 + m^2 I B)^2} \quad (18)$$

where  $V = 2Sl$  is the volume of the cores, and  $m = 2\omega L_0/R$  is the tangent of the impedance angle of the load.

On the basis of our assumptions it follows from Equation (17) that the second-harmonic power which is supplied to the load by the amplifier is proportional to the frequency of the excitation current, the volume of the core, and the permeability of the core material (for  $m = \text{const}$ ); it also depends in a more complex manner upon the power factor of the load and the magnitude of the exciting field.

In order to generalize our reasoning we shall introduce the concept of the normalized (specific) sensitivity  $S'_{P_2} = S_{P_2}/fV$  in determining the effect of the latter two factors (i.e., the sensitivity per unit volume of the core and per unit frequency of the excitation field):

$$S'_{P_2} = 5\mu_0 A^2 \frac{m[1 + m^2 D^2]}{(1 + m^2 D^2)^2}. \quad (19)$$

Let us determine the conditions governing the maximum normalized power sensitivity for specified excitation conditions.

Differentiating Expression (19) with respect to  $m$ , setting the result equal to zero and solving the resulting biquadratic equation with respect to  $m$ , we find

$$m_{\text{opt}} = \frac{1}{D} \sqrt{\frac{-3(B-D) + \sqrt{9(B-D)^2 + 4BD}}{2B}}. \quad (20)$$

After substituting Equation (20) into Equation (19), we obtain the expression for the maximum power sensitivity when the excitation conditions are specified:

$$\begin{aligned} (S'_{P_2})_{\text{max}} &= 5\mu_0 A^2 \sqrt{\frac{-3(B-D) + \sqrt{9(B-D)^2 + 4BD}}{2BD^2}} \times \\ &\times \frac{1 + \frac{-3(B-D) + \sqrt{9(B-D)^2 + 4BD}}{2B}}{\left[1 + \frac{-3(B-D) + \sqrt{9(B-D)^2 + 4BD}}{2D}\right]^2}. \end{aligned} \quad (21)$$

It follows from Equation (21) that when the amplifier is matched to the load the power sensitivity of the amplifier is a complex function of the quantity  $A$ ,  $B$ , and  $D$ , which are in turn complex functions of the excitation-field amplitude  $BH_{1m}$  [Equations (9a), (9b) and (9c)].

Taking this into account, it is advantageous to omit an analytical simultaneous investigation of Equations (9a), (9b), (9c) and (21) and to analyze the effect of the excitation-field amplitude upon the power sensitivity of the amplifier by means of graphical-analytical methods.

For this purpose we computed and plotted the dependence of the quantities  $A$ ,  $B$ ,  $D$ ,  $m_{\text{opt}}$  and  $(S'_{P_2})_{\text{max}}$  (which are determined by the equations indicated above) upon the amplitude of the exciting field (Figs. 4 and 5). Let us note that Equation (9a) and the curve in Fig. 4 which corresponds to it represent the dependence of the power sensitivity of the amplifier upon the amplitude of the excitation field at no load.

Thus the curves  $A = f(BH_1)$  and  $(S'_{P_2})_{\text{max}}/5\mu_0 = f(BH_1)$  provide a convenient description of the voltage sensitivity at no load and the power sensitivity for a matched load as functions of the excitation-field amplitude; thus they may serve as a basis for selecting the optimum operating mode of the magnetic amplifier.

### 3. Experimental Investigation

Figure 6 shows the circuit of the experimental unit. A. O. is an audio-oscillator of the type ZG-2A\*,  $R_1$  is a control rheostat of 1700 ohms,  $R_2$  is a current-limiting resistor of 1000 ohms,  $R_3$  is a complex of control

\* [Specifications for ZG-2A audio-oscillator: frequency range 20 to 20,000 cps. Beat-frequency oscillator with maximum output voltage of 150 v, maximum output power of 2 w.]

rheostats,  $R_4$  is a resistance box,  $V_1$  is a VTVM,  $V_2$  is a VTVM, S. A. is a selective amplifier with an attenuation of the order of 60 db with respect to adjacent harmonics and a calibrated gain. MA is the investigated magnetic amplifier with  $W_1 = 2 \times 160$  turns of 0.23 mm-diameter PEL wire,  $W_2 = 1500$  turns of 0.15 mm-diameter PEL wire,  $W_3 = 125$  turns of 0.23 mm-diameter PEL Wire (PEL wire is enameled lacquer-proof copper wire).

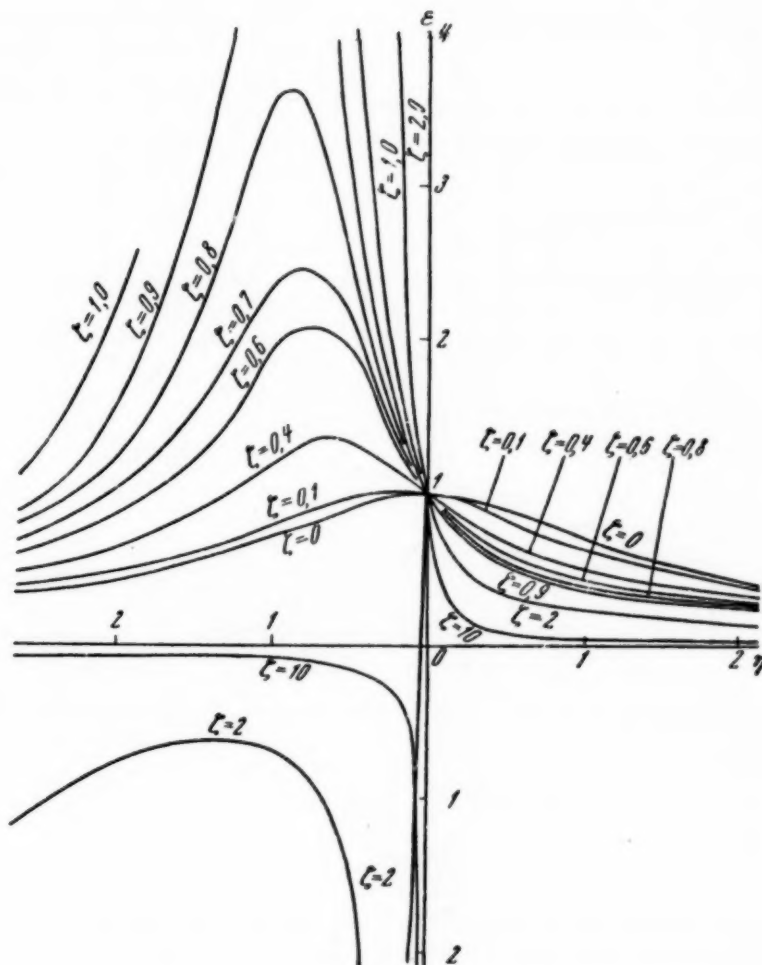


Fig. 3.

The core material of the magnetic amplifier consists of 79 HM4\*, the thickness of the core material is 0.1 mm, the cross-section of the core is  $S = 2 \times 256 \times 10^{-4} \text{ cm}^2$ , the mean diameter of the toroids is 27.5 mm. The measurements were performed for an excitation-current frequency of  $f = 500$  cps and a value of  $H_0 = 0.01$  oerst. for the constant magnetic field intensity created by the winding  $W_3$ .

First we obtained the basic magnetization curve for the investigated cores, plotted the function  $\mu_d = f(H)$  and determined the coefficients  $\mu_0 = 160 \times 10^3$  gauss/oerst. and  $B^2 = 1180$  oersted $^{-1}$  of the approximating function. The experimental results are denoted by the open circles on the corresponding curves (Figs. 4 and 5).

The function  $A = f(BH_1)$  [or the function  $E = f(BH_1)$  which is identical] was obtained for various excitation-field amplitudes according to the readings of the vacuum-tube voltmeter which was connected to the output of the unloaded amplifier.

\*[Characteristics of 79HM4: Based upon Mo-permalloy and has a high value of saturation induction.]



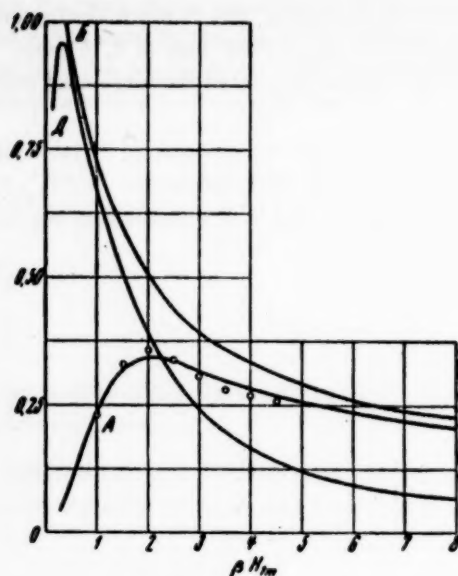


Fig. 4.

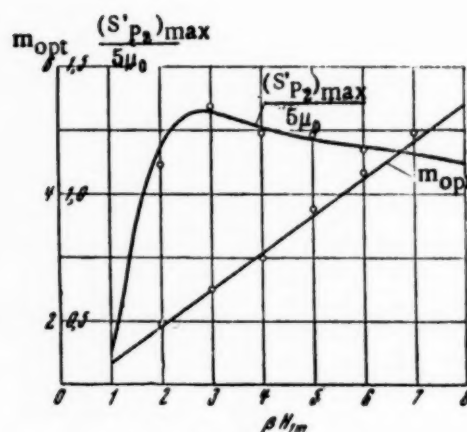


Fig. 5.

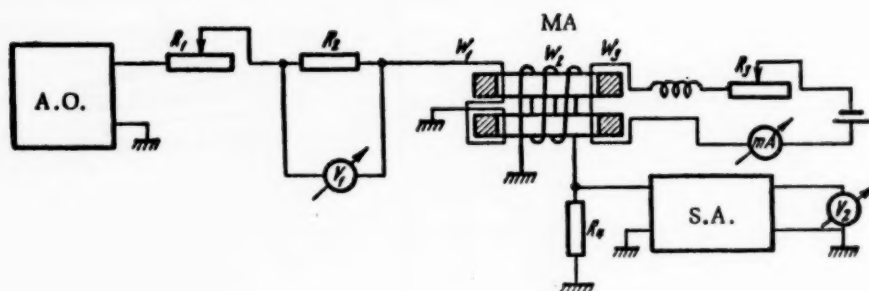


Fig. 6.

The function  $m_{opt} = f(\beta H_1)$  was determined from the value of the load impedance which corresponded to maximum power output to the load under fixed excitation conditions ( $\beta H_1 = 2, 3, 4$  etc.).

The scaled value of the sensitivity which corresponds to the optimum load for fixed excitation is then plotted on the curve  $(S'p_2)_{max} = f(\beta H_1)$ .

#### APPENDIX

##### Determining the Coefficients of the Second Harmonic Term in the Expansion of $\Delta B$ into a Fourier Series

$$\Delta B = \frac{2\mu [H_0 + H_{2m} \cos(2\omega t + \varphi)]}{1 + \alpha^2 \cos^2 \omega t}. \quad (1)$$

The term of interest to us in the expansion of the Function (1) can be written in the form

$$B_2 = B_{2a} \cos 2\omega t + B_{2b} \sin 2\omega t, \quad (2)$$



where

$$B_{2a} = \frac{1}{2\pi} \int_0^{2\pi} \frac{2\mu [H_0 + H_{2m} \cos(2\omega t + \varphi)]}{1 + \alpha^2 \cos^2 \omega t} \cos 2\omega t d\omega t, \quad (3)$$

$$B_{2b} = \frac{1}{2\pi} \int_0^{2\pi} \frac{2\mu [H_0 + H_{2m} \cos(2\omega t + \varphi)]}{1 + \alpha^2 \cos^2 \omega t} \sin 2\omega t d\omega t. \quad (4)$$

Let us compute Integrals (3) and (4) by means of the theory of residues. For this purpose we replace the real variable  $\omega t$  by the complex variable  $X = e^{j\omega t}$ .

When  $\omega t$  varies over the interval (0 to  $2\pi$ ) the complex variable  $X$  varies over a circle with a unit radius. After the new variables have been substituted and obvious transformations have been made, we obtain integrals of a rational fraction over the unit circle  $C$ :

$$B_{2a} = \frac{\mu}{\pi} \int_C \frac{H_0 + \frac{1}{2} H_{2m} \left( X^2 e^{j\varphi} + \frac{1}{X^2} e^{-j\varphi} \right)}{1 + \frac{1}{4} \alpha^2 \left( X^2 + 2 + \frac{1}{X^2} \right)} \left( X^2 + \frac{1}{X^2} \right) \frac{dX}{2jX}, \quad (5)$$

$$B_{2b} = -\frac{\mu}{\pi} \int_C \frac{H_0 + \frac{1}{2} H_{2m} \left( X^2 e^{j\varphi} + \frac{1}{X^2} e^{-j\varphi} \right)}{1 + \frac{1}{4} \alpha^2 \left( X^2 + 2 + \frac{1}{X^2} \right)} \left( X^2 - \frac{1}{X^2} \right) \frac{dX}{2X}. \quad (6)$$

Multiplying Equation (6) by  $j$  and adding it to Equation (5), we obtain

$$B_{2a} + jB_{2b} = \frac{\mu}{j\pi} \int_C \frac{H_0 + \frac{1}{2} H_{2m} \left( X^2 e^{j\varphi} + \frac{1}{X^2} e^{j\varphi} \right)}{1 + \frac{1}{4} \alpha^2 \left( X^2 + 2 + \frac{1}{X^2} \right)} X dX. \quad (7)$$

The poles of the integrand of (7) will coincide with the roots of the biquadratic equation

$$X^4 + 2 \left( 1 + \frac{2}{\alpha^2} \right) X^2 + 1 = 0. \quad (8)$$

Solving Equation (8), we find

$$X_1 = j \sqrt{\left( 1 + \frac{2}{\alpha^2} \right) - \frac{2}{\alpha^2} \sqrt{1 + \alpha^2}}, \quad X_3 = -X_1, \quad X_2 = j \sqrt{\left( 1 + \frac{2}{\alpha^2} \right) + \frac{2}{\alpha^2} \sqrt{1 + \alpha^2}}, \quad X_4 = -X_2. \quad (9)$$

By investigating the roots of Equation (8) we find that of the four roots only two ( $X_1$  and  $X_3$ ) lie within the unit circle for all values of  $\alpha$ . The two other roots  $X_2$  and  $X_4$  lie outside the unit circle for all values of  $\alpha$ . Thus

$$\begin{aligned} B_{2a} + jB_{2b} &= \frac{8\pi j\mu}{j\pi\alpha^2} \left\{ \text{res} \left[ \frac{(H_{2m} X^4 e^{j\varphi} + 2H_0 X^2 + H_{2m} e^{-j\varphi}) X}{(X - X_1)(X - X_2)(X - X_3)(X - X_4)} \right]_{X=X_1} + \right. \\ &\quad \left. + \text{res} \left[ \frac{(H_{2m} X^4 e^{j\varphi} + 2H_0 X^2 + H_{2m} e^{-j\varphi}) X}{(X - X_1)(X - X_2)(X - X_3)(X - X_4)} \right]_{X=X_3} \right\} = \\ &= \frac{8\mu}{\alpha^2} \left[ \frac{(H_{2m} X_1^4 e^{j\varphi} + 2H_0 X_1^2 + H_{2m} e^{-j\varphi}) X_1}{(X_1 - X_2)(X_1 - X_3)(X_1 - X_4)} + \frac{(H_{2m} X_3^4 e^{j\varphi} + 2H_0 X_3^2 + H_{2m} e^{-j\varphi}) X_3}{(X_3 - X_2)(X_3 - X_1)(X_3 - X_4)} \right]. \quad (10) \end{aligned}$$

After the values of  $X_1$  and  $X_3$  have been substituted into Equation (10) and obvious transformations have been made, we obtain

$$B_{2a} = -2\mu_0 \frac{(1 - \sqrt{1 + \alpha^2})^3}{\alpha^2 \sqrt{1 + \alpha^2}} \left( H_0 - \frac{2 + \alpha^2}{\alpha^2} H_{2m} \frac{e^{j\varphi} + e^{-j\varphi}}{2} \right),$$

$$B_{2b} = \mu H_{2m} \frac{(1 - \sqrt{1 + \alpha^2})^3}{\alpha^2 \sqrt{1 + \alpha^2}} \frac{3\alpha^2 + 2\sqrt{1 + \alpha^2} + 6}{\alpha^2} \frac{e^{j\varphi} - e^{-j\varphi}}{2j}.$$

by setting the real and imaginary portions of Equation (10) equal to each other.

Received April 17, 1956

#### LITERATURE CITED

- [1] V. K. Arkad'ev, *Electromagnetic Processes in Metals*. State Scientific and Tech. Press, Vol. 1, 1934; Vol. 2, 1936.\*
- [2] V. I. Kovalenkov, *Fundamentals of Magnetic Network Theory*. Acad. Sci. USSR Press, (1940).\*
- [3] M. A. Rozenblat, The Effect of Even Harmonics Upon the Characteristics of Ferromagnetic materials when they are Simultaneously Magnetized by DC and AC Magnetic Fields. *J. Tech. Phys.*, Vol. 18, No. 16 (1948).
- [4] L. A. Bessonov, *Electrical Circuits Containing Steel*, State Power Press, (1948).\*
- [5] F. C. Williams, The Fundamental Limitations of the second-harmonic Type of Magnetic Modulator. *Proceed. Instrum. Electrical Eng.* II, 97 August, (1950).
- [6] M. Wurm, Beiträge zur Theorie des Feldstärkedifferenzmessers für magnetische Felder nach Förster. *Zeitschrift angew. Phys* 2 (1950).
- [7] S. W. Noble, The Design of a Practical D.C. amplifier based on the second-harmonic Type of magnetic modulator. *PJEE*, Part II, August (1952).

\* In Russian.

## BLOCK DIAGRAMS FOR MAGNETIC AMPLIFIERS WITH "HARD" AND "SOFT" FEEDBACK LOOPS

L. A. Grigorian

(Erevan)

A method is proposed for composing and evaluating the parameters of block diagrams for magnetic amplifiers with "hard" and "soft" feedback loops. The paper examines amplifiers which work into a RL load that is connected after a rectifier; the fluctuations of the perturbation factor are considered small.

It is demonstrated that, depending upon the parameters of the amplifier and the load, the system can be replaced by seven different block diagrams. Expressions are derived which define the parameters of the block diagram for the general case, as well as for the case of an ideal magnetic circuit.

In investigating transient response in automatic control systems which contain magnetic amplifiers we often encounter the problem of determining what block diagrams can be used to replace the magnetic amplifiers.

In this paper we propose a method for composing and evaluating the parameters of block diagrams for magnetic amplifiers with "hard" and "soft" feedback loops which work into a RL load which is connected to the output of a rectifier (Fig. 1).

The basis of the method is an investigation of the transient response of magnetic amplifiers when the fluctuations of the perturbation factor are small; this makes it possible to linearize all the nonlinear equations of the system.

The following basic assumptions and postulates have been made.

1) Taking into account the fact that the transient response of magnetic amplifiers usually lasts over a period of several ac cycles, we use average values for the current values of currents, voltages and other quantities. For example, for the current we have

$$I_t = \frac{1}{T} \int_{t-\frac{T}{2}}^{t+\frac{T}{2}} |i| dt.$$

Here the mode of operation of the amplifier during each cycle can be assumed close to steady-state operation.

2) During the transient response the rectification coefficients of the rectifier with respect to current and voltage are assumed constant.

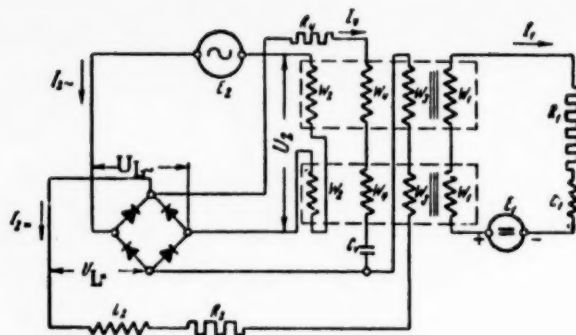


Fig. 1. Block diagram of the magnetic amplifier.

3) The reverse current of the rectifier is assumed equal to zero, and the forward voltage drop is added to the voltage across the resistive load. Thus an "ideal" rectifier is analyzed.

4) The effect of the current in a "soft" feedback loop upon the magnitude of the load current is neglected.

5) The emf induced in a "hard" feedback coil is not taken into account, since it is insignificant in comparison to the other voltages which affect the working circuit (see Appendix).

### 1. The General Differential Equation for the Magnetic Amplifier

For the assumptions we have made, the state of dynamic equilibrium is described by the following equations when we are analyzing the specified magnetic amplifier circuit:

$$R_1 I_1 + L_1 \frac{dI_1}{dt} + \frac{d\Psi_1}{dt} = E_1, \quad (1)$$

$$\Psi_1 = f_1(U_2, AW_-), \quad (2)$$

$$U_2 = f_2(E_2, U_{L-}), \quad (3)$$

$$U_{L-} = R_2 I_{2-} + L_2 \frac{dI_{2-}}{dt}, \quad (4)$$

$$I_{2-} = f_3(U_2, AW_-), \quad (5)$$

$$AW_- = I_1 W_1 + I_2 W_3 - I_4 W_4, \quad U_{L-} = R_4 I_4 + \frac{1}{C} \int I_4 dt - \frac{d\Psi_4}{dt}, \quad (6)$$

$$\Psi_4 = \Psi_1 \frac{W_1}{W_4}, \quad \alpha_1 = \frac{U_{L-}}{U_{L-}}, \quad \alpha_2 = \frac{I_{2-}}{I_{2-}}, \quad (7)$$

where  $\Psi_1$  and  $\Psi_4$  are the average values of the resultant flux linkages between the control winding and the "soft" feedback coil of the magnetic amplifier.

The remaining notation is evident from Fig. 1.

Linearizing Equations (2), (3) and (5) and making use of the expressions

$$H_{\sim} = \frac{I_{2-} W_2}{l}, \quad H_- = \frac{AW_-}{l}, \quad (8)$$

$$B_{\sim a} = \frac{U_2}{8fW_2 S}, \quad B_{\sim} = \frac{\Psi_1}{2W_1 S}, \quad (9)$$

we obtain

$$H_{\sim} = k_1 B_{\sim} + \frac{k_1}{k_2} H_- - k_1 A_1, \quad (10)$$

$$B_- = k_3 H_- - k_4 B_{\sim a} + A_2, \quad (11)$$

$$U_2 = k_5 E_2 - k_6 U_{L\sim} + A_3, \quad (12)$$

where

$$k_1 = \left. \frac{\partial H_-}{\partial B_{\sim a}} \right|_{H_{\sim 0}, B_{\sim a 0}}, \quad k_2 = - \left. \frac{\partial H_-}{\partial B_{\sim}} \right|_{H_{\sim 0}, B_{\sim 0}}, \quad A_1 = B_{\sim a} |_{H_{\sim 0}, H_{\sim 0}}, \quad (13)$$

$$k_3 = \left. \frac{\partial B_-}{\partial H_-} \right|_{B_{\sim 0}, H_{\sim 0}}, \quad k_4 = - \left. \frac{\partial B_-}{\partial B_{\sim}} \right|_{B_{\sim 0}, B_{\sim a 0}}, \quad A_2 = B_- |_{H_{\sim 0}, B_{\sim 0}}, \quad (14)$$

$$k_5 = \left. \frac{\partial U_2}{\partial E_2} \right|_{U_{20}, E_{20}}, \quad k_6 = - \left. \frac{\partial U_2}{\partial U_{L\sim}} \right|_{U_{20}, U_{L\sim 0}}, \quad A_3 = U_2 |_{E_{20}, U_{L\sim 0}}. \quad (15)$$

The subscript zero denotes the initial value of the quantity; small fluctuations occur in the vicinity of this value.

Solving Equations (1), (4)-(7), (10)-(12) simultaneously, we obtain the general differential equation for the magnetic amplifier:

$$\begin{aligned} & N_1 \frac{d^4 I'_{2-}}{dt^4} + N_2 \frac{d^3 I'_{2-}}{dt^3} + N_3 \frac{d^2 I'_{2-}}{dt^2} + N_4 \frac{d I'_{2-}}{dt} + N_5 I'_{2-} = \\ & = E'_1 + N_6 \frac{d E'_1}{dt} + N_7 E'_2 + N_8 \frac{d E'_2}{dt} + N_9 \frac{d^2 E'_2}{dt^2} + N_{10} \frac{d^3 E'_2}{dt^3} + N_{11}, \end{aligned} \quad (16)$$

where

$$I'_2 = I_{2-} W_2, \quad E'_1 = \frac{E_1}{W_1}, \quad E'_2 = \frac{E_2}{W_2},$$

$$N_1 = \frac{k_0 (k_2 k_3 + k_4) \beta^2 C'_4 L'_{2-}}{4 f \alpha_1}, \quad (17)$$

$$N_2 = \frac{k_0 (k_2 k_3 + k_4)}{4 f \alpha_1} [\beta^2 C'_4 (R'_1 L'_{2-} + R'_2 L'_1) + \tau_4 L'_{2-}] + \frac{2 k_2 k_3 \beta^2 F C'_4 L'_1}{k_1 \alpha_2 l} + \frac{k_2 k_3 \tau_4 L'_1 L'_2}{8 f F \alpha_1} + \beta C'_4 L'_1 L'_2, \quad (18)$$

$$\begin{aligned} N_3 = & \frac{k_0 (k_2 k_3 + k_4)}{4 f \alpha_1} (\beta^2 R'_1 R'_2 C'_4 + \tau_4 R'_2 + L'_{2-}) + \frac{2 k_2 k_3 F}{k_1 \alpha_2} \times \\ & \times (\beta^2 R'_1 C'_4 + \tau_4) + \frac{k_2 k_3}{8 f \alpha_1 F} [\tau_4 (R'_1 L'_{2-} + L'_1 R'_2) + L'_1 L'_{2-}] + \\ & + \beta C'_4 (R'_1 L'_{2-} + L'_1 R'_2) + \frac{\tau_4 L'_1}{\alpha_2} \left( \frac{k_2}{k_1} - \alpha_2 \gamma \right), \end{aligned} \quad (19)$$

$$\begin{aligned} N_4 = & \frac{k_2 k_3}{8 f \alpha_1 F} (R'_1 L'_{2-} + \tau_4 R'_1 R'_2 + L'_1 R'_2) + \frac{2 k_2 k_3 F}{k_1 \alpha_2} + \\ & + \frac{k_0 (k_2 k_3 + k_4) R'_2}{4 f \alpha_1} + \frac{1}{\alpha_2} (L'_1 + \tau_4 R'_1) \left( \frac{k_2}{k_1} - \alpha_2 \gamma \right) + \beta C'_4 R'_2 R'_1, \end{aligned} \quad (20)$$

$$N_5 = \frac{k_2 k_3 R'_1 R'_2}{8 f \alpha_1 F} + \frac{R'_1}{\alpha_2} \left( \frac{k_2}{k_1} - \alpha_2 \gamma \right), \quad N_6 = \tau_4, \quad (21)$$

$$N_7 = \frac{k_2 k_3 R'_1}{8 f F}, \quad N_8 = \frac{k_2 k_3}{8 f F} (\tau_4 R'_1 + L'_1) + \frac{k_0 (k_2 k_3 + k_4)}{4 f}, \quad (22)$$

$$N_9 = \frac{k_0 (k_2 k_3 + k_4)}{4 f} (\beta^2 R'_1 C'_4 + \tau_4) + \frac{k_2 k_3 \tau_4 L'_1}{8 f F}, \quad (23)$$

$$N_{10} = \frac{k_0 (k_2 k_3 + k_4) \beta^2 C'_4 L'_1}{4 f}, \quad N_{11} = k'_2 R'_1 \left( \frac{A'_3}{8 f F} + A_1 l \right), \quad (24)$$

where  $l$  is the mean length of a magnetic line of force,  $f$  is the frequency of the supply line,

$$\begin{aligned} A'_3 &= \frac{A_3}{W_2}, & R'_1 &= \frac{R_1}{W_1^2}, & R'_2 &= \frac{R_2}{W_2^2}, & R'_4 &= \frac{R_4}{W_2^2}, \\ L'_{2-} &= \frac{L_2}{W_2^2}, & L'_{1-} &= \frac{L_1}{W_1^2}, & C'_4 &= C_4 W_2^2, & \gamma &= \frac{W_3}{W_2}, \\ \beta &= \frac{W_4}{W_2}, & \tau_4 &= C_4 R_4, & F &= \frac{S}{l}, \end{aligned}$$

where  $S$  is the cross-section of the core.

The terms of the coefficients of the differential equation which contain  $\beta^2$  are produced as a result of considering flux linkage with the "soft" feedback coil.

In the case where hard feedback is connected through a separate rectifier the coefficient  $\alpha_2$  in front of  $\gamma$  must be assumed equal to unity.

Passing from the resultant values of the currents and voltages to their increments, we obtain

$$\begin{aligned} N_1 \frac{d^4 \Delta I'_{2-}}{dt^4} + N_2 \frac{d^3 \Delta I'_{2-}}{dt^3} + N_3 \frac{d^2 \Delta I'_{2-}}{dt^2} + \\ + N_4 \frac{d \Delta I'_{2-}}{dt} + N_5 \Delta I'_{2-} = \Delta E'_1 + N_6 \frac{d \Delta E'_1}{dt} + \\ + N_7 \Delta E'_2 + N_8 \frac{d \Delta E'_2}{dt} + N_9 \frac{d^2 \Delta E'_2}{dt^2} + N_{10} \frac{d^3 \Delta E'_2}{dt^3}, \end{aligned} \quad (16')$$

where

$$\Delta I'_{2-} = I'_{2-} - I_{2-0}, \quad \Delta E'_1 = E'_1 - E'_{10}, \quad \Delta E'_2 = E'_2 - E'_{20}.$$

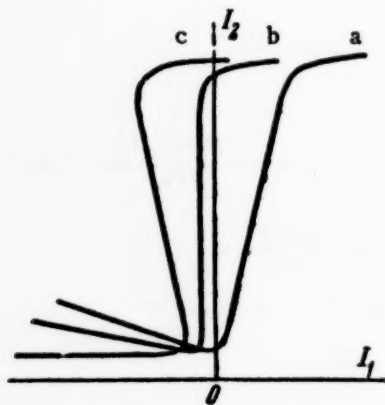


Fig. 2. Operating characteristics of the magnetic amplifier.

Let us determine the power-increment gain:

$$\xi_P = \Delta P_2 / \Delta P_1 \quad (25)$$

where

$$\Delta P_2 = \Delta I'^2_{2-} R'_2, \quad \Delta P_1 = \frac{\Delta E'^2_1}{R'_1}. \quad (26)$$

In a steady-state mode of operation when  $\Delta E'_2 = 0$ , Equation (16') acquires the form:

$$N_5 \Delta I'_{2-} = \Delta E'_1. \quad (27)$$

Solving Equations (25)-(27) simultaneously, we obtain

$$\xi_P = \frac{R'_1 R'_2}{N_5^2} = \frac{R'_2}{\left[ \frac{k_2 k_6}{8 f F \alpha_1} R'_2 + \frac{1}{\alpha_2} \left( \frac{k_2}{k_1} - \alpha_2 \gamma \right) \right]^2 R'_1}. \quad (28)$$

## 2. Block Diagrams of Magnetic Amplifiers

The coefficient  $N_5$  depends upon the coefficient of "hard" feedback and can acquire the following values.

1) When the feedback is under compensated (and also when there is no hard feedback; see Fig. 2, Curve a) we have  $N_5 > 0$ .

2) For compensated feedback (Fig. 2, Curve b) we have  $N_5 = 0$ .

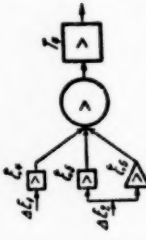





TABLE 1

Block Diagram for the Magnetic Amplifier in the Case Where there is no Soft Feedback

No.	$N_1$ $N_2$ and $L_{12}$	$\frac{\Delta N_1 N_2}{N_1^2}$	Differential equations of the system	Block diagrams of the magnetic amplifier	Values for the constants of the block diagram	Values for the constants of the block diagram for the case of an ideal magnetic circuit and natural magnetization
1	$N_1 > 0$ $N_2 > 0$ $L_{12} > 0$	$> 1$	$\left( \Omega^2 + \frac{1}{a^2} p^2 + \frac{2a}{\Omega^2 + a^2} p + 1 \right) \Delta I_{2-} = \xi_1 \Delta E_1 + \xi_2 \Delta E_2 + \xi_3 p \Delta E_3$		$\Omega = \frac{N_1}{2N_2} \sqrt{\frac{4N_1 N_2}{N_1^2}} - 1$ $\xi_1 = -\frac{N_1}{2N_2}, \xi_2 = \frac{N_2}{N_1}, \xi_3 = \frac{N_2}{N_1}$	$\Omega = \frac{1}{2T_L} \sqrt{\frac{16T_L R_1' \left( \frac{1}{a_2} - \gamma \right)}{R_2'}} - 1 = \frac{1}{2T_L} \sqrt{\frac{16T_L}{\xi_p \left( \frac{1}{a_2} - \gamma \right)}}$ $\xi_1 = \frac{1}{2T_L}, \xi_2 = \left( \frac{1}{a_2} - \gamma \right) R_1', \xi_3 = \frac{R_2'}{4f R_1' \left( \frac{1}{a_2} - \gamma \right)}$
2	$N_1 > 0$ $N_2 > 0$ $L_{12} > 0$	$< 1$	$(T_1 p + 1)(T_2 p + 1) \Delta I_{2-} = \xi_1 \Delta E_1 + \xi_2 \Delta E_2 + \xi_3 p \Delta E_3$		$T_{1,2} = \frac{2N_2}{N_1} \sqrt{\frac{4N_1 N_2}{N_1^2}} - 1$	$T_{1,2} = \frac{2T_L}{1 \pm \sqrt{\frac{16T_L R_1' \left( \frac{1}{a_2} - \gamma \right)}{R_2'}}}$ $= \frac{2T_L}{1 \pm \sqrt{1 - \frac{16/T_L}{\xi_p \left( \frac{1}{a_2} - \gamma \right)}}}$
3	$N_1 > 0$ $N_2 = 0$ $L_{12} = 0$		$(T_2 p + 1) \Delta I_{2-} = \xi_1 \Delta E_1 + \xi_2 \Delta E_2 + \xi_3 p \Delta E_3$		$T_2 = \frac{N_2}{N_1}$	$T_2 = \frac{R_2'}{4f R_1' \left( \frac{1}{a_2} - \gamma \right)} = \frac{\xi_p \left( \frac{1}{a_2} - \gamma \right)}{4f}$

TABLE 1 (Continued)

4	0	> 0		$p(T_{sp} + 1) \Delta I_{2-} = \xi_4 \Delta E_1 + \xi_4 p \Delta E_2$		$T_4 = \frac{N_2}{N_4}, \quad \xi_4 = \frac{1}{N_4}, \quad \xi_4 = \frac{1}{N_4}$	$T_4 = T_L, \quad \xi_4 = \frac{1}{R_2}, \quad \xi_4 = \frac{1}{R_2}$
5	0	0		$p \Delta I_{2-} = \xi_4 \Delta E_1 + \xi_4 p \Delta E_2$			
6	< 0	> 0	< 1	$(T_{sp} - 1)(T_{sp} + 1) \Delta I_{2-} = \xi_4 \Delta E_1 + \xi_4 p \Delta E_2$			
7	> 0	0		$(T_{sp} - 1) \Delta I_{2-} = \xi_4 \Delta E_1 + \xi_4 p \Delta E_2$		$T_{s,s} = \frac{2T_L}{\sqrt{1 + \frac{16/T_L R_1' (\frac{1}{a_2} - \gamma)}{R_2}}} \pm 1$ $= \frac{2T}{\sqrt{1 \pm \frac{16/T_L}{\xi_p (\frac{1}{a_2} - \gamma)}}} \pm 1$	

3) For overcompensated feedback (Fig. 2, Curve c) we have  $N_5 < 0$ .

Table 1 shows the block diagrams of the magnetic amplifier and their parameters for various values of the coefficients  $N_4$  and  $N_5$  (and for the expression  $4N_3N_5/N_4^2$  which determines the nature of transient response, i.e., whether the response is oscillatory or aperiodic). In order to simplify the investigation of the effect produced by individual factors, the case for which there is no soft feedback ( $\beta = 0$ ,  $\tau_4 = 0$ ) is analyzed. Here the coefficients  $N_1$ ,  $N_2$ ,  $N_6$ ,  $N_9$  and  $N_{10}$  of the differential equation are equal to zero.

It can be seen from the table that, depending upon the values of the coefficients of the differential equation, the block diagram of the examined magnetic amplifier can acquire seven different forms.

When a RL load with  $\cos \varphi > 0.16$  is present in the ac circuit, it is possible to assume that the load is resistive (to a certain approximation), since the time constant of such a load is less than the duration of one ac cycle and the transient response in the amplifier lasts for several cycles.

### 3. Determining the Coefficients of the Linearized Equations of the Magnetic Amplifier

The coefficients of the linearized equations of the magnetic amplifier can be determined in two different ways:

- 1) analytically, by means of approximating the magnetization curve of the magnetic material;
- 2) experimentally, by plotting a family of characteristics which correspond to Expressions (2), (3) and (5).

Below these coefficients are determined analytically when the magnetic circuit is ideal (Fig. 3); this analysis is made for the case of forced magnetization when the impedance of the control circuit to even harmonics is sufficiently great, and for the case of natural magnetization when the impedance of the control circuit is sufficiently small.

In the first case there are no even harmonics in the ampere-turns of the amplifier; in the second case there are no even harmonics in the flux.

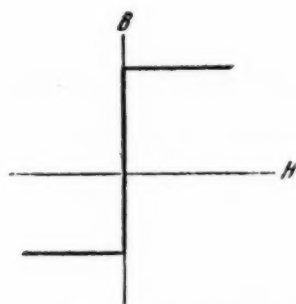


Fig. 3. Magnetization curves of an ideal magnetic circuit.

A. Forced Magnetization. As we know [3], in such an operating mode the curve representing current is rectangular (Fig. 4) and after rectification there will be no current pulsation, and therefore the inductance beyond the rectifier will not affect the operating regime of the amplifier; thus the load can be assumed to be a resistive load within the limits of one period.

Taking the assumption which we made at the beginning of the article into account, the coefficients of

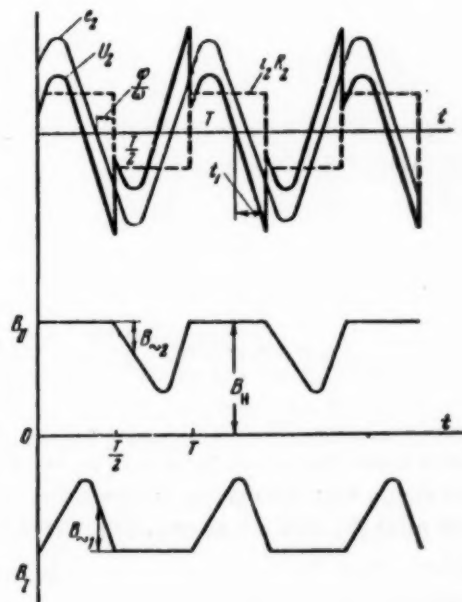


Fig. 4. Curves showing variation of basic quantities of amplifier for forced magnetization:  $e_2$  is emf applied to ac circuit,  $U_2$  is resultant voltage across ac windings of amplifier,  $i_2R_2$  is voltage drop across load,  $B_I$  and  $B_{II}$  are values of induction in first and second cores.

current and voltage rectification will prove to be equal to unity when the amplifier operates in a regime of forced magnetization:  $\alpha_1 = 1$ ,  $\alpha_2 = 1$ .

It is known [1], [2], [3] that for an ideal magnetic circuit we have

$$H_{\sim} = H_{\pm} \text{ and } \frac{\partial H_{\sim}}{\partial B_{\sim}} = 0. \quad (29)$$

on the working sector of the magnetic amplifier characteristic.

Taking (29) into account and making use of Expressions (10) and (13), it can be shown that  $k_1 = k_2 = 0$ . Here  $A_1$  can vary within the limits  $0 < A_1 < B_S$  ( $B_S$  is the saturation induction).

Let us pass over to determining the expression for the dc component of the magnetic induction  $B_{\pm}$ .

In accordance with [3] the instantaneous values of the alternating component of the induction will be

$$\begin{aligned} B_{\sim 1} &= \frac{E_2 a}{2\omega W_2 S} \left[ \left( 1 - \frac{2\omega t}{\pi} \right) \cos \varphi - \cos(\omega t + \varphi) \right], \\ B_{\sim 2} &= \frac{E_2 a}{2\omega W_2 S} \left[ \left( \frac{2\omega t}{\pi} - 1 \right) \cos \varphi - \cos(\omega t + \varphi) \right]. \end{aligned} \quad (30)$$

Figure 4 shows the curve for the variation of the inductions  $B_I$  and  $B_{II}$  in the first and second cores.

The dc component of the induction can be written as

$$B_{\pm} = B_S - \frac{2}{T} \int_0^{\frac{T}{2}} B_{\sim 1} dt. \quad (31)$$

over one half-cycle.

Substituting the value of  $B_{\sim 1}$  from (30) into (31), we obtain

$$B_{\pm} = B_S - \frac{E_2 \sin \varphi}{2W_2 \omega S}. \quad (32)$$

Making use of the expression for the instantaneous value of the voltage across the ac windings, we obtain the average value of this voltage:

$$U_2 = E_2 \eta, \quad (33)$$

where

$$\eta = \cos \arcsin \frac{2 \cos \varphi}{\pi} - \left[ 1 - \frac{2}{\pi} \arcsin \frac{2 \cos \varphi}{\pi} - \frac{2\varphi}{\pi} \right] \cos \varphi.$$

Figure 5 shows the curves for  $\eta = f(\varphi)$  and  $\sin \varphi$  plotted as functions of  $\varphi$ . It is evident from the curve shown in the figure that the maximum deviation of  $\eta$  from  $\sin \varphi$  in the working zone of variation of  $\varphi$  (from  $90^\circ$  to  $32^\circ 36'$ ) [3] does not exceed 13%. Thus we can assume to a certain approximation that  $\eta = \sin \varphi$ . Then

$$U_2 = E_2 \sin \varphi. \quad (34)$$

Solving Equations (9), (32) and (34) simultaneously, we obtain

$$B_{\pm} = B_S - \frac{2B_{\sim}}{\pi}. \quad (35)$$

Substituting Equation (35) into Equation (14), we obtain  $k_2 = 0$ ,  $k_4 = \frac{2}{\pi}$ , and  $A_2 = B_S$ . In accordance with [3] the average value of the load voltage is

$$U_L = E_2 \cos \varphi. \quad (36)$$

Solving Equations (34) and (36) simultaneously, we obtain

$$E_2 = \sqrt{U_2^2 + U_L^2} \quad (37)$$

Figure 6 shows the experimental curve  $U_2 = f(U_L)$  for a magnetic amplifier which operates in a regime of forced magnetization when  $E_2 = \text{const}$  (Curve a). The indicated curve verifies the correctness of Expression (37).

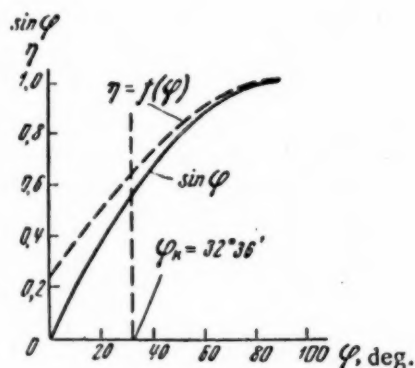


Fig. 5.

Making use of (37), we obtain the following results in accordance with Equation (15):

$$k_6 = \frac{1}{\sqrt{1 - I_2^{*2}}}, \quad k_8 = \frac{I_2^*}{\sqrt{1 - I_2^{*2}}}, \quad A_8 = 0, \quad (38)$$

$$I_2^* = \frac{I_2}{I_{2\max}}, \quad I_{2\max} = \frac{E_2}{R_2}.$$

In analogous fashion, we shall show that  $k_1 - k_2 = 0$ .

**B. Natural Magnetization.** Figure 7 shows the curves for the variation of the basic quantities of the amplifier for a regime of natural magnetization when the load is resistive. Figure 8 shows the same curves for an inductive load. The shape of the curves which represent the variation of the induction is identical for both cases.

As can be seen from the curves in Fig. 7, we have:

$$2B_- = 2B_S - 2B_{\sim a} \quad \text{or} \quad B_- = B_S - B_{\sim a}. \quad (39)$$

Substituting Equations (39) into (14), we obtain  $k_3 = 0$ ,  $k_4 = 1$  and  $A_2 = B_S$ .

Since the line voltage appears across the amplifier during one portion of the cycle and across the load during the other portion of the cycle, it is not difficult to show that the average values of these voltages are related by the following equation:

$$E_2 = U_2 + U_L \quad (40)$$

Figure 6 shows the experimental curve  $U_2 = f(U_L)$  for natural magnetization and  $E_2 = \text{const}$  (Curve b). The working portion of the characteristic verifies the correctness of Expression (40). The deviation from this law in the initial sector of the characteristic can be explained by the divergence between the actual magnetization curve and the ideal magnetization curve.

Substituting (40) into (15), we find that  $k_5 = 1$ ,  $k_6 = 1$  and  $A_3 = 0$ .

The rectification coefficients  $\alpha_1$  and  $\alpha_2$  for a resistive load are equal to unity. Let us determine these coefficients for the case of an inductive load. In the interval from  $t = 0$  to  $t = t_1$  (Fig. 8) the instantaneous value of the rectified current will be

$$i'_{2-} = \frac{E_{2a}}{R} \frac{\sin \varphi - \sin(\omega t_1 - \varphi) e^{-\frac{t_1}{T_L} - \frac{T}{2T_L}}}{1 - e^{-\frac{T}{2T_L}}} \cos \varphi e^{-\frac{t}{T_L}}, \quad (41)$$

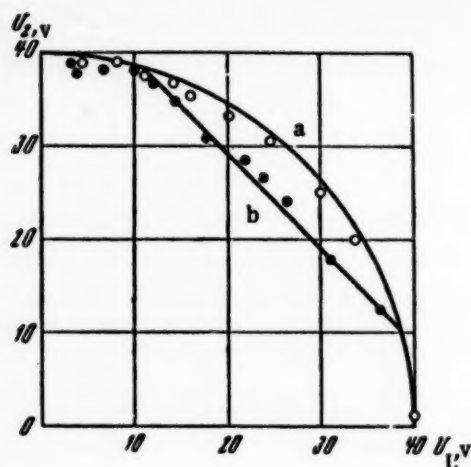


Fig. 6.

where

$$T_L = \frac{L_{2-}}{R_2}, \quad \varphi = \arctg \frac{\omega L_{2-}}{R_2}, \quad T = \frac{1}{f}.$$

The instantaneous value of the alternating and rectified current in the interval from  $t = t_1$  to  $t = T/2$  will be

$$i_{2-}^* = i_{2-} = \frac{E_{2a}}{R} \cos \varphi \left[ \sin(\omega t - \varphi) + \right.$$

$$\left. + \frac{\sin \varphi - \sin(\omega t_1 - \varphi) e^{-\frac{t_1}{T_L}}}{1 - e^{-\frac{T}{2T_L}}} e^{-\frac{t}{T_L}} \right]. \quad (42)$$

Making use of Expressions (41) and (42), we determine the relative magnitude of the average value of the ac current and the rectified current:

$$I_{2-}^* = \frac{I_{2-}}{I_{2\max}} = \frac{1}{2} \left[ \cos^2 \varphi + \cos \varphi \cos(\omega t_1 - \varphi) + \sin \varphi \times \frac{\sin \varphi - \sin(\omega t_1 - \varphi) e^{-\frac{t_1}{T_L}}}{1 - e^{-\frac{T}{2T_L}}} \left( e^{-\frac{t_1}{T_L}} - e^{-\frac{T}{2T_L}} \right) \right],$$

$$I_{2-}^* = \frac{I_{2-}}{I_{2\max}} = \frac{1}{2} [\cos^2 \varphi + \cos \varphi \cos(\omega t_1 - \varphi) + \sin^2 \varphi - \sin \varphi \sin(\omega t_1 - \varphi)]. \quad (43)$$

When the inductance beyond the rectifier is sufficiently great (i.e., when it is possible to assume that  $T_L \rightarrow \infty$  and  $\varphi \rightarrow \pi/2$ ) Expressions (43) acquire the form:

$$I_{2-}^* = \frac{1}{2} (1 + \cos \omega t_1) \left( 1 - \frac{2t_1}{T} \right), \quad I_{2-} = \frac{1}{2} (1 + \cos \omega t_1). \quad (43a)$$

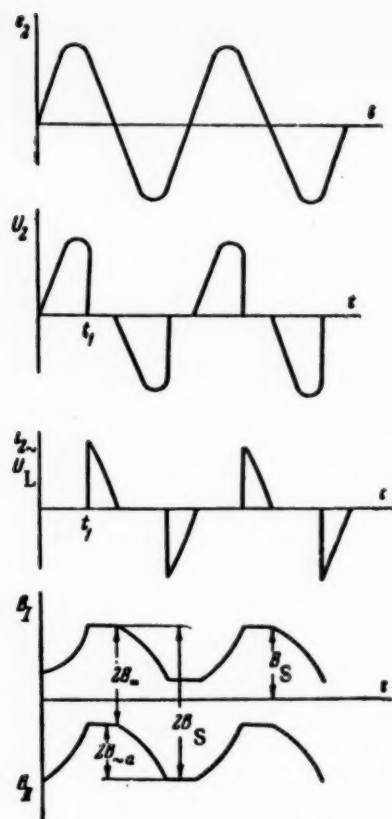


Fig. 7.



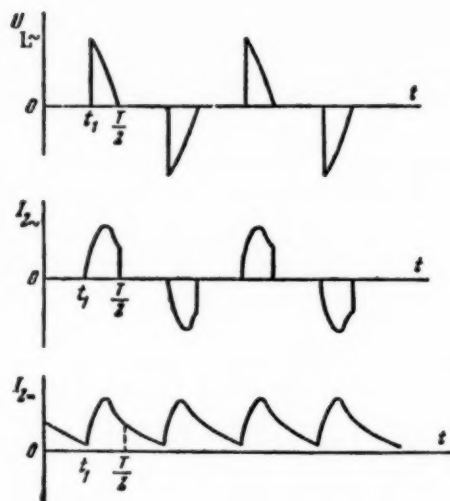


Fig. 8. Curves for the variation of the amplifier currents and voltages for natural magnetization and a RL load connected through a rectifier according to Fig. 1.

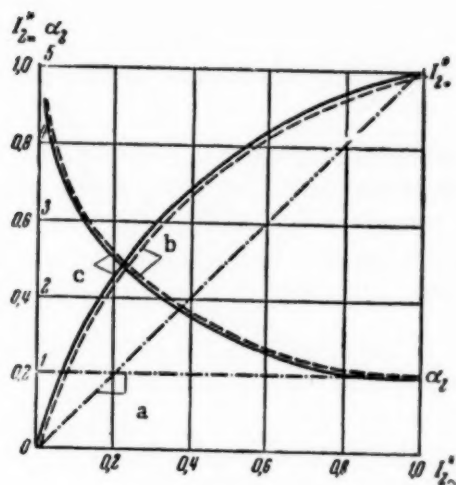


Fig. 9. a)  $\frac{\omega L_2}{R_2} = 0$ , b)  $\frac{\omega L_2}{R_2} = 5$ , c)  $\frac{\omega L_2}{R_2} = \infty$ .

In such a case the current-rectification coefficient will be

$$\alpha_2 = \frac{I_{2*}}{I_{2*}} = \frac{1}{1 - \frac{1}{180^\circ} \arccos(2I_{2*} - 1)} \quad (44)$$

Figure 9 shows the curves for the dependence of  $I_{2*}$  and  $\alpha_2$  upon  $I_{2*}$  for the cases  $\omega L_2/R_2 = 0.5$  and  $\infty$  (the dash-dot, dashed and solid lines respectively). It is evident from Fig. 9 that the curves  $\alpha_2 = f(I_{2*})$  for the cases  $\omega L_2/R_2 = 5$  and  $\omega L_2/R_2 = \infty$  almost coincide; therefore in the majority of cases it is possible to make use of Expression (44).

It is not difficult to show that the voltage-rectification coefficient is  $\alpha_1 = 1$ . Substituting the values which we have determined for the coefficients into Equations (17)-(24), we obtain the coefficients of the differential equation for an ideal magnetic conductor in the cases of forced and natural magnetization.

Thus for an ideal magnetic circuit the free term  $N_{11}$  of the differential equation is equal to zero; the remaining coefficients are constant and do not depend upon the magnitude of the current when the magnetization is natural and the load is resistive ( $\alpha_2 = 1$ ). Therefore in the indicated case the differential equation for the magnetic amplifier is also linear for the full values of the currents and voltages (within the limits of the working portion of the characteristic). Column 8 of Table 1 shows the values for the constants of the block diagram in the case of an ideal magnetic circuit and natural magnetization.

#### 4. Analysis of the Results and Conclusions

On the basis of our results we plotted curves for the dependence of the constants which characterized the block diagram of the amplifier upon the time constant of the load and the feedback coefficient for an ideal magnetic circuit, natural magnetization, the absence of "soft" feedback, and  $L_1 = 0$ ; these curves are shown in Figs. 10 and 11.

In order to facilitate an investigation of the effect of individual parameters upon the nature of the transient response, the coefficient of rectification  $\alpha_2$  is assumed equal to unity. The quantities  $T_1^*$ ,  $T_2^*$ ,  $T_7^*$  and  $T_8^*$  are the relative values of the time constants.

The base quantity is assumed to be the time constant of the amplifier when the load is resistive and there is no feedback:

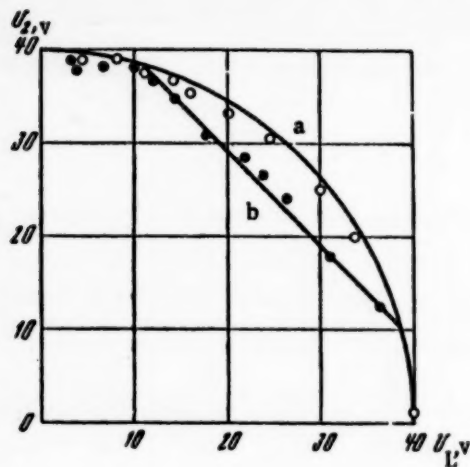


Fig. 6.

where

$$T_L = \frac{L_{2-}}{R_2}, \quad \varphi = \arctg \frac{\omega L_{2-}}{R_2}, \quad T = \frac{1}{f}.$$

The instantaneous value of the alternating and rectified current in the interval from  $t = t_1$  to  $t = T/2$  will be

$$i_{2-} = i_{2\sim} = \frac{E_{2a}}{R} \cos \varphi \left[ \sin(\omega t - \varphi) + \right.$$

$$\left. + \frac{\sin \varphi - \sin(\omega t_1 - \varphi) e^{-\frac{t_1}{T_L}}}{1 - e^{-\frac{T}{2T_L}}} e^{-\frac{t}{T_L}} \right]. \quad (42)$$

Making use of Expressions (41) and (42), we determine the relative magnitude of the average value of the ac current and the rectified current:

$$I_{2\sim}^* = \frac{I_{2\sim}}{I_{2\max}} = \frac{1}{2} \left[ \cos^2 \varphi + \cos \varphi \cos(\omega t_1 - \varphi) + \sin \varphi \times \frac{\sin \varphi - \sin(\omega t_1 - \varphi) e^{-\frac{t_1}{T_L}}}{1 - e^{-\frac{T}{2T_L}}} \left( e^{-\frac{t_1}{T_L}} - e^{-\frac{T}{2T_L}} \right) \right],$$

$$I_{2\sim}^* = \frac{I_{2-}}{I_{2\max}} = \frac{1}{2} [\cos^2 \varphi + \cos \varphi \cos(\omega t_1 - \varphi) + \sin^2 \varphi - \sin \varphi \sin(\omega t_1 - \varphi)]. \quad (43)$$

When the inductance beyond the rectifier is sufficiently great (i.e., when it is possible to assume that  $T_L \rightarrow \infty$  and  $\varphi \rightarrow \pi/2$ ) Expressions (43) acquire the form:

$$I_{2\sim}^* = \frac{1}{2} (1 + \cos \omega t_1) \left( 1 - \frac{2t_1}{T} \right), \quad I_{2-}^* = \frac{1}{2} (1 + \cos \omega t_1). \quad (43a)$$

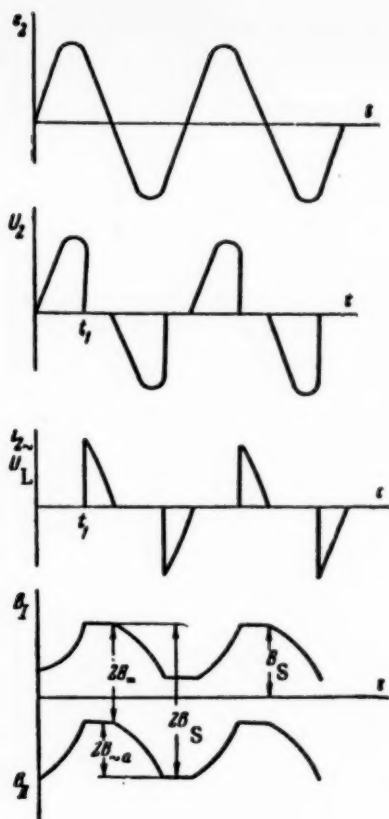


Fig. 7.

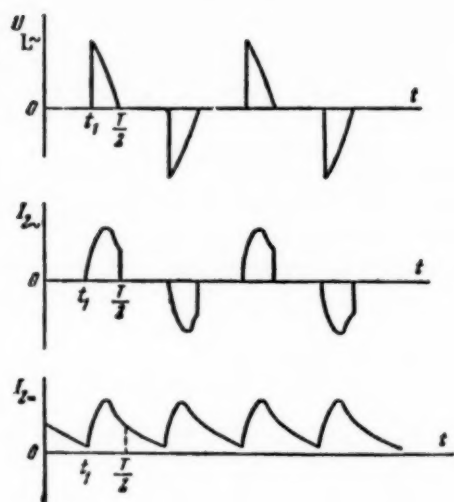


Fig. 8. Curves for the variation of the amplifier currents and voltages for natural magnetization and a RL load connected through a rectifier according to Fig. 1.

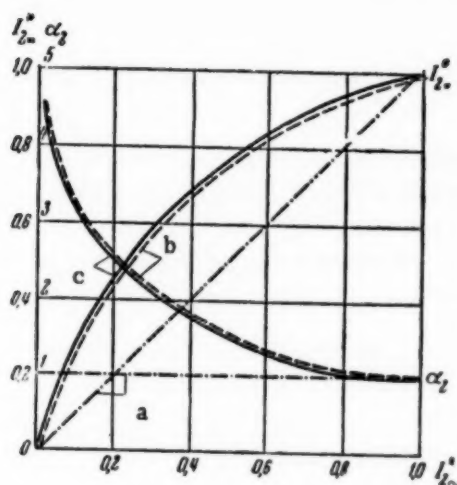


Fig. 9. a)  $\frac{\omega L_2}{R_2} = 0$ , b)  $\frac{\omega L_2}{R_2} = 5$ , c)  $\frac{\omega L_2}{R_2} = \infty$ .

In such a case the current-rectification coefficient will be

$$\alpha_2 = \frac{I_{2*}}{I_{2~}} = \frac{1}{1 - \frac{1}{180^\circ} \arccos(2I_{2*} - 1)} \quad (44)$$

Figure 9 shows the curves for the dependence of  $I_{2*}$  and  $\alpha_2$  upon  $I_{2~}$  for the cases  $\omega L_2/R_2 = 0.5$  and  $\infty$  (the dash-dot, dashed and solid lines respectively). It is evident from Fig. 9 that the curves  $\alpha_2 = f(I_{2~})$  for the cases  $\omega L_2/R_2 = 5$  and  $\omega L_2/R_2 = \infty$  almost coincide; therefore in the majority of cases it is possible to make use of Expression (44).

It is not difficult to show that the voltage-rectification coefficient is  $\alpha_1 = 1$ . Substituting the values which we have determined for the coefficients into Equations (17)-(24), we obtain the coefficients of the differential equation for an ideal magnetic conductor in the cases of forced and natural magnetization.

Thus for an ideal magnetic circuit the free term  $N_{11}$  of the differential equation is equal to zero; the remaining coefficients are constant and do not depend upon the magnitude of the current when the magnetization is natural and the load is resistive ( $\alpha_2 = 1$ ). Therefore in the indicated case the differential equation for the magnetic amplifier is also linear for the full values of the currents and voltages (within the limits of the working portion of the characteristic). Column 8 of Table 1 shows the values for the constants of the block diagram in the case of an ideal magnetic circuit and natural magnetization.

#### 4. Analysis of the Results and Conclusions

On the basis of our results we plotted curves for the dependence of the constants which characterized the block diagram of the amplifier upon the time constant of the load and the feedback coefficient for an ideal magnetic circuit, natural magnetization, the absence of "soft" feedback, and  $L_1 = 0$ ; these curves are shown in Figs. 10 and 11.

In order to facilitate an investigation of the effect of individual parameters upon the nature of the transient response, the coefficient of rectification  $\alpha_2$  is assumed equal to unity. The quantities  $T_1^*$ ,  $T_2^*$ ,  $T_7^*$  and  $T_8^*$  are the relative values of the time constants.

The base quantity is assumed to be the time constant of the amplifier when the load is resistive and there is no feedback;

$$T_b = \frac{R'_2}{4fR'_1}$$

As a result of analyzing results which we have obtained it is possible to draw the following basic conclusions.

1) For a resistive load the time constant of the amplifier increases with an increase in the impedance of the working circuit, in the coefficient of hard positive feedback  $\gamma$  and in the coefficient of soft negative feedback  $\beta$ ; the time constant of the amplifier decreases with an increase in the impedance of the control circuit and the frequency. For an ideal magnetic circuit this time constant does not depend upon the cross-section of the magnetic circuit.

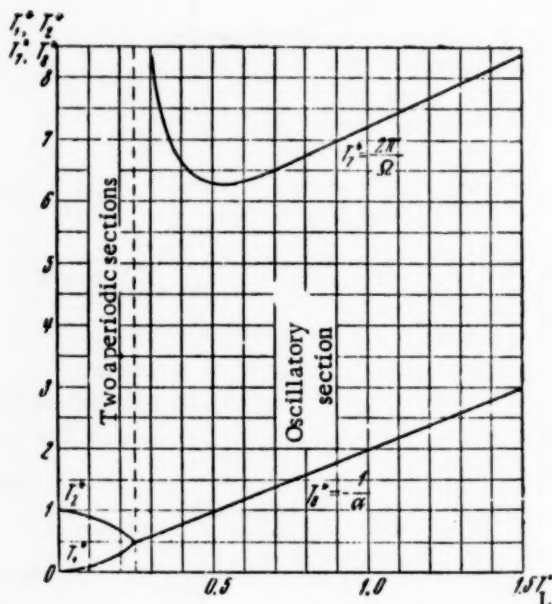


Fig. 10.

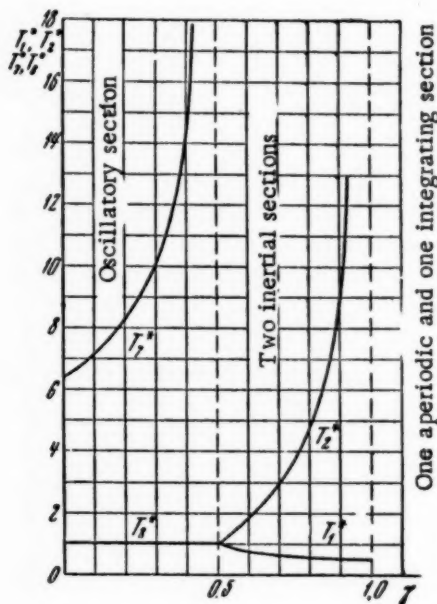


Fig. 11.

2) For a resistive load the ratio between the time constant of the amplifier and the power gain diminishes with an increase in the feedback factor and the frequency; for an ideal magnetic circuit and no soft feedback it does not depend upon the other parameters, but when soft negative feedback is present it increases with an increase in  $\beta$ ,  $C'_4$  and  $R'_1$ .

3) In the case where the block diagram of the system consists of two aperiodic sections an increase in the load time constant leads to a situation where the time constants of these sections approach each other; at the boundary of the transition from an aperiodic process to an oscillatory process they become equal. A further increase in the load time constant first leads to a decrease in the period of oscillation  $T_7$  from an infinite value to a certain minimal value, and then the period of oscillations increases again.

The quantity  $T_7^*$  which characterizes the damping time of the oscillatory process increases proportionally with an increase in the load time constant (Fig. 10).

4) For a resistive load the gain of the integral section is directly proportional to the frequency of the supply line and inversely proportional to the load impedance; for an ideal magnetic conductor and no soft feedback it does not depend upon the other parameters. The presence of negative soft feedback diminishes the gain; the degree of this decrease is proportional to  $\beta$ ,  $C'_4$ ,  $R'_1$  and  $R'_2$ .

5) If the system is replaced by an oscillatory section, then the intensification of hard positive feedback leads to an increase in the period of oscillations  $T_7$  when the attenuation time constant  $T_8$  of the oscillatory section remains constant.



At the boundary of the transition from an oscillatory process to an aperiodic process we have  $T_1 \rightarrow \infty$ , and the block diagram can be represented by two aperiodic sections with identical time constants.

A further intensification of feedback leads to an increase in the time constant of one section and a decrease in the time constant of the other section.

In the limit, for compensated feedback, one section becomes an integrating section, and the time constant of the other section becomes equal to the load time constant.

6) For undercompensated feedback (Fig. 2,a) the block diagram of the magnetic amplifier consists of aperiodic sections (one for  $L_L = 0$  and two for  $L_L \neq 0$ ), or it consists of an oscillatory section (see Table 1, Rows 1, 2 and 7).

For compensated feedback (Fig. 2,b) the system contains one integral and one aperiodic section (for  $L_L \neq 0$ ), or it contains only an integral section (for  $L_L = 0$ ) (Table 1, rows 4 and 5).

For overcompensated feedback (Fig. 2, c) we have one unstable section and one aperiodic section, (for  $L_L \neq 0$ ), or just one unstable section (for  $L_L = 0$ ).

The results cited above are verified by the fact that automatic control systems containing a magnetic amplifier which has undercompensated feedback (Fig. 2,a) have a static characteristic; when the magnetic amplifier has compensated feedback (Fig. 2, b) the system has a static characteristic, and finally, when the amplifier has overcompensated feedback the system has a characteristic with negative statism.

7) The physical meaning of the appearance of the integral and unstable sections can be explained in the following manner. In the case of compensated feedback the constant ampere-turns which are created by the feedback windings are compensated by the ampere-turns of the ac windings; the current in the control winding must be equal to the zero (for an ideal magnetic circuit) or it must have a constant value that corresponds to the shifting of the characteristics  $b$  in Fig. 2 (for an actual magnetic circuit).

When the voltage  $E_1$  is applied to the control windings of the amplifier, the applied voltage must be compensated by an emf which is induced in the control winding (since no current can appear in this circuit). Here it is true that the emf in the control winding must remain constant over the entire duration of the transient response (in the working sector of the characteristic).

The emf induced in the control windings is caused by a variation in the flux linkages of the control winding; this latter quantity is a function of the variation in the voltage across the ac windings [Formula (2), (35) and (39)]. The variation in the voltage across the ac windings is in turn a consequence of the variation of the load current  $I_2$ .

Thus, in order to guarantee a constant value of emf induced in the control winding the output current of the amplifier (within the limits of the linear region) must increase at a constant rate (i.e., the case of an integral section must obtain).

For overcompensated feedback the feedback winding creates more constant ampere-turns than alternating ampere-turns, and this difference increases to the degree that the output increases.

In order to compensate the extra feedback ampere-turns a negative current must flow in the control winding because of the fact that the emf induced in the control winding exceeds the input voltage  $E_1$ .

Since the emf induced in the control winding must increase when the load current  $I_2$  increases, it is natural that as the current  $I_2$  increases its rate of increase also rises. The magnetic amplifier will thus operate in an unstable manner.

## 5. Experimental Verification of the Results.

In order to perform an experimental verification of the results which we obtained by using the proposed method, we computed the time constants of a magnetic amplifier with the following specifications: the magnetic circuit consisted of 78% permalloy III-15 punchings with sheets 0.35 mm thick. The active cross-section of the saturable reactor was  $S = 2.85 \text{ cm}^2$ .

$$W_1 = 350, W_2 = 50, f = 500 \text{ cps}, L_1 = 0, R_1 = 16 \text{ ohm}, R_2 = 14.5 \text{ ohm}, L_2 = 0; 0.0044 \text{ and } 0.41 \text{ h.}$$

$$T_L = 0, 0.003 \text{ and } 0.028 \text{ sec, respectively.}$$

TABLE 2

Quantity	Units	Values of the quantities		
$T_L$	sec	0	0.003	0.028
$k_1$	$\frac{\text{amp}}{\text{gauss cm}}$	$0.4 \times 10^{-3}$	$0.9 \times 10^{-3}$	$0.9 \times 10^{-3}$
$k_2$	$\frac{\text{amp}}{\text{gauss cm}}$	$0.35 \times 10^{-3}$	$0.95 \times 10^{-3}$	$0.95 \times 10^{-3}$
$k_3$	$\frac{\text{gauss cm}}{\text{amp}}$	160	160	160
$k_4$		0.95	0.85	0.85
$k_5$		1.0	1.0	1.0
$k_6$		1.0	1.0	1.0
$\alpha_1$		1.0	1.0	1.0
$\alpha_2$		1.0	1.3	1.3

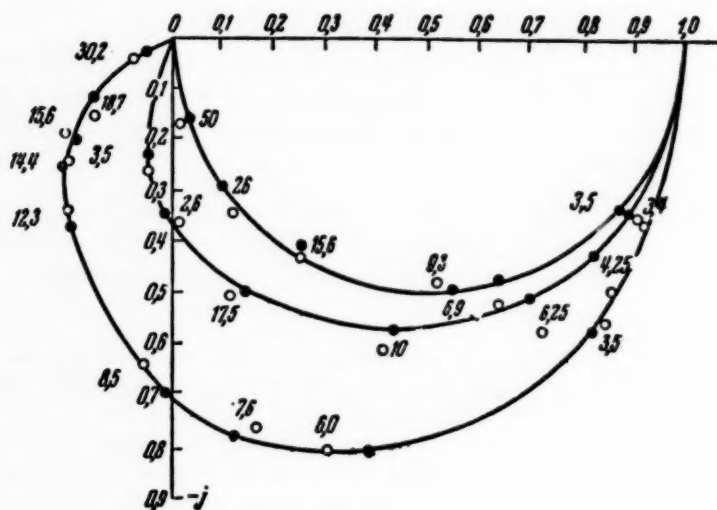


Fig. 12. Amplitude-phase characteristics of a magnetic amplifier for  $T_L = 0$ ,  $T_L = 0.003$ ,  $T_L = 0.028$  sec: ●) computed points, ○) experimental points.\*

TABLE 3

Quantities	Units	Values of the quantities		
$T_L$	sec	0	0.003	0.028
$T_1$	sec	—	0.0148	—
$T_2$	sec	—	0.00268	—
$T_3$	sec	0.0177	—	—
$\Omega$	rad/sec	—	—	36.7
$\alpha$	1/sec	—	—	-36.7

\*[The points (○, ●) on the curves are in cycles/sec.]



The linearization coefficients  $k_1, k_2, k_3$  and  $k_4$  are determined according to the corresponding curves which are obtained for the specified magnetic material and for natural magnetization. The coefficients  $k_5, k_6, \alpha_1$  and  $\alpha_2$  are determined from the circuit by direct computation.

Table 2 shows the values of the indicated coefficients for the various values of the load time constant.

On the basis of the data given in Table 2, the constants of the block diagram were computed for various values of the load time constant. The results of the computations are shown in Table 3.

Figure 12 shows the amplitude-phase characteristics.

As an example, Fig. 13 shows one of these oscillograms obtained for  $T_L = 0.0075$  sec. It is evident from this oscillogram that  $\Delta I_2$  varies according to an almost sinusoidal law. This verifies the correctness of analyzing the magnetic amplifier as a system which is linear at small perturbations. It is evident from Fig. 12 that the experimental and computed points on the amplitude-phase characteristics of the magnetic amplifier agree sufficiently well; this indicates that the proposed method of computation is correct and that the assumptions we have made are fully applicable.

## APPENDIX

### The Relationship Between the Emf Induced in the Hard Feedback Windings and the AC Current During Transients

The paper neglects the emf induced in the hard feedback winding in comparison to the voltage which appears in the working circuit.

In order to show the validity of this assumption we shall determine the relationship between the emf  $\Delta E_{fb}$  induced in the feedback winding and the increments of voltage  $\Delta U_2$  across the ac winding of the amplifier when the emf in the control circuit varies step-wise by an amount  $\Delta E_1$ . The magnetization of the amplifier is assumed to be natural, and the load is assumed to be resistive.

Figure 14 shows the curves for the variation of the corresponding quantities when the indicated conditions obtain.

The increment of flux linkage with the feedback winding is

$$\Delta \Psi_{fb} = \Delta \Psi_{fba} (1 - e^{-\frac{t}{\tau}}), \quad (1.1)$$

where  $\tau$  is the time constant of the amplifier. On the other hand,

$$\Delta E_{fb} = - \frac{d\Delta \Psi_{fb}}{dt}. \quad (1.2)$$

Let us substitute (1.1) into (1.2):

$$\Delta E_{fb} = - \frac{\Delta \Psi_{fba} e^{-\frac{t}{\tau}}}{\tau}. \quad (1.3)$$

When  $t = 0$

$$\Delta E_{fb_{max}} = \frac{\Delta \Psi_{fba}}{\tau}. \quad (1.4)$$

The voltage increment across the ac winding is

$$\Delta U_2 = 4/\Delta \Psi_{\sim a}, \quad (1.5)$$

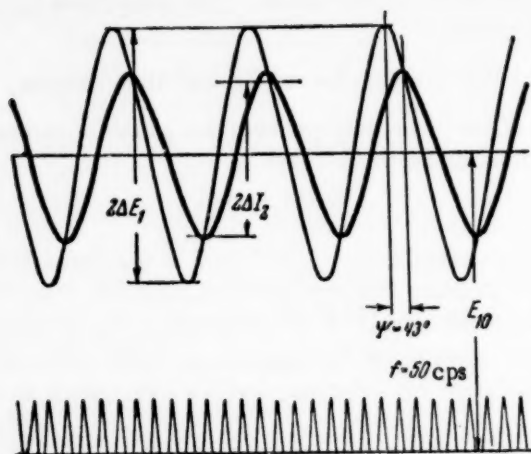


Fig. 13. Oscillogram of the curves for the control emf and the output current of the amplifier when sinusoidal oscillations at a frequency of 6.25 cps are superimposed upon the constant voltage  $E_{10}$ .

where  $\Delta \Psi_{\sim a}$  is the increment in the amplitude of the flux linkage with the ac winding.

On the basis of Equation (39) (for the condition  $W_2 = W_3$ ) it is possible to obtain the following result:

$$\Delta \Psi_{\sim a} = \Delta \Psi_{fb a}. \quad (1.6)$$

Solving Equations (1.4) - (1.6) simultaneously, we obtain

$$\frac{\Delta E_{fb \max}}{\Delta U_2} = \frac{T}{4\tau} \quad \left( T = \frac{1}{f} \right). \quad (1.7)$$

Since it is usually true that  $T < \tau$ , it follows that  $\Delta E_{fb \max} \ll \Delta U_2$ . For example, if we assume that  $\tau = 5T$ , then  $\Delta E_{fb \max}$  is 5% of  $\Delta U_2$ .

In conclusion the author considers it his pleasant duty to express his appreciation to A. G. Iosif'yan and E. A. Meerovich for the valuable advice which they gave during the writing of this paper.

Received June 26, 1956

#### LITERATURE CITED

- [1] M. A. Rozenblat, Magnetic Amplifiers, State Power Press, 1949.\*
- [2] A. G. Milnes, A New Theory of the Magnetic Amplifier, Proc. IEE, vol. 97, part II, p. 460, 1950.
- [3] Iu. G. Tolstov, Dc Instrument Transformers. State Power Press, 1951.\*
- [4] L. A. Bessonov, Transient Responses in Nonlinear Electrical Networks Containing Steel. State Power Press, 1951.

\* In Russian.

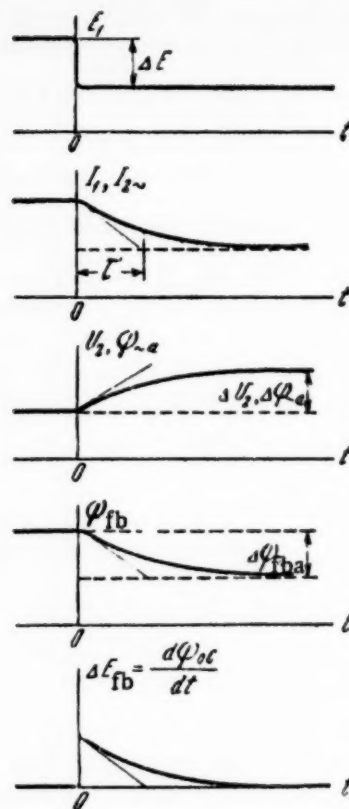


Fig. 14. Curves for the variation of the basic quantities of the magnetic amplifier for a step-wise variation of  $E_1$ .

[5] A. G. Milnes, The behavior of a series transductor magnetic amplifier with directly-connected or rectifier-fed leads. Proc. IEE, vol. 99, Part II, p. 13, 1952.

[6] L. A. Grigorian, Transient Responses in Magnetic Amplifiers which are Used in Control Circuits. Proceedings Acad. Sci. Armenian SSR, Vol. XV, No. 1, 1952.

[7] L. A. Grigorian, Transient Responses in Magnetic Amplifiers with Soft Feedback which are Utilized in Control Circuits. Proceedings Acad. Sci. Armenian SSR, Vol. XV, No. 3, 1952.

# THE COMPUTATION OF NONLINEAR NETWORKS BY THE METHOD OF TRANSFORMATION (TRANSFIGURATION) AND A CERTAIN ERROR WHICH ARISES IN THE APPLICATION OF THIS METHOD

P. A. Ionkin

(Moscow)

It is known that in order to compute linear circuits extensive use is made of transformation formulas for the purpose of transforming a passive or active multi-leg star into a polygon; extensive use is also made of Wye-Delta transformations. The utilization of these formulas makes it possible to transform the majority of branched linear networks to networks in which active and passive two-terminal networks are connected in series-parallel; the computation of such series-parallel networks is very simple. Such transformations and analogous ones (of which we shall speak below) are of still greater significance in the computation of networks containing nonlinear elements.

In a paper by V. E. Vartel'sky [1] a method was given by means of which the author asserts it is possible graphically to transform a Delta composed of nonlinear elements into an equivalent Wye in the general case.

However, in examining the proposed graphical method of transformation we detected a large error in it. In fact, in order to determine the magnitudes of the resistances (the volt-ampere characteristics of the equivalent Wye; Fig. 1) according to the specified resistances (volt-ampere characteristics) of the nonlinear elements of the Delta (Fig. 2) the author derives the following equations:

$$R'_0 + R'_2 = \frac{R_2(R_0 + R_4)}{R_0 + R_2 + R_4}, \quad R'_0 + R'_4 = \frac{R_4(R_0 + R_2)}{R_0 + R_2 + R_4}, \quad R'_2 + R'_4 = \frac{R_0(R_2 + R_4)}{R_0 + R_2 + R_4}. \quad (1)$$

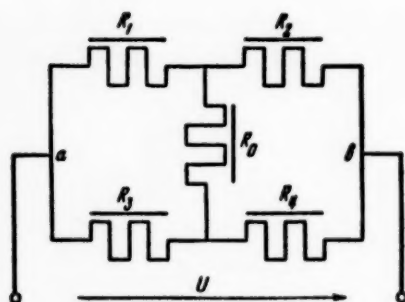


Fig. 1.

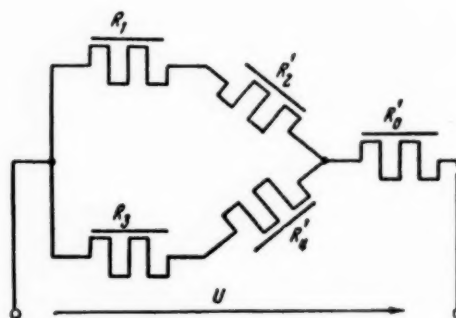


Fig. 2.

The error which the author [1] permitted consists of the fact that Equations (1) are valid only for linear circuits to which the principle of superposition can be applied. Only when the resistances of circuits shown in Figs. 1 and 2 are linear can the input resistances of the Wye and Delta across each pair of corresponding terminals

be set equal to one another. Therefore the reasoning of the author [1] concerning the solution of Equations (1) (Figs. 25 and 26 in [1]) and concerning the application of the results in the computation of branched networks by means of the transformation method are incorrect (Fig. 27 in [1]).

Let us examine the application of one of the transformations proposed by the author of this paper [2] for computing nonlinear networks that contain emf and current sources.

### Star Connection

Let us assume that the voltages  $U_{12}$ ,  $U_{13}$  and  $U_{14}$ , and the emfs  $E_{10}$ ,  $E_2$ ,  $E_3$  and  $E_4$  (as well as the volt-ampere characteristics of all the nonlinear elements which are connected to the emf sources in the Delta network; see Fig. 3) are specified. It is required to find the currents  $I_1$ ,  $I_2$ ,  $I_3$  and  $I_4$ . On the basis of the compensation theorem we replace the voltage across the terminals of, for example, the first element by an alternating emf  $E'_1(I_1)$  which opposes the current  $I_1$  (Fig. 3) and is equal to the voltage  $r_1(I_1)I_1$ . Then we connect an emf  $E_1(I_1) = E_{10} - E'_1(I_1)$  into every branch which is connected to the node 0 and establish the polarity of this emf so that current is directed away from this node (Fig. 4). As a result the currents in all of the branches will evidently remain unchanged, and the potential difference between 0 and 1 will be equal to zero. Here the unknown alternating emf  $E_1(I_1)$  is, as it were, "transferred" through the node 0 into all of the other branches which are connected to this node [2], and the specified voltages  $U_{12}$  and  $U_{14}$  will act at the terminals of these branches.

For example, in order to determine the current  $I_1$  we specify the values of this emf in accordance with the characteristic  $E_1(I_1)$  and find the currents  $I_2$ ,  $I_3$  and  $I_4$  for each value of  $E_1(I_1)$  according to the known voltages,  $U_2(I_2) = U_{12} + E_2 + E_1(I_1)$ ,  $U_3(I_3) = E_3 - U_{13} - E_1(I_1)$  and  $U_4(I_4) = E_4 + U_{14} + E_1(I_1)$  by making use of the corresponding volt-ampere characteristics. Then we plot the two characteristics  $E_1(I_2 + I_4 - I_3)$  and  $I_1(E_1)$  (Fig. 5) on the same coordinate axes. At the point where these characteristics intersect the current  $I_1$  of the first branch is equal to the algebraic sum of the currents  $I_2 + I_4 - I_3$  in the three other branches. As a result the ordinate of the point  $a$  yields the current  $I_1$  in the first branch, and the abscissa of the point yields the voltage across the terminals 1 and 0 of the first branch. After that the currents  $I_2$ ,  $I_3$  and  $I_4$  are determined from Fig. 4 on the basis of Kirchhoff's laws. The proposed method of computation can easily be applied to a star connection which has any other number of branches.

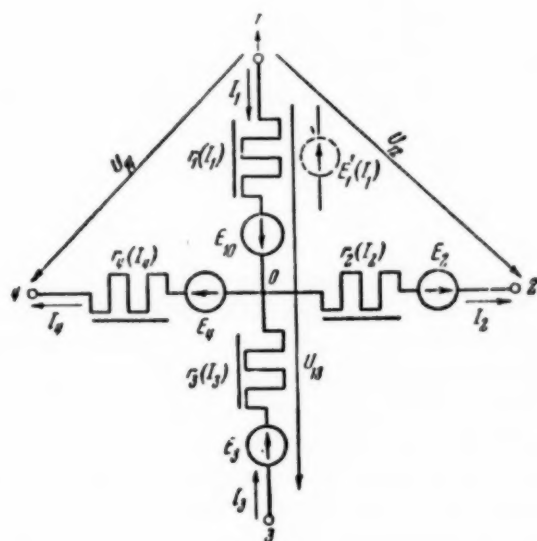


Fig. 3

teristics  $(-E_1(I_a + I_3))$  and  $I_1(E_1)$  or  $E_1(I_b - I_2)$  and  $I_1(E_1)$  yields the current  $I_1$ . After that it is easy to determine the currents  $I_2$  and  $I_3$  on the basis of Kirchhoff's laws.

### Complete-Rectangle Connection

Figure 11 shows the circuit of a complete rectangle in which the branches with the known currents

### Delta Connection

Figure 6, a shows the connection of the nonlinear elements  $r_1(I_1)$ ,  $r_2(I_2)$  and  $r_3(I_3)$  and the sources of emf  $E_2$  and  $E_3$  into a Delta network.

Let the currents  $I_a$ ,  $I_b$  and  $I_c$  be specified together with the emfs  $E_2$  and  $E_3$  and the volt-ampere characteristics of all the nonlinear elements. It is required to determine the currents  $I_1$ ,  $I_2$  and  $I_3$ . If the equivalent emf  $E_1(I_1) = r_1(I_1)I_1$  of the first branch is transferred through the node  $a$ , then we obtain a parallel circuit (Fig. 6, b). In order to determine, for example, the current  $I_1$  we specify the values of  $E_1(I_1)$  and graphically determine the currents  $I_2$  and  $I_3$  in accordance with the equations  $E_2 - r_2(I_2)I_2 = -[E_3 + E_1(I_1) - r_3(I_3)I_3]$  and  $I_c = I_2 - I_3$ . Then, just as for the star connection, we plot the characteristics  $-E_1(I_a + I_3)$  and  $I_1(E_1)$  or  $E_1(I_b - I_2)$  and  $I_1(E_1)$ , on one and the same coordinate axes. Since the current  $I_1 = -(I_a + I_3)$  or  $I_1 = I_b - I_2$ , it follows that the ordinates of the point of intersection of the charac-



$I_a$ ,  $I_b$ ,  $I_c$  and  $I_d$  are connected to its four nodes. Let us assume that the values of the emfs  $E_2$  and  $E_4$  and the volt-ampere characteristics of the nonlinear moments are also known. It is required to find the currents  $I_1$ ,  $I_2$ ,  $I_3$  etc. in all of the branches containing nonlinear elements.

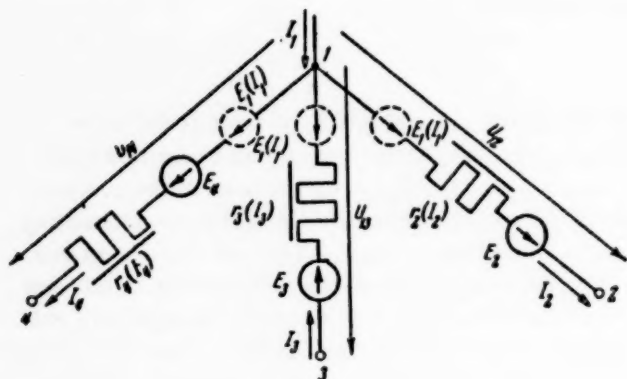


Fig. 4.

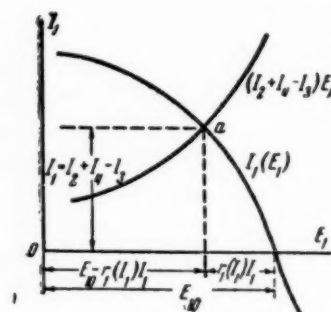


Fig. 5.

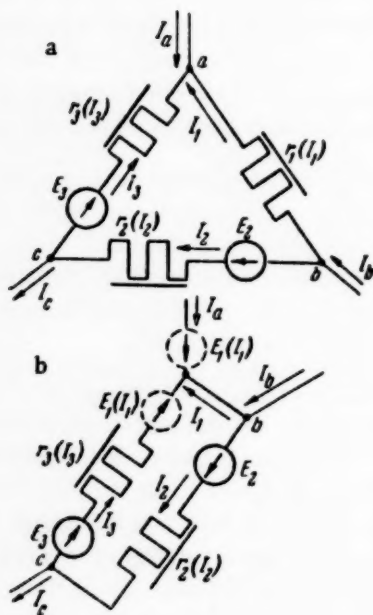


Fig. 6.

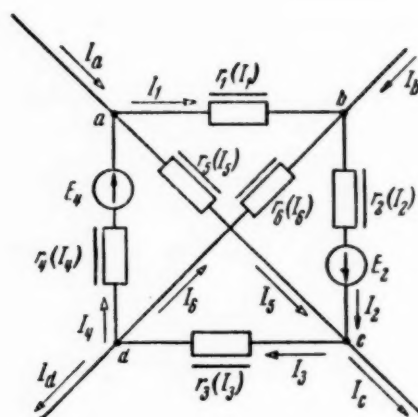


Fig. 7.

In order to determine the unknown currents let us replace the voltages across the terminals of the first and second branches by the emfs  $E_1(I_1)$  and  $E_2(I_2)$ ; we then transfer these emfs through the nodes  $b$  and  $d$  (respectively) into the other branches which are connected to these nodes. As a result we obtain the circuit

in Fig. 8 which has the form of a parallel connection of four branches. Then, in accordance with the volt-ampere characteristic  $E_1(I_1)$ , we assume a certain value of the emf  $E_1$  and then (assuming that this value is constant) use graphical-analytical methods to determine the branch currents of the circuit in Fig. 8 for various values of the emf  $E_3(I_3)$  in the same manner as we did for the circuit in Fig. 6,  $b$ . Since  $I_3 = -I_c + I_5 + I_2$  the intersection point of the curve  $E_3(-I_c + I_5 + I_2)$  with the characteristic  $I_3(E_3)$  yields the current  $I_3$ . The value of the current  $I_1 = I_b + I_6 - I_2$  which we obtain under these conditions does not satisfy the specified characteristic  $E_1(I_1)$  in the general case. Therefore we shall assume a new value of the emf  $E_1$  and shall again (utilizing the circuit of Fig. 8) perform the same type of graphical analysis in order to find a new value of the current  $I_1$ .



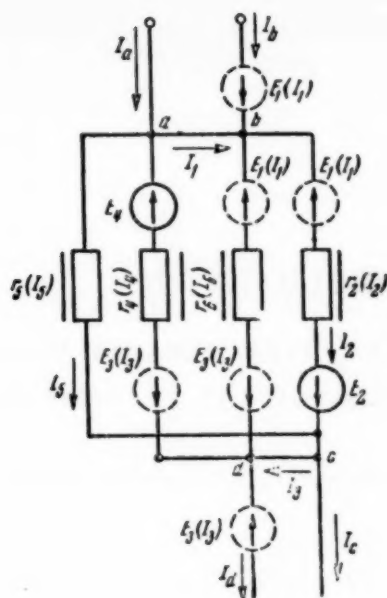


Fig. 8.

Performing a number of such computations, we shall obtain data for plotting the curve  $E_1(I_1 - I_5 - I_b)$  whose point of intersection with the characteristic  $E_1(I_1)$  yields the unknown current  $I_1$ . After that it is easy to determine the currents in the remaining branches of the circuit shown in Fig. 8.

Therefore by performing a preliminary transformation of the specified circuit to a circuit which consists of a series-parallel connection of active and passive nonlinear two-terminal networks, it is possible to use graphical-analytical methods to compute a whole series of branched electrical networks containing nonlinear elements.

In particular, in order to compute a bridge circuit with five nonlinear elements it is easy to obtain a network in the form of a mixed connection of two-terminal networks by means of transferring a specified external emf which is equal to voltage  $U$  through the node a or b and then shorting these nodes.

Received March 5, 1956

#### LITERATURE CITED

- [1] V. E. Vartel'sky, DC Circuits with Nonlinear Resistors, Automation and Remote Control No. 2, 1940.
- [2] G. V. Zeveke and P. A. Ionkin, Fundamentals of Electrical Engineering, Vol. 1, State Power Press, 1955.\*

\* In Russian.

## BIBLIOGRAPHY

### LIST OF SOVIET AND FOREIGN LITERATURE ON AUTOMATIC CONTROL AND ASSOCIATED PROBLEMS FOR THE YEAR 1955 (continuation)

#### STRUCTURES AND ELEMENTS OF AUTOMATIC CONTROL SYSTEMS

- Automatic Tirrill Voltage Regulator of the Type AVRN-3 Constructed by the All-Union Institute of Metrology. Temporary Instructions for Assembly, Mounting and Operation. Moscow, 1955, 24 pages (Moscow Electromechanical Institute).
- The Automatic Controller. Contained in the book: Information Material. Ministry of Transport Machine Building. USSR, No. 2, pp. 67-70, 1955.
- An Automatic Voltage Regulator of the Type UK-EMK. Technical Information and Instructions on Adjustment and Operation. Kiev, Acad. Sci. Ukrainian SSR, 61 pages, 16 figures, 1955.
- Automatic Temperature Controller for an Oxygen Meter Manufactured by the "Energopribor" Factory. In the book: Rationalization at Bashkirenergo Power Stations. Collection of Proposals for Rationalization, No. I. Ufa pp. 58-59, 1955.
- S. S. Alekseev, Two-Position Temperature Controller with a Lead Zone. In the collection titled: In Memory of A. A. Andronov. Moscow, Acad. Sci. USSR, pp. 45-76, 1955.
- A. N. Afanas'eva, B. M. Gurevich, A. I. Radgauz and K. I. Skorkin. A Unit for the Automatic Control of the Excitation of a Synchronized Induction Motor. Collection of Proposals for Rationalization, Ministry of the Electrical Industry of the USSR, No. 49, pp. 37-39, 1955.
- A. L. Ashkinazi, A Pressure Controller of the Plunger Type. In the book: Power and Transport. Materials on the Exchange of Production Engineering Experience, I. Moscow, Defense Press, pp. 12-20, 5 illustrations, 1955.
- A. I. Barkalov, M. V. Bezginsky and M. A. Duel', Mounting Thermal Control Instruments and Automatic Regulators. Moscow, State Power Press, 200 pages with illustrations, 20 references, 1955.
- G. A. Barchukov et al, An Electromechanical Frequency Stabilizer for a Klystron. Radio Engineering, Vol. 10, No. 3, pp. 29-32, 2 illustrations, 1955.
- S. F. Bereznikovsky, Metering Units in Automatic Control Systems for Electric Machines. In the Collection "Electrosila" No. 13. Moscow-Leningrad, State Power Press, pp. 49-58, 17 illustrations, one reference, 1955.
- V. O. Bogomolov and V. L. Benin, A Device Which Controls the Angle of Rotation of a Turbine as a Function of the Pressure. Bulletin of the Acad. Sci. Ukrainian SSR, No. 7, p. 47, 1955.
- A. E. Boltsov, D. I. Gerasenkov and K. A. Krivitsky, Voltage Regulators and Stabilizers. In their book: Electrical Supplies for Communications Units. Moscow, Railroad Transport Press, pp. 153-168, 13 illustrations, 4 tables, 1955.

- P. E. Boloban and G. N. Makhan'kov, A Device for Regulating the Steam Fed to the End Glands of Turbines. *Electric Power Stations*, No. 1, pp. 12-14, 3 illustrations, 1955.
- S. P. Bolarshtinov, Signalization of Operational Stoppage in a Supply Regulator of the ARI-IV type. *The Power Worker*, No. 7, pp. 11-12, 1955.
- A. A. Bulgakov, A Static Magnetic Phase Shifter and Peaking Transformers for the Automatic Control of Mercury-Pool Rectifiers. Moscow, Institute of Engineering and Economic Information of the Acad. Sci. USSR, 35 pages, 21 illustrations, 13 references, 1955.
- An Automatic Drilling Regulator. *Electricity*, No. 7, pp. 146-147, 1 illustration, 2 references, 1955.
- N. P. Vasili'eva and O. A. Sedykh, The Computation of Saturable-Reactor Magnetic Amplifiers with a Complex Load. *Automation and Remote Control*, Vol. 16, No. 1, pp. 47-63, 8 illustrations, 6 references, 1955.
- N. A. Venikov and I. V. Litkens, The Effect of Excitation Control Upon the Transmission Capability of Long-Range Electrical Transmission Lines. *Electricity*, No. 11, pp. 15-26, 8 references, 1955.
- I. A. Verebrusov, Synchronous Transmissions and Tracking Systems. Leningrad, Shipbuilding Industry Press, 237 pages, 104 illustrations, 15 references, 1954.
- M. E. Verkholat, A Duplicating-Metering Instrument for Automatic Tracking Systems. *Bulletin of Technical Information of the Ministry of Machine-Tool Building and Instrumentation Industry of the USSR*, No. 2, pp. 20-21, 1955.
- A. A. Vershinin and A. Kh. Pateev, An Automatic Controller for a Roasting Furnace. *The Fish Industry*, No. 9, pp. 30-33, 1955.
- V. I. Vinogradov, An Automatic Controller for Feeding Lubrication Oil into the Working Cylinders of Motors. *Power Bulletin of the Ministry of the Oil Industry of the USSR*, No. 8, pp. 19-22, 5 illustrations, 1955.
- B. I. Genkin, Quality-Quantity Control of the Operation of Central Heating Networks. In the collection: *Repair and Experimental Work of the "Orgres."* Moscow-Leningrad, State Power Press, No. 11, pp. 49-63, 9 illustrations, 1955.
- G. R. Gertenberg and Ia. N. Shtrafun, An Automatic Controller for the Excitation of Hydrogenerators in the Kulbyshev-Hydroelectric Station. *Journal of the Electrical Industry*, No. 5, pp. 3-8, 2 illustrations, 3 references, 1955.
- L. M. Gidon, Setting and Controlling Valve-Type Steam Distribution in Locomobiles. *The Power Worker*, No. 2, p. 30, 1955.
- Hydraulic Jet Diaphragm-Type Pressure Controllers. Mounting and Operational Instructions RD-MI. Moscow, Metallurgy Press, 36 pages with illustrations, 1955. (Energochermet).
- Hydraulic Jet Diaphragm-Type Ratio Controllers. Mounting and Operational Instructions RSMI. Moscow, Metallurgy Press, 35 pages, 1955.
- A. I. Glushko, A Mechanism for Pulling a Generator into Synchronism when Self-Synchronization Obtains. *Electricity*, No. 4, pp. 30-33, 57 illustrations, 3 references, 1955.
- L. S. Gol'dfarb and N. M. Aleksandrovsky, Certain Problems in Computing Corrective Elements in AC Tracking Systems. *Automation and Remote Control*, Vol. 16, No. 1, pp. 3-18, 14 illustrations, 9 references, 1955.
- N. A. Gorlachev and G. D. Baskakov, Automatic Temperature Control in Electrical Drying Closets and Thermostats. *Peat Industry*, No. 4, pp. 18-19, 2 illustrations, 1955.
- V. Ia. Grishin, A Transmitter with an Extra Pulse Which is Designed for a Thermal Controller. *Bulletin Acad. Sci. SSR*, No. 6, pp. 104-110, 7 illustrations, 4 references, 1955.

- V. N. Gritskov and Iu. V. Kozliuchenko, Dynamic Characteristics of a Proportional-Integral Controller of the type IR-130, TsAA. In the Collection of Articles by the Scientific Student Body. Moscow, pp. 3-18, 1955 (Moscow Power Institute).
- M. N. Gubanov, Unit for Controlling the Speed of Rotation of a Three-Phase Induction Motor. Bulletin of Inventions, No. 2, p. 15, Class 21d<sup>2</sup>, 224<sub>01</sub>, No. 99781, 1955.
- S. N. Delikishkin, A Device which Regulates the Amount of Mazut. Journal of Machine Building, No. 11, pp. 62-65, 6 illustrations, 1955.
- V. A. Deianov and V. V. Romantsev, Improving the Supply Circuit for Automatic Controllers in an Electro-mechanical System. Electric Power Stations, No. 8, pp. 53-54, 3 illustrations, 1955.
- V. I. Enin, Computations and Test Results for a Steam-Pressure Controller. In the collection: Problems of Designing and Operating Marine Power Units. Leningrad, "Ocean Transport," pp. 58-76, 10 illustrations, 3 references, 1955.
- V. A. Erofeev, Electronic Units for the Automatic Control and Regulation of Thermal Processes. Moscow-Leningrad, State Power Press, 72 pp., pp. 468-472, 1955.
- V. F. Zdor, A Temperature Controller in Thermal Aggregates. Technology of Transportation Machine Building, No. 5, pp. 39-42, 1955.
- I. I. Zotov and I. S. Lebedev, Automatic Controller for Maintaining the Water Level in a De-aerator Within Specified Limits. In the book: Information Materials of "Lenenergo" during 1954. Moscow-Leningrad, State Power Press, pages 107-110, 1955.
- I. P. Zubov, The "Kopir" Program Controller. Cutting Tools and Stands. Moscow, No. PS-55-433, pp. 8-11, 6 illustrations, 1955 (Inst. of Tech. and Economic Inf., Acad. Sci. USSR).
- L. S. Ivanov, I. A. Karmazin and Iu. A. Freiman, Reconstruction of a Speed Controller of the type UK for Hydroturbines of Intermediate Power Rating. Electrical Power Stations, No. 2, pp. 52-54, 2 illustrations, 1955.
- V. S. Ivanova and M. P. Vorob'ev, Improved Circuits for Temperature Control in Furnaces which are Contained in B P-8 installations. Factory Laboratory, No. 8, pp. 992-993, 1 illustration, 1955.
- Changing the Mounting Diagram for the Condensation Vessels and Pulse Lines in the Feed Controller of ARP-4 boilers. In the book: Rationalization Work at the Bashkirenergo Electric Power Stations. Collection of Rationalization Proposals, No. 1. Ufa, pp. 45-49, 1955.
- An Electrical Actuating Mechanism, IM-2/2.5. Mounting and Operational Instructions IM-2/2.5 MI. Moscow, Metallurgy Press, 9 pages, 1955. (Energochermet).
- Electrical Actuating Mechanisms IMT-12/120, IMT-25/120, IMT-12/60 and IMT-6/20. Mounting and Operational Instructions IMT-MI. Moscow, Metallurgy Press, 8 pages, 1955 (Energochermet).
- An Electrical Actuating Mechanism IM-2/120. Mounting and Operational Instructions IM 2/120 MI. Moscow, Metallurgy Press, 11 pages, 1955 (Ministry of Ferrous Metals of the USSR, Glavenergo, Energochermet).
- P. B. Kantor and B. S. Estrin, An Aqueous Thermostat with Automatic Temperature Control. Measuring Techniques, No. 5, pp. 50-52, 1955.
- K. B. Karandeev and E. P. Sokolovskii, Feedback in Amplifiers Containing an Electromechanical Transducer. Scientific Record of the Institute of Machinery and Automation of the Acad. Sci. of the Ukrainian SSR, Vol. 5, No. 4, pp. 64-82, 1955.
- A Combinatorial Solenoid Valve KSK. Mounting and Operational Instructions. KSK MI. Moscow, Metallurgy Press, 8 pages, 1955.
- O. B. Klebanov, Experience in Designing Automatic Pulp-Density Controllers. Kolyma, No. 7, pp. 24-31, 9 illustrations, 1955.



- S. D. Klement'ev, Automatic Control. In his book: Automation and Remote Control. Moscow, State Tech. and Theoret. Lit. Press, pp. 157-181, 15 illustrations, 1955.
- S. D. Klement'ev, Tracking Systems. In his book: Automation and Remote Control. Moscow, State Tech. and Theoret. Lit. Press, pp. 181-191, 5 illustrations, 1955.
- D. Kontorer, A Two-pulse Pneumatic Gas-Pressure Controller. Consumer Economy, No. 3, pp. 28-29, 1955.
- I. M. Krassov, An Automatic Pressure-Differential Controller. In his book: Automation of the Chemical Industry. Moscow, Acad. Sci. USSR, pp. 107-113, 8 illustrations, 1 reference, 1955.
- V. M. Krivosheev, An Inductive Relay Pulser for Automatic Speed Control of Furnace Gratings in a Boiler Aggregate. The Power Worker, No. 3, pp. 12, 14, 2 illustrations, 1955.
- I. Kruglak, The Thermal Regulator and the Temperature Modes of the "Zis-Moscow" Refrigerator. Refrigeration Engineering, No. 4, pp. 53-55, 3 illustrations, 1955.
- E. V. Kurlina and S. S. Rabinovich, A Mechanism for the Automatic Control of the Heating of an Electric Furnace. Moscow, Institute of Technical and Economic Information of the Acad. Sci. USSR, pp. 3-5, 2 illustrations, 1955.
- A. A. Lapshin, A Conductometric Level Controller. Cutting Tools and Stands. Subject No. 4, Moscow, 16 pages, Inst. Eng. and Economic Information, Acad. Sci. USSR, 1955.
- V. A. Leshchenko, Selecting the Parameters of a Hydraulic Servo Drive (Statics). Machine Tools and Cutting Tools, No. 8, pp. 3-7, 5 illustrations, 1955.
- A. B. Mansvetov, An Automatic Electrical Reversing Controller for a Production Cycle with Block Protection from Accidents. Moscow, Institute of Technical and Economic Information, Acad. Sci. USSR, 14 pages, 9 illustrations, 1955.
- V. D. Mironov and E. I. Stefani, Electronic Automatic Controllers for Thermal Processes. Moscow-Leningrad, State Power Press, 24 pages, 32 references, 1955.
- E. E. Mikhaliants, A Controller for Feeding Steam to the Labyrinth Glands of a Turbine. The Power Worker, No. 11, pp. 9-10, 1955.
- N. N. Nastenkov, A Controller for all Operating Modes of a IAAZ-204 motor. Automobile and Tractor Industry, No. 2, pp. 21-26, 5 references, 1955.
- N. A. Nechaev, An Automatic Excitation Controller for Low-Power Generators. The Power Worker, No. 12, pp. 7-9, 6 illustrations, 1955.
- M. A. Novozhilov, Additional Feed of Liquid into a Reciprocating Pump When the Controlling Organ is Displaced. Transactions of the Academy of Defense Industry, No. 2, pp. 65-78, 1955.
- A New Hydraulic Speed Controller. In the collection: Machine Building, No. 3, pp. 60-62, 2 illustrations, 1955.
- A Half-Cycle Time Controller for Low-Power Spot-Welding Machines. In the collection: Technical Information on Welding Equipment RI-65. Moscow, pp. 8-13, 4 illustrations, 1955. (Ministry of the Electrical Industry USSR, Central Bureau of Technical Information, and All-Union Scientific-Research Institute of Welding Equipment).
- V. A. Parail, The Effect of Saturation when the Speed of an Induction Motor is Controlled by DC Magnetization. Scientific Record of Odessa Polytechnical Institute, Vol. 8, pp. 37-49, 7 illustrations, 1955.
- V. A. Parail, Certain New Circuits for the Speed Control of an Induction Motor when it is Subjected to DC Magnetization. Scientific Record of the Odessa Polytechnical Institute, Vol. 8, pp. 55-62, 6 illustrations, 1955.
- V. A. Parail, Controlling the Speed of a Three-Phase Induction Motor when it is Subjected to DC Magnetization. Scientific Record of the Odessa Polytechnical Institute, Vol. 8, pp. 3-18, 7 illustrations, 5 references, 1955.

- N. V. Pautin, An Automatic Controller which Achieves Continuous Frequency and Power Control. *Journal of the Acad. Sci. USSR*, No. 10, pp. 59-62, 3 illustrations, 1955.
- N. V. Perchikhin and N. N. Fadeev, An Automatic Tirrill Voltage Regulator of the Type AVRN-3 Constructed by the All-Union Institute of Metrology. Temporary Instructions on the Arrangement, Mounting and Operation of the Device. Moscow, Ministry of State Farms of the USSR, 23 pages, 1955.
- N. B. Petrovsky, Controllers which Control the Number of Revolutions of a Motor. In his book: *Internal Combustion Engines for Ships*. Leningrad, "Ocean Transport" Press, Leningrad Division, pp. 382-397, 15 illustrations, 1955.
- B. A. Piontkovsky, L. A. Spasskaya and M. Z. Gol'dberg, An Automatic Voltage Regulation Rack (S ARN). *Communications Journal*, No. 4, pp. 3-5, 3 illustrations, 1955.
- B. V. Pistonov, A. D. Stepanov, S. M. Domanitsky and S. D. Popov, A Method for Testing Automatic Control Circuits. In his book: *Results of Comparative Tests Performed on Automatic Control Circuits for Locomotives*. Moscow, Transport Engineering Press, pp. 7-11, 1955. (Transactions of the All-Union Scientific-Research Institute of Railroad Engineering, No. 109).
- K. K. Plaude and V. E. Grislis, An Automatic Thermal Controller for Central Heating. *Bulletin of the Acad. Sci. of the Latvian SSR*, No. 7, pp. 113-118, 6 illustrations, 2 references, 1955.
- A Rotatable Controlling Vane PRZ. Mounting and Operational Instructions PRZ MI. Moscow, Metallurgy Press, 7 pages, 1955 (Energochermet).
- R. B. Popov, New Instruments for Automatizing the Control and Regulation of Hydrometallurgical, Hydrochemical and Central-heating Processes. *Non-Ferrous Metals*, No. 1, pp. 20-29, 10 illustrations, 1955.
- R. B. Popov, A New Automatic Weighing Density Meter and Density Controller for Solutions and Pulp. *Non-Ferrous Metals*, No. 6, pp. 25-29, 3 illustrations, 1955.
- I. N. Rabinovich, V. F. Baiko and A. A. Vavilov, Dynamoelectric Controllers with Longitudinal Fields. *Electricity*, No. 2, pp. 67-69, 1955.
- Time Controller of the type RVZ-7-1A. (Description and Instructions). Moscow, 16 pages, 1955 ("Elektrik" Factory).
- A DC Excitation Controller. (Description and Servicing Instructions). Moscow, 15 pages, 1955. (Ministry of the Electrical Engineering Industry of the USSR).
- Reconstruction of a Controller for the Automatic Feed of Water to Boilers (ARP-4). In the book: *Rationalization Work at the Bashkirenergo Electrical Power Stations*. Collection of Rationalization, No. 1, Ufa, pp. 49-51, 1955.
- A. A. Savin, An Automatic Device for Controlling the Operation of a Water-Heating Boiler which is Heated by Means of Gas. *The Power Worker*, No. 8, pp. 12-13, 1955.
- G. K. Salgus, An Electromagnetic Condensation Controller. *Transactions of the Moscow Power Institute*, No. 15, pp. 177-187, 1955.
- I. S. Svetlov, An Electronic-Electromagnetic Feed Controller for Paper-Making Machines. *The Paper Industry*, No. 2, pp. 19-20, 1 illustration, 1955.
- Piston and Hydraulic Servomotors. Mounting and Operation Instructions SPMI, Moscow, Metallurgy, Press, 23 pages with diagrams, 1955. (Energochermet Trust).
- Synchronous Transmissions and Tracking Systems for Aviation and Automobile Instruments. In the book: *Fundamentals of the Electrical Equipment for Airplanes and Automobiles*. Moscow-Leningrad, State Power Press, pp. 286-333, 1955.
- N. S. Sfunov and D. A. Arzamastsev, Fundamentals of Designing Controllers for Manual Three-Phase Arc Welding. *Automatic Welding*, No. 1, Kiev, Acad. Sci. Ukrainian SSR, pp. 25-38, 12 illustrations, 8 references, 1955.



- G. S. Skubathevsky, Supply and Control Aggregates. Operating Modes of Turbojet Engines and Control Problems. In his book: Aviation Engines. Moscow, Defense Press, pp. 505-527, 24 illustrations, 1955.
- M. M. Snegirev, An Electronic Liquid-Level Controller. Hydrolysis and Wood-Pulp Chemistry Industry, No. 6, p. 19, 1955.
- O. A. Stollarov, A Torque Meter with an Opposition Tachometer-Generator for Investigating Motors in Tracking Systems. Collection of Papers by the Scientific Student Body. Moscow, pp. 267-271, 1955. (Moscow Power Institute).
- I. N. Sulkhanishvili and B. M. Shkol'nikov, The Problem of the Controlled Drive of Sludge Pumps when the Turbine Drilling Method is Used. Power Bulletin of the Ministry of the Oil Industry of the USSR, No. 4, pp. 15-20, 6 illustrations, 1955.
- M. P. Suslov, Automatic Controller for the Filtration Rate of Rapid Open Filters. Moscow; Institute of Technical and Economic Information of the Acad. Sci. USSR, 14 pages, 10 illustrations, 1955. (Periodic Information).
- A. D. Talantsev, Decision Amplifiers with a Small Null Drift. Transactions of the Second All-Union Conference on the Theory of Automatic Control, Vol. 3, pp. 85-93, 10 illustrations, 5 references, 1955.
- M. V. Trubkin, Automatic Level Controller and Indicator for a Turbine Condenser. The Power Worker, No. 3, pp. 14-15, 3 illustrations, 1955.
- M. B. Tumarkin, Selecting the Parameters of Pneumatic Transmitters in Servosystems. Journal of Machine Building, No. 12, pp. 3-7, 8 illustrations, 1955.
- N. A. Utkin, Modification of the Combustion Controller in the Hydraulic System of the "Teploavtomat" Factory. The Power Worker, No. 8, pp. 7-9, 1955.
- Iu. M. Fainberg, On the Parameters of the Main Electric Drive in Continuous Rolling Mills. Electricity, No. 6, pp. 7-12, 1955.
- L. I. Fomkinsky, Supply Controllers for Marine Steam Boilers. Moscow, "River Fleet" Press, 111 pages, 55 illustrations, 1955.
- G. F. Kharlitsky, Steam Pressure Controller in the End Glands of a Steam Turbine. Heat-Power Engineering, No. 1, p. 51, 1 illustration, 1955.
- V. A. Khokhlov, The Power and Efficiency of Hydraulic Actuating Mechanisms with Restrictor (Slide-Valve) Control. Automation and Remote Control, Vol. 16, No. 6, pp. 530-535, 1955.
- V. A. Khokhlov, Speed Characteristics of Hydraulic Actuating Mechanisms with Slide-Valve Control. Automation and Remote Control, Vol. 16, No. 5, pp. 421-430, 1955.
- V. A. Khokhlov, Electrohydraulic Transducing Units for Use with Electronic DC Integrators. Transactions of the Second All-Union Conference on the Theory of Automatic Control, Vol. 3, pp. 94-104, 4 illustrations, 1955.
- L. V. Tsukernik and V. B. Rybinsky, An Automatic Excitation Controller for Low-Power and Intermediate-Power Generators. The Power Worker, No. 12, pp. 3-7, 5 illustrations, 2 tables, 1955.
- Ia. Z. Tsyarkin, On the Computation of Amplitude Responses for Limiters. Radio Engineering, No. 12, pp. 71-74, 5 references, 1955.
- G. V. Chaly, An Automatic Tuning-Fork Frequency Regulator. Bulletin of Technical and Economic Information, No. 8, pp. 12-15, 1 circuit, 1955. (Institute of Technical and Economic Information of the Acad. Sci. USSR).
- G. V. Chaly, An Automatic Tuning-Fork Frequency Regulator for Power Systems. Cutting Tools and Stands, Moscow, 35 pages, 32 illustrations, 1955. (Institute of Technical and Economic Information of the Acad. Sci. USSR).

- V. N. Chelomei, On Pneumatic Servomechanisms. In the book: Certain Problems of Mechanics. Collection of articles, Moscow, Defense Press, pp. 117-133, 4 illustrations, 1955.
- V. K. Chichinadze, An Electronic (gas-tube) Speed Controller for a Generator-Motor System. Transactions of the Power Institute of the Acad. Sci. Georgian SSR, Vol. 9, pp. 155-171, 11 illustrations, 1955.
- Iu. V. Shervin, An Automatic Controller for the Rate of Gas Evacuation. Factory Laboratory, No. 10, pp. 1261-1262, 1955.
- A. G. Shashkov, Experimental and Theoretical Investigation of Restrictor Elements and Hydraulic Relays of the "Nozzle-Vane" type which Operate in Oil. File of Dissertations for the Title of Candidate of Technical Sciences, Moscow, 10 pages, 5 references, 1955. (Institute of Automation and Remote Control of the Acad. Sci. USSR).
- V. N. Shestopalov and V. E. Rybinsky, A Unit for Measuring the Run-Down Angle of a Synchronous Machine, Electricity, No. 3, pp. 70-72, 2 illustrations, 1 table, 1955.
- V. Shcherbakov, Typical Circuits for the Automatization of Refrigeration Units by Means of Astatic Step Control. Refrigeration and Engineering, No. 4, pp. 8-16, 5 illustrations, 1955.
- Automatic Voltage-Regulation Panels of the type ShchML 9801-11A1, ShchML 9801-21A1 and ShchML 9081-22A2. Moscow, 15 pages, 1955.
- Dynamoelectric Amplifiers of the Type EMUZA and EMUEA (Description and Service Instructions). Moscow, Central Bureau of Engineering Information, 24 pages, 1955. (Ministry of Electrical Engineering Industry of the USSR).
- Electronic Units for Stabilizing AC Servo Drives. Electricity, No. 6, pp. 75-76, 1955.
- E. L. Ettinger and G. V. Chaly, A Test Gas-Tube (Electronic) Excitation Unit for a High-Power Hydroelectric Station. Electricity, No. 4, pp. 16-23, 15 illustrations, 1955.
- N. G. Iankilevich, Adjustment of Dynamoelectric Amplifiers (Amplidyne) "Periodic Information," Subject No. 30, No. K-55-83. Moscow, Institute of Technical and Economic Information of the Acad. Sci. USSR, 24 pages, 25 illustrations, 1955.
- AEG - New Control Relays, Elektropost, 1955, Vol. 8, No. 4, p. 68.
- L. W. Allen, Design and application of a peak voltage detector to industrial control system. Trans. Amer. Inst. Electr. Engrs., 1955, vol. 74, Part 2, p. 123-128; Appl. and Ind., 1955, No. 19, p. 129-134.
- Equipment for the Automatic Voltage Regulation of Electrical Distribution Networks, 1955, April, May, June, No. 101, p. 47-50.
- J. L. Auerbach and S. B. Disson, Magnetic elements in arithmetic and control circuits, Electr. Engng., 1955, Vol. 74, No. 9, pp. 766-770.
- J. E. Barkle and D. M. Santer, Magamps give close control of alternators, Mod. Power and Engng, 1955, Vol. 49, No. 4, pp. 74-75; R. Zh. Electrotehnika,\* , 1955, No. 2, pg. 85.
- Basic synchros and servomechanisms. By Van Valkenburgh, Nooger and Neville, Inc., New York, Rider 1955, Vol. 1, 137 pages; vol. 2, 122 pages.
- C. R. Bates, Electronic control of resistance welding. J. Brit. Inst. Radio Engrs., 1955, Jan., vol. 15, No. 1, pp. 31-46.
- J. Beczkoy, Direct-Acting Flow Controllers, Hungarian Power Industry, 1955, Vol. 8, No. 3, pp. 110-112.
- An Original AC Voltage Stabilizer. Feinwerktechnik, 1955, Vol. 59, No. 5, pp. 173-174.
- A. H. Benner and R. Drenick, An adaptive servo system. IRE Convent. Rec., 1955, Vol. 3, Pt. 4, pp. 8-14, 8 figs.
- F. A. Benson and M. S. Seaman, Saturated diodes. Electronic Engng, 1955, Aug., Vol. 27, pp. 360-365.

\*Journal of Abstracts, Electrical Engineering

- Birchler, Steam-Jet Refrigeration Units in Air-Conditioning Engineering (Controllers). *Techn. Rundschau*, 1955, Vol. 47, No. 4, p. 11.
- M. Body, A servosystem for Industrial Controllers Which Utilize a Selsyn in the Capacity of an Input-Signal Generator. *Bull. Scientifique de l'Assos. des Ingenieurs electriciens sortis de l'Inst. Electrotechn. Montefiore (AJM)*, 1955, Ann. 68, Nov., No. 11, pp. 749-750.
- H. Bonnhoff, Automatic voltage control of transformers by tapchange gear. *Elektrizitätswirtschaft*, 1955, June 20, Vol. 54, No. 12, pp. 395-398.
- H. Bonnhoff, Electrical Controllers. *Gaswarne*, 1955, Vol. 4, No. 4, pp. 114-117.
- K. Boop, A Simple Low-Power Servosystem. *AEG Mitt.*, 1955, Vol. 45, No. 1-2, pp. 155-157, 6 Abb.
- K. Brehm, Controlled Communications-System Supply Units. *AEG Mitt.*, 1955, Vol. 45, No. 1-2, pp. 100-103, 6 Abb., Bibliogr. 5.
- G. Brumby, The Leonard-System Controlled Drive. *AEG Mitt.*, 1955, Vol. 45, No. 1-2, 8 Abb.
- H. Burkhardt, The Control of Thermostatic Expansion Valves. *Kältetechnik*, 1955, Vol. 7, No. 1, pp. 4-5.
- O. E. Carlson, Regulate horsepower directly. *Control Engng.*, 1955, Febr., Vol. 2, No. 2, p. 58.
- W. P. Carpenter, AC voltage regulators. *Product. Engng.*, 1955, Febr., No. 2, pp. 135-139, 8 figs.
- H. Chestnut and R. W. Mayer, Servomechanisms and regulating system design., Vol. II. N.-Y., John Wiley and Sons, Inc., 1955, 384 p. ill.
- R. Cichon, Measuring and Controlling Liquid Levels. *Jeingeratetechnik*, 1955, Jan., Vol. 4, No. 1, p. 40, 2 Abb., Bibliogr. 1.
- E. C. Cowie and J. K. Gregson, Variable-speed Control for Integral HP. Motors. *Electronics*, 1955, April, Vol. 78, No. 4, pp. 162-163.
- P. U. Cronham, Automatic controls. *Process control*, 1955, Febr., Vol. 2, No. 2, pp. 51-56, 7 figs.
- M. Dätzel, A Hydraulic Controller with a Rotating Piston. *Gas (Wasser) Wärme*, 1955, Vol. 9, No. 6, pp. 124-130.
- E. Braunerstreuter and F. Kuhrt, A Metering Transducer for the Electronic Control of the Effective Value of an Alternating Voltage. *Regelungstechnik*, 1955, Vol. 3, pp. 90-94, 15 Abb.
- W. J. Brown, Wide-Angle Phase Shifter for Industrial Controls. *Elektronics*, 1955, March, Vol. 28, No. 3, pp. 188-193, 10 figs.
- A. de. Bruin, Electronic Switching and regulating apparatus for resistance welding machines. *Ingenieur*, 1955, March, 4, vol. 67, No. 9, pp. E 29-E41.
- M. M. Butel, Magnetic Power Amplifiers of the "Mutrou" Type and their Application in Control Problems, in particular, the tension and frequency of small Alternators. *Bull. Soc. Franc. Electriciens*, 1955, Oct., Vol. 5, No. 58, pp. 689-699, 16 figs.
- F. Buttner, Electrical Pump-Drives Which Control the Number of Revolutions; Their Application. *BBC Nachrichten*, 1955, Vol. 37, No. 3, pp. 88-104.
- J. Chytráček, Ferromagnetic Voltage Stabilizers. *Slaboproudý Obzor*, 1955, Vol. 16, No. 6, pp. 320-323, 14 Obr.
- F. Cibulka, Electronic Control of the Number of Revolutions of a Leonard Electric Drive. *Elektrotechnik (Praha)*, 1955, Vol. 10, No. 6, pp. 183-186, 60 figs., 1 tab.
- H. W. Collins and C. V. Fields, Magnetic Amplifiers for Indication and Control. *Elec. Mfg.* 1955, Sept., pp. 112-116.
- Constant pumping pressure automatically controlled without changing speed. *Engineering*, 1955, Vol. 179, No. 4663, p. 736..

- T. M. Dauphine and S. D. Woods, Low-Level Thermocouple Amplifier and a Temperature Regulation System. *Rev. Scient. Instrum.*, 1955, July, Vol. 26, No. 7, pp. 693-695, 4 figs.
- G. N. Davies, A voltage stabilizer for photomultiplier tubes. *Electronic Engng*, 1955, July, Vol. 27, No. 329, pp. 317-318.
- S. A. Davis, Using a two-phase servomotor as an induction tachometer. *Control Engng.*, 1955, Nov. Vol. 2, No. 11, pp. 75-76, 2 figs.
- J. P. DeBarber, A magnetic tape memory for decompositional servomechanisms. *Appl. and Ind.*, 1955, No. 16, pp. 373-374.
- J. J. De Mattels, Electronic facilities control. *Electr. Engng*, 1955, Vol. 74, No. 8, pp. 650-654.
- R. O. Decker and W. F. Horton, A 400 cps magnetic amplifier for a-c servomechanism application. *Proc. Nation. Electronics Conference*, Vol. 10. Chicago, 1955, pp. 35-39, 8 figs., Bibliogr. 4.
- W. R. Deichert, Regulator for constant current power supplies. *Electronics*, 1955, Aug., Vol. 28, No. 8, pp. 170-182, 4 figs.
- W. Dippel, Bimetallic Thermometers as Metering and Control Instruments. *Kaltetechnik*, 1955, Vol. 7, No. 1, pp. 14-15.
- W. Donner, Tape-controlled servos speed chemical analysis. *Electronics*, 1955, Febr., No. 2, pp. 136-141, 8 figs.
- Sh. Z. Dushkes, Applying fixed-displacement pumps to variable pressure hydraulic servomechanisms. *Machine Design*, 1955, Oct., Vol. 27, No. 10, pp. 171-175, 6 figs.
- Ch. Ecary, Servomechanisms with Speed Control. *Techn. et sci. aeronaut*, 1955, Vol. 3, p. 195.
- G. Ehrenberg, Automatic load-frequency control system for central station power. *Trans. Amer. Instn. Electr. Engrs*, 1955, Vol. 74, Pt. 3, pp. 787-795 (Pwr. Apparatus syst. No. 19, Aug. 1955).
- Electric winder with speed control; alternating current equipment installed at Avon Colliery. *Engineering*, 1955, Febr. 11, Vol. 179, No. 4646, pp. 186-187.
- Electronic control. *GEC. Journal*, 1955, Febr. Vol. 22, No. 1, p. 38, 1 fig.
- The Utilization of Electronics in Control Engineering. *Mesures et Controle Industr.*, 1955, Vol. 2, No. 214, pp. 211-218, ill.
- Electronics Place in Control. *McGraw-Hill Digest*, 1955, Vol. 10, No. 4, pp. 38-39.
- Electronic and Magnetic Control and Regulation Systems. 2. Auflage. Berlin, VDE - Verlag, 1955, 124 Seiten, 103 Abb.
- G. Erdösy, The design of centrifuge motors with speed control by pole change. *Elektrotechnika*, 1955, June, Vol. 48, No. 6, pp. 220-227.
- Error voltage detector. *Electr. J.*, 1955, vol. 154, No. 2, pp. 133-134; *R. Zh. Elektrotehnika*, 1955, No. 1, p. 114.
- H. Falderbaum, A Magnetic DSK2 Clutch as a Control Element Adapted for Long Through-Channels. *AEG Mitt.*, 1955, Vol. 45, No. 1-2, pp. 193-195, 5 Abb., Bibliogr. 6.
- Pressure Controller for the DRD-Compadyn System. *Regelungstechnik*, 1955, Vol. 3, No. 8, p. 205, 1 Abb.
- B. d'E Flagge and O. R. Harris, Individual dynode voltage regulator for photomultiplier tube. *Rev. Scient. Instrum.*, 1955, June, Vol. 26, No. 6, p. 610, 2 figs. Bibliogr. 1.
- A. E. Fleming, Level control. *Instruments and Automat.*, 1955, Vol. 28, No. 5, pp. 809-815.
- J. W. Forrest, H. W. Street and A. A. Shurkus, Optical servo detects refractive index to one part in 100000. *Control Engng*, 1955, Nov., Vol. 2, No. 11, pp. 103-105, 4 figs.



- H. Friedrich, A servomotor with a Pulse Controller. *Regelungstechnik*, 1955, Vol. 3, No. 8, pp. 200-204, 6 Abb.
- A. Fuchs, An ac voltage stabilizer. *Bull. Res. Count. Israel*, 1955, March, Vol. 4, No. 4, pp. 337-340.
- J. L. Gates, Electronic controllers. *Instruments and Automat.*, 1955, Vol. 28, No. 8, pp. 1338-1341.
- E. Gerecke, Three Examples of Electrical Servosystem Engineering. *A. angew. Math. u. Phys.*, 1955, Vol. 5, No. 6, pp. 443-465.
- F. Germann and E. Schroter, Controlling Selenium Rectifiers by Means of Magnetic Amplifiers. *AEG - Mitt.*, 1955, Vol. 45, No. 1-2, 16 Abb.
- F. Gerhart, Liquid-Mixing Controller with an Integrating Detector System. *Siemens-Zeitschr.*, 1955, Vol. 29, No. 5-6, pp. 238-241.
- W. Giertz, Controlling the Rate of a Self-Excited Mechanical Vibrator. *AEG Mitt.*, 1955, Vol. 45, No. 1-2, pp. 203-206, 5 Abb. Bibliogr. 2.
- E. Golde and W. Jentsch, Controlling Rectifiers by Means of Magnetic and Electronic Amplifiers. *AEG Mitt.*, 1955, Vol. 45, No. 1-2, 10 Abb.
- A. E. Goodwin and D. A. R. Morrison, Hydraulic servo actuation has low stand-by power. *Control Engng.*, 1955, Aug., Vol. 2, No. 8, p. 82, 3 fig.
- F. Gourash, A two-stage low-level magnetic amplifier with negative voltage feedback. *Proc. National Electron. Conference*, Vol. 10, Chicago, 1955, pp. 146-155, 7 figs., 1 table, Bibliogr. 4.
- D. Graham and R. C. Lathrop, Automatic feedback control and all weather flying. *Aeronaut. Engng. Rev.*, 1955, Oct., Vol. 14, No. 10, pp. 70-85, 21 figs. Bibliogr. 35.
- H. Graner, Controlling the Speed of Electrical Machines. *Regelungstechnik*, 1955, Vol. 3, No. 6, pp. 142-147, 4 Abb. Bibliogr.
- E. Grunwald, Designing Controllers and Feedback Loops. *Regelungstechnik*, 1955, Vol. 3, No. 6, pp. 147-152, 5 Abb.; No. 7, pp. 172-180, 6 Abb. Bibliogr.
- B. H. Hamilton, Semiconductor devices in regulated rectifiers. *Electr. Engng.*, 1955, Vol. 74, No. 2, p. 149.
- D. R. Hardy and T. E. Broadbent, The control of high-voltage impulse generators. *Beama Journal* 1955, Febr., Vol. 62, No. 2, pp. 63-68.
- J. E. Hart, An analytical method for the design of relay servomechanisms. *Applic. and Ind.*, 1955, No. 18, pp. 83-90.
- W. Hartel, Utilizing Thyratrons for Regulating the Fields of Electrical Machines. *Regelungstechnik*, 1955, Vol. 3, No. 3, pp. 66-69, 8 Abb. Bibliogr. 7.
- R. K. Hayward, J. C. Jennings and R. C. Barker, Regulated d.c. power supplies at low voltages. *Electronic Engng.*, 1955, July, Vol. 27, No. 329, pp. 304-307.
- H. Helbig, Position Controllers for Continuous-Loop Machines. *AEG Mitt.*, 1955, Vol. 45, No. 1-2, pp. 168-173, 17 Abb. Bibliogr. 4.
- G. W. Heumann, How to select today's high-voltage a.c.-motor controllers. *Power*, 1955, Oct., Vol. 99, No. 10, pp. 98-100, 4 figs.
- K. Horneber, Automatic Controller for a Piston Pump., *Polygraph*, 1955, Vol. 8, No. 3, pp. 115-116.
- A. B. Hulse and R. Aymer, Applications of differential winch to control systems. *Product Engng.*, 1955, June, No. 6, pp. 184-185.
- W. Hunsinger, Metering and Controlling Instruments. *Z. Vereines dtsch. Ingr.*, 1955, No. 31, pp. 1101-1104.
- W. Hunsinger, Control Engineering. *Z. Vereines dtsch. Ingr.*, 1955, Vol. 97, No. 19-20, pp. 657-662, Bibliogr. 243.

- G. Hutarew, Power Output and Performance Indices of Pumps. *Techn. Rundschau*, 1955, Vol. 47, No. 5, pp. 1-2.
- Hydraulic governors Woodward. *Diesel Engine Catalog*, 1955, Vol. 20, pp. 298-299, 6 figs.
- Hydraulic relay governors Marquette. *Diesel Engine Catalog*, 1955, Vol. 20, pp. 296-297, 5 figs.
- Instrumentation as a service designing and building automatic control systems. *Engineering*, 1955, No. 25, Vol. 180, No. 4687, p. 728, 2 figs.
- A. L. Jaumotte, Control of single shaft, open cycle, gas turbines for constant speed and constant maximum temperature. *Acad. Roy. Belgique, Bull. Cl. Sci.*, 1955, Vol. 41, No. 5, pp. 486-499.
- P. G. Johanessen, Application of a magnetic amplifier to a high performance instrument servo. *JRE Convent. Rec.*, 1955, Vol. 3, Pt. 4, pp. 15-22, 13 figs. Bibliogr. 4.
- A. J. Young, An introduction to process control system design. London, Longmans, Green and Co., 1955, 378 pp., fig. Bibliogr. 95.
- H. Junior, Controlling an AC Source by Means of a Magnetic Amplifier. *AEG Mitt.*, 1955, Vol. 45, No. 1-2, pp. 79-81, 6 Abb. Bibliogr. 1.
- E. Karg, The Technique of Controlling Electrical Heating Devices. *Elektrowarmetechnik*, 1955, Vol. 6, No. 3, pp. 49-52.
- H. F. Karlsruhe, A Pulse-Controlled Servomotor. *Regelungstechnik*, 1955, No. 8, pp. 200-204, 6 Abb. Bibliogr. 1.
- A. B. Kaufman, Electronic temperature controller. *Radio Electronic Engng.*, 1955, March, Vol. 24, No. 3, pp. 10-11, 30 ill.
- V. C. Kennedy, Measurement and control by electronic weighing. *Instruments and Automat.*, 1955, Vol. 28, No. 2, pp. 272-276.
- R. W. Ketchledge, Distortion in Feedback Amplifiers. *Bell system Techn. J.*, 1955, Nov., Vol. 34, No. 6, pp. 1265-1286, 3 figs.
- H. Kindler, Control Techniques and Instrument-Design Techniques. *Jeingeratetechnik*, 1955, Sept., No. 9, pp. 407-410.
- H. Kleinrath, Designing AC Collector Motors with Fixed Brushes and Simple RPM Controllers. *Elektrotechnik und Maschinenbau*, 1955, 1. Juni, Vol. 72, No. 11, pp. 249-256, 13 Abb. Bibliogr. 4.
- R. B. D. Knight, K. M. Poole and J. H. Sanders, A voltage stabilizer for a radiofrequency extra high tension set. *J. Scient. Instrum.*, 1955, April, Vol. 32, No. 4, pp. 134-136.
- Temperature Control. *Regelungstechnik*, 1955, Vol. 3, No. 8, p. 204, 1 Abb.
- H. Krantz, A Controller for Boiler Furnaces. *Gesundh., Ingr.*, 1955, Vol. 76, No. 1-2, p. 28.
- J. Krenmayr, New Developments in the Field of Program Control. *Techn. Rundschau*, 1955, 11 Febr., Vol. 42, No. 6, 2 Blatt., pp. 9-10, 12 Abb.
- R. Kretzmann, An Electronic Thermostat. *Elektron. Rundschau*, 1955, Jan., Vol. 9, No. 1, pp. 17-18.
- F. Kretzschmer, An Engineering Analysis of Pneumatic Controllers. *Regelungstechnik*, 1955, Vol. 3, No. 8, pp. 206-209, 9 Abb.; No. 9, pp. 232-234, 2 Abb.; No. 10, pp. 256-258, 1 Abb.
- K. Kreuter, Control of Industrial Turbines. *Das Papier*, 1955, Vol. 9, No. 9-10, pp. 193-198.
- A. Kusko and J. G. Nelson, Magnetic-Amplifier Control of D-C Motors. *Electr. Engng.*, 1955, May, Vol. 74, No. 5, p. 404, 2 figs; *Trans. Amer. Instn. Elektr. Engrs.*, 1955, Vol. 74, Pt. 1, pp. 326-333.
- W. La Pierre, Magnetic amplifiers as control components. *Product Engng.*, 1955, Aug., No. 8, pp. 129-133, 3 figs.



- J. Lagasse and R. Mezencev, A Servosystem for a High-Voltage Shock-Wave Oscillator. C. R. Acad. Sci., Paris, 1955, 16 May, Vol. 240, No. 20, pp. 1973-1975.
- A. Lang, Synchronous Generators with Controlled Compounding Without Exciters. AEG Mitt., 1955, Vol. 45, No. 1-2, pp. 59-63, 7 Abb. Bibliogr. 4.
- H. S. Lewis, A compact relay for automatic control of power factor. G. E. C. J., 1955, April, Vol. 22, No. 2, pp. 71-78.
- H. J. Lindenhovius Fundamentals of Electronic Measurements and Control in Industry. Microtechnik, 1955, Vol. 9, No. 3, pp. 159-165.
- Liquid level controller. Engineering, 1955, Vol. 180, No. 4667, p. 62.
- G. Loocke, Design of DC Machines for Automatic Control Systems. Regelungstechnik, 1955, Vol. 3, No. 4, pp. 84-90, 8 Abb. Bibliogr. 6.
- R. E. Lynch, Reliable voltage regulator tubes. Proc. Nation. Electronics Conference, Vol. 10, Chicago, 1955, pp. 714-722, 57 p., Bibliogr. 4.
- The Magnestat Voltage regulator automatic device for large alternators. Engineering, 1955, March 11, Vol. 179, No. 4650, p. 319, 1 fig.
- P. Marsilli, Improvements to automatic voltage regulators with magnetic amplifiers. Elettrotecnica, 1955, April, Vol. 42, No. 3, bis, pp. 165-167.
- C. E. Mathewson, Advantages of Electronic Process Control. Instruments and Automat., 1955, Vol. 28, No. 2, pp. 258-265.
- J. J. Mattels, Electronic facilities control. Electr. Engng., 1955, Aug., Vol. 74, No. 8, pp. 650-654, 6 figs.
- H. Matuschka, Metering Instruments for Temperature Controllers. Siemens Zeitschr., 1955, Vol. 29, No. 5/6, pp. 222-228.
- W. Mecklenburg, A Tuned Controller for the Automatic Control of Petersen Coils. AEG-Mitt., 1955, Vol. 45, No. 1-2, pp. 126-129, 4 Abb. Bibliogr. 2.
- P. Ménager, General Description of Pneumatic Controllers. Mesures et Controle Industr., 1955, Vol. 20 Annee, No. 213, pp. 93-98, 9 figs.
- C. L. Mershon and N. F. Schuh, A.C. control for aircraft electrical systems. Westinghouse Engr., 1955, Sept., Vol. 15, No. 5, pp. 146-151.
- Metering and Control Instruments for Boilers and Solid-Fuel Central Heating Units. Heizg. (Luftg.) Haus-technik, 1955, Vol. 6, p. I - XIV.
- J. T. Miller, Control handbook. Section I. Elements of process controllers and servomechanisms. Instrument Practice, 1955, Jan., Vol. 9, No. 1, pp. 50-56, 17 figs. Bibliogr. 9. R. Zh. Electrotechnika, 1955, No. 1, p. 94.
- J. T. Miller, Control handbook. Section 2. Servomechanism components. Instrument Practice 1955, Febr., Vol. 9, No. 2, pp. 142-147, 29 figs.
- J. T. Miller, Control handbook. Section 3. Amplifiers. Instrument Practice, 1955, Vol. 9, No. 3, pp. 246-251.
- J. T. Miller, Control handbook. Section 4. Simple computing devices in process measurement and control. Instrument Practice, 1955, Vol. 9, No. 4, pp. 342-348.
- J. T. Miller, Control handbook, Section 5. Electrical analogies in process control. Instrument Practice, 1955, Vol. 9, No. 5, pp. 441-444.
- J. T. Miller, Control handbook, Section 6. Reduced capacity trim for double seated diaphragm operated control valve. Instrument Practice, 1955, Vol. 9, No. 6, pp. 563-567.

- J. T. Miller, Control handbook. Section 7. Computers. Instrument Practice, 1955, Vol. 9, No. 9, pp. 890-894.
- J. T. Miller, Control handbook, Section 8. Computers. Storage devices. Instrument Practice, 1955, Vol. 9, No. 10, pp. 989-993.
- G. R. Mohr and R. Lee, Magnetic amplifier control of radiofrequency generators. *Appl. and Ind.*, 1955, No. 16, pp. 374-378.
- A New Standard Controller for Pressures, Amounts and Ratios. *Regelungstechnik*, 1955, Vol. 3, No. 9, pp. 234-235, 5 Abb.
- New Instruments for Controlling the Composition of Fluids and Gases. *Regelungstechnik*, 1955, Vol. 3, No. 5, p. 126, 3 Abb.
- A New Pneumatic Pressure Controller. *Regelungstechnik*, 1955, Vol. 3, No. 9, pp. 204-205, 1 Abb.
- New Control Instruments. *J. Franklin Inst.*, 1955, Vol. 259, No. 1, p. 80.
- New mag amplifiers for servosystems. *Aviat. Week*, 1955, Vol. 62, No. 13, pp. 50, 52; 1955, No. 2, p. 81.
- B. R. Nichols, Hydraulic-turbine governors developed to reduce outage time. *Mech. Eng.*, 1955, Febr., Vol. 77, No. 2, pp. 137-140, 5 figs.
- A Level Controller without a Packing Gland. *Regelungstechnik*, 1955, Vol. 3, No. 2, p. 49.
- J. W. O'Hara and R. A. Lundholm, Power station controls frequency electronically. *Nat. Engr.*, 1955, Vol. 59, No. 2, pp. 25-27; *R. Zh. Electrotechnika*, 1955, No. 1.
- E. W. Otto, H. Gold and R. W. Hiller, Design and performance of throttle-type fuel controls for engine dynamic studies. *NACA T*, No. 3445, 1955, 39 pages.
- F. M. Partridge and G. C. Wilson, Hydraulic techniques for piston-operated valves. *Instruments and Autom.*, 1955, Vol. 28, No. 2, pp. 286-287.
- E. B. Pearson and G. J. Lingwood, A servomechanism layout designed for instructional purposes. *Instrument Practice*, 1955, Apr., Vol. 9, No. 4, pp. 324-330, 6 figs.; No. 6, pp. 540-550.
- A Pneumatic Differentiating Device. *Regelungstechnik*, 1955, Vol. 3, No. 4, pp. 100-101, 1 Abb.
- J. Preminger, Frequency changes in electric power systems and requirements of automatic frequency and active power regulators. *Energetika*, 1955, Vol. 9, No. 3, pp. 127-130.
- Control Engineering. Control-Problem Analyses and their Practical Application. Berlin, 1955, 228 pages. (*Regelungst.*, 1956, No. 1, pp. 24-25.)
- A Pneumatic Recording Controller. *Mesures et Controle Industr.*, 1955, Sept. 20, Annee. No. 220, pp. 626-631.
- The "Sensilab" Temperature Controller. *Mesures et Controle Industr.*, 1955, avril, No. 215, pp. 283-295.
- Controllers and Servosystems with Magnetic Amplifiers. *Mesures et Controle Industr.*, 1955, No. 214, pp. 197-200, 4 figs.
- An Inductive Controller. *Mesures et Controle Industr.*, 1955, Fevr., Annee 20, No. 213, pp. 131-137, 23 figs.
- Pneumatic Controllers with a Compensator. *Mesures et Controle Industr.*, 1955, Fevr., 20, Annee, No. 213, pp. 117-121, ill.
- The Shoppe-and-Faeser Inductive Controller System. *Mesures et Controle Industr.*, 1955, Mars, No. 214, p. 211-218; Avril, No. 215, pp. 265-270.
- Remote Control. *Engineering*, 1955, Vol. 178, No. 4652, p. 370.
- R. Richter, The "Relo" Rotary Controller. *AEG Mitt.*, 1955, Marz-April, Vol. 45, No. 3/4, pp. 260-261, 3 Abb.

- E. J. Rogers, Current regulator for van de Graaft Magnet. *Electronics*, 1955, Oct., Vol. 28, No. 10, pp. 151-153, ill. Bibliogr. 1.
- F. Rub, Automatic Temperature Control Applied to Industrial Furnaces. *Werkstatt und Betrieb*, 1955, No. 4, pp. 163-164, 3 Abb.
- E. Samal, Application of the Rotary Pulse Controller. *AEG Mitt*, 1955, Vol. 55, No. 1-2, pp. 216-224, 16 Abb. Bibliogr. 4.
- E. Samal, A Rotary Controller Combined with Pneumatic and Electrical Actuating Mechanisms. *Regelungstechnik*, 1955, Vol. 3, No. 10, pp. 258-261, 11 Abb. Bibliogr. 2.
- Fr. Sauter, Simple Pneumatic Controllers. *Schweiz. Bauzeitung*, 1955, Vol. 73, No. 16, pp. 230/234.
- H. Schaal, Electronic and Transducer Regulators. *Lichttechnik*, 1955, Sept., Vol. 7, No. 9, pp. 342-348.
- Scharla, An Automatic Furnace Controller for Water-Heating Systems. *Gesundheits-Ingenieur*, 1955, Vol. 76, No. 9-10, p. 160.
- W. Schilling, Electrical Elements in a Control System. Teil II. *Regelungstechnik*, 1955, Vol. 3, No. 11, p. 281-282. Abb.
- W. Schilling, Techniques of Applying Magnetic Amplifiers. II. Utilizing Controllers for Voltage Stabilization. *Regelungstechnik*, 1955, Vol. 3, No. 2, pp. 28-36, 24 Abb. Bibliogr. 6.
- H. Schonfeld, Problems in Control Engineering. *Feingeratetechnik*, 1955, Dez., No. 12, pp. 534-570, 16 Abb. Abb.
- K. Schwarz, An Instrument for Determining the Stability of Servomechanisms. *Electr. Eng. Rev.*, 1955, No. 5, pp. 292-293, 306.
- J. Skotnicky, An Electronic Thermal Controller. *Communications Rev.*, 1955, No. 8, pp. 422-424, 2 Obr., Bibliogr. 3.
- Cl. Soule, A New Type of Low-Inertia Motor for Servosystems. *Mesures et Controle Industr.*, 1955, Mars, No. 214, pp. 181-186, 16 figs.
- M. C. Spencer, Squirrel-cage motor speed control system. *Electronics*, 1955, Aug., Vol. 28, No. 8, pp. 126-129.
- An Electroplate with Two Temperature Controllers. *Elektropost*, 1955, Vol. 8, No. 4, pp. 69-70.
- H. F. Storm, Magnetic Amplifiers. N.Y., Wiley; London, Chapman and Hall, 1955, 545 pages, figs. Bibliogr. pp. 508-527.
- R. Suss, Controllers with a Minimum Reset Frequency and an Actuator Mechanism. *Regelungstechnik*, 1955, No. 5, pp. 106-109, 4 Abb.
- O. Suter, Pneumatic Controllers. *Gaswarme*, 1955, Vol. 4, No. 4, pp. 120-124.
- Controller Construction. *Mesures et controle Industr.*, 1955, Vol. 2, No. 214, pp. 197-200, ill.
- These 7 steps design a tach stabilized servo: 1. Select motor-generator. 2. Specify gear ratio. 3. Determine design constants. 4. Find velocity error constant. 5. Calculate gain and feedback. 6. Calculate allowable backlash. 7. Correct for quadrature and phase shift. *Control Engng.* 1955, Aug. Vol. 2, No. 8, pp. 72-79, 7 figs.
- Synchronous transmission in automatic level control in watersheds. *Mesures et Contrôle Industr.*, Vol. 20, No. 214, pp. 189-194, 11 figures, 1955.
- G. Unterkircher, Static regulator holds engine-generator frequency constant. *Westinghouse Eng.*, 1955, Vol. 15, No. 1, p. 18.
- J. A. Van Den Broek, Isochronal spiral regulator. *Amer. J. Phys.*, 1955, Apr., Vol. 23, No. 4, pp. 224-239.

- Van Valkenburgh, Nooger and Nevill, Inc., Basic synchros and servomechanisms. N. Y., Rider, 1955, Vol. 1, 137 pages; Vol. 2, 122 pages.
- The "Visko" Unit for Automatic Control. Regelungstechnik, 1955, Vol. 3, No. 5, pp. 130-131.
- Walter W. Vergleich, Comparison of Contact-Type and Magnetic Controllers for Synchronous Generators. ETZ - A, 1955, Vol. 71, No. 9, May, pp. 327-330, 9 Abb. Bibliogr. 3.
- W. Weber, Instrument for Measurement and Control in Hydro-Heat-Power. Z. Vereines dtsch. Ingr., 1955, Vol. 97, No. 19-20, pp. 652-656, 4 Abb. Bibliogr. 100.
- E. Wenzel, Time Control of Electric Laboratory Furnaces. Chemie Ing. Technik, 1955, Vol. 27, No. 2, pp. 75-77.
- R. R. West, Do you know your basic low-cost controller? Instruments and Automat., 1955, Vol. 28, No. 2, pp. 280-284.
- H. Wicke, Pressure Controllers for Extraordinary Conditions. Askania Warte, 1955, Vol. 13, No. 47, p. 18.
- E. Winkler and R. Jaquero, An Electronic Controller for a Smelting Furnace. Neue Zürcher Zeitung, Bellage Technik, 1955, 30 marz, No. 830.
- R. Wobser, A Temperature Controller for Instrument Manufacture. Feingeratetechnik, 1955, Vol. 4, May, No. 5, pp. 200-205, Abb.
- G. Wunsch, The Alphabet of Control. Askania Warte, 1955, Vol. 13, No. 47, pp. 8-17; No. 48, pp. 13-15, 18-19.
- H. Ziebolz, An Improved Pneumatic Nozzle-Vane Controller. Regelungstechnik, 1955, Vol. 3, No. 1, pp. 22-23, 4 Abb.
- M. Zucchini, Autopilot magnetic servo amplifier. Electronics, 1955, Vol. 28, No. 5, pp. 208, 210, 212, 214; R. Zh. Elektrotehnika, 1955, No. 2, p. 82.

#### APPLICATION OF AUTOMATIC CONTROL SYSTEMS

- Automatization of Production Processes. Collection of Papers. Moscow, Acad. Sci. USSR, 91 pages, 1955. (Institute of Automation and Remote Control of the Acad. Sci. of the USSR).
- Automatic Control in the Process Industry. Collaboration between Process and Instrument Engineers - Engineering, 1955, Nov. 4, No. 4684, p. 631.
- D. M. Boyd, Why is Electronic Control of Technological Processes Used in Industry? Regelungstechnik, 1955, Vol. 3, No. 10, pp. 239-243, 8 Abb.
- W. Britall, The Intensive Introduction of Metering and Control Techniques into Production. Feingeratetechnik, 1955, May, Vol. 4, No. 5, pp. 193-194, 1 Abb.
- Industrial Control and Regulation. Mesures et controle industr., 1955, April, No. 215, pp. 275-278.
- Controls aid production at Ford Motor Co., Ltd. Process Control and Automat., 1955, June, No. 6, pp. 197-201, fig.
- L. J. Delaney, Maintenance of gas pressure regulators. Instruments and Automat., 1955, April, Vol. 28, No. 4, pp. 633-635, 3 figs.
- G. Hutarew, Control Engineering (An Example is Given of Controlling the Number of Revolutions of Hydro-Turbines). Berlin (Gottingen, Heidelberg, Springer Verlag, 1955, p. 177, 198 Abb.
- The Gap Between Theory and Practice. Regelungstechnik, 1955, Vol. 3, No. 5, p. 105.
- G. L. D'Ombra, Automatic process control. Process Control, 1955, Vol. 2, Febr., No. 2, pp. 66-68, 5 figs.; March, No. 3, pp. 102-103, 6 figs.; Nov., No. 11, pp. 430-433.
- G. L. D'Ombra, Automatic process control. Part 7. Three-term controllers. Process Control, 1955, April, No. 4, pp. 135-137, 5 figs.



- G. L. D'Ombraiu, Automatic process control. Part 13. Three-term response. *Process Control and Automation*, 1955, Vol. 2, No. 10, pp. 386-387, 3 figs.
- W. Palmer, Some practical application of servomechanisms. *Sperry Eng. Rev.*, 1955, July - August, pp. 2-8.
- W. Pontow, The Field of Application of the Siemens Type ZR5 Controller with an Indicating Needle. *Siemens-Zeitschrift*, 1955, Vol. 29, No. 3-4, pp. 100-103.
- Control in Industry. *Mesures et controle Industr.*, 1955, Vol. 2, No. 214, pp. 203-207, III.
- H. J. Roosdorp, Electronic Control of Technological Processes. *Philips technische Rundschau*, 1955, Aug., No. 2, pp. 63-73, 17 Abb.
- Two Ideas for Users of Contactor servos. *Control Engng.*, 1955, December, Vol. 2, No. 12, pp. 79-81.
- A Comparison of Control Processes in the Consumer Industry and in Engineering. *Regelungstechnik*, 1955, Vol. 3, No. 2, p. 27.
- L. Walter, The care of process control instruments. *Electr. J.*, 1955, Vol. 104, No. 1, pp. 37-39;
- R. Zh. Electrotechnika*, 1955, No. 1, p. 97.

#### a) In Industry

##### In Power

- V. L. Ankhimiuk, Computing the Currents of an Asynchronous-Synchronous Stage in Two-Zone Control. *Transactions of the Central Asian Polytechnical Institute*, pp. 379-390, 6 illustrations, 1955.
- M. R. Arshtein, Steam Pressure Control in Condenser Manifolds. *Power Worker*, No. 7, p. 17, 1955.
- S. P. Boiarshinov, Signalization of Operational Breakdown in a ARI-IV Controller. *Power Worker*, No. 7, pp. 11-12, 1955.
- V. N. Veller, Controlling Steam Turbines. Moscow-Leningrad, State Power Press, 252 pages, 126 illustrations, 26 references, 1955.
- V. A. Venikov and I. V. Litkens, The Effect of Excitation Control Upon the Transmissive Capability of Long-Range Electrical Transmission. *Electricity*, No. 11, pp. 15-26, 8 references, 1955.
- V. L. Dejanov and V. V. Romantsov, Improving the Supply Circuits of the Self-Compensators of an Electro-mechanical System. *Electrical Power Station*, No. 8, pp. 53-54, 3 illustrations, 1955.
- M. A. Duel' and N. R. Litvak, Experience in Determining the Economic Effects of Automatic Control of the Combustion Process. *Electrical Power Stations*, No. 6, pp. 4-6, 2 illustrations, 2 tables, 1955.
- A. G. Zaparin, Problems of Automatic Control in Local Power Systems. In the collection: *Electrical Power Equipment and Automatization in Rural Electrical Power Installations*. Moscow-Leningrad, State Power Press, pp. 25-31, 1955.
- B. M. Zvenigorodsky and A. P. Kopelovich, Automatic Combustion Control in Boiler Installations which Burn Two Types of Fuel. ——— *Electrical Power Station*, No. 8, pp. 9-15, 11 illustrations, 1955.
- L. M. Ivanov and Iu. A. Freiman, Experience in Applying the Method of Self-Synchronization of Generators at a Hydroelectric Station. *Electricity*, No. 5, pp. 61-62, 1955.
- N. Kh. Kanaian and N. G. Miridzhamian, Group Control and Aggregate Control. *Technical Bulletin of the Central Laboratory of "Armenenergo"*, No. 1, pp. 10-26, 12 illustrations, 1955.
- A. K. Kirsh, The Reception of Steam from the Controlled Stage of a Turbine. *The Power Worker*, No. 7, p. 29, 1955.
- B. D. Kosharsky, Handbook on Thermal Metering Instruments and Automatic Controllers for Electrical Power Stations. Second Edition, Modified. Moscow-Leningrad, State Power Press, 352 pages, 47 references, 1955.

- A. B. Krikunchik, Motors and the Control of the Efficiency of the Mechanisms which Satisfy the Intrinsic Needs of New Thermal Electric Power Stations in the USA. *Electrical Power Stations*, No. 6, pp. 59-62, 4 tables, 1955.
- O. S. Lindorf, On Controlling the Speed of Rotation of an Electric Motor, the Efficiency of Compressors, and the Practicality of Loading Synchronous Compensators with a Resistive Load. *The Power Worker*, No. 3, pp. 39-40, 1955.
- M. V. Melkmer, Control of Steam Superheating when High-Pressure Boilers are Stoked. *The Power Worker*, No. 1, p. 4, 1955.
- V. D. Mironov and E. P. Stefani, Automatic Electronic Controllers for Thermal Processes, Moscow, State Power Press, 224 pages, 32 references, 1955.
- A. V. Naumov, A New Circuit for Controlling the Combustion Process. *Heat-Power Engineering*, No. 10, pp. 57-58, 1955.
- L. N. Pupyshv, A Unit for Stabilizing and Controlling Frequency. *Electrical Power Stations*, No. 11, p. 57, 1955.
- A. A. Ravkind, Utilizing the ID-8 Controller for the DSG-38 "Enterprise" Motor. *Power Bulletin of the Ministry of the Oil Industry of the USSR*, No. 1, pp. 5-9, 7 illustrations, 2 references, 1955.
- A. Ia. Riabkov, Voltage Regulation in Electrical Distribution Networks. In his book: *Electrical Networks*. Moscow-Leningrad, State Power Press, pp. 272-307, 1955.
- A. A. Savin, An Automatic Unit for Controlling the Operation of a Water-Heating Boiler which is Gas-Fueled. *The Power Worker*, No. 8, pp. 12-13, 1955.
- M. A. Seleznev, The Application of Gas-Analyzers in Control Circuits which Economize the Combustion Process. The Jubilee Scientific-Engineering Conference. Theses of the Reports. Moscow, pp. 13-14, 1955 (Ministry of Higher Education of the USSR, (Moscow Power Institute)).
- G. T. Ter-Arutiunian and L. M. Khurshudlian, Automatic Water-Flow Power Control (ARMV) in an Operating High-Pressure Hydroelectric Station. *Technical Bulletin of the Central Laboratory of Armennergo*. No. 1, pp. 38-48, 1955.
- S. M. Timofeev, An Automatic Electrical Regulator for the Speed of Rotation of Hydroturbines with Small and Intermediate Power Ratings. Tashkent, Acad. Sci. Uzbek SSR, 20 pages, 7 illustrations, 1955, (Power Institute of the Acad. Sci. Uzbek SSR).
- G. N. Ul'ianov, Controller for the Combustion Process in the VTI System when Low-Power Boilers are Used. *Bulletin of Technical and Economic Information of the Institute of Technical and Economic Information of the Acad. Sci. USSR*, No. 10, pp. 17-19, 1955.
- G. L. Khundadze, Automatic Frequency Control in Power Systems Where the Control is Performed with Respect to the Deviation and Rate of Change of the Frequency. *Transactions of the Power Institute of the Acad. Sci. Georgian SSR*, Vol. 9, pp. 205-213, 1955.
- S. S. Tsimbal, Controlling the Water Level in a Steam Boiler. *The Power Worker*, No. 10, pp. 15-16, 1955.
- N. M. Shchapov, Automatic Turbine Control. In the book: *Turbine Equipment in Hydroelectric Power Stations*. Moscow-Leningrad, State Power Press, pp. 186-212, 34 illustrations, 1955.
- R. M. Epshtein, Increasing the Speed of Response of Hydroturbine Speed Controllers. *Electrical Power Stations*, No. 3, pp. 22-25, 1955.
- K. Bodekker, Condenser Installations which are Automatically Controlled. *Deutsche Elektrotechnik*, 1955, Vol. 9, No. 9, September, pp. 322-325.
- The Automatic Control of Boiler Auxiliaries. *Steam Engr.*, 1955, Febr., Vol. 24, No. 281, pp. 174-176, 5 figs. *J. of Abstracts, Machine Construction*, 1956, No. 3, p. 15.



- E. Bornitz and A. Schmidt, Control of Reactive Power by Means of Capacitors in Industrial Enterprises and in Distribution Networks. AEG Mitt., 1955, Vol. 45, No. 1-2, 15 Abb.
- H. Braun, The Application of Modern Controllers in Electrical Engineering. Mitteilungsblatt des VDE, Bez. Ver. Frankfurt n/Main, 1955, Vol. 4, No. 13, p. 1-3.
- J. A. Dever, Control of nuclear Reactors. Control Engng., 1955, Aug., No. 8, pp. 54-62, fig. Bibliogr. 9.
- H. Dickinson, Unified Boiler Control at East Yelland. Engineering, 1955, Oct. 14, Vol. 180, pp. 546-548.
- G. Evangelisti, The Problems of Speed-Acceleration Governing in Hydro-Electric Plant. Ingegneria, 1955, Sept., Vol. 29, No. 9, pp. 1013-1021.
- G. Fabritz, Steam Turbine Control. Regelungstechnik, 1955, Vol. 3, No. 9, pp. 214-219, 13 Abb. Bibliogr. 7.
- G. Fabritz, Gas Turbine Control. Regelungstechnik, 1955, Vol. 3, No. 11, pp. 266-268, 2 Abb. Bibliogr. 5.
- G. Fabritz, Hydroturbine Control. Regelungstechnik, 1955, Vol. 3, No. 3, pp. 58-66, 12 Abb. Bibliogr. 7.
- L. W. Fitzpatrick, Electrical Control Adopts Tankless Deaerator to Swing-Loads. Power, 1955, Vol. 99, No. 1, pp. 124-125.
- L. R. Girling, Automatic Regulation of Excitation of Small a.c. Generators Running in Parallel with Public Supplies. Metropolitan-Vickers Gazette, 1955, No. 435, pp. 315-318, 6 figs.
- J. M. Harrer, Nuclear reactor control. Electr. Engng., 1955, Vol. 74, No. 3, pp. 230-233.
- J. Heisuck and H. R. Eggers, Controlling the Condenser Vacuum of an Air-Cooled Steam Turbine. AEG Mitt., 1955, Vol. 45, No. 1-2, pp. 206-211, 4 Abb. Bibliogr. 6.
- G. Kirchberg and A. Raab, Steam Turbine Control. AEG Mitt., 1955, Vol. 45, No. 1-2, pp. 212-216, 11 Abb. Bibliogr. 2.
- H. Kupfer, Small Electrical Machines and their Control. Feingeratetechnik, 1955, Vol. 4, No. 1, pp. 21-23, 5 Abb.
- M. Ledinegg, Design of Atomic Reactors. Part VII. Control Methods. Elektrotechnik u. Maschinenbau, 1955, Vol. 72, No. 15-16, pp. 373-380.
- H. E. Lokay, Controlling Voltage in Distribution Systems. Westinghouse Eng., 1955, Vol. 15, No. 2, pp. 50-55; No. 3, pp. 86-88.
- S. F. Maleker and E. Rathje, Nuclear Reactor Control Systems Utilizing Solid State Devices. JRE-Convent. Rec., 1955, part 10, pp. 218-223, 6 figs. Bibliogr. 6.
- J. J. Owens and J. H. Pigott, Safety Aspects of Nuclear Reactor Control. Electrical Engineering, 1955, Vol. 74, No. 4, pp. 307-309.
- C. J. Penescu, Techniques of Power-System Control. Energetica si hidrotehnica, 1955, Anul III, No. 3, pp. 144-150, 19 figs.
- Ste Saint-Chaumont-Granat, Synchronous Transmission for Automatic Level Controllers in Reserve Water Sheds. Mesures et Controle Industry, 1955, March, No. 214, pp. 189-194, 11 figs.
- H. F. Steinmuller, A Controller with a Magnetic Amplifier which is Used to Charge Large Storage Batteries. AEG Mitt., 1955, Vol. 45, No. 1-2, pp. 96-99, 4 Abb. Bibliogr.
- D. C. Swift, Pay Close Attention to Feedwater Regulators, Heaters, Evaporators. Power, 1955, April., Vol. 99, No. 4, pp. 118-119, 222.

#### In Metallurgy

- Automatic Control of Mold-Packing Density in Molding Machines. In the book: The All-Ukrainian Scientific-Production Conference on the Problem on Technology and Mechanization of the Foundry Industry. December 7-11, 1955. (Theses of Reports and Papers). Kiev, Institute of Machine Building and Agricultural Mechanics of the Acad. Sci. USSR, pp. 23-24, 1955.

- Automatic Control of Blast-Furnace Operation.** Bulletin of the Central Institute of Information of Ferrous Metals, Ministry of Ferrous Metals of the USSR, No. 5-6, pp. 67-68, 1955.
- D. M. Amstislavsky,** Automatic Control of the Air-Feed in Coke-Furnace Heating. Steel, No. 6, pp. 483-487, 1955.
- V. P. Borodin, V. F. Demenkov, P. E. Darmanian and A. A. Iudson,** The Introduction of a Complex System for the Automatic Control of the Thermal Regime of a Mazut Open-Hearth Furnace. Steel, No. 11, pp. 977-983, 8 illustrations, 3 tables, 1955.
- I. A. Burovol,** On the Automatic Control of Furnaces Which are Designed for Annealing in the Bolling Layer. Ferrous Metals, No. 3, pp. 38-43, 3 illustrations, 1955.
- V. G. Kamennov,** Automatic Control of the Thermal Regime of Gas Furnaces. Moscow, Central Bulletin of Technical Information of the Ministry of Machine-Tool Building and Cutting-Tool Industry of the USSR, 8 pages, 1955.
- L. V. Karniushin and M. G. Liukov,** The Problem of Designing Rational Automatic Control Systems for Steel-Smelting Arc Furnaces. In the book: Proceedings of the Lvov Polytechnical Institute, Vol. 1, No. 1, pp. 111-117, 1955 (Lvov State University).  
Kiev-Moscow, Machinery Press, pp. 215-221, 5 illustrations, 1955. (All Union Scientific Engineering-Technical Society. Machinery, Kiev Regional Division).  
Regional Division).
- I. P. Kuklenkova,** Temperature Control in Electrical Furnaces and Resistance Baths. Collection of Rationalization Proposals, No. 49, pp. 20-21, 1 diagram, 1955.
- E. V. Kurmina and S. S. Rabinovich,** A Mechanism for the Automatic Control of the Temperature to which an Electrical Furnace Is Heated. Cutting Tools and Stands. Subject No. 9. Moscow, 11 pages, 1955. Institute of Technical and Economic Information of the Acad. Sci. USSR.
- F. K. Makarov and A. A. Novitsky,** Contactless Electronic-Ionic (Gas-Tube) Power Controller for the Arc of an Electric Furnace. Journal of Technical Information of the Ministry of Tractor and Agricultural Building Machine of the USSR, No. 1, pp. 22-24, 1955.
- M. I. Panfilov and M. V. Shavel'zon,** New Circuits for the Control of Combustion in Open-Hearth Furnaces. Steel, No. 1, pp. 84-86, 1955.
- B. E. Paton,** Automatic Control of Electric Slag Welding. Automatic Welding, No. 3, pp. 39-50, 10 illustrations, 3 references, 1955.
- P. F. Sabaneev,** Automatic Control of the Cooling of Arc Furnaces. Steel, No. 7, pp. 612-616, 9 illustrations, 1955.
- A. S. Filatov,** Automatic Control of Strip Thickness in Cold-Rolling Mills. In the collection: Rolling Mills. Moscow, Machinery Press, pp. 127-157, 22 illustrations, 7 references, 1955.
- S. M. Emdina,** The Effect of Technological Perturbations Upon the Formation of a Seam and Upon the Operation of Controllers. Welding Production, No. 12, pp. 6-7, 3 illustrations, 1955.
- Application of Control Regulators to Steel Operation.** Iron and Steel Eng., 1955, Aug., Vol. 32, No. 8, pp. 132-142.
- Automatic Control of the Heating of Electric Furnaces.** Elektrotechnik und Maschinenbau, 1955, May, Vol. 72, No. 10, p. 235, 1 Abb.
- R. G. Beadle,** Application of Control Regulators to Steel Operations. Iron and Steel Engr., 1955, Aug., Vol. 32, No. 8, pp. 132-135, 3 figs.
- H. Becker,** The Application of Electronic Control to the Processing of Sheet Metal. Blech, 1955, Vol. 2, No. 3, pp. 17-19.

- G. Elchert, The State of Metering and Control Engineering with Respect to Small Forging Arcs. *Werkstattstechnik und Maschinenbau*, 1955, Oct., Vol. 45, No. 10, pp. 548-552, 7 Abb.
- Gage Controlled Automatically on Tandem Cold Reduction Mill. *Iron and Steel Engr.*, 1955, Dec., Vol. 32, No. 12, pp. 136, 139, 140, 3 Abb.
- J. R. Ilckmott, Automatic Control for heating Systems. *Electr. Times*, 1955, Vol. 127, No. 3298, pp. 89-90; *R. Zh. Elektrotehnika*, 1955, No. 1, p. 95 1955, No. 1, p. 95
- H. Kind and J. Wetger, Controlling Strip Rolling Mills. *ETZ-B*, 1955, Vol. 7, No. 9, pp. 317-320, 8 Abb.
- W. Litterscheidt and Th. Schmidt, On Controlling Industrial Gas Furnaces. The Gas-Air System as a Section of the Control System. *Gaswarne*, 1955, Vol. 4, No. 1, pp. 1-14.
- F. Mertz, The Development of Instrumentation and Control Engineering with Regard to Hot Blasts. *Kupolofenanlagen. Glasserel*, 1955, Sept., No. 40, pp. 549-551, 6 Abb.
- H. Molter, Control and Regulation in an Enterprise Manufacturing Metal Parts. *Industrie. Elektrizitätswirtschaft*, 1955, March 5, Vol. 54, No. 5, pp. 123-127.
- Open-Hearth Furnace Controllers. *Regelungstechnik*, 1955, Vol. 3, No. 6, pp. 152-153, 2 Abb.
- A. W. Robinson, Blast-Furnace Automation. *Instruments and Automat.*, 1955, Vol. 28, No. 2, pp. 266-269.
- W. Runter, Drive System and Control for the Centrifugal Air Blower of a Blast Furnace. *Stahl und Eisen*, 1955, April 21, Vol. 75, No. 8, pp. 461-474, 27 Abb.
- G. Sachs, Automatic Signaller for the Purpose of Protecting Automatically Controlled Electric Industrial Furnaces. *Draht*, 1955, Vol. 6, No. 4, pp. 140-141.
- G. Stepken, Electrical Equipment for Strip Mills During Hot Rolling. (Control is Affected by Means of an Amplidyne). *Stahl und Eisen*, 1955, Vol. 75, No. 5, pp. 291-292.
- W. H. Stuck, Strip Pickling Requires Acid Control. *Instruments and Automat.*, 1955, Vol. 28, No. 3, pp. 444-446.
- J. E. Weber, Distribution Control of Mixed Gas. *Instruments and Automat.*, 1955, Vol. 28, No. 9, pp. 1528-1531.
- J. Wetzger, Installing a Magnetic Amplifier for the Rapid Control of Rolling-Mill Drives. *Stahl und Eisen*, 1955, Vol. 75, No. 8, pp. 478-485.
- A. J. Winchester, Reel Control Systems for Mills and Process Lines. *Iron and Steel Engr.*, 1955, Vol. 32, No. 11, pp. 125, 134, 18 figs.; *Steel*, 1955, Dec. 5, Vol. 137, No. 23, pp. 130, 134, 3 figs.; *Automatic Control*, 1955, Nov., Vol. 3, No. 5, pp. 26-27, 3 figs.

#### In Machine Building

- P. R. Malakhov, Automatic Control of Cutting Speed as a Function of the Temperature of the Cutting-Edge of the Tool. *Journal of Machine Building*, No. 4, pp. 26-30, 1955.
- P. N. Malakhov, Increasing the Efficiency of Metal-Cutting Machine-Tools when the Cutting Speed is Automatically Controlled. *Transactions of the Bezhets Institute of Transport Machine Building*, No. 14, pp. 51-72, 5 illustrations, 1955.
- M. B. Tumarkin, Duplication Processing with Contact Servosystems. *Machine Tools and Cutting Tools*, No. 10, pp. 21-23, 5 illustrations, 1955.
- C. E. Johansson, Continuous Monitoring and the Automatic Control of Machine Tools. *Mesure et controle Industr.*, 1955, April, No. 215, pp. 259-262, 5 figs.
- H. G. Lott, A Position Controller for Controlling the Speed of an Automatic Lathe. *AEG-Mitt.*, 1955, Vol. 45, No. 1-2, pp. 152-155, 7 Abb. Bibliogr. 6.

J. B. Mohler, Automatic Rinsing. Control. Metal Industry, 1955, Oct. 21, Vol. 87, No. 17, pp. 343-346, 8 figs.

Automatic Control of the Number of Revolutions in Order to Guarantee a Constant Cutting Speed. Werkstattstechnik und Maschinenbau, 1955, Vol. 45, No. 1, p. 27.

M. Steinebrunner, Leonard-System Drives and Their Special Applicability to Machine Tools. Werkstatt und Betrieb, 1955, Vol. 88, No. 10, pp. 639-643.

J. A. Stokes, Electronic tracer control of Machine Tools. Engineer, 1955, Febr. 25, Vol. 199, No. 5170, pp. 268-270, 7 figs.; BT-H Actv., 1955, March-April, Vol. 26, No. 2, pp. 53-57.

W. Sussebach and B. Dahm, Installations with Automatic Control for Cutting Sheet Iron for Automobile Chassis. AEG-Mitt., 1955, Vol. 45, No. 1-2, pp. 149-151, 2 Abb. Bibliogr.

#### In the Chemical Industry

A. F. Andreev and L. A. Kostromitin, Automatic Control of the Feed of Flotation Pyrite into a Furnace. Chemical Industry, No. 5, pp. 41-42, 1955.

A. I. Apakhov, A. V. Baleev, I. G. Perevezentsev and G. M. Fialko, Automatic Control of the Preparation of Ozone Oxides for Absorption in Sulphate Concrete Production. Chemical Industry, No. 8, pp. 28-29, 1955.

M. R. Arshtein, Program Control of Thermal Processes in Vulcanizing Boilers (in Factories of the Chemical Industry) Chemical Industry, No. 5, pp. 42-44, 1955.

G. V. Bukhantsev, Theoretical Investigation of the Application of Automatic Control in Soda Production Processes. In the Book: Automation of the Chemical Industry, Moscow, Acad. Sci. USSR, pp. 82-96, 1955.

Papers on the Technology of Inorganic Substances and the Automatic Control of Processes, Leningrad, State Chemical Press, 277 pages, 1955. (Transactions of the Ural Scientific-Research Chemical Institute, No. 3).

A. V. Smirnova, Automatic Control of the Concentration of Sulphuric Acid. Chemical Industry, No. 5, pp. 40-41, 1955.

G. M. Fialko and D. I. Mil'man, Mutually Associated Control of the Technological Parameters in the Drying-Absorbing Divisions of Sulfuric-Acid Contact Factories. Transactions of the Ural Scientific-Research Chemical Institute, No. 3, pp. 235-255, 1955.

G. M. Fialko, Papers of the Ural Scientific Research Chemical Institute on the Automatic Control of Sulfuric-Acid Production Processes. In the book: Automation of the Chemical Industry. Moscow, Acad. Sci. USSR, pp. 47-55, 1955.

G. M. Fialko and D. I. Mil'man, Controllers for the Mutually-Associated Control of Concentration and Level of the Acid in the Drying-Absorption Divisions of Contact Factories which Produce Sulfuric Acid. Transactions of the Ural Scientific-Research Institute, No. 3, pp. 229-235, 1955.

Chemical Feed Control Features Adjustability. Chem. and Engng. News, 1955, 28 Febr., Vol. 33, No. 9, p. 900.

Application of Automatic Control in the Production of Sodium Nitrate Monocrystals. Mesures et controle Industr., 1955, Fevr., 20 Annee, No. 213, pp. 125-128. Bibliogr. 5.

J. Hansen, New Techniques for Measurement, Monitoring and Control in the Chemical Industry. Industriekurier, Techn. und Forschg., 1955, Vol. 8, No. 73, pp. 200, 201, 203.

K. Hengst and A. Meier, Experiments on the Automatic Control of Distilled Cubes. Regelungstechnik, 1955, Vol. 3, No. 9, pp. 219-225, 10 Abb.; No. 10, pp. 243-248, 27 Abb. Bibliogr. 5.

E. F. Johnson, How to Use Frequency Response in Chemical Process Control. Chem. Engng. Progr., 1955, Vol. 51, No. 8, pp. 353-356.



A. Rose, Automatic Control in Continuous Distillation. *Industr. and Engng. Chem.*, 1955, Nov., Vol. 47, No. 11, pp. 2284-2289, 12 figs. Bibliogr. 14.

Round Table on Process Control. *Chem. Engng. Progr.*, 1955, Vol. 51, No. 8, pp. 343-347.

U. Seiffert, Controlling the  $P_{H_2}$ -Value During the Electrolysis of Chlorine. *Anlage. Siemens-Zeitschr.*, 1955, Vol. 29, No. 5/6, pp. 209-212.

G. J. Sleutelberg, Automatic Control in the Chemical Industry. *Teknisk Tidskrift*, 1955, Dec., No. 46, pp. 1031-1032, 1 fig.

B. Sturm, Metering and Control in Chemical Engineering. Berlin, Springer, 1955.

#### In the Oil Industry

A. A. Abdullaev, Automatic Control of a Group of Compressor Wells which are Coupled Through a Common Main Feed Line. *Automation and Remote Control*, Vol. 16, No. 2, pp. 158-171, 1955.

L. V. Karniushin, On Levels and Methods of Investigating the Stability of Automatic Systems for Controlling the Regimes of Oil-Well Drilling Equipment. *Scientific Record of the Lvov Polytechnical Institute*, No. 8, pp. 205-232, 1955.

F. C. Somers and R. C. Fuhs, Here's the First Report of Atlantic Refining's Experience with Electronic Control of a Catformer Unit. *Oil and Gas J.*, 1955, June 27, Vol. 54, No. 8, pp. 82-86, 4 figs.

#### In the Mining Industry

K. F. Bakanov, Remote Automatic Control of Stationary Belt Conveyors by Means of Transmission Lines. Moscow, Central Institute of Technical Information of the Ministry of the Coal Industry of the USSR, 46 pages, 1955.

S. S. Bogutsky, Automatic Control of Mining Machinery. In the book: *Automation of Coal-Mining Process in the Kuzbass Mines*. Kemerov Book Press, pp. 13-16, 1955.

O. B. Klebanov, The Industrial Utilization of New Automatic Pulp-Density Controllers. *Kolyma*, No. 8, pp. 22-28, 1955.

M. F. Lokonov, The State of Automatic Control and Regulation Engineering with Regard to Enrichment Processes. *Bulletin of the Central Institute of Information of Ferrous Metals of the Ministry of Ferrous Metals*, No. 3, (44), pp. 21-27, 1955.

I. L. Faibisovich, Automatic Control of the Feed Rate of Coal-Cutting Machines and Coal Combines. Moscow, 18 pages, 1955 (All-Union Polytechnical Correspondence Institute).

M. J. Defroy, Controlling the Speed of AC Hoisting Machines. *Bull. Soc. franc. Electriciens*, 1955, May, Vol. 5, No. 53, pp. 295-300, 7 figs.

V. Korsgaard, Electric temperatures Regulation of Ventilating Equipment. *Ingeniren*, 1955, Aug. 23, Vol. 64, No. 17, pp. 362-366.

R. Vandaele, Application of Frequency Changers to the Speed Control of Hoist Motors (3-ph Induction Type) *Bull. Soc. Franc. Electr.*, 1955, May, Ser. 7, Vol. 5, pp. 301-304.

H. Sick, A Hydrostatic Controlled Drive for Hoists. *Fordern und Heben*, 1955, Vol. 5, No. 1, pp. 40-43.

#### In the Construction Industry

A. G. Bolko, Continuous-Production Concrete Factories with Automatic Control of the Plasticity of the Concrete Mixture. *Mechanization of Construction*, No. 7, pp. 23-28, 1955.

D. Braun, Automatic Control in a Concrete Factory. *Fordern und Heben*, 1955, Vol. 5, Messe-Sonderausgabe, pp. 113-117.

W. Bury, Control Board for Rotary Kilns in the Cement Industry. *Siemens-Zeitschr.*, 1955, April, Vol. 29, No. 3-4, pp. 145-147.

B. Egberts, Controlling the Efficiency of Tunnel-Type Kilns for Annealing Ceramic. *Elektrizitätswirtschaft*, 1955, Vol. 54, No. 5, pp. 137-138.

#### In the Textile Industry

A. N. Rlabchikov, Automatic Control of Ventilation, Moisture and Central-Heating in Textile Factories. Moscow, Trade Union Press, 94 pages, 46 illustrations, 19 references, 1955.

V. Khokhlov, Automatic Program Control of Temperature in Coloring Silk Fabrics. *Bulletin of Technical and Economic Information of the Institute of Technical and Economic Information of the Acad. Sci. USSR*, No. 9, pp. 19-20, 1955.

R. D. Atchley, Control Stretch with Synchros. *Control Engng.*, 1955, Nov., Vol. 2, No. 11, p. 101.

R. Fahrbeck, Control Sectors in a Silk-Spinning Factory. *Textil-Praxis*, 1955, Vol. 10, No. 5, pp. 425-427.

K. Kreisel, Metering and Regulating the Temperature in Order to Control the Operation of Textile Enterprises. *Textil-Praxis*, 1955, Vol. 10, No. 6, pp. 604-607.

A Thermal Controller for the Automatic Temperature Control of Coloring Baths. *Mesures et controle Industr.*, 1955, Vol. 20, March, No. 214, pp. 203-207, ill.

#### In the Paper Industry

E. Ia. Balmasov, The Automatic Control of the Processes Involved in Cellulose-Paper Production. Leningrad, State Pulp and Paper Press, 248 pages, 85 illustrations, 23 references, 1955.

M. M. Snegirev, Automatic Control of the Vapor Pressure and Humidities of a Paper Strip. *Paper Industries*, No. 5, 13 pages, 1955.

N. Bockmann and G. Robert, Controlling the RPM of the Machinery in the Paper Industry. *Regelungstechnik*, 1955, Vol. 3, No. 2, pp. 36-40, 6 Abb. Bibliogr. 3.

Automatic Control of the Position of the Edges of Paper Sheeting When it is Wound on a Spool. *Techn. Mod.*, 1955, Febr., Vol. 47, No. 2, p. 78, 1 fig.

#### In the Refrigeration Industry

V. Fünér, The State of Development of Techniques for the Regulation and Control of Refrigeration Installations in the USSR. *Kältetechnik*, 1955, Vol. 7, No. 1, pp. 24-25.

D. Metzenauer, American Switching Devices and Controllers for the Refrigeration Industry. *Kältetechnik*, 1955, Jan., Vol. 7, No. 1, pp. 12-13.

O. Møller-Olsen, Automatic Utilization of Large Refrigeration Units. *Kältetechnik*, 1955, Vol. 7, No. 1, pp. 5-8.

W. Niebergall, Processes and Methods for the Control of Adsorption-Type Refrigeration Units. *Kältetechnik*, 1955, Vol. 7, No. 5, pp. 128-133.

#### In the Food Industry

C. Bruhn, Control in Yeast Production. *Siemens-Z.*, 1955, Vol. 29, No. 5-6, pp. 250-251.

H. P. Kaeding, A Milk-Temperature Controller. *Siemens-Z.*, 1955, Vol. 29, No. 1, pp. 11-14.

The Application of Francel-System Controllers in the Sugar Industry. *Mesures et controle Industr.*, 1955, April, Vol. 215, pp. 279-281.

J. P. Rumles, Control of Vaporizers in the Sugar Industry. *Mesures et controle Industr.*, 1955, Febr., 20 année, No. 213, pp. 107-113, 4 figs.



A System for the Automatic Temperature Control of Diffusion Units in Sugar Factories. *Mesures et Controle Industr.*, 1955, Vol. 20, No. 215, pp. 251-255, 3 figs.

G. W. Van Santen, Automatic Regulation of Temperature in a Milk Pasteurizing Plant with the Aid of Electronic Equipment. *Ingenieur*, 1955, April, Vol. 67, No. 14, pp. 0-51-0-55.

#### b) In Transportation

##### In Railroad Transportation

An Automatic Controller for the Excitation of Generators in Railroad Electric Power Stations. Moscow, Railroad Transportation Press, 6 pages, 1955.

N. A. Korchagin and A. B. Fel'dman, Rectifier Units with Automatic Voltage Regulation; Types VU-24/25 and VU-60/2.5. Moscow, Railroad Transportation Press, 22 pages, 1955.

H. Ofverholdm, Recent Swedish Single-Phase Locomotives. *ASEA Journ.*, 1955, Vol. 28, No. 1-2, pp. 3-35.

##### In Marine Transportation

M. Ia. Khabensky, Automatic Temperature Control in Marine Cooling Systems. *River Transportation*, No. 12, pp. 23-24, 1955.

P. S. Dickey and C. H. Barnard, Automatic Control for Marine Boilers. *J. Amer. Soc. Naval Engrs.*, 1955, Aug., Vol. 67, No. 3, pp. 687-696, 5 figs.

##### Air Transportation

N. V. Inozemtsev, Fundamentals of Turbojet Motor Control. In his book: *Gas-Turbine Aviation Engines*. Moscow, Defense Press, pp. 234-268, 47 illustrations, 1955.

M. J. Lawrence, Automatic Control of Aircraft Center of Gravity. *Aeron. Eng. Rev.*, 1955, Oct., Vol. 14, No. 10, pp. 61-65, 5 figs.

J. B. Schrock, Launching Control for Guided Missiles. *Electronics*, 1955, Vol. 28, No. 2, pp. 122-127.

D. F. Winters, The Control of Turbojet Engines. *Aeron. Eng. Rev.*, 1955, June, No. 6, pp. 62-65.

#### c) In Radio Communication

Automatic Gain Control with Alternate Switching. *Journal of Information*, No. 6, pp. 6-8, 1955.

V. I. Siforov, Automatic Control Units in Radio Receivers. In his book: *Ultra-High-Frequency Radio Receivers*. Moscow, Defense Press, pp. 540-550, 12 illustrations, 1955.

W. Donner, Spectrometer regulator Stabilizes R. F. *Electronics*, 1955, Nov., Vol. 28, No. 11, pp. 137-139.

#### d) In Consumer Economy

V. F. Kozhinov, G. S. Popkovich and M. I. Karlinskaia, Automatic Control. In their book: *Automation of the Operation of Tap-Water Channelizing Equipment*. Moscow, State Industrial Press, pp. 96-130, 1955.

G. A. Maksimov, Controlling the Operation of Ventilation Units. In his book: *Central Heating and Ventilation II. Ventilation*. Moscow, State Construction and Architectural Lit. Press, pp. 290-296, 1955.

H. Bock, Optimum Conditions for Utilizing a Refrigeration Unit in Order to Moisten the Air. *Kaltetechnik*, 1955, Vol. 7, No. 6, pp. 159-161.

W. Ende, Automatic Temperature Control of Coke Central Heating. *Industriekurier, Techn. und Forsch.*, 1955, Vol. 8, No. 42 (II), pp. 98-100.

G. Gabrysch, Control of Exhaust-Fan and Suction-Fan Ventilators in Utilizing Steam Boilers. *Energietechnik*, 1955, March, Vol. 5, No. 3, pp. 118-124, 16 Abb. Bibliogr. 27.

- Ch. Kessler and G. Schildt, New Controllers for Central-Heating and Ventilation Engineering. Siemens-Z., 1955, Vol. 29, No. 10, pp. 456-461.
- H. J. Kress, Underground Hospitals. Their Ventilation and the Control of Air-Conditioning. Z. Vereinesdtsch Ingr., 1955, Vol. 97, No. 14, pp. 429-434.
- O. Peter, An Electrical Aggregate for Central Heating. A Temperature Controller. Elektropost, 1955, Vol. 8, No. 1, pp. 10-11.
- G. Spahr, Increasing the Efficiency of a Biological Station which Purifies Stagnant Water by Means of an Electro-Pneumatic Controller. Gesundh. Ing., 1955, Vol. 76, No. 15-16, pp. 240-242.
- E. Sprenger, Problems of Control in Ventilation Engineering and Air-Conditioning Engineering. Regelungstechnik, 1955, Vol. 3, No. 8, pp. 188-193, 13 Abb.
- E. Strempel, Increase the Economy of Heat Consumption in Central Heating Systems. Geschwindh. Ingr., 1955, Vol. 76, No. 13-14, pp. 199-204.
- W. Thilo, A Compensated Pneumatic Controller for Adjusting Air-Conditioning. Sanitare Techn. 1955, No. 20, pp. 81-82.

#### e) In Agriculture

- A. B. Balakhanian, The Development and Testing of an Electrical Tractor with an Automatic Control System for Cable Feed and Tension. In the Collection: Electric-Power Equipment and Automatization of Rural Electric Power Installations. Moscow-Leningrad, State Power Press, pp. 110-116, 1955.
- N. I. Kaletozishvili, Automatic Control of the Power Output of Rural Hydroelectric Stations According to the Water-Flow Regime. In the collection: Electric-Power Equipment and Automatization of Rural Electric Power Installations. Moscow-Leningrad, State Power Press, pp. 32-38, 1955.
- N. N. Nastenka, Methods for Improving the Basic Characteristics of Controllers for Auto-Tractor Motors from the point of View of Increasing the Performance Quality of Agricultural Machines. In the book: Transactions of the Second All-Union Conference on the Theory of Automatic Control, Vol. 1, pp. 543-561, 1955.

#### f) In Other Fields

- S. I. Lomaka, I. Ia. Pleshch and L. Ia. Fel'dman, Investigation of the Mechanism which Governs Automatic Feed Control. In the book: Collection of Student Scientific Papers. Khar'kov Automobile-Highway Institute, No. 9, pp. 41-43, 1955.
- V. M. Obukhov, A Simplified Method for the Automatic Control of Pressure in a Glass Furnace. Glass and Ceramics, No. 7, pp. 23-25, 1955.
- L. P. Podol'sky, Automatic Temperature Control in Drying Furnaces. Railroad Transportation, No. 11, pp. 76-77, 1955.
- M. S. Rozenberg and A. O. Pusen, Two-Pulse Automatic Control of the Parameters of the Drying Agent. Wood-Pulp Processing Industry, No. 12, pp. 7-9, 1955.
- E. D. Besser and E. L. Piret, Controlled Temperature Dielectric Drying. Chem. Engng. Progress, 1955, Vol. 51, No. 9, pp. 405-410.
- H. Dietz and W. Hartel, Controlling the Brightness of the Stage (Theatre) by Means of Low-Voltage Lamps. Siemens - Z., 1955, Vol. 29, No. 1, pp. 4-11.
- R. Holter, Experience in the Utilization of Photoelectric Controllers in the Printing Industry. Polygraph, 1955, Vol. 8, No. 3, pp. 72-73.
- M. A. Hyde and W. A. Derr, Basic Circuitry for Electrically Powered Pipe-Line Pump Stations under Automatic or Remote Control. Trans. AIEE, 1955, Vol. 74, Pt. II, pp. 4-14.

Bibliography Composed by: E. O. Vil'dt and R. S. Landsberg.

Edited by Candidate of Technical Sciences A. V. Khramoi

L 7 5 6 4

